2011 HysplRI Science Workshop

Objectives, Overview and Update

Woody Turner

HysplRI co-Program Scientist

Earth Science Division

NASA Headquarters

August 23, 2011

HyspIRI

HyspIRI is a Tier 2 NASA Decadal Survey ***global*** mission concept featuring:

- a VSWIR imaging spectrometer at 380 to 2500 nm with 10 nm sampling, capturing the Earth's complete terrestrial surface and coastal regions at 60m spatial resolution every 19 days and
- an 8-channel multispectral TIR instrument operating between 3 and 12 microns capturing the same area at 60m spatial resolution every 5 days.

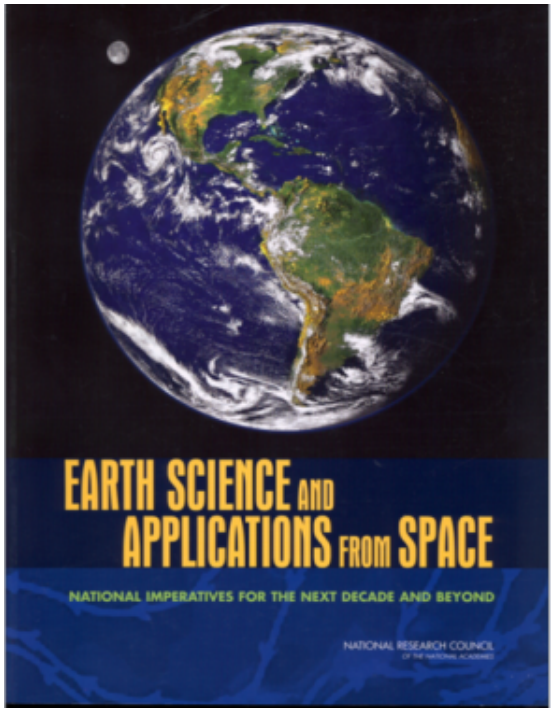

As a global mission, HyspIRI meets the needs of the Earth System Science community.

HyspIRI Management Structure

Earth Science Division
Michael Freilich, Director
Peg Luce, Deputy Director

Research	Flight Programs	Applied Sciences	Technology (ESTO)
Jack Kaye, Associate Director Lucia Tsaoussi, Deputy A.D.	Steve Volz, Associate Director Steve Neeck, Deputy A.D.	Lawrence Friedl, Associate Director	George Komar, Associate Director Bob Bauer, Deputy A.D.

HyspIRI Steering Committee
W. Turner, J. LaBrecque (PS Co-leads); S. Neeck (PE Lead); W. Turner (AS Lead);
R. Green/JPL; S. Hook/JPL; E. Middleton/GSFC;
S. Ungar/GSFC ret.; C. Bruce/JPL; B. Oaida/JPL; B. Knox/GSFC;
B. Edwards (Data); C. Norton (ESTO); A. Mason/C. Wu (Program Office);
M. Fladeland (Airborne)
D. Wickland (Terrestrial Ecology); P. Bontempi (Ocean Biology)

HyspIRI Science Study Group
Co-Chairs R. Green, S. Hook, B. Middleton

HyspIRI International Science Group

HysplRI Science Study Group

Mike Abrams	JPL
Rick Allen	UID
Martha Anderson	USDA
Greg Asner	Carnegie
Paul Bissett	FERI
Alex Chekalyuk	LDEO
James Crowley	USGS
Ivan Csiszar	UMD
Heidi Dierssen	U. Connecticut
Friedmann Freund	NASA Ames
John Gamon	U. Alberta
Louis Giglio	UMD
Greg Glass	JHU
Robert Green	JPL
Simon Hook	JPL
James Irons	NASA GSFC
Bob Knox	NASA GSFC
John Mars	USGS
David Meyer	USGS EROS
Betsy Middleton	NASA GSFC
Peter Minnett	U. Miami
Frank Muller-Karger	USF
Scott Ollinger	UNH
Thomas Painter	JPL
Anupma Prakash	UAF
Jeff Privette	NOAA
Dale Quattrochi	NASA MSFC
Mike Ramsey	U. Pittsburgh
Vince Realmuto	JPL
Dar Roberts	UCSB
Dave Siegel	UCSB
Phil Townsend	U. Wisconsin
Kevin Turpie	NASA GSFC
Steve Ungar	NASA GSFC
Susan Ustin	UC Davis
Rob Wright	UHI

Workshop Objectives

- Update Community on HyspIRI Status
- Review recent projects addressing HyspIRI precursor science
- Focus on applications for HyspIRI Data
- Present Technologies, Tools, and Products supporting a HyspIRI Mission
- Explore Domestic and International Partnership Opportunities
- Examine options for a HyspIRI mission

Workshop Overview

Tuesday:

Programmatic Context, Measurement Concepts, Mission Requirements, Advances in HyspIRI Science

Wednesday:

Global and Regional Applications of HyspIRI data, including: volcanology, mineralogy, fires, agriculture, urban development, energy; along with a few talks on ecosystem science and an overview of Japan's HISUI mission

Thursday:

Mission Design and Precursor Activities, Partnership Opportunities, Cool Coastal Science, Lessons Learned from Previous Missions, Requirements Review, Wrap Up

Past HysplRI Science Workshops

Since the Last Workshop

- ROSES 2010 *HyspIRI Preparatory Activities Using Existing Imagery*
- Regular Steering Committee and Science Study Group Teleconferences
- Reports from two Subgroups addressing issues raised in earlier workshop
  - Sun Glint
  - High-Temperature Saturation
- 2 Workshops on Global HyspIRI Products for Climate Science Research
- 2nd HyspIRI Science Symposium on Ecosystem and Climate Data Products
  - May 2011, NASA GSFC
- Summative Briefing to NASA Management
  - November 2010, NASA HQ
  - Continue focused and limited technology maturation
  - Proceed with excellent community interactions and workshops planned
  - Work with ESD across missions on delivery of low-latency data
  - Support Program Office on TRL assessments of critical HyspIRI technologies
- Finalizing Formation of HyspIRI International Science Group

HysplRI Next Steps

Remember what we are:

- A *global* mission providing VSWIR imaging spectrometry (380 to 2500nm) and multispectral day/night thermal imaging in 8 bands at 60m spatial resolution for global lands and waters <50m depth, with a 19-day repeat for the VSWIR and 5-day repeat for the TIR, and ice sheets and open oceans averaged to 1km
- A broad-based Earth System Science mission
- A mission with mature technologies

Work on:

- Cost reduction
- Retiring risk
- Developing precursor scientific opportunities
- Seek partnerships with domestic and international partners for:
  - joint scientific campaigns; calibration/validation; data product development and use; spacecraft; launch
- Work with other NASA missions
- Be Ready!

THANK YOU

HyspIRI VSWIR Science Measurement and Instrument Concept Baseline

Robert O. Green*, Carl Bruce*, Elizabeth Middleton** and The HyspIRI Team

23 August 2011

*Jet Propulsion Laboratory, California Institute of Technology

**Goddard Space Flight Center

NRD Decadal Survey
HysplRI Mission Concept

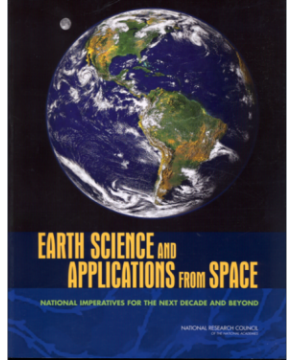

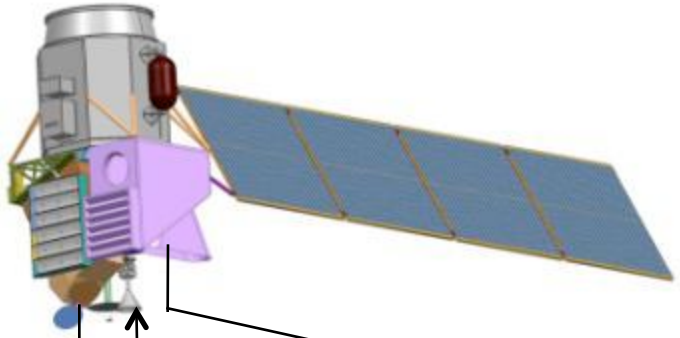

Visible ShortWave InfraRed (VSWIR) Imaging Spectrometer

Multispectral Thermal InfraRed (TIR) Scanner

IPM Low Latency Data

Map of dominant tree species, Bartlett Forest, NH

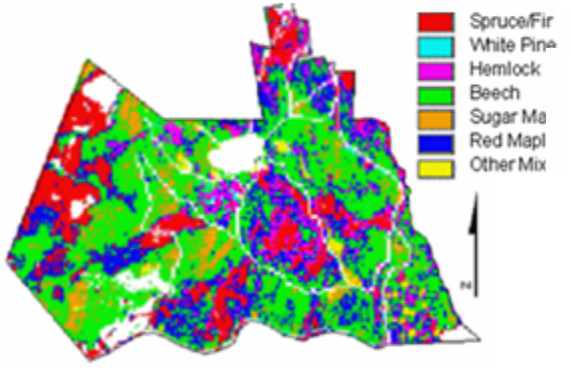

Soil C:N Ratio
White Mountain National Forest, NH

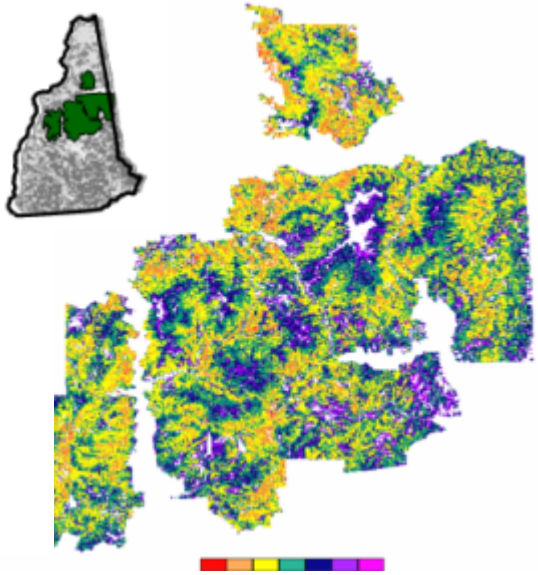

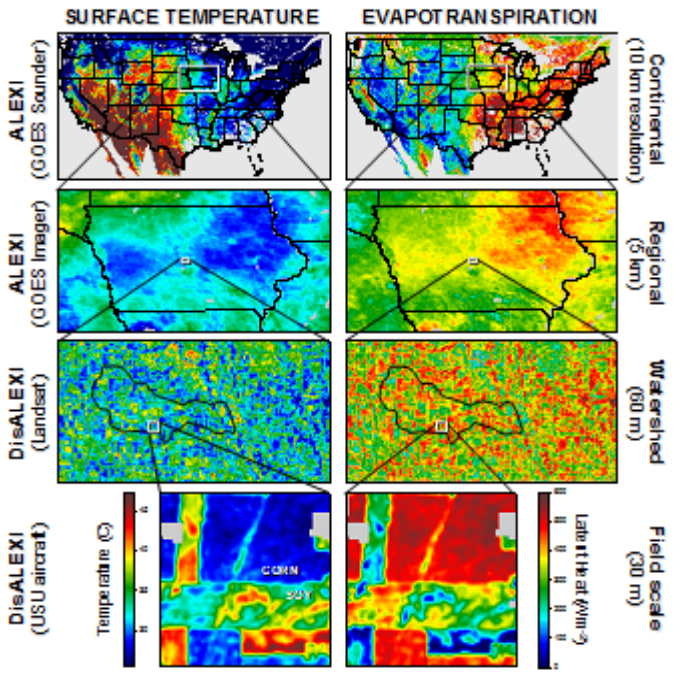

HysplRI Measures the Optical Spectrum

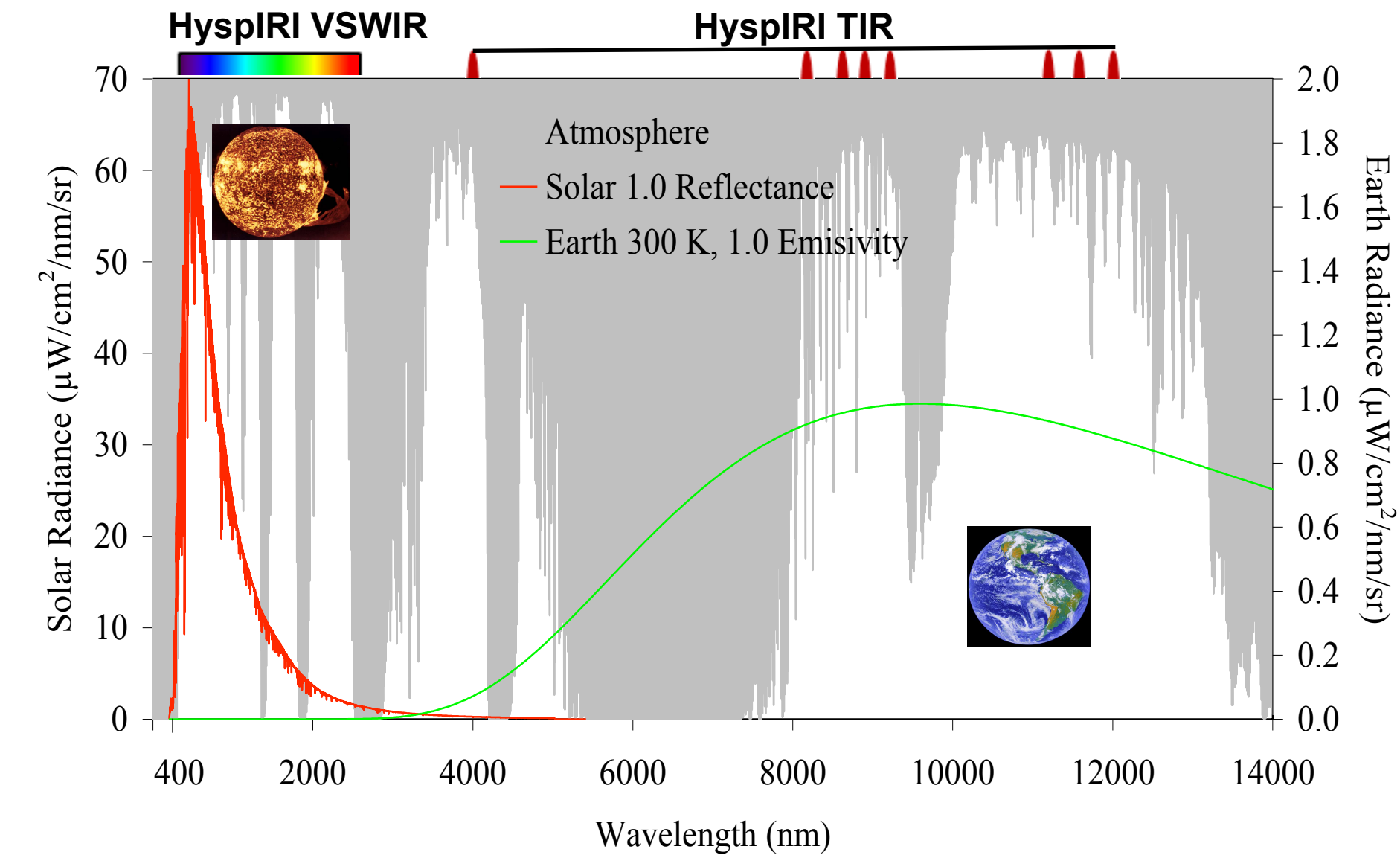

HysplRI VSWIR Decadal Survey Science and Decadal Survey Climate Science

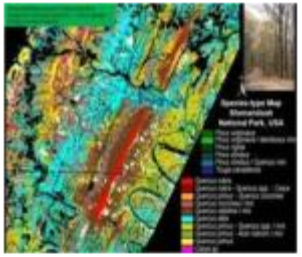

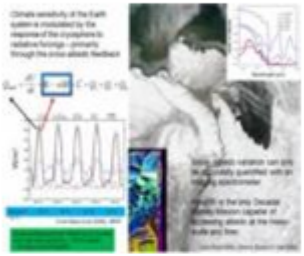

- Key HysplRI climate objectives from the Decadal Survey and IPCC
  - Ecosystem Measurement for Climate Feedback
  - Black Carbon/Dust Effects on Snow and Ice
  - Carbon Release from Biomass Burning
  - Evapotranspiration and Water Use and Availability
  - Critical Volcanic Eruption Parameters
- Imaging Spectrometer (VSWIR)
  - Pattern and Spatial Distribution of Ecosystems and their Components
  - Ecosystem Function, Physiology and Seasonal Activity
  - Biogeochemical Cycles
  - Changes in Disturbance Activity
  - Ecosystem and Human Health
  - Earth Surface and Shallow Water Substrate Composition
- Combined Imaging Spectrometer and Multi-Spectral Thermal Science
  - Coastal habitats, and inland aquatic environments
  - Wildfires
  - Volcanoes
  - Ecosystem Function and Diversity
  - Land surface composition and change
  - Human Health and Urbanization

Example: Imaging Spectroscopy Mapping Wetland Dominants 2010 LA

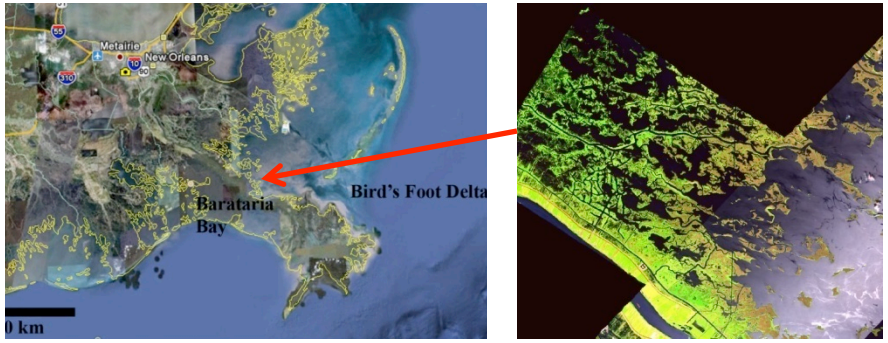

AVIRIS Vegetation Spectra

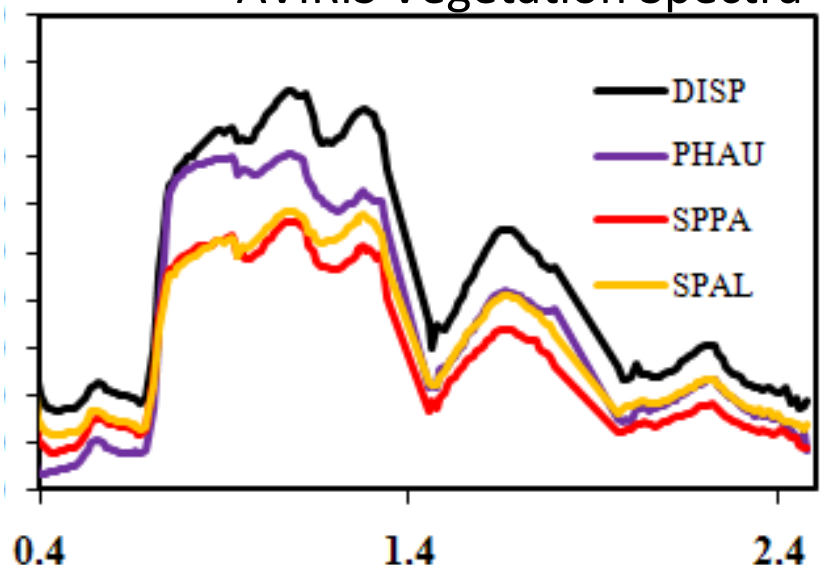

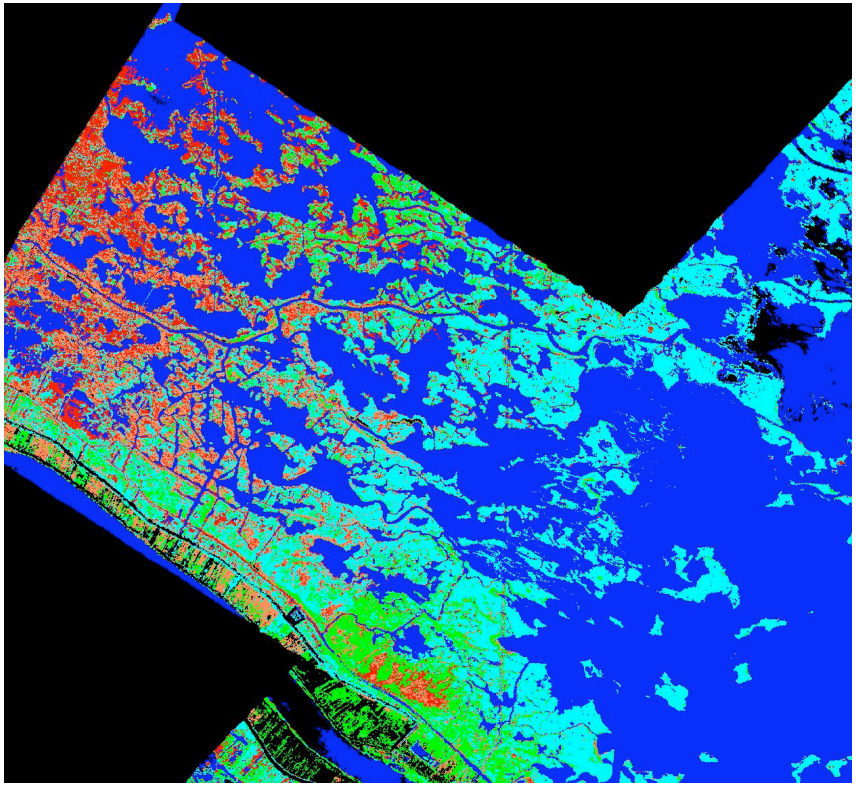

Water/ glint | phau | spal

sppa | vilu | Unclass

Vegetation mapped cleanly across scene boundaries

- *Phragmites (phau)*
- *Spartina alterniflora (spal)*
- *Spartina patens (sppa)*
- *Vigna luteola (vilu)*

D. Roberts, UCSB

Spectroscopy for Species/Functional-type, Biogeochemistry and Physiological Condition

PLSR weighting for foliar Nitrogen

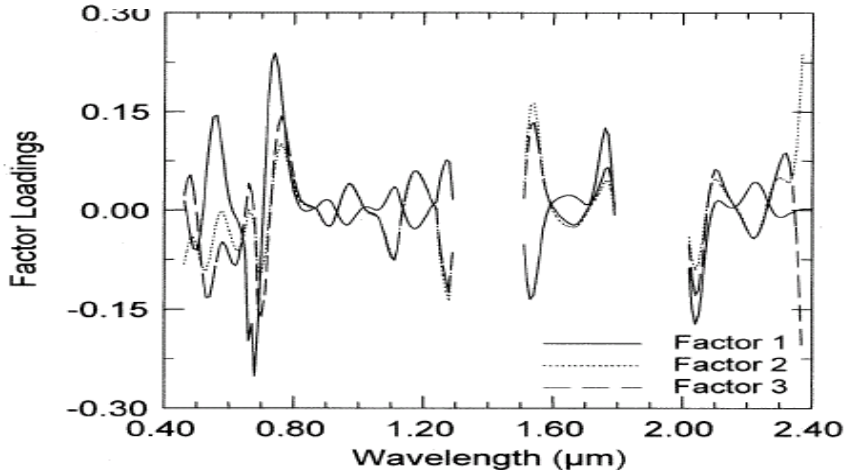

PLSR wavelength selection for one species

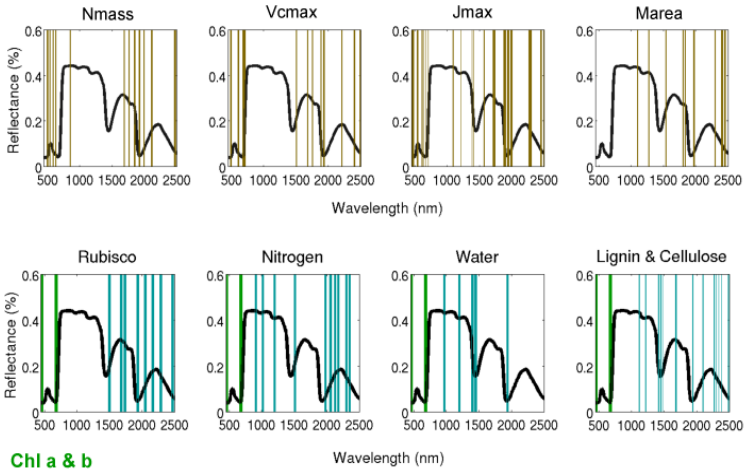

Measuring spectral shift from Lignin : Cellulose ratio

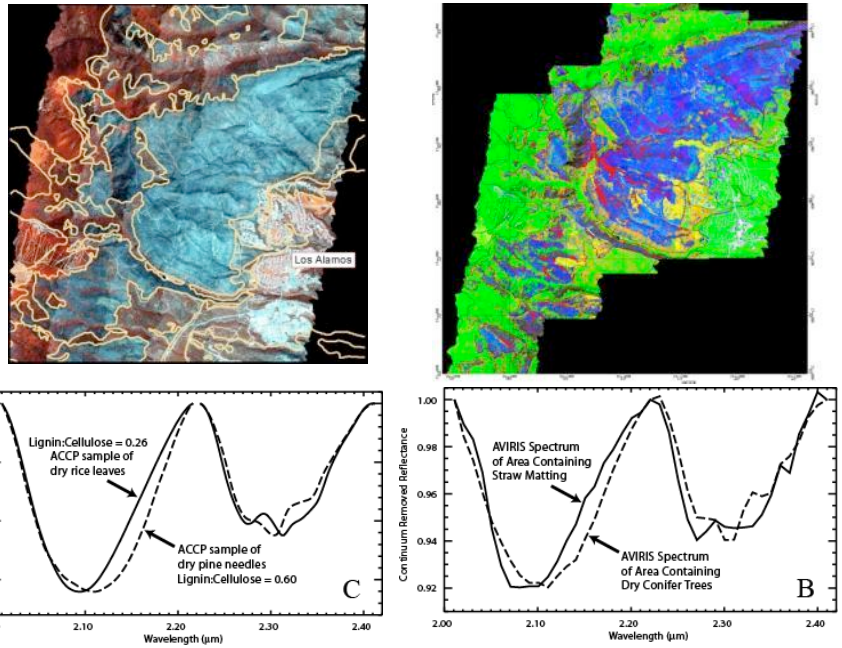

Chl a & b

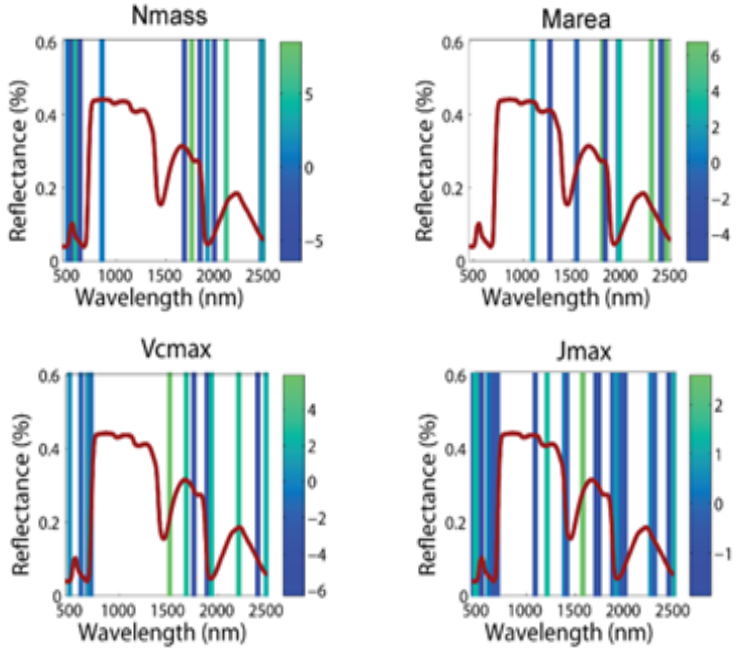

Surface Compositional Derived with Imaging Spectrometer Measurements

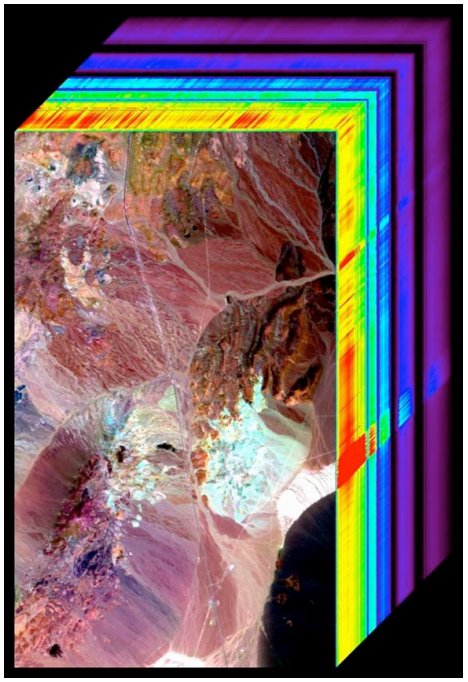

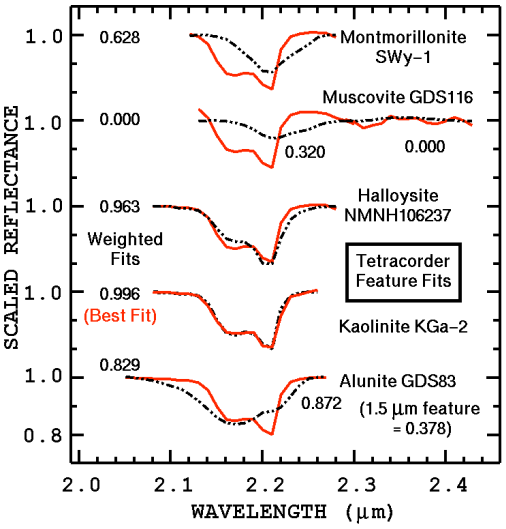

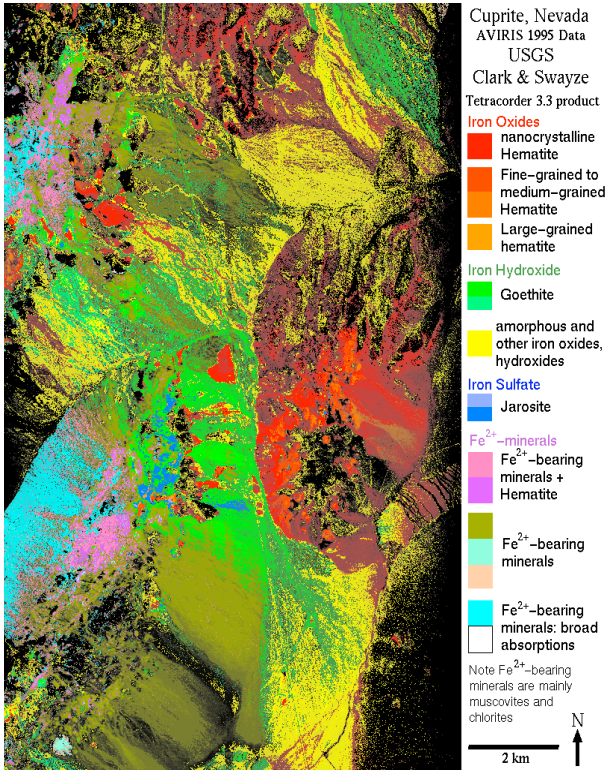

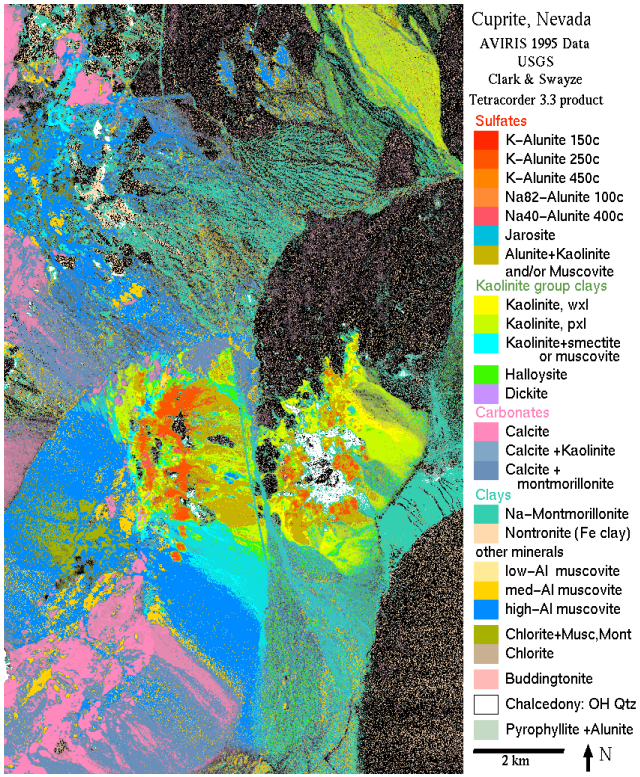

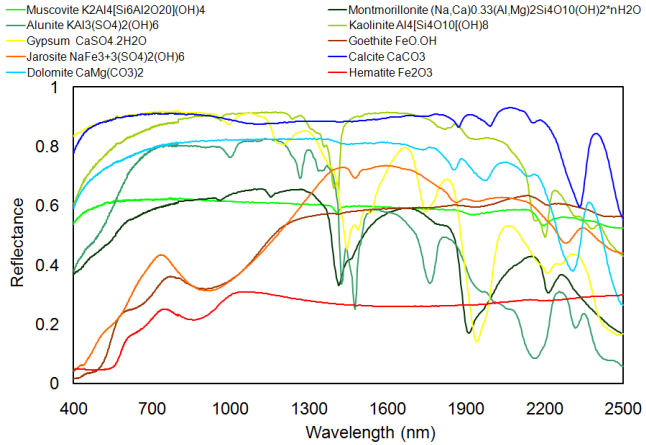

Albedo and Black Carbon/Dust Effects on Snow/Ice

What is causing the downwasting and retreat of Himalayan glaciers and elsewhere?

For snow and ice in the Himalaya, increasing temperatures and increasing dust and soot combine in unknown proportions to accelerate melt through their changes in albedo. Imaging Spectrosocpy is the only approach that allows us to attribute changes in albedo into effects from temperature and dust/black carbon and at a fine enough spatial resolution that heterogeneous terrain can be resolved. Multi-band sensors such as NPOESS VIIRS have neither capacity.

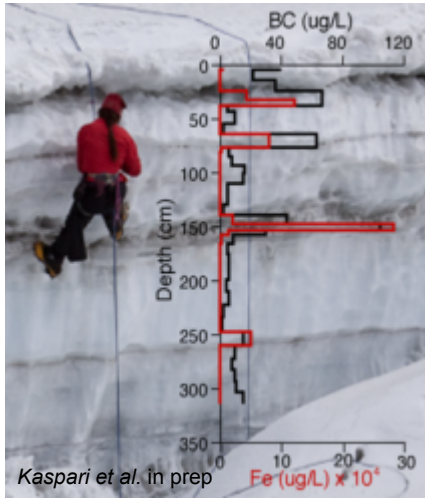

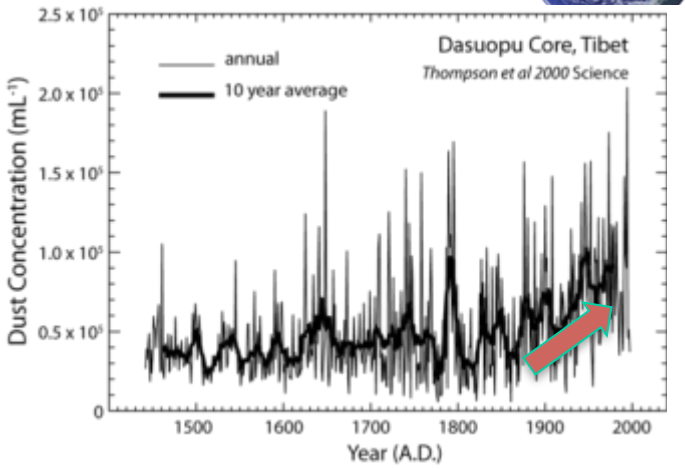

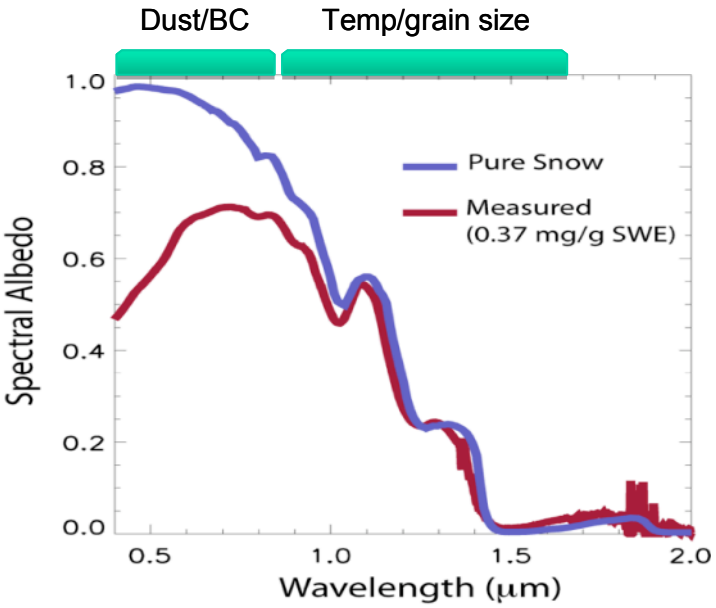

Required Measurement: Global glacial covered area, full solar spectrum, < 100 m spatial, <20 days revisit

HyspIRI: Coral, Benthic Composition, and Aquatic Vegetation

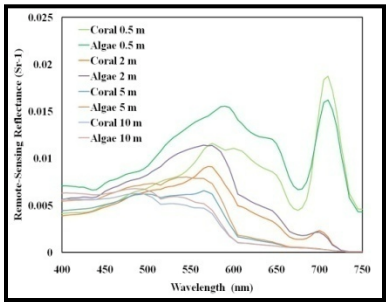

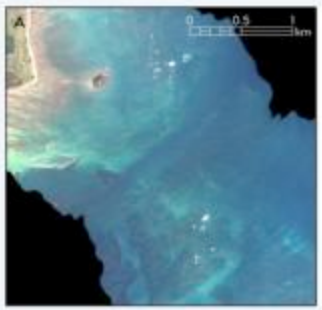

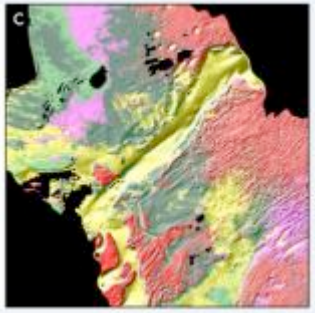

Variation in shallow water HyspIRI-type spectral signatures in coral environments.

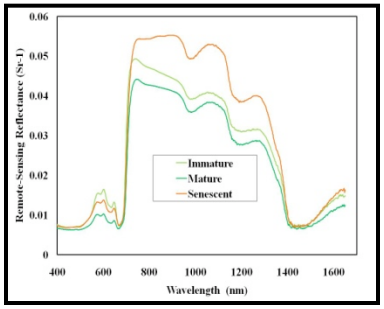

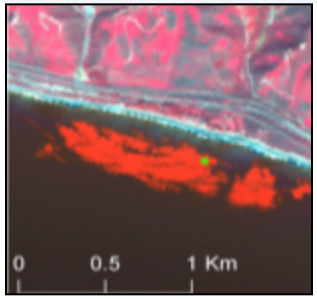

Variation in HyspIRI-type spectral signatures of floating aquatic vegetation (e.g. Kelp)

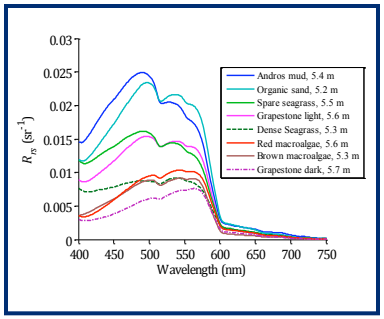

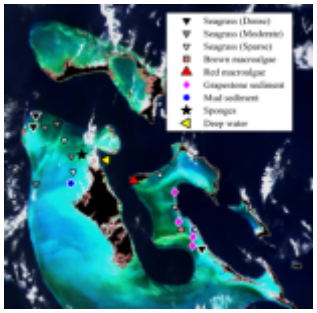

Variation in shallow water HyspIRI-type spectral signatures in seagrass beds and benthic habitat materials

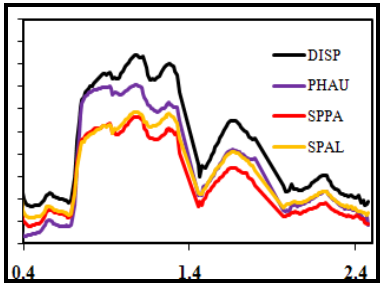

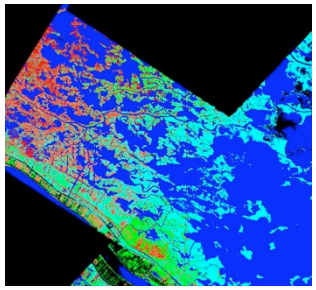

Emergent vegetation signatures are well suited to the HyspIRI measurement. For example mapping in the Gulf of Mexico coastal region with AVIRIS measurements.

HysplRI VSWIR Science Measurements

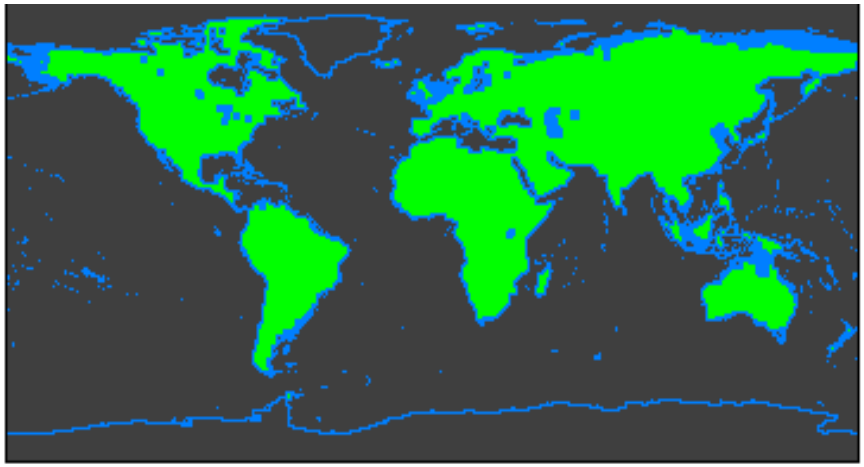

HysplRI is a global mission, measuring land and shallow aquatic habitats at 60 meters and deep oceans and ice sheets at 1km every 19 days (VSWIR)

HysplRI's VSWIR imaging spectrometer directly measures the full solar reflected spectrum of the Earth from 380 – 2500nm at 10 nm.

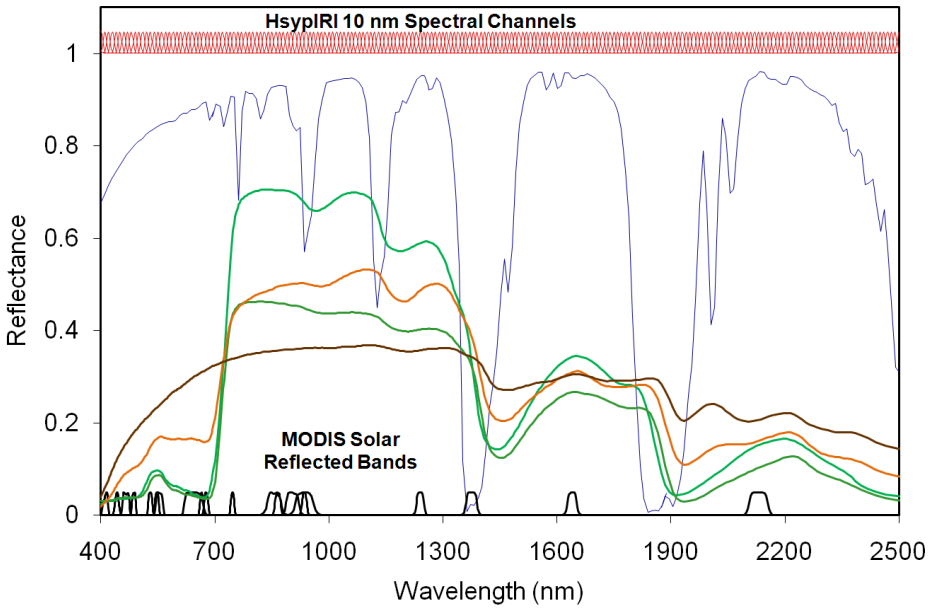

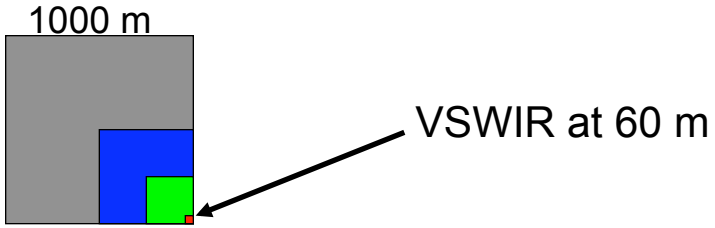

HysplRI VSWIR SNR and Uniformity Characteristics

Benchmark Radiances

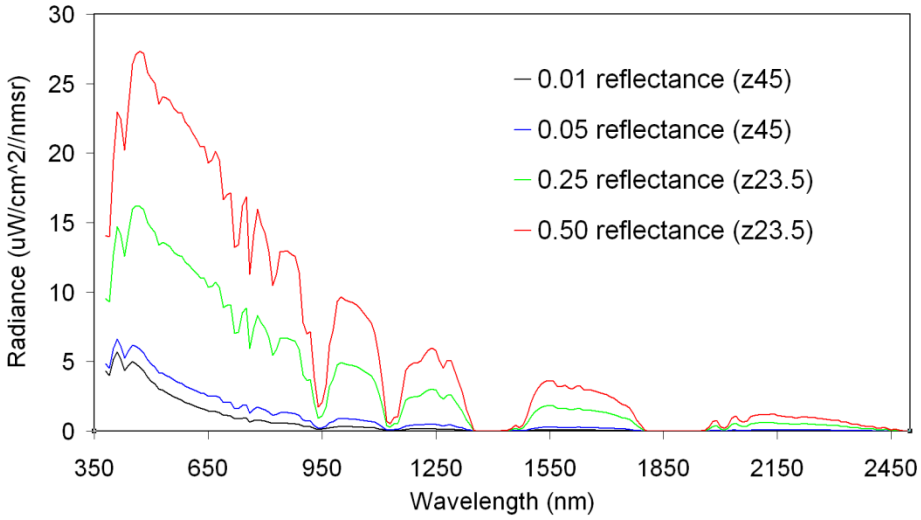

Signal-to-Noise Ratio

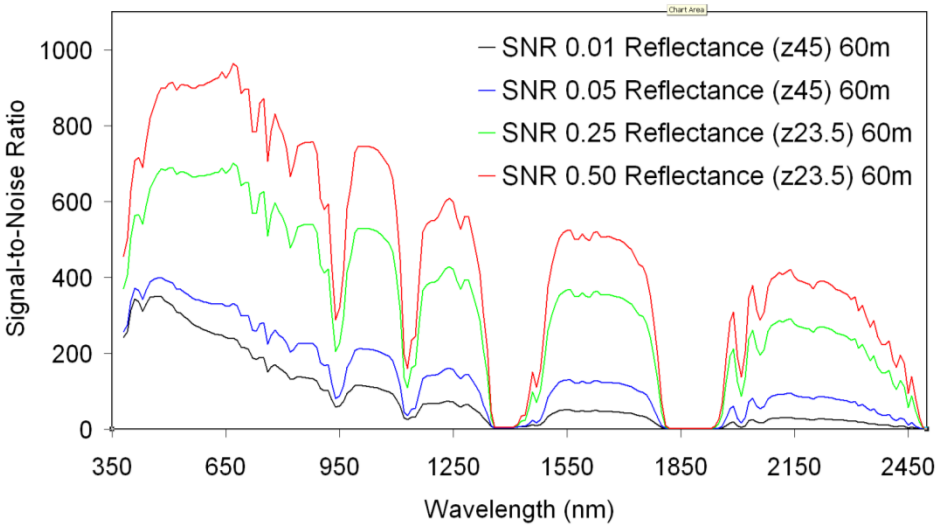

Uniformity Requirement

Cross Track Sample

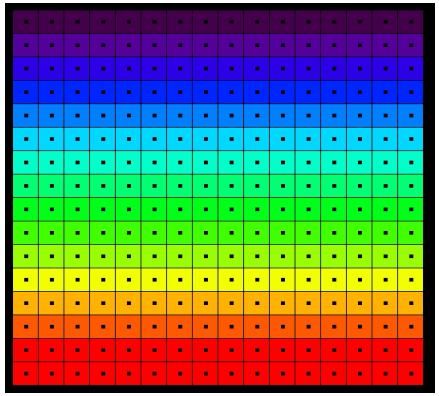

Depiction

-Grids are the detectors
-Dots are the IFOV centers
-Colors are the wavelengths

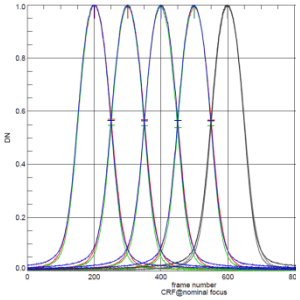

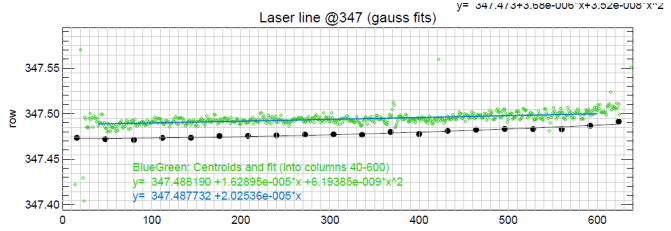

Requirement

Spectral Cross-Track	>95% cross-track uniformity {<0.5 nm min-max over swath}
Spectral-IFOV-Variation	>95% spectral IFOV uniformity {<5% variation over spectral range}

Seasonal and Annual Cloud Probability Maps Validate the HyspIRI Coverage Requirements

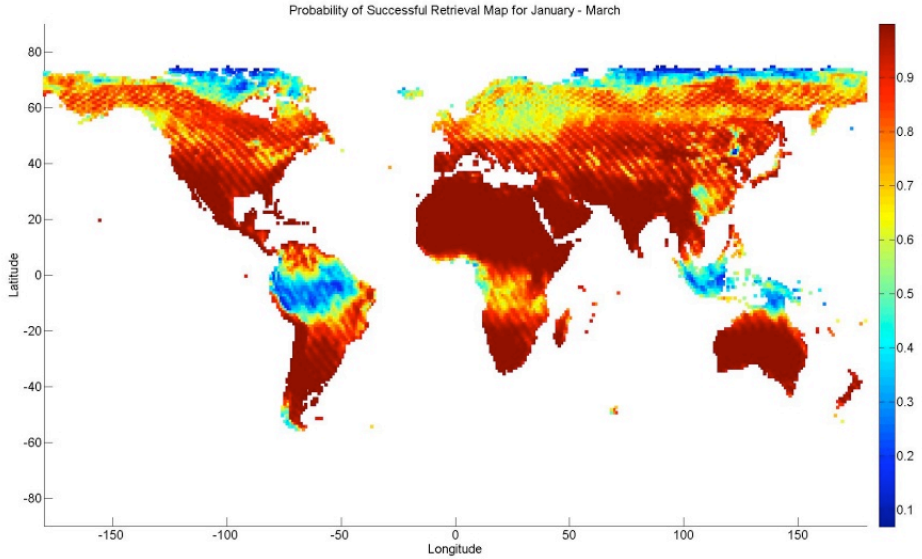

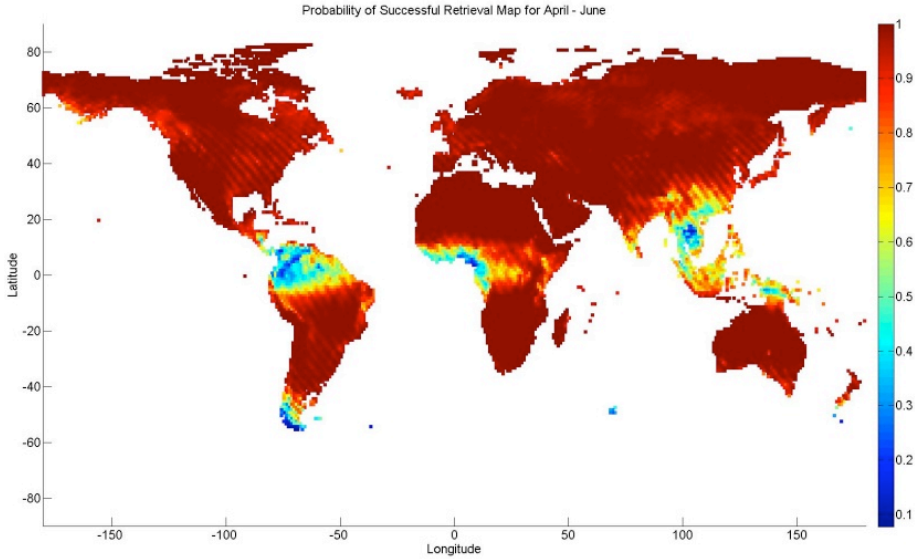

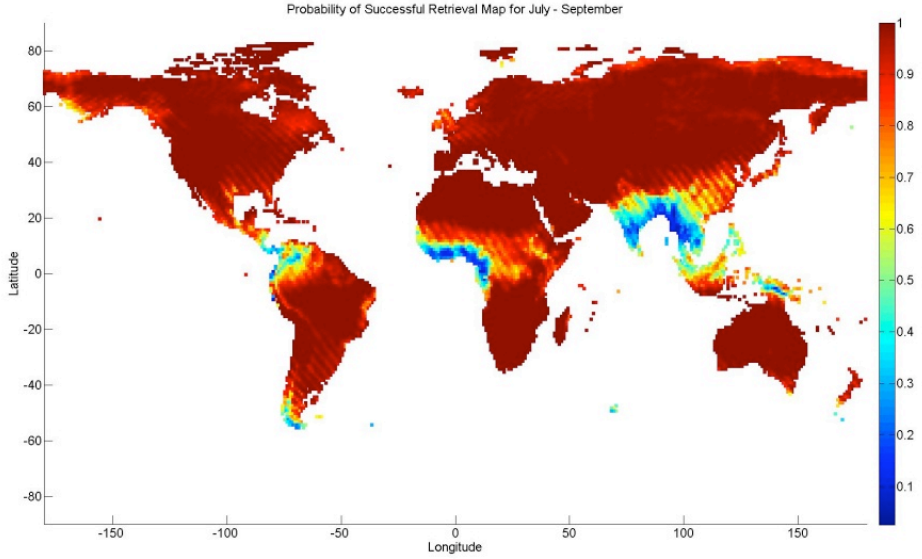

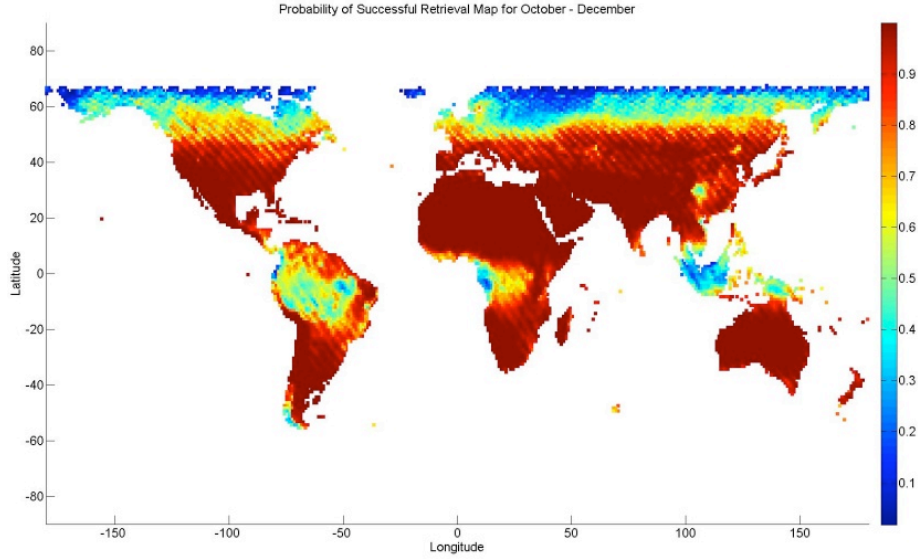

HyspIRI VSWIR Coverage

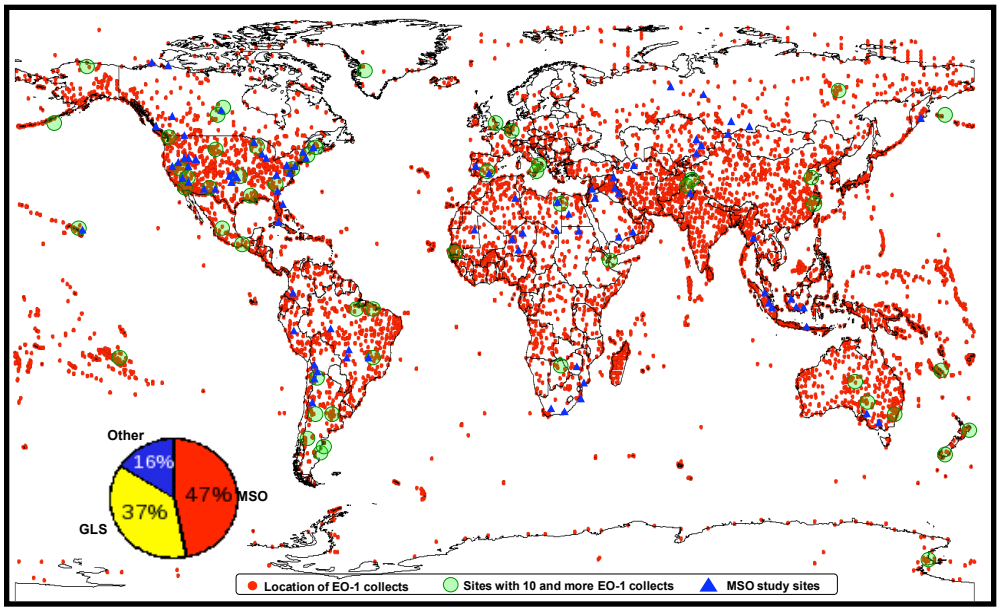

- EO-1 Hyperion acquisitions in 10 years. Technology demonstration sampling mission with deep ESTO contribution.

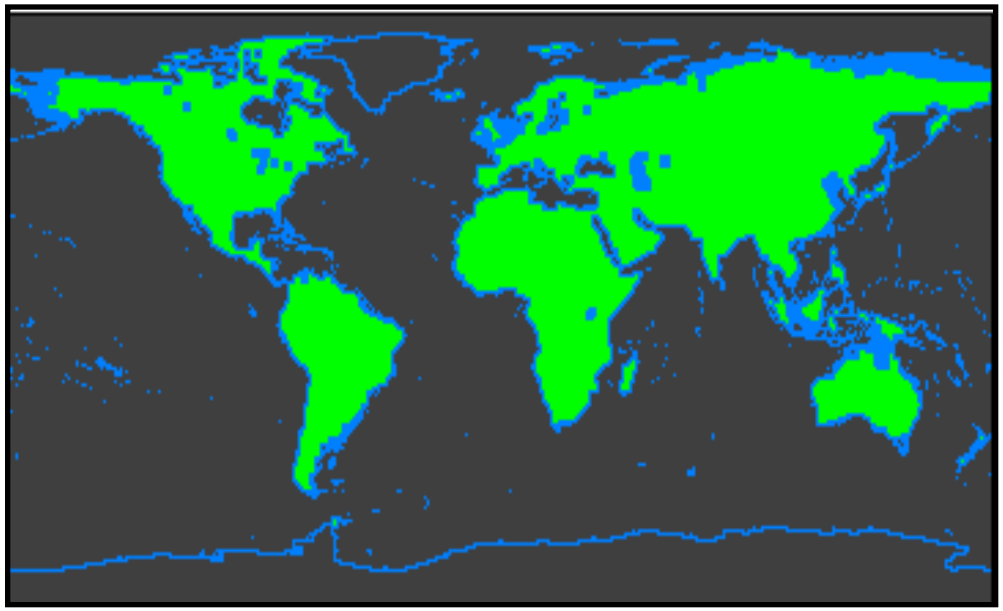

- HyspIRI VSWIR provides complete terrestrial coverage every 19 days.
- It would take Hyperion 100 years to acquire what HyspIRI measures in 1 year.

VSWIR - Instrument Concept

OUTLINE

1. Introduction
2. Key Requirements & Performance
3. VSWIR Concept
4. Technology Readiness & Heritage

HysplRI – VSWIR

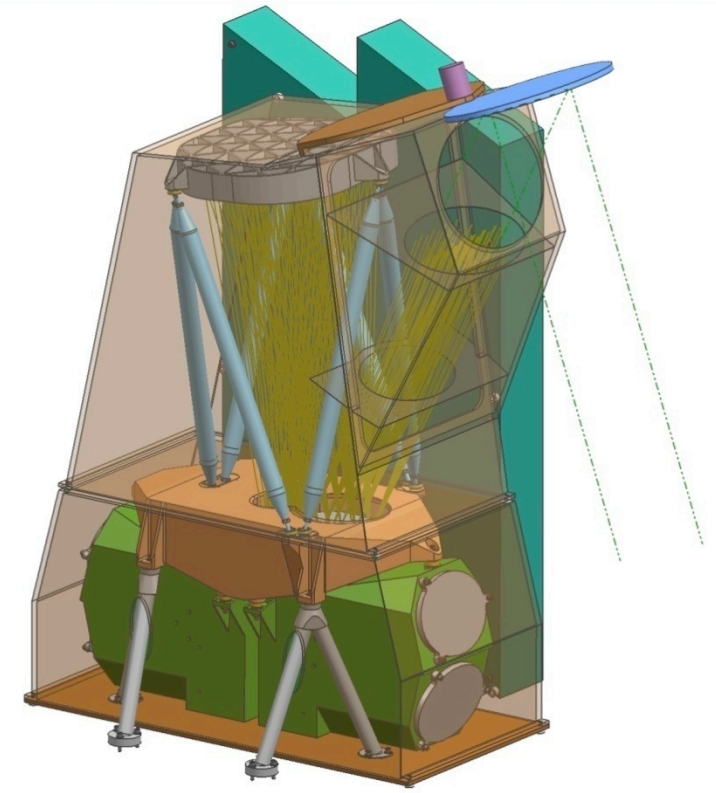

Mass (CBE) ***55Kg***
Power (Ave.) ***41Watts***

Key VSWIR Requirements

Spectral	Requirement	Status
Range	380 to 2500 nm (solar reflected spectrum)	Demonstrated – AVRIS, MaRS, M3
Sampling	<= 10 nm {uniform over range}	Demonstrated – MaRS, M3
Response	<= 13 nm (FWHM) {uniform over range}	Demonstrated – MaRS, M3
Accuracy	<0.5 nm	Demonstrated – MaRS, M3, CAO-VSWIR

Radiometric	Requirement	Status
Range & Sampling	0 to 1.5 x benchmark radiance, 14 bits	Demonstrated via analysis and 14 bit ADC bread board electronics
Accuracy	>95% absolute radiometric, 98% on-orbit reflectance, 99.5% stability	Demonstrated – AVIRIS, MaRS
Precision (SNR)	See spectral plots at benchmark radiances	Demonstrated via analysis
Linearity	>99% characterized to 0.1 %	Demonstrated via test, MaRS and CAO-VSWIR
Polarization	<2% sensitivity, characterized to 0.5 %	Demonstrated via analysis of design and test data on the grating
Scattered Light	<1:200 characterized to 0.1%	Demonstrated in MaRS and CAO-VSWIR

Key VSWIR Requirements

Spatial	Requirement	Status
Range	>145 km	Demonstrated by design and analysis (150 km)
X-track Sampling	>2400	Demonstrated by design and analysis (2500)
Sampling	<= 60m (Nadir)	Demonstrated by design and analysis
Response	<= 1.2X sampling (FWHM)	Demonstrated by MaRS and M3
Uniformity		
Spectral Cross-Track	>95% cross-track uniformity {<0.5 nm min-max over swath}	Demonstrated by MaRS and M3
Spectral-IFOV-Variation	>95% spectral IFOV uniformity {<5% variation over spectral range}	Demonstrated by MaRS and M3

Other Key	Requirement	Status
Data rate	~ 300 Mbits per second	Met by preliminary architecture and parts selection – all required parts are at or above TRL 6
Compression	3:1 lossless	Met by algorithm test on MaRS data. Algorithms implemented in breadboard electronics and flight FPGA
Pointing Knowledge	60m radius (3σ)	Met by analysis and the use of ground tie points
Mass	<55 kg	Met by current design with 30% margin – working to increase margin

Instrument Approach

- **Selected: Offner spectrometer (Hyperion, CRISM, M3, ARTEMIS, COMPASS^{air}, NG^{air})**
  - Full range from 380 to 2500 nm demonstrated. Efficiency for high SNR optimized with multiple blaze grating demonstrated. Uniformity from design through alignment demonstrated. Snapshot acquisition detector. Dispersion efficiency tunable to optimize use of detector.

- Prism dispersion spectrometer
  - Dispersion is non-uniform. Cross-track and spectral-IFOV uniformity not inherent in optical design. Dispersion efficiency not tunable in detail to optimize use of detector full well.
- Wedge/Linear-variable filter spectrometer
  - Full spectral range coverage from 380 to 2500 nm has not been demonstrated maintaining 10 nm spectral sampling and response function. Filter uniformity is a concern over wide spectral and spatial domain. Fast, high throughput, beams interplay with filter spectral bandpass undermines uniformity.
- Fourier Transform Spectrometer
  - Dispersion is non constant with wavelength. Not typically built to operate below 1 micron. Detector dynamic range and photon shot noise concern. Architecture for > 2000 cross track elements and >200 spectral channels not identified. Not well suited for wide or moderate field of view. Requires IMC.
- Liquid Crystal Tunable & Acousto-Optical Tunable
  - Time sequential acquisition undermines uniformity. Low TRL, polarization sensitive. Limited spectral range. Requires IMC.

HyspIRI VSWIR Concept

Optics
• Front End Telescope consists of a primary spherical mirror and a secondary aspherical mirror

• Back End Spectrometers consist of 2 optimized Offner spectrometers

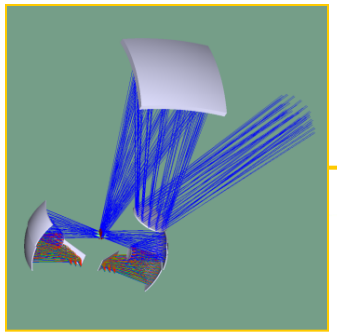

Spectrometers (2x)
- 2 identical Offner spectrometers
- Each contains:
  - E-Beam grating
  - Si air slits
  - FPA assembly

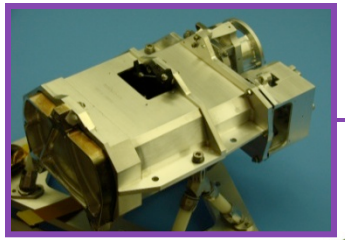

Radiator
• Area 0.6m^2
• M3 technology heritage

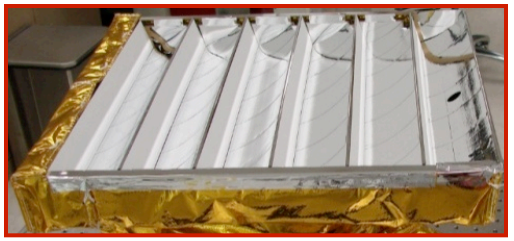

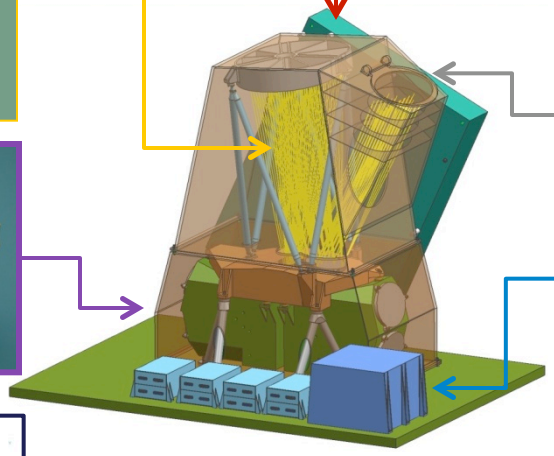

Baffle/Cover/Cal Panel
• *Launch cover*
•*Used as a solar reflectance calibration target*
•*Hyperion Heritage*

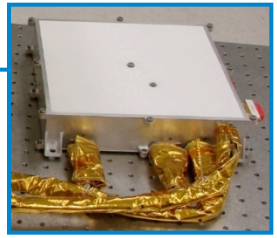

Electronics
• M3 Derivative 4x

• Electronic concept is based upon available flight approved parts

• Ins. control, Data Compression, mode control

FP A (2x)
• Mount is adjustable in 6 DOF

• Thermal strap connects mount to radiator

•Includes integral OSF

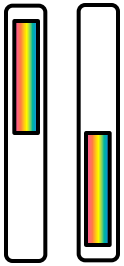

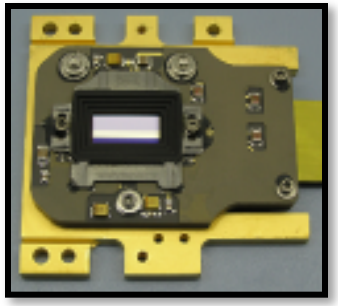

Detectors
- Teledyne 6604b detectors, scaled from 6604a detectors flown on M3
- Analog output
- Each spectrum readout as snapshot, so that there is no time delay, yaw, or jitter impact to the spectral-IFOV-uniformity.

Concept Technologies are Proven Work Continues to Lower Risk

1) Uniform Offner spectrometer (Mouroulis Design)

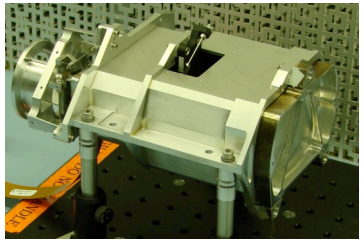

2) Finely adjustable optics and detector mounts that can be locked within fraction of a micron (0.1 microns)

3) Electron beam fabricated gratings (large ruling period)

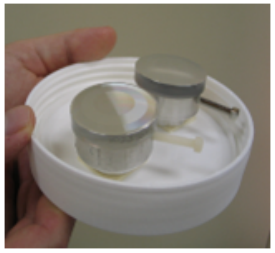

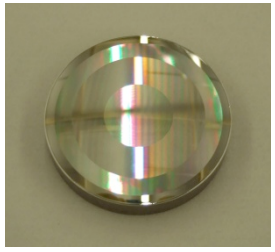

4) Electron beam fabricated air slits (non-uniformity < .05 microns)

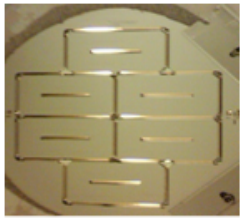

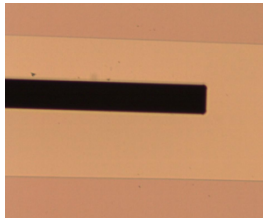

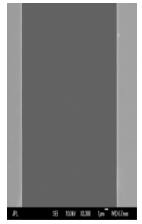

5) Alignment and calibration sources and methodologies to achieve and verify requirements.

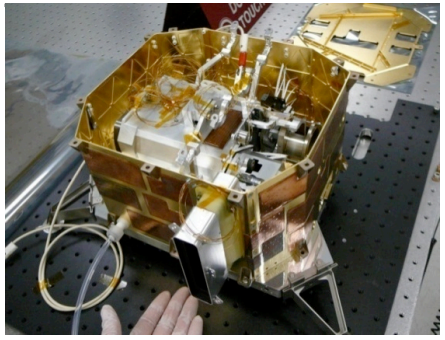

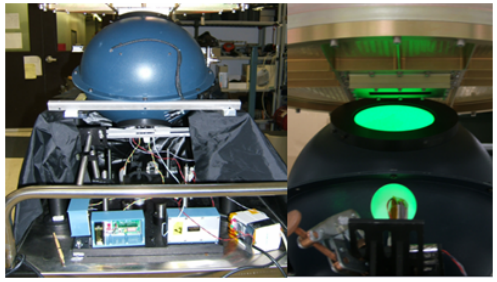

The HyspIRI VSWIR Concept Enables the Full Set of Decadal Survey Science and Science Applications and Climate Science

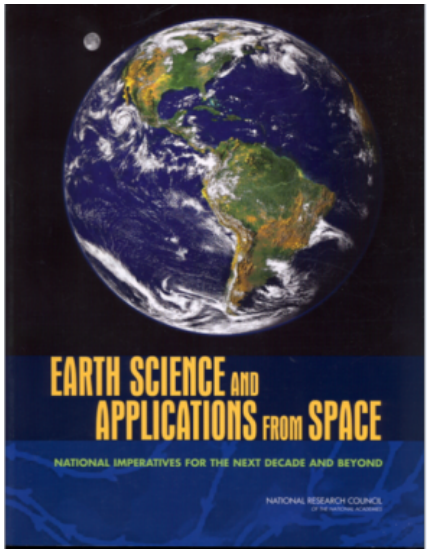

- Key HyspIRI climate objectives from the Decadal Survey and IPCC
  - Ecosystem Measurement for Climate Feedback
  - Black Carbon/Dust Effects on Snow and Ice
  - Carbon Release from Biomass Burning
  - Evapotranspiration and Water Use and Availability
  - Critical Volcanic Eruption Parameters

Imaging Spectrometer (VSWIR)

- Pattern and Spatial Distribution of Ecosystems and their Components
- Ecosystem Function, Physiology and Seasonal Activity
- Biogeochemical Cycles
- Changes in Disturbance Activity
- Ecosystem and Human Health
- Earth Surface and Shallow Water Substrate Composition

Combined Imaging Spectrometer and Multi-Spectral Thermal Science

- Coastal habitats, and inland aquatic environments
- Wildfires
- Volcanoes
- Ecosystem Function and Diversity
- Land surface composition and change
- Human Health and Urbanization

Questions?

Backup

Concept Technologies are Proven Work Continues to Lower Risk

1) Uniform Offner spectrometer (Mouroulis Design)

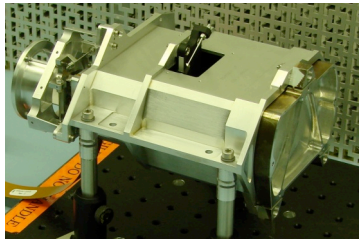

2) Finely adjustable optics and detector mounts that can be locked within fraction of a micron (0.1 microns)

3) Electron beam fabricated gratings (large ruling period)

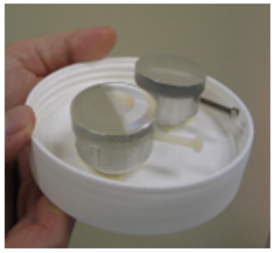

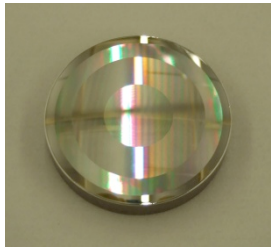

4) Electron beam fabricated air slits (non-uniformity < .05 microns)

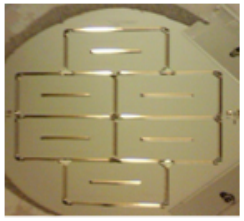

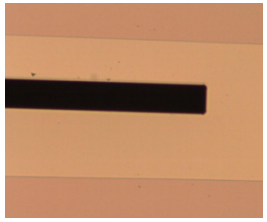

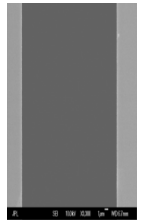

5) Alignment and calibration sources and methodologies to achieve and verify requirements.

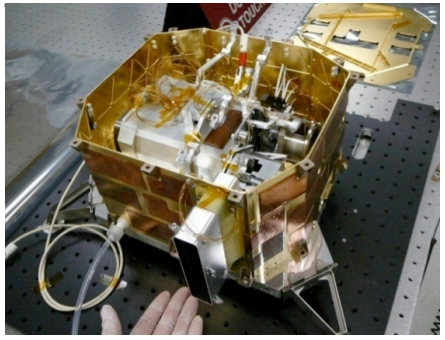

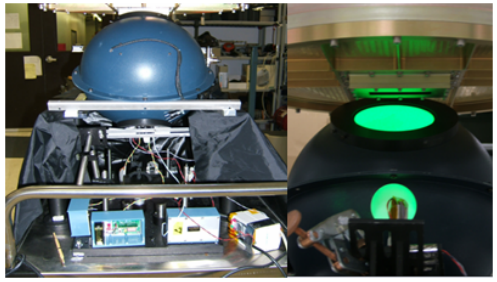

HyspIRI

TIR Science Measurement Baseline and Instrument Concept

NASA Earth Science and Applications Decadal Survey

Simon J. Hook and HyspIRI Team

© 2011 California Institute of Technology. Jet Propulsion Laboratory, California Institute of Technology. Government sponsorship acknowledged.

NRC Decadal Survey HyspIRI

Visible ShortWave InfraRed (VSWIR) Imaging Spectrometer
+
Multispectral Thermal InfraRed (TIR) Scanner

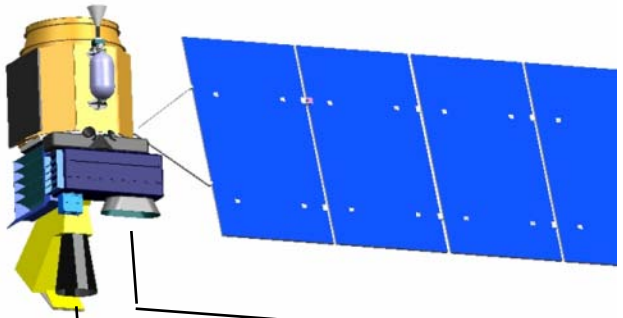

VSWIR: Plant Physiology and Function Types (PPFT)

Multispectral TIR Scanner

Map of dominant tree species, Bartlett Forest, NH

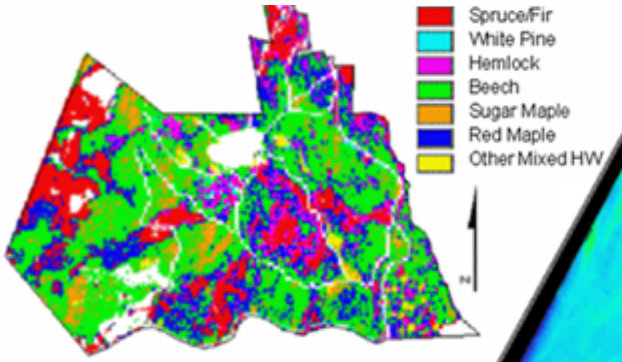

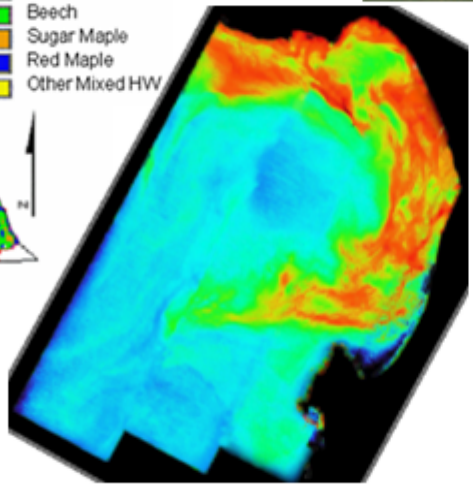

Red tide algal bloom in Monterey Bay, CA

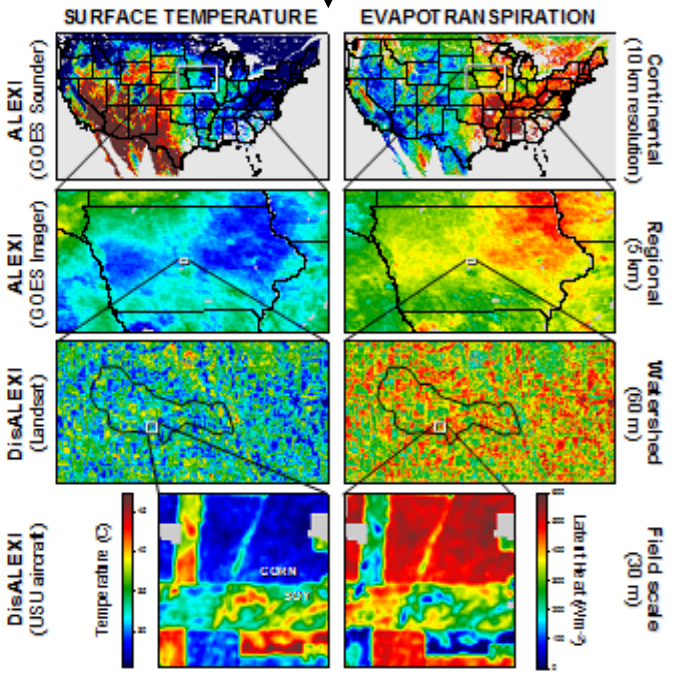

HyspIRI Thermal Infrared Multispectral (TIR) Science Measurements

Science Questions:

TQ1. Volcanoes/Earthquakes (MA,FF)

– How can we help predict and mitigate earthquake and volcanic hazards through detection of transient thermal phenomena?

• TQ2. Wildfires (LG,DR)

– What is the impact of global biomass burning on the terrestrial biosphere and atmosphere, and how is this impact changing over time?

• TQ3. Water Use and Availability, (MA,RA)

– How is consumptive use of global freshwater supplies responding to changes in climate and demand, and what are the implications for sustainable management of water resources?

• TQ4. Urbanization/Human Health, (DQ,GG)

– How does urbanization affect the local, regional and global environment? Can we characterize this effect to help mitigate its impact on human health and welfare?

• TQ5. Earth surface composition and change, (AP,JC)

– What is the composition and temperature of the exposed surface of the Earth? How do these factors change over time and affect land use and habitability?

Measurement:

- 7 bands between 7.5-12 µm and 1 band at 4 µm. (4 um band for hot targets)
- 60 m resolution, 5 days revisit
- Global land and shallow water

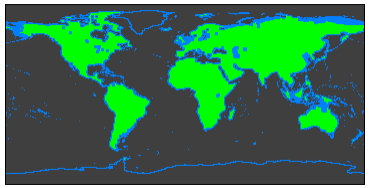

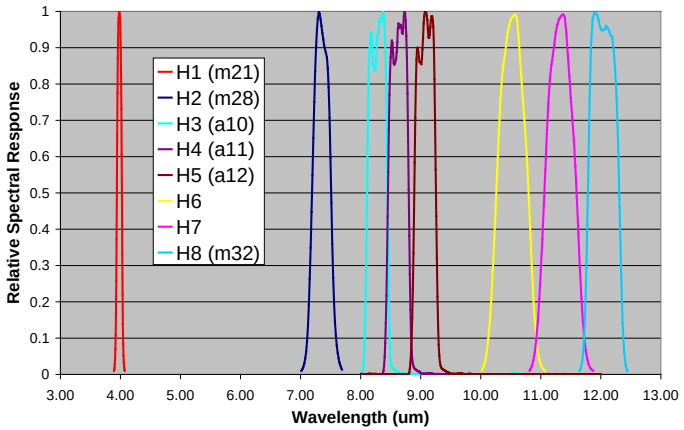

Andean volcano heats up

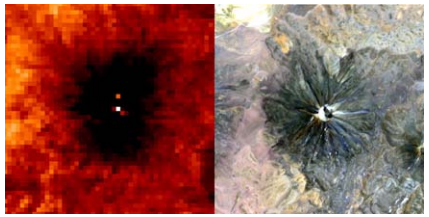

Volcanoes

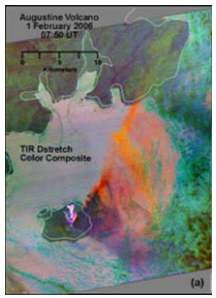

Urbanization

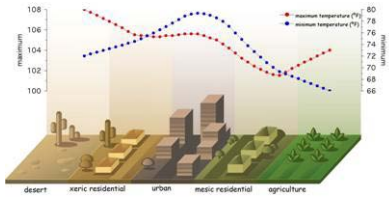

Water Use and Availability

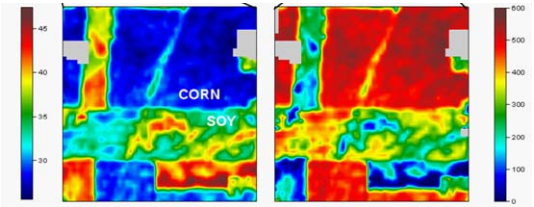

Surface Temperature

Evapotranspiration

TIR Overarching Science Questions

- **TQ1. Volcanoes/Earthquakes (MA,FF)**
  - How can we help predict and mitigate earthquake and volcanic hazards through detection of transient thermal phenomena?
- **TQ2. Wildfires (LG,DR)**
  - What is the impact of global biomass burning on the terrestrial biosphere and atmosphere, and how is this impact changing over time?
- **TQ3. Water Use and Availability, (MA,RA)**
  - How is consumptive use of global freshwater supplies responding to changes in climate and demand, and what are the implications for sustainable management of water resources?
- **TQ4. Urbanization/Human Health, (DQ,GG)**
  - How does urbanization affect the local, regional and global environment? Can we characterize this effect to help mitigate its impact on human health and welfare?
- **TQ5. Earth surface composition and change, (AP,JC)**
  - What is the composition and temperature of the exposed surface of the Earth? How do these factors change over time and affect land use and habitability?

Gas and thermal anomalies, plume composition including SO2 and ash content on weekly basis

Characterizing and Understanding Volcanic Eruptions

"Likewise, the Tier 2 **Hyperspectral Infrared Imager (HyspIRI)** mission would include measurements over a range of optical and infrared wavelengths useful for detecting volcanic eruptions, determining the ash content of volcanic plumes, and identifying the occurrence and effects of associated landslides."

Source: Dr Jack Kaye, Presented to
Subcommittee on Space and Aeronautics
Committee on Science and Technology
United States House of Representatives,
May 5, 2010

Characterizing and Understanding Volcanic Eruptions

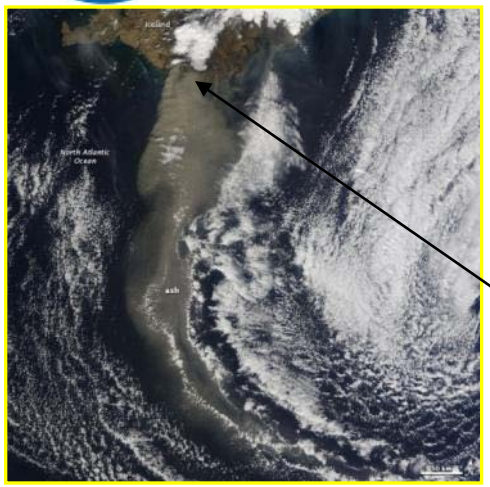

Eyjafjallajökull Iceland Volcano Eruption

April 19 2010 MODIS image of ash plume.

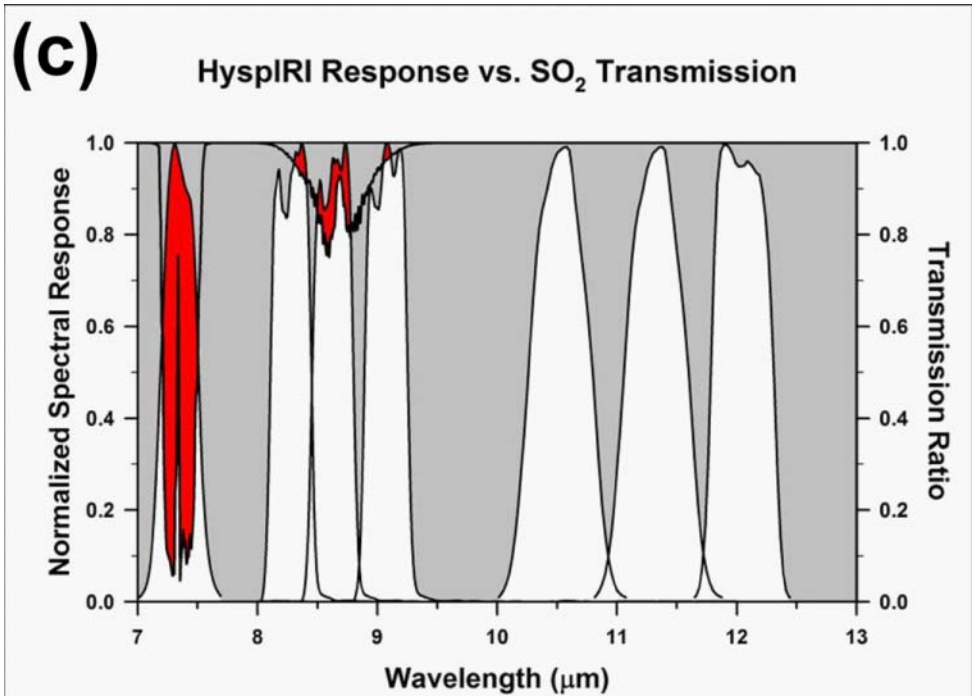

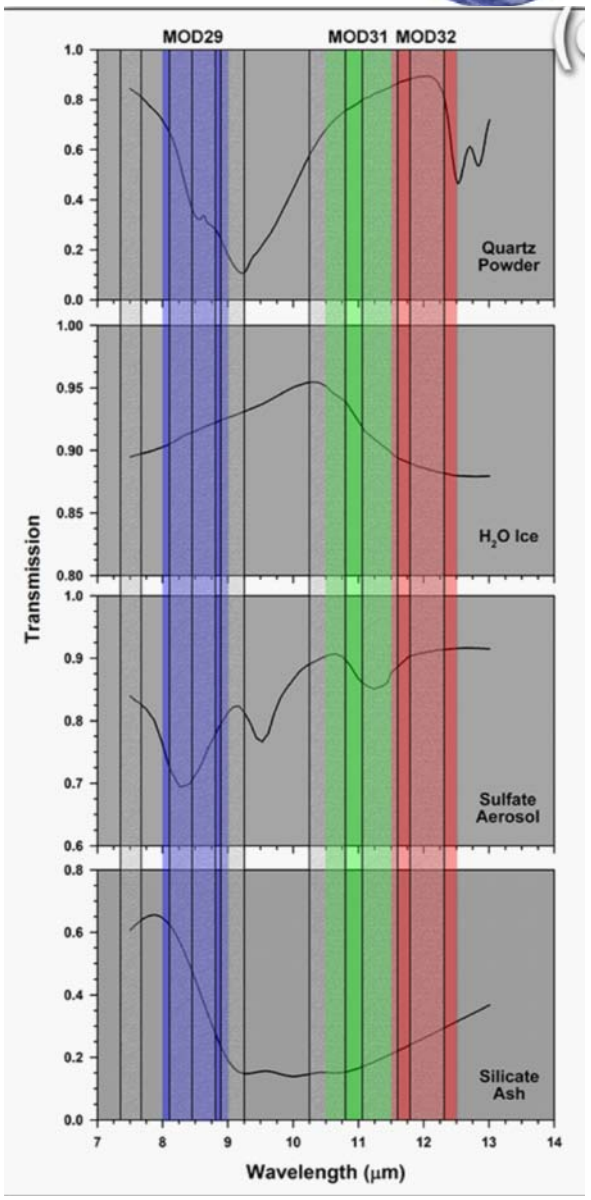

Characterizing and Understanding Volcanic Eruptions

ASTER Observations of the Eyjafjallajökull Eruption
19 April 2010 - 12:51 UTC

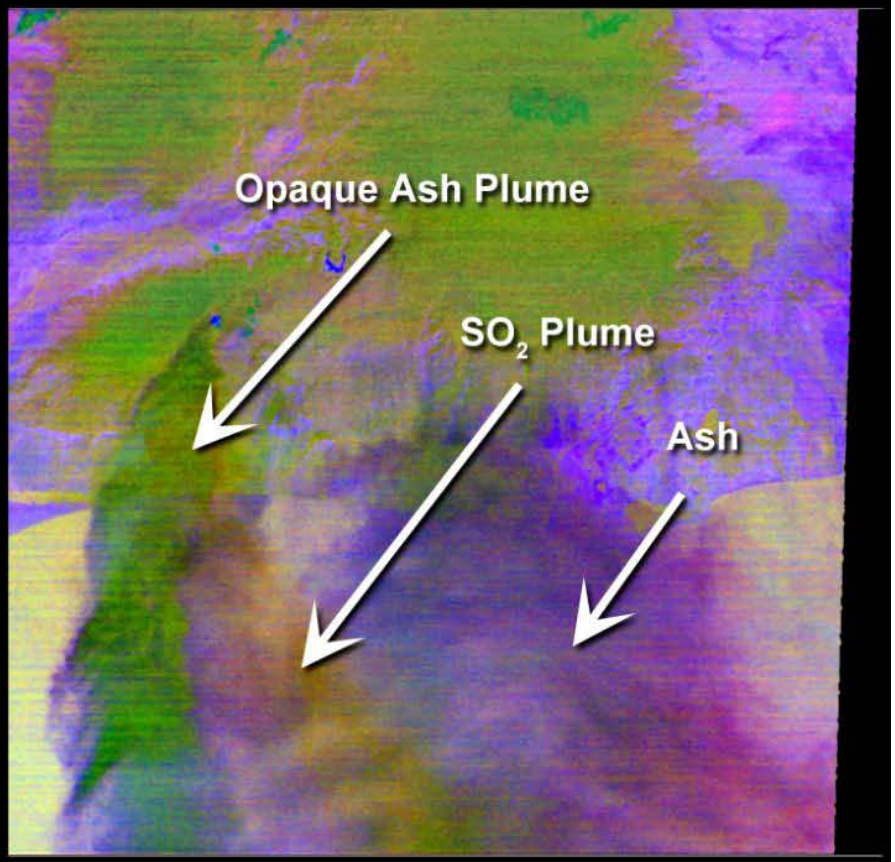

Visible - Near Infrared

kilometers

0 36

Thermal Infrared

Wildfires

- How are global fire regimes changing in response to, and driven by, changing climate, vegetation, and land use practices? [DS 198]
- Is regional and local scale fire frequency changing? [DS 196]
- What is the role of fire in global biogeochemical cycling, particularly trace gas emissions? [DS 195]
- Are there regional feedbacks between fire and climate change?

Large error in carbon budget exists due to poor knowledge of Carbon release from fires

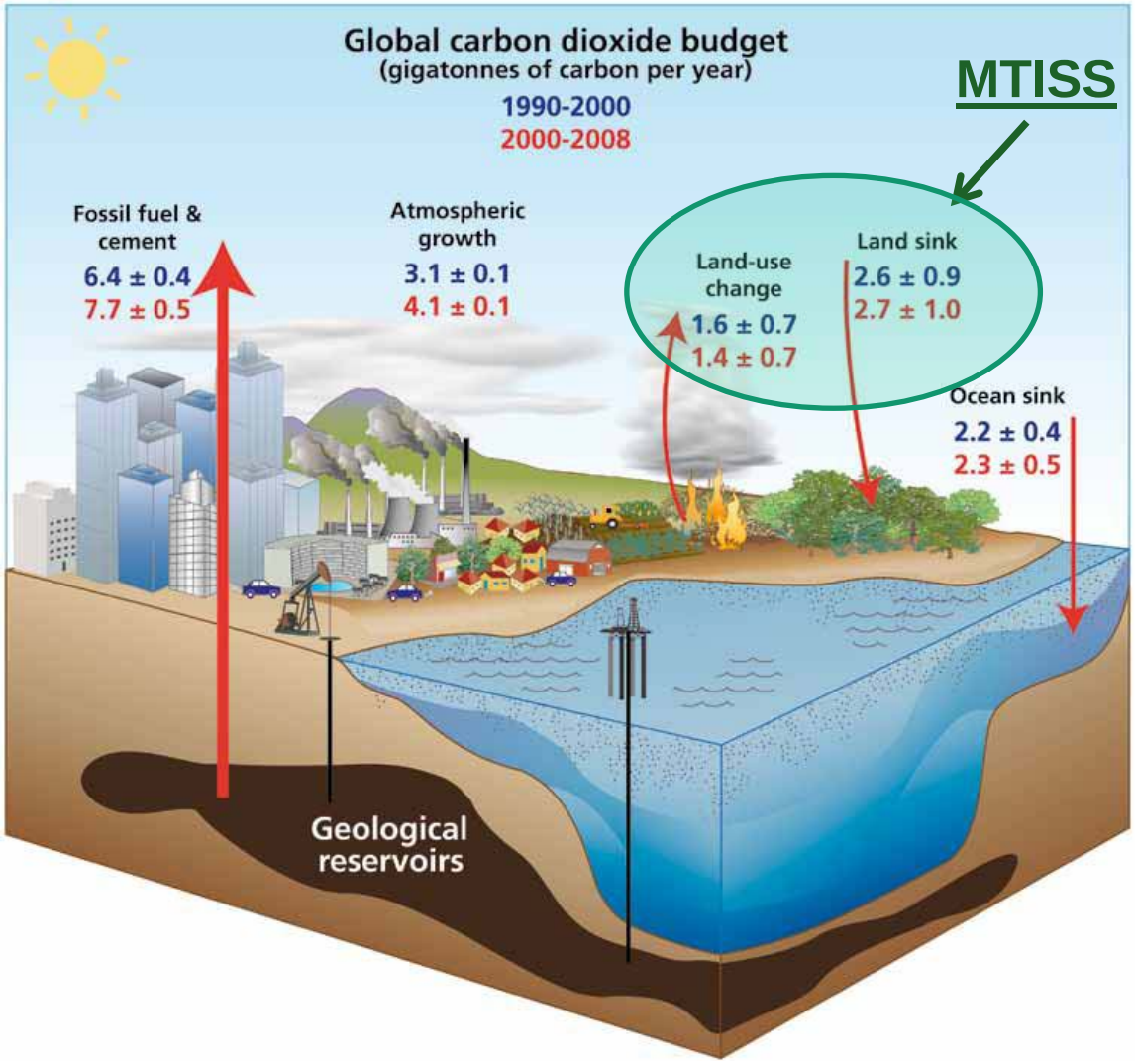

Global CO2 budget for 1990-2000 (blue) and 2000-2008 (red) (GtC per year). Emissions from fossil-fuel and land-use change are based on economic and deforestation statistics. Atmospheric CO2 growth is measured directly. The land and ocean CO2 sinks are estimated using observations for 1990-2000 (Denman *et al.* IPCC 2007). For 2000-2008, the ocean CO2 sink is estimated using an average of several models, while the land CO2 sink is estimated from the balance of the other terms.

Measuring global fire emission is necessary for reducing the uncertainty in carbon emissions from biomass burning

Global average biomass burning estimates range from 20 – 40 % of all global C emissions.

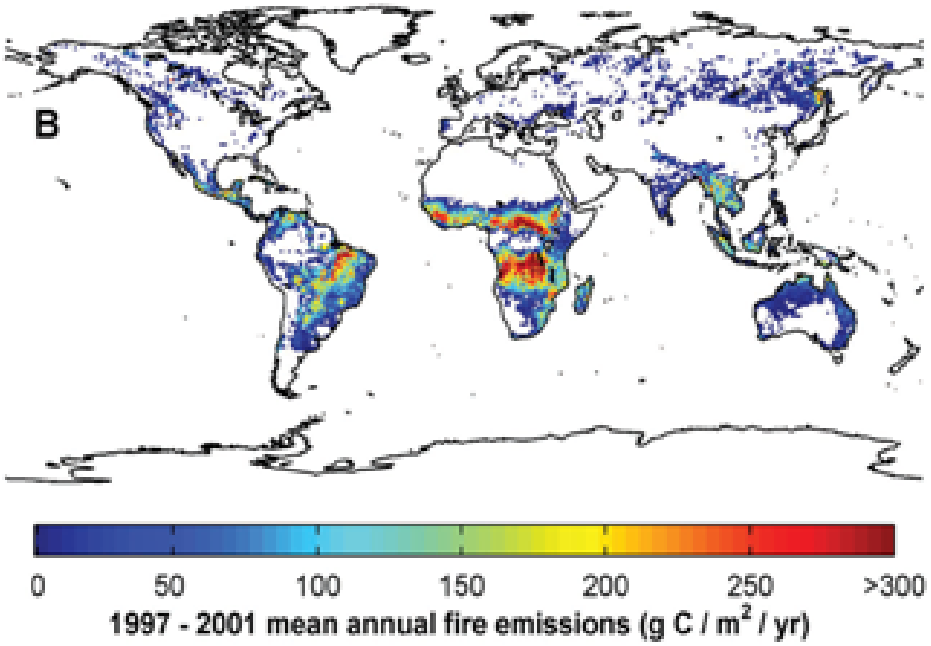

Van der Werf et al., 2010

Fires occur worldwide need a GLOBAL Mapping Mission, emissions vary regionally

HyspIRI-TIR will measure Radiative Energy that has been shown to yield precise estimates of Biomass Combusted

- Historically calculated using Seiler & Crutzen (1980) approach:

Biomass combusted = Area Burnt x Fuel Load x Combustion Efficiency

- More recently Fire Radiative Energy approach

Biomass combusted = Radiative energy or heat yield

(Since the heat yield (*kJ/kg*) of vegetation fuel is ~ constant, measuring the energy released on burning and knowing the heat yield allows the amount of biomass burned to be calculated.)

- For both methods:

Biomass combusted x Emission factor = Carbon released

Emission factors are obtained for given cover type e.g. forest vs peat

HyspIRI-TIR Provides Orders of Magnitude Improvement in Measurement Capability

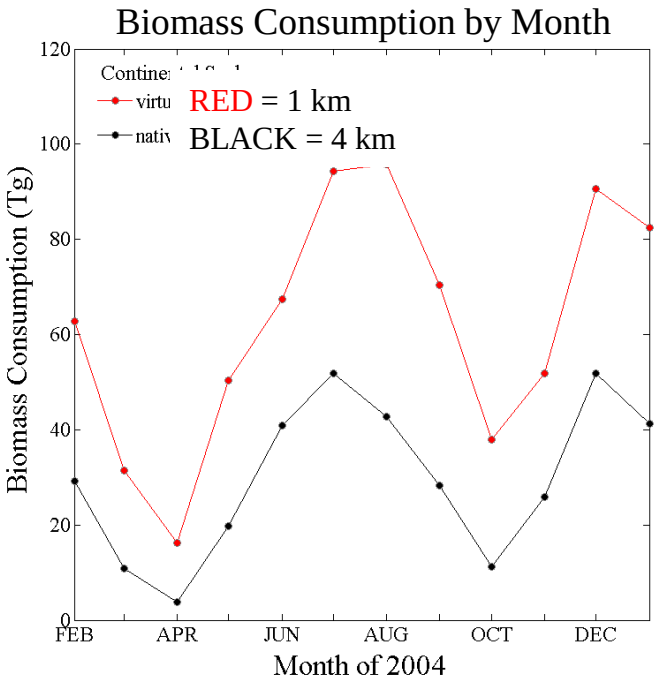

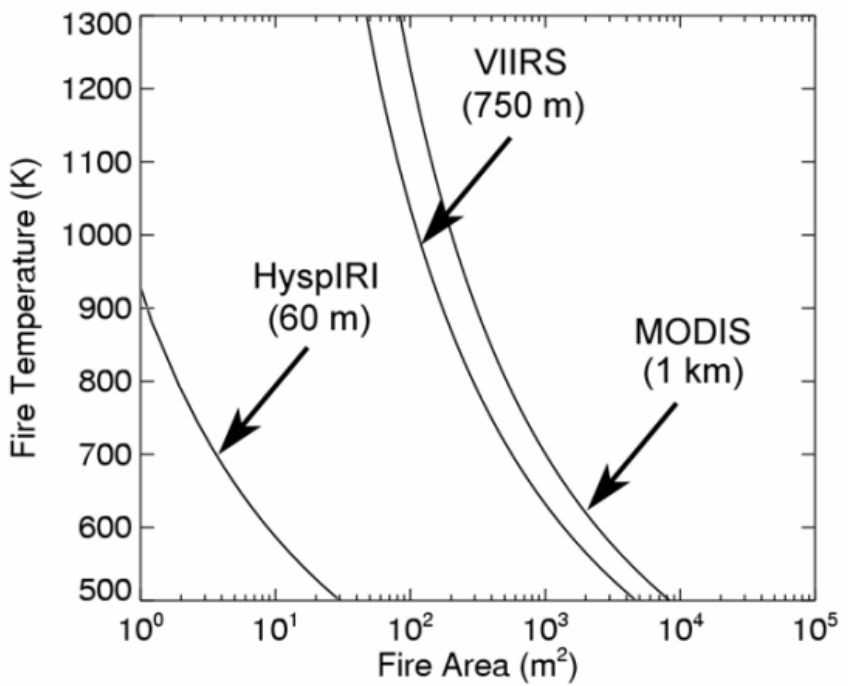

- HyspIRI-TIR measures very small fires as well as large fires. Small fires have a disproportionately large carbon contribution
- Global carbon contribution from peat, agricultural and deforestation fires unknown because cannot be measured with current sensors but see a large discrepancy between 1km MODIS and 4km GOES

Measuring carbon fire emissions requires measurements in the Mid and Thermal Infrared

- Greater sensitivity due to shift in emission peak with temperature
- Measure radiance rather than temperature and avoid mixed pixel problem

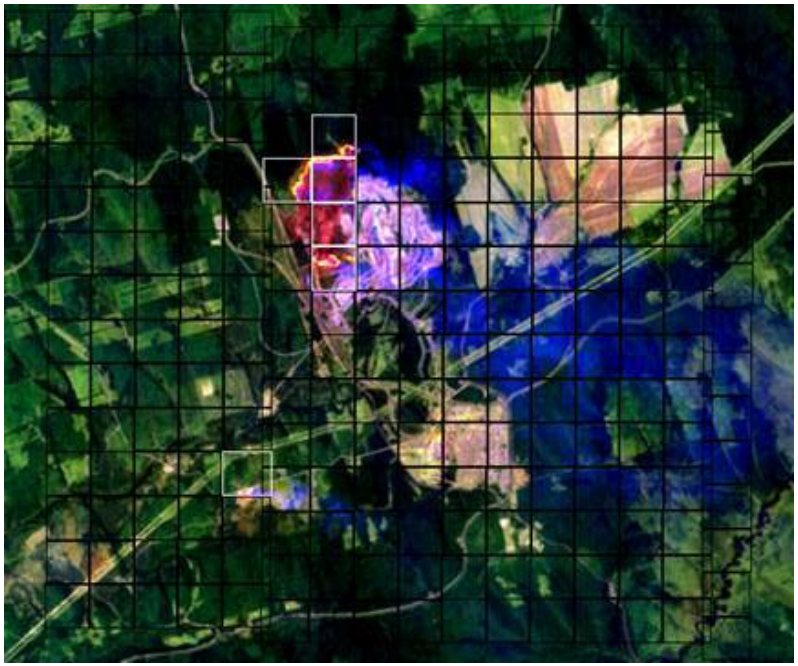

MODIS only detects white boxes (1kmX1km) does not provide information on the fire front or smouldering part of fire

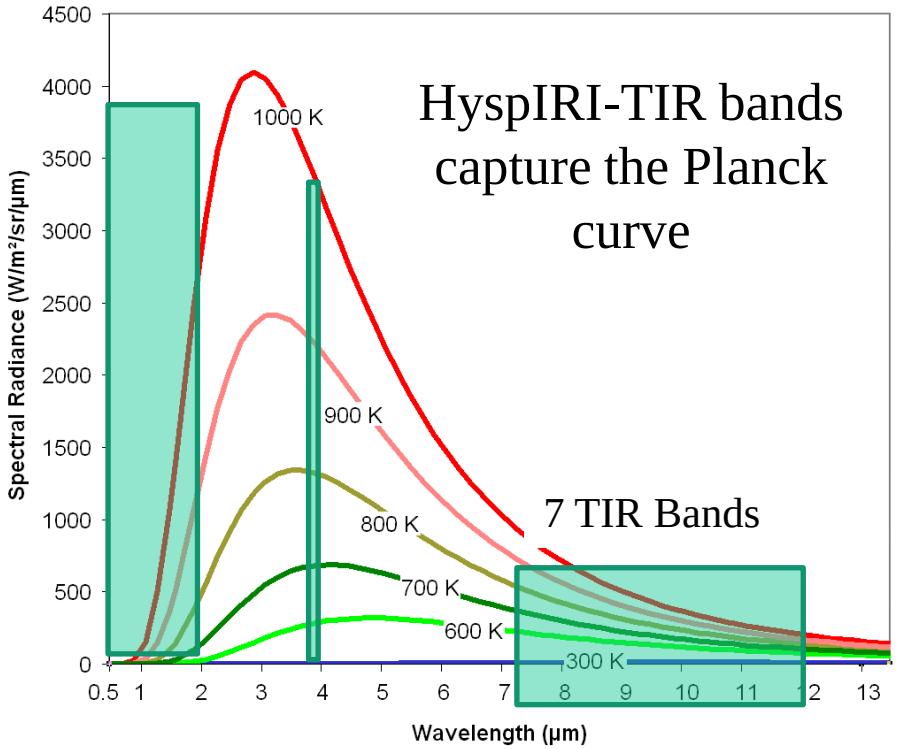

Thermal emission peaks in the MIR (3-5 µm) region for fire temperatures ranging from ~ 650 K (weak smouldering) to ~ 1400 K (strong flaming). MIR is far more sensitive to hot targets than TIR.

Water Use and Availability

- How is climate variability (and ENSO) impacting the evaporative component of the global water cycle over natural and managed landscapes? [DS 166, 196, 203, 257, 368]
- What are relationships between spatial and temporal variation in evapotranspiration and land-use/land-cover and freshwater resource management? [DS 196, 203, 368]
- Can we improve early detection, mitigation, and impact assessment of droughts at local to regional scales anywhere on the globe? [DS 166, 196, 203, 368]; How does the partitioning of Precipitation into ET, surface runoff and ground-water recharge change during drought?
- What areas of Earth have water consumption by irrigated agriculture that is out of balance with sustainable water availability? [DS 196, 368]
- Can we increase food production in water-scarce agricultural regions while improving or sustaining quality and quantity of water for ecosystem function and other human uses? [DS 196, 368]

High Spatial and Temporal Resolution Required to Accurately Measure Evapotranspiration (ET)

High spatial resolution: access to the local scale (field, urban district…)

1 km box

1 km data does not capture field scale variation

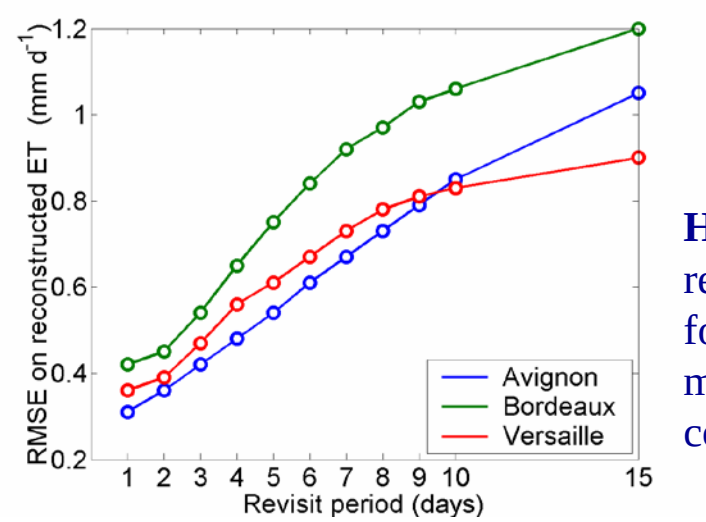

5-day revisit minimizes error on ET Estimation

High revisit: rapid response to surface forcing (water status, meteorological conditions…)

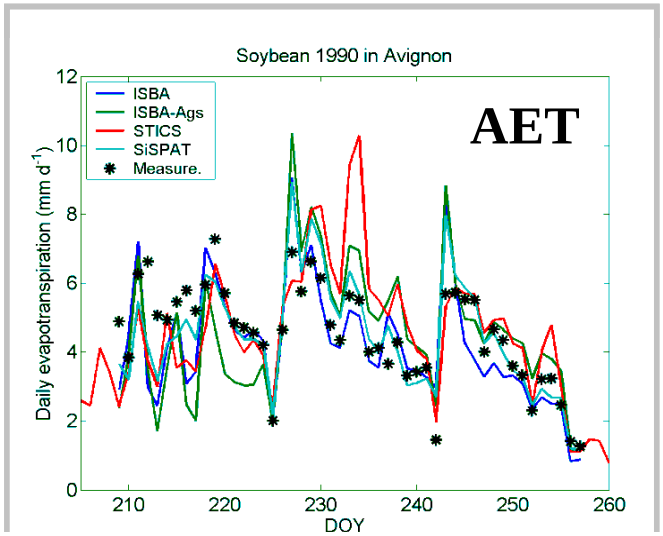

ET is very dynamic compared with LAI

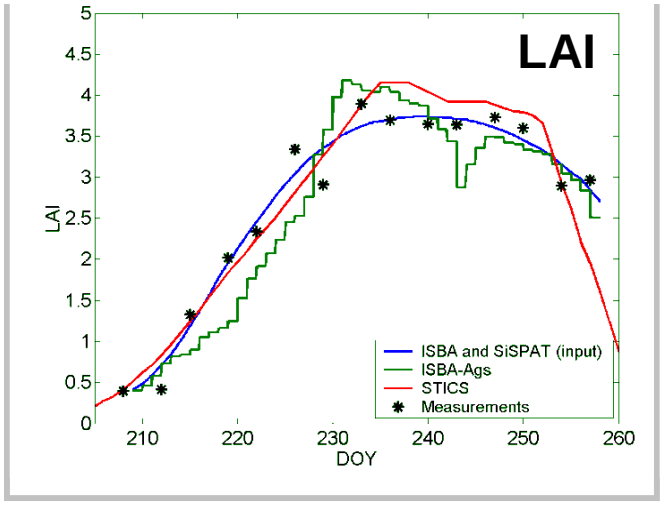

Courtesy Jean-Pierre Lagouarde, INRA, France

Evapotranspiration and Water Use and Availability

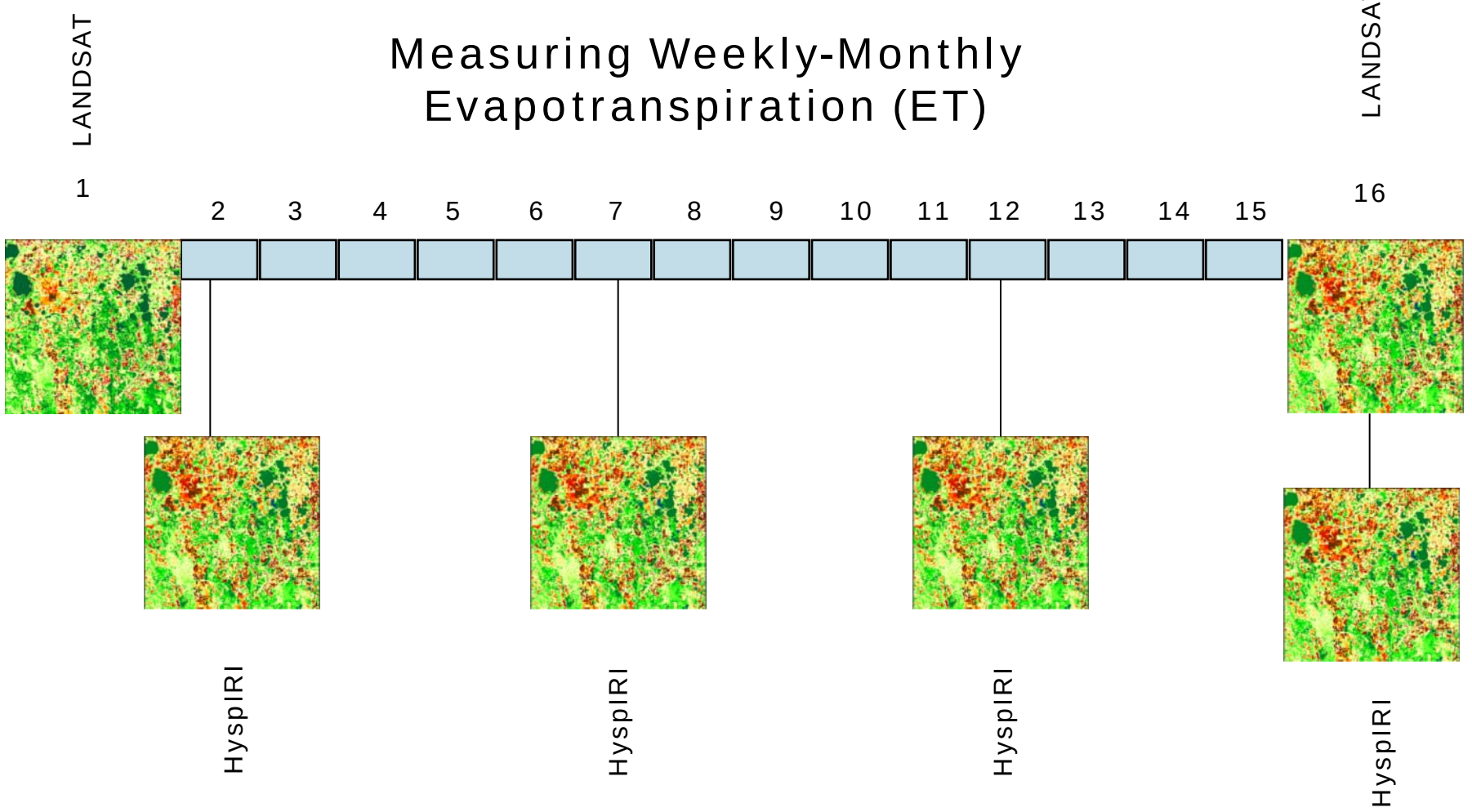

HyspIRI-TIR provides ET data every 5 days, allows weekly-monthly measurement
And expectation for a cloud-free scene (typically 1 in every 3 data takes)

Mission Concept and Instrument
Operational Scenario

- Following arrival at science orbit, the baseline data acquisition plan is established. Collect data for entire land surface excluding sea ice (Arctic and Antarctic) every 5 days at 60 m spatial resolution in 8 spectral bands
- Data are downlinked and transferred to the science data processing center where calibration and baseline processing algorithms are applied.
- Level 1, 2 products are delivered to the scientific community and general users to pursue the science questions
  - With appropriate cloud screening, compositing, spatial, and temporal subsetting

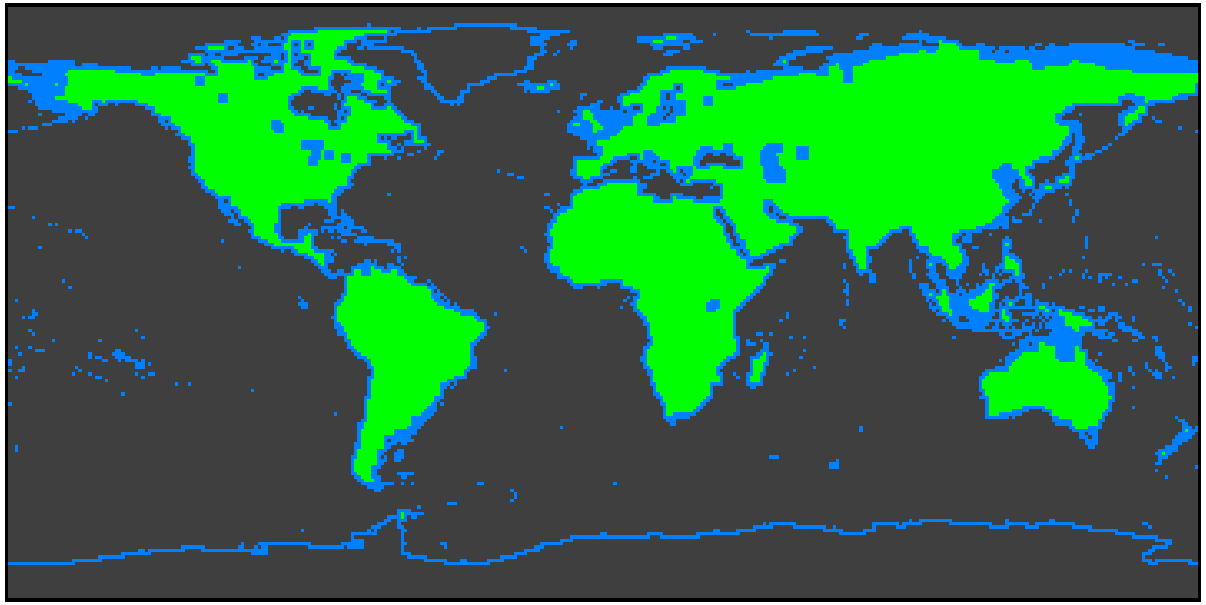

Land and coastal acquisition

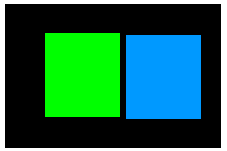

Annual TIR imaging opportunities in a 5-day near-repeating orbit, 1 yr. simulation

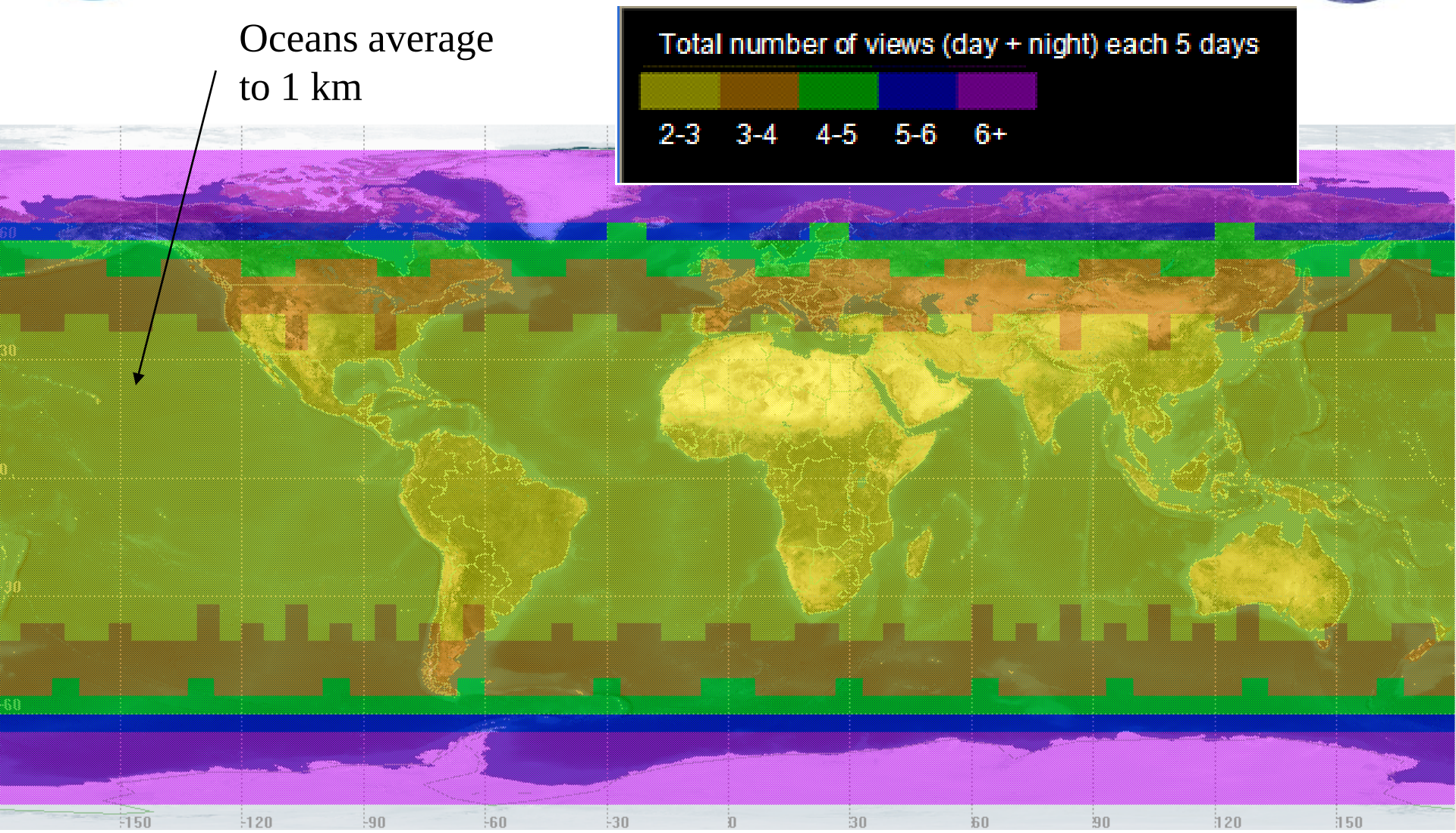

Nominal orbit: average alt. 626.8 km, inclination 97.8°. TIR imager FOV: +/- 25.46° (60 m pixel GSD at nadir, 9272 cross-track pixels).

Science Measurements
Summary Measurement Characteristics

Spectral	
Bands (8) µm	3.98 µm, 7.35 µm, 8.28 µm, 8.63 µm, 9.07 µm, 10.53 µm, 11.33 µm, 12.05
Bandwidth	0.084 µm, 0.32 µm, 0.34 µm, 0.35 µm, 0.36 µm, 0.54 µm, 0.54 µm, 0.52 µm
Accuracy	<0.01 µm
Radiometric	
Range	Bands 2-8= 200K – 500K; Band 1= 1200K
Resolution	< 0.05 K, Linear Quantization to 14 bits
Accuracy	< 0.5 K 3-sigma at 250K
Precision (NEdT)	< 0.2K
Linearity	>99% characterized to 0.1 %
Spatial	
IFOV	60 m
MTF	>0.65 at FNy
Scan Type	Push-Whisk
Swath Width	600 km (±25.5° at 623 km altitude)
Cross-Track Samples	10,000
Swath Length	15.4 km (+/- 0.7-degrees at 623km altitude)
Down-Track Samples	256
Band-to-Band Co-registraion	0.2 pixels (12 m)
Pointing Knowledge	1.5 arcsec (0.1 pixels)

Science Measurements

Characteristics Continued

Temporal	
Orbit Crossing	10:30 am sun synchronous descending
Global Land Repeat	5 days at equator
OnOrbit Calibration	
Lunar View	1 per month {radiometric}
Blackbody Views	1 per scan {radiometric}
Deep Space Views	1 per scan {radiometric}
Surface Cal Experiments	2 (d/n) every 5 days {radiometric}
Spectral Surface Cal Experiments	1 per year
Data Collection	
Time Coverage	Day and Night
Land Coverage	Land surface above sea level
Water Coverage	Coastal zone -50 m and shallower
Open Ocean	Averaged to 1km spatial sampling
Compression	2:1 lossless

TIR Instrument Concept

Scanning and Data Rate

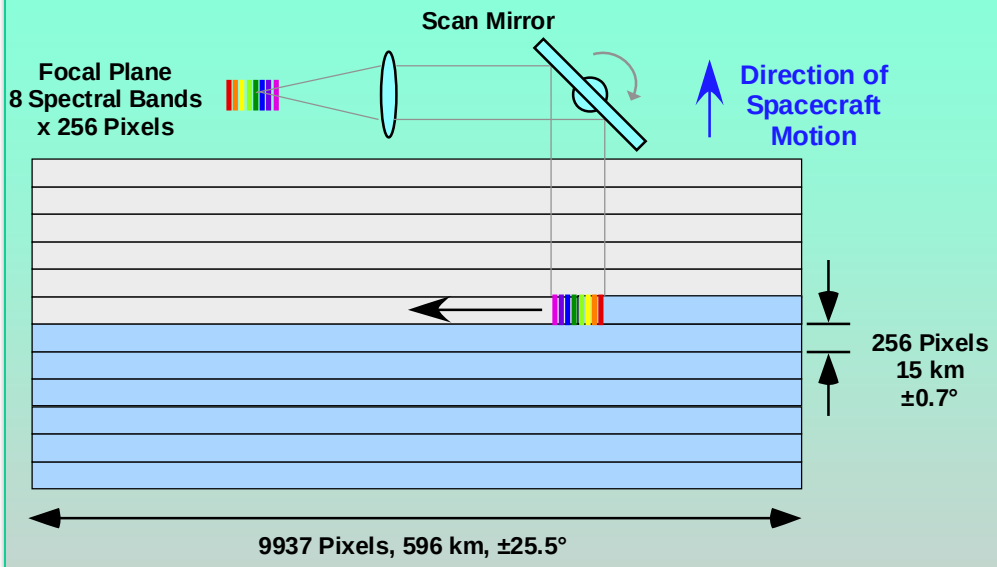

- 60 m Pixel Footprint
- Time-Averaged Science Data Rate 0.024 Gbps
- Assuming 14 bits, 2:1 Compression
- Scan Mirror Rotation Rate 13 RPM
- Pixel Dwell Time 32 microseconds

Mass and Power (JPL Team X)

- Mass CBE 60 kg
- Power CBE 109 W

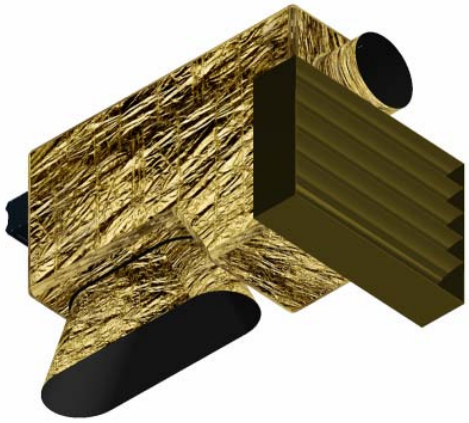

Spectral Bands

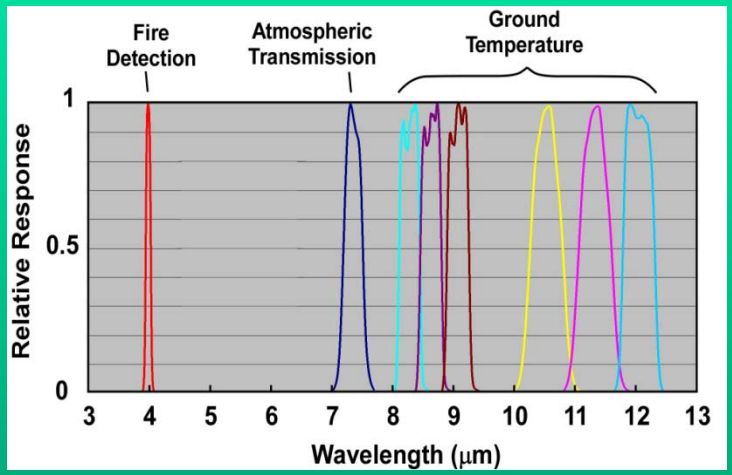

Mission Concept
TIR Overview

- Duration: 4 years development, 3 years science
- Coverage: Global land every 5 days
- Day and Night imaging (1 day and night image at a given location obtained every 5 days)
- Data download using dual-polarization X-band at high-latitude stations
- Spacecraft: LEO RSDO bus (SA-200HP)
- Launch: Taurus-class launch vehicle

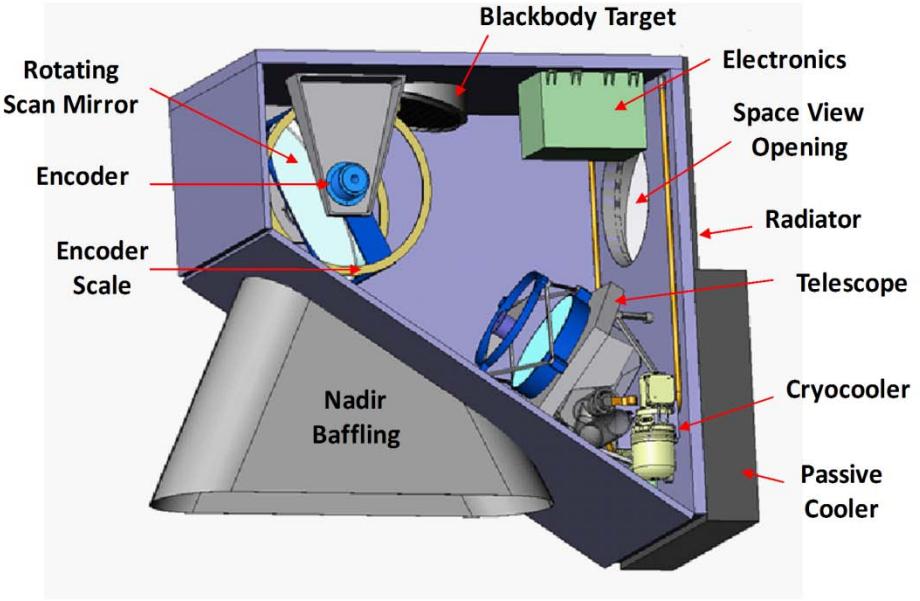

Technology Readiness

Hyperspectral Thermal Emission Spectrometer (HyTES)

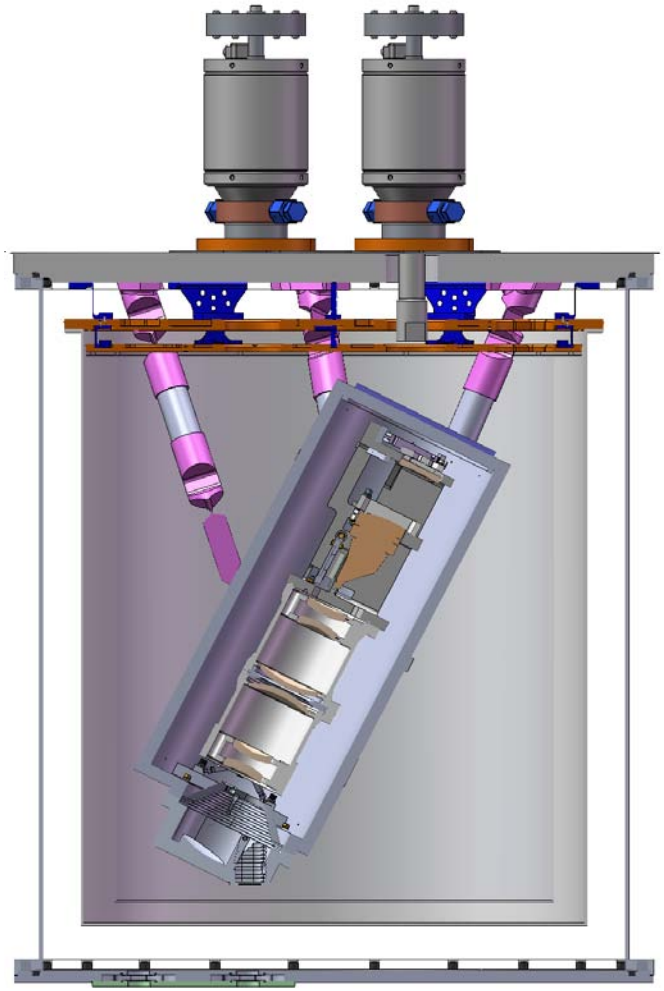

Prototype HyspIRI Thermal Infrared Radiometer (PHyTIR)

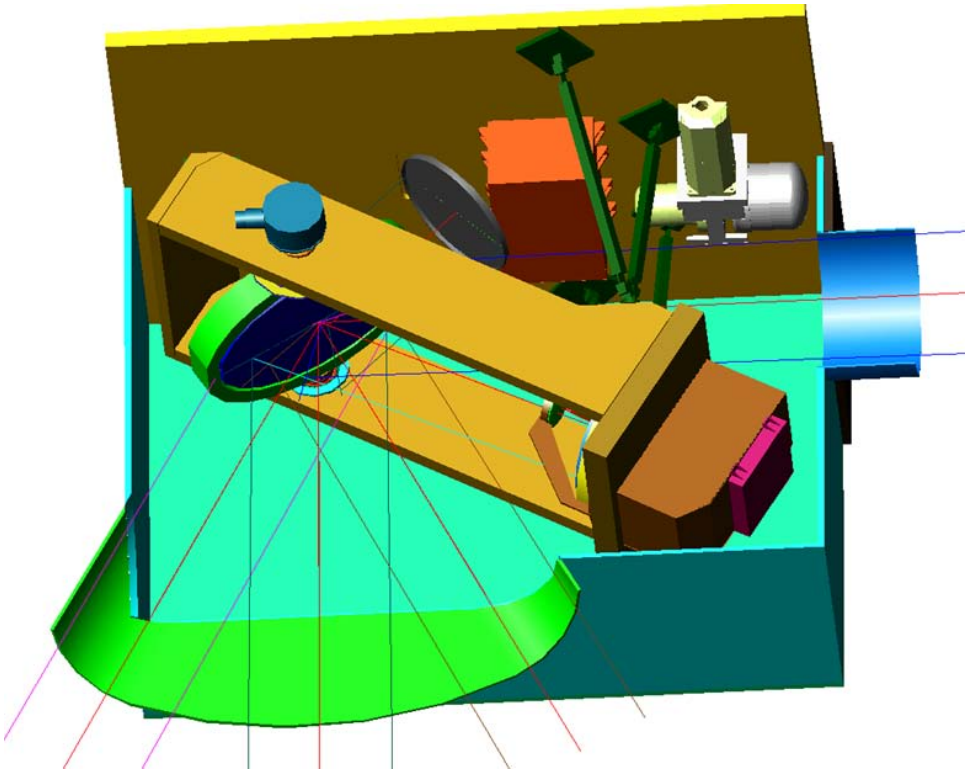

Elevator Speech

- ***Quantify carbon and other emissions from fires to balance carbon budget***

- ***Determine if heat, gas and lava emissions from volcanoes can be used to understand their future behavior***

- ***Quantify evaporative loss from vegetated regions to balance water budget***

Summary

We have developed a sets of science questions that are well aligned with the HyspIRI Mission called for in the NASA Earth Science and Applications Decadal Survey. The mission has strong relevance to both climate and society.

We have reviewed and refined these questions that relate to both science and applications objectives and developed traceability to a set of science measurements.

We have established a high heritage and low risk approach for acquiring the HyspIRI VSWIR and TIR science measurements

Backup

Measuring global fire emission is necessary for reducing the uncertainty in carbon emissions from biomass burning

Global average biomass burning estimates range from 20 – 40 % of all global C emissions.

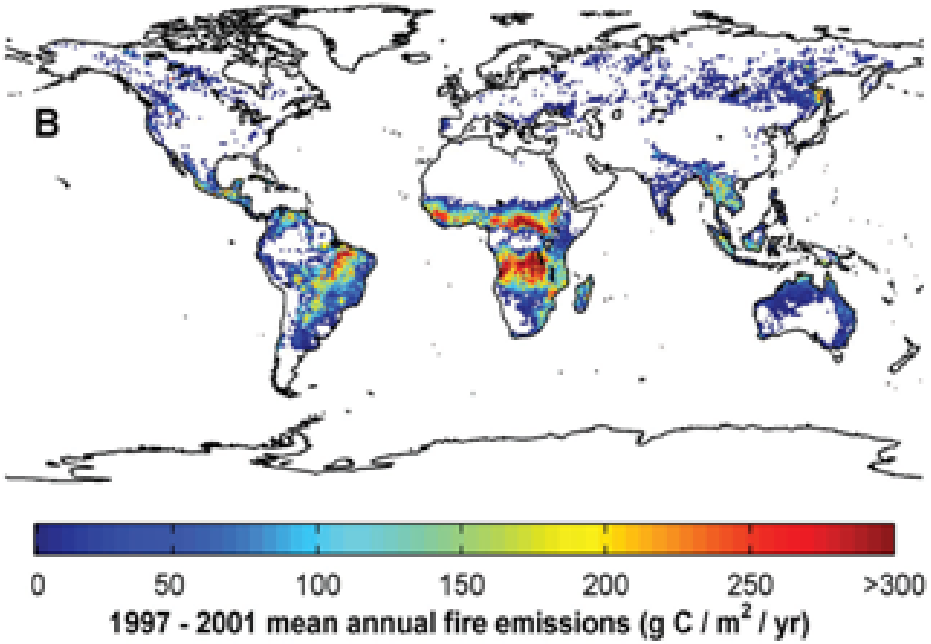

Van der Werf et al., 2010

Fires occur worldwide need a GLOBAL Mapping Mission, emissions vary regionally

HyspIRI Mission Concept

Bogdan Oaida,
with contributions from
Michael Mercury [JPL]

[bogdan.oaida@jpl.nasa.gov]

Jet Propulsion Laboratory
California Institute of Technology

National Aeronautics and
Space Administration

Jet Propulsion Laboratory
California Institute of Technology
Pasadena, California

Copyright 2011 California Institute of Technology. Government sponsorship acknowledged.

National Aeronautics and Space Administration

Jet Propulsion Laboratory
California Institute of Technology
Pasadena, California

HyspIRI Mission Architecture

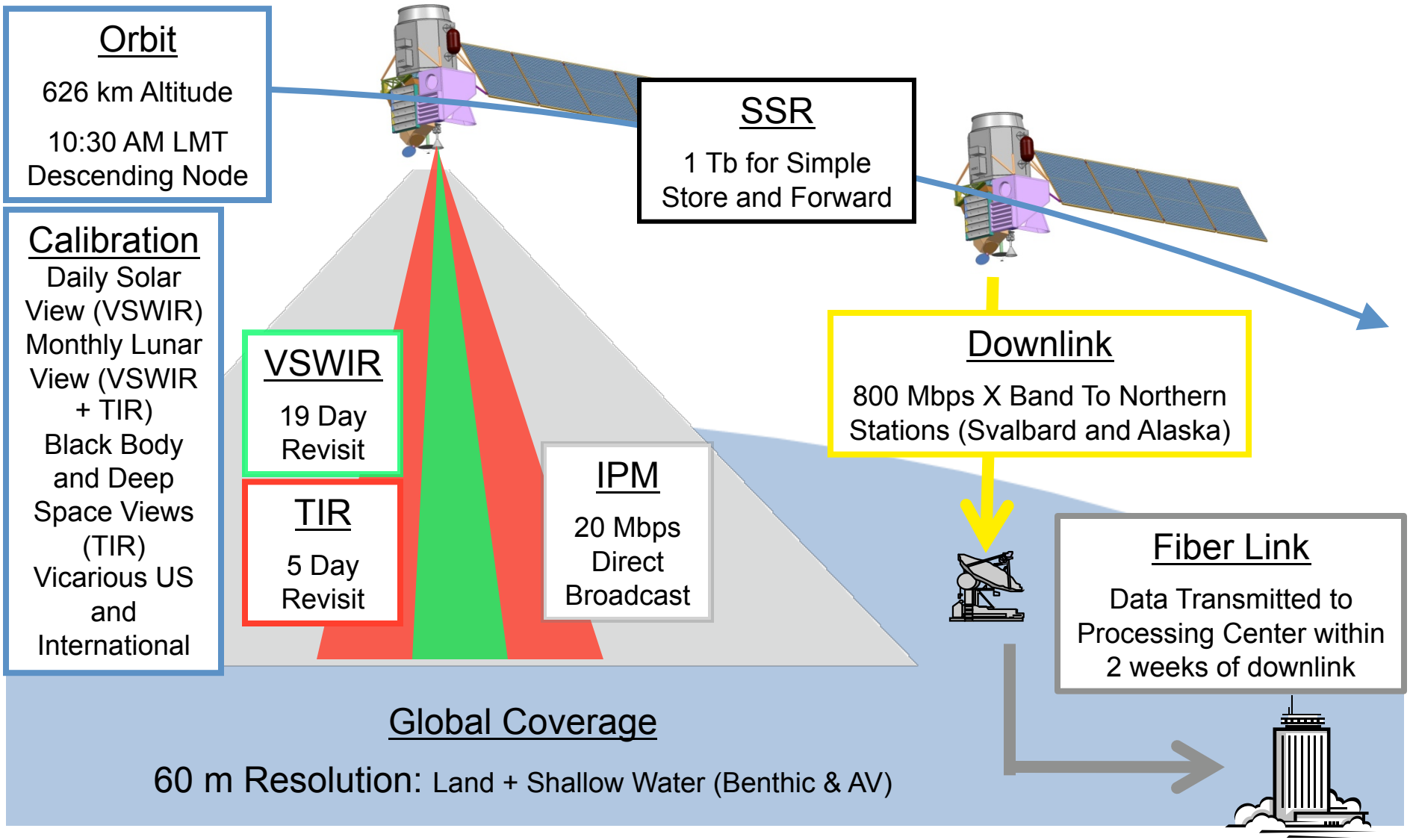

National Aeronautics and Space Administration

Jet Propulsion Laboratory
California Institute of Technology
Pasadena, California

HyspIRI Global Coverage

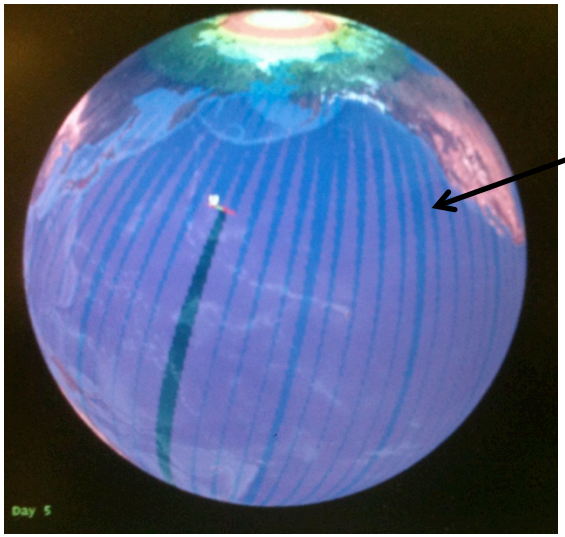

TIR Coverage after 5 days

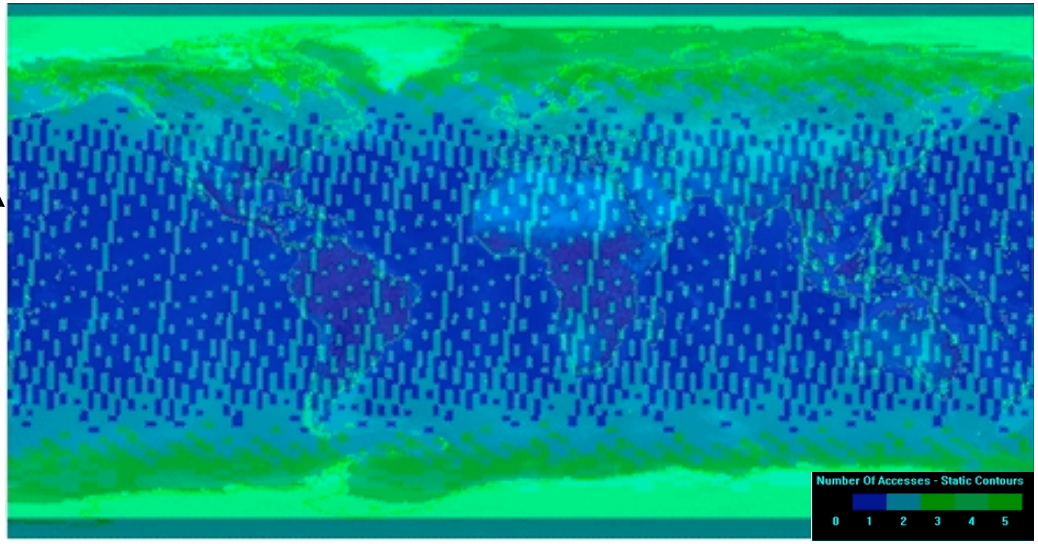

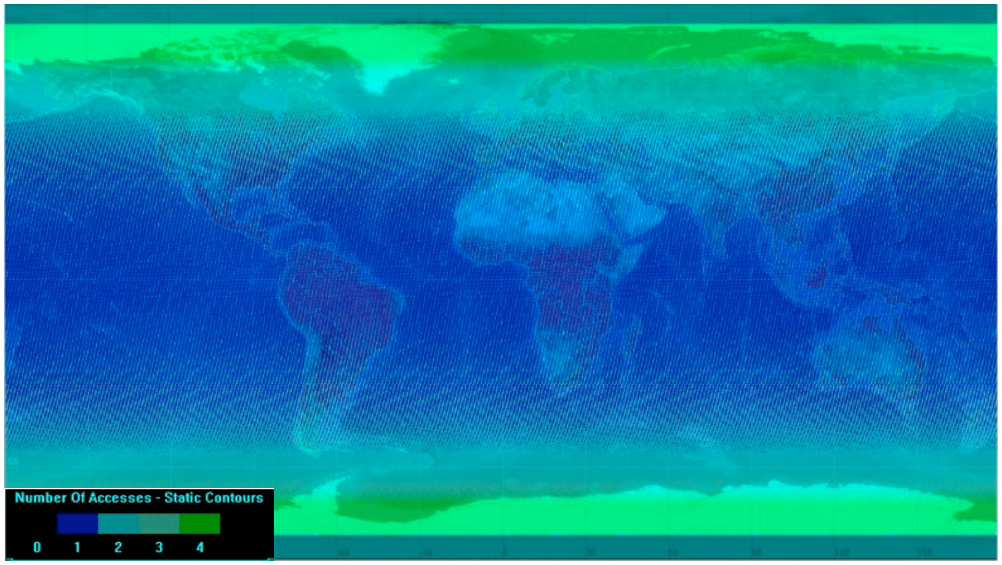

VSWIR Coverage after 19 days

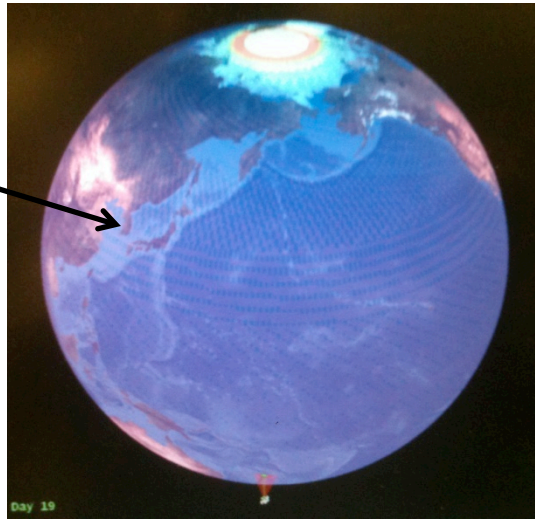

Due to the min 20 deg Sun elevation angle constraint on the VSWIR acquisition, the latitudes covered change with the seasons

National Aeronautics and Space Administration
Jet Propulsion Laboratory
California Institute of Technology
Pasadena, California

Data Acquisition Strategy

- Instrument modes change multiple times each orbit, but are clearly defined by geography and spacecraft location

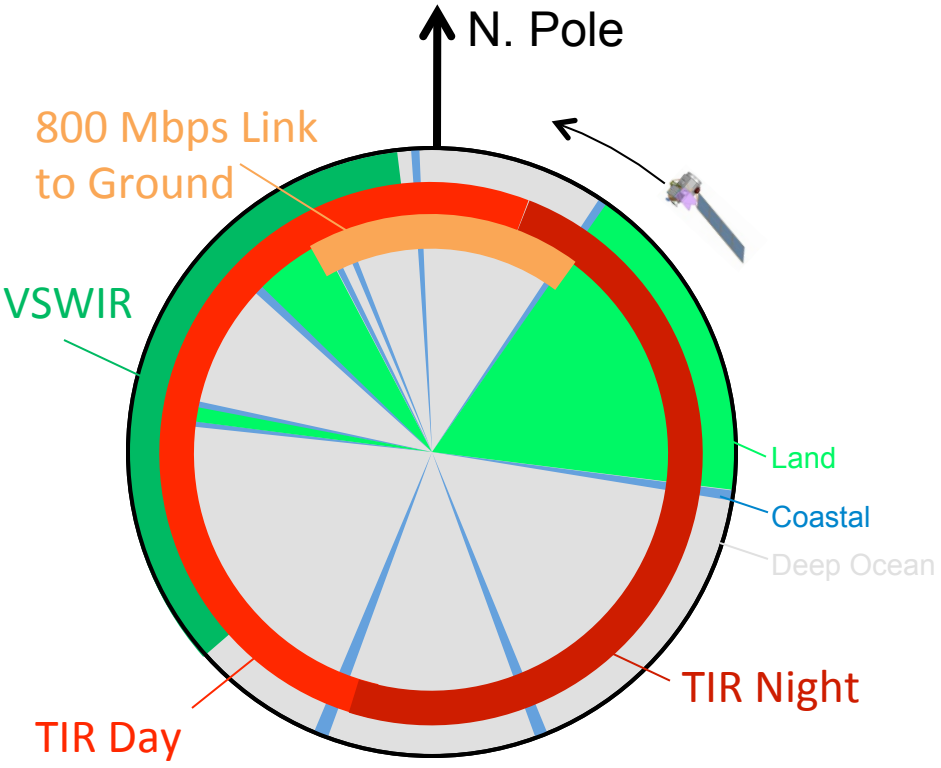

Cut away of earth with slice taken along plane of orbit

Imaging Mode

Instrument	Land	Coastal	Deep Ocean	Greenland	Antarctica
VSWIR	60 m	60 m	1 km	1 km	1 km
TIR	60 m	60 m	1 km	1 km	1 km

Target Map

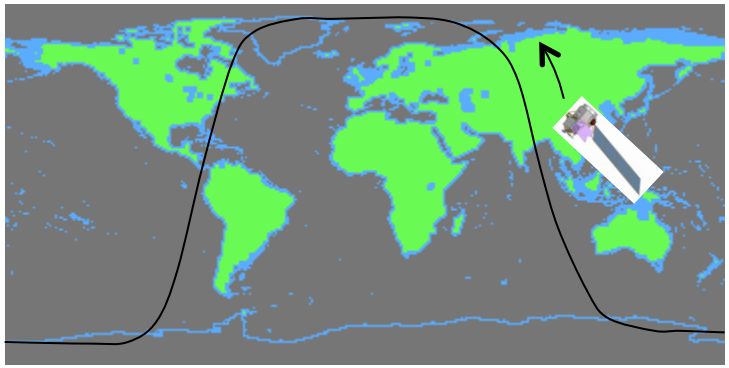

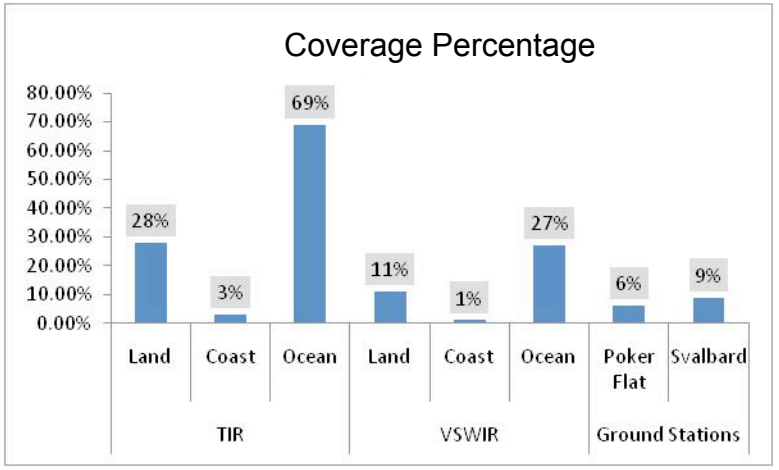

National Aeronautics and Space Administration
Jet Propulsion Laboratory
California Institute of Technology
Pasadena, California

HyspIRI Downlink Data Volume

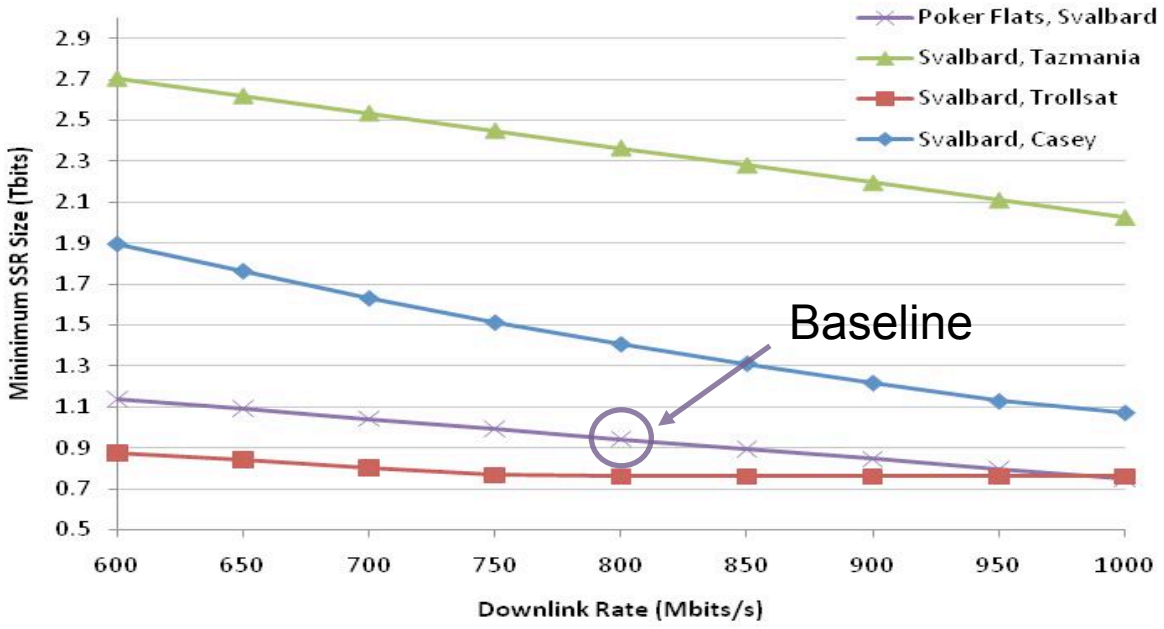

	Rate	On-board Compression
VSWIR_land	804.1 Mb/s	3:1
VSWIR_shallow	865.9 Mb/s	3:1
VSWIR_ocean	3.9 Mb/s	3:1
TIR_land	130.2 Mb/s	2:1
TIR_shallow	130.2 Mb/s	2:1
TIR_ocean	0.6 Mb/s	2:1

	Avg (Tb)	Min (Tb)	Max (Tb)
Per Day	4.64	3.59	5.29
Per Orbit	0.31	0.00	0.81

Total downlinked data volume for the 3 year mission: 5024 Tbits

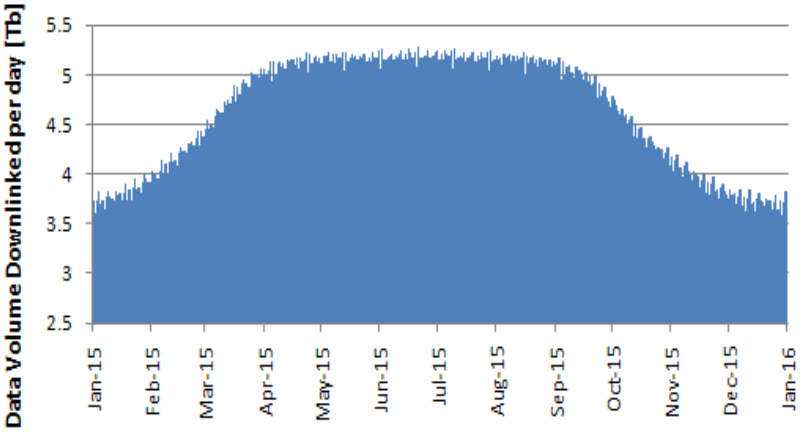

- Baseline selected to minimize system level cost and risk
- On-board storage capacity
  - 1 Tb
  - 0.31 Tb/orbit
- WorldView-1 and -2 have 2.2 Tb SSR
  - WorldView1: 0.33 Tb/orbit
    - Different downlink strategy requires larger SSR than HyspIRI
  - WorldView2: 0.52 Tb/orbit
- 30% margin added to calculated required SSR size

National Aeronautics and Space Administration
Jet Propulsion Laboratory
California Institute of Technology
Pasadena, California

Baseline Flight System Concept

- Industry procured spacecraft bus
  - SA-200HP used as an example for the study to identify and cost needed modifications
- HyspIRI specific
  - Payload integrated on the top plate (TIR, VSWIR) and inside the S/C
  - Configuration chosen to minimize/eliminate thermal impacts on the payload radiators
  - Spacecraft Dry Mass (CBE): 520 kg
  - Launch Mass: 681 kg
  - JPL DP Margin: 31%
  - Required Power (CBE): 620W
  - Available Power: 965W, 7.2 m^2 array

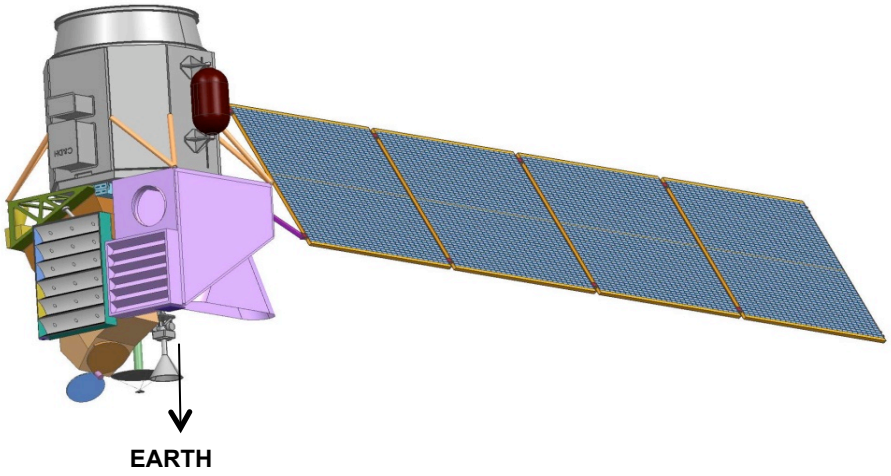

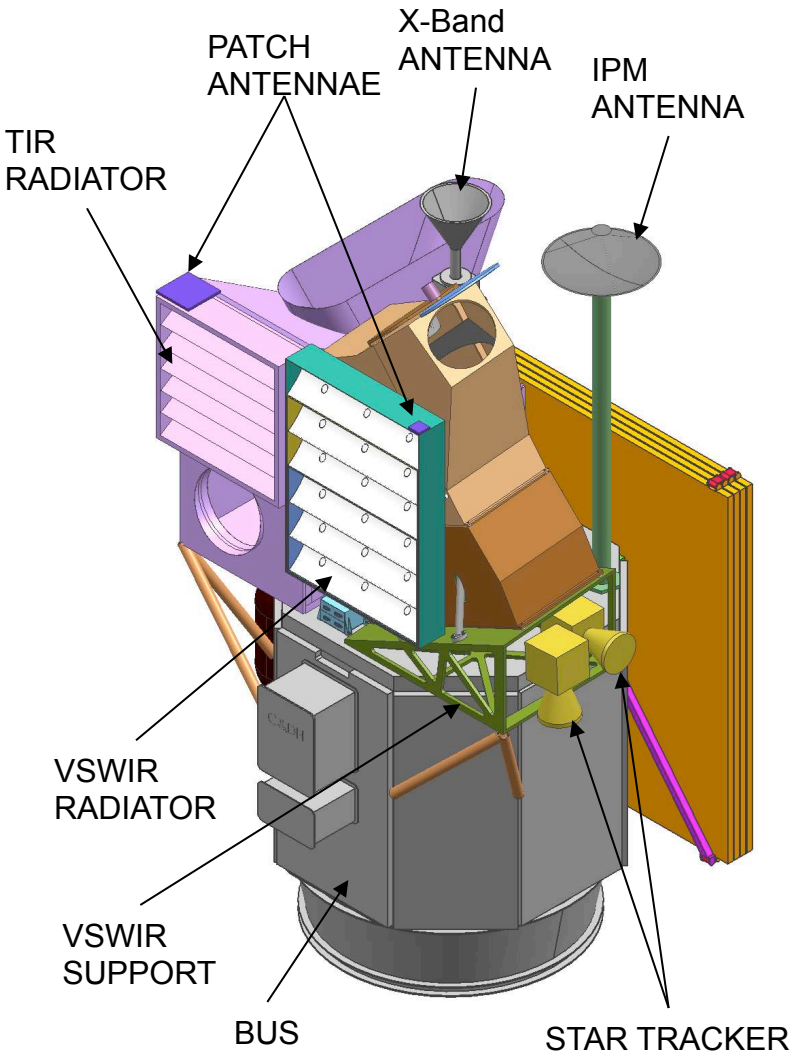

National Aeronautics and Space Administration

Jet Propulsion Laboratory
California Institute of Technology
Pasadena, California

Baseline Flight System Concept

	Requirements	RSDO SA-200HP	HyspIRI SA-200HP	Modifications
Orbit	626 km 10:30 LTDN	✓	✓	-
Mission duration	3 years, selective redundancy	4 years, selective redundancy	3 years, single string	Remove redundancy to reduce cost
Thermal	Passive architecture	✓	✓	-
Downlink	800 Mbps	80Mbps	800 Mbps	Dual-pol X-band
Propellant	75 m/s 37 kg	131 m/s 67 kg tank	131 m/s 67 kg tank	-
Onboard recorder	1 Tbit	134 Gbits	1Tbit	SEAKR SSP-R
Payload mass	126kg	666 kg	666 kg	Support structure for Instuments
Payload Power	885 W	650 W	965 W	Single wing configuration, add one panel
Pointing Knowledge	See table below	0.5 arcsec (3σ)	<=0.5 arcsec (3σ)	Replaced one of two coarse Ball CT-602 star tracker with one fine Lockheed Martin AST-301 star tracker.
Pointing Accuracy		16 arcsec (3σ)	<=16 arcsec (3σ)	
Pointing Stability		0.1 arcsec/sec (3σ)	<=0.1 arcsec/sec (3σ)	

Pointing	VSWIR Requirement	TIR Requirement	Rationale	Driver
Knowledge	< 48 μrad (3σ/ axis)	< 48 μrad (3σ/ axis)	<30m (3σ) post-reconstruction orthorectification knowledge at 626km altitude	TIR
Accuracy	<4.5 mrad (3σ/axis)	<4.5 mrad (3σ/ axis)	VSWIR: Limits cross-track error to < 3 km on the surface	VSWIR
Stability	±0.1 mrad/sec (3σ)	±24.7 mrad/sec (3σ)	VSWIR: Limit smear to < 0.6 meters as one pixel crosses a spot on the surface in 8.8 msec TIR: Time for 6 pixels in TDI string to cross a point on the surface at nadir is 0.39 msec.	VSWIR

National Aeronautics and Space Administration
Jet Propulsion Laboratory
California Institute of Technology
Pasadena, California

Alternative Flight System Concept

- Based on RFI response from ATK
  - Uses Responsive Space Modular Bus (RSMB) architecture
- HyspIRI specific
  - Spacecraft Dry Mass (CBE): 511 kg
  - Launch Mass: 671 kg
  - JPL DP Margin: 35% (assumes Taurus 3210)
  - Required Power (CBE): 640W
  - Available Power: 1028W

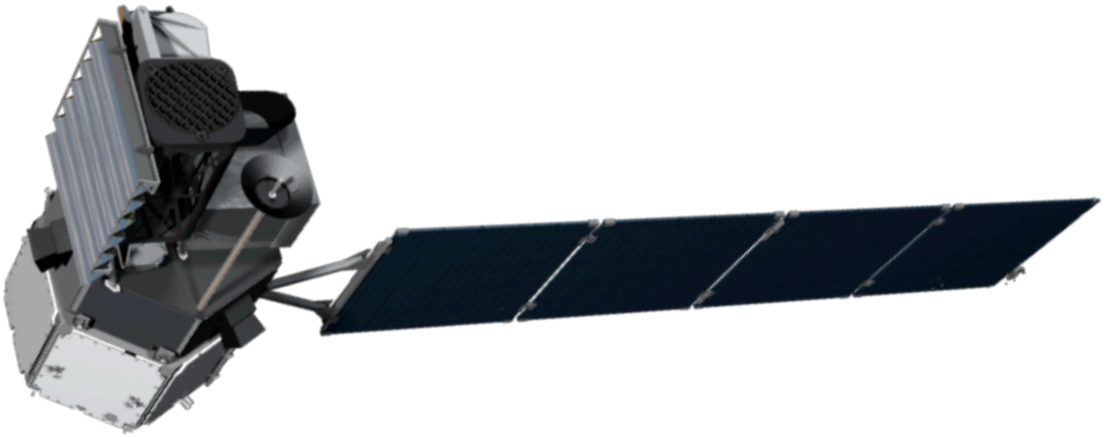

National Aeronautics and Space Administration

Jet Propulsion Laboratory
California Institute of Technology
Pasadena, California

Science Payload Accommodation and System Margins

Accommodations	VSWIR	TIR
Mass (CBE)	55 kg	60 kg
Volume	1.1 x 0.5 x 0.8 m	1.2 x 1.1 x 0.6 m
Power	41 W	103 W
FOV (crosstrack)	13.62 deg	50.7 deg
FOV (alongtrack)	95.9 microrad	95.9 microrad
Orientation	4 deg to starboard	nadir

	Required	Design	Margin (D-R)/D
Swath width VSWIR	141km	151 km	6%
Swath width TIR	536km	600 km	11%
Recorder capacity	0.8 Tb	1.0 Tb	20%
Power	620 W (CBE)	965 W	36%
LV mass capability	520 (CBE, dry)	790 kg	34%

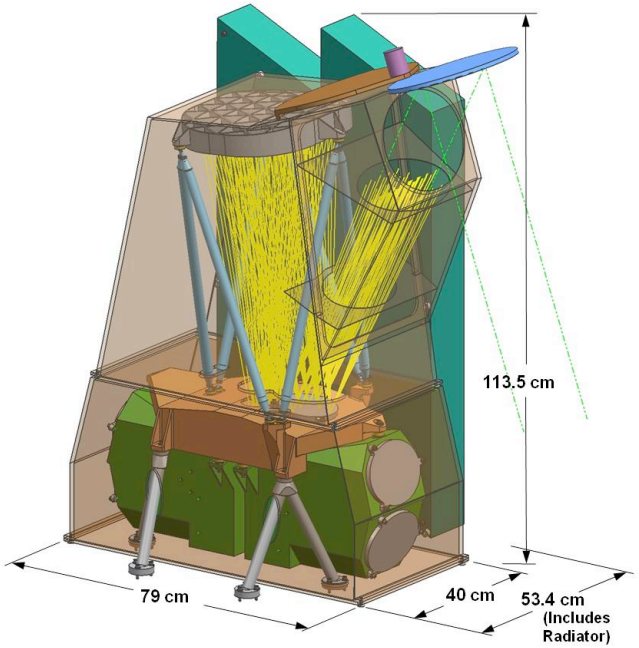

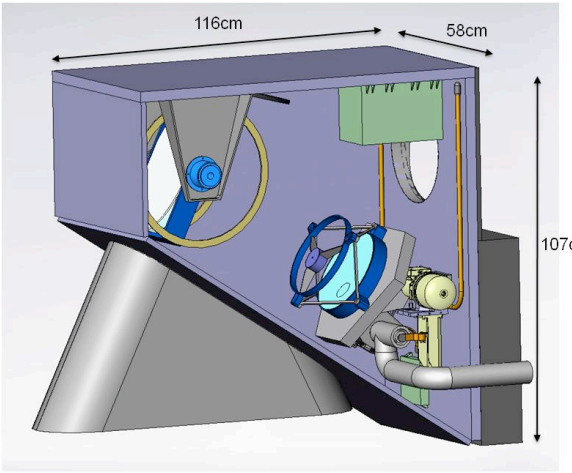

National Aeronautics and Space Administration
Jet Propulsion Laboratory
California Institute of Technology
Pasadena, California

Launch Vehicle Concept

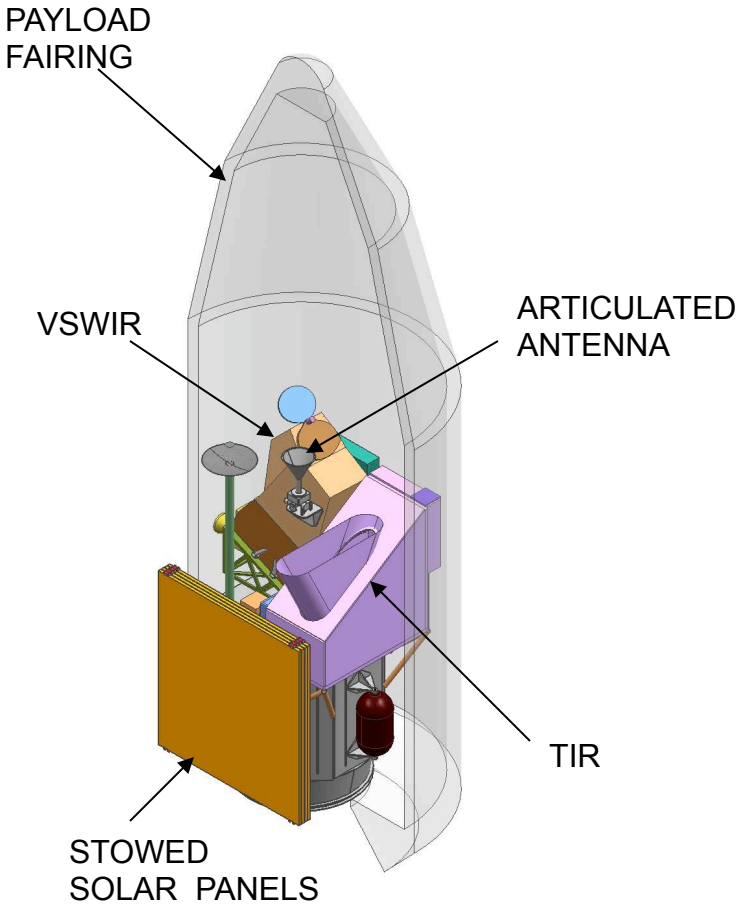

- Taurus 3210 can meet the mission needs
  - Closest fit among currently NASA approved launchers
  - 31% margin (per JPL Design Principles) with a Taurus-class launch vehicle
  - Fits dynamic volume envelope
  - 790 Kg launch capacity for HyspIRI Orbit
- Launch window
  - Mapping orbit reachable once per day

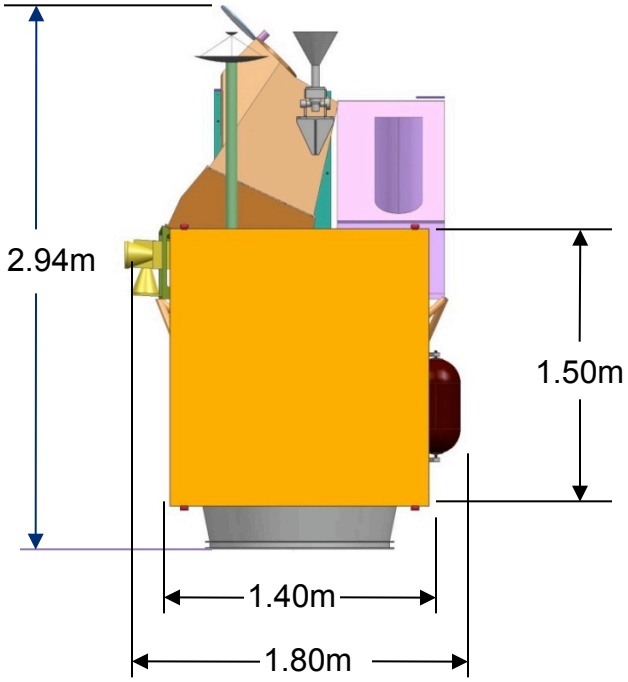

National Aeronautics and Space Administration
Jet Propulsion Laboratory
California Institute of Technology
Pasadena, California

Alternate Orbits Compatible with HyspIRI

There is flexibility in the HyspIRI orbit design to accommodate a shared launch, should one be available, without sacrifices to science return

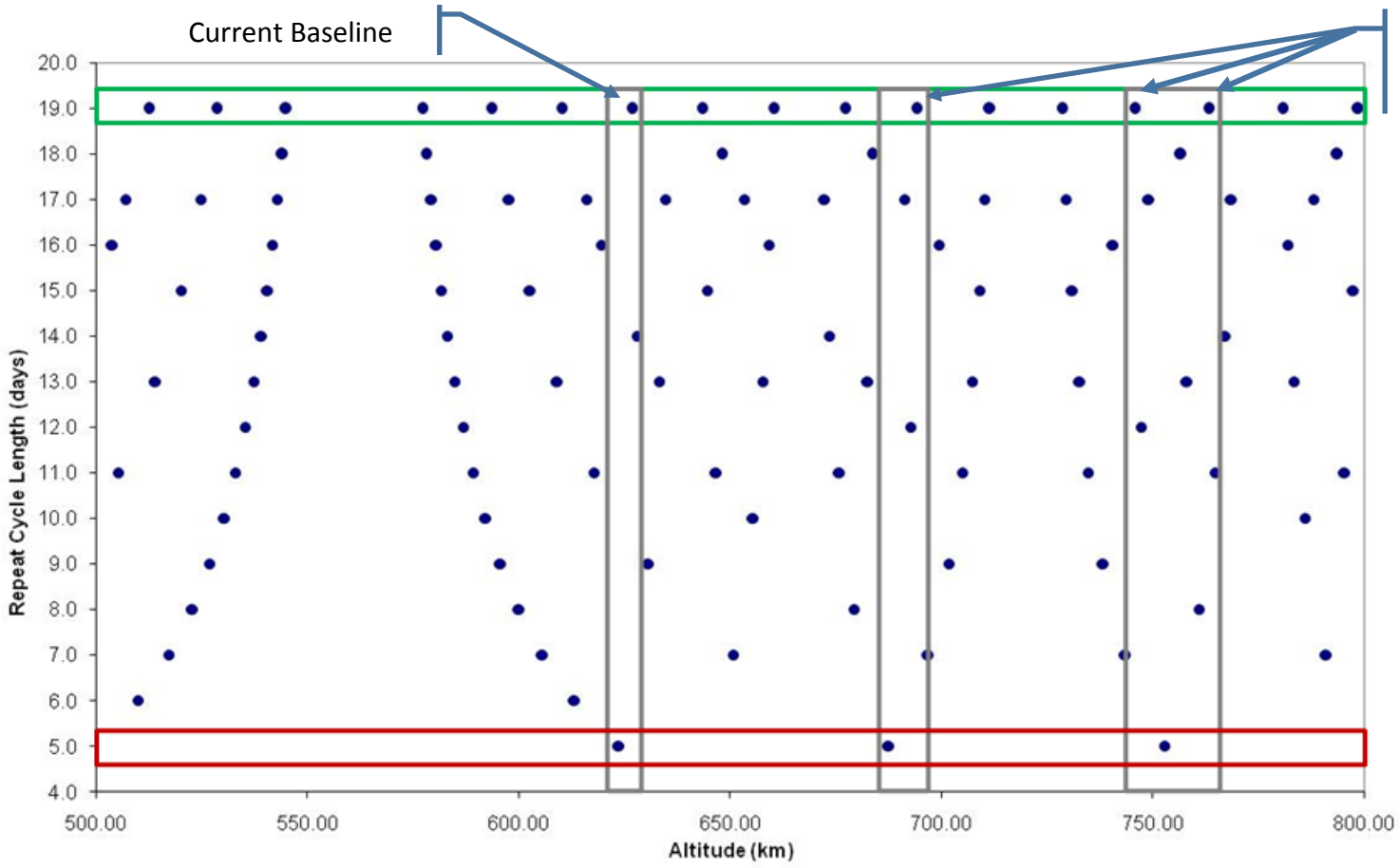

The VSWIR and TIR telescopes can be scaled to maintain 60 m spatial sampling at each of these orbits.

National Aeronautics and Space Administration
Jet Propulsion Laboratory
California Institute of Technology
Pasadena, California

U.S. Launch Vehicle Compatibility

LV	Throw Mass* (kg)	JPL Margin	Fairing (in)	Successful Launches	Availability	Estimated Cost	Comments
Taurus (3210)	790	31%	92	6/9 (1/1)	Yes	~$54M	Baseline; only one 3210 launch
Minotaur IV	1100	49%	92	2/2	DoD Only	~$50M	
Falcon 9	7500	>90%	204	2/2	Yes	~$55M	both flights were with Dragon capsule
Atlas V 4xx	~10000	>90%	157	17/18	TBD	TBD	401 had 9/10 launches
Delta IV Medium	8600	>90%	157	3/3	Yes	~$140	
Athena IIc	1700	69%	92	0/0	2012	TBD	2/3 launches of the II version

* For HyspIRI Orbit: 626km, sun-sync

National Aeronautics and Space Administration
Jet Propulsion Laboratory
California Institute of Technology
Pasadena, California

Deorbit Analysis

NASA mandates compliance with NASA-STD 8719.14 Orbit Debris & Reentry

"A spacecraft or orbital stage with a perigee altitude below 2000 km shall be disposed of by … :"

- "Atmospheric reentry option:
  Leave the space structure in an orbit in which natural forces will lead to atmospheric reentry within 25 years after the completion of mission but no more than 30 years after launch"
- HyspIRI is compliant as analysis of the spacecraft orbit and the geometry of the observatory indicates reentry within 18 years from EOL

"The potential for human casualty is assumed for any object with an impacting kinetic energy in excess of 15 Joules: "

- "For uncontrolled reentry, the risk of human casualty from surviving debris shall not exceed 0.0001 (1:10,000)."
- HyspIRI is currently compliant as simulation performed with NASA's Debris Assessment Software (DAS 2.0.1) shows a probability of 1:42,300

National Aeronautics and Space Administration
Jet Propulsion Laboratory
California Institute of Technology
Pasadena, California

Ground System Concept

- Data Downlink
  - KSAT Ground network
    - Svalbard @ 800 Mbps Dual-pole X-Band (existing)
    - Poker Flats @ 800 Mbps Dual-pole X-Band (in development)
    - Other stations available
  - Almost 100% data return with 1 Tbit SSR on spacecraft
- Data Processing
  - SDS sized to process L0 through L2 data for both instruments
  - Deliver L2 data products to DAAC
  - L3 data products produced by users

HyspIRI will utilize existing infrastructure with proven capability to downlink and process all science data

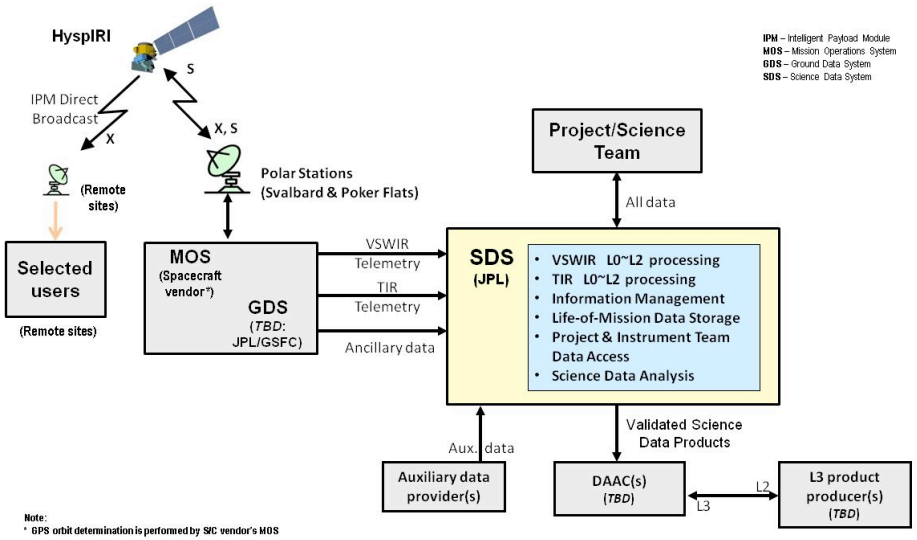

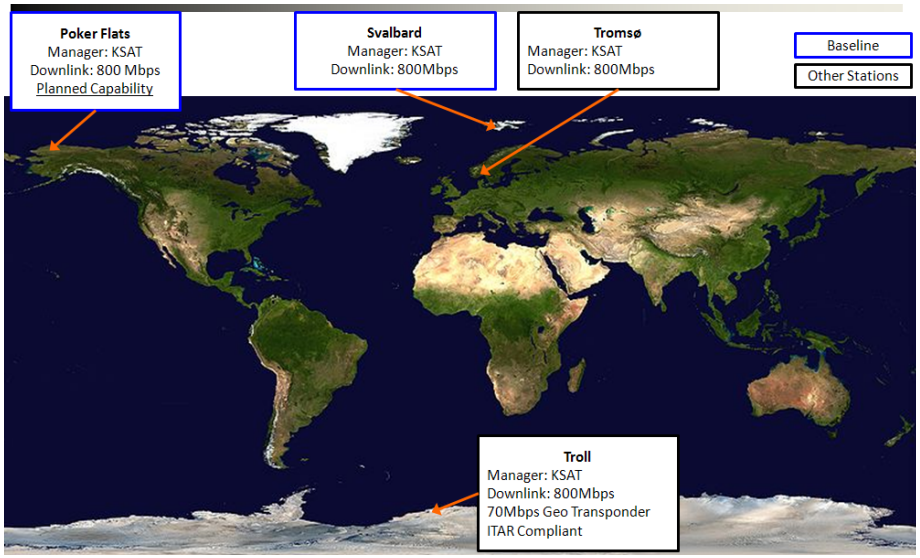

BACKUP

National Aeronautics and
Space Administration

Jet Propulsion Laboratory
California Institute of Technology
Pasadena, California

National Aeronautics and Space Administration
Jet Propulsion Laboratory
California Institute of Technology
Pasadena, California

HyspIRI Mission Concept

Orbit Selection

- Key Orbit Design Considerations
  - Local time of observations
    - Sun-synchronous
    - 10:30 AM LTDN
  - Altitude
    - Low Earth Orbit
    - Repeating Ground track
  - Global coverage in a minimum number of days given the swath-width of each instrument.
    - VSWIR: 19 days revisit at the equator
    - TIR: 5 day revisit at the equator (1 day + 1 night)
- 626 km altitude at equator suits the needs of both instruments

Orbit selection and operations concept meet science requirements with infrequent ground commanding or maintenance.

Operations Concept

- Systematic mapping vs. pointing capability
- Target map driven - No need for uploading acquisition sequences
- High resolution mode and Low resolution mode
- Direct Broadcast capability
  - Uses Intelligent Payload Module
  - Applications-driven

Operational Requirement	VSWIR	TIR
10:30 am sun-sync orbit	✓	✓
626 km altitude at equator	✓	✓
19 days revisit at the equator	✓	
5 day revisit at the equator		✓
Day Observation	✓	✓
Night Observation		✓
Pointing strategy to reduce sun glint	✓	
Surface reflectance in the solar reflected spectrum for elevation angles >20	✓	
Avoid terrestrial hot spot	✓	
Monthly Lunar View calibration	✓	✓
Weekly Solar View Calibration	✓	
Blackbody View Calibration		✓
Deep Space View Calibration		✓

National Aeronautics and Space Administration
Jet Propulsion Laboratory
California Institute of Technology
Pasadena, California

Key Driving SDS Design Requirements

- Data Downlink Volumes: 5.3 Tb/day Max. (4.6 Tb/day Mean)
- Data Product Types: 2 Level 0's, 2 Level 1's, 2 Level 2's, *tbd* L3
- Data Product Availability:

Product Application	Nominal Latency From Receipt of Required L0a Data at Processing Node	Comments
Routine Science	1 week – 2 weeks	Products meet science/calibration specifications
Priority Target Events	1 day	Data acquisitions are not routinely planned but event-driven Products are L1 and L2/3 in limited quantity Products may not meet science/calibration specifications
Intelligent Payload Module Direct Broadcast	No latency requirement for SDS	Data broadcast via the IPM will not end up at the SDS

- **Total Mission Data Volume***: 47.2 Tbits (6.2 Tb L0B's, 18.6 Tb L1B's, 22.5 Tb L2's) per day
  58.2 Pb over mission life
- **Processing Loading:** Sized to meet respective product latency requirements (no backlog and with margin to include *one* reprocessing campaign
- **SDS sized for 5.2 Tb/day**
  - 98.1% of the time, less than 5.2 Tb is downlinked per day

Notes: * Mission data volume based on maximum L0A downlink volume; exclusive of data from Direct Broadcast;
Assumes all L0 processed to L1 & L2; all in 16-bit per sample;
Assumes data compression ratios of 3:1 for all VSWIR and 2:1 for all TIR image bands; assumes no compression for ancillary bands;
Tb – Terabits (10^12 bits); Pb – Petabits (10^15 bits)

HyspIRI

DRAFT PRELIMINARY Level 1 Requirements

NASA Earth Science and Applications Decadal Survey

Robert O. Green, Simon Hook, Betsy Middleton, Stephen Ungar, Bob Knox, Woody Turner, John LaBrecque and the HyspIRI Team

Overview

Beginning in January 2007 a Mission Concept effort for HyspIRI Mission has been under way with involvement of NASA HQ, JPL, GSFC, and a broad Science Study Group and the 2008 workshop, 2009 workshop, 2010 symposium.

With the call of the NASA Earth Science and Applications Decadal Survey this team has worked to develop a end-to-end concept for implementation of the HyspIRI Mission.

Based on this effort and with input from SSG and the relevant communities a set of Level 1 Requirements and Success Criteria have been develop in accordance with the required NASA process.

The Level 1 Requirements are a NASA Headquarters Document and provide an important basis for tracking the progress and judging the success of HyspIRI

HyspIRI Science Study Group
(Selected by NASA Program Science Leadership)

- Request list from authors

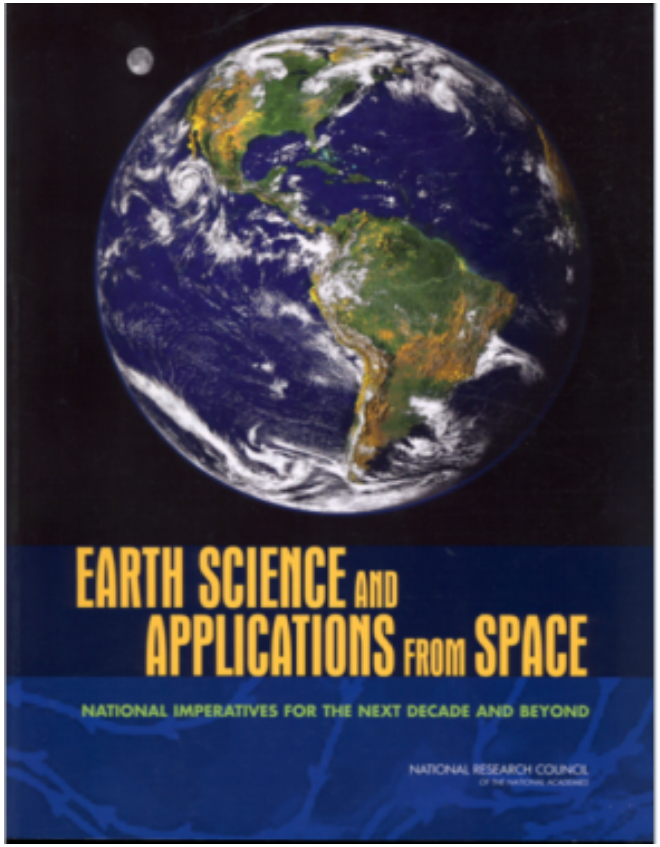

Level 1 Requirements Outline

1.0 Scope

2.0 Science Definition
- 2.1 Baseline Science Objectives
- 2.2 Science Instrument Summary Description

3.0 Project Definition
- 3.1 Project Organization and Management
- 3.2 Project Acquisition Strategy

4.0 Performance Requirements
- 4.1 Science Requirements
- 4.2 Mission and Spacecraft Performance
- 4.3 Launch Requirements
- 4.4 Ground System Requirements
- 4.5 Mission Data Requirements

5.0 NASA Mission Cost Requirement Program Requirement
- 5.1 Cost
- 5.2 Cost Management and Scope Reduction

6.0 Multi-Mission NASA Facilities

7.0 External Agreements

8.0 Public Outreach and Education

9.0 Special Independent Evaluation

10.0 Waivers

11.0 Approvals and Concurrences

Level 1 Requirements

Draft Preliminary

HyspIRI

Visible to Short Wavelength Infrared Imaging Spectrometer and Thermal Infrared Imager (HyspIRI) Decadal Survey Earth Science and Applications Mission

Level 1 Requirements and Mission Success Criteria

Version X-8.0
Date: August 27, 2010

Owner: NASA Decadal Survey HyspIRI Program Executive and Program Scientist

Draft Preliminary

Level 1 Requirements

- ***2.2. Science Objectives***

- The HyspIRI Project will implement an earth observation space mission designed to collect and deliver global surface spectral reflectance, remote sensing reflectance over shallow water, thermal emissivity and surface temperature imaging measurements that will enable science and applications users to advance the current understanding of the Earth's ecology, biogeochemistry, biodiversity, coastal and inland water research, geology, natural hazards, hydrology, climate, climate change impact and adaptation, and studies of the carbon cycle[NRC DS].

Level 1 Requirements

4. Performance Requirements

4.1 Science Requirements

The science objectives in Section 2.2 can be achieved by either the baseline or minimum science mission requirements listed here, but the baseline mission provides substantially more value to NASA and the Earth Science Community.

- **4.1.1 Requirement: Baseline Science Mission**
- *The scientific requirements that must be achieved in order to fully satisfy the baseline science objectives.*

- a) VSWIR

- b) TIR

- c) Combined

Level 1 Requirements

VSWIR

- a) To address the Decadal Survey and community identified science and application questions related to terrestrial and coastal ocean ecosystem composition, function, and change as well as surface composition (DS113-115), the baseline science mission shall provide global mapping measurements of the surface reflectance or remote sensing reflectance for shallow water regions across the solar reflected spectrum from 380 to 2500 nm at ≤10 nm sampling at the specified signal-to-noise ratio and accuracy with >95% spectral/spatial uniformity at ≤60 m nadir spatial sampling with <20 day revisit to provide >60% seasonal and >80% annual coverage of the terrestrial and shallow water regions of the Earth for at least three years with a subset of measurements available near-real-time for designated science and applications.

Level 1 Requirements

Benchmark Radiances

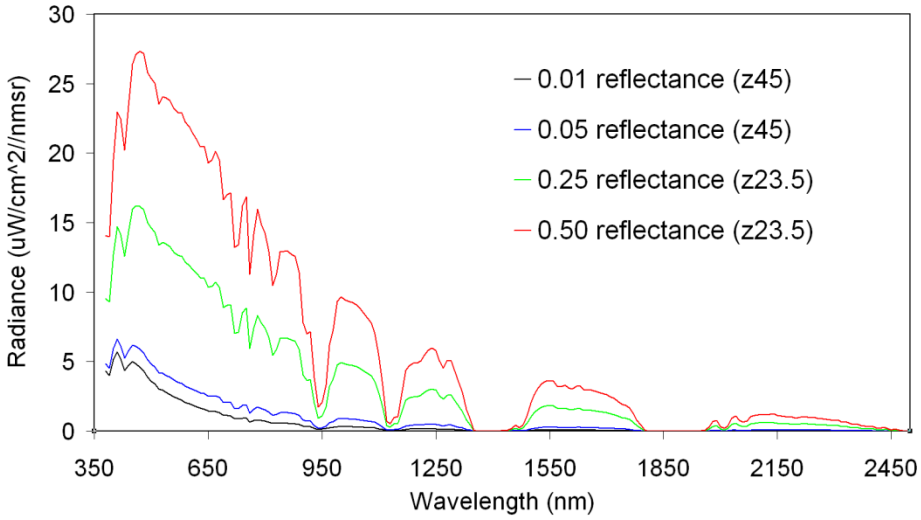

Required SNR

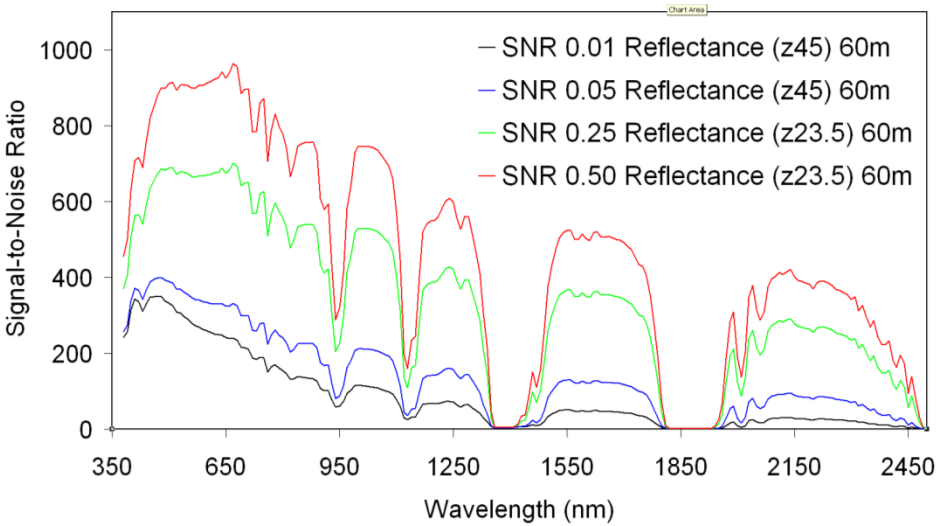

Uniformity Requirement

Cross Track Sample

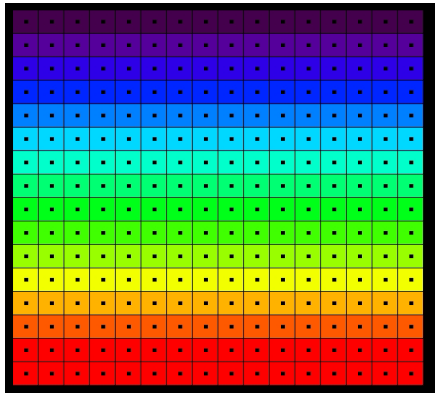

Wavelength

Depiction

-Grids are the detectors
-Dots are the IFOV centers
-Colors are the wavelengths

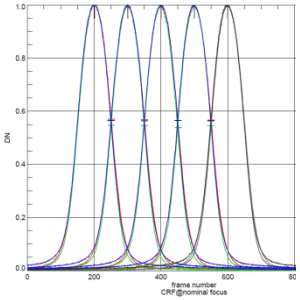

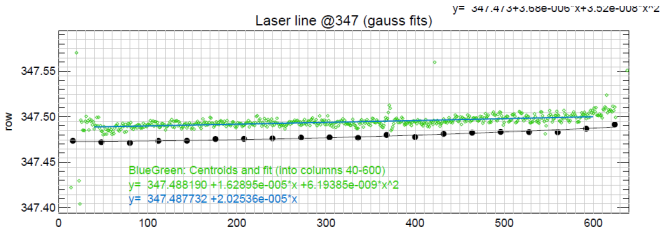

Requirement

Spectral Cross-Track	>95% cross-track uniformity {<0.5 nm min-max over swath}
Spectral-IFOV-Variation	>95% spectral IFOV uniformity {<5% variation over spectral range}

TIR

Level 1 Requirements

TIR

b) To address the Decadal Survey and community-identified science and application questions related to volcanoes, wild fires, water usage, urbanization and surface composition (DS113-115), the baseline science mission shall provide global mapping measurements of the surface radiance, temperature and emissivity with 8 spectral bands from the 3-5 micron and 8-12 micron regions of the spectrum at the specified noise-equivalent-delta-temperature and accuracy at ≤60 m nadir spatial sampling with ≤5 day revisit to provide >60% Monthly, >70% seasonal and >85% annual coverage of the terrestrial and shallow water regions of the Earth for at least three years with a subset of measurements available near-real-time for designated science and applications.

Specified NEdT

	Wavelength	Spectral Bandwidth	Min Nominal Radiance and Temperature	Max Nominal Radiance and Temperature	NEdT at Min nominal Temperature	NEdT at Max Nominal Temperature	NEdT at 300 K
	(microns)	(microns)	(W/m^2/micron/sr)	(W/m^2/micron/sr)	Kelvin	Kelvin	Kelvin
Band 1	3.98	0.08	14 (400 K)	9600 (1400 K)	1	0.12	11.2
Band 2	7.35	0.32	0.34 (200 K)	110 (500 K)	2.8	0.22	0.28
Band 3	8.28	0.34	0.45 (200 K)	100 (500 K)	2	0.22	0.24
Band 4	8.63	0.35	0.57 (200 K)	94 (560 K)	1.6	0.24	0.24
Band 5	9.07	0.36	0.68 (200 K)	86 (500 K)	1.2	0.24	0.22
Band 6	10.53	0.54	0.89 (200 K)	71 (500 K)	0.64	0.22	0.16
Band 7	11.33	0.54	1.1 (200 K)	58 (500 K)	0.56	0.26	0.16
Band 8	12.05	0.52	1.2 (200 K)	48 (500 K)	0.52	0.3	0.18

Digitization @ min radiance	Digitization @ max radiance	Digitization @ 300 K
(W/m^2/micron/sr)	(W/m^2/micron/sr)	(W/m^2/micron/sr)
4.0e-2 (0.12 K)	4.0e-2 (0.01 K)	5.0e-2 (1.4 K)
5.6e-3 (0.30 K)	5.6e-3 (0.009 K)	5.6e-3 (0.03 K)
4.8e-3 (0.23 K)	4.8e-3 (0.009 K)	4.8e-3 (0.03 K)
4.5e-3 (0.19 K)	4.5e-3 (0.009 K)	4.5e-3 (0.03 K)
4.1e-3 (0.15 K)	4.1e-3 (0.010 K)	4.1e-3 (0.03 K)
2.5e-3 (0.08 K)	2.5e-3 (0.008 K)	2.5e-3 (0.02 K)
2.2e-3 (0.07 K)	2.2e-3 (0.010 K)	2.2e-3 (0.02 K)
2.1e-3 (0.06 K)	2.1e-3 (0.012 K)	2.1e-3 (0.02 K)

Notes

Center wavelength is the average of the max and min wavelengths at the FWHM
Spectral bandwidth is the FWHM
Minimum nominal radiance is 200K except for 4 um band where it is 400K
Maximum nominal radiance is 500K except for 4 um band where it is 1400K

Level 1 Requirements

COMBINED

c) To address Decadal Survey and community-identified science and application questions (DS113-115), requiring combined reflectance, emissivity and temperature measurements, the baseline mission shall provide combined global mapping data sets.

Level 1 Requirements

Threshold Science Requirements

- Threshold (or minimum) scientific requirements (the “science floor”) that are required to scientifically justify performing the mission.

Level 1 Requirements

Threshold Science Requirements

4.1.2 Threshold Science Requirements

a) [VSWIR] To address the Decadal Survey and community identified science and application questions related to terrestrial and coastal ocean ecosystem composition, function, and change as well as surface composition (DS113-115), the baseline science mission shall provide global global mapping measurements of the surface reflectance or remote sensing reflectance for shallow water regions across the solar reflected spectrum from 380 to 2500 nm at ≤10 nm sampling at >80% of the specified signal-to-noise ratio and accuracy with > 90% spectral/ spatial uniformity at ≤60 m nadir spatial sampling with <20 day revisit to provide > 50% seasonal and >70% annual coverage of the terrestrial and shallow water regions of the Earth for at least two years.

Level 1 Requirements

Threshold Science Requirements

b) [TIR]To address the Decadal Survey and community identified science and application questions related to volcanoes, wild fires, water usage, urbanization and surface composition (DS113-115), the baseline science mission shall provide global mapping measurements of the surface temperature as well as emissivity and surface radiance in 8 spectral bands from the 3-5 micron and 8-12 micron regions of the spectrum at >80% the specified noise-equivalent-delta-temperature and accuracy at ≤60 m nadir spatial sampling with ≤5 day revisit to provide > 40% Monthly, > 60% seasonal and >70% annual coverage of the terrestrial and shallow water regions of the Earth for at least two years.

c) [COMBINED] To address Decadal Survey and community identified science and application questions requiring combined reflectance, emissivity and temperature measurements, the threshold mission shall provide combined global mapping data sets.

Summary

Program Level Requirements (or Level 1 Requirements) are a required gate product
KDP-A: Draft
KDP-B: Updated Draft Baseline
KDP-C: Baseline Update

In the pre Phase A period of the HyspIRI Mission concept input to the Level 1 Requirements will be requested from the SSG and Community.

The Level 1 Requirements are a NASA Headquarters Document and provide an important basis for tracking the progress and judging the success of HyspIRI

Questions?

NRC Decadal Survey
HysplRI Mission Concept

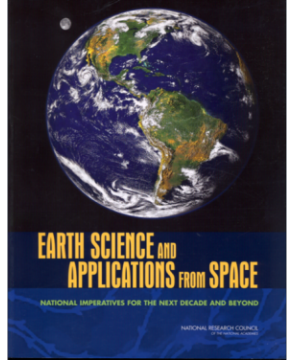

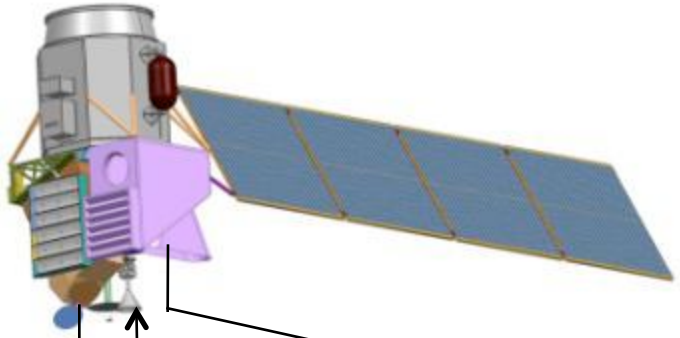

Visible ShortWave InfraRed (VSWIR) Imaging Spectrometer

Multispectral Thermal InfraRed (TIR) Scanner

IPM Low Latency Data

Map of dominant tree species, Bartlett Forest, NH

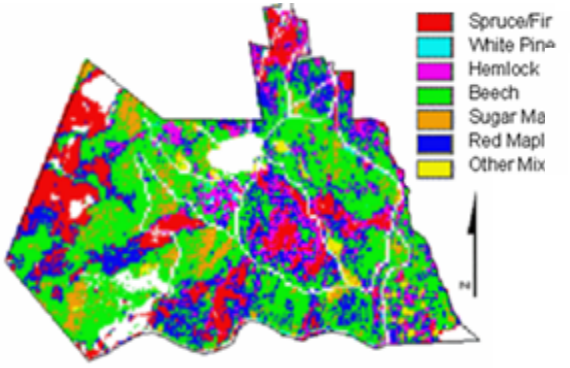

Soil C:N Ratio

White Mountain National Forest, NH

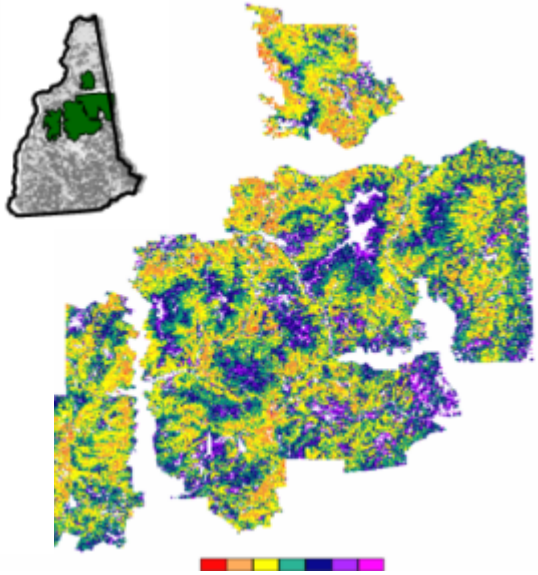

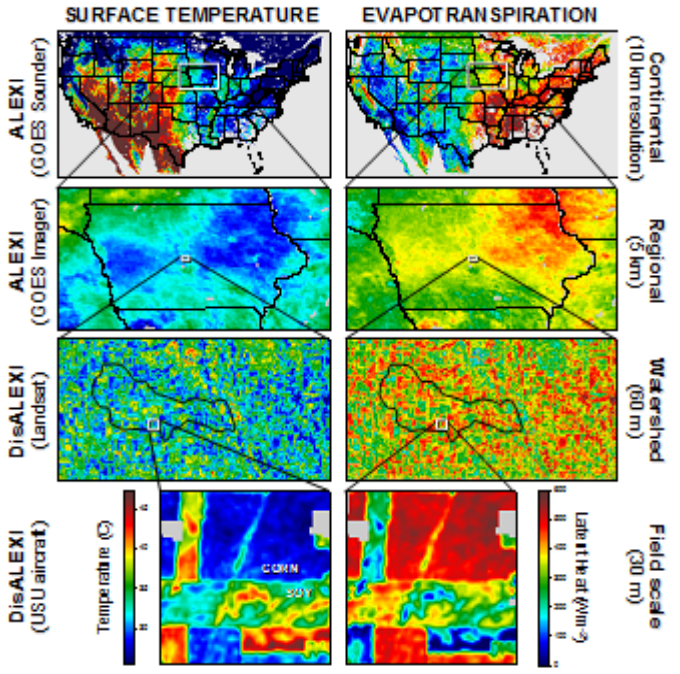

2011 HyspIRI Decadal Survey Mission Science Workshop
Washington, DC, August 23-25, 2011

A unique role for HyspIRI in Earth System Science Dynamical Global Vegetation Models

Jose F. Moreno
Depart. Earth Physics and Thermodynamics
Faculty of Physics
University of Valencia, Spain

Presentation outline:

- Background and motivation
- Status of Dynamical Global Vegetation Models
- Uniqueness of HyspIRI data
- **First approach:** Land cover mapping, classification and tables of assigned biophysical variables
- **Second approach:** Retrievals of biophysical variables as direct inputs to models
- **Third approach:** direct assimilation of radiances/reflectances into models
- Perspectives: current trends and way forward

BACKGROUND:

- Developments in the framework of SPECTRA mission within ESA Earth Explorer Programme

  Now discarded
- Current activities in preparation of the FLuorescence EXplorer (FLEX) ESA Earth Explorer mission

  in Phase A / B1
- Preparatory activities for data exploitation of global time series of high resolution data within the Global Monitoring for Environment and Security (GMES) programme, including data assimilation of Sentinels data for land applications.
- TERRABITES – *Terrestrial biosphere in the Earth System*, Carbon Model Reference Dataset, Climate Change Initiative, Essential Climate Variables, Glob-data series, etc.

The meaning of EARTH SYSTEM MODEL

(a) Technology side

Big powerfull computers running monster programs and producing huge amounts of output data that are better visualised in nice 3D animations (vector/parallel machines, code optimisation, distributed computer nodes grid, Fortran 2000+)

(b) Science side

Trying to make a "Theory of Everything" about the Earth (including solid Earth: volcanoes, earthquakes, etc. Oceans: temperature, salinity, circulation, etc., Atmosphere: all physics and dynamical chemistry, but also Live: ***a dynamical model of the Biosphere***)

In practice, the real problem is to define an adequate parameterization for the actual available inputs !

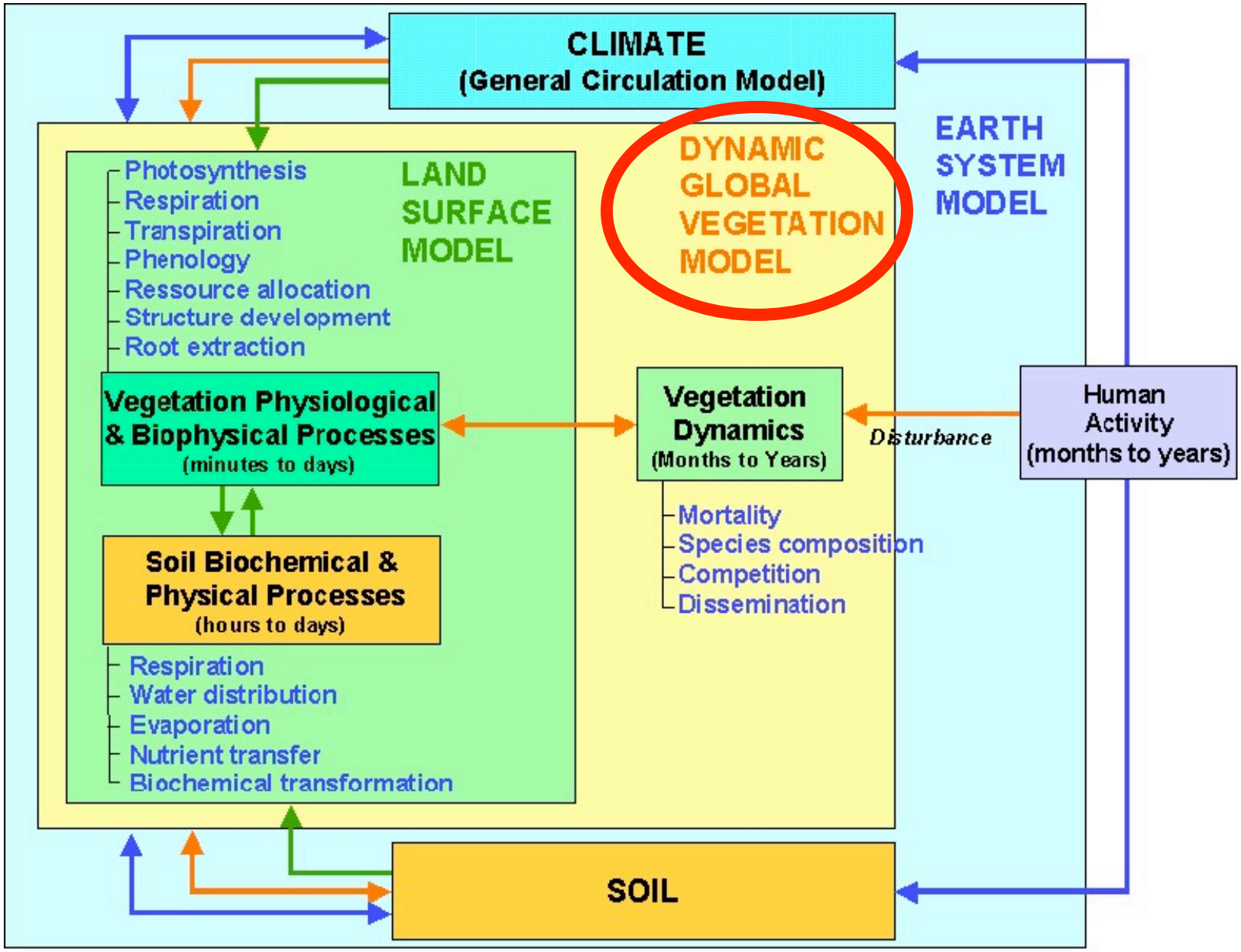
CLIMATE
(General Circulation Model)
EARTH SYSTEM MODEL
DYNAMIC GLOBAL VEGETATION MODEL
LAND SURFACE MODEL
Photosynthesis
Respiration
Transpiration
Phenology
Ressource allocation
Structure development
Root extraction
Vegetation Physiological & Biophysical Processes
(minutes to days)
Vegetation Dynamics
(Months to Years)
Disturbance
Human Activity
(months to years)
Mortality
Species composition
Competition
Dissemination
Soil Biochemical & Physical Processes
(hours to days)
Respiration
Water distribution
Evaporation
Nutrient transfer
Biochemical transformation
SOIL

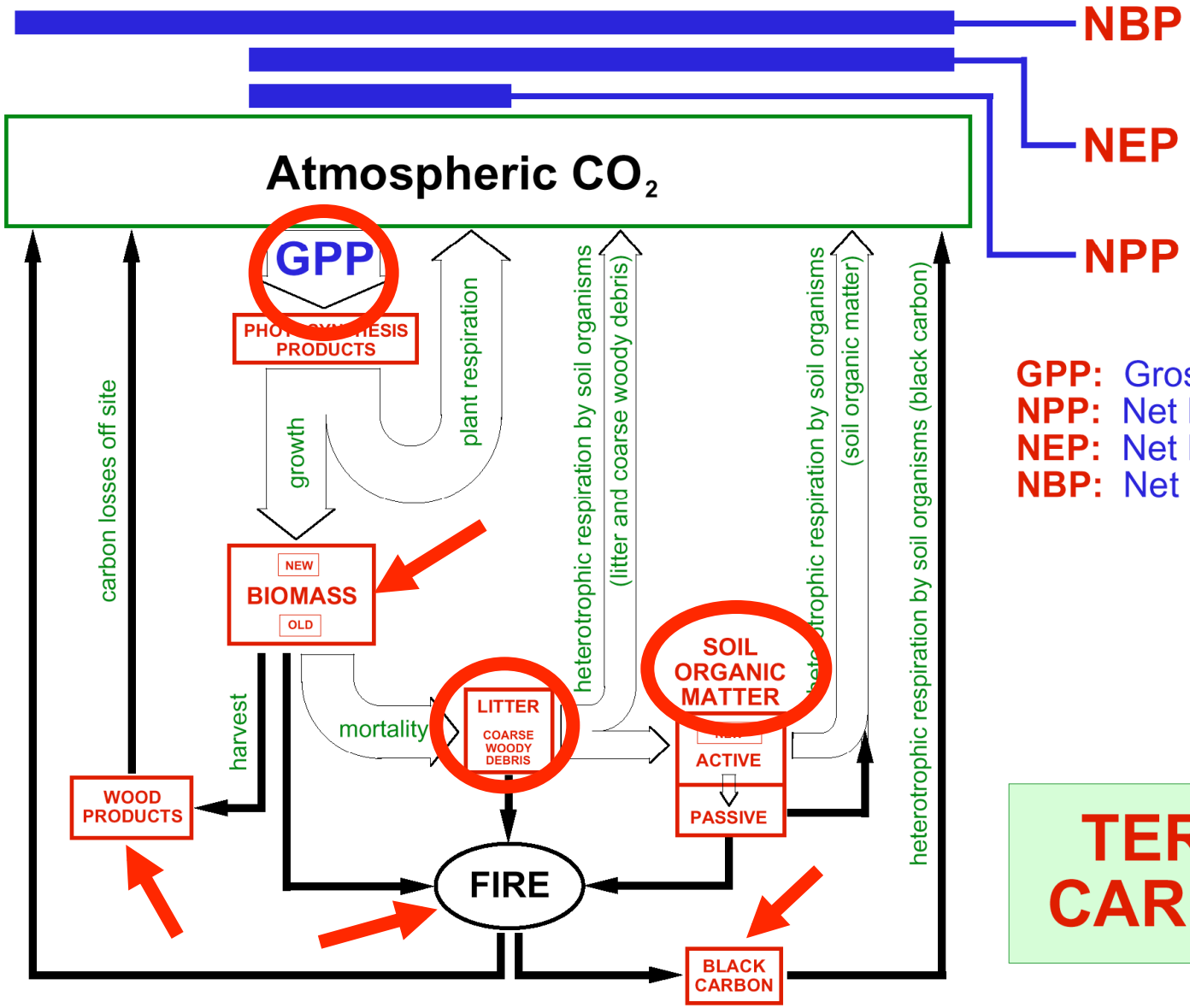

GPP: Gross Primary Production
NPP: Net Primary Production
NEP: Net Ecosystem Production
NBP: Net Biome Production

⇨ fluxes
▭ pools

TERRESTRIAL CARBON CYCLE

Getting the whole picture:

(a) Photosynthesis / CO_2 assimilation

Light absorption by plants

Different use by the plants of the absorbed light

Changes in land-use & physiology (growth/senescence)

→ **Imaging spectrometers VIS/NIR/SWIR + TIR**

(b) Biomass allocation / long-term carbon accumulation

Respiration terms for each biomass type (total biomass)

Net carbon accumulation (seasonal + multi-annual)

→ **SAR (L-inf, P-pol), Canopy lidars, BRDF sensors**

(c) Atmospheric CO_2 concentration

Net CO_2 balance (bottom of atmospheric column)

+ CO_2 atmospheric transport

→ **Dedicated atmospheric spectrometers + lidars ?**

Photosynthesis modelling approaches in LSM/GCM-DGVM

	POSITIVE	NEGATIVE
Biochemical	- Physical model (useful for climate change simulations at all scales) - Makes possible the explicit coupling of energy, water and carbon fluxes	- Computationally expensive for long-term climate simulations
Light-use efficiency	- Conceptual model (few parameters) - Interersting approach when APAR is measured (mostly over time scales of constant LUE)	- Empirical approach (useful for long timescales but accounting for LUE changes) - Not possible the explicit coupling of energy, water and carbon fluxes
Carbon assimilation	- Simplistic approach (useful for very long timescales) - To be used with coupled conceptual models	- Empirical approach (calibration needed for each environment) - Explicit coupling of processes not possible due to necessary large time steps

OPEN ISSUES IN LAND SCIENCE – Modelling aspects

- Model structure improvements:
  - parameterisation of surface heterogeneity
  - horizontal transport at the boundaries
  - vertical transport in 3D structures
- Coupling to ecological processes
  - phenology cycles / multiannual growth
  - vegetation dynamics (sucession, regeneration)
  - soil processes (decomposition, mineralisation)
- Coupling to hydrological processes
  - surface/sub-surface transport
  - river flow
  - lake/wetland dynamics
- Coupling to chemical cycles (CO_2, CH_4, N_2O, …)
- Link to atmospheric dynamics (wind at surface)

OPEN ISSUES IN LAND SCIENCE – Data availability

- Global data available mostly are of low spatial resolution, with limited capabilities to observe variables directly related to some key processes, though indirect observation is possible via the coupling of different processes through modelling.

- There is a definite need for global data at high spatial resolution (< 300 m) to be able to describe surface heterogeneity at relevant scales with adequate temporal resolution to describe dynamics

- Full spectral resolution (VIS, NIR, SWIR + TIR) highly desirable to constraint models with a full set of observations for each given model parameterization.

Unique information provided by HysplRI:

Explicit mapping of how plants absorb light, as a function of the temperature of leaves

- *spectrally resolved PAR (400-700 nm)*
- *canopy chemistry and structural effects, decoupling non-photosynthetic elements*
- *high data quality is expected*

- **Monitoring vegetation changes (time series)**

But we not only need to get data to be ingested in existing models but also to develop models that can ingest the new available data !

Different spatial sampling observational approaches:

(a) Discrete sampling of identified reference sites

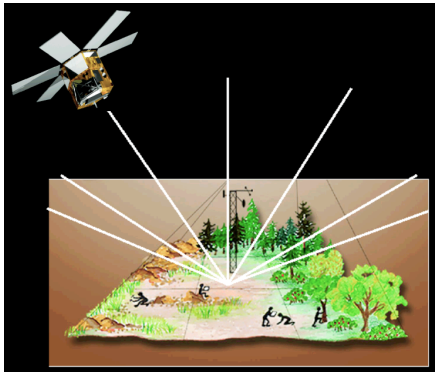

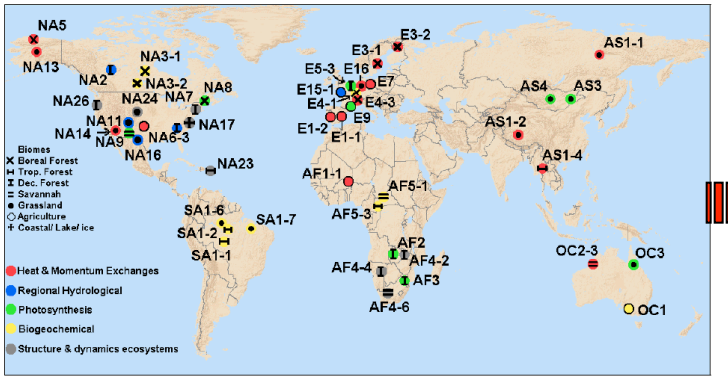

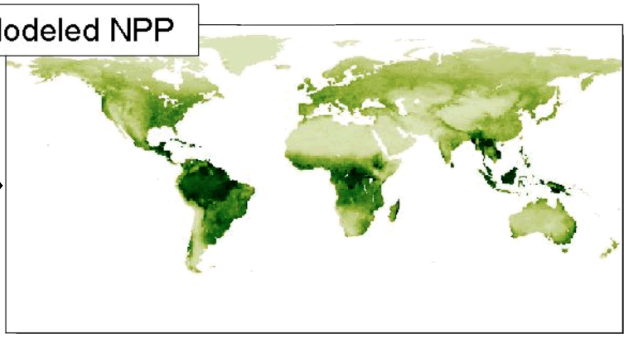

(b) Systematic global sampling

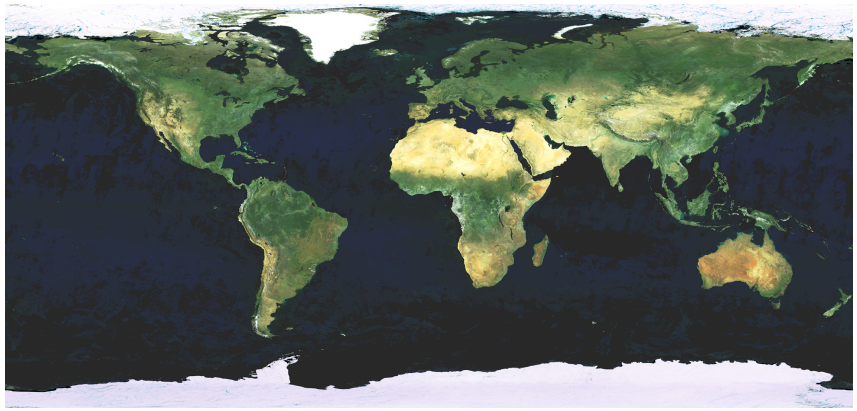

HysplRI approach

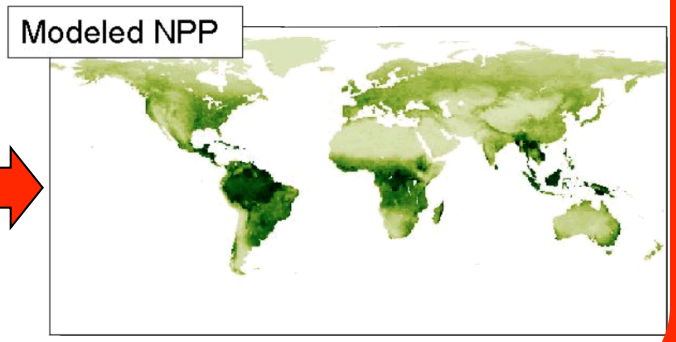

Temporal scales in DGVM

From 15-30 minutes time-step (to capture diurnal cycle) to long-time scale processes (centuries, millennia) both for past and future dynamics

≥ 5 - 19 days

Temporal scales resolved by HysplRI

≤ 5 / 10 years

Minutes / Months	Photosynthesis and leaf respiration
Minutes / Months	Growth respiration Stem and root maintenance respiration
Daily / Monthly	Phenology
Daily / Annual	Allocation
Monthly / Annual	Nitrogen cycle
Decades / Centuries	Competition between Plant Functional Types

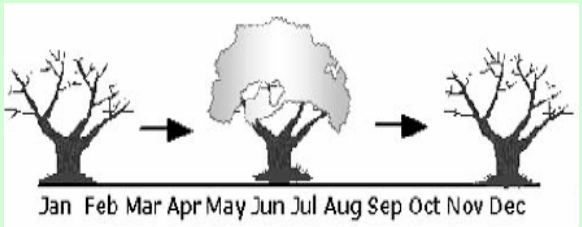

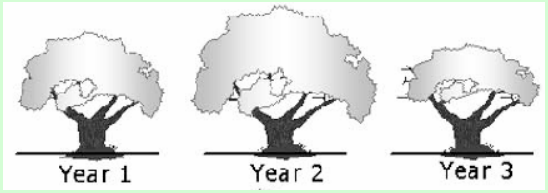

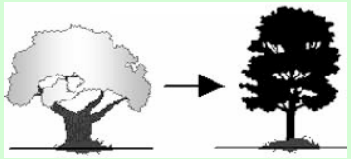

First approach:
LAND COVER MAPPING, CLASSIFICATION AND TABLES OF BIOPHYSICAL VARIABLES ASSIGNED TO EACH CLASS

Global land cover maps

Feature-Based Parametric Object Oriented Land Cover databases

- Cultivated and Managed areas / Rainfed cropland
- Post-flooding or irrigated croplands
- Mosaic cropland (50-70%) / vegetation (grassland/shrubland/forest) (20-50%)
- Mosaic vegetation (grassland/shrubland/forest) (50-70%) / cropland (20-50%)
- Closed to open (>15%) broadleaved evergreen and/or semi-deciduous forest (>5m)
- Closed (>40%) broadleaved deciduous forest (>5m)
- Open (15-40%) broadleaved deciduous forest/woodland (>5m)
- Closed (>40%) needle-leaved evergreen forest (>5m)
- Closed (>40%) needle-leaved deciduous forest (>5m)
- Open (15-40%) needle-leaved deciduous or evergreen forest (>5m)
- Closed to open (>15%) mixed broadleaved and needleleaved forest
- Mosaic forest or shrubland (50-70%) and grassland (20-50%)
- Mosaic grassland (50-70%) and forest or shrubland (20-50%)
- Closed to open (>15%) shrubland (<5m)
- Closed to open (>15%) grassland
- Sparse (<15%) vegetation
- Closed (>40%) broadleaved forest regularly flooded, fresh water
- Closed (>40%) broadleaved semi-deciduous and/or evergreen forest regularly flooded, saline water
- Closed to open (>15%) grassland or shrubland or woody vgt on regularly flooded or waterlogged soil, fresh, brakish or saline water
- Artificial surfaces and associated areas (Urban areas >50%)
- Bare areas
- Water bodies
- Permanent Snow and Ice

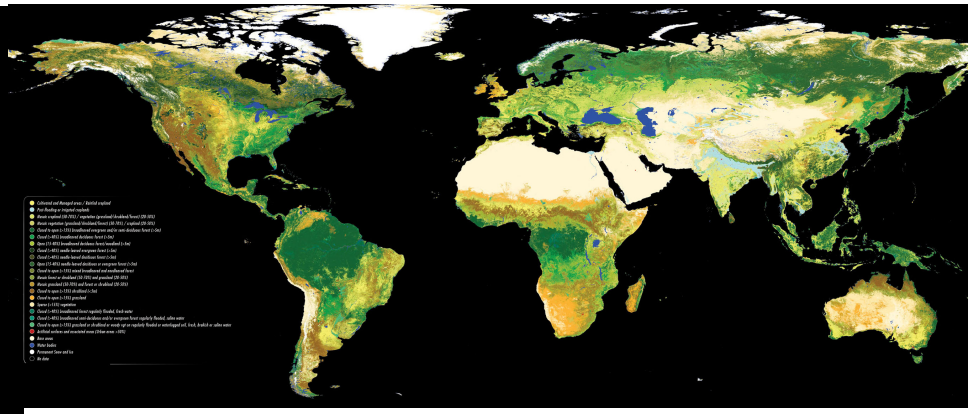

Plant functional types and temporal profiles

Disturbances described by multi-annual classifications

Second approach:
RETRIEVALS OF BIOPHYSICAL VARIABLES AS DIRECT INPUTS TO MODELS

- Global spatially distributed inputs assumed necessary by most modeling approaches (APAR, LAI, fCover, Chl, temperature, etc.)
- Specific variables retrieved from remote sensing data used either for initialisation, forcing, updating or validation

Use of constrained minimization procedures that guarantee the minimal variation of model variables to produce the same output, and a robust initialization procedure of such variables (consistency even if model has global bias).

$$f(\bar{\mathbf{x}}) = \frac{1}{2}\bar{\mathbf{x}}^T \bar{\mathbf{W}}_\mathbf{x} \bar{\mathbf{x}} + \frac{1}{2}\left(\bar{\mathbf{z}} - \bar{\mathbf{H}}\bar{\mathbf{x}}\right)^T \bar{\mathbf{W}}_\mathbf{d} \left(\bar{\mathbf{z}} - \bar{\mathbf{H}}\bar{\mathbf{x}}\right)$$

Open issues:

- Specific Leaf Area (currently normally PFT fixed) is a key parameter that need spatialization (current parameterizations assume carbon derived from SLA).
- Non photosynthetic elements in canopy structure not yet described (i.e. celullose, lignin)

→ **Potential for new variables to be provided by HysplRI**

How well the spectral reflectance signal is understood?

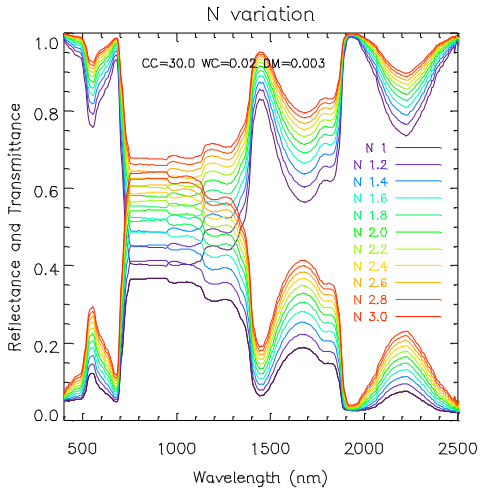

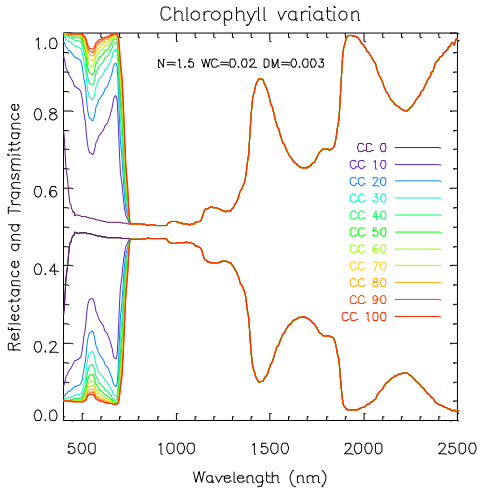

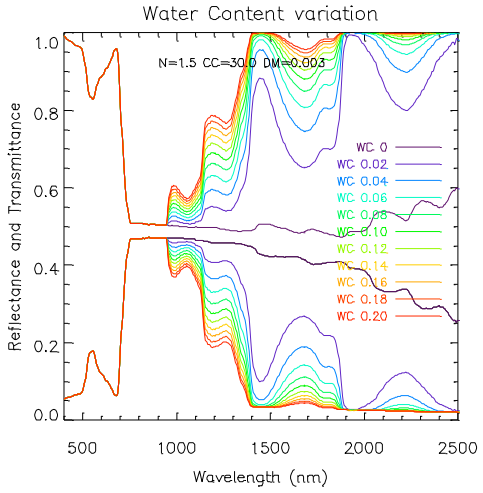

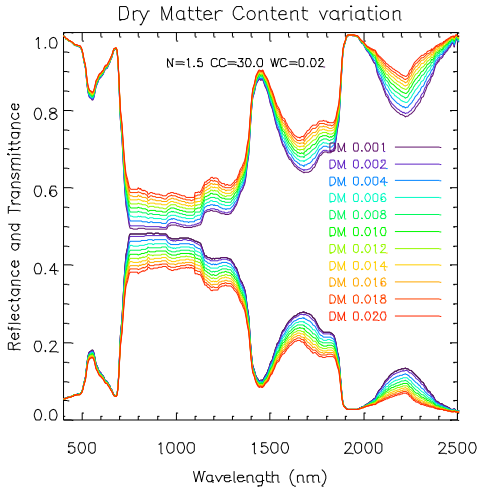

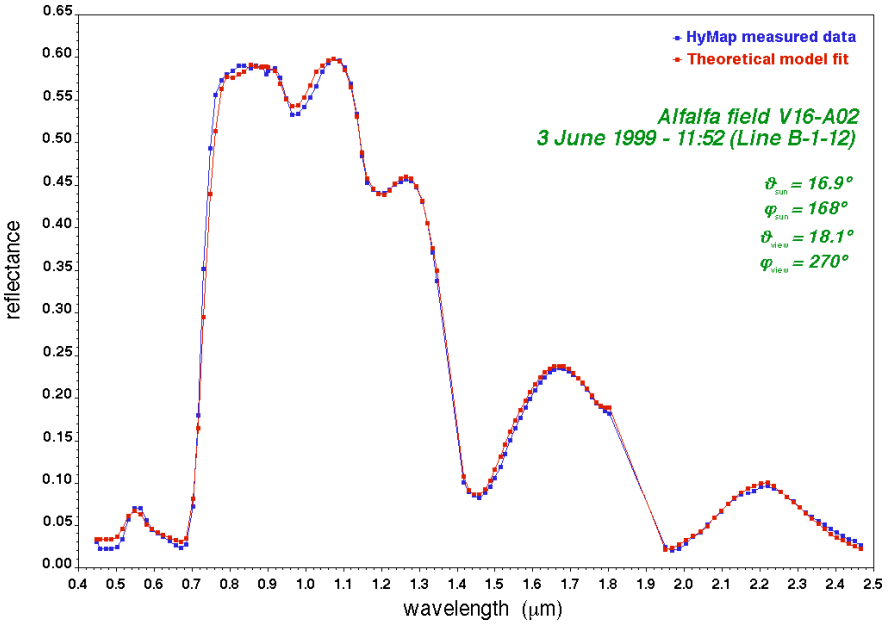

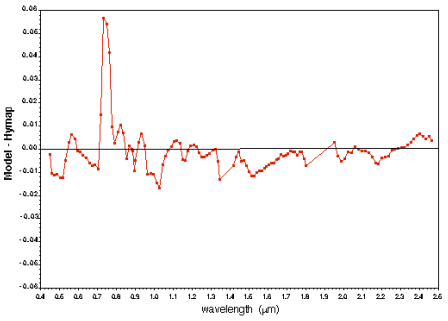

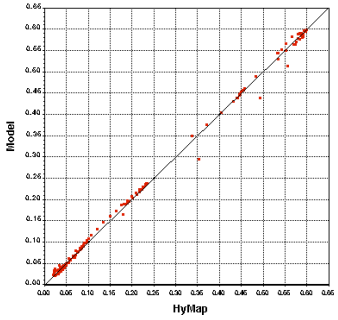

Third approach:
DIRECT ASSIMILATION OF RADIANCES/REFLECTANCESINTO MODELS

- The function that relates the set of observables to the state variables -forward operator or mathematical model- is not always well defined; variables tend to have different meaning.
- For instance, LAI is an important variable in the DGVMs, but remote sensing products not yet used properly used to inconsistency (green/total, true/effective, clumping)
- Light absorption: chlorophyll content used instead of APAR (APAR computed instead of input) new remote sensing products are necessary.
- Consistent description canopy structure (used in photosynthesis modules to separate sunlit and shadowed leaves) and absorption by photosynthetic pigments and by other non-photosynthetic elements.

The physical laws that relate the state variables and the observables are rather empirical in most cases (weak conservation laws).

Direct data assimilation is a tendency to avoid problems and inconsistencies.

Is it possible to assimilate TOA radiances in Dynamical Global Vegetation Models?

- In principle yes, if one can deal with atmospheric effects (aerosols, water vapour, ozone), but dynamical effects are too challenging (i.e., statistical cloudiness versus actual clouds). Assimilation of TOA radiances in dynamical models is a challenge.

- A more realistic approach is to assimilate normalized time series of surface reflectance (enhancement in the radiative transfer component of the models is needed).

- An even more realistic approach is to assimilate maps of surface variables consistently retrieved.

- An even more realistic approach is to assimilate 'constant' (or with low time variation) surface parameters instead of relying on fixed parameterisations (i.e., V_{max})

CURRENT TRENDS IN GDVMs – 1 : Resolutions

GCMs typically use 15-30 min as time-step, DGVMs use time-steps from 30 min to one day (up to a month).

GCMs operate with resolutions in the order of 100-500 km resolution, DGVMs use resolutions in the order of 50 km.
Processes on a scale < 1 km (including vegetation patterns and wetlands, permafrost, urbanization, etc.) are parameterized as sub-grid scale processes (not explicitly resolved).

Spatial resolution is an issue. Tiling (fractional horizontal cover) and spatial sampling techniques are common approaches. The alternative to go for fine resolution without tiling is being seriously considered, at least for test relevant scenarios of using GDVM outside GCMs.

The assumed sub-grid scale parameterizations are not thoroughly calibrated. Explicit modelling of traits (explicit spatially distributed data) is an emerging approach that definitely needs the link with global datasets derived from remote sensing data.

CURRENT TRENDS IN GDVMs – 2 : Parameterizations

- The key problem right now is the large number of parameters and the large uncertainty in such parameters, which limits the capability to run predictive analyses based on perturbations of free model parameters to test future climate scenarios including plant adaptation / acclimation to climate change.
- The only way to have better confidence is to run models over "current" datasets to get good model parameterization to run future predictions.
- Model intercomparison (C4MIP, etc.) is a common approach to estimate structural uncertainty in the models (driven by model parameterization) and benchmarking are designed to indicate "best" parameterizations strategies.

But a *reference dataset* is needed which is: global, high spatial resolution, spectrally complete, good temporal resolution, covering several years to describe several seasonal cycles

NOTE: Reference datasets are needed to fix parameterizations, not necessarily as "inputs" to run the models.

THE WAY FORWARD:
What activities are needed to achieve these goals?

- The DGVM modellers are already too busy with model improvements in other aspects and will not adapt their models to ingest these new type of data.
- Direct radiance/reflectance data assimilation is an adequate efficient way, but model adaptations are needed.
- Remote sensing specialists with some background on modelling are in a better position to establish the link between data and models.
- The HyspIRI community must be active developing the necessary modelling and data assimilation tools.

Thank you !

Discriminating dominant plant species and functional types across ecosystems

Keely L. Roth[1], Dar A. Roberts[1], Philip E. Dennison[2], & Greg K. Fryer[2]

HyspIRI Science Workshop, 2011

[1]Dept. of Geography, University of California, Santa Barbara

[2]Dept. of Geography, University of Utah

Mapping Plant Species & Functional Types

- Rationale/Relevance to HyspIRI
- Research Objectives
- Study Ecosystems
- MESMA at native and 60 m resolutions
  - Individual sites
  - Combined-sites
- Findings & Conclusions

HyspIRI Mission Goals

- VQ1) What is the global spatial pattern of ecosystem and diversity distributions, and how do ecosystems differ in their composition or biodiversity?...*What is the current spatial distribution of ecosystems, functional groups, or key species within major biomes?*

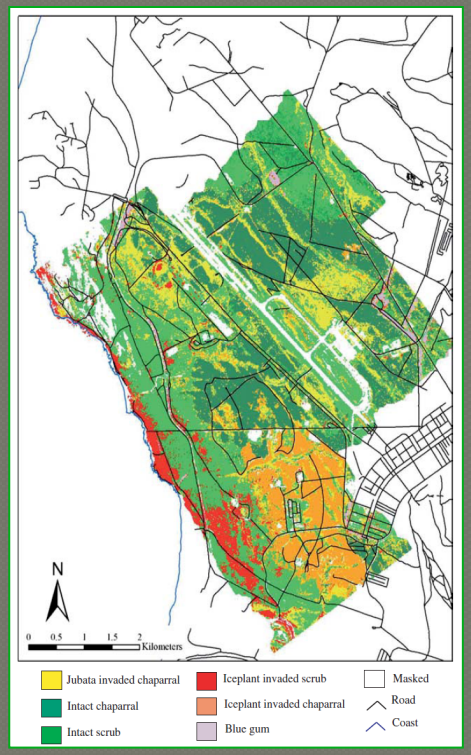

Underwood et al., 2007, *Environ Manage*

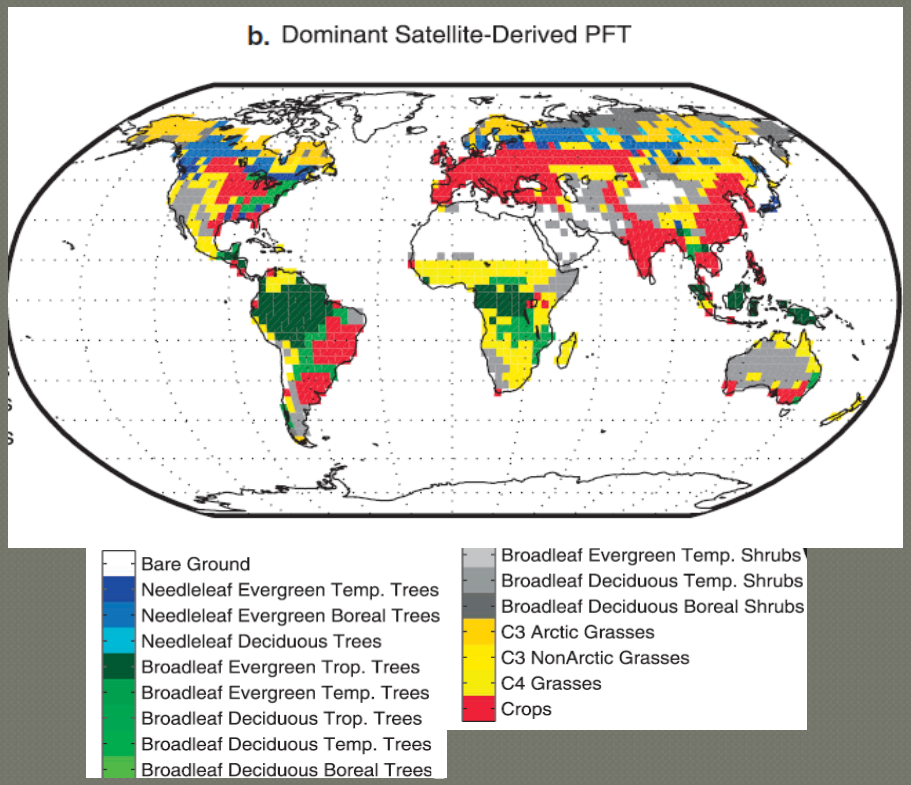

Bonan et al., 2002

Research Objectives

What are the *spatial*, spectral and temporal data requirements for discriminating plant species & functional types across diverse ecosystems?

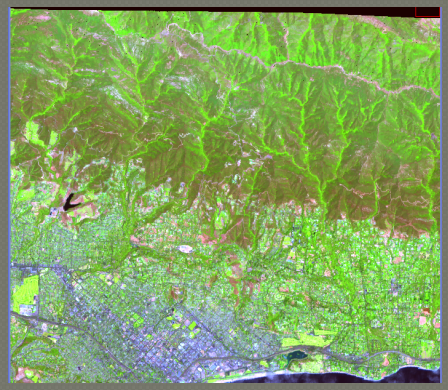

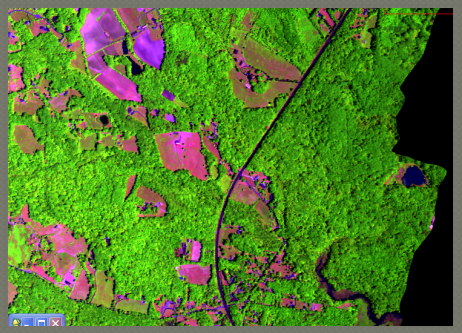

Impact of 60 m?

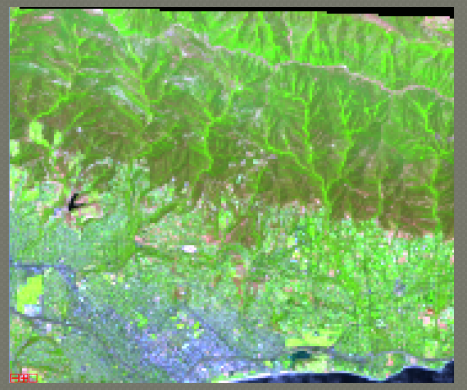

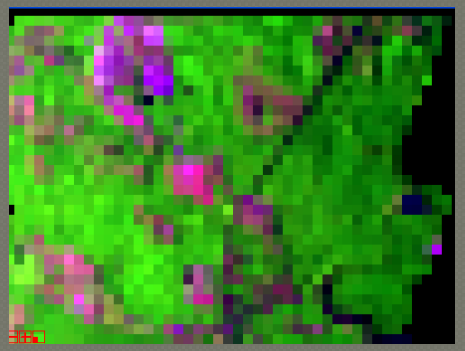

Study Sites

Canada
Wind River
Sierra Nevada
Santa Barbara
SERC
Atlantic Ocean
Pacific Ocean
Mexico
Gulf of Mexico

Smithsonian Environmental Research Center (SERC)

Santa Barbara Front Range (SBFR)

Wind River Experimental Forest (WR)

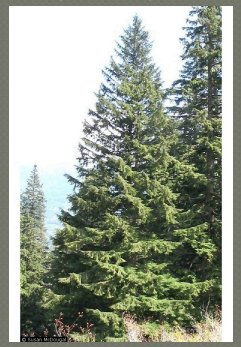

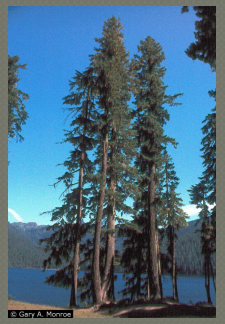
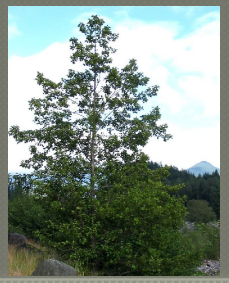

Southern Sierra National Forest (SNev)

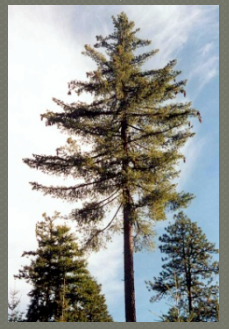

Image & Library Processing

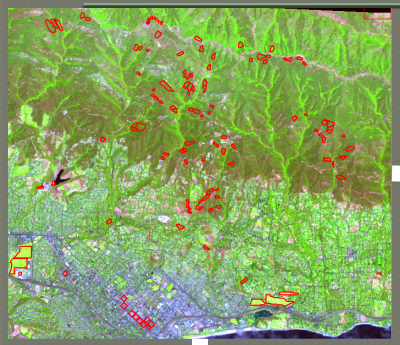

native

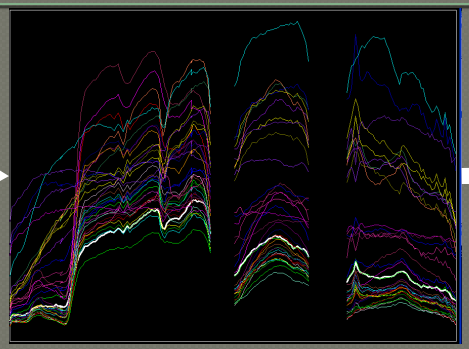

full library

random sampling

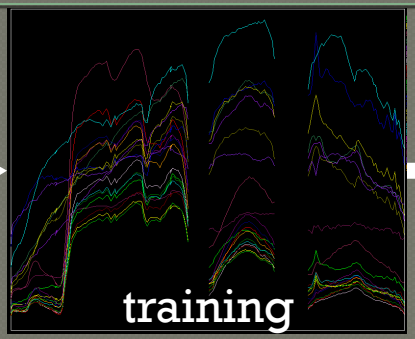

training

validation

Iterative Endmember Selection

spatial aggregation

60 m

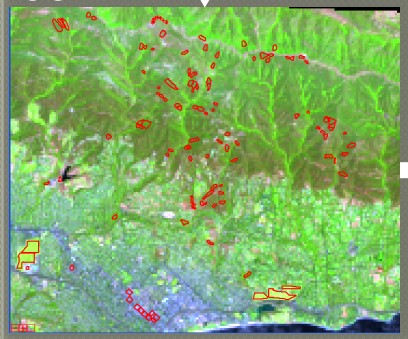

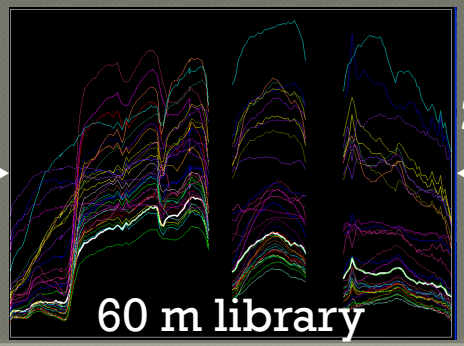

60 m library

2-EM MESMA

2-EM MESMA

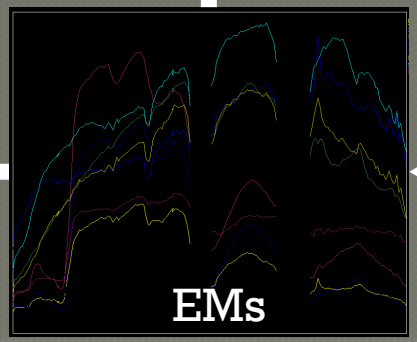

EMs

Temperate Broadleaf Deciduous Forest (SERC)

acquired 29 May 2006 at 3.5 m

EMs = 68

Species-level

	native	60 m
# classes	11	8
kappa	0.778	0.823
overall accuracy	82.6%	85.7%

PFT-level

	native	60 m
# classes	5	5
kappa	0.909	0.872
overall accuracy	93.3%	90.5%

60 m species

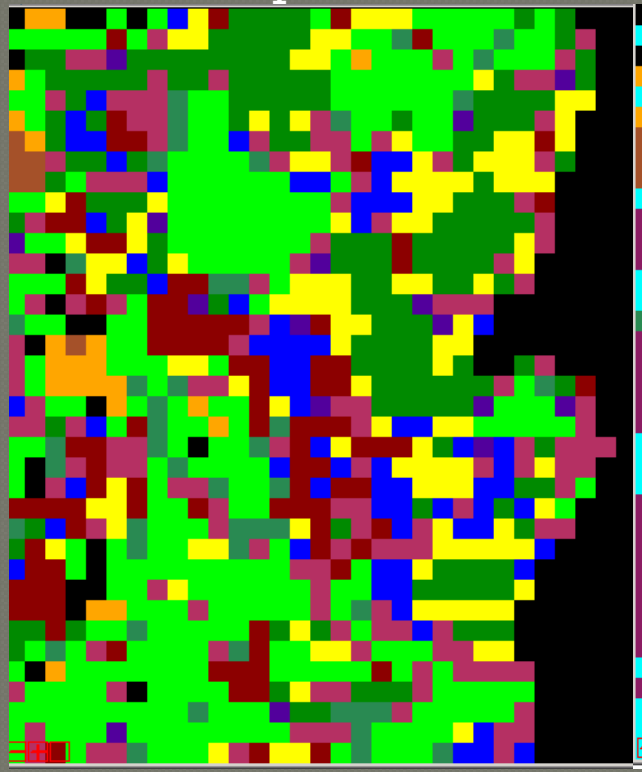

60 m PFT

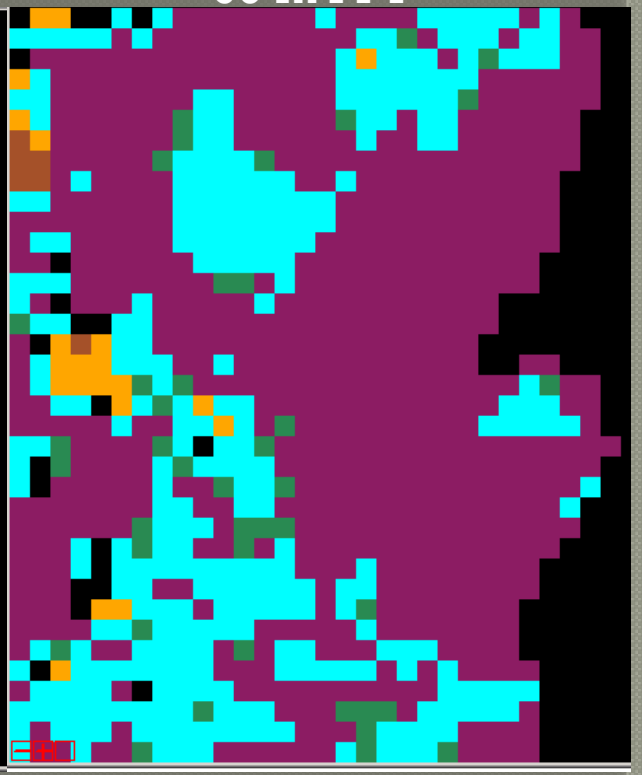

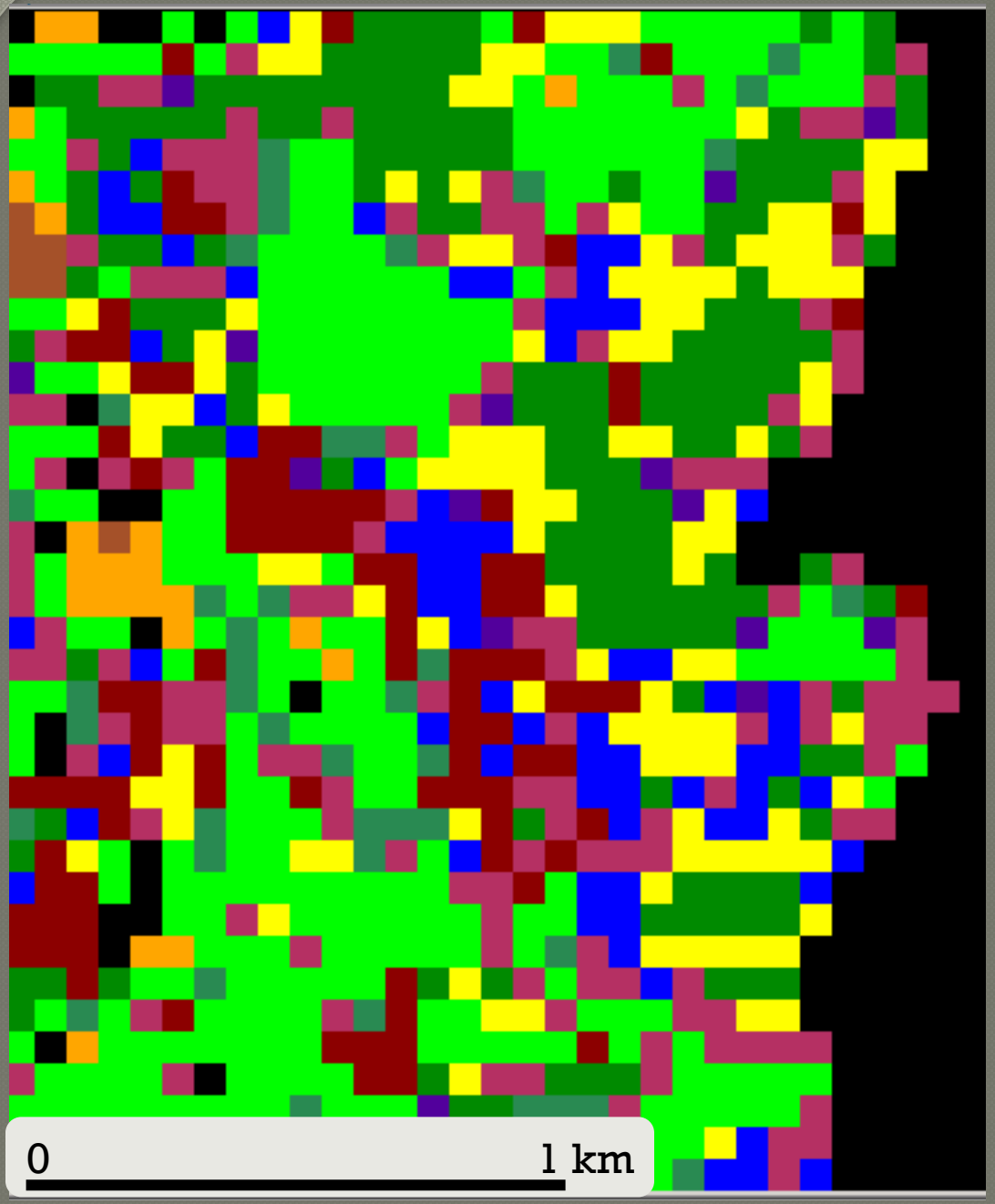

unclassified

~~Acer rubrum~~

crop

soil

Carya

Fagus grandifolia

Pinus

litter

Quercus

~~Platanus occidentalis~~

~~Liquidambar styraciflua~~

Liriodendron tulipifera

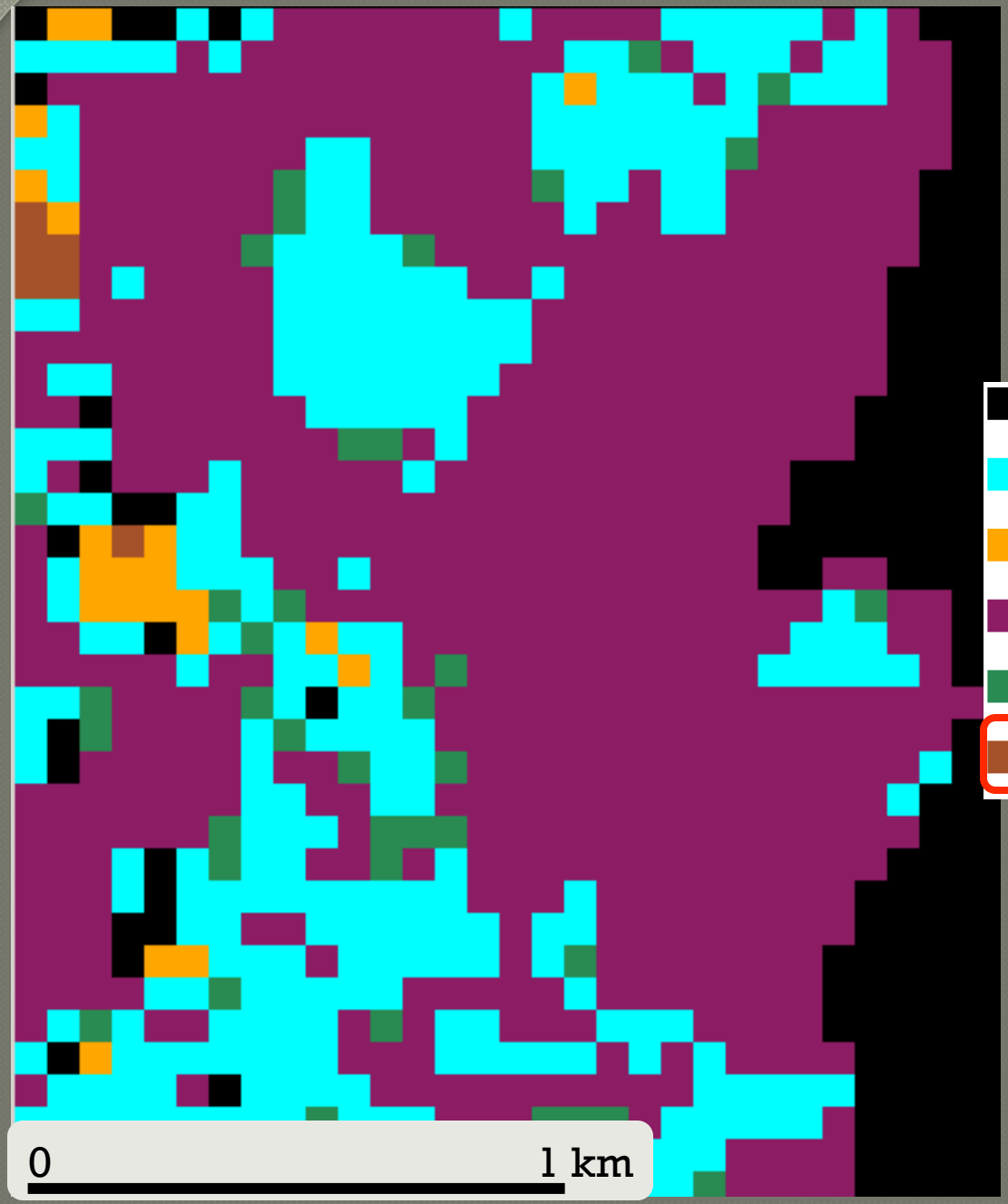
unmodeled
annual broadleaf herb
litter
deciduous broadleaf tree
evergreen needleleaf tree
soil
0
1 km

Temperate Broadleaf Deciduous Forest (SERC)

acquired 29 May 2006 at 3.5 m

EMs = 68

Species-level

	native	60 m
# classes	11	8
kappa	0.778	0.823
overall accuracy	82.6%	85.7%

PFT-level

	native	60 m
# classes	5	5
kappa	0.909	0.872
overall accuracy	93.3%	90.5%

Key Results

- canopy dominants separable at 60 m, but smaller classes become too mixed
- discrimination among deciduous broadleaf tree species is moderate
- good discrimination among functional types at 60 m

Chaparral Shrubland/Oak Woodland/Urban (SBFR)

acquired 06 Aug 2004 at 16 m

EMs = 310

Species-level

	native	60 m
# classes	22	22
kappa	0.793	0.767
overall accuracy	82.3%	79.6%

60 m species

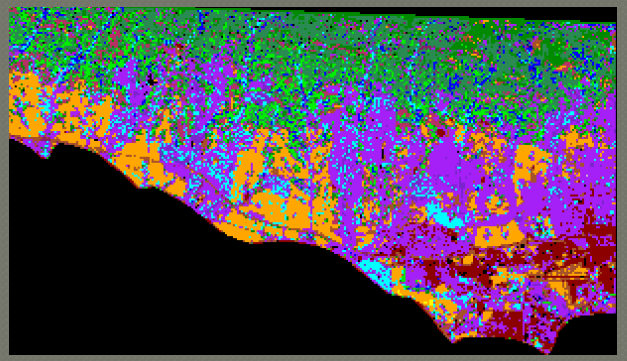

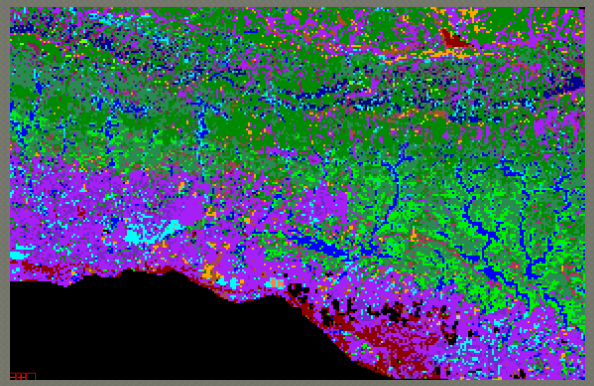

PFT-level

	native	60 m
# classes	12	12
kappa	0.842	0.819
overall accuracy	87.6%	85.6%

60 m PFT

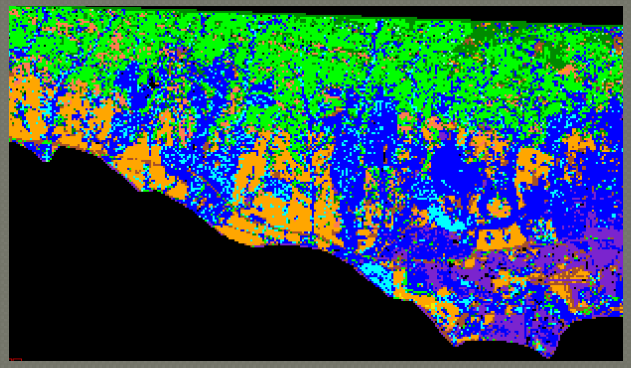

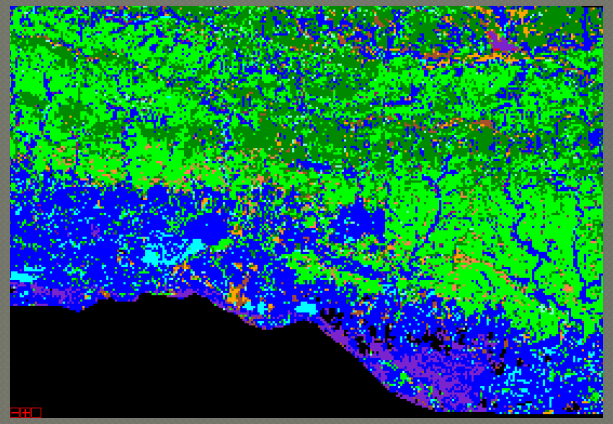

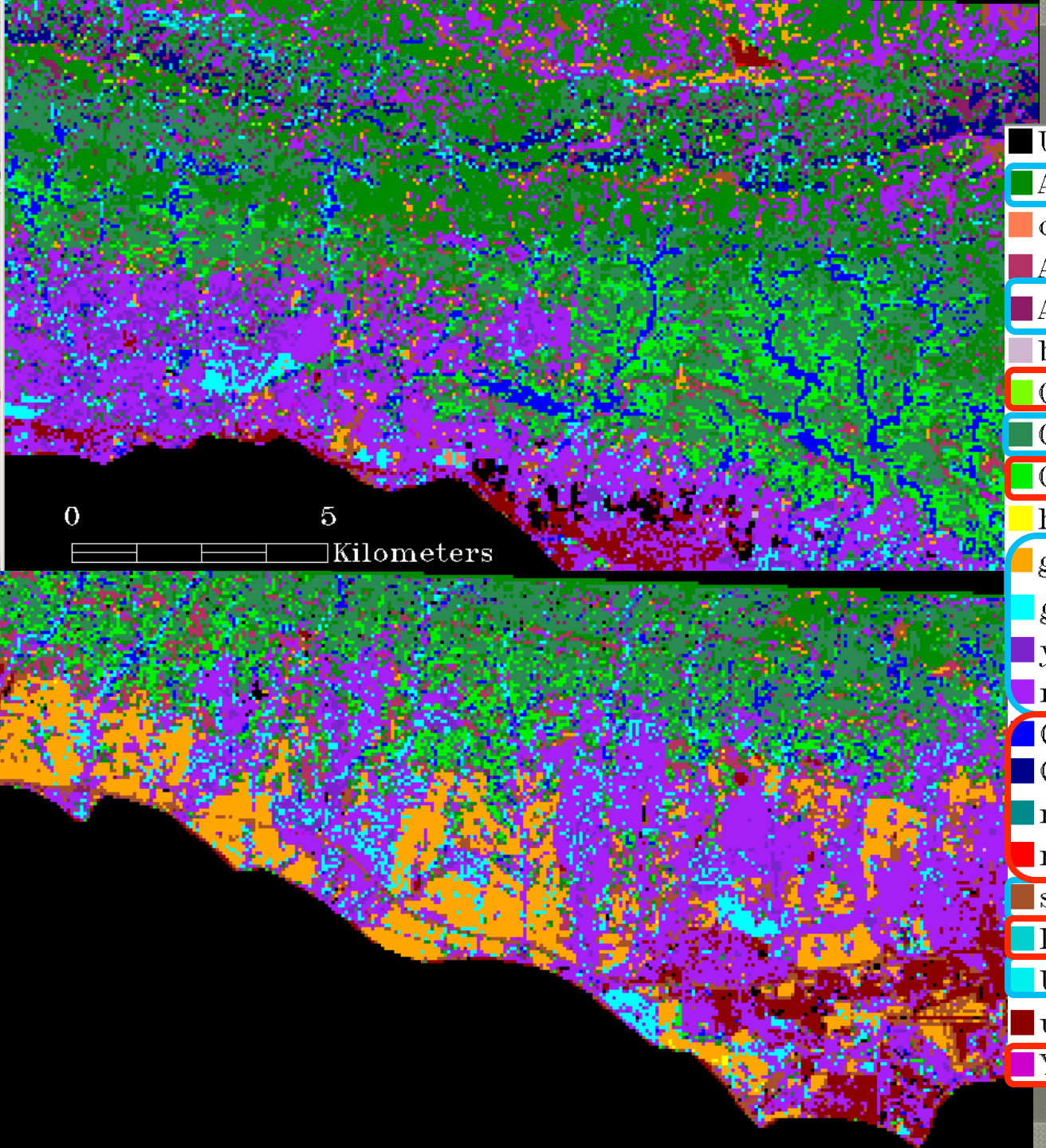

Unclassified
Adenostoma fasciculatum
crop
Artemisia californica
Arctostaphylos gl.
burn scar
Ceanothus cuneatus
Ceanothus megacarpus
Ceanothus spinosus
herb litter
grass litter
golf course
young orchard
mature orchard
Quercus agrifolia
Quercus dumosa
riparian
rock
soil
Platanus racemosa
Umbellularia californica
urban
Yucca whipplei

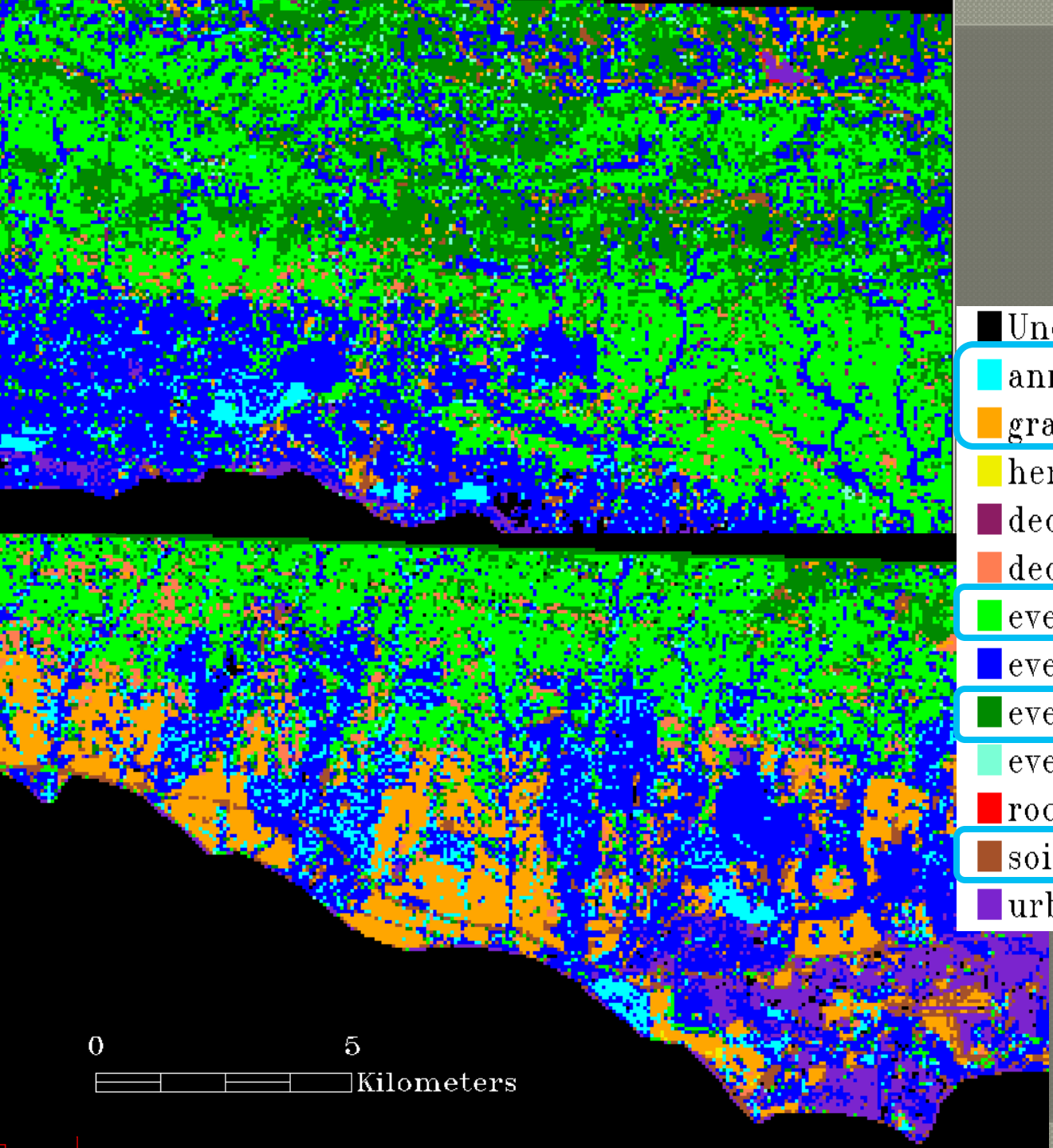

- Unclassified
- annual broadleaf herb
- grass litter
- herb litter
- deciduous broadleaf tree
- deciduous needleleaf shrub
- evergreen broadleaf shrub
- evergreen broadleaf tree
- evergreen needleleaf shrub
- evergreen succulent shrub
- rock
- soil
- urban

Chaparral Shrubland/Oak Woodland/Urban (SBFR)

acquired 06 Aug 2004 at 16 m

EMs = 310

Species-level

	native	60 m
# classes	22	22
kappa	0.793	0.767
overall accuracy	82.3%	79.6%

PFT-level

	native	60 m
# classes	12	12
kappa	0.842	0.819
overall accuracy	87.6%	85.6%

Key Results

- overall accuracy diminishes slightly at 60 m, but spatial patterns in distribution are preserved

- most classes improve or stay stable from native to 60 m

- classes which become less accurate at 60 m tend to occur in thin patches with higher perimeter to area ratios

Mixed Conifer Forest (SNev)

acquired 11 July 2003 at 4 m

EMs = 99

Species-level

	native	60 m
# classes	14	14
kappa	0.327	0.395
overall accuracy	41.6%	47.5%

PFT-level

	native	60 m
# classes	6	6
kappa	0.471	0.526
overall accuracy	63.9%	68.4%

60 m species

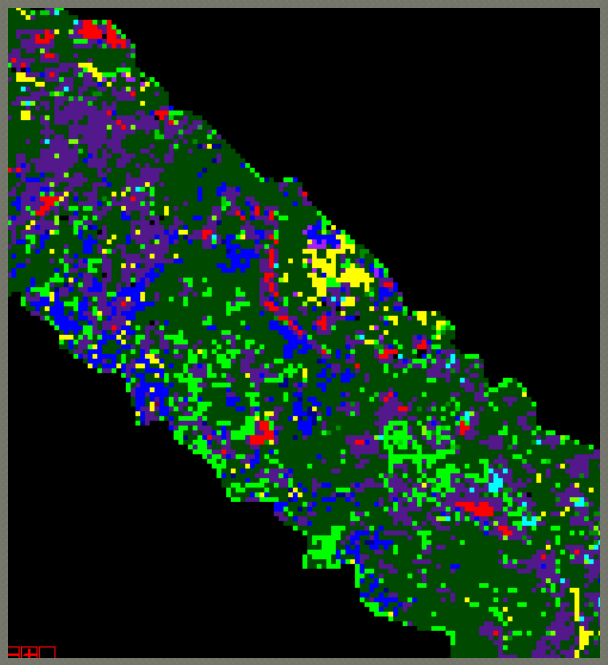

60 m PFT

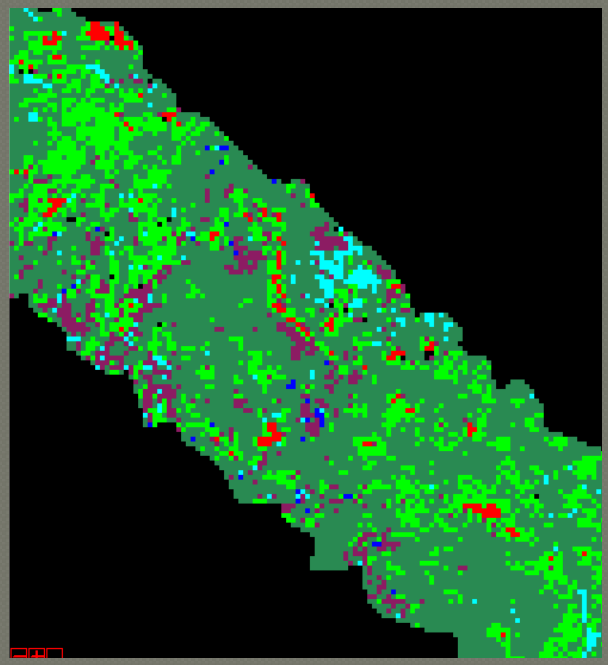

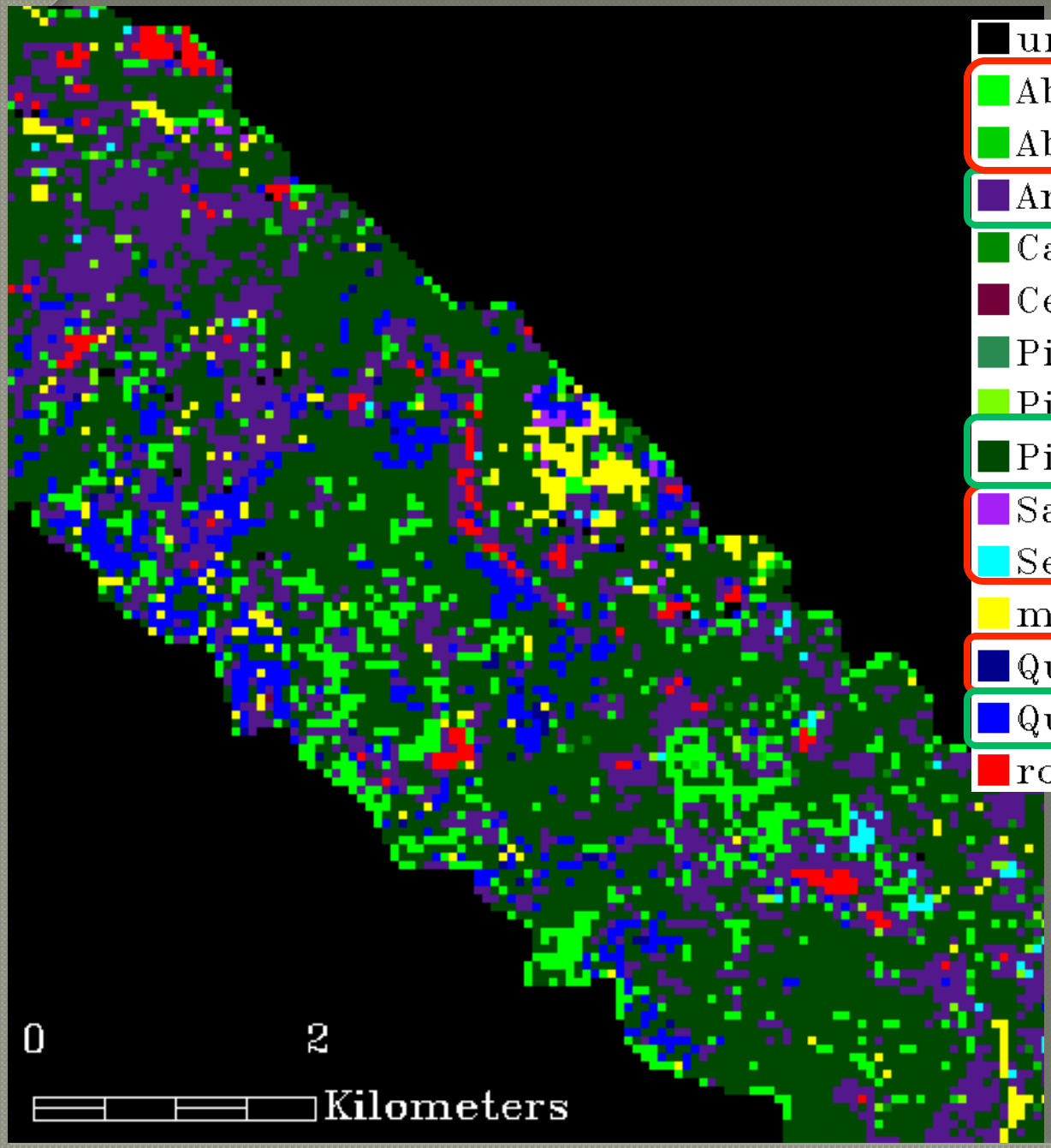

unmodeled
Abies concolor
Abies magnifica
Arctostaphylos glauca
Calocedrus decurrens
Ceanothus cordulatus
Pinus jeffreyi
Pinus lambertiana
Pinus ponderosa
Salix spp.
Sequoiadendron giganteum
meadow
Quercus chrysolepsis
Quercus kelloggii
rock

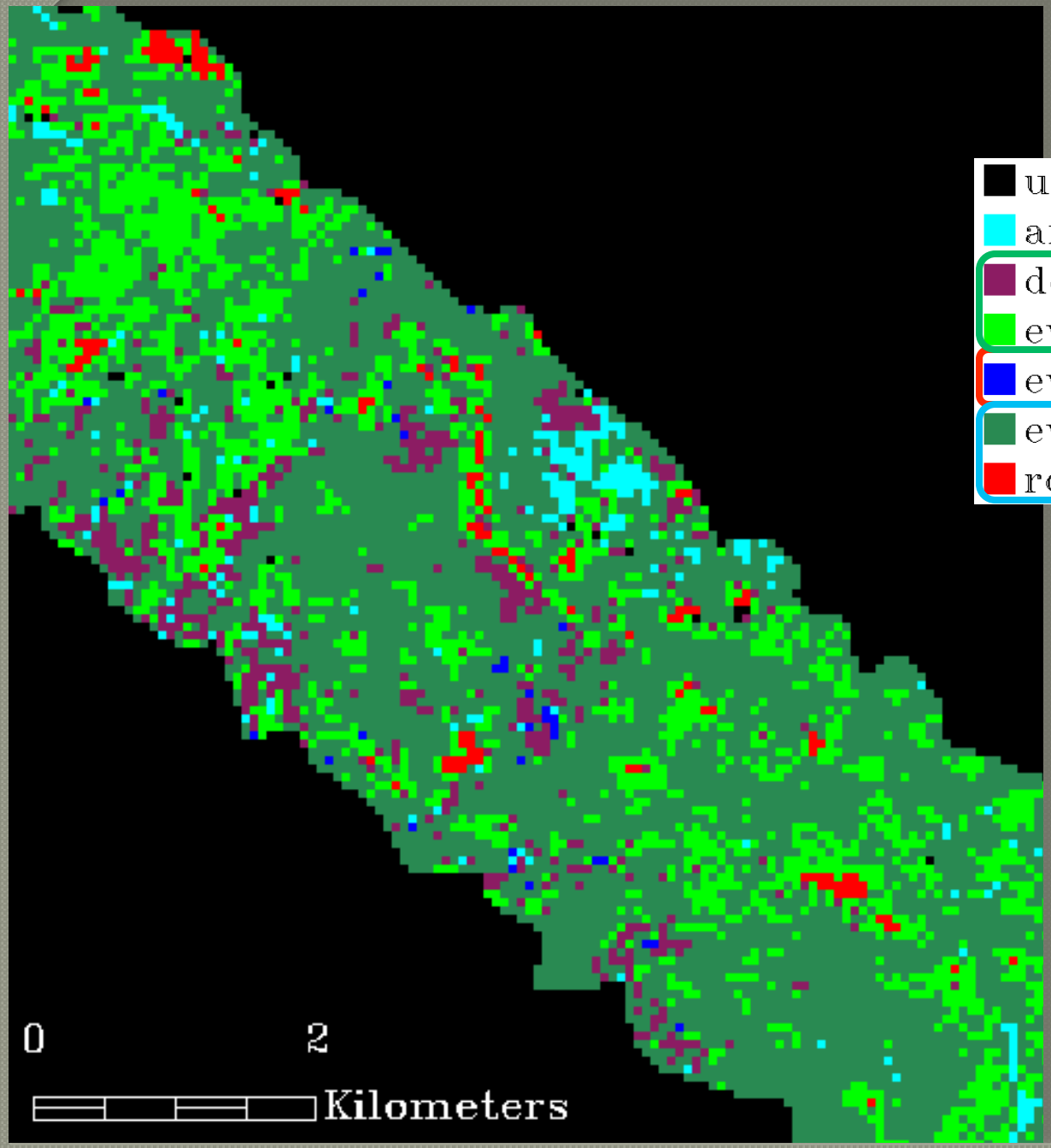
unmodeled
annual broadleaf herb
deciduous broadleaf tree
evergreen broadleaf shrub
evergreen broadleaf tree
evergreen needleleaf tree
rock
0
2
Kilometers

Mixed Conifer Forest (SNev)

acquired 11 July 2003 at 4 m

EMs = 99

Species-level

	native	60 m
# classes	14	14
kappa	0.327	0.395
overall accuracy	41.6%	47.5%

PFT-level

	native	60 m
# classes	6	6
kappa	0.471	0.526
overall accuracy	63.9%	68.4%

Key Results

- poor accuracy at species level may be due to high spectral variability (likely reflectance retrieval)
- much confusion among conifer tree species
- highly mixed stands make classification more challenging

Mixed Conifer/Broadleaf Temperate Rainforest (WR)

acquired 18 July 2003 at 3.3 m

EMs = 66

Species-level

	native	60 m
# classes	11	6
kappa	0.533	0.751
overall accuracy	66.4%	82.1%

PFT-level

	native	60 m
# classes	6	3
kappa	0.815	0.957
overall accuracy	91.4%	98.0%

60 m species

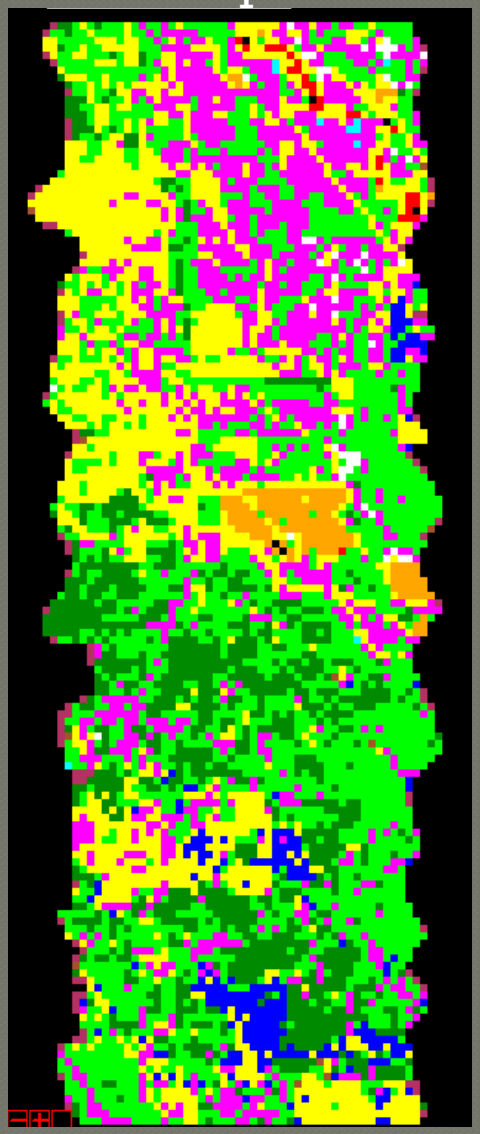

60 m PFT

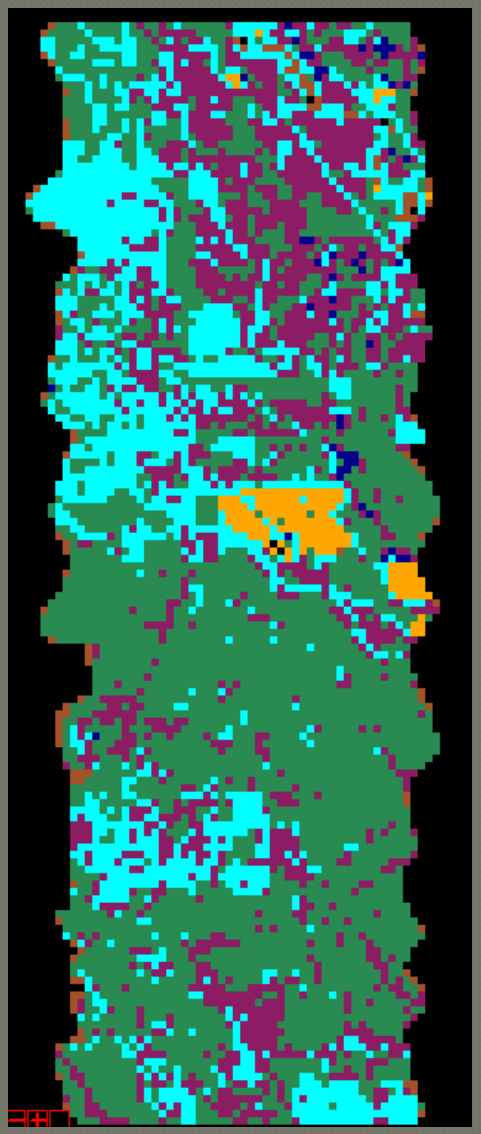

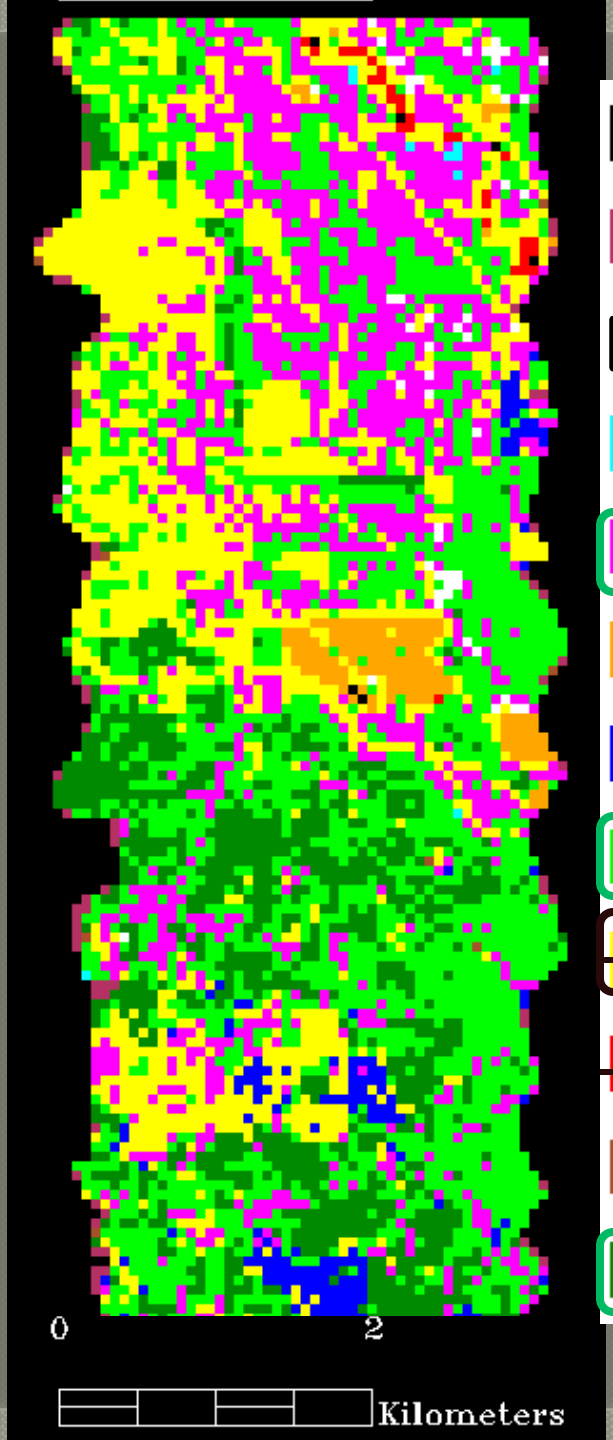

unmodeled

~~Abies grandis~~

~~Acer circinatum~~

Acer macrophylla

Alnus rubra

litter

Populus trichocarpa

Psuedotsuga menziesii

~~Pteridium aquilinum~~

~~rock/soil~~

~~Thuja plicata~~

Tsuga heterophylla

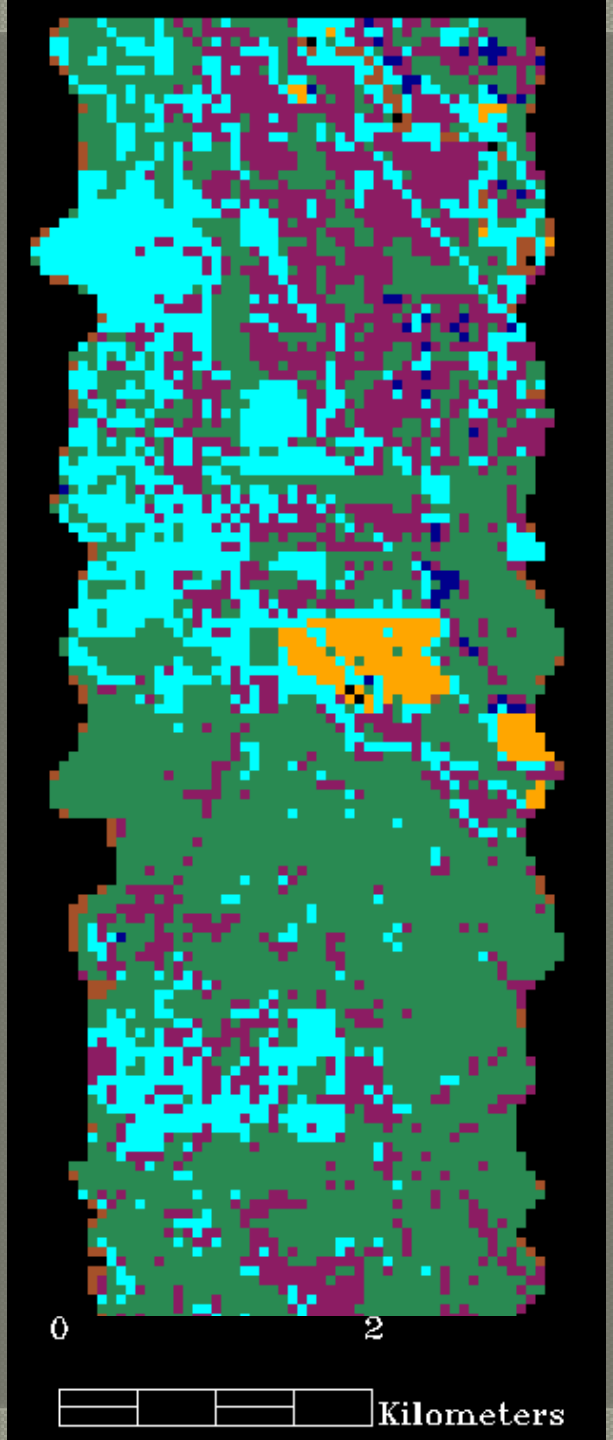

unmodeled

litter

~~deciduous broadleaf shrub~~

deciduous broadleaf tree

~~annual broadleaf herb~~

evergreen needleleaf tree

~~rock~~

Mixed Conifer/Broadleaf Temperate Rainforest (WR)

acquired 18 July 2003 at 3.3 m

EMs = 66

Species-level

	native	60 m
# classes	11	6
kappa	0.533	0.751
overall accuracy	66.4%	82.1%

PFT-level

	native	60 m
# classes	6	3
kappa	0.815	0.957
overall accuracy	91.4%	98.0%

Key Results

- sunlit canopy frequently mistaken for fern, leading to over-mapping of this class
- some confusion between two most dominant classes (TSHE & PSME)
- excellent discrimination of functional types

Combined-Sites (C-S) Analysis

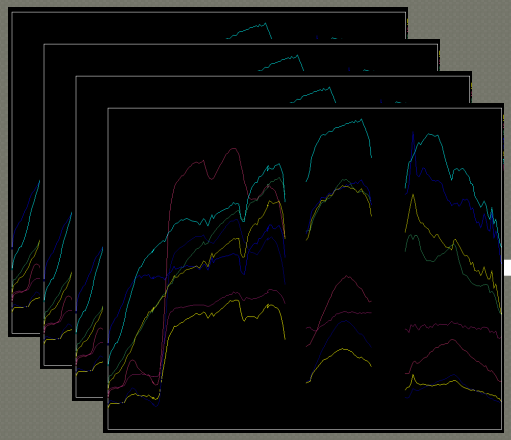

site-specific EMs

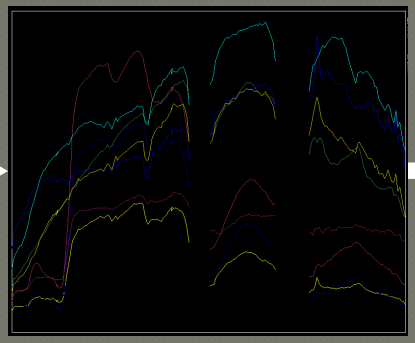

combined EM library

site-level native validation libraries

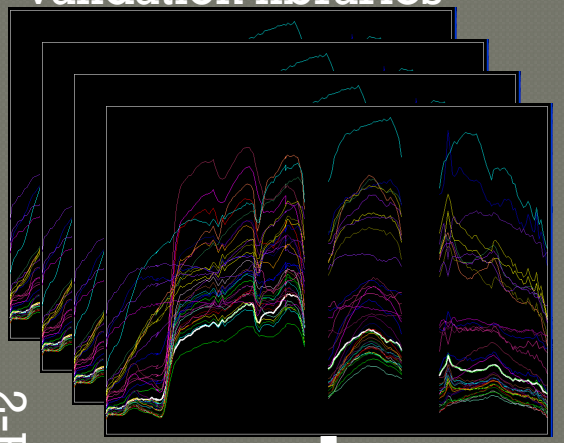

random sample

2-EM MESMA

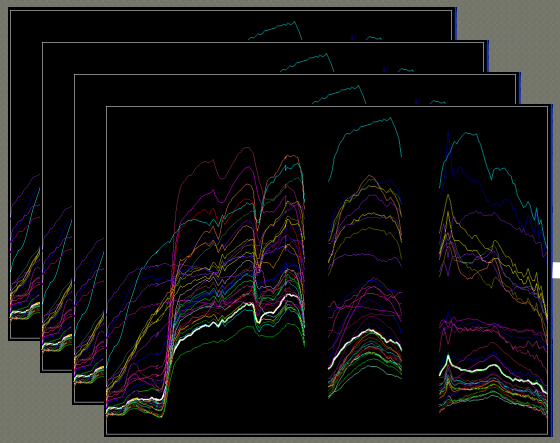

site-level 60 m libraries

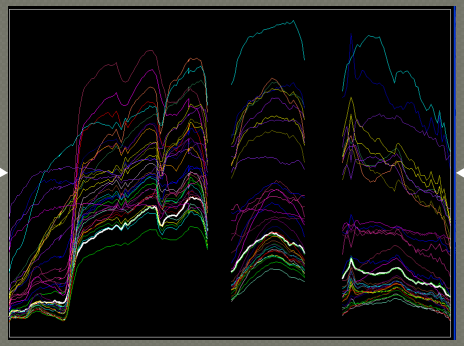

combined 60 m library

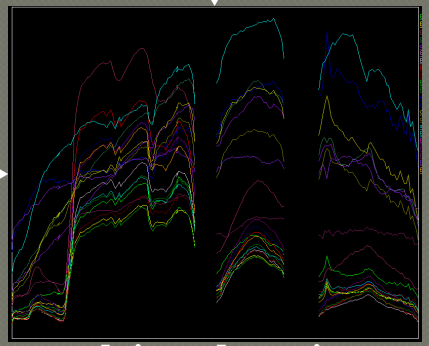

combined native validation library

Combined-Sites Results

EMs = 475 (pooled)

Species-level

# classes = 33	native	60 m
Kappa	0.580	0.702
overall accuracy	60.2%	72.9%

8 classes

15 classes

10 classes

PFT-level

# classes = 9	native	60 m
Kappa	0.686	0.776
overall accuracy	73.2%	81.2%

3 classes

4 classes

2 classes

Cross-Ecosystem Results

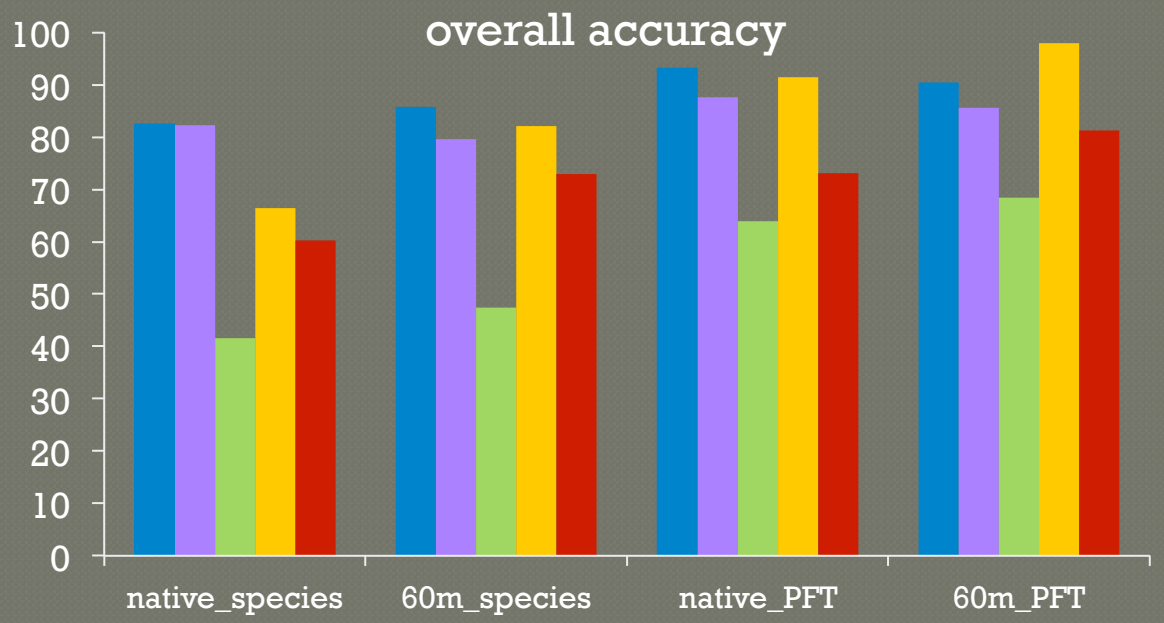

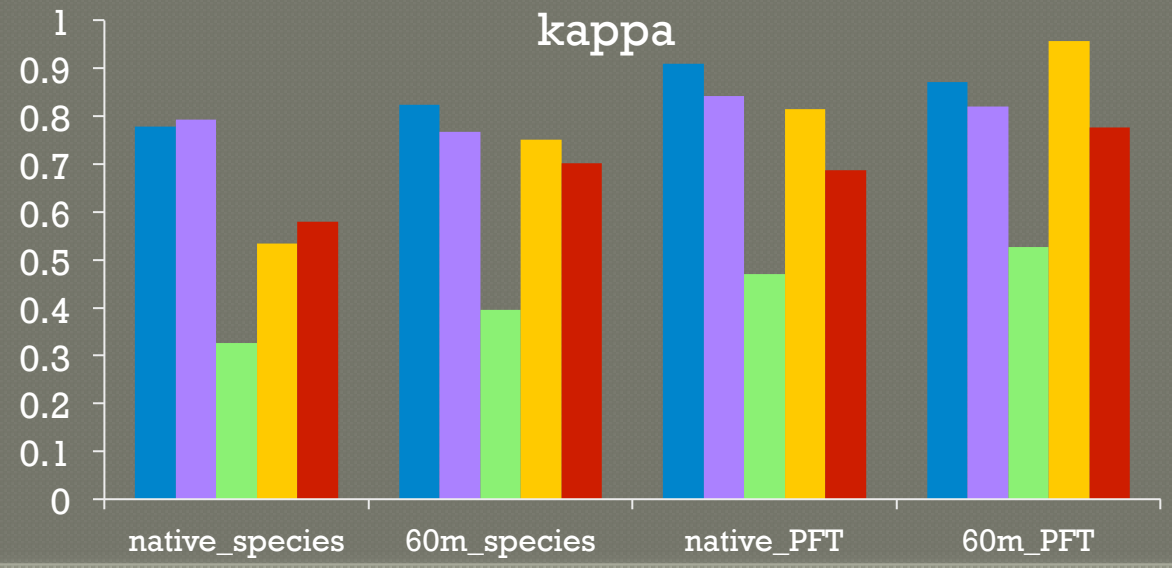

Limitations & Assumptions

- reference data
  - assumes a minimize patch size
  - maps may be more accurate than is reflected in results
- reflectance retrieval: need a robust algorithm
- greater global diversity in ecosystems than examined here

Conclusions

- accuracy stable/improved from native to 60 m spatial resolution

- EMs selected from fine resolution regional data can be applied to 60 m data from multiple ecosystems

- future work:
  - intermediate spatial scales (20 m & 40 m)
  - species/PFT spectral separability analysis

Thanks!
Questions?

Keely L. Roth
klroth@geog.ucsb.edu

Visualization & Image Processing for Environmental Research (VIPER) Lab
Department of Geography
University of California, Santa Barbara

Sub-selection from pooled EMs

	native species		60 m species		native PFT		60 m PFT	
	all EMs	subset EMs	all EMs	subset EMs	all EMs	subset EMs	all EMs	subset EMs
kappa	0.580	0.471	0.702	0.580	0.686	0.554	0.776	0.634
overall accuracy	60.2%	49.6%	72.9%	61.4%	73.2%	61.9%	81.2%	68.7%

native combined-sites PFT error matrix

	ABH	litter	DBT	EBS	EBT	ENS	ENT	rock/soil	urban	unmodeled	User's Accuracy
ABH	2153	41	132	172	212	0	780	2	1	0	**61.6**
litter	13	1707	2	18	2	13	29	37	4	0	**93.5**
DBT	81	11	2946	33	29	0	1032	0	0	0	**71.3**
EBS	6	36	84	1681	137	161	240	20	1	0	**71.1**
EBT	352	38	316	453	2778	19	903	9	7	0	**57.0**
ENS	0	30	1	303	13	593	39	2	0	0	**60.5**
ENT	60	20	293	87	1	0	3993	0	2	0	**89.6**
rock/soil	1	118	1	15	4	2	6	1651	36	0	**90.0**
urban	3	9	0	0	0	0	7	15	396	0	**92.1**
unmodeled	13	2	6	2	3	0	6	29	10	0	
Producer's Accuracy	**80.3**	**84.8**	**77.9**	**60.8**	**87.4**	**75.3**	**56.8**	**93.5**	**86.7**		**73.2%**

60 m combined-sites PFT error matrix

	ABH	litter	DBT	EBS	EBT	ENS	ENT	rock/soil	urban	unmodeled	User's Accuracy
ABH	379	3	12	5	24	0	69	0	0	0	**77.0**
litter	0	103	0	0	0	0	0	3	0	0	**97.2**
DBT	4	0	38	0	4	0	9	0	0	0	**69.1**
EBS	0	1	3	163	19	16	7	0	0	0	**78.0**
EBT	54	1	10	23	349	1	39	7	0	0	**72.1**
ENS	0	1	0	32	2	63	2	0	0	0	**63.0**
ENT	0	1	0	2	0	1	174	0	0	0	**97.8**
rock/soil	0	4	0	0	2	1	0	258	1	0	**97.0**
urban	0	0	0	0	0	0	0	0	51	0	**100.0**
unmodeled	1	0	0	0	0	0	0	1	0	0	
Producer's Accuracy	**86.5**	**90.4**	**60.3**	**72.4**	**87.3**	**76.8**	**58.0**	**95.9**	**98.1**		**81.2%**

Multiple Endmember Spectral Mixture Analysis (MESMA)

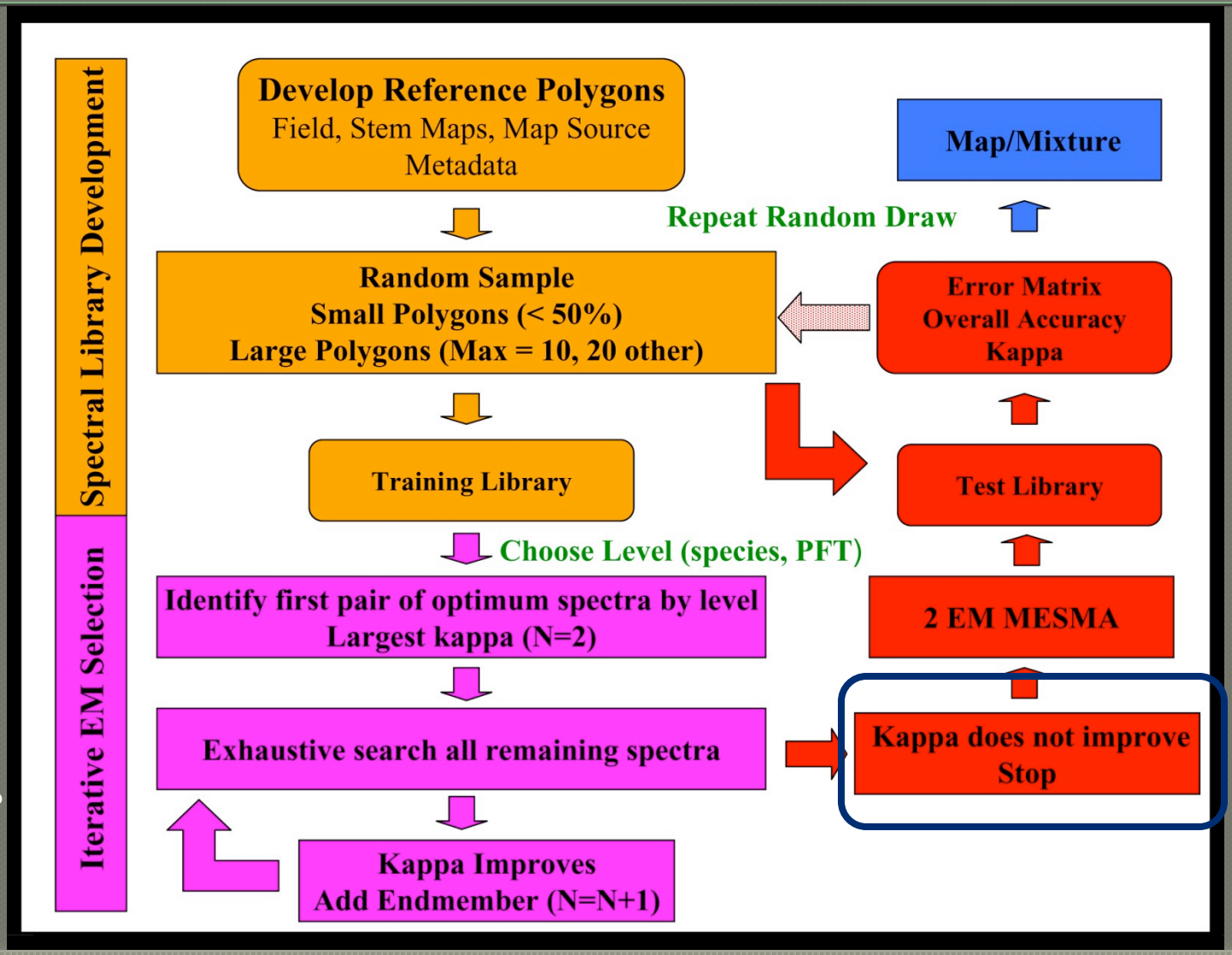

figure from Roberts et al., 2010

SERC EMs

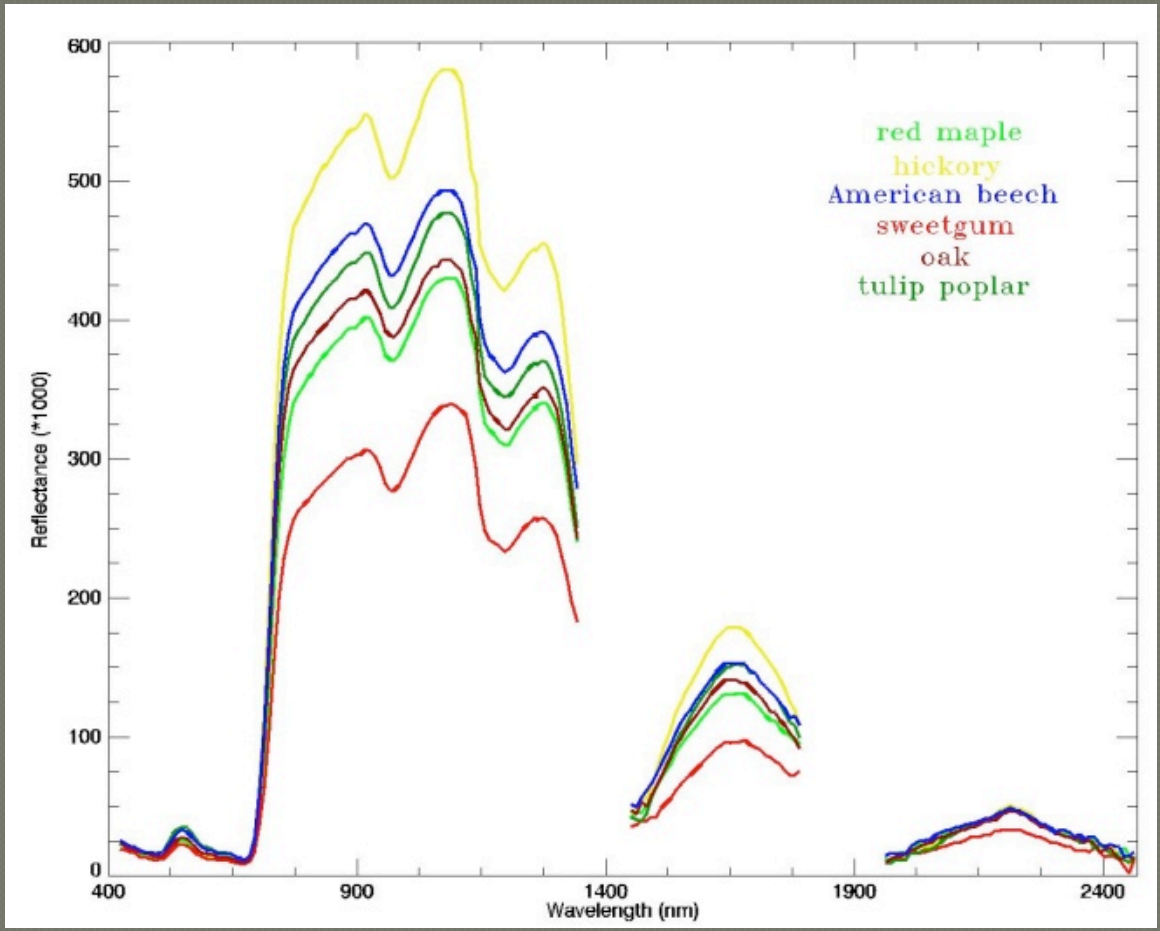
red maple
hickory
American beech
sweetgum
oak
tulip poplar
Reflectance (*1000)
Wavelength (nm)
0
100
200
300
400
500
600
400
900
1400
1900
2400

Santa Barbara Front Range EMs

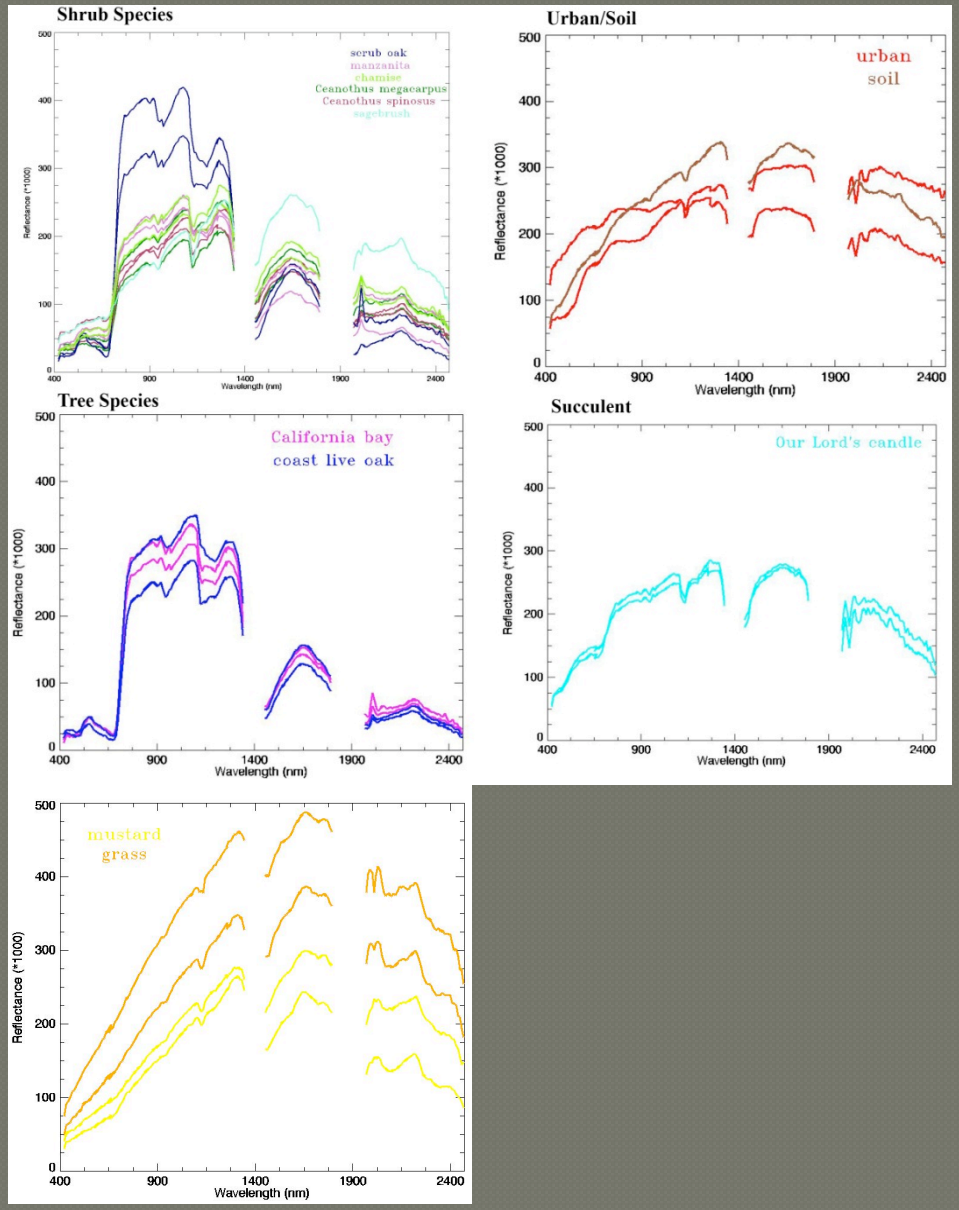

Wind River EMs

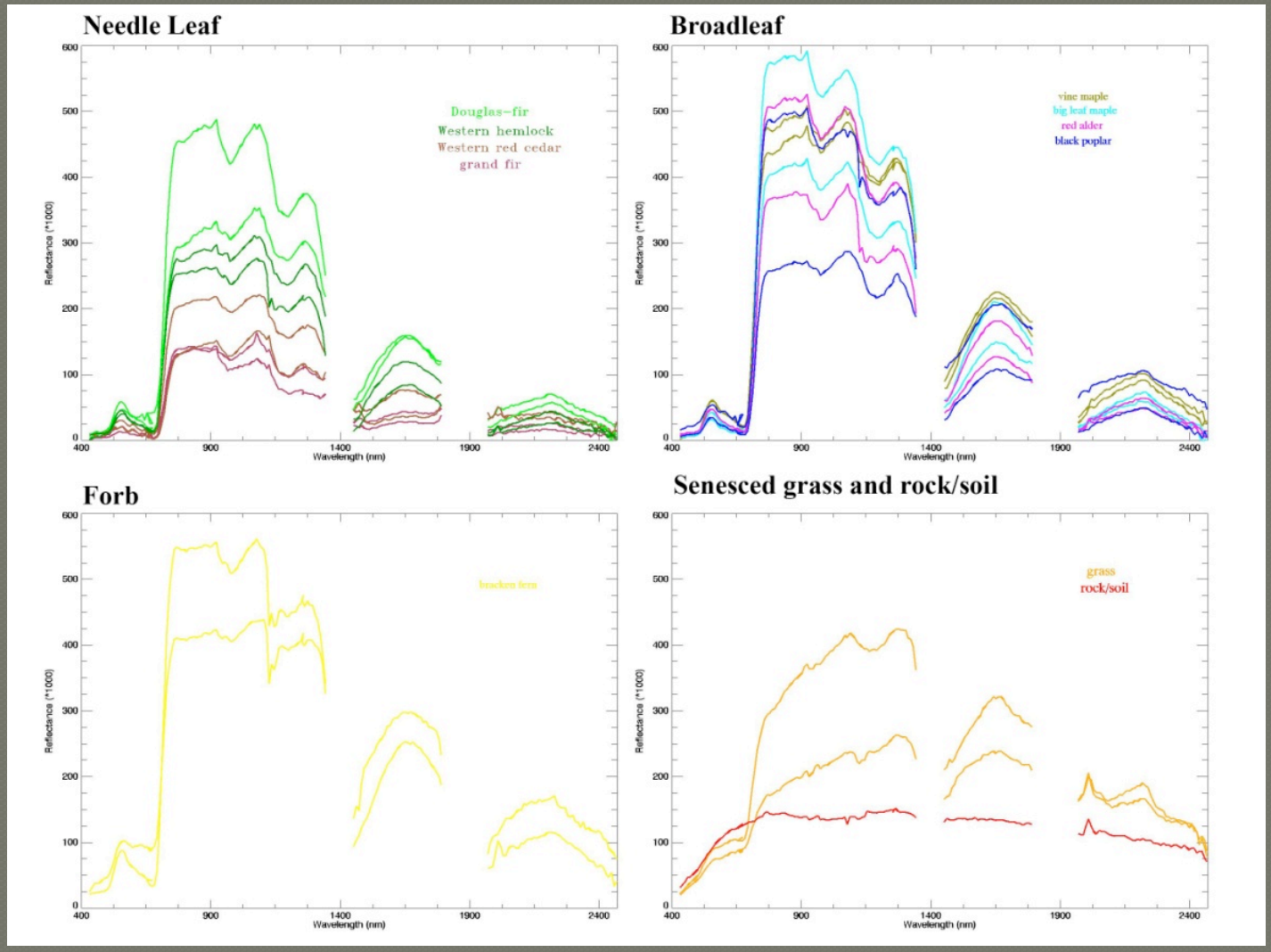

Status of HyTES/PHyTIR Concepts and Technologies being Validated for the HysplRI TIR Instrument Concept

Presented at:

2011 HysplRI Science Workshop
Washington, D.C.

Simon Hook & The HyTES/PHyTIR Team
Organization: NASA/Jet Propulsion Laboratory
Co-Authors: William R. Johnson, Marc C. Foote, Renaud Goullioud, Bjorn T. Eng, Bruno M. Jau

© 2011 California Institute of Technology. Jet Propulsion Laboratory, California Institute of Technology. Government sponsorship acknowledged.

Outline

- HyspIRI Background
- Prototype Hyperspectral Thermal Infrared Radiometer (PHyTIR)
- Hyperspectral Thermal Emission Spectrometer (HyTES)
- Summary

HyspIRI Background

Visible ShortWave InfraRed (VSWIR) Imaging Spectrometer

+

Multispectral Thermal InfraRed (TIR) Scanner

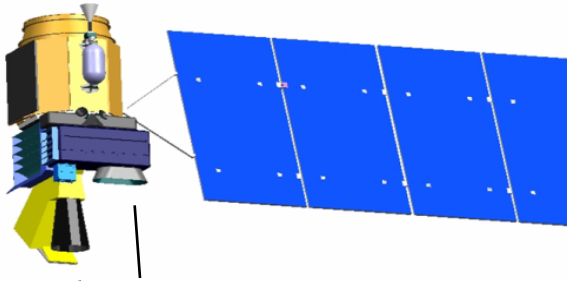

VSWIR: Plant Physiology and Function Types (PPFT)

Multispectral TIR Scanner

Map of dominant tree species, Bartlett Forest, NH

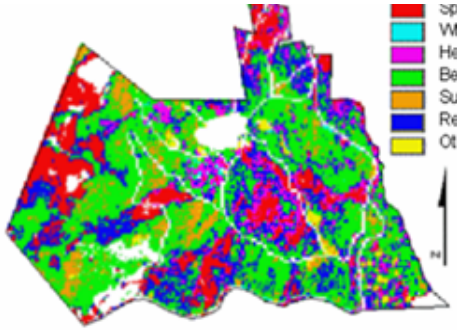

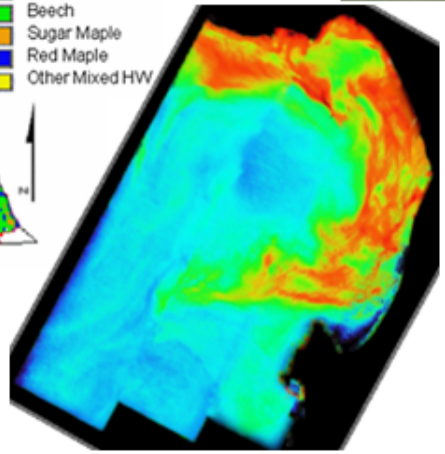

Red tide algal bloom in Monterey Bay, CA

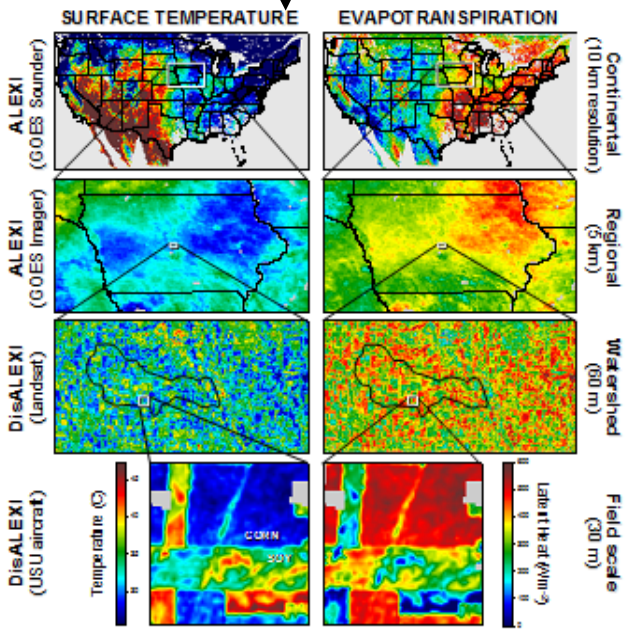

http://hyspiri.jpl.nasa.gov/

HyspIRI Background

Science Questions:

TQ1. Volcanoes/Earthquakes (MA,FF)

– How can we help predict and mitigate earthquake and volcanic hazards through detection of transient thermal phenomena?

• TQ2. Wildfires (LG,DR)

– What is the impact of global biomass burning on the terrestrial biosphere and atmosphere, and how is this impact changing over time?

• TQ3. Water Use and Availability, (MA,RA)

– How is consumptive use of global freshwater supplies responding to changes in climate and demand, and what are the implications for sustainable management of water resources?

• TQ4. Urbanization/Human Health, (DQ,GG)

– How does urbanization affect the local, regional and global environment? Can we characterize this effect to help mitigate its impact on human health and welfare?

• TQ5. Earth surface composition and change, (AP,JC)

– What is the composition and temperature of the exposed surface of the Earth? How do these factors change over time and affect land use and habitability?

Measurement:

- 7 bands between 7.5-12 μm and 1 band at 4 μm
- 60 m resolution, 5 days revisit
- Global land and shallow water

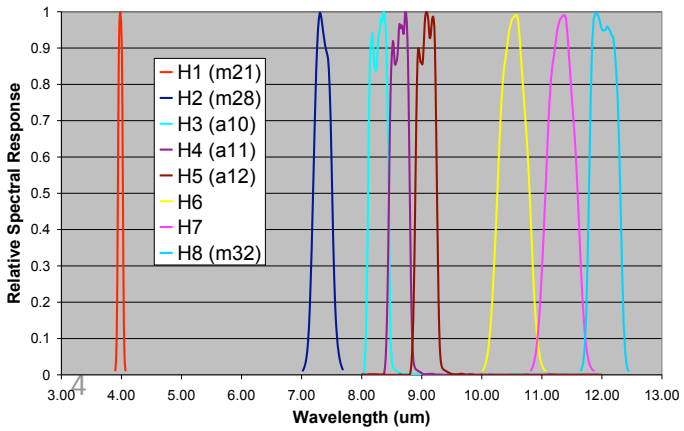

Andean volcano heats up

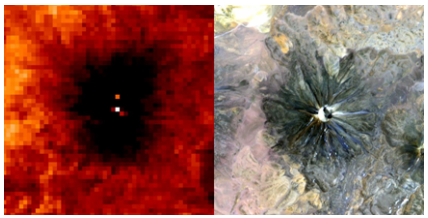

Volcanoes

Urbanization

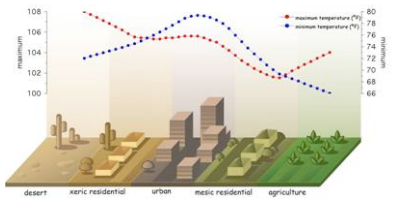

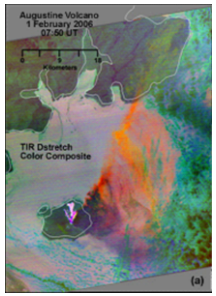

Water Use and Availability

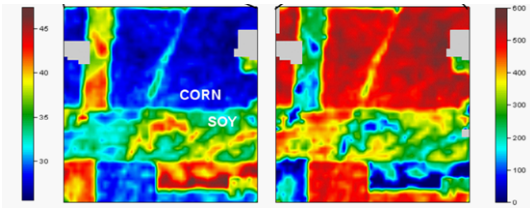

Surface Temperature

Evapotranspiration

HyspIRI-TIR Instrument Concept

Science Requirements
60 m Resolution
5-Day repeat

→

Instrument Requirements
~10,000 pixels cross track
~600 km swath
51° Cross-track swath

Whiskbroom (Push-Whisk)
- Single telescope with scanning mirror
- Single detector array with 256 pixels per band

Pushbroom
- ~10 detector arrays, each with ~1,000 pixels per band
- ≥3 telescopes

Science Requirements
0.5% Radiometric accuracy for 300 K scenes

→

Instrument Requirements
Frequent 2-point calibrations (space and blackbody)

Whiskbroom (Push-Whisk)
- Scanning mirror allows easy and frequent 2-point calibrations
- No mapping gaps

Pushbroom
- Calibration mechanism required – must enable multiple telescopes to view space and blackbody
- Gap in mapping during calibration

HyspIRI-TIR Instrument Concept

Science / Instrument Requirement
0.2 K resolution for 300 K scene

MCT Detectors
- Quantum efficiency ≥ 70%
- 0.06 K resolution at 60 K
  (69 W cooler power)

QWIPs
- Quantum efficiency ~3%
- > 0.3 K resolution at 40 K
  (225 W cooler power)

Uncooled Microbolometers
- Too slow for push-whisk method
- Even with pushbroom, resolution ~0.8 K

Science / Instrument Requirement
8 spectral bands 4-12 μm

MCT Detectors
- Single band-gap material can cover full spectral range

QWIPs
- Multiple arrays required to cover all bands

Uncooled Microbolometers
- Not sensitive to 4 μm band

HyspIRI-TIR Optical Assumptions

Optical Design Assumptions

- Altitude: 623km (5-day repeat)
- Ground Sample Distance: 60m (@ NADIR)
- Pixel pitch: 40μm
- Aperture: F/2
- IFOV: 96.308 μrad
- FOV: 1.413° (along track)
- FOV: 51° (cross track scanning)
- Focal Length: 415.3mm
- Aperture Size: 207.7m
- Cross track pixels: 9242 pixels
- Swath: 600km (R_{earth} = 9378km)
- Swath overlap: 10% along track pixels
- Dwell time: 32microseconds
- Scan Mirror Rotation Rate: 14.15rpm (double sided scan mirror)
- Spectral coverage (Passband) = 4 to12mm
- $MTF_{Nyquist}$ = 60% for all fields and wavelengths
- Obscuration <15% (by area)
- 3 aspheric mirrors (telescope and relay)
- 2 flat mirrors (fold and scan)
- 2 transmissive elements (window and interference filter)
- chromatic aberration negligible

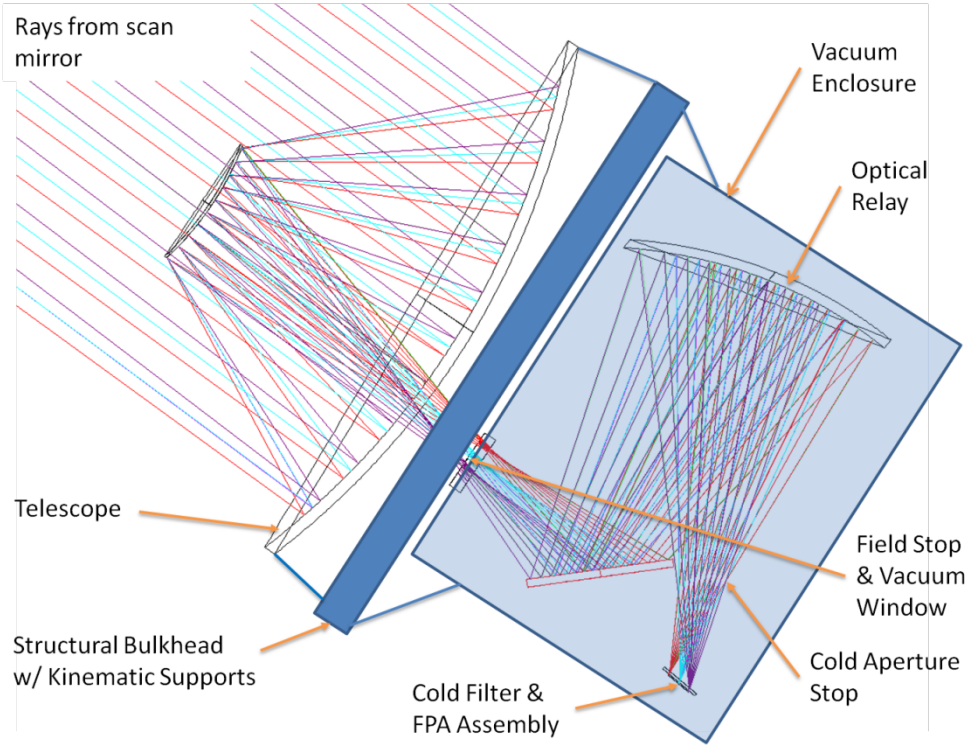

Summary

Parameter	Value
Aperture Size	208 mm (<10% obstruction)
F/#	2
Focal Length	416mm
Optical Throughput w/ Filters	66%

HyspIRI-TIR Instrument Concept

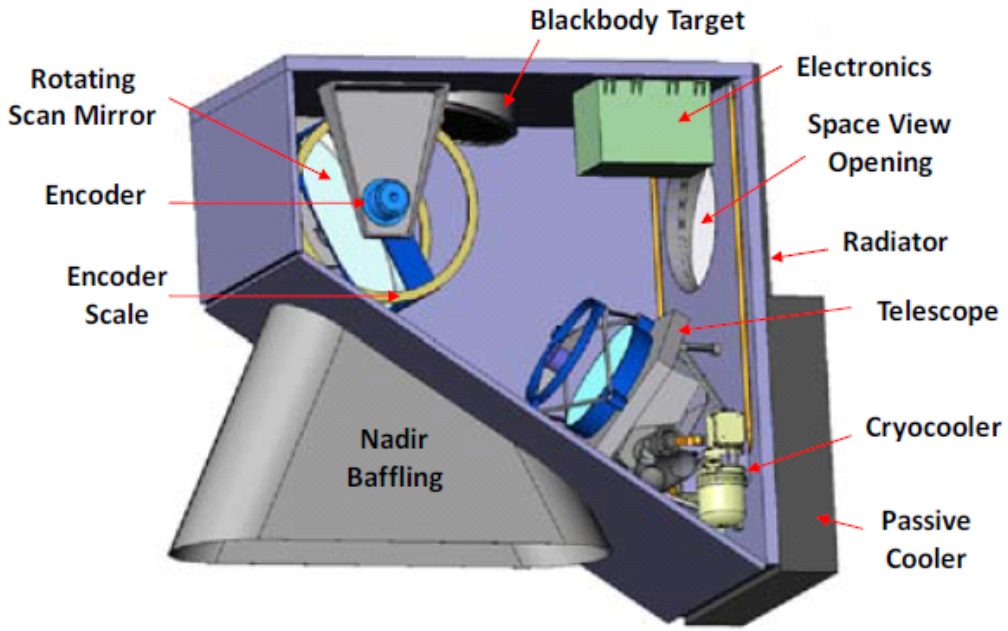

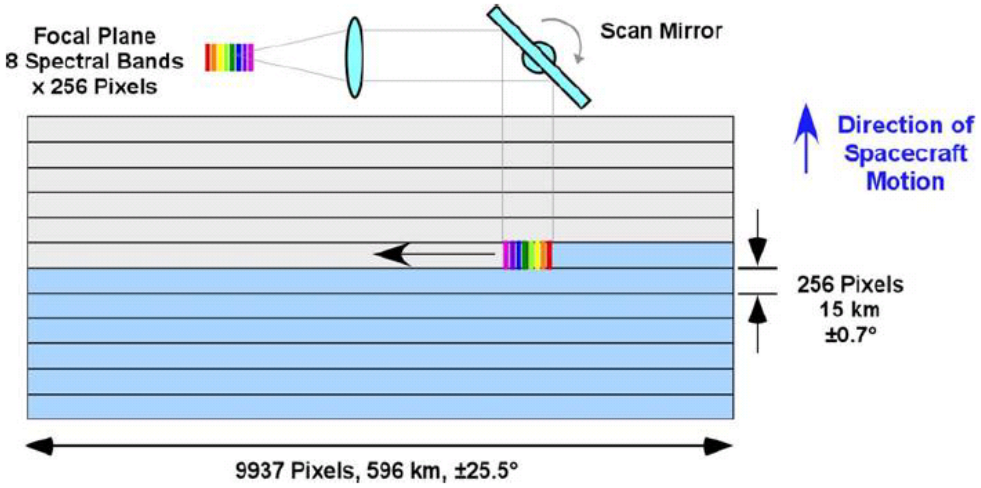

HyspIRI-TIR Instrument Concept

HyspIRI TIR Instrument Characteristics			
Spectral		**Spatial**	
Bands (8)	3.98 µm, 7.35 µm, 8.28 µm, 8.63 µm, 9.07 µm, 10.53 µm, 11.33 µm, 12.05 µm	IFOV	100 µrad; 60 m at nadir
Bandwidths	0.084 µm, 0.32 µm, 0.34 µm, 0.35 µm, 0.36 µm, 0.54 µm, 0.54 µm, 0.52 µm	MTF	>0.60 at FNy
Accuracy	<0.01 µm	Scan Type	Push-Whisk, 14.2 RPM mirror rotation
Radiometric		Cross-Whisk Samples	256
Temperature Range	Channel 1: 400-1200 K Channel 2–8: 200 K – 480 K	Samples in Whisk Direction (Cross Track)	9,300
Resolution	< 0.05 K, linear quantization to 14 bits	Cross-Whisk Swath Width	15.4 km (±0.7° at 623 km altitude)
Accuracy	< 0.5 K at 250 K	Swath Length in Whisk Direction	596 km (±25.5° at 623 km altitude)
Precision (NETD)	< 0.2 K	Band to Band Co-Registration	0.2 pixels (12 m)
Linearity	>99% characterized to 0.1 %	Pointing Knowledge	10 arcsec (0.5 pixels, 30 m)

- Butcher-Block Filter Assembly
- Baffles to Prevent Crosstalk Between Spectral Channels

- MCT Detector Array – 256 elements cross-sweep
- 1 Bandgap to Cover Full Spectral Range
- ≥ 4 Detector Columns per Spectral Channel to Allow Time Delay and Integration (TDI)

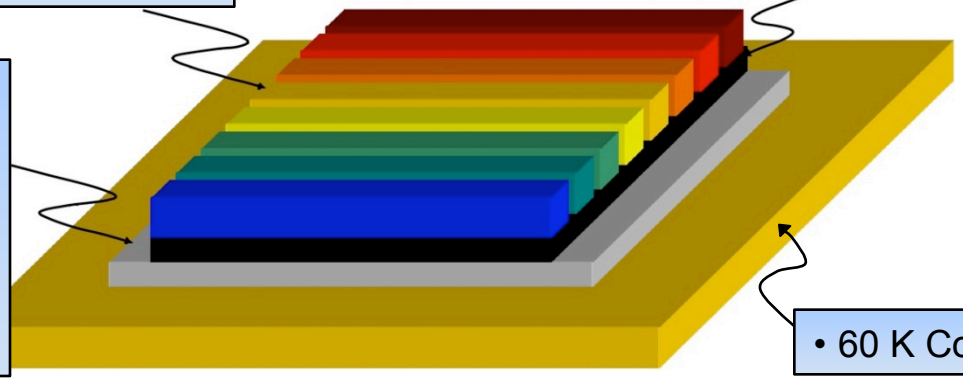

- CMOS Read-Out Integrated Circuit (ROIC)
- Multiple Output Signals to Enable Necessary Pixel Read Rate
- On-Chip Digitization Under Study

- 60 K Cold Tip of Cryocooler

HyspIRI-TIR will use a Butcher-block filter layout on top of focal plane. PHyTIR will not use focal plane filers but will spin a filter wheel in the optical path.

HyspIRI-TIR Instrument Concept

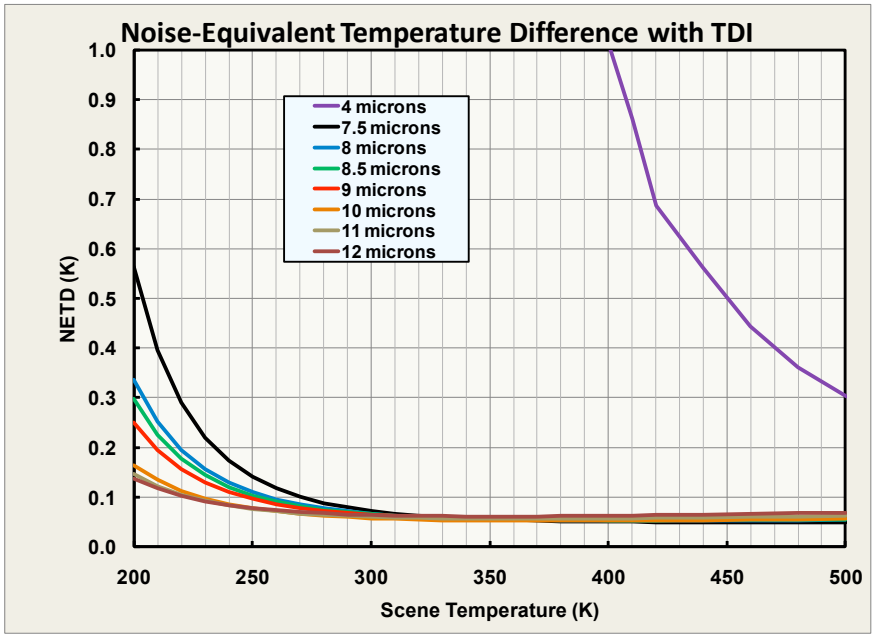

Expected HyspIRI-TIR Sensitivity Metric expressed as Noise Equivalent Delta Temperature (NEDT)

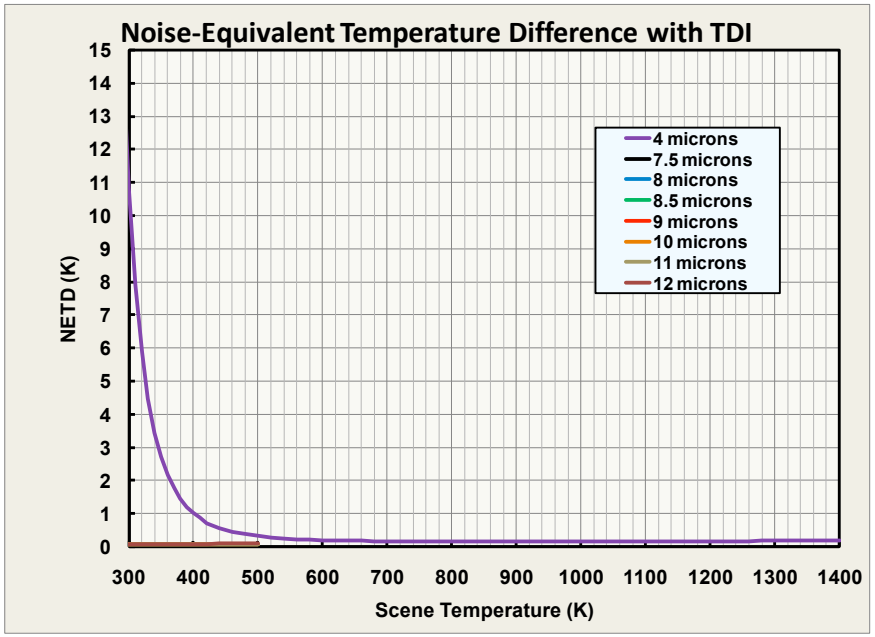

Expected HyspIRI-TIR Sensitivity Metric expressed as Noise Equivalent Delta Temperature (NEDT)

- Predicted sensitivity better than 0.2 K @ 300 K requirement.
- Good sensitivity in overlap region between channel 1 and channels 2-8.
- Expected saturation temperature of 1200K based on HyspIRI: Hot Target Saturation Subgroup (HTSS)

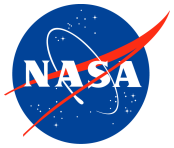

The Prototype HysplRI Thermal Infrared Radiometer (PHyTIR)

PHyTIR Rational

- HyspIRI-TIR requires a high throughput FPA and scanning approach to meet the revisit time (5 days), the high spatial resolution (60m), and the number of spectral channels (8).
- PHyTIR will demonstrate that:
  - The detectors and readouts meet all signal-to-noise and speed specifications
  - The scan mirror, together with the structural stability, meets the pointing knowledge requirements
  - The long-wavelength channels do not saturate below 480 K
  - The cold shielding allows the use of ambient temperature optics on the HyspIRI-TIR instrument without impacting instrument performance.

PHyTIR Implementation

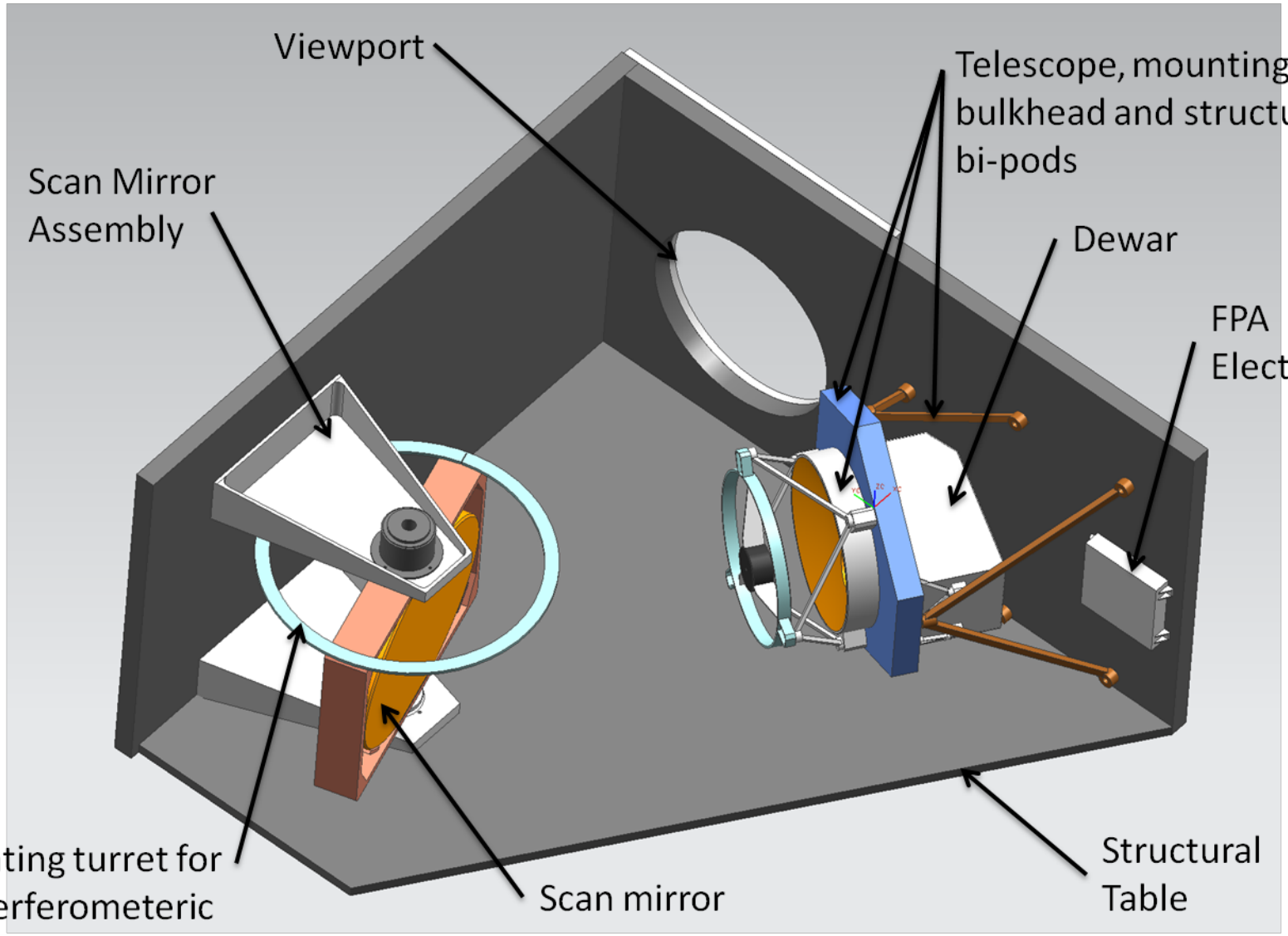

PHyTIR Implementation

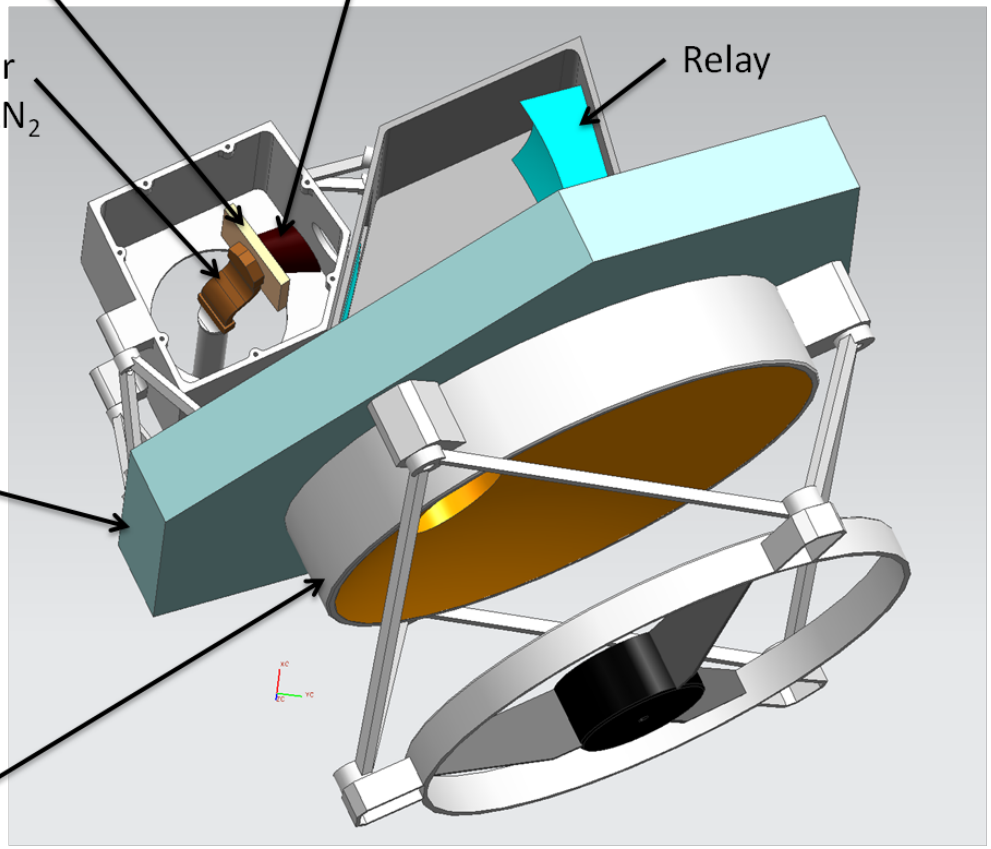

Dewar removed to show internal components

PHyTIR Implementation

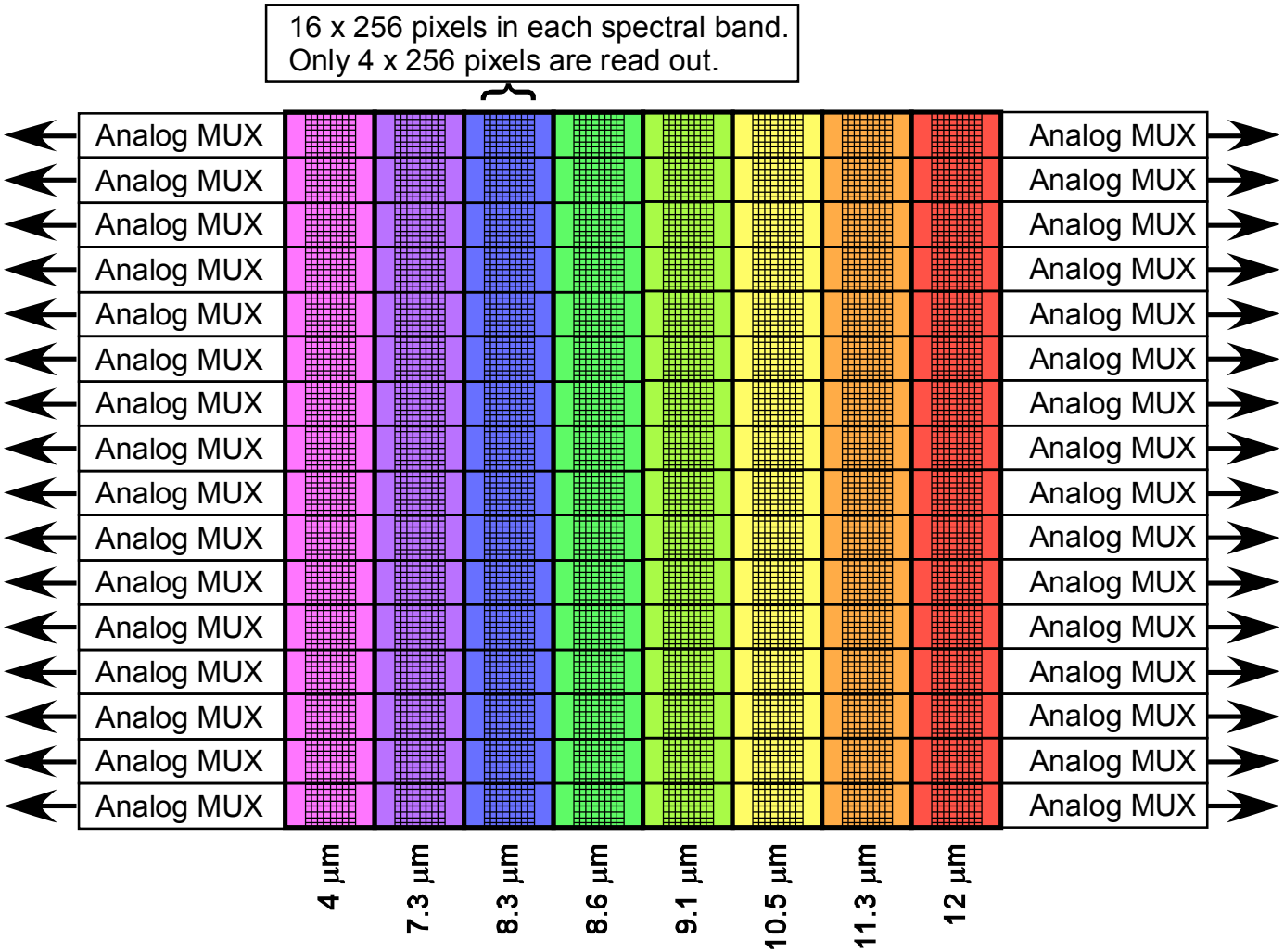

PHyTIR will not have focal plane filters but will implement the identical ROIC design to HyspIRI-TIR.
32 parallel output at ≥ 10 MHz allow 32 µs frame times.

PHyTIR Current Design

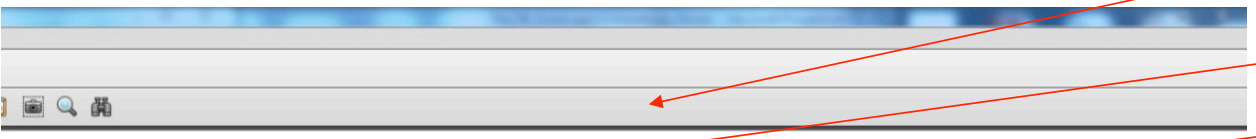

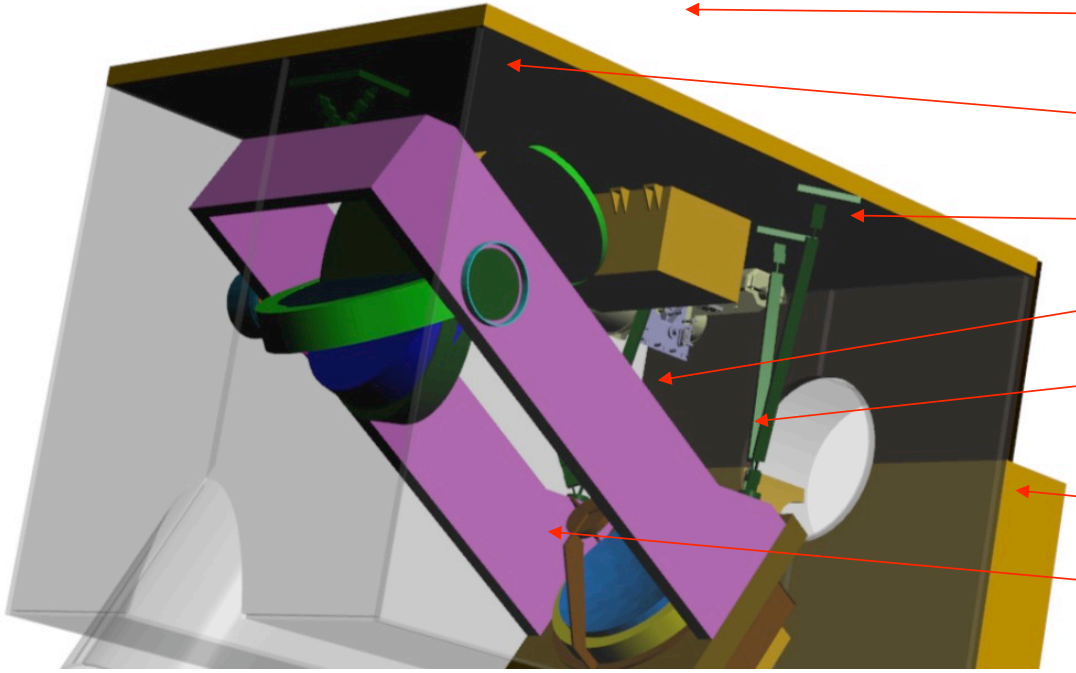

Common spacecraft interface

Bi-pod struts

Kinematic yoke mounting

Onboard blackbody

Electronics

Fine and coarse encoding scan mirror

Space view port

Telescope

Relay optics enclosure

Passive radiator/cooler

Baffling

PHyTIR Testing

- PHyTIR Prototype Consists of
  - Full HyspIRI TIR MCT detector array
  - Spectral range 4-12 μm (TIR spectral range)
  - Scan mirror prototype with precise encoder
- Testing of PHyTIR Prototype
  - Measuring response to two blackbody targets, combined with detector noise, will provide S/N (tested at full frame rate)
  - Imaging of target-projector slit while inducing T gradients will test pointing stability
  - Increasing blackbody T will determine saturation T and high-T S/N
  - Measuring background, noise, and drift will show effects of uncooled optics

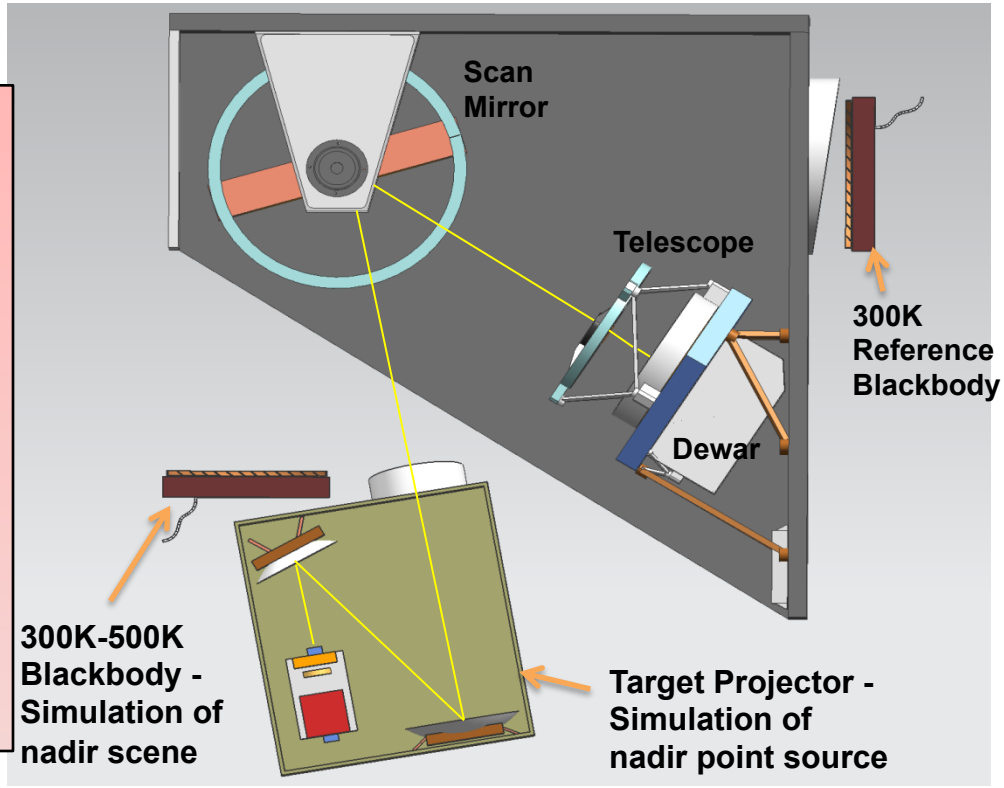

PHyTIR Summary

The following steps are currently being undertaken to build PHyTIR:

1) Design and Build the Scan Mechanism
2) Design and Build a Scan Mirror
3) Integrate the Spectral Filters with Focal Plane Array and ROIC
4) Assemble the Dewar with external telescope, internal relay and focal plane assembly
5) Build the prototype Electronics
6) Assemble PHyTIR

Once PHyTIR is assembled it will be used to retire the four key risks as noted earlier. A key part of this effort is the final testing to prove these four key risks.

a) **Detectors and readout meet all signal-to-noise and speed specifications.**
b) **Scan mirror and structure meet pointing knowledge requirements.**
c) **Long-wavelength channels will not saturate below 480 K.**
d) **Background from ambient temperature optics does not affect instrument performance.**

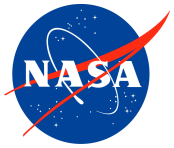

The Hyperspectral Thermal Emission Spectrometer (HyTES)

HyTES Rational

- Determine of the optimum position for the band filters for HyspIRI
- Provide antecedent data for testing HyspIRI algorithms
- Provide a new measurement capability, with high spectral and spatial imaging data useful for a range of applications such as volcanic gas detection
- Capitalize on the Quantum Well Earth Science Testbed (QWEST) an internally funded laboratory demonstration system for component testing, e.g. Detectors (QWIP), diffraction gratings, and slits at the system level.

HyTES Instrument Design

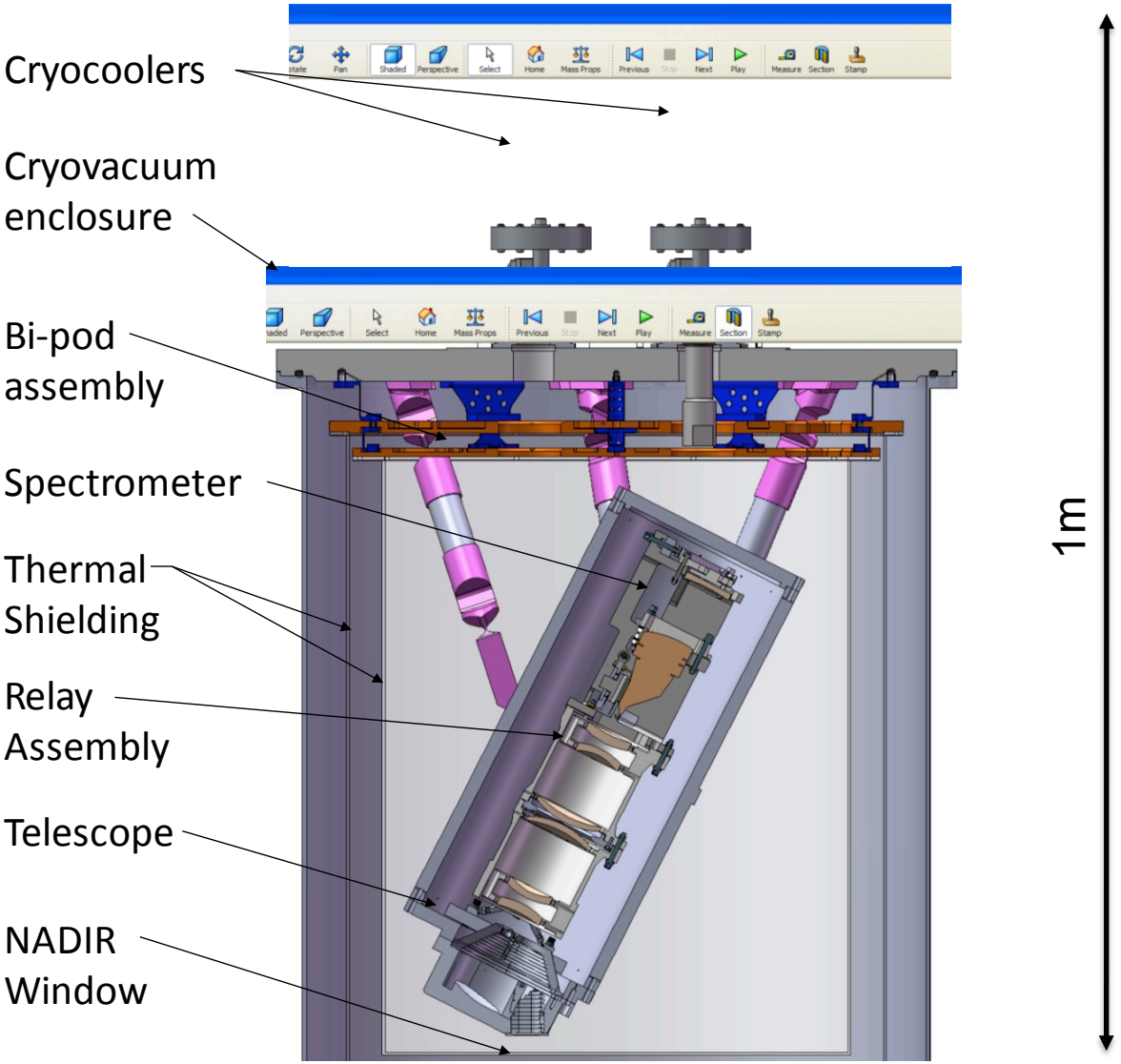

HyTES & QWEST Characteristics

Instrument Characteristic	QWEST	HyTES
Number of pixels x track	320	512
Number of bands	256	256
Spectral Range	8-12 um	7.5-12 um
Integration time (1 scanline)	30 ms	30 ms
Total Field of View	40 degrees	50 degrees
Calibration (preflight)	Full aperture blackbody	Full aperture blackbody
QWIP Array Size	640x512	1024x512
QWIP Pitch *	25 um	19.5um
QWIP Temperature	40K	40K
Spectrometer Temperature	40K	100K
Slit Width	50 um	39 um
Pixel size at 2000 m flight altitude	4.5 m	3.64
Pixel size at 20,000 m flight altitude	45 m	36.4
	Operational	**Late 2011**

HyTES Optics

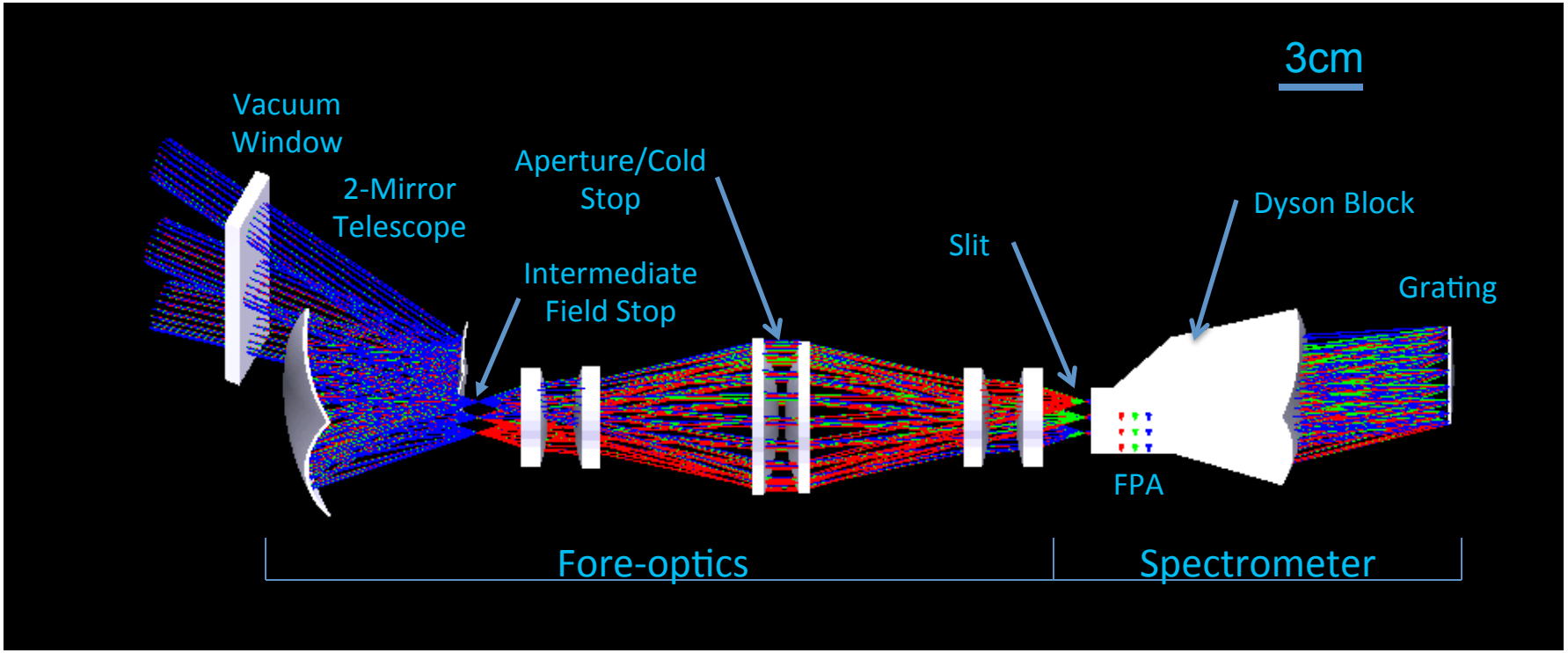

HyTES Optical Layout
(i.e. The entire system is cold, so there's no real "cold stop" in the traditional fashion)

HyTES Precursor: Technology Demo

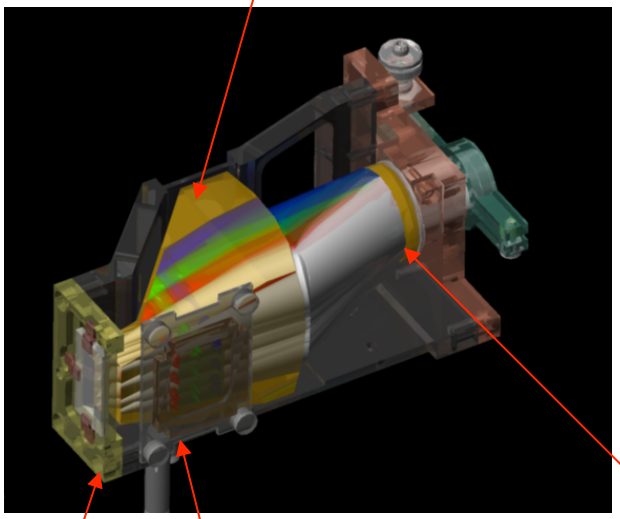

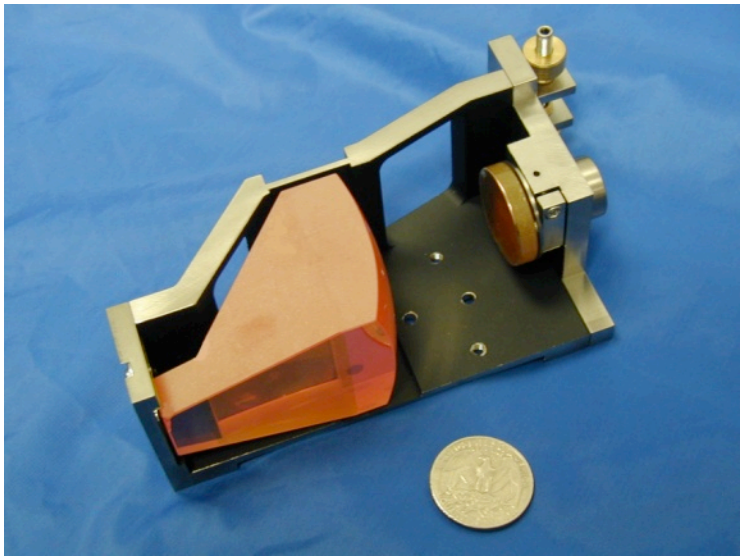

Compact Thermal Spectrometer Designs and Hardware

HyTES Precursor: Data Train

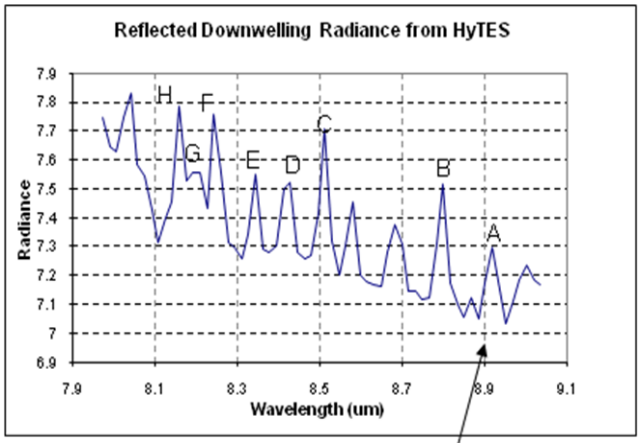

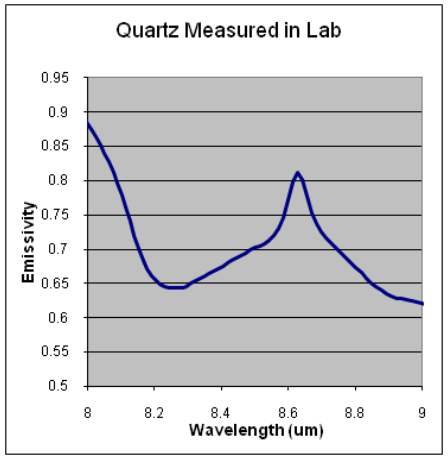

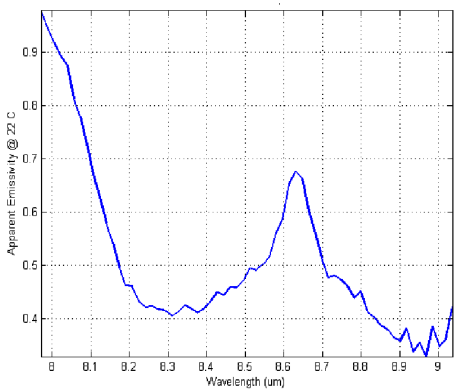

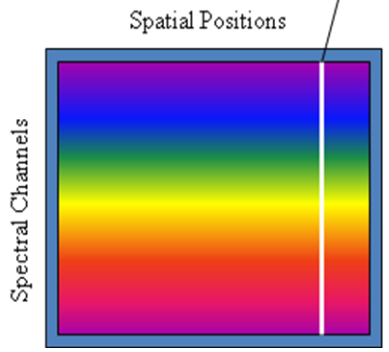

	Model	QWEST	Delta
A	8.92061	8.9179	0.00271
B	8.79894	8.7995	-0.00056
C	8.51426	8.5121	0.00216
D	8.4246	8.4276	-0.003
E	8.34725	8.3431	0.00415
F	8.25082	8.2418	0.00902
G	8.20345	8.208	-0.00455
H	8.16327	8.1573	0.00597

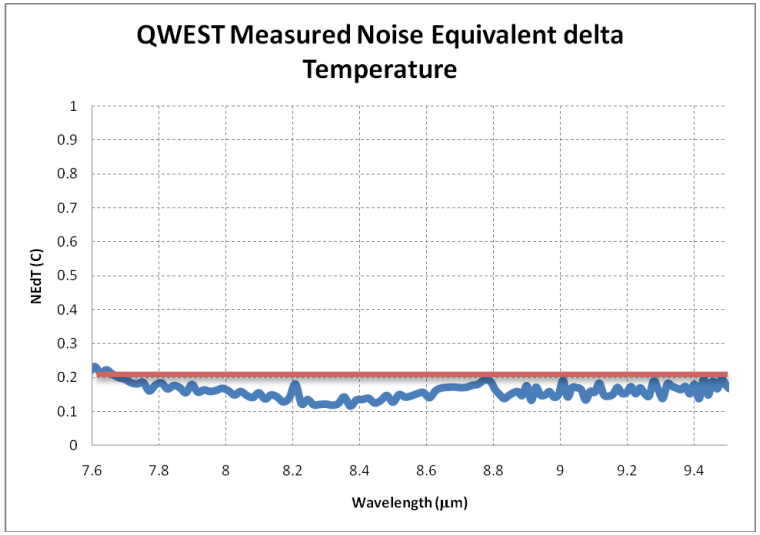

HyTES Diffraction Grating

- Grating successfully fabricated (ZnSe substrate, grooves etched in PMMA resist, gold reflective coating)

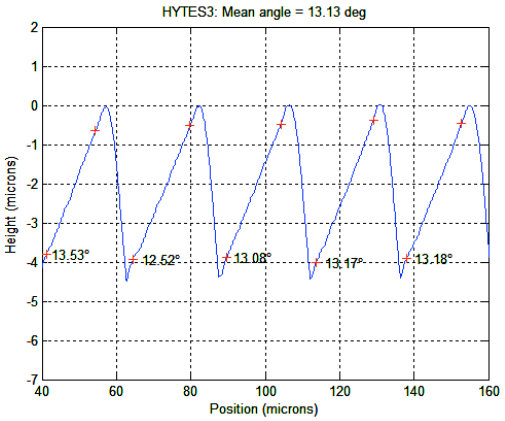

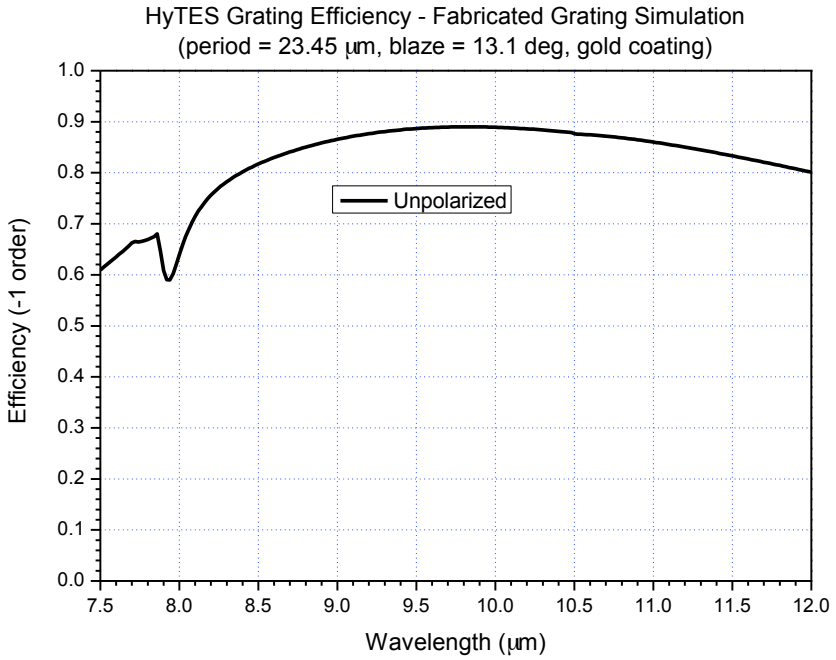

- Measured blaze angle is 9% deeper than 12° design – will decrease efficiency at 7.5 µm and increase efficiency at 12 µm as simulated above

HyTES Focal Plane Array

- HyTES will use a 1024x1024 pixel array covering the 7.5-12μm spectral band (typical array package shown at top right)
- JPL has fabricated and delivered similar large area and multi-band (dual color, three color and four color) arrays in the past
- This is not a commercially available technology, and only JPL delivers large format, high performance multi-band QWIP arrays
- The detector array has the following requirements:
  - 1kx1k format, SBF 184 ROIC
  - Operating temperature 40K
  - Performance such that in each of the 2x2 superpixels in the 7.5-12μm band the NEDT is less than 200 mK

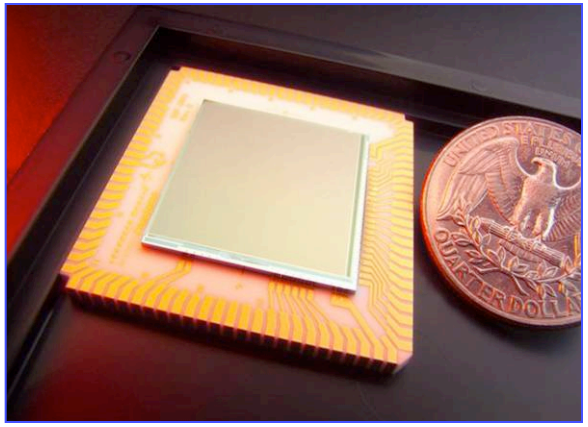

1024x1024 pixel single-band QWIP FPA

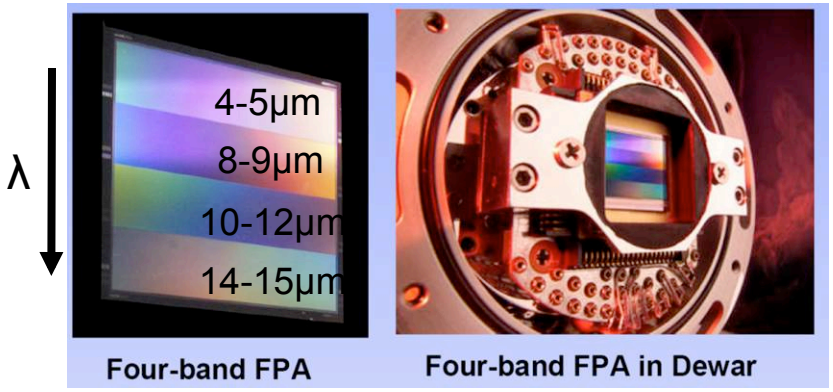

Four-band FPA

Four-band FPA in Dewar

HyTES Focal Plane Array

- A cross section of the two-band quantum well infrared photodetector (QWIP) used as the detector material is shown below
- This is similar to the previous three-band design but much simpler to process
- Roughly half of the illuminated area of the array will respond in the 7.5-10µm range, and the other half will cover the 10-12 µm range
- Different fabrication approaches on each half of the array are required to achieve the 7.5-12µm operation

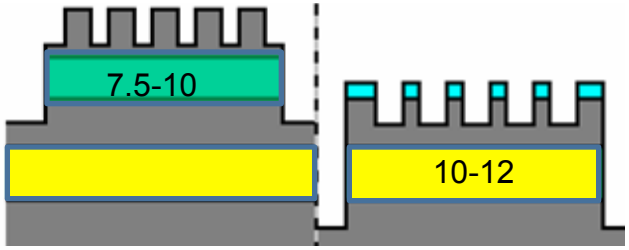

HyTES pixel design – cross-sectional zoom at the transition point, showing two bands with ¼ lamda gratings on each

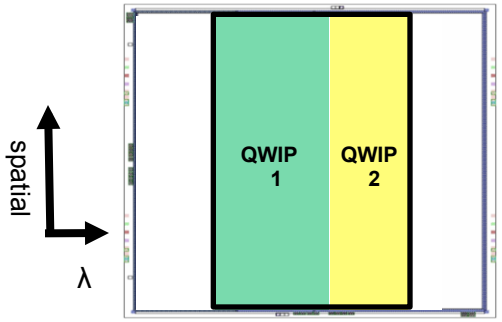

Top-down view of FPA
Illuminated area shown in green and yellow

HyTES Focal Plane Array

Measured noise equivalent delta temperature (NEΔT) for existing focal plane array. Single pixel data.

19.2 mK

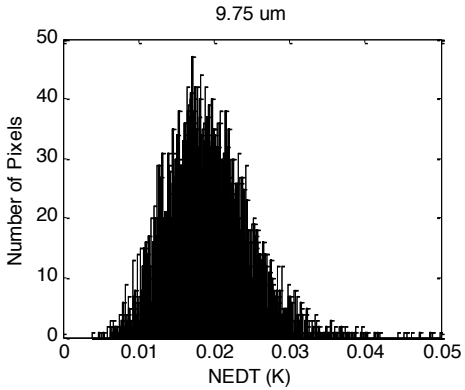

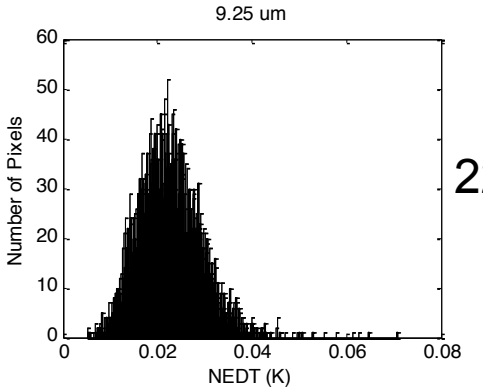

22.5 mK

22.7 mK

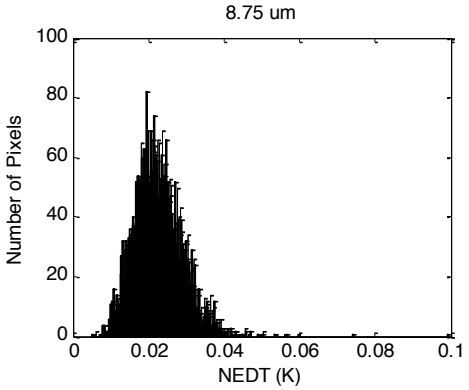

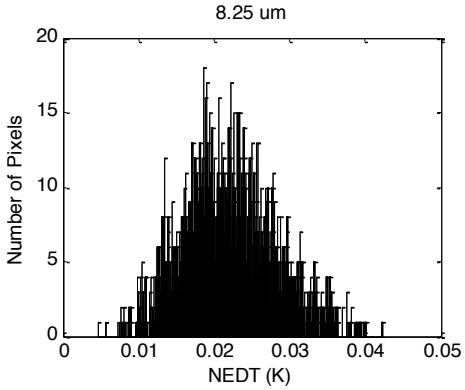

22.0 mK

HyTES Sensor Modeling

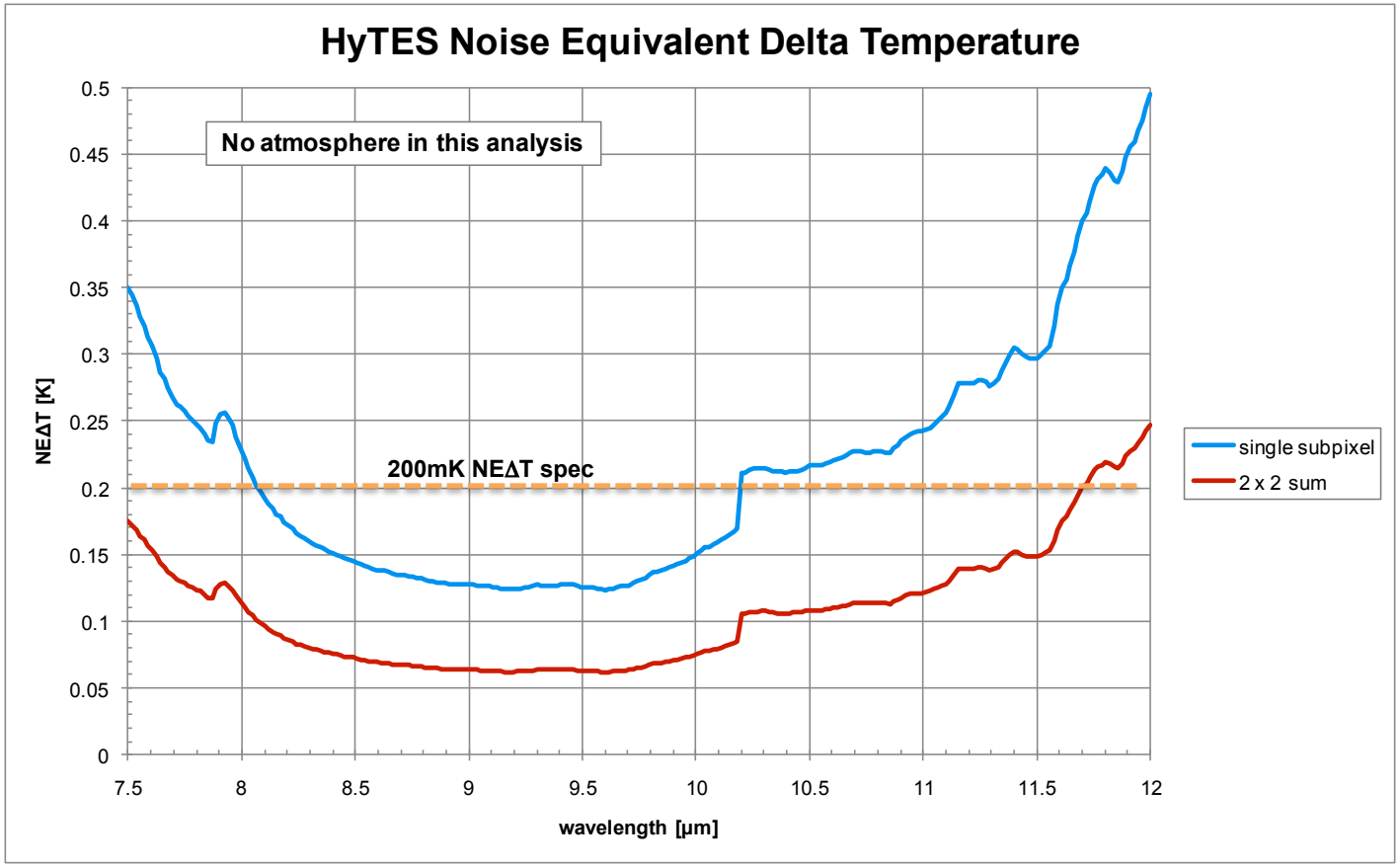

- The final design exhibits a smoother transition between bands than the original three-color version and meets spec (2x2 pixel summation NEΔT < 200mK) in nearly all of the 7.5-12µm band

HyTES System

Focal Plane Electronics

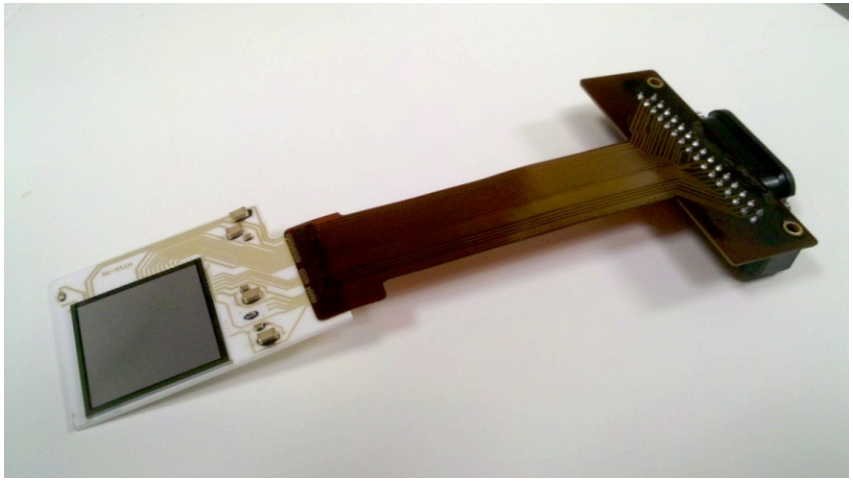

Spectrometer housing and Relay Assembly

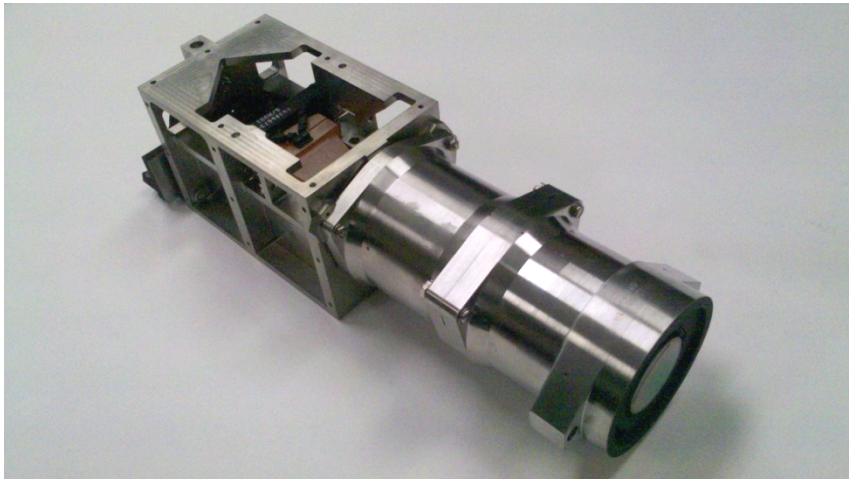

Airborne Cryovacuum Enclosure

Various delivered hardware. The current effort is focused on integration and testing.

HyTES Summary

- HyTES will allow the determination of the optimum position for the band filters for HyspIRI
- HyTES will provide antecedent data for testing HyspIRI algorithms
- HyTES will provide a new measurement capability, with high spectral and spatial imaging data useful for a range of applications such as volcanic gas detection
- HyTES instrument laboratory testing will begin in the next few weeks
- HyTES airborne flights are planned for mid 2011

Overall Summary

- Exciting technology development and risk reduction underway for the HyspIRI-TIR program
- PHyTIR provides instrument risk reduction for key components of HyspIRI-TIR in particular the scan mirror and detectors
- HyTES provides science risk reduction for HyspIRI-TIR by allowing the optimum band positions to be determined as well as providing antecedent data at higher spectral and spatial resolution for algorithm development

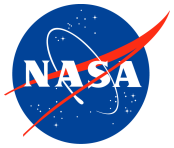

Backup

PHyTIR Summary

This activity will benefit the development of any airborne or spaceborne system that will utilize a high speed scanning mirror coupled with a MCT detector array to obtain a wide swath width, high spatial resolution, thermal infrared measurement with an NEΔT of approximately 0.2K.

Similar systems have been used in the Moderate Resolution Imaging Spectroradiometer (MODIS), Visible Infrared Imaging Radiometer Suite (VIIRS), Advanced Spaceborne Thermal Emission Radiometer (ASTER) and Landsat (TM5/ ETM+) instruments (Barnes et. al. 1998; Mitchel 2008; Ohmae and Kitamure, 1994; Barsi et al. 2003).

However, none of these existing systems has sufficient performance to meet the measurement requirements of the HyspIRI-TIR instrument. PHyTIR will demonstrate that HyspIRI-TIR required high accuracy measurements can be made and help enable both the HyspIRI-TIR instrument as well as other future instruments built by Governments or Commercial Companies that utilize similar technology.

HyTES Diffraction Grating

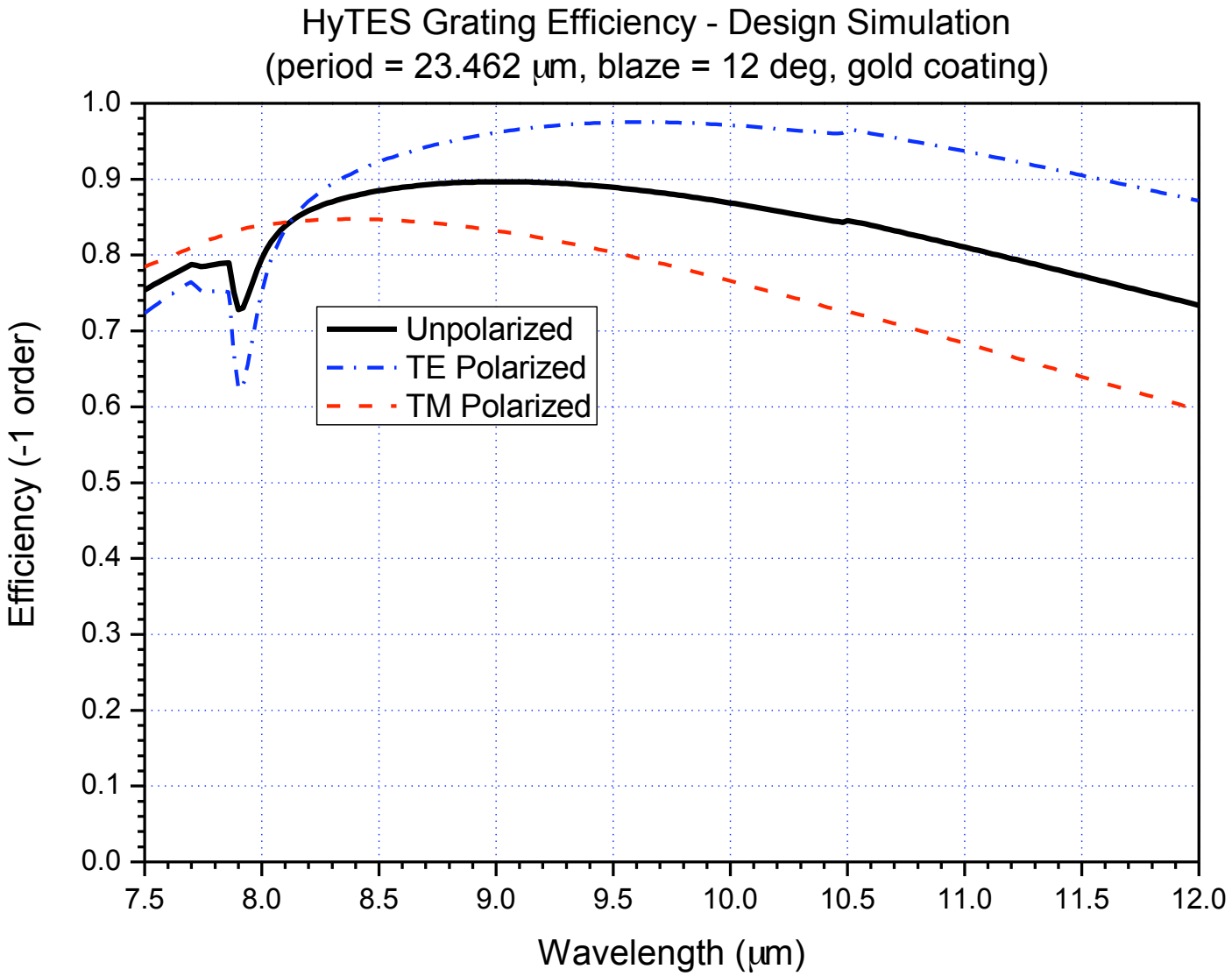

Status of AVIRIS Next Generation and Technologies Validated for the HysplRI VSWIR Instrument Concept

Robert O. Green, The AVIRIS-NG Team

23 August 2011

Jet Propulsion Laboratory, California Institute of Technology

Overview

- Science Objectives
- AVIRIS-classic and AVIRIS-NG Measurement Characteristics
- AVIRIS-NG Concept
- AVIRIS-NG Current Development Status
- Summary and Conclusion

Science Objectives

- Support imaging spectroscopy based NASA Earth science and science applications
- Test imaging spectrometer elements that may be used in space instruments
- Provide a calibration/validation under flight resource for HyspIRI

AVIRIS Next Generation Compared to AVIRIS

	AVIRIS-Next Generation	AVIRIS-Classic
SPECTRAL		
Range	380 to 2510 nm	380 to 2500 nm
Position	5 nm	10 nm
Response	1 to 1.5 X sampling	1 to 1.5 X sampling
Calibration	+-0.1 nm	+-0.1 nm
RADIOMETRIC		
Range	0 to max Lambertian	0 to max Lambertian
Precision (SNR)	>2000 @ 600 nm	>1000 @ 600 nm
	>1000 @ 2200 nm	>400 @ 2200 nm
Accuracy	95% (<5% uncertainty)	90% (<10% uncertainty)
Linearity	>=99% characterization	>=99% characterization
SPATIAL		
Range	34° field-of-view	34° field-of-view
Sampling	1 milliradian	1 milliradian
Response	1 to 1.5 X sampling	1 to 1.5 X sampling
Sample Distance	0.3 m to 20 m	4 m to 20 m
Geom Model	Full 3 Axes cosines	Full 3 Axes cosines
UNIFORMITY		
Spectral Cross-Track	>95% across FOV	>98% across FOV
Spectral-IFOV-Variation	>95% Spectral Direction	>98% Spectral Direction

NGIS Reference Radiances

Reference Radiances for SNR Benchmark

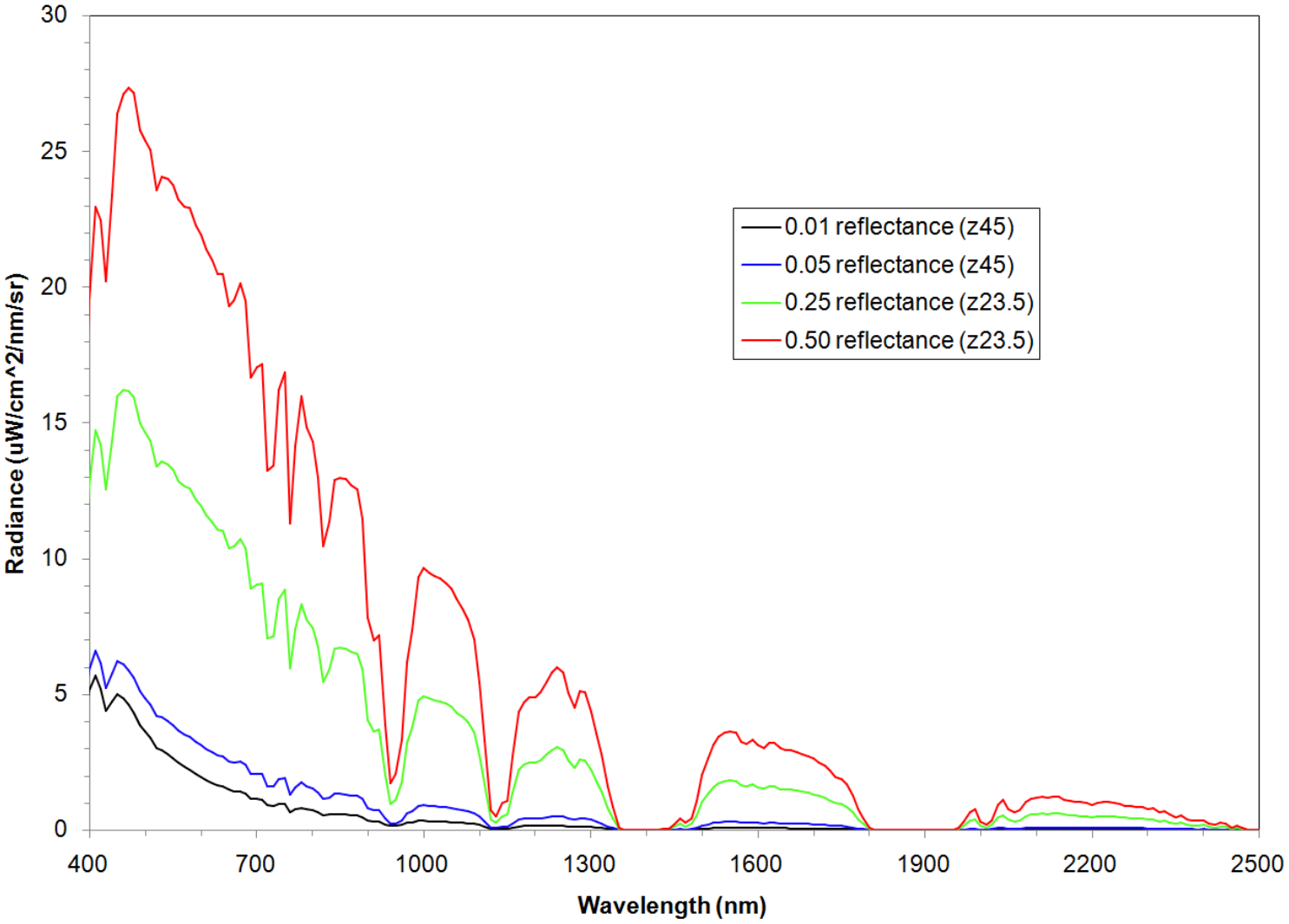

NGIS SNR Modeled Performance

SNR at 10 nm and AVIRIS scan line rate

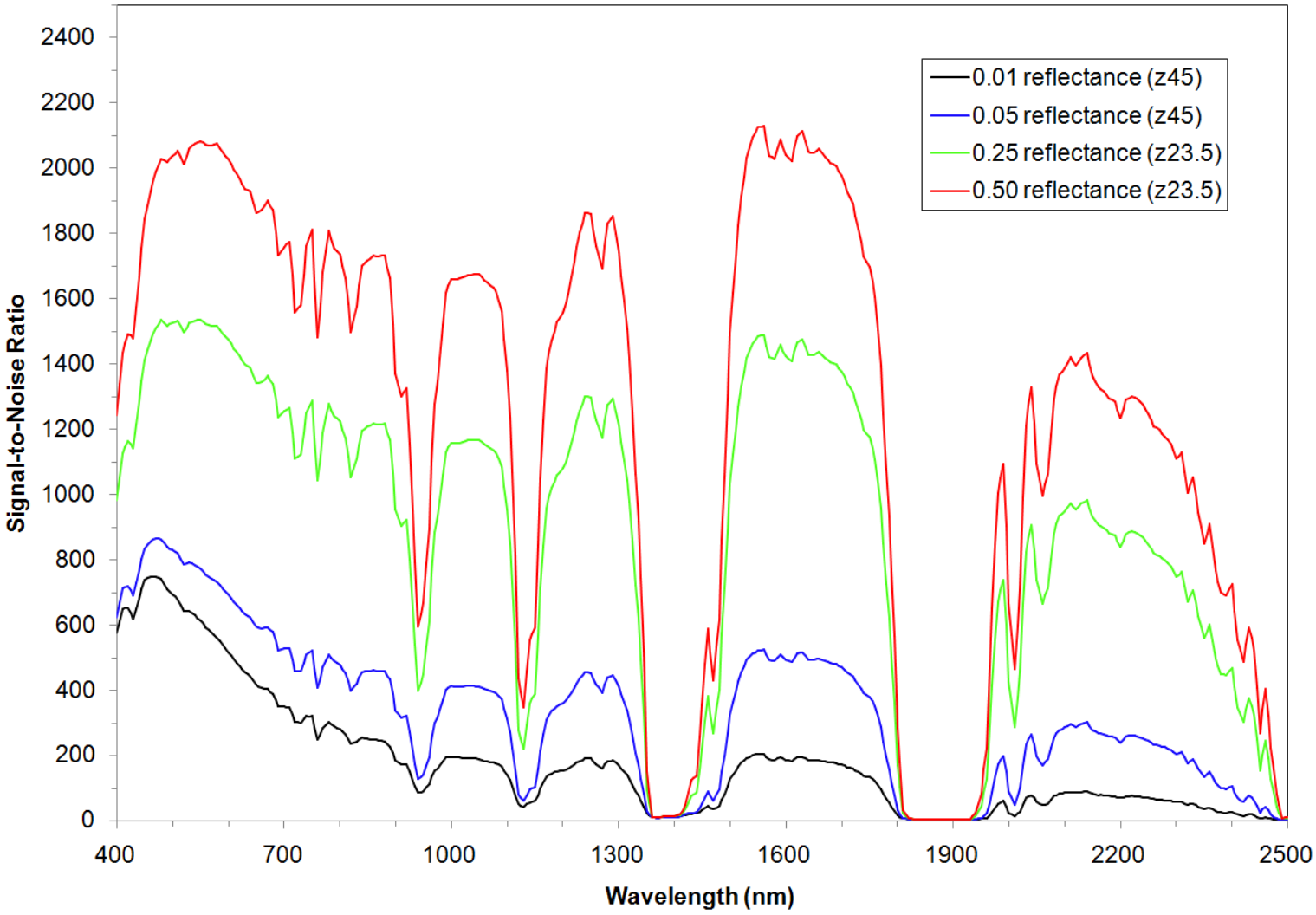

AVIRIS-NG Uniformity

Depiction

-Grids are the detectors
-Spots are the IFOV centers
-Colors are the wavelengths

>95% spectral cross-track

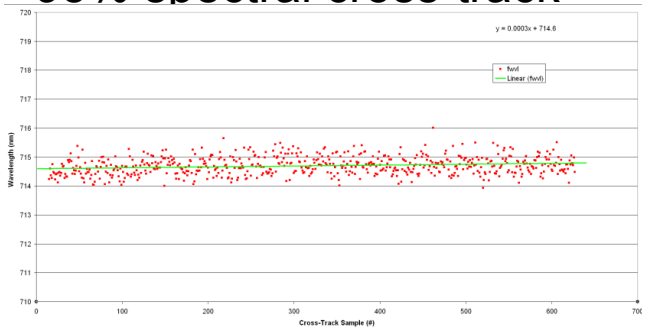

M3

>95% spectral IFOV

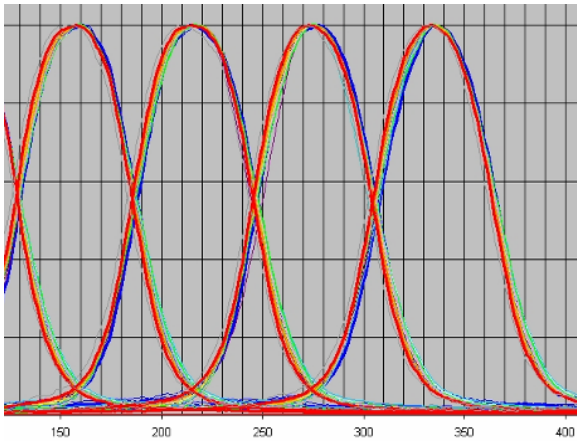

M3

Cross-Track

Wavelength (nm)

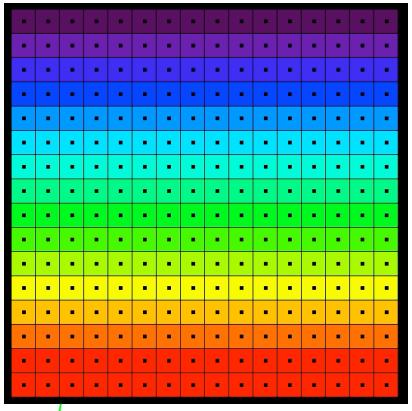

√ Required Uniformity

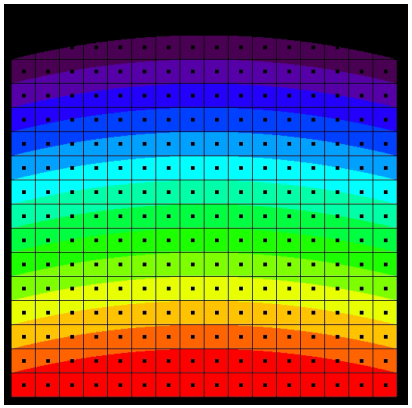

X Failure by "frown"

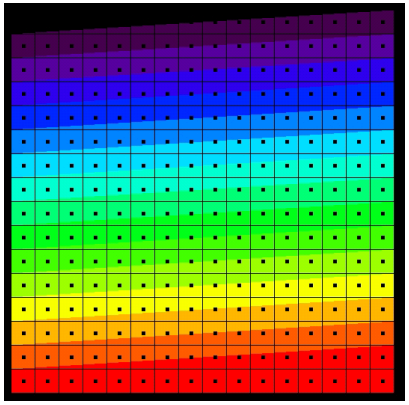

X Failure by twist

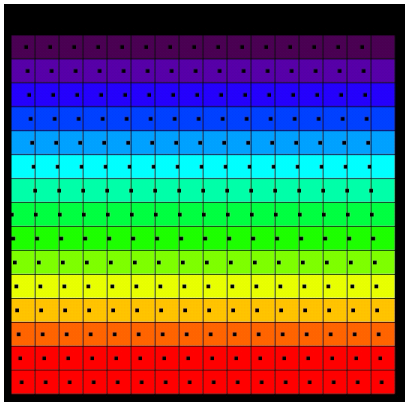

X Failure by Spectral-IFOV-shift

AVIRIS Next Generation Optical Concept

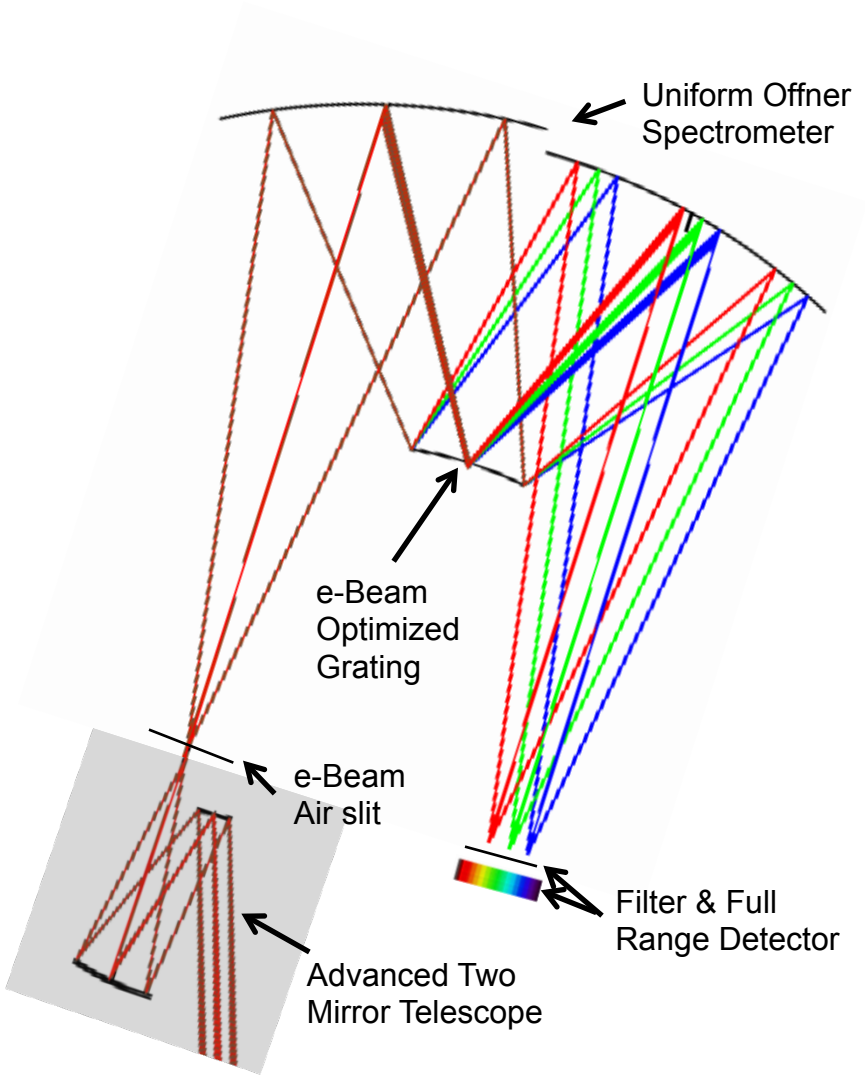

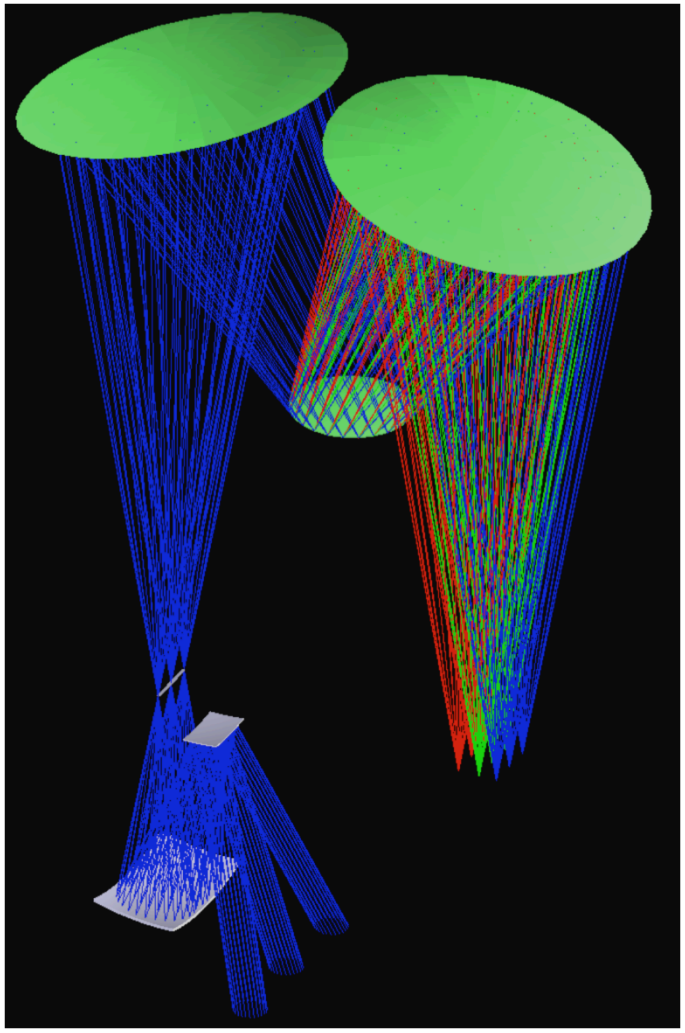

Enabling Elements

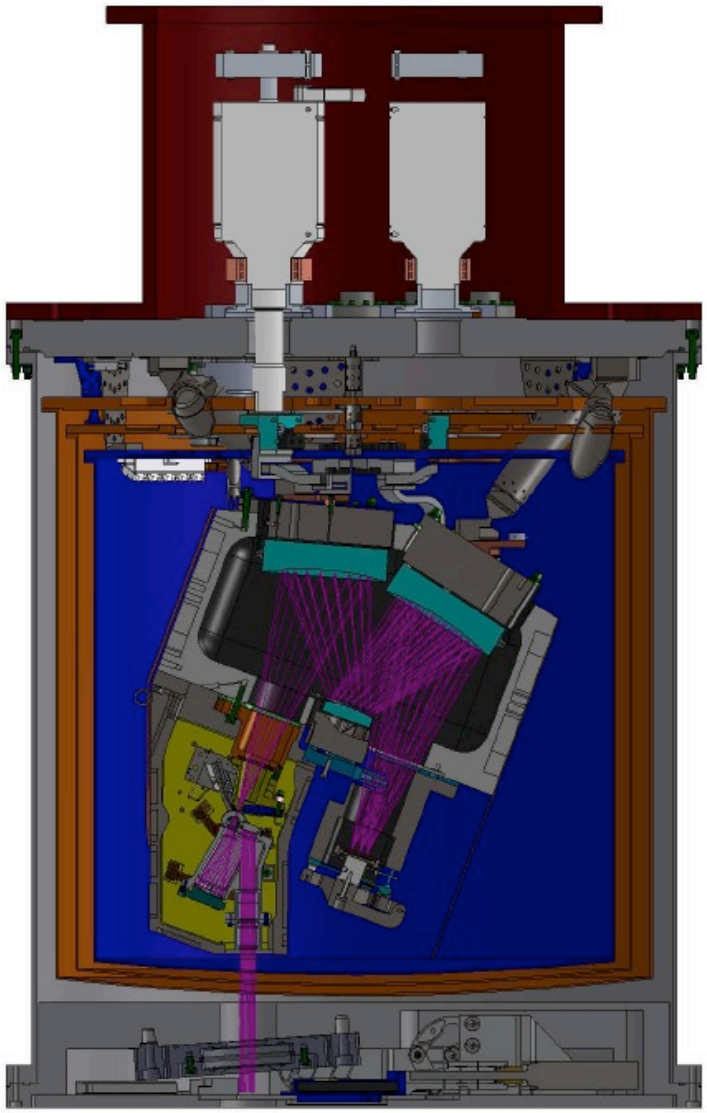

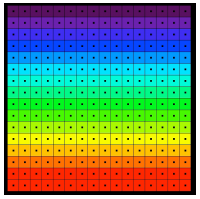

High SNR and high uniformity imaging spectrometer designs (Mouroulis et al., 2000)*

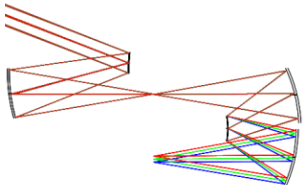

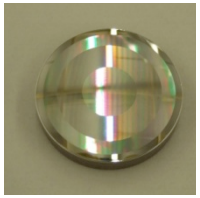

Electron-beam lithography low-scatter tuned-high-efficiency gratings on curved surfaces for space

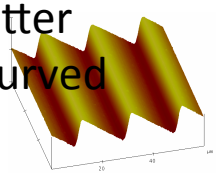

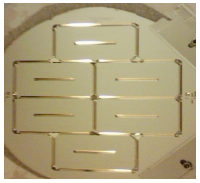

Ultra uniform 27 µm x 20 mm electron-beam lithography slit for space flight

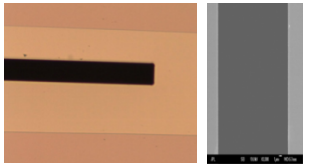

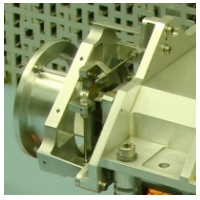

Component mounts with 0.25 micron feedback adjustment that are lockable for space flight

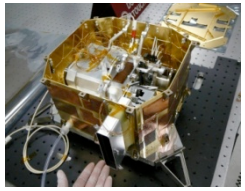

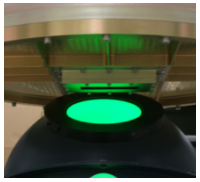

Unique set of alignment and calibration sources and tools for imaging spectrometer development

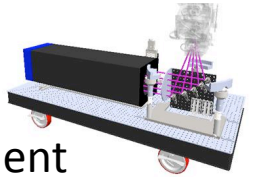

*Mouroulis P., Green R. O., Chrien T. G., “Design of pushbroom imaging spectrometers for optimum recovery of spectroscopic and spatial information,” APPL OPTICS 39: (13) 2210-2220 MAY 1 2000

AVIRIS Next Generation Spectrometer
Installation of First Mirror

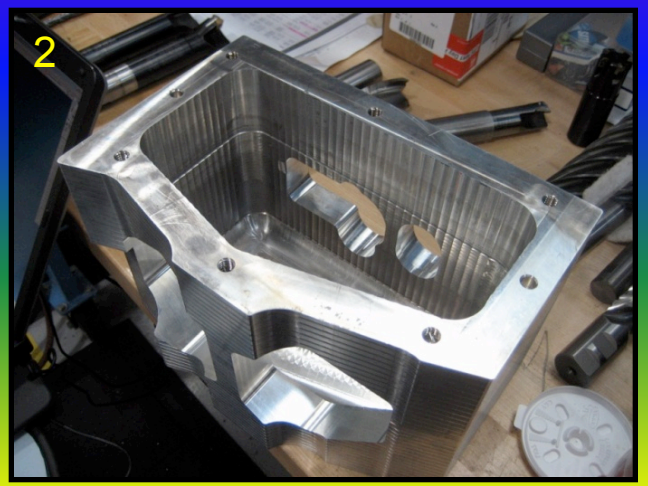

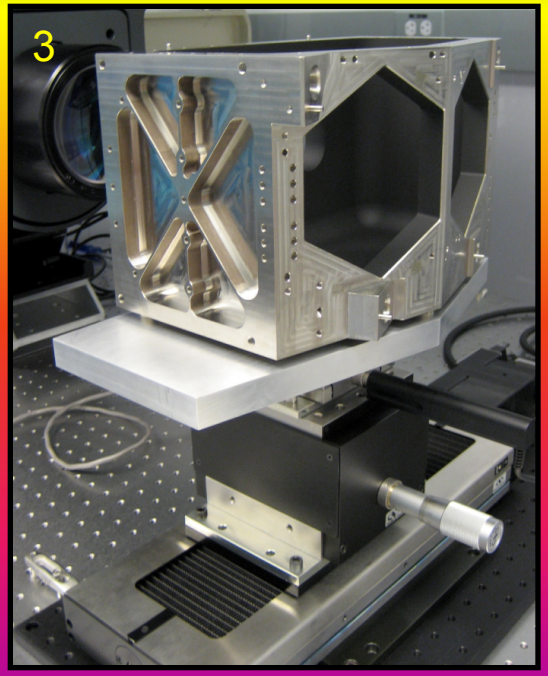

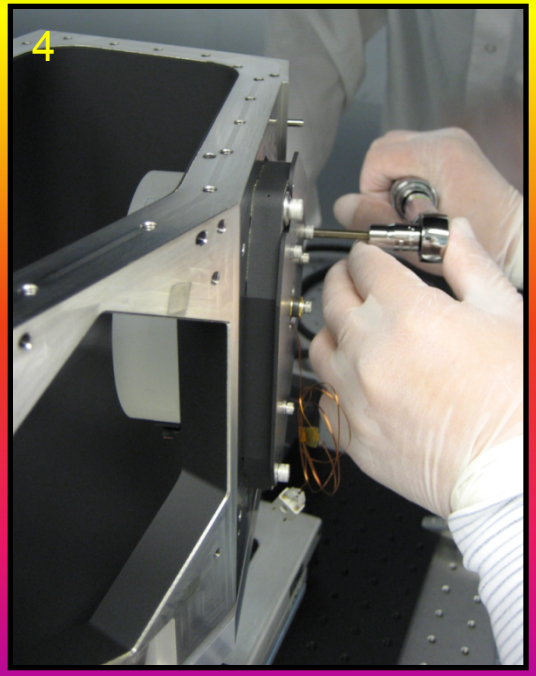

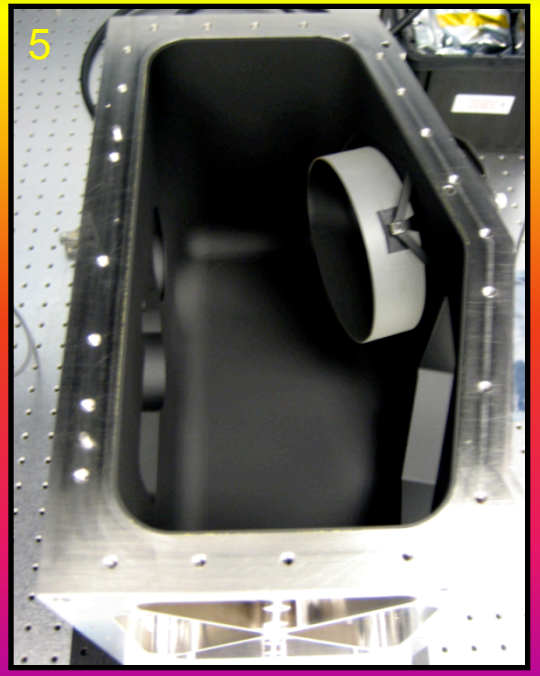

AVIRIS Next Generation Telescope
Fully Aligned

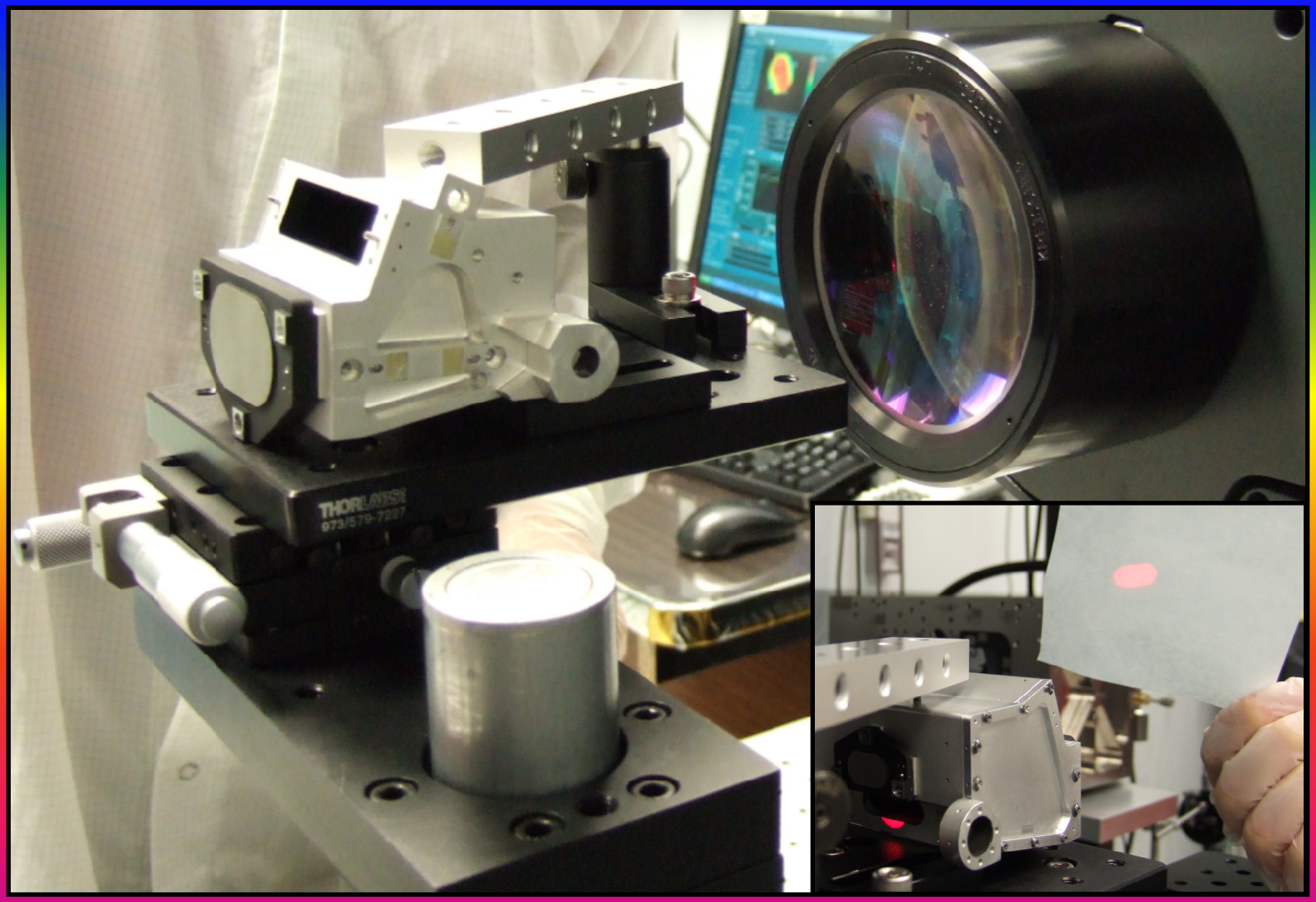

Spectrometer toThermal Shields

Alignment Understanding

> 95% Uniformity (Precursor Instrument)

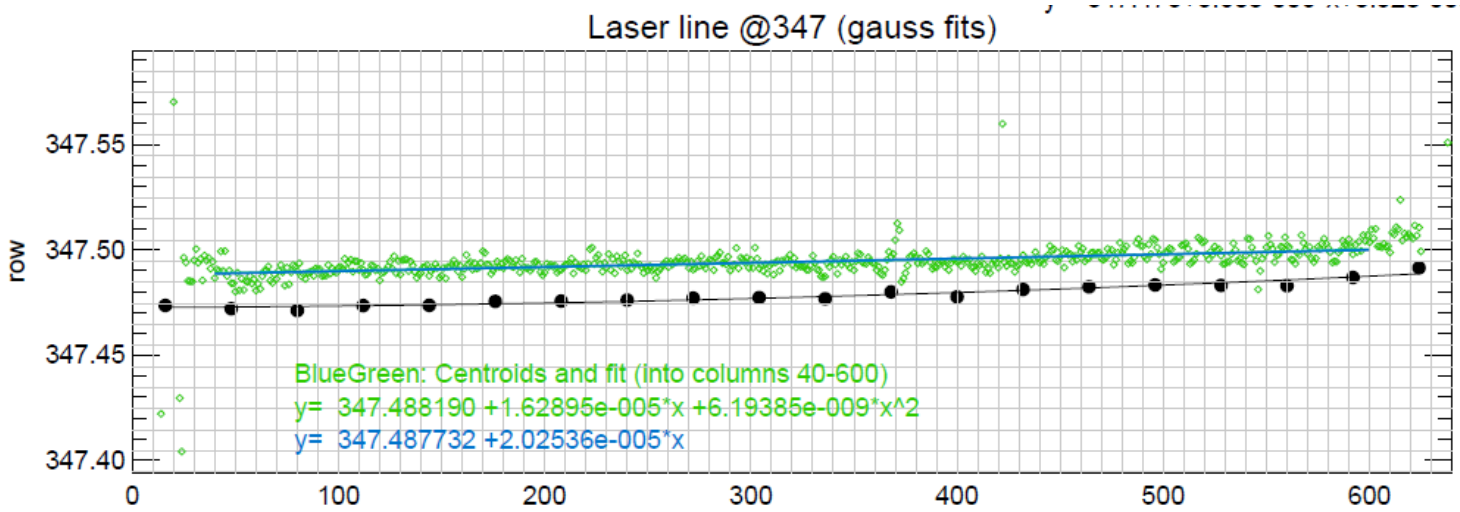

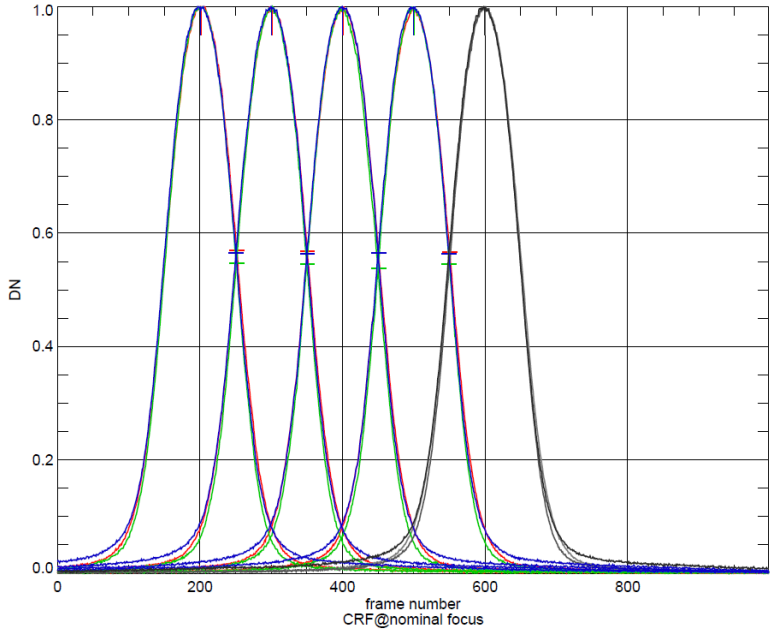

Laboratory Test Spectrum

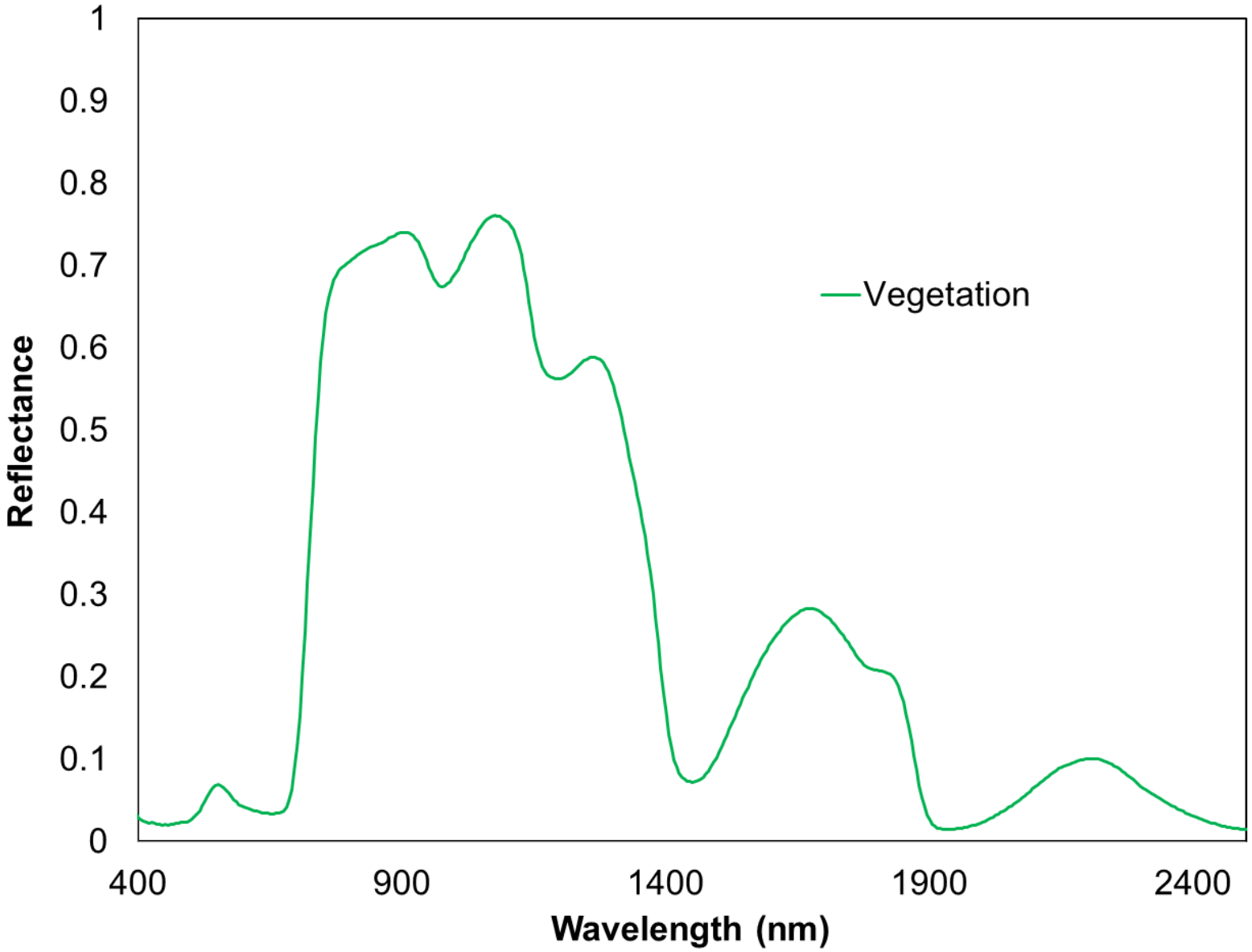

Precursor to AVIRIS-NG in Testing

Measurements from the Precursor Imaging Spectrometer

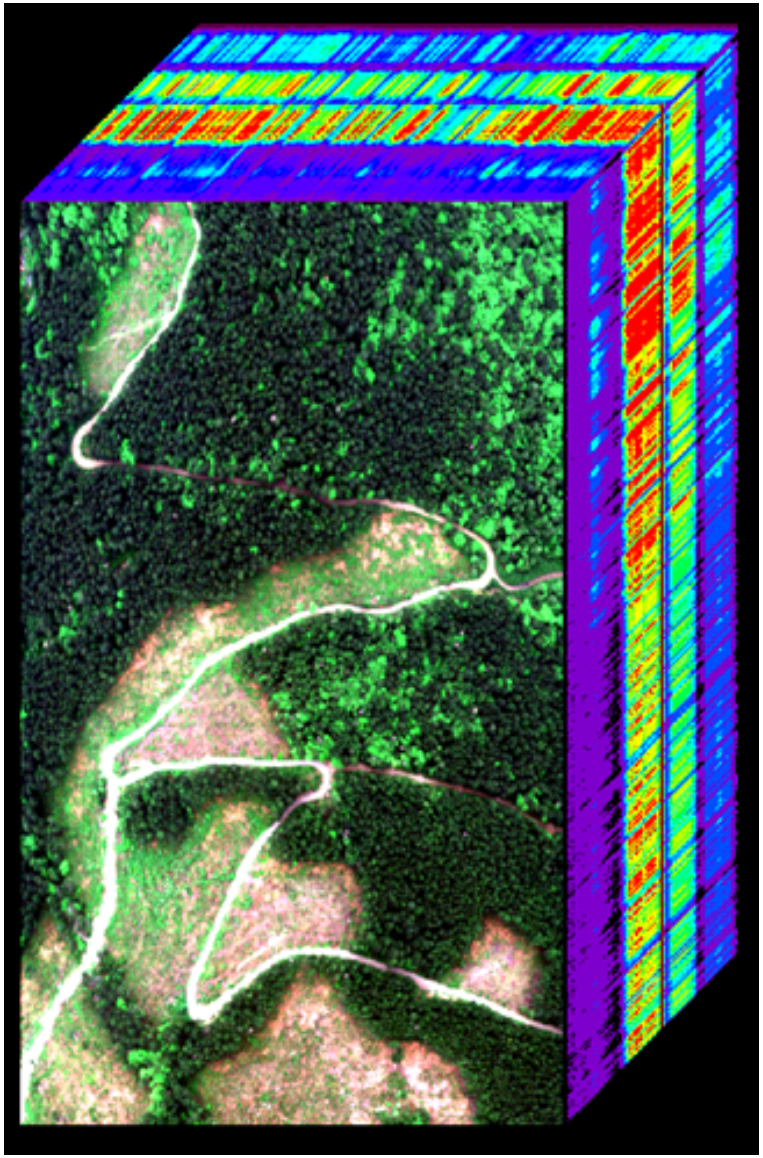

Full solar reflected spectral range 380 to 2500 nm at 5 nm
95% spectral cross-track and IFOV uniformity
High signal-to-noise ratio

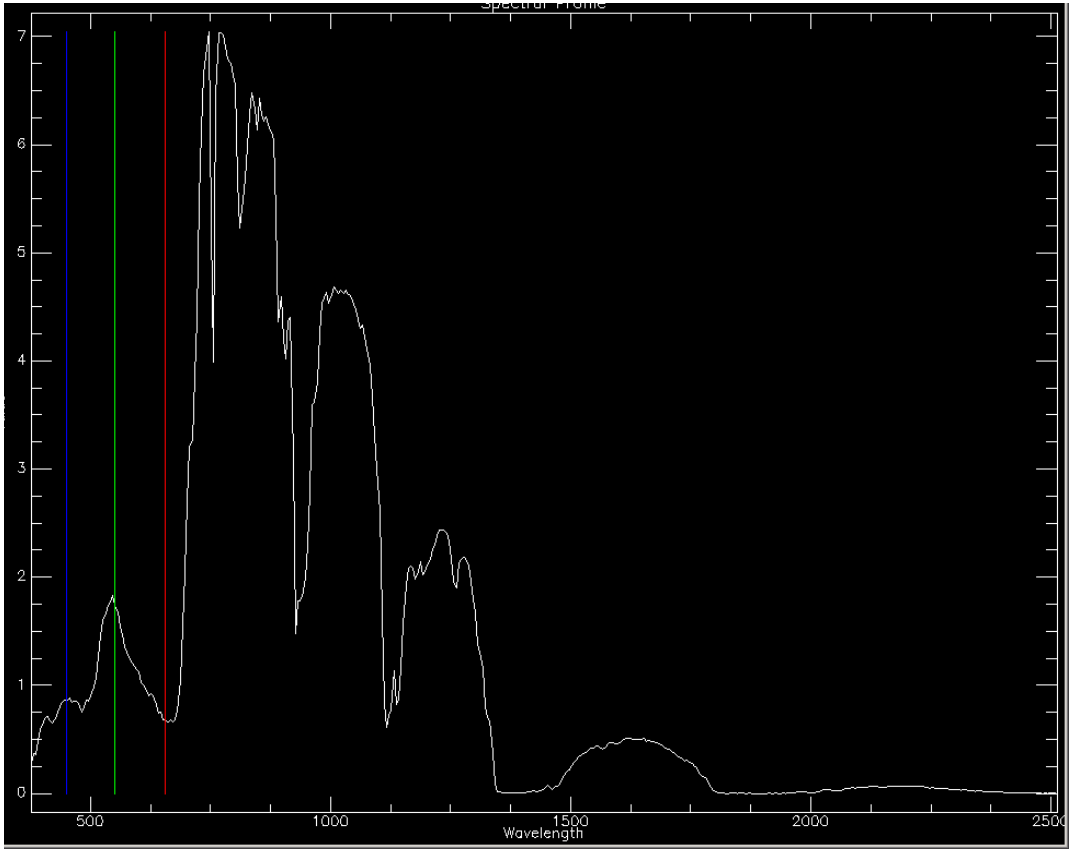

Summary and Conclusion

- AVIRIS-NG development is nearly complete.
- AVIRIS-NG is on track to begin cold alignment and then calibration.
- At present all of the requirements are on track to be met.
- Test flights of AVIRIS Next Generation should occur in the Autumn of 2011.
- AVIRIS-NG is expected to be available in 2012 for science validation activities

QUESTIONS?

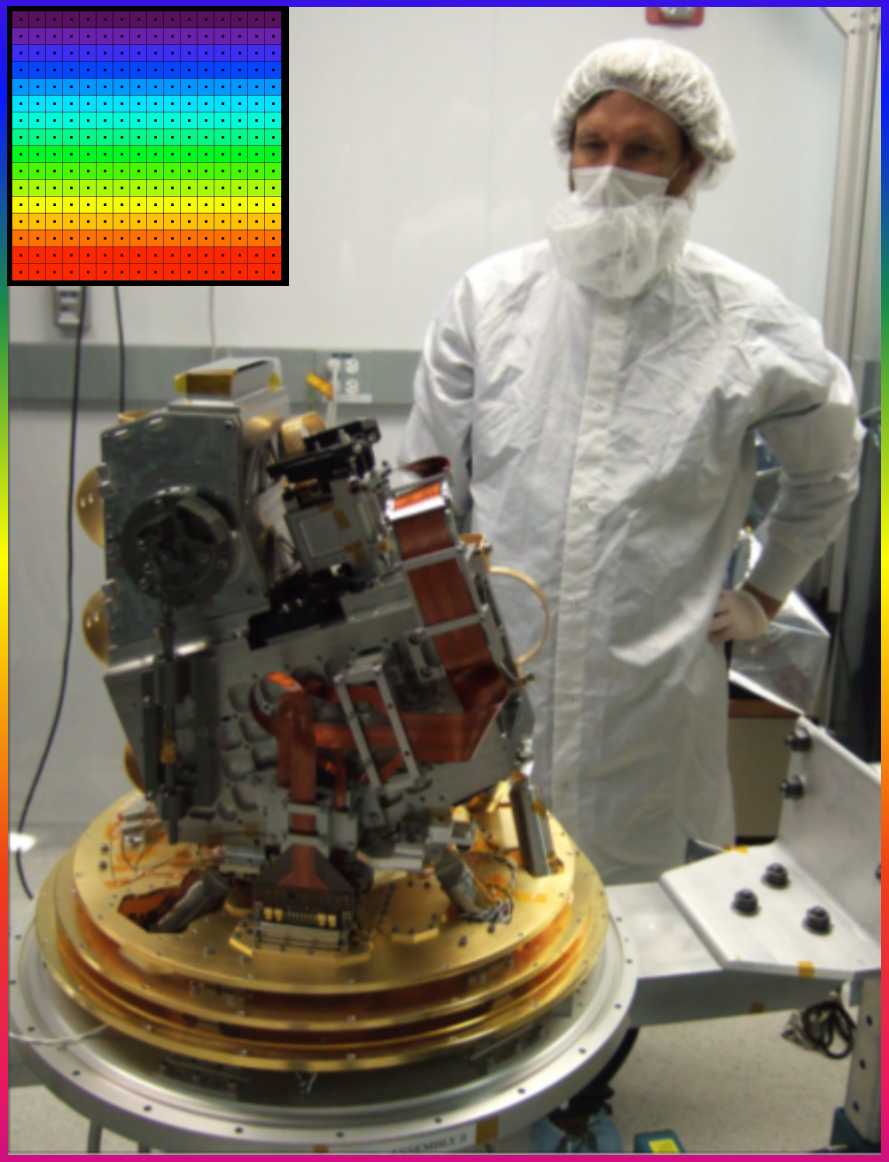

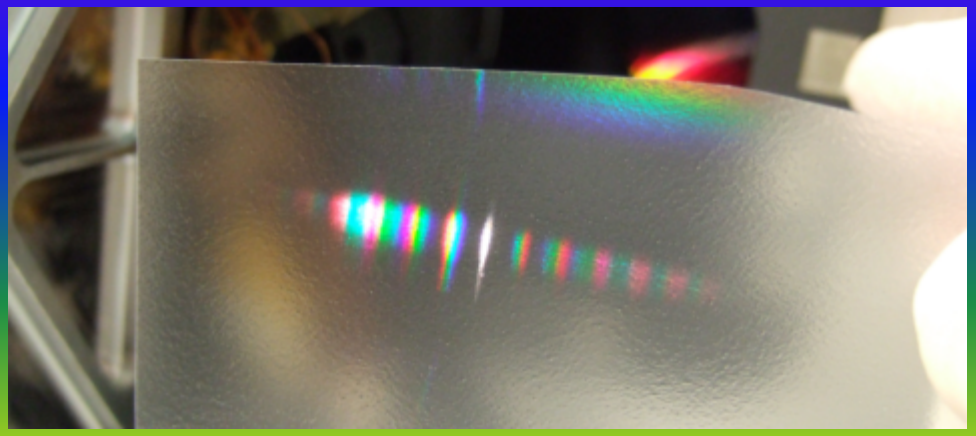

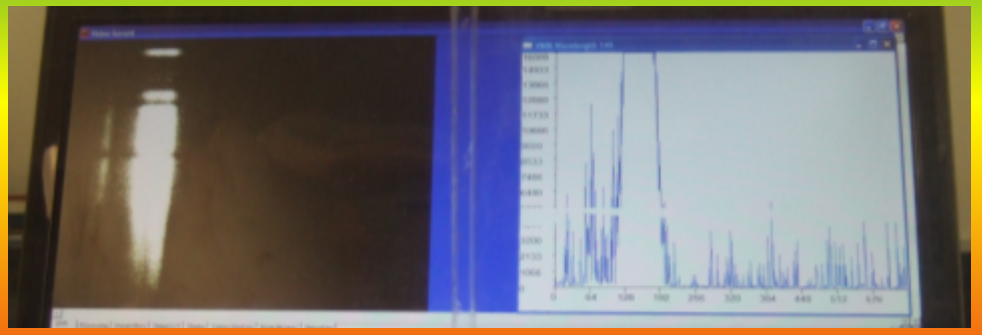

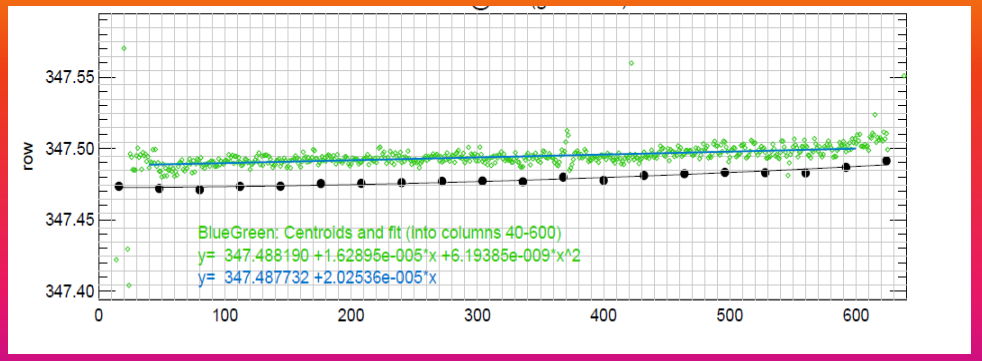
347.55
347.50
347.45
347.40
row
0
100
200
300
400
500
600
BlueGreen: Centroids and fit (into columns 40-600)
y= 347.488190 +1.62895e-005*x +6.19385e-009*x^2
y= 347.487732 +2.02536e-005*x

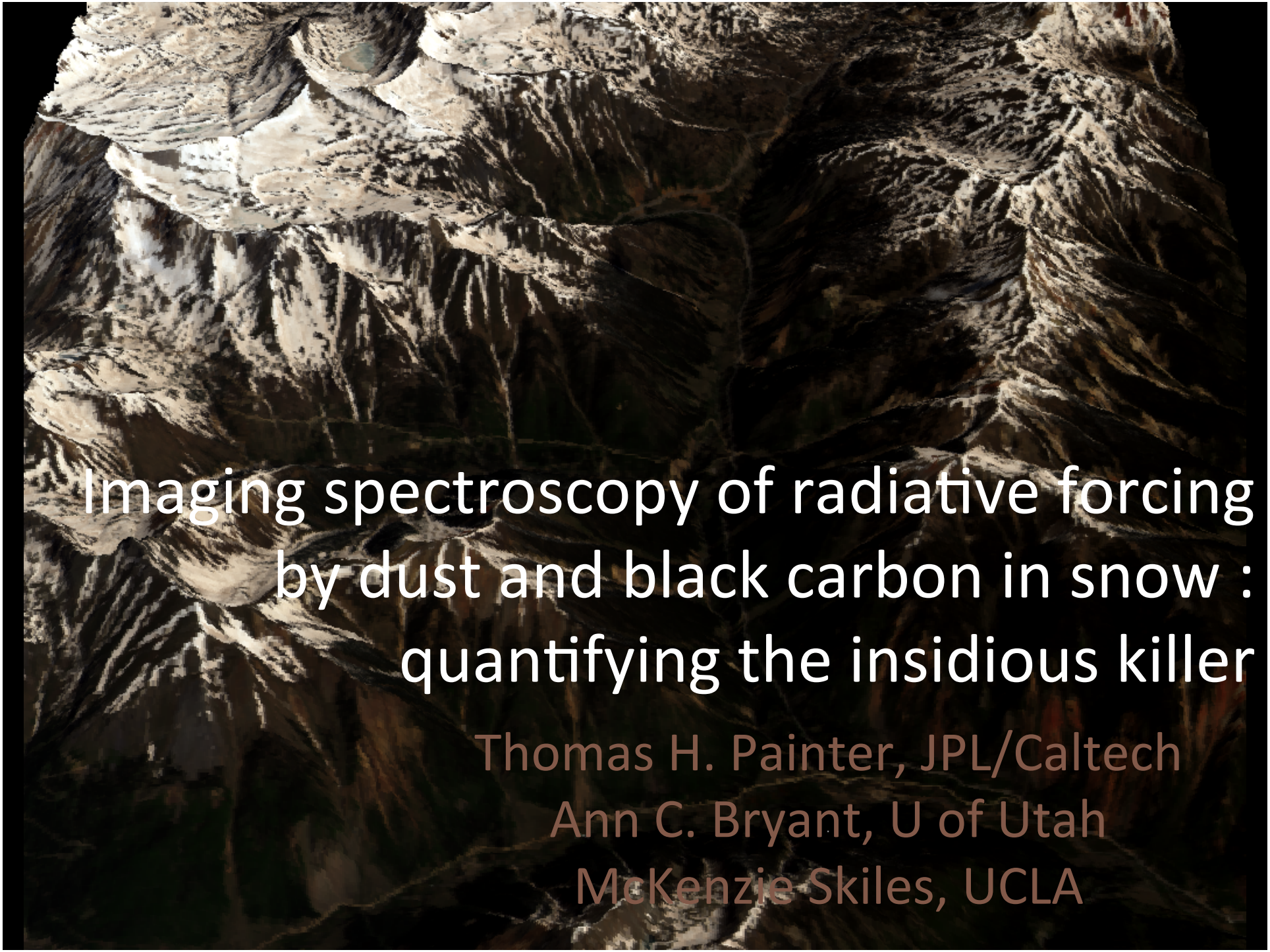

Imaging spectroscopy of radiative forcing by dust and black carbon in snow : quantifying the insidious killer

Thomas H. Painter, JPL/Caltech
Ann C. Bryant, U of Utah
McKenzie Skiles, UCLA

Snow Pit Speech

Guiding Science Questions

How does variation in snow albedo modulate river runoff and glacier mass balance?

How has radiative forcing by increases in dust and black carbon loading in the Anthropocene changed river runoff and glacier mass balance?

Outline

- Perspective on snow and ice melt
- Impacts of changes in albedo
- Global changes in dust and BC loading
- Global need for HyspIRI (USGCRP goals 1&2, Advance Science and Inform Decisions)
- Imaging spectroscopy of radiative forcing
- Upper Colorado River Basin, Spring 2011

Mountain Snow and Ice

- In the Western US, ~75% of freshwater comes from mountain snowmelt.
- Mountain snow and ice of the globe provides freshwater to nearly 2 billion people

Global Glacier Retreat

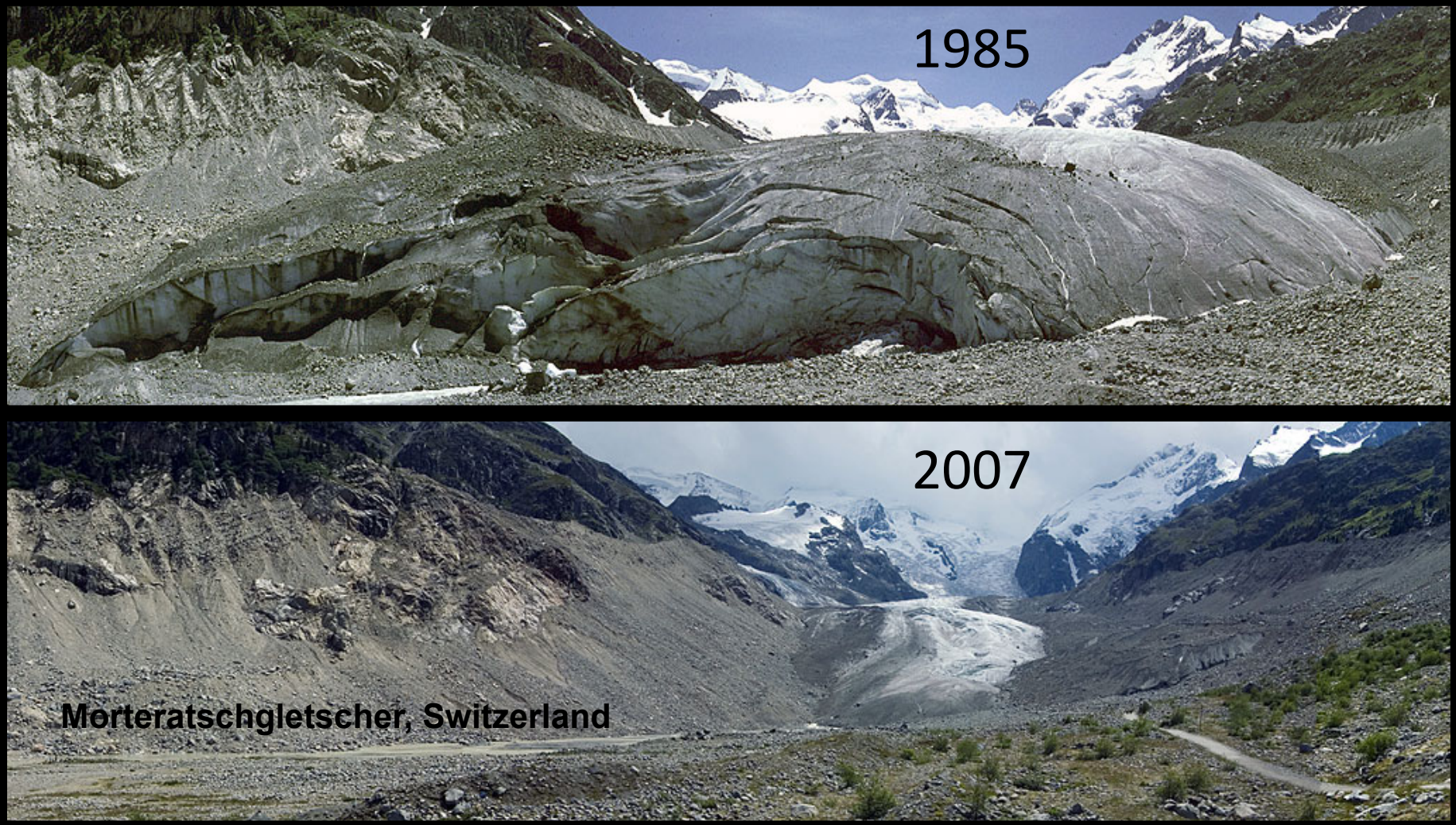

Global Water Stress

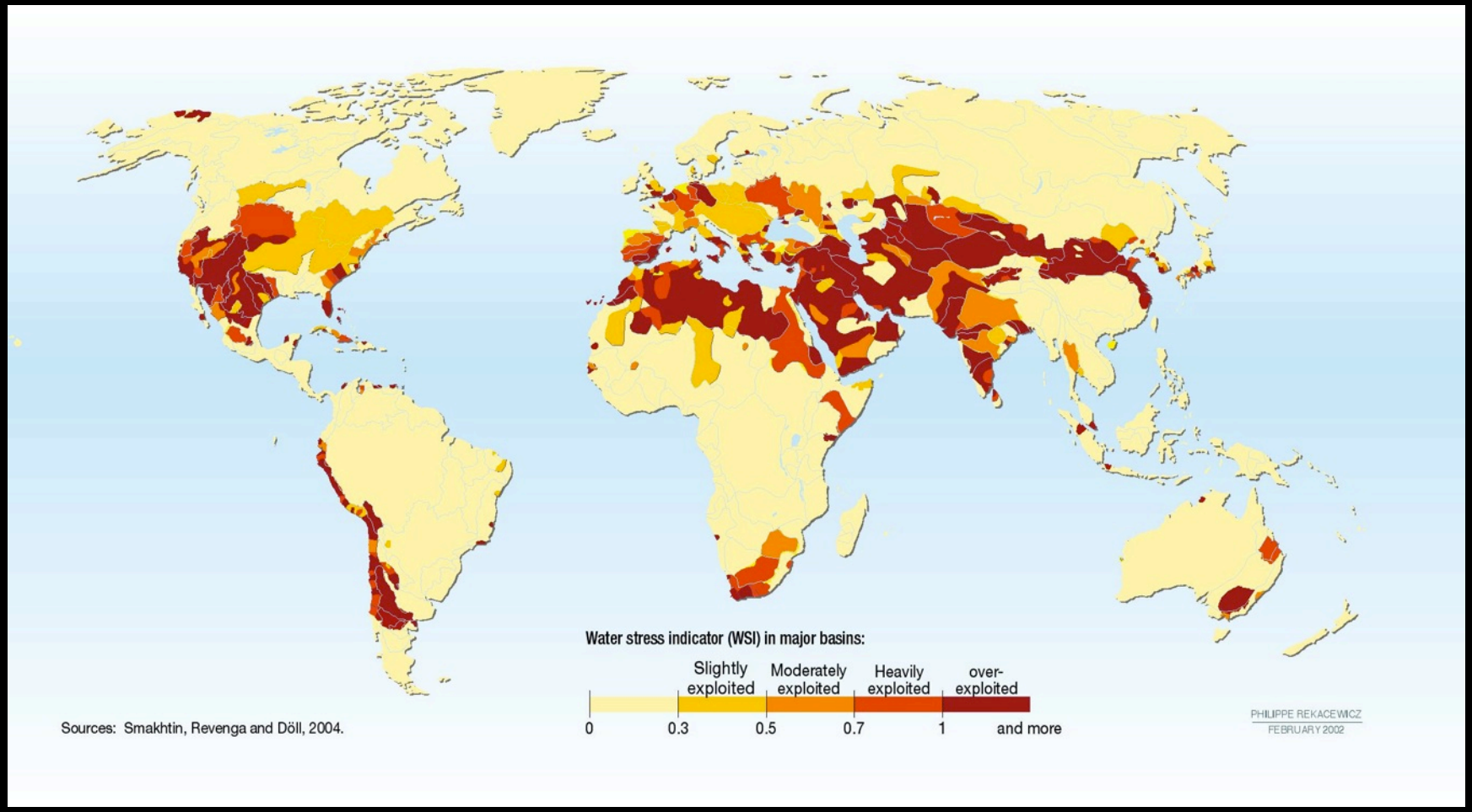

Source: http://www.unep.org/

$$\frac{dU}{dt} + Q_m = (1-\alpha)S + L^* + Q_s + Q_v + Q_g + Q_r$$

What controls snowmelt?

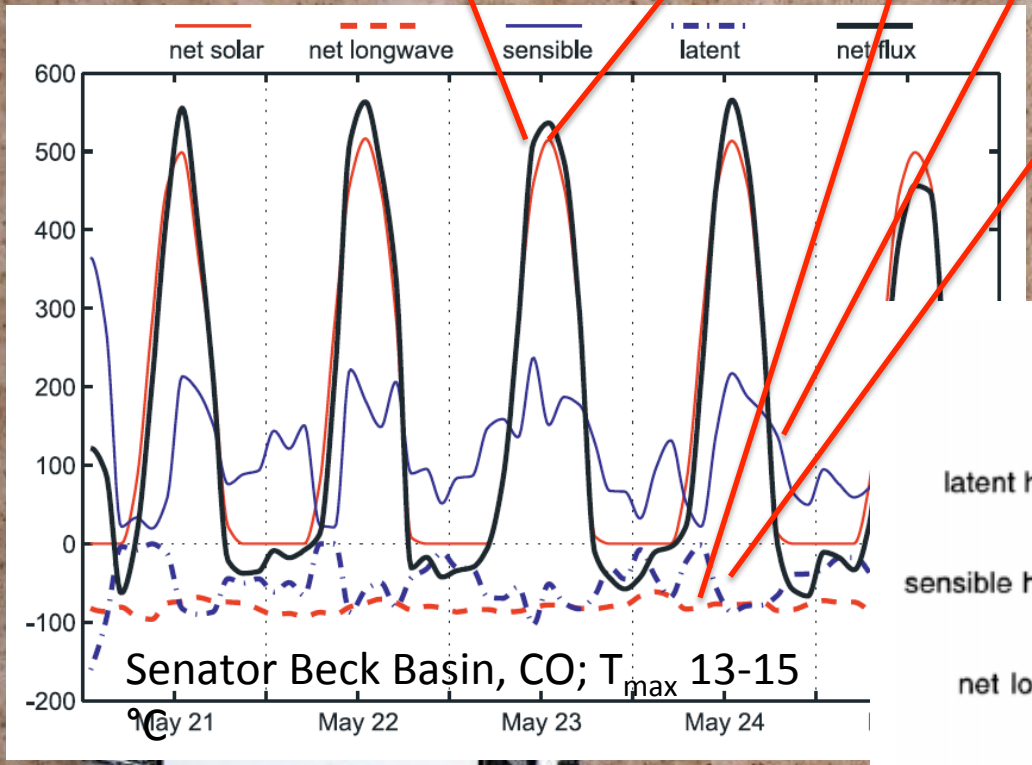

Senator Beck Basin, CO; T_{max} 13-15

Elk Range, Colorado River Basin, April 2009

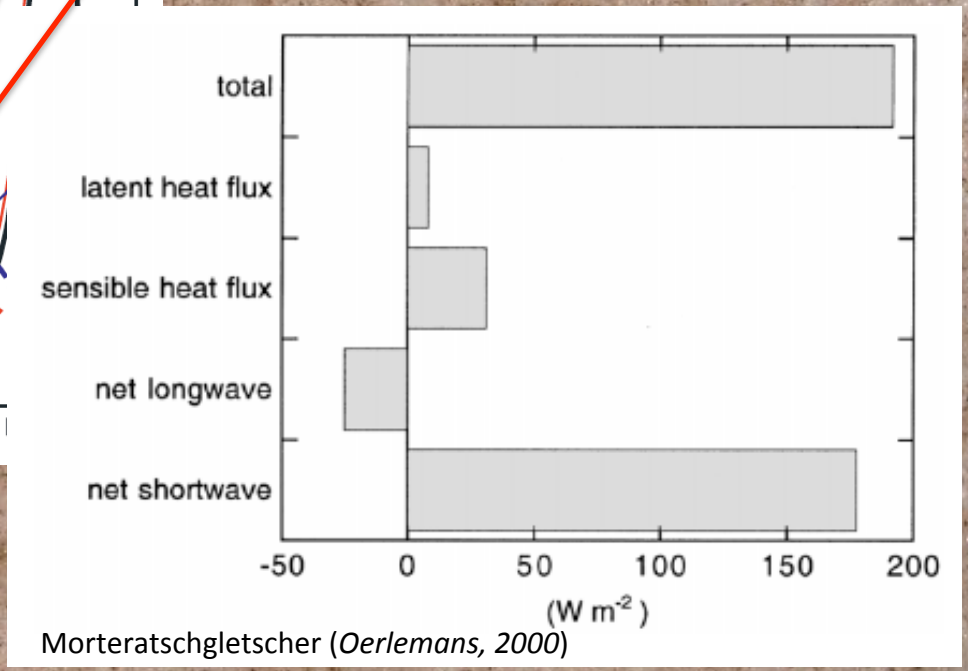

Morteratschgletscher (*Oerlemans, 2000*)

Upper Colorado River Basin

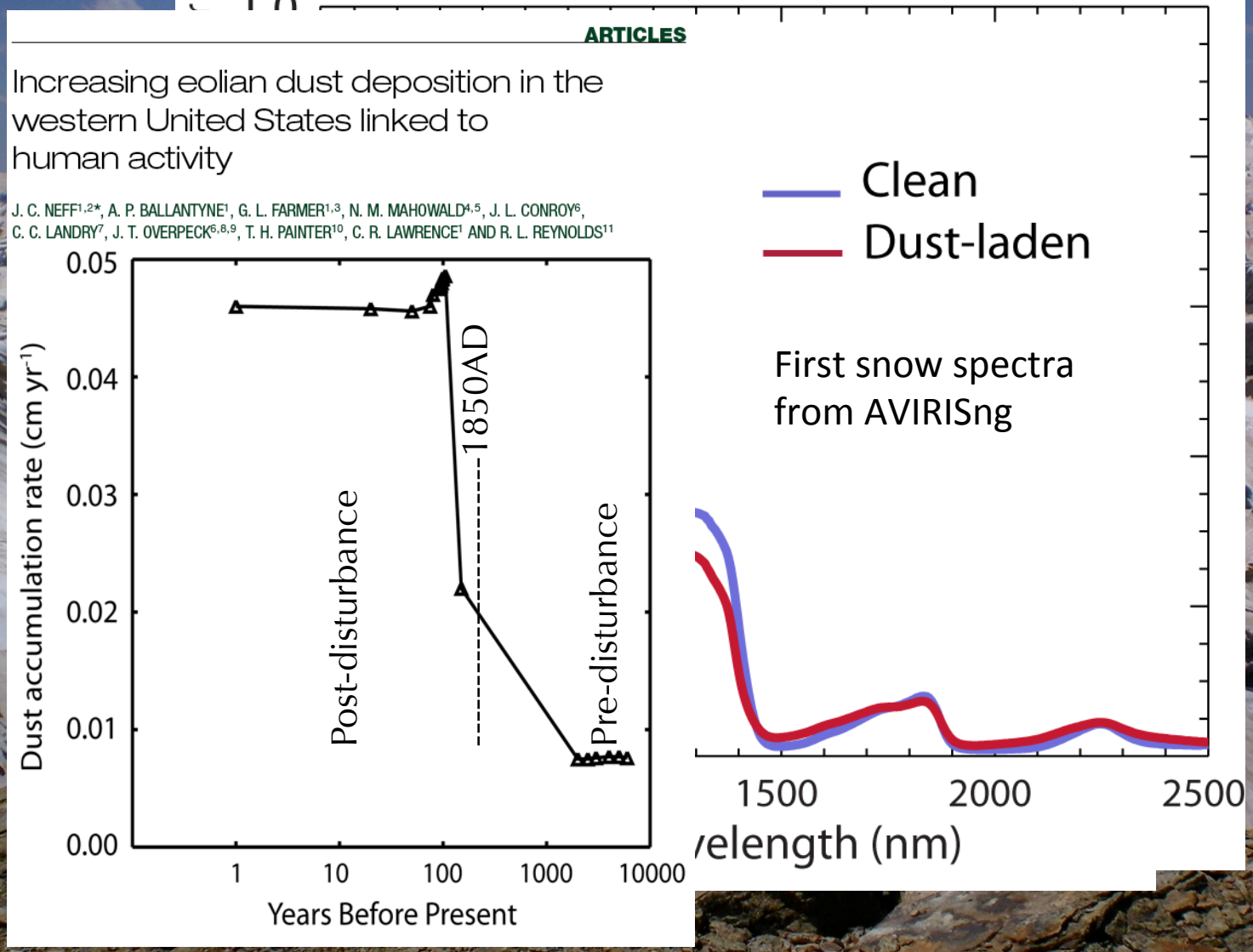

Response of Colorado River runoff to dust radiative forcing in snow

Thomas H. Painter[a,b,1], Jeffrey S. Deems[c,d], Jayne Belnap[e], Alan F. Hamlet[f], Christopher C. Landry[g], and Bradley Udall[d]

[a]Jet Propulsion Laboratory, California Institute of Technology, Pasadena, CA 91109; [b]Joint Institute for Regional Earth System Science and Engineering, University of California, Los Angeles, CA 90095; [c]National Snow and Ice Data Center, Boulder, CO 80309; [d]National Oceanic and Atmospheric Administration Western Water Assessment, Boulder, CO 80309; [e]United States Geological Survey, Southwest Biological Center, Moab, UT 84532; [f]University of Washington, Department of Civil and Environmental Engineering, Seattle, WA 98195; and [g]Center for Snow and Avalanche Studies, Silverton, CO 81433

Government and Manager Briefings:

- Anne Castle, Asst Secretary of Interior for Water and Science, Nov 2010
- US Global Change Research Program, Nov 2010
- NOAA HQ, Nov 2010
- Colorado River Water Users Association, Dec 2010
- EPA Section 8 + BLM, Dec 2010

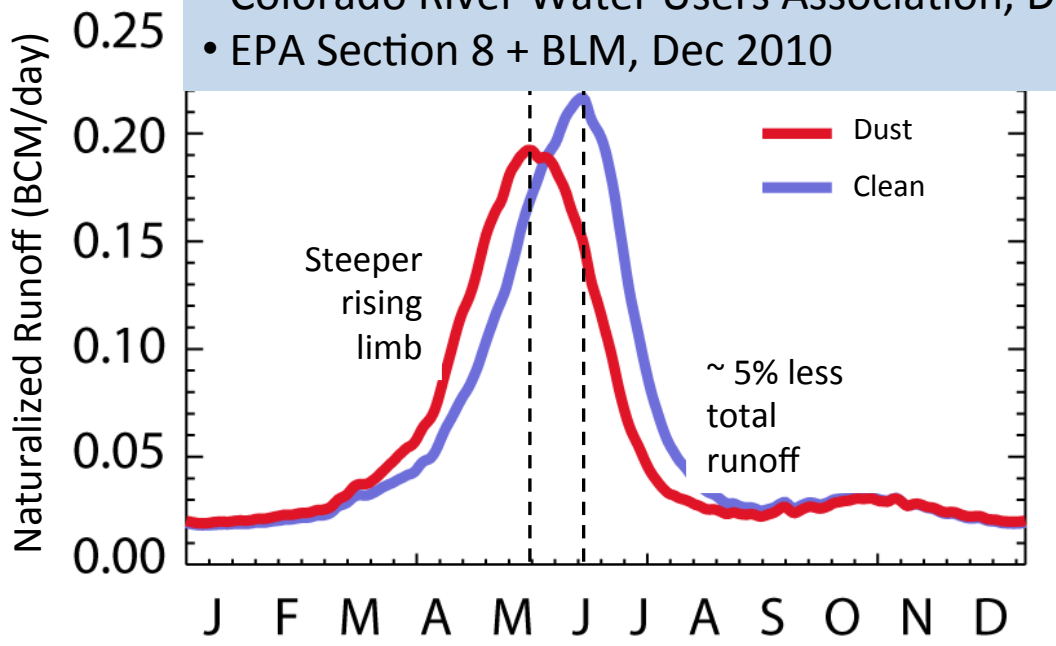

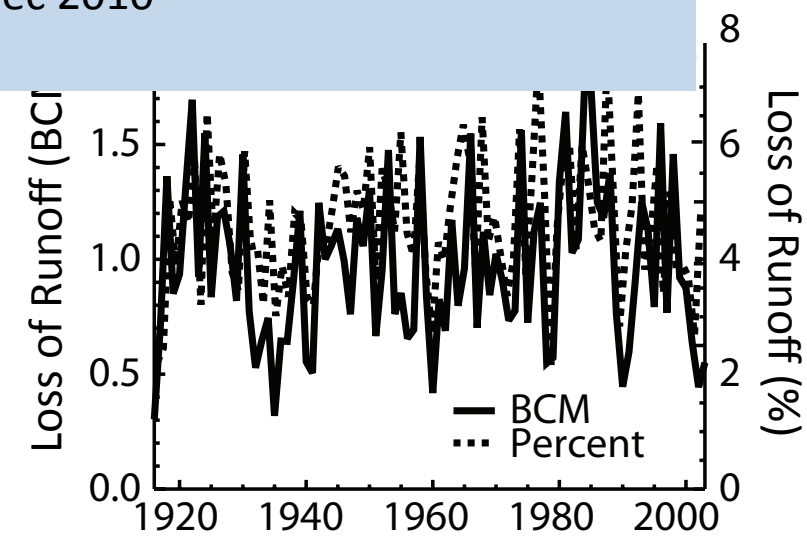

ıst radiative forcing in snow in the Upper Colorado River Basin duces annual runoff by ~5% or more than half of Mexico's annual otment under treaty. **Painter et al 2010, *PNAS***

Snowmelt Runoff and Dust Forcing

Uncompahgre River, Colorado
Upper Colorado River Basin
Ordinate

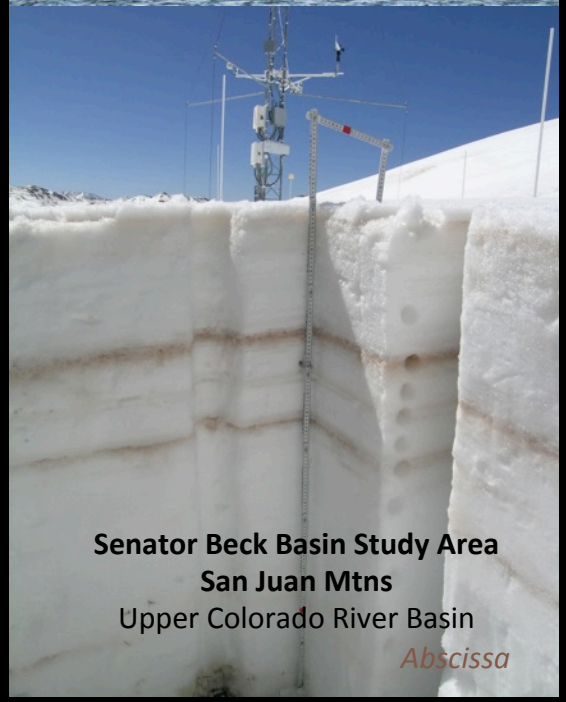

Senator Beck Basin Study Area
San Juan Mtns
Upper Colorado River Basin
Abscissa

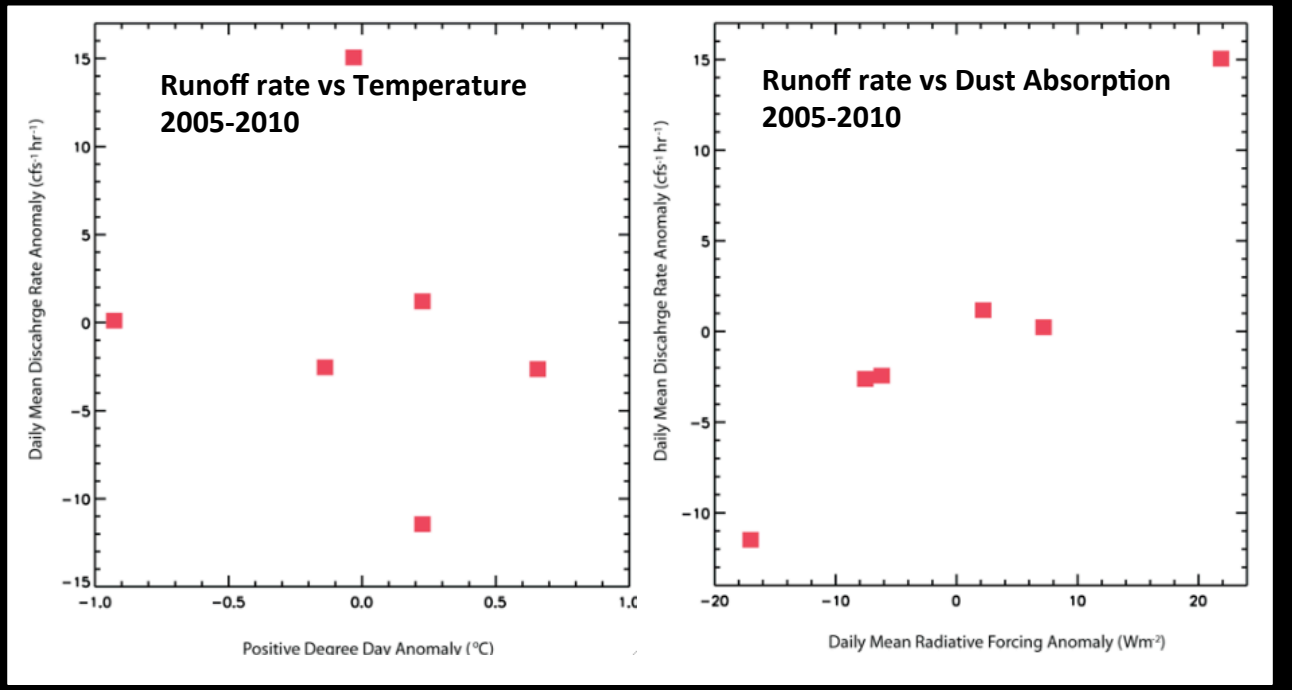

Take Home: Albedo and radiative forcing drive

Painter et al (in preparation)
Funding: *NASA Interdisciplinary Science*

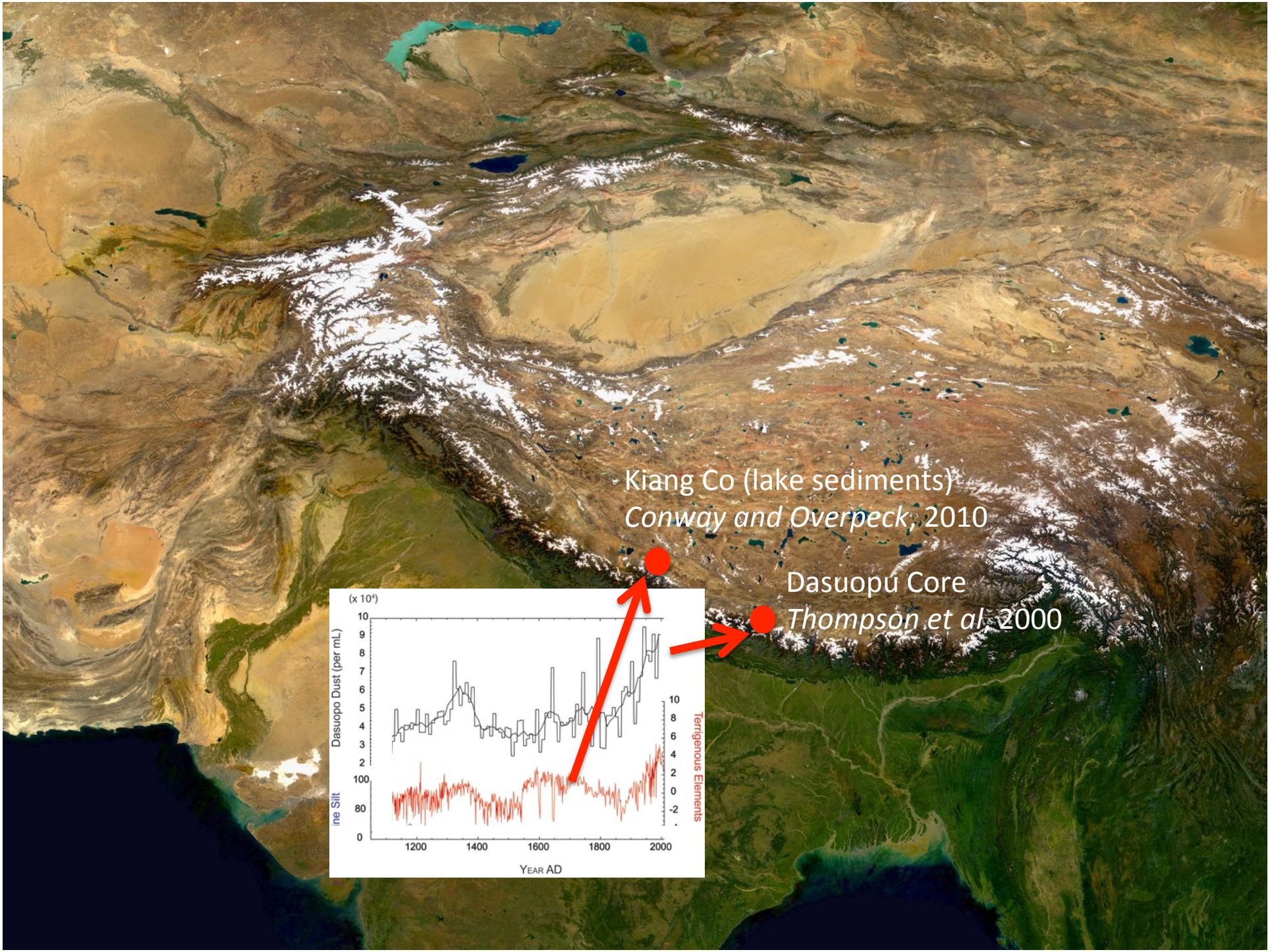
Kiang Co (lake sediments)
Conway and Overpeck, 2010
Dasuopu Core
Thompson et al. 2000
(x 10⁴)
Dasuopo Dust (per mL)
ine Silt
Terrigenous Elements
Year AD
1200
1400
1600
1800
2000

Caucasus Mountains

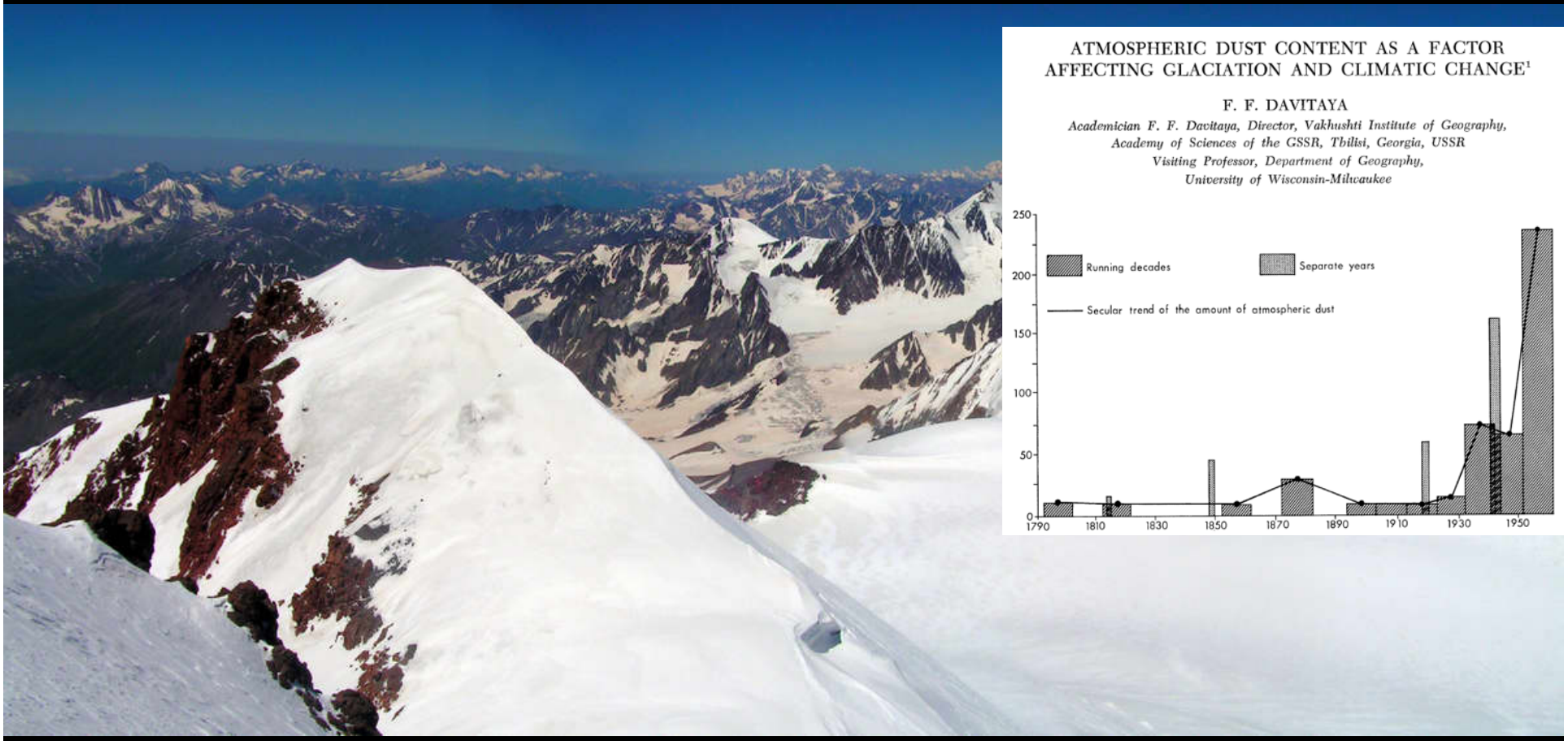

ATMOSPHERIC DUST CONTENT AS A FACTOR AFFECTING GLACIATION AND CLIMATIC CHANGE[1]

F. F. DAVITAYA

Academician F. F. Davitaya, Director, Vakhushti Institute of Geography, Academy of Sciences of the GSSR, Tbilisi, Georgia, USSR
Visiting Professor, Department of Geography, University of Wisconsin-Milwaukee

Black Carbon

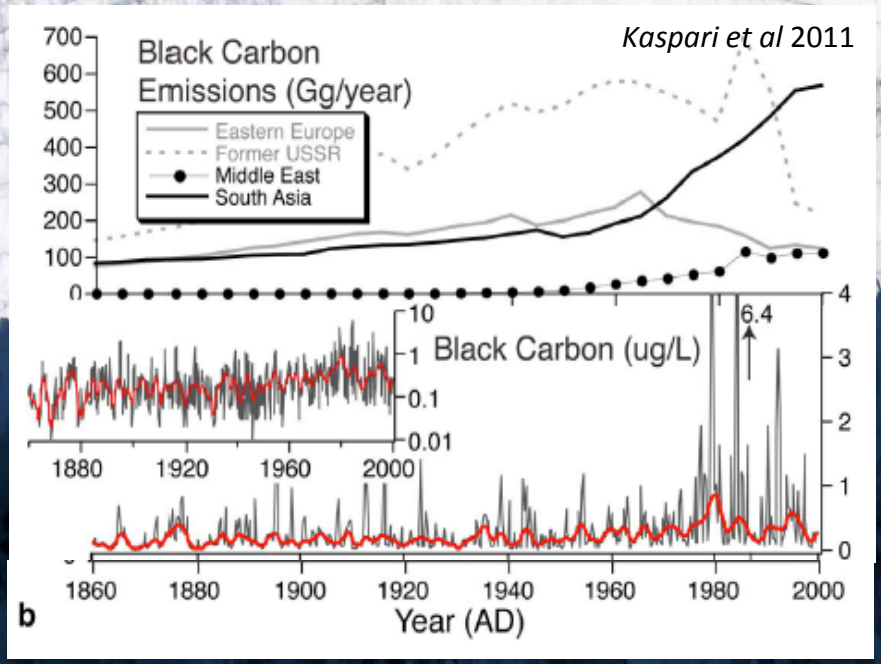

Kaspari et al 2011

PNAS

Black soot and the survival of Tibetan glaciers

Baiqing Xu[a,b], Junji Cao[b], James Hansen[c,1], Tandong Yao[a], Daniel R. Joswia[a], Ninglian Wang[d], Guangjian Wu[a], Mo Wang[a], Huabiao Zhao[a], Wei Yang[a], Xiaoqin Liu[e], and Jiangiao He[d]

JOURNAL OF GEOPHYSICAL RESEARCH, VOL. 114, D03108, doi:10.1029/2008JD011039, 2009

Click Here for Full Article

Effects of soot-induced snow albedo change on snowpack and hydrological cycle in western United States based on Weather Research and Forecasting chemistry and regional climate simulations

PNAS

Soot climate forcing via snow and ice albedos

James Hansen*†‡ and Larissa Nazarenko*†

Atmospheric Research 92 (2009) 114–123

Contents lists available at ScienceDirect

Atmospheric Research

journal homepage: www.elsevier.com/locate/atmos

ELSEVIER

Black Carbon (BC) in the snow of glaciers in west China and its potential effects on albedos

Jing Ming [a,b,c,d,e,*], Cunde Xiao [b,c], Helene Cachier [f], Dahe Qin [a,c], Xiang Qin [c], Zhongqi Li [c], Jianchen Pu [c]

Vol 448|2 August 2007|doi:10.1038/nature06019 nature

LETTERS

Warming trends in Asia amplified by brown cloud solar absorption

Veerabhadran Ramanathan[1], Muvva V. Ramana[1], Gregory Roberts[1], Dohyeong Kim[1], Craig Corrigan[1], Chul Chung[1] & David Winker[2]

We propose that the combined warming trend of 0.25 K per decade may be sufficient to account for the observed retreat of the Himalayan glaciers[4–6].

What about MODIS and VIIRS?

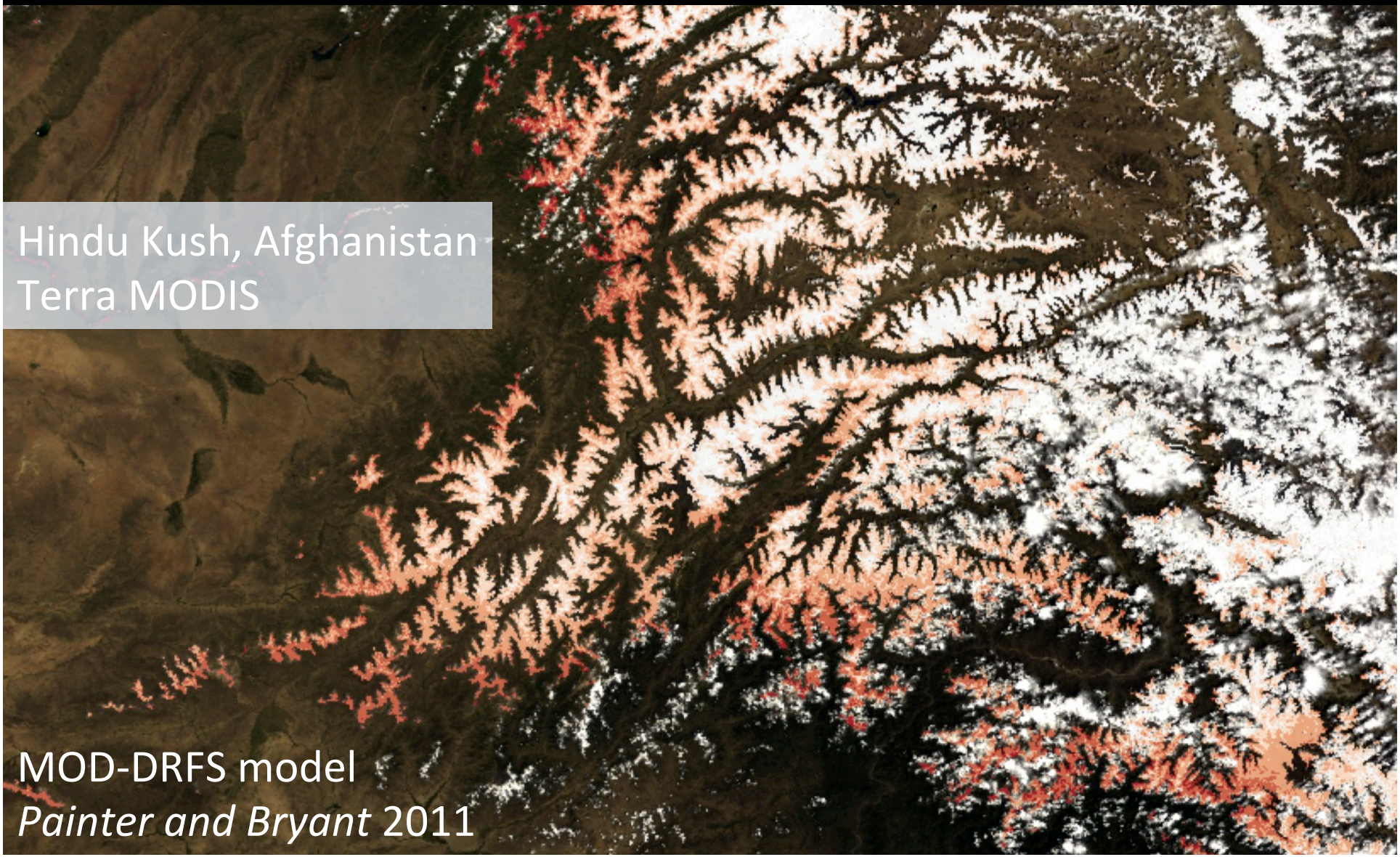

Spectrometer vs MODIS

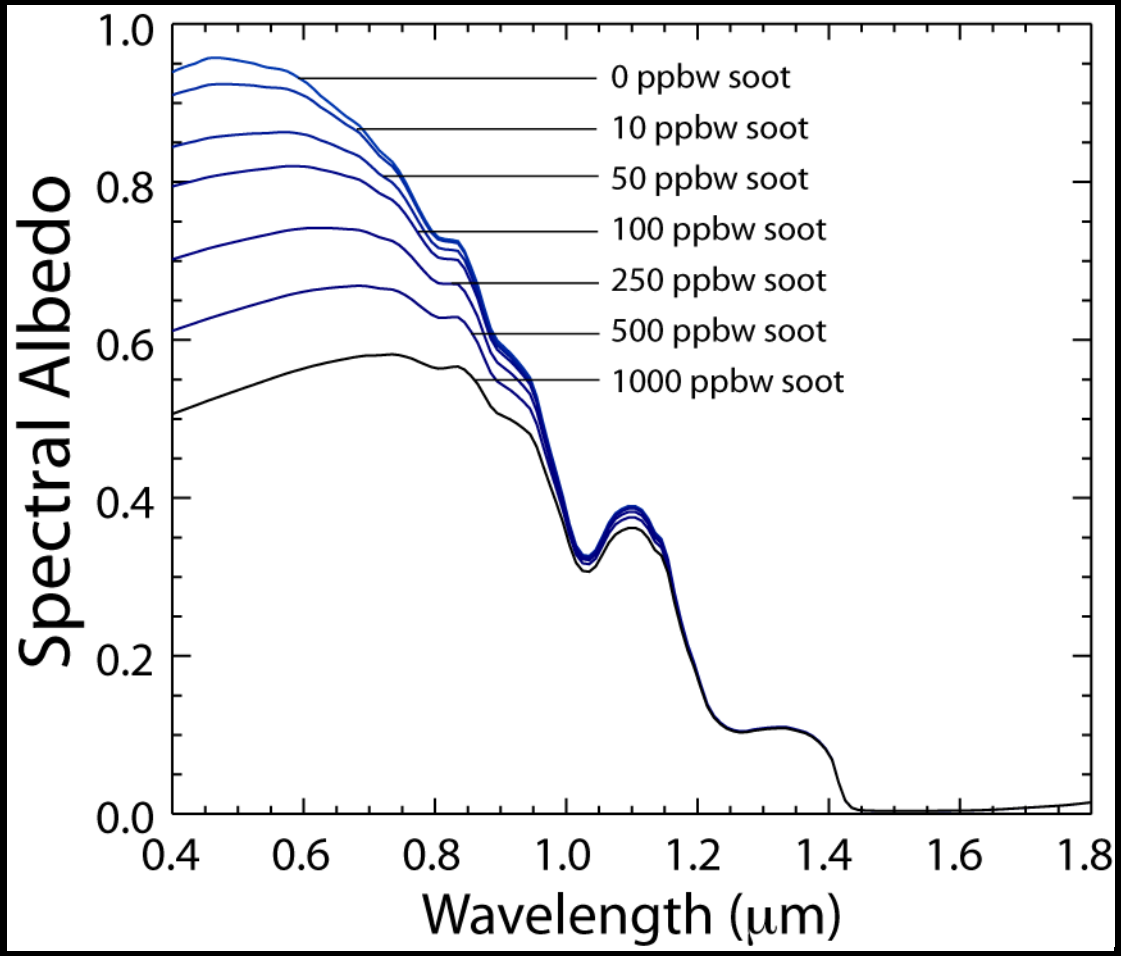

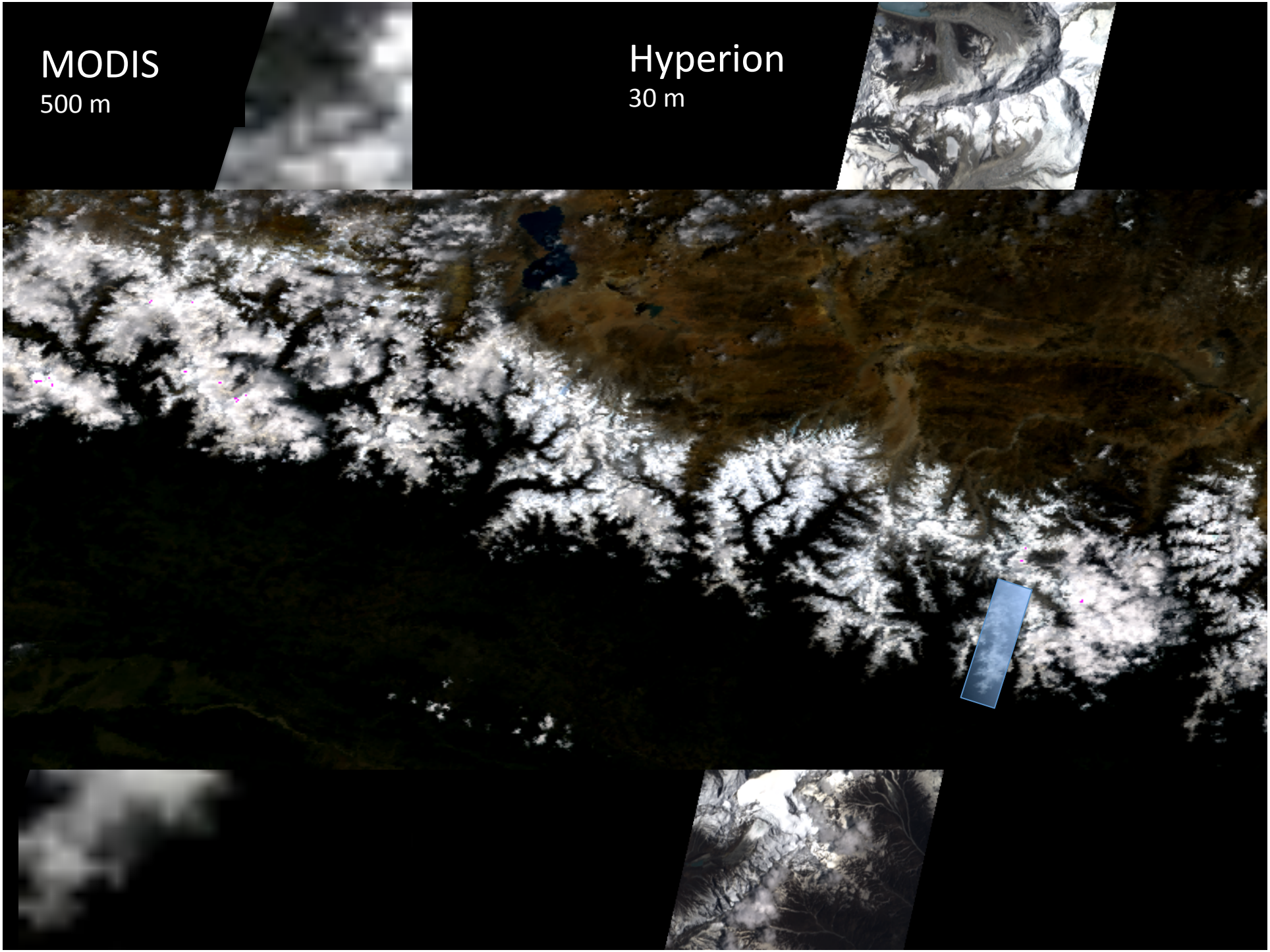
MODIS
500 m
Hyperion
30 m

Radiative Forcing in Snow

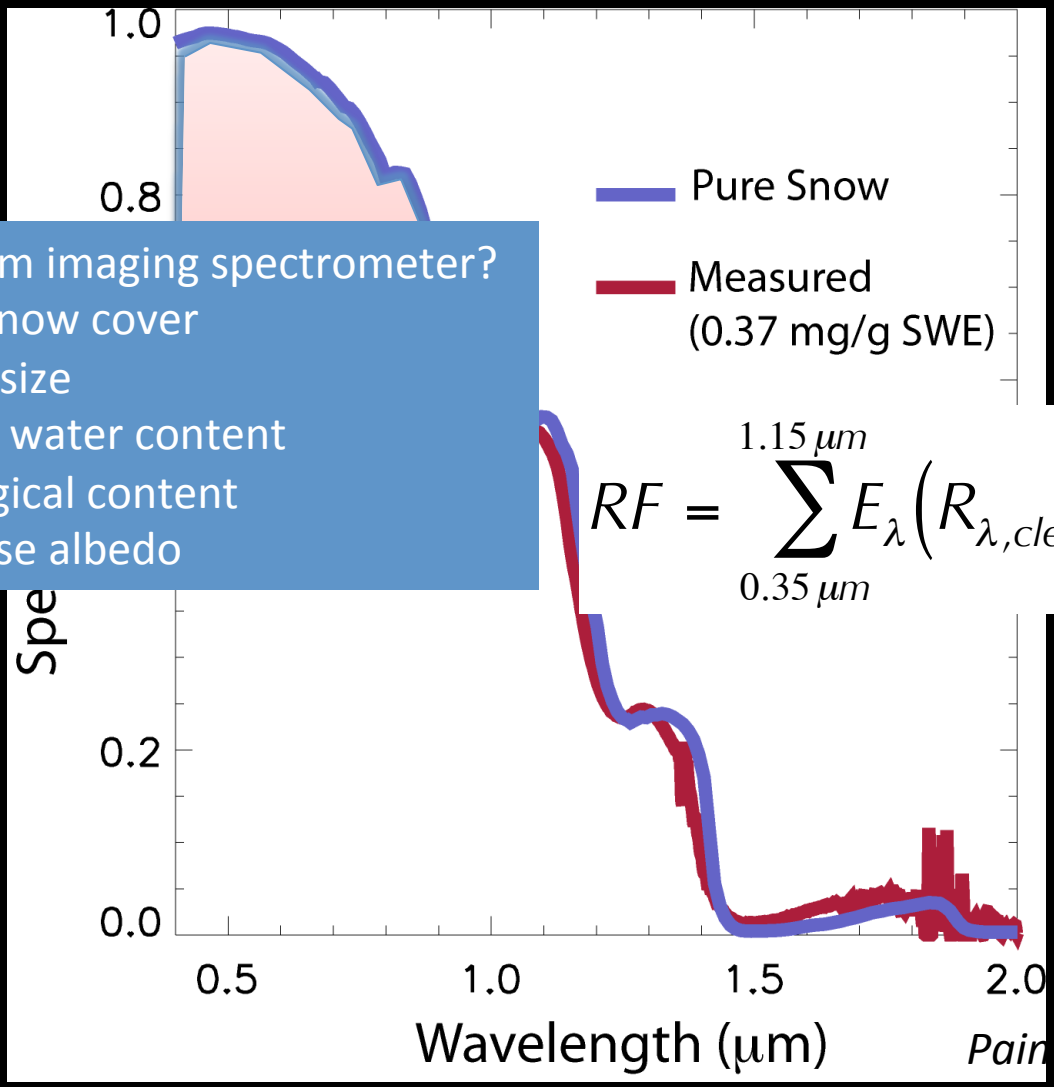

What else from imaging spectrometer?

- Fractional snow cover
- Snow grain size
- Snow liquid water content
- Snow biological content
- and of course albedo

$$RF = \sum_{0.35\,\mu m}^{1.15\,\mu m} E_\lambda \left(R_{\lambda,clean} - R_{\lambda,dust} \right) d\lambda$$

NASA IDS *Integrated hydrologic response to extreme dust deposition to mountain snowcover of the Colorado River Basin*

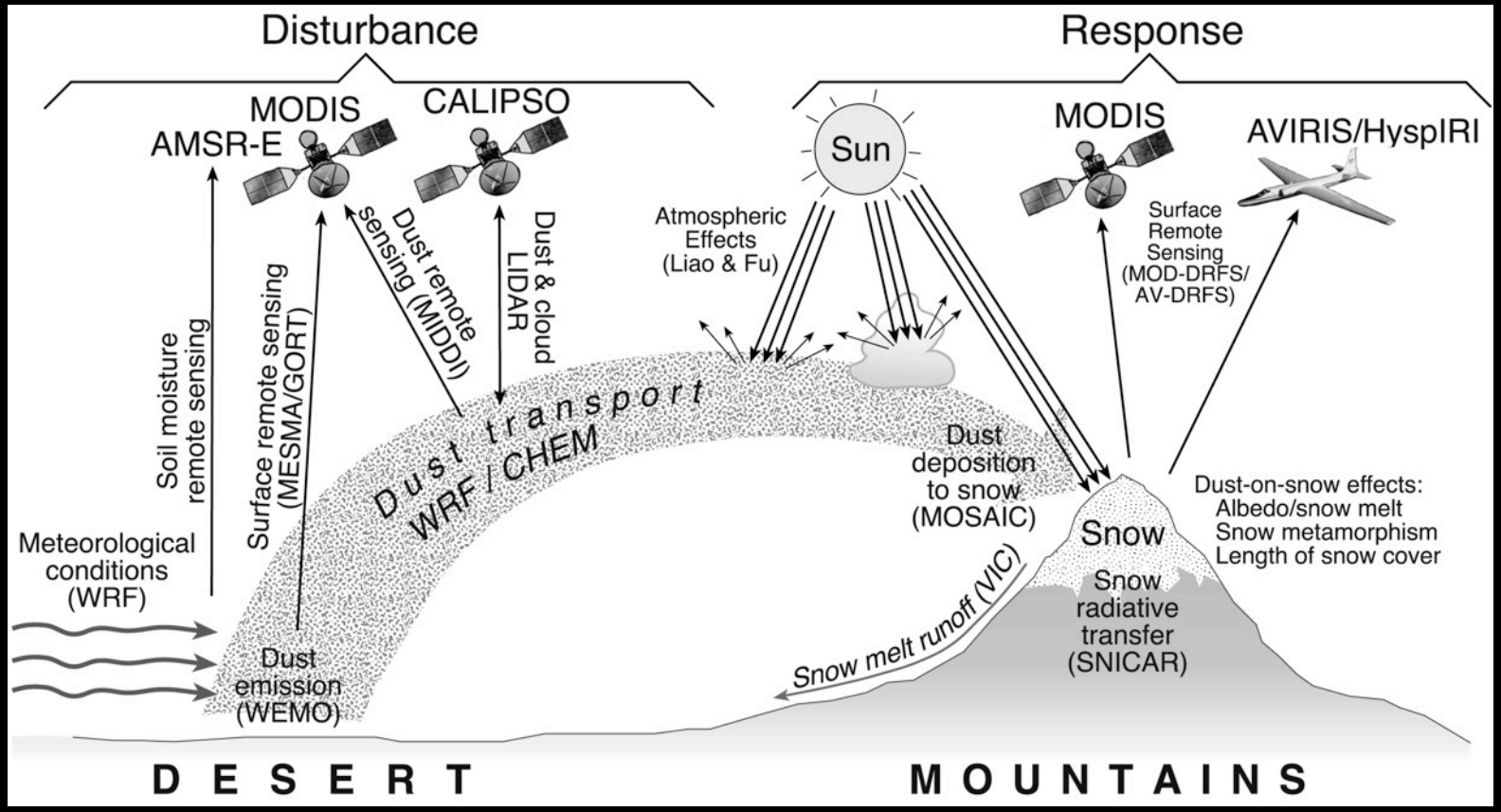

AVIRISclassic
6/23/2011

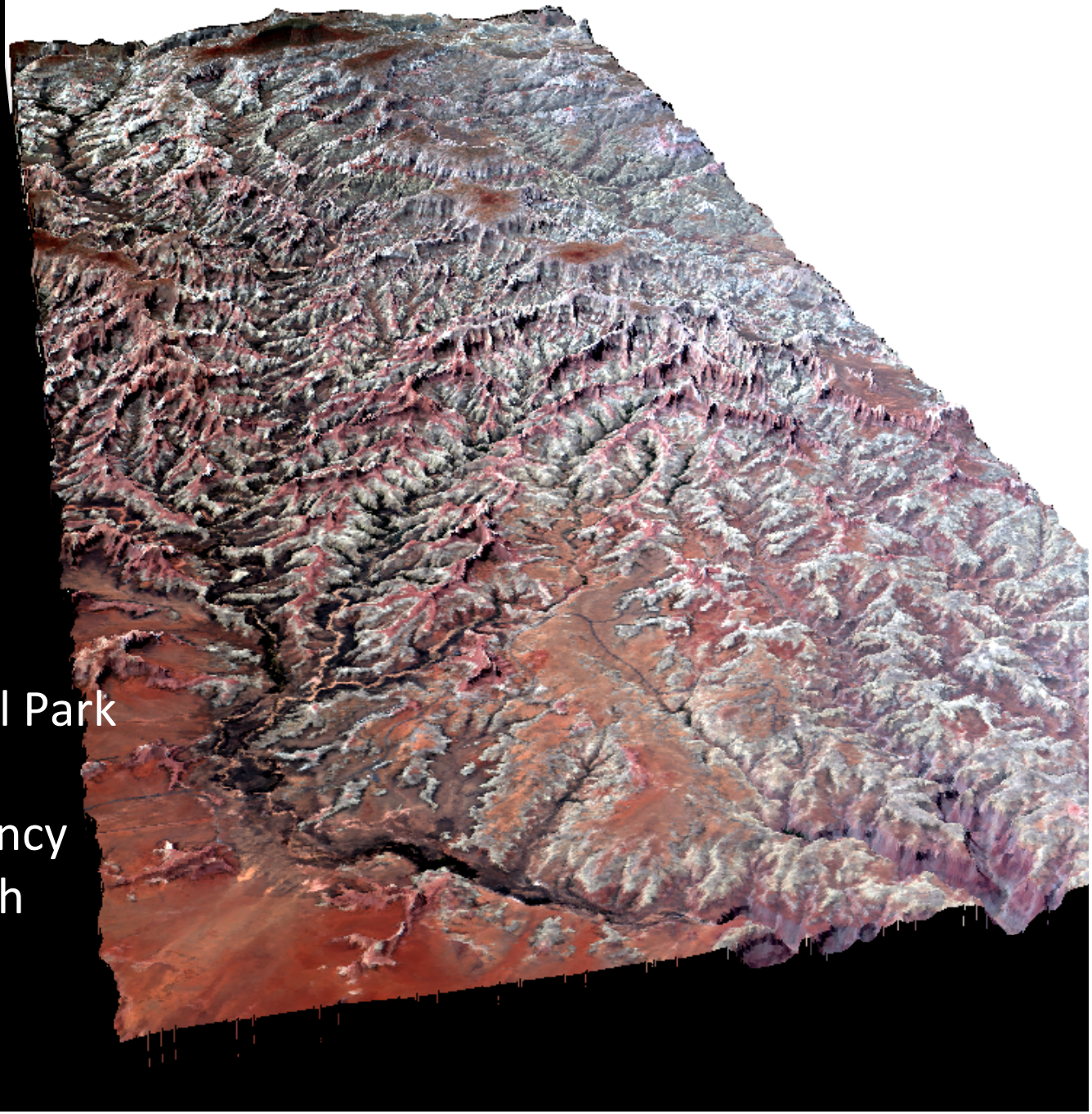

Canyonlands National Park
and
The Nature Conservancy
Canyonlands Research
Center

Upper Colorado River Basin

San Juan Mountains, CO

15 June 2011

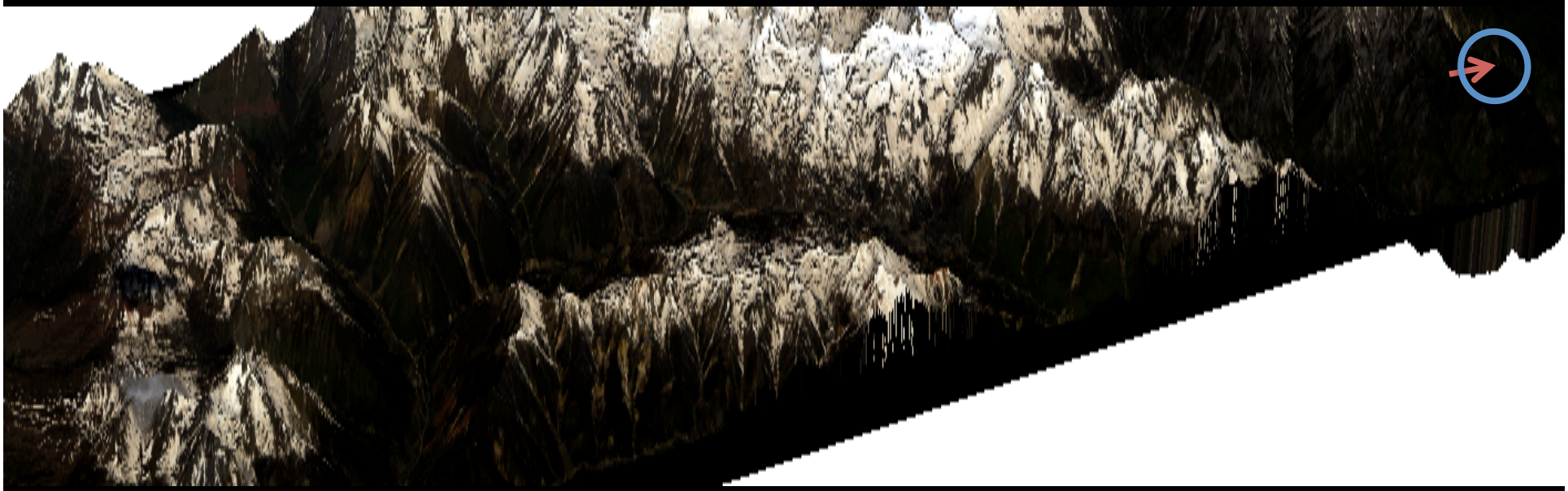

Atmospheric Correction in Rough Terrain

- AVIRISclassic acquisitions over spring 2011 (only 15 June presented here)
- ReSe Applications ATCOR4.0
- Rugged terrain model
- Variable visibility calculation
- Full spatial/spectral irradiance (direct & diffuse) reportage

Constrained by sunphotometer

Red Mountain Pass AERONET site
Swamp Angel Study Plot

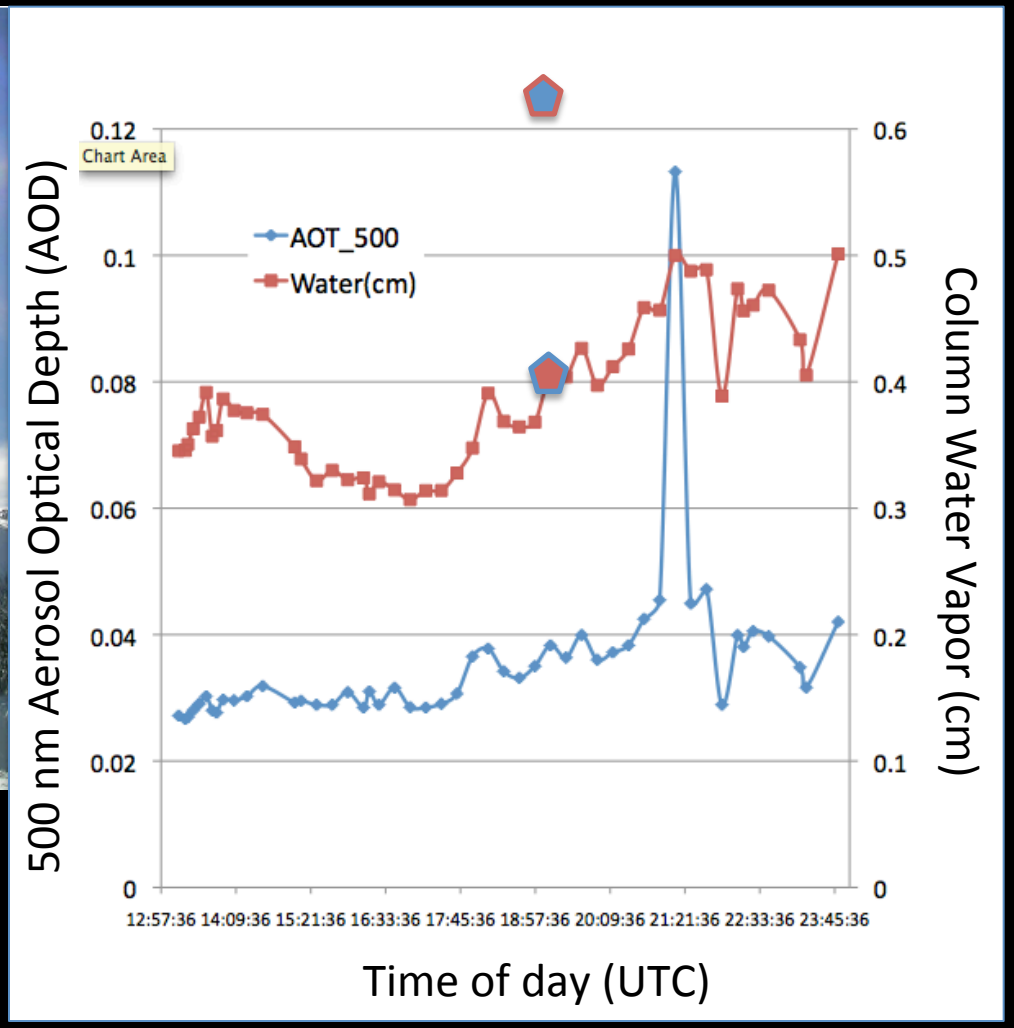

15 June 2011

Irradiances

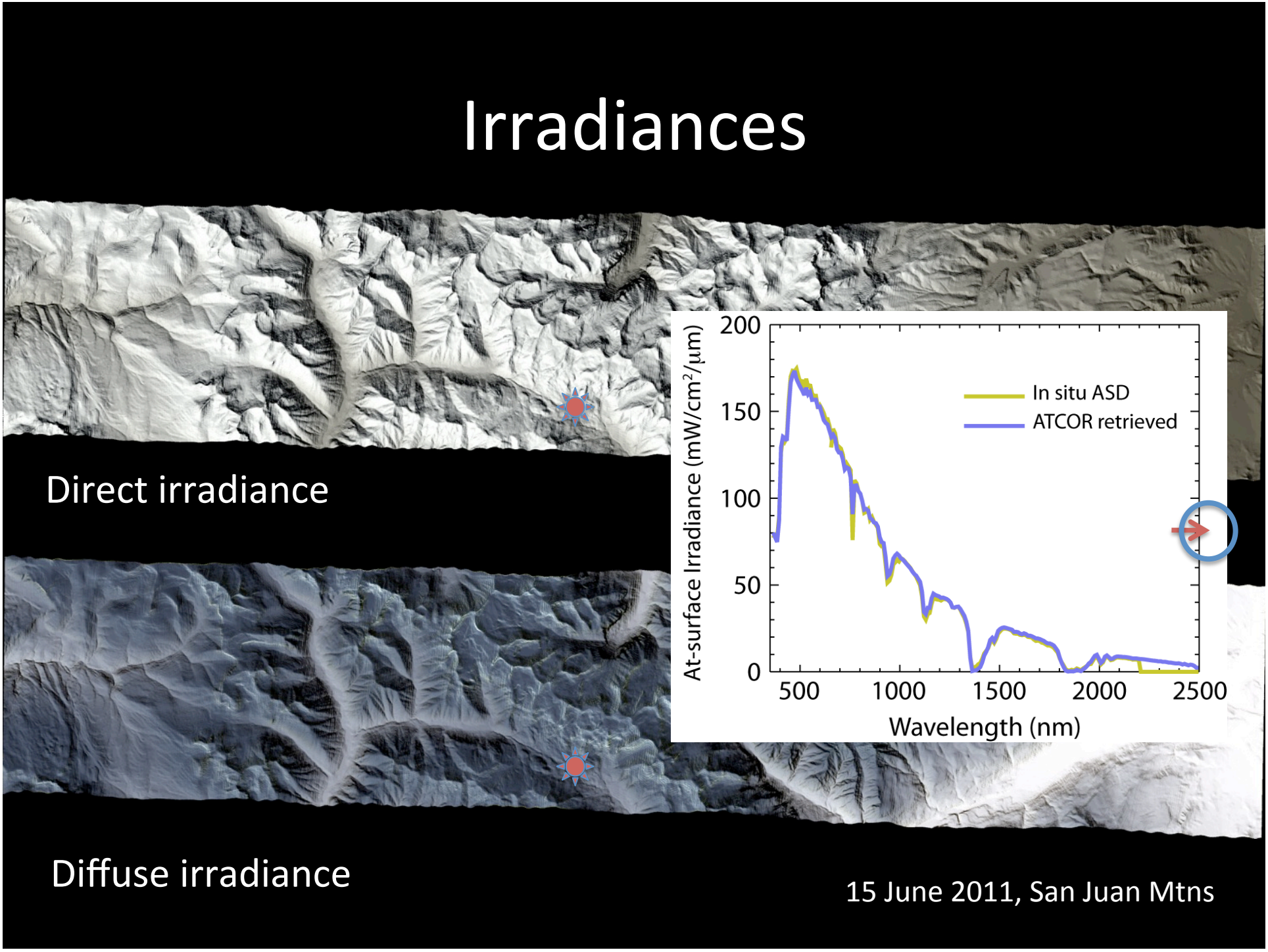

Reflectance

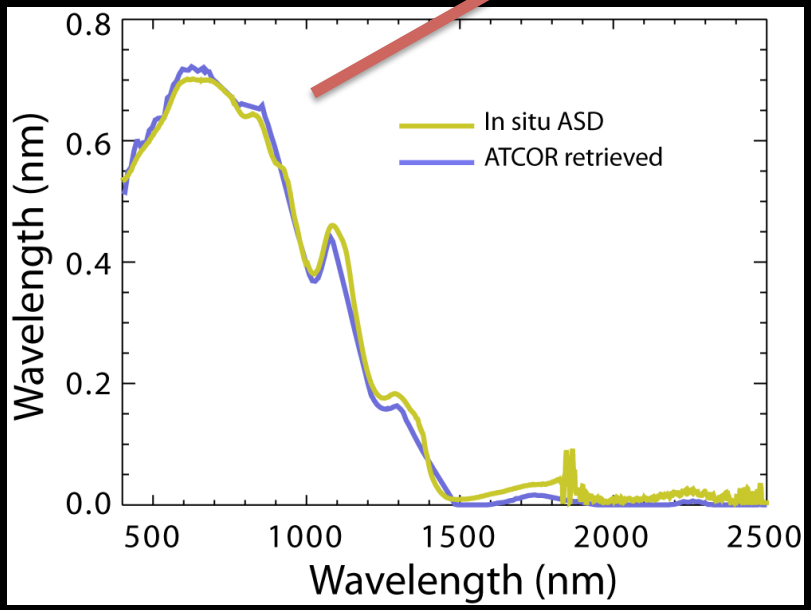

Albedo and radiative forcing

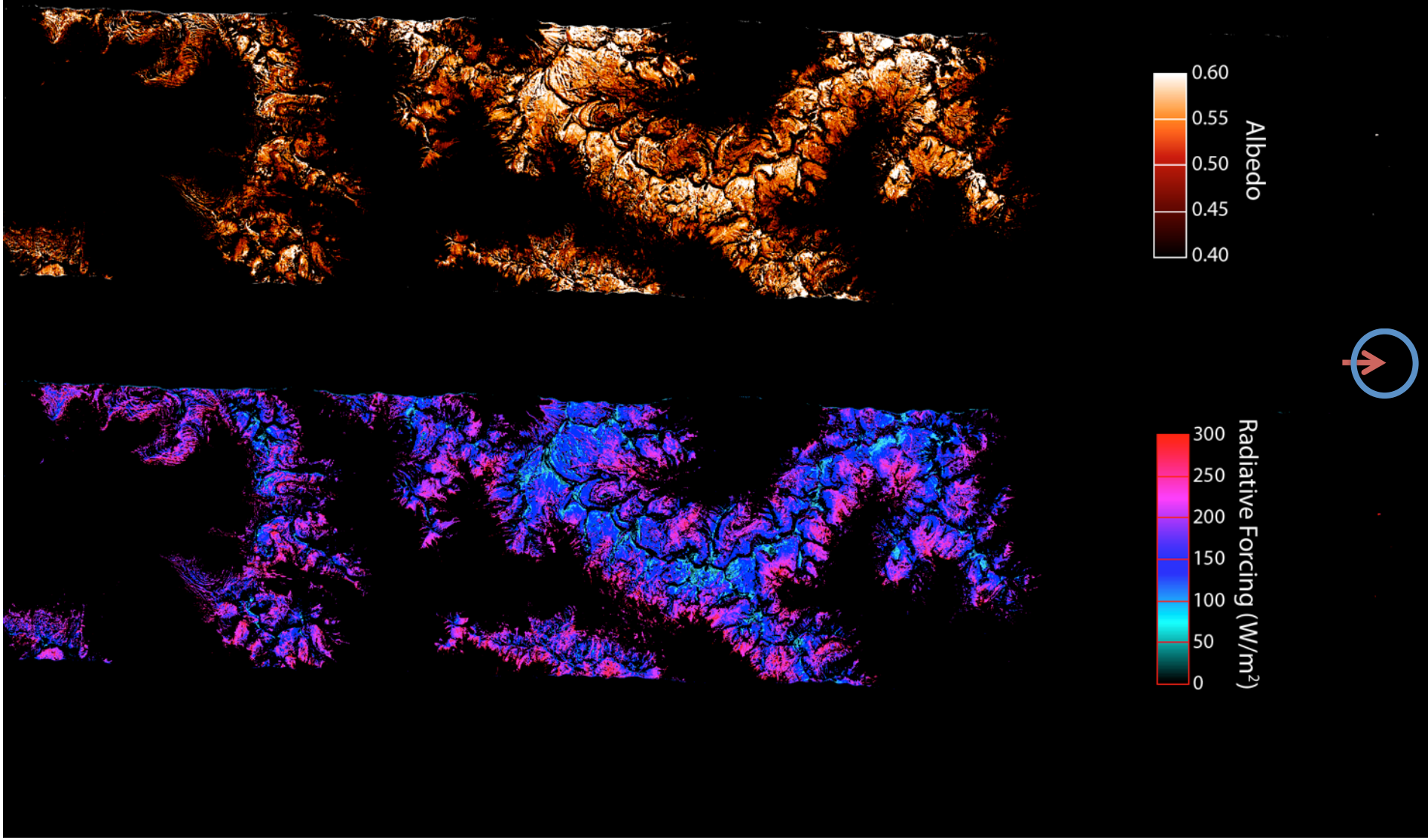

From West

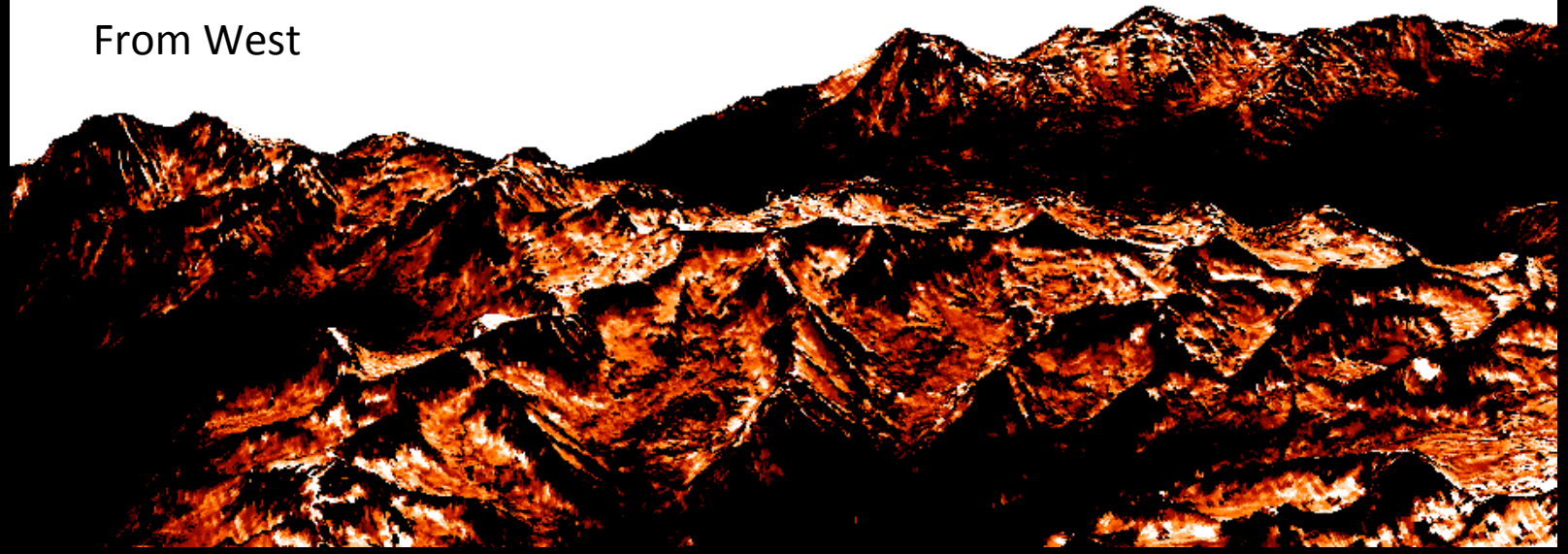

From East

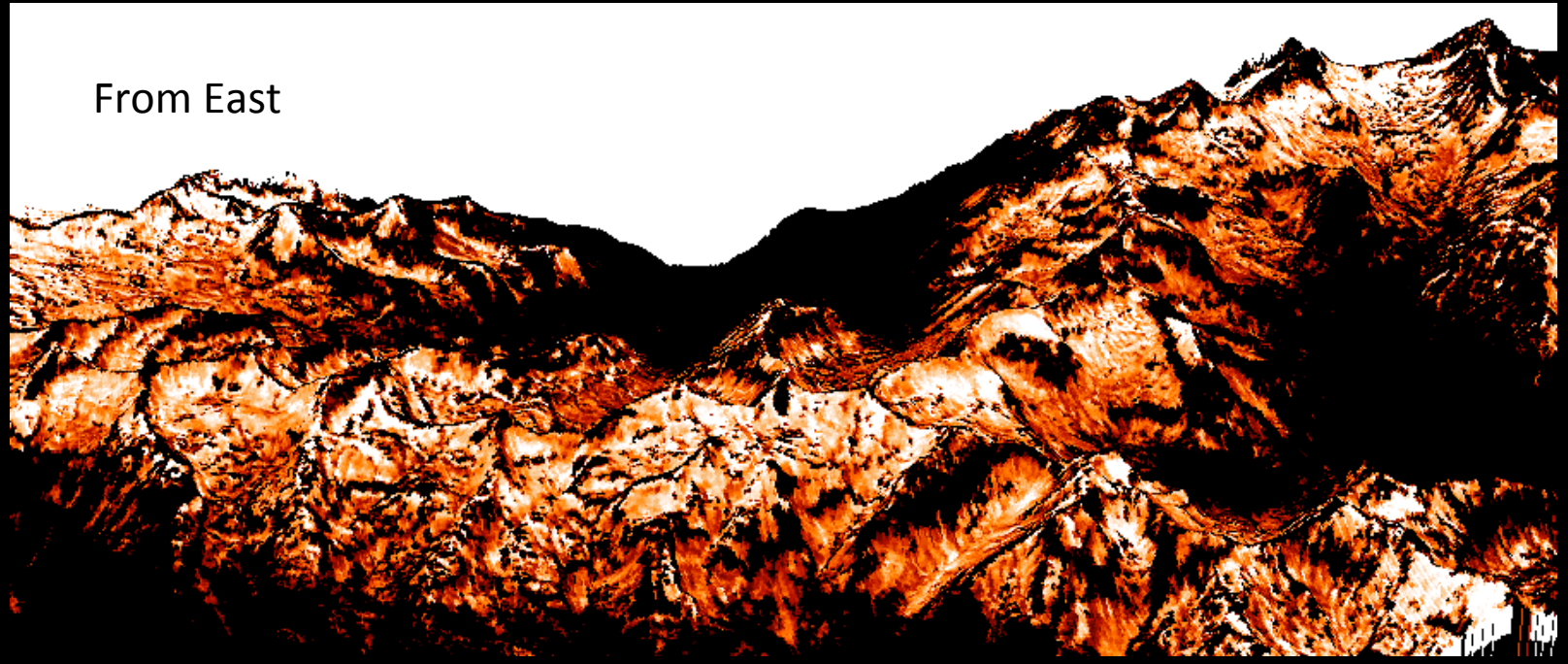

What about the thermal bands?

$$\frac{dU}{dt} + Q_m = (1-\alpha)S + L^* + Q_s + Q_v + Q_g + Q_r$$

Snow Temp < 0 °C

Snow Temp = 0 °C

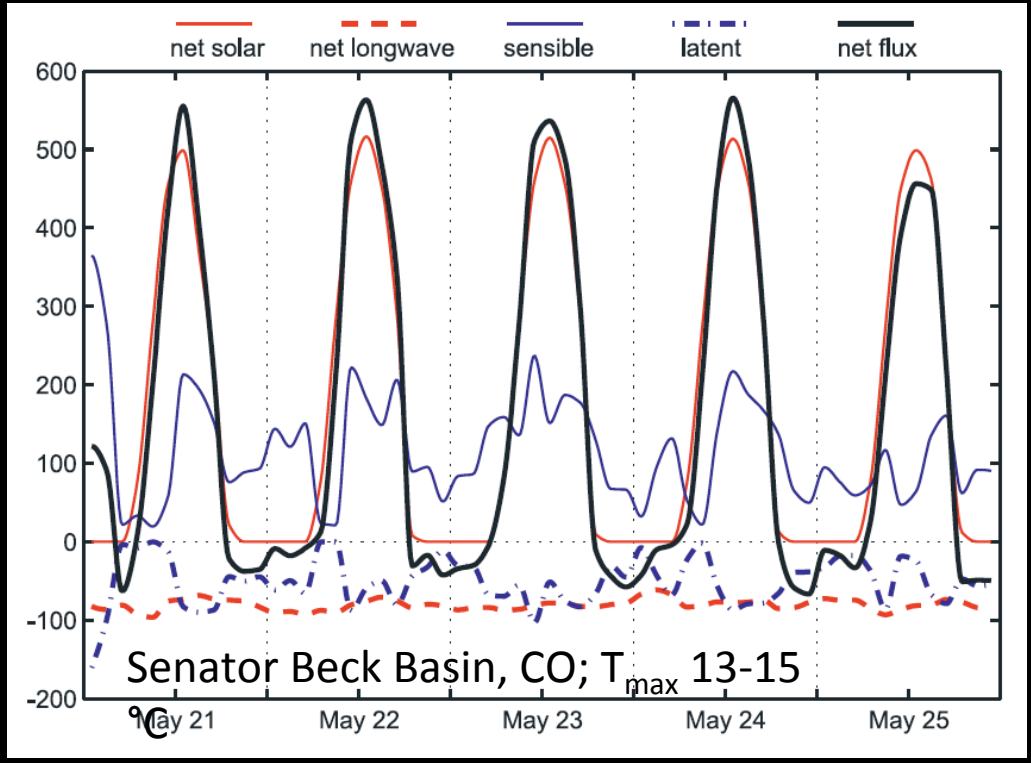

Summary

- Changes in global snow and ice drive powerful positive feedbacks in the Earth system and
- HyspIRI will provide global direct access to snow albedo, radiative forcing by dust and BC, and the snow thermal response
- HyspIRI will also provide a baseline against which reductions in dust loading and BC may be assessed
- Aerosol model remains the powerful challenge for reflectance retrievals, particularly in rough mountain terrain
- Thanks to Diane Wickland, Jared Entin, Rob Green, Ian McCubbin, Michael Eastwood, Sarah Lundeen

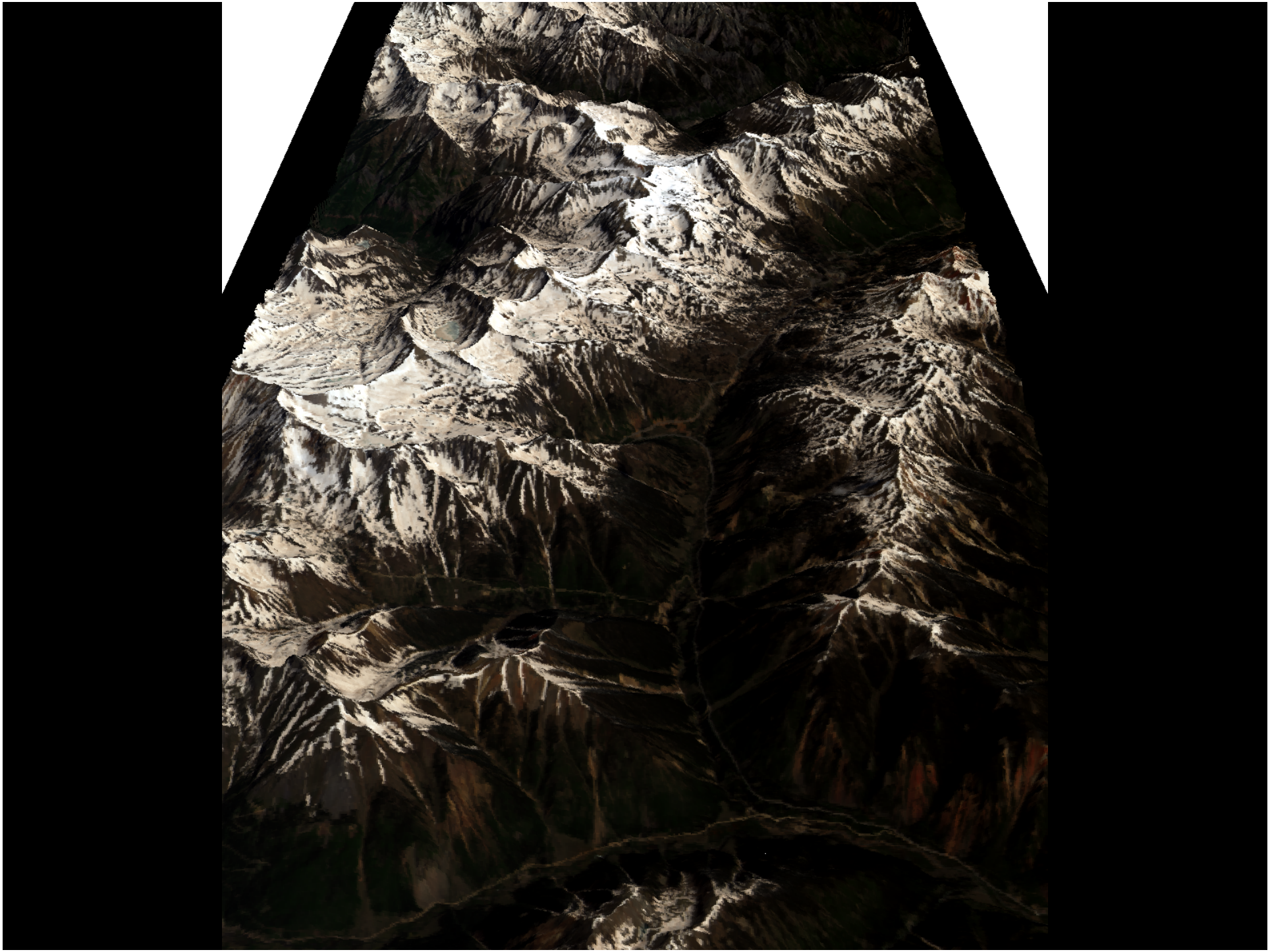

Characterization of Glint and Its Impact on HyspIRI Aquatic Science

2011 HyspIRI Science Workshop, Washington, D.C., 23 August 2011

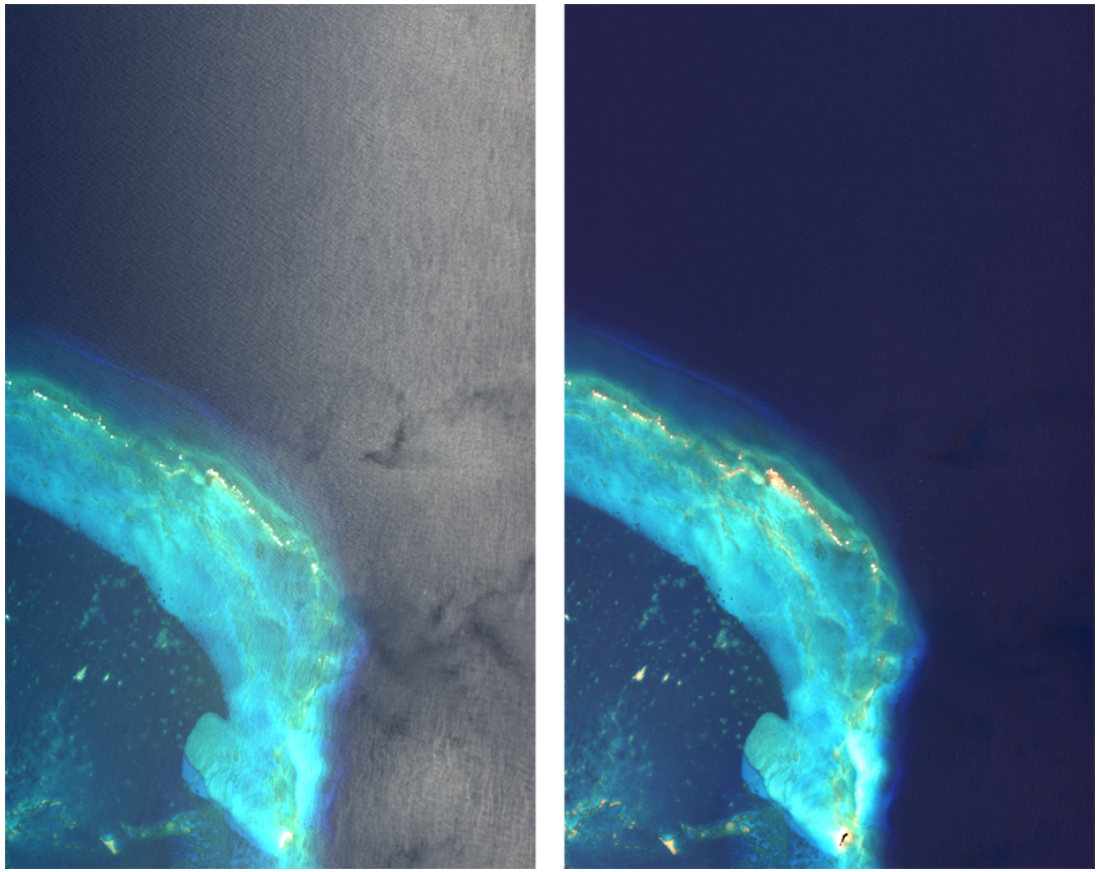

Contributors

Eric J. Hochberg, Curtis D. Mobley, Youngje Park, James Goodman, Kevin R. Turpie, Bo-Cai Gao, Carl F. Bruce, Robert O. Green, Robert G. Knox, Frank E. Muller-Karger, Elizabeth M. Middleton, Peter J. Minnet, Chelle Gentemann, Bogdan V. Oaida, Richard C. Zimmerman

Background

Sources of light contributing to the remotely sensed signal

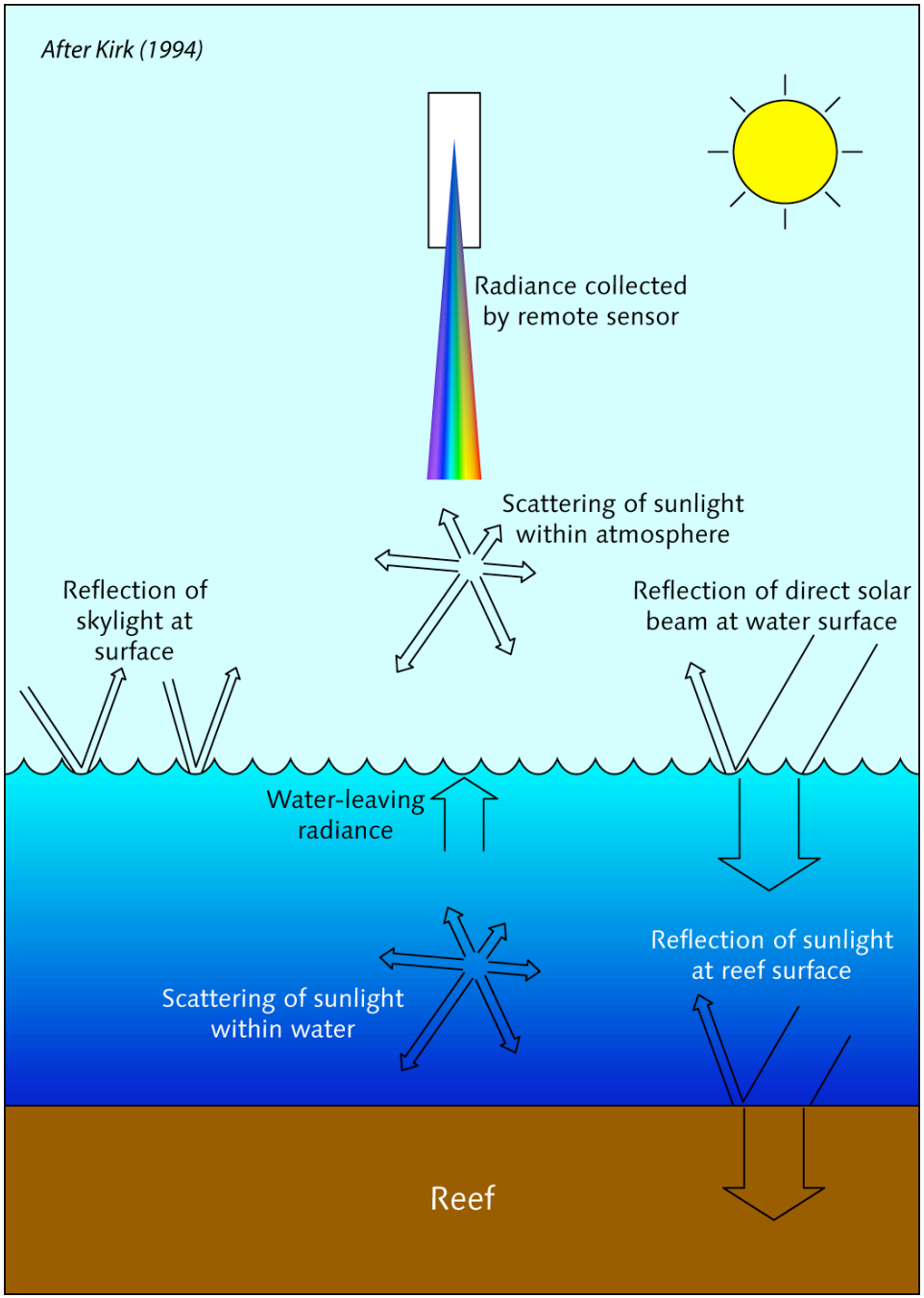

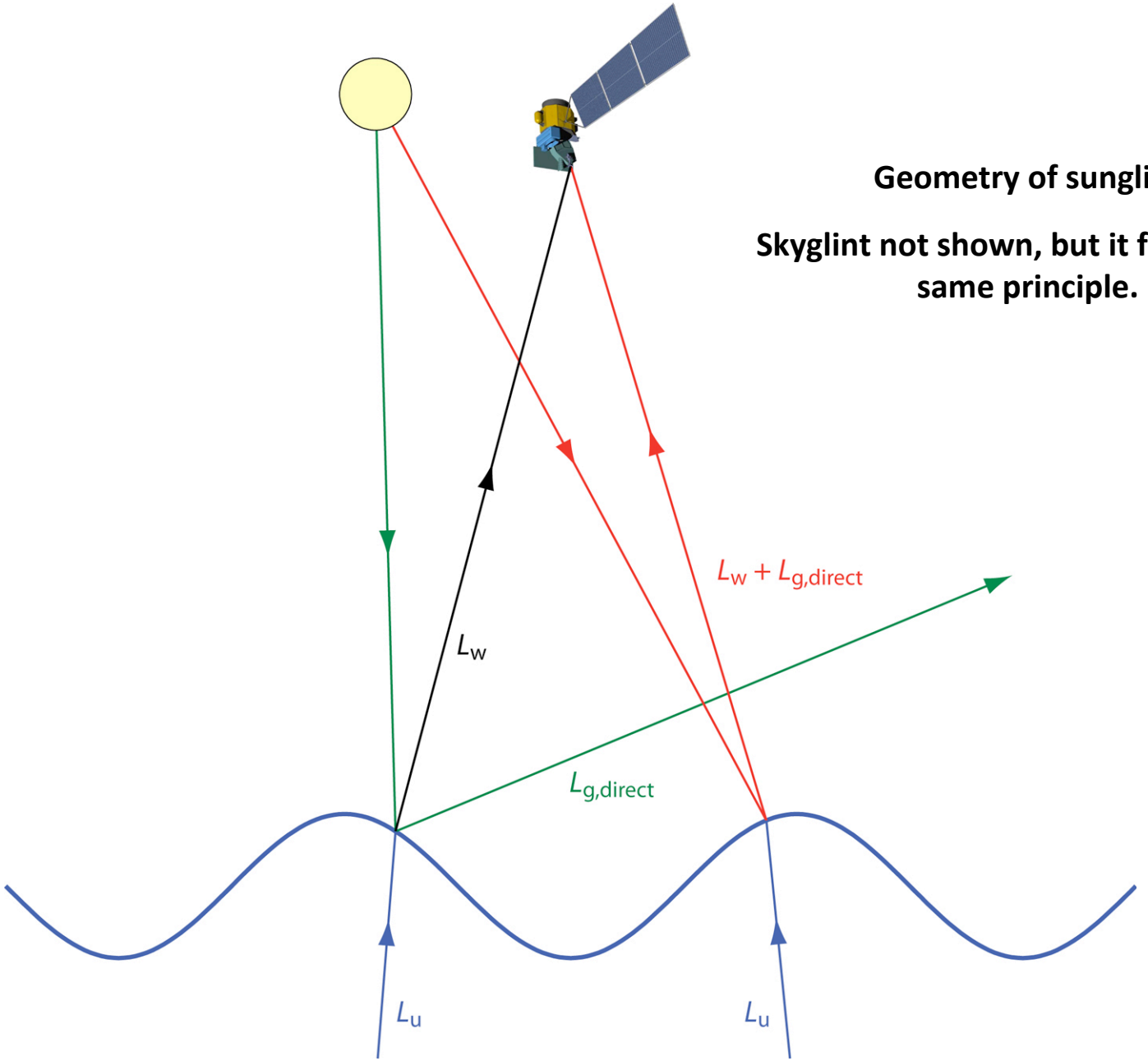

Geometry of sunglint

Skyglint not shown, but it follows the same principle.

Background: Quickbird Examples

Tampa Bay, Florida. Very calm water. No apparent sunglint, only skyglint.

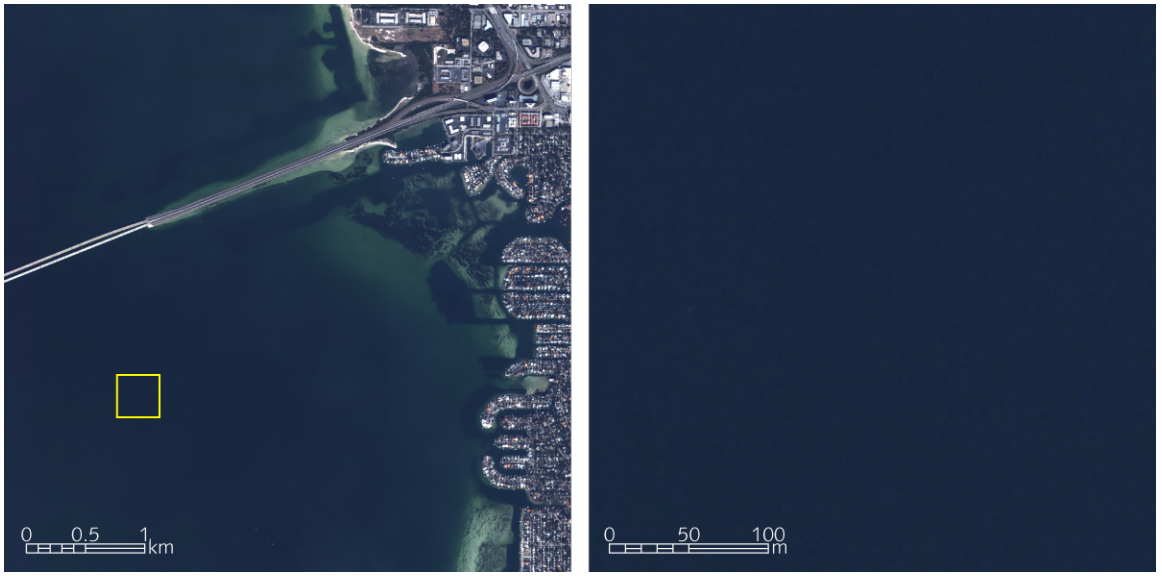

Bermuda. Fairly confused sea state. Sunglint on wave faces, skyglint implicit.

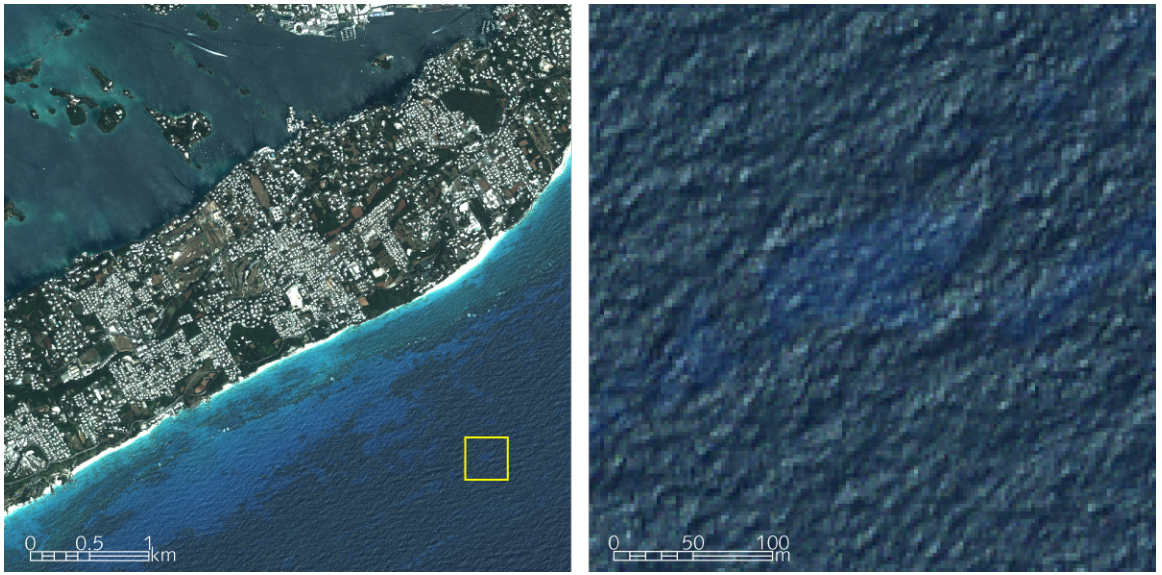

Background

HyspIRI observation geometry. The satellite is moving south (outward from the page).

These view angles, coupled with sun angles, may lead to glint in HyspIRI aquatic scenes.

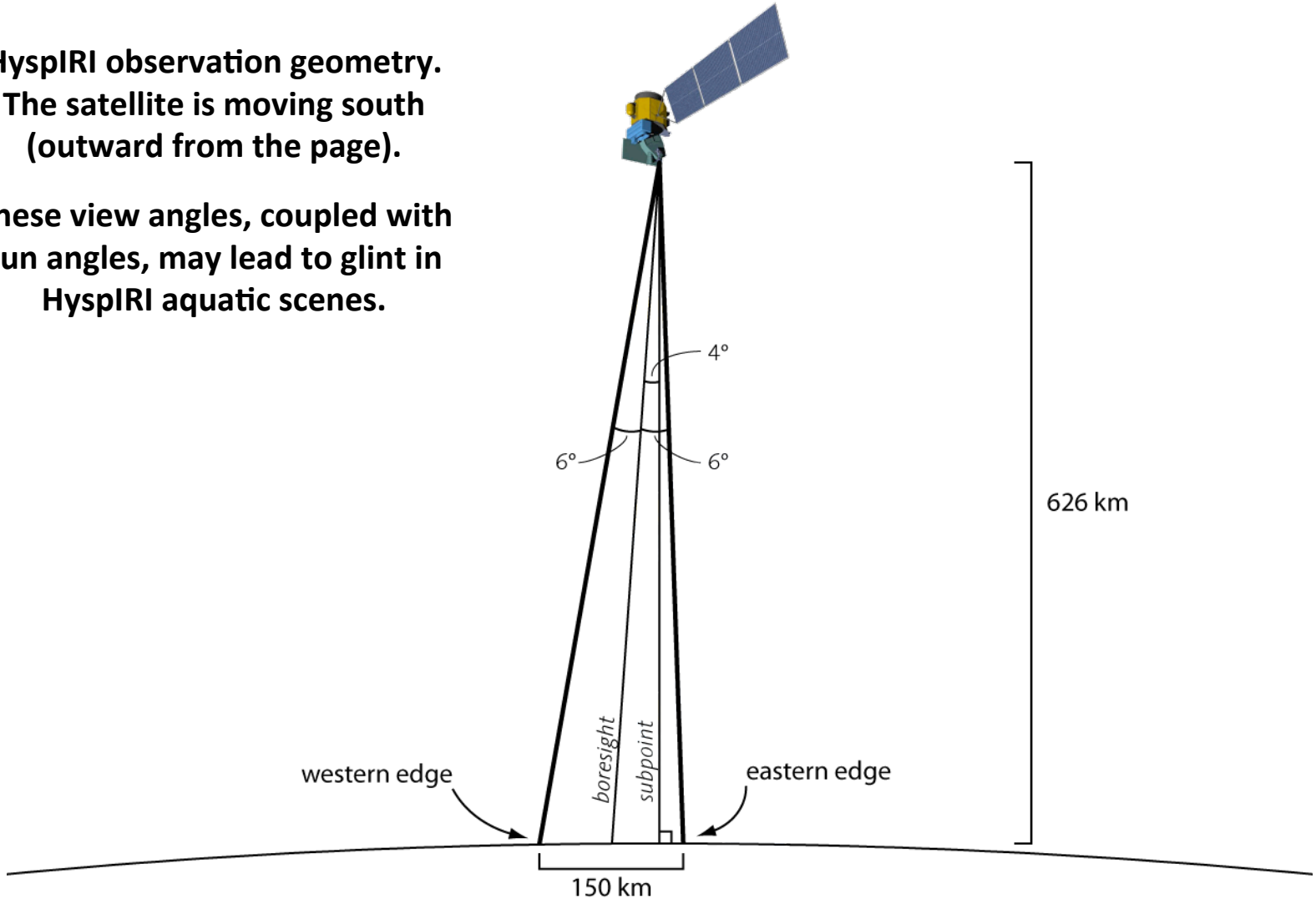

Literature Review

- Glint has been recognized as a potentially confounding factor from the outset of ocean remote sensing.

- There is a fair amount of research on the subject.

- Review of glint and some mitigation strategies:

  Kay S, Hedley JD, Lavender S (2009) Sun glint correction of high and low spatial resolution images of aquatic scenes: a review of methods for visible and near-infrared wavelengths. *Remote Sensing* 1:697-730

Approaches to glint mitigation

(A) Avoidance

- Physically pointing the remote sensor toward the ocean at an angle that minimizes specular reflection at the sea surface
- Pointing angle is determined by the position of the sensor relative to the position of the sun, generally assuming the ocean is smooth

(B) Correction

- Even in cases where the bulk of direct specular reflection can be avoided, skyglint contamination remains, as does sunglint that arises due to deviations from the level-surface ocean, i.e., waves

Two basic approaches to glint correction

(1) Statistical modeling of sea surface state to infer glint contribution

- Traced to Cox and Munk (1954), who analyzed aerial photographs of sun glint to infer statistics of the sea surface wave slope distribution as a function of wind speed

- Basis for modern ocean color glint correction

(2) Direct estimation of glint from remote sensing image data

- Based on common assumption that there is no water-leaving radiance in the NIR, especially at $\lambda > 900$ nm: after atmosphere corrections, remaining NIR signals must originate from the sea surface, i.e., glint

Literature Review

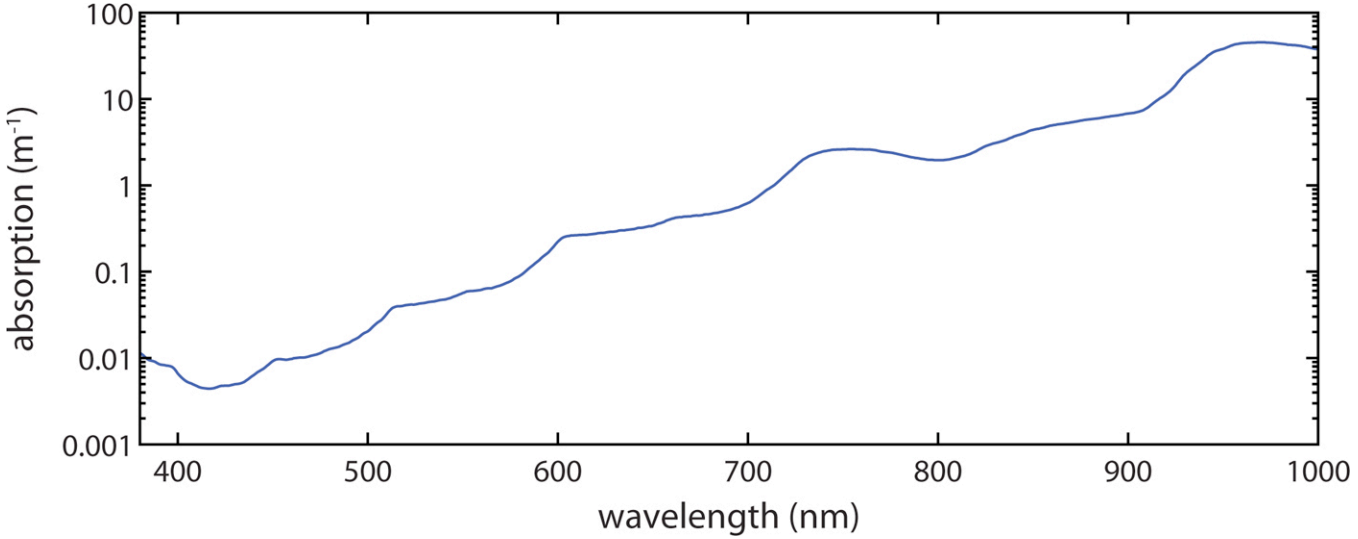

Water absorbs light very strongly at NIR wavelengths, especially >900 nm. Water-leaving radiance at these wavelengths is negligible. VIS data from Pope and Fry (1997); NIR data from Kou et al. (1993).

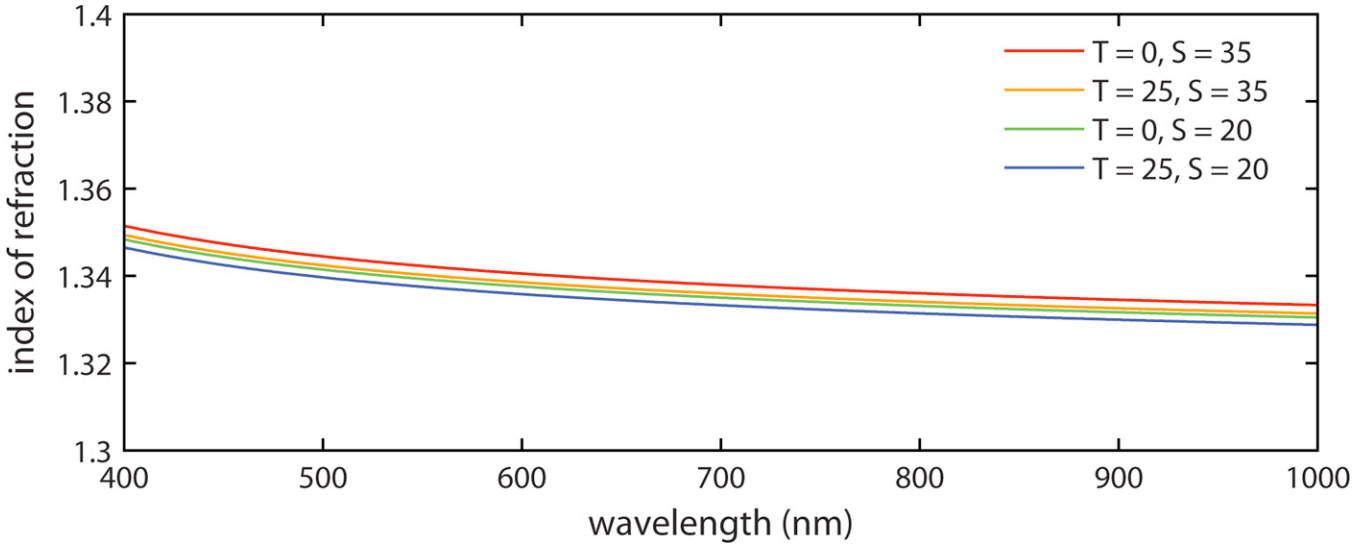

Index of refraction of water. Values are calculated following empirical model of Quan and Fry (1995). Values are modeled for four combinations of temperature (T, °C) and salinity (S, ‰).

Literature Review

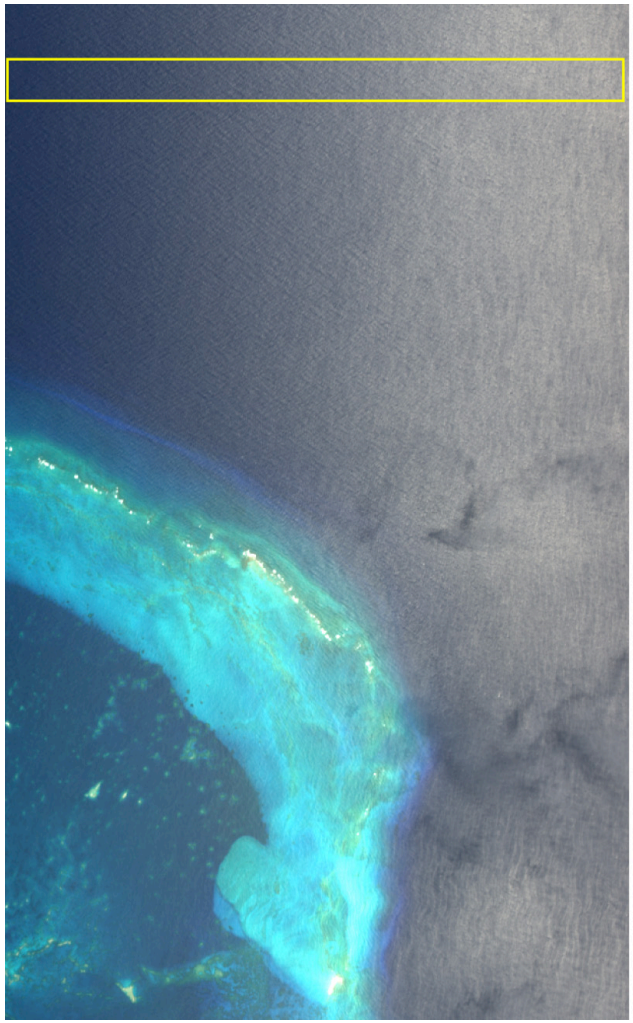

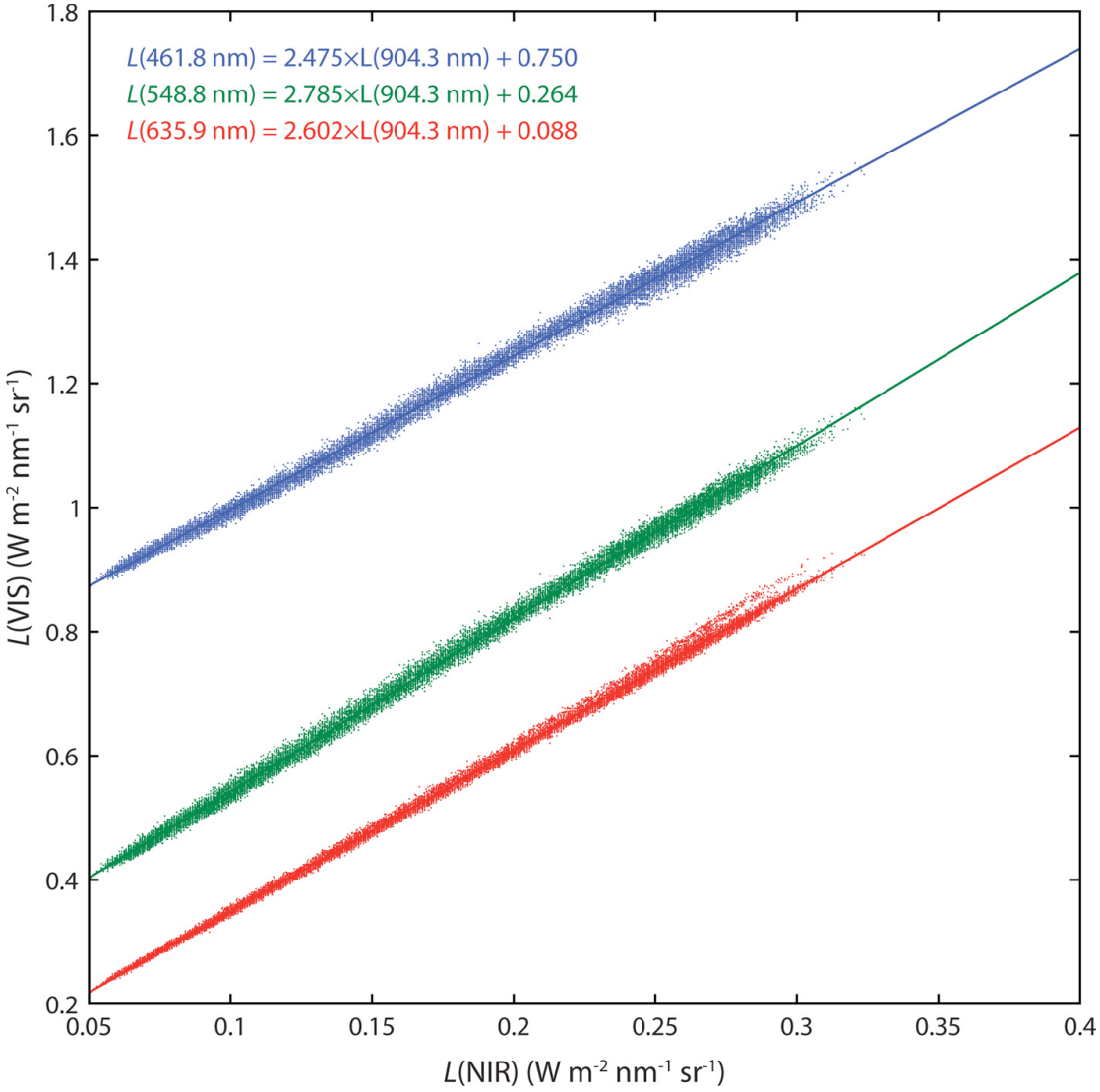

Quantitative Glint Characterization:
Modeling Based on Latitude, Date, and Wind

Global longitudinal variability of sea-surface sun glint reflectance for the HyspIRI orbit for (a) three levels of wind speed, which were used to compute sea-surface glint at (b) the west edge, (c) the middle point, and (d) the east edge of the HyspIRI field of view.

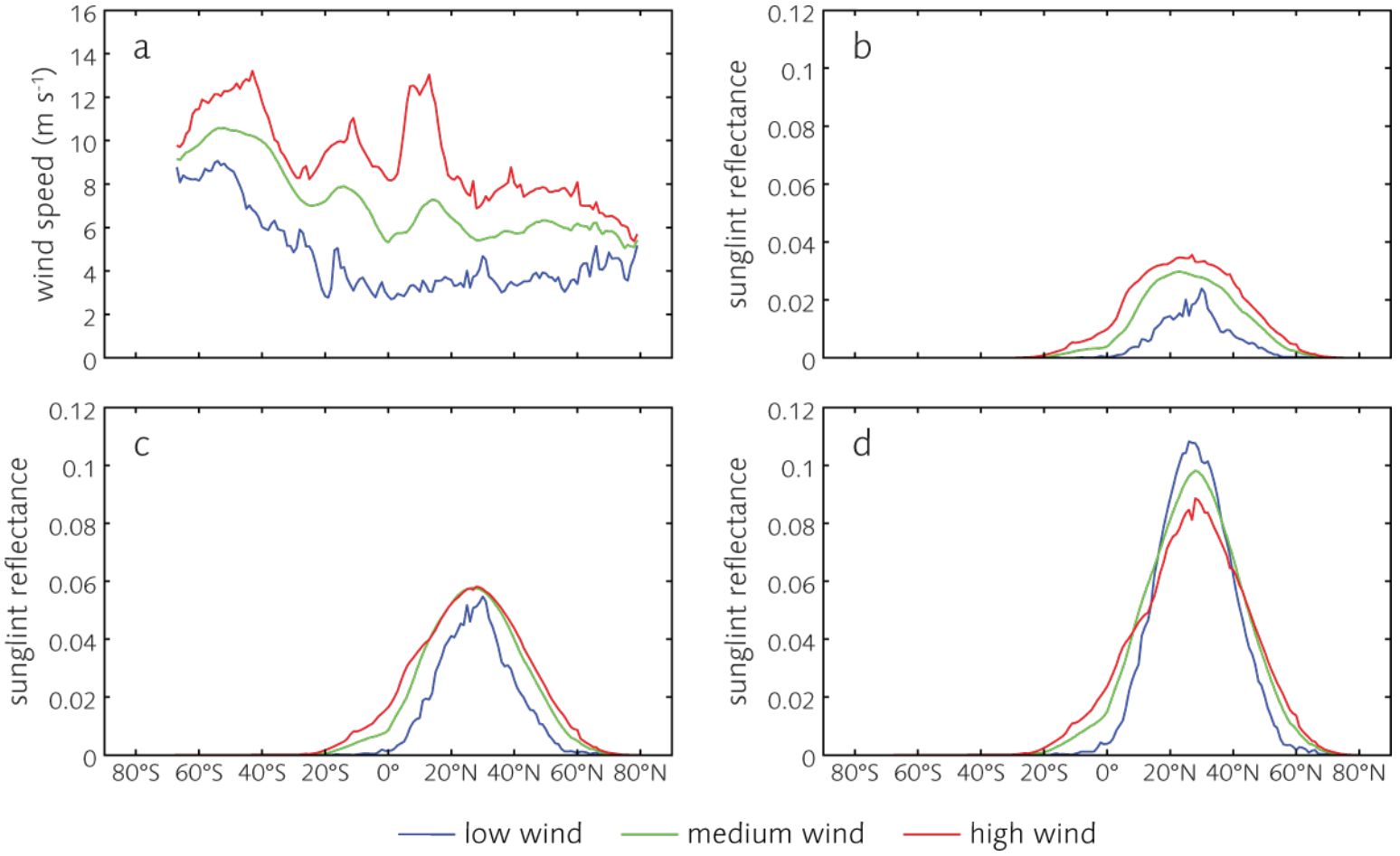

21 June

Source: Youngje Park

Quantitative Glint Characterization:
Modeling Based on Sun/View Angles, Atmosphere and Wind

Example Hydrolight/HydroMod discretized output. Radiance travels outward from center of hemispheres.

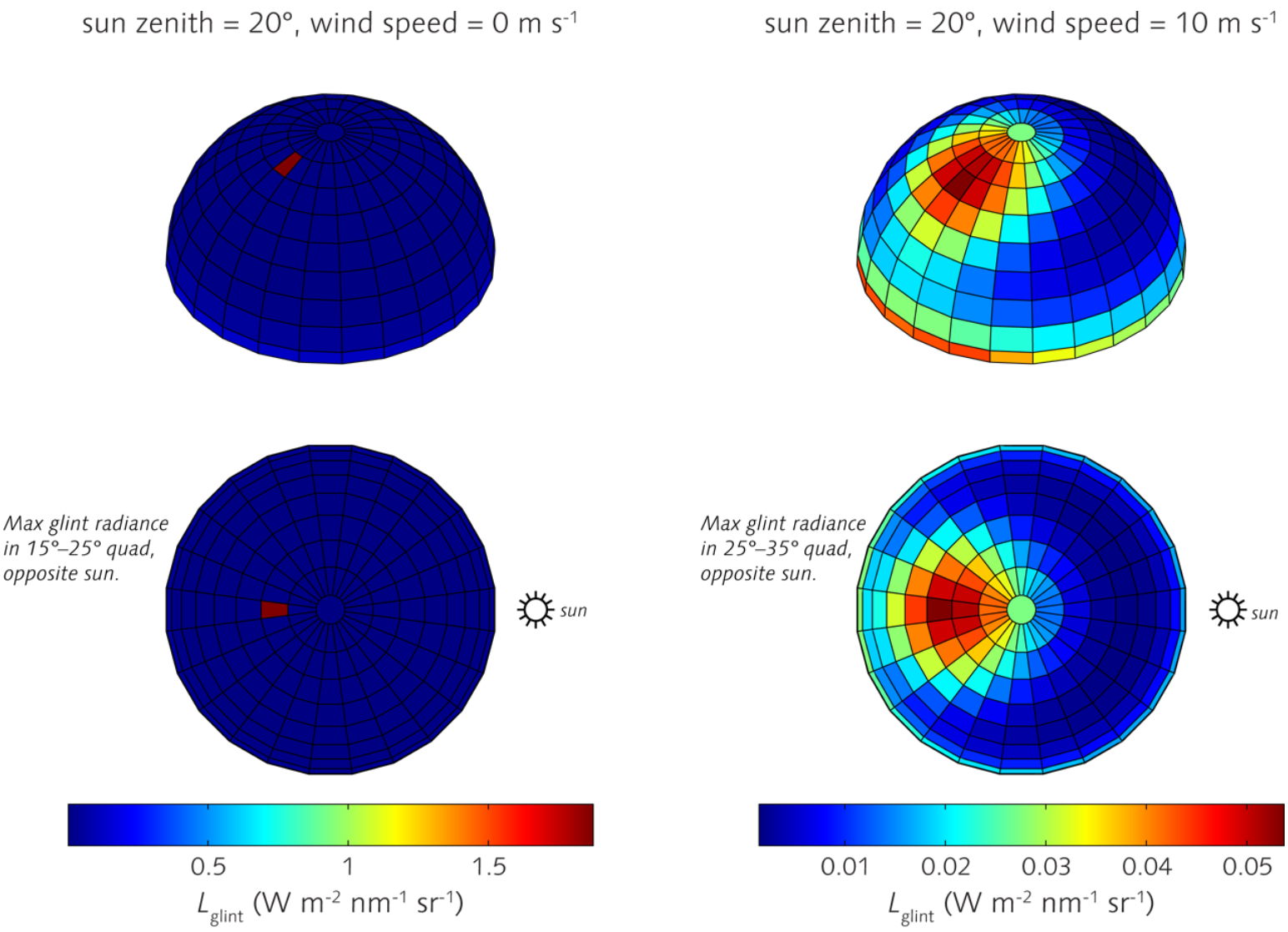

Note difference in radiance scales.

Quantitative Glint Characterization:
Modeling Based on Sun/View Angles, Atmosphere and Wind

HydroMod simulation of shallow water, mixed bottom spectrum, case 1 inherent optical properties, and comparing east vs. west side of HyspIRI field of view

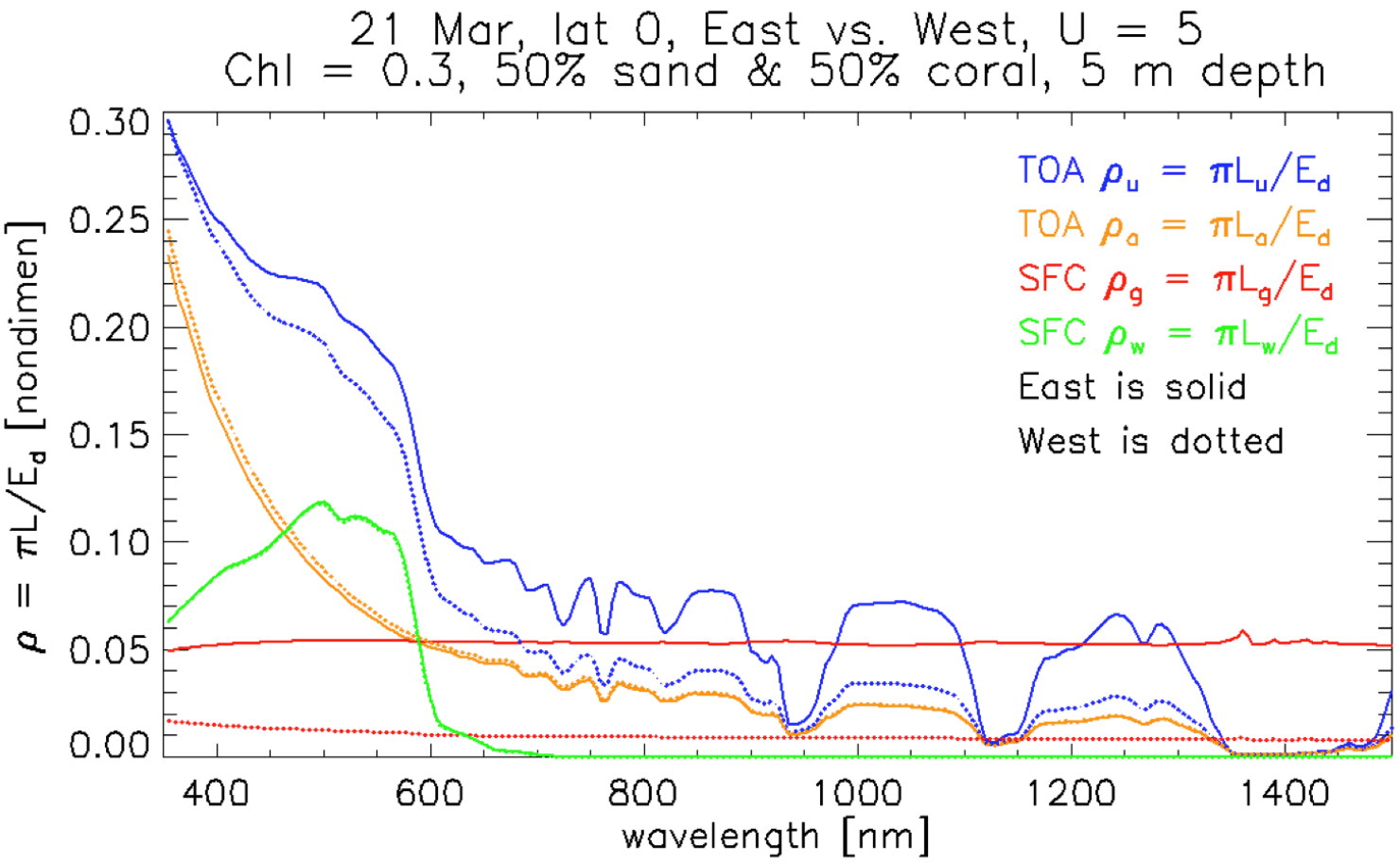

Source: Curtis Mobley

Quantitative Glint Characterization:
Deriving Glint Statistics from AVIRIS Imagery

AVIRIS scenes used to estimate glint reflectance for comparison with modeled values. Yellow regions are deep-water areas used to extract glint statistics.

f000411t01p03_r01

f000412t01p03_r08

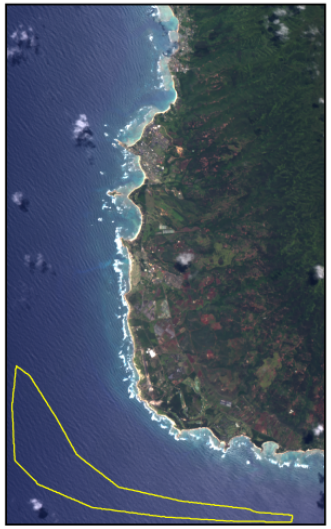

f000416t01p03_r02

f000416t01p03_r03

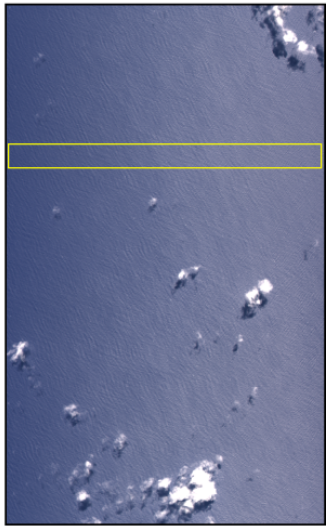

f000418t01p03_r01

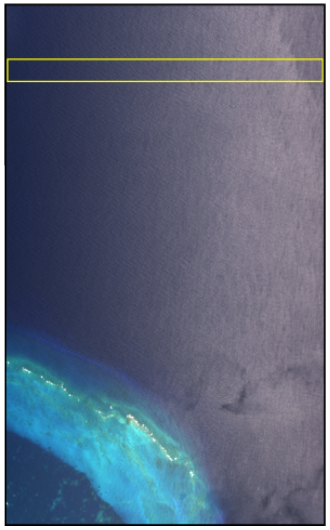

f000424t01p03_r09

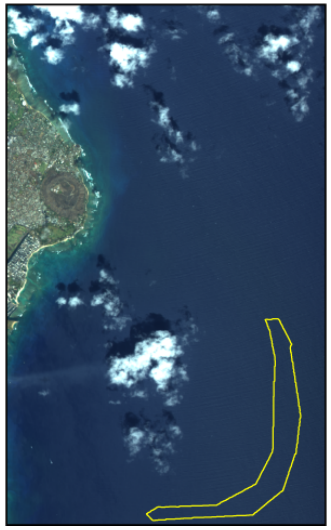

f000425t01p03_r07

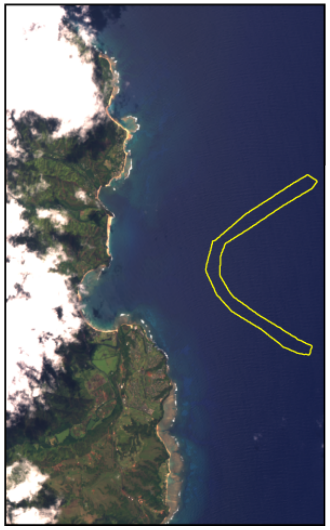

Quantitative Glint Characterization:
Deriving Glint Statistics from AVIRIS Imagery

Estimated TOA maximum glint reflectances for seven AVIRIS scenes.
These values are comparable to modeled values.

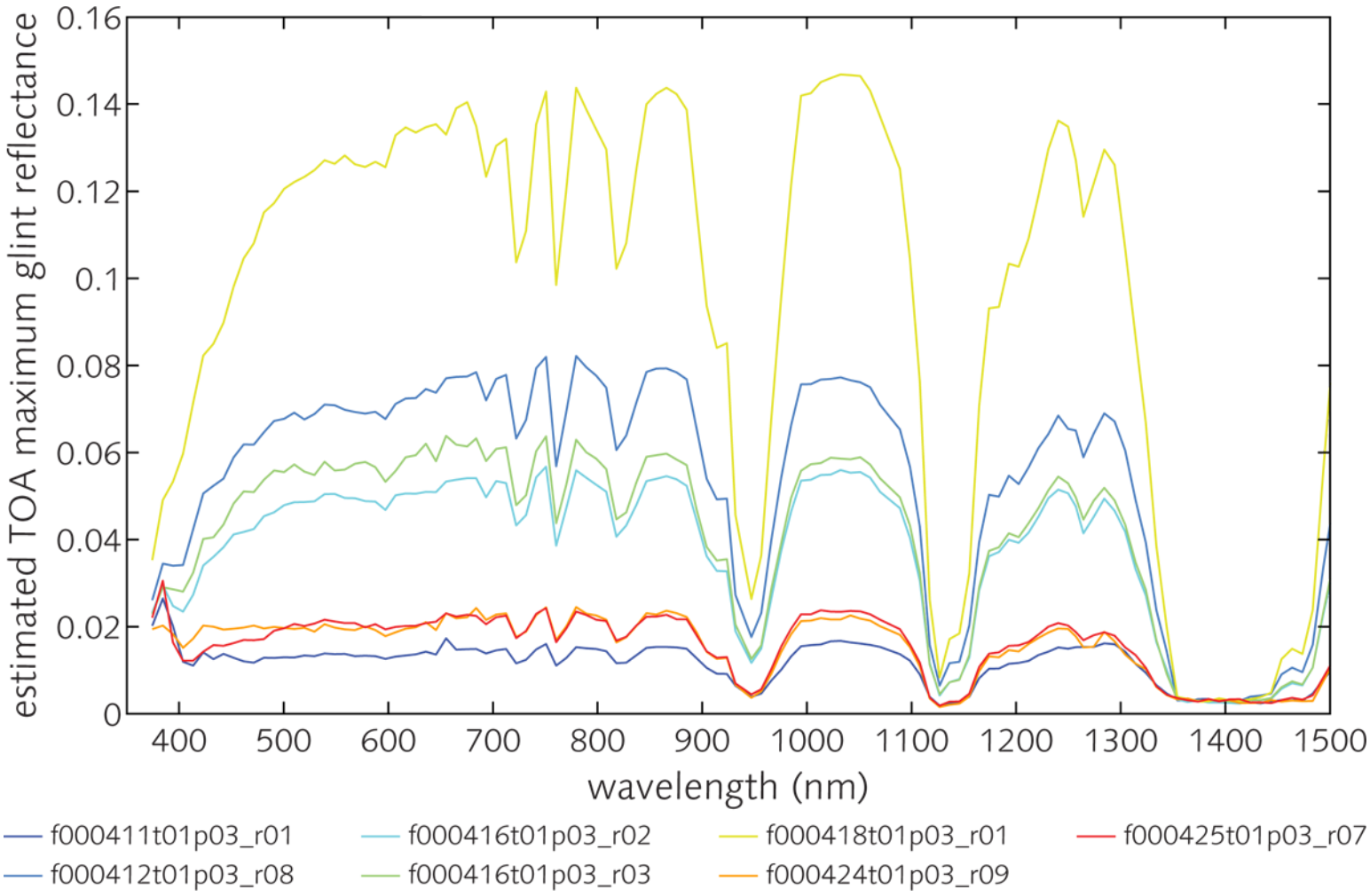

Quantitative Glint Characterization:
Deriving Glint Statistics from AVIRIS Imagery

AVIRIS scene f000418t01p03_r01 for demonstration of glint-aerosol discimination
Yellow line shows location of cross-track sample in analysis

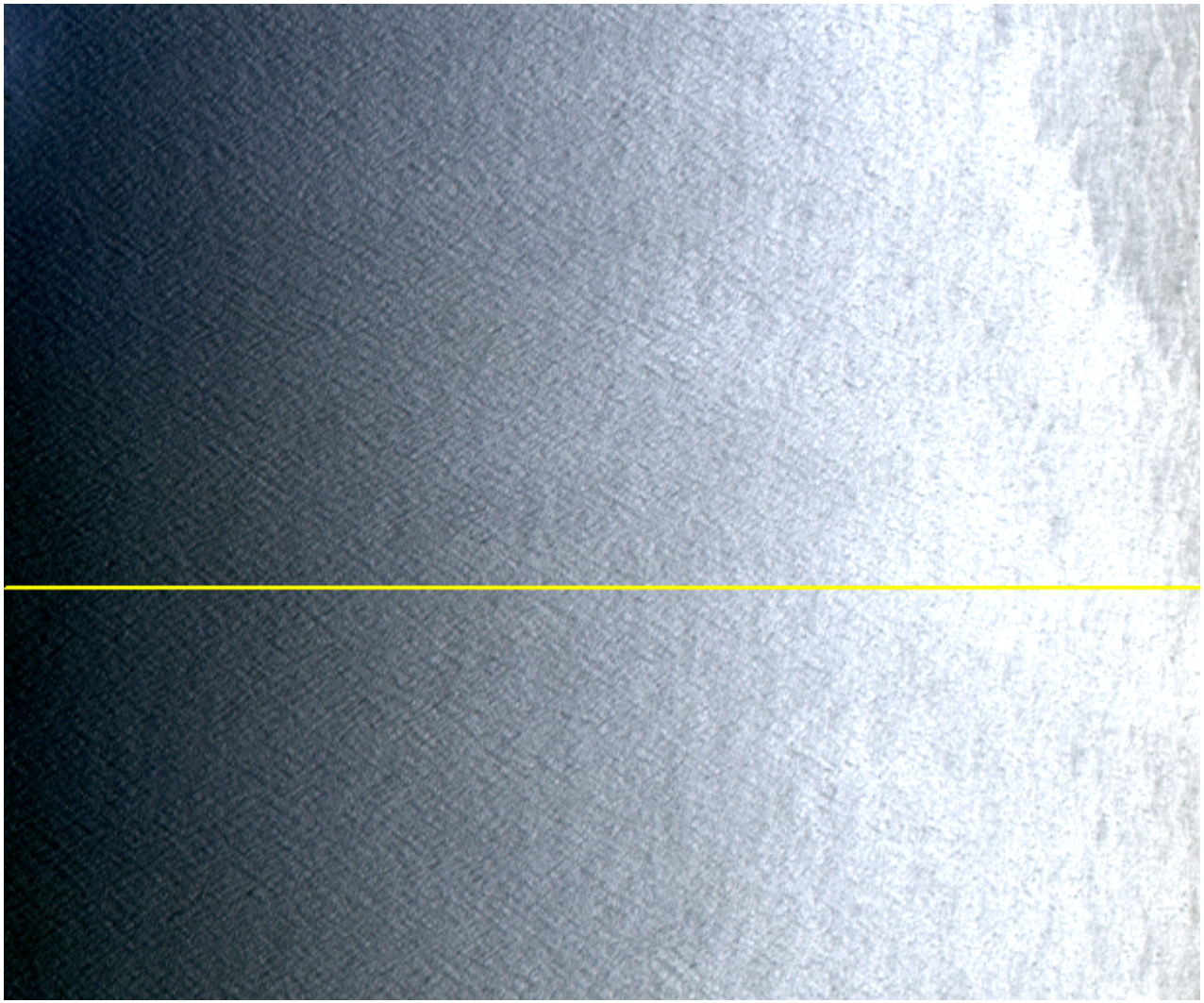

Source: Youngje Park

Quantitative Glint Characterization:
Deriving Glint Statistics from AVIRIS Imagery

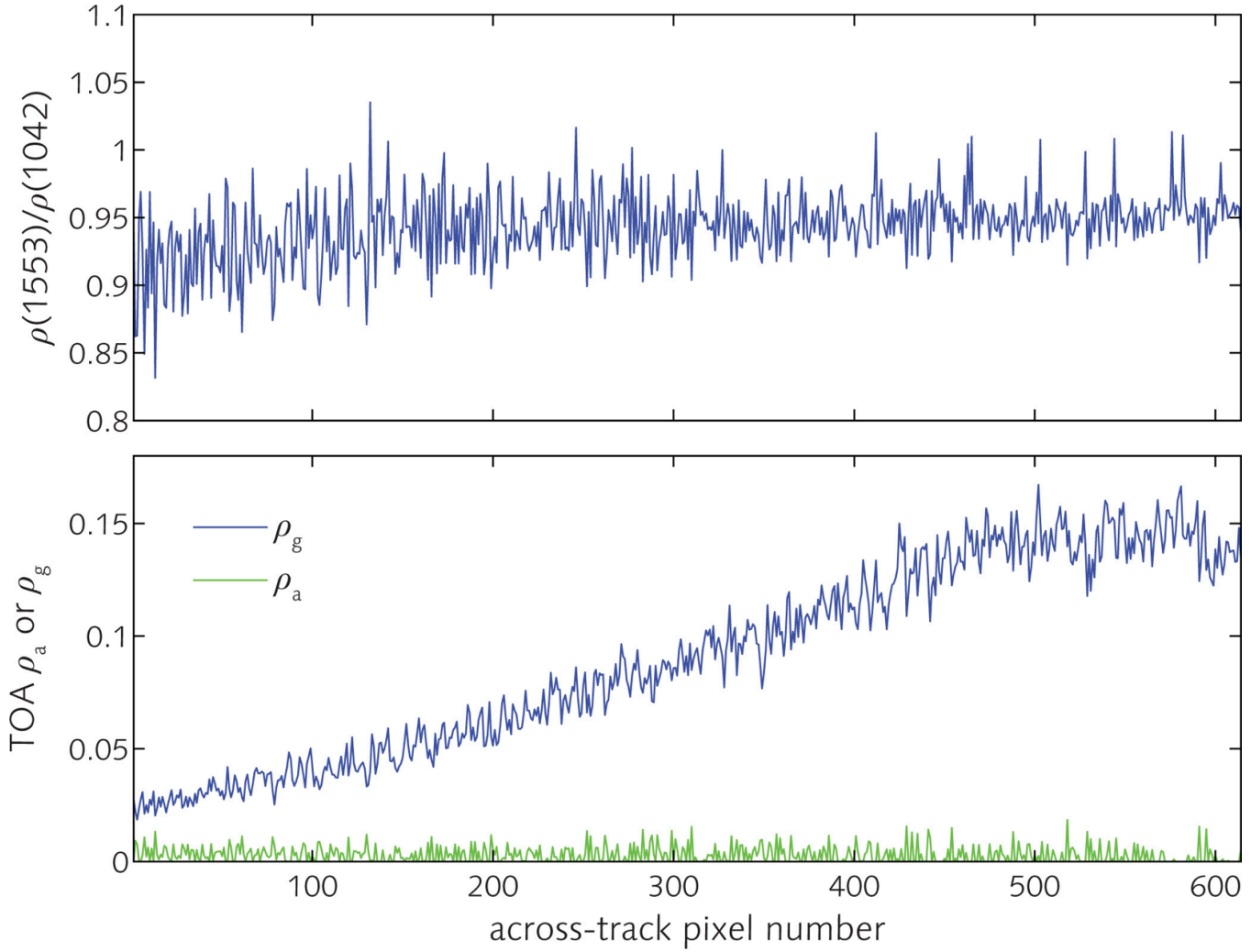

Source: Youngje Park

Quantitative Glint Characterization: Summary

Several summary observations can be made from model and image analysis:

- The effect of latitude is very clear. Sun glint is stronger where the sun is high, because HyspIRI looks almost straight down. Sun glint effects are apparent across a latitude band of 50° to 100° (i.e., 25°S–25°N to 50°S–50°N), depending on wind speed and the across-track pixel location.
- Sun glint is sensitive to wind speed for low to moderate glint strength and less sensitive for high glint.
- Sun glint at the east edge of the HyspIRI field of view is consistently stronger (a factor of two) than at the west edge.
- Sun glint is high in summer due to high sun and low in winter due to low sun. At the equator in the middle point of the swath, sun glint reflectance takes values of 0.025, 0.01, 0.04 to 0.01 for March, June, September and December respectively.
- Regional temporal variability appears similar to global longitudinal variability in magnitude.
- Large differences in glint reflectance than can occur from the east to the west edges of the HyspIRI field of view for moderate wind speeds in equatorial regions.
- Glint intensity can surpass that of water-leaving radiance.
- Glint radiance is function of incident irradiance.
- Glint reflectance is a function of the index of refraction of the water body.
- *Glint reflectance at the sea surface, to first order, is spectrally flat.* This is particularly important, because it is the basis for virtually all glint correction strategies.

Glint Impact on HysplRI Science:
Coral Reefs: Hydrolight Modeling & Classification

Scenario 1: Clear reef water, sun zenith 20°, wind 5 m s^{-1}

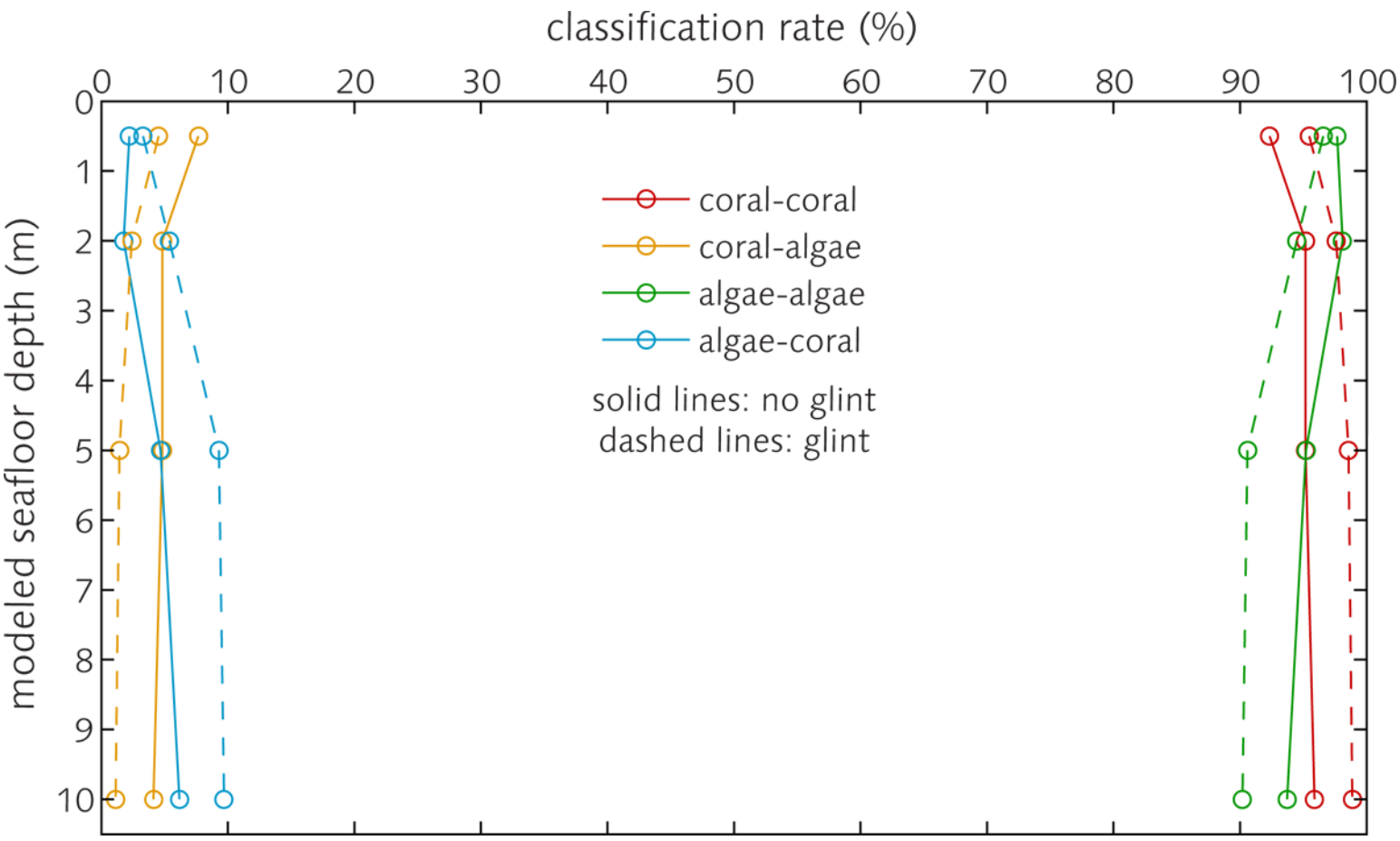

Values indicate classification rates for specific bottom-type/depth combinations classified as bottom-type at any depth. Solid lines show results of R_{rs} modeled without glint; dashed lines show results of R_{rs} modeled with full glint. Under the given water column and view conditions, glint actually increases the correct classification rate of coral at all depths, but it also increases the misclassification of algae as coral at all depths.

Glint Impact on HysplRI Science:
Coral Reefs: Hydrolight Modeling & Classification

Scenario 2: Turbid reef water, sun zenith 40°, wind 10 m s^{-1}

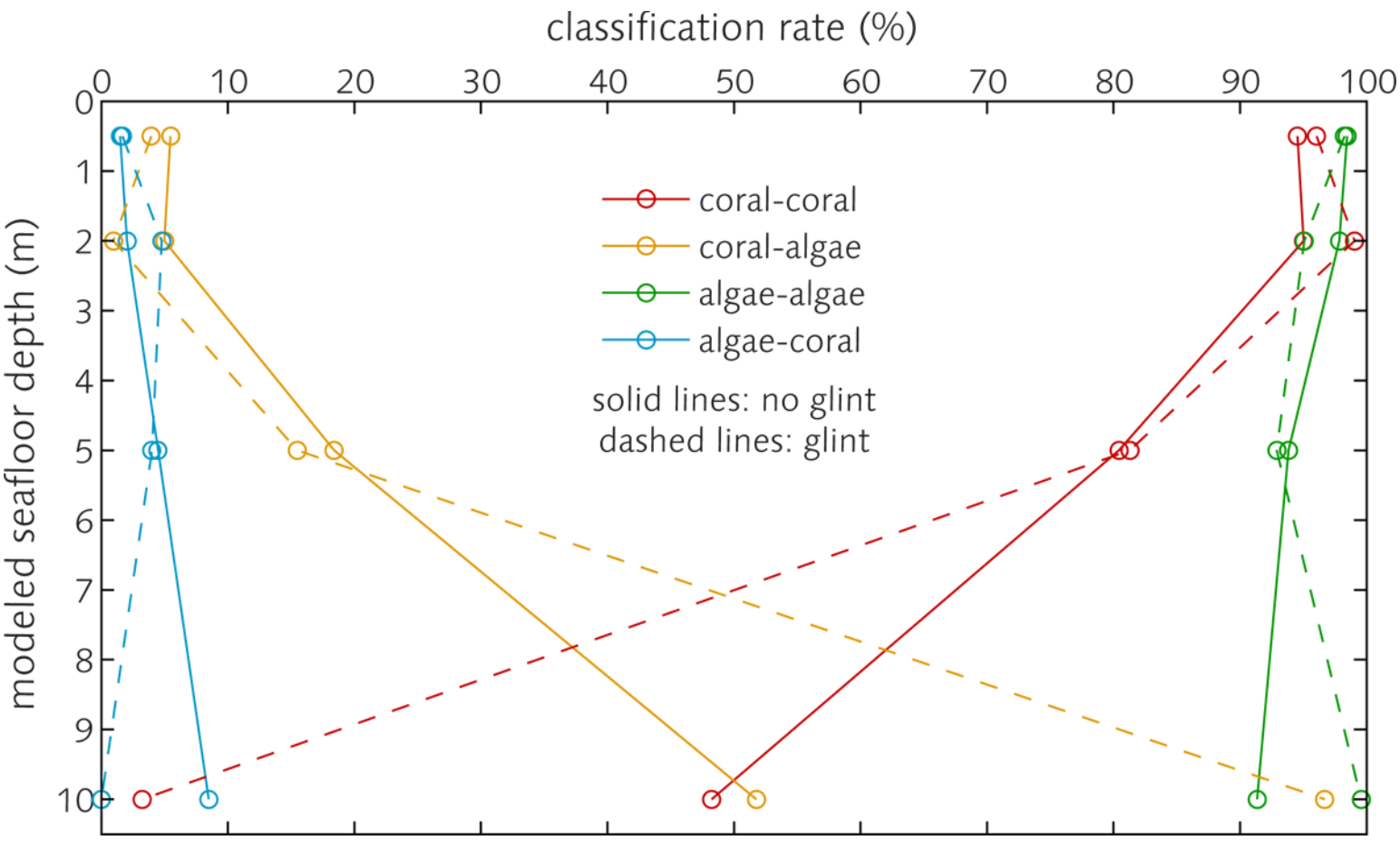

Under these conditions, glint increases the correct classification rate of coral at 0.5 and 2 m, but but greatly reduces correct coral classifications at 10 m.

Glint Impact on HysplRI Science:
Ocean Color: HydroMod Modeling, Inversion & Analysis

HydroMod parameterization

Location:	Station ALOHA, 22°45' N, 158°W
Date:	21 June
Sun Azimuth wrt Along Track:	107.78°
Sun Zeinth:	17.99°
Suspended Chlorophyll:	0.05 µg l^{-1}
Wind Speed:	two values modeled, 0 and 10 m s^{-1}
Atmosphere Conditions:	Clear sky with marine aerosols
Bottom Boundary:	Infinitely deep ocean

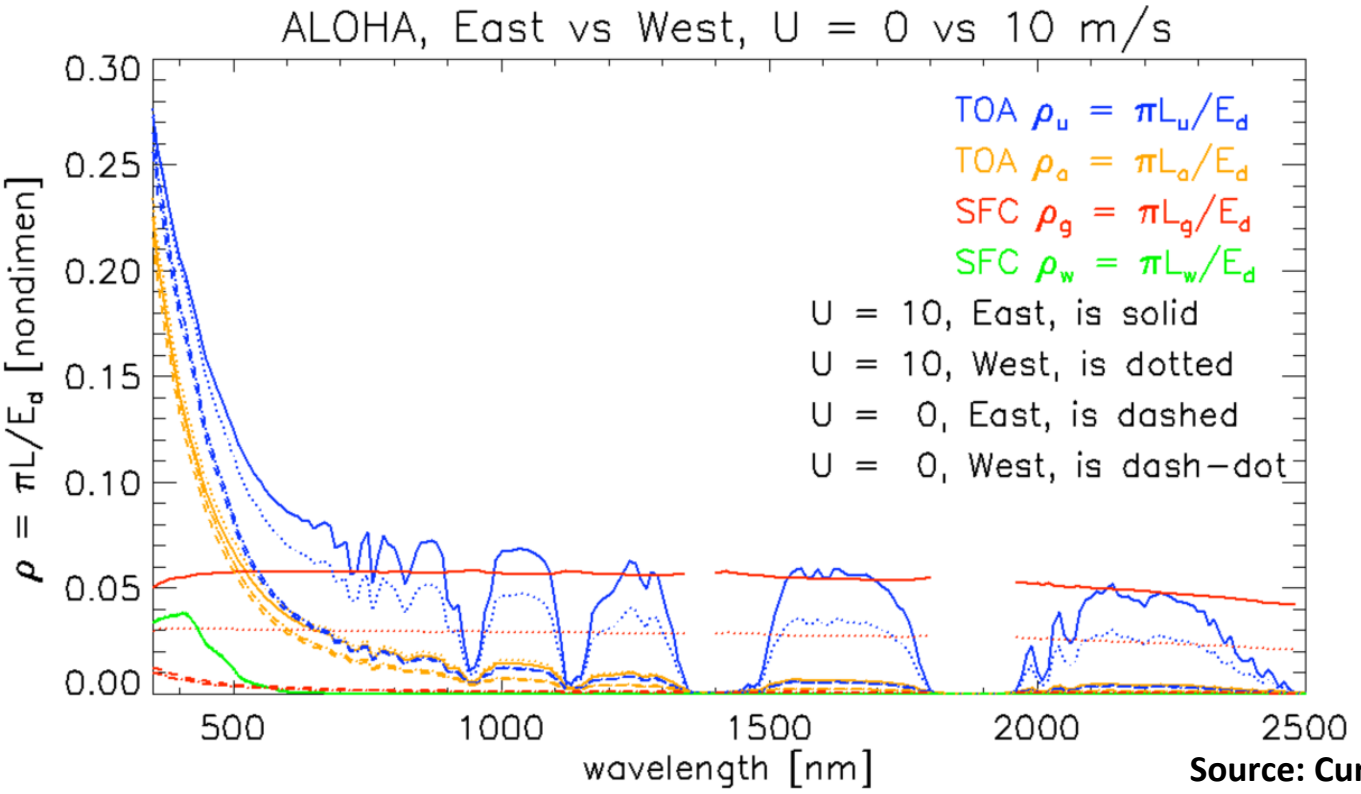

Source: Curtis D. Mobley

Glint Impact on HysplRI Science:
Ocean Color: HydroMod Modeling, Inversion & Analysis

Radiometrically inverted water-leaving reflectance spectra for Station ALOHA 21 June simulation. (A) West edge of HysplRI field of view, *U* = 0 m s^{-1}, (B) east edge, *U* = 0 m s^{-1}, (C) west edge, *U* = 10 m s^{-1}, (D) east edge, *U* = 10 m s^{-1}.

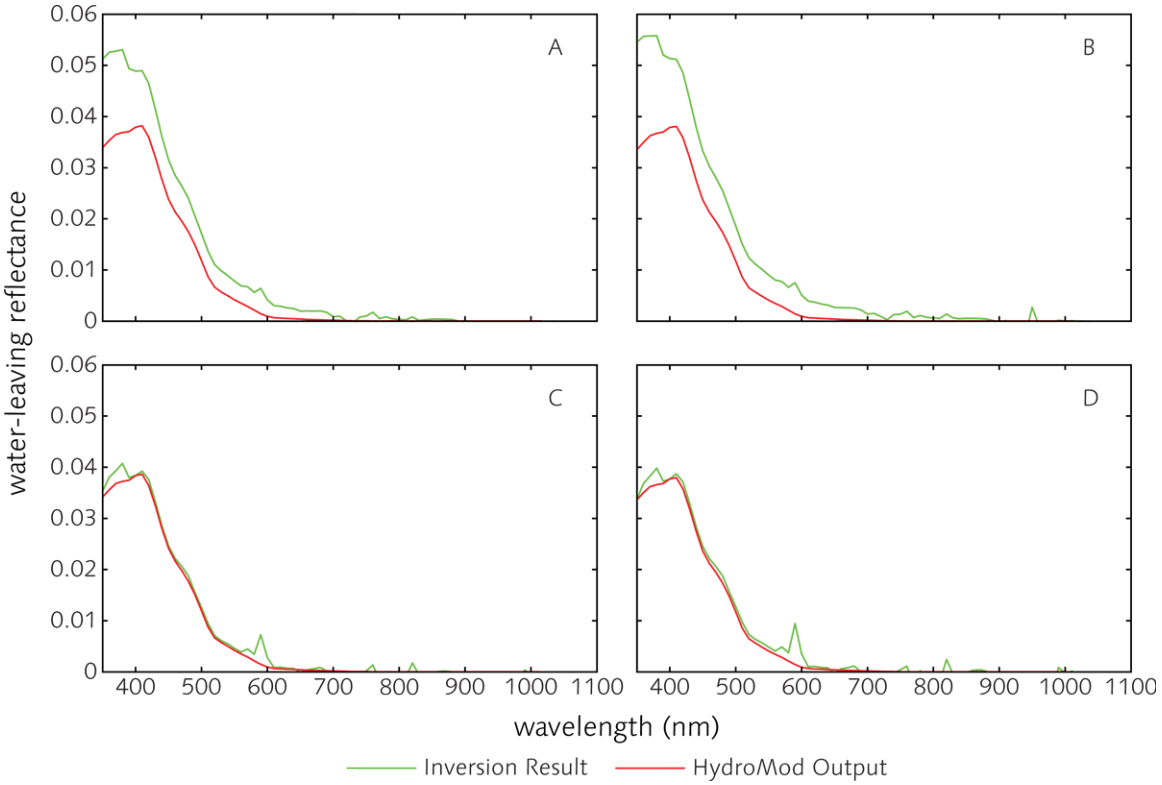

Chlorophyll values (mg m^{-3}) retrieved using OC4 and OC3M algorithms applied to R_{rs} data derived from Figure 4.3.3-2. "Edge" refers to position in HysplRI field of view. "*U*" refers to wind speed. Actual chlorophyll concentration used in HydroMod biooptical model is 0.05 mg m^{-3}.

Edge	*U* (m s^{-1})	Algorithm	
		OC4	OC3M
West	0	0.12	0.12
East	0	0.14	0.13
West	10	0.08	0.07
East	10	0.08	0.08

Source: Youngje Park

Glint Impact on HysplRI Science:
Emergent Vegetation: Examples & Challenges

Multi-angle CHRIS/Proba images of Fishing Bay Wildlife Management Area, Maryland. (a) At 0° nominal view zenith angle glint is visually apparent on water bodies interspersed amongst subaerial vegetation. (b) At 55° nominal view zenith angle glint is much less apparent. Boxes cover same ground area in (a) and (b).

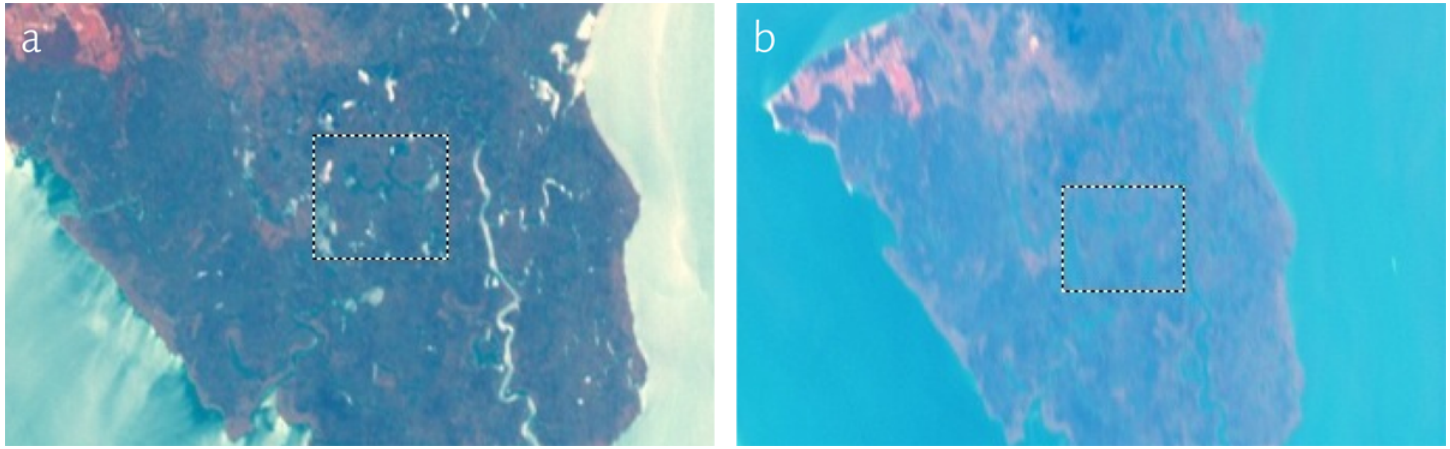

Spectra extracted from regions highlighted by boxes above. (a) At 0° nominal view zenith angle, glint produces very high values across the spectrum, evidenced by the maximum spectral curve. (b) At 55° nominal view zenith angle, the glint effect is greatly reduced.

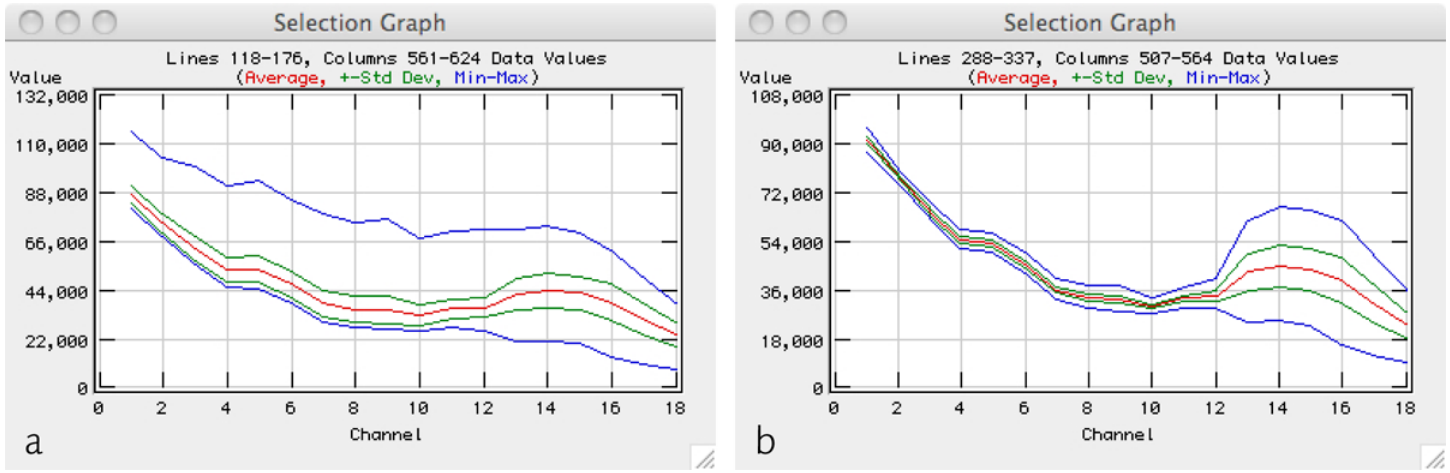

Source: Kevin Turpie

Glint Impact on HyspIRI Science: Summary

- For two basic HyspIRI science objectives, coral reefs and seagrass, expected levels of glint do not appear to dramatically impact classification retrievals.
- Glint has the greatest impact when retrieval conditions are already marginal, for example when water column optical properties limit penetration depth.
- Potential for improvement via mitigation for glint was not investigated.

- For the open ocean, with very low suspended chlorophyll levels, it is clear that glint correction must be tied to correction for atmospheric aerosols.
- Thus, both are fundamental requirements for accurate retrieval of spectral remote sensing reflectance.

- The situation is less clear for glint effects in emergent vegetation.
- Measurement and modeling capabilities for these systems lag those for shallow and deep oceans.
- At the same time, emergent vegetation has the benefit of usefully observable NIR and SWIR spectral features.

Mitigation Options
Avoidance

- Avoidance is the simplest method for mitigation of glint impacts, and it is the method of choice in operational ocean color.
- Any portions of imagery that exhibit significant glint can merely be ignored, then re-imaged on subsequent satellite overpasses.
- Nearshore and benthic applications typically require higher spatial resolution, i.e., 1–100 m vs. 1 km.
- The higher spatial resolution required closer to shore is offset by narrower fields of view and longer revisit times.
- The data rate for a given area of Earth surface is much lower, and it is generally not possible to ignore image data that exhibit glint effects.
- Thus, glint avoidance is a luxury not often afforded to nearshore and benthic applications.

Mitigation Options
NIR-VIS Empirical Linear Relationships

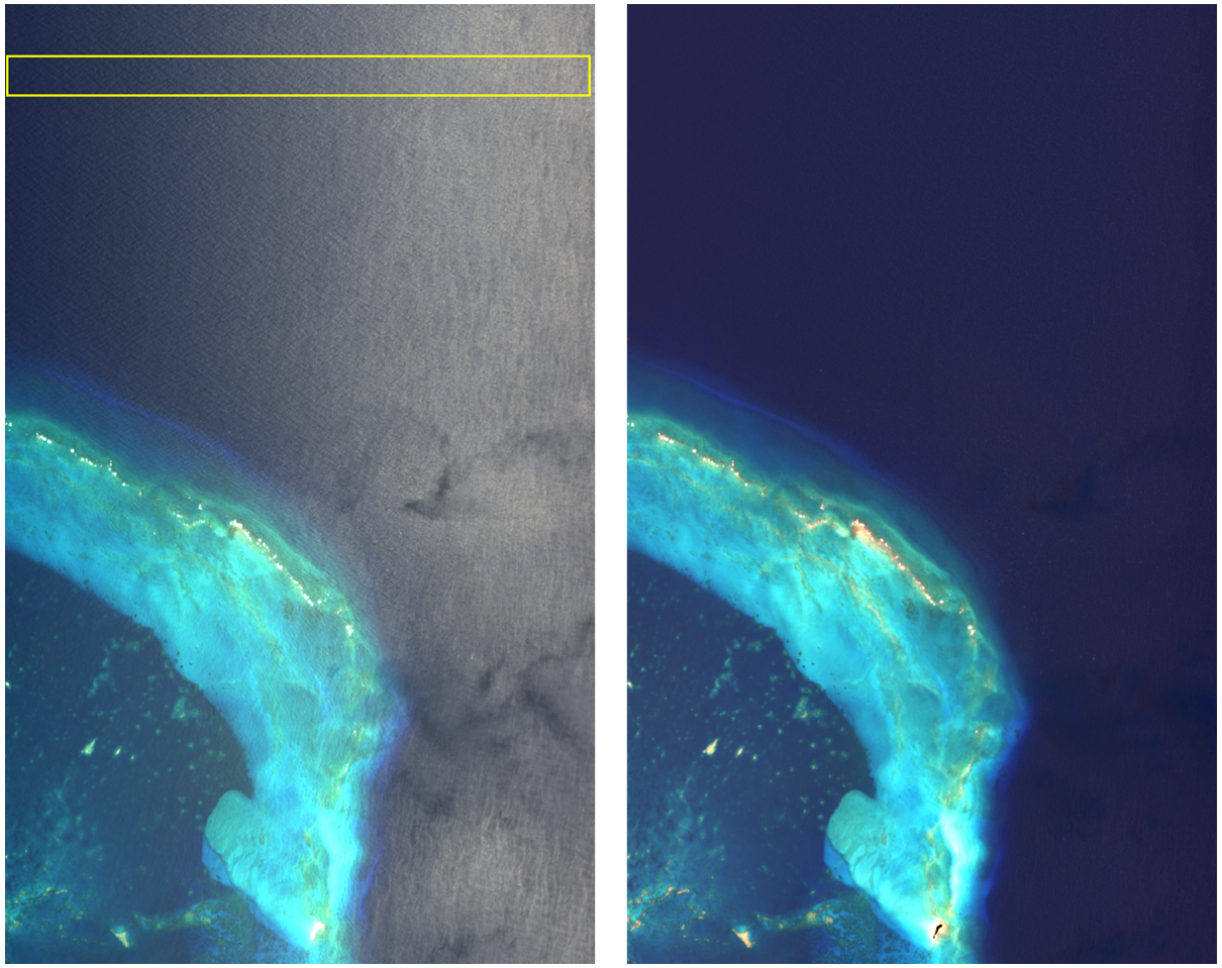

AVIRIS scene f000418t01p03_r01 covering the southeast portion of French Frigate Shoals, Hawaii and surrounding deep ocean. Image is rotated so that north is to the left of the scene. (Left) Original scene shows very strong glint effects. Yellow box highlights region from which empirical linear relationships are derived. (Right) The scene after application of glint correction. Glint effects are very effectively removed.

Mitigation Options
Subtraction of NIR Reflectance

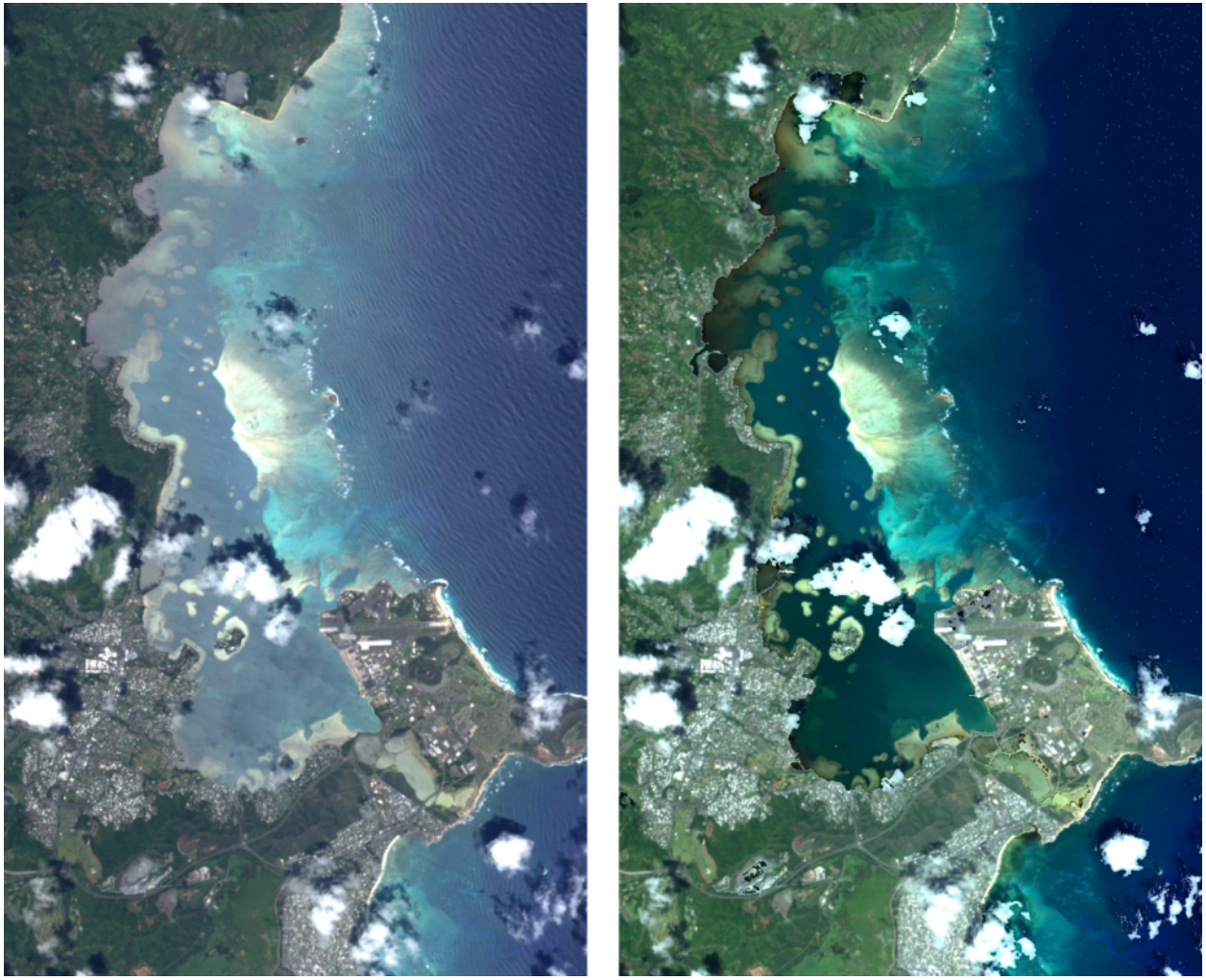

Example of glint correction using subtraction of NIR reflectance. (Left) Original AVIRIS scene of Kaneohe Bay, Hawaii (f000412t01p03_r08). (Right) The scene after atmosphere and glint correction. Clouds and some sea surface features remain; this is due to automated masking. Overall, glint correction performs quite well.

Source: Bo-Cai Gao

Conclusions and Recommendations

Conclusions

- The literature and present examples demonstrate that glint correction is feasible.
- Present examples further demonstrate that key HyspIRI science objectives are achievable even in the presence of glint.
- Therefore, it is very reasonable that active glint correction can be a part of a successful HyspIRI processing flow.

Near-Term Recommendations

- The glint correction procedures described here each demonstrate strong potential. Each also requires further refinement.
- The presented analyses have touched on some key points about glint and its impact on remote sensing retrievals of certain biophysical parameters. These issues could certainly benefit from deeper investigation.
- It would be very desirable to perform field validation for model results of selected, important HyspIRI science objectives.

Long-Term Recommendations

- Environmental (aquatic) optics would be greatly advanced by the collection of a few comprehensive data sets that provide all inputs and outputs to the RTE.
- As glint correction procedures become codified, it would be useful to have a glint toolbox utility from which a user could select among a suite of glint correction techniques.

Autonomous forecasting of lava flow hazards using HyspIRI

Robert Wright

Hawai'i Institute of Geophysics and Planetology

UNIVERSITY of HAWAI'I®
MĀNOA

Forecasting lava flow hazards

- Along which paths, and to what distance from the vent, will lava flow, and how long will it take to get there?

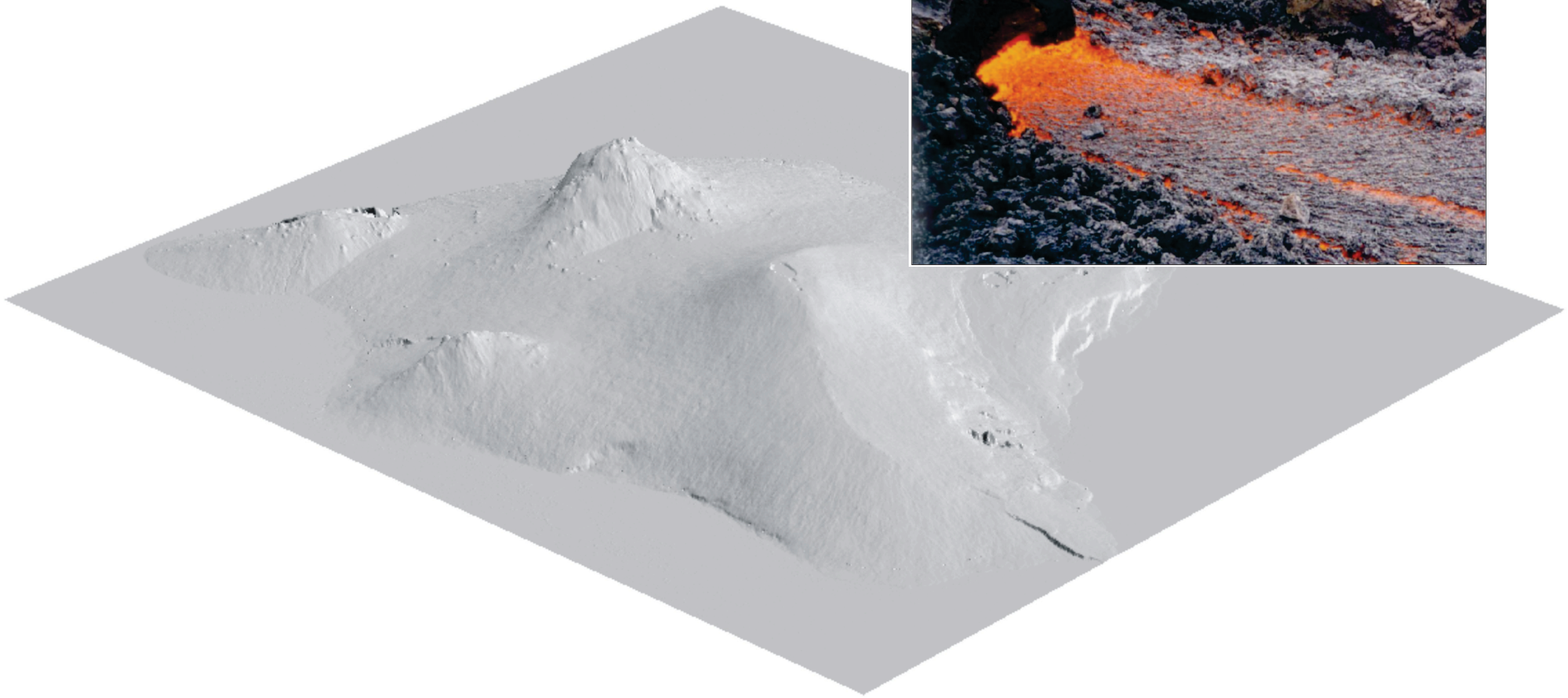

Predicting potential flow paths using a drainage model

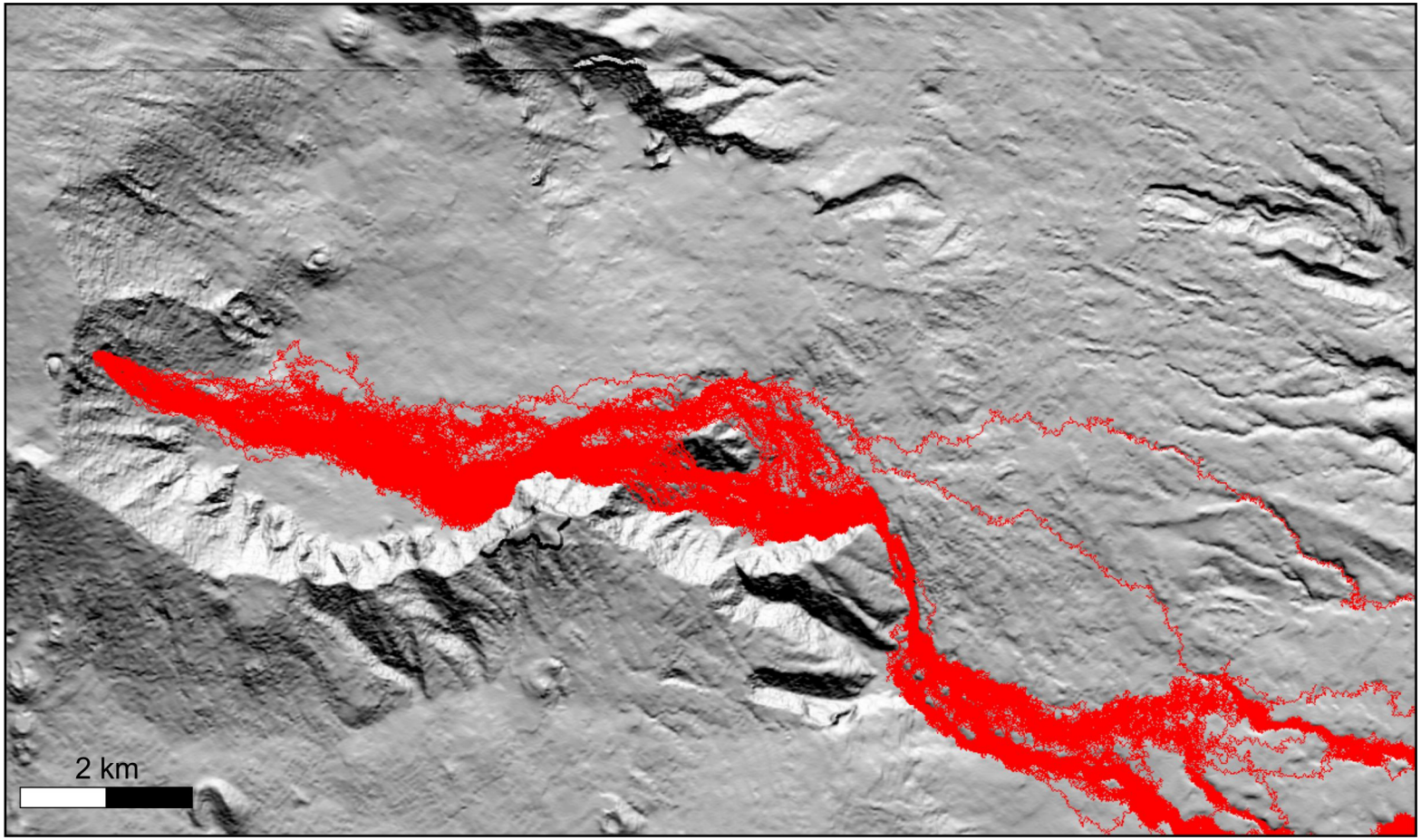

Favalli et al., 2005

Lava flows downhill, but which way is downhill? A stochastic drainage model can be used with a DEM (SRTM, ASTER GDEM) to simulate the most likely paths a lava flow will take given a vent location

Predicting potential flow paths using a drainage model

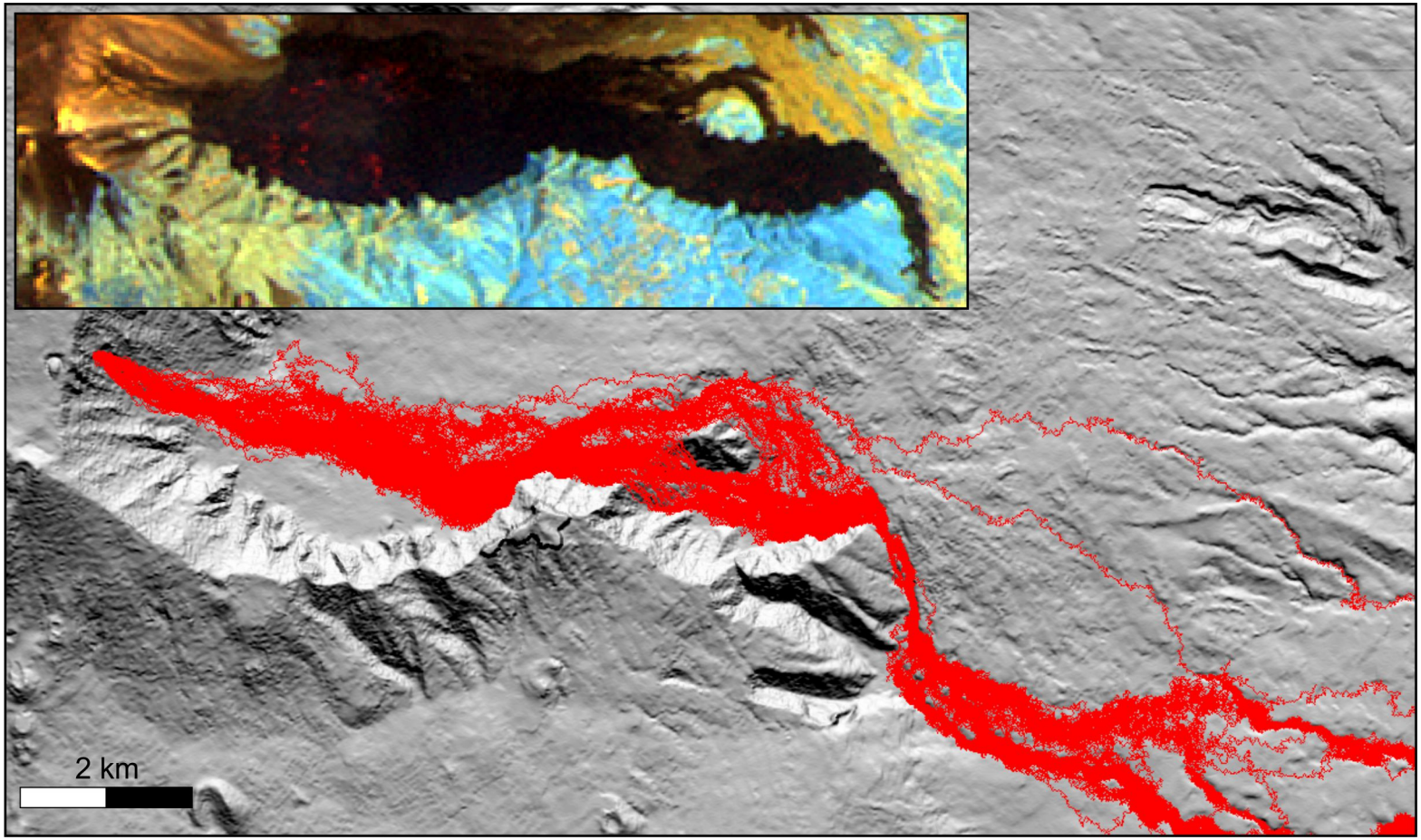

But, this approach does not predict the likely length a lava flow will attain

Predicting potential flow lengths using a thermo-rheological model

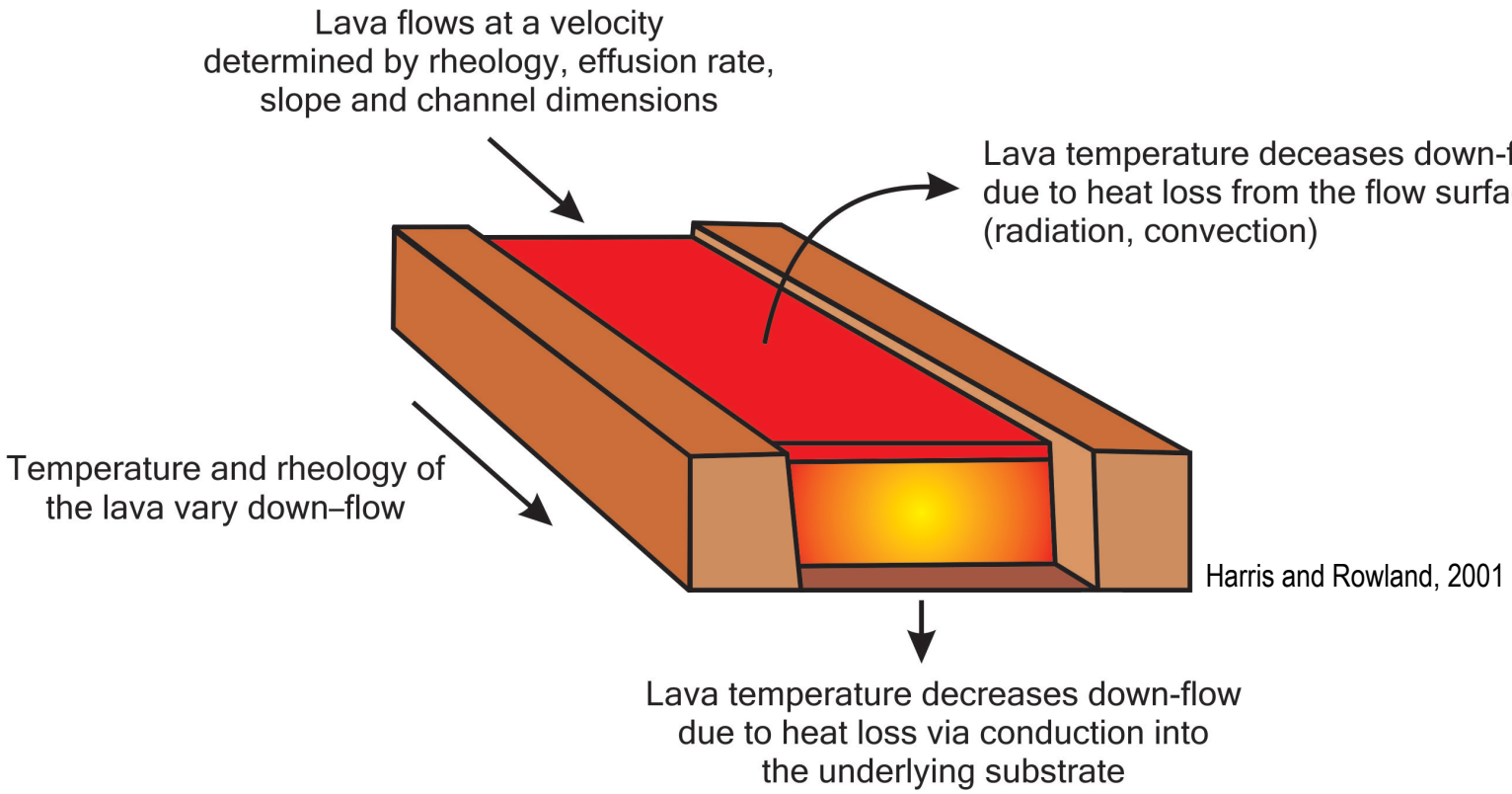

By modeling the stiffening of a control volume of lava flowing in a channel, the time (and hence distance) from the vent that the lava becomes too stiff to flow any further can be predicted using a numerical model

A thermo-rheological/stochastic approach for modeling lava flow hazards

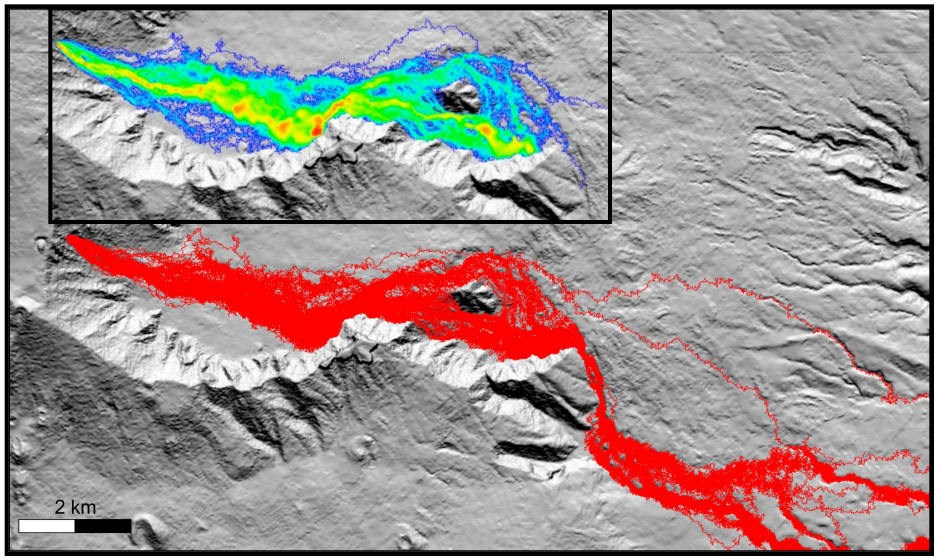

Eruption intensity can change rapidly, and reliable lava flow hazard predictions rely on timely and accurate information regarding the nature and intensity of the eruption and how this varies

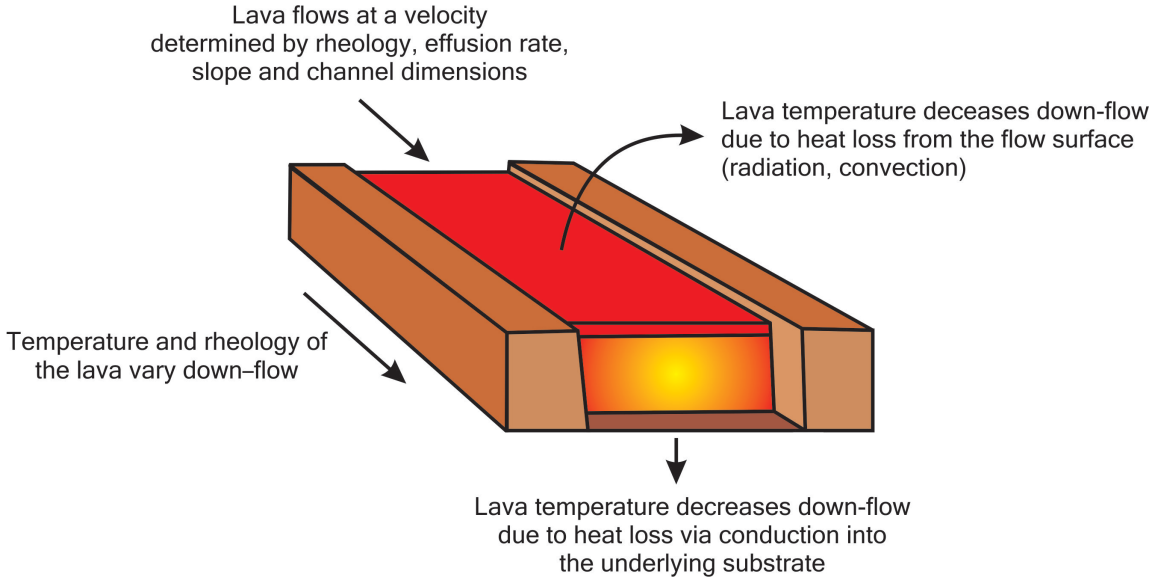

Much of the relevant information can be obtained from remote sensing data, in a manner not possible in the field

The importance of effusion rates

Effusion rates:

- Determine (largely) final flow length
- Vary during an eruption and between eruptions by1-2 o.o.m.
- Are difficult to estimate in the field

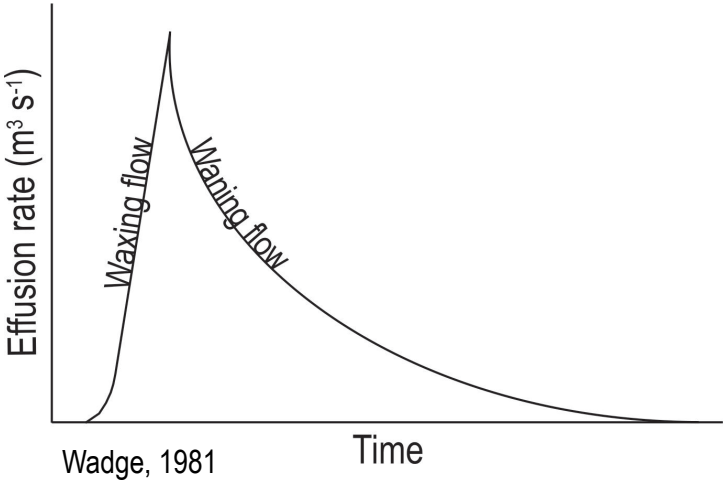

Wadge, 1981

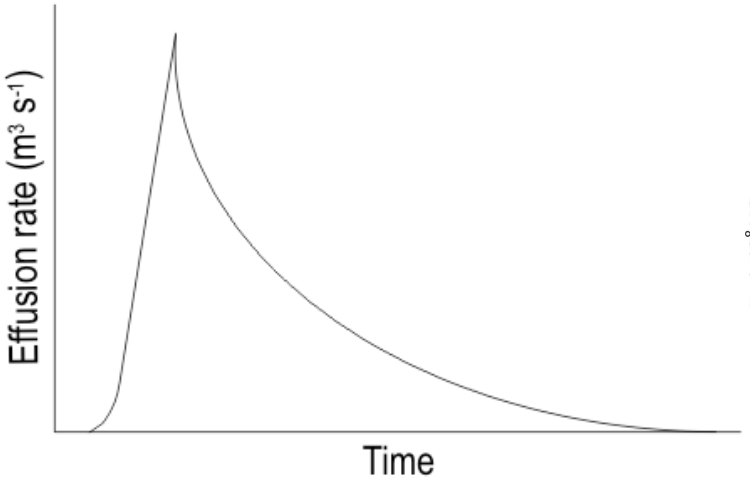

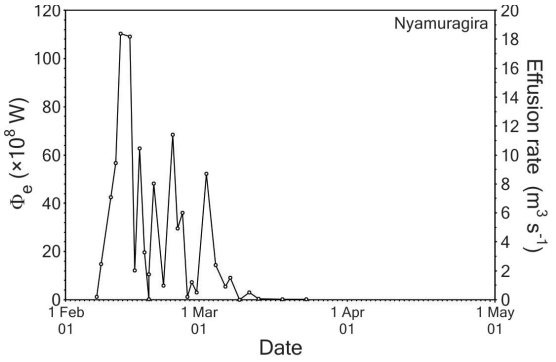

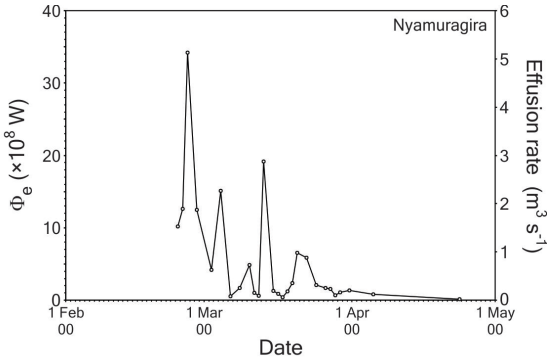

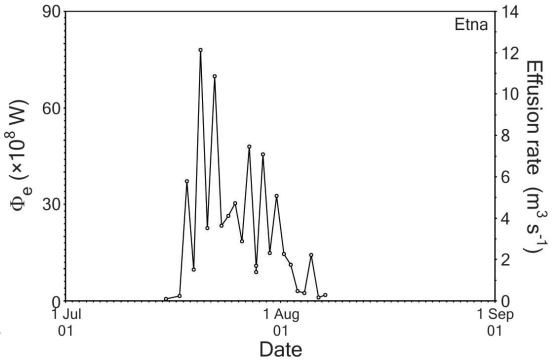

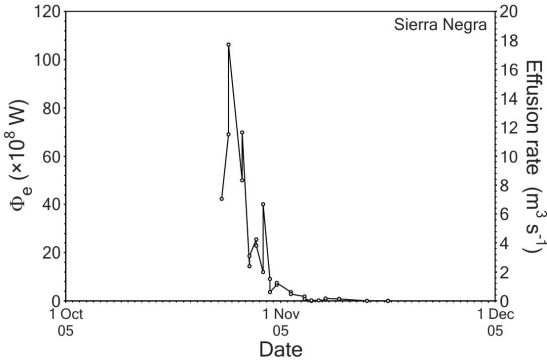

Calculating lava effusion rates from infrared satellite data

The higher the volumetric flux of lava from the vent, the greater the length (area) it can spread over before it solidifies

$$\text{Lava effusion rate} = \frac{\text{Heat loss from flow surface}}{\text{Enthalpy of the mass of lava}}$$

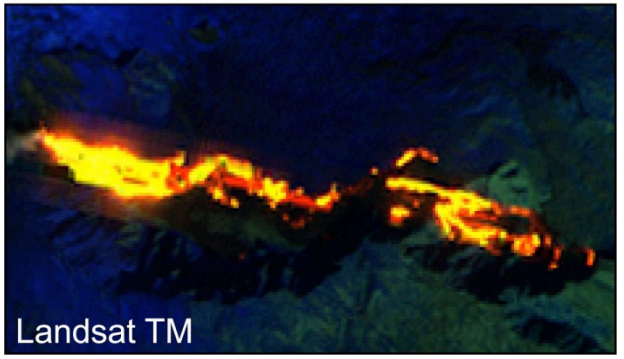

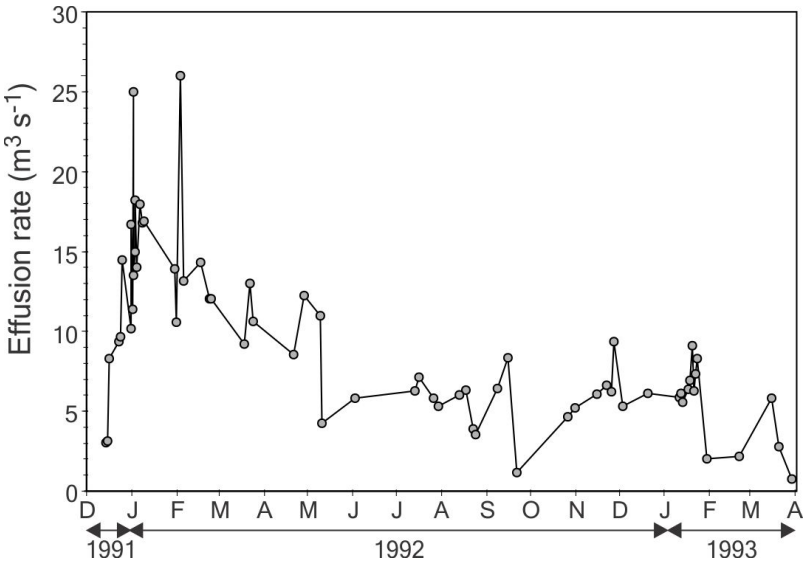

Walker, 1973; Pieri and Baloga, 1986; Harris et al., 1997; Wright et al., 2001

Calculating lava flow cooling from HyspIRI's 4 μm channel

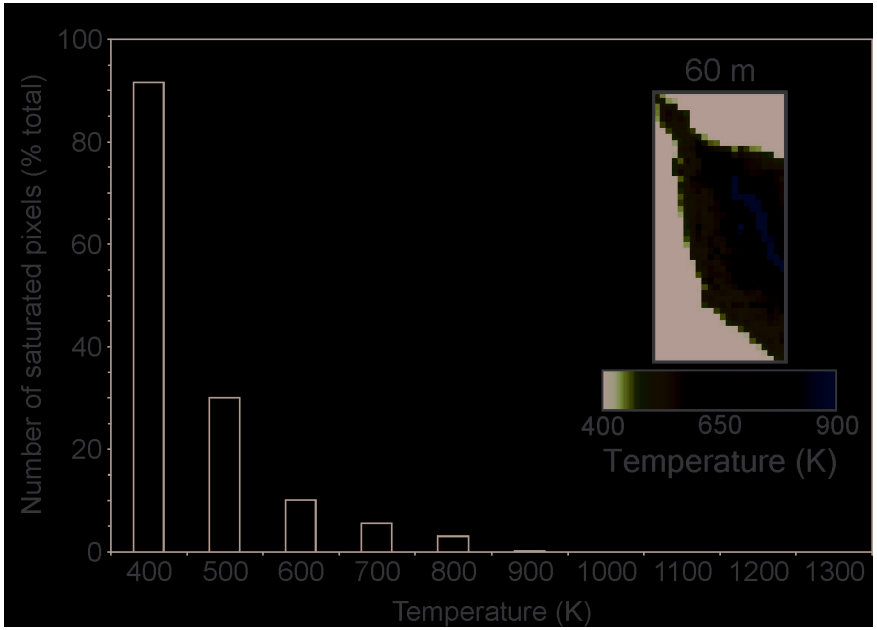

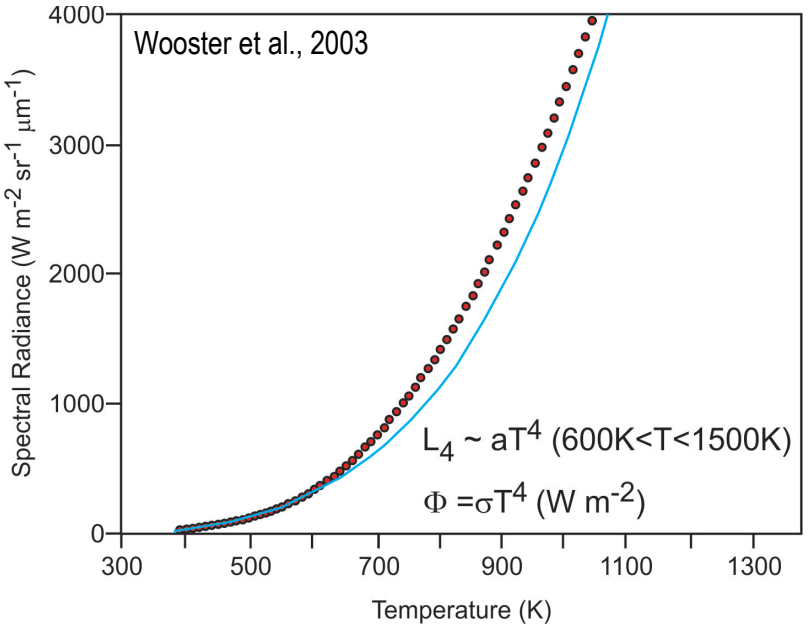

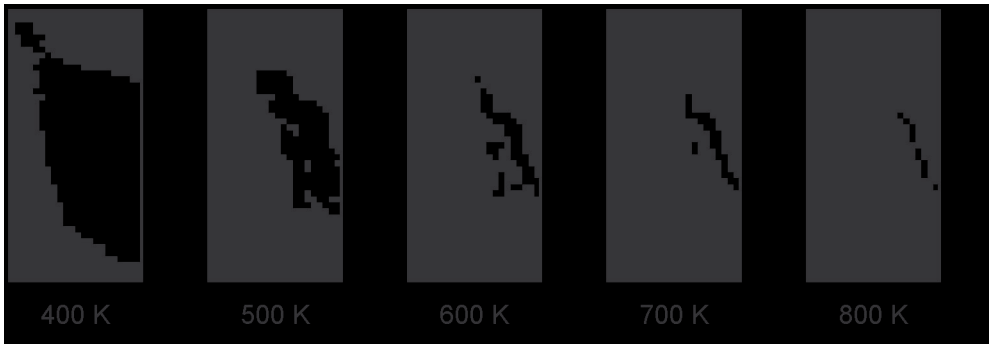

HyspIRI's high saturation temperature 4 μm channel will allow us to estimate lava flow cooling (and area) twice in each 5 day period

Surface heat loss along the length of an active lava channel

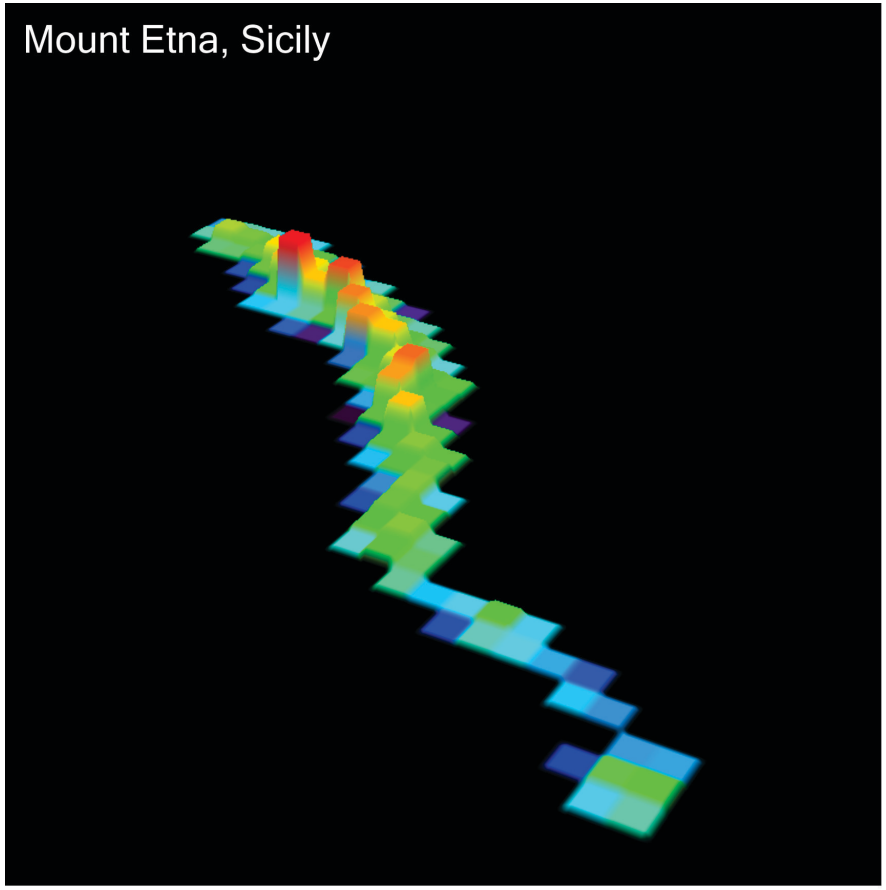

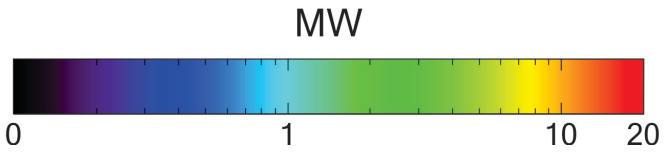

HyspIRI bridges the gap between high/low, spatial/temporal resolution sensors

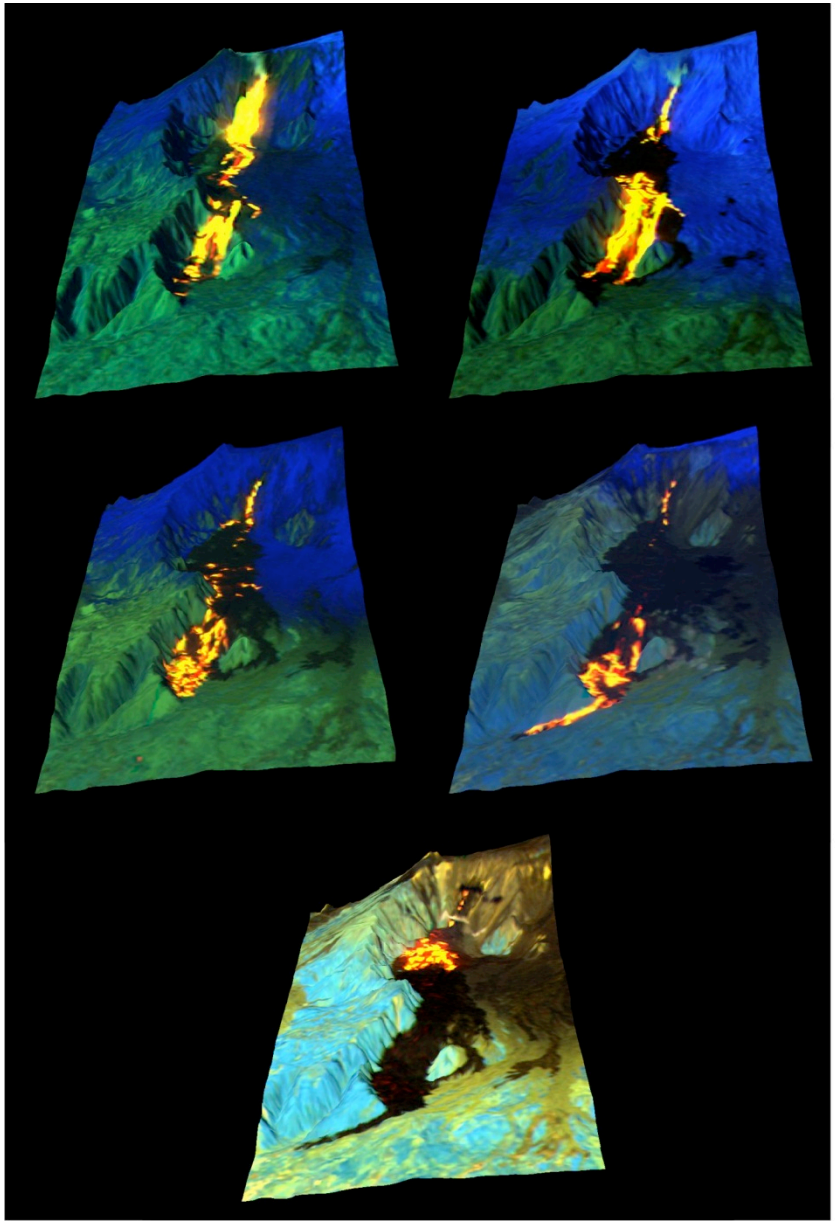

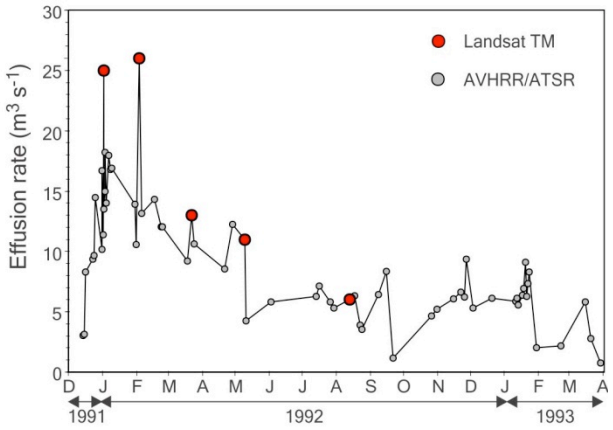

HyspIRI will give us MODIS-class temporal resolution with Landsat-class spatial resolution, allowing us to determine the important effusion rate parameter by day and night every five days

Driving numerical lava flow hazard models using satellite-derived effusion rates

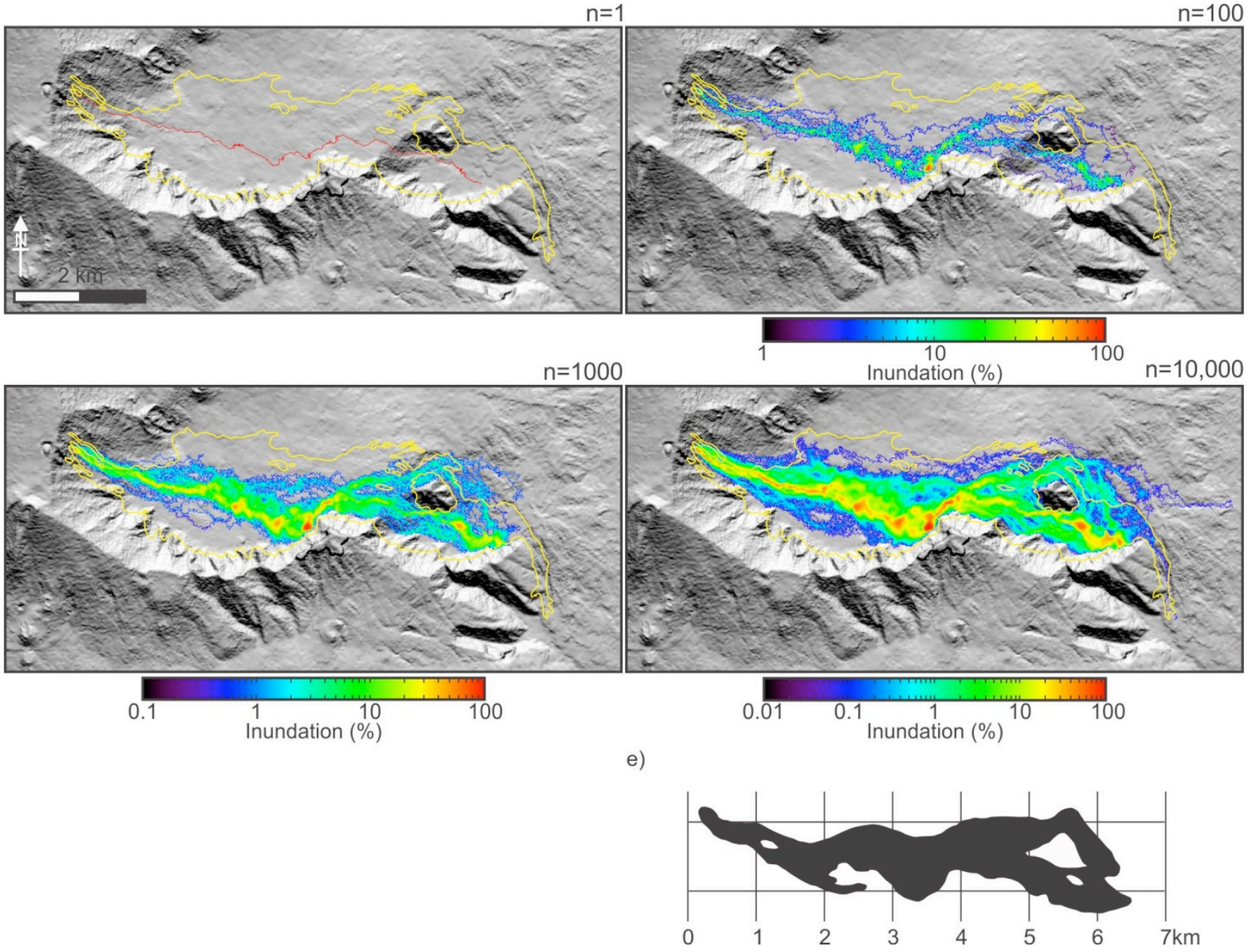

Wright et al., 2008

Driving numerical lava flow hazard models using satellite-derived effusion rates

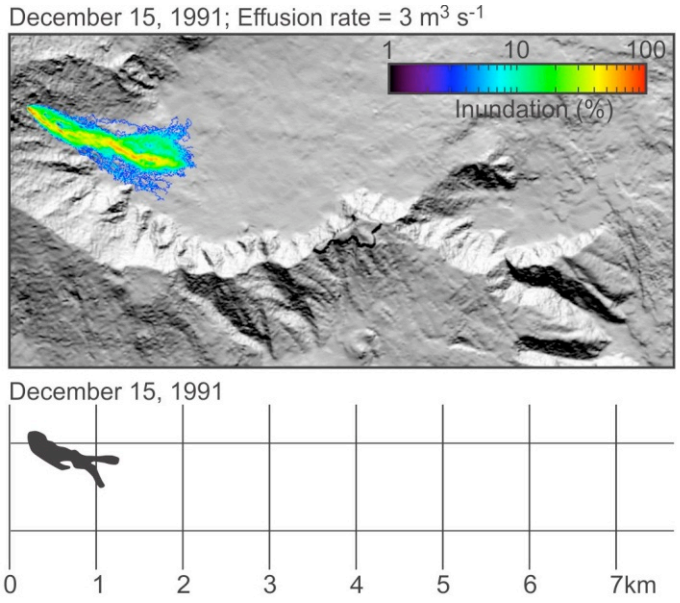

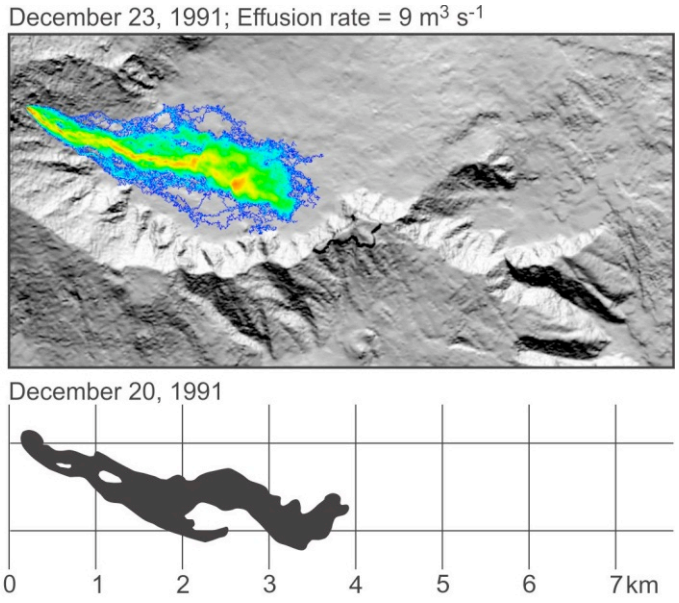

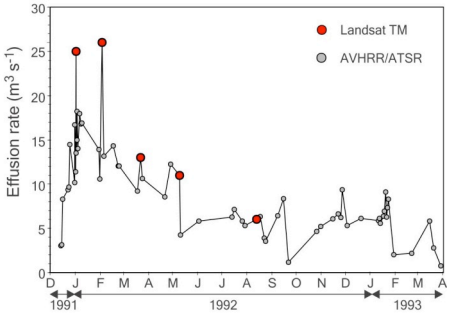

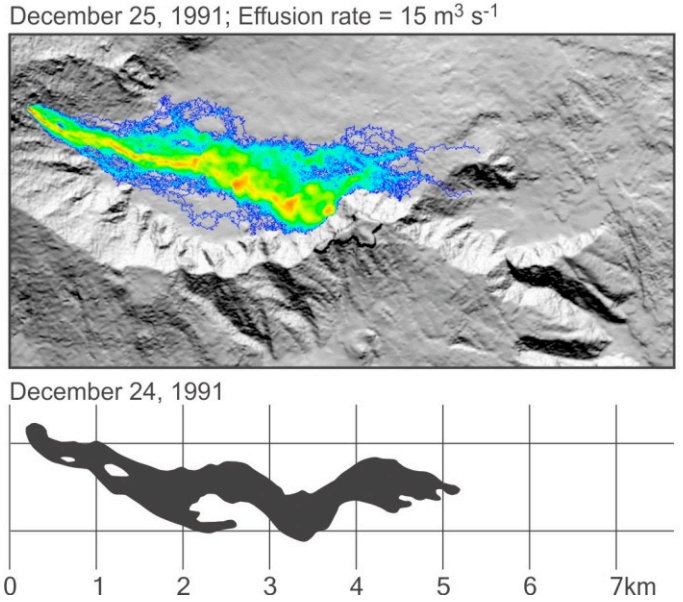

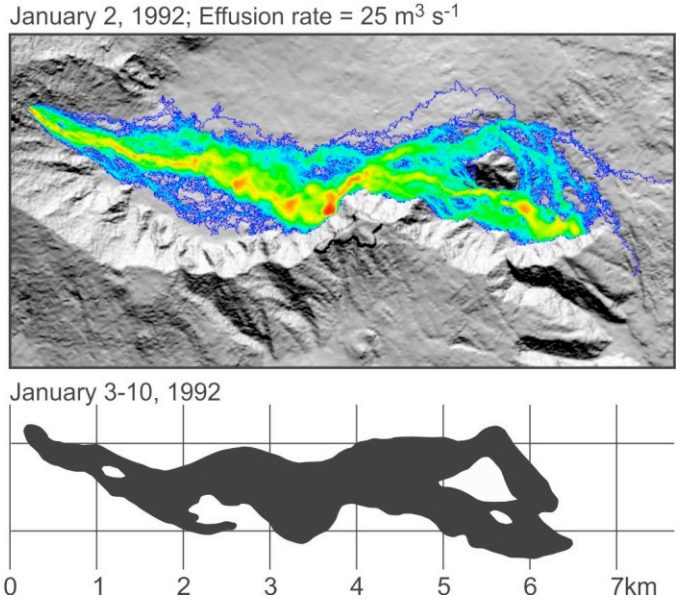

Wright et al., 2008

Parameterizing lava flow forecasting models using HyspIRI

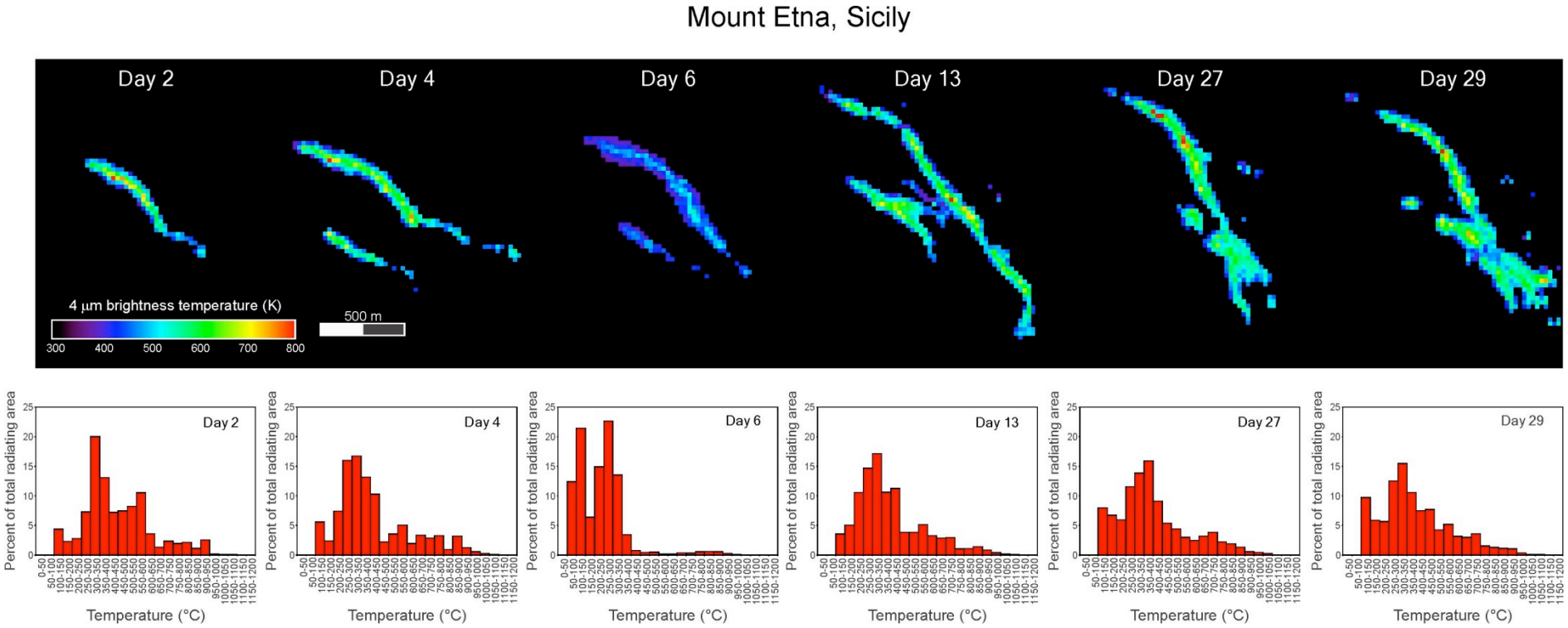

Wright, unpublished data

Lava flow surface temperature, and hence cooling rate, are important controls on how quickly lava solidifies. At present, these are poorly constrained inputs to numerical flow simulations. HyspIRI will allow us to fill this knowledge gap

Lava surface temperatures can be retrieved from an imaging spectrometer

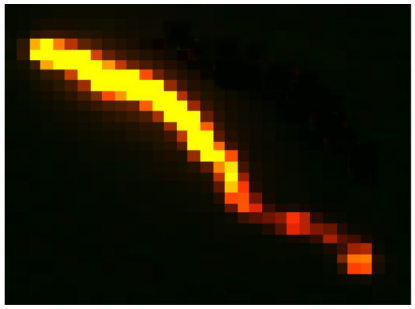

$$L_\lambda = \sum_{i=1}^{n} f_i(L, T_i)$$

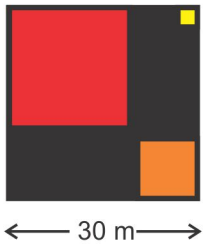

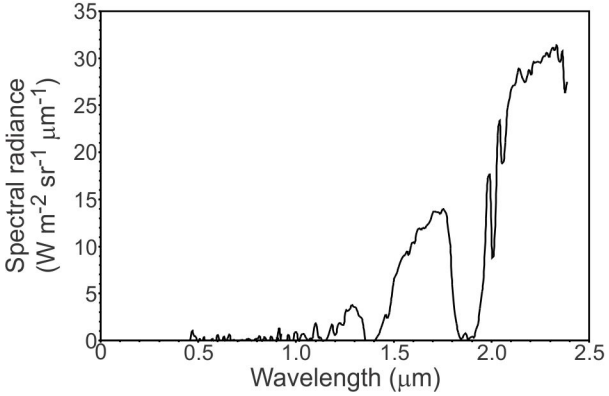

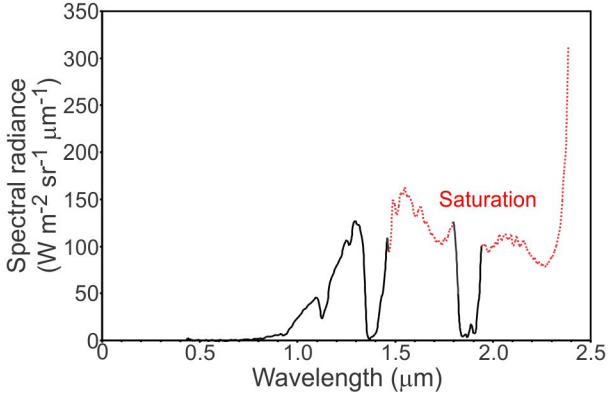

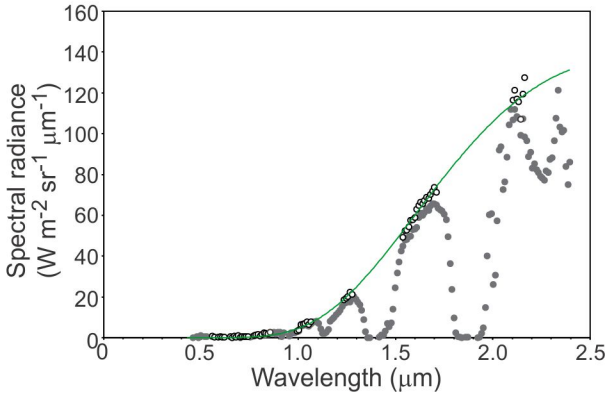

An imaging spectrometer always provides several tens of unsaturated spectral radiance measurements, at all points on the lava flow surface, from which lava surface temperatures can be determined

Autonomous forecasting of lava flow hazards using HyspIRI

1. HyspIRI autonomously detects the onset of the eruption, pinpoints the vent location and acquires an image.....

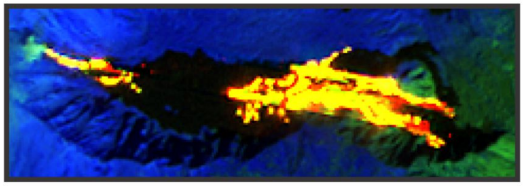

2. which allows us to compute the prevailing lava effusion rate.....

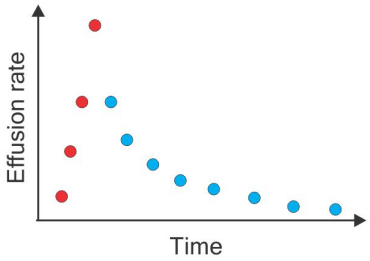

3. which we can use to drive a forecast of where the lava is likely to inundate.

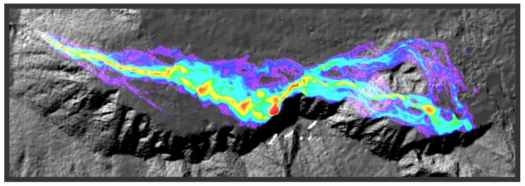

4. The next time HyspIRI passes over the target another image is acquired.....

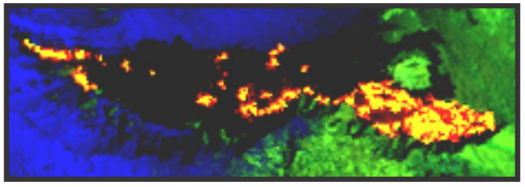

5. which can be used to compute the new prevailing effusion rate.....

6. as well as calibrate and validate the model predictions

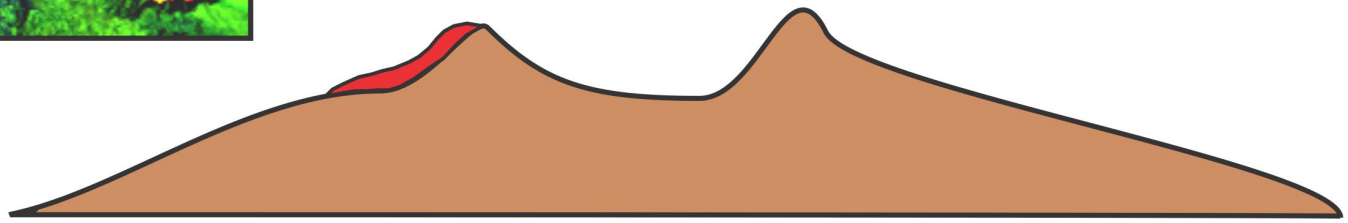

End

Simulated HyspIRI Volcanology Data Sets

Michael Abrams, Dave Pieri, Vince Realmuto,
NASA/Jet Propulsion Laboratory
Robert Wright
University of Hawaii

Goals of Project

The primary objective of this proposal is to create precursor HyspIRI-like data sets to examine several important volcanological questions:

1 What do changes in SO_2 emissions tell us about a volcano's activity?

2 How do we use measurements of lava flow temperatures and volume to predict advances of the flow front?

3 What do changes in lava lake temperatures and energy emissions tell us about possible eruptive behavior?

A second objective is to determine the saturation temperature for the Mid-IR band

ETNA

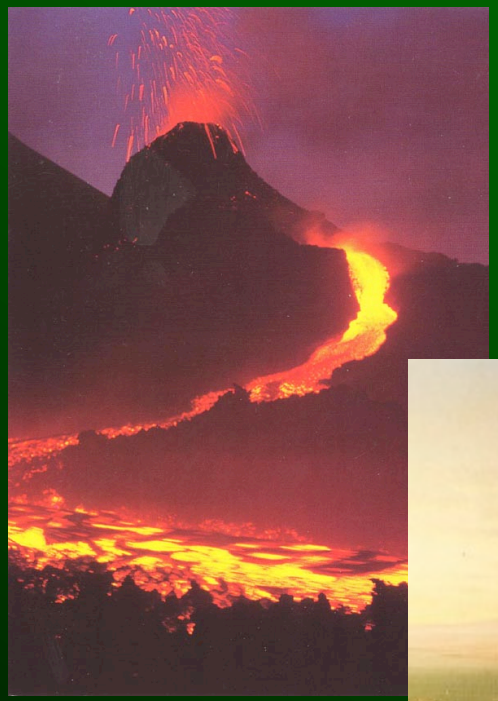

Why Mt. Etna?

- Europe's most active volcano
- Explosive and effusive eruptions
- Massive SO_2 emitter
- Extraordinarily frequent remote sensing data acquisitions
- Very well monitored by INGV
- Co-I at INGV will provide all ancillary data needed

Characteristics of Input Data Sets

	EO-1 Hyperion	ASTER TIR
Bands	196 unique in 0.4-2.5 micron region	5 in 8-12 micron region
Spatial resolution	30 m	90 m
Swath	7.5 km	60 km
Quantization	16 bit	12 bit

Ancillary Data Sets

	COSPEC SO_2	Flow field Topography	Eruption chronology
Eruptions and gas emissions	X		X
Lava flow modeling		X	X
Lava lake energy release			X

ASTER Daytime Scenes (1 2 3)

2000	2001	2002	2003	2004	2005	2006	2007	2008	2009	2010
7 May	29 July	5 June	15 Jan	7 Apr	26 Apr	3 Aug	19 Jun	21 Jun	7 Oct	26 May
		7 July	13 Mar	10 June		12 Aug	21 Jun	8 Aug		7 Aug
		23 July	19 July	26 June		7 Nov	14 Jul	21 Nov		
		3 Nov	11 Aug	6 Aug			21 Jul			
		30 Dec		13 Aug			30 Jul			
				22 Aug			2 Oct			

Multispectral TIR from Daytime ASTER (1 2 3)

VNIR image: plume is gray;
flows are not incandescent

TIR image: plume composition
is mostly ash; flows are obvious

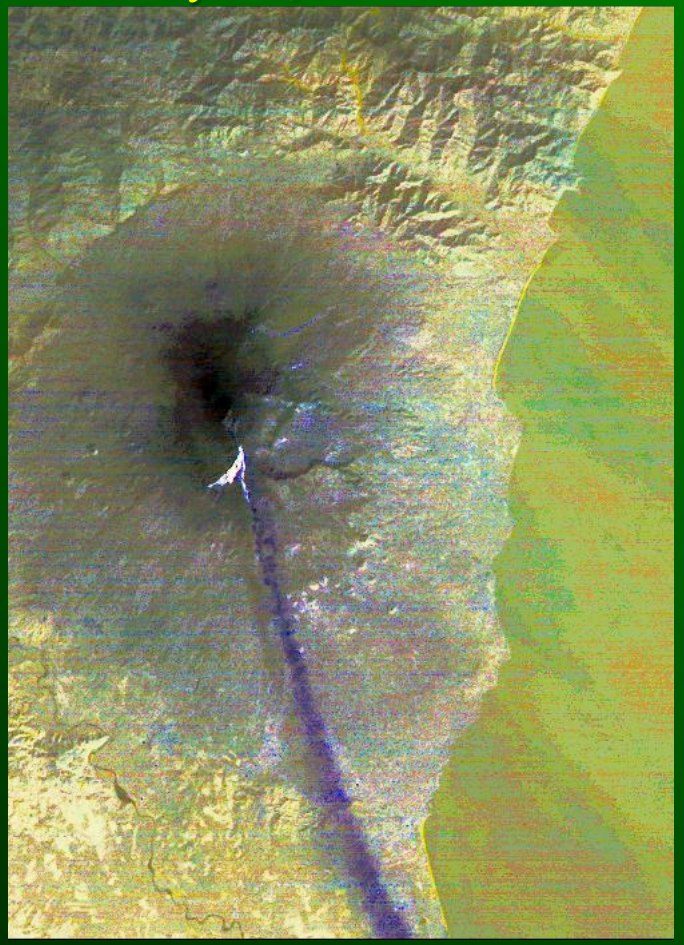

Multispectral Daytime ASTER (2 3)

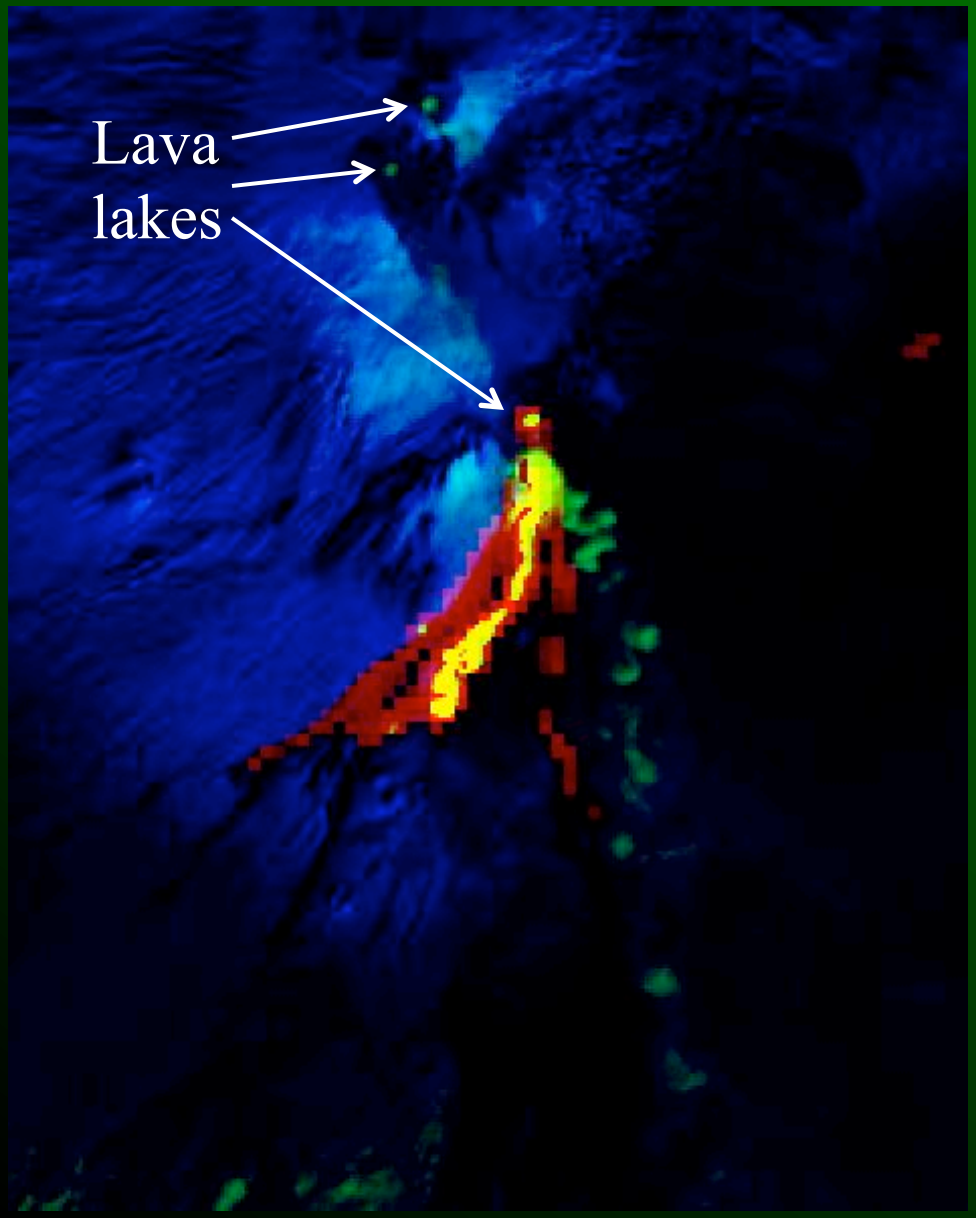

R=11um G=1.5um B=0.84um

Lava flows vary in temperature; multispectral data allow better estimation of temperatures than TIR alone.

ASTER Nighttime TIR Scenes (1 2 3)

2000	2001	2002	2003	2004	2005	2006	2007	2008	2009	2010
6-Jun	9-Jan	19-Jan	7-Feb	13-Mar	5-Feb	29-Apr	15-Mar	21-Jun	6-Jan	2-Jan
22-Jun	25-Jun	22-Jan	20-Mar	15-Jun	4-Nov	31-May	18-May	11-Oct	15-Jun	3-Feb
8-Jul	11-Jul	28-Jan	14-May	26-Jun	11-Nov	2-Jul	19-Jun	5-Dec	24-Jun	1-May
24-Jul	15-Oct	4-Feb	17-Jul	3-Jul	27-Nov	25-Jul	26-Jun		10-Jul	10-May
10-Sep	24-Oct	12-Jan	26-Jul	14-Sep		3-Aug	12-Jul		2-Aug	
28-Oct		11-May	18-Aug			10-Aug	12-Dec		15-Nov	
		20-May				4-Sep				
		28-Jun				13-Oct				
		23-Jul				7-Nov				
		16-Sep								
		18-Oct								
		27-Oct								
		19-Nov								
		28-Nov								

Selected 2002 ASTER Night TIR (1 2 3)

January 19

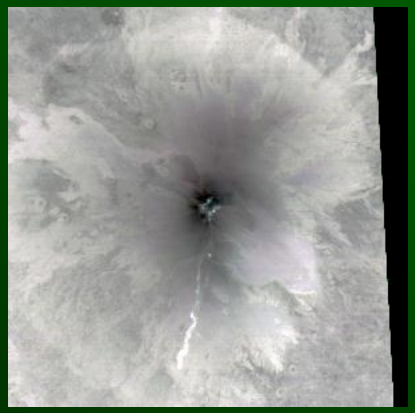

January 28

May 11

May 20

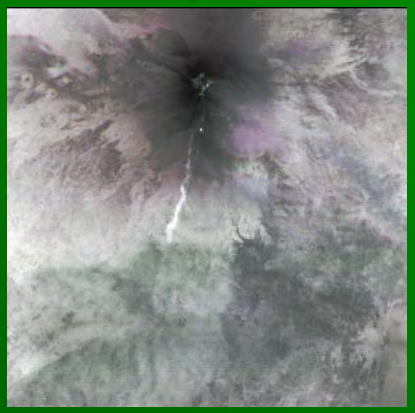

June 28

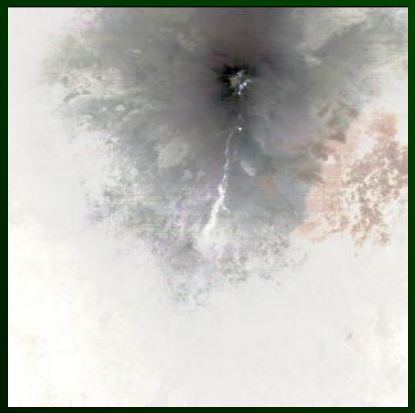

July 23

October 27

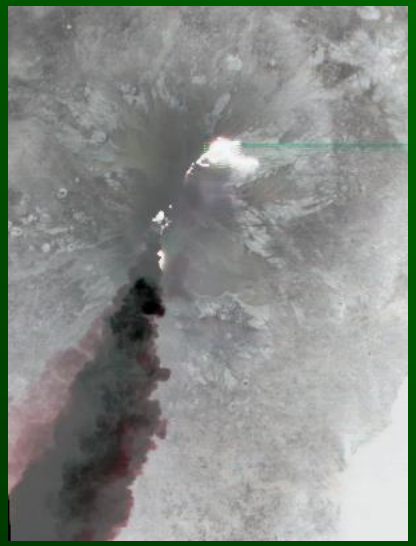

EO-1 Hyperion Daytime Scenes (2 3)

EO1H1880342009281110pf_sgs_01
EO1H1880342008206110kf_sgs_01
EO1H1880342008152110kf_sgs_01
EO1H1880342007190110kf_sgs_01
EO1H1880342007134110kf_sgs_01
EO1H1880342006303110pf_sgs_01
EO1H1880342006298110pf_sgs_01
EO1H1880342005316110kf_sgs
EO1H1880342005302110kf_sgs
EO1H1880342005205110pf_hgs
EO1H1880342004283110pw_sgs
EO1H1880342004260110kw_pf1
EO1H1880342003223110kf_sgs
EO1H1880342003207110kx_hgs
EO1H1880342003177110ky_sgs
EO1H1880342001267110kp_sgs
EO1H1880342001242110po_sgs
EO1H1880342001203110kp_sgs
EO1H1880342001194110po_sgs

July 22, 2001 Hyperion Etna Data (2 3)

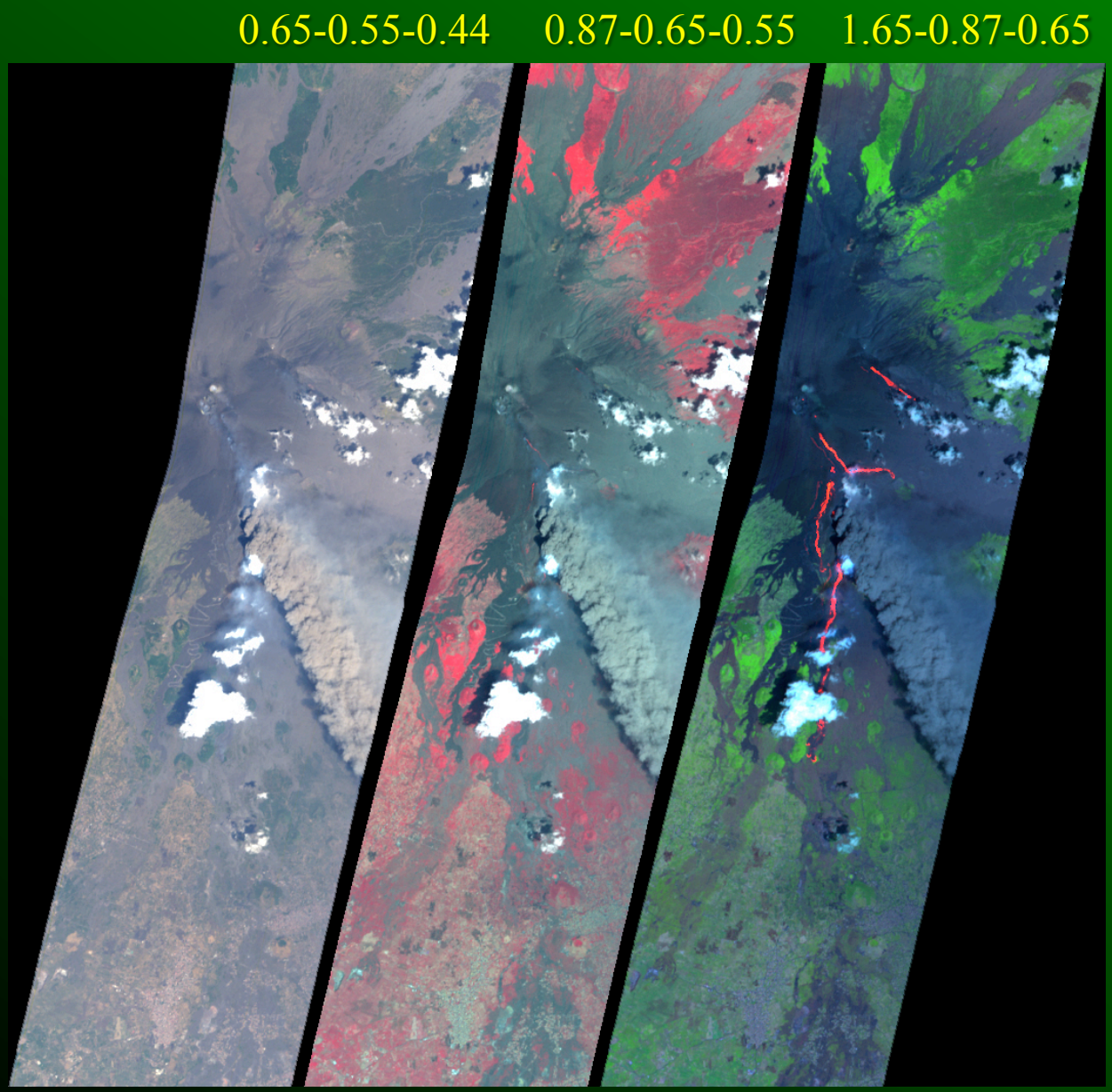

SO_2 Determination with ASTER TIR(1)**

Will be discussed
in following talk
by Vince Realmuto

Lava Flows, Energy Radiated, Extent (2)

Lava flow models require DEM data, effusion rates, and Temperature distributions

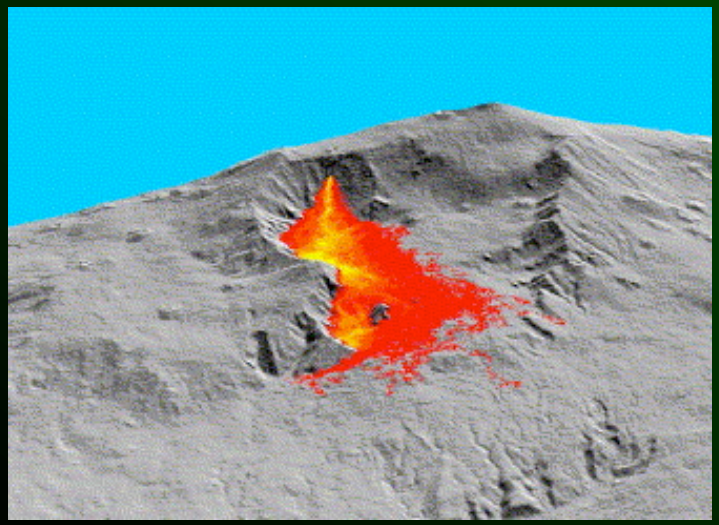

Damiani et al., 2006

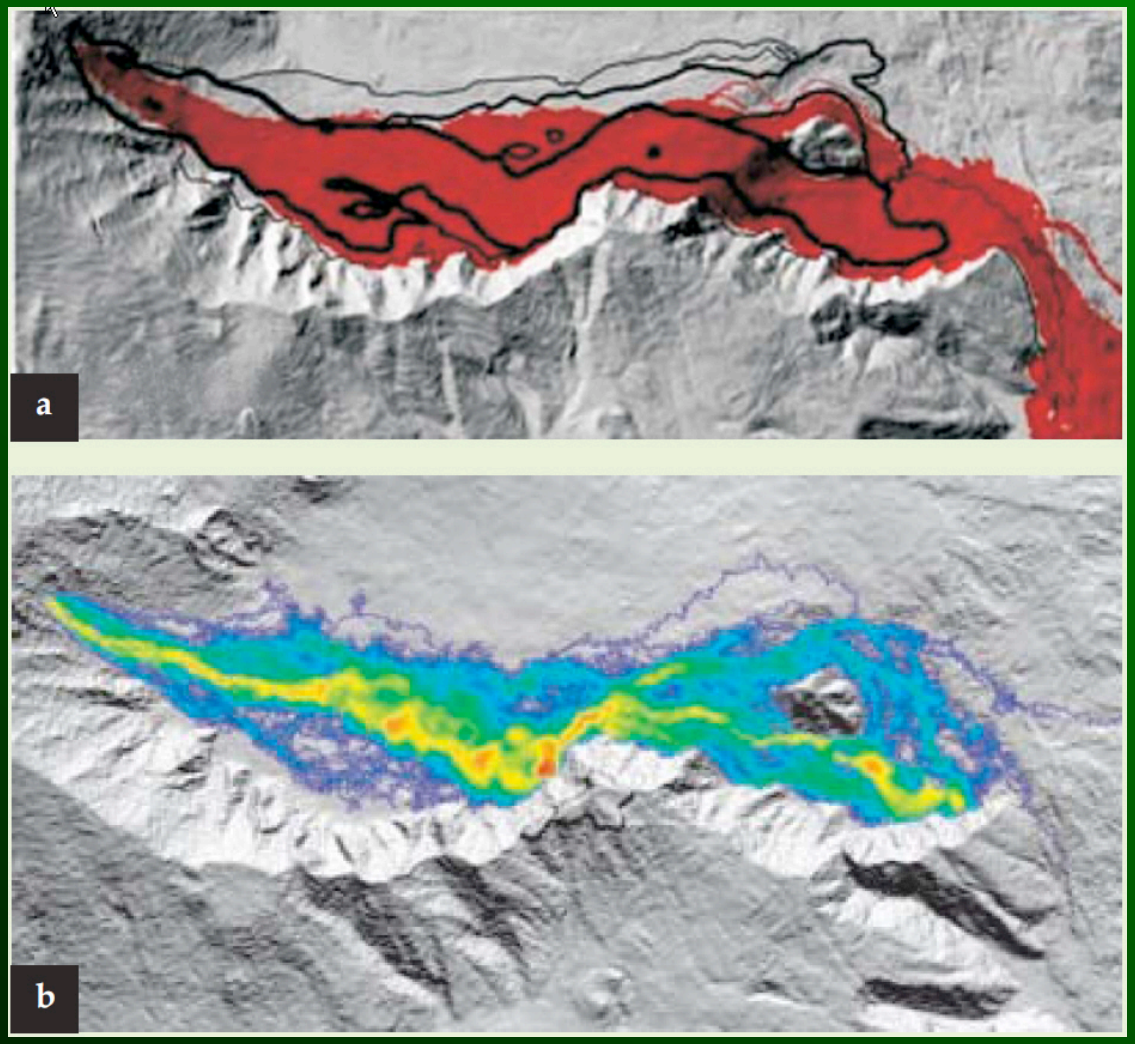

Wright et al., 2008

Lava Flows, Energy Fluxes (2)

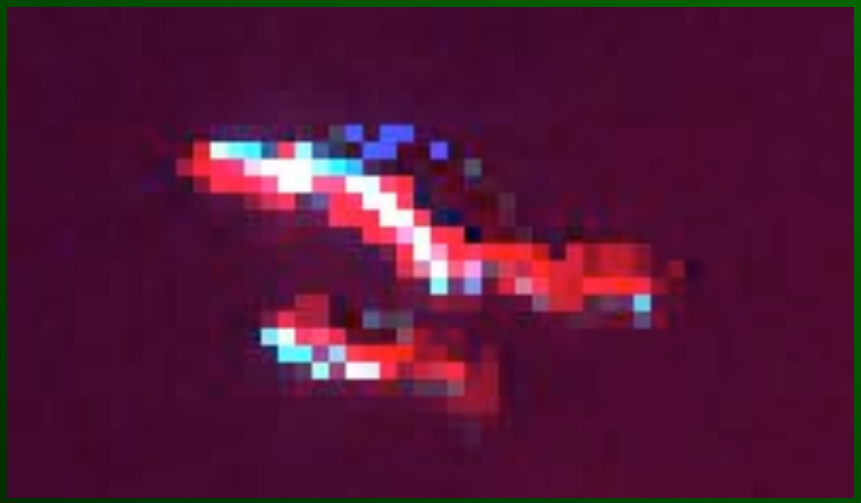

Sept 14, 2004 nighttime combined ASTER + EO-1 Hyperion data for lava flows; most TIR pixels are saturated.

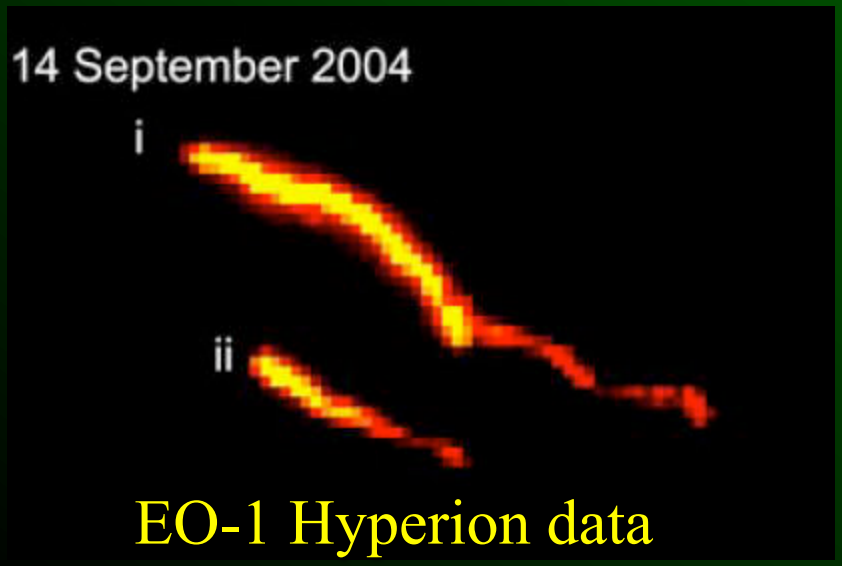

EO-1 Hyperion data

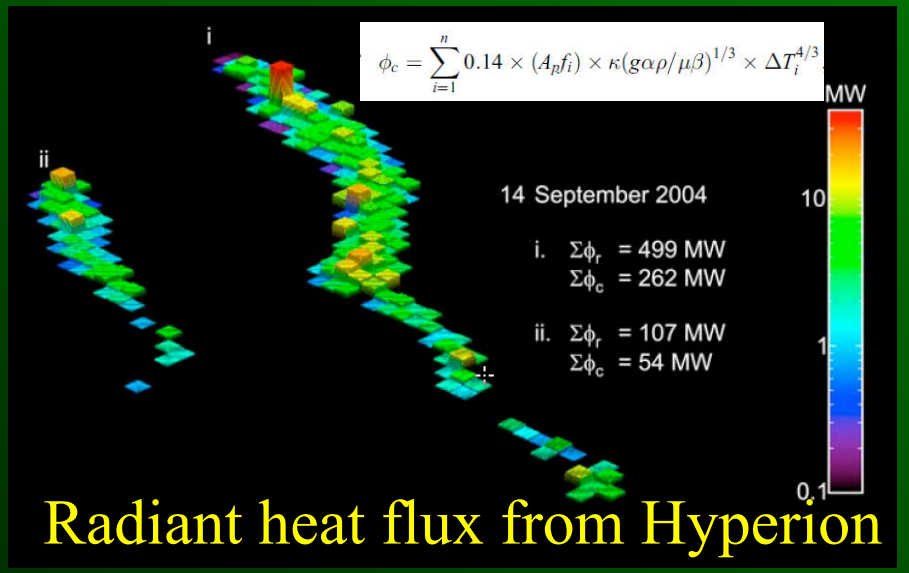

Radiant heat flux from Hyperion

Wright et al., 2010, JGR

Lava Flows, Energy Fluxes (2)

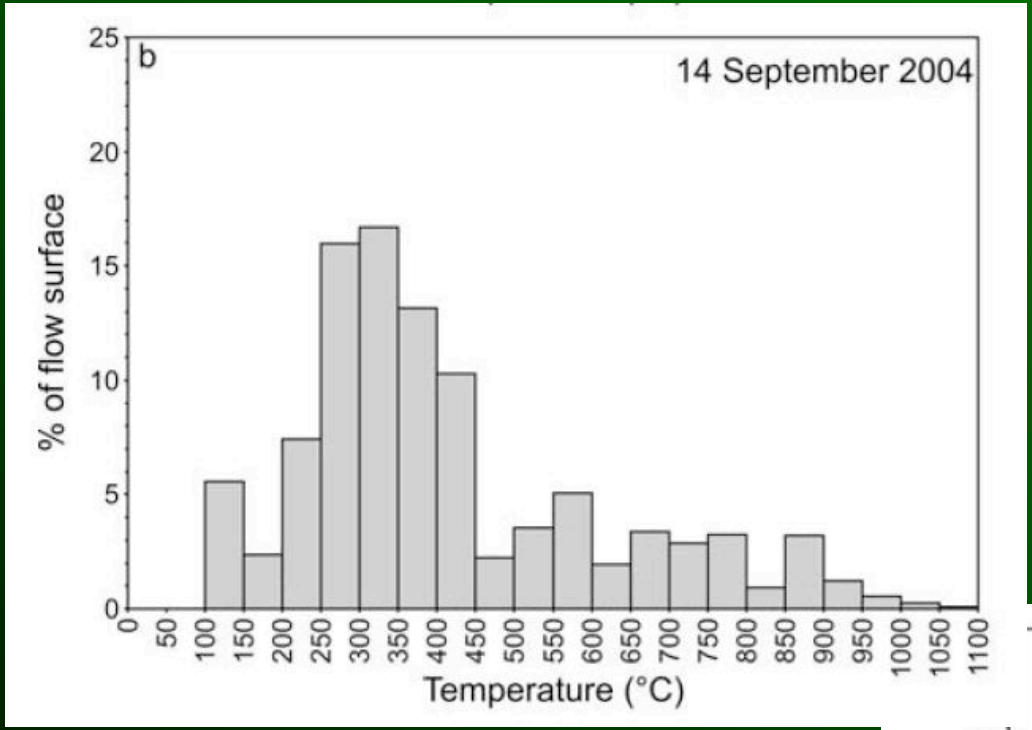

Temperature histogram for flow unit I from Hyperion data

Radiant heat flux as a function of distance from the vent. September 14 is red curve.

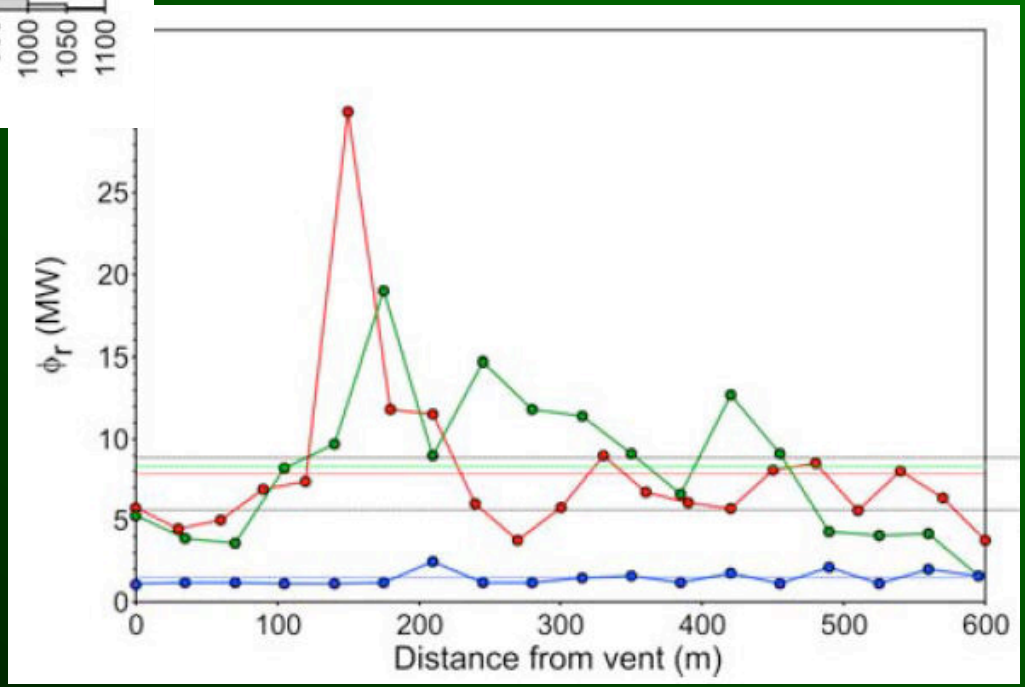

Wright et al., 2010, JGR

Lava Flow Dynamics (2)

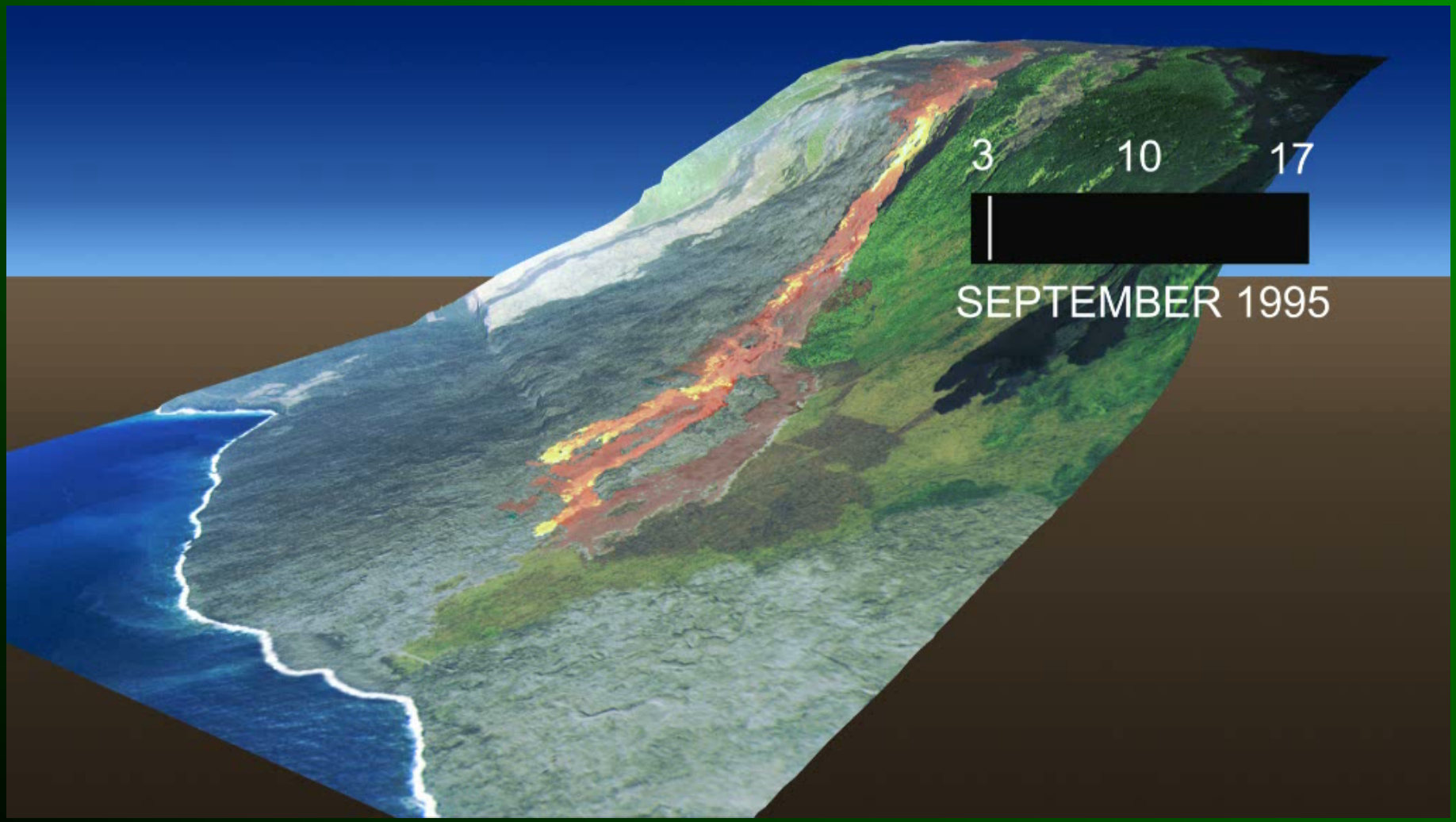

Courtesy of Vince Realmuto

Lava Flow Dynamics (2)

To Do: Use Temperature and energy measurements in lava flow model (FLOWZ) to predict flow extent.

ETNA Craters

Central Crater:
Bocca Nuova & La Voragine

Northeast Crater

Southeast Crater

Craters, Energy Fluxes (3)**

July 22, 2001 EO-1 daytime image of craters and flows. Radiance of incandescent craters fills one pixel; 60m size allows only pixel integrated temperature to be estimated.

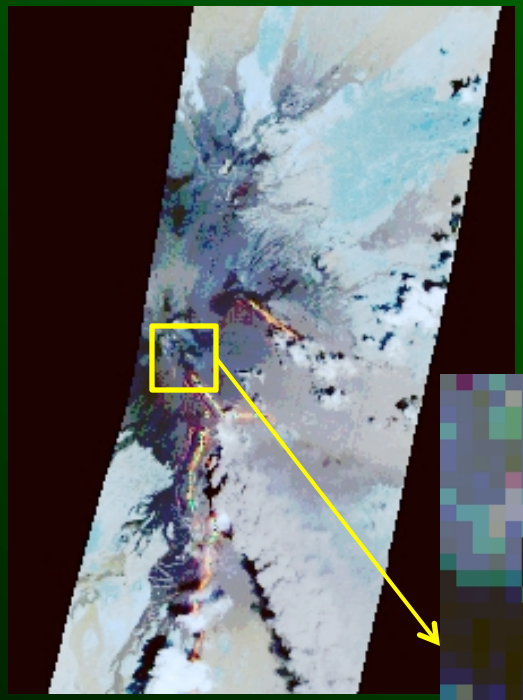

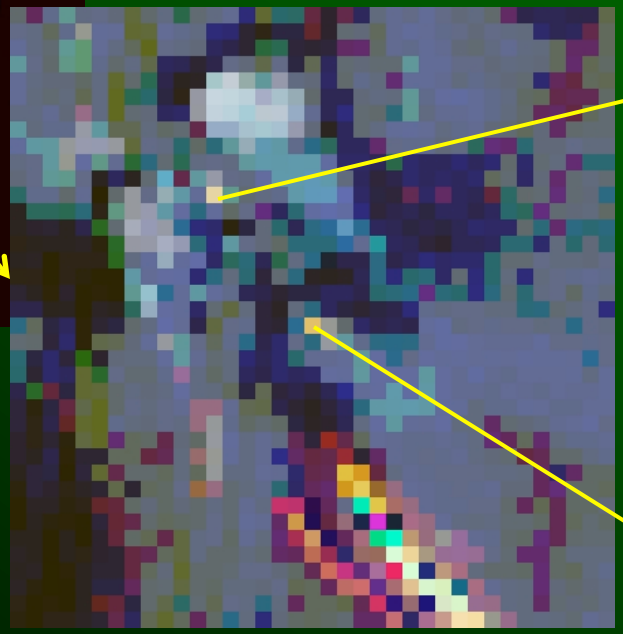

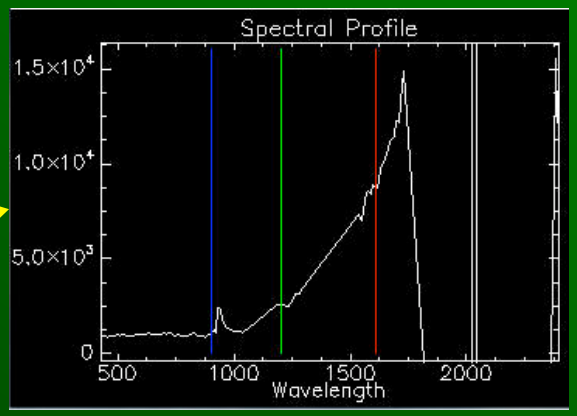

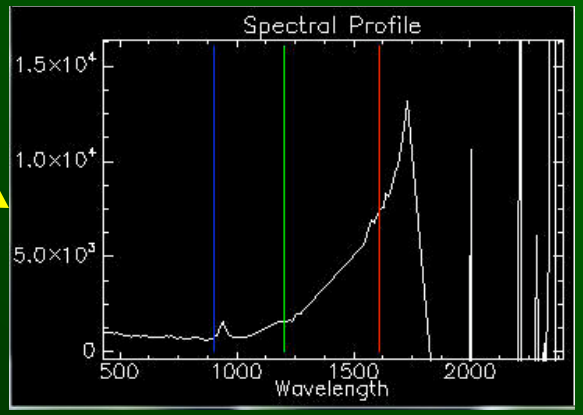

Craters, Energy Fluxes (3)**

- Between 2000 and 2010, 61 ASTER cloud-free nighttime TIR scenes were acquired (~6/yr, or one scene every 2 months)
- Summit area was extracted, and maximum radiance of craters was determined.
- *Still to do: compute total flux from craters*

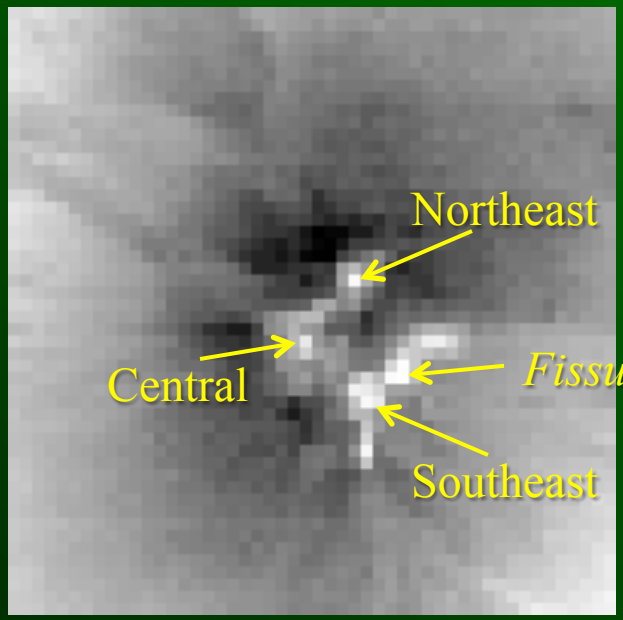

Craters, Energy Fluxes (3)** 2000-2002

La

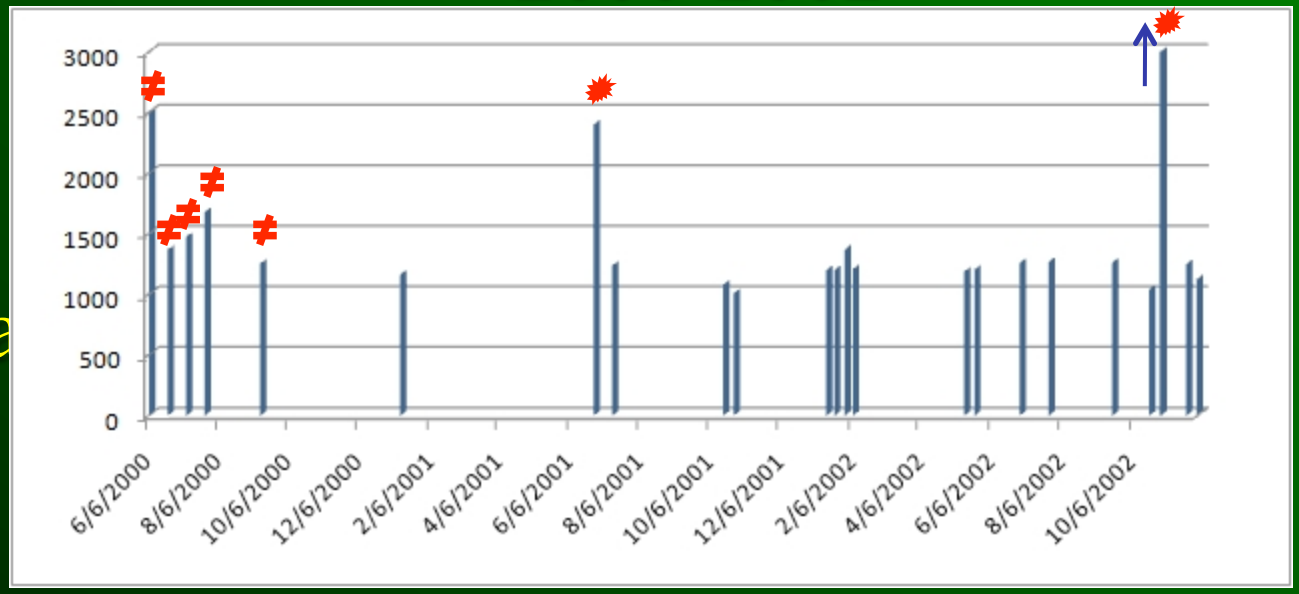

Large eruption

No data

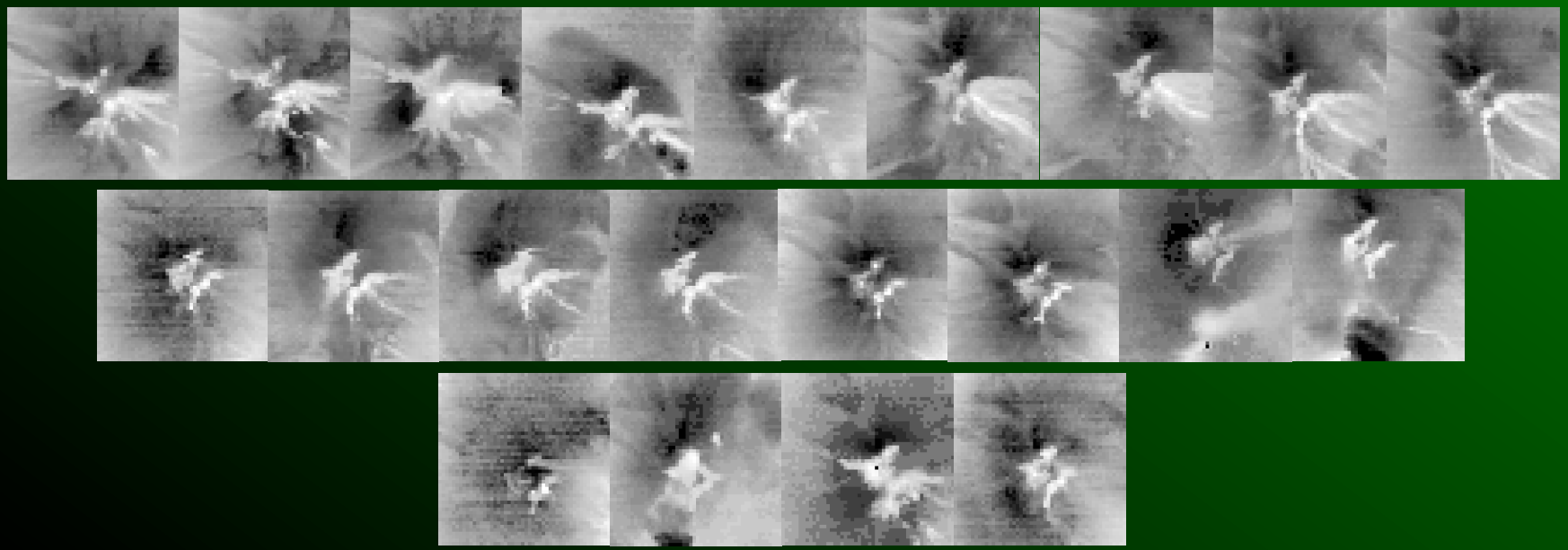

Craters, Energy Fluxes (3)** 2003-2005

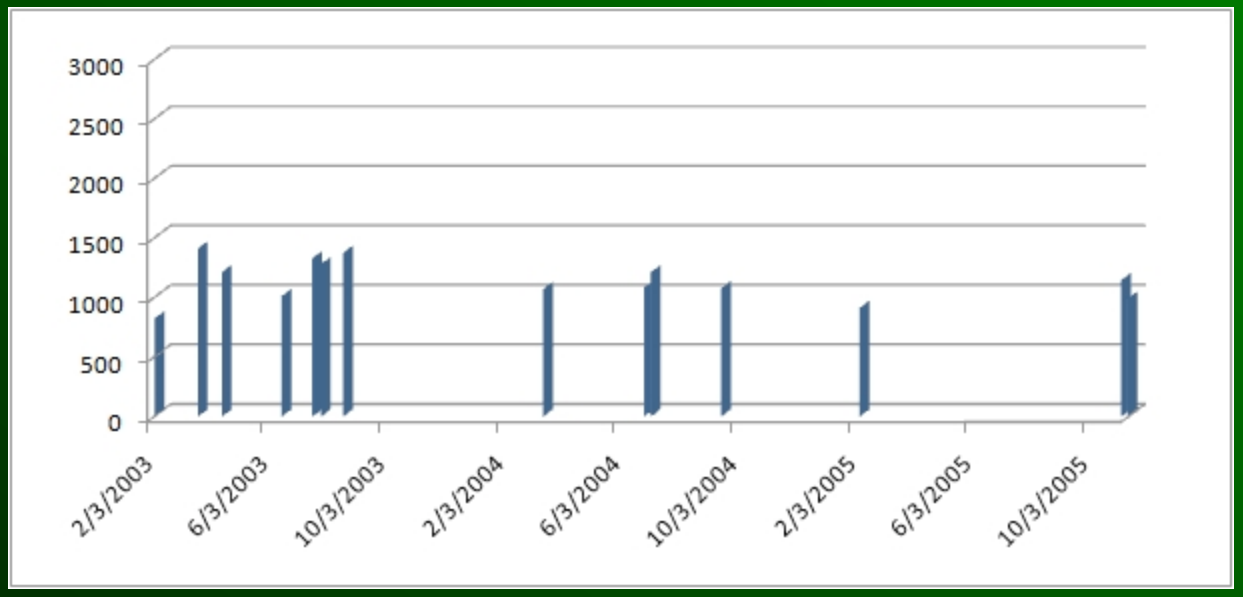

- Large eruption
- No data

All dates reported gas and ash emissions

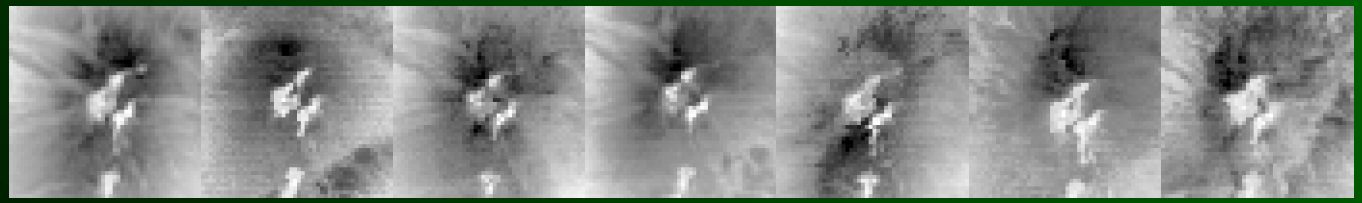

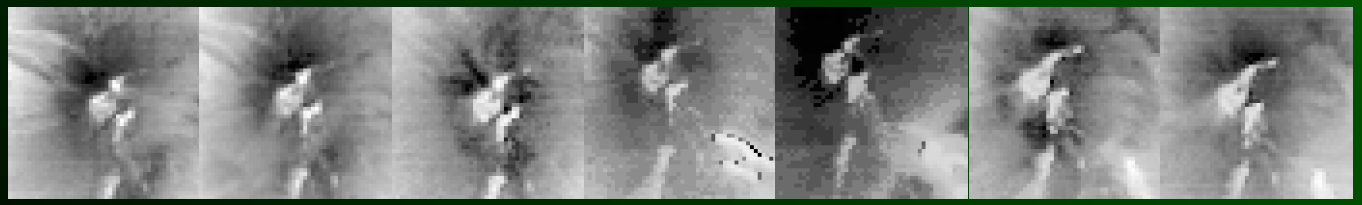

Craters, Energy Fluxes (3)** 2006-2010

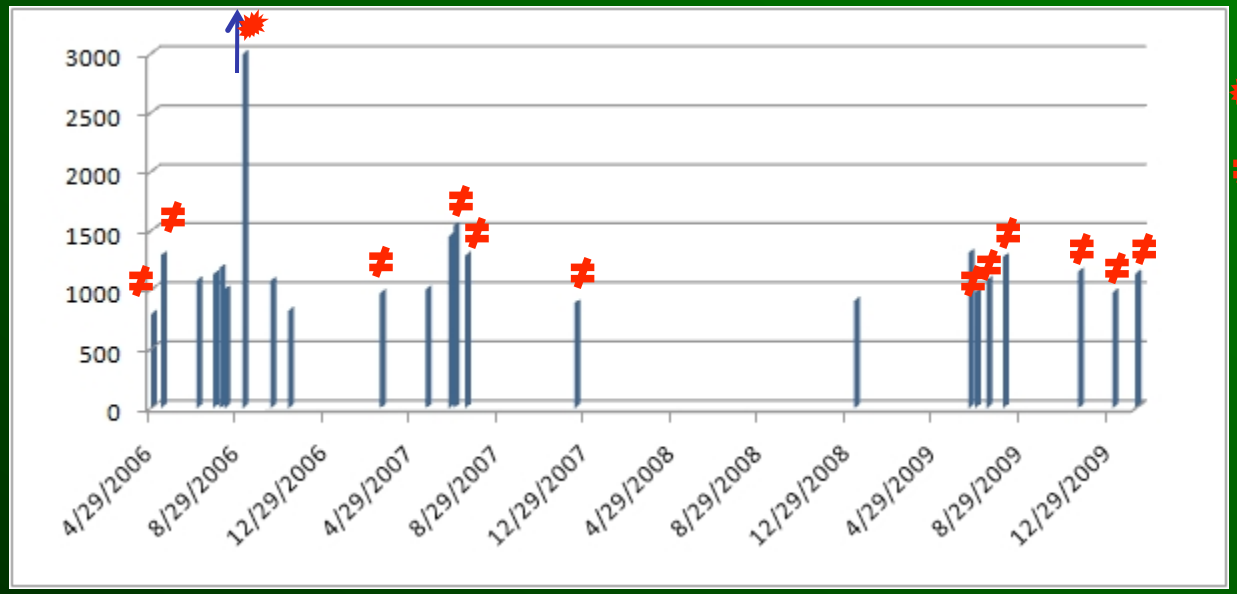

Large eruption

No data/actvity

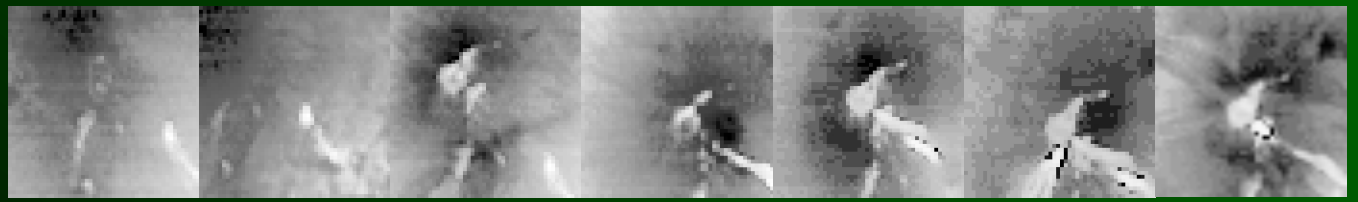

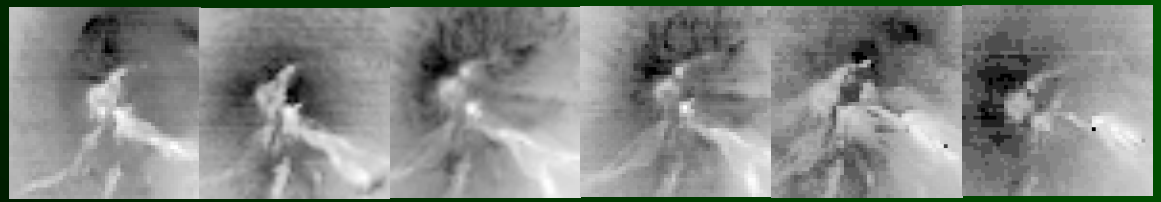

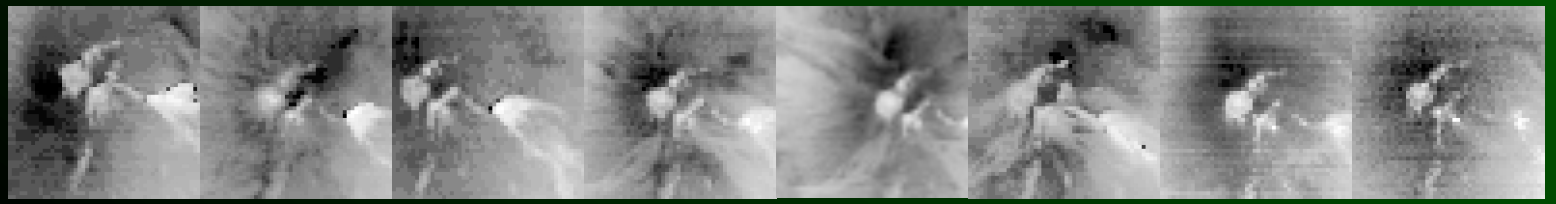

Simulated HyspIRI Data Sets

- 5 daytime dates and 1 nighttime date were selected that were cloud-free, and had simultaneous Hyperion and ASTER acquisitions; only 1 coincided with eruption activity

- Hyperion data were re-sampled to 60m, duplicate channels removed, data scaled to radiance-at-sensor

- ASTER TIR bands were re-sampled to 60m, registered to Hyperion, data scaled to radiance-at-sensor

- 226-band images created with ENVI header files

Simulated HyspIRI Daytime Data Sets

Cloud-free Hyperion and ASTER Data

Hyperion	ASTER
2001-7-13	2001-7-29
2001-7-22	
2001-8-5	
2001-8-14	2002-6-5
2001-8-30	2002-7-7
2001-9-24	2002-7-23
	2002-11-3
2002-11-12	2002-12-30
2003-1-15	2003-1-15
2003-3-20	2003-3-13
2003-6-26	2003-7-19
2003-7-19	2003-8-11
2003-7-26	2003-1-15
2003-8-11	
2004-9-16	2004-6-26
2004-10-9	2004-8-6
	2004-8-22

Hyperion	ASTER
2005-3-16	2005-4-26
2005-3-18	
2005-7-24	2006-8-3
2005-10-29	2006-8-12
2005-11-5	2006-11-17
2005-11-12	2006-11-30
2005-11-30	
	2007-6-19
2006-10-25	2007-6-21
2006-11-24	2007-7-14
2006-11-29	2007-7-21
	2007-7-30
2007-5-14	2007-10-2
2007-7-9	
	2008-6-21
2008-5-31	2008-8-8
2009-10-8	2009-5-23
	2009-10-8
	2010-5-10
2011-6-30	2011-2-6
	2011-4-4
	2011-6-30

Simulated HyspIRI Daytime Data Sets
January 15, 2003

- On 15 January 2003, ash emission increased at the 2,750-m-elevation pyroclastic cone on the volcano's upper S flank. There was also an associated increase in lava emission towards the south
- The volcano was snow covered down to the 1500m level

- Smithsonian/USGS Weekly Volcanic Activity Report

Simulated HyspIRI Data Sets
January 15, 2003

.91, .65, .55

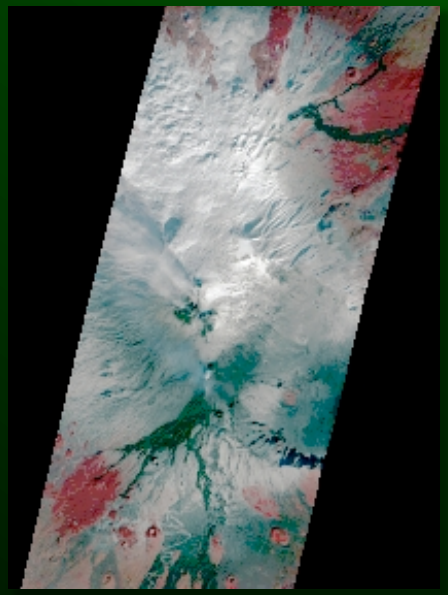

1.2, .91, .65

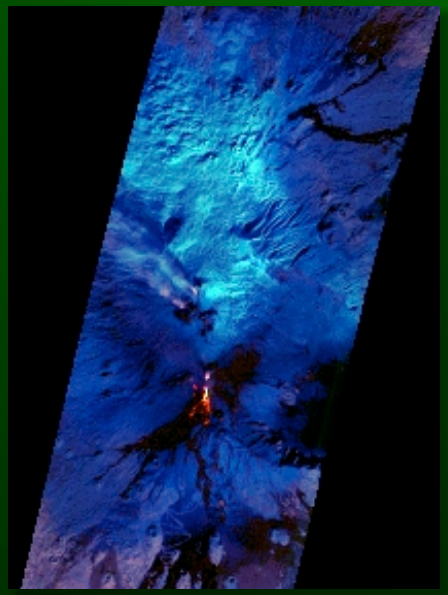

1.6, 1.2, .91

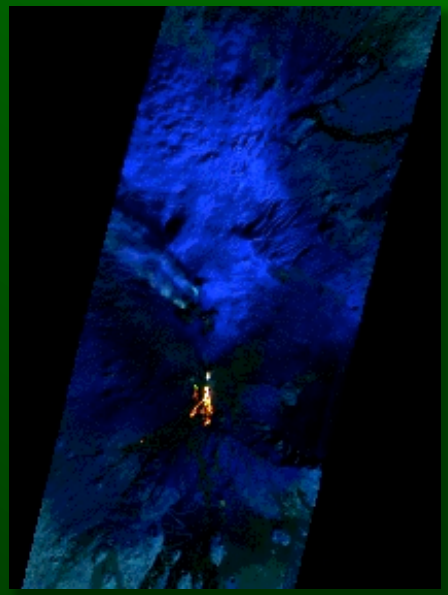

9.0, 1.6, 1.2

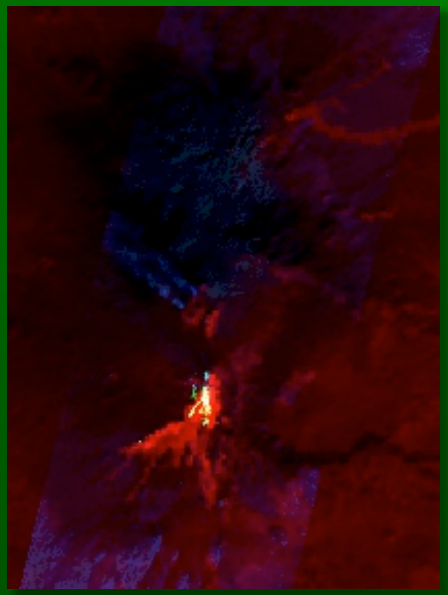

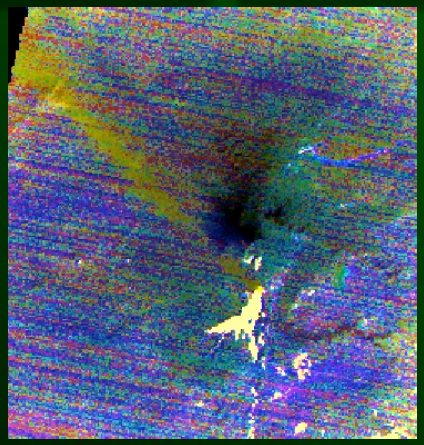

11.3, 10.6, .8.6

Simulated HyspIRI Data Sets**
January 15, 2003

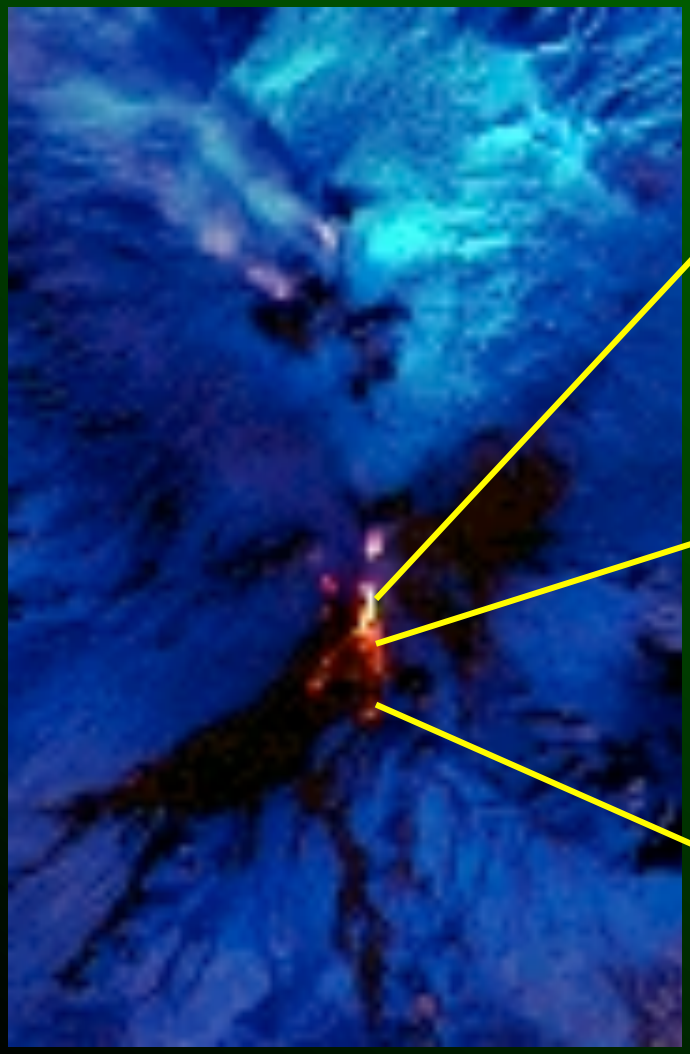

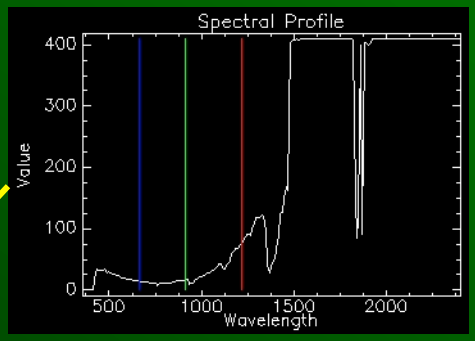

Hottest, “saturated” lava

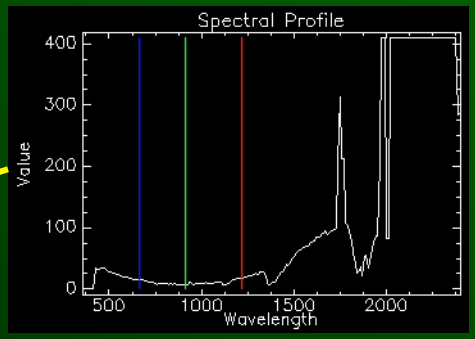

Hot lava

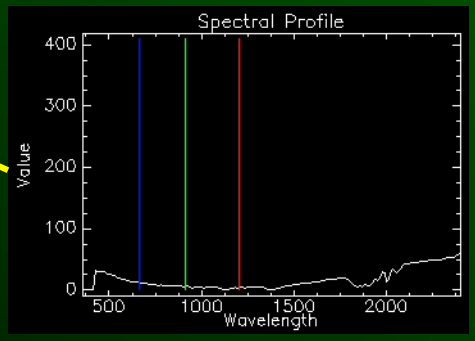

“Warm” lava

Simulated HyspIRI Data Sets
January 15, 2003: ASTER TIR

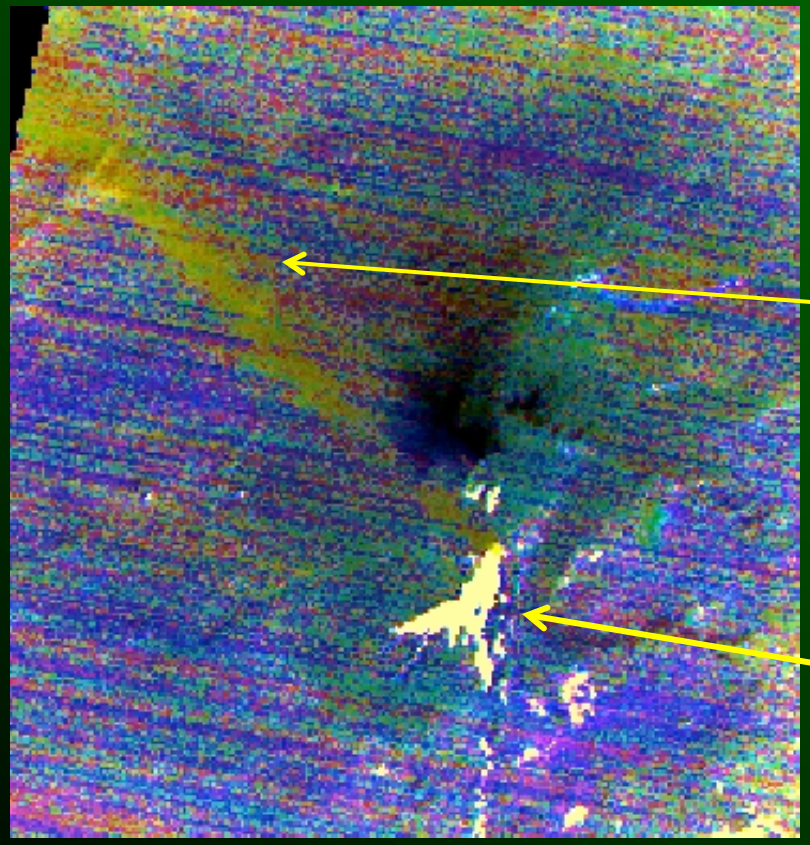

11.3, 10.6, .8.6

Yellow color of plume in this d-stretch image indicates that the dominant components are SO_2 and ash

Most of lave flow is saturated in ASTER TIR channels

4 micron Channel Saturation

Retrieving lava surface temperatures using Hyperion

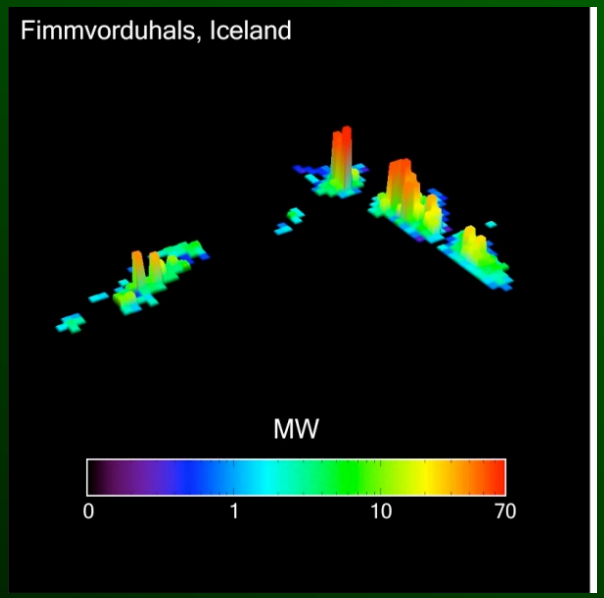

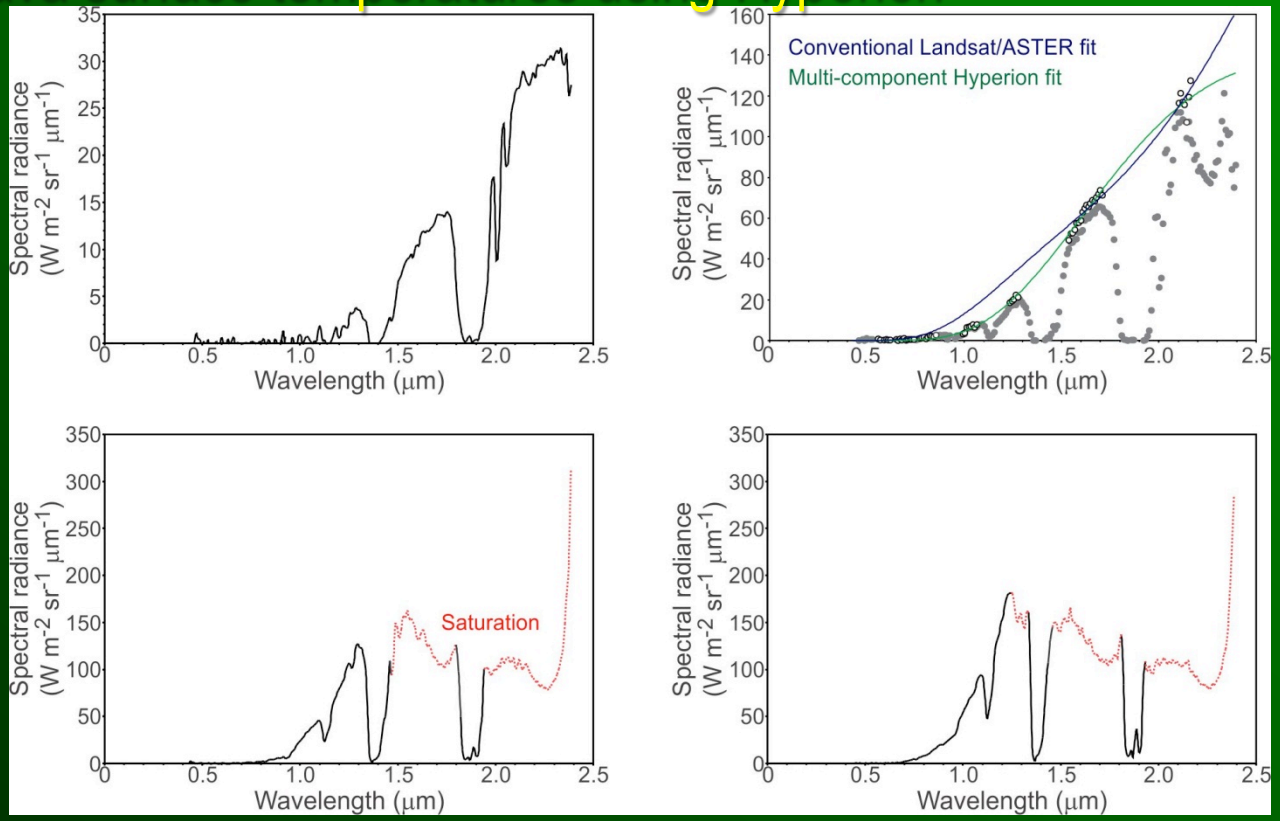

- Used Hyperion images (nighttime data) to calculate the sub-pixel temperature distributions of active lavas as a first step to retrieving surface leaving radiance at 4 μm at 30 m scale.
- Unsaturated data are always available from an imaging spectrometer, so Hyperion resolves the temperatures of even the hottest lava flows

How hot are Earth's lava flows, domes and lakes?

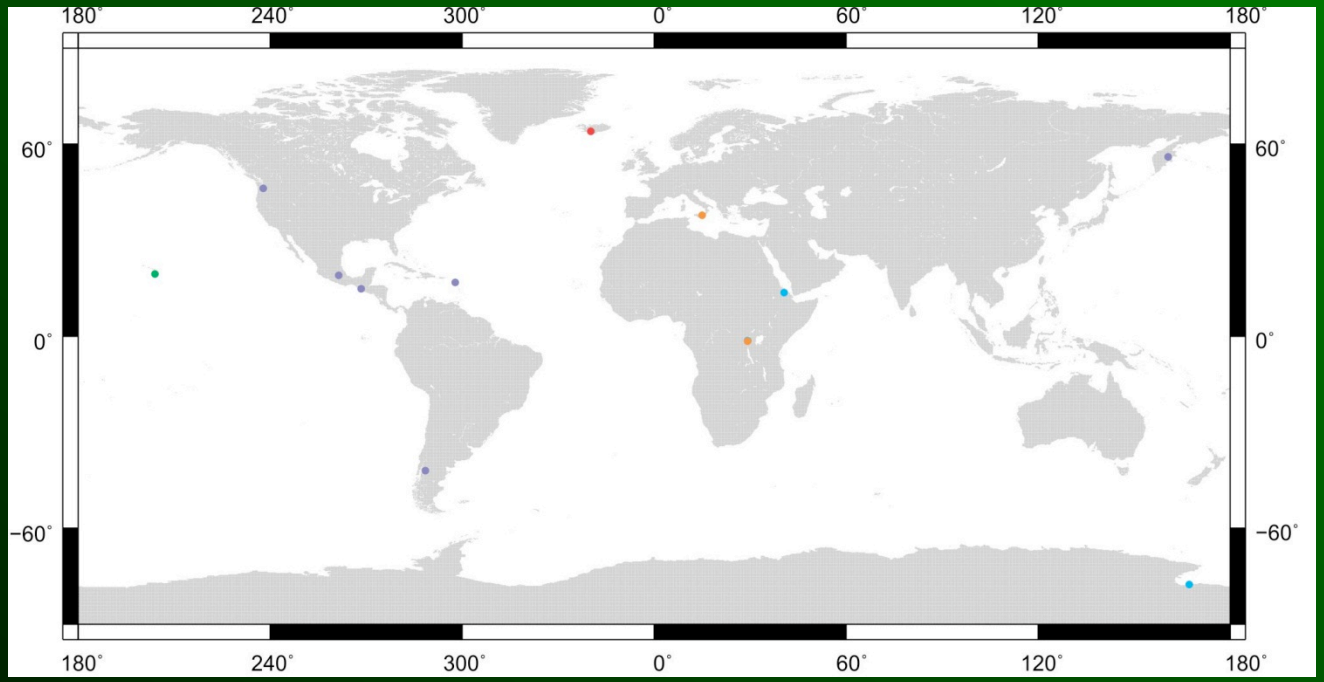

10 images of ʻaʻā lava flows
10 images of pāhoehoe lava flows
20 images of domes
20 images of lakes
1 image of fountains

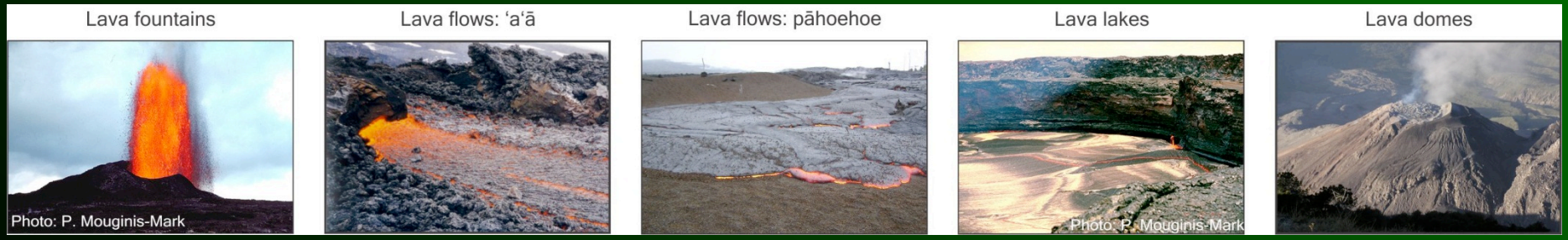

•Analyzed Hyperion images acquired at 16 different volcanoes, exhibiting the full range of common eruption styles to ensure the results were representative

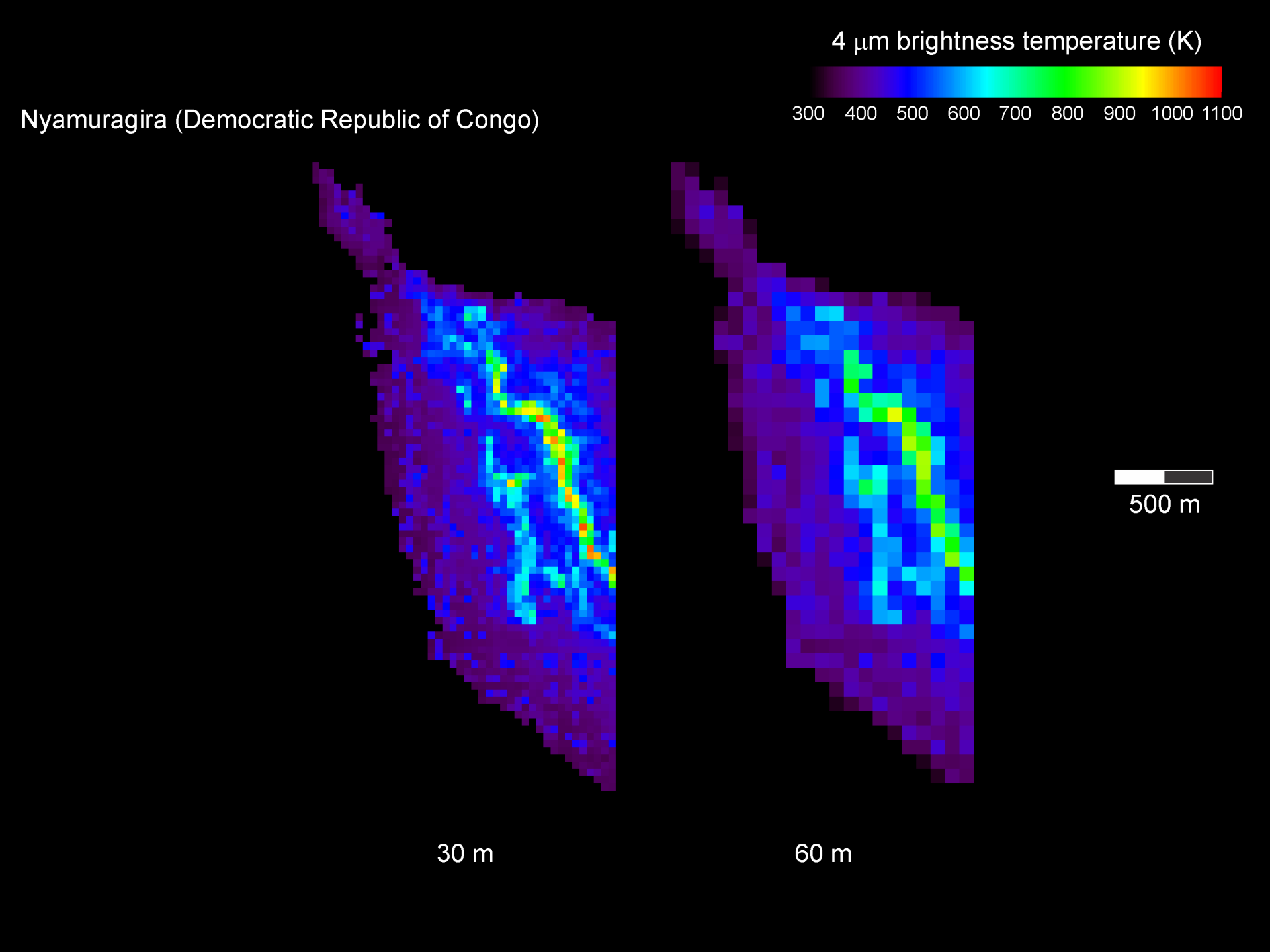
4 μm brightness temperature (K)
300 400 500 600 700 800 900 1000 1100
Nyamuragira (Democratic Republic of Congo)
500 m
30 m
60 m

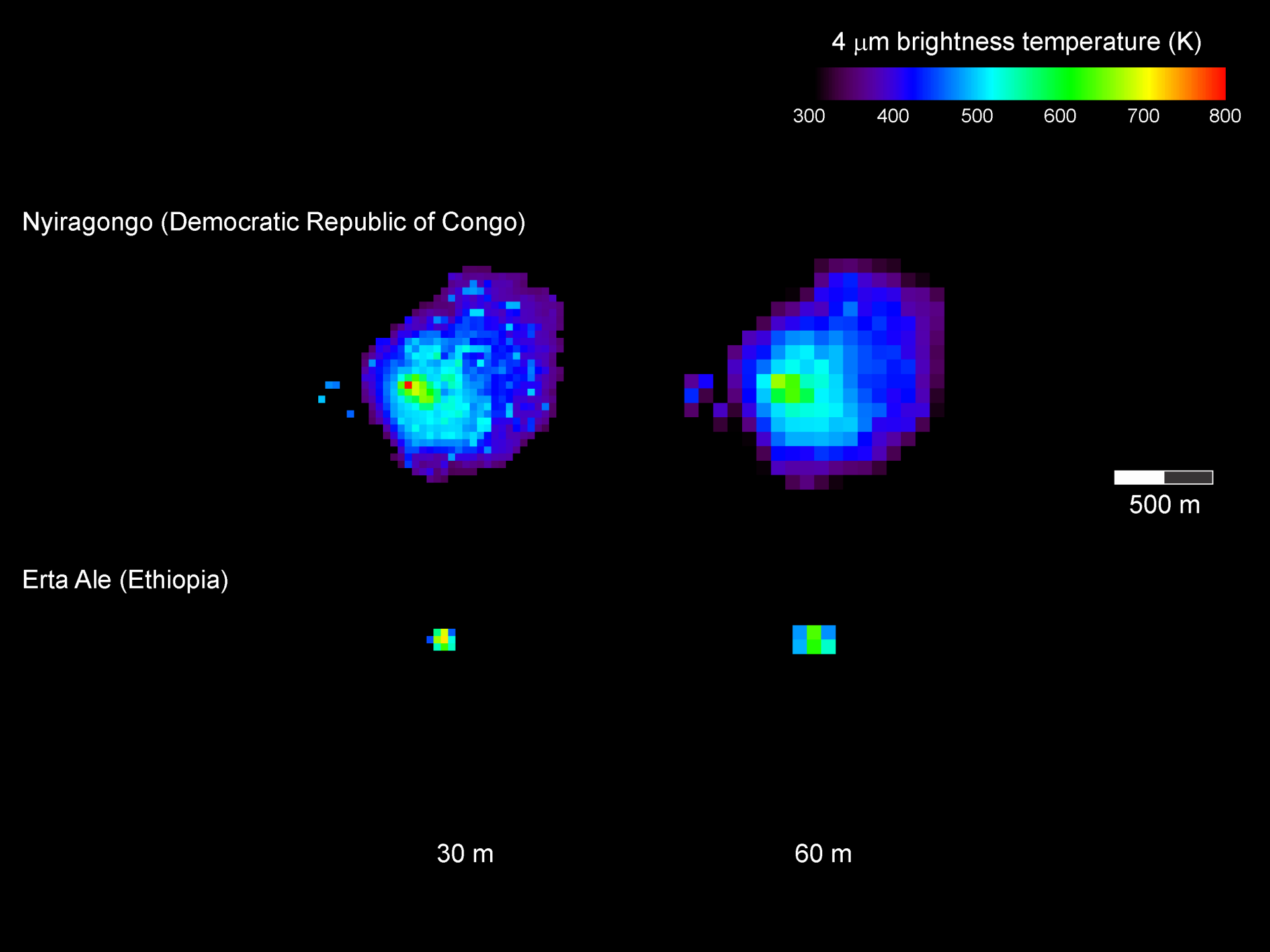
4 μm brightness temperature (K)
300
400
500
600
700
800
Nyiragongo (Democratic Republic of Congo)
500 m
Erta Ale (Ethiopia)
30 m
60 m

Calculated incidence of HysplRI 4 μm channel saturation as a function of L/T_{sat}

T_{sat}(K)	$\#_{sat}$(i)	$\#_{sat}$(ii)
400	471	432
500	163	142
600	55	48
700	30	26
800	11	14
900	0	1
1000	0	0

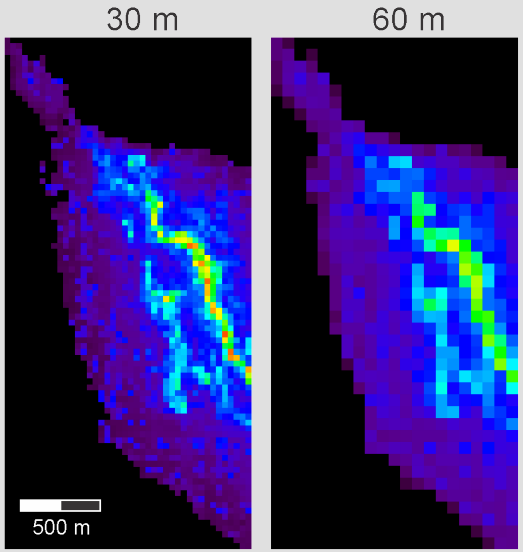

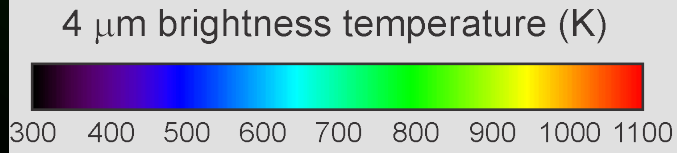

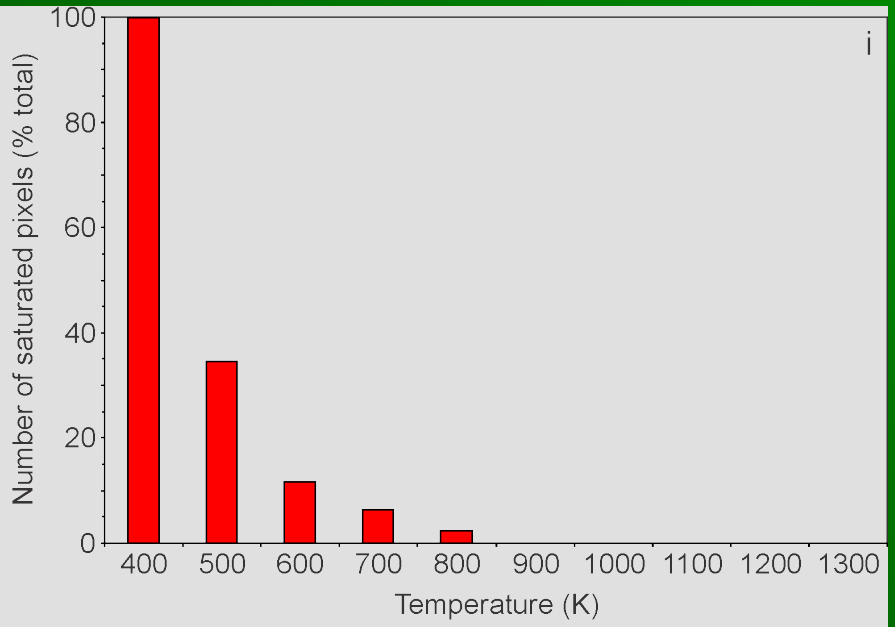

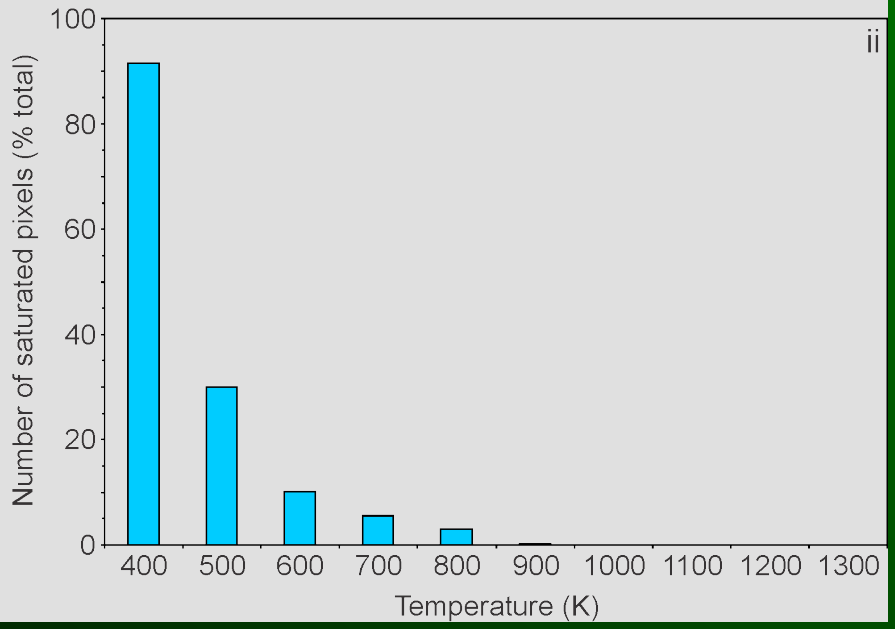

Conclusion: set 4 μm T_{sat} no less than 1100 K

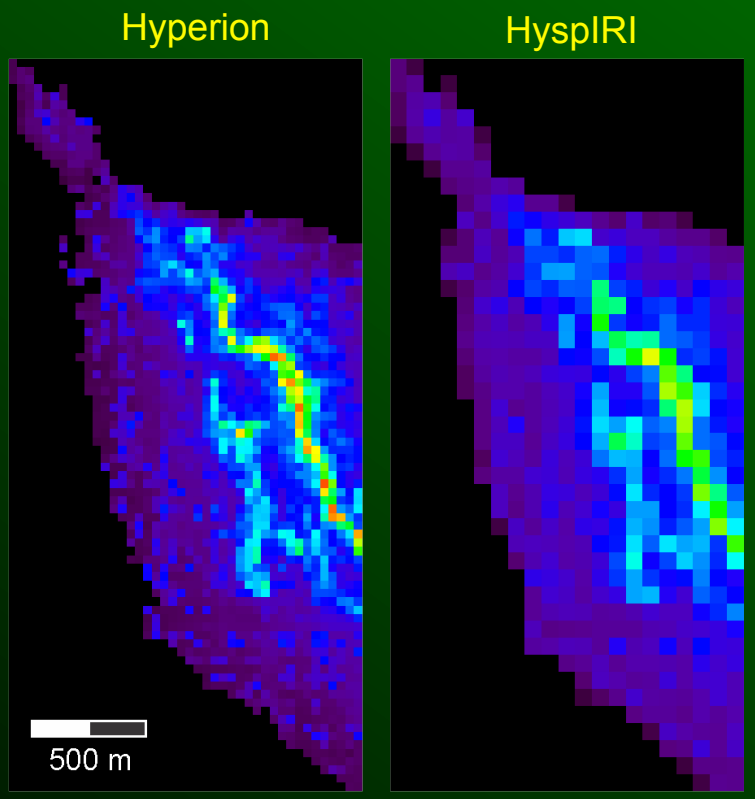

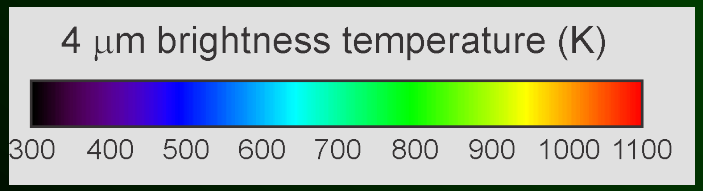

- Aggregation of four most radiant pixels at HyspIRI resolution yields a $T_{4\mu m}$ of 1041 K

HyspIRI Volcanology Project Outreach

Jet Propulsion Laboratory
California Institute of Technology

JPL HOME | EARTH | SOLAR SYSTEM | STARS & GALAXIES | SCIENCE & TECHNOLOGY
BRING THE UNIVERSE TO YOU: JPL Email News | RSS | Podcast | Video

HyspIRI Volcanology Project

Home | Events | Science | Science Study Group | Documents | Related Links

NASA/JPL

You are here: Home

Navigation

- Home
- Events
- Science
- Science Study Group
- Documents
- Related Links

« August 2011 »

Mo	Tu	We	Th	Fr	Sa	Su
1	2	3	4	5	6	7
8	9	10	11	12	13	14
15	16	17	18	19	20	21
22	23	24	25	26	27	28
29	30	31				

HyspIRI Volcanology Precursor Data for Mt. Etna

The Hyperspectral Infrared Imager or HyspIRI mission will study the world's ecosystems and provide critical information on natural disasters such as volcanoes, wildfires and drought. HyspIRI will be able to identify the type of vegetation that is present and whether the vegetation is healthy. The mission will provide a benchmark on the state of the worlds ecosystems against which future changes can be assessed. The mission will also assess the pre-eruptive behavior of volcanoes and the likelihood of future eruptions as well as the carbon and other gases released from wildfires.

The HyspIRI mission includes two instruments mounted on a satellite in Low Earth Orbit. There is an imaging spectrometer measuring from t visible to short wave infrared (VSWIR: 380 nm - 2500 nm) in 10 nm contiguous bands and a multispectral imager measuring from 3 to 12 um in the mid and thermal infrared (TIR). The VSWIR and TIR instruments both have a spatial resolution of 60 m at nadir. The VSWI will have a revisit of of 19 days and the TIR will have a revisit of 5 days HyspIRI also includes an Intelligent Payload Module (IPM) which will enable direct broadcast of a subset of the data.

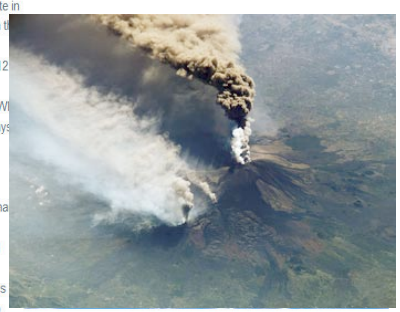

The data from HyspIRI will be used for a wide variety of studies prima in the Carbon Cycle and Ecosystem and Earth Surface and Interior focus areas. The mission was recommended in the recent National Research Council Decadal Survey requested by NASA, NOAA, and USGS.The mission is currently at the study stage and this website is being provided as a focal point for information on the mission and to keep the community informed on the mission activities.

Click to find out more about the 2011 HyspIRI Science Workshop and sign up

Click to view 2010 Workshop Agenda, Presentations and Report

Click to view 2009 Workshop Agenda, Presentations and Report

Click to view 2008 Workshop Agenda, Presentations and Report

ALL RIGHTS RESERVED Copyright California Institute of Technology U.S. Government Sponsorship Acknowledged under NAS7-1260 CL 08-2417

Powered by Plone & Python

http://HyspIRI-Volcanology.jpl.nasa.gov

NEX NASA Earth Exchange

Login | Register

Search

HOME | RESEARCH AREAS | PROJECTS | RESOURCES | MEMBERS

HyspIRI Preparatory Data Sets for Volcanology

Home

Members

Resources
N/A

Related Research Areas
Earth Surface & Interior

HyspIRI is a Tier 2 mission recommended to NASA by the National Research Council's Decadal Survey report. One of the main goals of the HyspIRI mission is to provide global observations of surface attributes at local and landscape spatial scales (10's of meters to hundreds of kilometers) to map volcanic gases and surface temperatures, which are identified as indicators of impending volcanic hazards; as well as plume ejecta which pose risks to aircraft and people and property downwind. We will create precursor HyspIRI data sets for volcanological analyses, using existing data over Mt. Etna, Italy. We have identified 12 EO-1 Hyperion data acquisitions, 12 near-coincident ASTER data acquisitions, and a MIVIS aircraft data acquisition, covering six eruptive periods between 2001 and 2007. These three data sets provide us with 30 m hyperspectral VSWIR data and 90 m multispectral TIR data (satellite) and 10 m multispectral TIR data (aircraft). They will allow us to examine temporal sequences of several Etnaean eruptions. We will address the following critical questions, directly related to understanding eruption hazards: 1) What do changes in SO2 emissions tell us about a volcano's activity? How well do these measurements compare with ground-based COSPEC measurements? 2) How do we use measurements of lava flow temperature and volume to predict advances of the flow front? 3) What do changes in lava lake temperatures and energy emissions tell us about possible eruptive behavior? Mapping SO2 emissions will be done using REALMUTO Software applied to our precursor HyspIRI data sets. We will calculate, through data analysis and models, the column abundance of SO2 all along Etna's plumes. Results will be compared with coincident COSPEC ground measurements at Etna obtained daily by Istituto Nazionale del Geofisica e Vulcanologia in Catania, Sicily. Examining the time history of SO2, compared with eruption history, will provide us some indication of the correlation between the two.

Data from the VSWIR and TIR will allow us to determine radiant temperatures over a wide range: edges of lava flows at 100C, to magmatic lava at 1100C. This improved characterization of flows is a crucial input into flow models for predicting run-out lengths. Similarly, improved accuracy for determining temperatures of lava lakes will provide better insight into the internal plumbing of Etna, and the state of magma ascent from depths.

Project Highlight

1 members
Started: Aug 09, 2010
Last Activity: Dec 09, 2010

Admin:
NDC-cmilesi

What can I do on this project?

New Member

Cristina Milesi
Joined 1 year ago

Related Projects

- Using Advanced Geodetic Imaging ... 1 members
- Geodetic Imaging of Earth's ... 1 members
- Improvements to the Accuracy ... 1 members

Need help?
Visit our help center

https://c3.nasa.gov/nex/

SELECTED CONCLUSIONS

- T_{sat} 4μm channel >1100K

- Short repeat time mandatory for volcano monitoring: Hyperion and ASTER do not provide sufficient frequency at 10-16 days, given cloud cover. HyspIRI repeat of 5 days (daytime) PLUS nighttime acquisitions will be stunning for volcanology.

- Lava flow energy fluxes with topo and flow models can be used to estimate flow duration and extent. Requires very frequent flow observations (~several days) to measure dynamics.

- Crater activity (T, energy flux) monitoring requires very frequent observations to investigate correlation with eruption potential; questionable at present.

Potential Contributions of HyspIRI to the Remote Sensing of Volcanic Plumes

Vincent J. Realmuto
Jet Propulsion Laboratory
23 August 2011

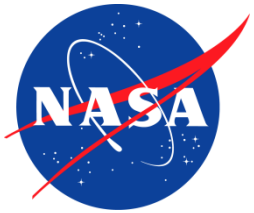

H_2O Vapor vs. SO_2 Absorption

H_2O Vapor Absorption Affects the Entire 8-12 μm Atmospheric Window:

- **Add Channel Sensitive to H_2O to Facilitate Atm. "Corrections"**

Considerable Variation in H_2O Within a Scene:

- **Can We Characterize These Variations?**

Very Strong H_2O Vapor and SO_2 Absorption in HysplRI 7.3 μm Channel:

- **Can We Separate Effects of H_2O and SO_2?**

7.3 μm Not Suitable for Mapping Plumes Below 5 km? [Prata et al., 2003]

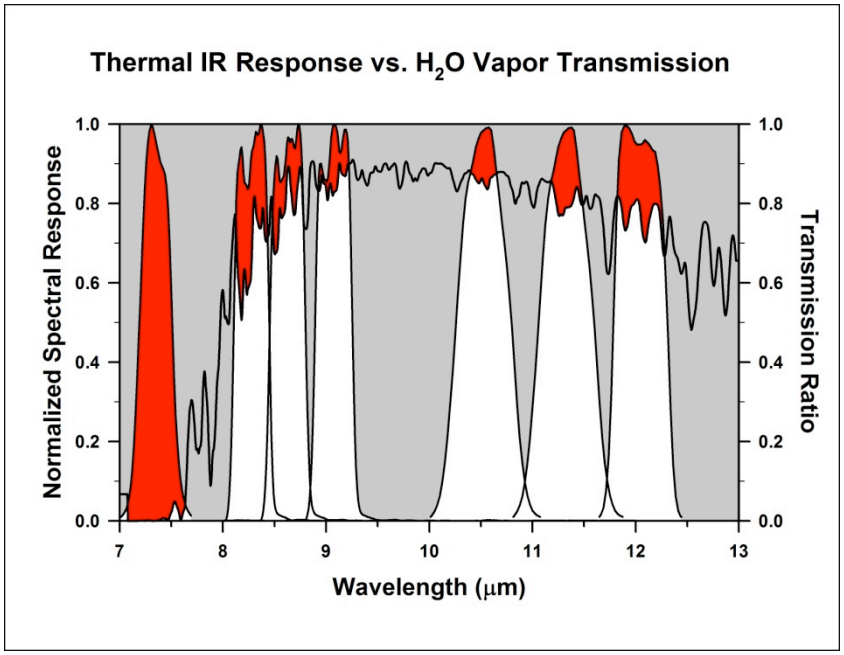

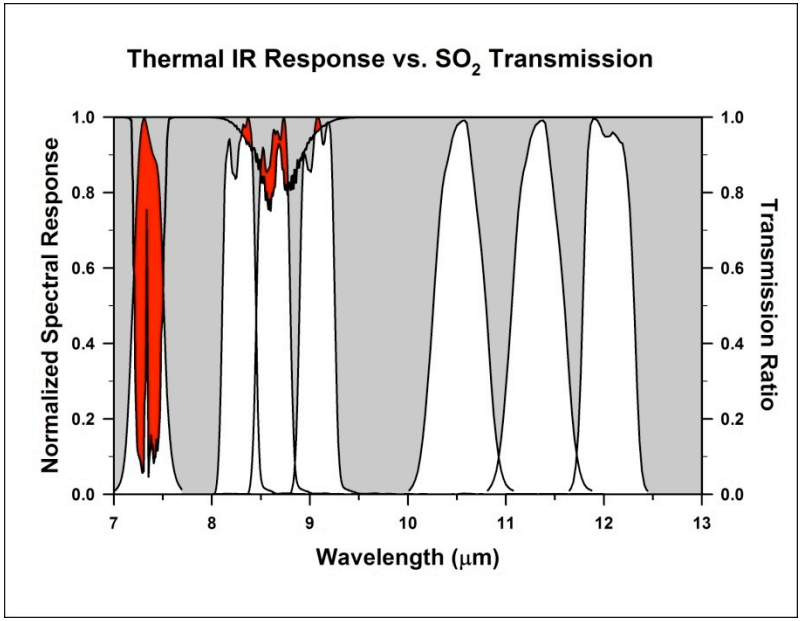

Heritage for HysplRI Spectral Response

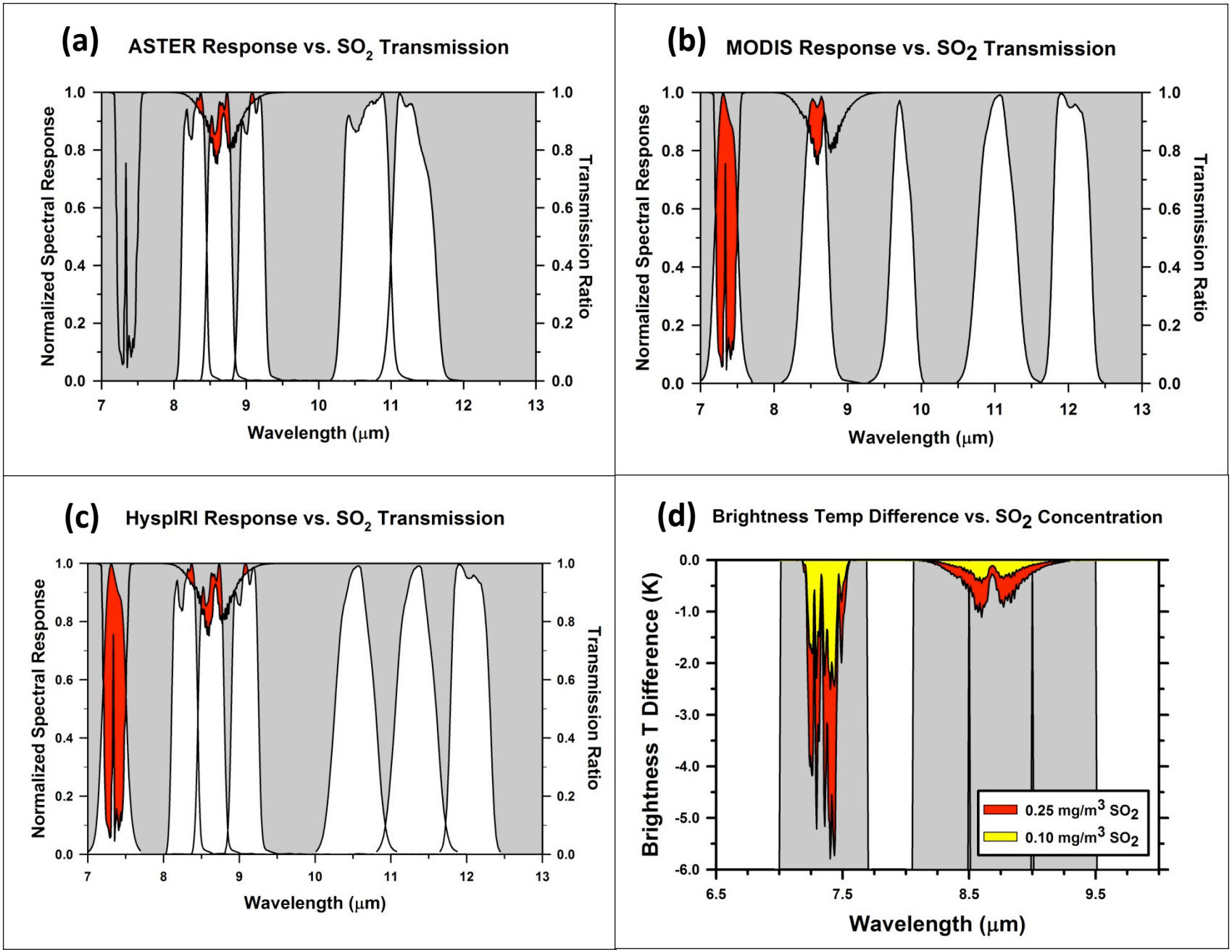

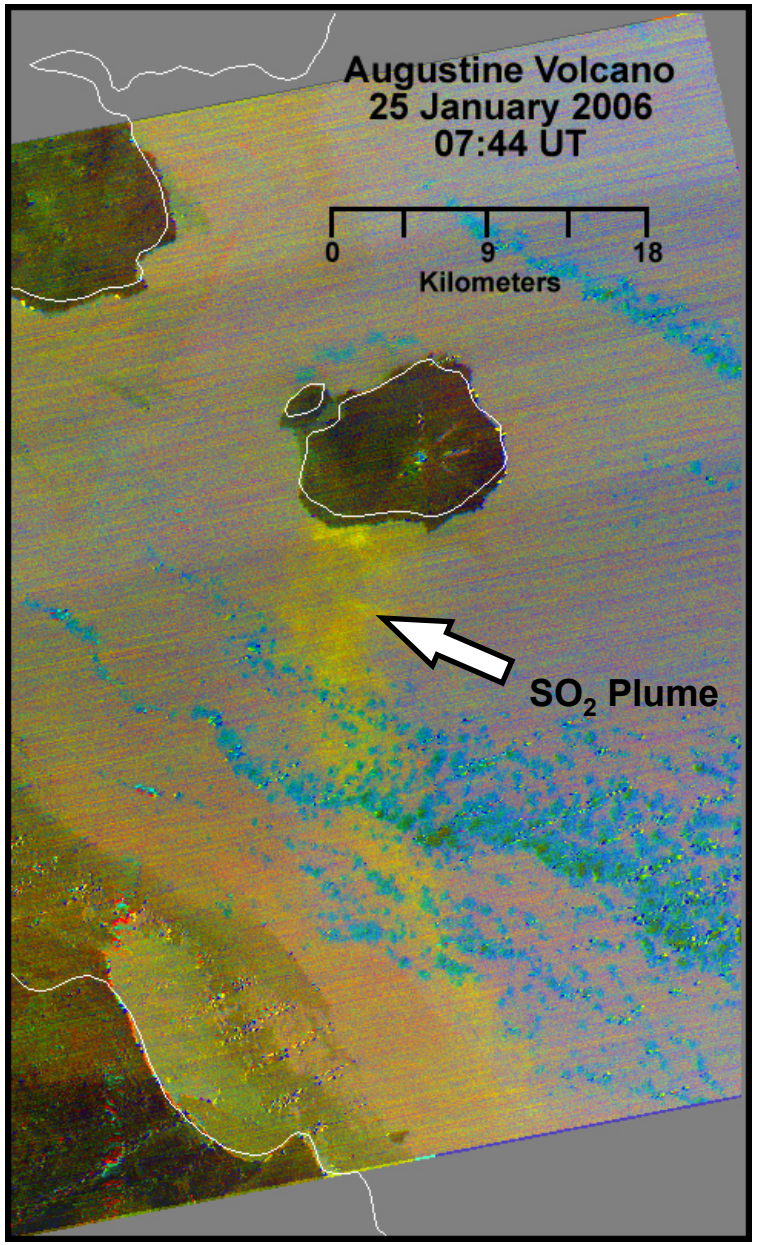

ASTER D-Stretch Depicting the Passive Emission of SO_2

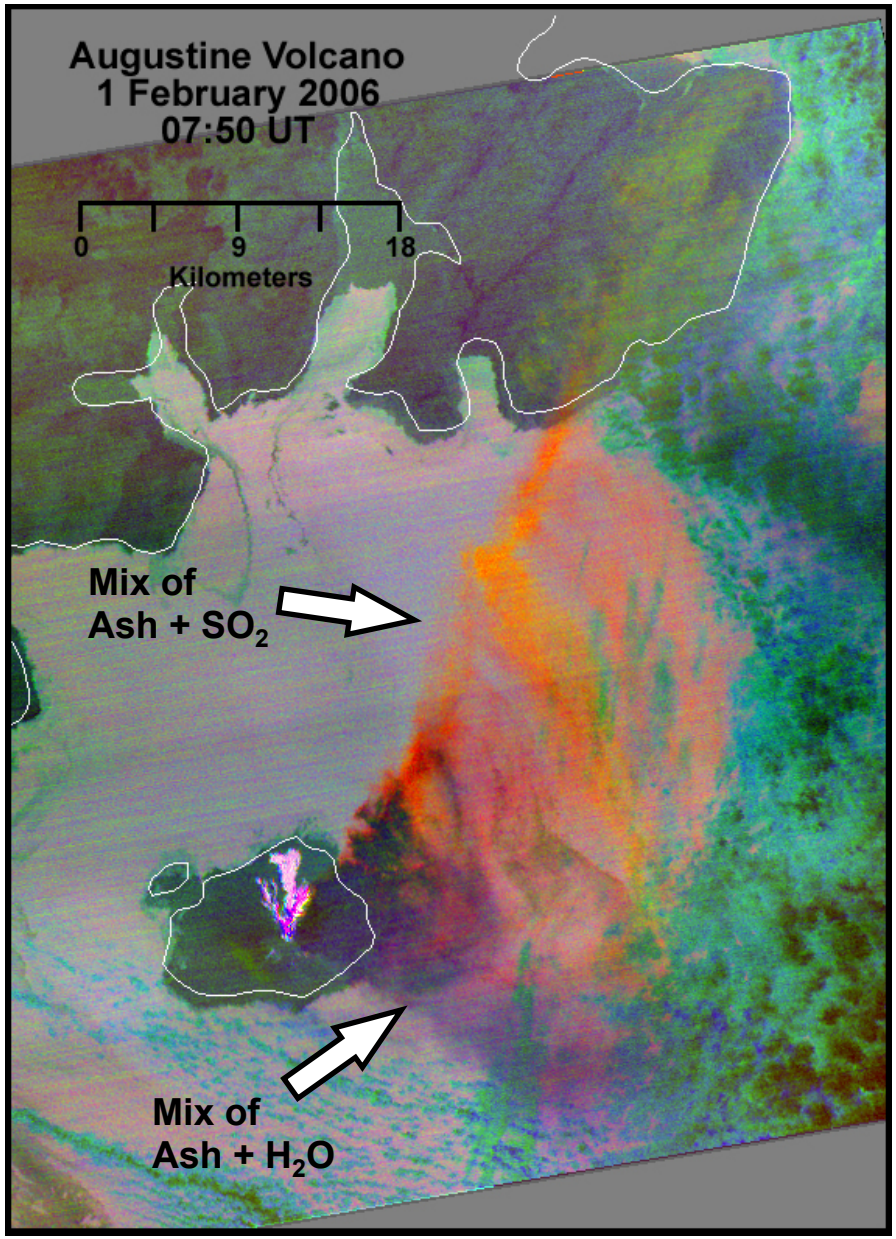

ASTER D-Stretch Depicting Ash, water/ice, and SO_2 Released by Explosive Eruption

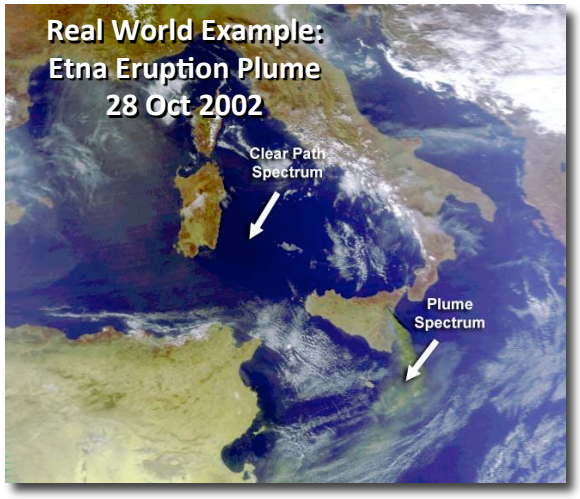

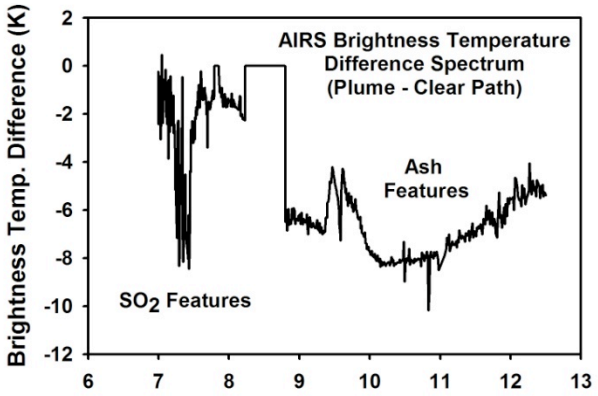

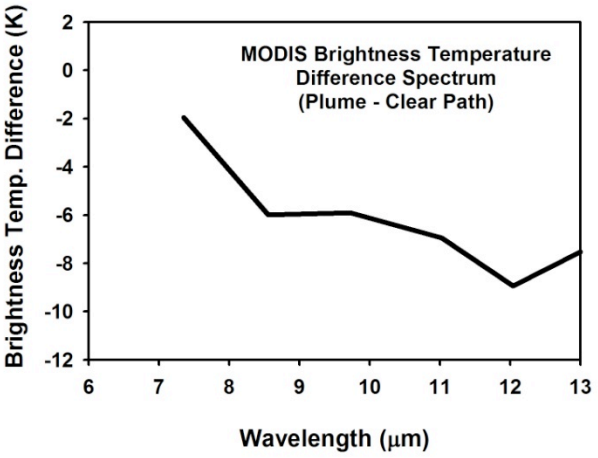

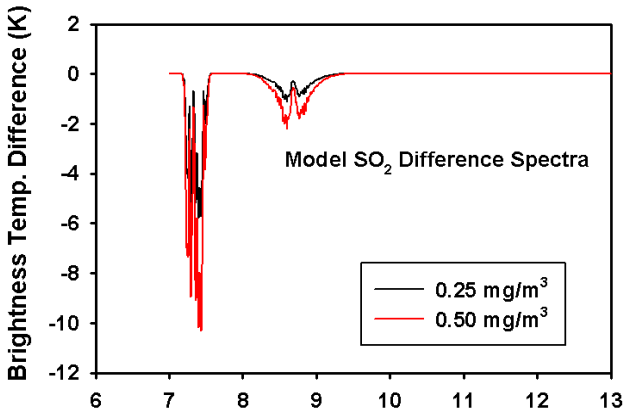

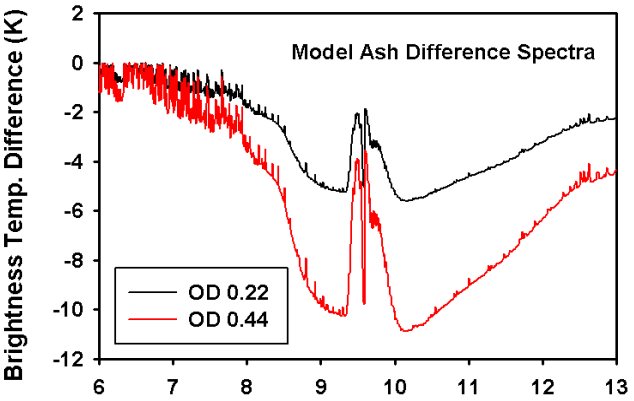

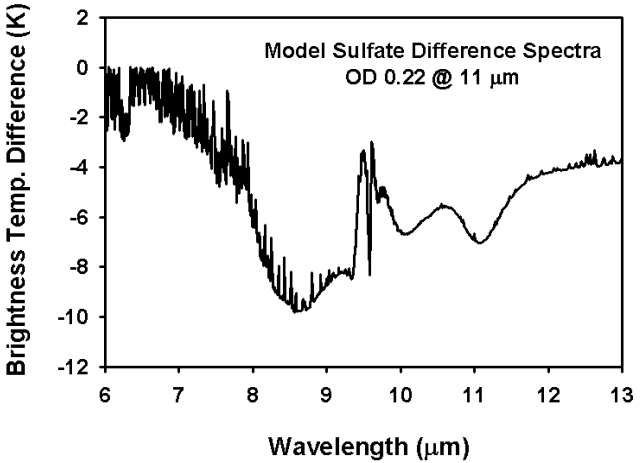

Notional HyspIRI TIR Response vs. Spectra of Plume Materials

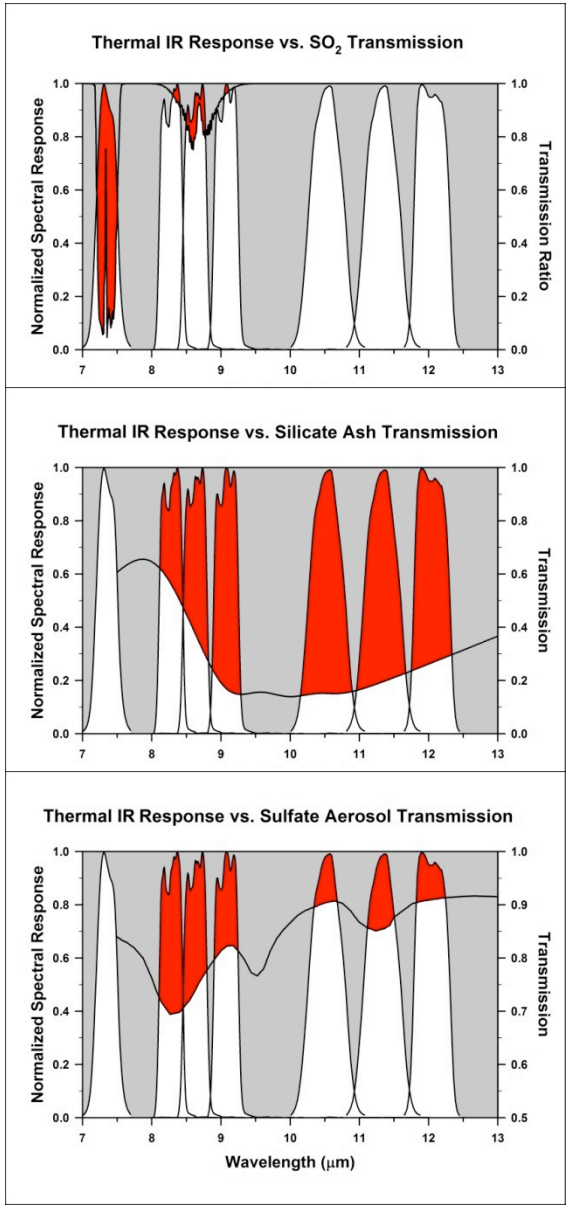

Retrieval of Surface Temperature and SO_2 Concentration

Ground Temperature has Stronger Influence on Perceived Radiance Than the SO_2 Concentration

Simultaneous Retrieval of Temperature and SO_2 is Difficult; Temperature is Well-Constrained but SO_2 is Poorly-Constrained

Cascading (Serial) Retrieval is a Better Option:

- **Estimate Surface Temperature**
- ***(Estimate H_2O Vapor Factor)***
- **Estimate SO_2 Concentration**
- **Repeat Temperature Estimation w/ Prior H_2O and/ or SO_2 Estimates**
- **Repeat H_2O and/or SO_2 Estimation with New Temperature**
- **Exit When $\Delta T <$ Threshold**

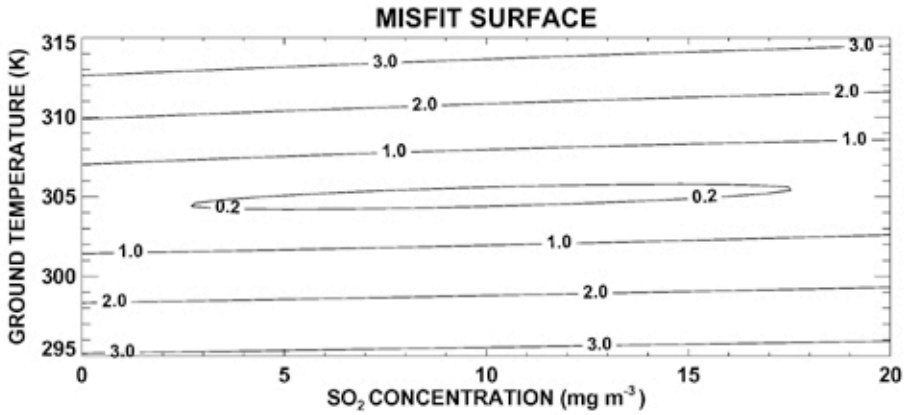

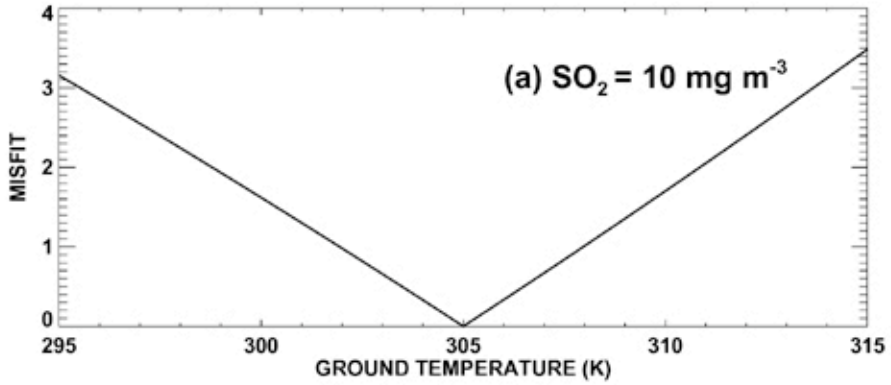

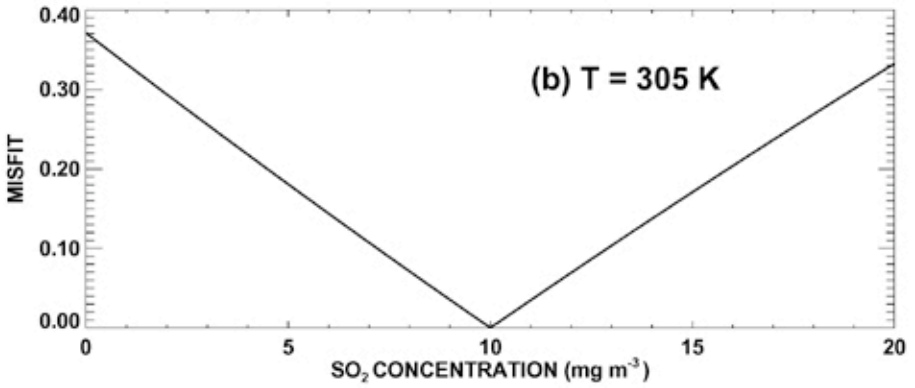

Retrieval Procedure Requires Profiles of Atm. Temp, H_2O, and O_3 as Input

Radiance Spectra from Clear Path (Plume-Free) Regions are used to "Tune" the H_2O and O_3 Profiles

Tuning is a Time-Consuming Process: Retrieval of H_2O is More Efficient and a Better Characterization of Variations in H_2O

Two Candidates for H_2O Channel:
MODIS 28 (7.3 μm) and MODIS 33 (13.3 μm)

Strong H_2O Absorption in MODIS 28 Obscures the Surface

Moderate H_2O Absorption in MODIS 33 Does Not Obscure the Surface

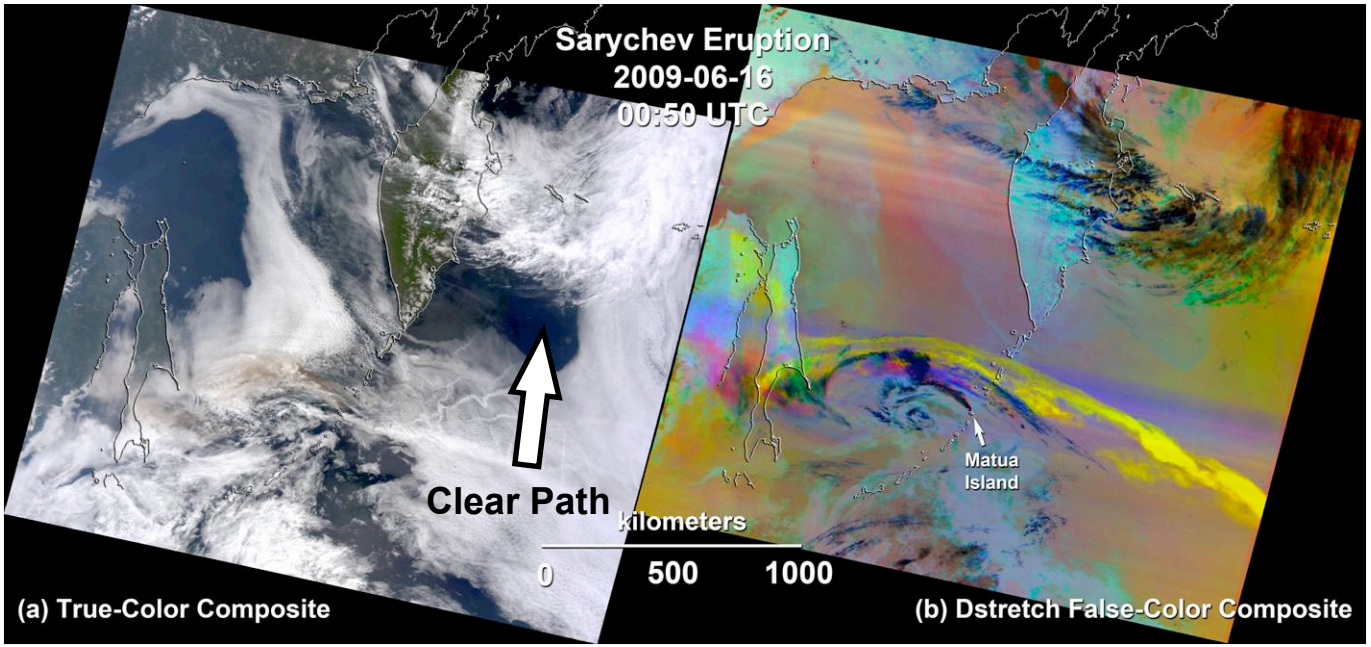

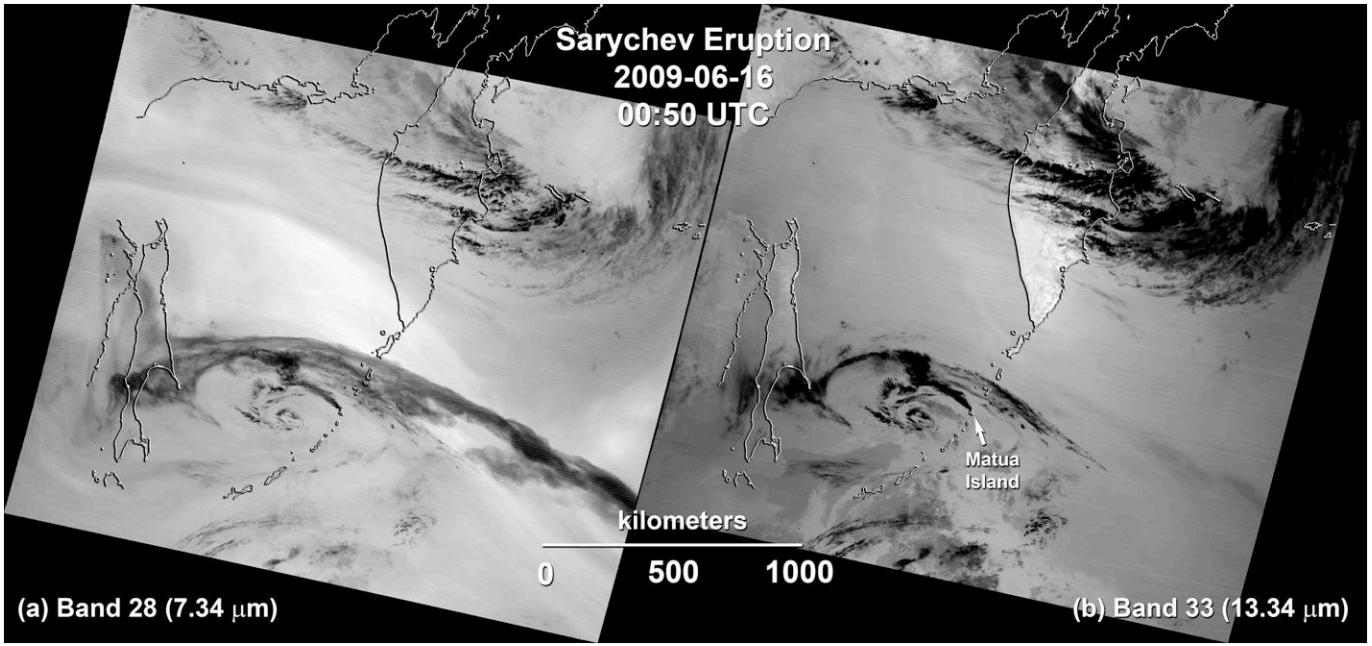

Simulated Retrievals of H_2O and SO_2

Evaluate Five Configurations of Channels

- **ASTER, HyspIRI, MODIS 29-32, MODIS 28-32, and MODIS 29-33**

Synthetic Radiance Spectra as "Observations"

- **Surface Temp = 275 K, SO_2 Conc = 2.5 mg/m^3, H_2O Factor = 0.75**
- **Plume Altitude = 15 km, Sea Surface Background, Sarychev Atm. Profiles**

Three Retrieval Modes/Configuration

- **Temperature: Assume SO_2 = 0, H_2O = 0.75 (Tuning Mode)**
- **H_2O Factor: Assume SO_2 = 0 (Potential New Tuning Mode)**
- **H_2O + SO_2: Potential New Retrieval Mode**

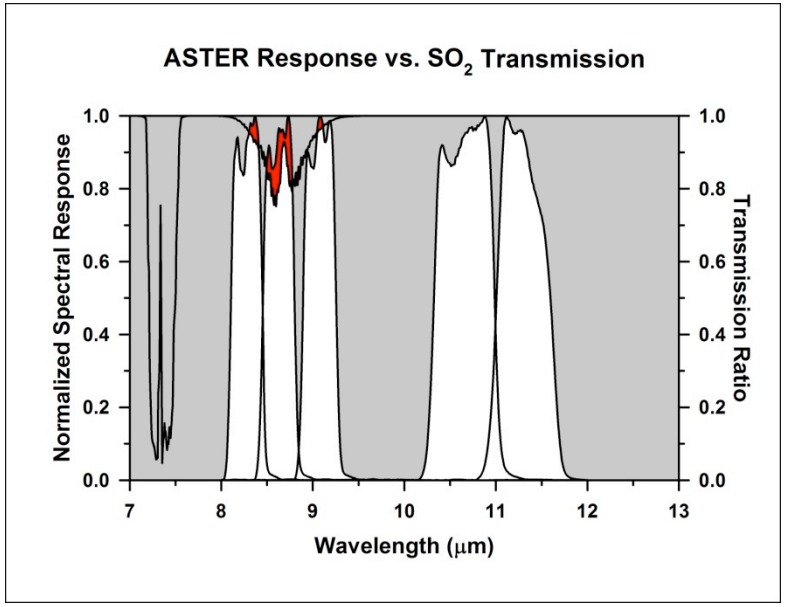

ASTER Simulation Results

Temperature Under-Estimated, Misfit Spectrum 4 – 10%

H_2O: Misfit Spectrum < 6%

$H_2O + SO_2$: Misfit Spectrum < 2%

Δ% Axis Range = 24%

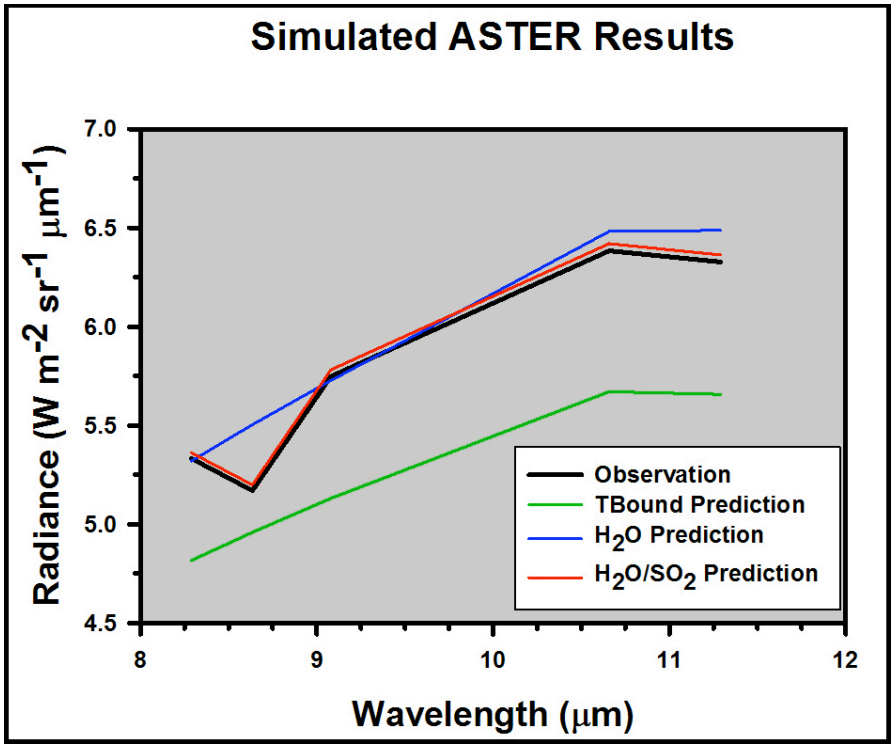

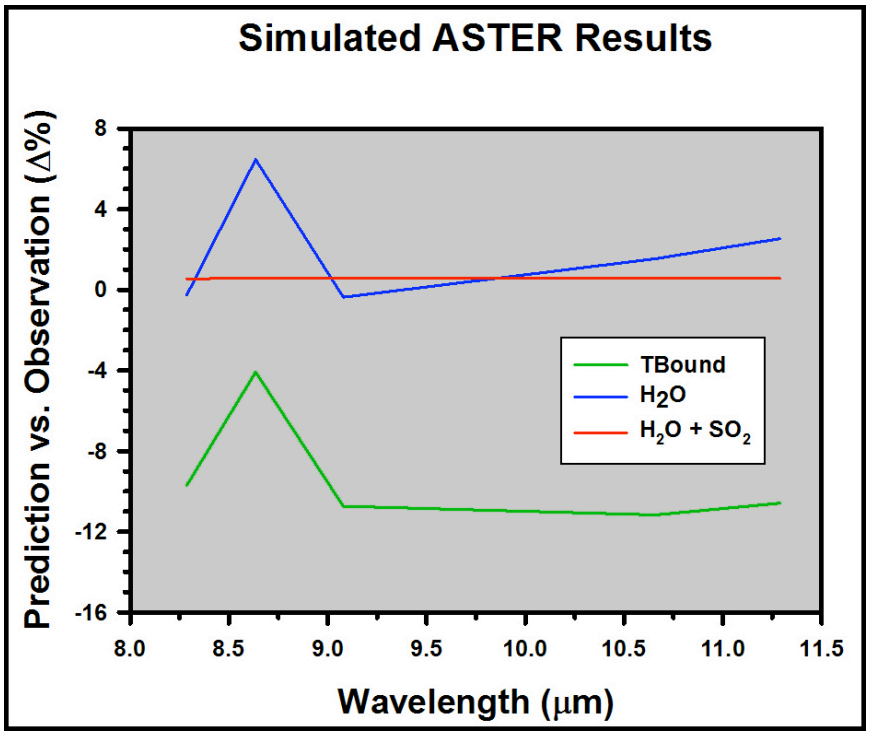

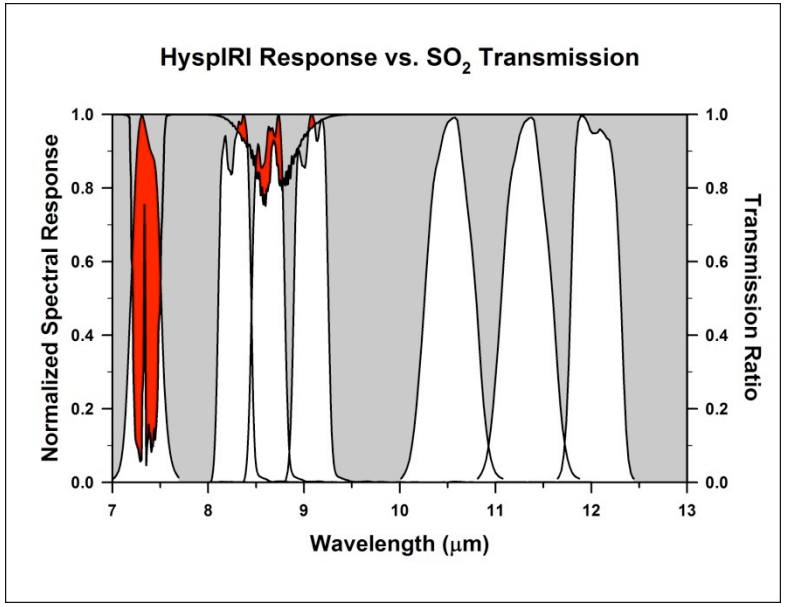

HysplRI Simulation Results

Temperature Over-Estimated, Misfit Spectrum ~75% at 7.3 μm

H_2O: Misfit ~20% at 7.3 μm

H_2O + SO_2: Misfit Spectrum < 2%

Δ% Axis Range = 100%

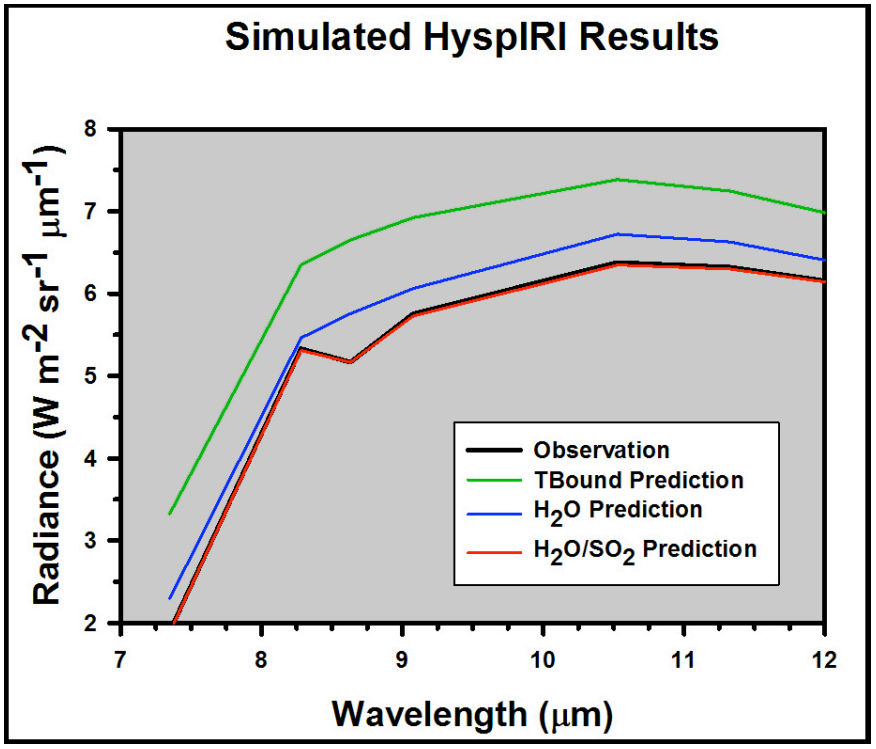

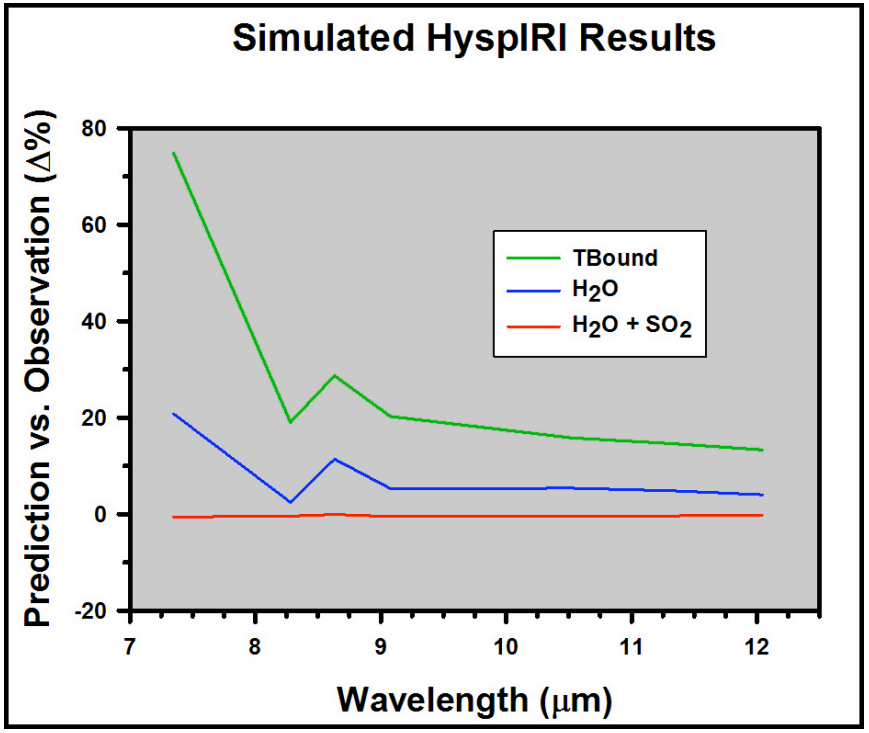

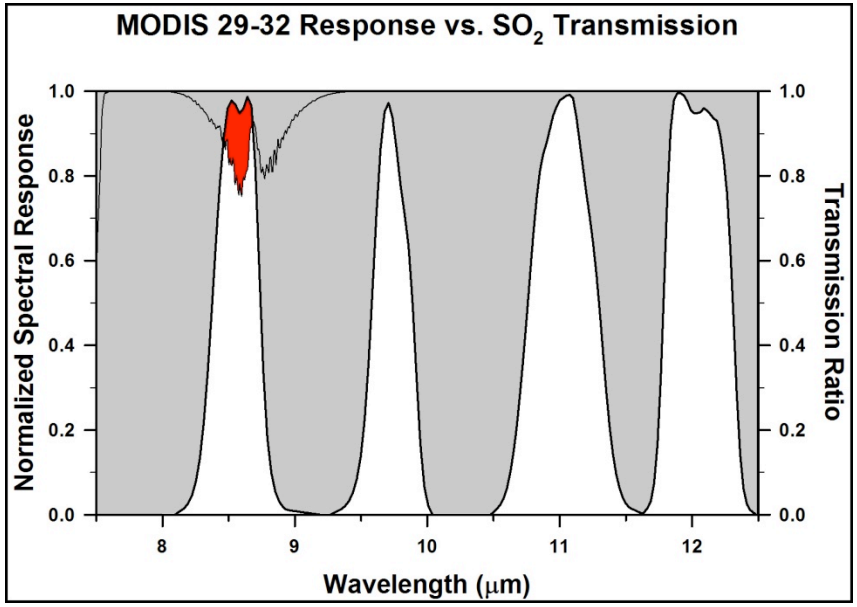

MODIS 29-32 Simulation Results

Temperature Under-Estimated, Misfit Spectrum Between 5 – 11%

H_2O: Misfit Within ±3%

H_2O + SO_2: Misfit Spectrum < 1%

Δ% Axis Range = 19%

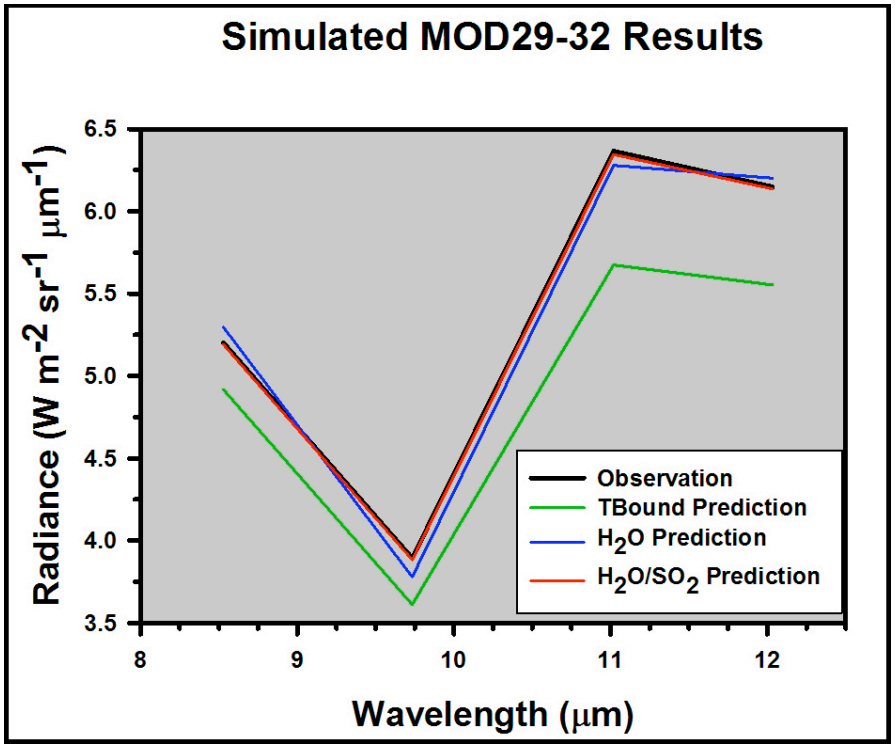

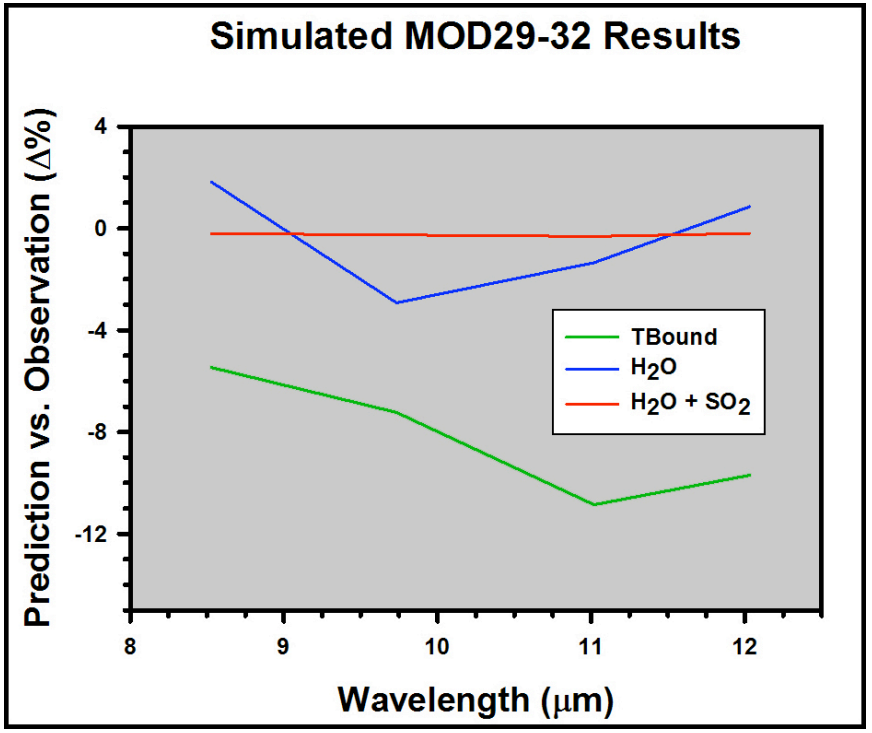

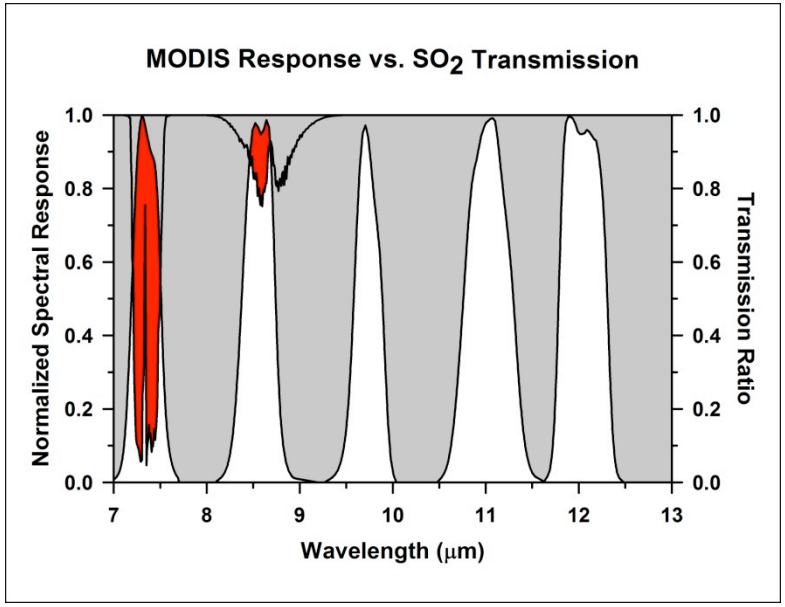

MODIS 28-32 Simulation Results

Temperature Over-Estimated, Misfit Spectrum ~80% at 7.3 μm

H_2O: Misfit ~20% at 7.3 μm

H_2O + SO_2: Misfit Spectrum < 10%

Δ% Axis Range = 120% (Worst Misfit)

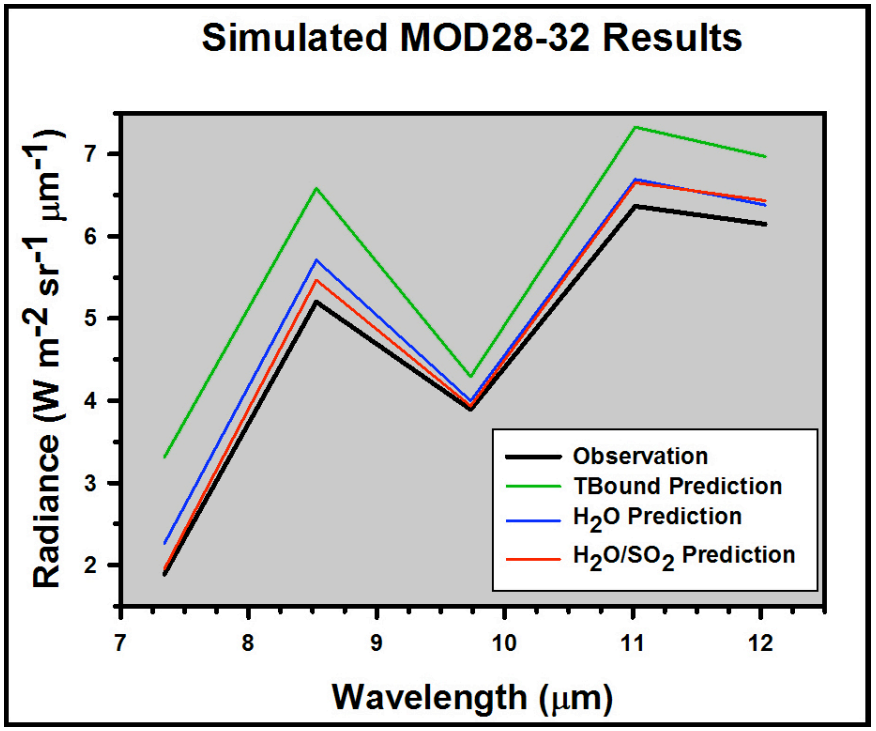

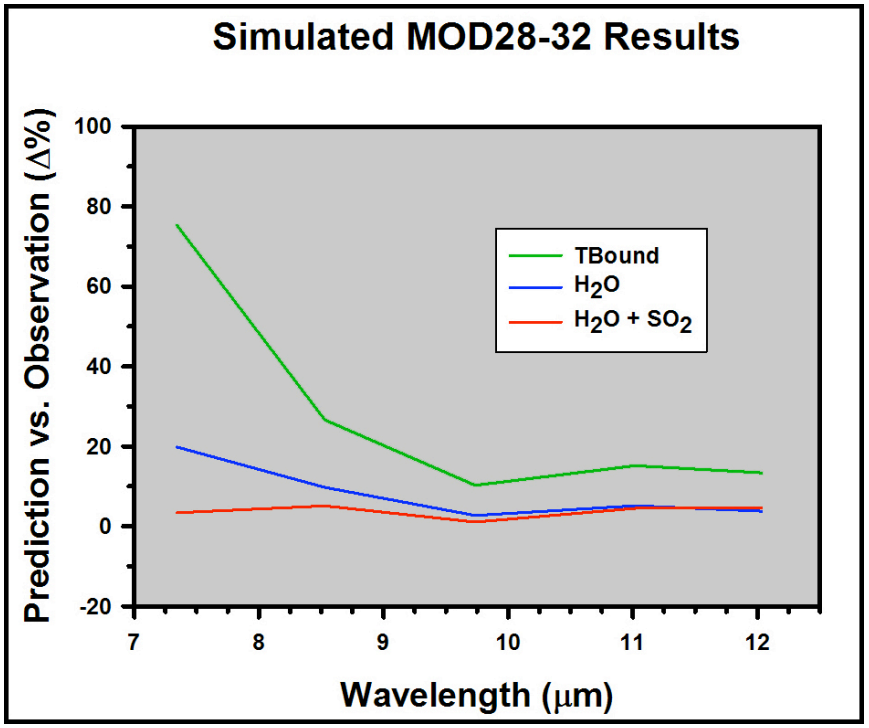

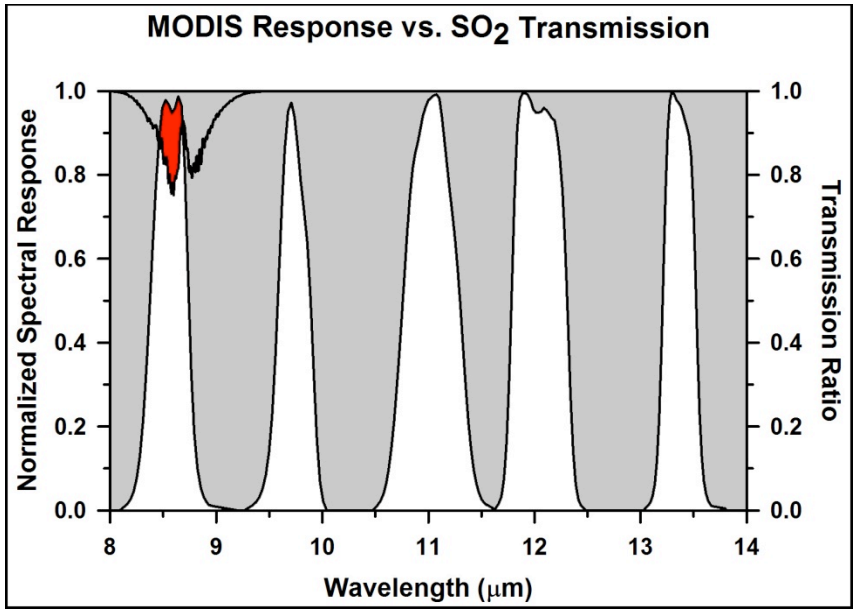

MODIS 29-33 Simulation Results

Temperature Under-Estimated, Misfit Spectrum < 6%

H_2O: Misfit < 3%

H_2O + SO_2: Misfit Spectrum < 1%

Δ% Axis Range = 8% (Best Misfit)

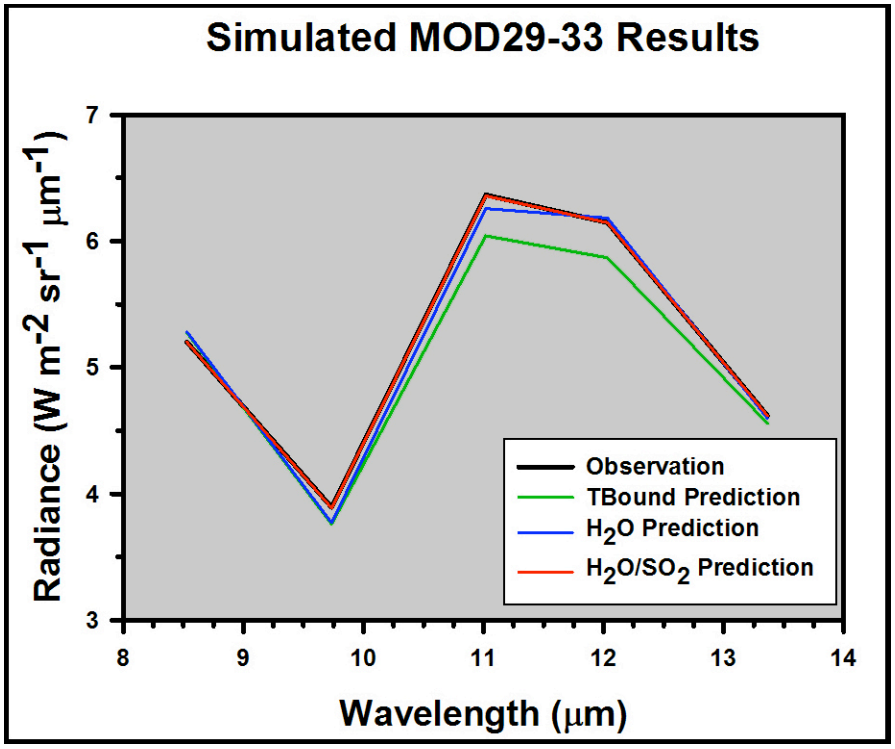

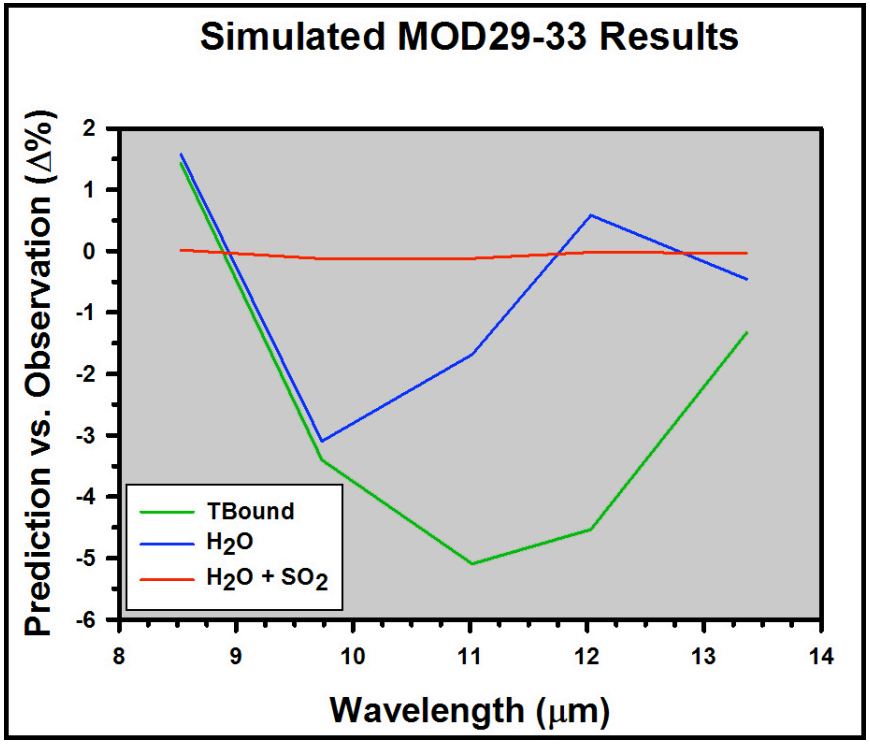

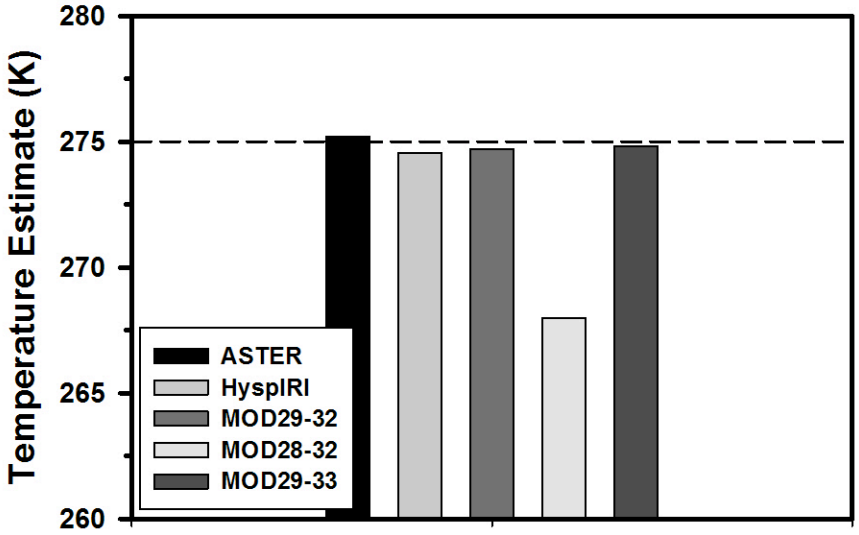

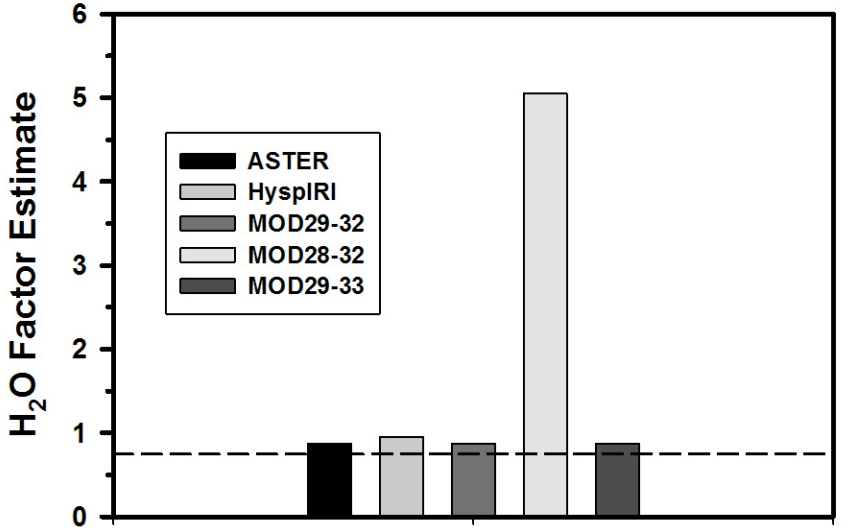

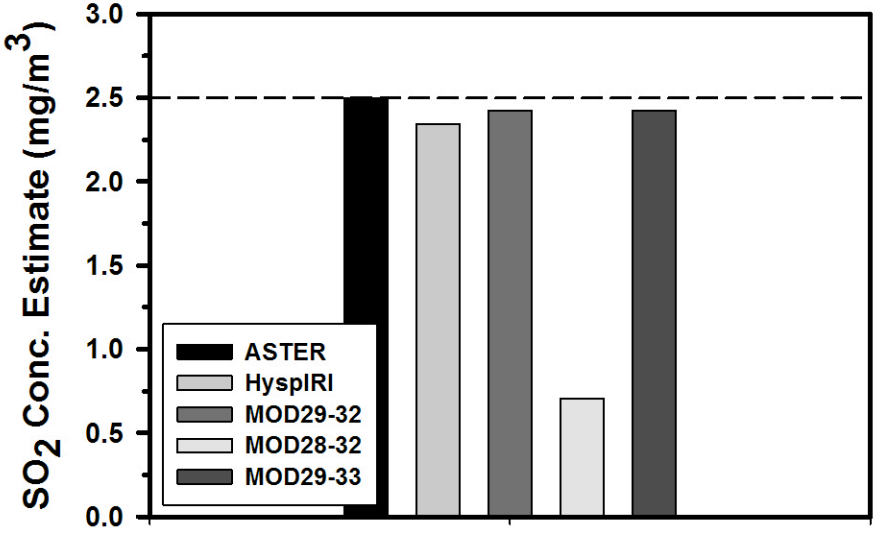

Retrieval Accuracy

ASTER: Best Overall Performance

MODIS 28-32: Worst Overall Performance

MODIS 29-32/MODIS 29-33: Roughly Equal Performance; Slightly Better Than HyspIRI

Presence of 7.3 μm Channel Degrades Performance

Note: All Configurations Produced Exact Retrievals in Traditional (TBound + SO_2) Mode

MODIS-Based Retrievals of H_2O and SO_2

Evaluate Three Configurations of Channels
- **MODIS 29-32, MODIS 28-32, and MODIS 29-33**

Compare Temperature and SO_2 Retrievals with Fixed and Free H_2O Factors
- **Region-of-Interest Included SO_2, Ash, and Clear-Path Pixels**

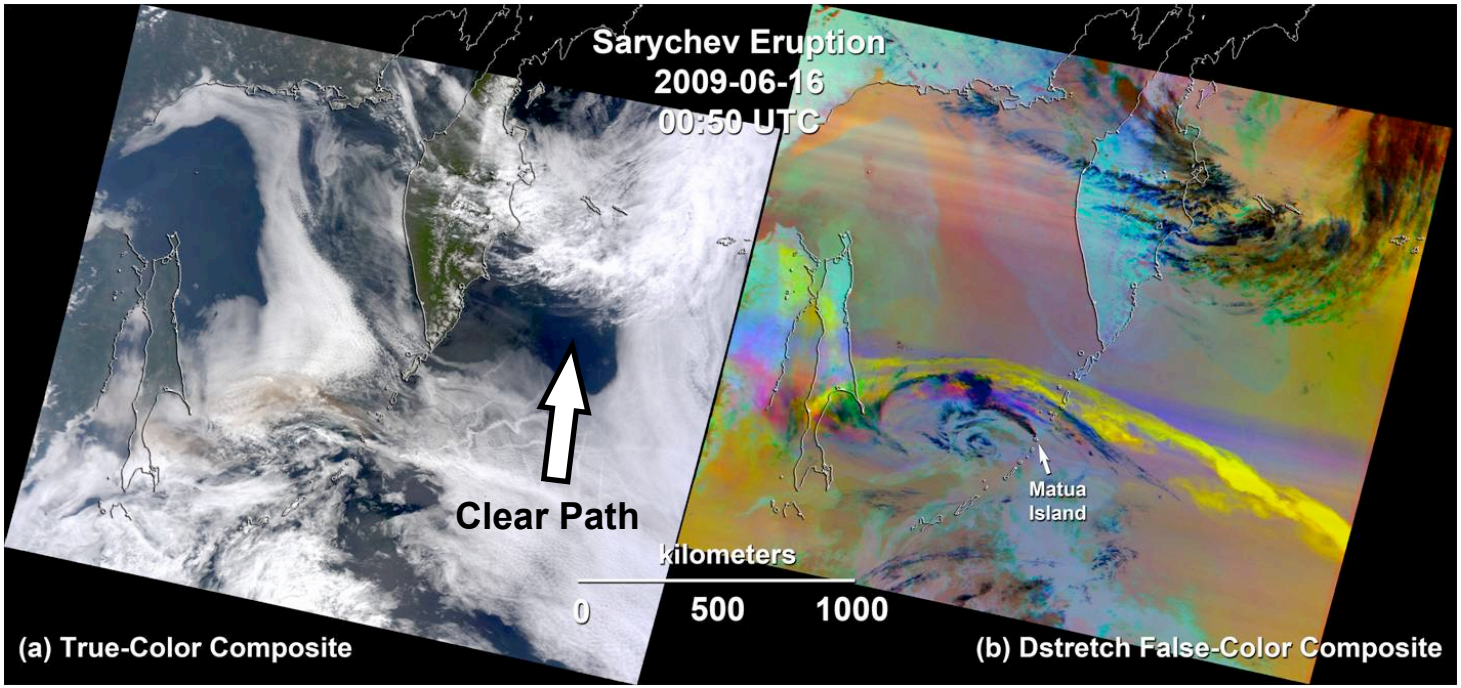

MODIS 29 – 32 Results

Fixed H_2O Factor

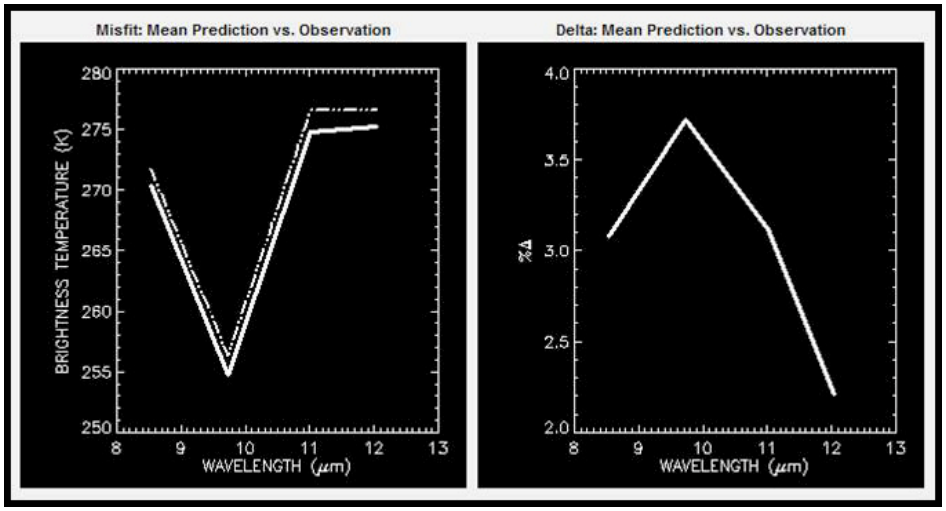

Free H_2O Factor

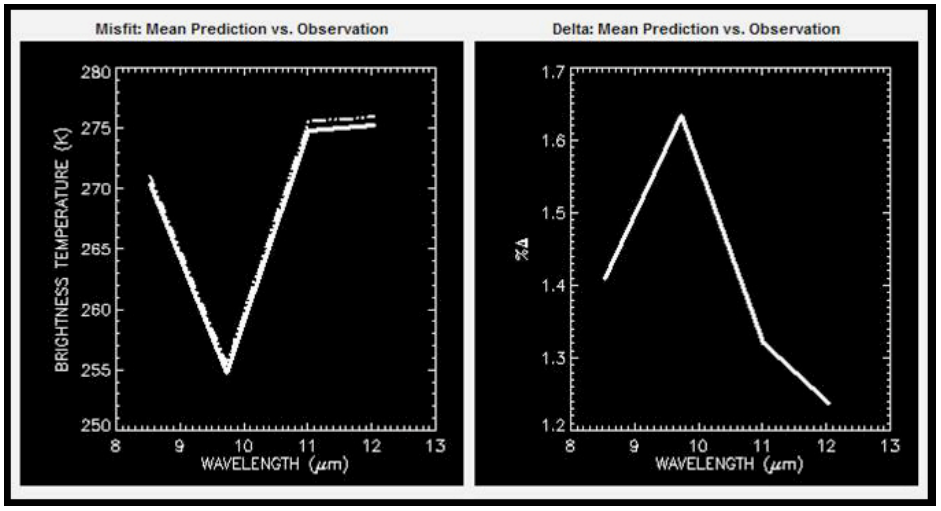

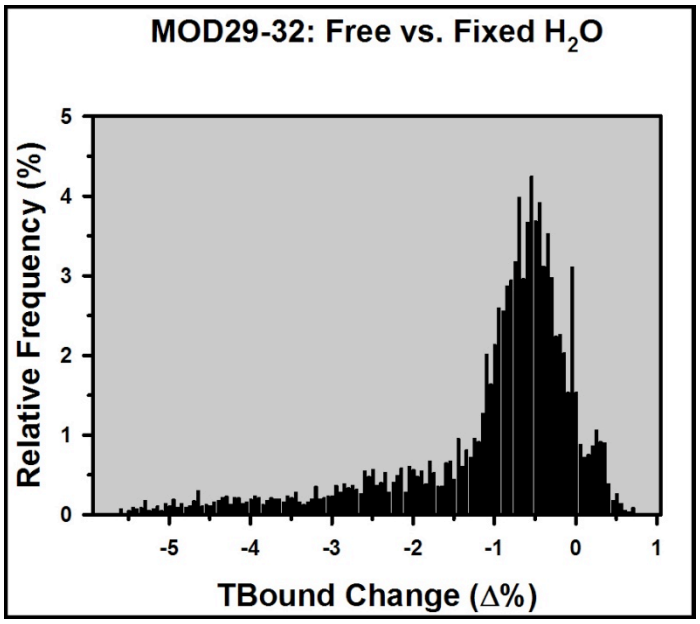

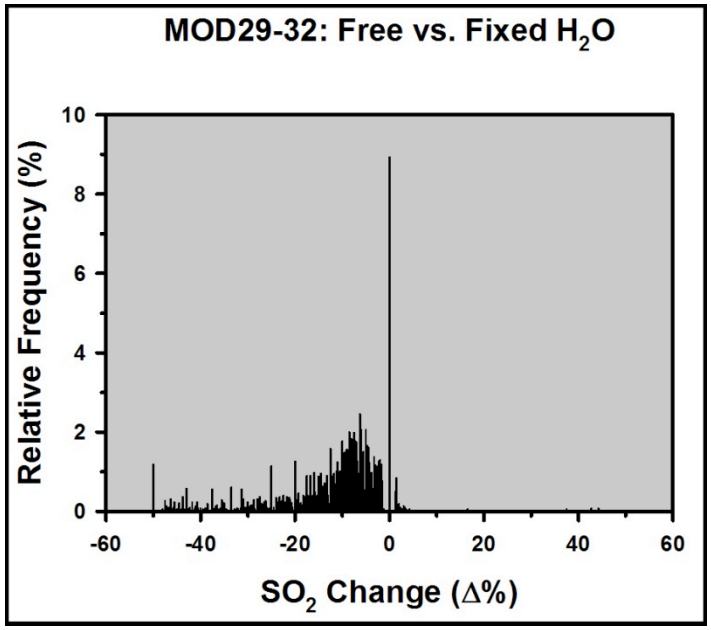

Improved Fit: Δ% Range Reduced from 2% to 0.5%

TBound Estimates Decreased ~0.5%

SO_2 Estimates Decreased 5 – 10%

MODIS 28 – 32 Results

Fixed H_2O Factor

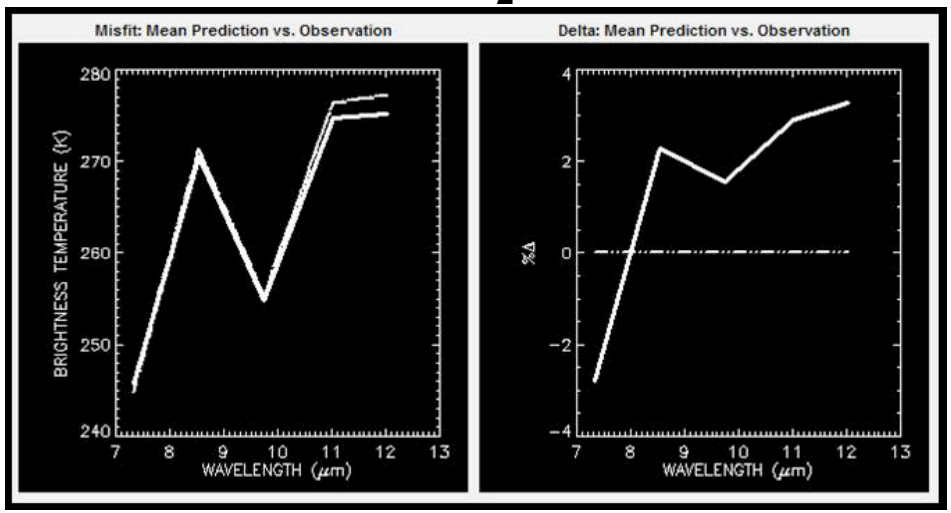

Free H_2O Factor

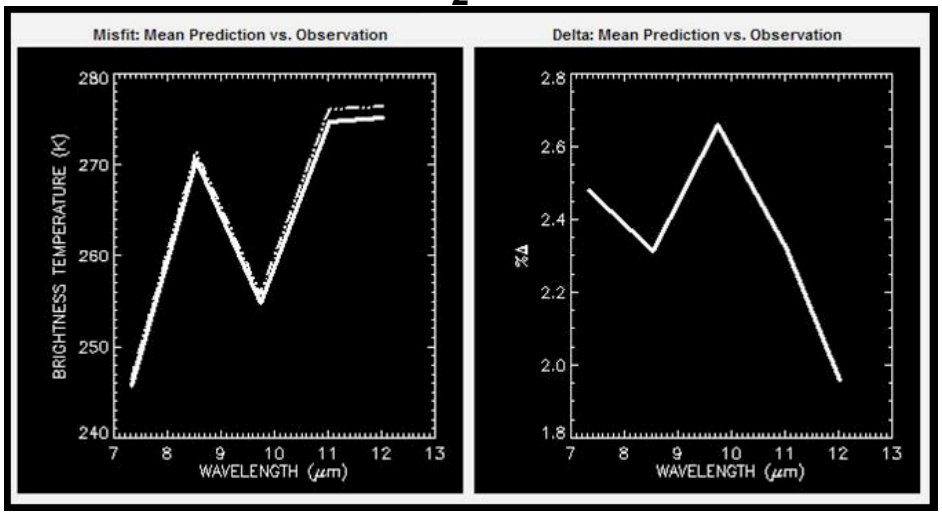

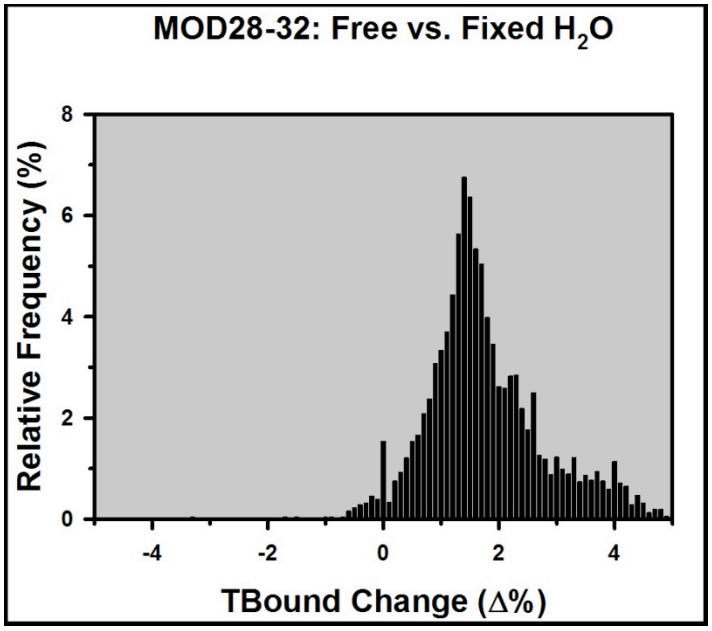

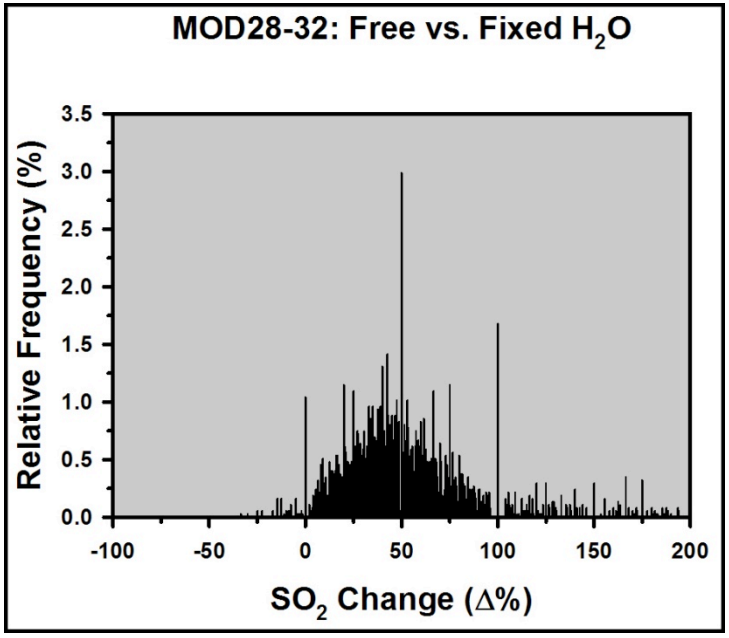

Improved Fit: Δ% Range Reduced from 8% to 1%

TBound Estimates Increased ~1.5%

SO_2 Estimates Increased ~ 50%

MODIS 29 – 33 Results

Fixed H_2O Factor

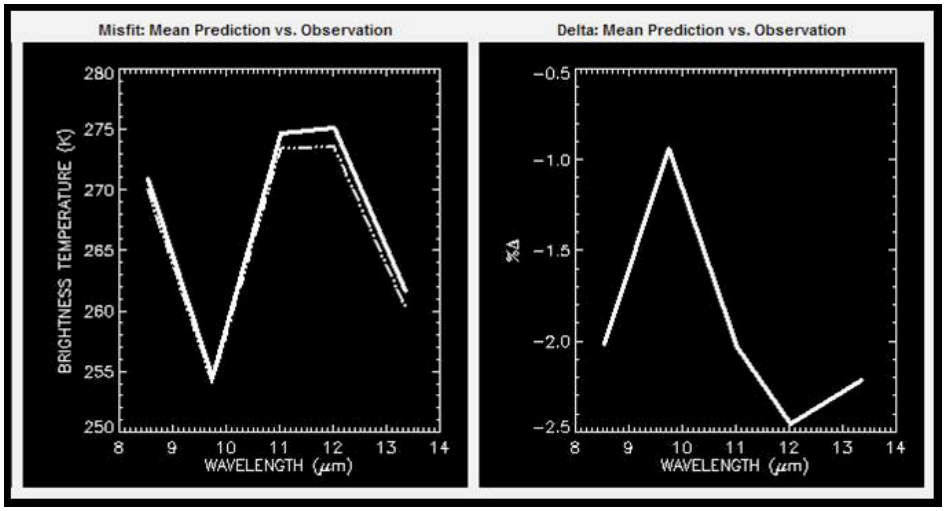

Free H_2O Factor

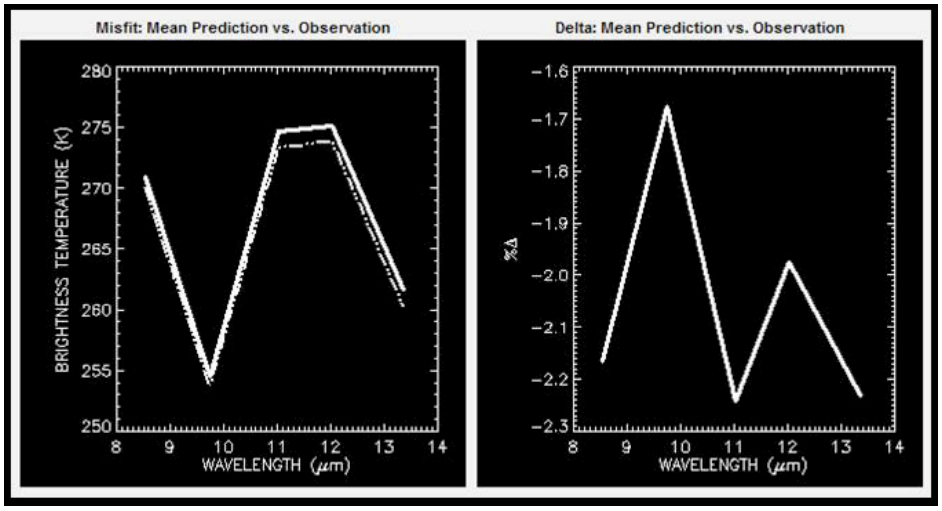

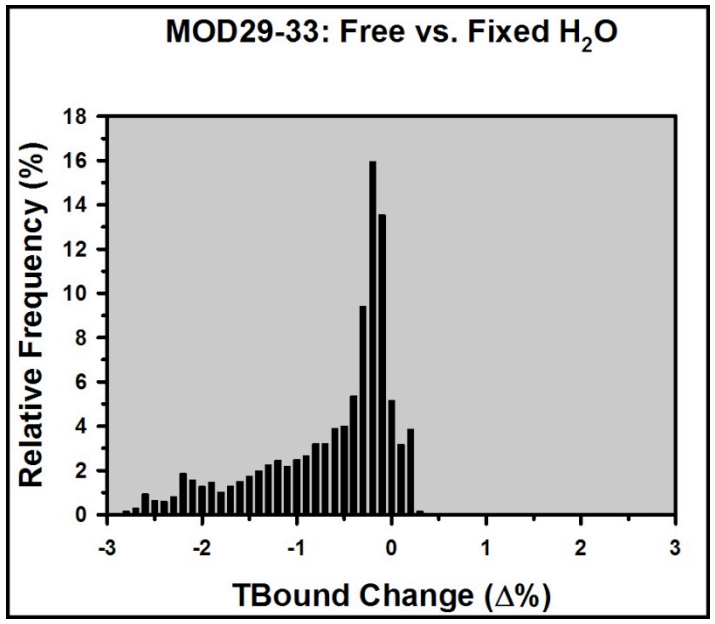

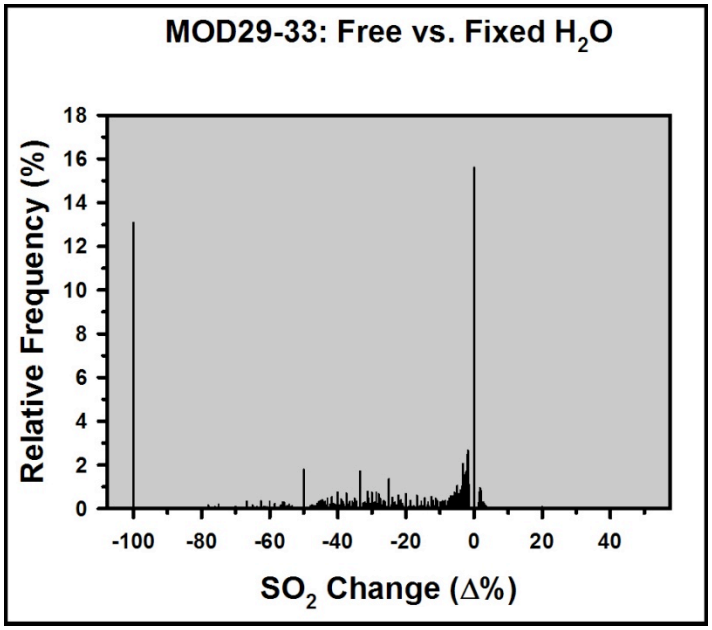

Improved Fit: Δ% Range Reduced from 3% to 0.7%

TBound Estimates Decreased < 0.5%

Problematic Interpretation of SO_2 Results:
Reduction in Estimates < 10% ?

Spike @ -100% is Significant!

Spike @ 0 Change Significant?

Notional HysplRI TIR Response vs. Spectra of Plume Materials

Summary Remarks

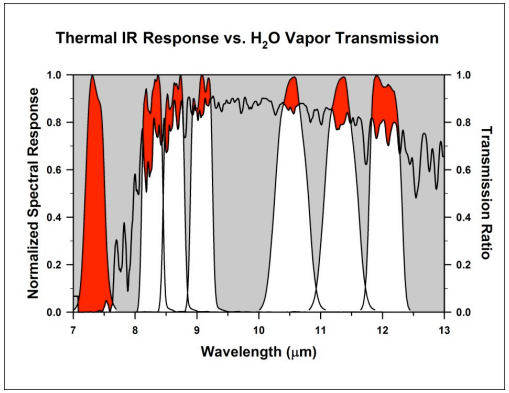

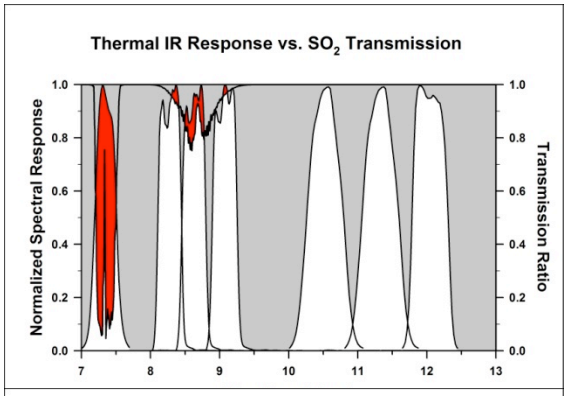

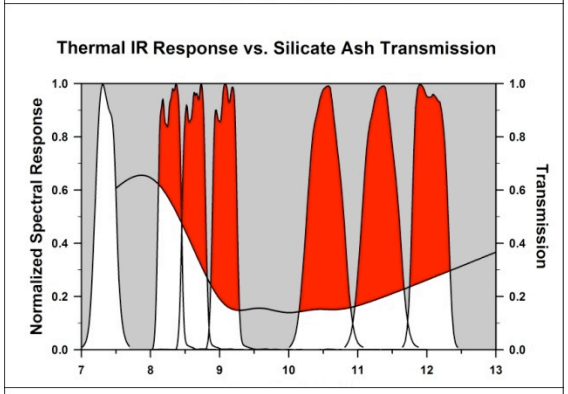

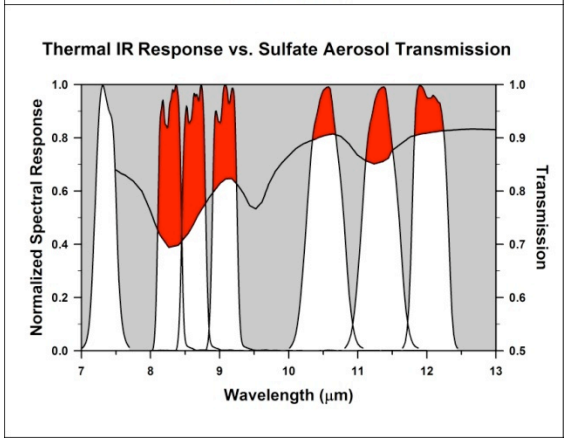

Single Channel @ 7.3 μm Does Not Provide Sufficient Resolution to Separate the Effects of H_2O and SO_2

Characterizing Spatial Variations in H_2O Has Broader Science Impact than SO_2 Detection:

- **Shift Channel to Longer Wavelength (~ 8.0 μm)**
- **Definitive Solution to Channel Position Requires HyTES Data**

Adopting 13.3 μm Channel (MOD 33) for MODIS-Based Plume Mapping

- **Not Necessary for HysplRI Due to High Spectral Resolution Between 8 and 9 μm**

Food For Thought: HysplRI Channel Between 9.5 and 10 μm Would Help Discriminate Sulfate Aerosols from SO_2 or Ash

Update on NEON (National Ecological Observatory Network) and Complimentarily with HyspIRI

Thomas Kampe and the AOP Team

National Ecological Observatory Network, Inc.,
1685 38 St, Suite 100, Boulder, CO 80301

Aug 25, 2011

Introduction

The overarching goal of NEON is to enable understanding and forecasting of climate change, land use change, and invasive species on continental-scale ecology *by providing infrastructure* to support research in these areas.

- NEON design is in response to NRC Grand Challenges in Environmental Sciences: Biodiversity, Biogeochemical cycles, Climate change, Ecohydrology, Infectious disease, Invasive species, Land use
- The NEON Project is the observatory funded by the U.S. National Science Foundation (NSF)
- NEON Inc. is a not-for-profit corporation that is funded by the NSF to plan, design, build and operate NEON

Addressing Grand Challenges in Ecology

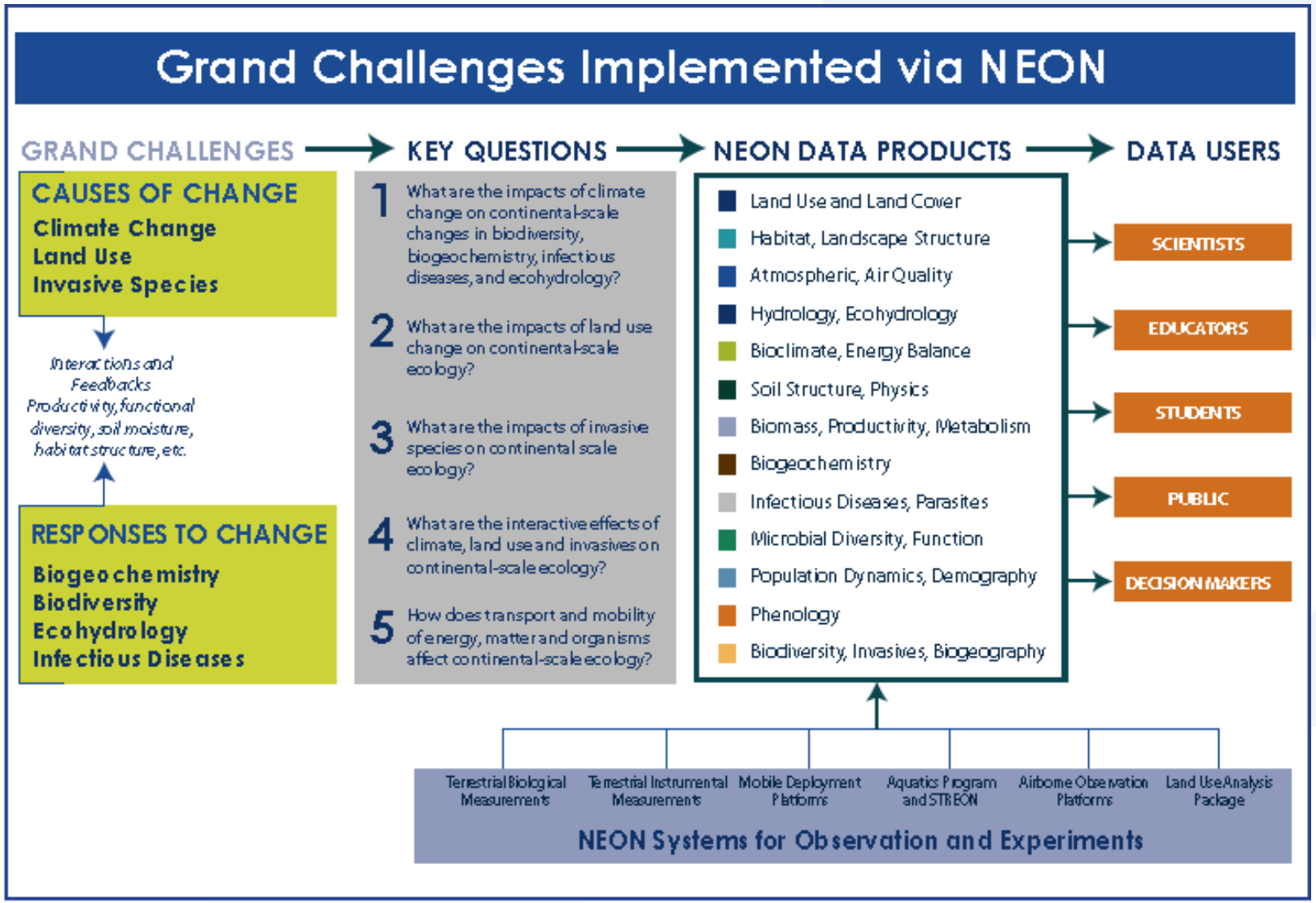

NEON Infrastructure

- Headquarters (incl. CI, labs, etc.) – Boulder, CO
- 20 Domains
- 20 Core sites (wildland)
- 40 Relocatable sites (land-use sites)
- 36 Aquatic sites
- 3 Airborne Observation Platforms
- 10 Mobile Deployment Platforms (AK, HI, CONUS+PR)
- Cyberinfrastructure/Data Center/LUAP
- STREON Experiment

- 542 Primary (i.e., raw) observations
- 118 Continental scale data products
- ~500 Terabytes data/year
- 5 year construction
- 30 year operations

NEON Science Facilities

Fundamental Sentinel Unit – measurement of key response variables in selected taxa (e.g. plants, birds, insects, …)

Field sampling

Fundamental Instrument Unit – automated sensor for climate & climate-related physical variables in the atmosphere and soil

Towers

Aquatics– field sampling and automated sensors for Algal cell count, macroinvertebrate biovolume, stream discharge, water height

Surface and ground water

Airborne Observation Platform – remote sensing observations of land-use change, and vegetation biochemistry and structure

Aircraft

Land Use Analysis Package – land-use, land management and other national datasets plus satellite observations

Satellite Data

National Observatory: 20 Eco-climatic Domains

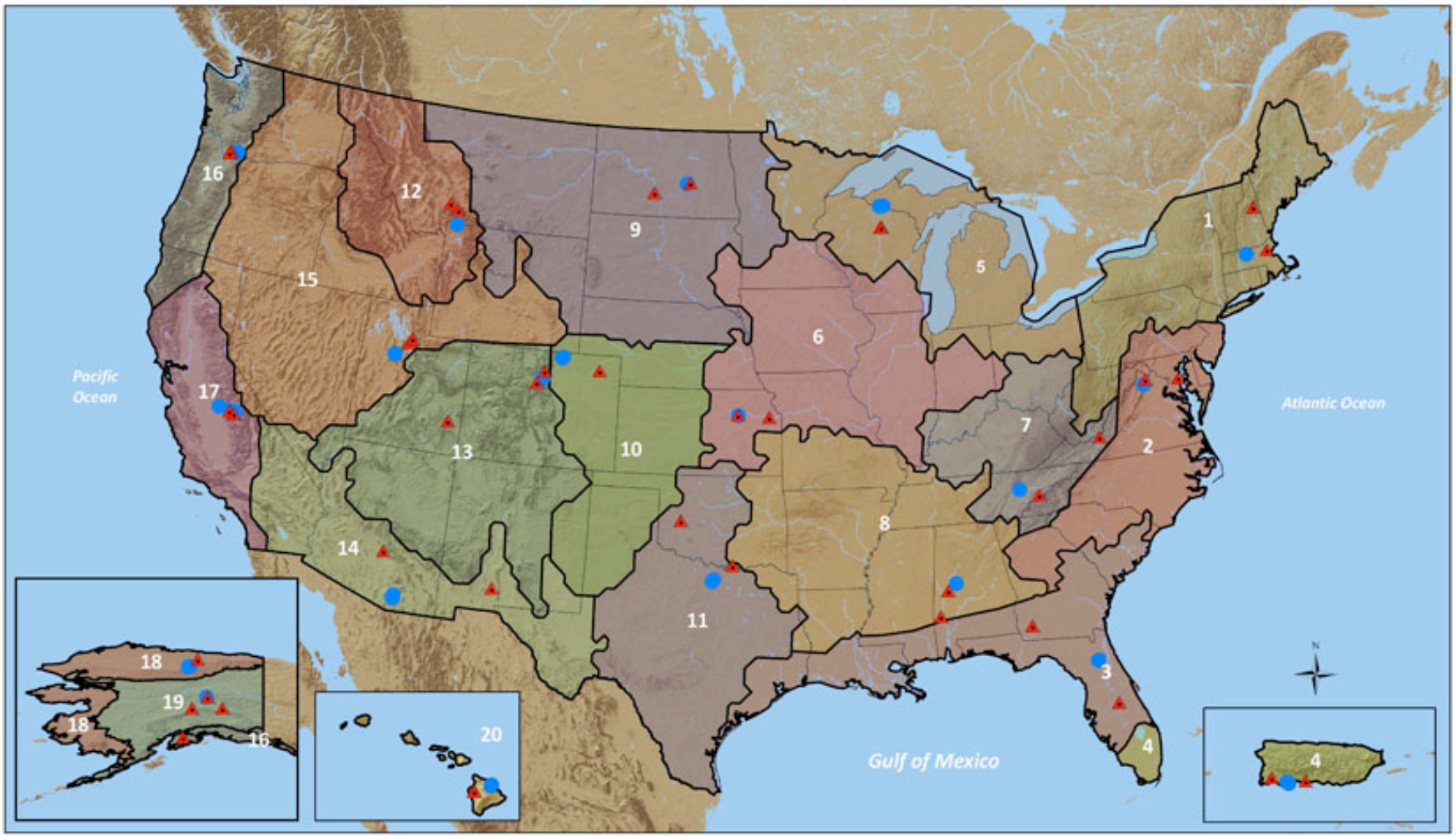

Terrestrial Instrument Measurements

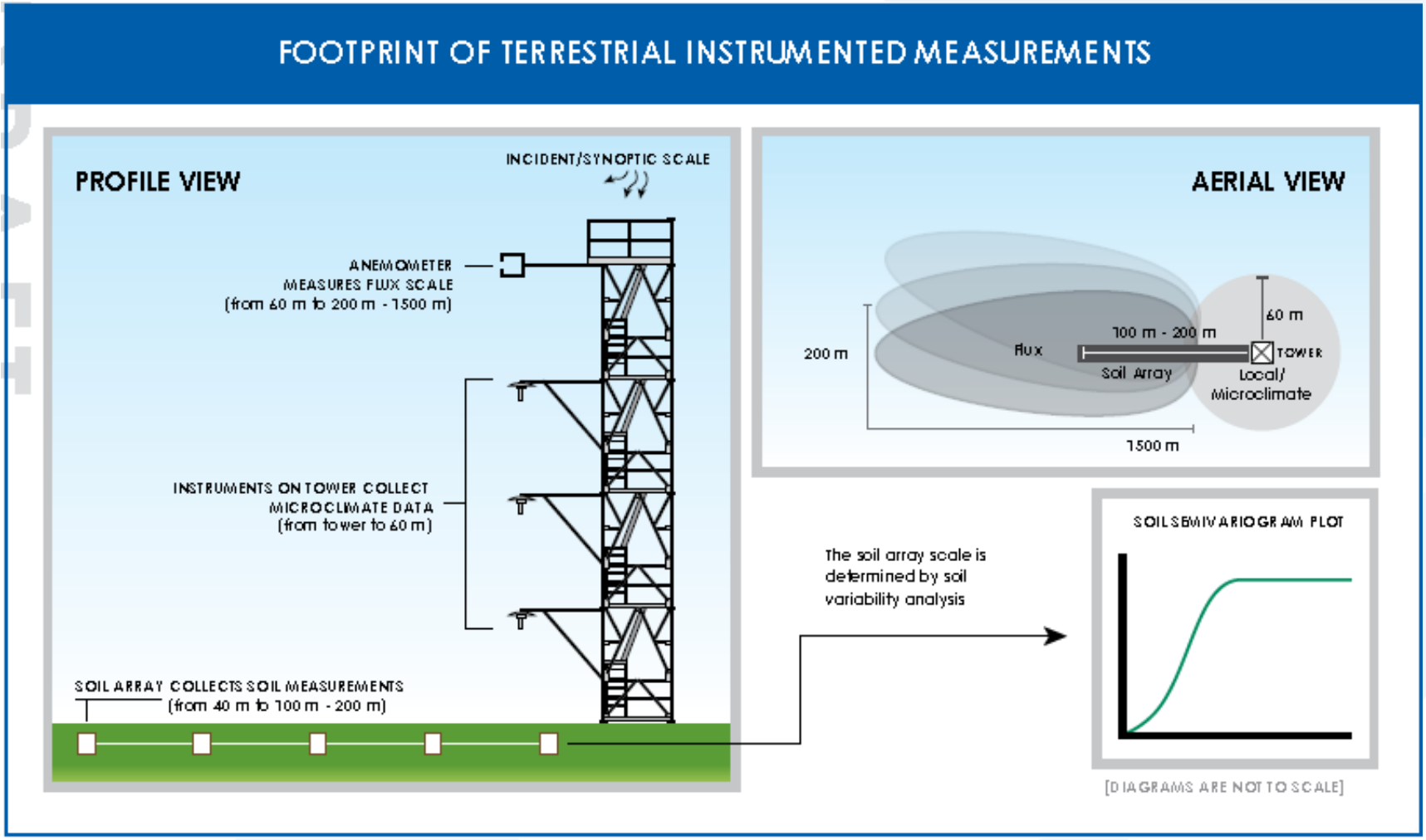

Role of the Airborne Observation Platform

- AOP will observe land use drivers and ecosystem responses surrounding NEON flux tower sites
  - Land cover
  - Vegetation structure
  - Invasive plant species
  - Biochemical and biophysical properties
  - Ecosystem functioning

- Bridge scales from organism and stand scales (e.g., meter-scale) to the scale of satellite-based remote sensing
- Connection to satellite observations (coverage of 300 km^2 about each site)

NEON Airborne Observation Platform (AOP)

- Three airborne remote sensing payloads:
  - Waveform-LiDAR altimeter
  - Imaging spectrometer
  - High-resolution digital camera
  - GPS-Inertial measurement unit
- Leased Twin Otter aircraft
- Instrumentation maintenance and calibration facility
- Science and flight operations

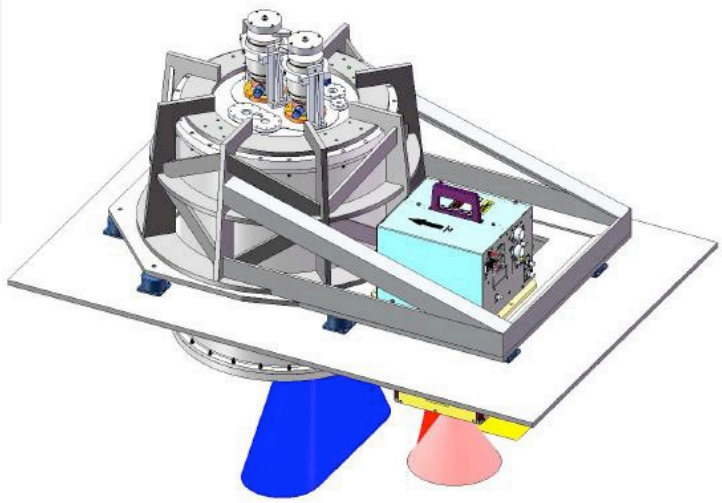

9

Integrated Airborne Observations

Waveform Light Detection and Ranging

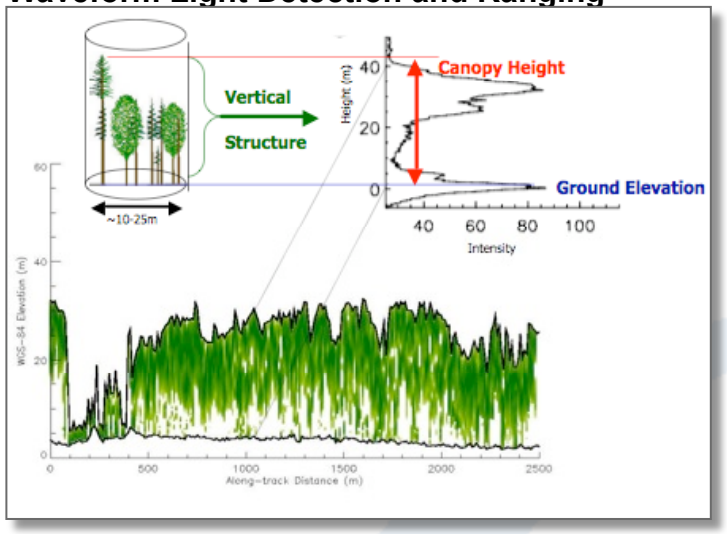

+

High-fidelity Imaging Spectroscopy

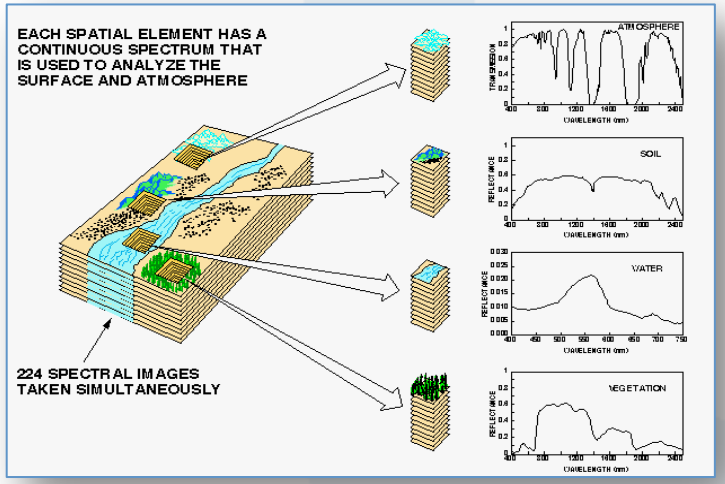

- LiDAR Altimetry to measure 3-D vegetation structure
  - —sub-canopy topography
  - —mapping of vegetation height
  - — Mapping of cover and canopy structure
  - —Biomass

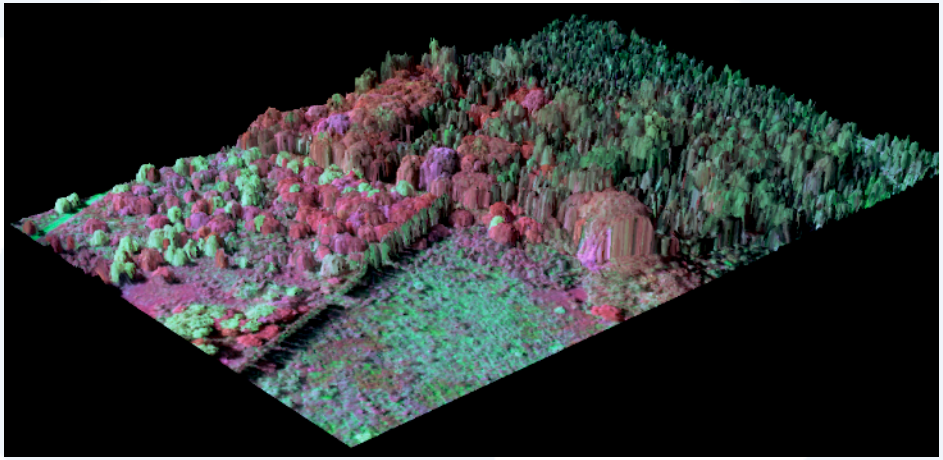

- Spectroscopy
  - —Determine biochemical & biophysical properties of vegetation
  - —Cover type/fraction
- Information contained in subtle variations in surface reflectance

Spatial Scaling Strategy

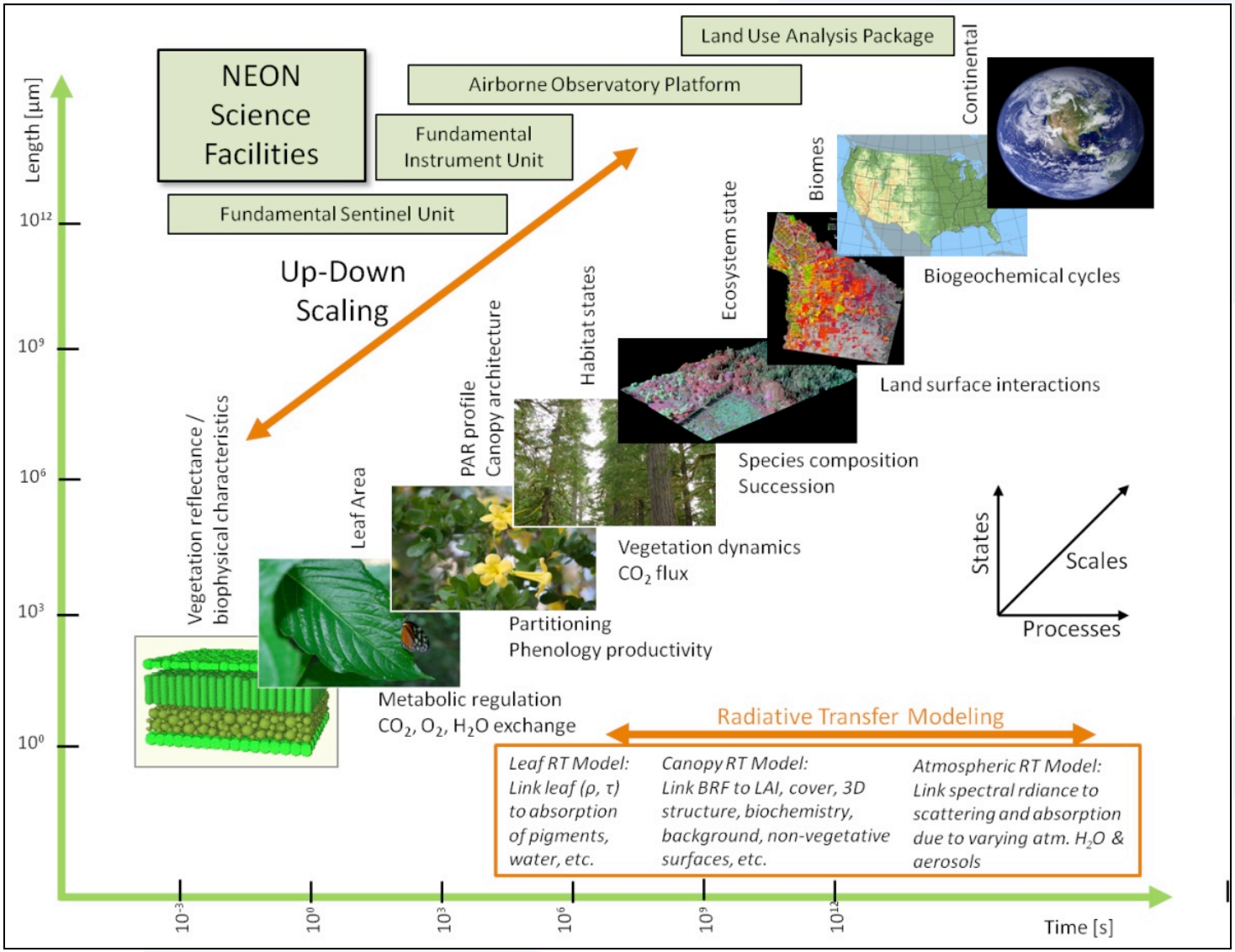

AOP Flight Operations

- 7-months, 1,000 flight hrs flight season
- 2.3 aircraft with identical payloads required for annual survey of NEON sites
- 3rd Payload for reserve & new science opportunities

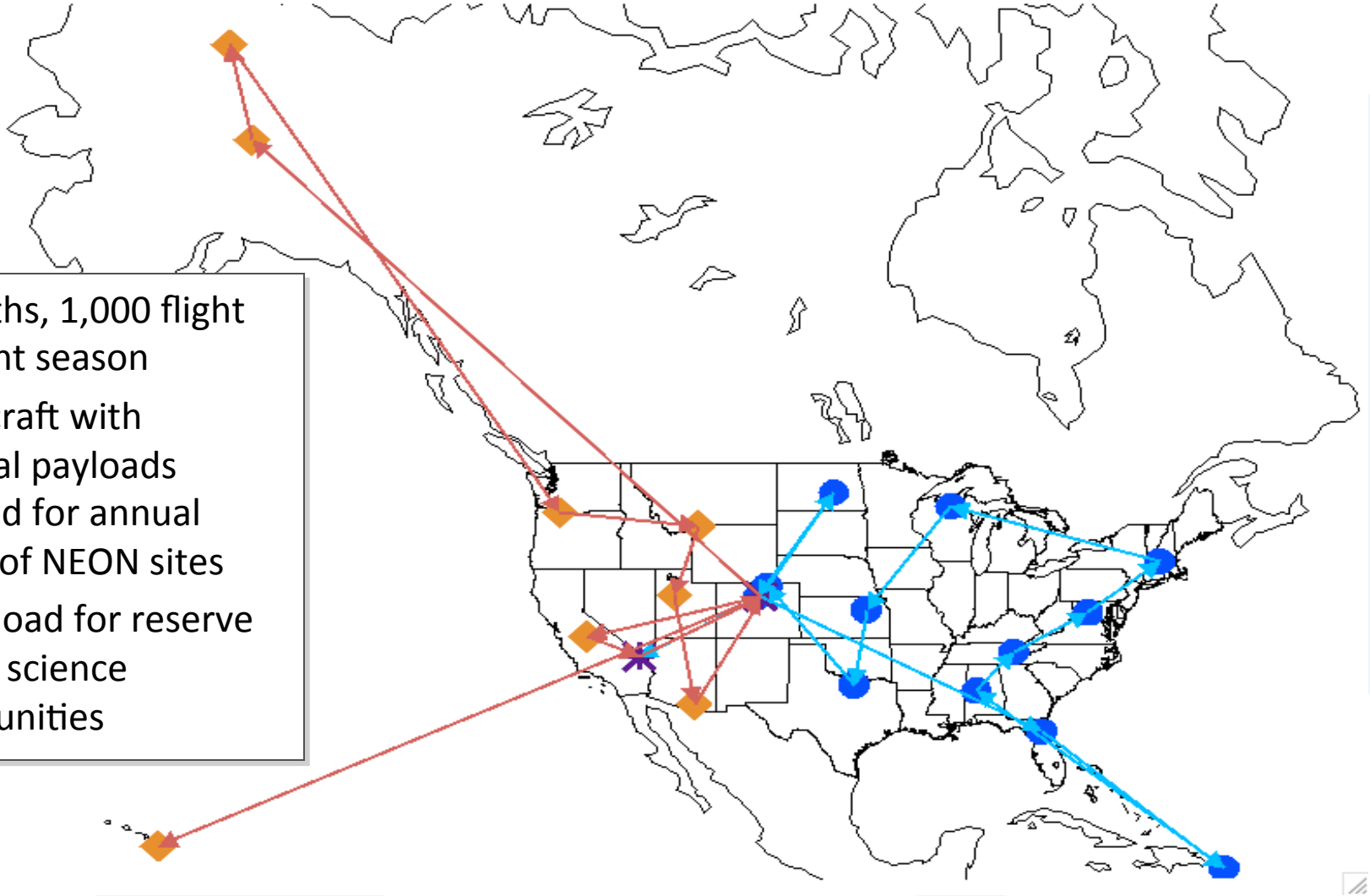

Imaging Spectrometer Development Status

- In Sept 2009, NEON Inc. received Stimulus funding for the development of the NEON Imaging Spectrometer Design Verification Unit (NISDVU)
- The NISDVU is currently being developed at NASA JPL
- Goals:
  - Verification of imaging spectrometer design, performance, and operations
  - Provide a clear demonstration that a significant portion of AOP development risk has been retired
  - Ensure that imaging spectrometer performance requirements are met prior to committing to the build of NIS units 2 and 3
- Prototype science algorithm development
- Test flights to validate laboratory radiometric calibration of the DVU and instrument boresight and cross-calibration with existing heritage instruments (i.e., AVIRIS)
- 24-month program - complete in December 2011

NEON Imaging Spectrometer

Spectral range	380 to 2510 nm
Spectral resolution	10 nm
Spectral sampling	5 nm
Spatial Registration	≤ 0.05 pixel
Radiometric Accuracy	> 95% absolute
Radiometric precision	SNR > 1000 @ 550 nm SNR > 1000 @ 2100 nm
Dynamic Range	0 to saturation radiance
Sensor IFOV	1 milliradian
Sensor FOV	34 degrees
Spectral & Spatial response uniformity	≥ 95%
Cross-track pixels	> 600 pixels
Cross-track swath	1.0 km @ 1000 altitude

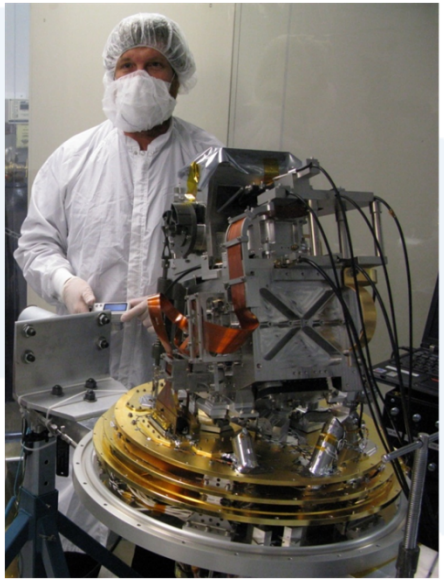

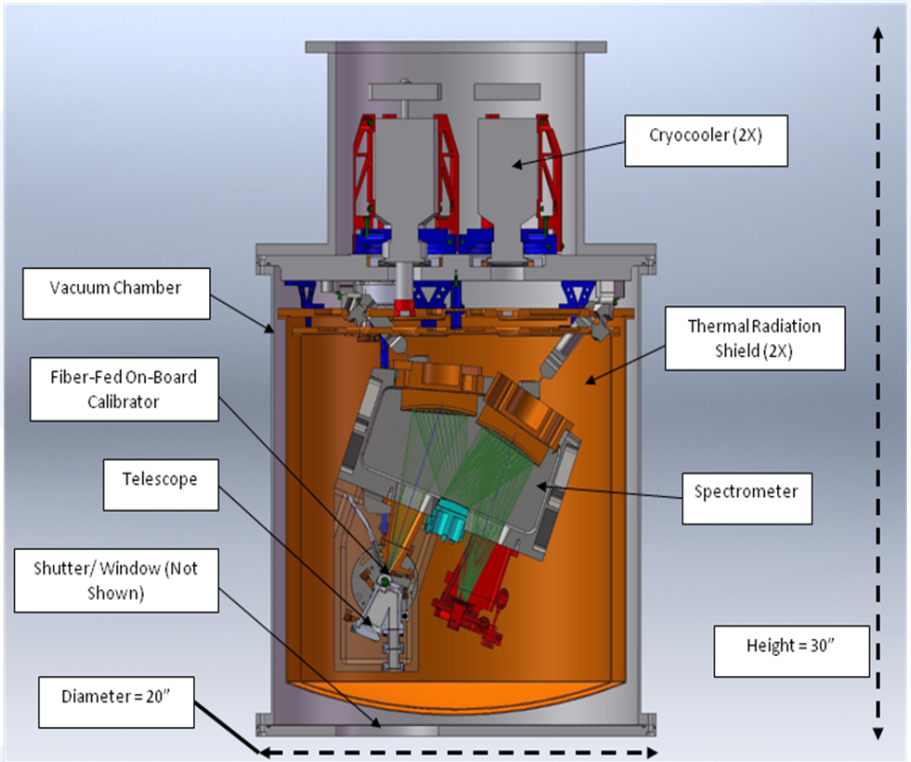

Current Status and Measured Performance

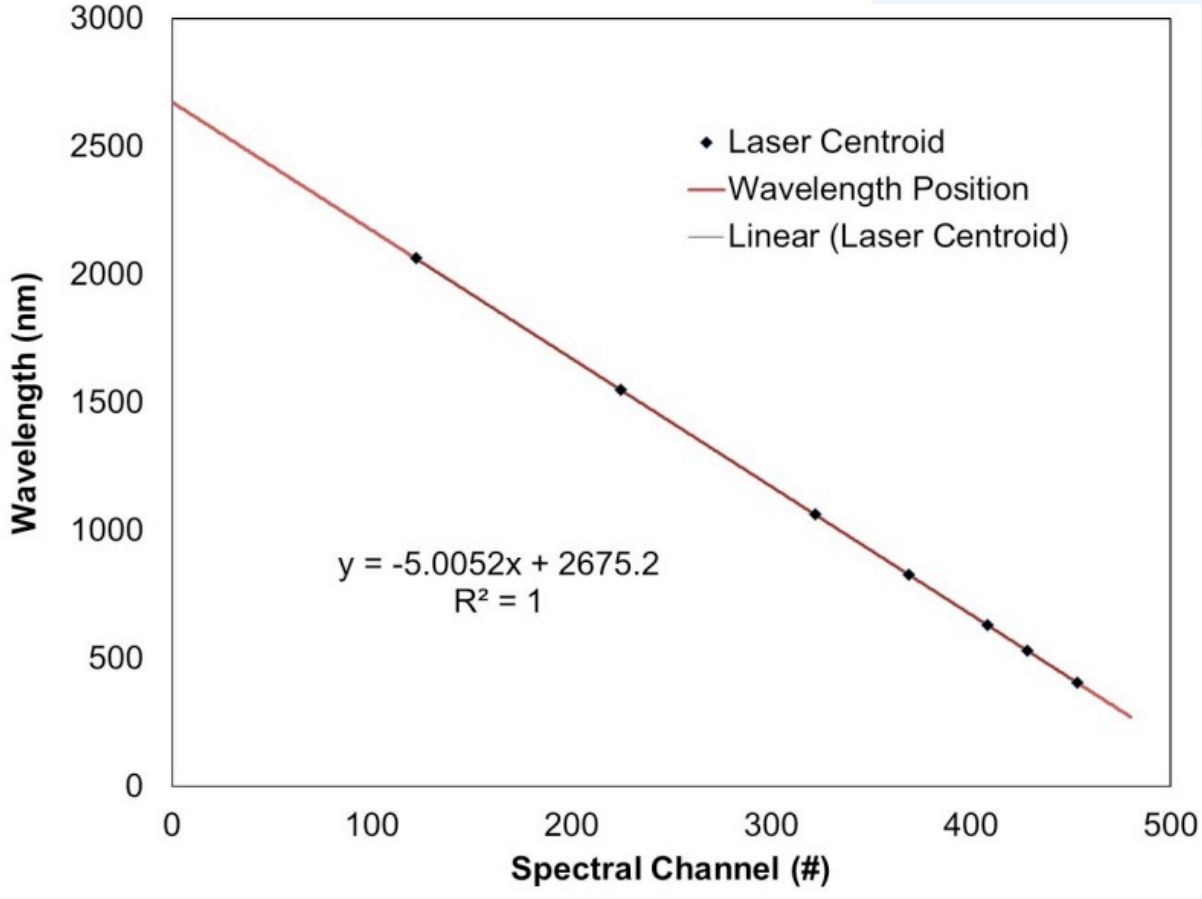

Current Status and Measured Performance

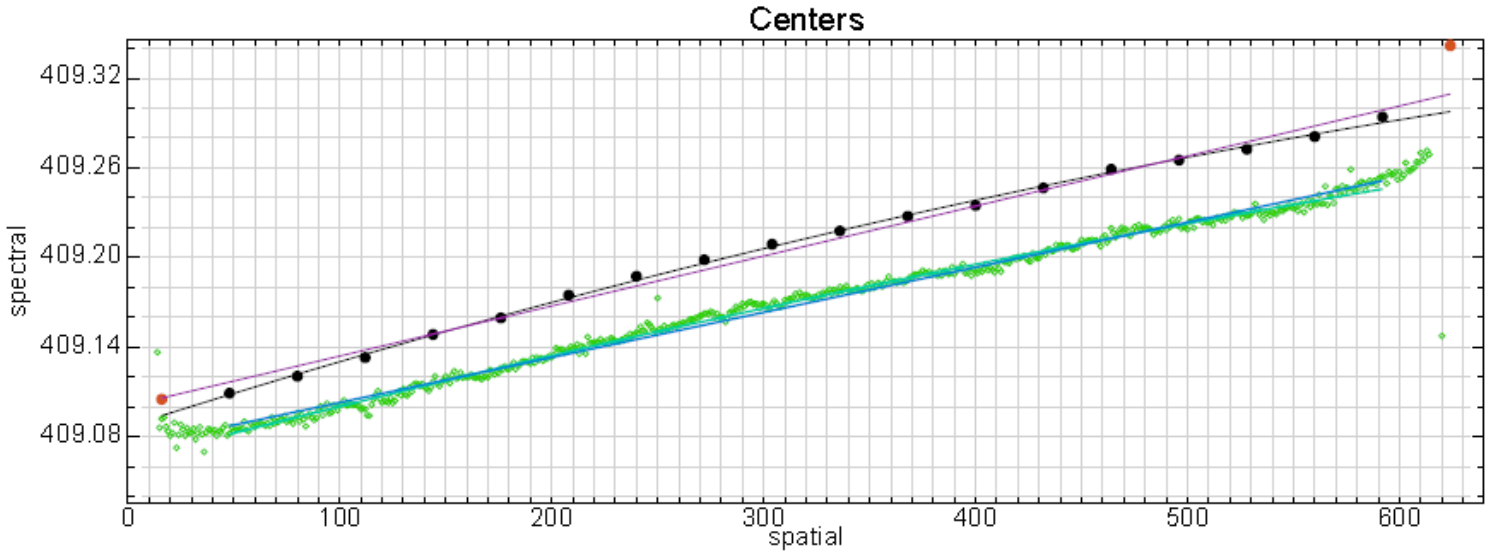

- NISDVU in cold alignment and nearly complete
- Results from cold cycle 5
  - Spectral smile <1%
  - Small amount of FPA clocking required (15-20% pixel)

Predicted System-Level Performance

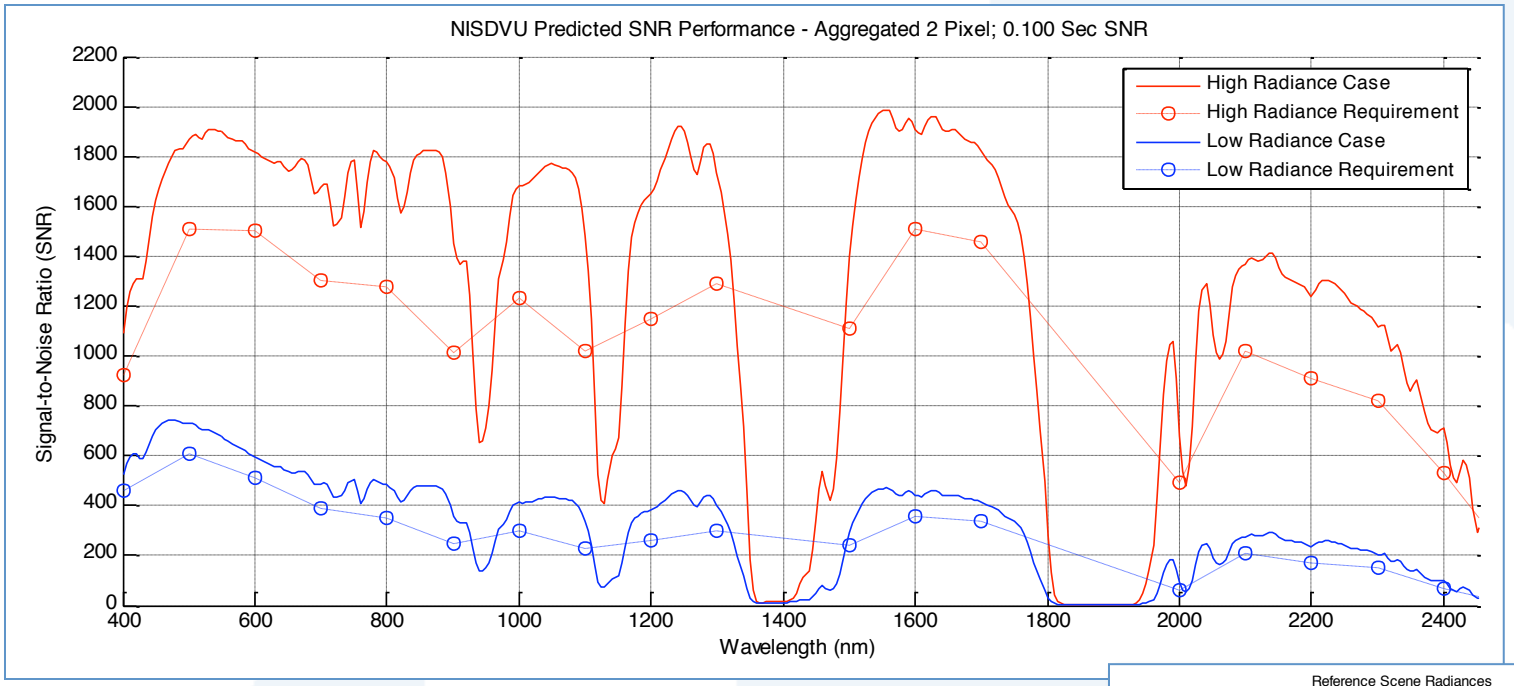

- Predicted SNR exceeds requirement over full VIS to SWIR band
- Predictions account for measured component data

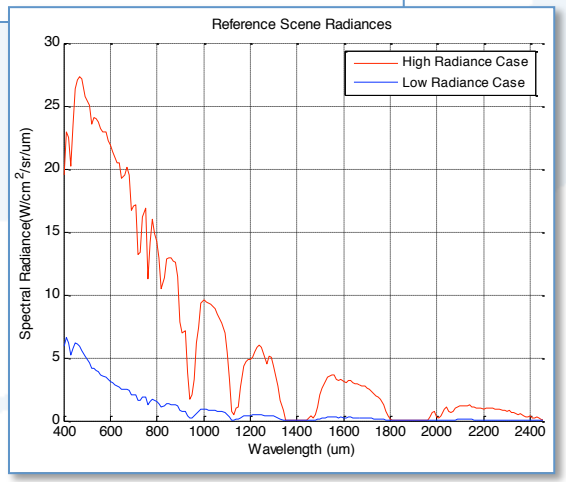

Representative Data Acquisitions

- **NEON 2010 Pathfinder Campaign**

High-Level Goals

Collect a combined waveform LiDAR and spectrometer dataset
Prototype ground truth measurement & field sampling techniques that will be required for validation of higher level data products

AOP Goals

Reduce sensor data product development risk
Develop prototype field and airborne measurement techniques
Develop ground validation techniques
Develop data processing algorithms
Inform validation of atmospheric correction methodologies in a humid environment

Terrestrial Biology Goals

Develop field training and data collection protocols
Collect ground-based data to calibrate airborne data
Determine time-frame in which ground data must be collected
Prototype plot design for measuring plant biodiversity
Assess ability of airborne platform to monitor invasive species

- Twin Otter Aircraft
- NASA AVIRIS Spectrometer
- NCALM LiDAR

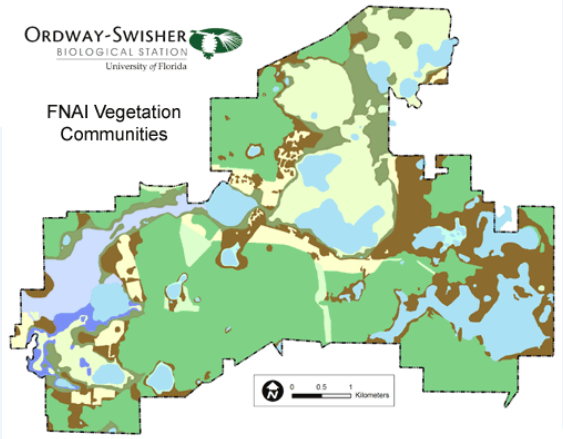

- Florida study areas:
  - Ordway-Swisher Biological Station
  - Donaldson Plantation
  - Calibration Sites

Pathfinder 2010 Airborne and Satellite Observations

- JPL AVIRIS
  - 9/4/10 OSBS morning flight
  - 9/6/10 Donaldson Plantation
  - 9/10/10 OSBS mid-day flight
- NCALM flying an Optech Gemini
  - 8/31/10 Aquatic Sites
  - 9/1/10 OSBS
  - 9/2/10 Donaldson Plantation
  - 9/3/10 Ashley Prairie
- Satellite Observations
  - Hyperion and ALI tasked
  - Landsat 5 and 7 overpasses
  - MODIS overpasses

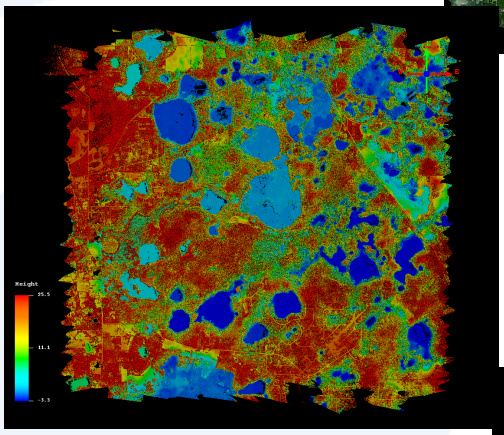

Pathfinder 2010 Ground Measurements

- Airborne Observation Team
  - Atmospheric - CIMEL
  - Weather – Kestrel pocket weather station
  - Reflectance – ASD measurements
    - Above canopy long-leaf pine, turkey oak, and mix from an aerial boom lift
    - Ground measurements of short wire grass, fennel, and pindo palm
    - Radiometric calibration sites
  - Leaf Area Index (along several 500m long transects)
  - Differential GPS base stations

- Terrestrial Biology Team
  - Leaf Area Index (along several 500m long transects)
  - Vegetation Structure (along small plot 20m x 120m)
    - Canopy diameter
    - Diameter at breast height, DBH
    - Height
    - Height to first branch
    - Species ID
  - Biodiversity (several locations across site)
    - Plant species richness
    - Locations of invasive Pindo Palm

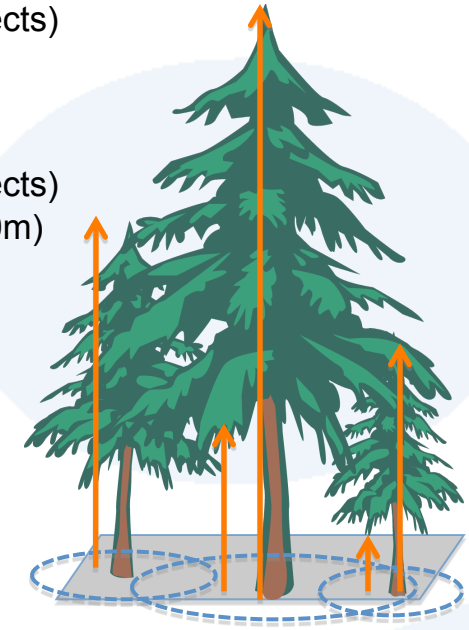

Comparison of JPL AVIRIS Spectral Reflectance With ASD Ground Measurements

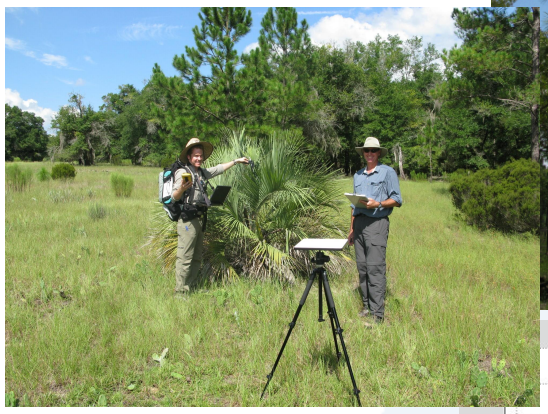

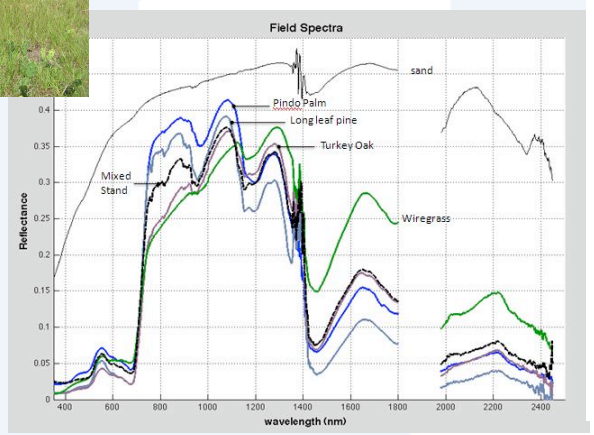

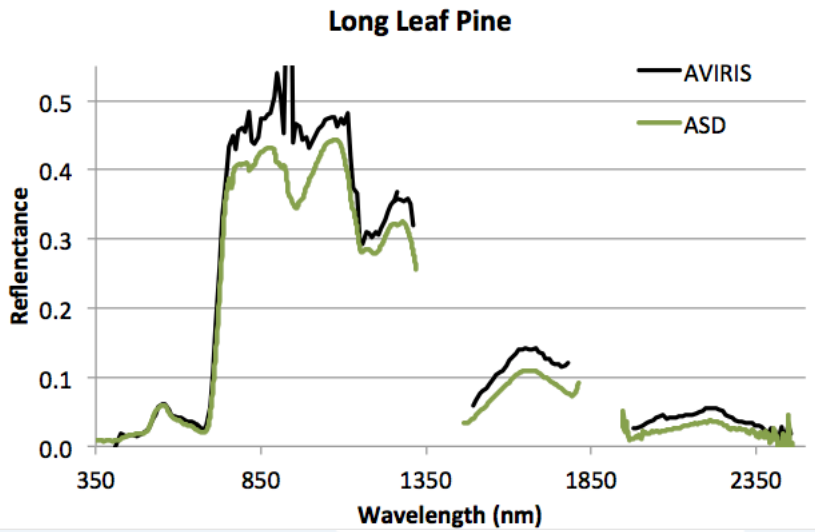

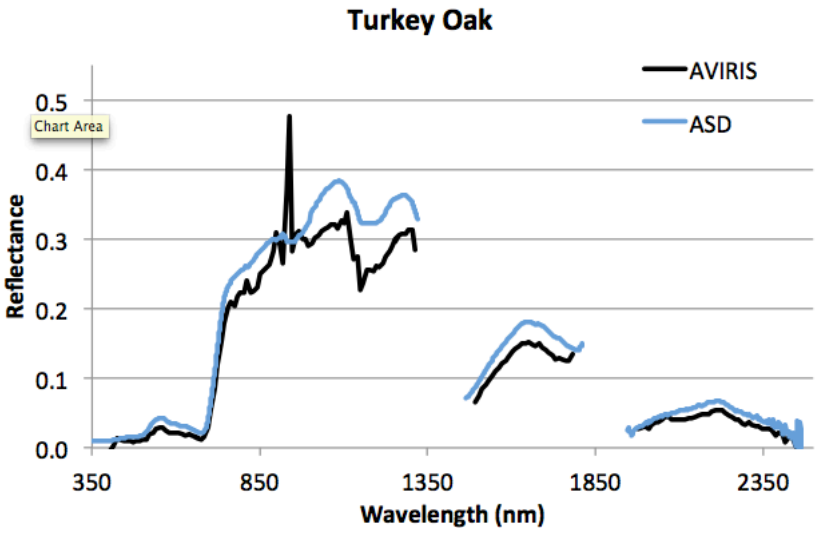

Pathfinder 2010 Prototype Results To Date

- Use the Pathfinder 2010 data collected over Ordway-Swisher Biological Station and Donaldson Plantation to inform spectrometer and LiDAR algorithm flow and identify required algorithm/ processing steps
  - Full end-to-end view of Level 0 raw data through Level 4 science data products

- Spectrometer and LiDAR Prototype Data Sets
  - Nine spectral inversion algorithms are applied to the imagery to prototype six AOP Level 4 products including:
    - Bioclimate_004 Leaf Area Index
    - Biogeochemistry_009 Canopy Nitrogen
    - Biogeochemistry_010 Canopy Water Content
    - Biogeochemistry_011 Canopy Xanthophyll Cycle (PRI)
    - Biogeochemistry_012 Canopy Chlorophyll
    - Biogeochemistry_013 Canopy Lignin
    - Cellulose
  - A basic ground finding algorithm is applied along with COTS software processing in Quick Terrain Modeler and ENVI to prototype three AOP Level 4 products including:
    - Land_Use_002 Elevation (digital elevation model DEM)
    - Land_Use_004 Slope and Aspect
    - Biodiversity_018 Ecosystem Structure (canopy height model CHM)
    - Digital surface models (DSM) are also required in order to create the canopy height models

22

Spectrometer Prototype Data Sets:

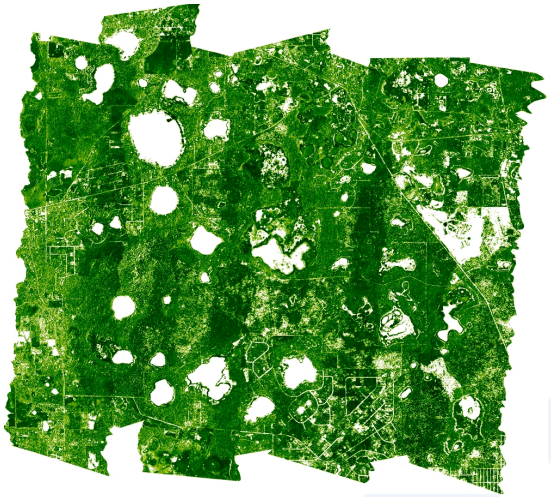

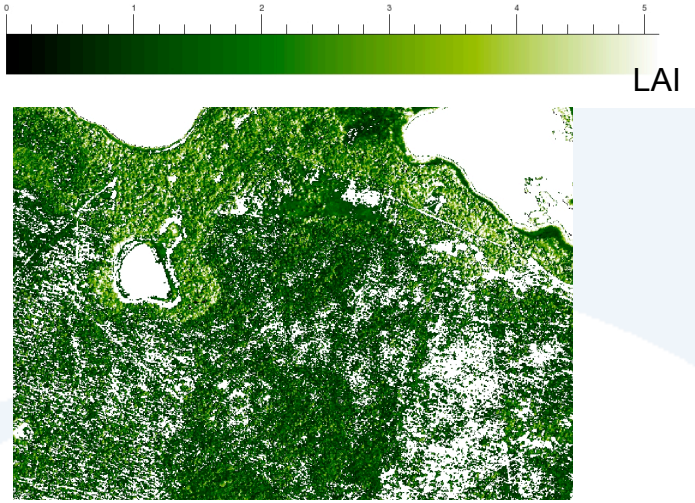

Spectrometer Prototype Data Sets: Leaf Area Index

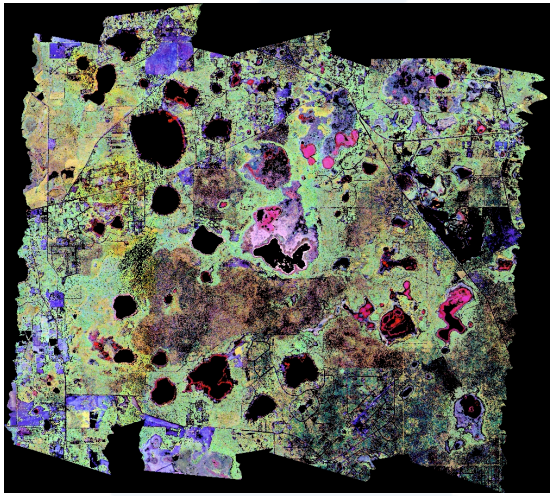

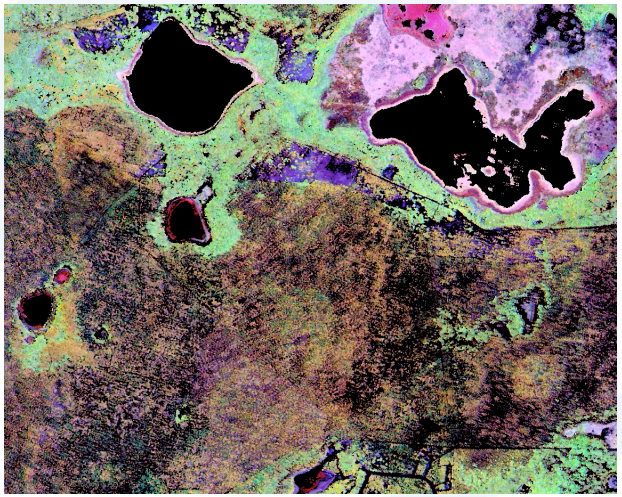

Spectrometer Prototype Data Sets: R,G,B: Water, Chlorophyll, Nitrogen

Discrete LiDAR Point Cloud Visualization:

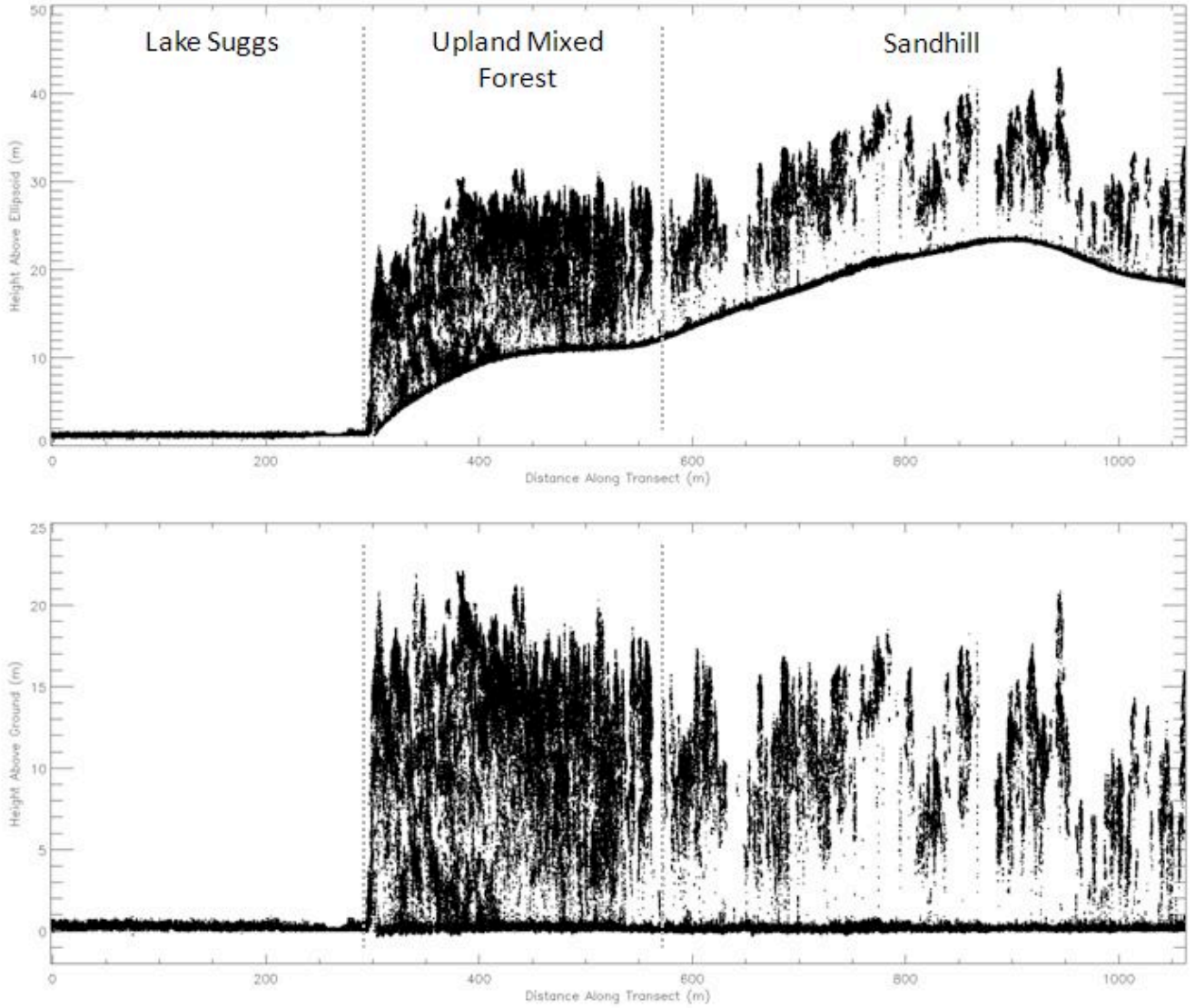

Data from Prototype Campaign available at:

http://neoninc.org/pds/

Prototype Data Sharing - Windows Internet Explorer provided by NEON

http://neoninc.org/pds/

View Favorites Tools Help

NEON Prototype Data Sharing

National Ecological Observatory Network

Prototype Data Sharing

Welcome to NEON's Prototype Data Sharing (PDS) system. The PDS allows you to browse various "prototype" data sets that are available for limited use. It is important to understand that the data, metadata, and file formats distributed do not necessarily correspond to those planned for Operations.

The grid below lists the datasets that are currently available, along with descriptions of their spatial and temporal range as well as format and size. You may sort the list by any of the columns by clicking on its heading. Entering search terms in the box provided will immediately filter the list to show only those items that match, regardless of the column in which the match appears.

To request access to any of the datasets, please click the appropriate [Request] link below. You will then be presented with a page containing the detailed metadata associated with the data and instructions of how to request the data for your use.

Copy CSV Excel PDF Print

Search:

Link	Description	Contact	Size	Format	Notes
Request	Reaeration & Discharge Rating Curve Data	K. Goodman	20.5 MB	.xls	Single archive file contining .xls files for water chemestry, reaeration rates, and discharge rating curves.
Request	Leaf Area Index & Vegetation Structure Data from D3	C. Meier	500 KB	ASCII (csv)	Single archive file containing individual data files (LAI & VS for Ordway-Swisher and Donaldson sites).
Request	NEON Terrestrial Insect DNA Barcode Library	C. Gibson	1.9 GB	jpg; ab1; xls	CO1 gene reads (images and both traces) and associated metadata, averaging 1.2 MB per specimen.
Request	Soil Temperature And Soil Moisture Data From NEON Candidate Sites	E. Ayres	1.2 MB	.txt (tab delimited)	Single archive file containing 60 site files each detailing ~130 locations in the expected airshed.
Request	Pathfinder Discrete LIDAR, Donaldson Plantation	T. Kampe	5.5 GB	.las	17 separate flightline archives, averaging 340 MB each.
Request	Pathfinder Discrete LIDAR, Ashley Prairie	T. Kampe	1.9 GB	.las	10 separate flightline archives, averaging 190 MB each.
Request	Pathfinder Spectrometer, OSBS Morning Flight	T. Kampe	18 GB	ENVI	16 separate flightline archives, averaging 1.2 GB each.
Request	Pathfinder Discrete LIDAR, OSBS	T. Kampe	15 GB	.las	33 separate flightline archives, averaging 450 MB each.
Request	Pathfinder Spectrometer, OSBS Mid-day Flight	T. Kampe	21 GB	ENVI	16 separate flightline archives, averaging 1.4 GB each.
Request	Pathfinder Spectrometer, Donaldson Plantation	T. Kampe	11 GB	ENVI	14 separate flightline archives, averaging 800 MB each.
Request	Pathfinder Discrete LIDAR, Aquatic Sites	T. Kampe	4.2 GB	.las	18 separate flightline archives, averaging 233 MB each.
Request	Pathfinder Ancillary Ground Data	T. Kampe	10.1 MB	various	Atmospheric, meteorological, and spectral reflectance measurements collected on the ground during the Pathfinder Campaign.

There are currently 12 prototype datasets available.

The National Ecological Observatory Network is a project sponsored by the National Science Foundation and managed under cooperative agreement by NEON, Inc. This material is based upon work supported by the National Science Foundation under Grant #0080752017. Any opinions, findings, and conclusions or recommendations expressed in this material are those of the author(s) and do not necessarily reflect the views of the National Science Foundation.

Upcoming 2011 Pathfinder Flight Campaign

- Domain 17 Sites (Southern Sierra, California)
- Flying the NASA AVIRIS imaging spectrometer
- San Joaquin Experimental Range
  - Open woodland dominated by oaks (blue and interior live oaks) and gray pine with scattered shrubs
  - 1000 ft. elevation
- Soaproot Saddle, Upper Teakettle
  - Southern Sierra pine/fir forests
  - 5000 – 7500 ft. elevation
- Science focus:
  - Assessing rangeland dry matter
  - Species distributions

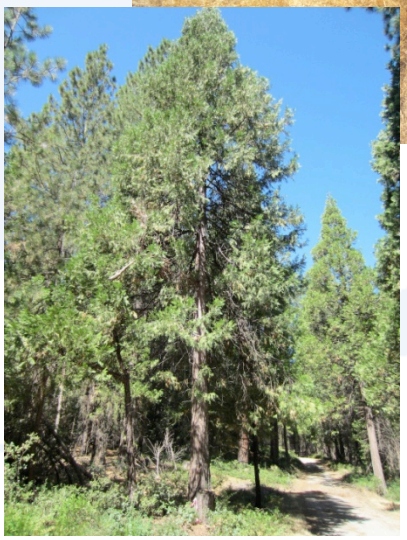

Candidate Opportunity for Interaction with HyspIRI

- **HyspIRI Preparatory Airborne Activities (Summer of 2012)**
  - Obtain precursor science data representative of what could be expected from HyspIRI
  - Fly regions with large climate gradients and diversity
  - Large areas; 3 seasons; ≥ 2 years
  - Acquisition from ER-2 (20 km native resolution; aggregated to 60 km to match HyspIRI)
- **NEON's Role**
  - Early AVIRIS flight over Domain 17 sites (2011) – 4m resolution
  - Underflights of ER-2 AVIRIS (20km) with NISDVU @ 1-km altitude (1m res)
  - Concurrent satellite acquisitions (MODIS, Landsat, Hyperion)
  - Supporting ground measurements (field spectroscopic measurements, LAI, radiometric calibration, AOD, etc)

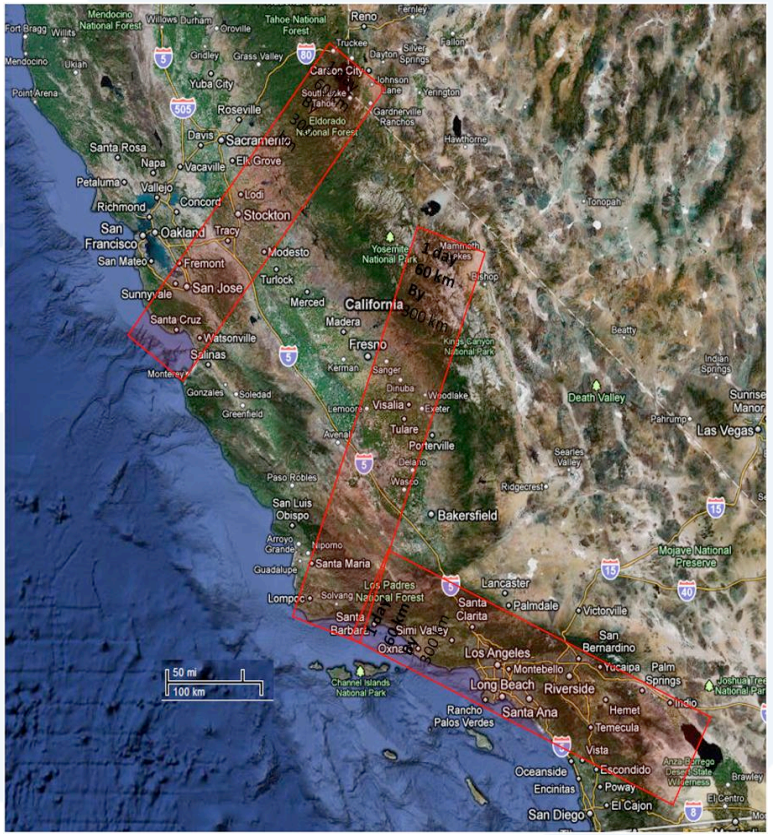

Goals:

- Obtain spectroscopic data at multiple spatial scales useful for assessing sampling strategies for the extrapolation of biophysical processes
- Spectroscopic and lidar data at 1-m resolution to support HyspIRI science product development

Potential NEON Synergy with HyspIRI

- **NEON Ground/Airborne Validation of HyspIRI**
  - Well-validated annual measurements at 60 sites across the continental US –grasslands, deserts, agricultural areas, deciduous forest, conifer forest, tundra and Arctic
  - Vegetation chemical & structural information measured at all sites; site-specific spectral databases developed
  - FSU can provide ground validation of AOP and HyspIRI measurements
  - FIU towers provide point or airshed measurements of CO_2, aerosol optical depth and other atmospheric constituents
- **Bridging to Continental Scale**
  - HyspIRI continental-wide 60 m spectroscopic data will support NEON's mission to bridge from AOP plot scale to continental scale

28

Potential NEON Synergy with HyspIRI

- **Operational Science Algorithm Development**
  - NEON science algorithms developed over a broad range of ecoregions
  - Algorithms and associated error budgets documented in publically-available ATBDs
  - NEON science algorithms and associated software code to be developed to an operational level
- **Calibration Comparisons with Spaceborne Sensors**
  - Yearly vicarious calibration flights by NEON over well-characterized ground validation sites (e.g., Railroad Valley, Ivanpah Playa)
  - Multi-decadal record of spectral reflectance measurements suitable for calibration comparisons with satellite and other airborne sensors
  - 3rd AOP platform potentially available to support dedicated under-flights of satellite sensors (Landsat, OLI, MODIS, NPOESS VIRRS, HyspIRI)
- **Education**
  - NEON data will be openly available to all potential users
  - NEON AOP data will provide the opportunity for developing broad scientific user community of terrestrial remote sensing information in anticipation of the HyspIRI launch

Current Status

- Design Phase completed in June 2011
- On July 20, 2011, the Natl. Science Foundation announced that it will fund the Construction of the NEON Observatory beginning in late Summer 2011
  - The construction phase, during which the observatory infrastructure will be built out, is expected to extend over five years
  - NEON anticipates beginning to construct the first of its sites in Colorado and New England over the next 12 months
- Test flights of the1st AOP remote sensing payload test flights begin in Spring 2012
  - Remote sensing payload “checkout” flight
  - Vicarious calibration campaign
  - First flight campaigns over NEON sites

The National Ecological Observatory Network (NEON) is a project sponsored by the National Science Foundation and managed under cooperative agreement by NEON, Inc. This material is based in part upon work supported by the National Science Foundation. Any opinions, findings, and conclusions or recommendations expressed in this material are those of the authors and do not necessarily reflect the views of the National Science Foundation.

In situ observations of volcanic emissions for sub-orbital calibration and validation

David Pieri
Jet Propulsion Laboratory, Pasadena, CA
Jorge Andres Diaz
University of Costa Rica, San Jose
Geoffrey Bland
NASA Wallops Flight Facility/Goddard SFC, Wallops Island, VA
Matthew Fladeland
NASA Ames Research Center, Mountain View, CA

Puyehue-Cordon Caulle Volcano, Chile
04 June 2011
Courtesy Agence France-Presse

2011 HyspIRI Science Workshop, 23-25 August 2011, Washington, DC

Outline

1. The problem:
How can we conveniently, accurately, responsively, and relatively cheaply, sample volcanic ash and gas emissions in situ?

2. One solution: Use small unmanned aerial vehicles (UAVs).

Volcano Hazards

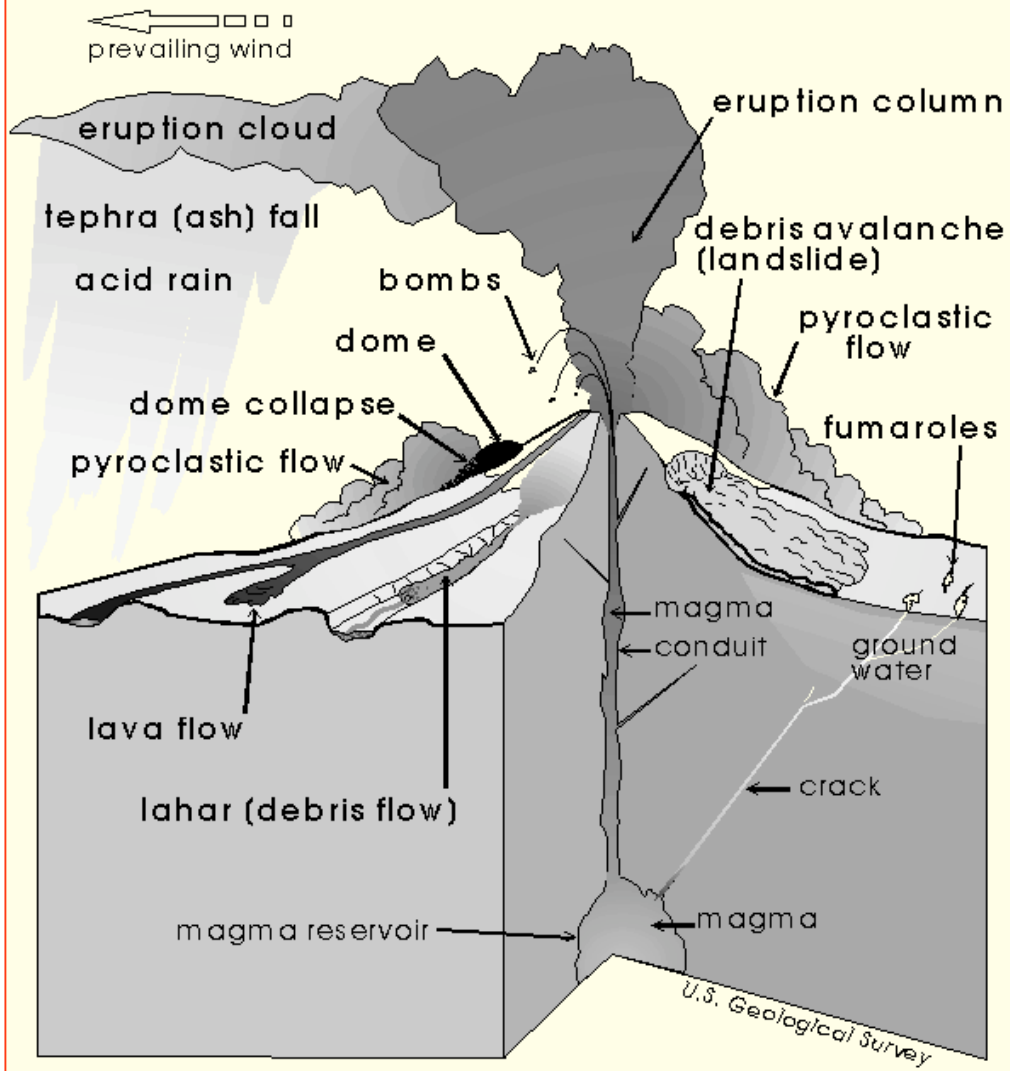

USGS

Topinka, USGS/CVO, 1998, Modified from: Myers and Brantley, 1995, USGS Open-File Report 95-231

Eruption column processes

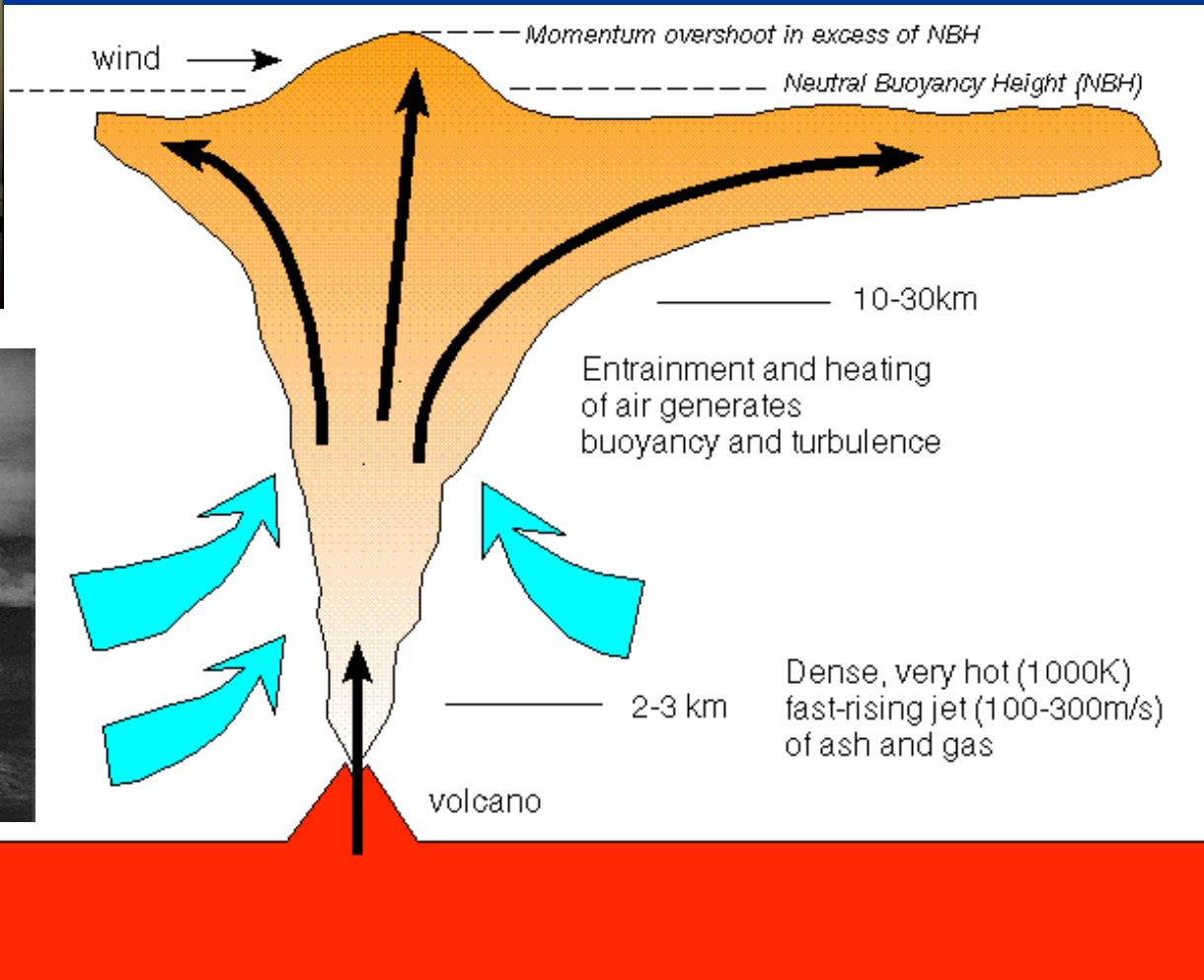

Importance of In Situ Sampling of Volcanic Plumes?

- Basic science

  Better knowledge of instrument response

  How well are detection, mass-loading, and trajectory prediction models doing in characterizing volcanic airborne emissions, both gases and aerosols?

- Applied Science (Emphasis of this talk)

  ☠ Understand the physical properties of airborne volcanogenic emissions in the context of airborne hazards to aviation.

Ash is a serious regional to global threat to aircraft

"…the 2010 eruptions of Eyjafjallajökull in Iceland have highlighted the frailties of global aviation…"

"…today it is recognized that one of the more serious direct threats of airborne ash clouds is to aircraft in flight…"

"…the threat of volcanic ash clouds to aviation is significant in thinking about the multidimensional hazards of large eruptions in the future…"

excerpts from new book by Clive Oppenheimer, 2011, *Eruptions that Shook the World,* Cambridge University Press

The collision between volcanic eruptions and aviation: stimulus and response

- **The Stimulus: Airborne Hazards**
  - Eruption effects—injection of large amounts of volcanic gas, particulate ash, water vapor, and ice into the troposphere and stratosphere.
  - Volcanic plumes and clouds—drifting over major sections of the globe, disruptive, dangerous.
  - Effects on Aircraft—obvious prompt and more subtle delayed engine and airframe problems.

- **The Operational Response—Airlines, VAACs, First responders**
  - Where is the stuff? Where's it going?
  - Aviation—go around! OK for North America, parts of Asia, and maybe Australia/New Zealand but can't easily do it in Europe or Central/South America, for instance.
  - What concentration levels are safe to fly through and for how long?

The collision between volcanic eruptions and aviation: stimulus and response

- **The Observational Response—National weather and science agencies**
  - Remote sensing—get data!
  - Mainly satellite observations—from LEO and GEO. (HyspIRI will vastly help).
  - How do we interpret our data?
  - How much is there?
  - Could we have seen it coming--precursors? (HyspIRI will vastly help here, too.)
- ***The Critique (the role of in situ observations—focus of this talk)***
  - ***How good are our remote sensing data?***
  - ***What do our data mean in terms of "tangible" physical properties of volcanic clouds?***
  - ***How well can we validate our results and how can we improve them?***

Emergent Airborne Ash Issues 2009 and now

Jet Propulsion Laboratory
California Institute of Technology

The challenges:

Historical context: Pre-Eyjafyallajokull
In situ validation of ash-cloud models—R&D
First *Support to Aviation for Volcanic Ash Avoidance (SAVAA) Workshop* - Rome – Italy, 6-7 April, 2009

- **Rapidly dispersing ash clouds present an aviation threat that widens minute by minute during and after an eruption.**
- **First, at local scale—then rapidly becomes regional, and large eruptions can become continental to global in effect.**
- ****Physical characteristics of the eruption clouds are inferred from remote sensing data with few validation measurements.**
- ****Ash concentration, trajectory, altitude, and lateral extent estimates are highly dependent on**
    - **Dispersion models**
    - **Radiative transfer models**
    - **Remote sensing data reduction models**

An Inventory of handicaps-1

"…there are **no standard data products** specifically designed for volcanic ash and volcanic gases…" (Prata et al., IEEE, 2009)

"…There are also no internationally agreed satellite-based volcanic product standards and no protocols or procedures in place to permit specification of safe limits for aviation encountering airborne volcanic substances. Part of this problem lies with **the lack of sufficient information regarding what constitutes safe operating limits when flying near to volcanic clouds. Part of the solution lies in being able to provide quantitative satellite information and some means for validation."** (Prata et al., IEEE, 2009)

"…Currently, there is **no objective means for determining the injection height** of a volcanic eruption, and usually multiple dispersion simulations must be run and matched "by eye" to current or prior satellite imagery." (Prata et al., IEEE, 2009)

An Inventory of handicaps-2

"…Sensitivity analyses by Wen and Rose [1994] suggest **mass loading errors of 40–50%.**" (Prata and Kerkmann, GRL, 2007)

"…We emphasize here that **neither of these SEVIRI retrieval schemes have been properly validated against independent measurements.** Based on an error budget for the TOVS/HIRS SO_2 retrieval scheme [Prata et al., 2003], a conservative error for SEVIRI is ±10 D.U. on a single pixel basis. This gives a mass loading retrieval error of approximately ±0.01 Tg(S), for the SO_2 clouds discussed here. (Prata and Kerkmann, GRL, 2007)

Questions :

- **How crucial are the validations of models and data reduction techniques? Is just knowing the ash is there "enough" to manage safety concerns?**

- **What are the consequences of establishing better confidence on knowledge of ash concentrations? Will this propagate to smaller safety margins as air carriers make more finely tuned risk-benefit analyses? "Don't ask, don't tell?"**

- *****How strongly are we willing to advocate for possibly heroic or expensive efforts to collect high altitude in situ validation data?**

==========

- **Ad hoc Airborne In Situ Sampling Working Group was to start in 2011 at Melbourne IAVCEI Congress—now planned for 2012 in Costa Rica**

Eruption column processes

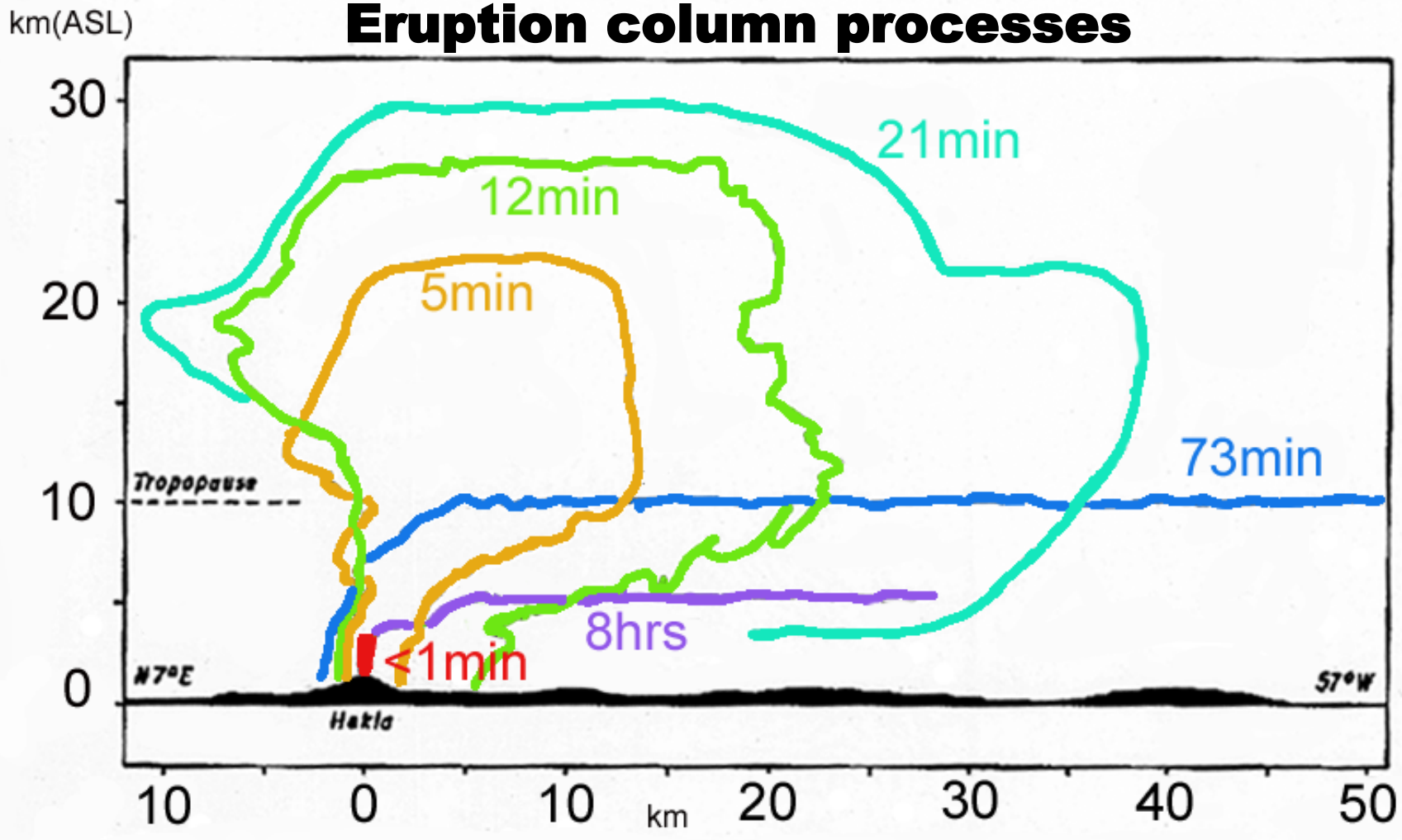

Growth of the 1947 Hekla Plume

(after Thorarinsson, 1954)

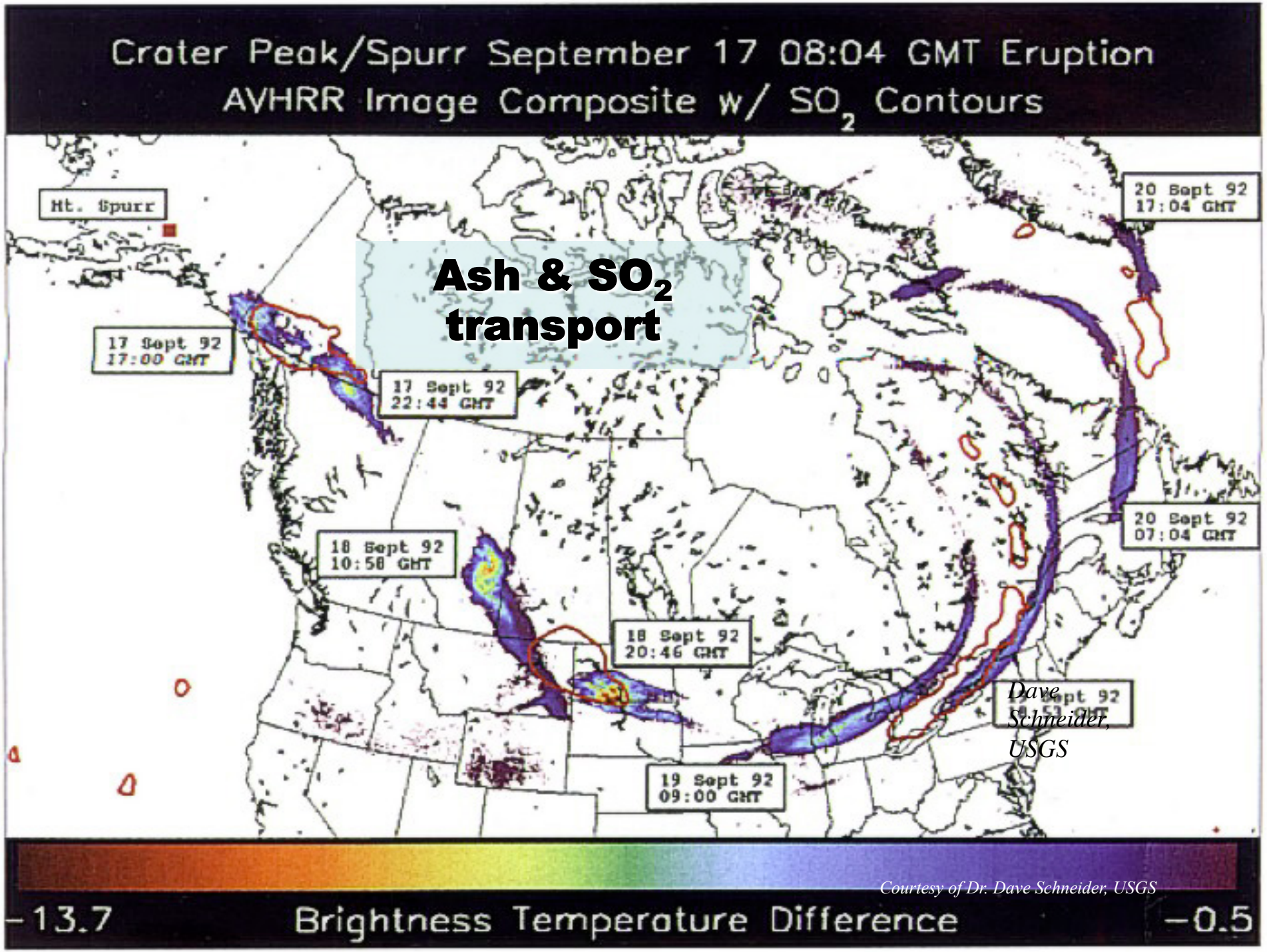

Courtesy of Dr. Dave Schneider, USGS

Ash effects on aircraft

The effect of volcanic ash on aircraft--Exterior

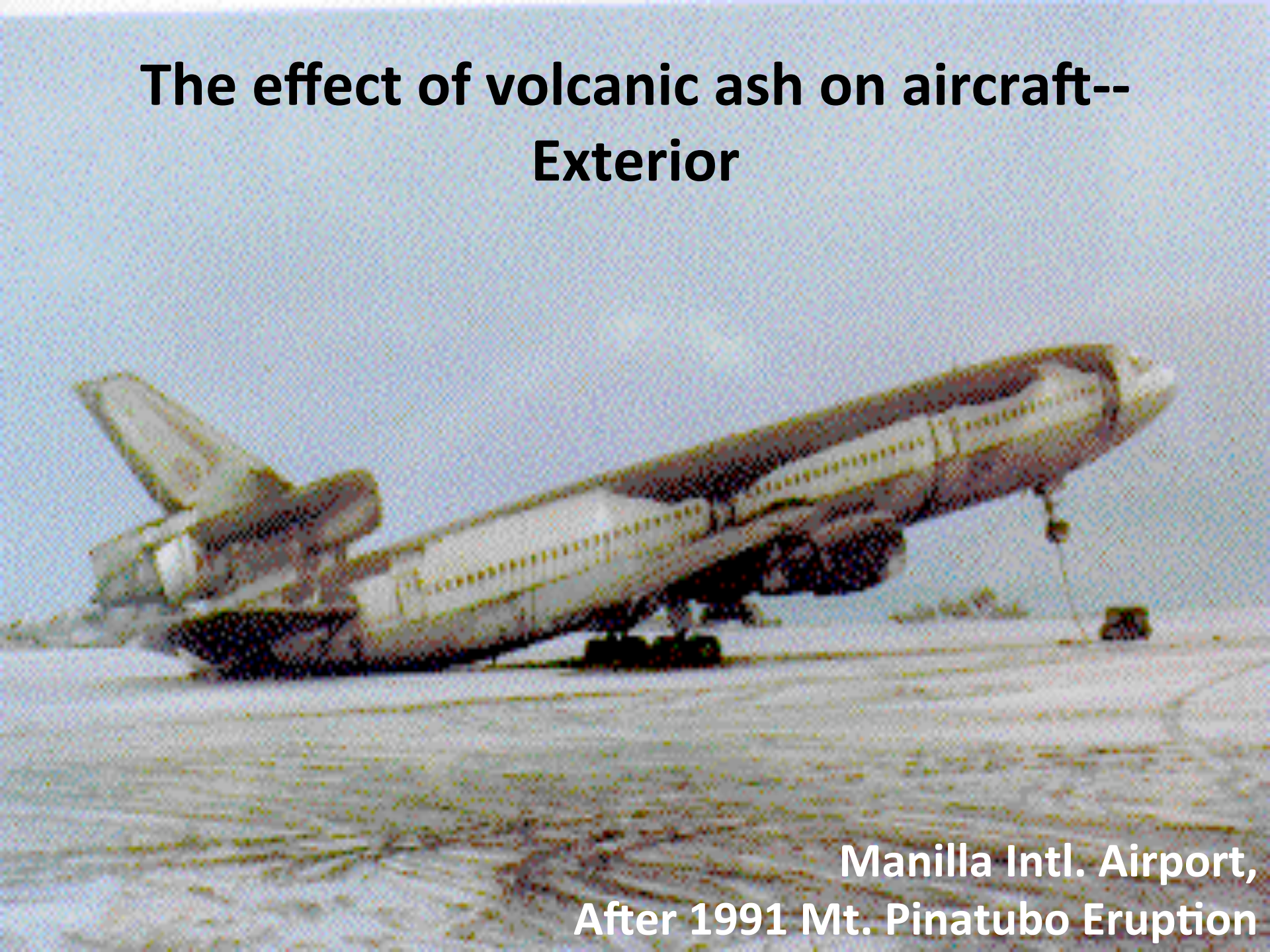

Manilla Intl. Airport,
After 1991 Mt. Pinatubo Eruption

PILOT KLM B-747 – "KLM 867 HEAVY IS REACHING {FLIGHT} LEVEL 250 HEADING 140"

ANCHORAGE CENTER - "OKAY, DO YOU HAVE GOOD SIGHT ON THE ASH PLUME AT THIS TIME?"

PILOT KLM B-747 – "YEA, IT'S JUST CLOUDY IT COULD BE ASHES. IT'S JUST A LITTLE BROWNER THAN THE NORMAL CLOUD."

PILOT KLM B-747 – "WE HAVE TO GO LEFT NOW... IT'S SMOKY IN THE COCKPIT AT THE MOMENT SIR."

ANCHORAGE CENTER – "KLM 867 HEAVY, ROGER, LEFT AT YOUR DISCRETION."

PILOT KLM B-747 – "CLIMBING TO {FLIGHT} LEVEL 390, WE'RE IN A BLACK CLOUD, HEADING 130."

PILOT KLM B-747 – "KLM 867 WE HAVE FLAME OUT ALL ENGINES AND WE ARE DESCENDING NOW!"

ANCHORAGE CENTER – "KLM 867 HEAVY ANCHORAGE?"

PILOT KLM B747 – "KLM 867 HEAVY WE ARE DESCENDING NOW … WE ARE IN A FALL!"

PILOT KLM B-747 – "KLM 867 WE NEED ALL THE ASSISTANCE YOU HAVE SIR. GIVE US RADAR VECTORS PLEASE!"

NASA DC-8 Research Aircraft Engine Parts after disassembly upon return from the SOLVE experiment (Courtesy NASA Dryden FRC)

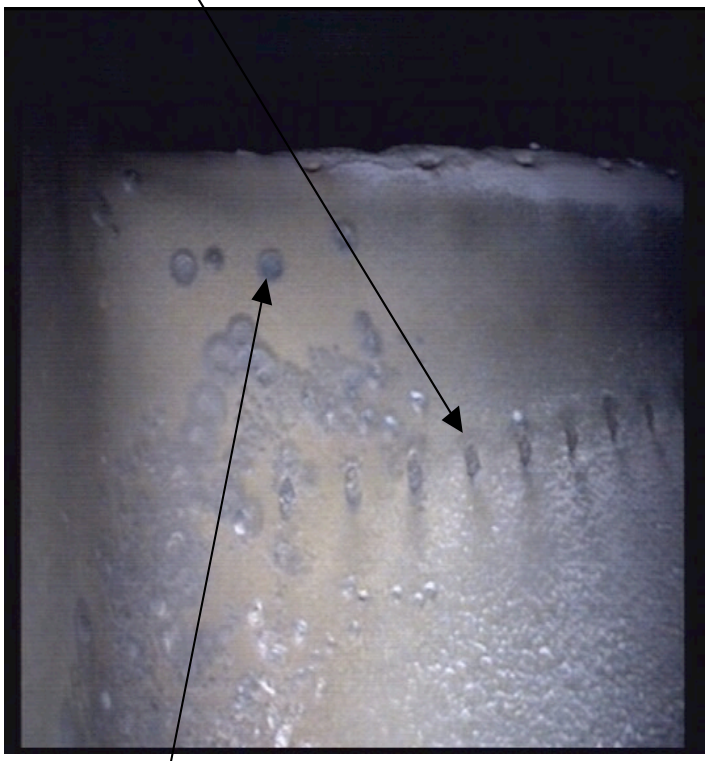

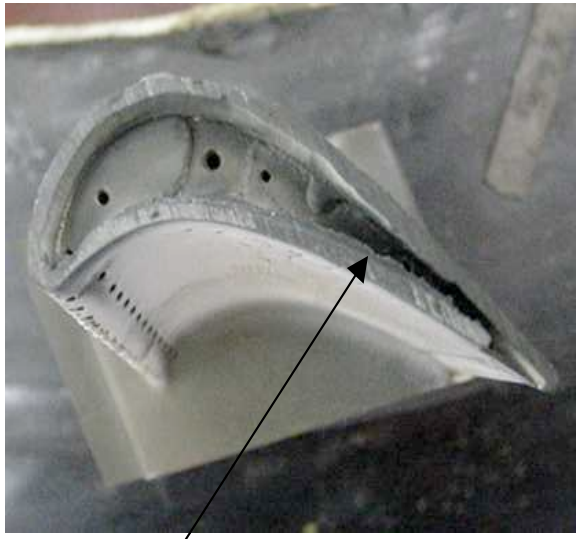

2. VIEW OF GRID THROUGH HAZE

The effect of volcanic ash on aircraft – Windscreens

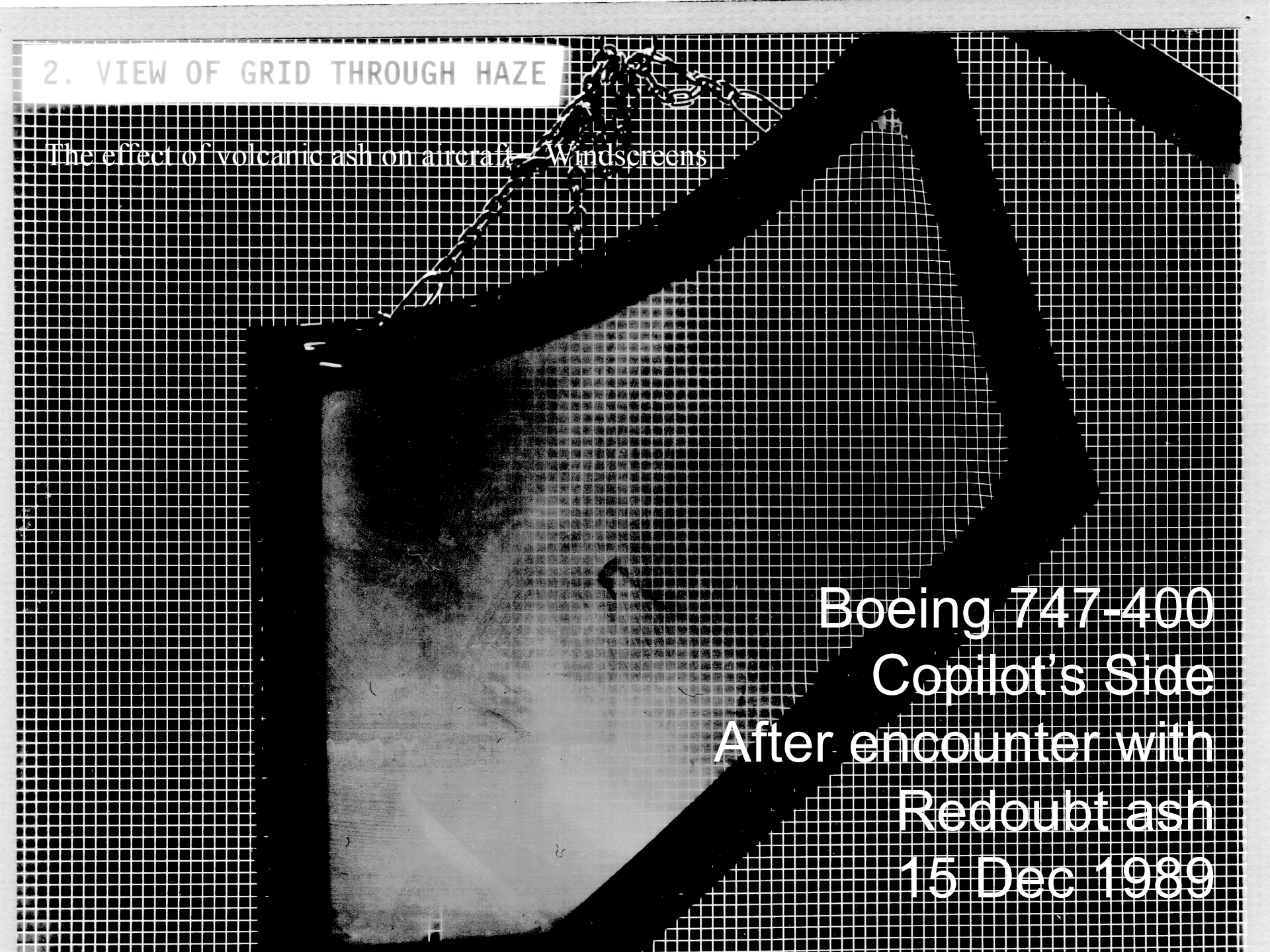

Boeing 747-400
Copilot's Side
After encounter with
Redoubt ash
15 Dec 1989

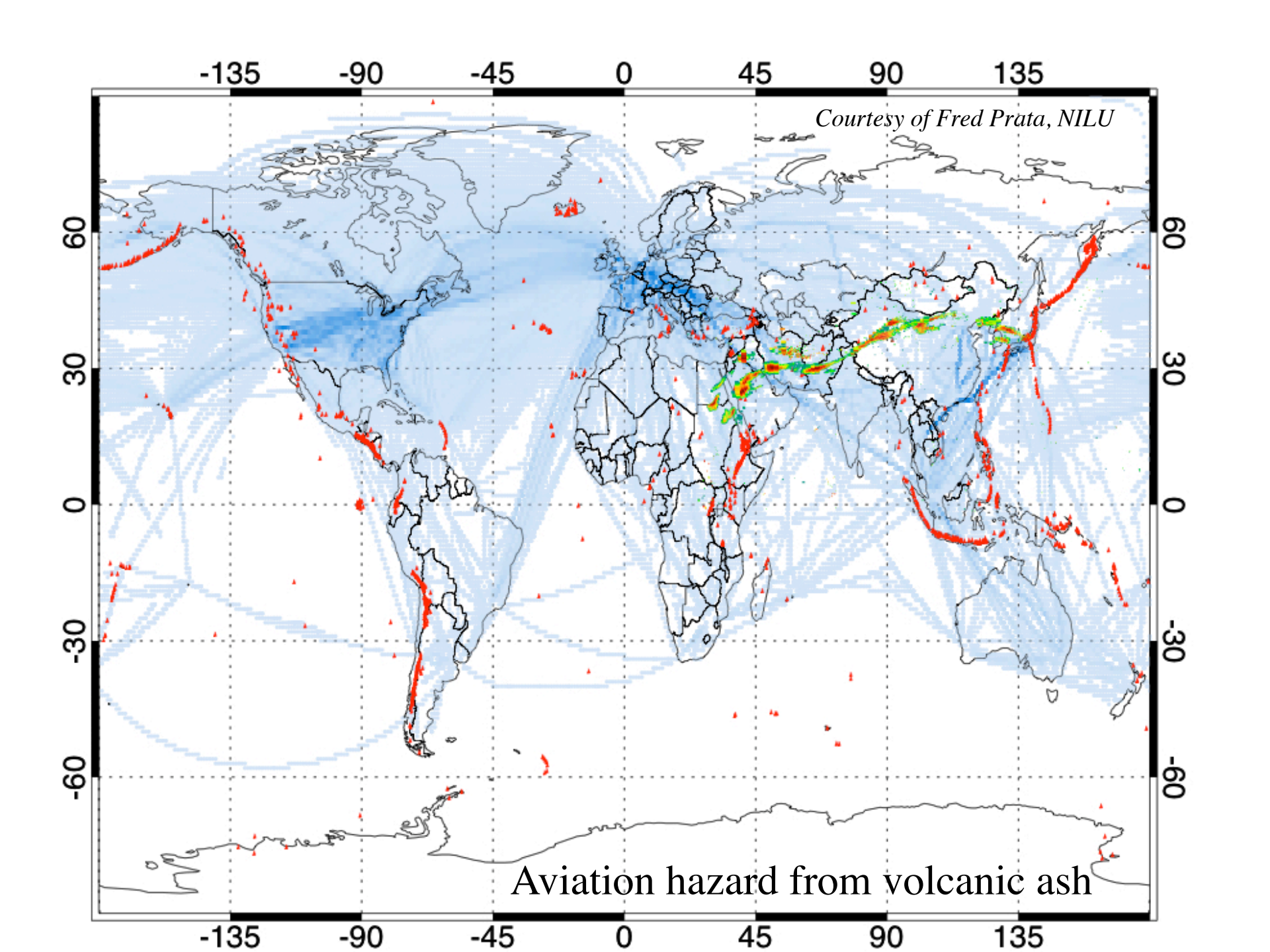
-135
-90
-45
0
45
90
135
60
30
0
-30
-60
Courtesy of Fred Prata, NILU
Aviation hazard from volcanic ash

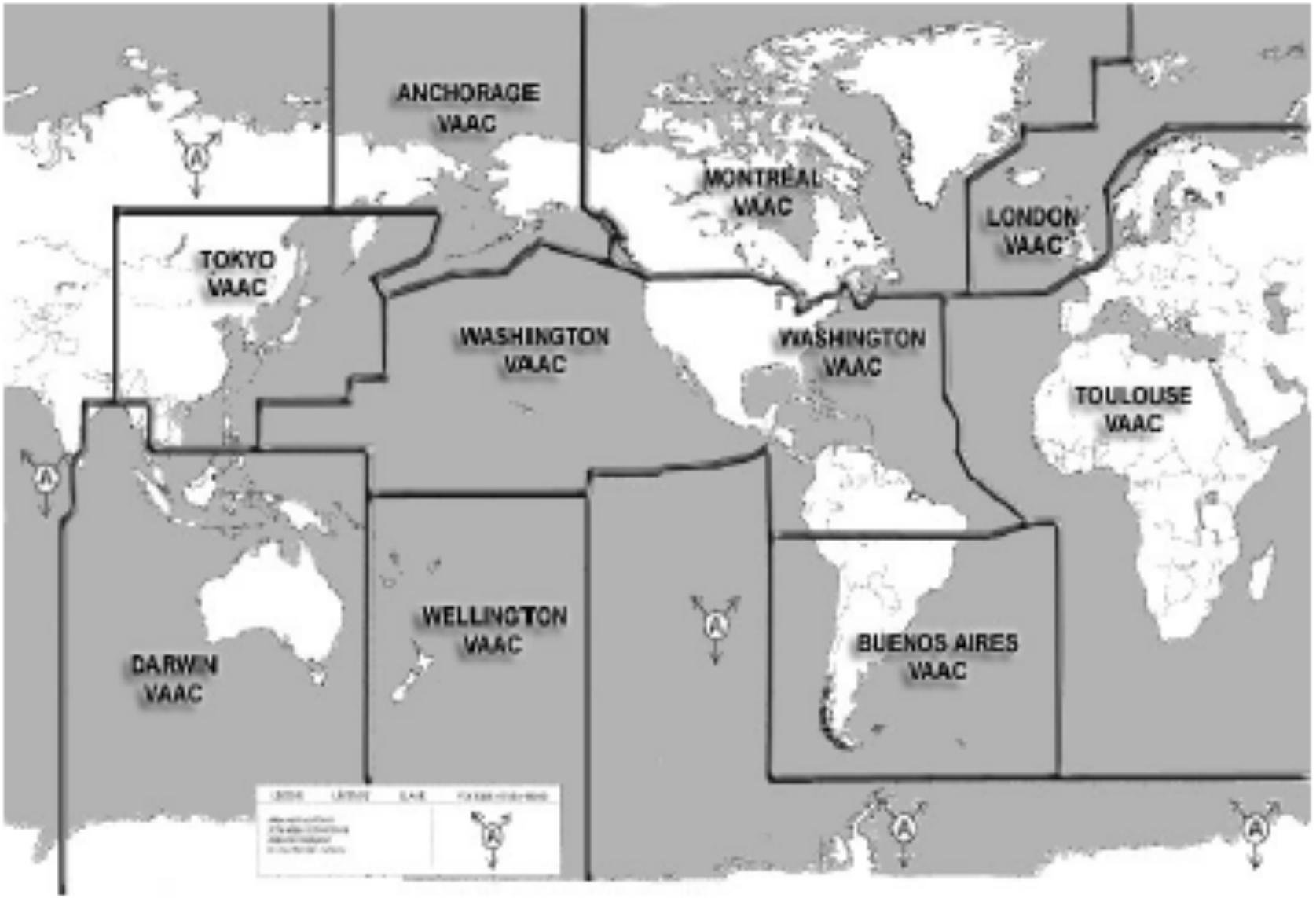

Chris Newhall, USGS

Properties of Volcanic Clouds

What do we know about ash particles?

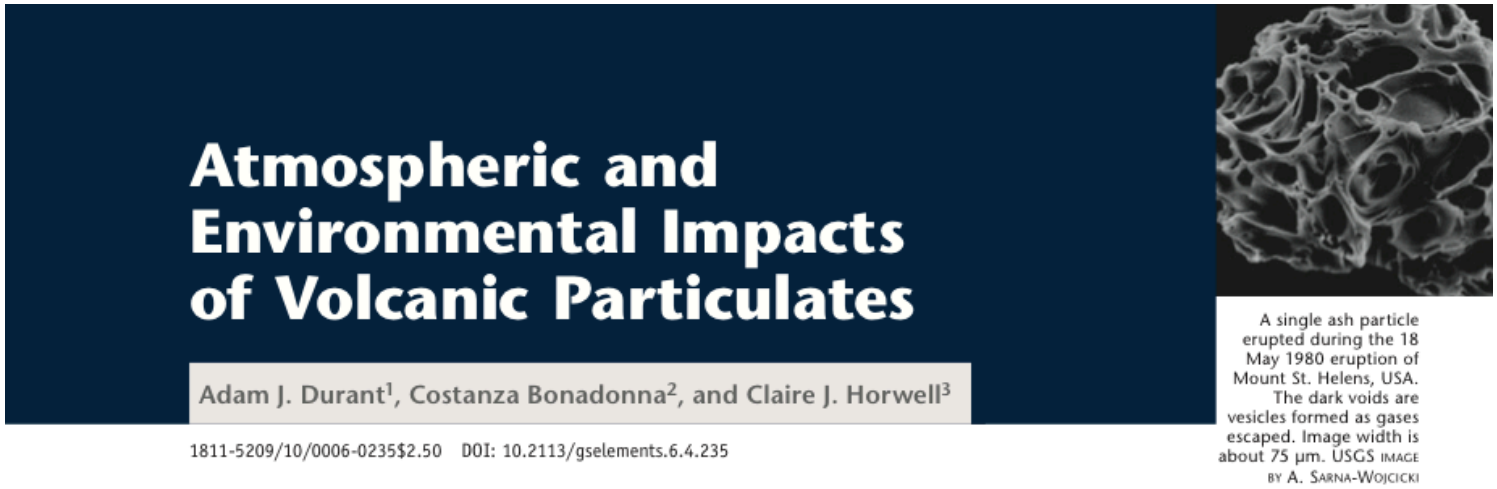

High silicate content

Particle size (radius) ranges from 0.01–500 μm (typically)

Irregular shape

Melting point ~1100 ºC (800–1200 ºC).

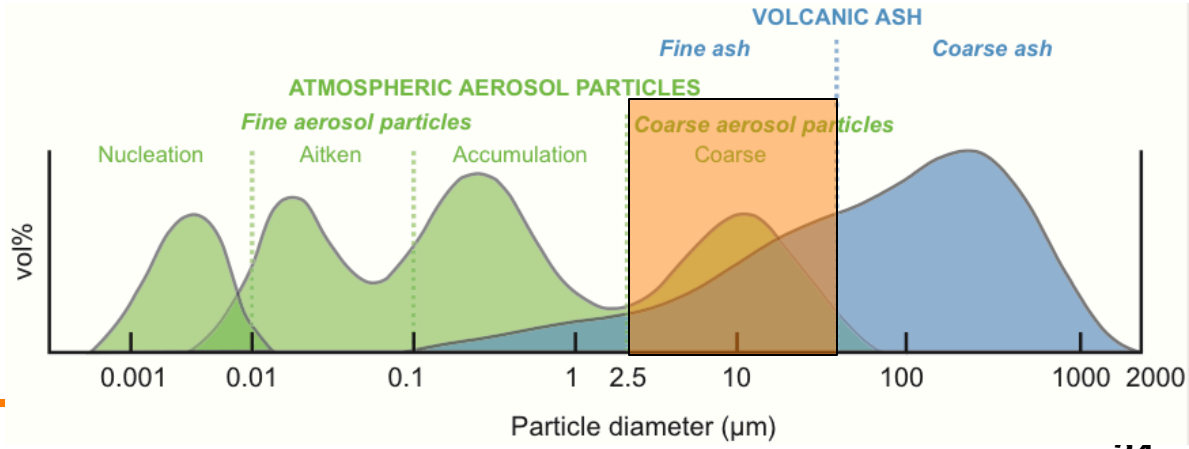

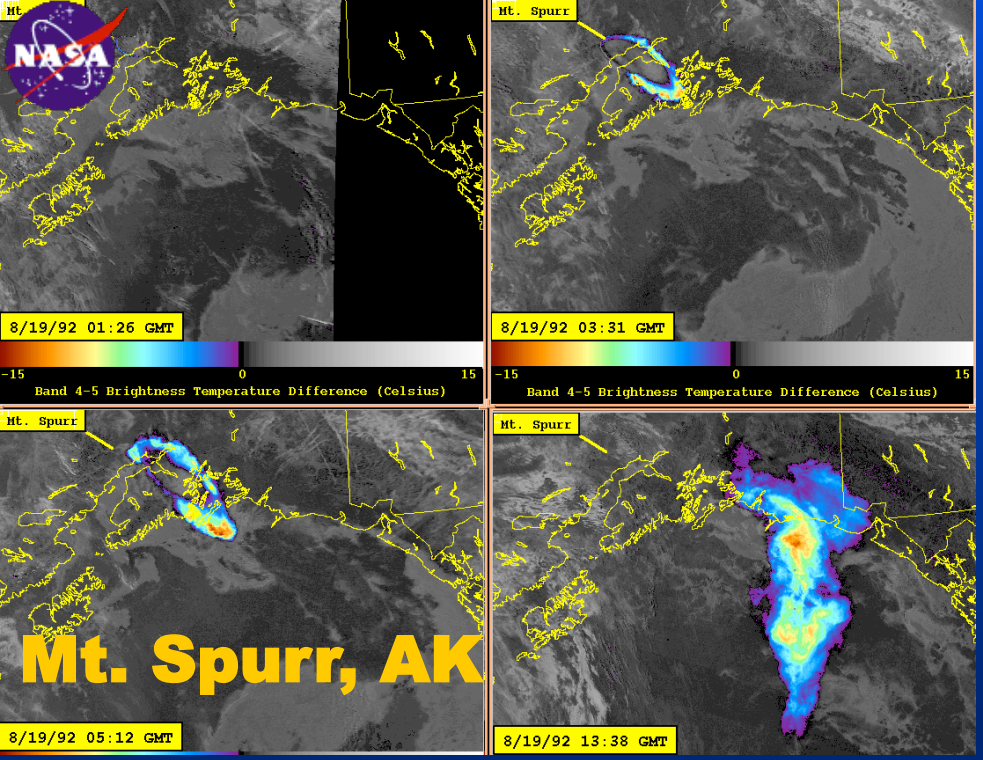

Seeing Ash with TIR Split Window

- Comparison of Mt. Spurr '92 (polar dry) plume detection with La Soufriere (Montserrat) '96 (tropical wet) –
- Band 4 (10μm) minus 5 (12 μm) "subtraction technique" or "split window technique."

·Split Window technique only works after plume has become translucent to upwelling TIR radiation.

·Water vapor is confounding.

·Use of shorter TIR bands (e.g., 7-9 μm) could improve things.

·***HyspIRI may improve this***

Montserrat, West Indies

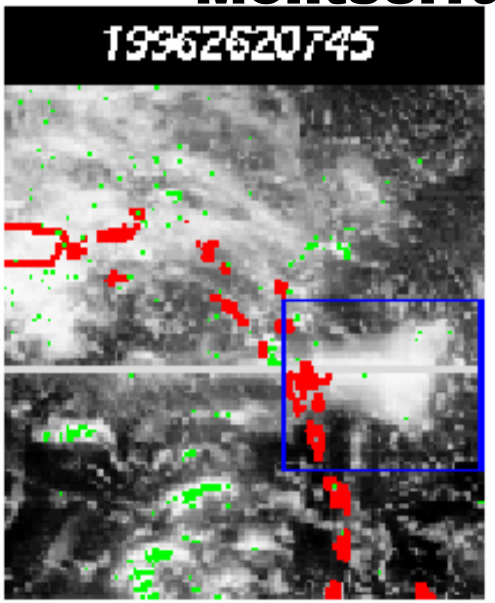

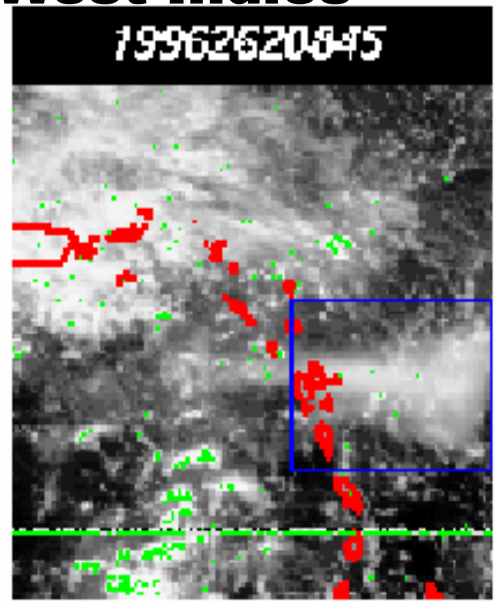

ΔT_{4-5}

Positive

Negative

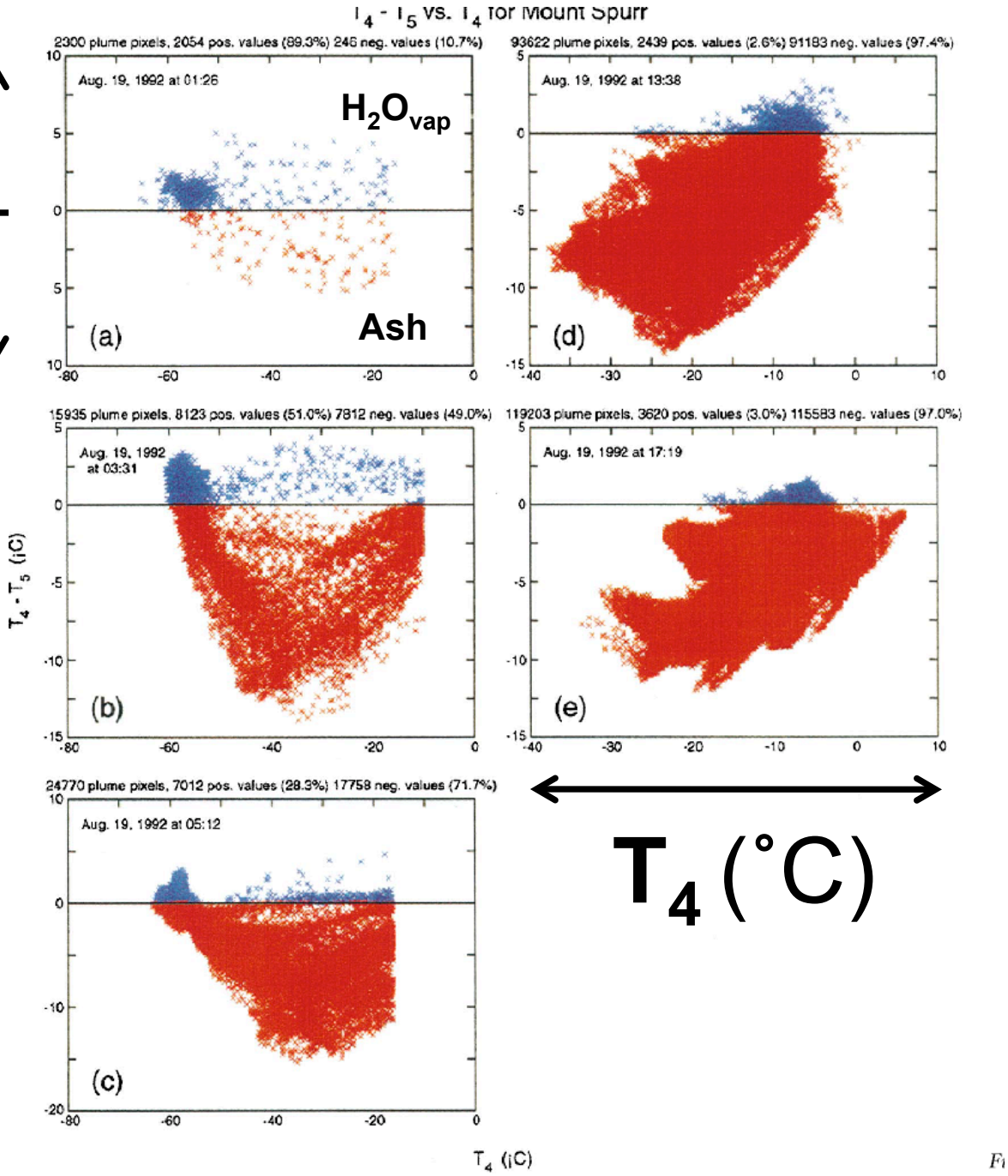

T_4 (˚C)

Statistics for Mt. Spurr Ash Plume

(from Simpson *et al.*, 2000)

Statistics for Monserrat Ash Plume

(from Simpson *et al.*, 2000)

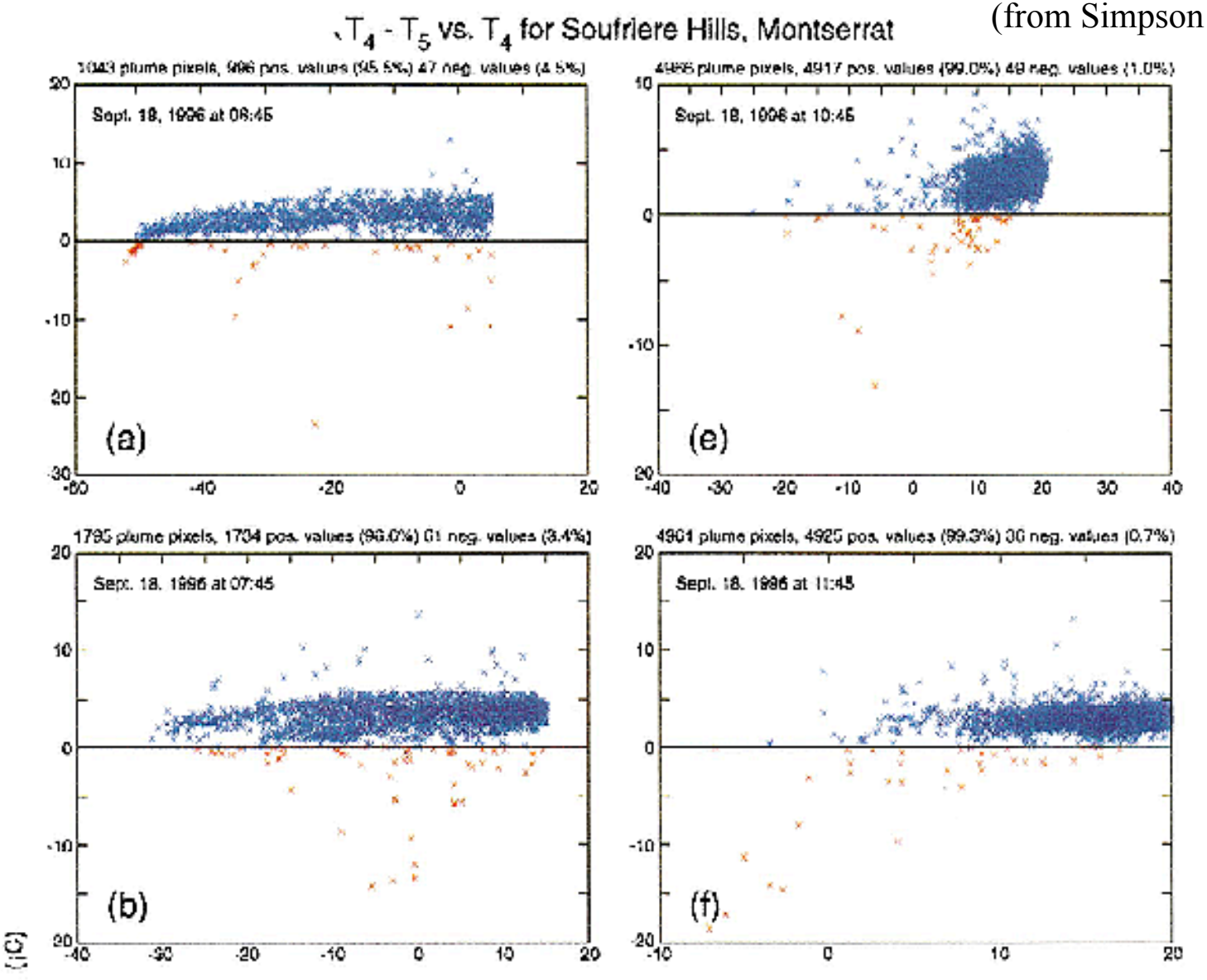

SO_2 Detection and Tracking
Passive emission precursors:
HysplRI Targets

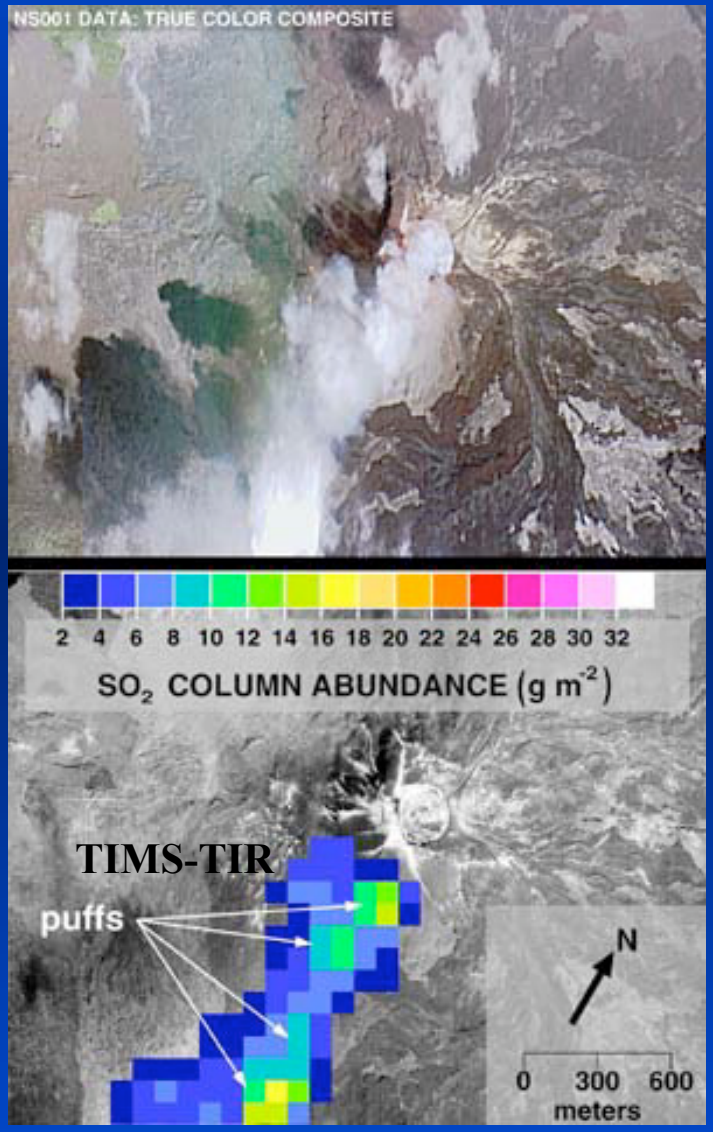

Airborne Detection from NASA C130 in over PuuOo Vent, Kilauea (left)

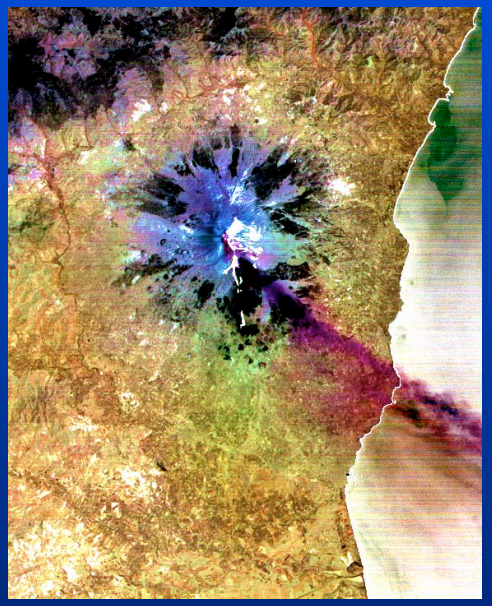

Orbital Detection of Tropospheric SO_2
ASTER over Hawaii (below) and Mt. Etna, Italy (above)

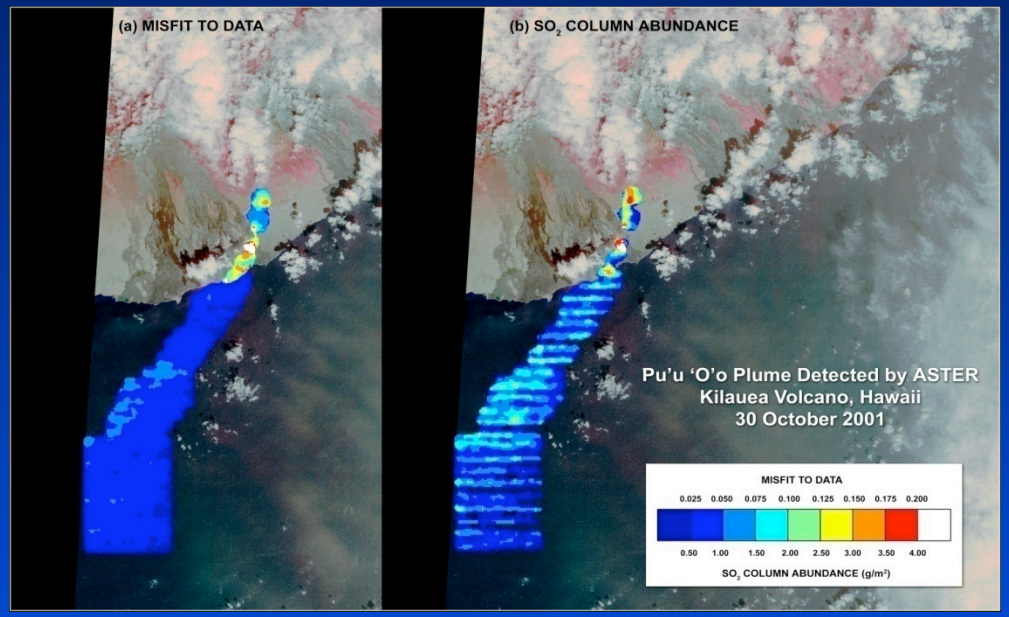

Courtesy Vince Realmuto, JPL

Case Study—NASA DC-8 Ash Encounter The Hekla February 2000 Eruption

- An ash encounter with a very dilute ash plume-- fine grained (<1-10μm diameter solid aerosols), ice-coated ash particles.
- A minimum “economic damage” encounter.
- Significant because of “silent damage”

Jet Propulsion Laboratory
California Institute of Technology

Onboard solid aerosol collection data from the NASA DC-8 Research Aircraft engaged in the Kiruna SOLVE experiment (Courtesy NASA Langley RC)

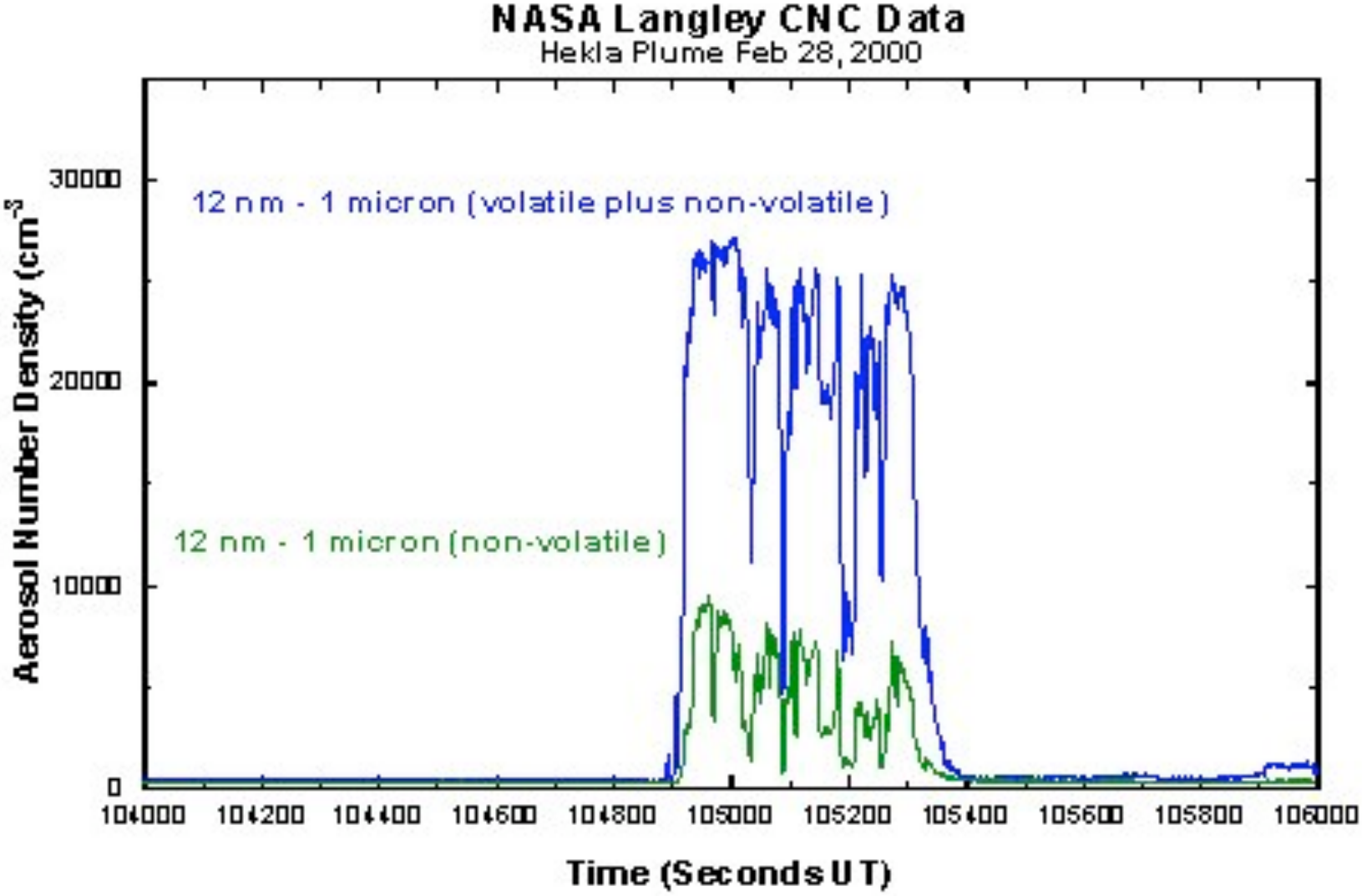

Jet Propulsion Laboratory
California Institute of Technology

Caltech Scanning Electron Microscope imaging of the Keddeg Air Conditioning Filters from NASA DC-8 Research Aircraft (from Pieri et al., 2002; GRL)

JPL

Unused | **Normal use** | **After ash encounter**

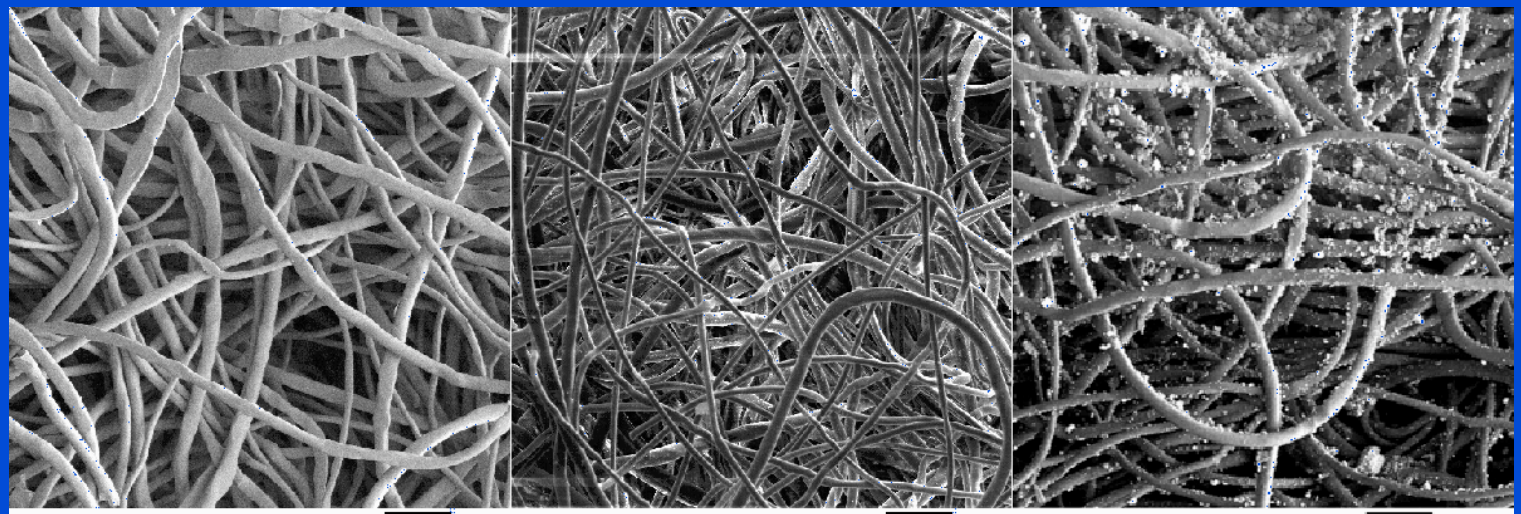

Figure 1a. 100µm 150X

Figure 1b. 100µm 150X

Figure 1c. 100µm 150X

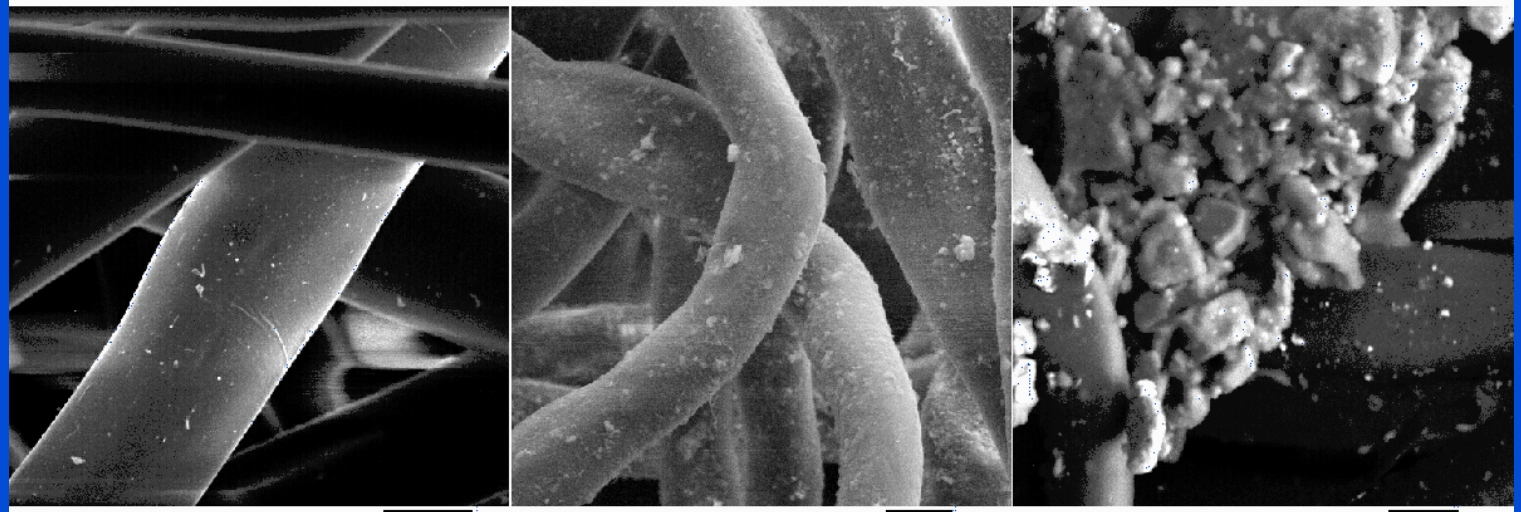

Figure 1d. 10µm 2000X

Figure 1e. 10µm 1500X

Figure 1f. 10µm 1500X

Recirculation Filter

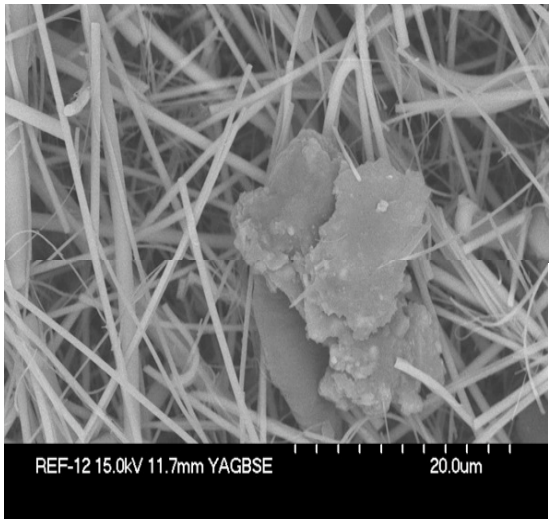

SEM & EDX results from easyJet filters, Eyjafyallajokull 2010

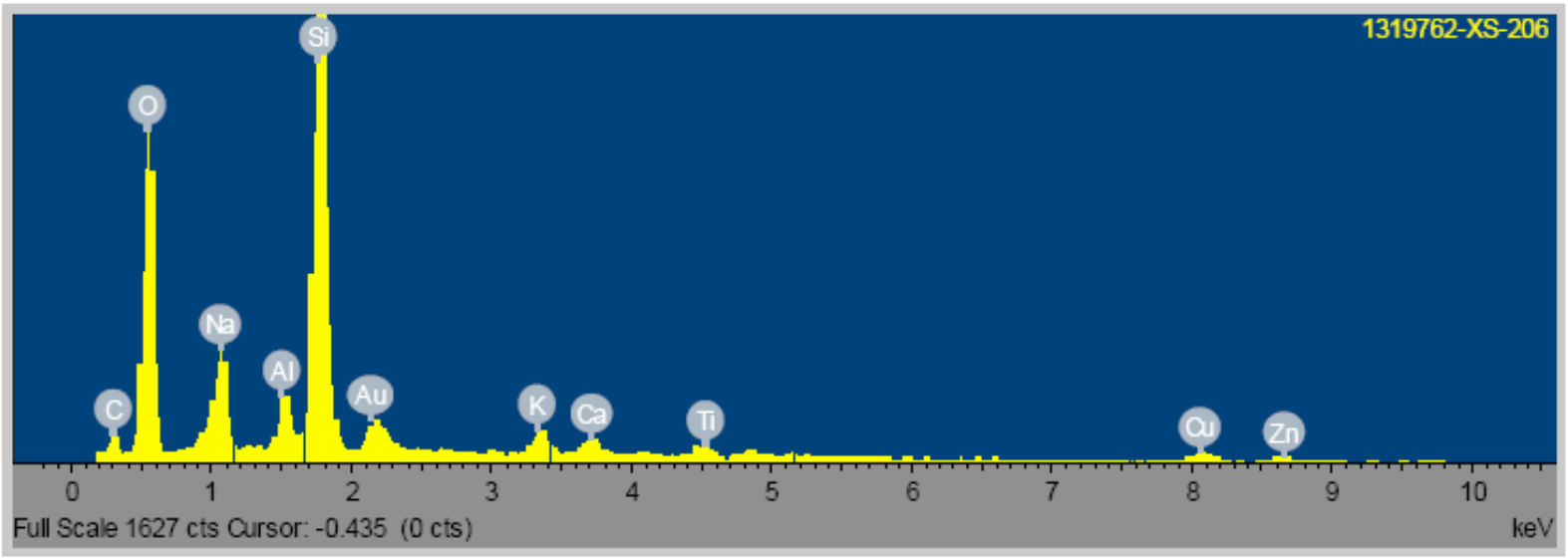

easyJet plc

Courtesy: Ian Davies

NILU

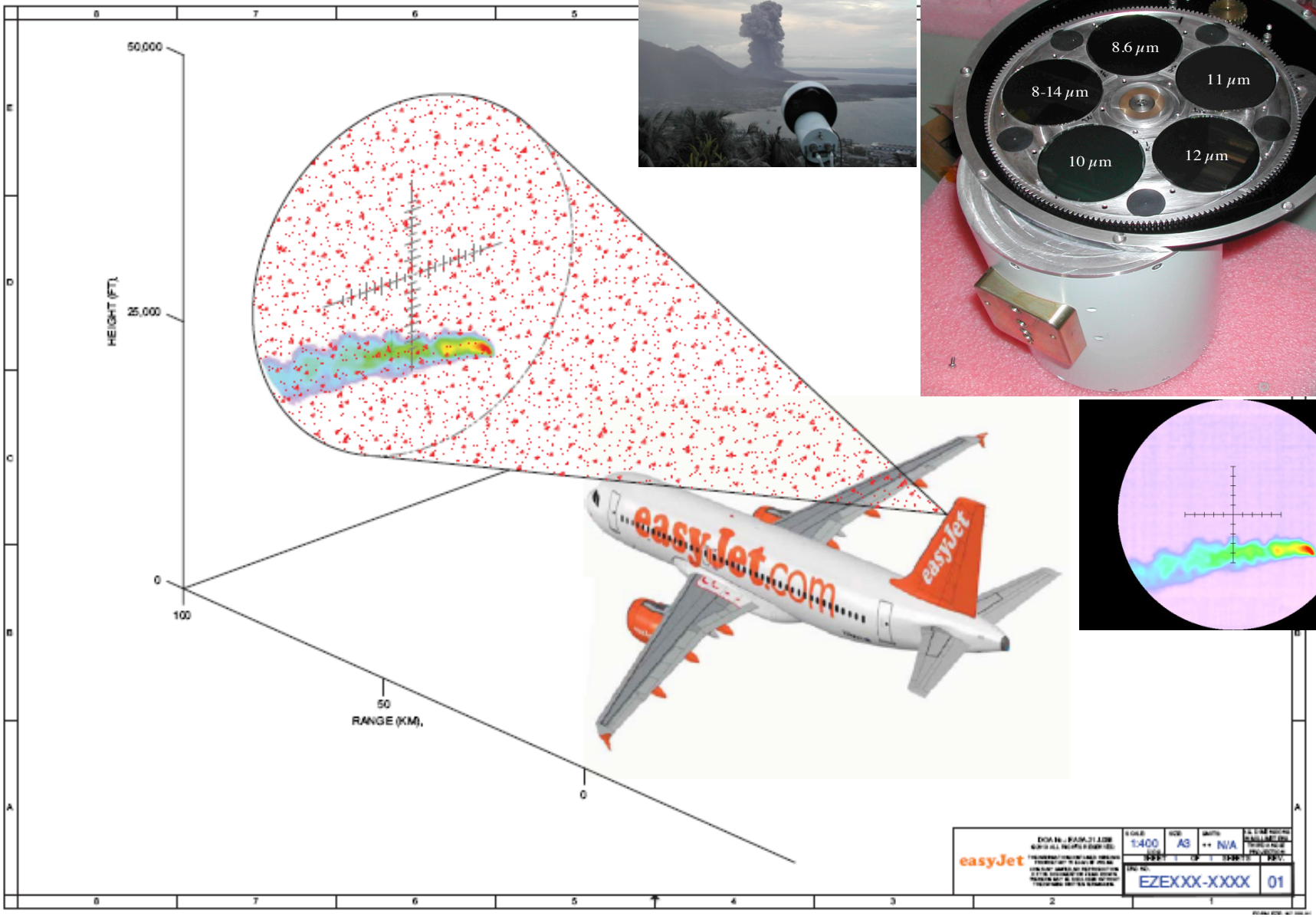

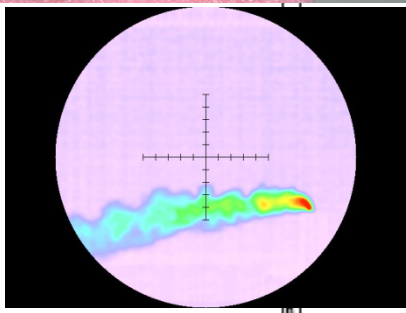

easyJet plc

NILU

Small UAV approach to sampling volcanic plumes:

1. Relatively cheap and less complicated
2. Quick response to dynamic events
3. Risk-appropriate tools for hazardous missions
4. Humble start (troposphere), aiming to evolve to larger (tropopause & stratosphere)

UAVs over volcanoes in Costa Rica

Project Scope : In-Situ + remote sensing integration of active volcanic plumes data for CAL/VAL of satellite remote sensing information

Approach:

- Simultaneous fixed-wing, blimp, and tethered aerostats UAS airborne observations, integrated with in-situ instrumentation with simultaneous orbital and ground-based remote sensing
- Operate in airspace too dangerous for manned aircraft—over and around actively erupting volcanoes.

Measurements:

- *In situ ash, SO2, H2S, CO2, He, and other gas concentration;*
- *Temperature + pressure + humidity;*
- *GPS location and altitude;*
- *Particle count by size*
- *Solid aerosol (ash) sampling for post-flight SEM analysis*

Instruments:

- *Electro-chem MEMS based SO2, CO2, H2S sensors; radiometers; particle drum-impactors, laser diode/optical particle counters, size-frequency analyzer, samplers; mini-mass spectrometer*

Where: ▶ *Turrialba and Arenal Volcanoes*

CR ACTIVE VOLCANOES
Active and stable volcanic plume conditions visible from space
Easy access and logistics to sites
UAV friendly environment
Local scientific collaborators
National Airborne Research Hangar
Rincon de la Vieja Volcano
Miravalles Volcano
Tenorio Volcano
Arenal Volcano
Poas Volcano
Irazu Volcano
Turrilaba Volcano
Why
Costa Rica
=► Natural Laboratory for Calibration and Validation of Satellite Remote Sensing Observations

In situ Compact Airborne Mass Spectrometer in Costa Rica--NASA WB-57 and Cessna 206 (CARTA I & II)

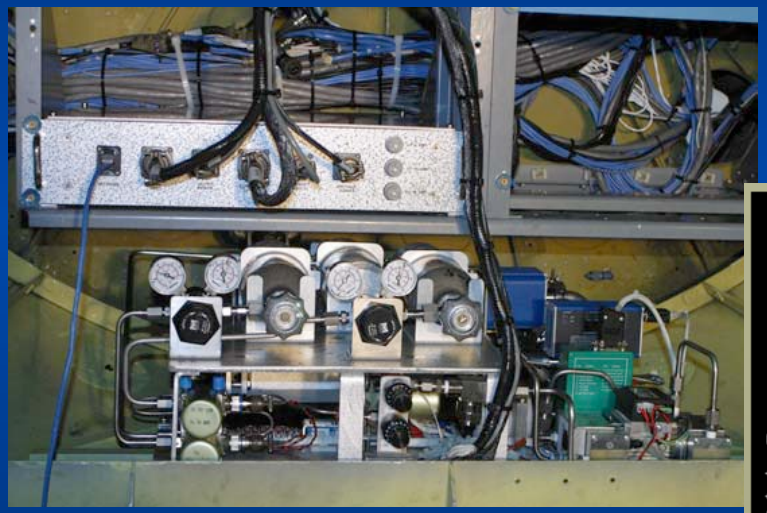

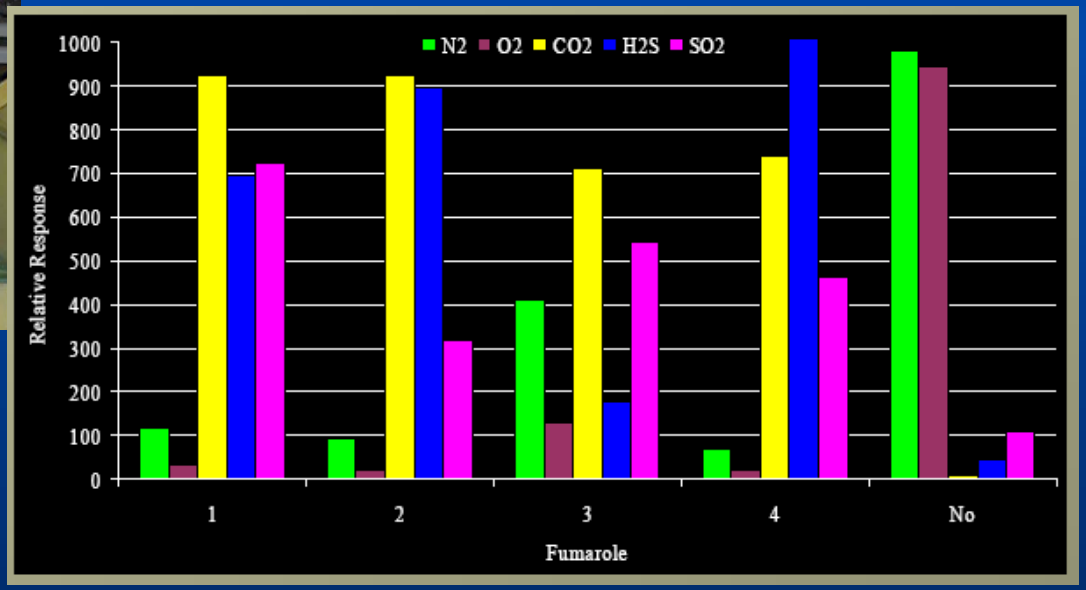

From Griffin et al., 2008 & Arkin, et al., 2009

Sampling at Turrialba fumarole in main crater

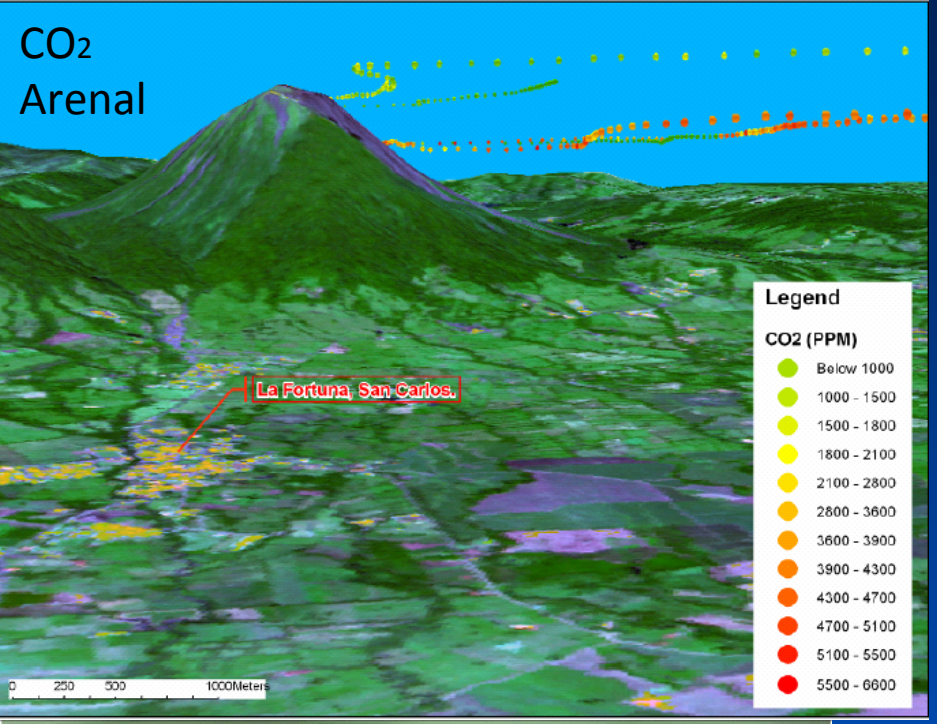

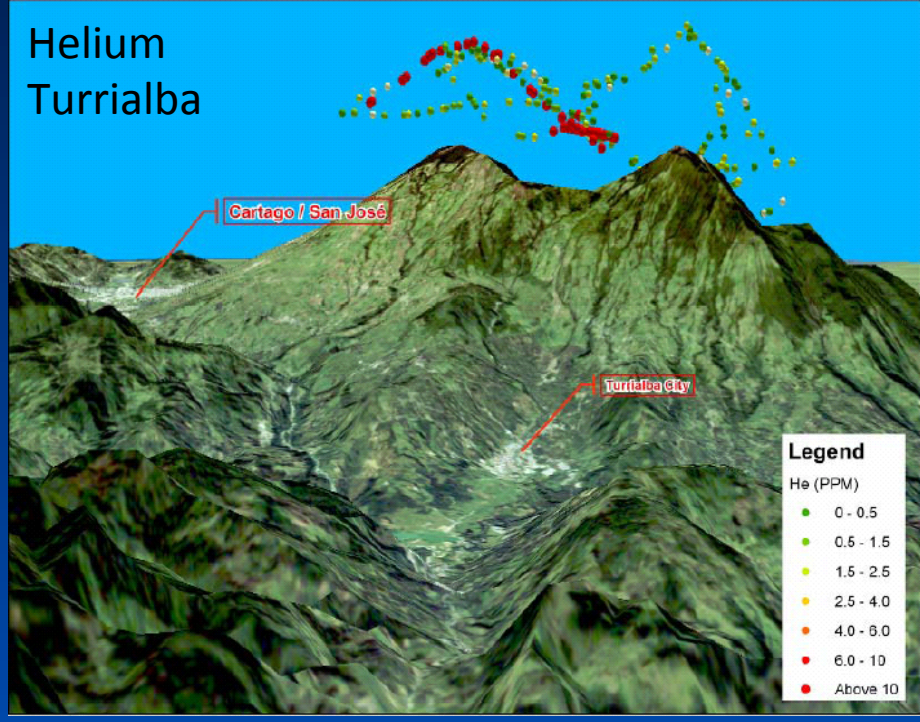

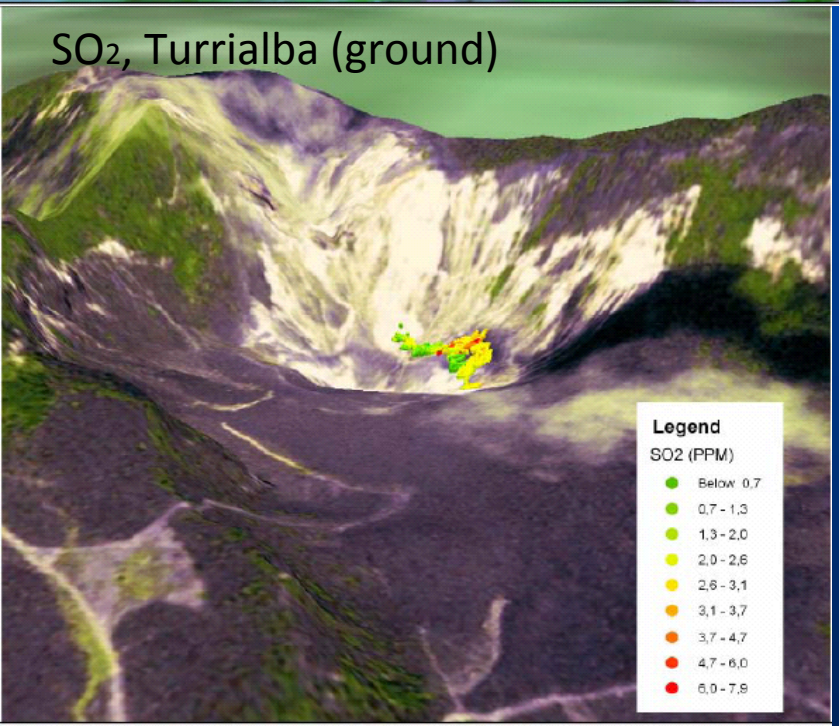

3-D Concentration Mapping with Portable Mass Spectrometer Systems in Costa Rica—airborne and ground

Courtesy of Andres Diaz, UCR

In Situ Gas Sampling
Turrialba Volcano—Costa Rica

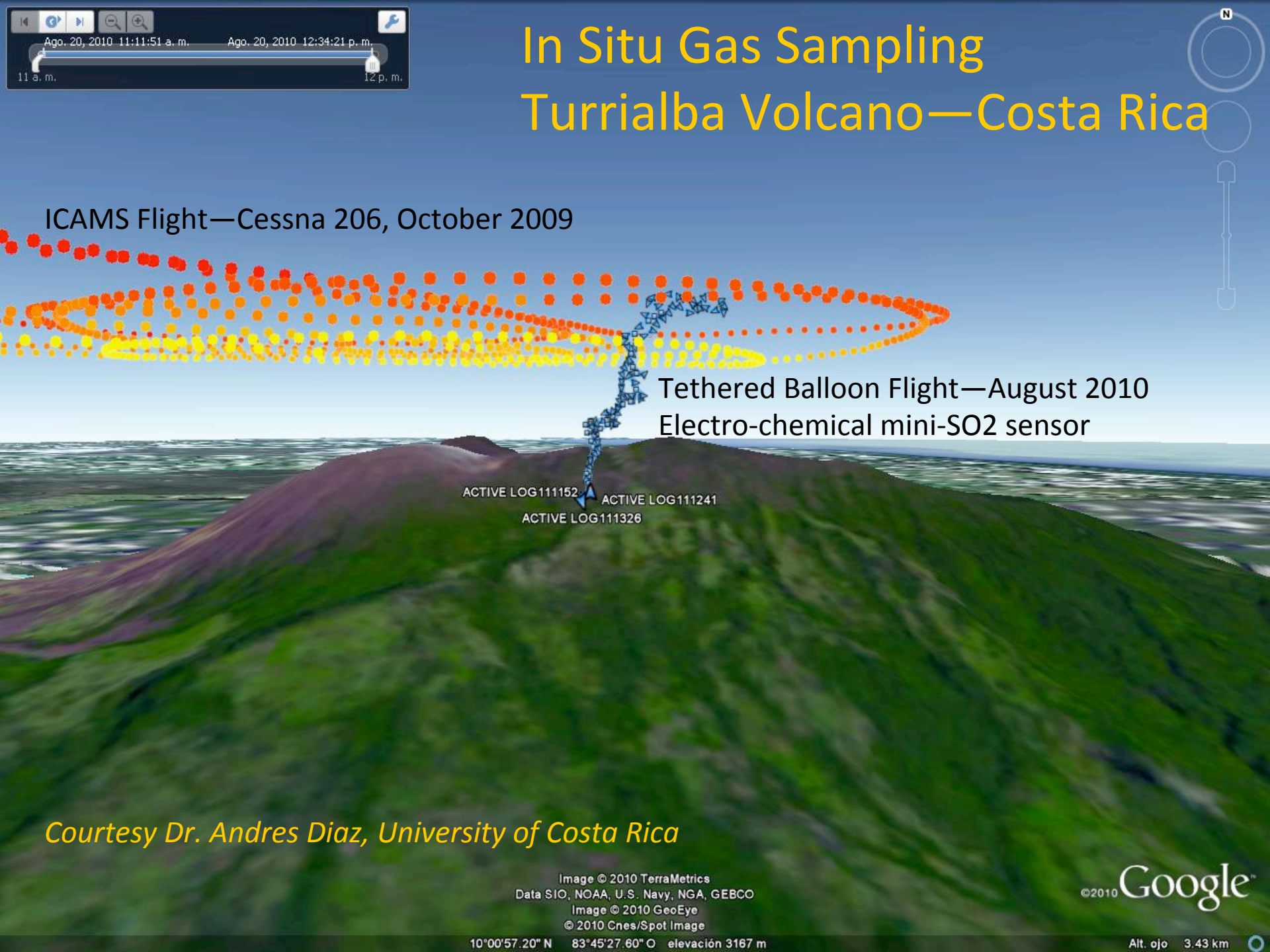

Courtesy Dr. Andres Diaz, University of Costa Rica

Turrialba Volcano, Costa Rica
Hard working UCR graduate student, January 2011

Satellite and Balloon-Based Measurements of Turrialba Volcano, Costa Rica—2010 & 2011

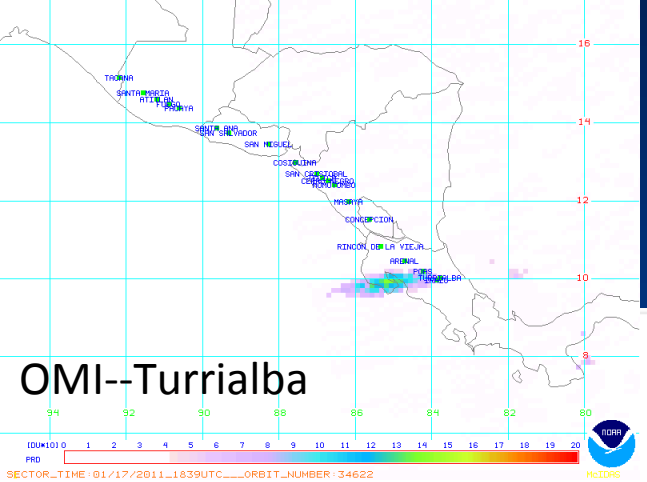

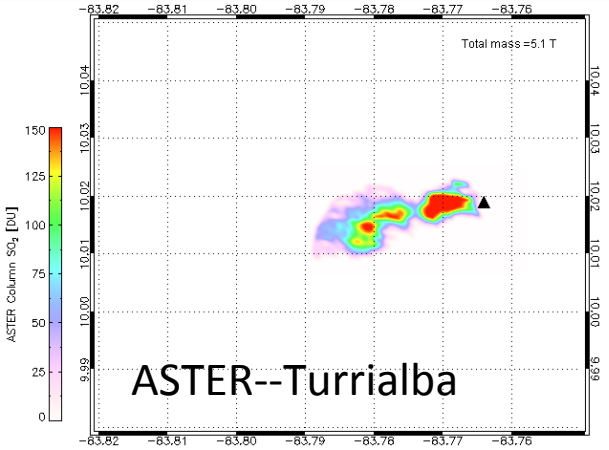

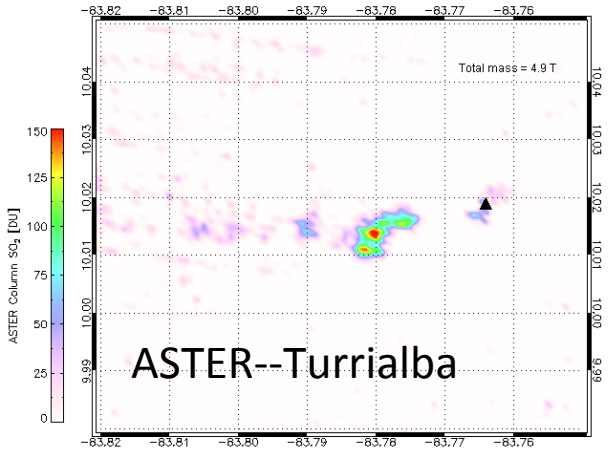

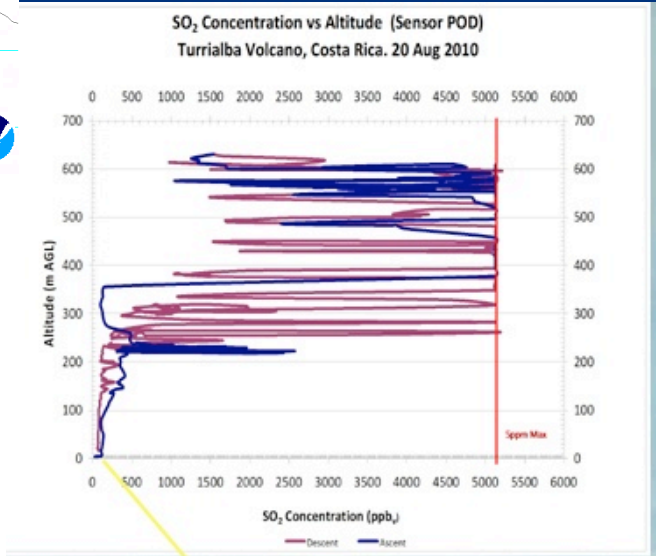

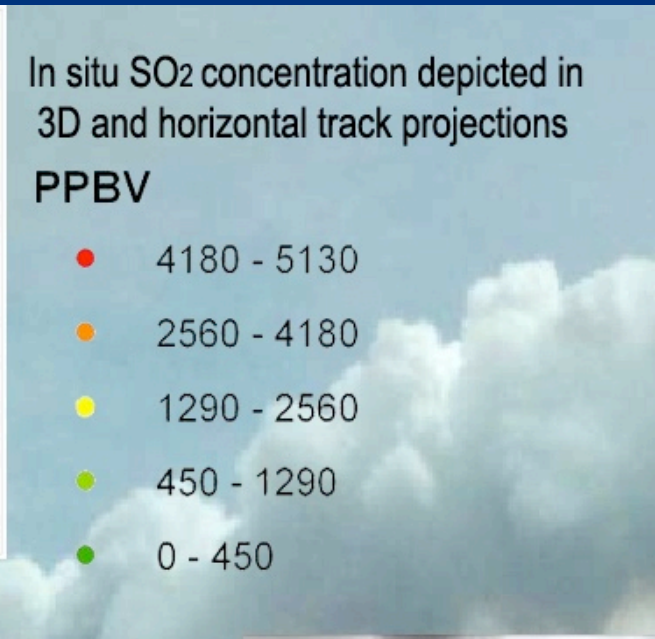

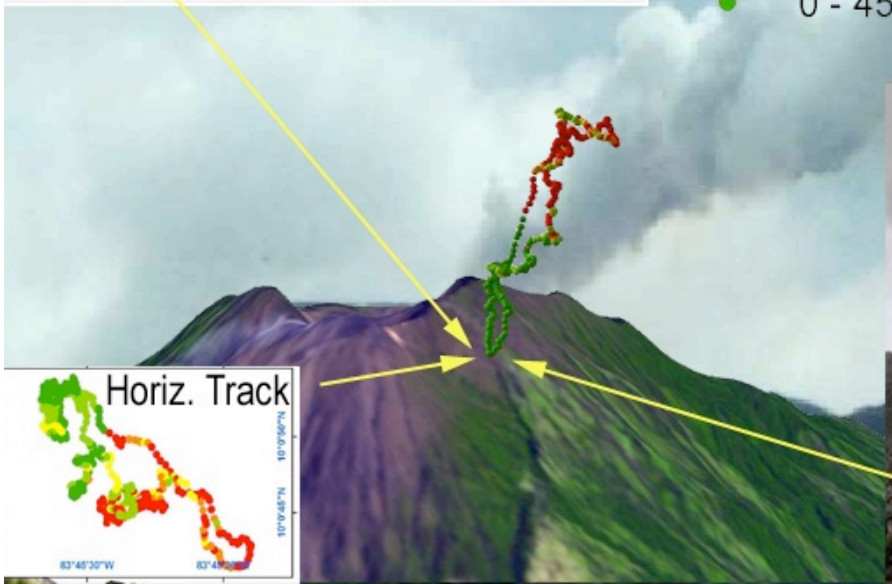

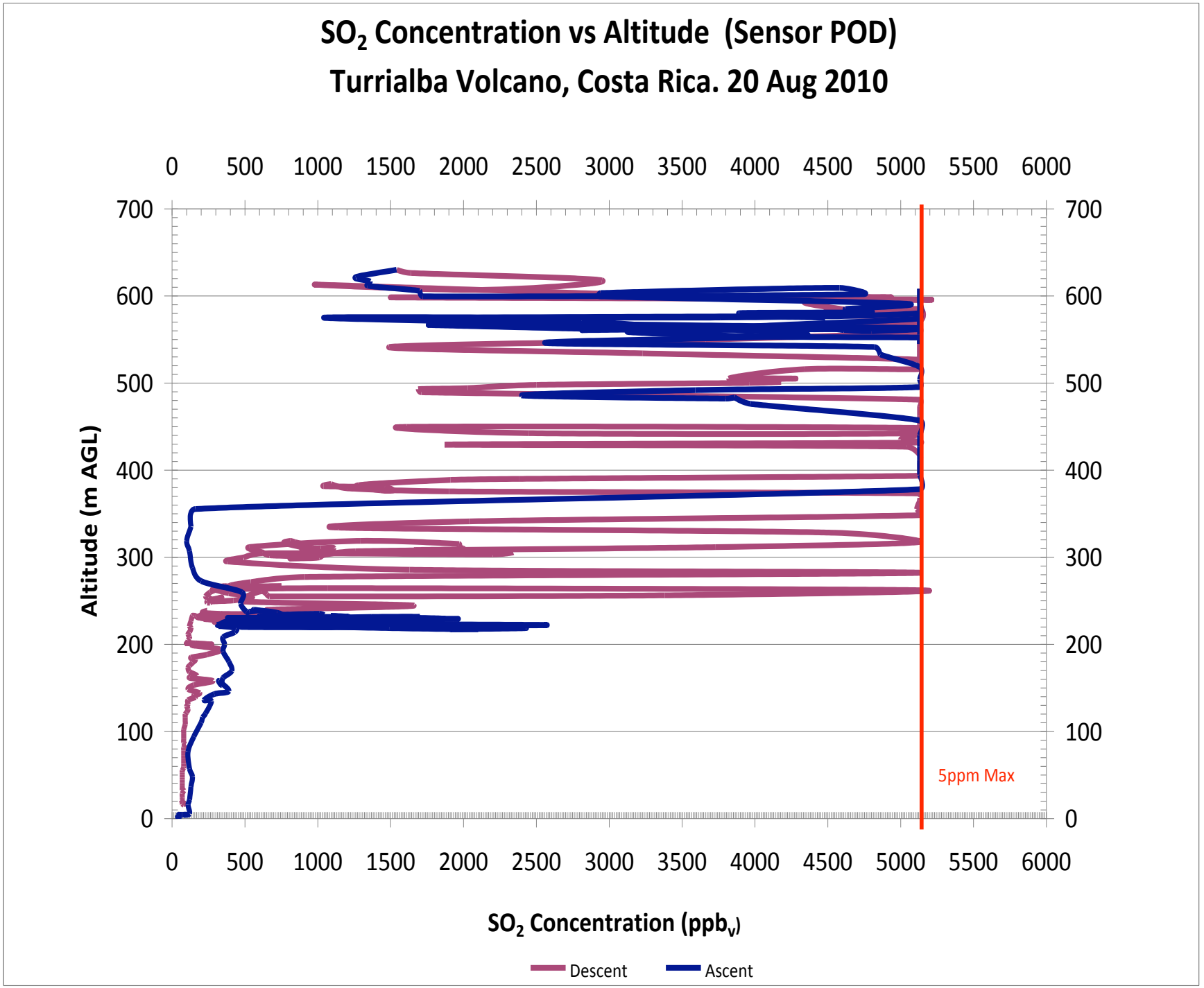
SO2 Concentration vs Altitude (Sensor POD)
Turrialba Volcano, Costa Rica. 20 Aug 2010
0
500
1000
1500
2000
2500
3000
3500
4000
4500
5000
5500
6000
700
600
500
400
300
200
100
0
Altitude (m AGL)
5ppm Max
SO2 Concentration (ppbv)
Descent
Ascent

Turrialba Volcano, Costa Rica
Intrepid International Field Team
January 2011

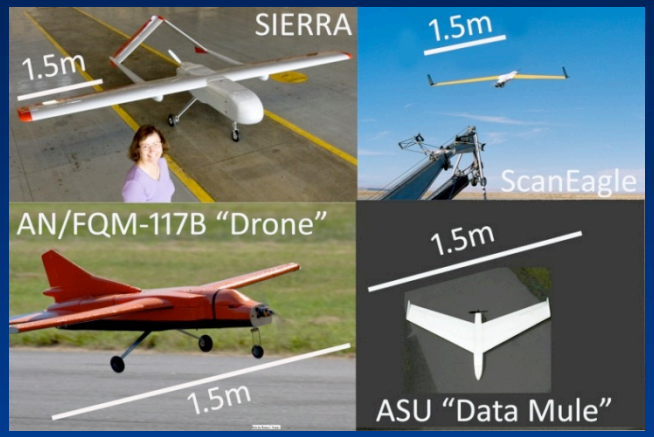

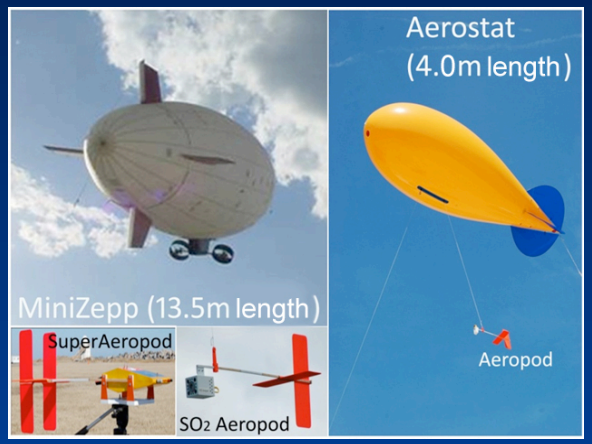

Allocation of instruments to CARTA 2012-2013 UAS platforms

UAS	Type (FW-Fixed Wing)	Load (kg)	Instruments	Radius & Endurance (km)&(hrs)	Each UAS has a Unique Mission
SIERRA	Gas, FW	45	ULISSES; Ames Particle Suite; T,P,%H_2O,SO_2,Aerosol size-freq., sampler; drum sampler.	100 & 8	Accurately define plume physical vs. photometric edges (e.g., in ASTER)
ScanEagle	Gas/Elec, FW Wing	6	Drum sampler, T,P,%H_2O,SO_2, Aerosol size-freq., sampler.	100 & 20+	Fast longitudinal, lateral and vertical profiles
AN/ FQM-117B	Elec, FW	1-2	T,P,%H_2O,SO_2, Aerosol size-freq., sampler.	10 & 2	Penetrate the eruption column—risky.
Data Mules	Elec FW	1	Digital stereo cameras (1 on ea.)	2 & 0.5	Plume topograhy
MiniZepp	Gas, Blimp	100	T,P,%H_2O,SO_2, Aerosol size-freq., sampler; real-time video	5 & 2	Slow Lagrangian temporal samples
Aerostats	Tethered Balloon	1	T,P,%H_2O,SO_2, Aerosol size-frequency, sampler.	2km vert & indef.	Static temporal sampling

Notional diagram of the CARTA deployment strategy at Arenal Volcano:
***Vent Zone: Data Mules circle above eruption column, while F117B flies through it;**
***Transitional Zone: ScanEagle profiles through it and Aerostats monitor within plume;**
***Distal Zone: MiniZepp drifts with an air parcel--SIERRA prowls plume edges.**

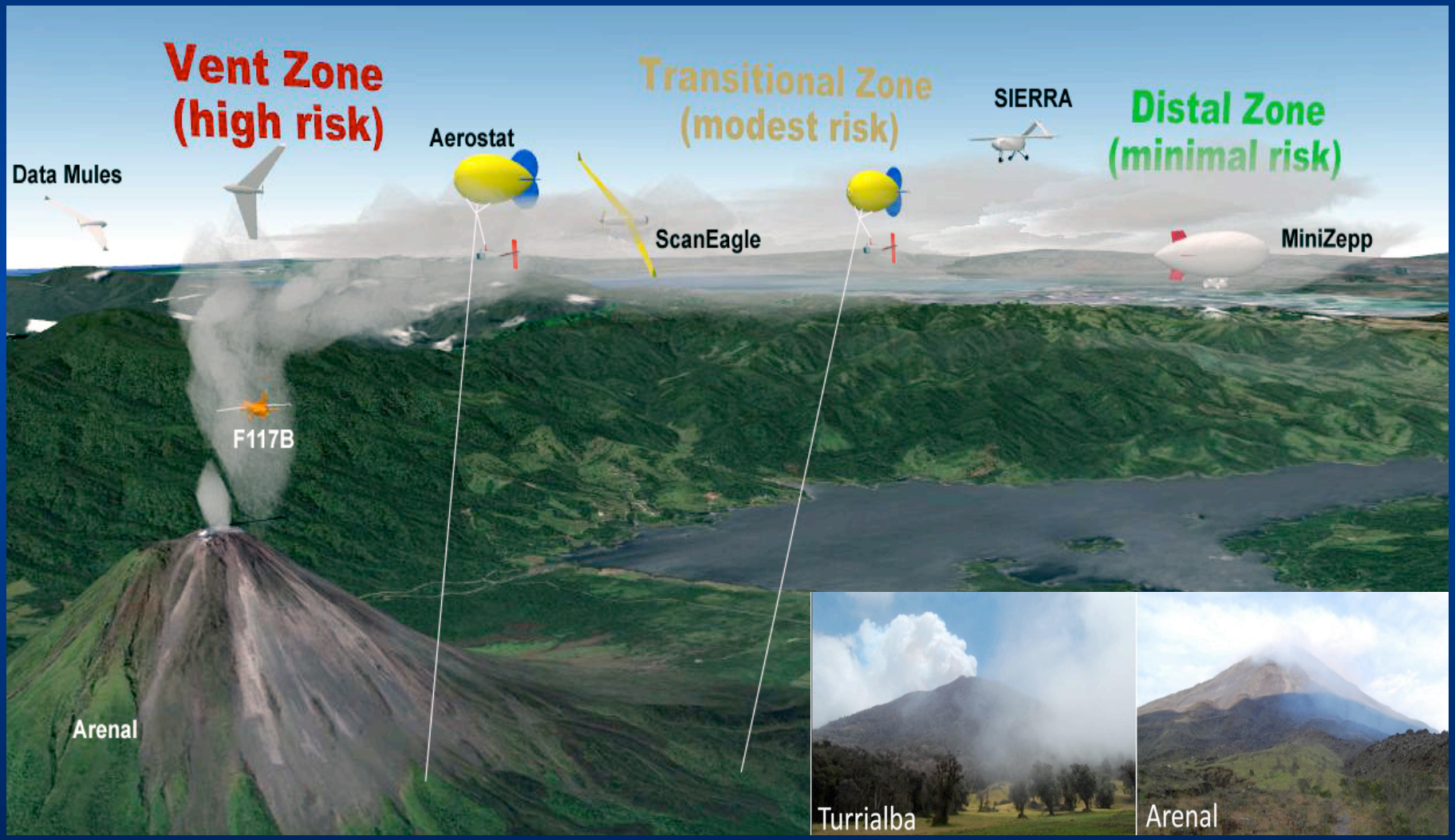

SIERRA, NASA Ames Research Center

Wing Span	**20 ft.**
Length	**11.8 ft.**
Height	**4.6 ft.**
Wing Area	**42.4 sq. ft.**
Empty Weight	**215 lbs.**
Gross Weight	**445 lbs.**
Max Speed	**79 kts.**
Cruise Speed	**55 kts.**
Stall Speed	**30 kts.**
(clean)	**9.43**
Aspect ratio	**545 ft./min.**
Rate of Climb	**29-32% Chord**
CG Position	**~100lbs**
Payload weight	**28V DC**
Payload power	**8-10 hours**
Duration	

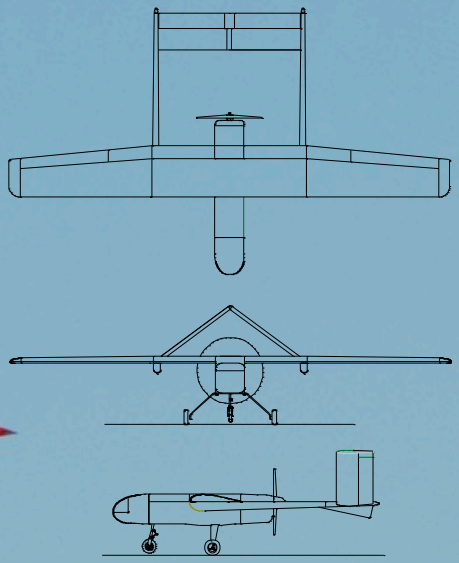

CAD model of ULISSES mini-mass spec gas analyzer integrated into the SIERRA nosecone

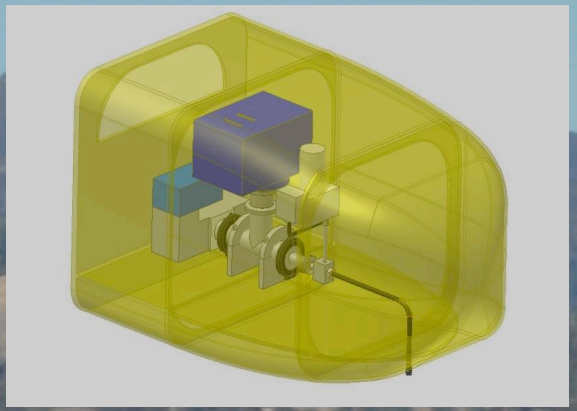

Maryland Aerospace Wing-100 UAV, University of Costa Rica

Small UAV Instrument and Platform Development under the *NASA Small Business Innovative Research* (SBIR) Program

ICE-WATER-ASH DISCRIMINATION

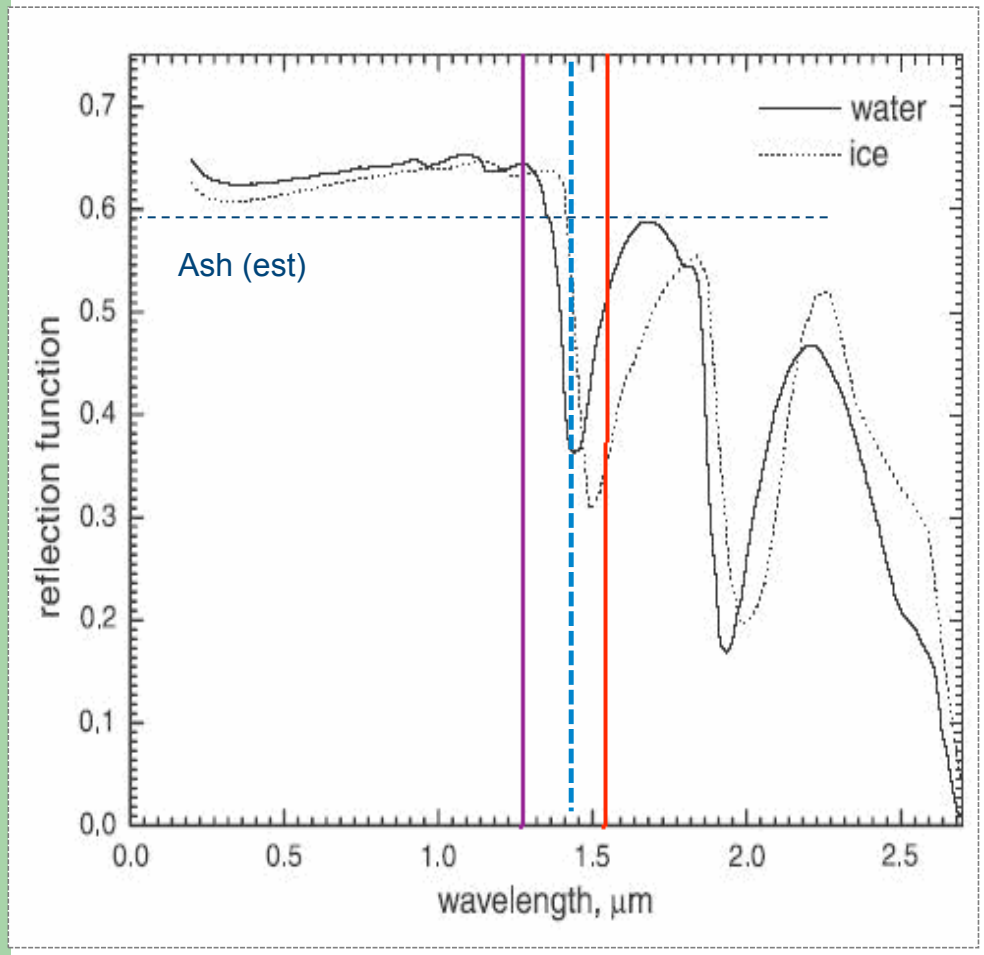

Laser probing wavelengths:
1310 nm
1550 nm
1430 nm (Phase 2)

Reflectivity relationships for discrimination:
@ 1310 nm: Ice ≈ Water ≈ SiO2
@ 1430 nm: Water < Ice < SiO2
@ 1550 nm: Ice < Water < SiO2

Ash reflectivity approximately the same for all wavelengths

Courtesy of Joe Gerardi

PROTOTYPE NEPHELOMETER

- Prototype dual wavelength active IR sensor used for tests at the NASA Glenn Icing Research Tunnel as well as tests in IDI's cloud chamber
- Plastic embodiment – light weight

Courtesy of Joe Gerardi

IDI CLOUD CHAMBER

Sonaer nozzle

liquid nitrogen

Sonaer nozzles for water generation:
- three calibrated water particle sizes
- range of flow rates

Vibrating sifter for ash generation:
-calibrated size and mass

Liquid nitrogen for ice crystal generation:
-insulated, double walled
-can cool chamber to below -40°C

Long path length:
- 16ft long fall distance
- high signal return
- averaging over many particles

Courtesy of Joe Gerardi

First powered flight

Courtesy of Jeremy Novara

Vanilla Aircraft VA02-experimental, Fort Pickett, VA; 26 Jul 2011; SBIR Phase I

Vanilla Aircraft VA02-experimental—pre-launch.

Vanilla Aircraft VA02-experimental—launch!

Conclusions

• Validation and calibration of models of volcanogenic cloud transport and composition are important for basic volcanological science and application to air safety issues in the context of volcanic hazards.

• Low-cost field deployable airborne platforms and miniaturized instrumentation to sample and analyze volcanic ash and gas emissions, both during eruptions and as eruption precursors, can provide important correlative data to support other airborne and orbital observations.

• **In situ observations can materially enhance the utility and applicability of HysplRI observations for the detection and monitoring of volcanic phenomena.**

• It is important to carry out proof-of-concept activities at relatively benign, low altitude active volcanoes, such as is the current situation in Costa Rica, in order to minimize risk to equipment and researchers.

• Such preliminary confidence-building and risk-reduction activities are part of a strategy to develop economical, quick-reaction high altitude in situ measurement capabilities in response to large explosive eruptions.

Attainable? Perhaps.

Wildfire Mapping and Decision Support, Capabilities, Gaps & Opportunities

2011 HyspIRI Science Workshop
NASA Decadal Survey Mission
February 14, 2011

Everett Hinkley
National Remote Sensing Program Manager
USDA Forest Service
Geospatial Management Office

Hyspiri

From the Hyspiri web page:

"The HyspIRI mission will study the world's ecosystems and provide critical information on natural disasters such as volcanoes, wildfires and drought."

Discussion Points

- Introduction
- Fire stages and key needs
- Current & near term capabilities
- Gaps & Opportunities
- Current areas of R&D

Introduction

- Wildland fire is an important challenge facing land managers in the United States.
- In recent years, increased fire size and severity together with an increase in the number of people living in the wildland–urban interface has resulted in billions of dollars of damage to property and significant loss of life in the United States.

Fire Phases & Key Needs

- Pre-Fire
  - Pre-burn fuels mapping
- Detection / Ignition
  - Tipoff Information – Lat/Long/Level of Confidence
- Active Fire
  - Fire perimeter and active fire fronts
  - Problem areas – hot spots outside line
  - Where the fire has been
  - Lines of containment
  - Effectiveness of backfire operations
  - Hot-spots during the mop-up phase
  - Carbon flux!
  - Fire Modeling
- Post-fire
  - Burn severity and mitigation strategies

Pre-Fire Fuels Mapping

- Land managers want cost-effective methods for mapping and characterizing forest fuels quickly and accurately.
- Fuels have traditionally been mapped through extensive field inventory with sampling and statistical inference.
  - Takes a lot of time
  - Very expensive
- Data derived from remote sensing data can be input into fire models to assess fire hazard and risk, and to predict fire behavior.
- Potential remote sensing sources include:
  - LiDAR
  - Imagery (multi-spectral and hyperspectral / air & space sensors)
  - Radar (Synthetic Aperture Radar)
- Caveat: The availability of low-cost satellite hyperspectral and LiDAR datasets is currently limited.

Fire Detection

- Fast and effective detection is a key factor in wildfire fighting. Detection efforts should be focused on early response, accurate (location) results in both daytime and nighttime, and the ability to prioritize fire danger.
- Early detection methods included:
  - Fire lookout towers (early 20th Century)
  - Aerial and land photography using instant cameras (1950s)
  - Infrared scanning (Developed in the 1960s).

Fire Detection

Current Methodologies

- Small area / high value assets at risk
  - The public (public hotlines, cell phones)
  - Watchtowers (manned)
  - Ground based sensor networks
- Large area / low value assets at risk
  - MODIS / satellite detection
  - Electronic lightning detection
  - Aerial patrols: planes, helicopter, and/or UAVs

Fire Detection

- Caveats
  - Satellite detection is prone to positional offsets.
  - Cloud cover and spatial resolution often limit the effectiveness of satellite imagery.
  - Ground and near earth observations can be expensive.
  - Improved fire detection is generally a low priority for federal land managers.
- Opportunities
  - GOES – R
  - Other future satellite systems
  - Military and IC capabilities

Active Fire Mapping

- Current capabilities for tactical fire mapping
  - National Infrared Operations (NIROPS)
  - Vendor aircraft
  - Military and IC assets
  - Unmanned aircraft (UAS)
  - *Commercial satellite imagery*
- Future Opportunities
  - Future satellite systems, GOES-R

Active Fire Mapping

Phoenix Sensor Workstation on Citation Jet

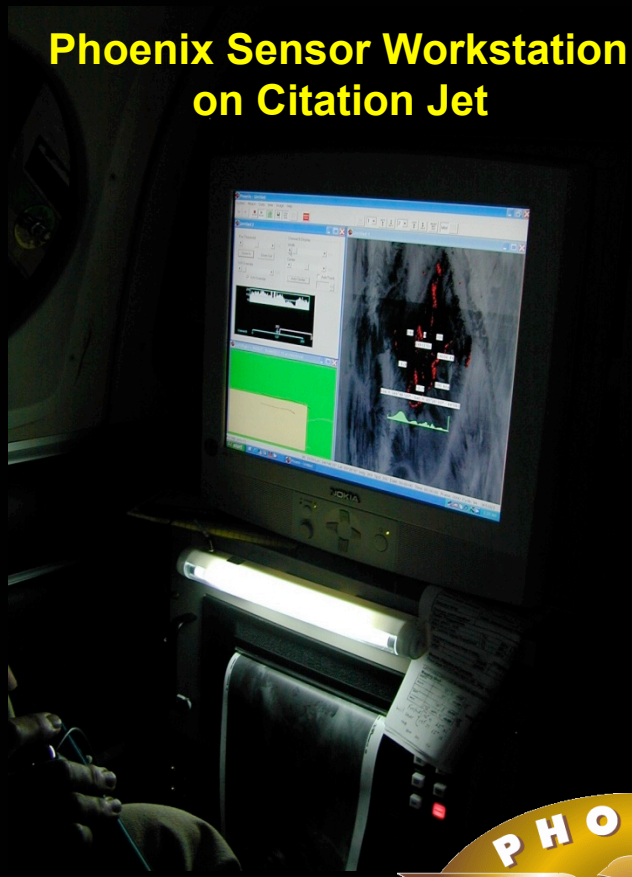

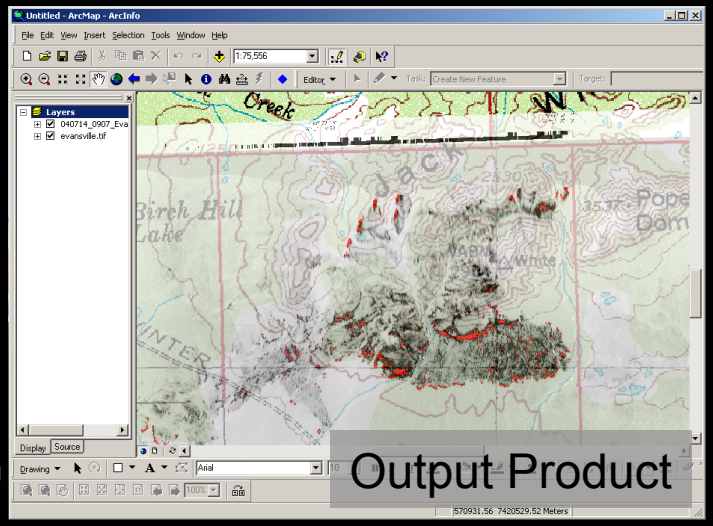

PHOENIX
INFRARED FIRE DETECTION AND MAPPING

GMO

Active Fire Mapping

PHOENIX Output Products

- GeoTiffs
  - Color
  - Grayscale
  - “255 Pixel Layer
- JPEGS
- Mosaics
- Active Heat Areas shape file

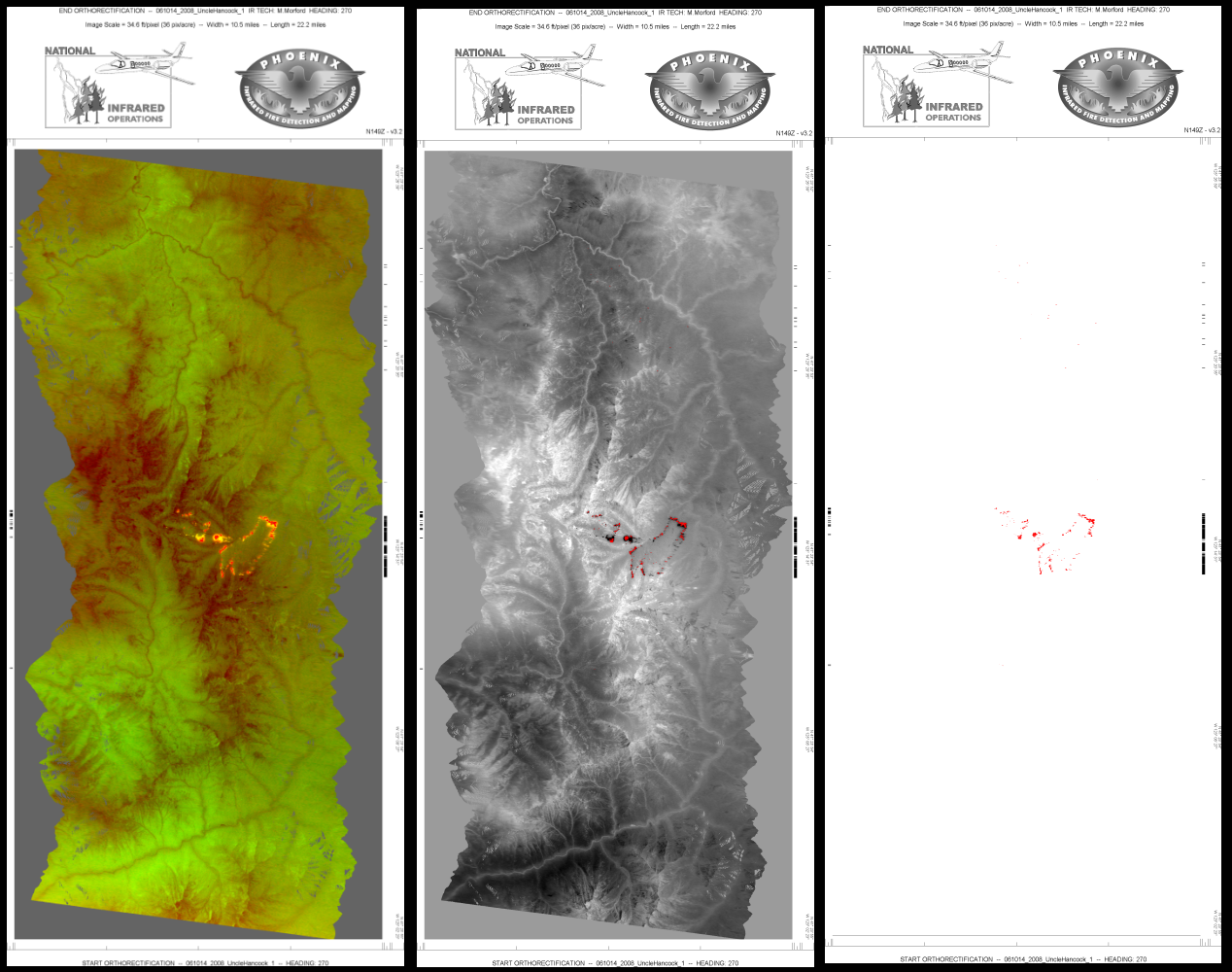

Burned Area Emergency Response

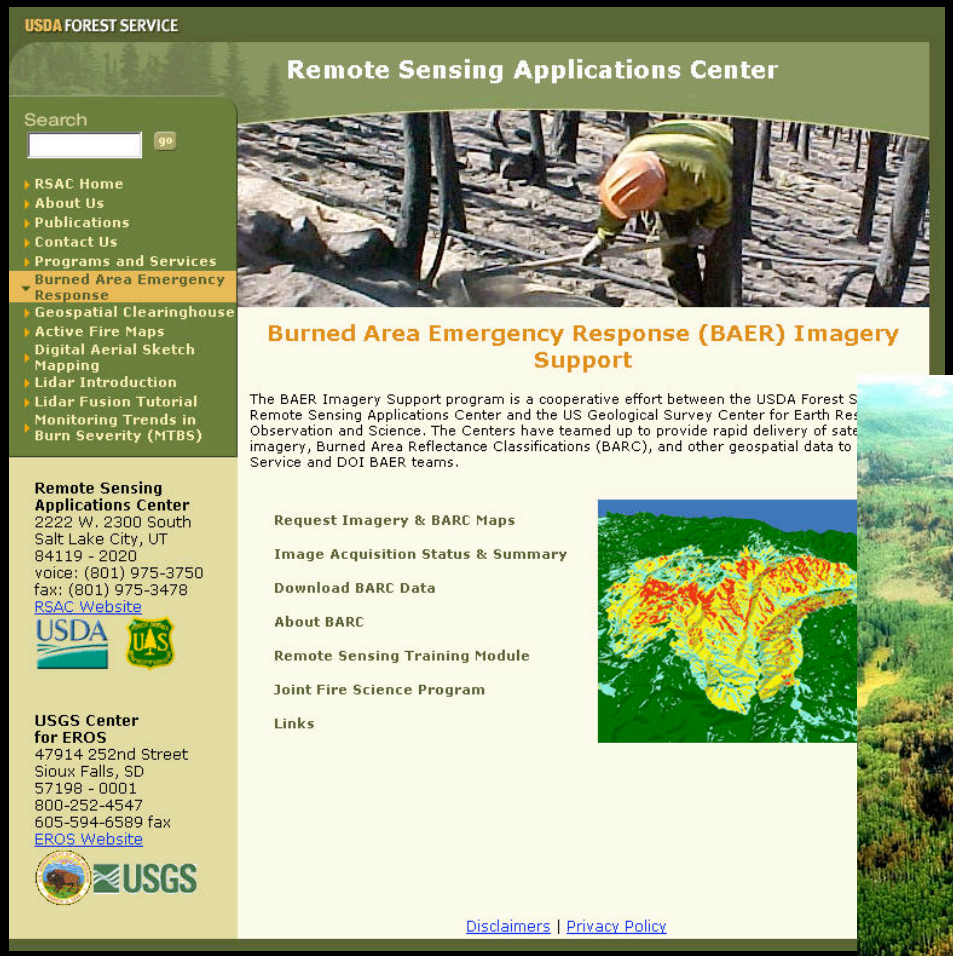

USFS

Burned Area Emergency Response

- Fast track emergency assessment
  - BAER response plan is required within 7 days of fire containment
- Utilizes change detection methods from satellite imagery
- Assess fire effects on the soil and watershed hydrologic function (erosion and flood potential)
- Prescribe and implement emergency stabilization measures to mitigate potential hazards to:
  - Life
  - Property
  - Long-term soil productivity
  - Water quality
  - Natural resources

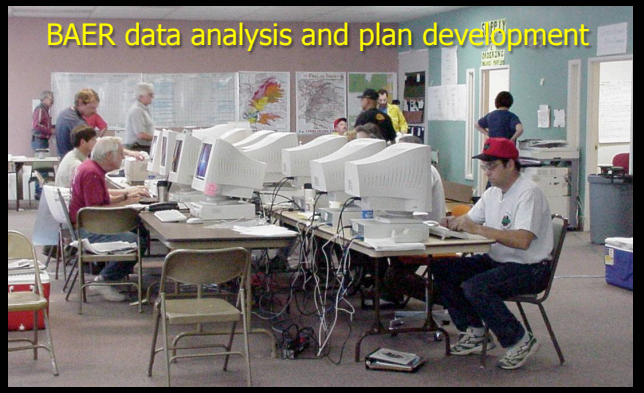

Burned Area Emergency Response

- Post-fire situations of concern for BAER teams…

High burn severity – Robert Fire 2003 (Carl Key, USGS)

Hydrophobic soils, USFS

High burn severity – Station Fire 2009 (USGS)

Burned Area Emergency Response

- Potential consequences of unmitigated post-fire hazard situations…

Burned Area Emergency Response

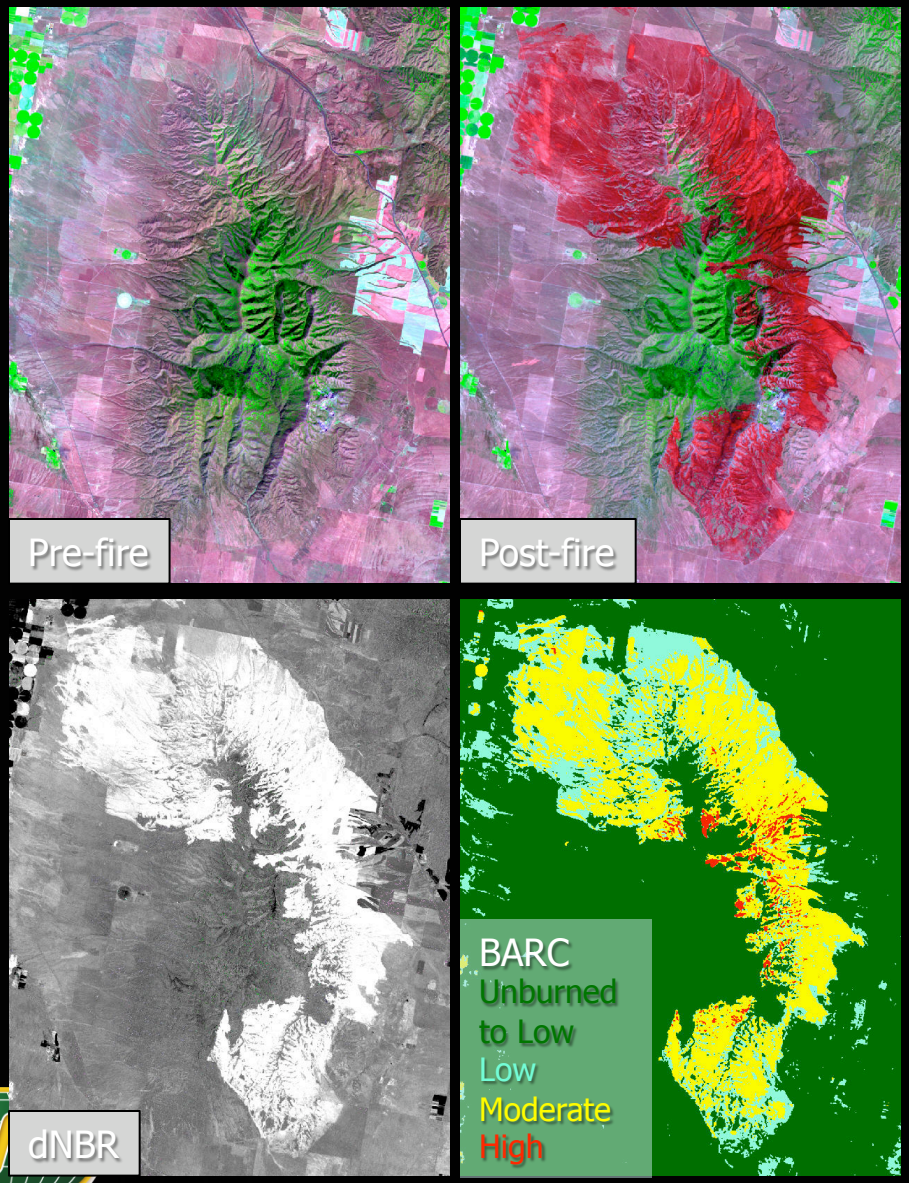

- ~860 fires mapped since 2001 (~27.5 million acres)
- Imagery, BARC and other data products provided within 2 hours of receiving image from provider

Burned Area Reflectance Classification (BARC)
Normalized Burn Ratio (NBR)
Differenced Normalized Burn Ratio (dNBR)

NBR = (NIR – SWIR) / (NIR + SWIR)
dNBR = Pre NBR – Post NBR

BARC = Continuous dNBR data thresholded into severity classes

Burned Area Emergency Response

Leveraged Sensor Assets – Use Best Available

Sensor	Platform Type	Spatial Resolution (Reflectance Bands)	Temporal Resolution (per instrument)	Data Source
Landsat 5 TM	Polar orbiting	30m	16 days	USGS EROS
Landsat 7 ETM+[1]	Polar orbiting	30m	16 days	USGS EROS
AWiFS	Polar orbiting	56m	5 days	USDA-FAS-SIA
SPOT 4	Polar orbiting	20m	2-3 days (pointable)	SPOT Image/USGS EROS
SPOT 5	Polar orbiting	10m/20m	2-3 days (pointable)	SPOT Image/USGS EROS
ASTER[2]	Polar orbiting	15m/30m	4-16 days (pointable)	NASA/USGS EROS
NASA AMS	Airborne (UAV)	~ 21m	--	NASA
LDCM[3]	Polar orbiting	30m	16 days	USGS EROS

1 – SLC failure in May 2003; 2 – SWIR band issues since April 2008; 3 – launch scheduled for December 2012

Fire Phases & Key Needs

- Pre-Fire
  - **Pre-burn fuels mapping**
- Detection / Ignition
  - **Tipoff Information** – Lat/Long/Level of Confidence
- Active Fire
  - Fire perimeter and active fire fronts
  - Problem areas – hot spots outside line
  - Where the fire has been
  - Lines of containment
  - Effectiveness of backfire operations
  - Hot-spots during the mop-up phase
  - **Carbon flux!**
  - **Fire Modeling**
- Post-fire
  - Burn severity and mitigation strategies

New Technology Evaluation

- Sensors
- Platforms
- Data Distribution & Decision Support Systems
- The golden age of mapping & remote sensing
  - GPS & GIS
  - The Internet
  - Powerful desktop computing
  - National data sets
  - Decision support systems

- Working with NASA, other federal agencies, academia, commercial vendors, and international partners.

Data Delivery

- Traditional Delivery Methods
  - "Land and Hand"
    - IRIN at central location
    - "Pod" at central location
  - Land and upload to ftp.nifc.gov/NIROPS
    - IRIN or IR technician

- AirCell Data Downlink System
  - Terrestrial based telecomm system
  - Broadband level connectivity
  - Is being installed on both NIROPS aircraft
  - Planned for use this summer
  - Phoenix data will be down linked to fitp.nifc.gov for retrieval by IRINs

gogo Inflight Internet

Autonomous Modular Sensor (AMS)

Band	Wavelength µm	
1	0.42-0.45	
2	0.45-0.52	(TM1)
3	0.52-0.60	(TM2)
4	0.60-0.62	
5	0.63-0.69	(TM3)
6	0.69-0.75	
7	0.76-0.90	(TM4)
8	0.91-1.05	
9	1.55-1.75	(TM5)
10	2.08-2.35	(TM7)
11	3.60-3.79	(VIIRS M12)
12	10.26-11.26	(VIIRS M13)

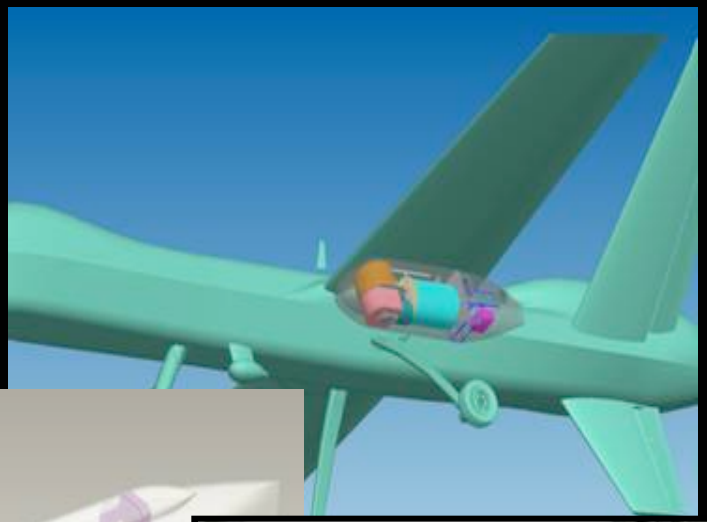

Total Field of View: 42.5 or 85.9 degrees (selectable)
IFOV: 1.25 mrad or 2.5 mrad (selectable)
Spatial Resolution: 3 – 50 meters (variable)

EnablingTechnologies

New Fire Mapping Sensors

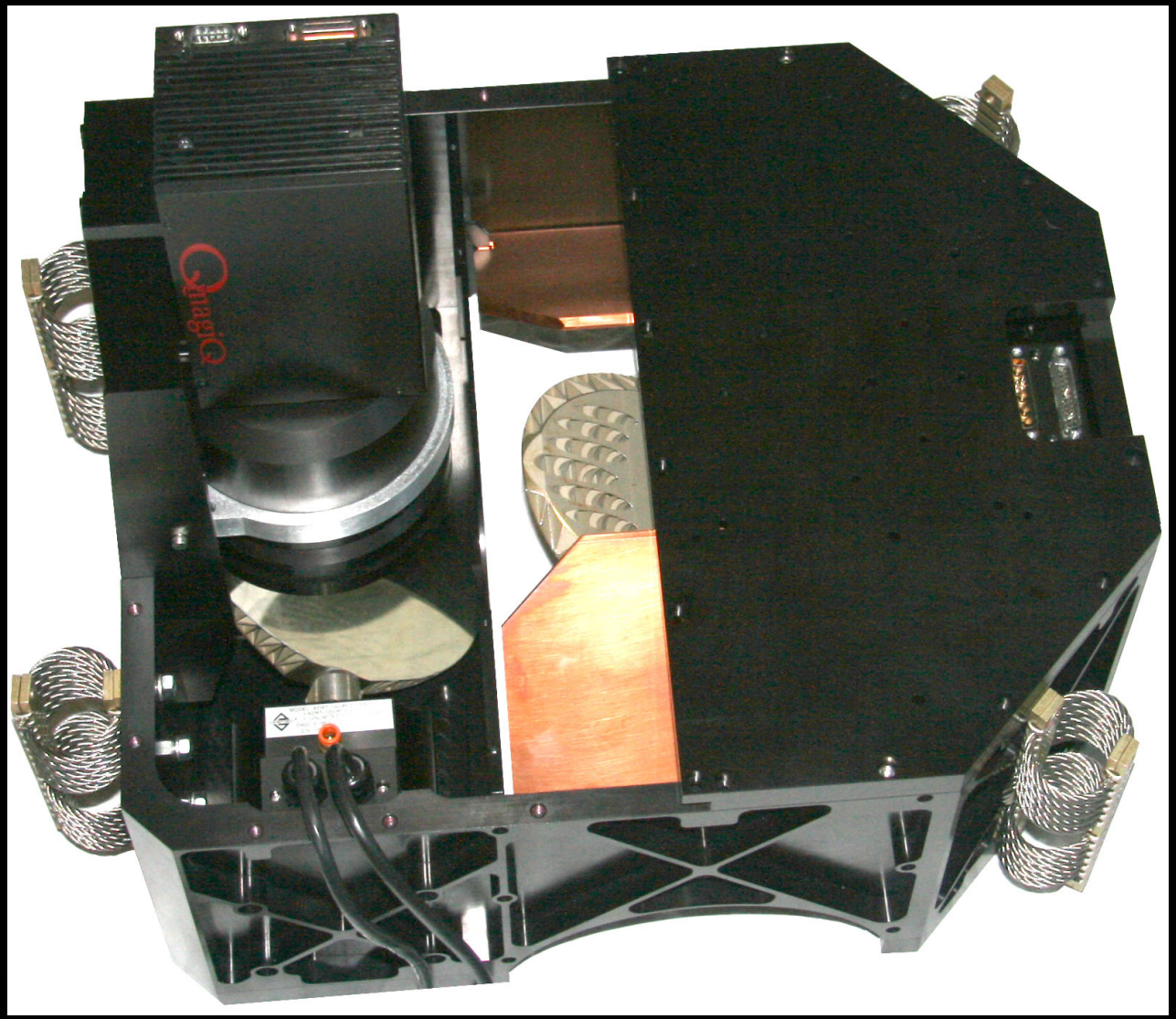

Unmanned Aircraft

Two Track Approach

Small UAS

Desired Features

- Fully autonomous takeoff and landing
- Operable from small, unimproved locations!!
- Man or light truck portable
- Capable imaging systems and guidance systems
- VTOL Preferred

UAS: Image Products

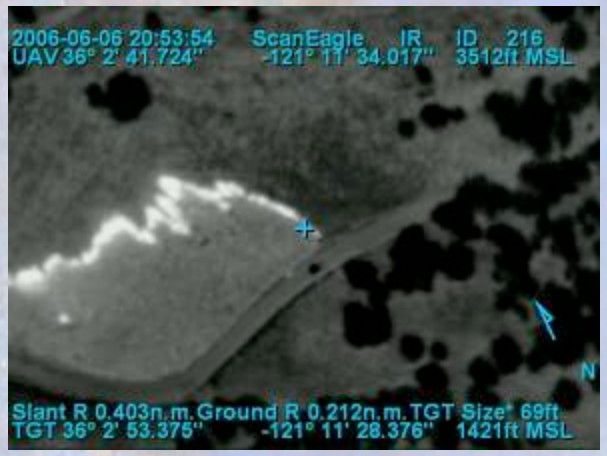

NASA Ikhana

- Continuation of objectives in-place from 2007-2009 missions.
- Missions using NASA Ikhana UAS in 2007, 2008, and 2009.
- Ikhana on standby and funded for emergency fire response in 2010

New Processes

- Multiple sensing systems working together can be used to merge satellite data, aerial imagery, and personnel GPS position/imagery into a collective whole for near-realtime use by Incident Command centers.
  - Decision support tools / geospatial mash-ups
  - NASA's SensorWeb concept!

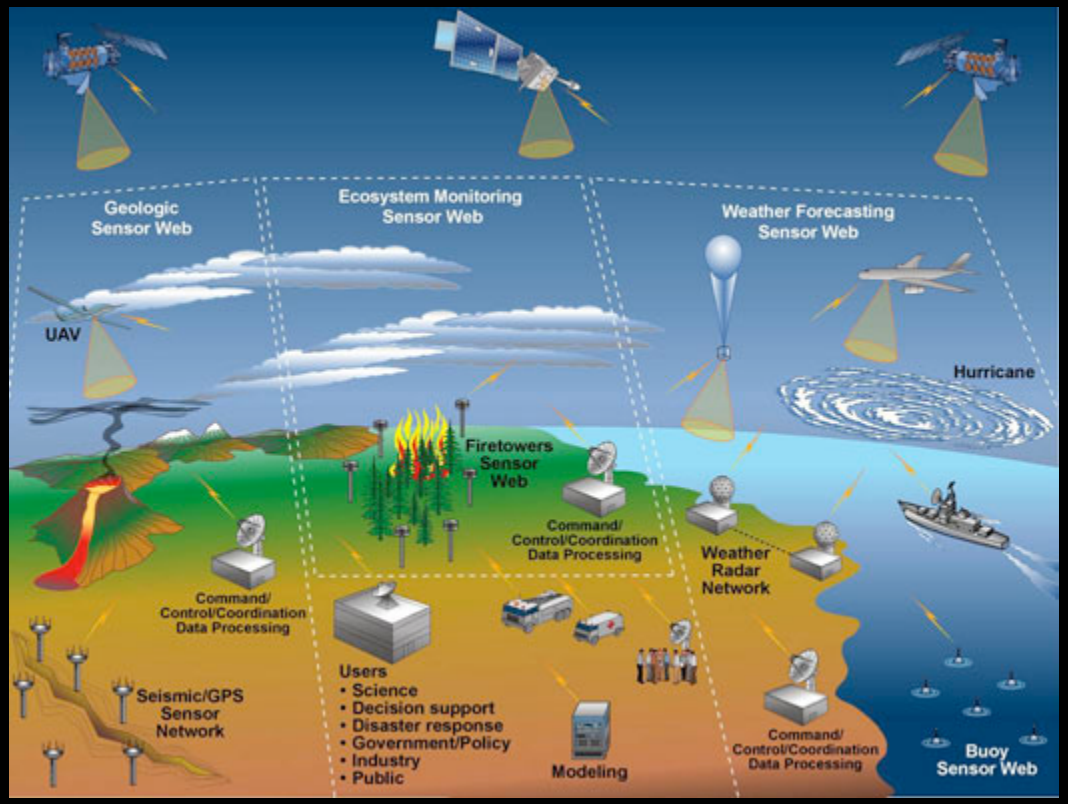

SensorWeb

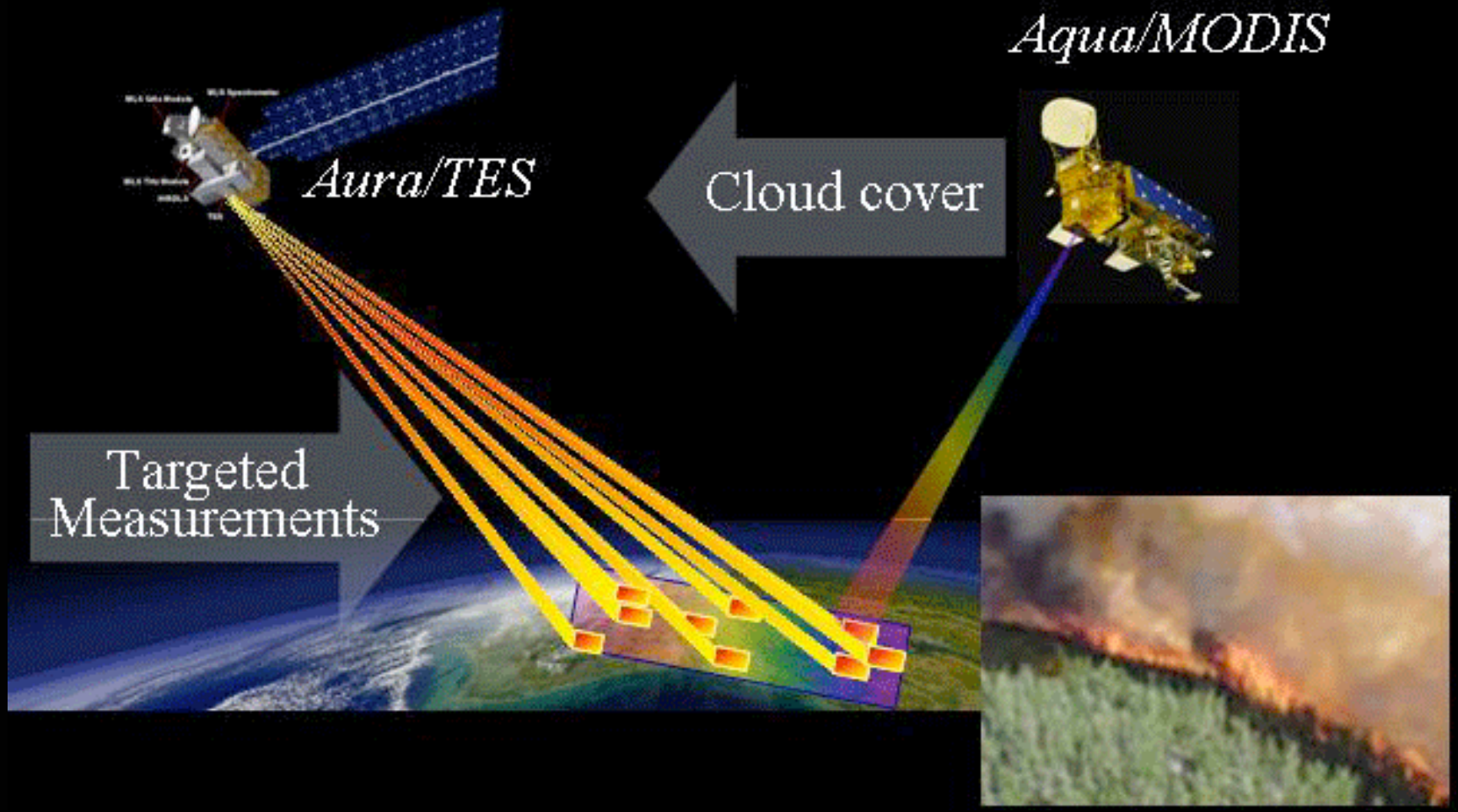

Enabling Technologies: Google Earth

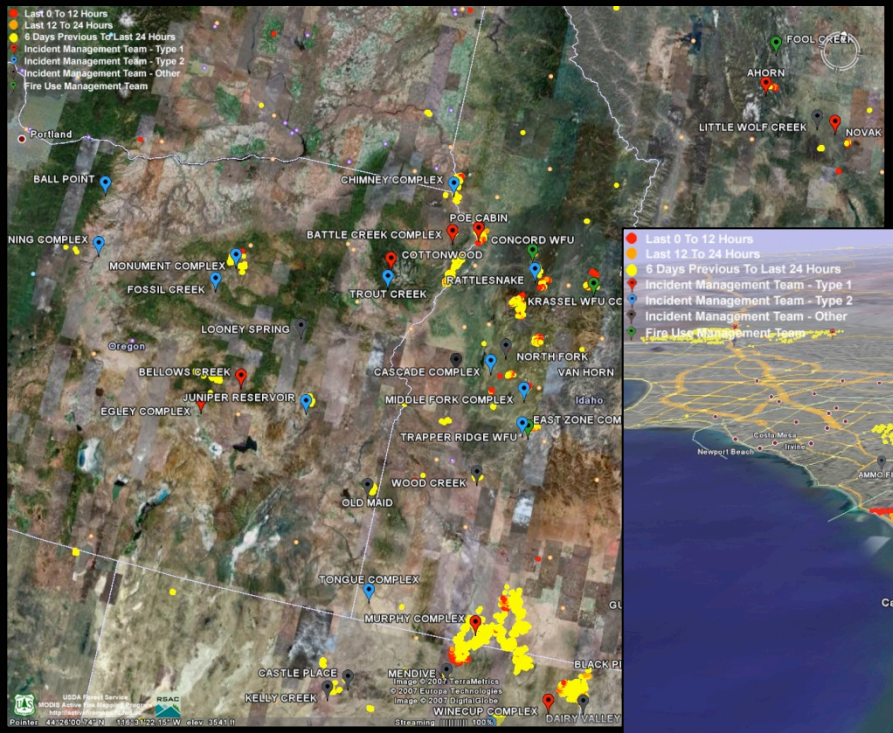

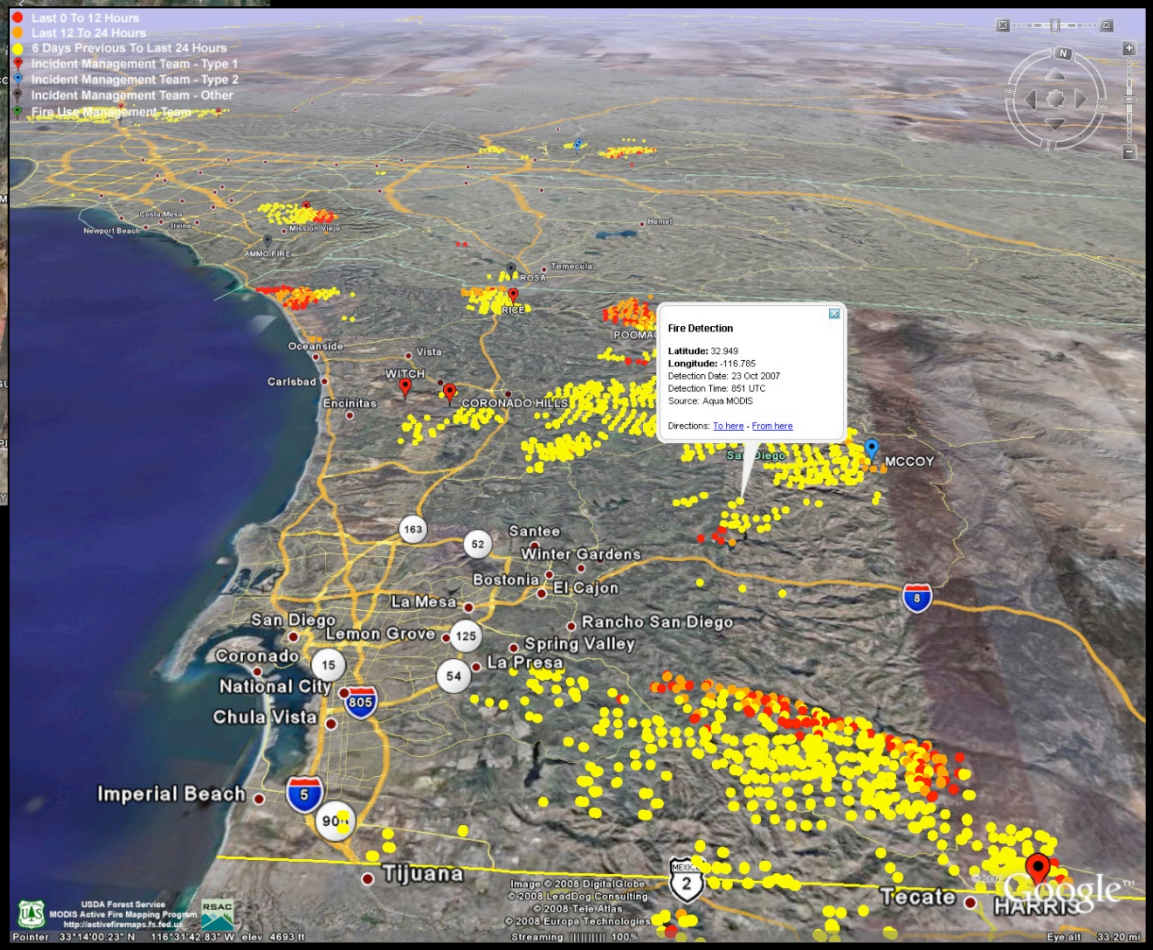

Enabling Technologies: GPS Enabled Phones

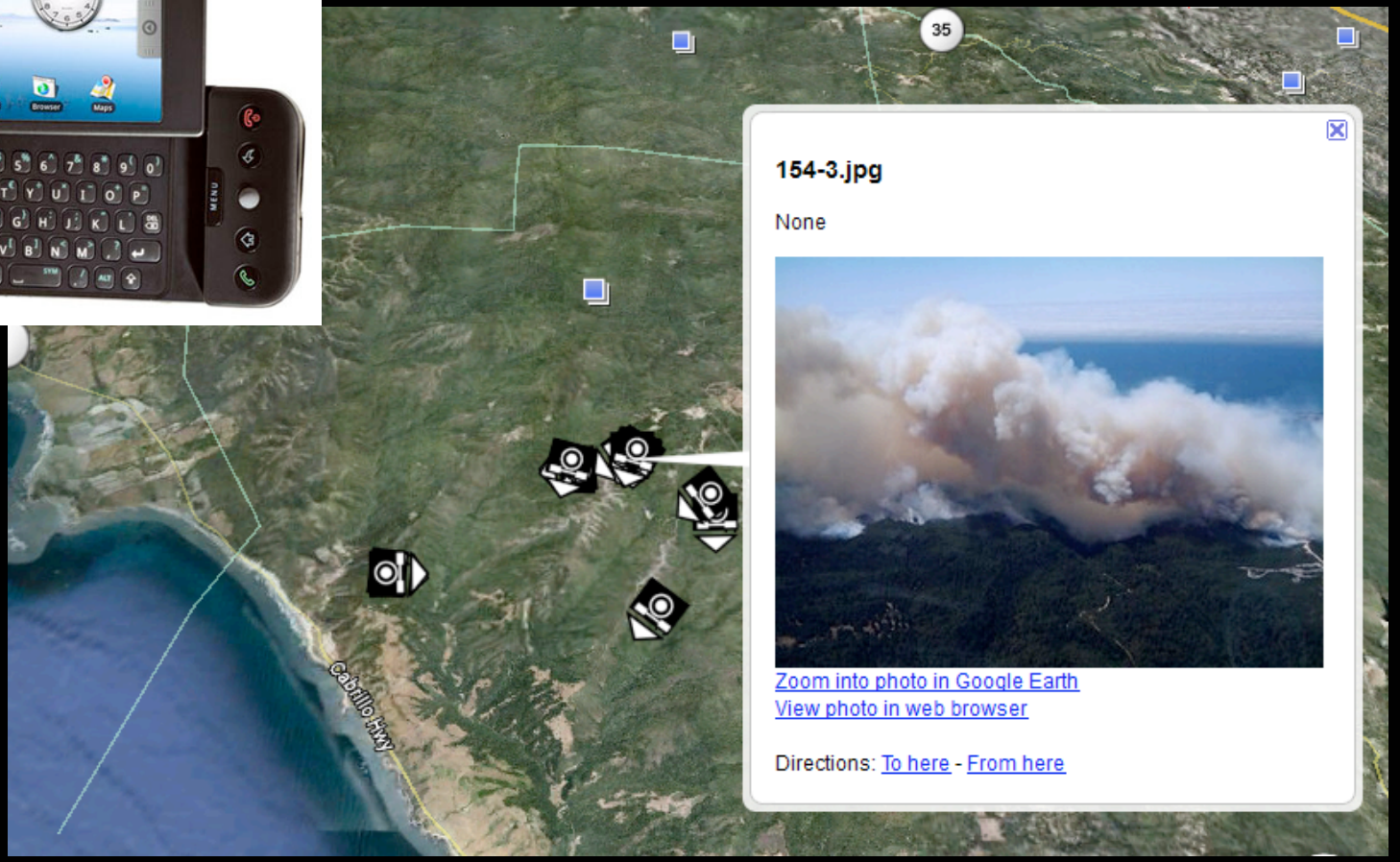

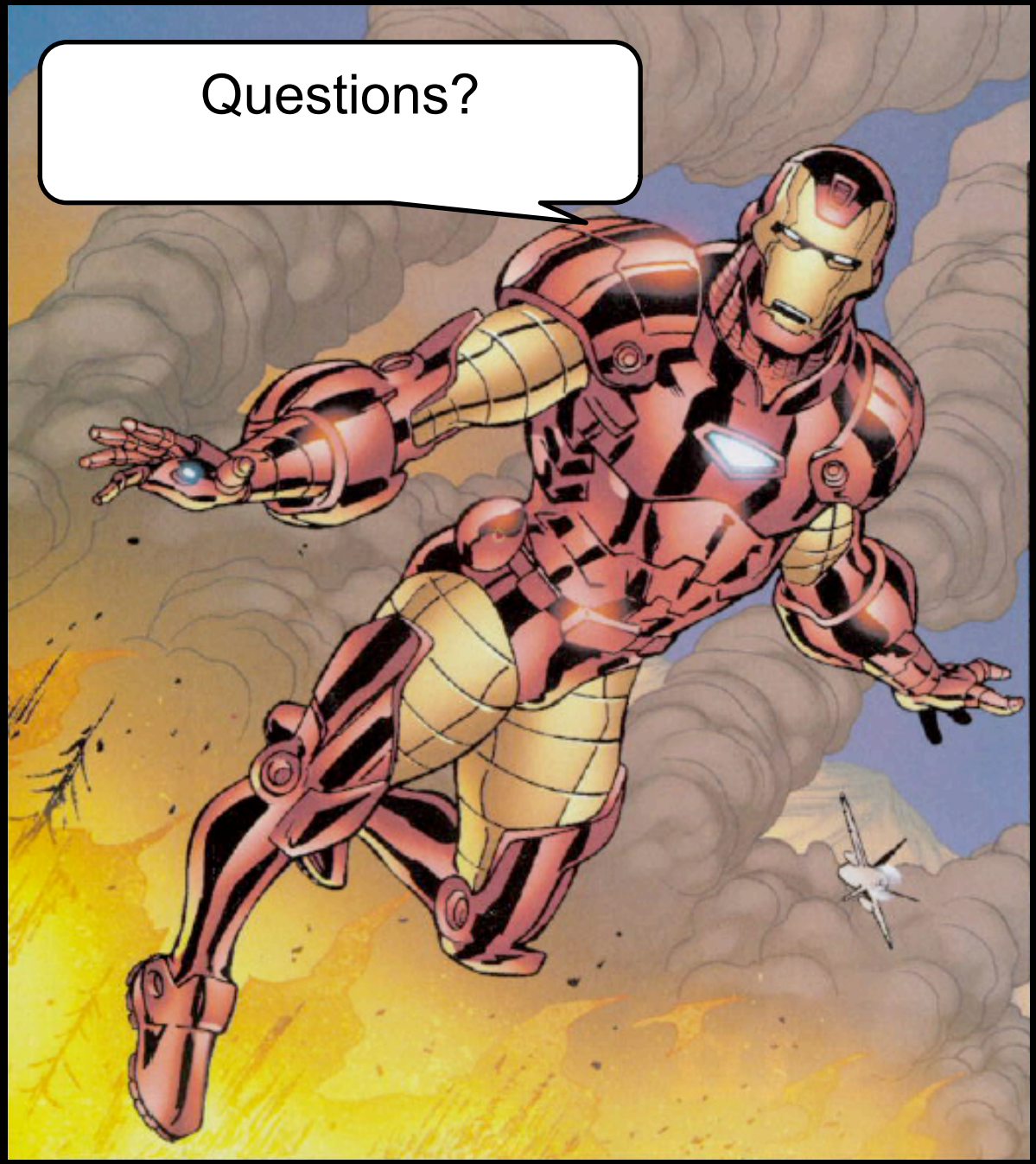
Questions?

Practical considerations regarding the use of HyspIRI for fire monitoring

Evan Ellicott (University of Maryland)
Louis Giglio (University of Maryland)
Ivan Csiszar (NOAA/NESDIS)
Wilfrid Schroeder (NOAA)
August 24th, 2011

Biomass Burning

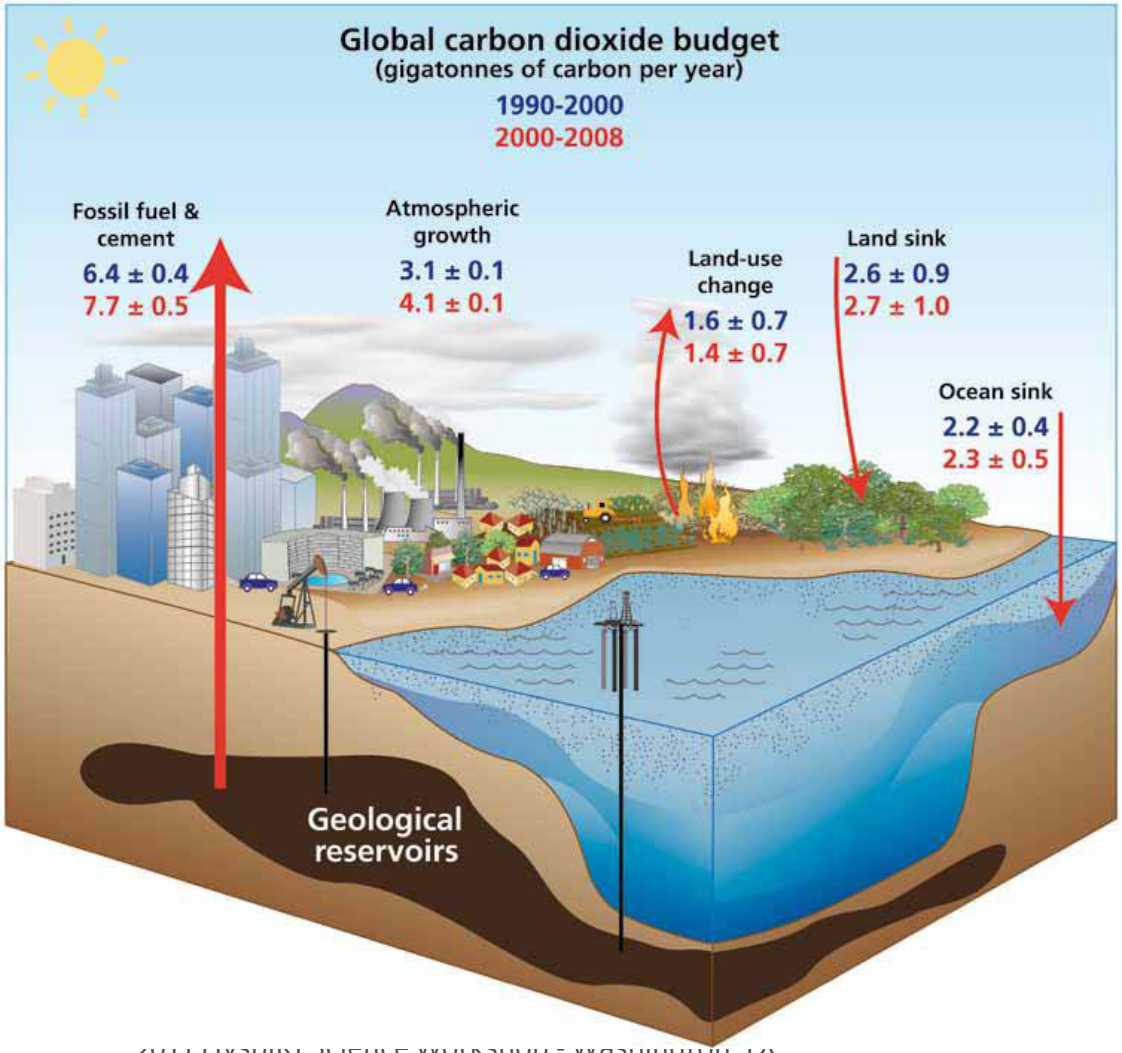

Decadal Survey – Thematic Questions

TQ2. Wildfires

- How are global fire regimes changing in response to, and driven by, changing climate, vegetation, and land use practices?
- Is regional and local scale fire frequency changing?
- What is the role of fire in global biogeochemical cycling, particularly trace gas emissions?
- Are there regional feedbacks between fire and climate change?

Decadal Survey – Thematic Questions

CQ2. Wildfires

- How does the timing, temperature and frequency of fires affect long-term ecosystem health?
- How does vegetation composition and fire temperature impact trace gas emissions?
- What are the feedbacks between fire temperature and frequency and vegetation composition and recovery?
- How does vegetation composition influence wildfire severity?
- How does invasive vegetation cope with fire in comparison to native species?

Active Fires

- Current detection scheme for coarse resolution polar-orbiting platforms exploits the strong emission response in the MIR (4µm) channel (ideally placed to limited atmospheric perturbation)

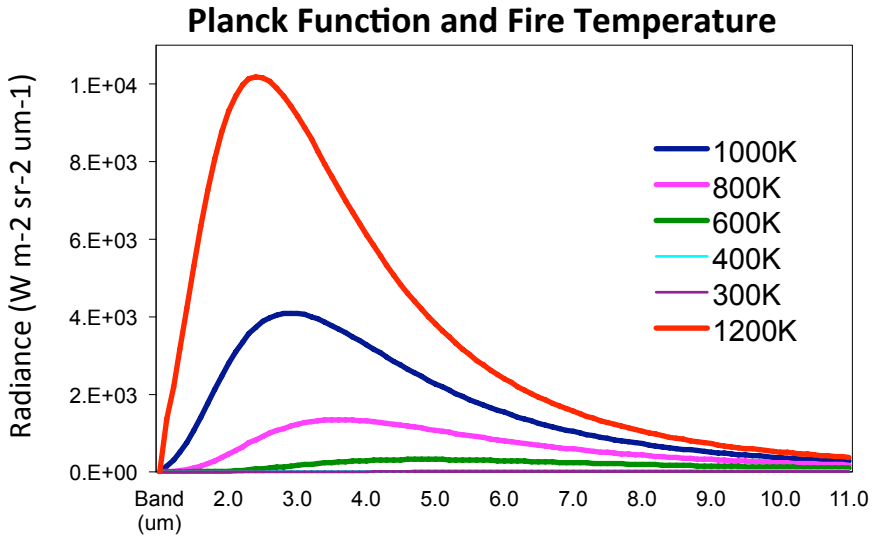

Channel number	Central wavelength (µm)	Purpose
1	0.65	Sun glint and coastal false alarm rejection; cloud masking.
2	0.86	Bright surface, sun glint, and coastal false alarm rejection; cloud masking.
7	2.1	Sun glint and coastal false alarm rejection.
21	4.0	High-range channel for active fire detection.
22	4.0	Low-range channel for active fire detection.
31	11.0	Active fire detection, cloud masking.
32	12.0	Cloud masking.

Benefits

HyspIRI Active Fires

- Measure the land surface temperature and emissivity
- 5 day equatorial revisit to generate monthly, seasonal and annual products.
- 60 m spatial resolution
- 4µm band saturates at 1400K
- 7.5-12 µm bands saturate at 400K

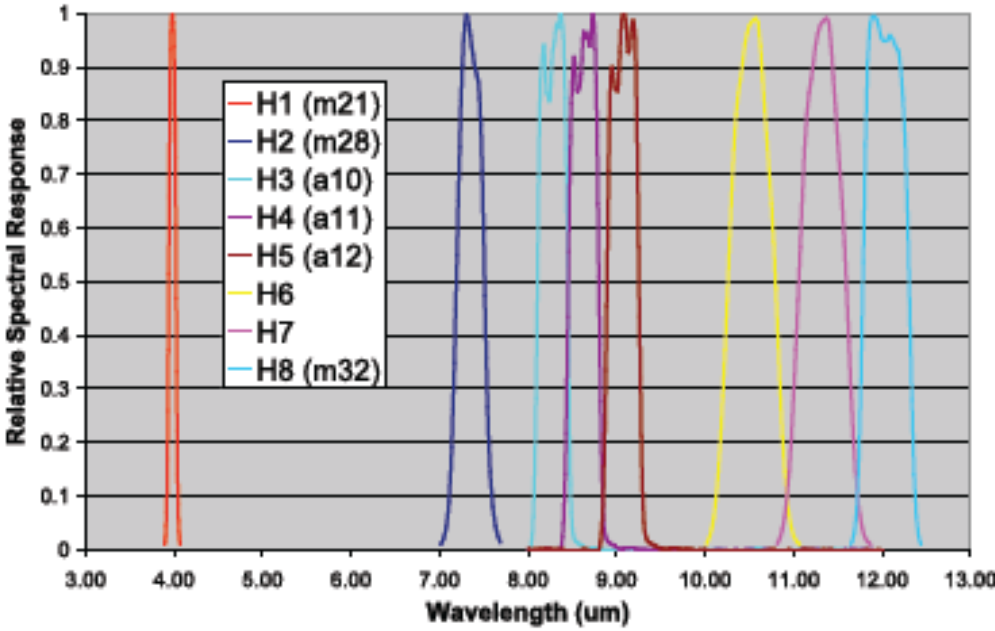

Hyperspectral Fire Detection

- Dennison, P.E., and D.S. Matheson, 2011.
  - Comparison of fire temperature and fractional area modeled from SWIR, MIR, and TIR multispectral and SWIR hyperspectral airborne data. Remote Sensing of Environment, 115, 876-886.
- Dennison, P.E. and D.A. Roberts, 2009.
  - Daytime fire detection using airborne hyperspectral data. Remote Sensing of Environment, 113, 1646-1657.

$$\mathrm{HFDI} = \frac{\left(L_{2.43\mu m} - L_{2.06\mu m}\right)}{\left(L_{2.43\mu m} + L_{2.06\mu m}\right)}$$

- Dennison, P.E., 2006
  - Fire detection in imaging spectrometer data using atmospheric carbon dioxide absorption. International Journal of Remote Sensing, 27, 3049-3055.

$$\mathrm{CO_2\ Absorp.\ Index} = \frac{L_{2010}}{0.666 \cdot L_{1990} + 0.334 \cdot L_{2040}}.$$

- Vodacek, A., et al., 2002.
  - Remote optical detection of biomass burning using a potassium emission signature. International Journal of Remote Sensing, 13, 2721–2726.

$$\text{potassium emission index} = \frac{L_{770}}{L_{780}}$$

Detection Envelopes

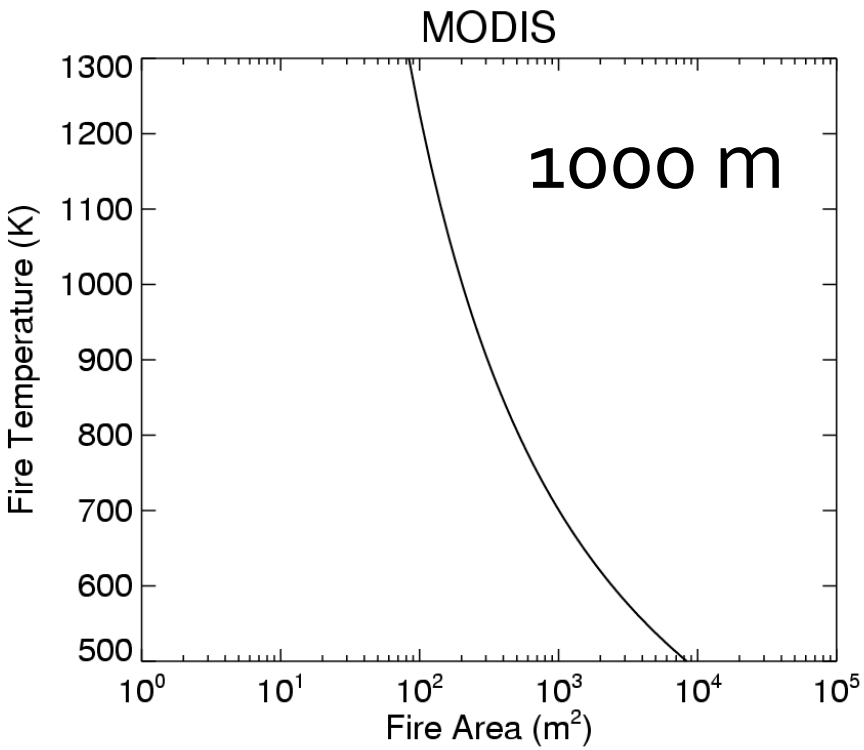

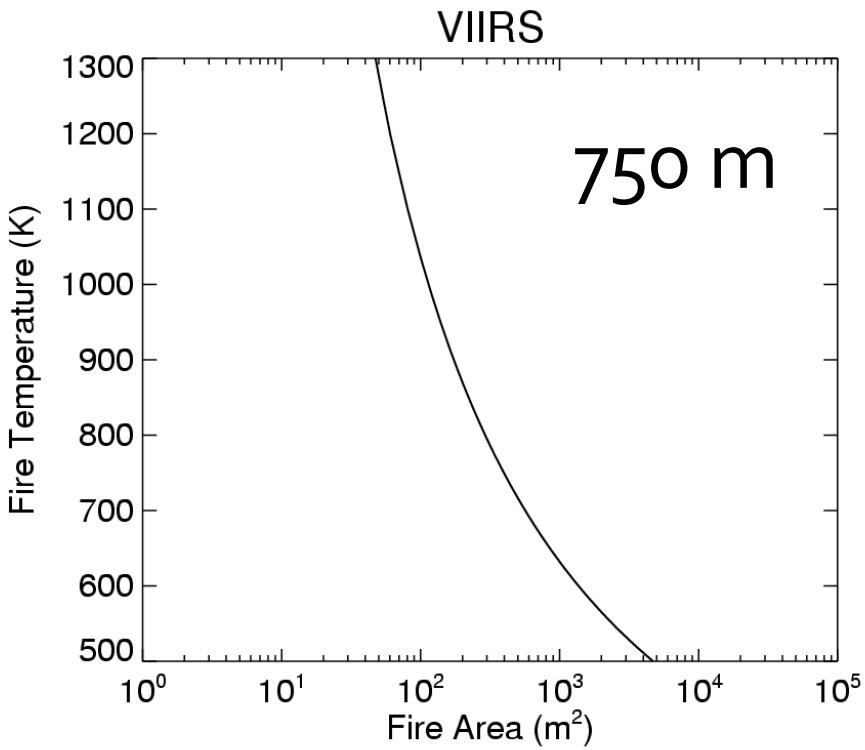

90% probability of detection; boreal forest; nadir view

L. Giglio

Detection Envelopes

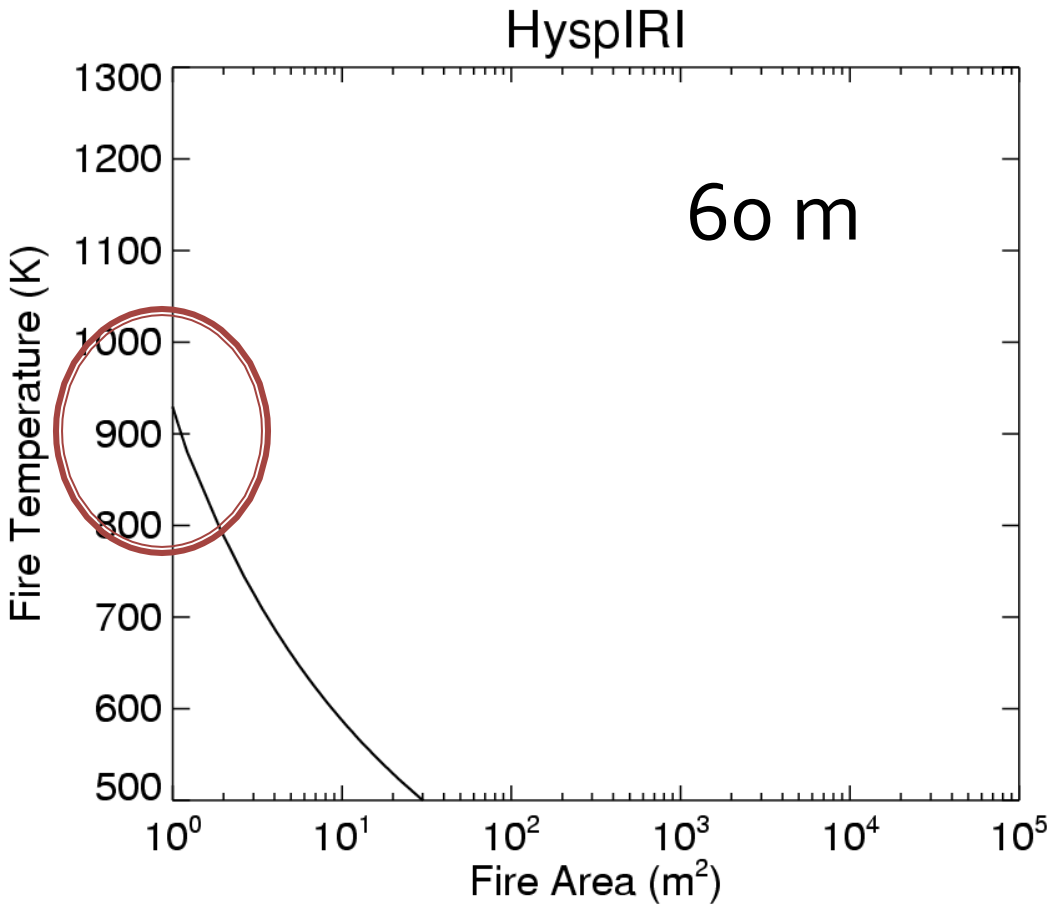

90% probability of detection; boreal forest; nadir view

L. Giglio

Cal/Val

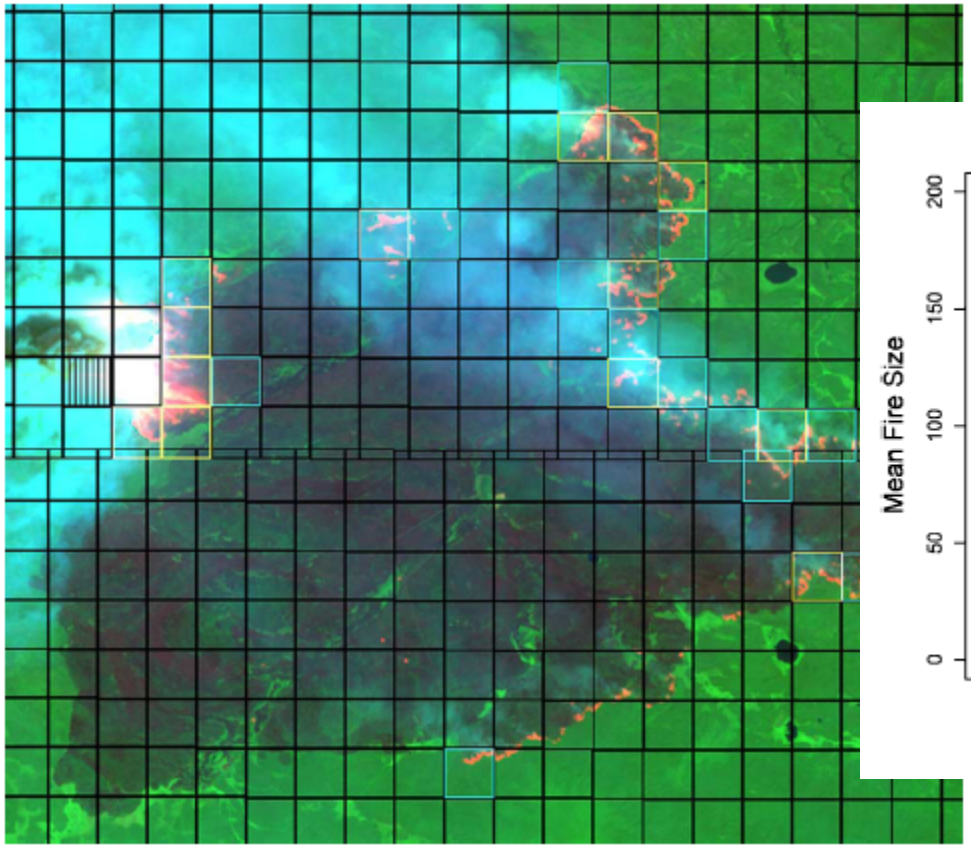

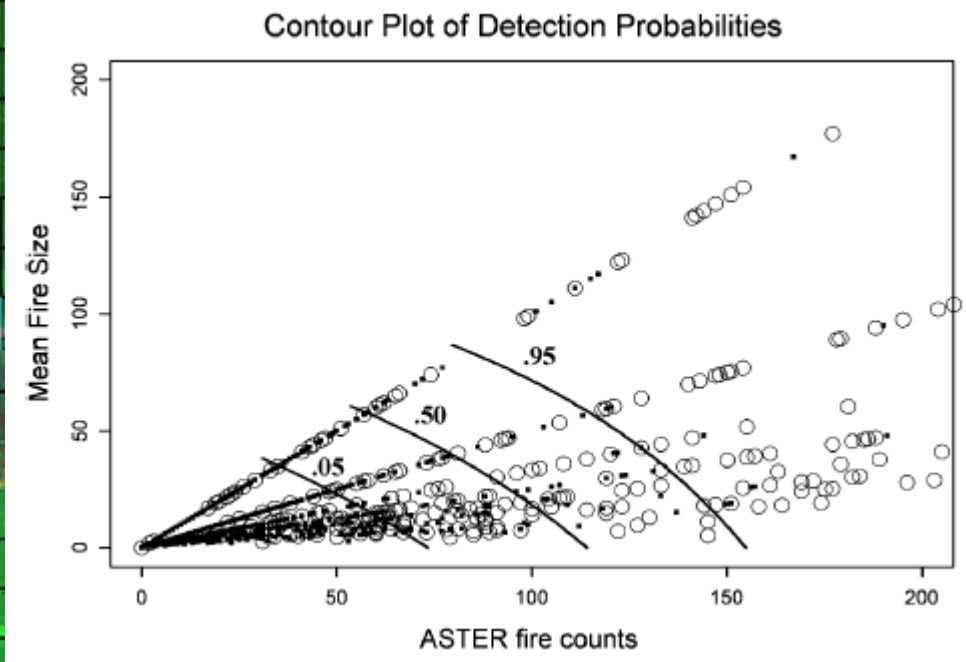

Csiszar et al., 2006

Cal/Val

False Color Composites: 30m ASTER MOD14: False (c) and True (d) Detections

30m ETM+ WFABBA False (e) and True (f) Detections

Schroeder et al., 2008

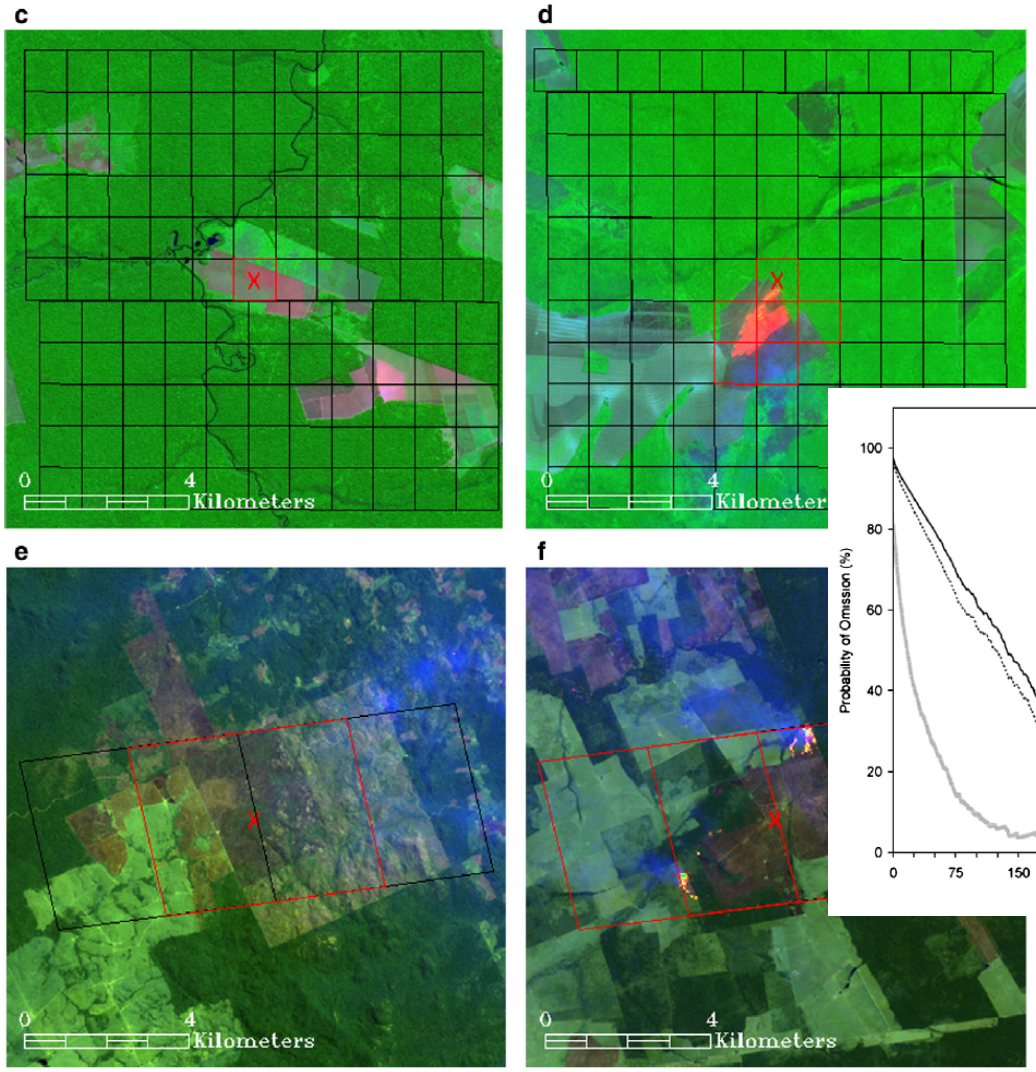

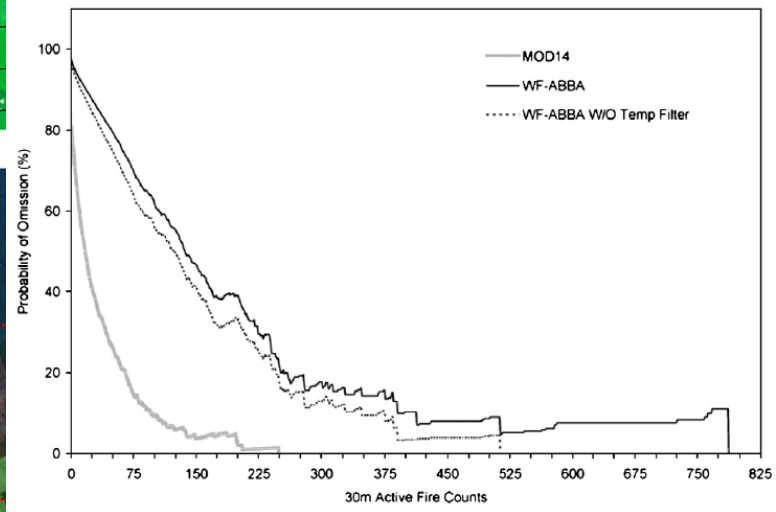

Fig. 11 (*continued*).

Emissions

CO_2 emissions from forest loss

G. R. van der Werf, D. C. Morton, R. S. DeFries, J. G. J. Olivier, P. S. Kasibhatla, R. B. Jackson, G. J. Collatz and J. T. Randerson

Deforestation is the second largest anthropogenic source of carbon dioxide to the atmosphere, after fossil fuel combustion. Following a budget reanalysis, the contribution from deforestation is revised downwards, but tropical peatlands emerge as a notable carbon dioxide source.

"The combined contribution of deforestation, forest degradation and peatland emissions to total anthropogenic CO2 emissions is about 15% (range 8–20%)"

Emissions

Atmos. Chem. Phys., 10, 11707–11735, 2010
www.atmos-chem-phys.net/10/11707/2010/
doi:10.5194/acp-10-11707-2010
© Author(s) 2010. CC Attribution 3.0 License.

Atmospheric Chemistry and Physics

Global fire emissions and the contribution of deforestation, savanna, forest, agricultural, and peat fires (1997–2009)

G. R. van der Werf[1], J. T. Randerson[2], L. Giglio[3,4], G. J. Collatz[4], M. Mu[2], P. S. Kasibhatla[5], D. C. Morton[4], R. S. DeFries[6], Y. Jin[2], and T. T. van Leeuwen[1]

"While the sum of deforestation, degradation, and peat fire emissions accounted for about a quarter of total C emissions, for CH_4 these sources were key **contributing to 44% of total CH_4 emissions** of 20 Tg CH_4 year–1. This was mostly due to the large EF for CH_4 in **peat areas**, which was 3x as high as the EF for tropical deforestation fires, and almost 10x that of the EF for grassland and savanna fires"

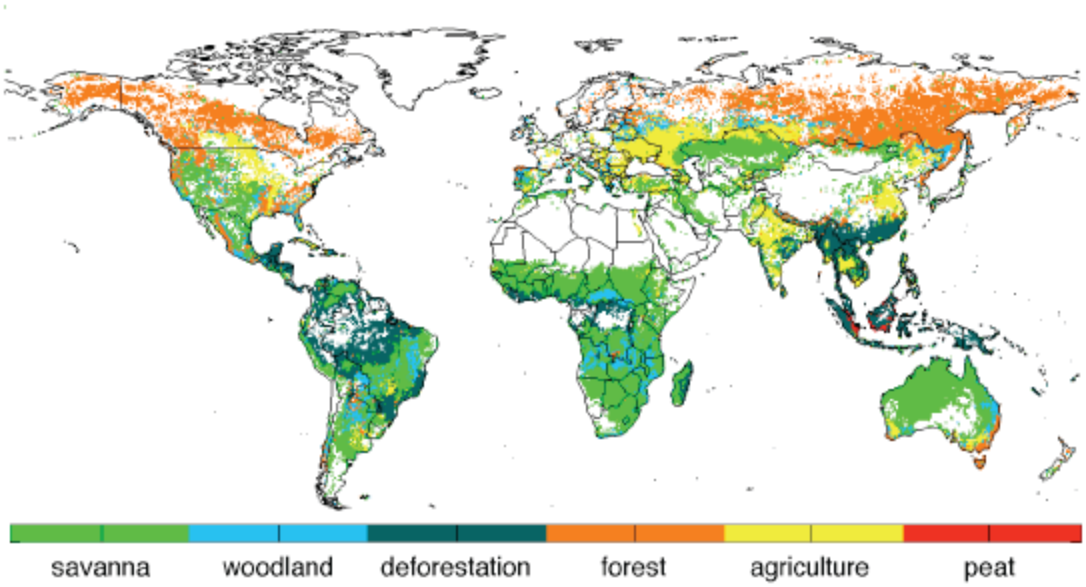

Emissions

- Fuels (type, moisture)
- Inventory (bottom-up) vs. Fire Energy
- Emission factors (related to fuel type) and relationship with temperature
- Combustion completeness
- Flaming : Smoldering ratio

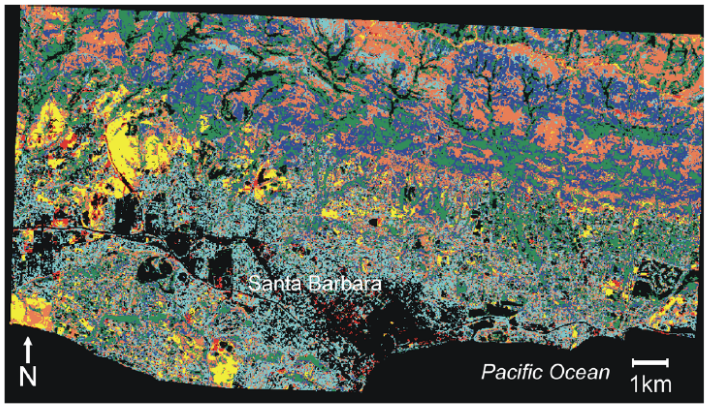

Dennison & Roberts, 2003

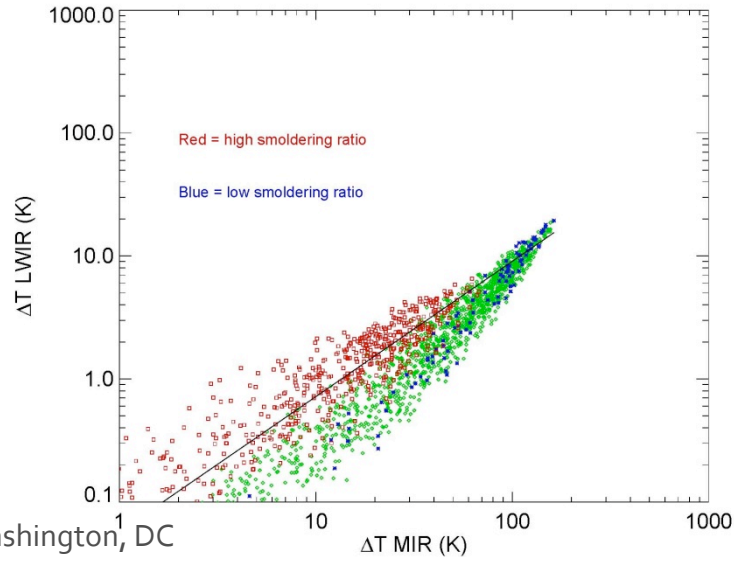

FRP

- Reconcile discrepancies between sensors
  - Errors due to spatial distribution of fires, sensor characteristics (PSF), spatial/temporal resolution

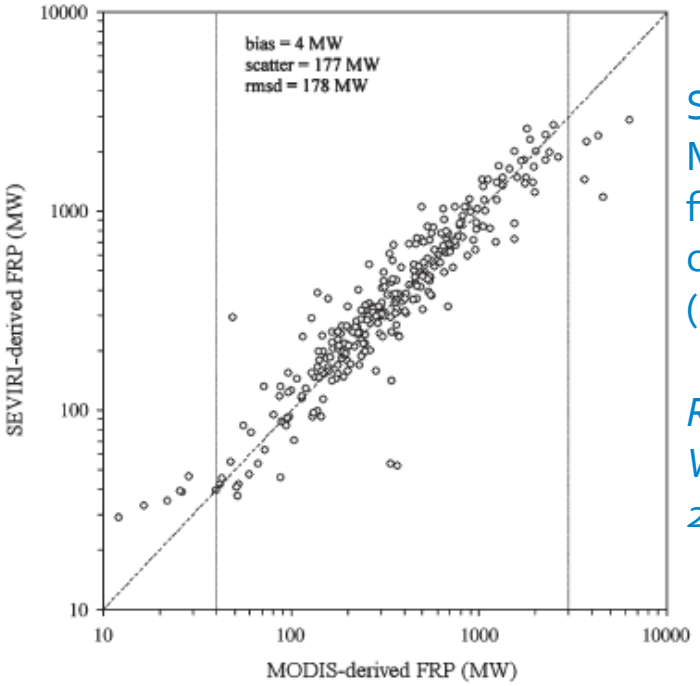

SEVIRI vs. MODIS per-fire FRP comparison (289 "fires").

Roberts & Wooster, 2008

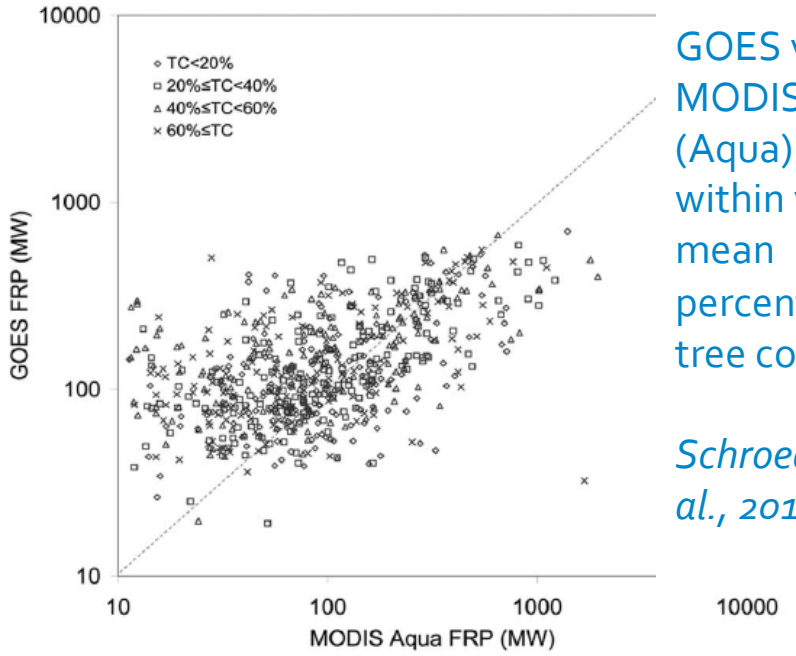

GOES vs. MODIS (Aqua) FRP within varying mean percentage of tree cover

Schroeder et al., 2010

FRP > FRE > Emissions

- Fire Radiative Energy

Ellicott et al., 2009; Vermote et al., 2009

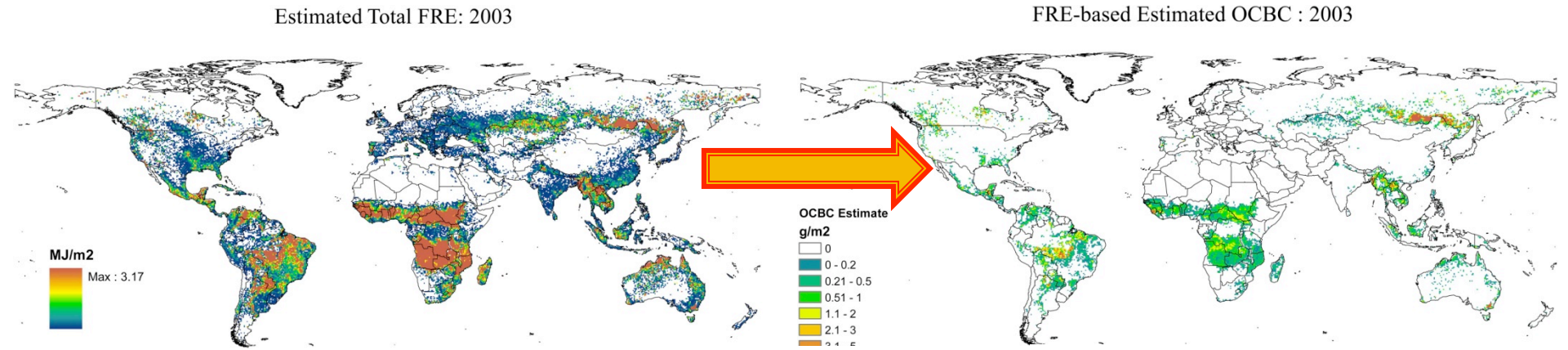

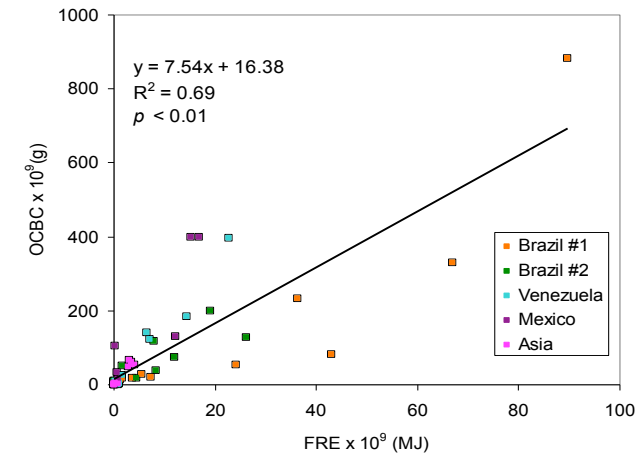

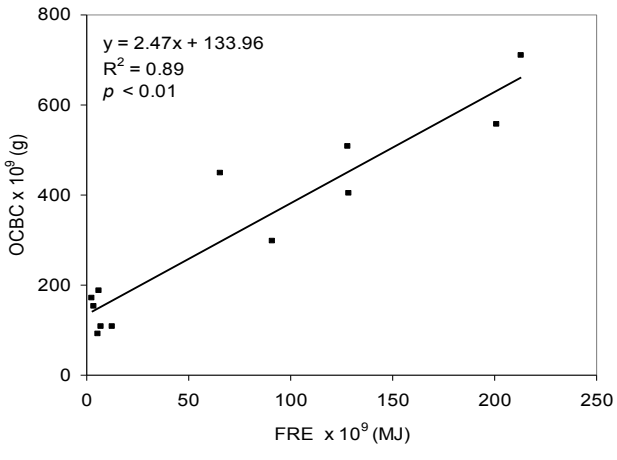

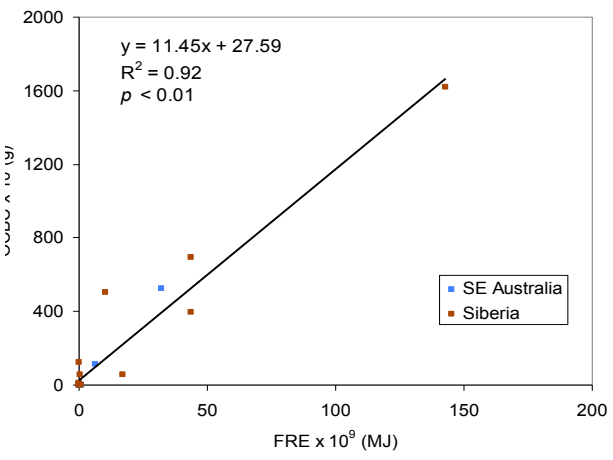

Burned Area

- Agriculture fires
  - Till vs. No-Till
  - Till vs. Harvested
  - Harvested vs. Burnt
  - Burnt vs. Till

Example of the mosaic of recently burned fields, newly harvested, plowed fields where the spectral resolution of Landsat ETM+ is insufficient for producing an accurate thematic map

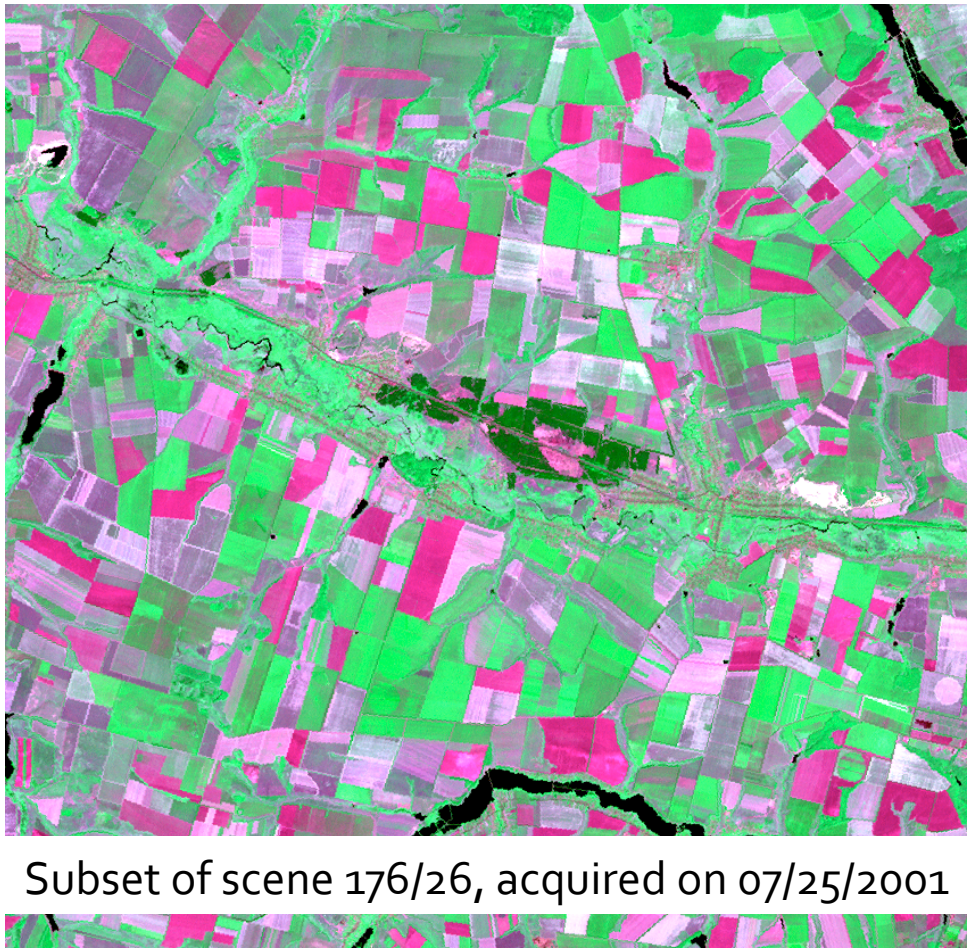

Subset of scene 176/26, acquired on 07/25/2001

Courtesy of Luigi Boschetti

Limitations

VSWIR – TIR swath mismatch

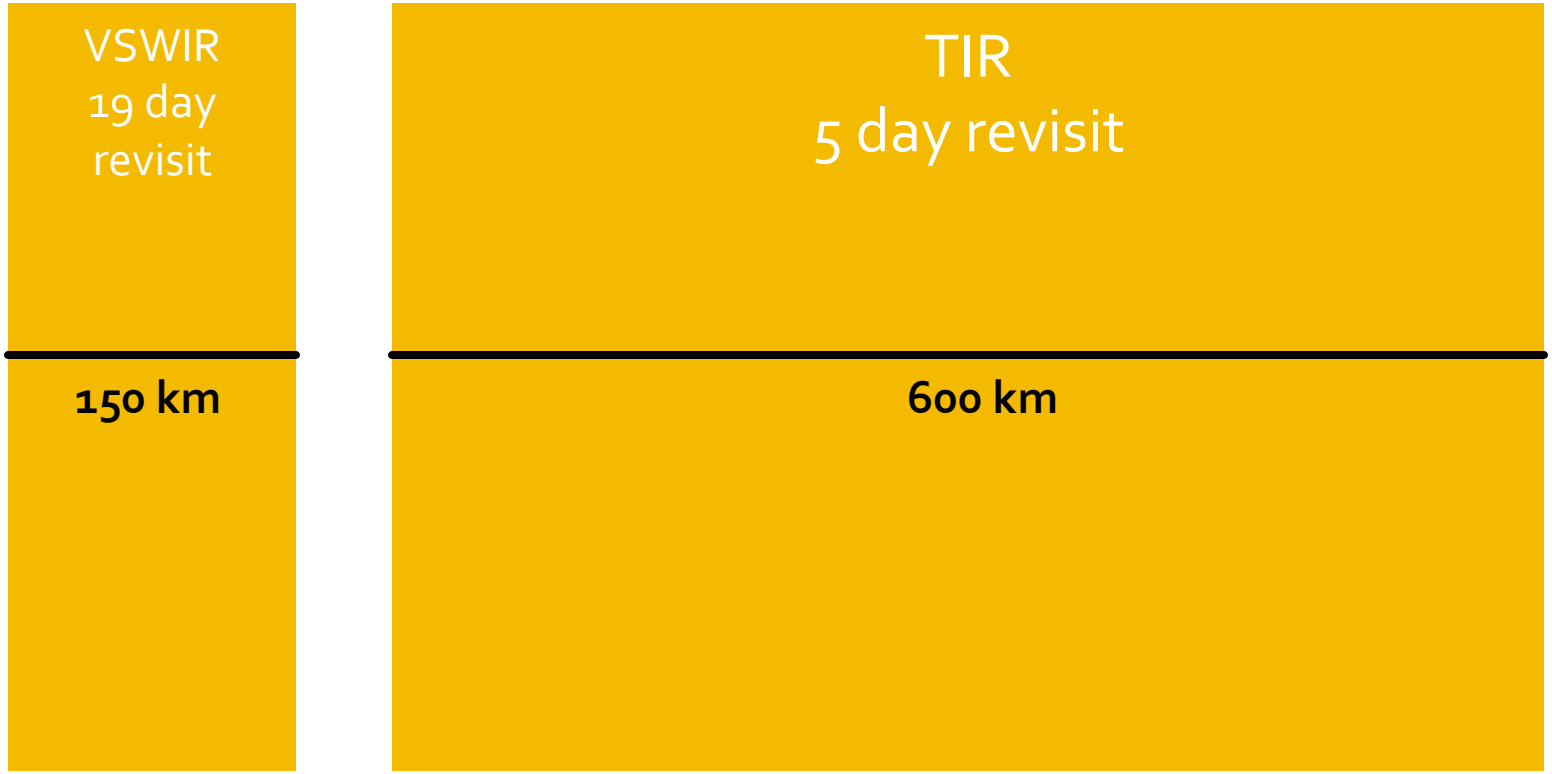

Cloud Cover

5 – 19 day repeat at the equator, the region most responsible for biomass burning and LCLUC

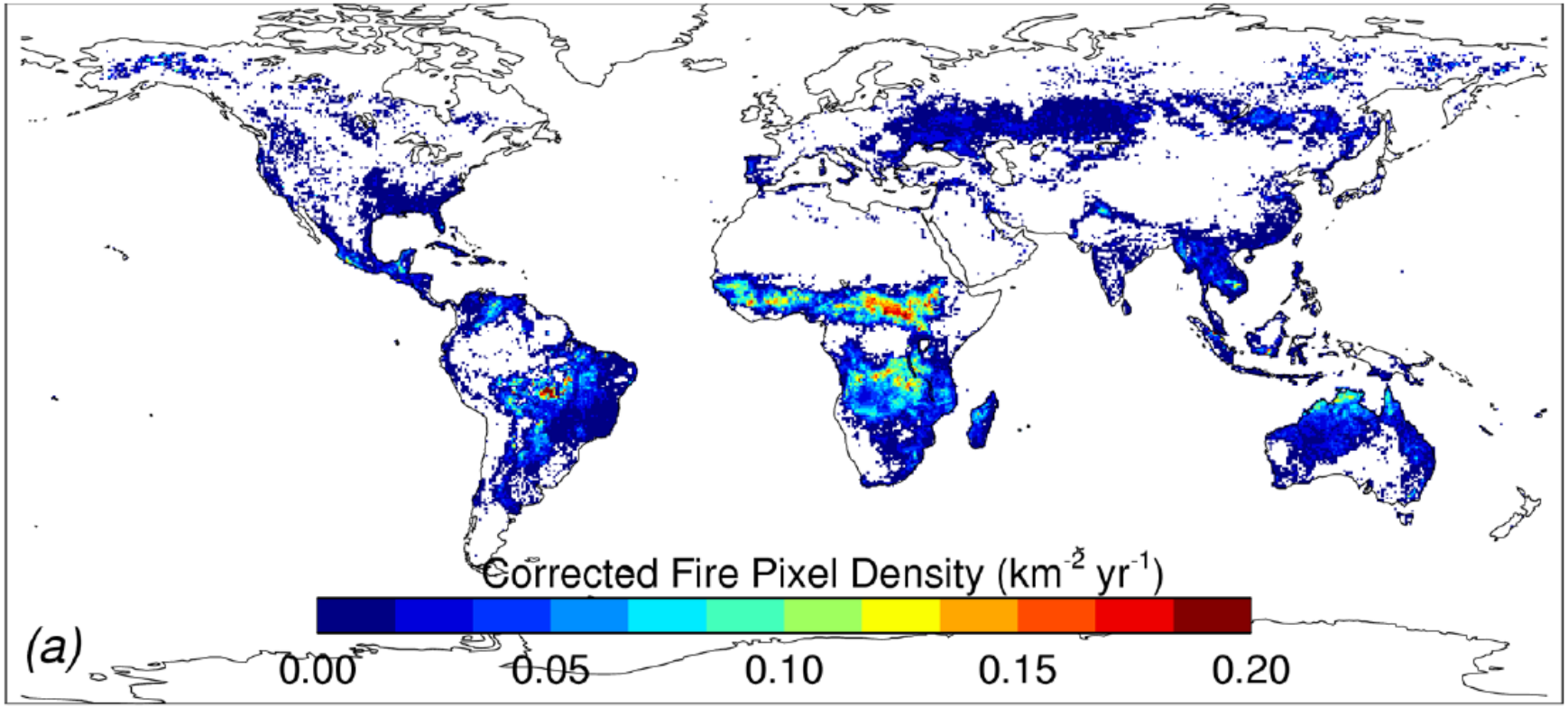

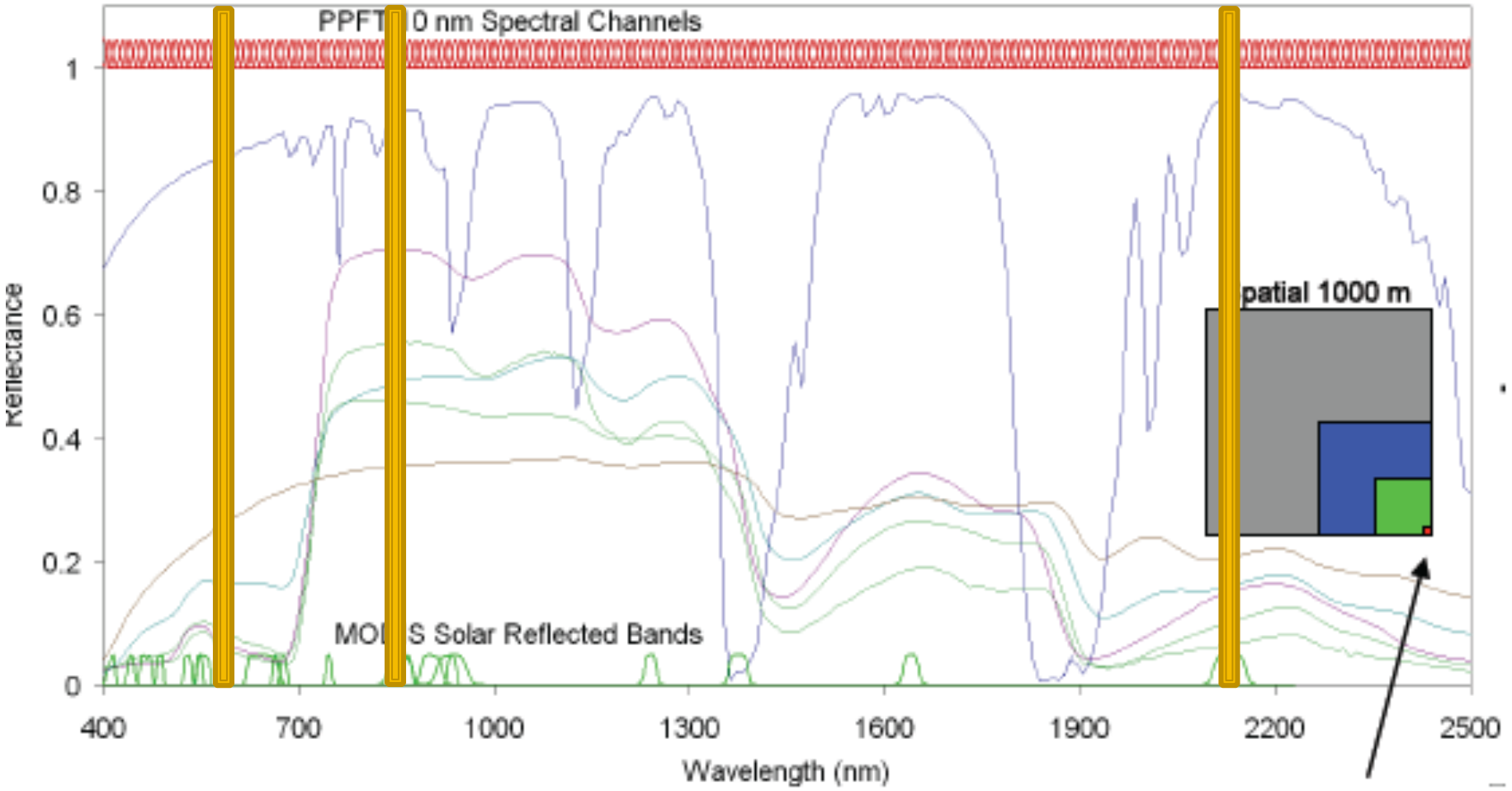

0.65 - Sun glint and coastal false alarm rejection, cloud masking
0.86 - Bright surface, sun glint, coastal alarm rejection, cloud masking
2.1 - Sun glint and coastal alarm rejection

Sun Glint

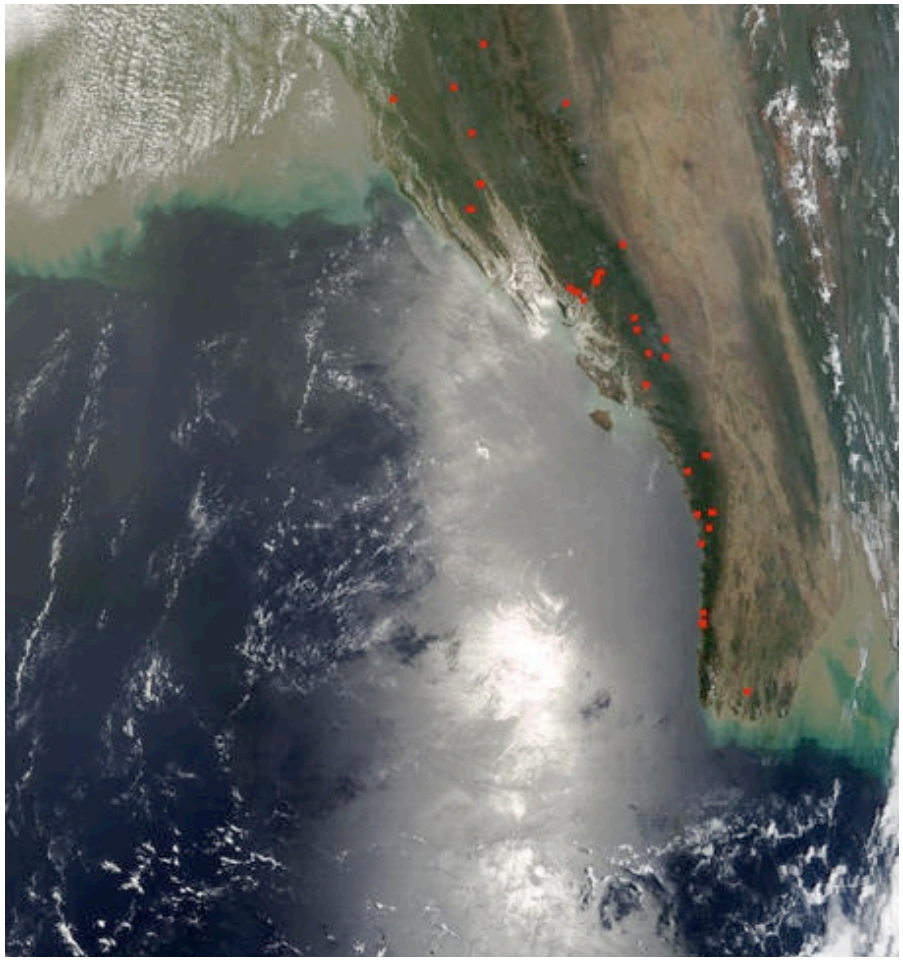

Need reflective bands to identify glint, otherwise detection algorithm can be fooled into thinking that glint-contaminated pixels contain fires.

Most, if not all, of the fire pixels in this scene are true fires. Note how MODIS algorithm continues to function (albeit in a degraded mode) in areas affected by sun glint.

Cloud Mask

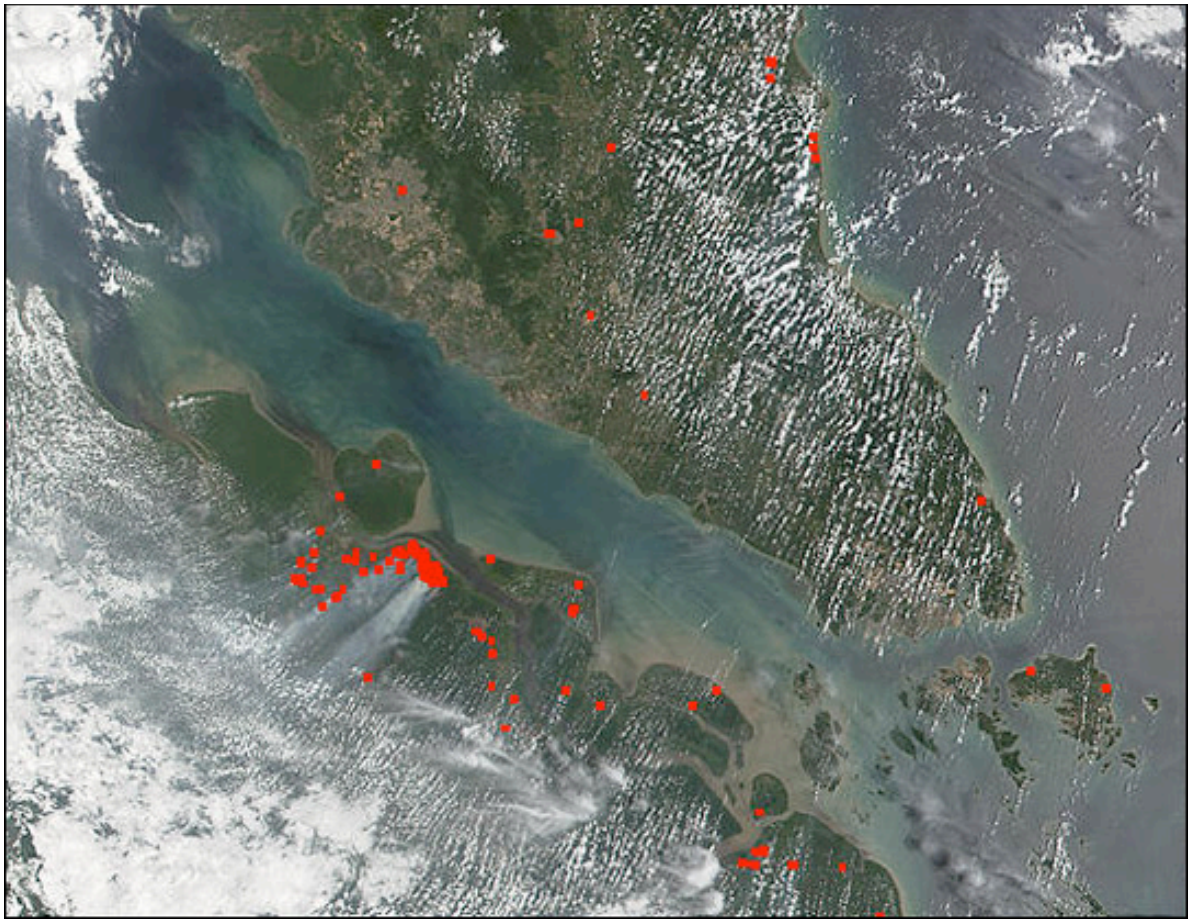

Detection algorithm must function in the presence of small, convective clouds, which in some ways resemble small fires during the daytime.

Coastal Alarm Rejection

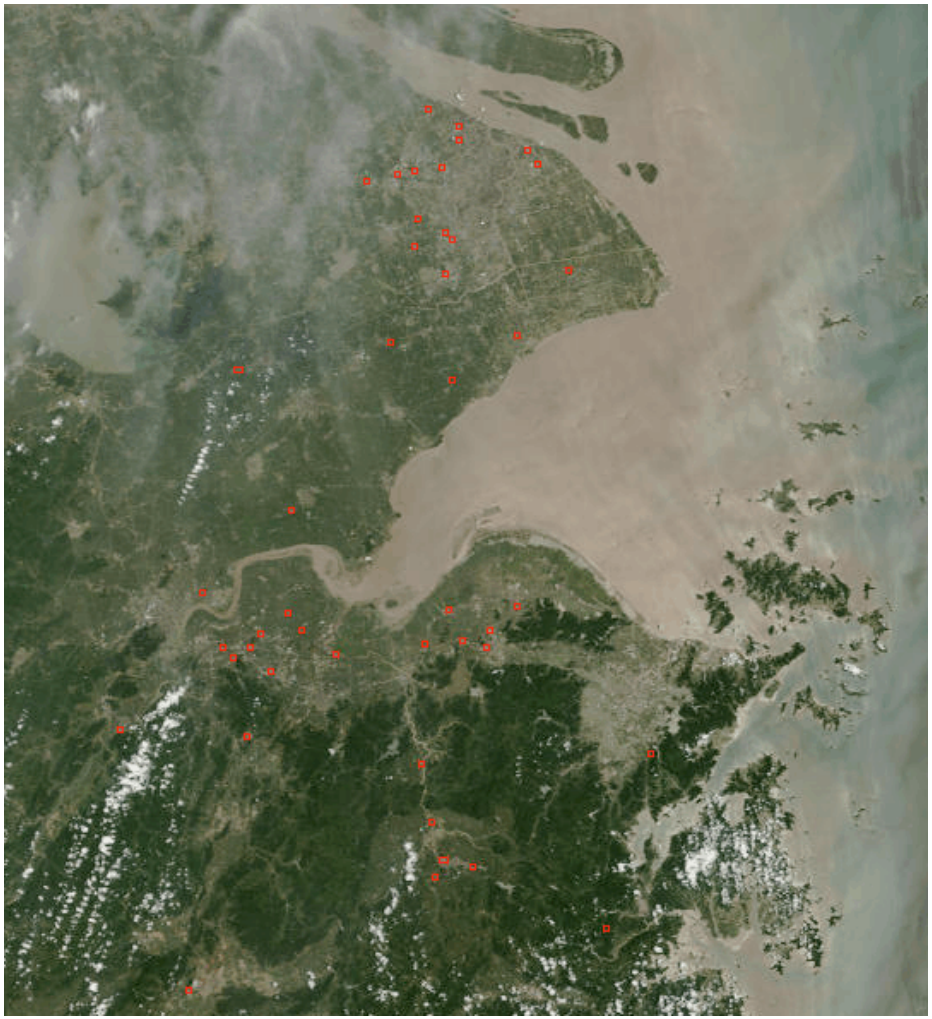

This rejection test helps to eliminate false alarms caused by cooler water pixels contaminating the contextual background. Note: We will need a 60 m land/sea mask for HyspIRI active fire detection and burned area mapping.

Terra MODIS
Shanghai - 18 July
2004, 02:45 UTC

Conclusions

- HyspIRI will provide unique capabilities for fine spectral and spatial characterization of wildfires (fuels, energy, emissions)
- While offering cal/val opportunities for coarser resolution sensors
- Improve our understanding of fire behavior as a function vegetative condition, microclimate conditions, land cover / land use, etc.

Conclusions

- Science, not operational
- Regular monitoring of wildfires not possible with such a large gap in repeat visits
  - Rather, the opportunities will exist to generate a robust snapshot of data understanding fires in a given time and place.
- 3 year mission (hopefully to see add-on missions) is too short for long term records needed.
- Persistent cloud cover and 19-day repeat time means the tropics will have limited "looks".

Potential of HyspIRI for post-fire assessments

Sander Veraverbeke, S. Harris, G. Hulley and S. Hook (JPL)

© 2011 California Institute of Technology. Jet Propulsion Laboratory, California Institute of Technology. Government sponsorship acknowledged.

Some terminology

Veraverbeke, S., Lhermitte, S., Verstraeten, W.W., & Goossens, R., (2010). *The temporal dimension of differenced Normalized Burn Ratio (dNBR) fire/burn severity studies: the case of the large 2007 Peloponnese wildfires in Greece*. Remote Sensing of Environment 114, 2548-2563

SEVERITY: degree of environmental change caused by a fire

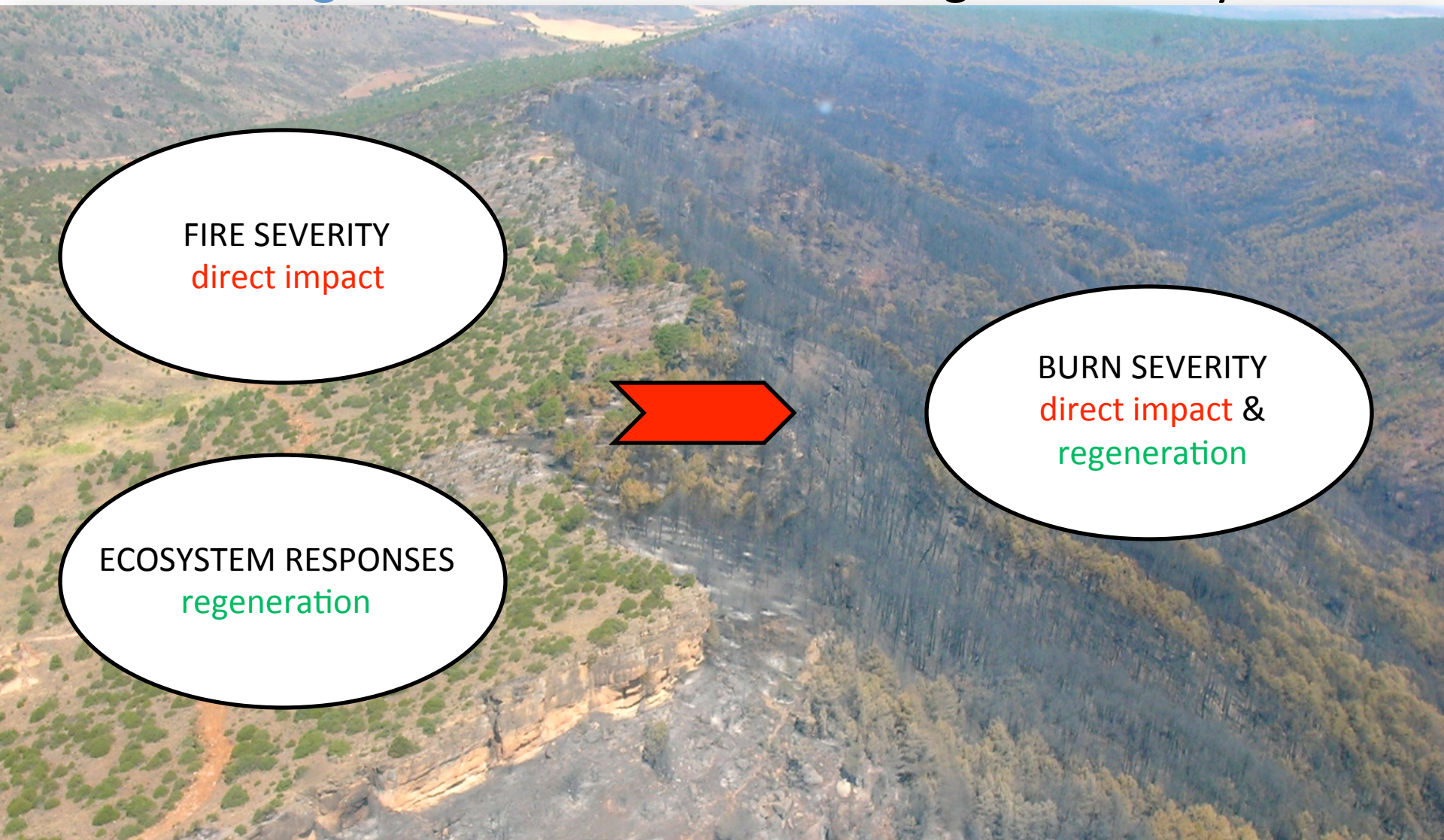

Importance

Trace gas emission estimates and carbon sequestration → Earth's carbon budget

Post-fire management (erosion prevention, rehabilitation)

Are they changing?

Airborne MASTER

As a surrogate to study HyspIRI's potential…

MASTER	HyspIRI
11 VNIR bands	Hyperspectral VSWIR
14 SWIR bands	
15 MIR bands	8 MTIR bands
10 TIR bands	
5-50 m pixel size	60 m pixel size

Application 1: Burned area mapping

Whole bunch of indices currently in use, most of them relying on the VSWIR region

e.g. NDVI, NBR, BAI, SAVI, etc.

Which indices are the best to map burned areas?

And what could the MIR-TIR regions add?

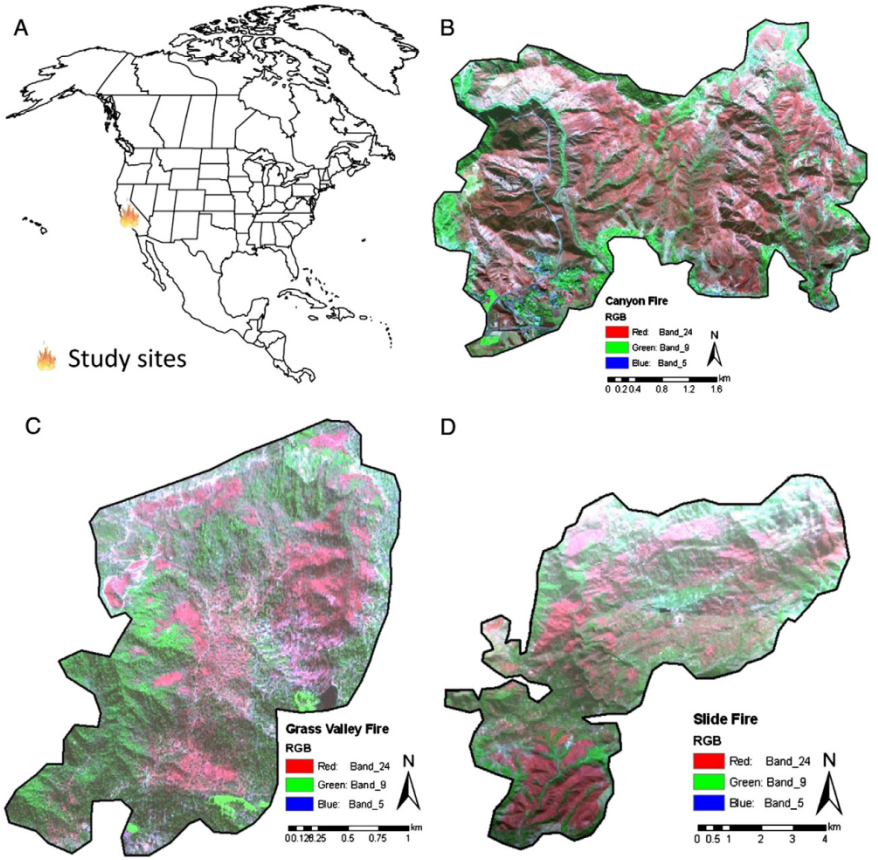

Spectral separability measured by:

$$M = \frac{\mu_b - \mu_u}{\sigma_b - \sigma_u}$$

The higher M, the better

Veraverbeke, S., Harris, S. & Hook, S. (2011). *Evaluating spectral indices for burned area discrimination using MODIS/ASTER (MASTER) airborne simulator data*. Remote Sensing of Environment 115, 2702-2709

Application 1: Burned area mapping

Table 3
Spectral indices tested in this study (B: Blue, R: Red, NIR: Near Infrared, SSWIR: shorter short wave infrared, LSWIR: longer short wave infrared, MIR: mid infrared, TIR: thermal infrared, E: emissivity and T_s: surface temperature, see Section 2.3 for specifications on wavelength intervals).

Index	Abbreviation	Formula	Reference
Normalized Difference Vegetation Index	NDVI	$NDVI = \frac{NIR-R}{NIR+R}$	Tucker, 1979
Global Environment Monitoring Index	GEMI	$GEMI = \gamma(1-0.25\gamma) - \frac{R-0.125}{1-R}$ with $\gamma = \frac{2(NIR^2-R^2)+1.5NIR+0.5R}{NIR+R+0.5}$	Pinty and Verstraete, 1992
Enhanced Vegetation Index	EVI	$EVI = 2.5\frac{NIR-R}{NIR-6R-7.5B+1}$	Huete et al., 2002
Vegetation Index 3	VI3	$VI3 = \frac{NIR-MIR}{NIR+MIR}$	Kaufman and Remer, 1994
Soil Adjusted Vegetation Index	SAVI	$SAVI = (1+L)\frac{NIR-R}{NIR+R+L}$ with L=0.5	Huete, 1988
Modified Soil Adjusted Vegetation Index	MSAVI	$MSAVI = \frac{2NIR+1-\sqrt{(2NIR+1)^2-8(NIR-R)}}{2}$	Qi et al., 1994
Burned Area Index	BAI	$BAI = \frac{1}{(0.1+R)^2+(0.06+NIR)^2}$	Chuvieco et al., 2002
Global Environment Monitoring Index 3	GEMI3	$GEMI3 = \gamma(1-0.25\gamma) - \frac{MIR-0.125}{1-MIR}$ with $\gamma = \frac{2(NIR^2-MIR^2)+1.5NIR+0.5MIR}{NIR+MIR+0.5}$	Barbosa et al. 1999b
Normalized Burn Ratio	NBR	$NBR = \frac{NIR-LSWIR}{NIR+LSWIR}$	Key and Benson, 2005
Char Soil Index	CSI	$CSI = \frac{NIR}{SWIR}$	Smith et al., 2007
Mid Infrared Burn Index	MIRBI	$MIRBI = 10LSWIR - 9.8SSWIR + 2$	Trigg and Flasse, 2001
Normalized Difference Vegetation Index Thermal	NDVIT	$NDVIT = \frac{NIR-R\times TIR}{NIR+R\times TIR}$	Smith et al., 2007
Soil Adjusted Vegetation Index Thermal	SAVIT	$SAVIT = (1+L)\frac{NIR-R\times TIR}{NIR+R\times TIR+L}$ with L=0.5	Smith et al., 2007
Normalized Burn Ratio Thermal	NBRT	$NBRT = \frac{NIR-LSWIR\times TIR}{NIR+LSWIR\times TIR}$	Holden et al., 2005
Char Soil Index Thermal	CSIT	$CSIT = \frac{NIR}{SWIR\times TIR}$	Smith et al., 2007
Vegetation Index 6 Thermal	VI6T	$VI6T = \frac{NIR-TIR}{NIR+TIR}$	Holden et al., 2005
NIR-SWIR-Emissivity Version 1	NSEv1	$NSEv1 = \frac{NIR-LSWIR}{NIR+LSWIR}\times E$	This study
NIR-SWIR-Emissivity Version 2	NSEv2	$NSEv2 = \frac{NIR-(LSWIR+E)}{NIR+LSWIR+E}$	This study
NIR-SWIR-Temperature Version 1	NSTv1	$NSTv1 = \frac{NIR-LSWIR}{NIR+LSWIR}\times T_S$	This study
NIR-SWIR-Temperature Version 2	NSTv2	$NSTv2 = \frac{NIR-(LSWIR+T_s)}{NIR+LSWIR+T_s}$	This study

Table 4
MODIS/ASTER (MASTER) airborne simulator bands revealing the best spectral separability M for each spectral region. These bands were used to generate the indices listed in Table 3 (B: Blue, R: Red, NIR: Near Infrared, SSWIR: shorter short wave infrared, LSWIR: longer short wave infrared, MIR: mid infrared, TIR: thermal infrared, E: emissivity and T_s: surface temperature, see Section 2.3 for specifications on wavelength intervals).

Spectral region	MASTER band (μm)	M statistic (average over three fires)
B	0.45 to 0.48	0.15
R	0.65 to 0.68	0.13
NIR	0.86 to 0.88	0.64
SSWIR	1.59 to 1.62	0.09
LSWIR	2.31 to 2.36	0.58
MIR	3.54 to 3.64	0.71
TIR	8.51 to 8.76	0.58

Table 5
M values of the spectral indices over the Canyon, Grass Valley and Slide fires. Values higher than one are given in bold. For explanation on the indices, reference is made to Table 3 and Section 2.3.

Spectral indices	Canyon fire	Grass Valley fire	Slide fire	Average over three fires
NDVI	**1.22**	0.42	0.78	0.80
GEMI	0.07	0.04	0.06	0.06
EVI	0.28	0.10	0.04	0.14
VI3	**1.30**	**1.29**	0.83	**1.14**
SAVI	**1.42**	0.55	0.83	0.94
MSAVI	0.23	0.25	0.13	0.21
BAI	0.34	0.47	0.07	0.29
GEMI3	0.04	0.03	0.01	0.03
NBR	**1.46**	**1.00**	0.94	**1.13**
CSI	0.04	0.00	0.00	0.01
MIRBI	0.67	0.76	0.55	0.66
NDVIT	0.92	0.22	0.42	0.52
SAVIT	0.88	0.21	0.41	0.50
NBRT	0.08	0.03	0.16	0.09
CSIT	0.04	0.00	0.00	0.01
VI6T	0.66	0.92	0.36	0.65
NSEv1	**1.47**	0.88	**1.06**	**1.13**
NSEv2	**1.57**	**1.02**	**1.07**	**1.22**
NSTv1	**1.47**	0.88	**1.06**	**1.14**
NSTv2	0.71	0.96	0.41	0.69

Application 1: Burned area mapping

Potential of MIR and TIR data in synergy with the traditionally used NIR and SWIR regions

Slightly better results than NBR

Tough currently unavailable on moderate resolution spaceborne sensors

HyspIRI will meet the requirements

Application 2: Fire severity

Traditionally assessed with Landsat dNBR

$$NBR = \frac{NIR - LSWIR}{NIR + LSWIR}$$

Caveats
- bi-temporal differencing requires image-to-image normalization
- rapid assessments over active fires impeded as the NIR band is affected by smoke

MASTER imagery over the active Wallow fire, AZ

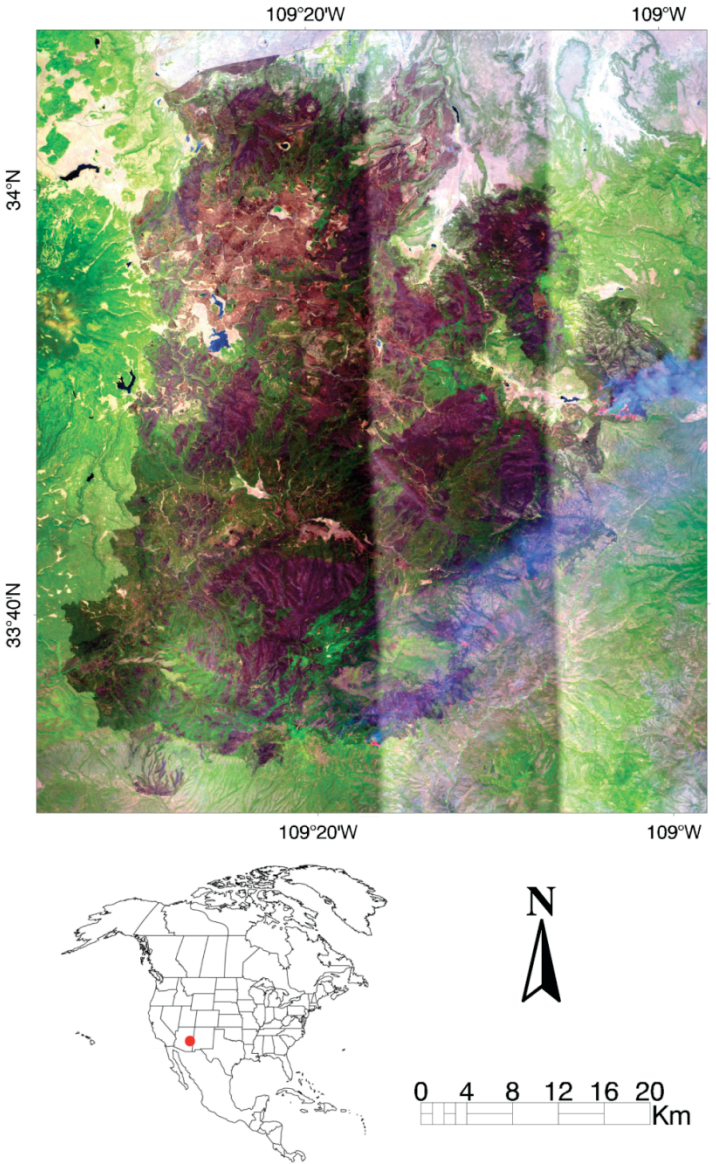

Application 2: Fire severity

We want maximal discrimination between fire-related and non-fire related terrain features
Does NBR do so?
An alternative index, unimpeded by smoke, the SWIR-MIR index: $SMI = \frac{SSWIR - MIR}{SSWIR + MIR}$

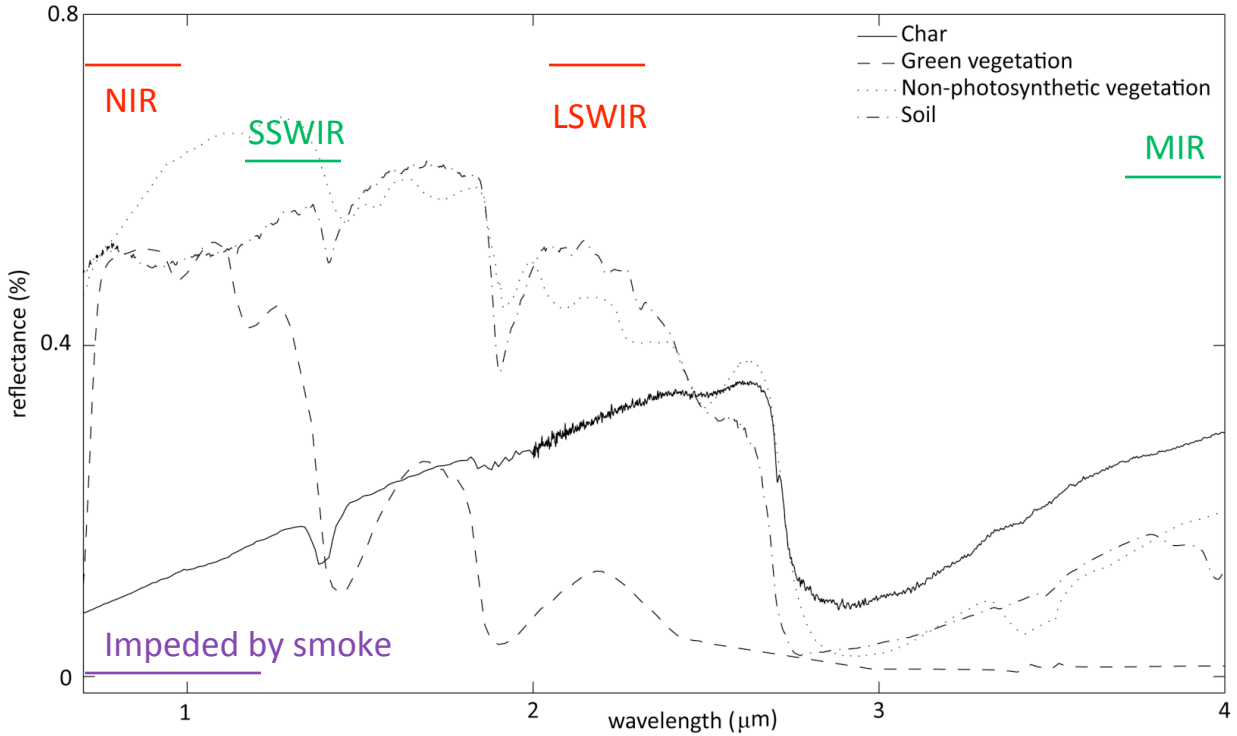

	NIR	SSWIR	LSWIR	MIR	*NBR*	*SMI*
Char	0.107	0.235	0.316	0.241	*-0.494*	*-0.013*
Green vegetation	0.517	0.225	0.124	0.012	*0.612*	*0.899*
Non-photosynthetic vegetation	0.577	0.595	0.453	0.122	*0.120*	*0.660*
Soil	0.501	0.610	0.494	0.139	*0.007*	*0.629*

Application 2: Fire severity

SMI

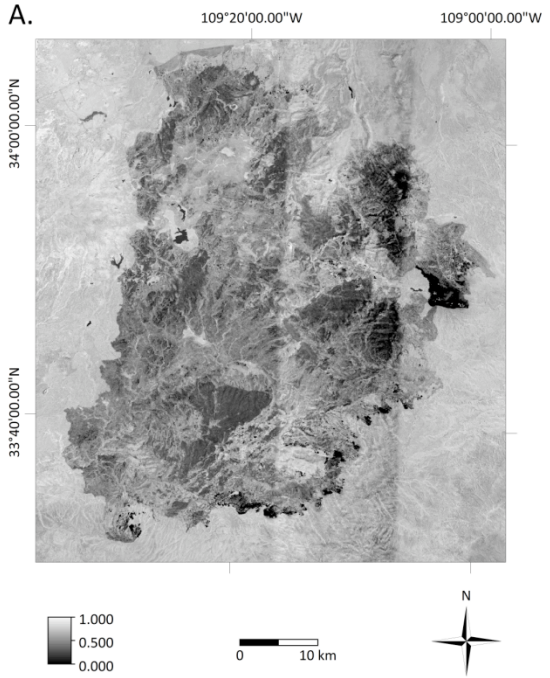

SMI-approach

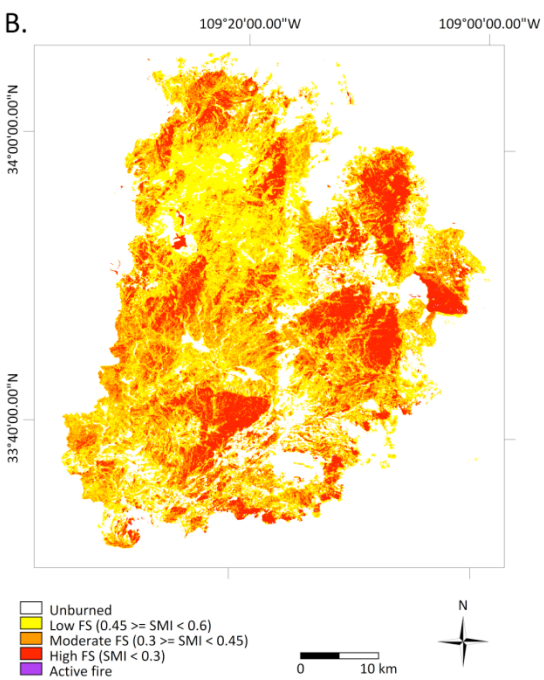

BARC-approach

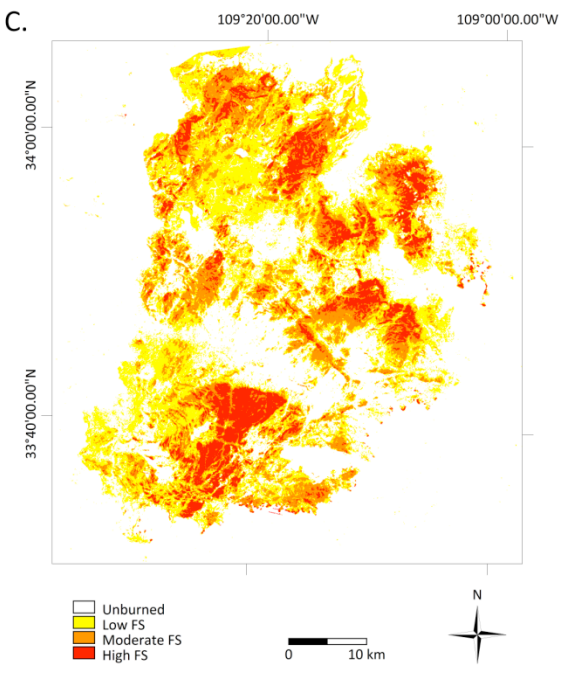

		BARC approach			
		Unburned	Low FS	Moderate FS	High FS
SMI approach	Unburned	0.54	0.03	0.01	0.00
	Low FS	0.08	0.08	0.03	0.01
	Moderate FS	0.04	0.04	0.04	0.02
	High FS	0.02	0.02	0.03	0.03

Total agreement	0.68
Kappa coefficient	0.43

Application 2: Fire severity

Benefits of SMI:
- not impeded by smoke
- mono-temporal

→ Allows timely assessments

Further testing required (field data, different ecosystems)

Tough currently unavailable on moderate resolution spaceborne sensors

HyspIRI will fill the gap

Application 2: Further research

92 GeoCBI (Composite Burn Index) plots, sampled August 2-15, 2011

$$GeoCBI = \frac{\sum_{m_1}^{m_n} CBI_m \cdot FCOV_m}{\text{of strata } \sum_{m_1}^{m_n} FCOV_m}$$

where m refers to each vegetation stratum and n is the number

GeoCBI 3

GeoCBI 2.39

GeoCBI 1.14

Stratum	Burn severity scale						
	No effect	Low		Moderate		High	
	0	0.5	1	1.5	2	2.5	3
Substrates				FCOV			
Litter (l)/Light Fuel (lf) Consumed	0 %	--	50 % l	--	100 % l	> 80 % lf	98 % lf
Duff	0 %	--	Light char	--	50 %	--	Consumed
Medium/Heavy Fuel	0 %	--	20 %	--	40 %	--	> 60 %
Soil & Rock Cover/Colour	0 %	--	10 %	--	40 %	--	> 80 %
Herbs, low shrubs and trees less than 1 m				FCOV			
% Foliage Altered	0 %	--	30 %	--	80 %	95 %	100 %
Frequency % Living	100 %	--	90 %	--	50 %	< 20 %	0 %
New sprouts	Abundant	--	Moderate-high	--	Moderate	--	Low-none
Tall shrubs and trees 1 to 5 m				FCOV			
% Foliage Altered	0 %	--	20 %	--	60-90 %	> 95 %	branch loss
Frequency % Living	100 %	--	90 %	--	30 %	< 15 %	< 1 %
LAI Change %	0 %	--	15 %	--	70 %	90 %	100 %
Intermediate trees 5 to 20 m				FCOV			
% Green (Unaltered)	100 %	--	80 %	--	40 %	< 10 %	none
% Black/Brown	0 %	--	20 %	--	60-90 %	> 95 %	branch loss
Frequency % Living	100 %	--	90 %	--	30 %	< 15 %	< 1 %
LAI Change %	0 %	--	15 %	--	70 %	90 %	100 %
Char Height	none	--	1.5 m	--	2.8 m	--	> 5 m
Big trees >20 m				FCOV			
% Green (Unaltered)	100 %	--	80 %	--	50 %	< 10 %	none
% Black/Brown	0 %	--	20 %	--	60-90 %	> 95 %	branch loss
Frequency % Living	100 %	--	90 %	--	30 %	< 15 %	< 1 %
LAI Change %	0 %	--	15 %	--	70 %	90 %	100 %
Char Height	none	--	1.8 m	--	4 m	--	> 7 m

Summary

Current post-fire effects rely heavily on the VSWIR region, especially NBR

MIR and TIR data can add valuable information

Tough the VSWIR-MIR-TIR combination is current not available in moderate resolution (< 100 m)

The VSWIR-MTIR synergy will be available on HyspIRI

DON'T START FIRES YOU CAN'T STOP.
BE FIREWISE.
FIREWISE
WILDFIRE
MOVES
QUICKER
THAN YOU
THI

Spatial Scaling of Fire Detection and Temperature Modeling Using SWIR Imaging Spectrometer Data

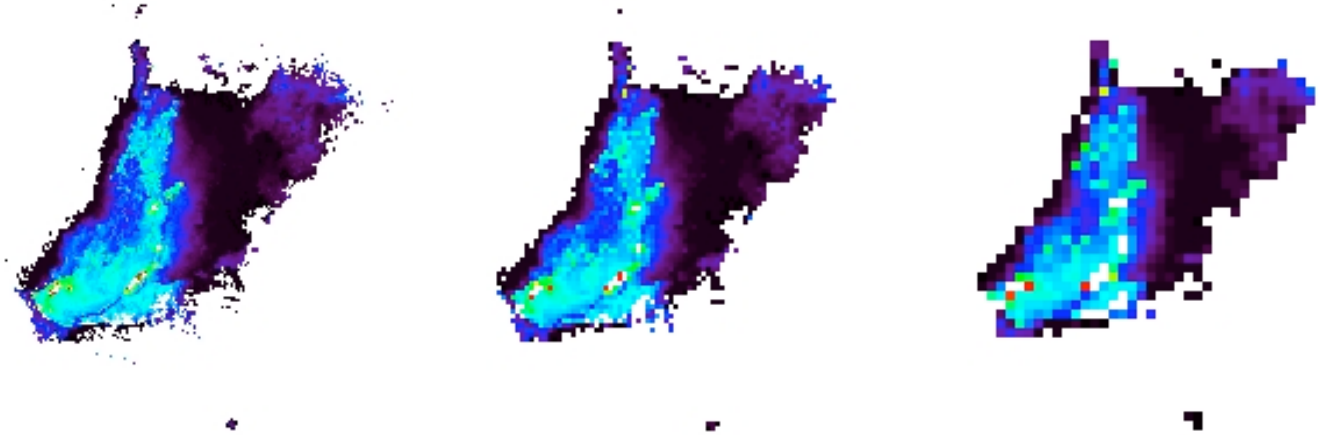

Scott Matheson

Philip Dennison

URSA

Utah Remote Sensing Applications Lab
University of Utah

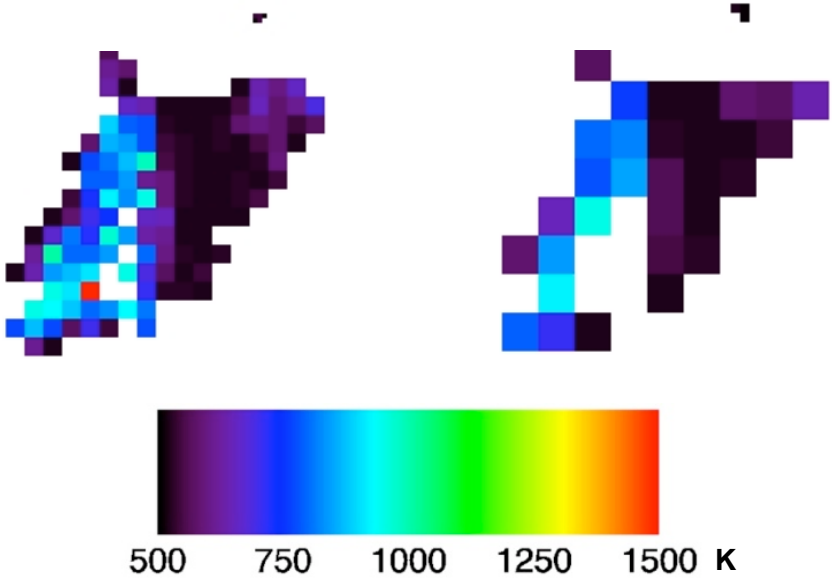

HyspIRI and Fire

- Fire is central to multiple HyspIRI science questions (CQ2, TQ2, VQ3, VQ4)
- Fire properties can be measured using emitted radiance in SWIR, MIR, and TIR spectral regions

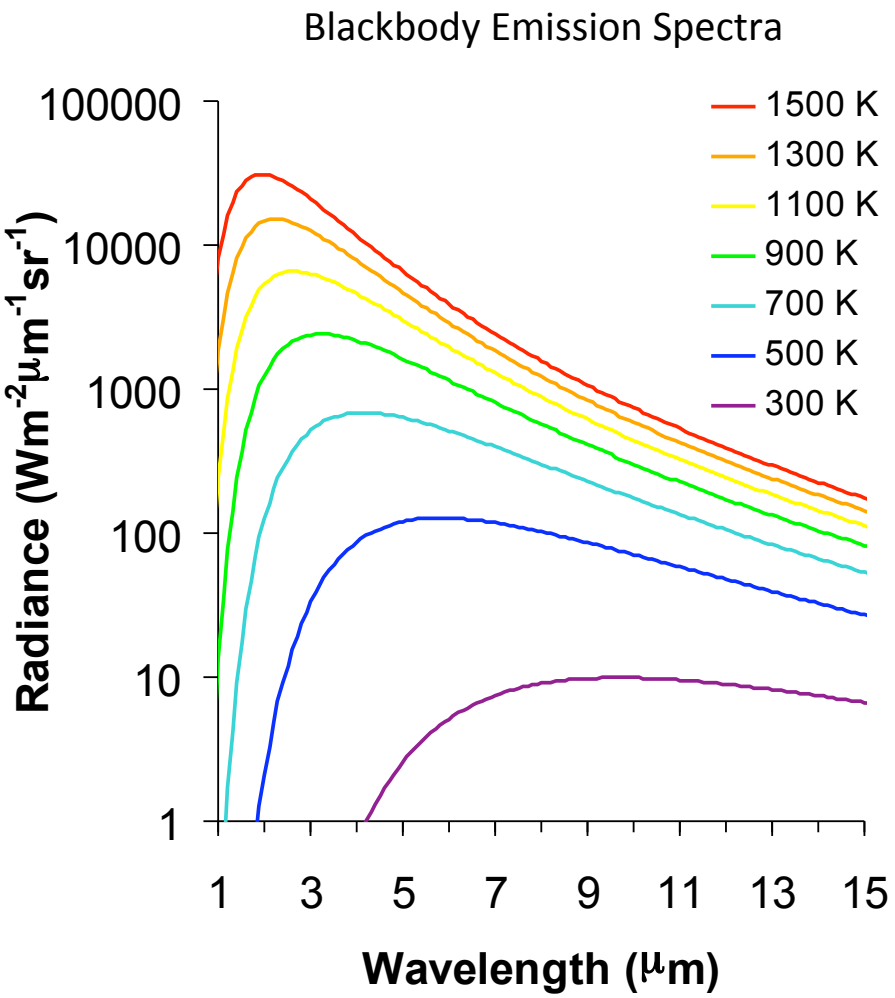

HyspIRI and Fire

- HyspIRI should be able to resolve important science questions related to fire and carbon emissions
  - Multiple bands covering spectral regions with strong emitted radiance
  - 60 m spatial resolution will map small fires

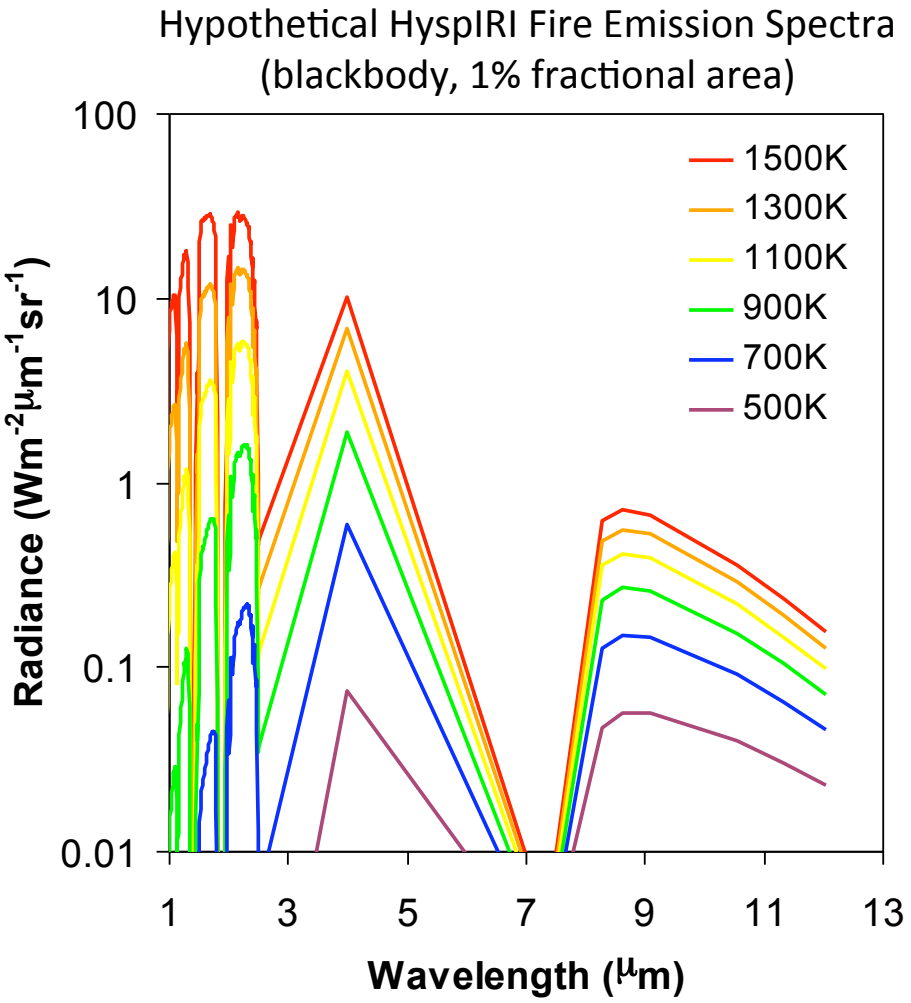

HysplRI and Fire

- The 4 µm channel will continue a legacy of fire radiative power and fire detection
- VSWIR data can offer complementary capabilities for fire characterization
  - More than 100 10 nm bands with low attenuation from smoke will capture detailed spectral shape of fire emission
  - Potential for separation of flaming and smoldering combustion

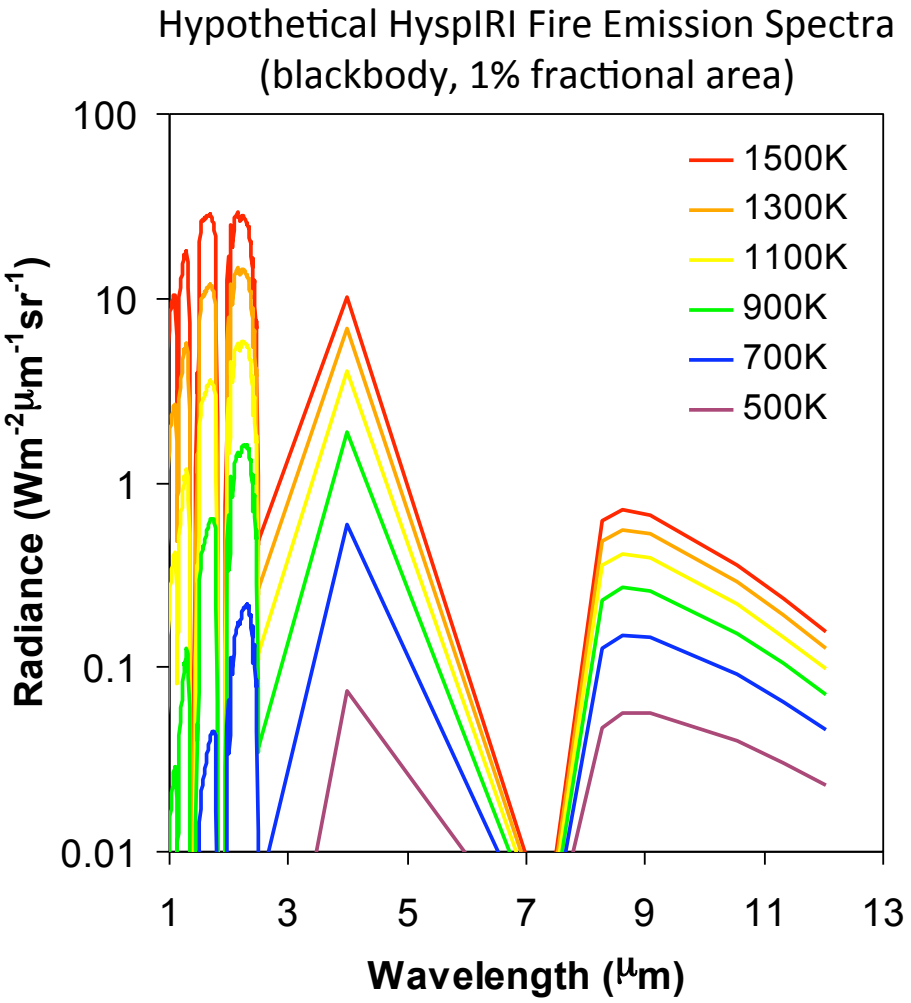

Hyperspectral Fire Detection Index (HFDI)

- Normalized difference ratio using 2060 and 2430 nm bands (Dennison and Roberts, 2009)

2008 Indians Fire

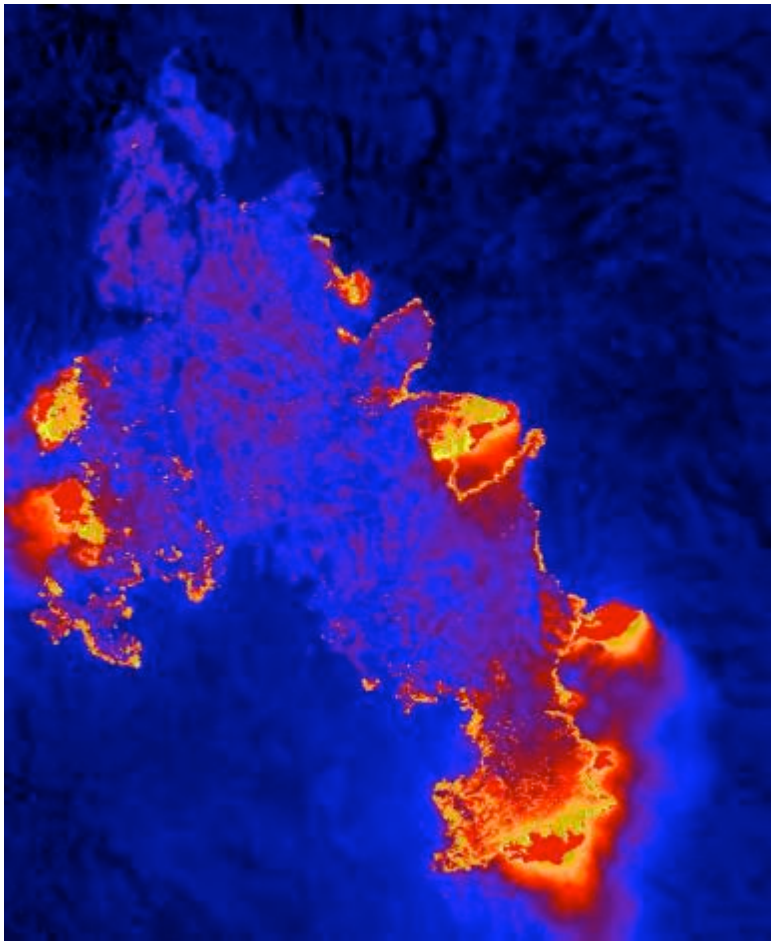

2009 Station Fire

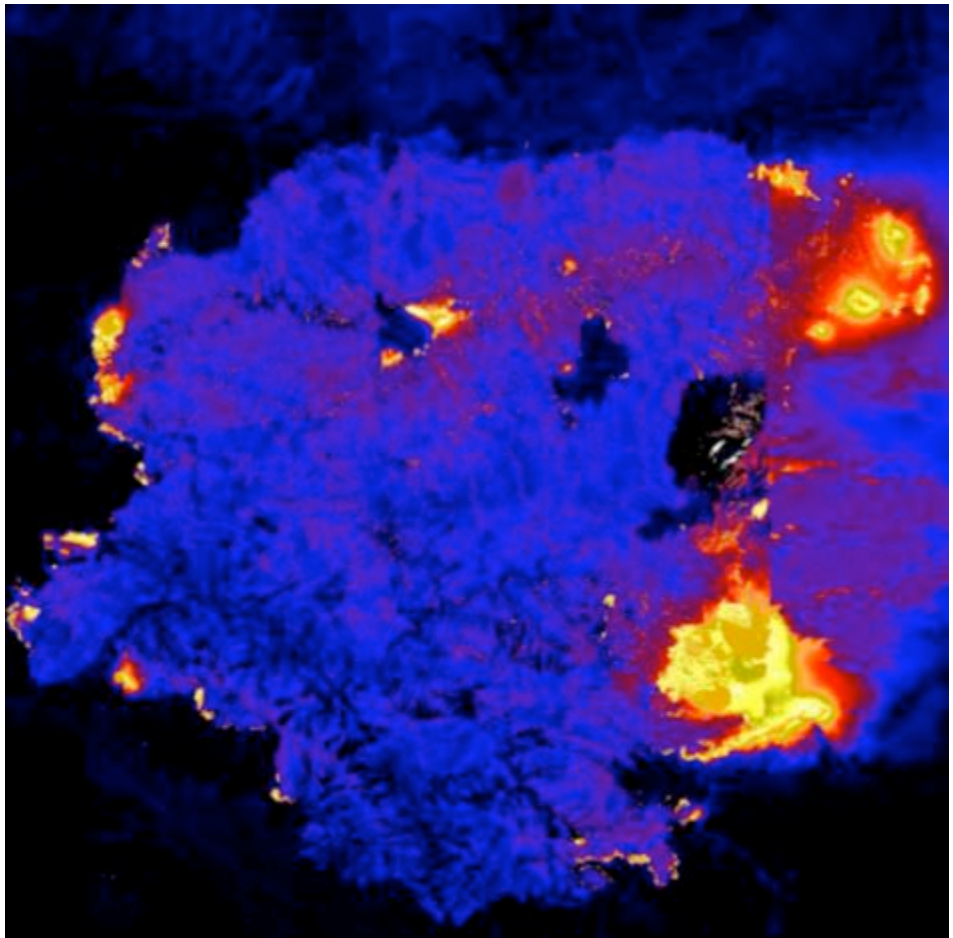

Effective Fire Temperature

- Multiple endmember mixing models can be used to simultaneously retrieve effective fire temperature, fire fractional area, and background land cover (Dennison et al., 2006; Dennison and Matheson, 2011)

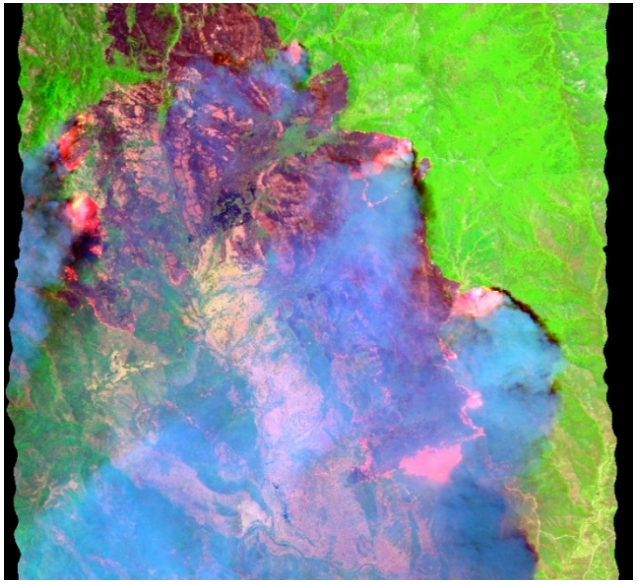

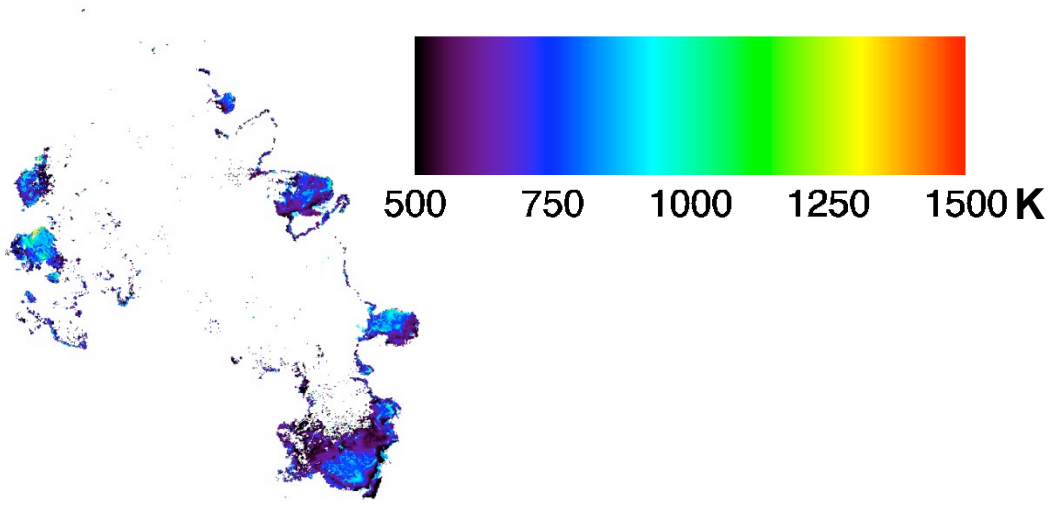

Questions

- How do SWIR fire detection and modeled fire temperature change with coarsening spatial resolution out to 60 m?
- Can AVIRIS data acquired over actives fires provide an approximate SWIR fire saturation threshold at 60 m?

AVIRIS Data

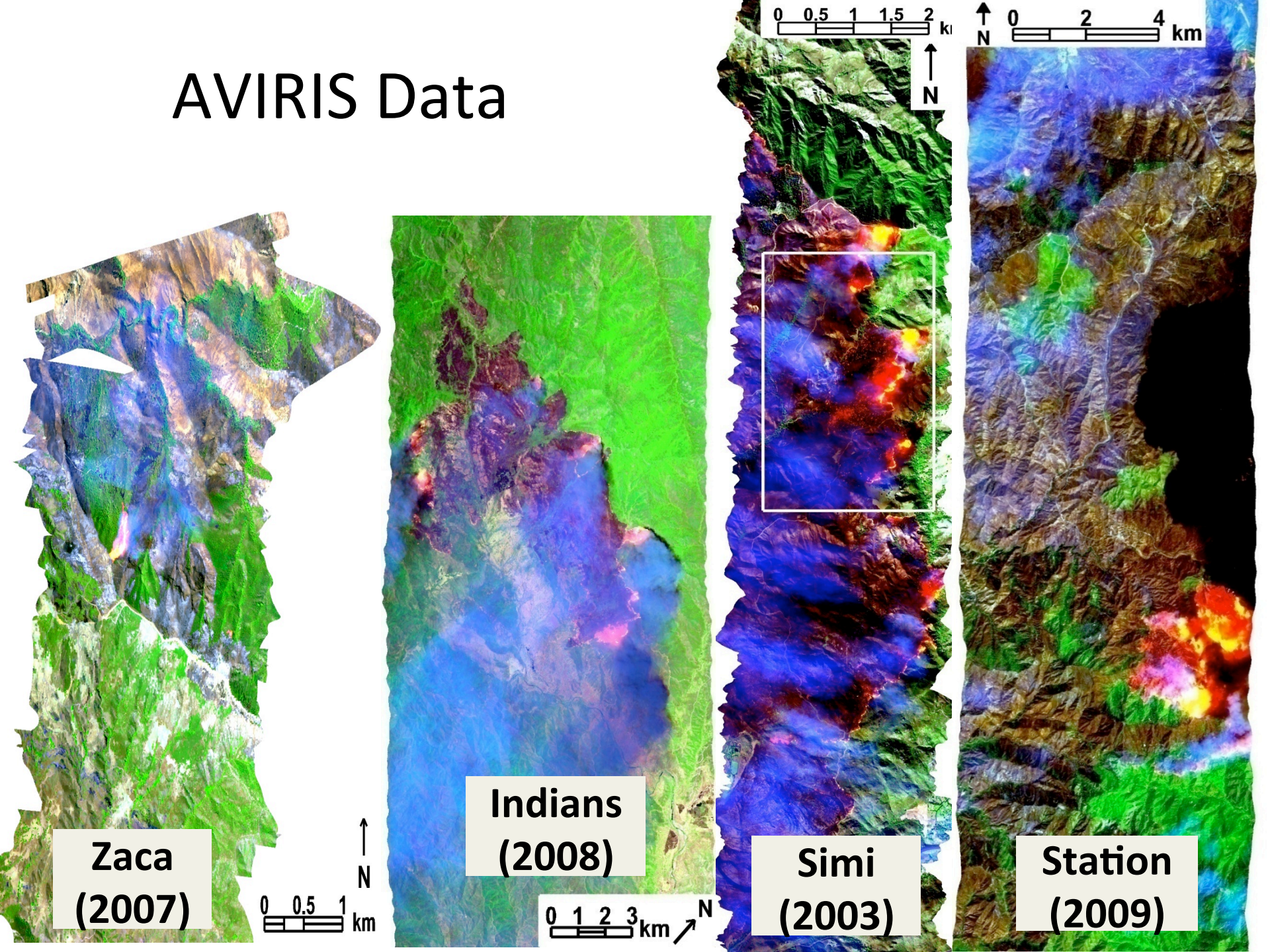
Zaca
(2007)
0 0.5 1
km
N
Indians
(2008)
0 1 2 3
km
N
0 0.5 1 1.5 2
N
Simi
(2003)
N
0 2 4
km
Station
(2009)

Spatial Resampling

- Aggregation and Gaussian resampling were compared for the Simi Fire
- Fire detection and temperature modeling results were similar, so aggregation resampling was used to resample 4 AVIRIS scenes to ~ 60 m
- Saturated bands were excluded from resampling

Fire	Simi	Zaca	Indians	Station
Original Resolution (m)	4.0	3.8	16.1	10.7
Resampled resolutions (m)	8.0, 16.0, 32.0, 64.0	7.6, 15.2, 30.4, 60.8	32.2, 64.4	21.4, 42.8, 64.2

Fire Detection and Temperature Modeling

- HFDI was used to detect burning pixels
- Burning pixels were modeled using a three endmember linear mixing model
  1. Fire emitted radiance
  2. Background reflected radiance
  3. Shade endmember
- Non-burning pixels were modeled using a two endmember model
  1. Background reflected radiance
  2. Shade endmember

Fire Detection and Temperature Modeling

- Background reflected radiance endmembers
  - Selected using iterative endmember selection
  - Selected only at the finest spatial resolution, then used for all resolutions (Schaaf et al., 2011)
  - Partitioned into smoke and non-smoke endmembers for improved background modeling
- Fire emitted radiance endmembers
  - Modeled using MODTRAN, 300-1500 K single temperature blackbody emission at 10 K interval
- Shade endmember modeled using MODTRAN to account for scattered radiance

Results

- HFDI fire detection area increased with coarsening spatial resolution

Resolution	Total HFDI-Flagged Area (km^2)
Simi	
4.0 m	3.379
8.0 m	3.471
16.0 m	3.720
32.0 m	4.154
64.0 m	4.976
Zaca	
3.8 m	0.169
7.6 m	0.168
15.2 m	0.169
30.4 m	0.177
60.8 m	0.192
Indians	
16.1 m	9.745
32.2 m	10.125
64.4 m	10.837
Station	
10.7 m	20.067
21.4 m	20.236
42.8 m	20.525
64.2 m	20.612

AVIRIS Data

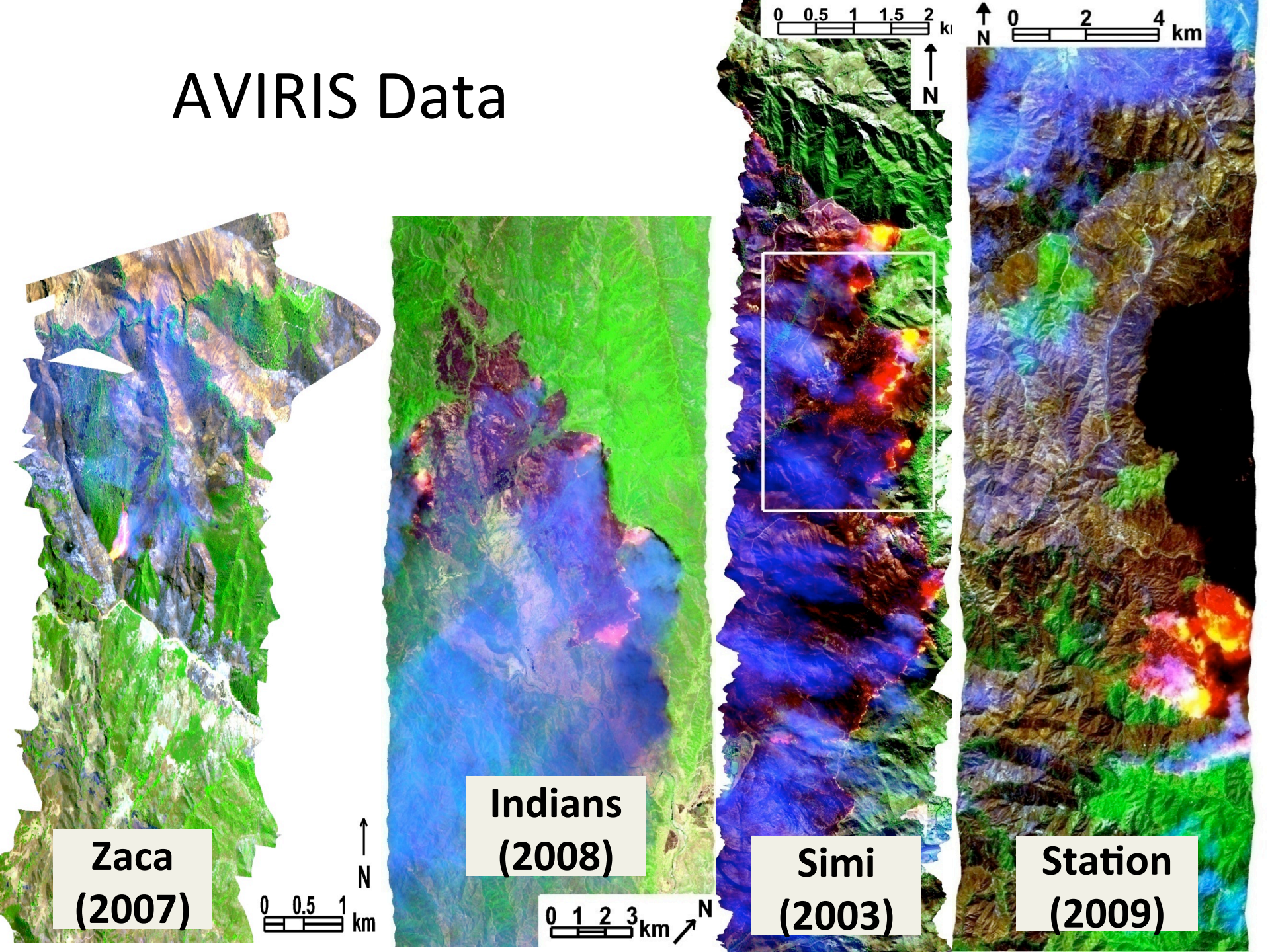
Zaca
(2007)
0 0.5 1
km
N
Indians
(2008)
0 1 2 3
km
N
0 0.5 1 1.5 2
N
Simi
(2003)
N
0 2 4
km
Station
(2009)

Modeled Temperature
Simi 4 m

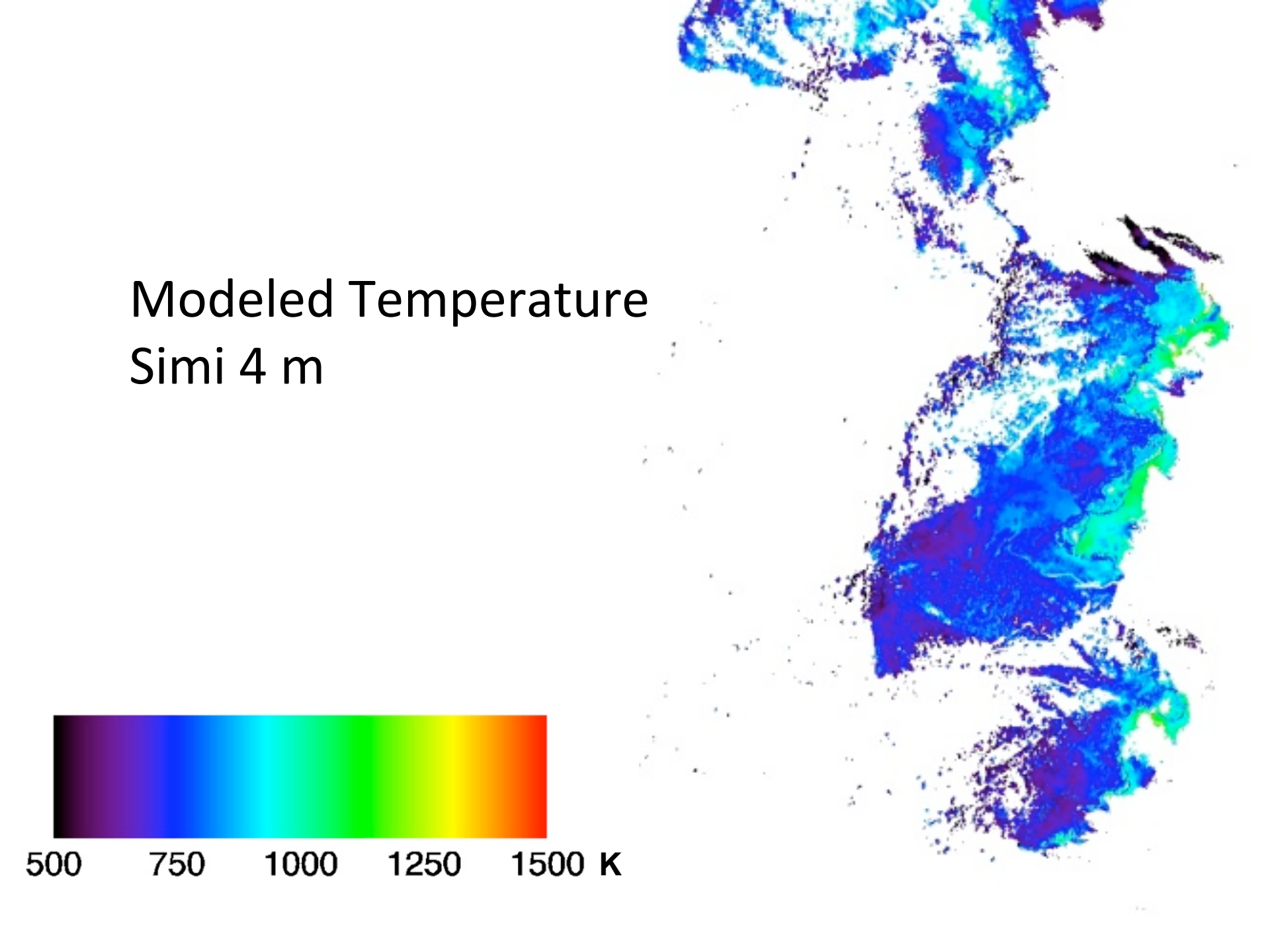

Modeled Temperature
Simi 8 m

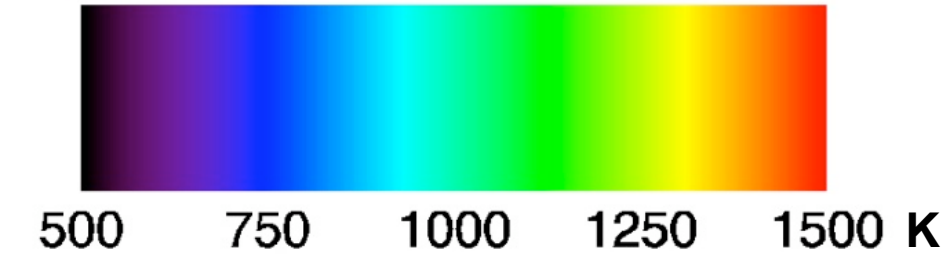

Modeled Temperature
Simi 16 m

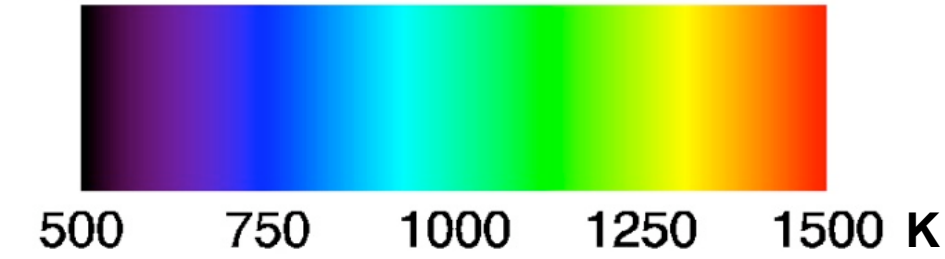

Modeled Temperature
Simi 32 m

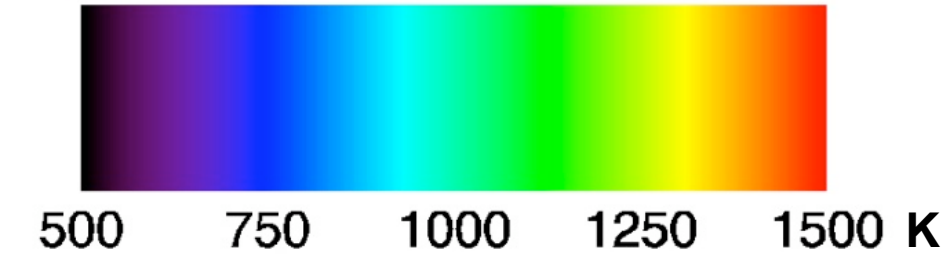

Modeled Temperature
Simi 64 m

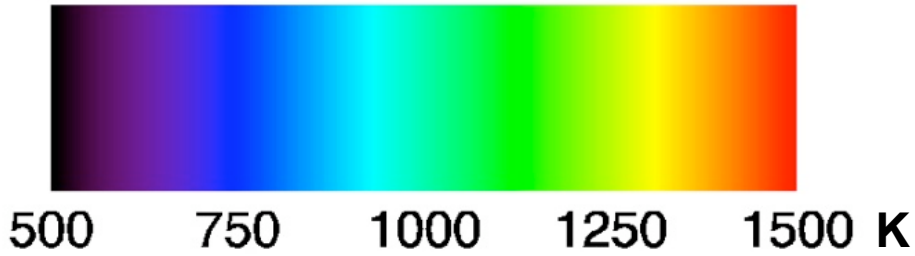

Fire Fractional Area
Simi 4 m

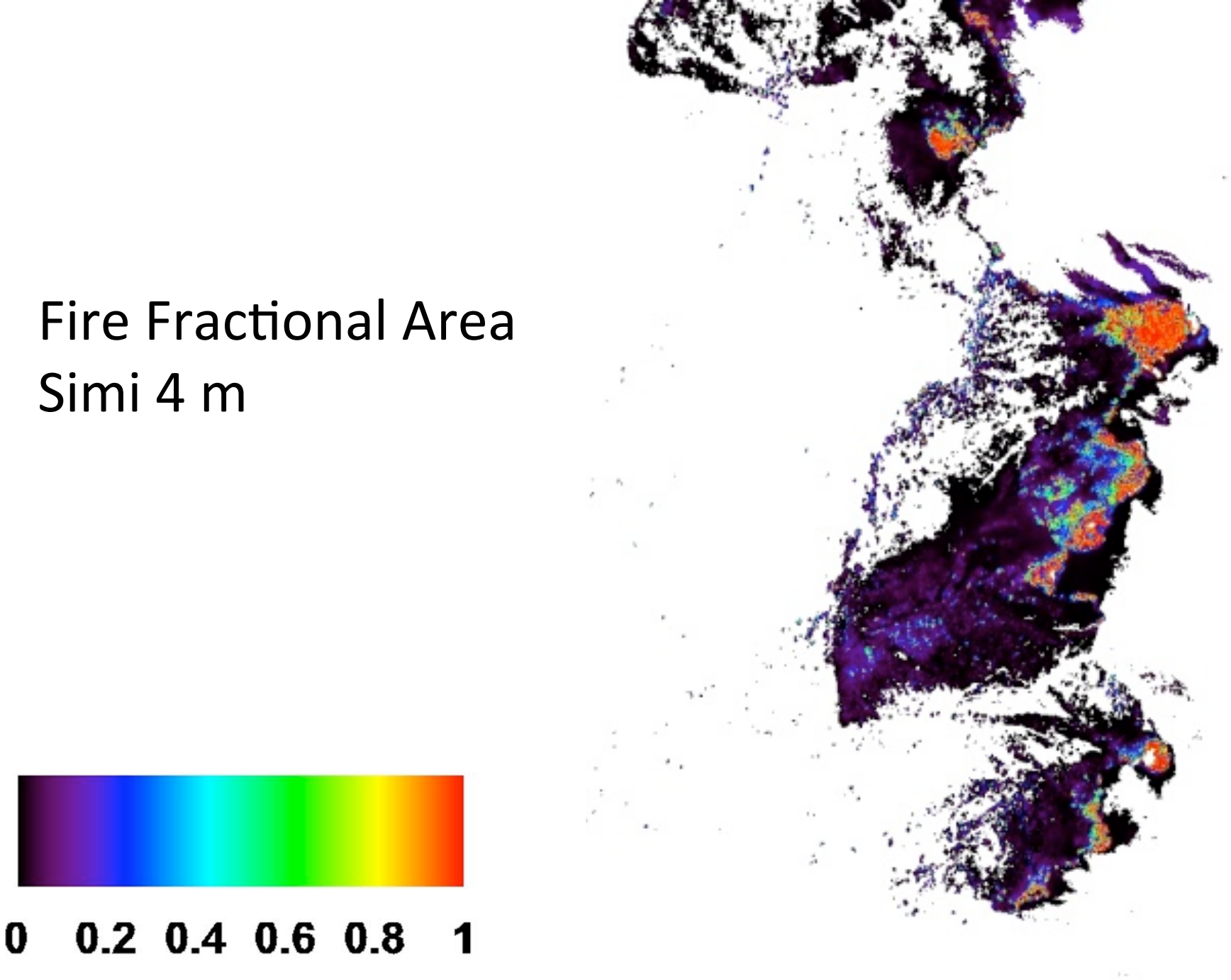

Fire Fractional Area
Simi 8 m

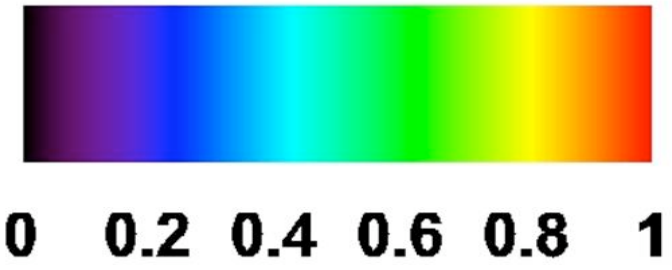

Fire Fractional Area
Simi 16 m

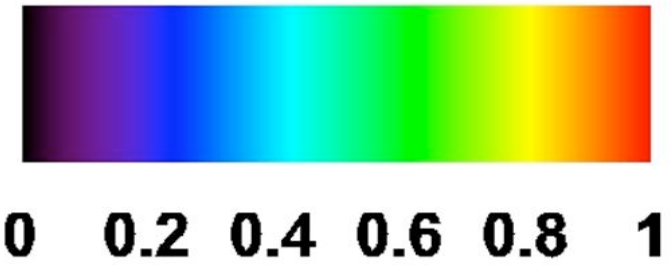

Fire Fractional Area
Simi 32 m

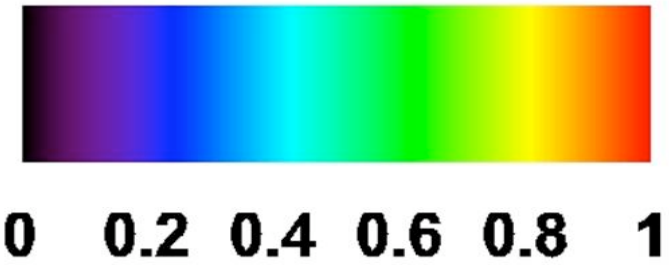

Fire Fractional Area
Simi 64 m

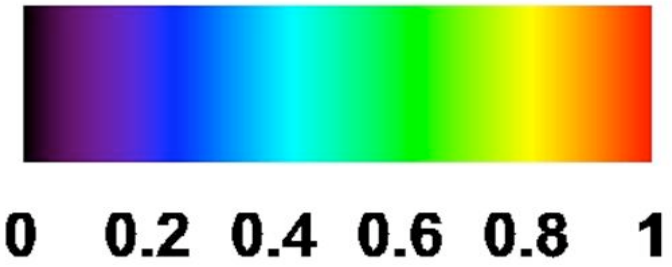

Simi Fire

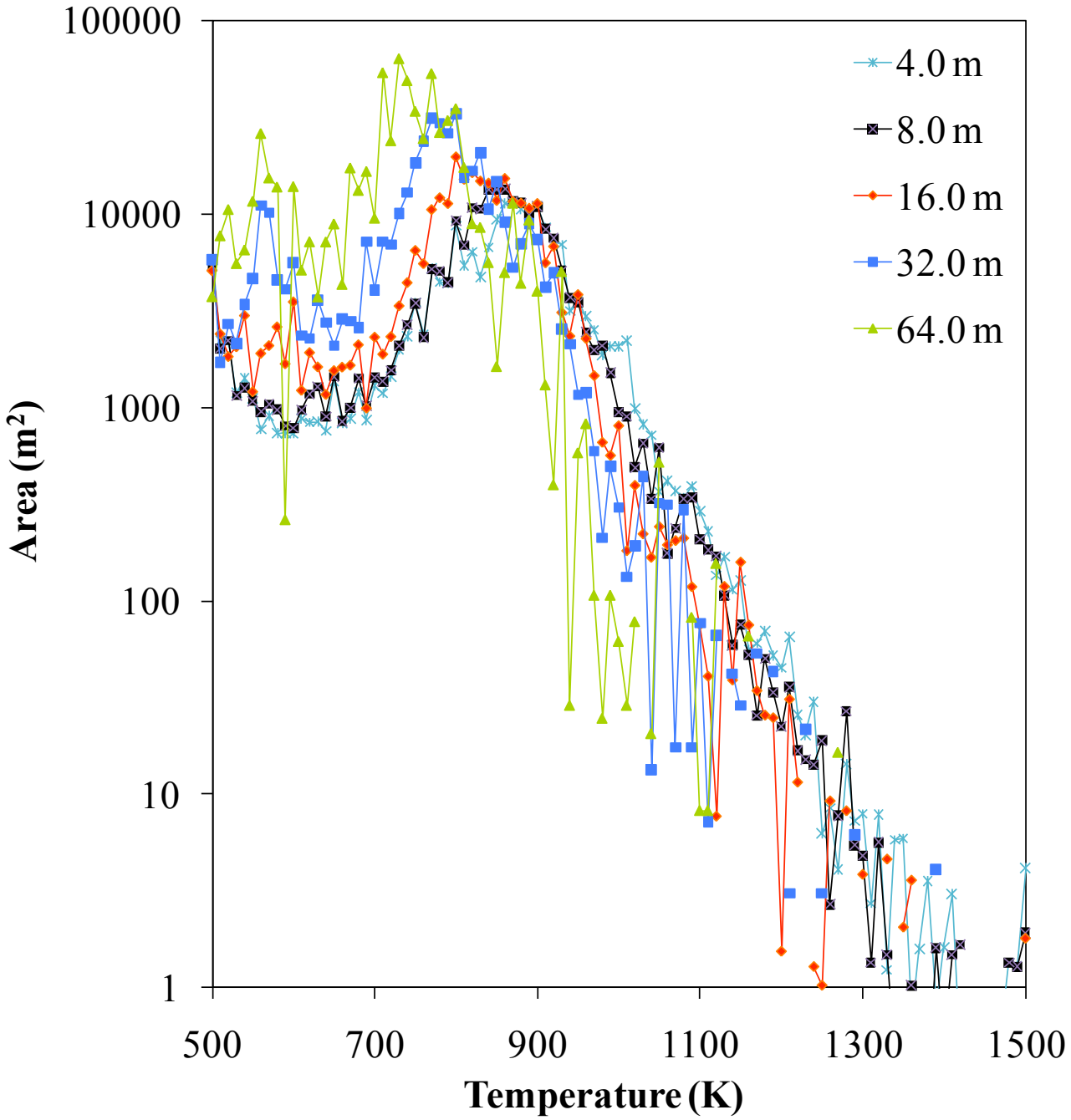
100000
10000
1000
100
10
1
Area (m²)
500
700
900
1100
1300
1500
Temperature (K)
4.0 m
8.0 m
16.0 m
32.0 m
64.0 m

Zaca Fire

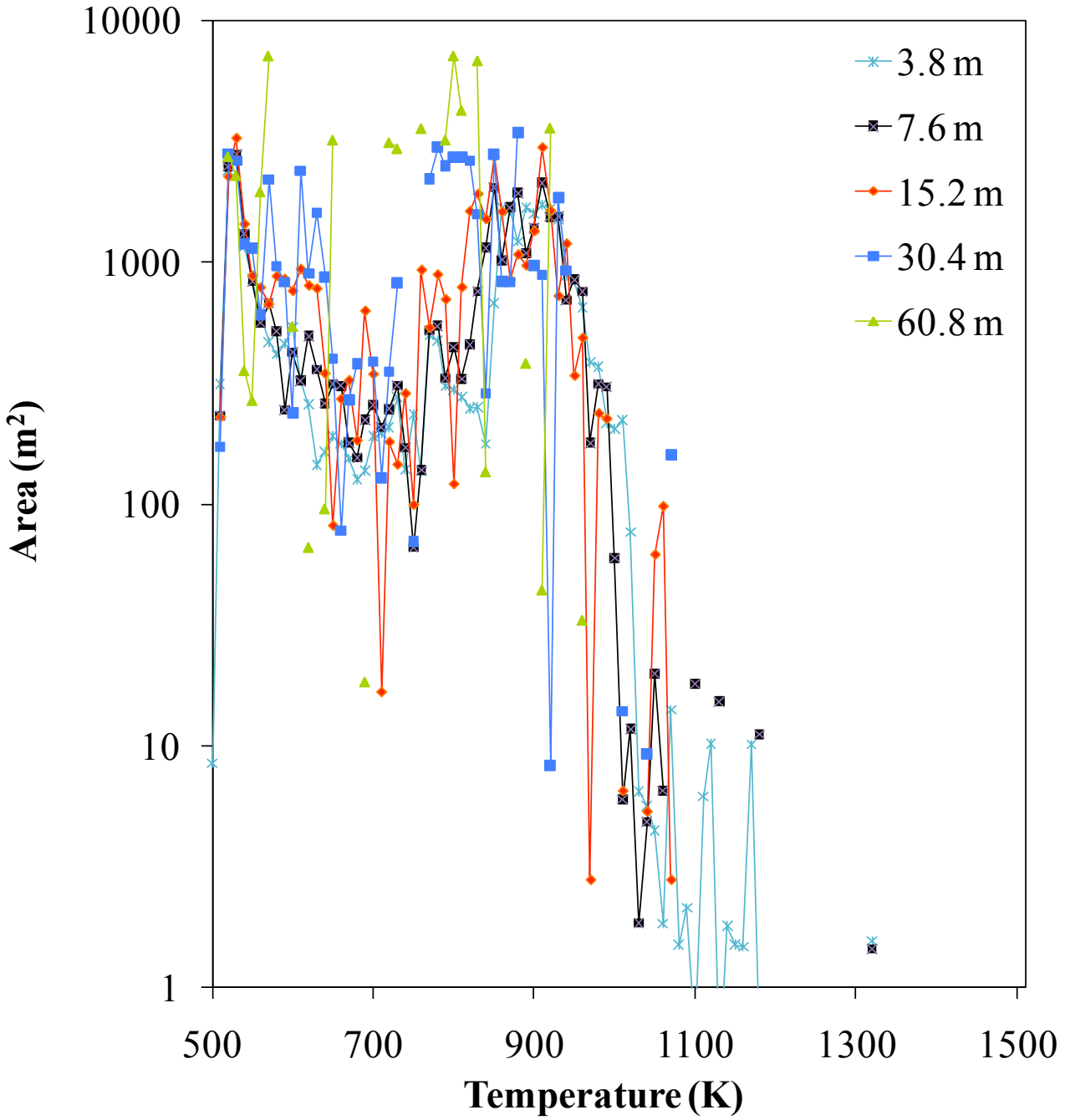
10000
1000
100
10
1
Area (m²)
500
700
900
1100
1300
1500
Temperature (K)
3.8 m
7.6 m
15.2 m
30.4 m
60.8 m

Indians Fire

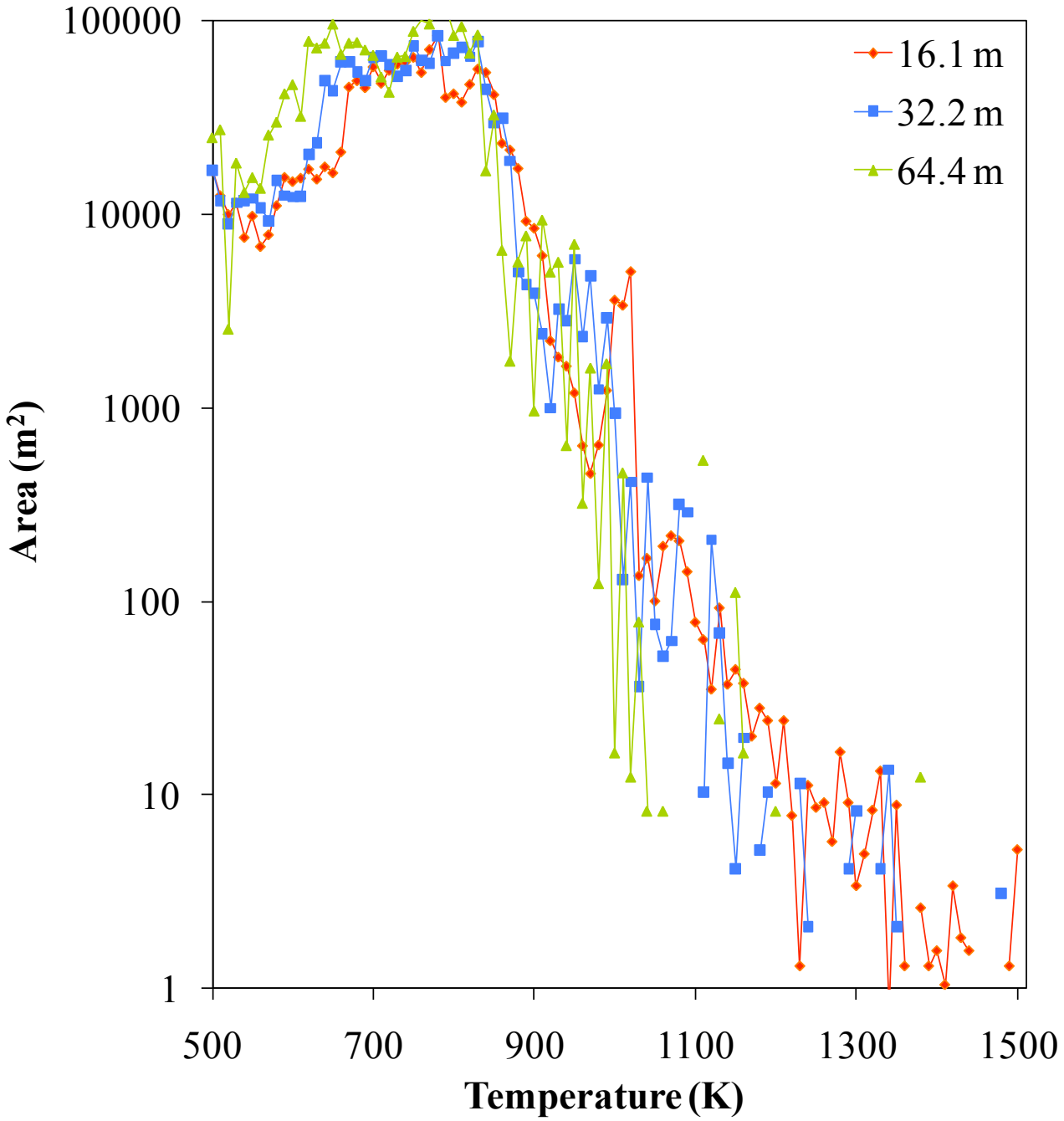

Station Fire

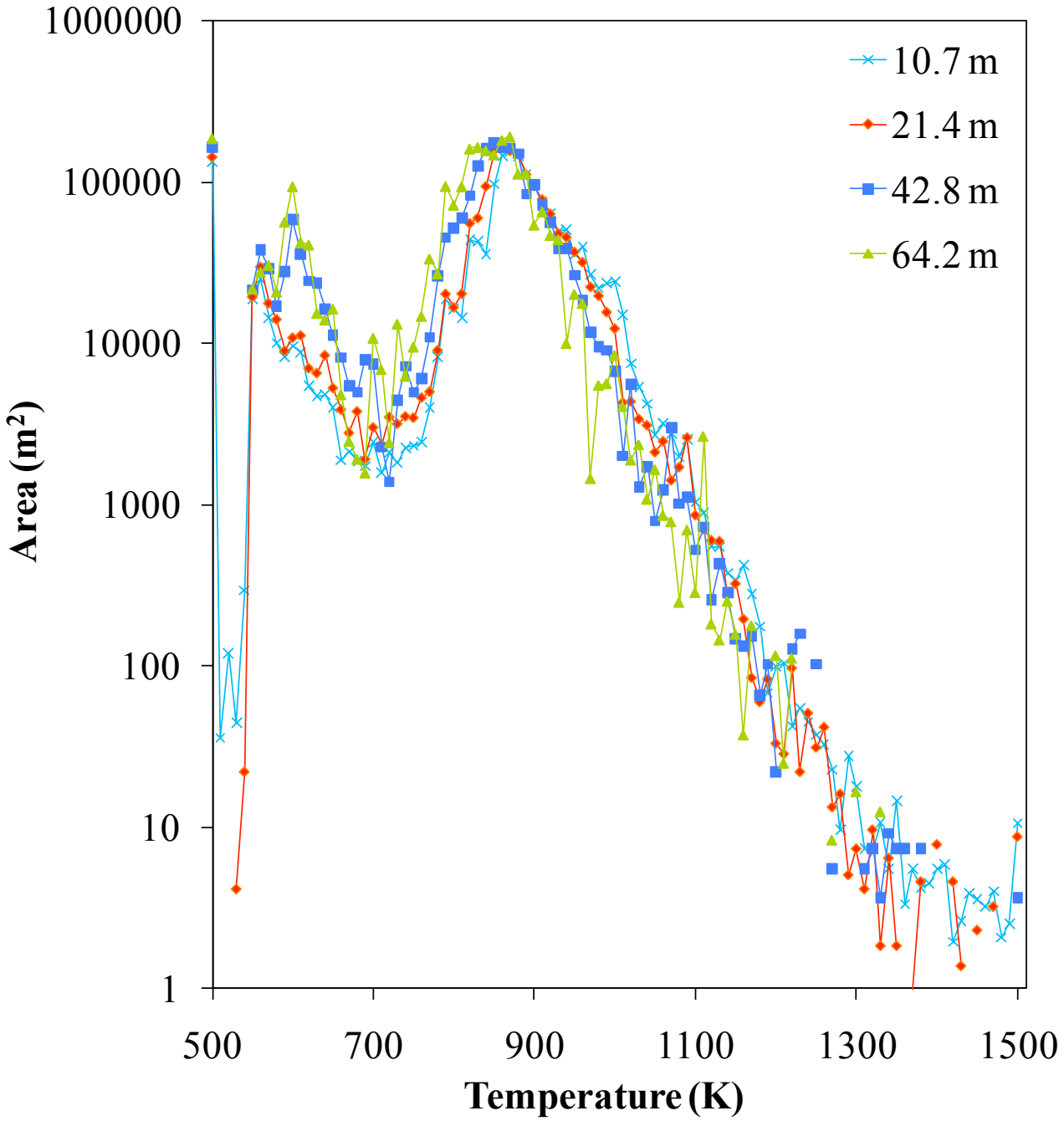

Resolution and Modeled Fire Characteristics

- As spatial resolution coarsens, modeled temperature decreases and modeled fractional area increases
  - Areas of higher emitted radiance are mixed with areas of lower emitted radiance
  - High temperature emission is “spectrally diluted”
  - More common low temperature emission dominates

Modeled Background
Simi 4 m

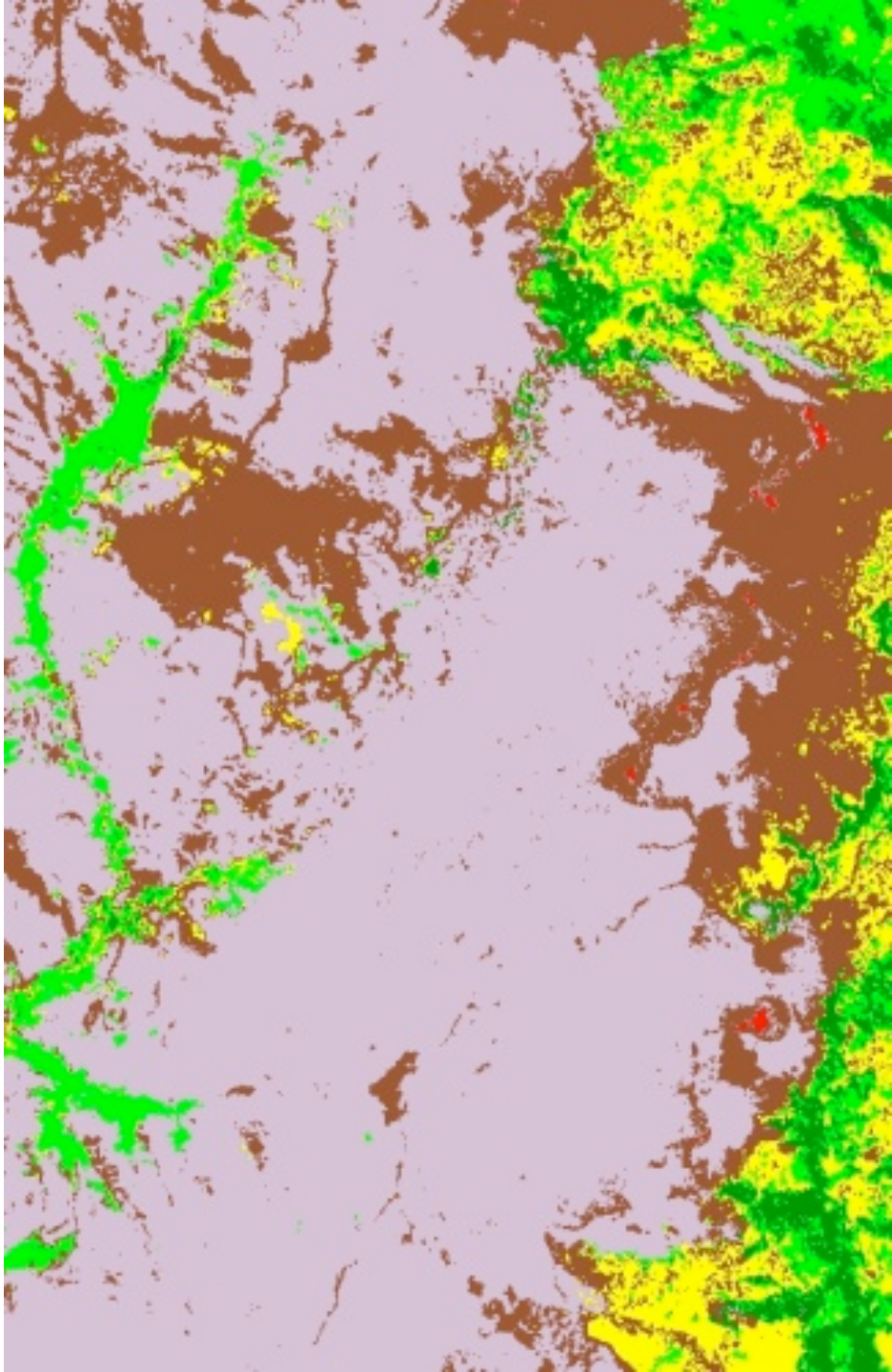

Modeled Background
Simi 8 m

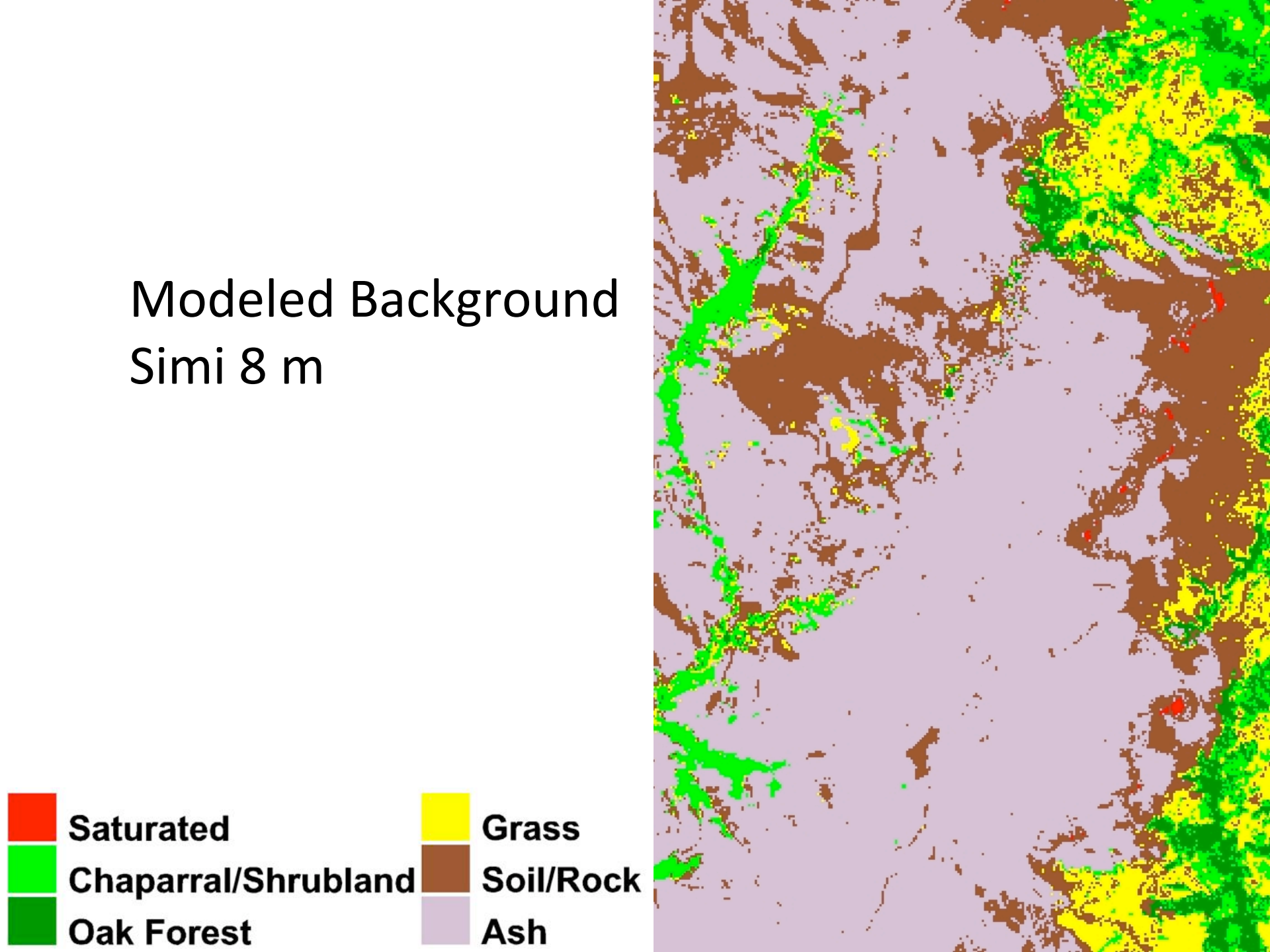

Modeled Background
Simi 16 m

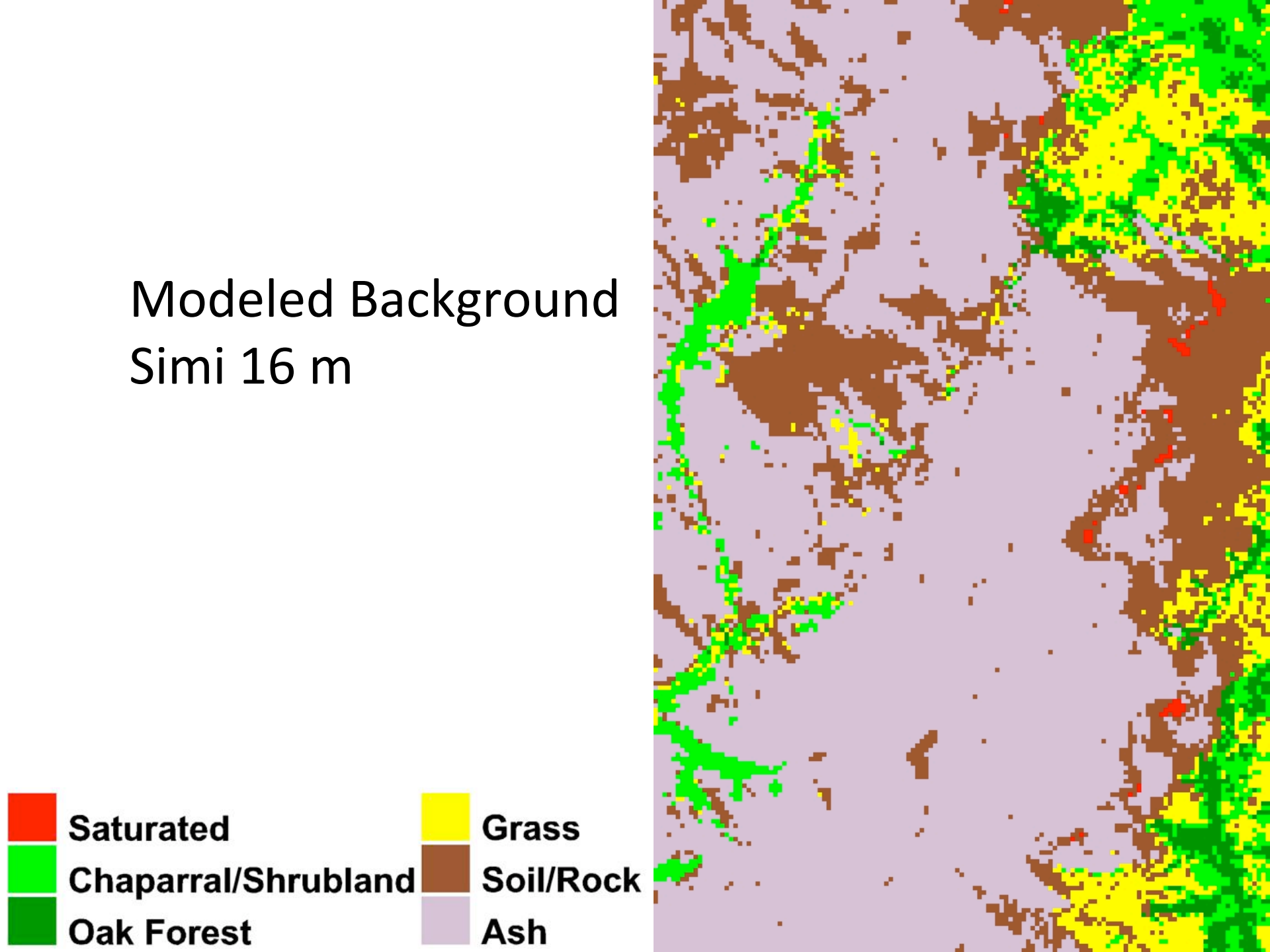

Modeled Background
Simi 32 m

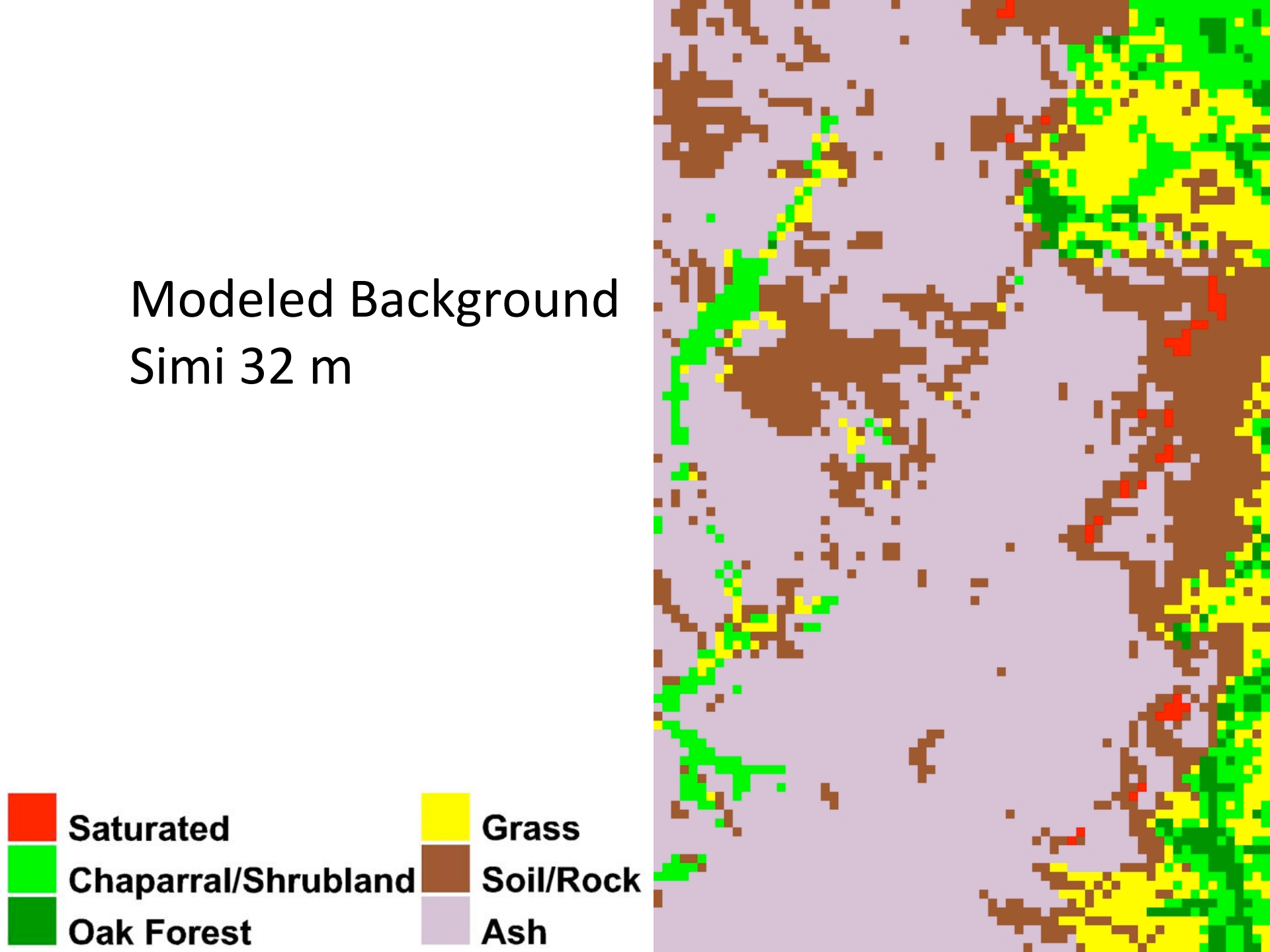

Modeled Background
Simi 64 m

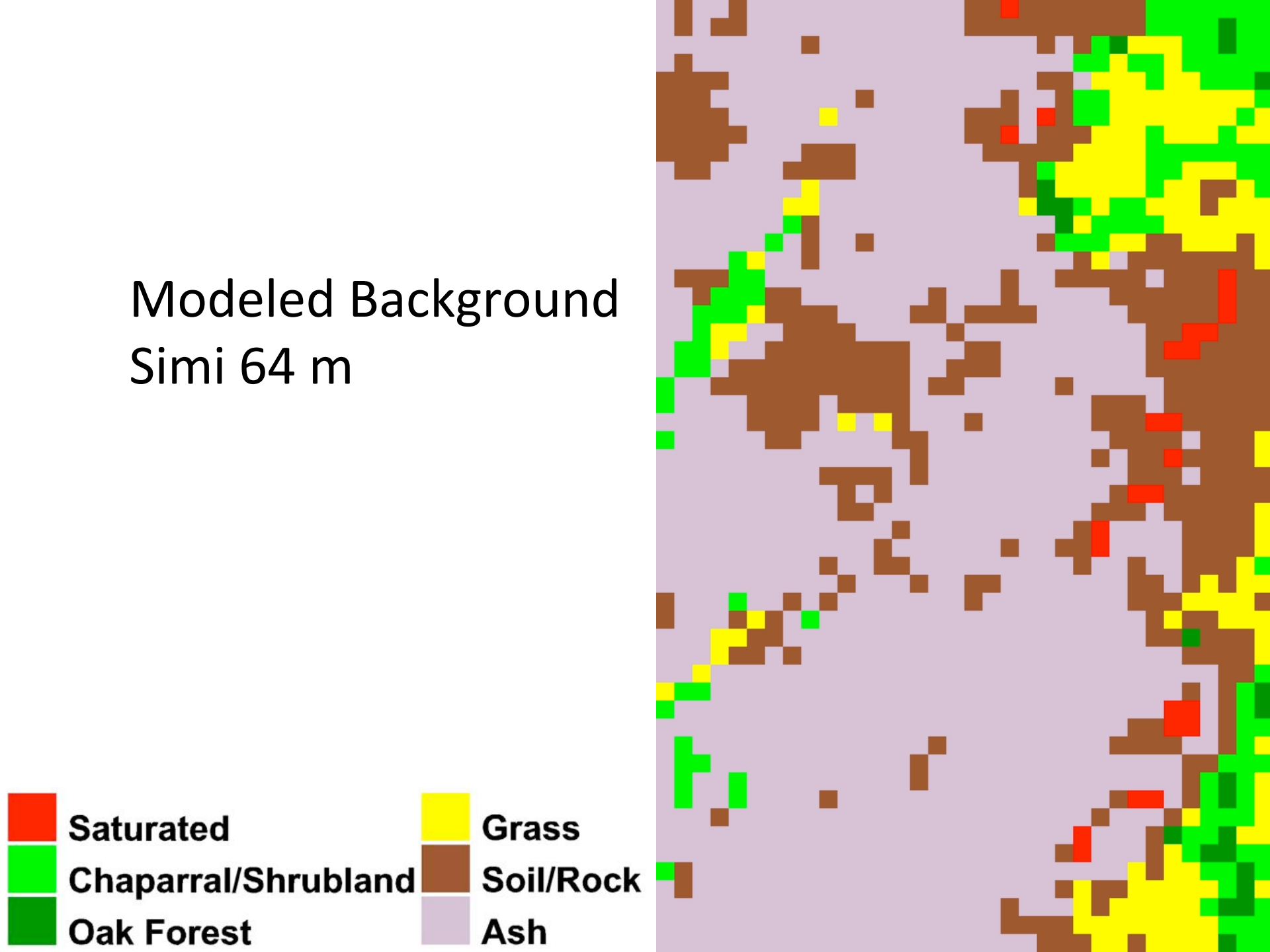

Saturation Threshold

- In the hottest areas of all four fires, most SWIR bands were saturated
- We calculated blackbody emission for all modeled fire temperatures and fractions using Simi Fire 60 m Gaussian resampled data
- Maximum radiance from a single pixel was modeled at 920 K and 98.7% fire fractional area
- After incorporating atmospheric attenuation, maximum modeled blackbody emitted radiance was 189 $\mu W\ cm^{-2}\ sr^{-1}\ nm^{-1}$
- Calculated SWIR saturation thresholds for AVIRIS ranged from 5 $\mu W\ cm^{-2}\ sr^{-1}\ nm^{-1}$ (2003 Simi Fire) to 8 $\mu W\ cm^{-2}\ sr^{-1}\ nm^{-1}$ (2009 Station Fire)

Conclusions

- Distributions of modeled temperature and area are broadly similar as spatial resolution is coarsened
- Coarsening spatial resolution tends to produce:
  - Higher detected fire area
  - Cooler modeled fire temperatures
  - Higher modeled fire fractional area
  - Lower RMSE
- Fire saturation is likely to be an issue for HyspIRI VSWIR at 60 m resolution

Monitoring Evapotranspiration Over Arid Lands of the U.S. Southwest

Andrew N. French[1], Juan Manuel Sanchez[2], Vicente Garcia-Santos[3], Enric Valor[3], Cesar Coll[3], Kelly Thorp[1] & Tom Schmugge[4]

1. USDA/ARS Maricopa, AZ
2. Univ Castilla La Mancha
3. Univ Valencia
4. NMSU/ret.

Need for Arid Land Evapotranspiration Remote Sensing Research

- Increasing population in water scarce regions
- Drought & climate change exacerbating water supplies
- Irrigated agriculture in arid lands are highly productive but will be the first to sacrifice water use.
- Ag. Use 40% of freshwater withdrawals (Hutson et al. 2004)
- Irrigated crops 53% of market value on 17% of crop land (Clemmens et al., 2008)
- Trend: In Arizona annual water supply 2.4 M ac-ft; enough to support 8 M people with no agriculture (Watering the Sun Corridor, Morrison Inst. Public Policy 2011)
- Remote sensing is only way to synoptically observe & estimate land cover and water use changes.

Need for High Spatial & Temporal Resolution

- Arid Lands are highly heterogeneous in space and time
- For water use studies mixed-pixels poorly represent actual conditions
- Better than 100 m needed for VNIR and TIR
- Remote sensing cannot be part of a decision support system if land and water use changes are not up-to-date
- Daily to weekly estimates for croplands, weekly to monthly for rangelands.

Managed Cropland & Urban Interface

Managed (& Un-managed) Rangeland

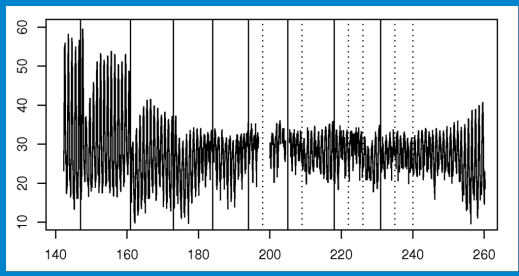

Cropland LST

Need for Multispectral/Hyperspectral Remote Sensing

- More accurate energy balance estimates
- Better land cover discrimination
- Observe land surface changes and states unobservable with single or several broadband channels

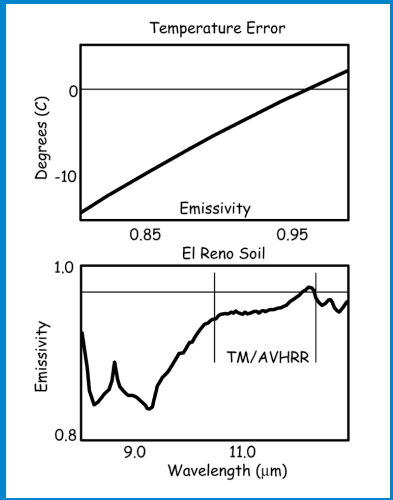

Energy Balance Modeling for Water Use Estimation

$$R_n - G = H + LE$$

Available **Turbulent Flux**

- Physically based
  - Generality
  - Estimates closely linked to vegetation/soil/atmospheric processes & detects water stress vegetation
  - Complex & computationally demanding
- Empirical & Parameterized
  - Locally calibrated
  - Applies to standardized conditions

$$\mathrm{LE} = \frac{\Delta}{\Delta + \gamma}\left[\mathrm{R_n} - \mathrm{G}\right] + \frac{\gamma}{\Delta + \gamma}\rho \mathrm{c_p}\left[\mathrm{e^{\star}} - \mathrm{e_a}\right]/\mathrm{r_a}$$

Penman-Monteith ET (N.B.- no surface temperature)

Available Energy: Net Radiation

$$R_n = (1\text{-albedo})R_{solar} + \varepsilon_{air} R_{L\downarrow} - \varepsilon_{surface} L_{BB,\uparrow}$$

- Single most important component of surface energy balance
- HyspIRI design can improve estimation of R_n beyond broadband sensors
- Error/uncertainty needs to be less the 10%
- Shortwave component dominant term & can be improved with hyperspectral VNIR
- Surface longwave component also important and dependent upon accurate land surface emissivities

Available Energy: Soil Heat Flux

Remote sensing can't directly retrieve G
Typically estimated with Rn and vegetation index
Diurnally variable with time lag
Small : < 50 W m-2
G = c * Rn_soil

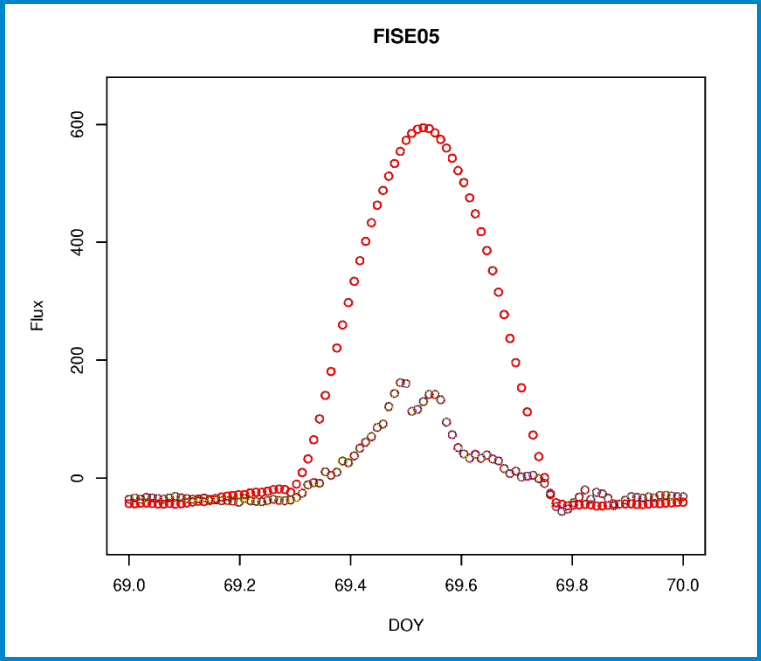

Turbulent Energy Flux: Sensible Heat

Energy flux due to surface temperature gradients

Can be estimated using remotely sensed thermal infrared

Sensible heat related to surface and sub-surface water content

Linked in a non-trivial way to radiometric temperature

$$H = \rho\, c_p\, \Delta T/(r_a + r_s)$$

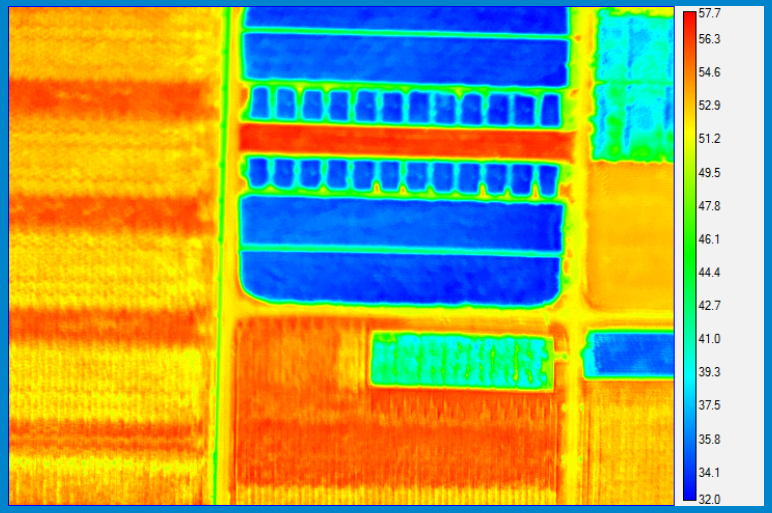

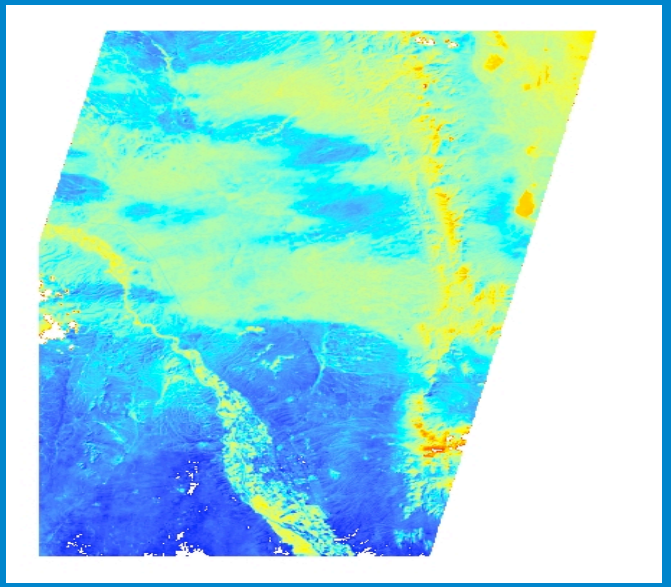

Turbulent Energy Flux: Latent Heat -> Evapotranspiration <-

- Component of surface energy balance representing conversion of liquid water to vapor from soil and plants
- Indicator of plant water use and plant water stress
- Estimated from energy balance residual
- Current ET model examples: SEBAL/METRIC, SEBS, TSEB

$$\mathrm{LE_C} = \mathrm{f_g}\alpha\left[\frac{\Delta}{\Delta+\gamma}\right]\mathrm{R_{n,C}}$$

$$H \cong H_{soil}(\Delta T) + H_{canopy}(PT)$$

$$\mathrm{LE_S} = \mathrm{R_{n,S}} - \mathrm{G} - \rho \mathrm{c_p}\frac{\mathrm{T_s} - \mathrm{T_a}}{\mathrm{r_a} + \mathrm{r_s}}$$

$$\mathrm{LE} = \mathrm{R_n} - \mathrm{G} - \rho \mathrm{c_p}\left[\frac{\Delta \mathrm{T}}{\mathrm{r_a}}\right]$$

Energy balance modeling to get daily ET

LST

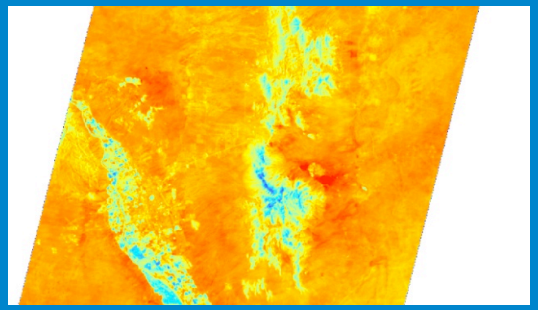

NDVI

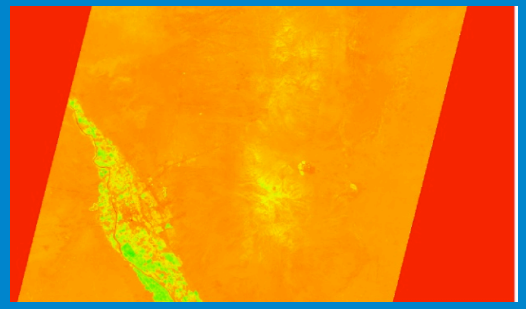

Emissivity

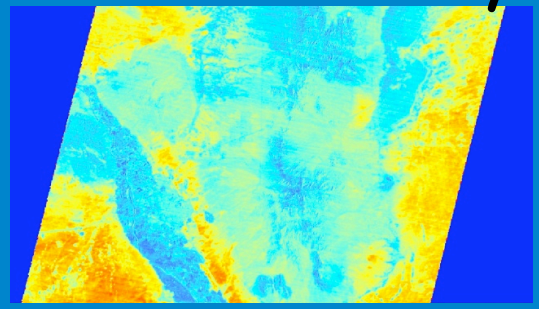

+Land Use
+Meteorology+…

ASTER
6 Oct 2002

H

LE

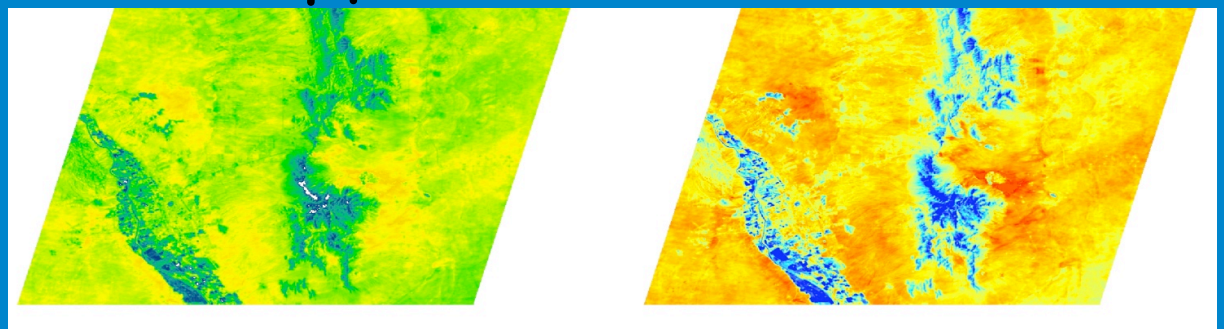

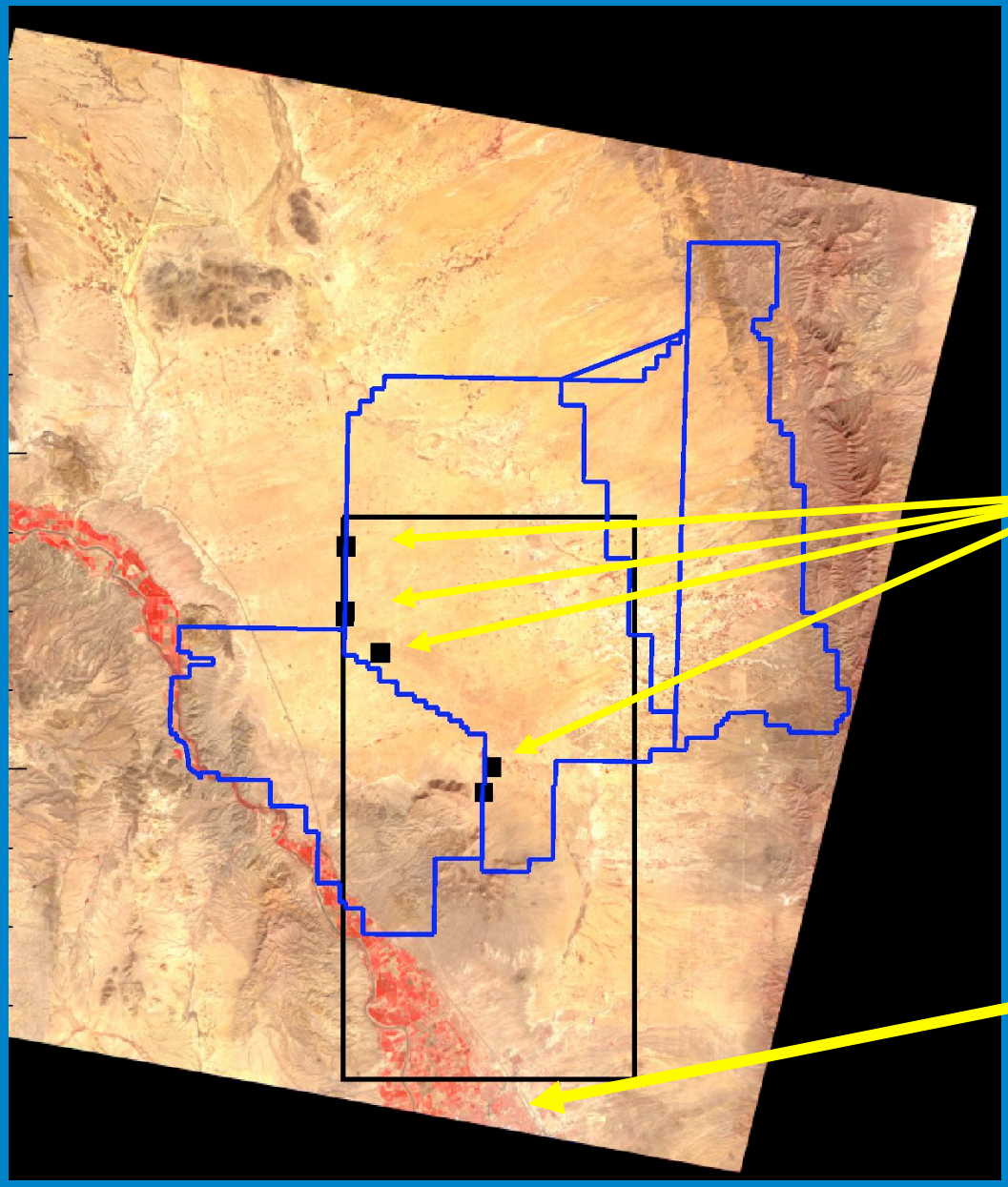

Jornada Region

6 October 2002

ASTER VNIR

Ground Stations

Las Cruces, NM

NDVI for Jornada & Rio Grande 2001-2003

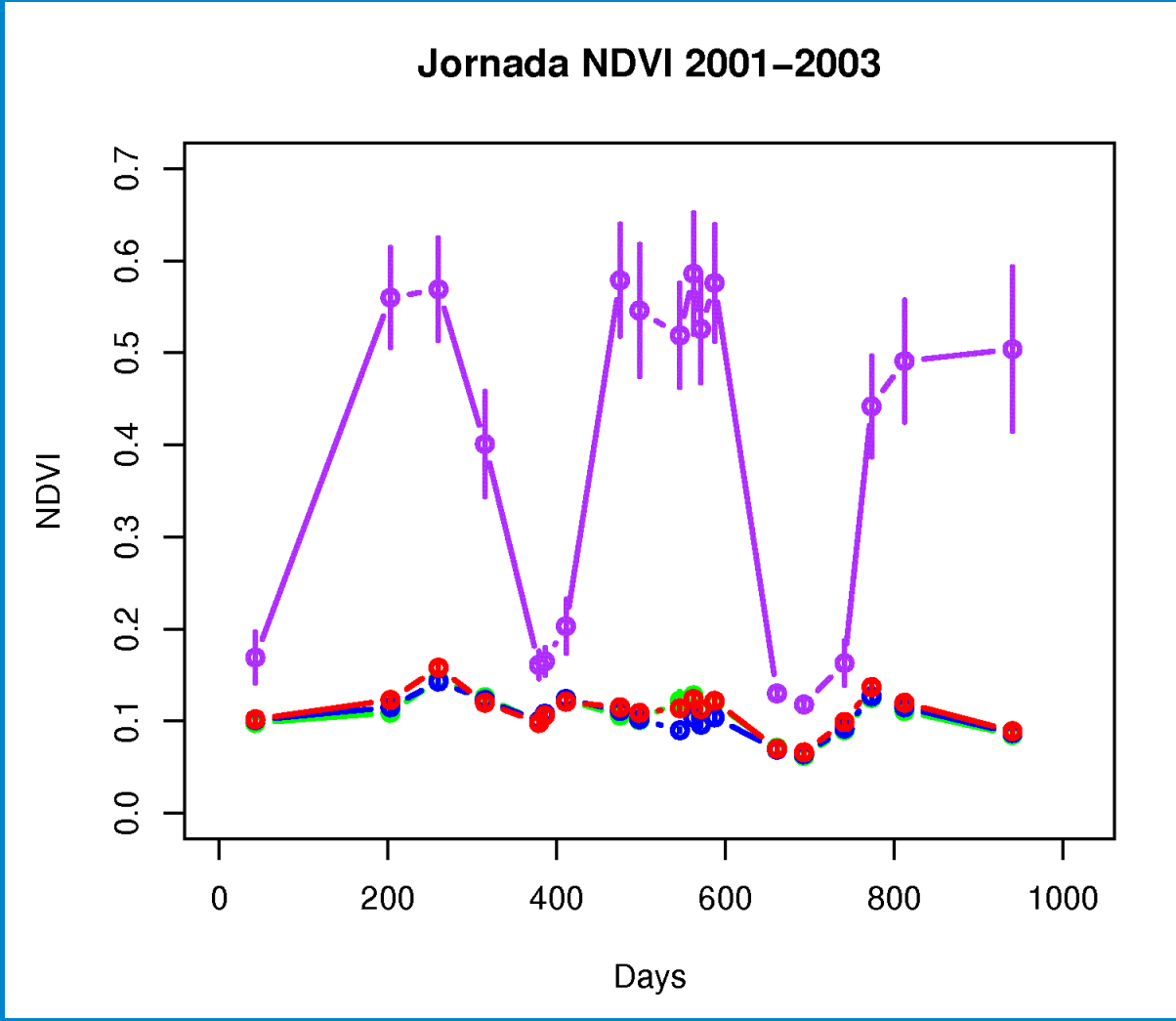

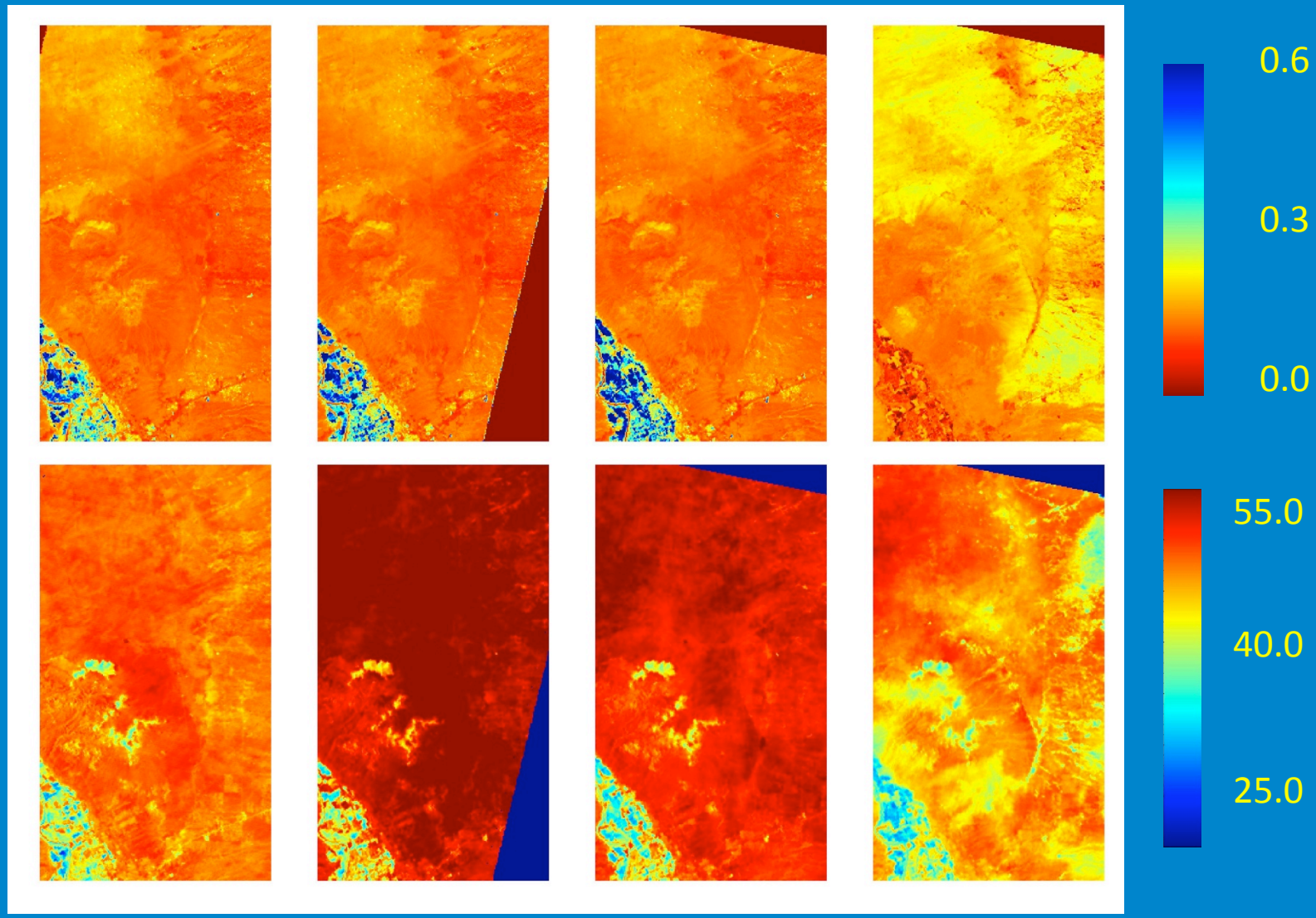
May 15
May 31
June 23
Aug 10
NDVI
Temp.
0.6
0.3
0.0
55.0
40.0
25.0

ET estimates at 90 m Resolution

Site	H	LE	G	R_n
Grass	411 (7) 377	0 8	92 (2) N/A	505 (1) N/A
Transition (Bowen)	419 (7) 326	0 91	88 (2) 121	509 (1) 538
Mesquite	418 (35) 364	0 22	89 (8) N/A	508 (7) N/A

ASTER TSEB Ground Observation

Emissivity Contrast at Jornada

Emissivity data are dynamic
Provide additional information about the land surface
Obtainable only from multispectral TIR

May 15 | Aug 10 | Sep 20 | Oct 6

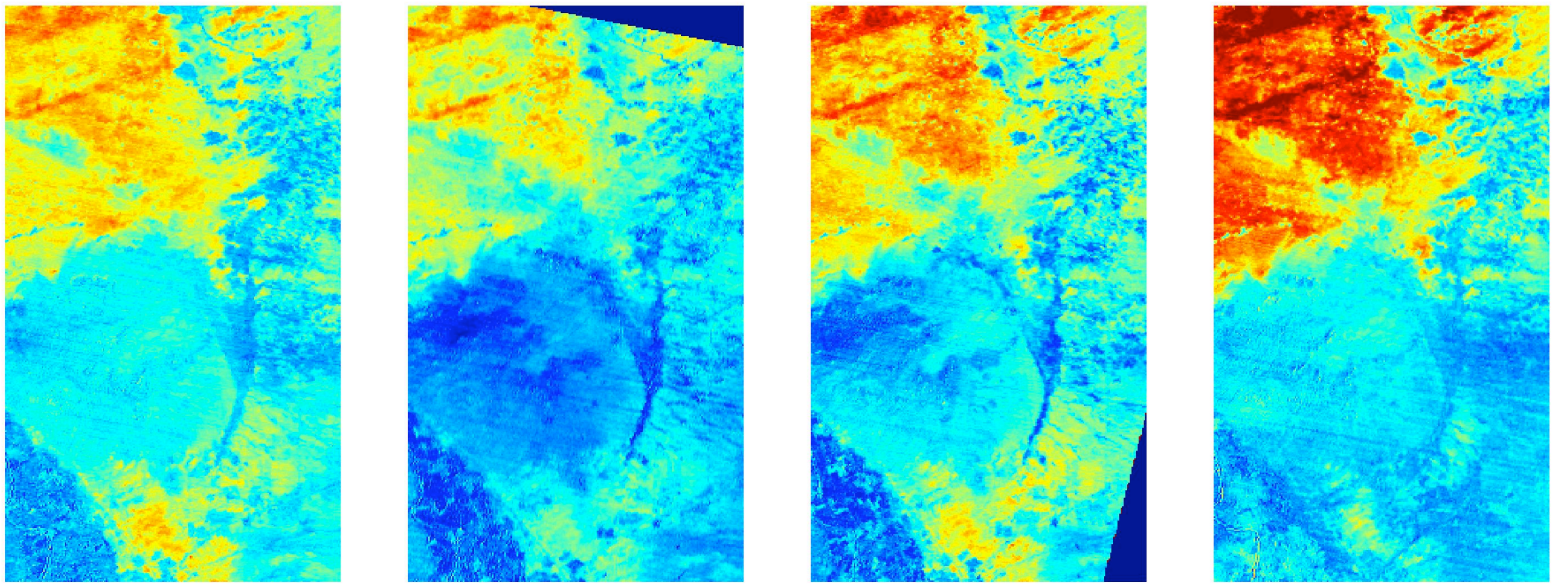

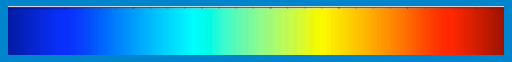

0.0 0.05 0.1 0.15

-Soil moisture effects
-Atmospheric correction errors

Remote Sensing of ET with Multispectral TIR

Dynamic Emissivity & Land Cover Change

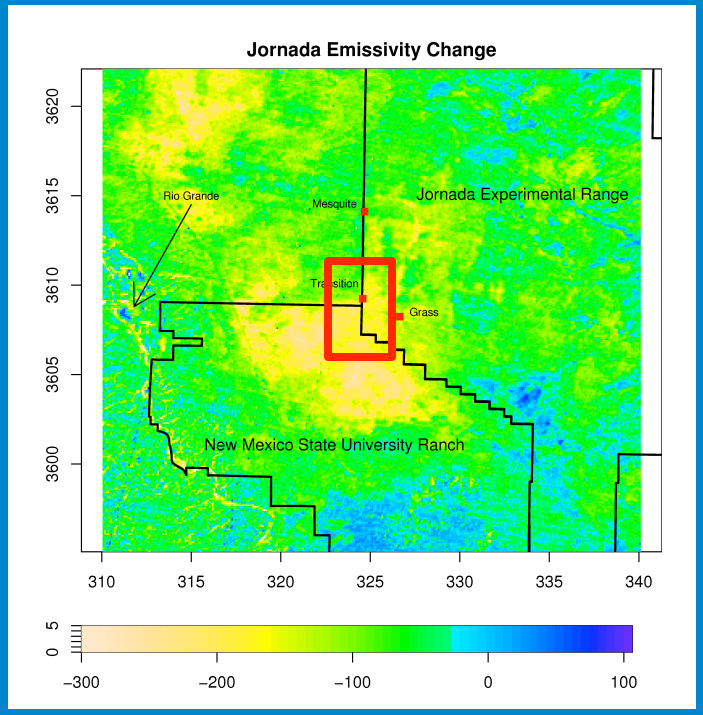

R^2

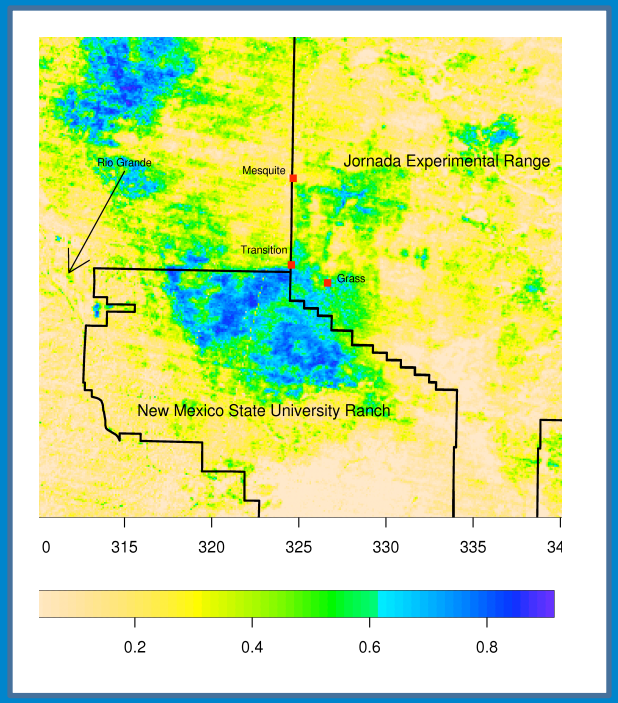

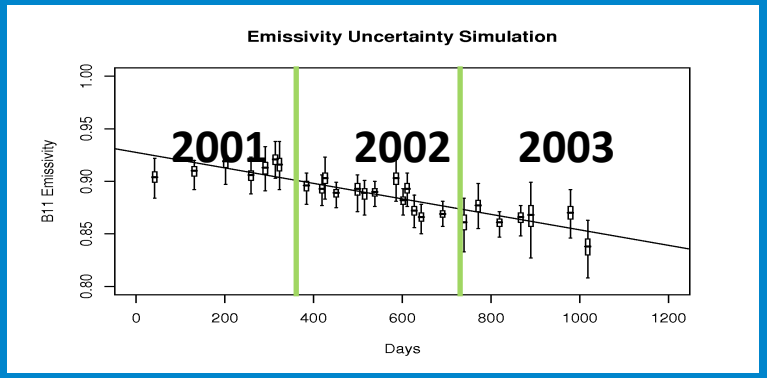

200 m extract

MASTER Confirms Emissivity Changes

6-12 m resolution

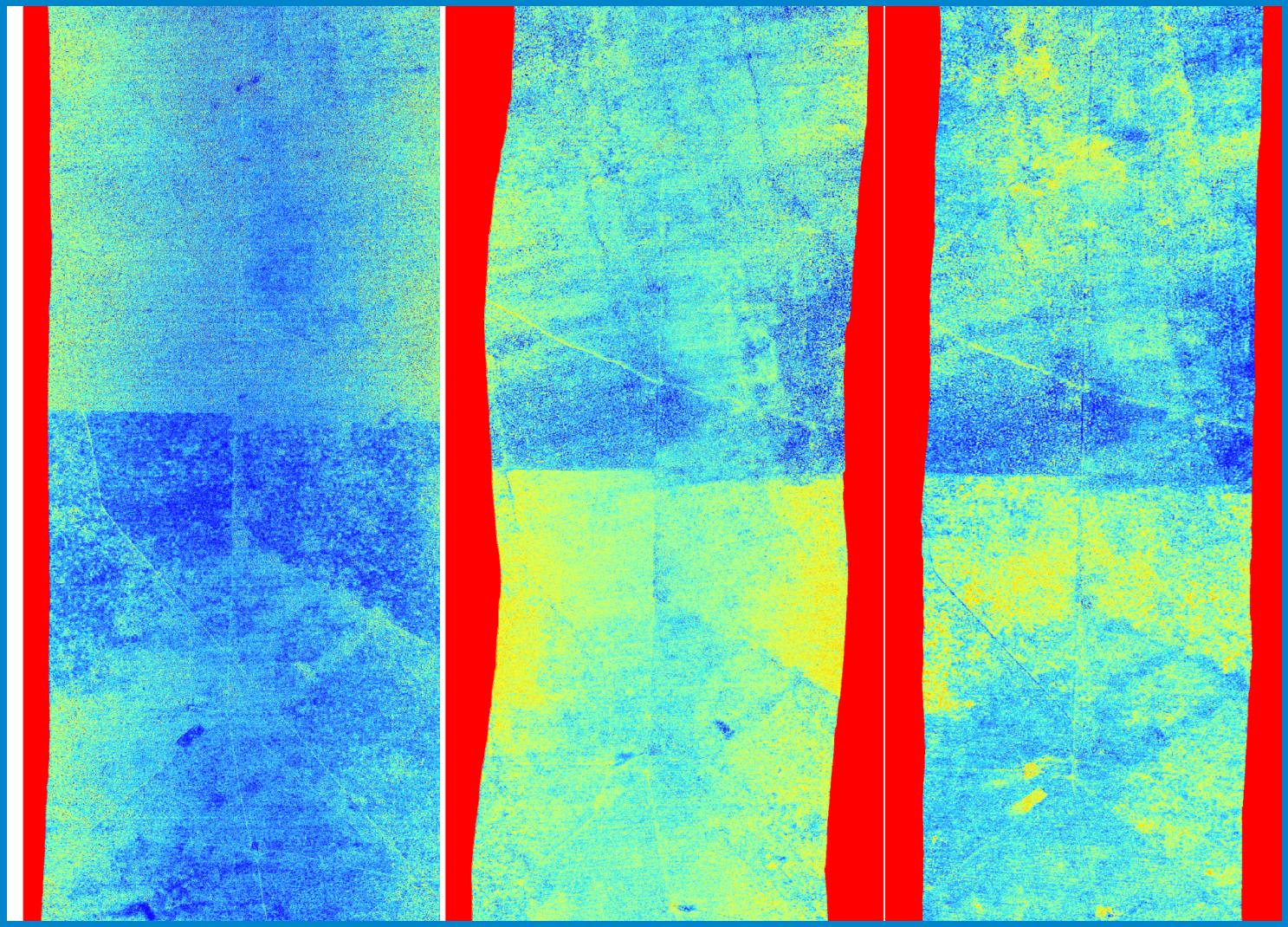

May 2001 May 2002 May 2003

Importance of Spatial Resolution: Scaling of Land Surface Temperatures

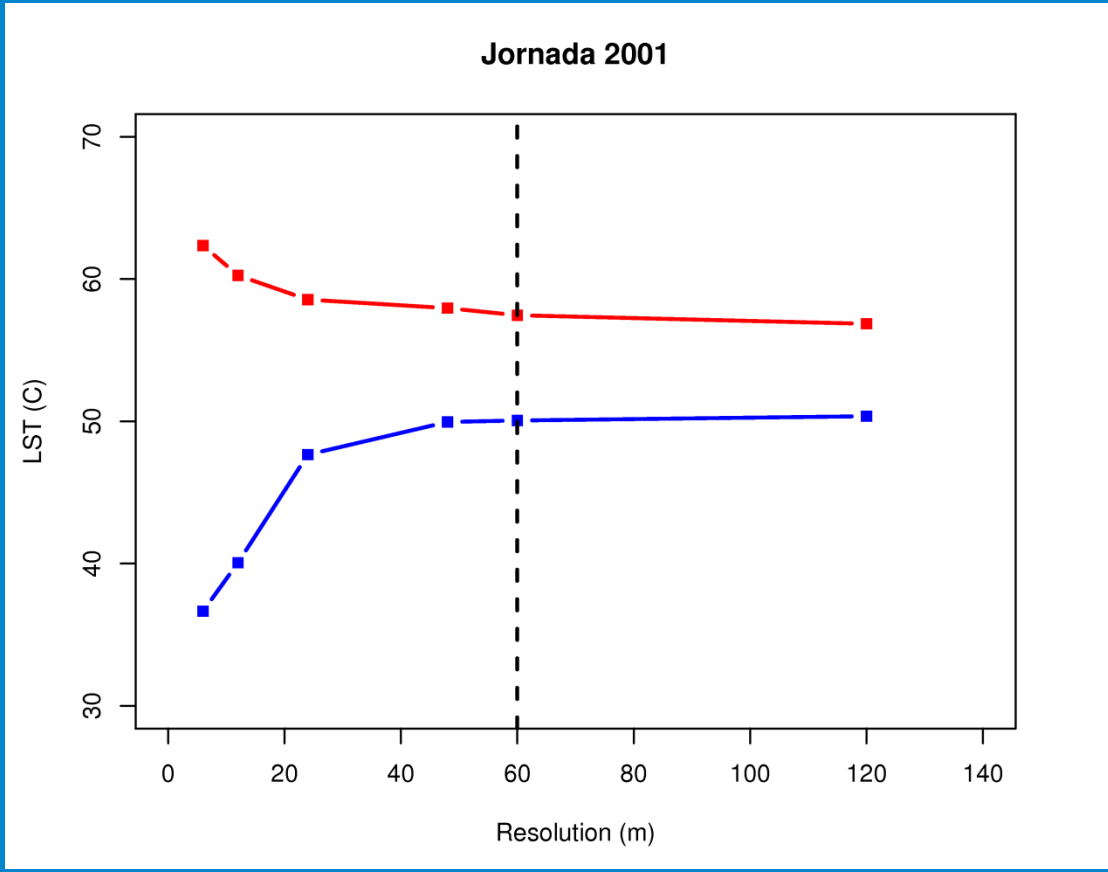

- Most of LST dynamic range lost ~50m
- LST contrast loss mainly over cooler surfaces
- HyspIRI resolution will discriminate land used changes, but not individual shrubs
- Loss of range needs to be considered when modeling surface energy fluxes

NDVI an Unsatisfactory LST Estimator

Rangeland has limited NDVI range

Cropland has broad variance of LST

Cannot discriminate plant stress

NDVI

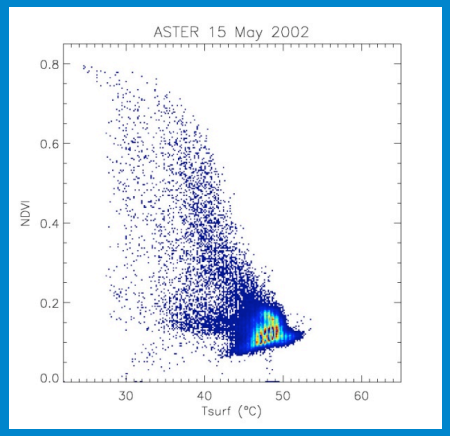

15 May

NDVI

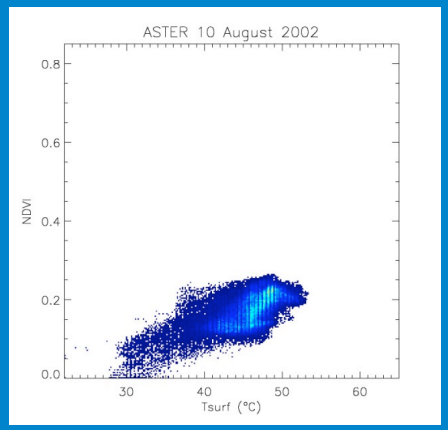

10 August

Tsurf

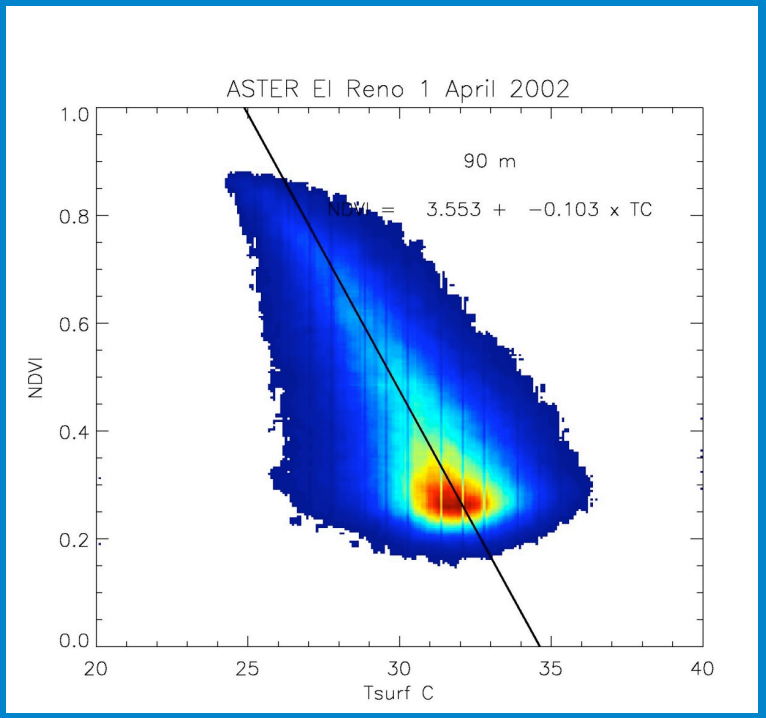

Slope is time of day dependent

Emissivities May Help Disaggregation

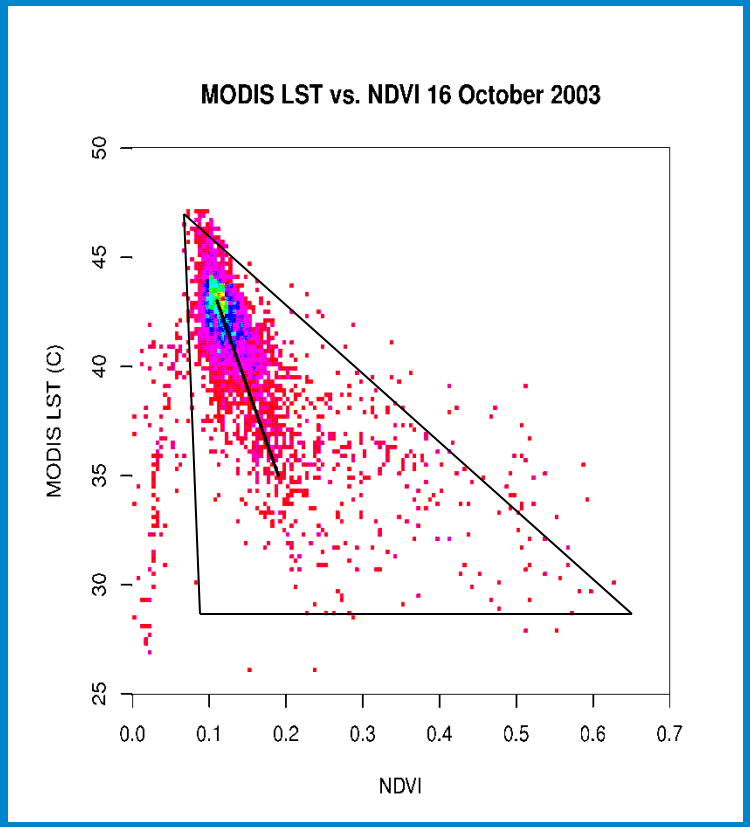

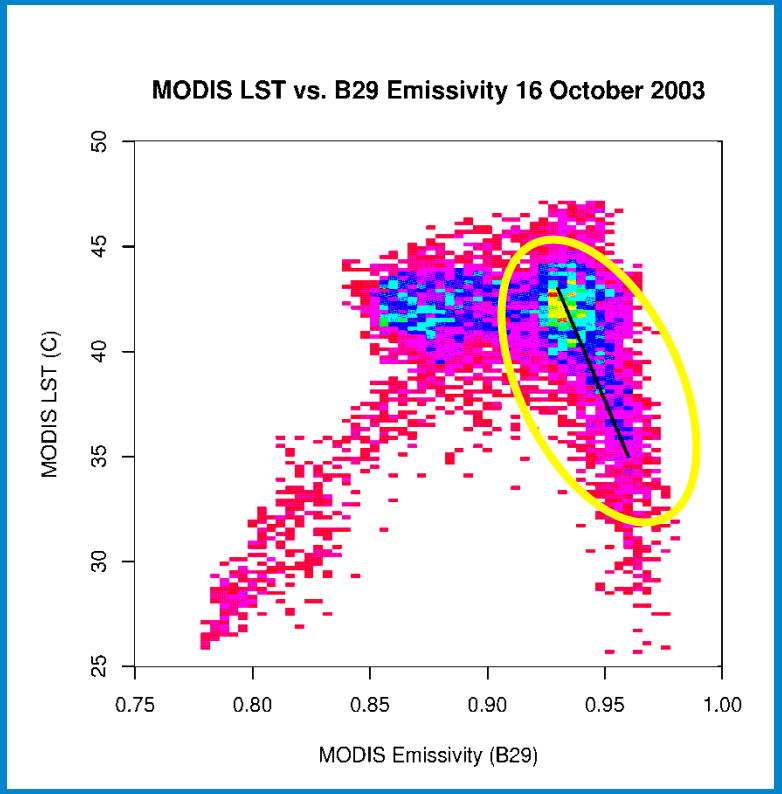

$$LST = k\left[b_0 + b_1 NDVI\right] + (1-k)\left[c_0 + c_1 Emiss.\right]$$

ET Estimation for Croplands

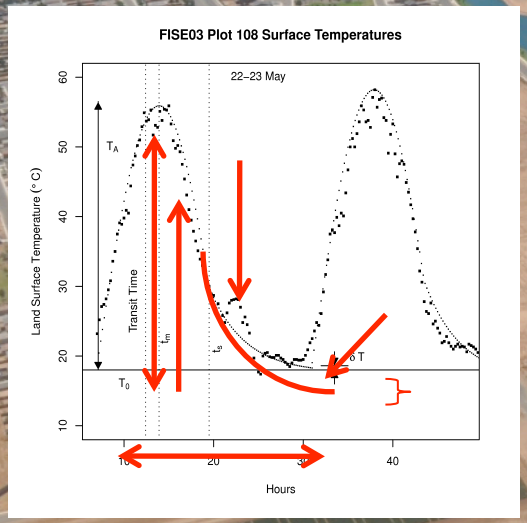

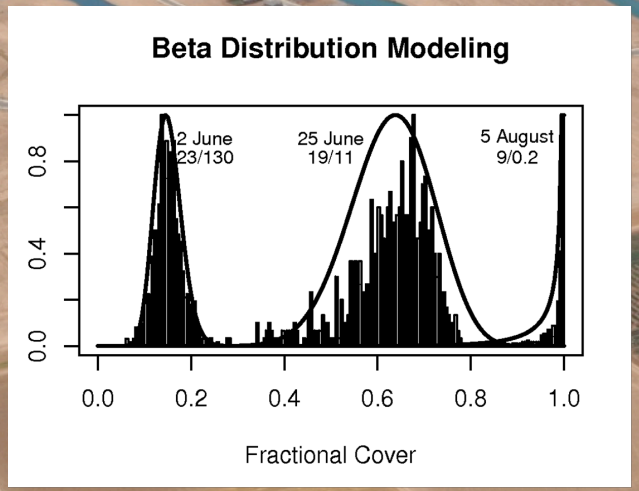

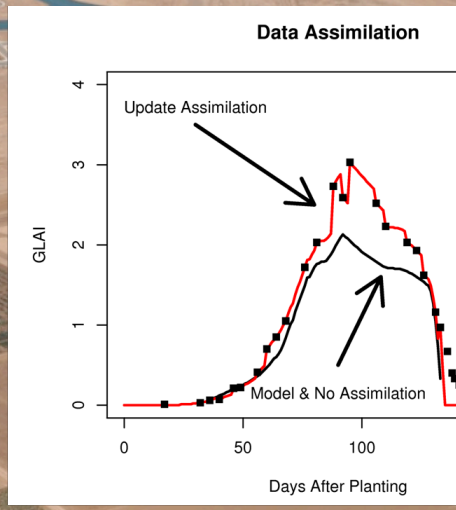

Diurnal LST modeling

Weekly vegetation Cover modeling

Daily biophysical mo

- Integration of multiple sensors, ground-based information & models re
- Decision support tools require <weekly estimates & spatial resolution <

Remote Sensing of ET with Simulated HysplRI

- Implement ET methodology at 60m using MASTER data (11 Flights 1999-2010) and AVIRIS (6 flights 1998-2002)
- Investigate ways to improve LST retrieval for low emissivity contrast surfaces
- Incorporate hyperspectral data to improve vegetation detection, classification and albedo

Conclusions

- Finding accurate ways to estimate ET is vital for monitoring water use & building decision support tools to manage freshwater supplies.
- Remote sensing essential for global scale studies
- HyspIRI will advance these goals by providing frequent high spectral & spatial resolution spanning multiple thermal bands & contiguous VSWIR bands needed for resolving the surface energy balance components.

ASTER Composite over Jornada 2001-2003

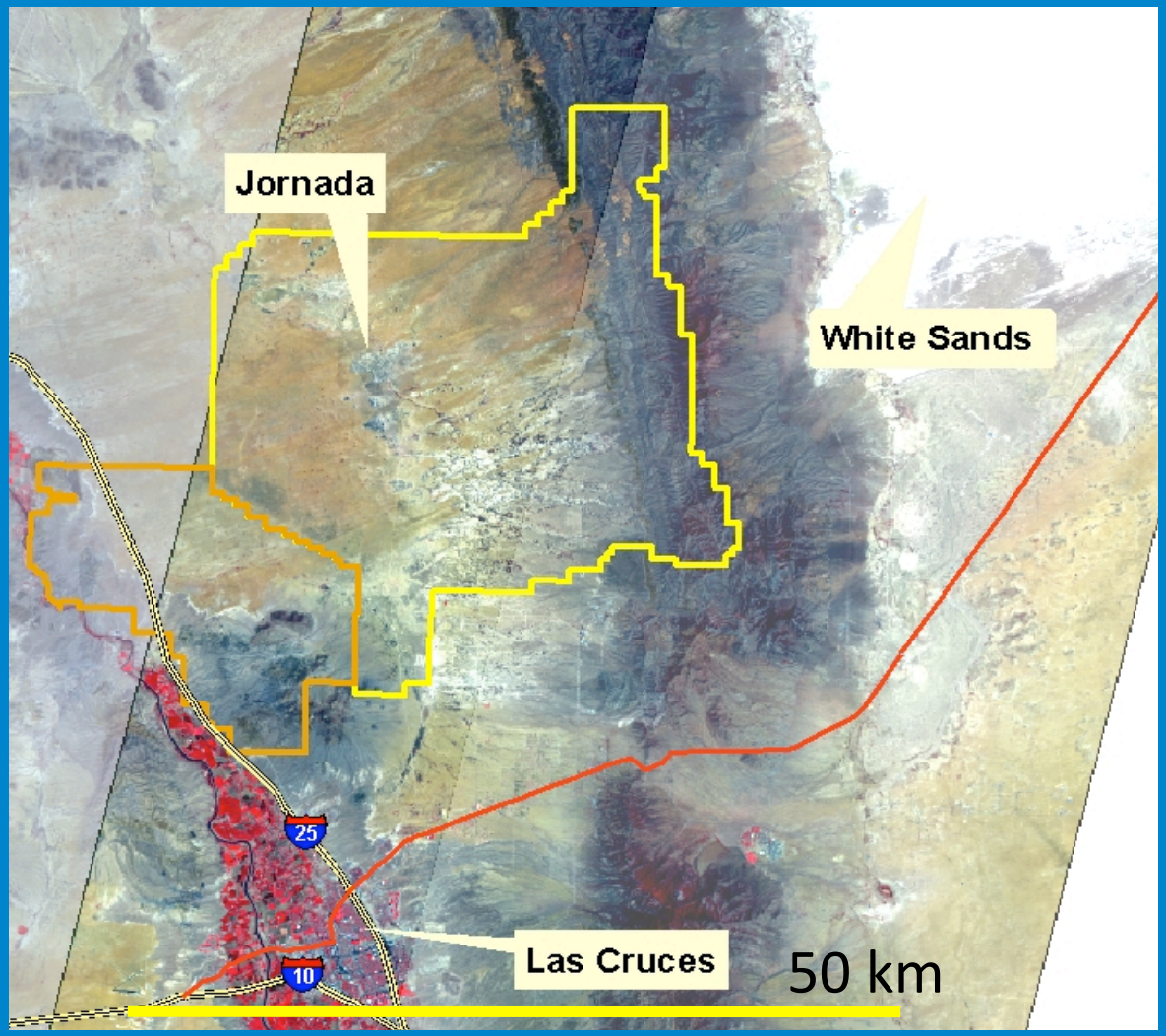

Update ET estimates beyond Remote Sensing Times

- Image data not available frequently enough, nor with sufficient resolution
- Background crop model constrains growth to physiological plausible ranges
- But process model not spatial, so need image data to map ET
- Update with observables such as LAI and LST

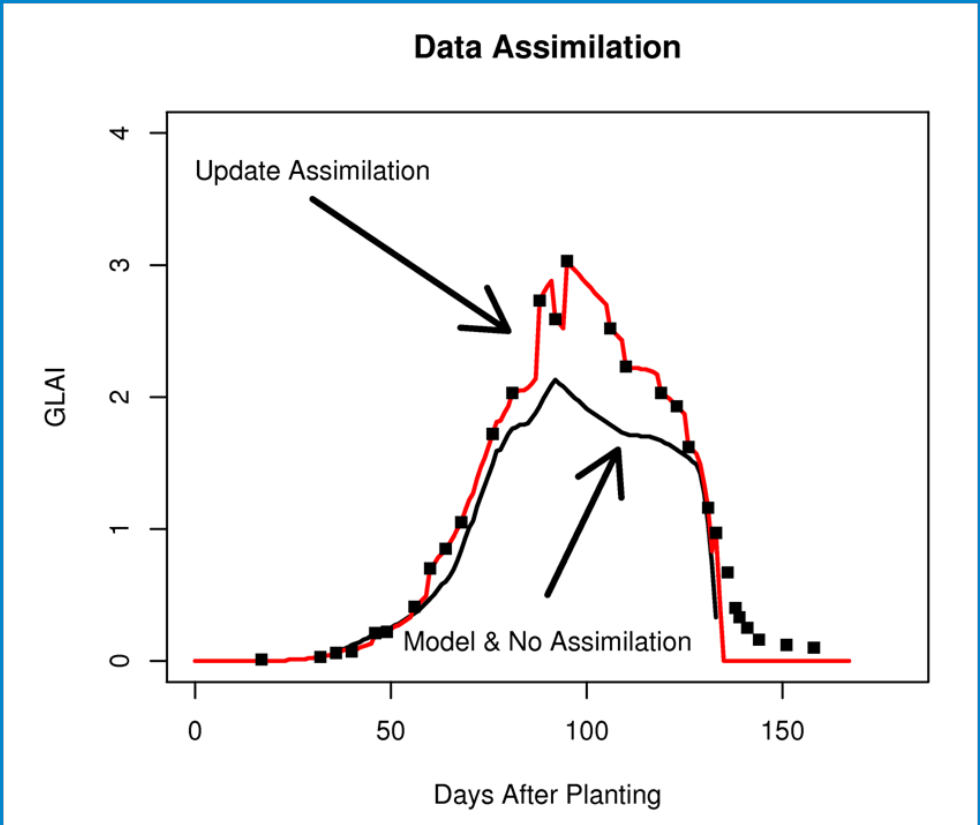

Land surface temperature modeling

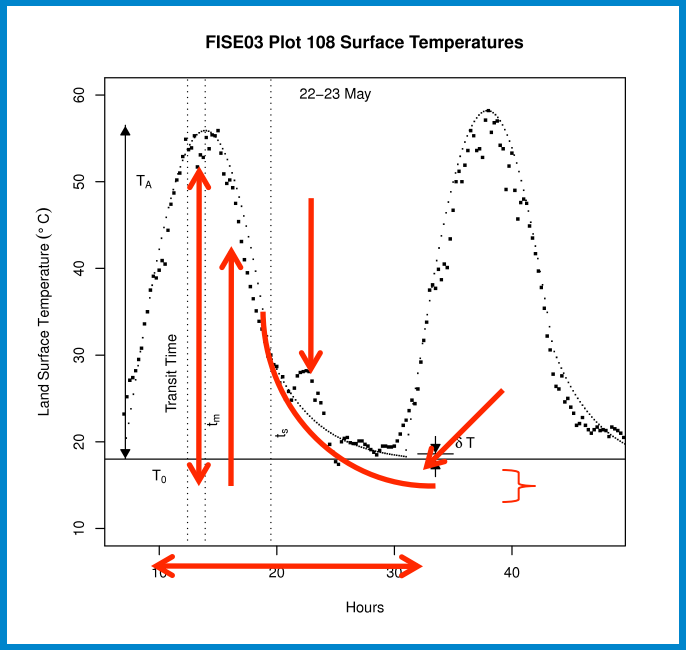

7 Parameter Composite Diurnal Function

- Day length
- Time of maximum temperature
- Time of cosine/exp transition
- Newton cooling decay constant
- Residual temperature difference
- Temperature at sunrise
- Temperature amplitude

$$T(t) = \begin{cases} T_0 + T_a \cos\left[\frac{\pi}{\omega}(t - t_m)\right] & t < t_s \\ (T_0 + \delta T) + \left[T_a \cos\left[\frac{\pi}{\omega}(t_s - t_m)\right] - \delta T\right] \exp\frac{-(t-t_s)}{k} & t \geq t_s \end{cases}$$

How to extrapolate spatially distributed plant cover?

- Updates needed at least weekly
- Some (most?)process models don't handle spatial effects
- Extrapolation needed for 2-week periods
- Model needs to accommodate plot means and variabilities

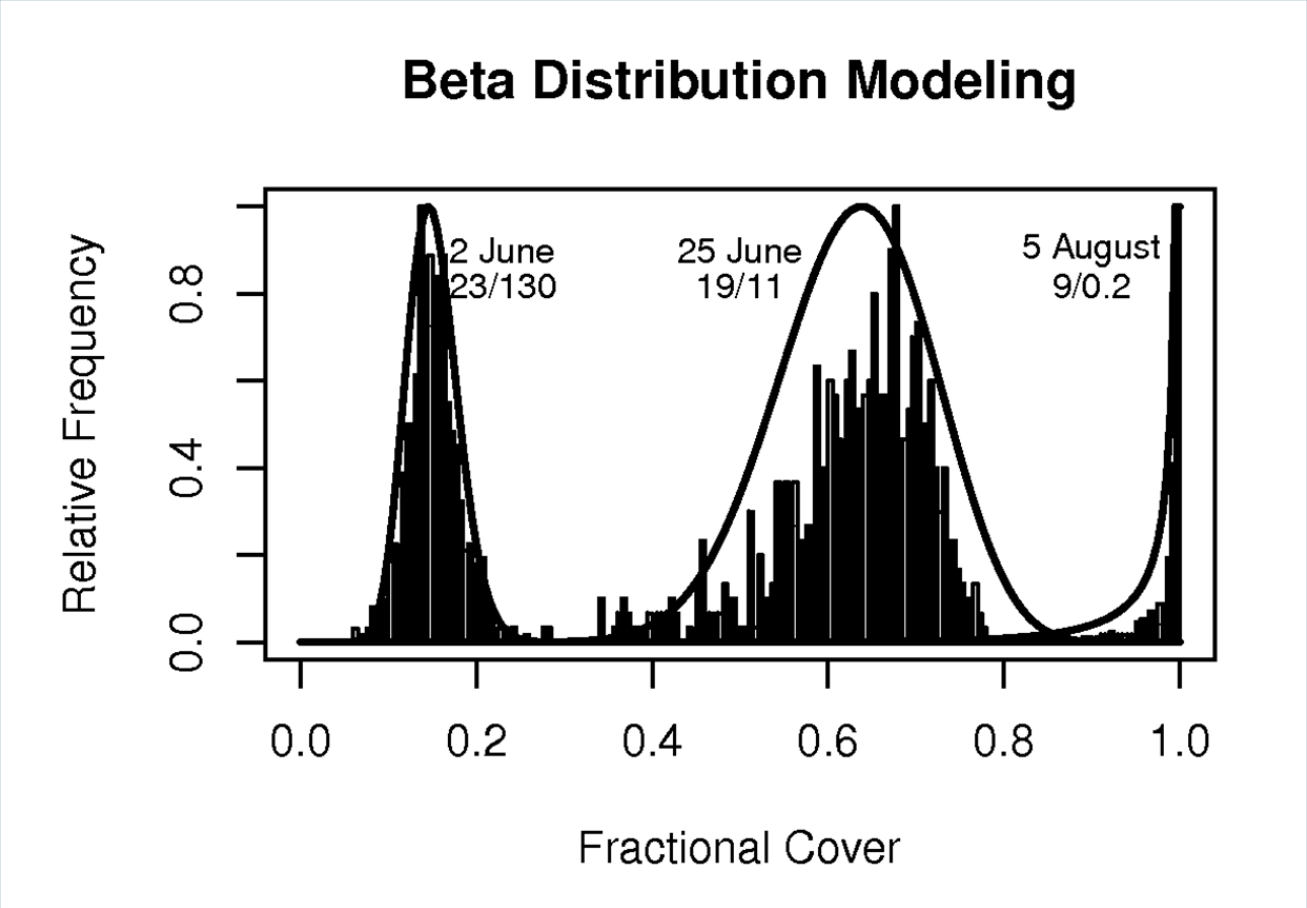

LST Disaggregation & Diurnal LST/NDVI variability

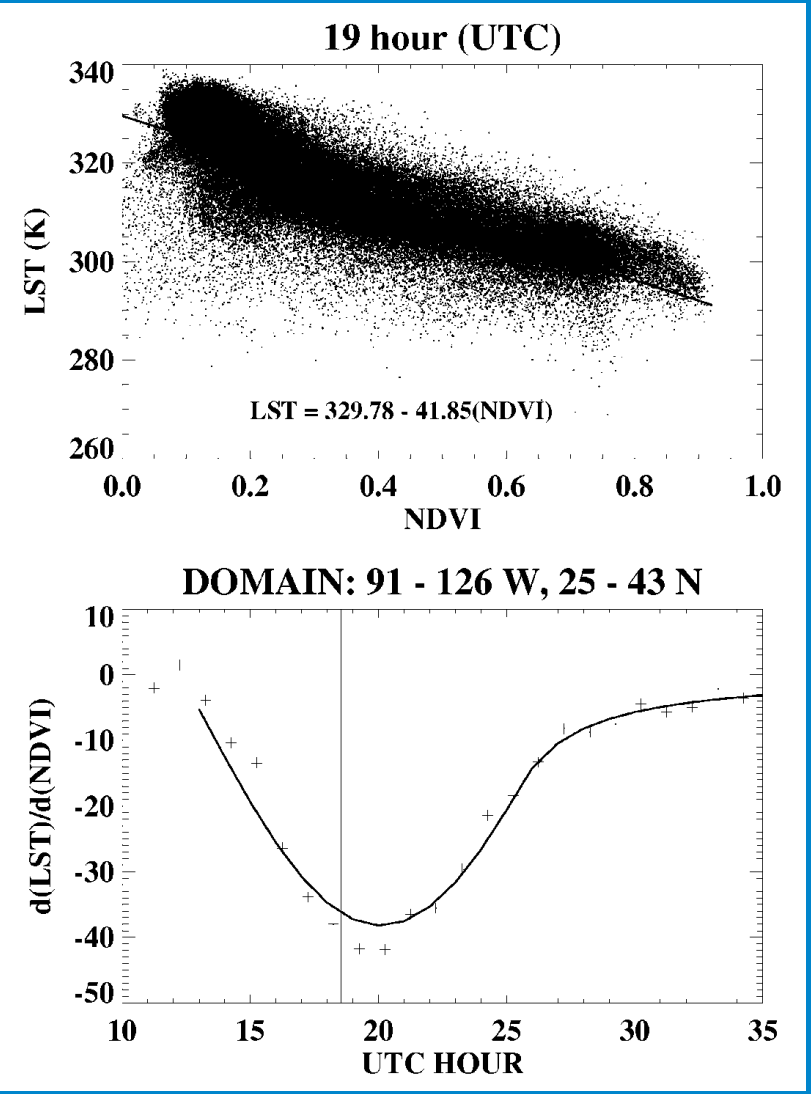

How to Spatially Extrapolate Land Surface Temperatures?

•Empirical approach scales ground observations based on vegetative cover

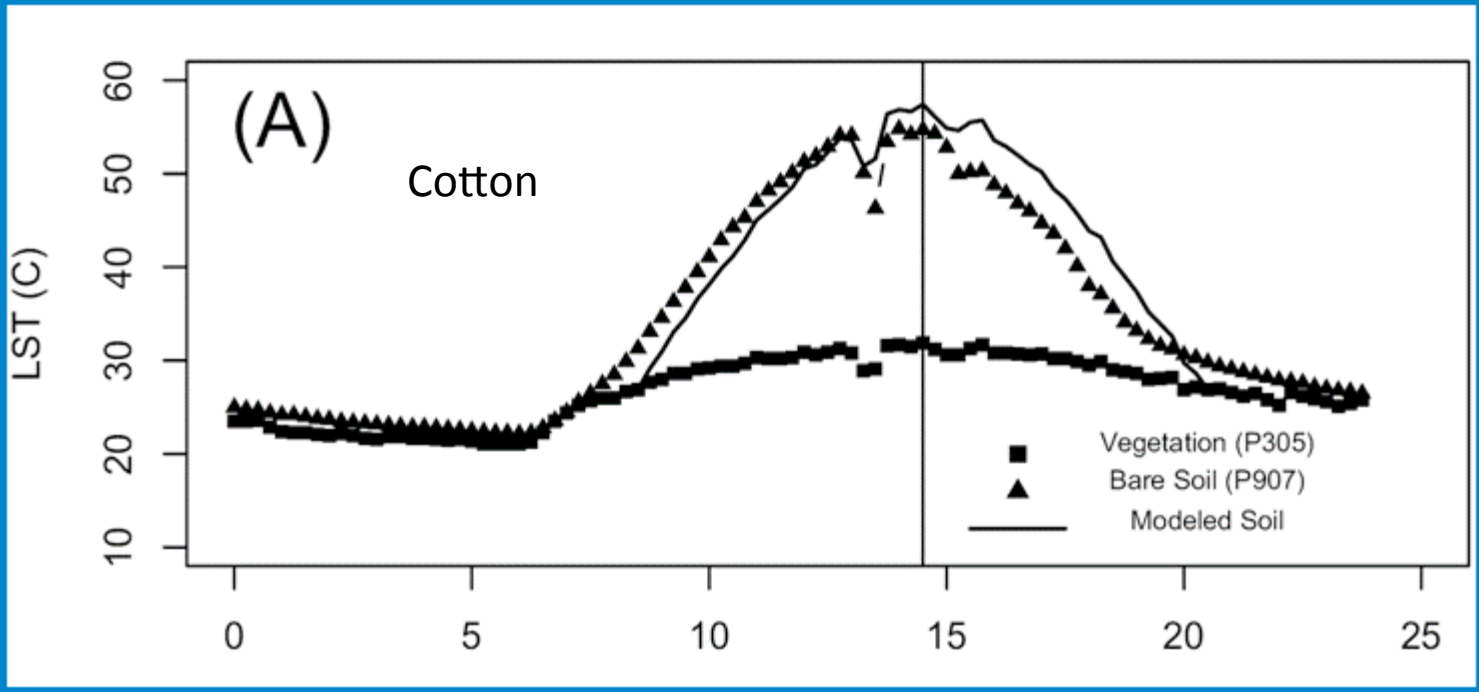

LST's observations from 2-min radiometric observations of plant/soil

Partitioning of Composite Radiometric Temperature

T4 = f*Tveg4 + (1-f)*Tsoil4

- Need additional information to solve
- Sensitive to errors when one fraction is < 0.2
- Some compensation due to corresponding decrease in component Rn

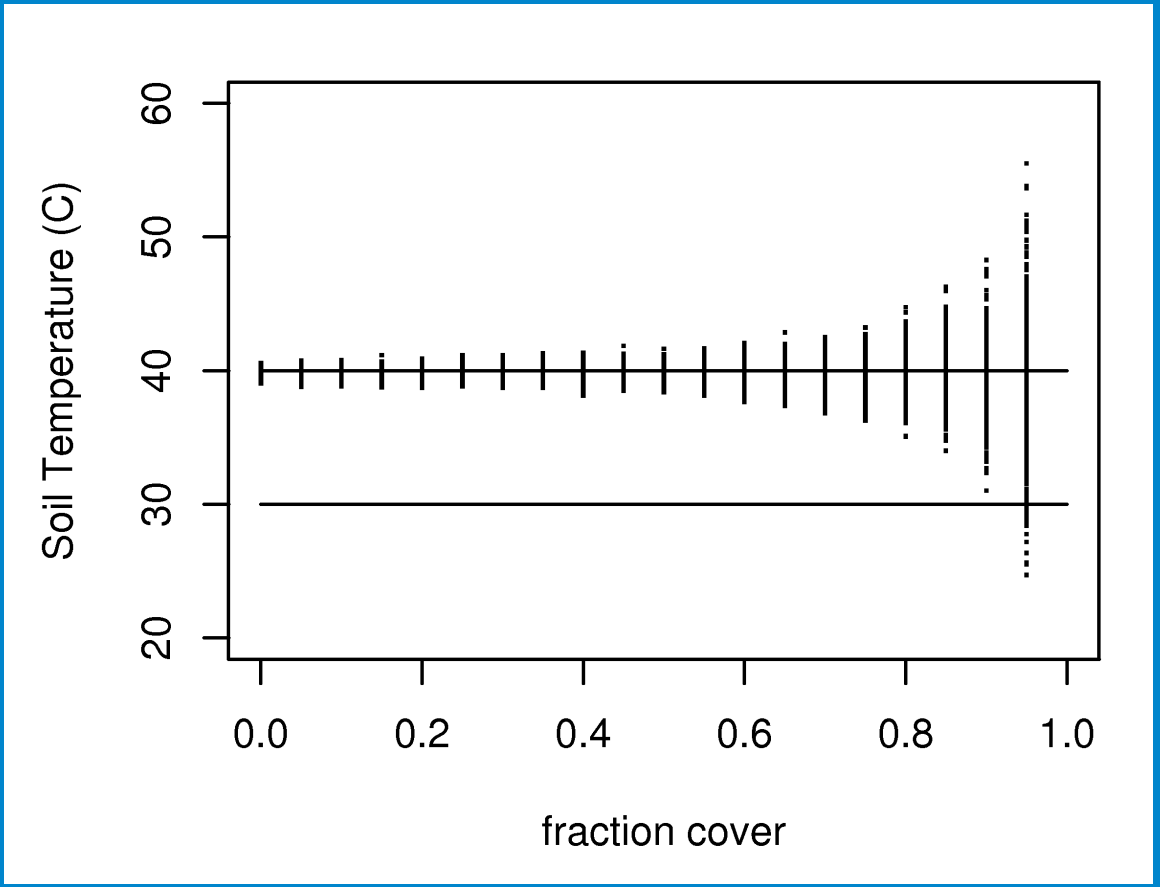

UNCERTAINTIES IN THE RELATIONSHIP BETWEEN HYPERSPECTRAL DATA AND LEAF NITROGEN CONTENT IN TEMPERATE AND BOREAL FORESTS

Y. Knyazikhin[1], M.A. Schull[1], S.V. Ollinger[2], L.Lepine[2], R.B.Myneni[1], P.Stenberg[3], M.Mõttus[4], M. Rautiainen[3], P.L. Carmona[5], R.Kaufmann[1]

[1]Department of Geography and Environment, Boston University
[2]Complex System Research Center, Institute for the Study of Earth, Oceans and Space, University of New Hampshire
[3]Department of Forest Sciences, University of Helsinki
[4]Department of Geosciences and Geography, University of Helsinki
[5]Departamento de Lenguajes y Sistemas Informaticos, Universidad Jaume I, Castellón

HYSPIRI DECADAL SURVEY MISSION SCIENCE WORKSHOP
Washington, DC, August 23-25, 2011

MOTIVATION

- The importance of nitrogen for terrestrial ecosystem carbon dynamics and its climate feedback has been well recognized
- Interaction between carbon and nitrogen at leaf level is among the fundamental mechanisms that directly control the dynamics of terrestrial vegetation carbon
- This process influences absorption and scattering of solar radiation by foliage, which in turn impacts radiation reflected by the vegetation and measured by satellite sensors

How much information about foliar nitrogen do hyperspectral data convey?

SITE AND DATA DESCRIPTION

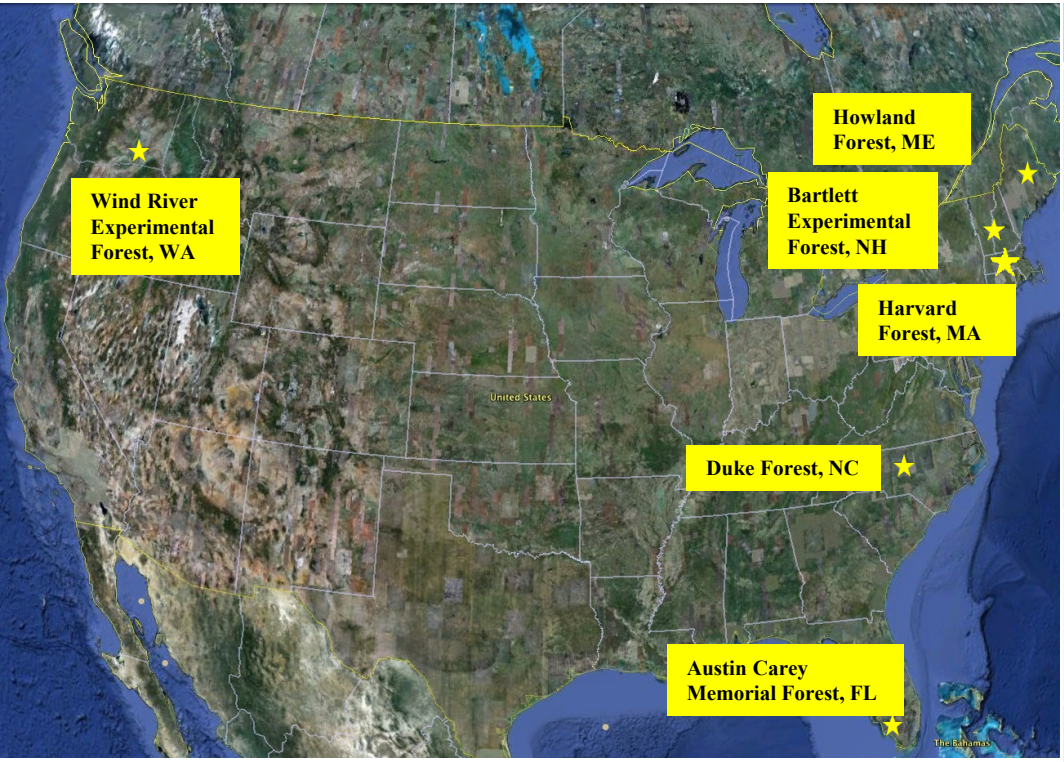

Site	Airborne data	Description
Austin Carey Memorial Forest, FL	AVIRIS	Planted and natural pine
Bartlett Experimental Forest, NH	AVIRIS AirMISR LVIS CHRIS/PROBA	Mixed northern hardwood
Duke Forest, NC	AVIRIS	Pine, pine-hardwood
Harvard Forest, MA	AVIRIS AirMISR LVIS CHRIS/PROBA	Mixed temperate deciduous forest
Howland Forest, ME	AVIRIS AirMISR LVIS CHRIS/PROBA	Boreal-northern hardwood forest
Wind River Experimental Forest, WA	AVIRIS	Temperate evergreen

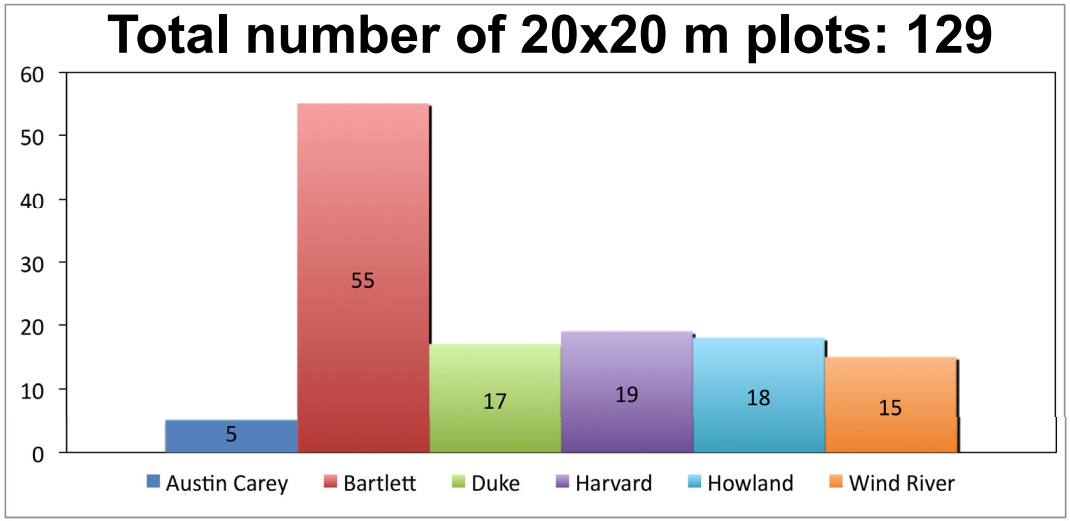

Ground data was collected at 20x20 m plots

Smith, M.L., & Martin, M.E. (2001). A plot-based method for rapid estimation of forest canopy chemistry. *Can. J. of For. Res., 31, 549-555.*

DENSE VEGETATION CANOPY

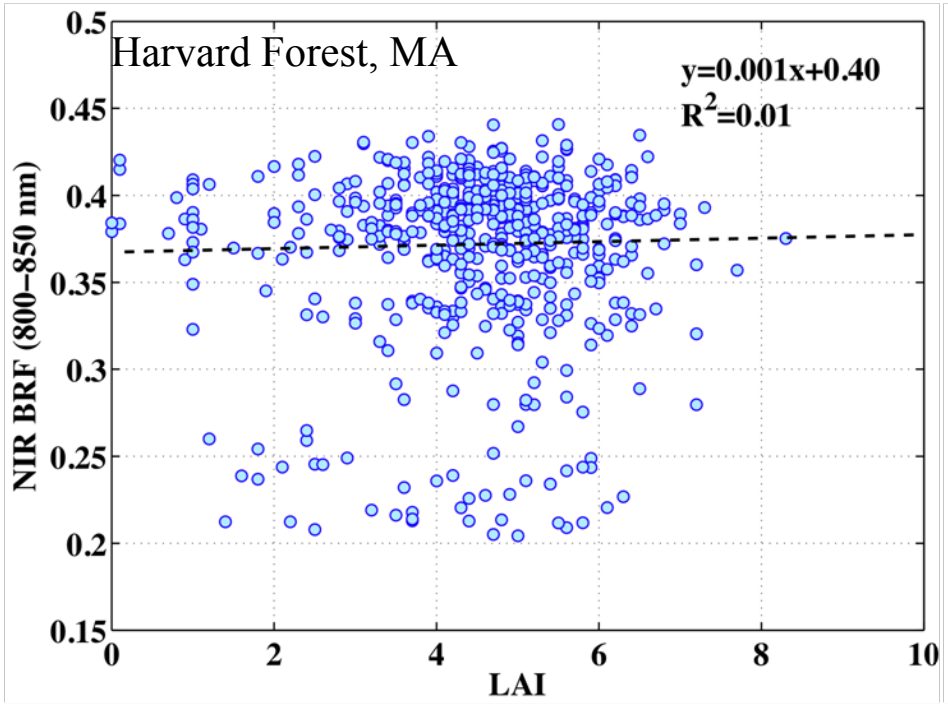

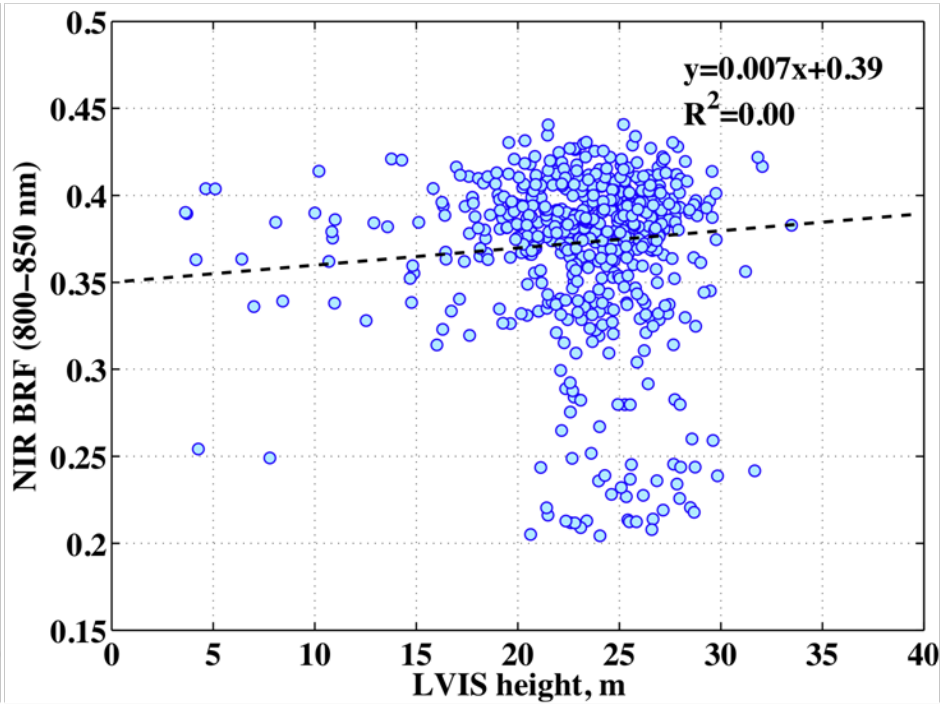

- Sites represent closed canopy forests (LAI~5)
- Impact of canopy background is negligible
- No correlation between BRF, LAI and height

Schull, M.A. (2010). Application of spectral invariants for monitoring forest across multiple scales. PhD Thesis. Department of Geography and Environment, Boston University, November 2nd, 2010, 137 pp., http://library.bu.edu/search/X

DENSE VEGETATION CANOPY

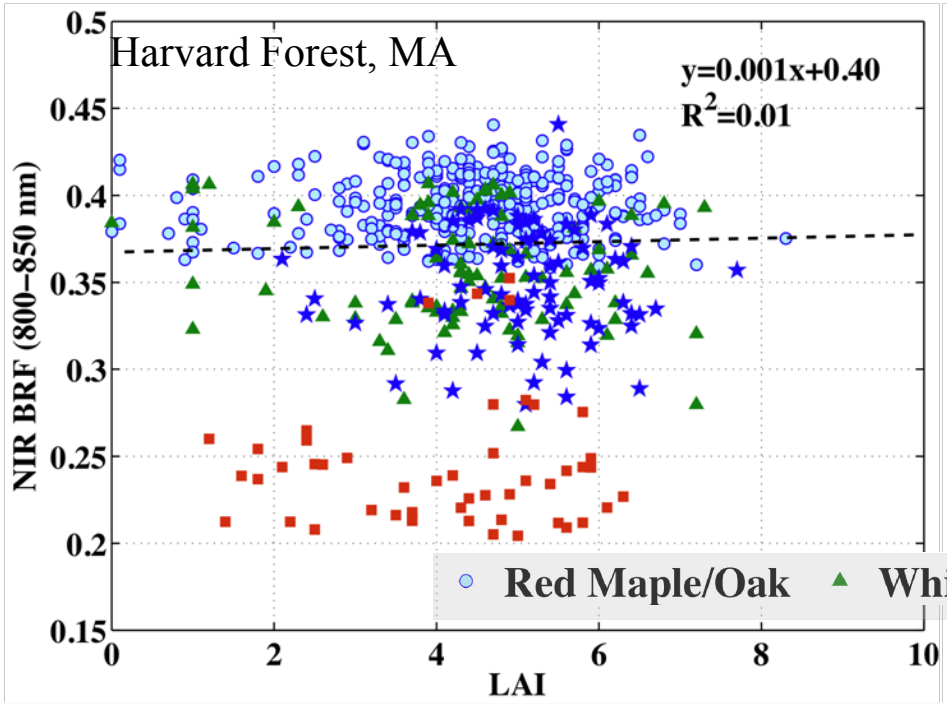

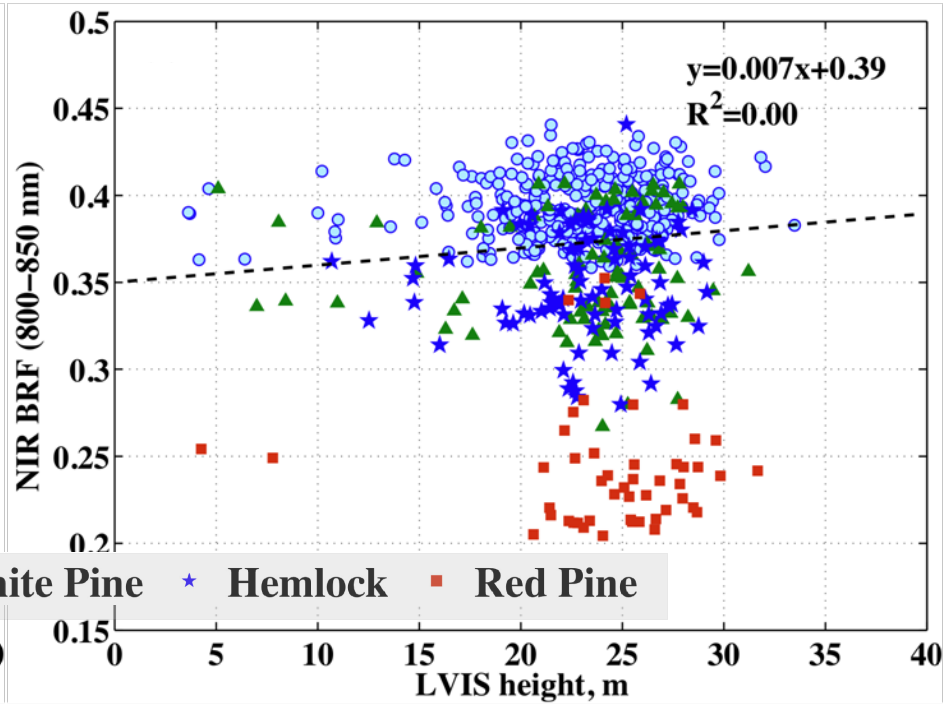

- Sites represent closed canopy forests (LAI~5)
- Impact of canopy background is negligible
- No correlation between BRF, LAI and height

But there are 3D effects of structure

Schull, M.A. (2010). Application of spectral invariants for monitoring forest across multiple scales. PhD Thesis. Department of Geography and Environment, Boston University, November 2nd, 2010, 137 pp., http://library.bu.edu/search/X

Huang et al., (2008). Stochastic transport theory for investigating the three-dimensional canopy structure from space measurements. Remote Sens. Environ. 112, 35-50.

FOREST REFLECTANCE AND FOLIAR NITROGEN

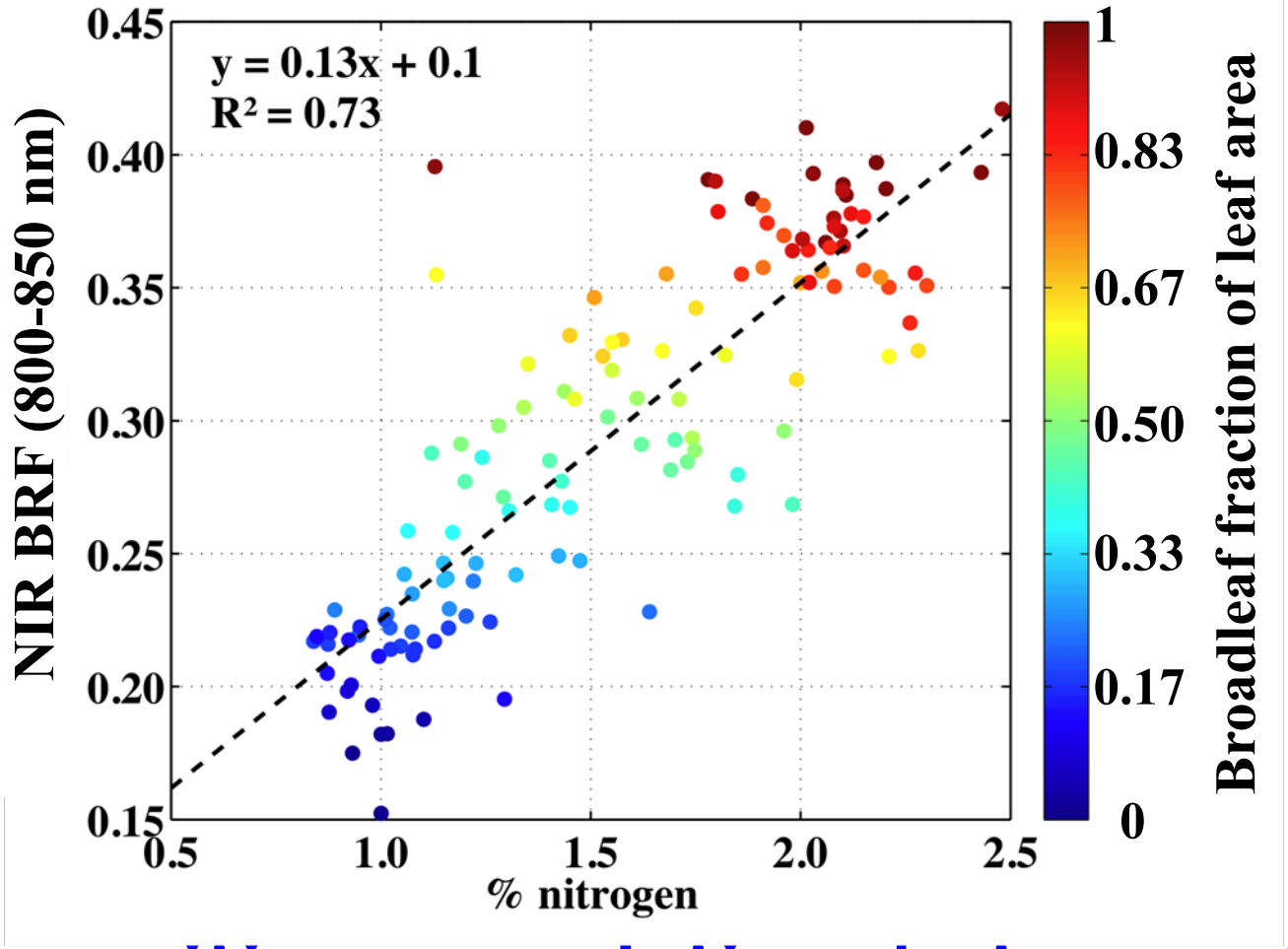

- Strong positive correlation between forest NIR zenith reflectance and foliar N
- Valid for the global SW radiation (400-2,500nm)

Ollinger, S.V. et al. (2008). Canopy nitrogen, carbon assimilation, and albedo in temperate and boreal forests: Functional relations and potential climate feedbacks. Proc. Natl. Acad. of Sci., 105, 19336-19341.

MONITORING FOLIAR NITROGEN FROM SPACE

- **Does the positive BRF vs. N relationship provide a basis for monitoring the foliar nitrogen from space using NIR and/or SW surface reflectance data?**
  - Canopy structure is the dominant factor that positively relates NIR BRF and N
  - The observed BRF vs. N correlation conveys no information about foliar N.

- **What about hyperspectral data?**
  - 3D effects of canopy structure can easily be removed
  - provide a link to leaf optics
  - leaf surface properties have an impact on forest reflectivity, lowering its sensitivity to leaf absorbing pigments …

N AND BRF ARE STRONGLY AND POSITIVELY RELATED TO BfLAI

Bartlett Forest

Mean N (std), in g per 100g of dry leaf mass[1]	
needle	1.24 (0.26)
flat leaf	2.17 (0.40)

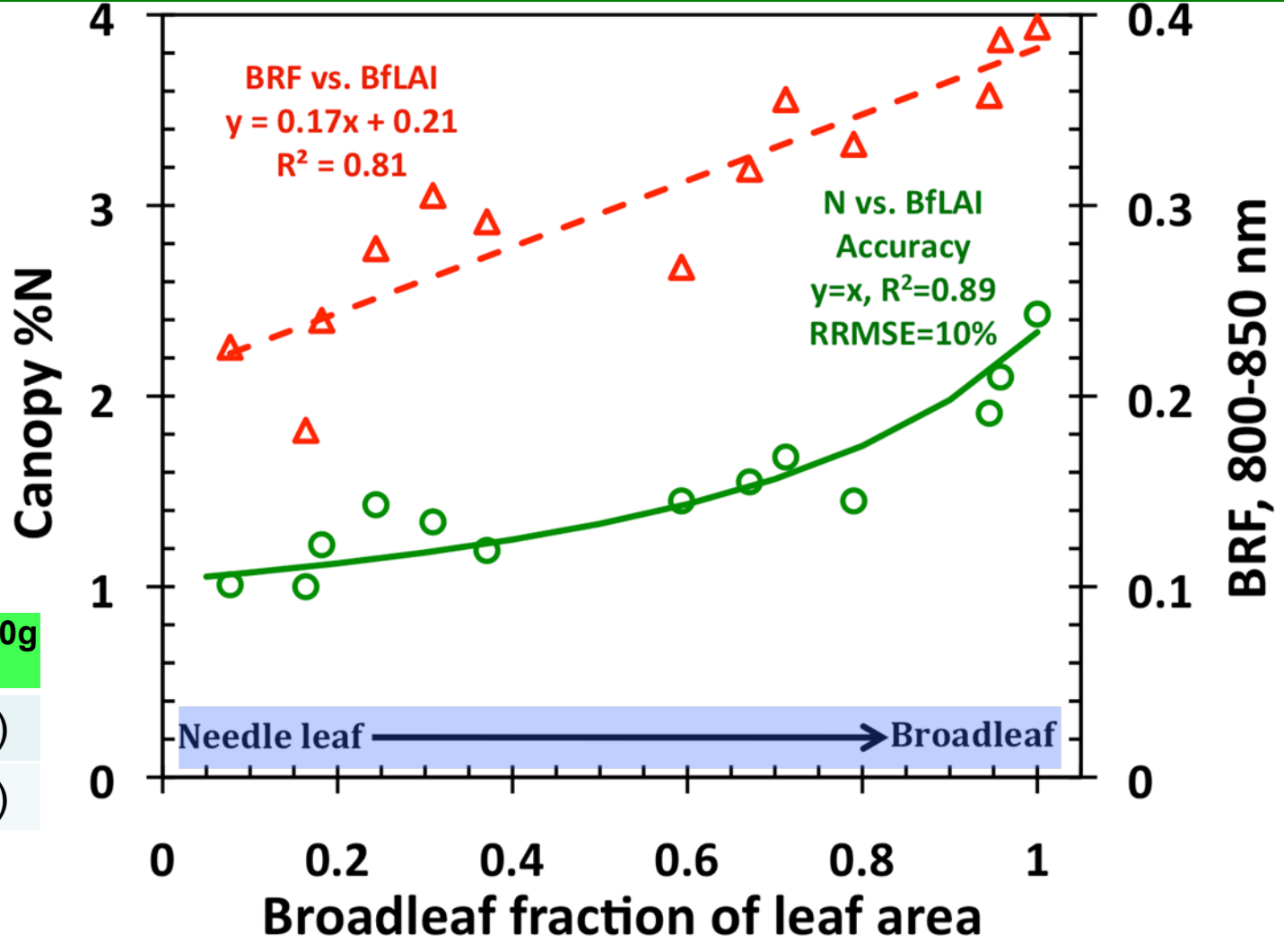

Structure positively relates NIR BRF(zenith) and N

[1]Smith, M.L., & Martin, M.E. (2001). A plot-based method for rapid estimation of forest canopy chemistry. Can. J. of For. Res., 31, 549-555

Rautiainen&Stenberg (2005). Application of photon recollision probability in coniferous canopy reflectance simulations. Remote Sens. Environ. 96, 98-107.

OUT-OF-SAMPLE TEST

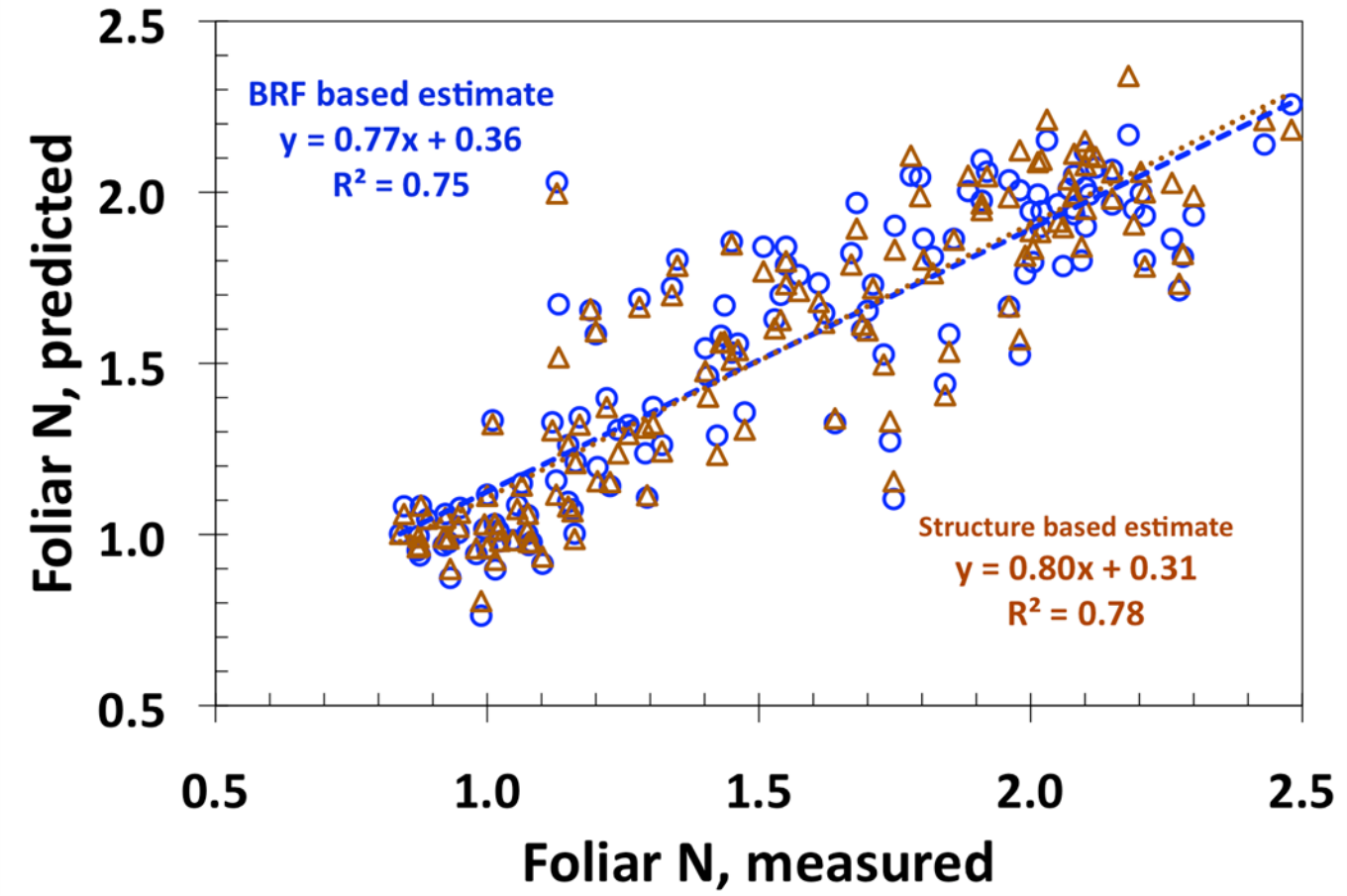

Method 1: Use the empirical NIR BRF vs. N relationship to estimate N

Method 2: Use spectral interval [710,790] to estimate canopy structure first and then N

Schull, M.A. (2010). Application of spectral invariants for monitoring forest across multiple scales. PhD Thesis. Department of Geography and Environment, Boston University, November 2nd, 2010, 137 pp., http://library.bu.edu/search/X

PARAMETERIZATION OF CANOPY STRUCTURE

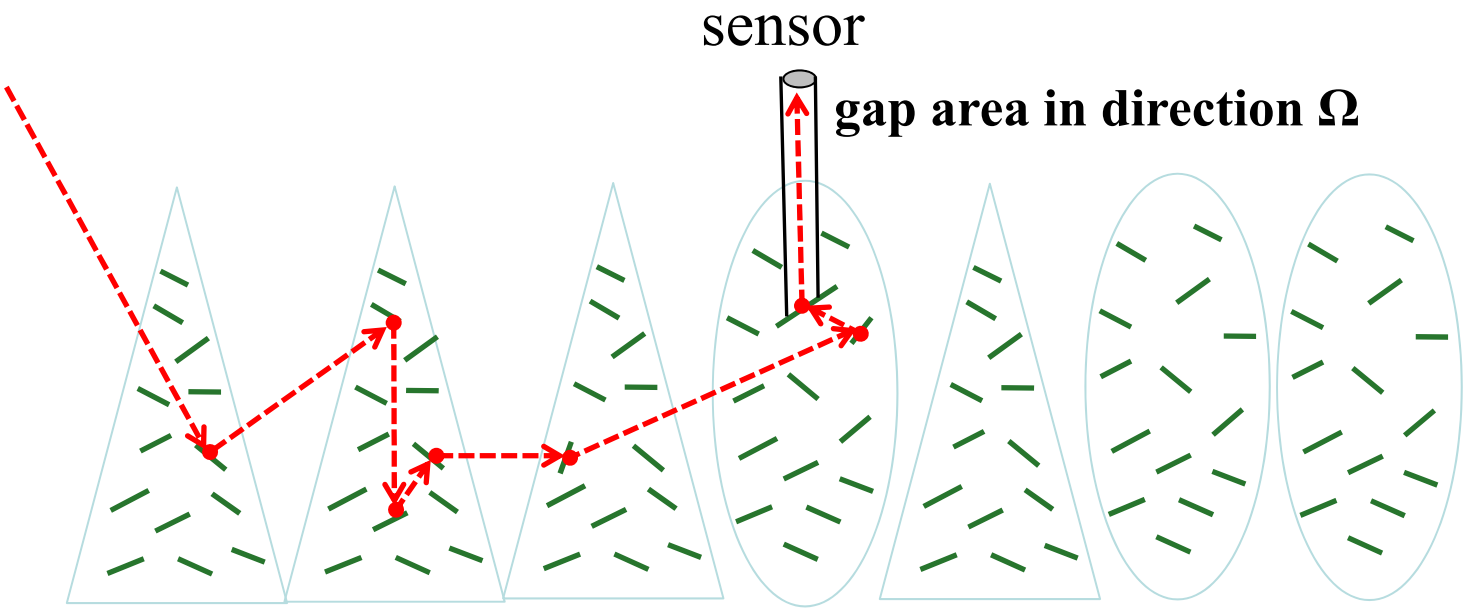

- Gap area fraction: total gap area in Ω normalized by the total leaf area = fraction of leaf area that "sensor sees" in a given direction
- Can directly be estimated from BRF spectrum in [710,790nm] (no models are needed!)
- Physics[1]: (a) multiple scattering dominates; (b) minimal impact of absorbing pigments; (c) sharp jump in leaf albedo

[1]See our poster "Retrieval of distribution of gaps in vegetation canopies using hyperspectral data"

GAP AREA FRACTION AND SPECIES COMPOSITION

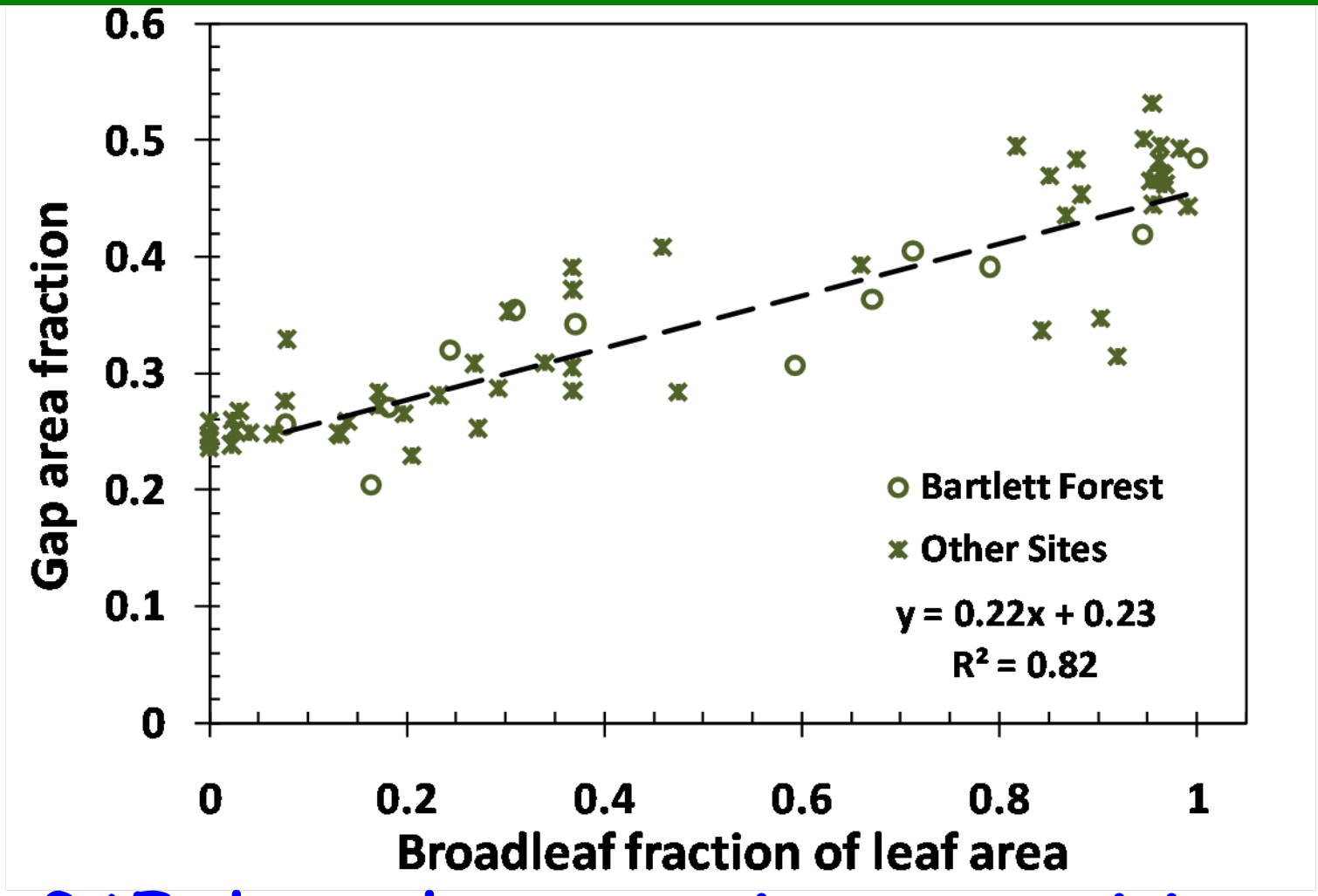

- GAF depends on species composition
- Useful in interpretation of LIDAR data
- BfLAI is labor intensive while GAF not

NIR BRF AND GAP AREA FRACTION

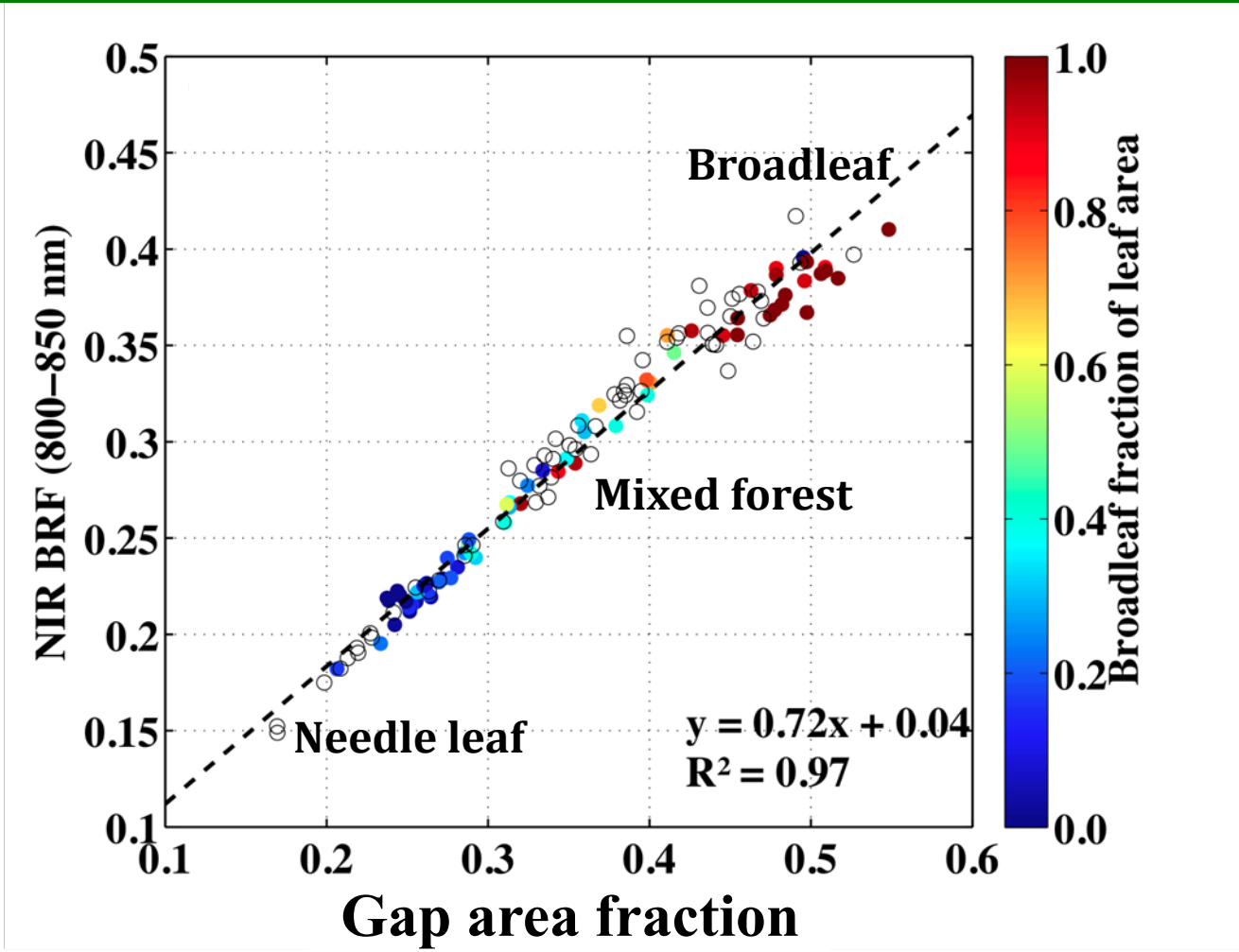

The GAF explains variation in NIR BRF due to variation in canopy structure.

CANOPY SCATTERING

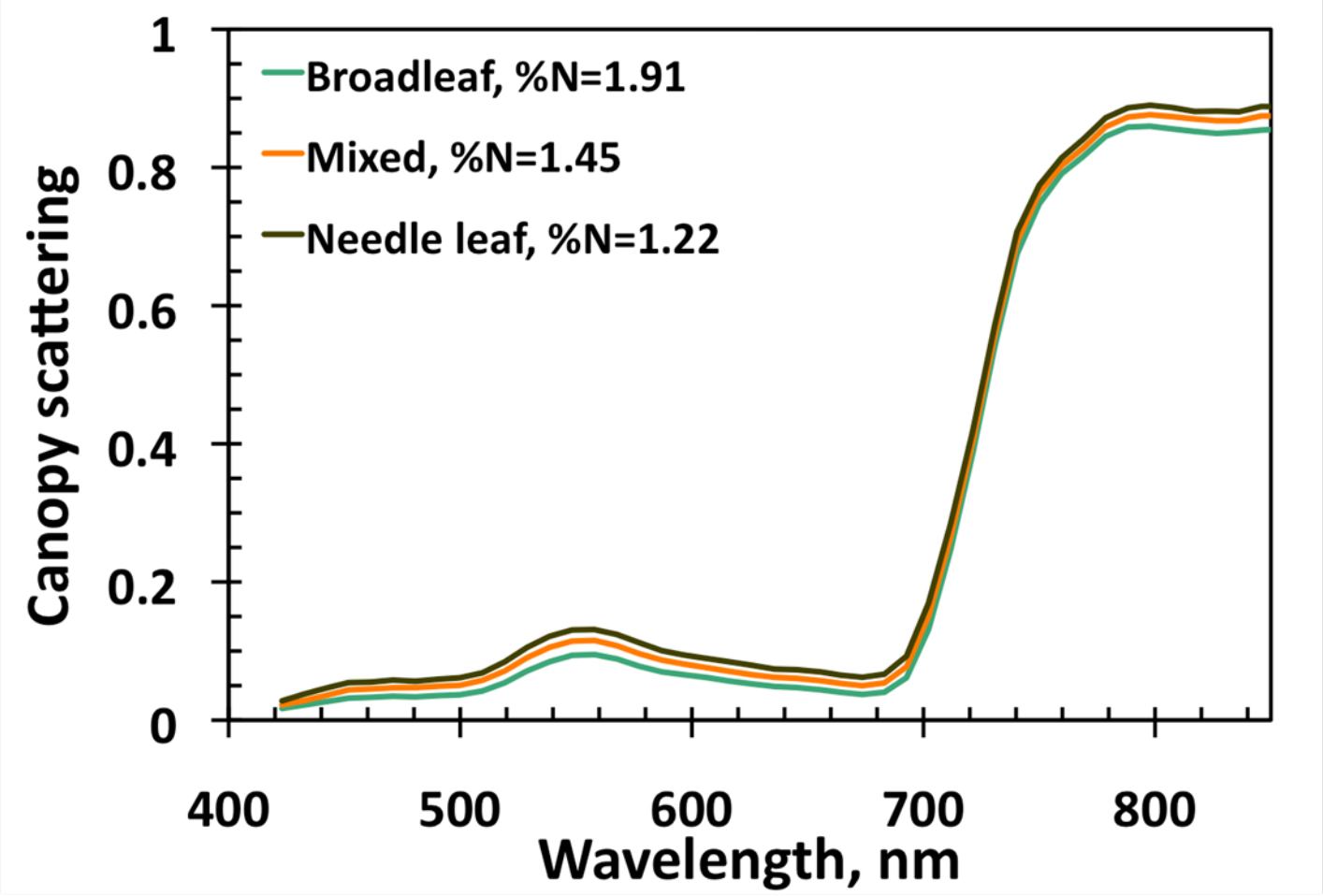

- mimics shape and magnitude of leaf albedo spectrum
- negatively related to N for all wavelength in the interval [420,900 nm]

SENSITIVITY TO LEAF ABSORBING CONSTITUENTS

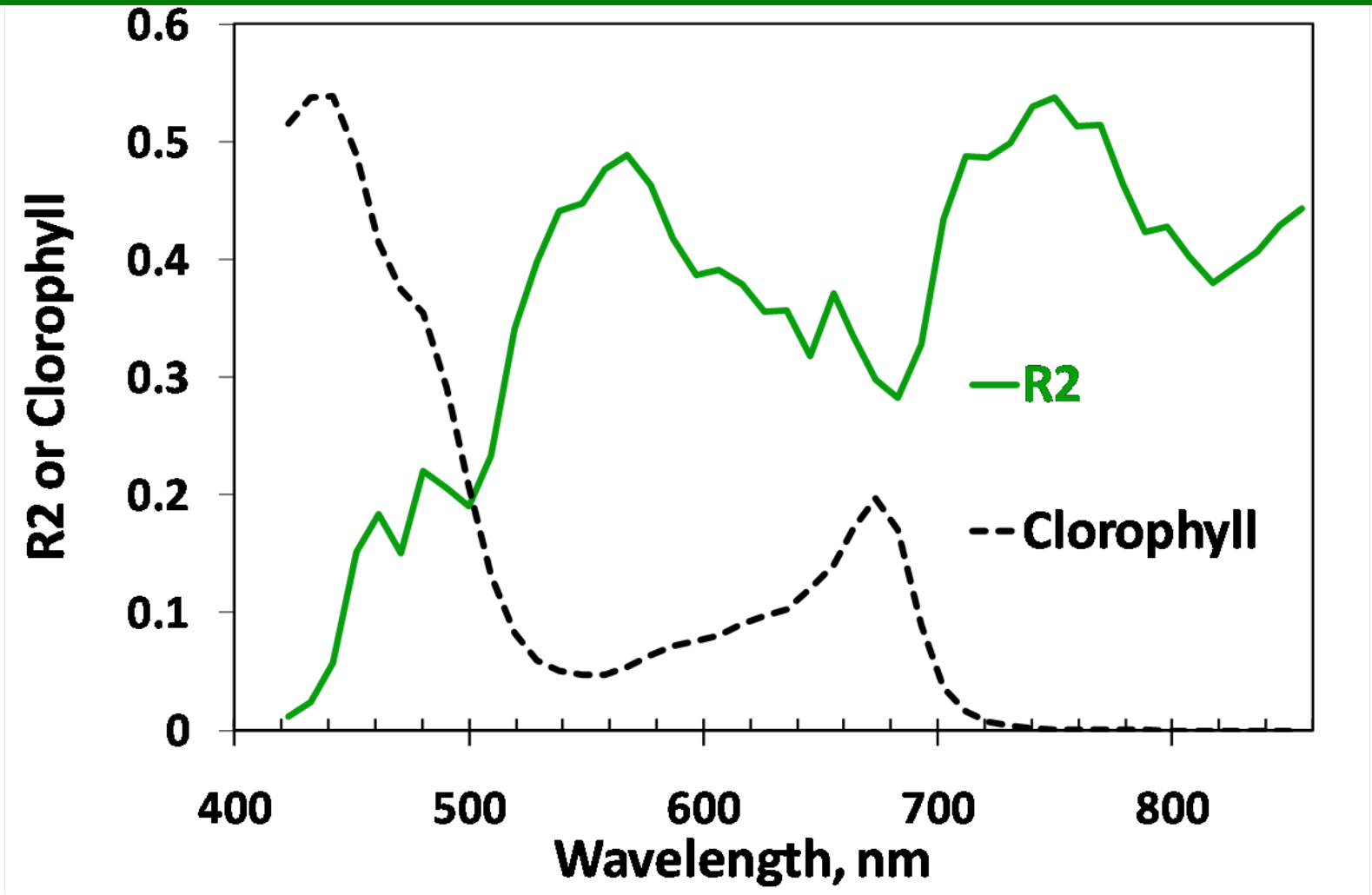

Foliar N can explain up to 55% of variation in AVIRIS spectra in the interval between 400nm and 900nm

REFLECTION AND POLARIZATION

Airborne MultiangleSpectroPolarimetric Imager: georectified Image of Palmdale

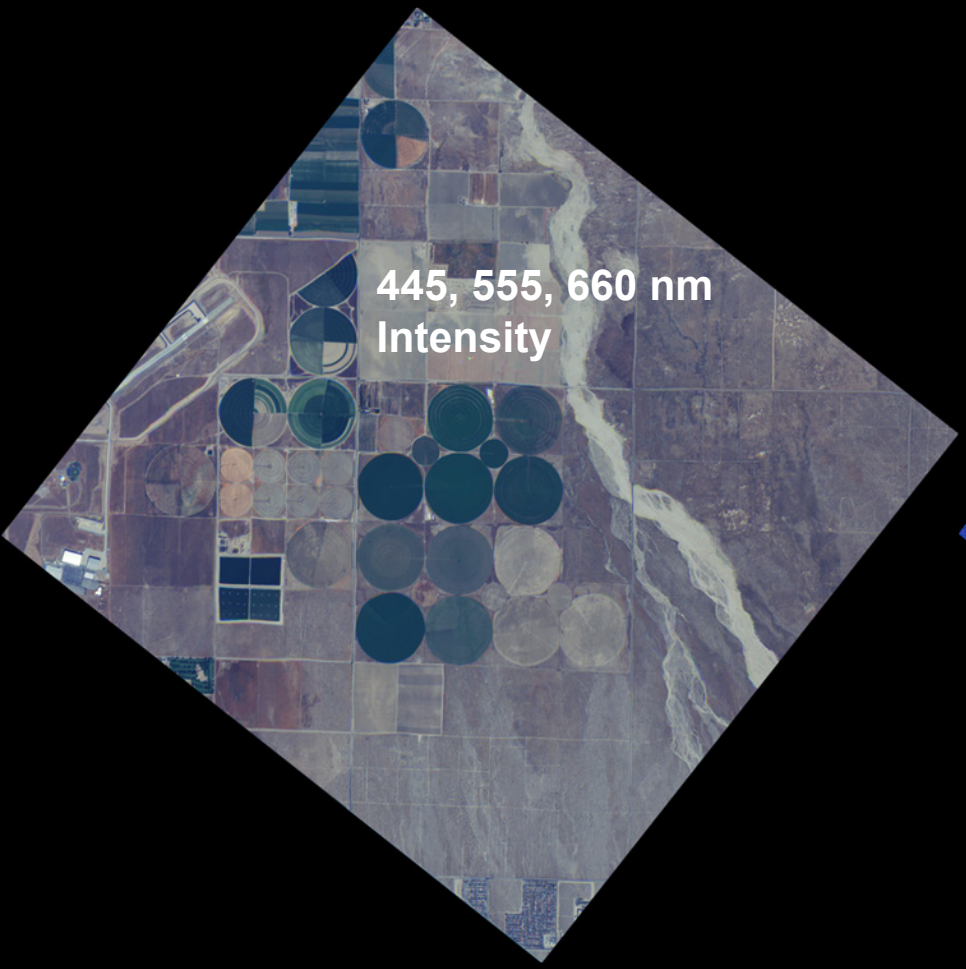

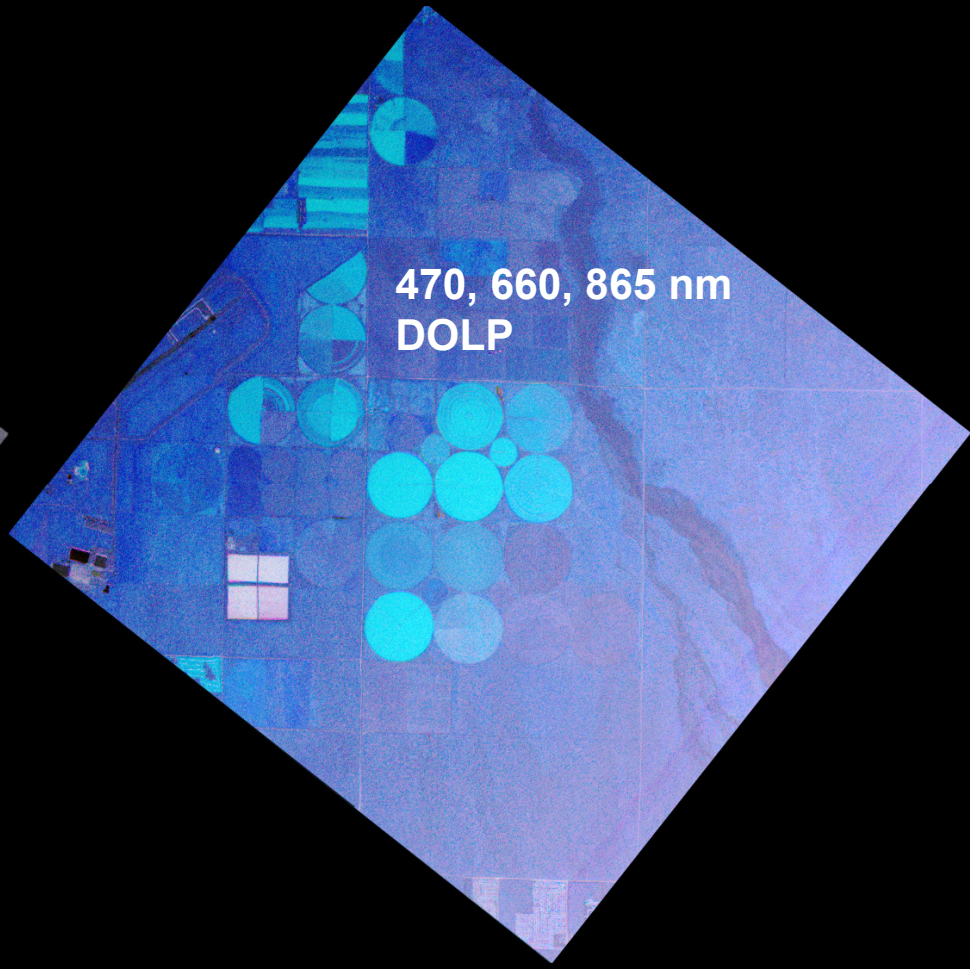

Images from D.Diner et al., Early results from Ground MSPI and AirMSPI, MISR Data Users Science Symposium, Dec. 2010.

SURFACE AND DIFFUSE LEAF SCATTERING

Airborne MultiangleSpectroPolarimetric Imager: georectified Image of Palmdale

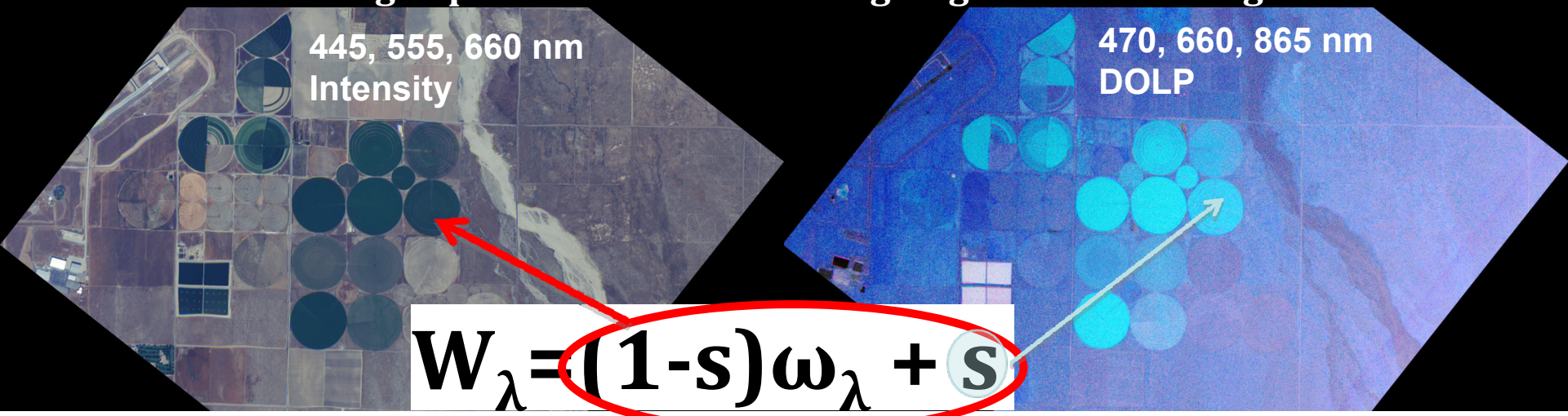

Radiation scattered by a leaf includes two components

1) Radiation reflected at the air-cuticle interface
   - ❑ polarized; weak spectral variation; depends on the leaf surface properties; no info about leaf interior
2) Diffuse radiation due to "within leaf photon interactions"
   - ❑ non-polarized, depends on absorption spectra of leaf pigments; conveys info about leaf interior

Polarized reflectance of 9% can account for 68% of the total leaf reflection[1]

[1]Grant et al.,(1993) Polarized and Specular Reflectance Variation with Leaf Surface-Features. Physiol Plantarum 88(1):1-9.
Images from D.Diner et al., Early results from Ground MSPI and AirMSPI, MISR Data Users Science Symposium, Dec. 2010.

LEAF BIOCHEMISTRY FROM SPACE

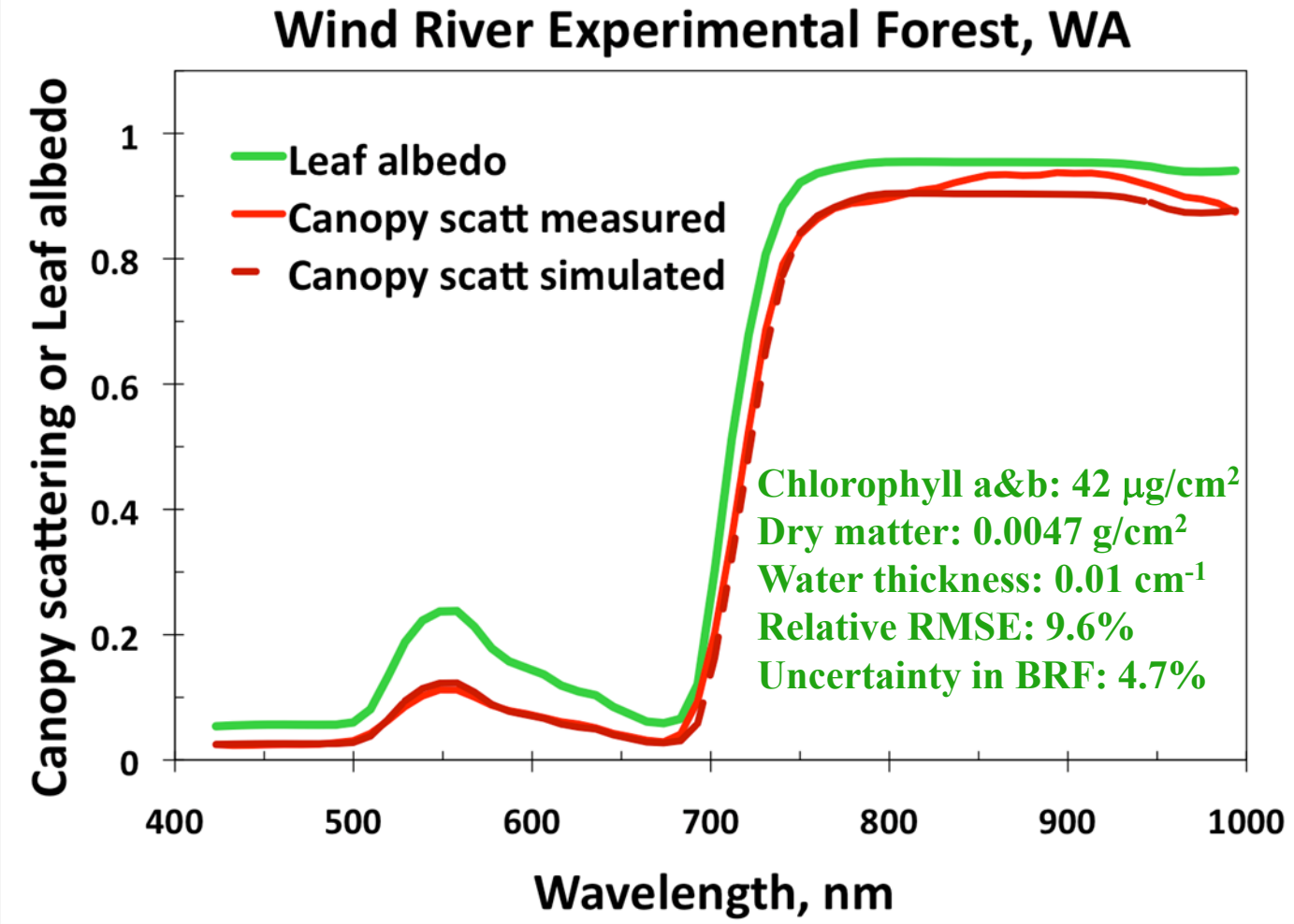

Information about leaf surface properties may require to fully remove impact of canopy structure

SUMMARY

- Canopy structure can significantly suppress the sensitivity of hyperspectral data to leaf optics
- Reflectance spectra in the interval [710, 790 nm] are required to obtain the Gap Area Fraction
- The Gap Area Fraction explains variation in measured reflectance spectra due to variation in canopy structure
- Leaf surface properties may have an impact on forest reflectivity, lowering its sensitivity to leaf absorbing pigments
- Foliar nitrogen concentration can explain up to 55% of variation in AVIRIS spectra. The remaining factors could be due to

  a) impact of leaf surface properties and/or

  b) under-sampling of leaf optical properties due to the single view of the AVIRIS sensor

Measurement of Urban Land Surface Temperatures as Related to Land Cover Change Dynamics: The HysplRI Advantage

Moving Towards an Integrated Interdisciplinary Urban Science

Dale A. Quattrochi

NASA

Earth Science Office

Marshall Space Flight Center

Huntsville, Alabama

The Talk

Perceptions of HyspIRI Data Applications to Urban Land Use/Land Cover Change, Analysis of the Urban Heat Island Effect, and Climate Impacts

- HyspIRI VSWIR-TIR data for Land Cover/Land Use Change (LULCC) relationships with Land Surface Temperature (LST) for analysis of Urban Heat Island (UHI) at the local scale

- HyspIRI LULCC and LST relationships for UHI analysis at local to regional, or potentially even global, scales

- Integration of HyspIRI data with multi-scaled geospatial data for modeling and assessment of urbanization impacts on the peri-urban environment and climate

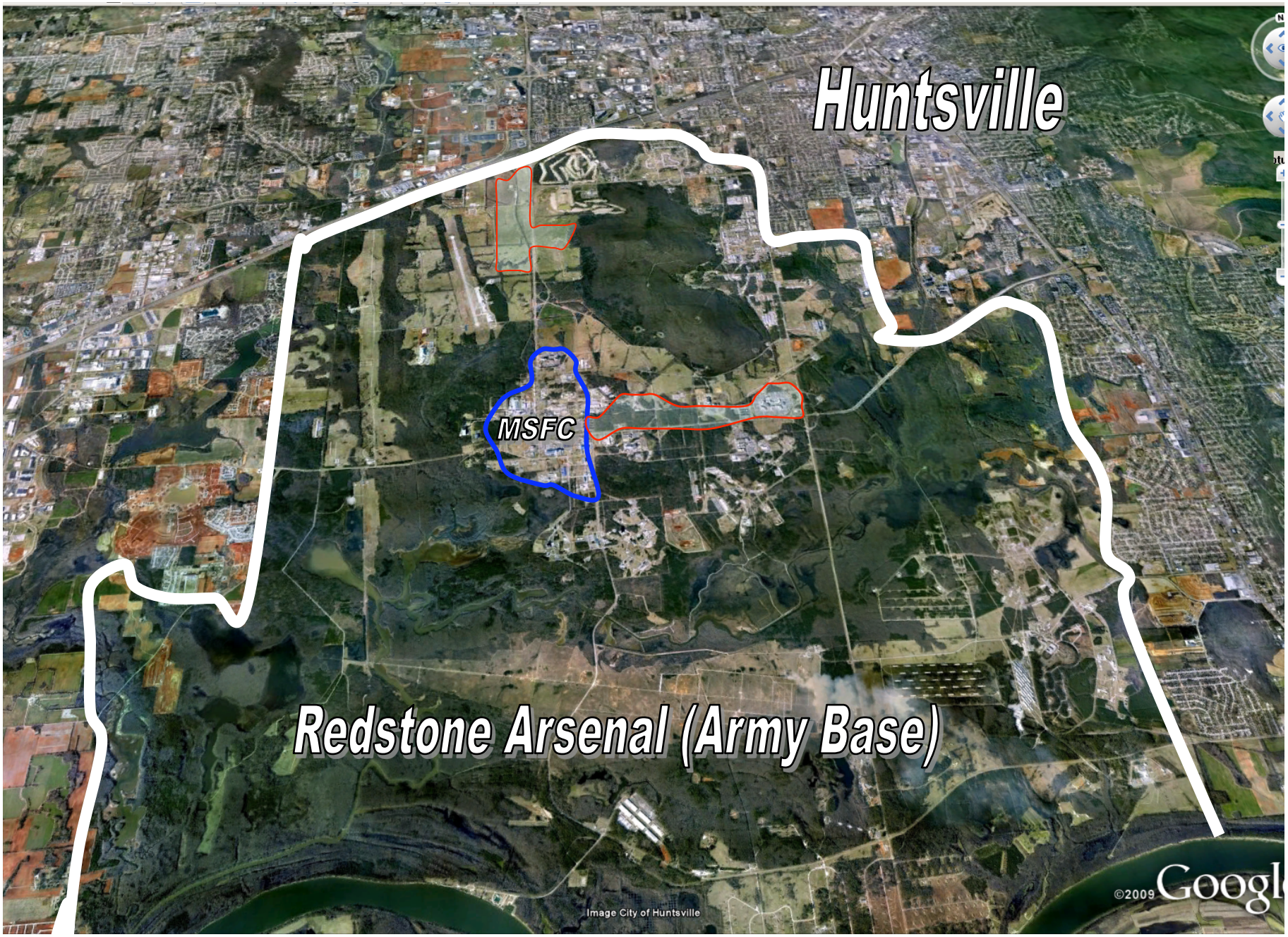
Huntsville
MSFC
Redstone Arsenal (Army Base)
Image City of Huntsville
©2009 Google

Weather Station Installation

- 11 sites across MSFC
- 10m wind speed and direction (not shown)
- 2m temperature, humidity, rainfall (below)

Real-time transmission (1-5 min intervals)

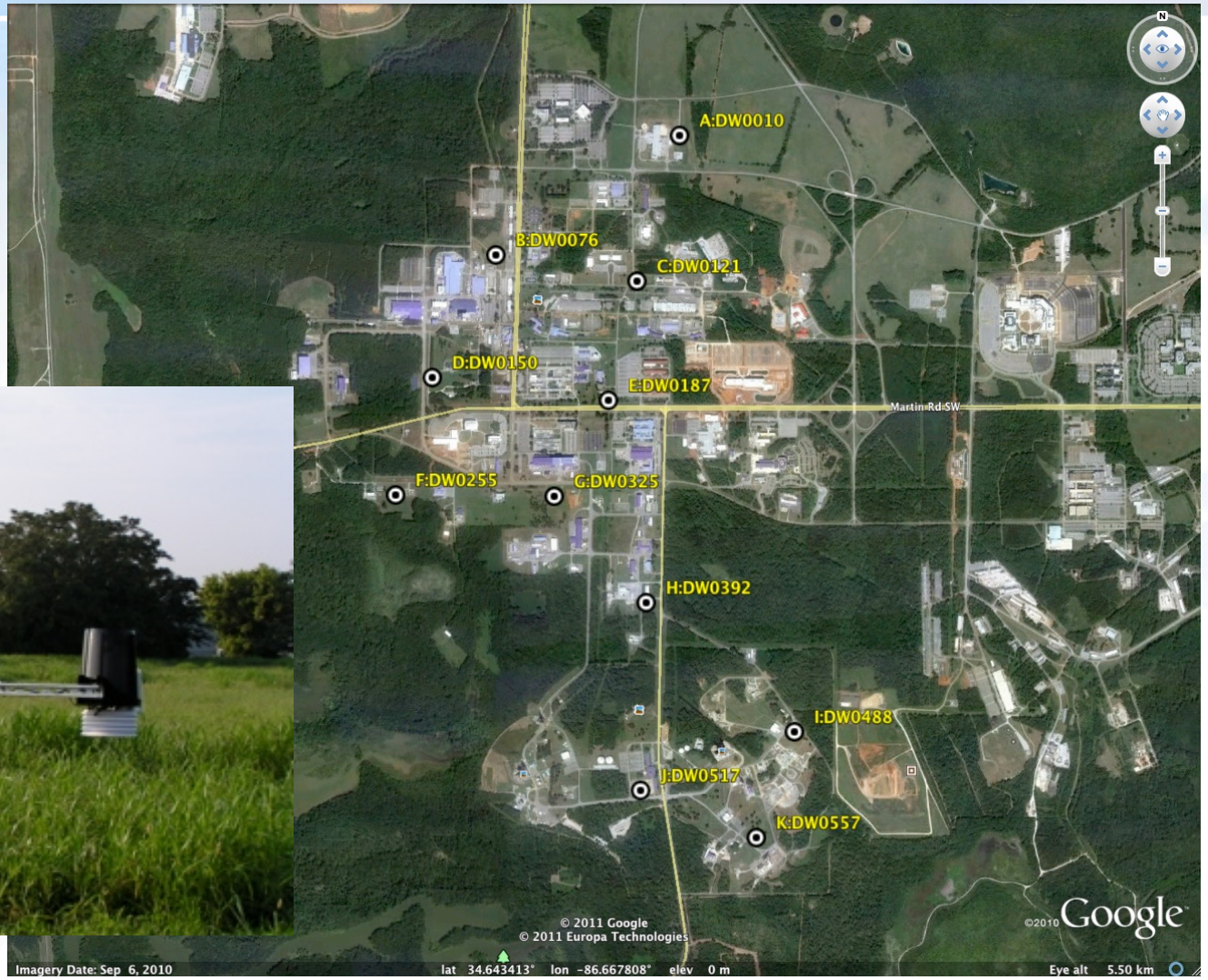

Land Cover and Climate Change Impacts

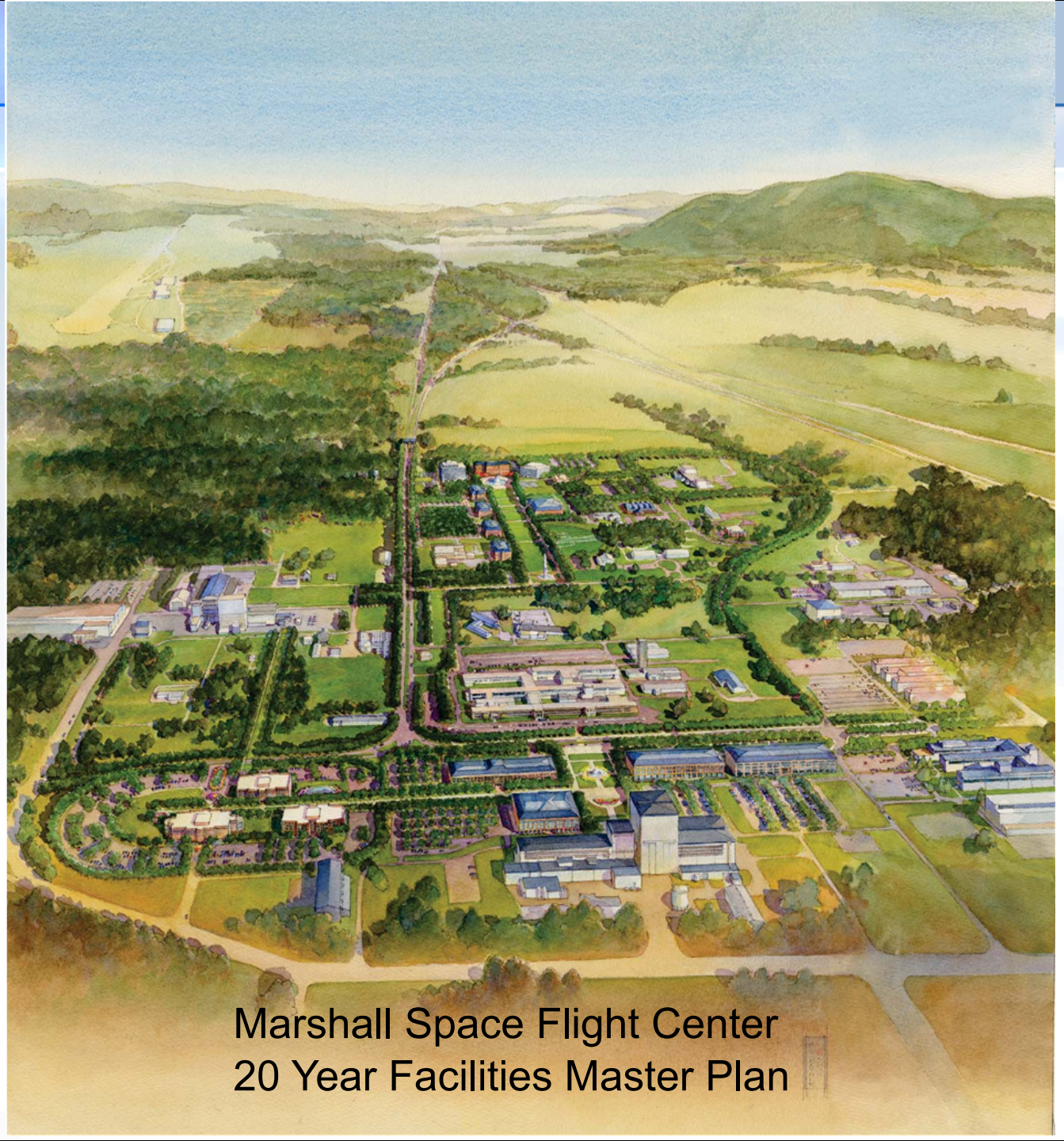

Marshall Space Flight Center
20 Year Facilities Master Plan

Land Use Change around MSFC

Dramatic increase in urban-residential land use category from 1992-2001

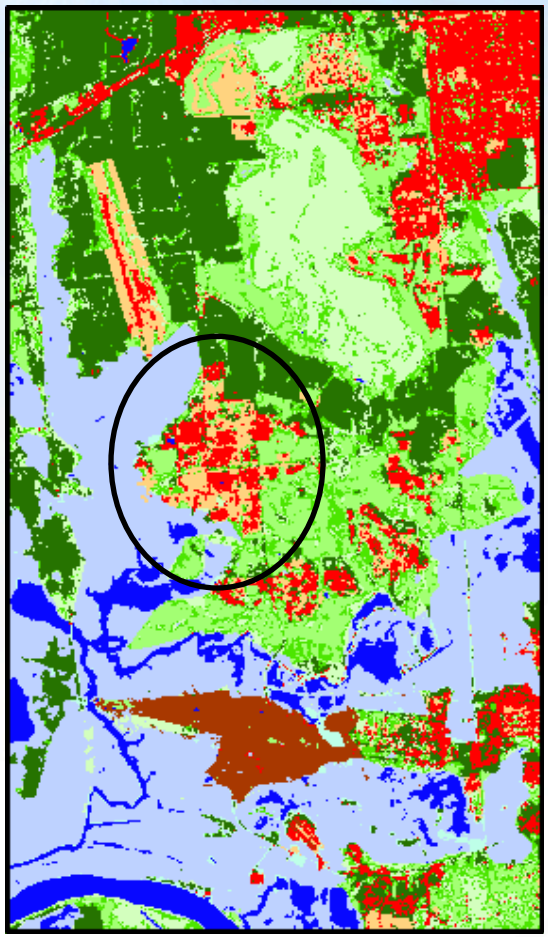

1992

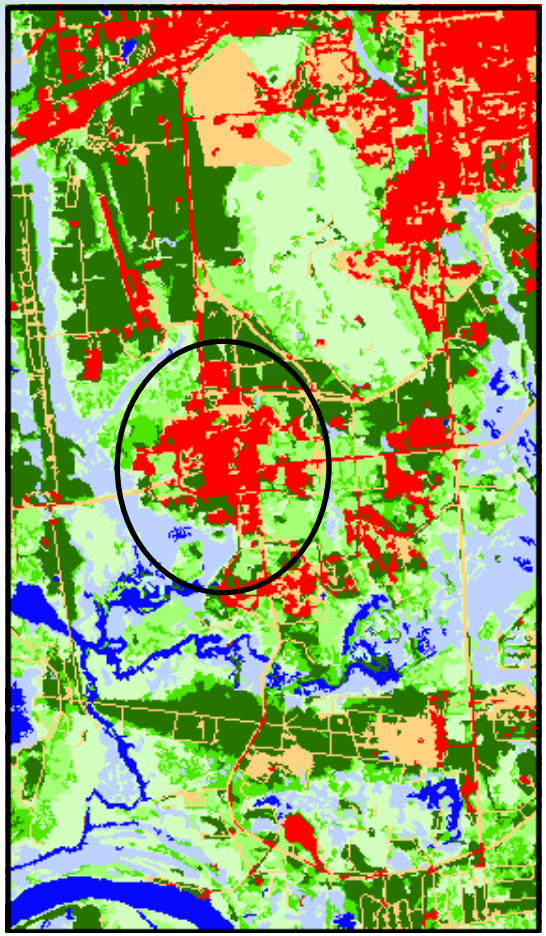

2001

- Water
- Developed Open Space/Recreational Grasses
- Residential/Commercial
- Bare Soil / Transitional
- Deciduous Forest
- Evergreen Forest
- Mixed Forest / Shrub
- Agricultural / Pasture
- Woody Wetlands
- Emergent Herbaceous Wetlands

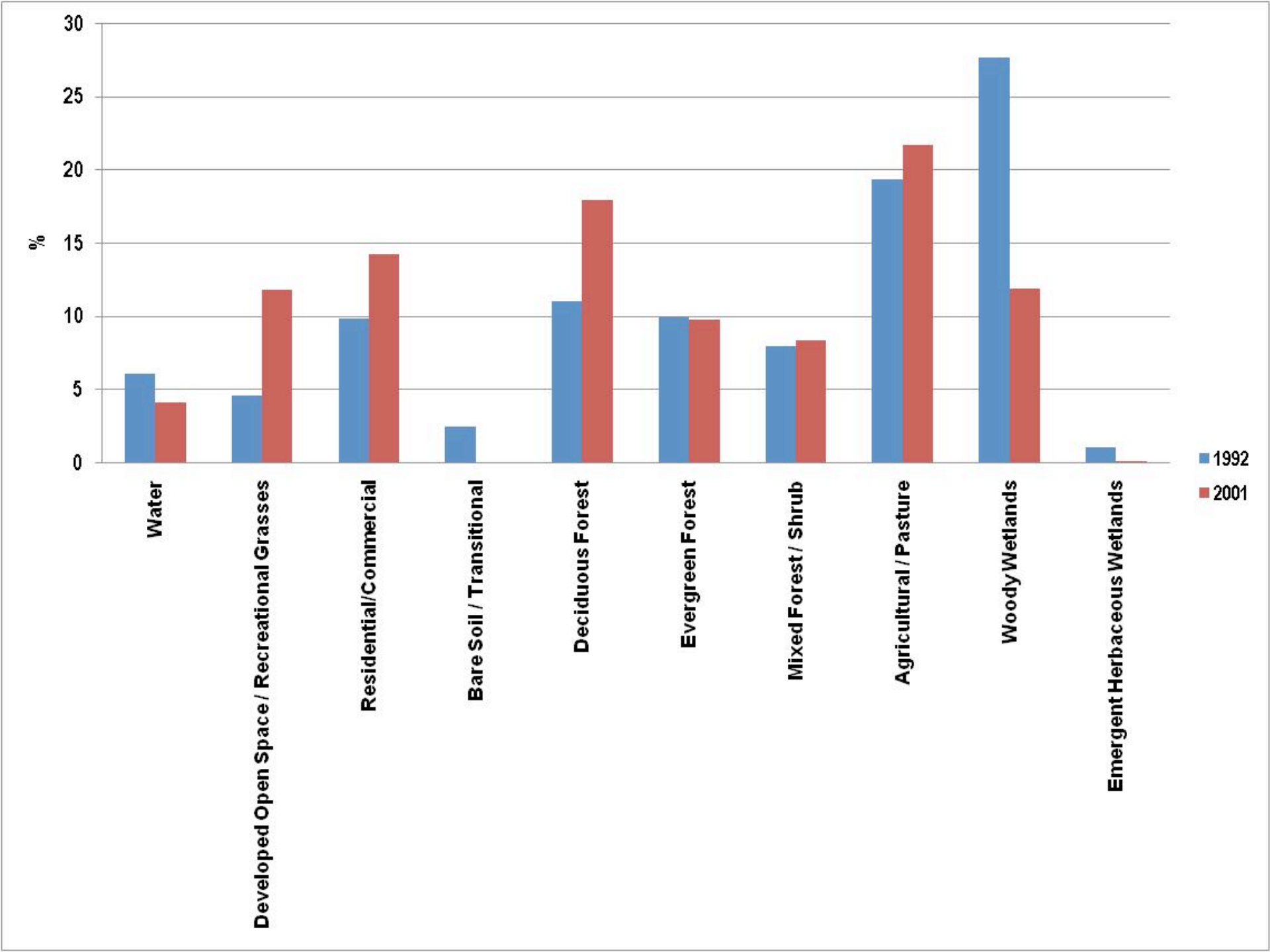
30
25
20
15
10
5
0
%
Water
Developed Open Space / Recreational Grasses
Residential/Commercial
Bare Soil / Transitional
Deciduous Forest
Evergreen Forest
Mixed Forest / Shrub
Agricultural / Pasture
Woody Wetlands
Emergent Herbaceous Wetlands
1992
2001

Land Use Change Drives Thermal Change

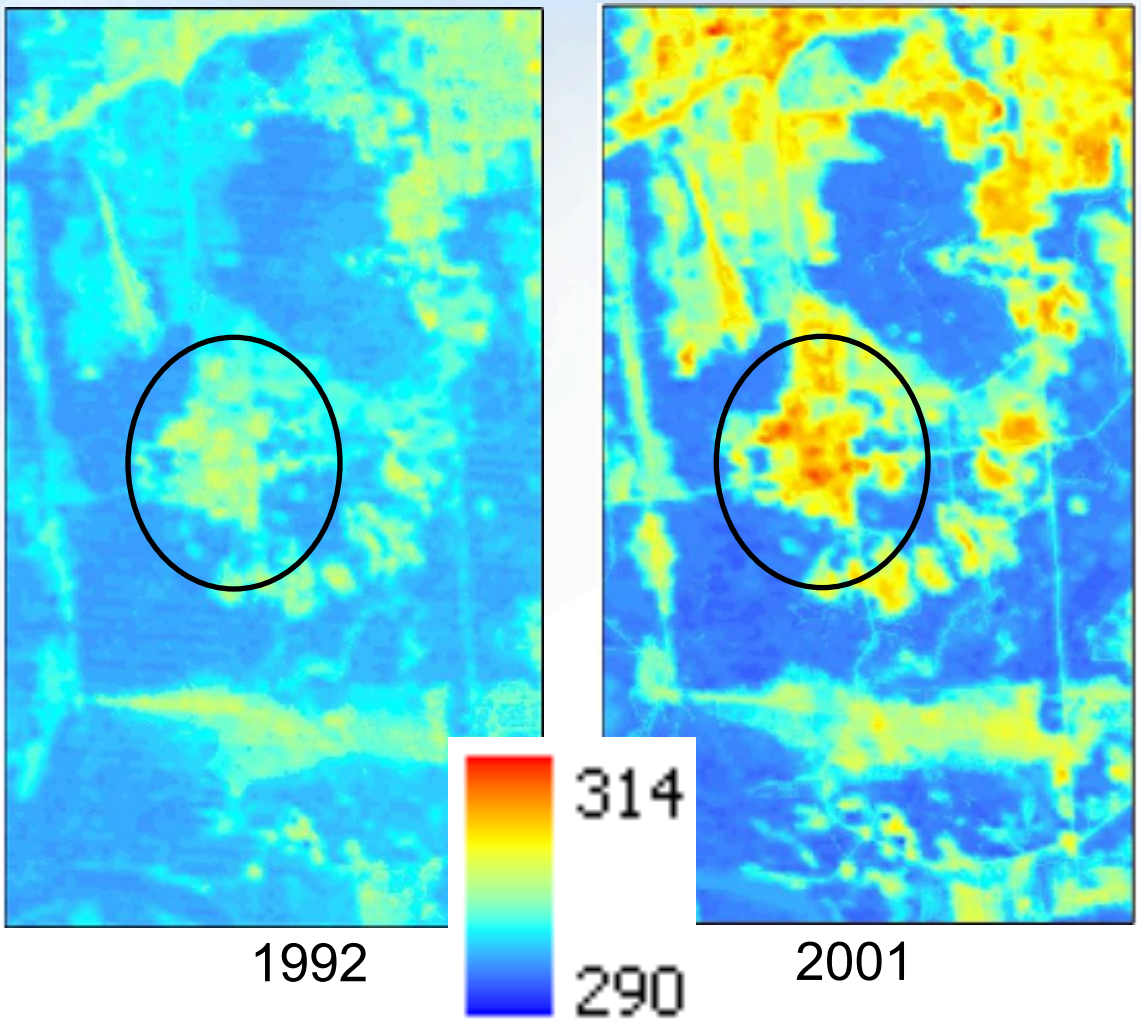

Conversion of forest, shrub, and agricultural land to MSFC infrastructure substantially changes surface thermal signatures

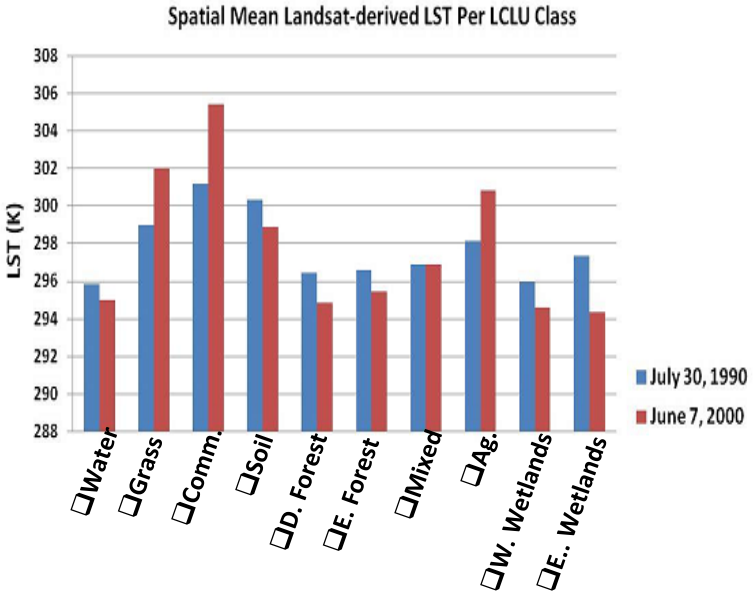

Need to determine impact on local temperatures

Emissivity 1992

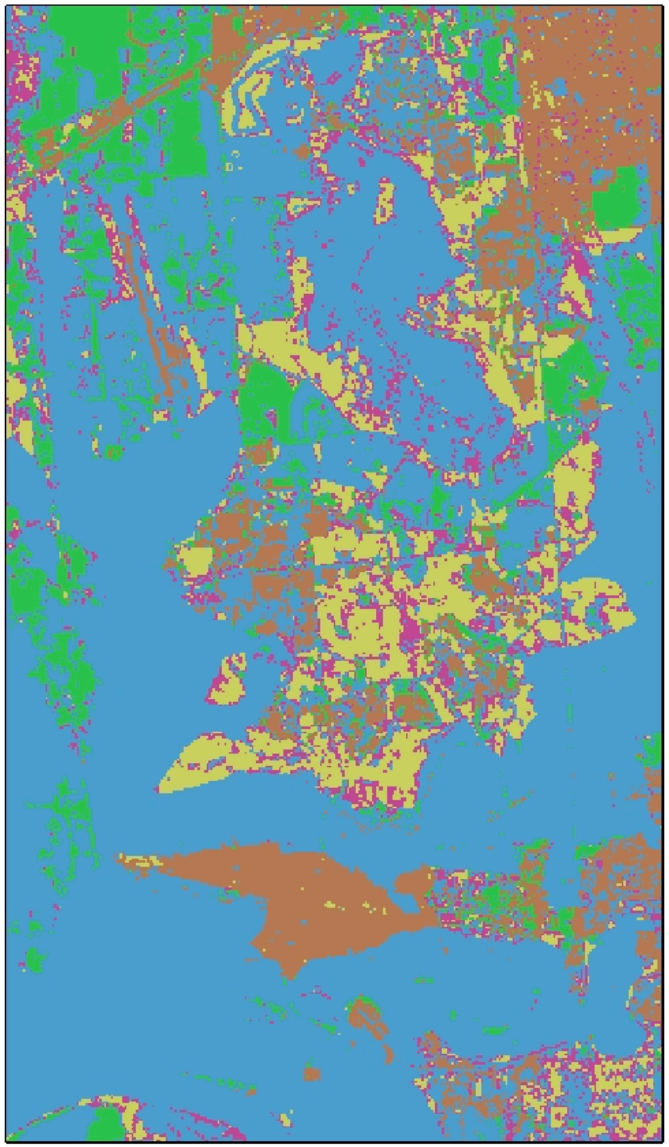

❑**Emissivity**

- 0.969 (Used for Bare Soil; and Developed Pixels)
- 0.974 (Used for Shrub Pixels)
- 0.980 (Used for Crops Pixels)
- 0.989 (Used for Deciduous Forests (assuming they're mostly Broadleaf); Wetlands, and Water Pixels)
- 0.9895 (Used for Mixed Forests Pixels)
- 0.990 (Used for Evergreen Pixels (assuming they're mostly Needle))

❑Based on a look-up table in Snyder et al. 1998 and given that our analysis is for a period when the vegetation is green.

Emissivity 2001

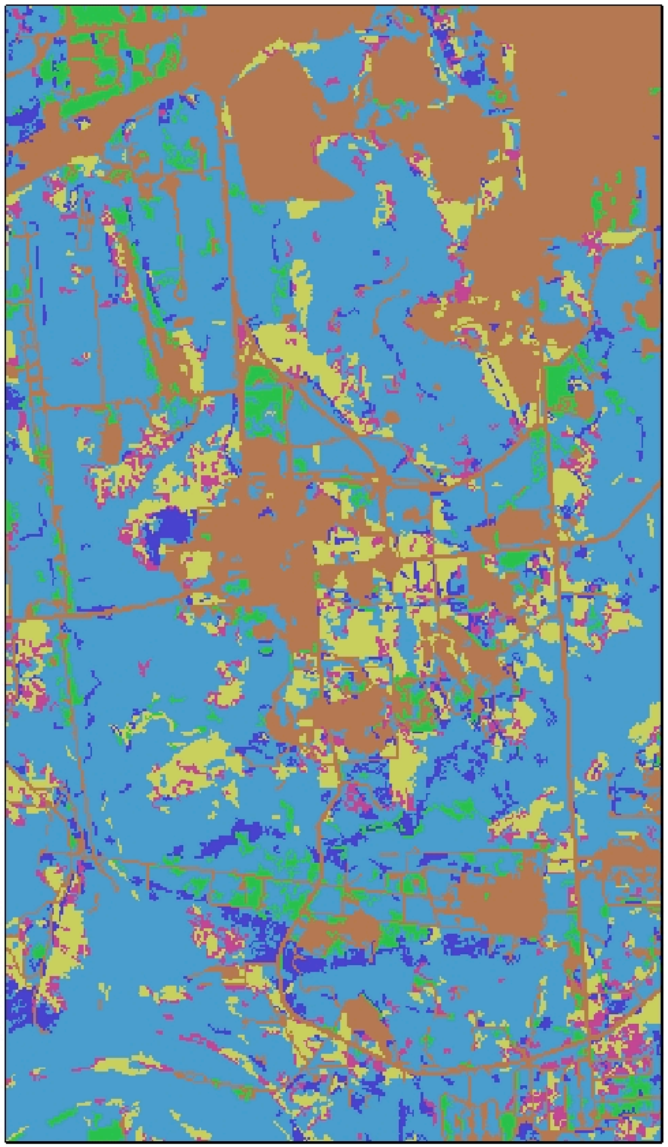

❑**Emissivity**

- 0.969 (Used for Bare Soil; and Developed Pixels)
- 0.974 (Used for Shrub Pixels)
- 0.980 (Used for Crops Pixels)
- 0.989 (Used for Deciduous Forests (assuming they're mostly Broadleaf); Wetlands, and Water Pixels)
- 0.9895 (Used for Mixed Forests Pixels)
- 0.990 (Used for Evergreen Pixels (assuming they're mostly Needle))

❑Based on a look-up table in Snyder et al. 1998 and given that our analysis is for a period when the vegetation is green.

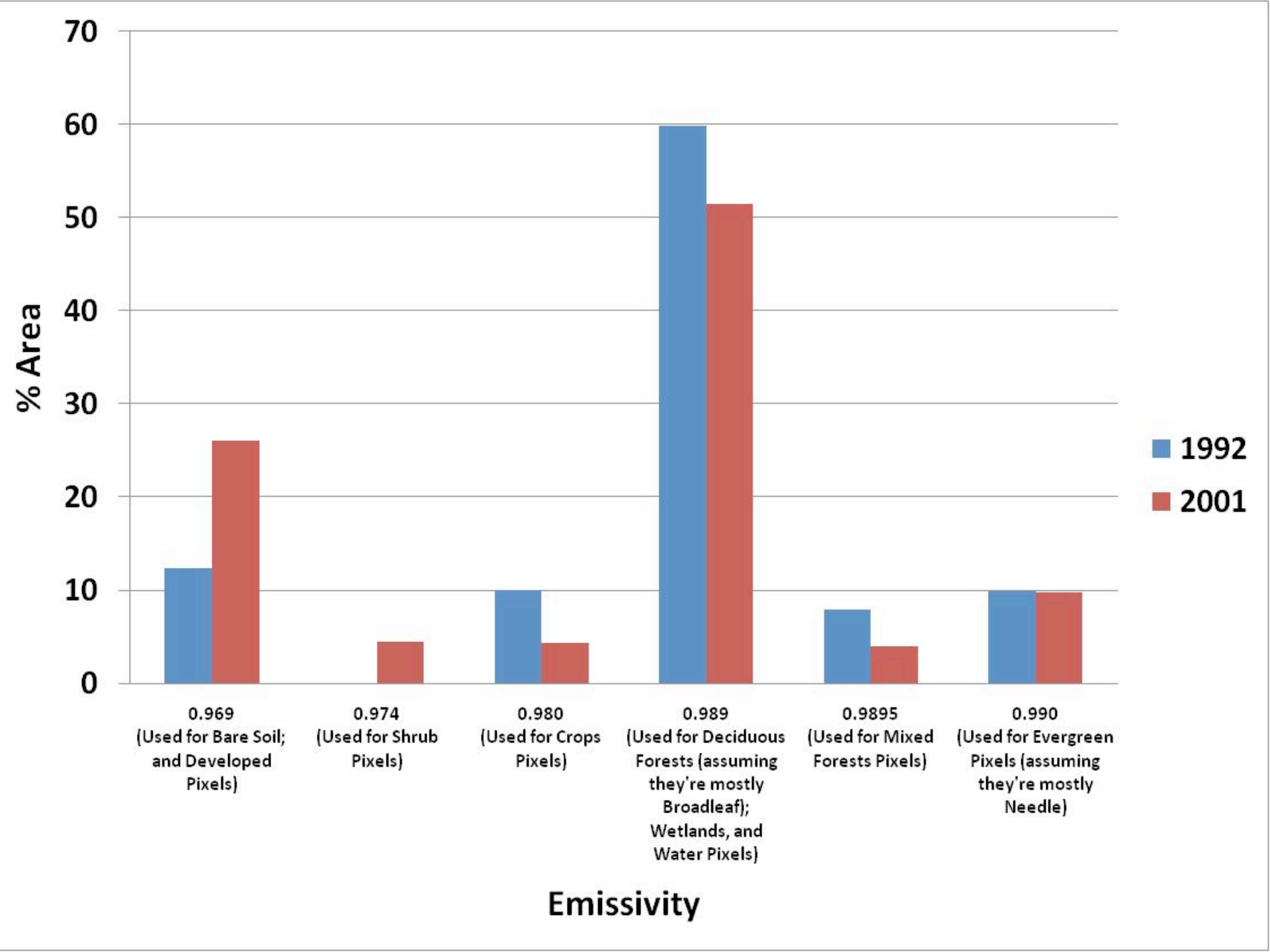
70
60
50
40
30
20
10
0
% Area
1992
2001
0.969 (Used for Bare Soil; and Developed Pixels)
0.974 (Used for Shrub Pixels)
0.980 (Used for Crops Pixels)
0.989 (Used for Deciduous Forests (assuming they're mostly Broadleaf); Wetlands, and Water Pixels)
0.9895 (Used for Mixed Forests Pixels)
0.990 (Used for Evergreen Pixels (assuming they're mostly Needle)
Emissivity

ASTER LULC (APR 6, 2001)

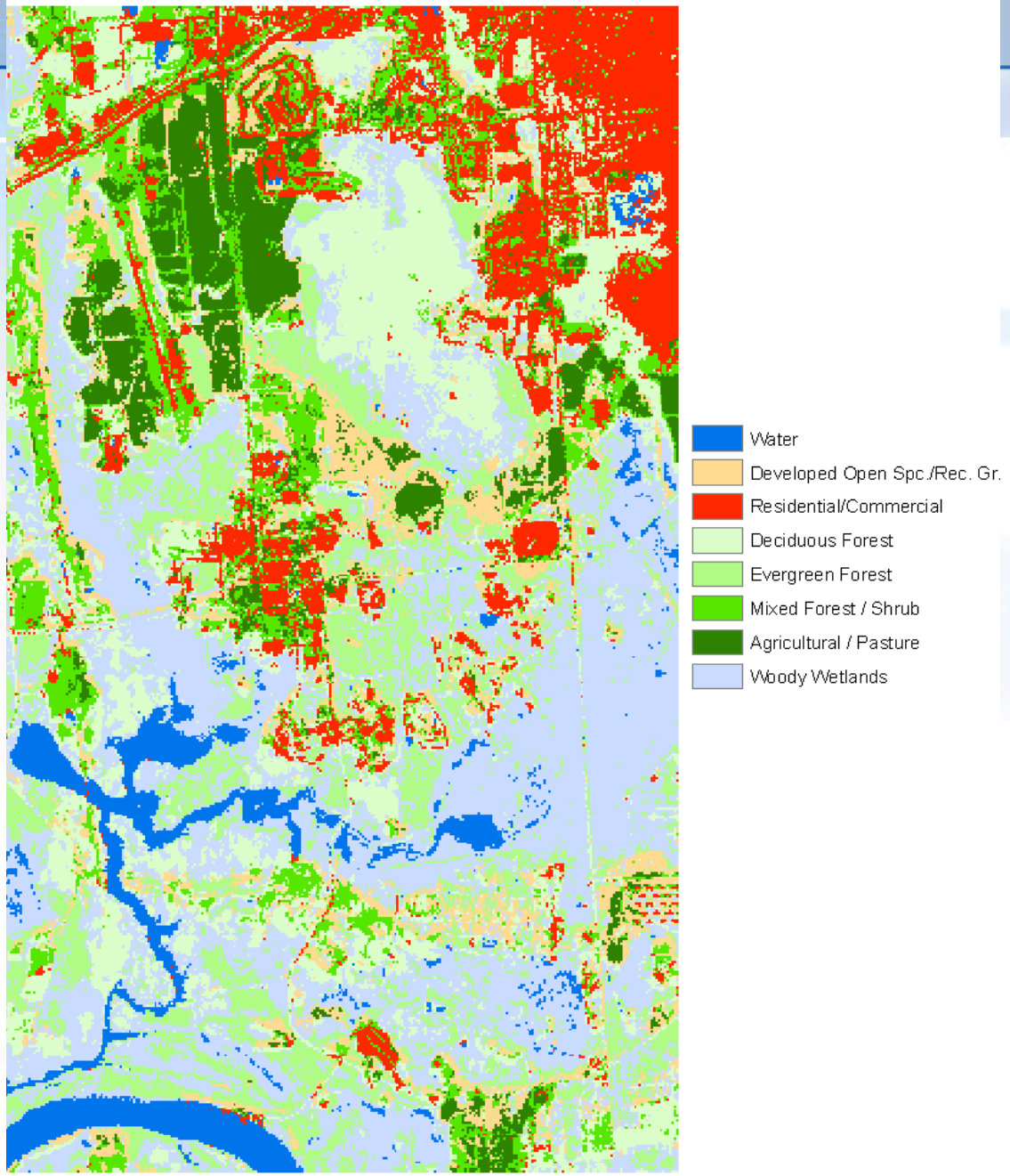

ASTER LULC (MAR 1, 2011)

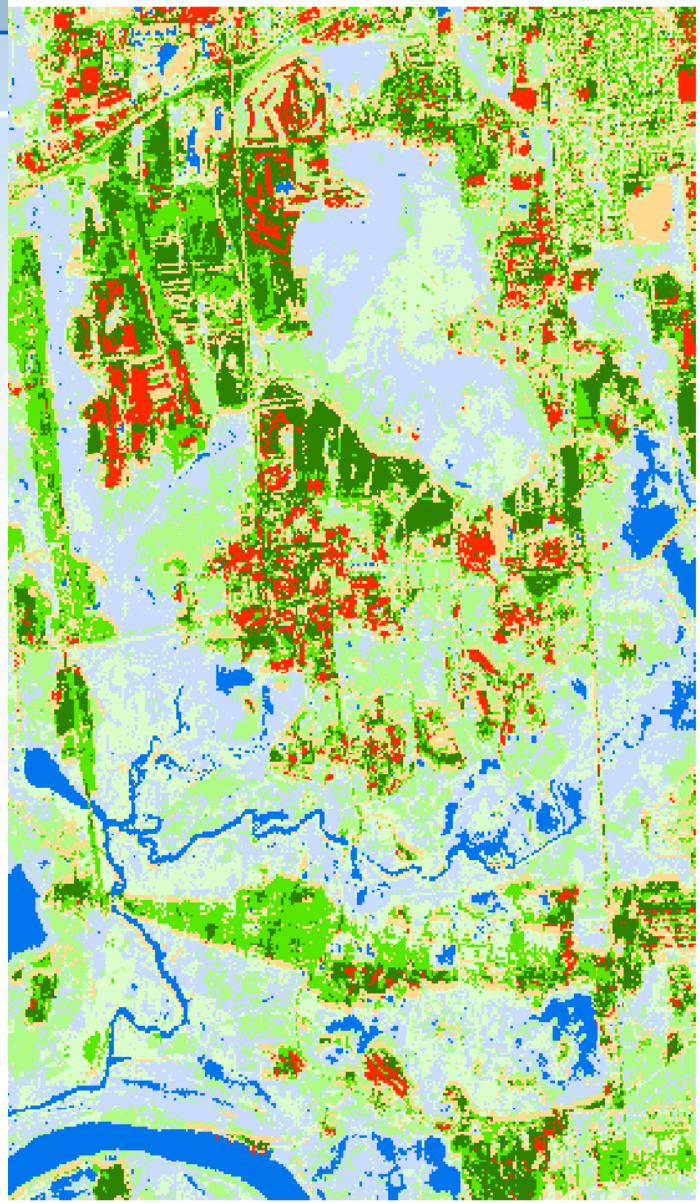

ASTER LST (K) (APR 6, 2001)

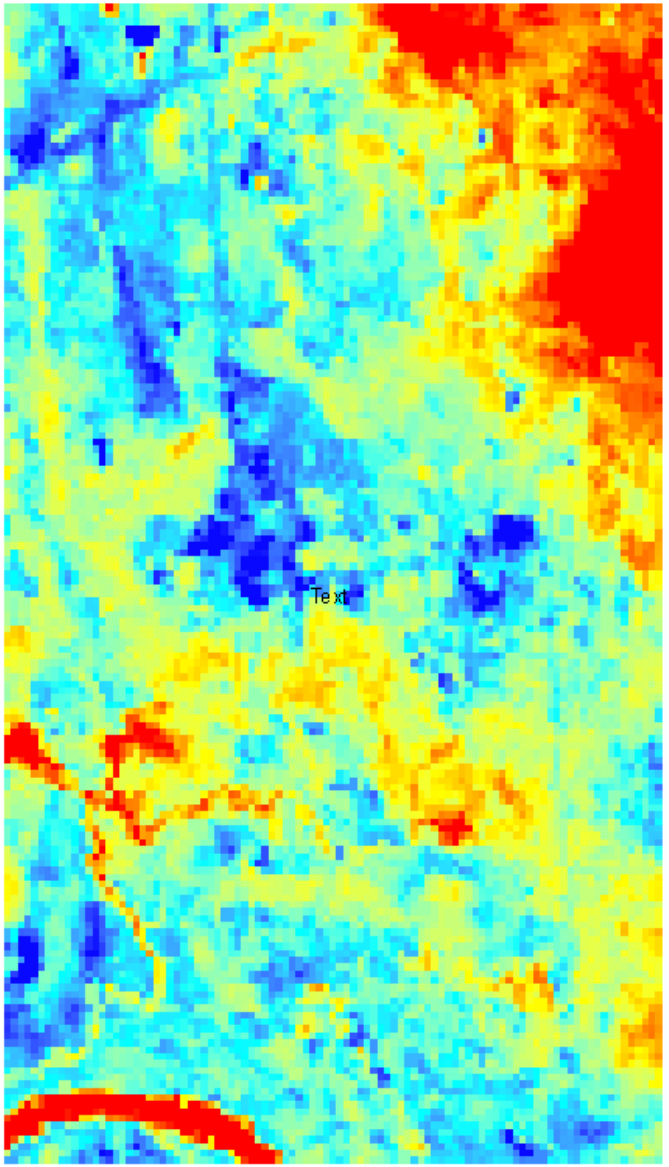

ASTER LST (K) (MAR 1, 201 l)

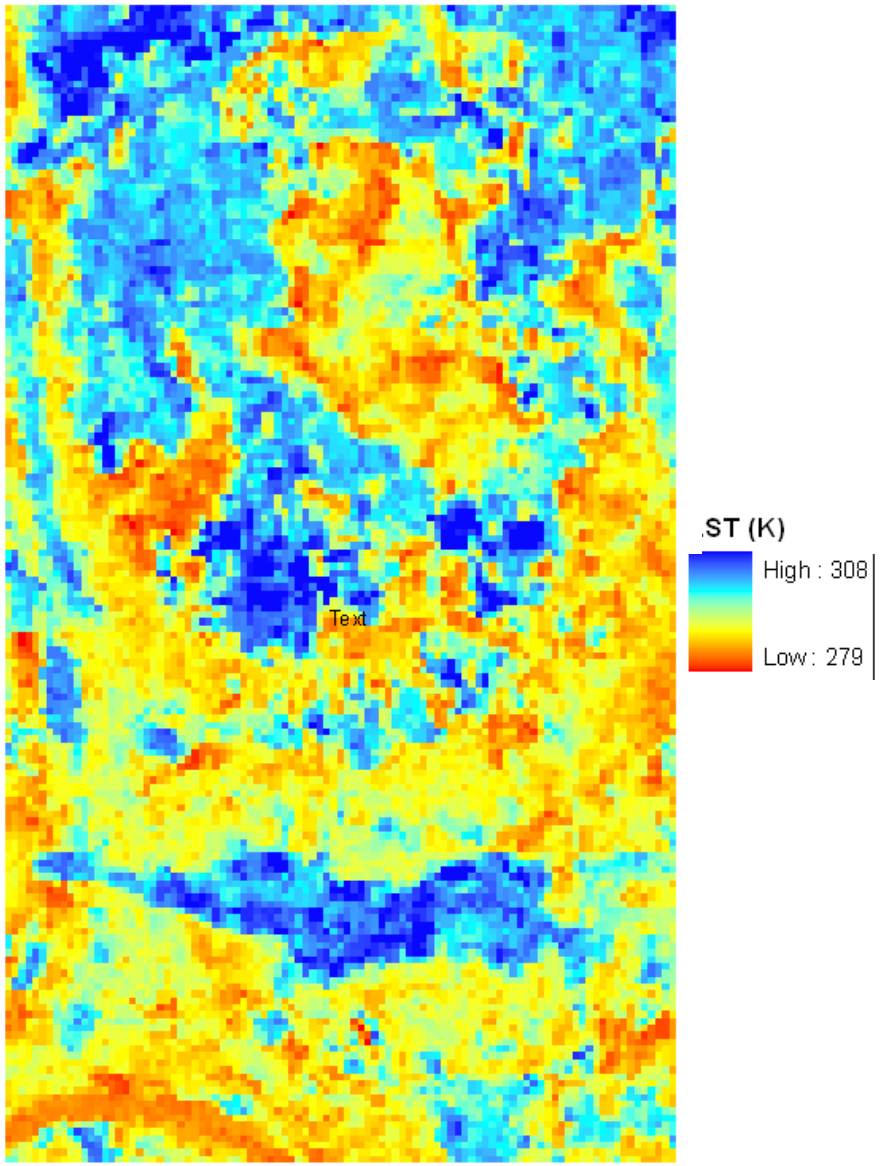

Land Cover and Climate Change Impacts

Spatial Mean ASTER-derived LULC per Class

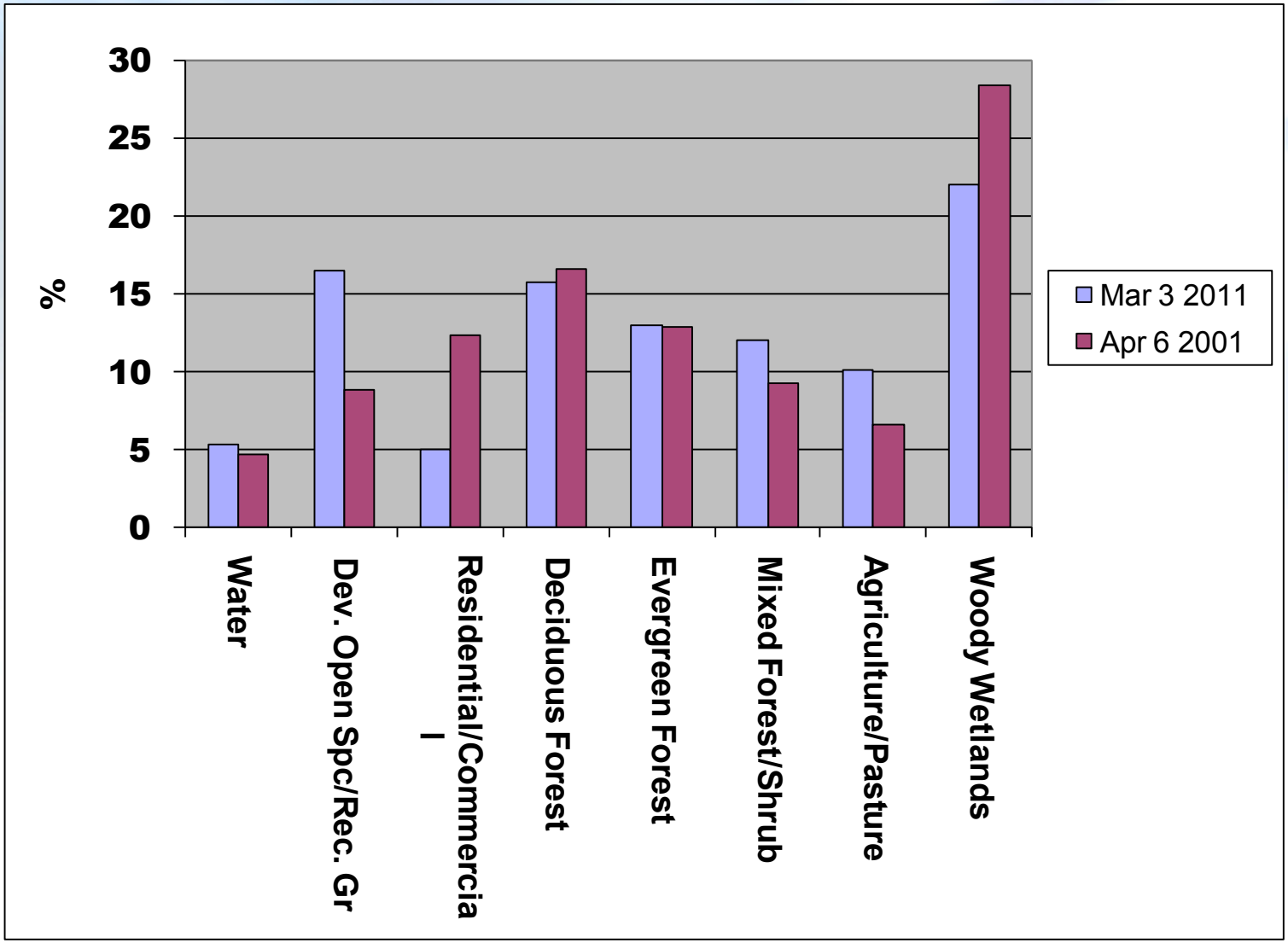

Land Cover and Climate Change Impacts

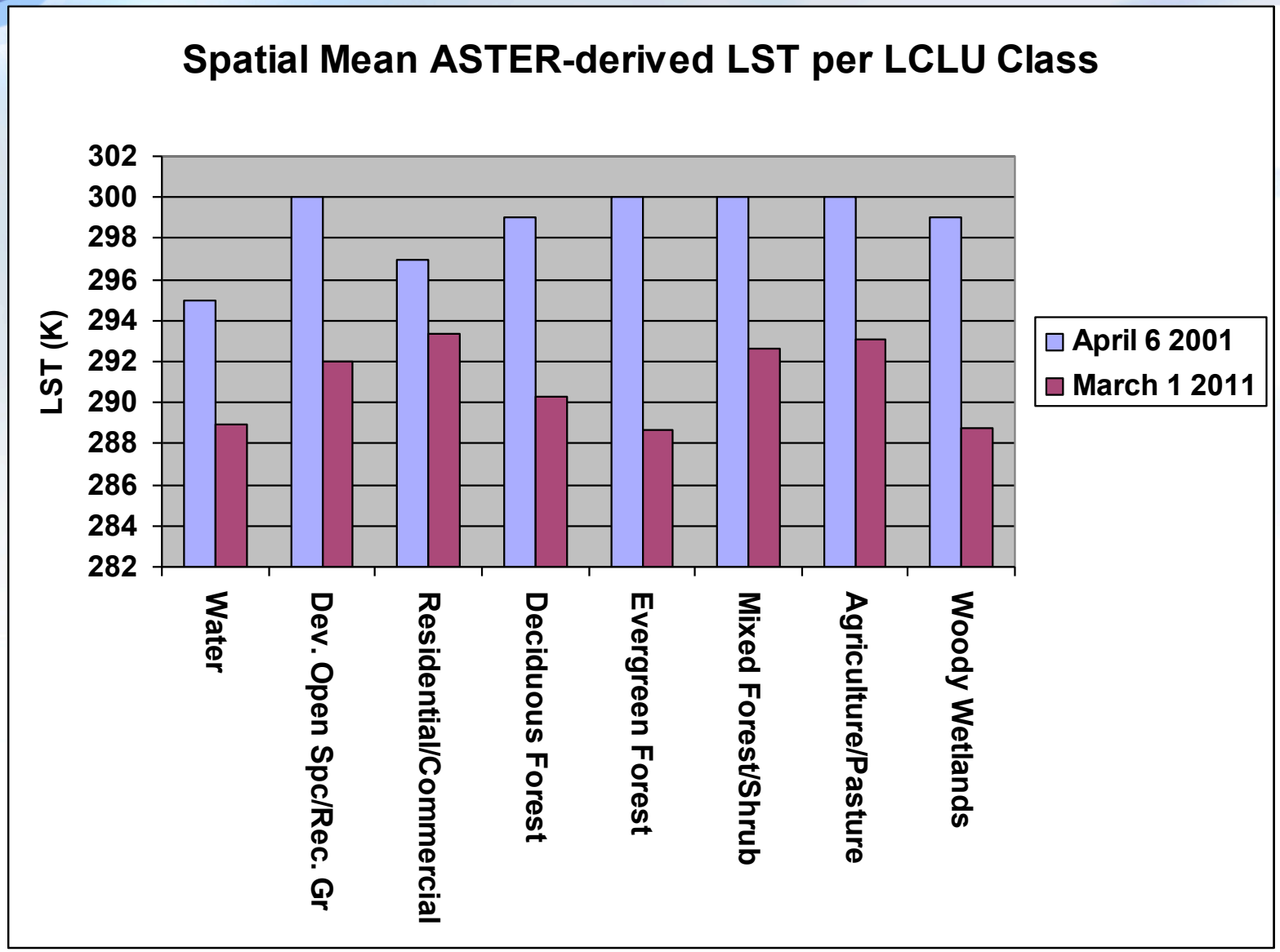

ASTER LULC (MAY 4, 2011)

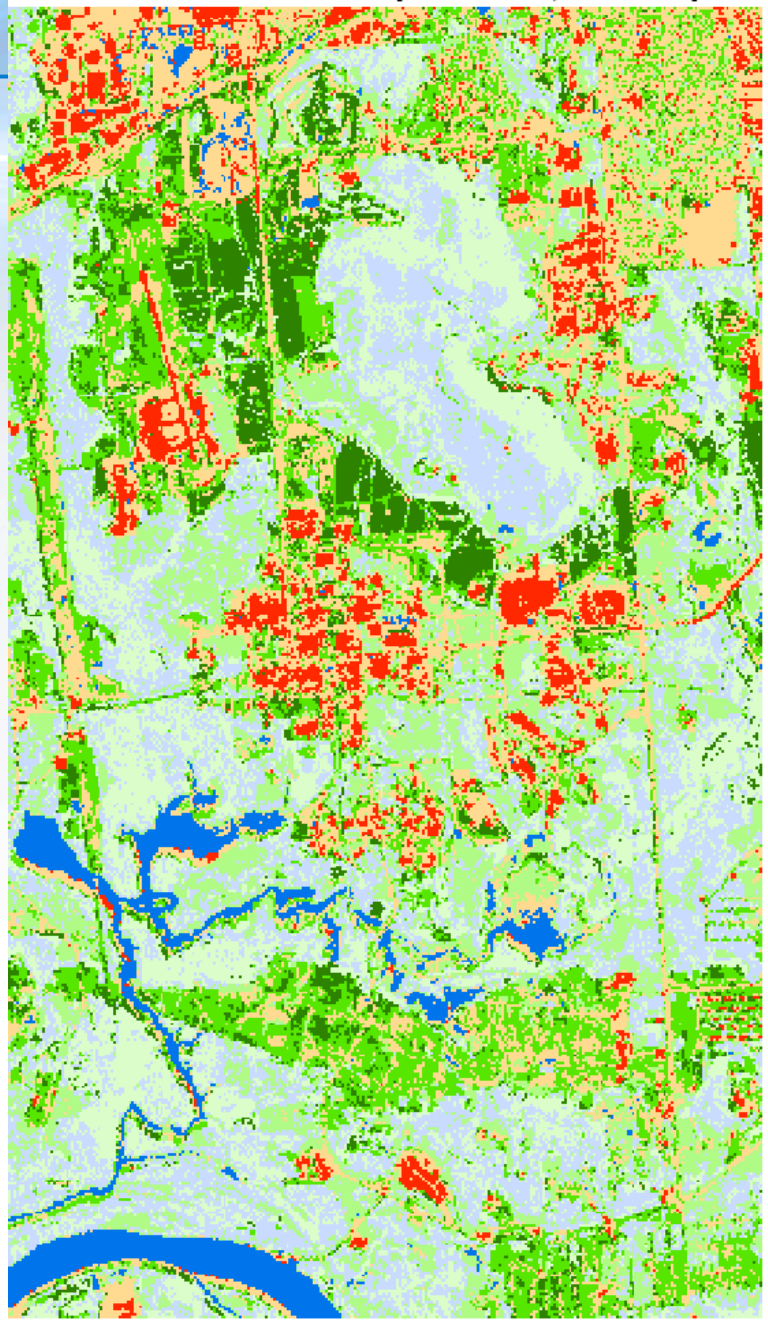

- Water
- Developed Open Spc./Rec. Gr.
- Residential/Commercial
- Deciduous Forest
- Evergreen Forest
- Mixed Forest / Shrub
- Agricultural / Pasture
- Woody Wetlands

ASTER LST (K) (MAY 4, 2011)

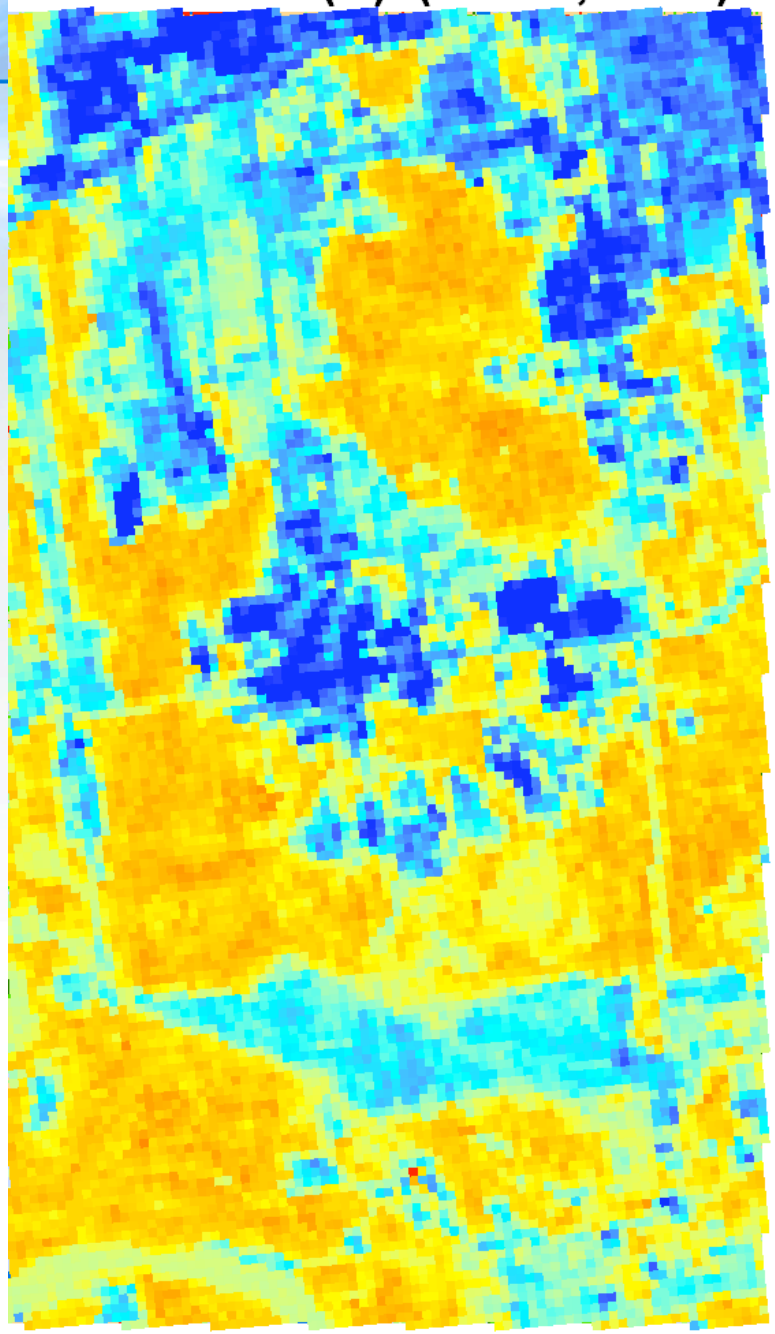

LST(K)

High : 3173

Low : 2860

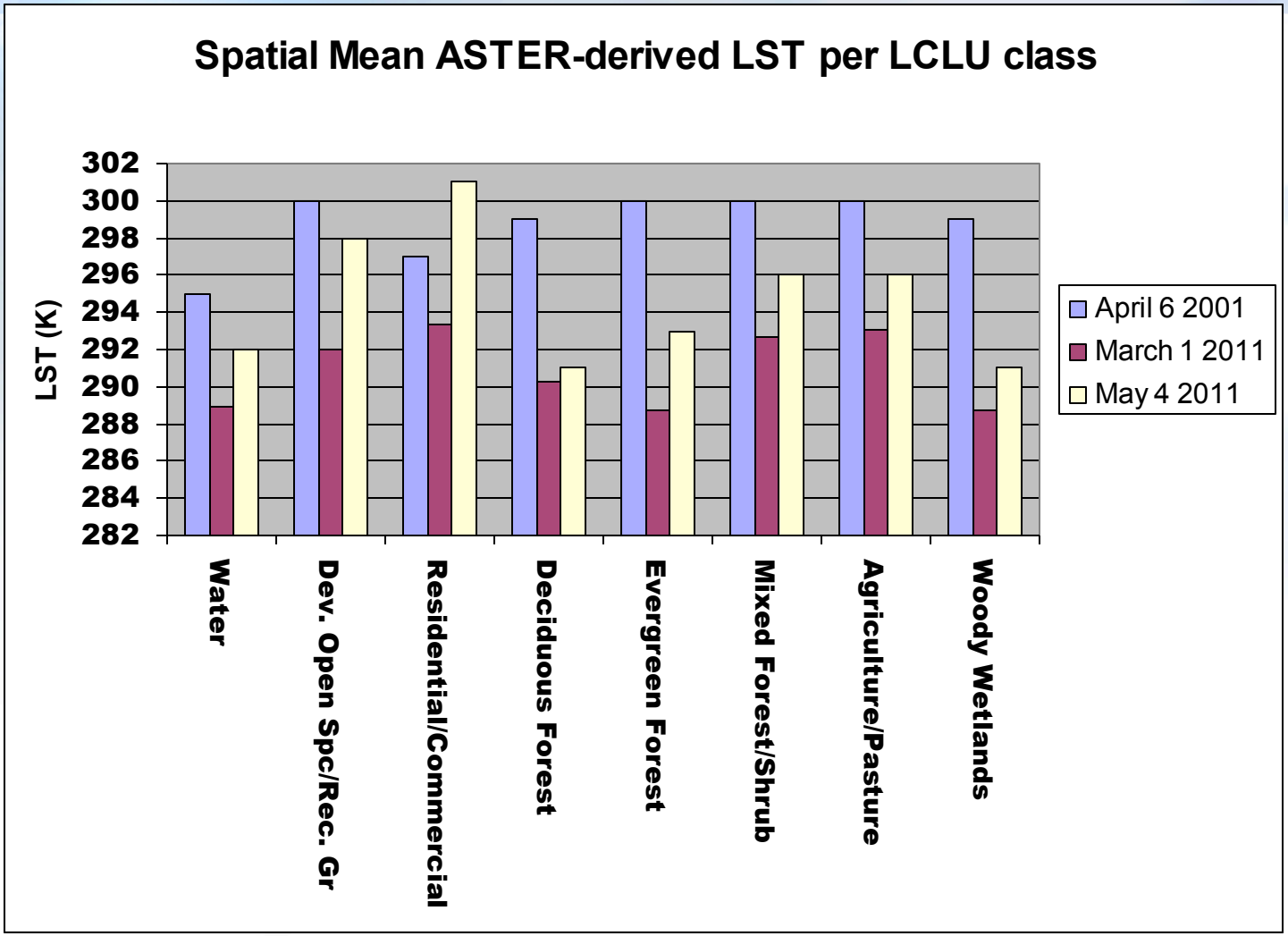
Spatial Mean ASTER-derived LST per LCLU class
LST (K)
302
300
298
296
294
292
290
288
286
284
282
Water
Dev. Open Spc/Rec. Gr
Residential/Commercial
Deciduous Forest
Evergreen Forest
Mixed Forest/Shrub
Agriculture/Pasture
Woody Wetlands
April 6 2001
March 1 2011
May 4 2011

The Need For HyspIRI Data for More Quantitative Analysis of Urban Land Change and Affects on LSTs and the Urban Heat Island:

- NASA Earth science satellites currently in orbit are aging and are beginning to have sensor difficulties (e.g., ASTER SWIR Bands)

- More hyperspectral bands needed for analysis of urban vs. non-urban land cover/landscape attributers (e.g., detailed identification of urban surfaces)

- Planned satellites (e.g., LDCM) will not have multispectral thermal IR bands with 60m spatial resolution to derive thermal responses from urban vs. non-urban surfaces (e.g., separation of bare soil vs. other impervious surfaces)

- 5 day revisit time and day/night collection of thermal IR data will greatly increase the opportunity for diurnal analysis of urban LSTs at frequent time intervals

- SWIR channels will provide for excellent analysis of albedo from urban surface types

Growth of Global Megacities

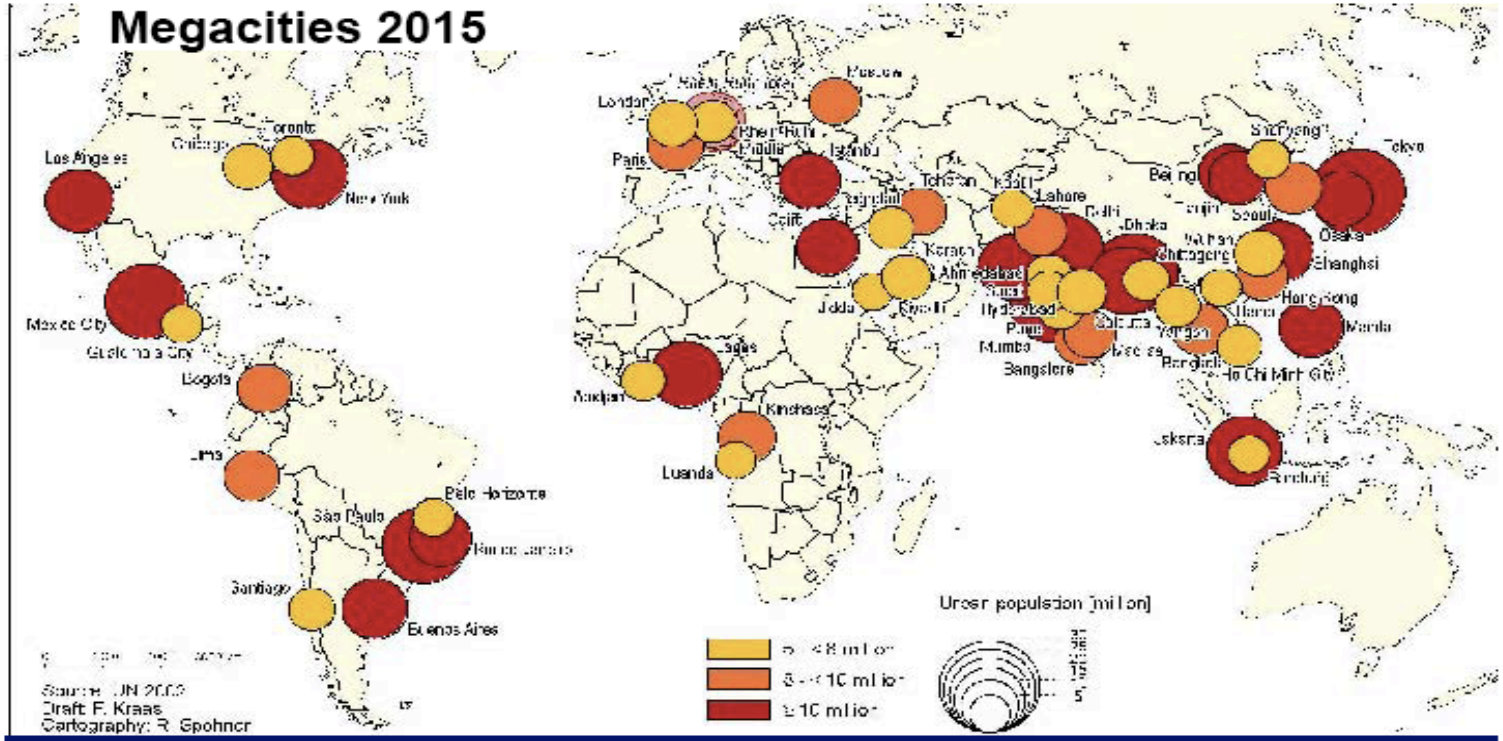

- 1950: 4, 1980: 28, 2002: 39, 2015: 59 megacities worldwide; 2/3 in developing countries, resp. South and East Asia
- 2002: 394 Mio. people, of these: 246 Mio. in developing countries, oder 215 Mio. in Asia; in the year 2015: 604 Mio. worldwide
- Population data tripled between 1970 and 2000: e.g. Mexico City, São Paulo, Seoul, Mumbai, Jakarta, Teheran

The Urban Dynamic

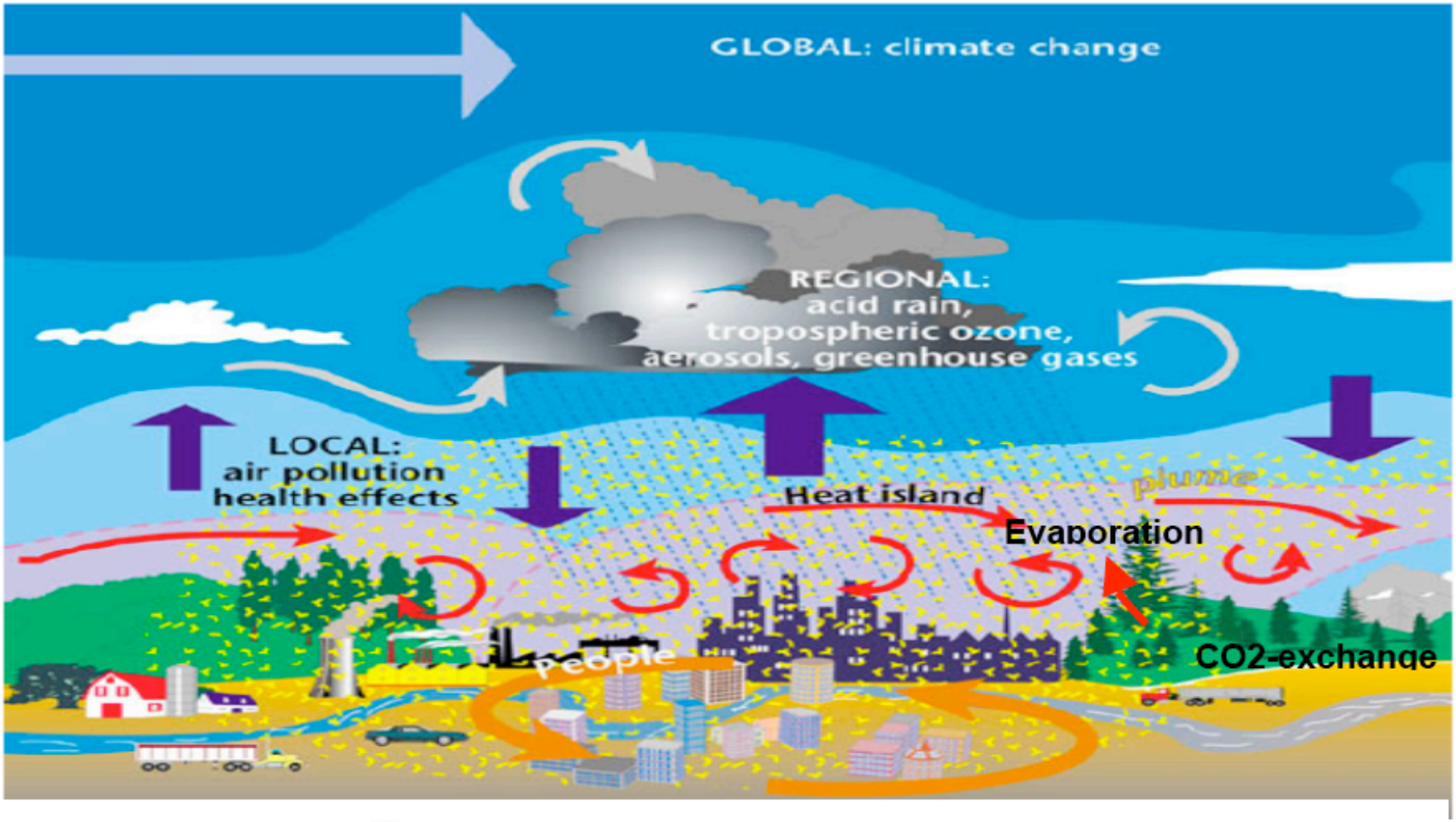

Seto and Shepherd (2009) originally in Hidalgo et al--38. Hidalgo J, Masson V, Baklanov A, Pigeon G, Gimenoa L: Advances in Urban Climate Modeling:Trends and Directions in Climate Research. *Annual New York Academy of Sciences* 2008, 1146.

Urban Heat Islands and Emissions?

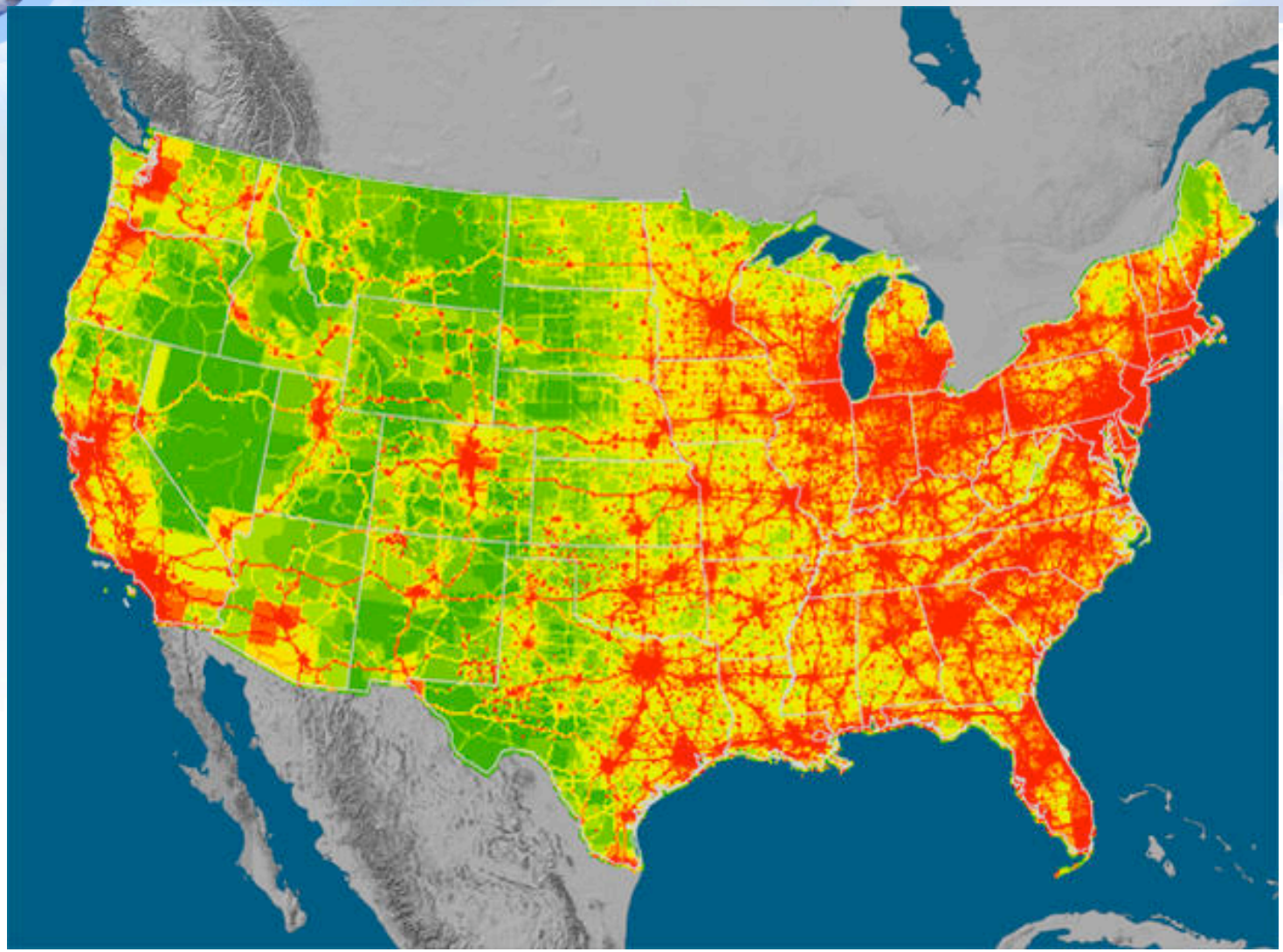

- Emission Sources (Source: Purdue University)

Consequences of Urbanization on NPP-Carbon in the United States

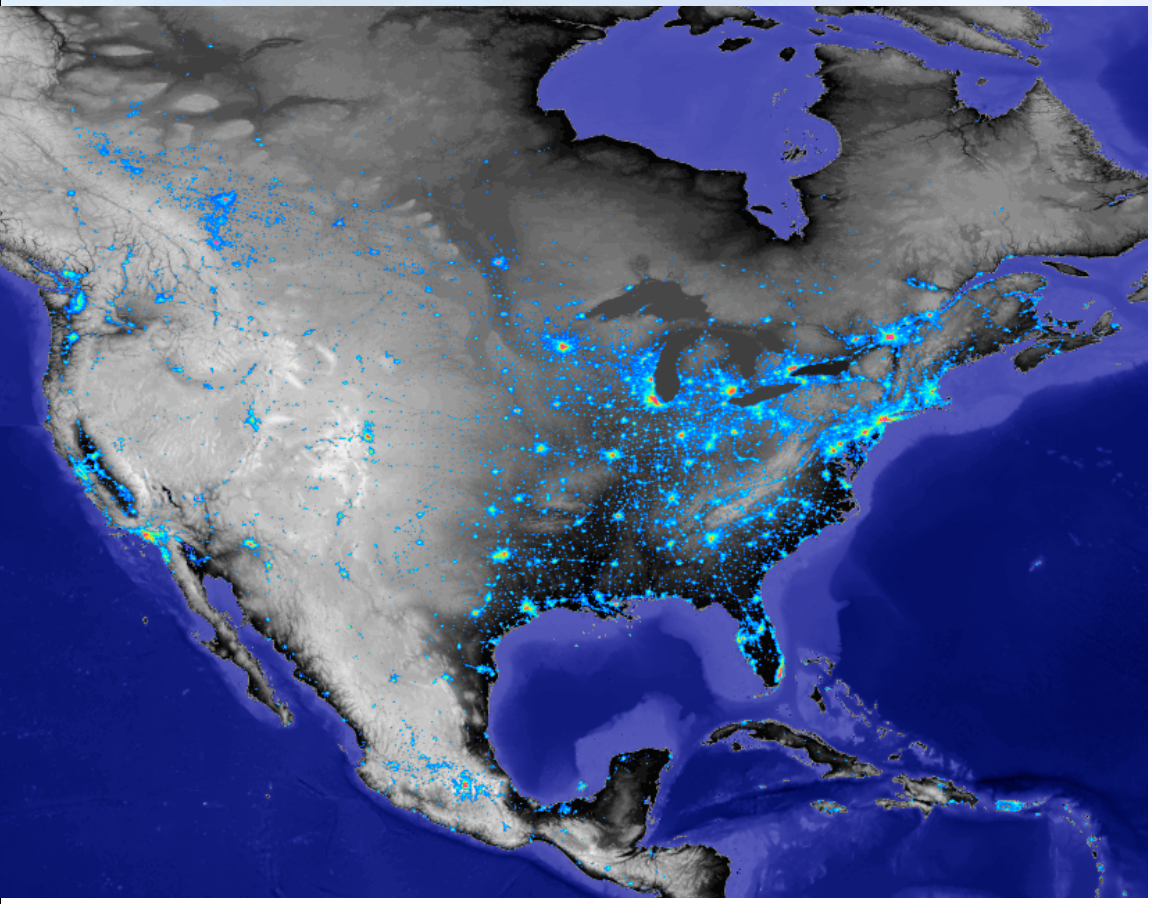

- What is the overall impact in North America?
  - Has the NPP-carbon sink been reduced?
  - What are the consequences?
- How does urbanization interact with climate locally?
  - Is there a recognizable effect in the NDVI signal at 1km spatial resolution?
  - What are the seasonal dynamics?
  - Is urbanization's impact on NPP balance positive or negative?

Consequences of Urbanization on NPP-Carbon in the U.S.

Urbanization and NPP

- NPP decreased <u>41.5 M tons C / year</u>.
- Roughly equivalent to the increase
  - ❑ created by 300 years of agricultural
  - ❑ development.

❑How can this happen when urban areas occupy only 3% of the land surface and agriculture occupies 29%?

<u>Location, Location, Location.</u>

Urbanization is taking place on the most fertile lands

❑Reduction of NPP may have biological significance:

NPP Lost or Gained (annual)

Due to Urbanization

❑Going from a pre-urban to a post urban world

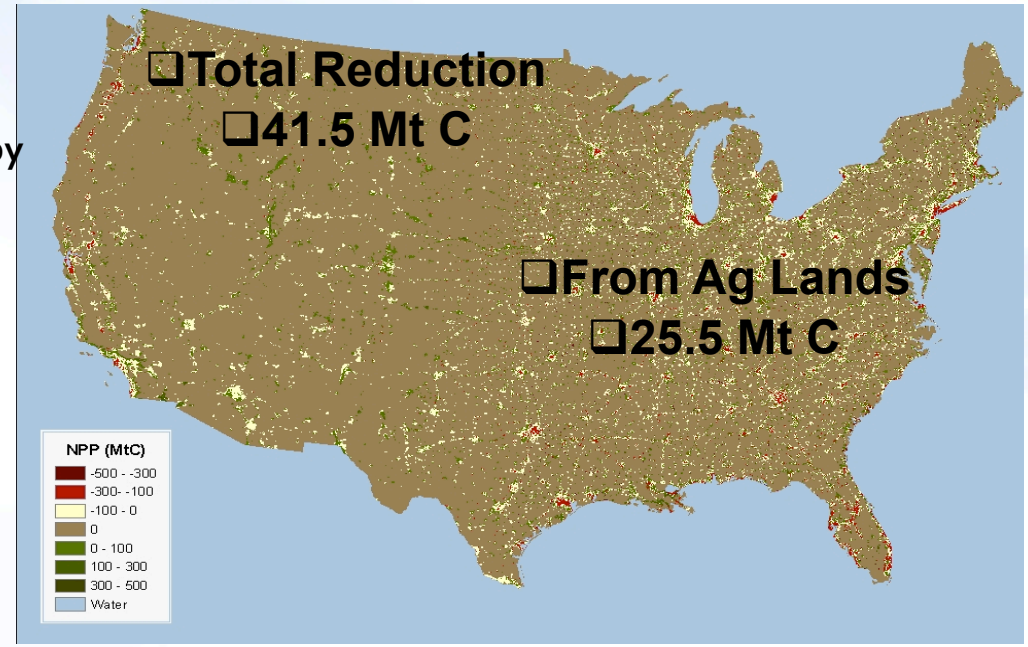

-Annual loss of food web energy 400 Trillion kilocalories

- ❑ (roughly equal to food energy requirement for 448 million people).
- Reduction of actual food products equivalent to needs of 16.5 million persons annually
- ❑ (about 6% of US population).

Mechanisms: Convergence and Fluxes?

Difference in Divergence (Atlanta - No Atlanta)

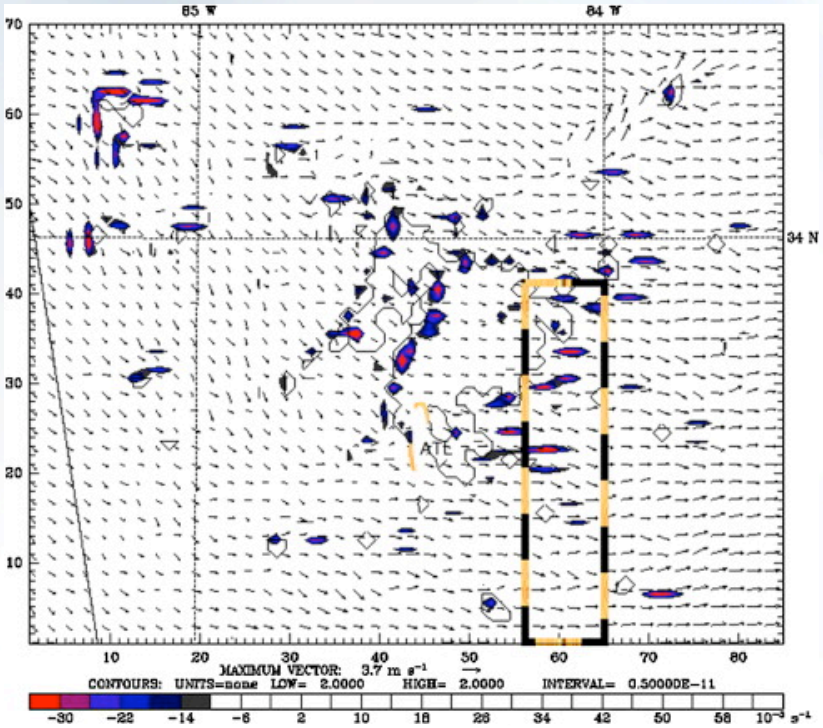

Atlanta

No Atlanta

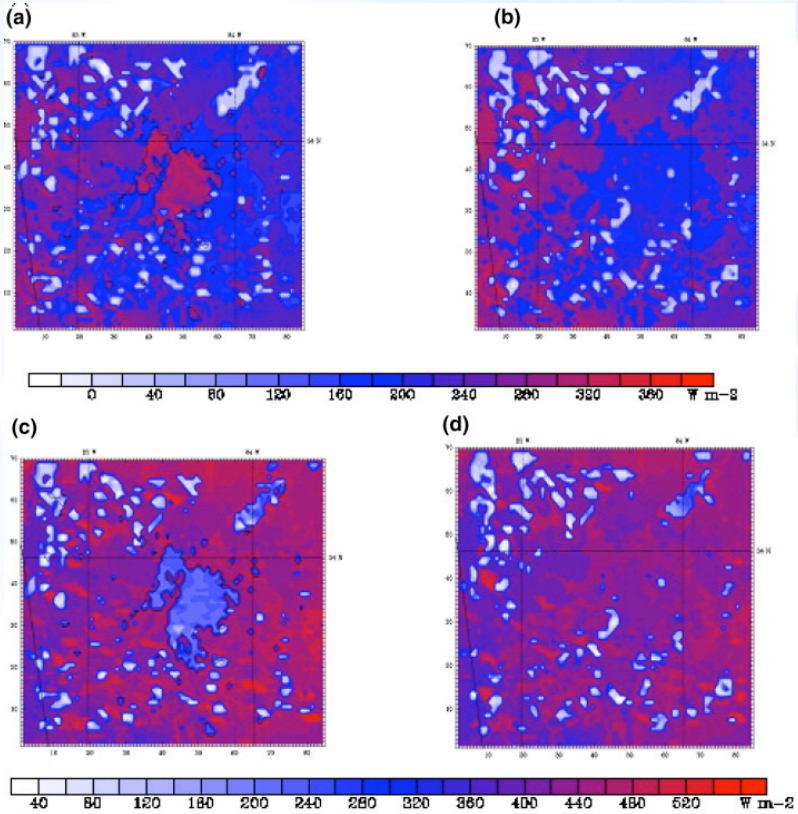

- Shem and Shepherd (2009) found that Atlanta can initiate or enhance pre-existing convection through enhanced convergence (left) and sensible heat flux (right and top)

Urban Surfaces and Morphological Parameters

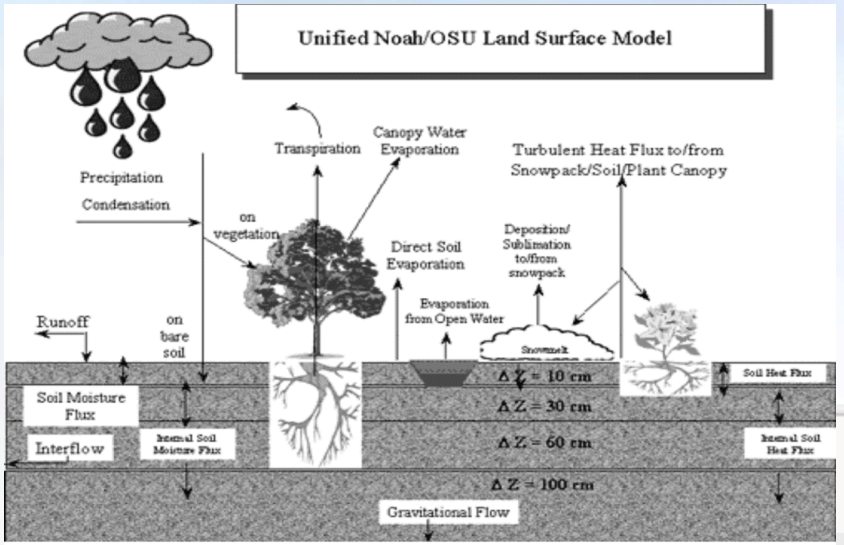

Urban surfaces and morphological parameters are still poorly represented in most studies of urban effects

Shepherd, Burian, and colleagues (2009) have used lidar derived urban canopy parameters and an Urban Canopy Model embedded in WRF NOAH.

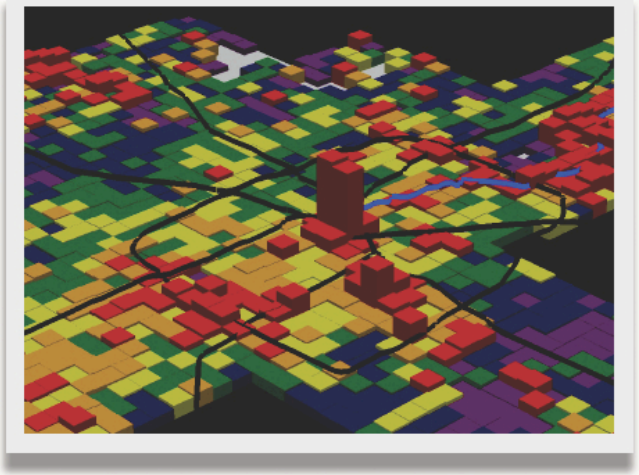

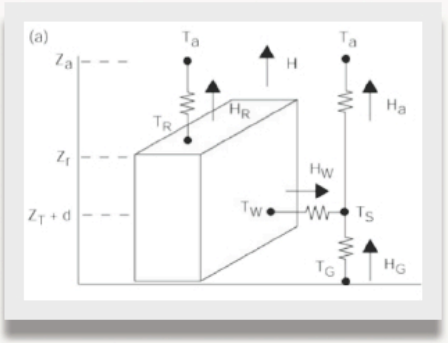

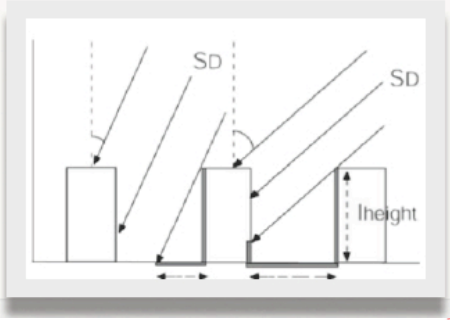

HyspIRI Combined with other RS/GIS data to generate Urban Morphological Datasets

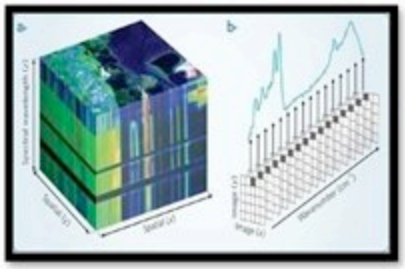

HyspIRI VSWIR data Products

Urban morphological datasets

GIS datasets

Lidar

Digital photogrammetry

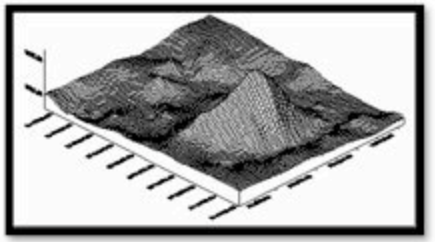

Digital elevation model

Weng et al., 2010

Moving Towards and Integrated Interdisciplinary Urban Science – The Need for HysplRI Data

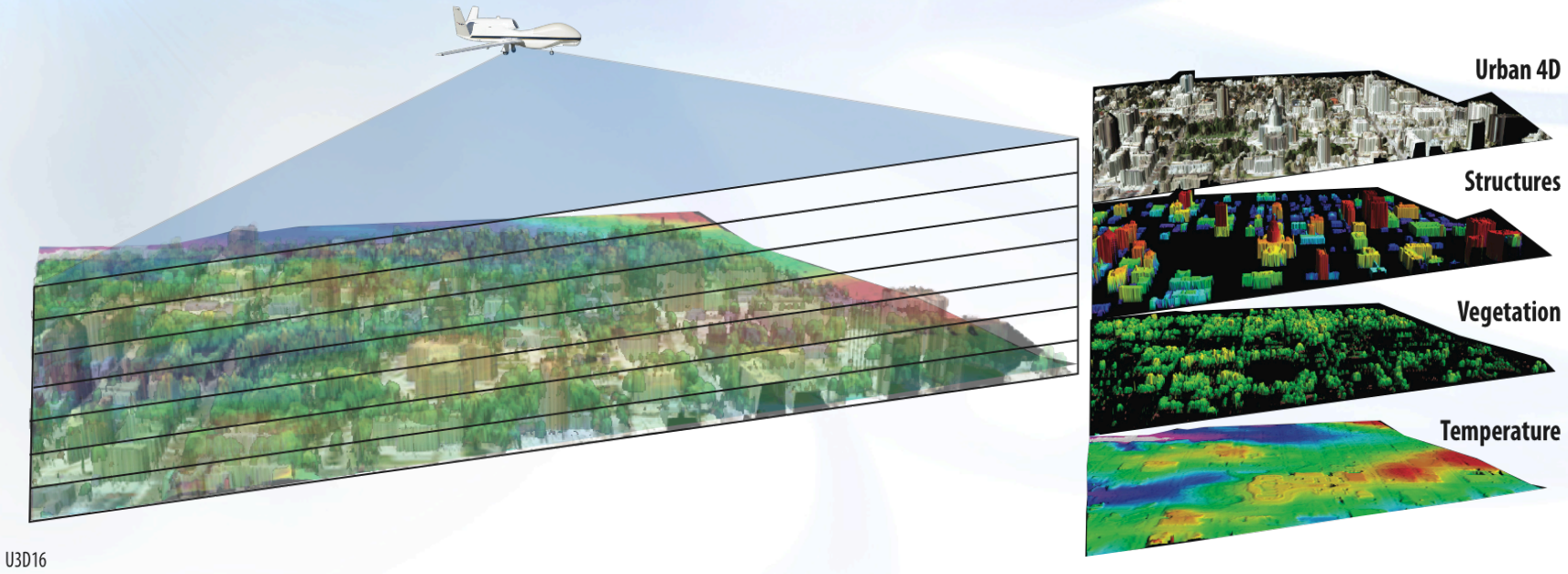

- Time series of airborne lidar, multispectral, and thermal sensors to provide the 4-dimensional (space and time) observations required to parameterize, test, and further develop models that explain and predict the influence of urbanization on earth system processes at the local, regional, and global scales.
  - **MASTER (MODIS/ASTER Simulator (50 channels 0.4 - 13 μm @ 12 m –diurnal)**
  - **LVIS full waveform and elevation products at (7.5m spot size)**

The Need for HyspIRI Data

Summary

- HyspIRI data will greatly advance our scientific understanding of the coupling between urban surface materials, land covers/ land uses, and LSTs as they drive the formation of the UHI

- HyspIRI data will for the first time, help us to measure UHI dynamics at frequent time intervals and on a diurnal basis across seasons from a synoptic perspective

- HyspIRI data will help us to measure and model the impacts of urbanization on land-atmosphere interactions that affect local to regional meteorology and ultimately, the urban climate

The Need for HyspIRI Data

- HyspIRI data will offer a unique opportunity to better measure the albedo and thermal responses from different building/ surface materials ubiquitous to the urban environment (e.g., rooftops)

- HyspIRI data will be of critical importance in providing LCLU and land surface energy measurements (LSTs) that are key to the emerging “Science of the City” (i.e., the interdisciplinary study of the physical, atmospheric, biological, environmental and socioeconomic interactions that comprise “the city” as an entity)

BACK UP

HyspIRI Combined Composite Data Set Advanced Product for Urban Ecosystems Analysis

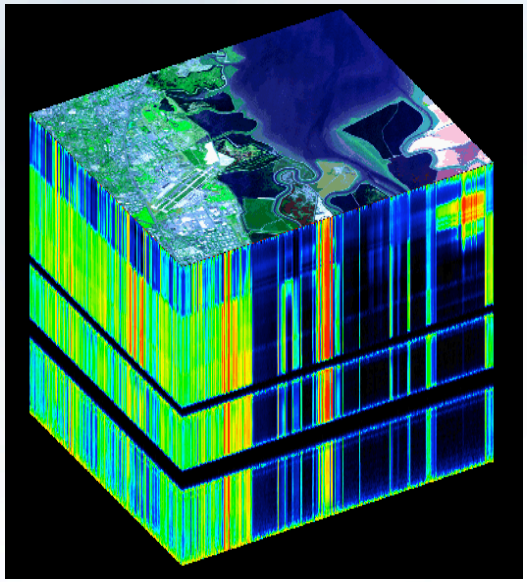

HyspIRI Hyperspectral VSWIR Level II Product
(NDVI, fPAR, surface reflectance characteristics)

+

HyspIRI TIR multispectral Level II product (8 TIR Bands)
(surface temperature, radiance, [day/night], emissivity)

=

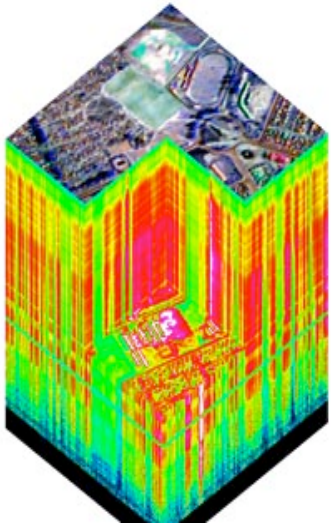

HyspIRI VSWIR/TIR composite data set
(quantitative integrative measurement of urban surface reflectances, temperatures, and emissivity across the urban ecosystem)

HyspIRI Combined Composite Land Use Change Advanced Product for Urban Ecosystems Analysis

Through Time

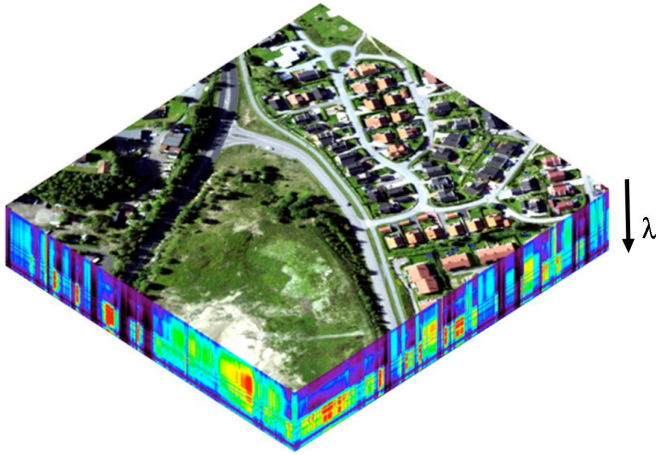

HyspIRI Hyperspectral VSWIR Level II Product

(NDVI, fPAR, surface reflectance characteristics)

+

HyspIRI TIR multispectral Level II product (8 TIR Bands)

(surface temperature, radiance, [day/night], emissivity)

=

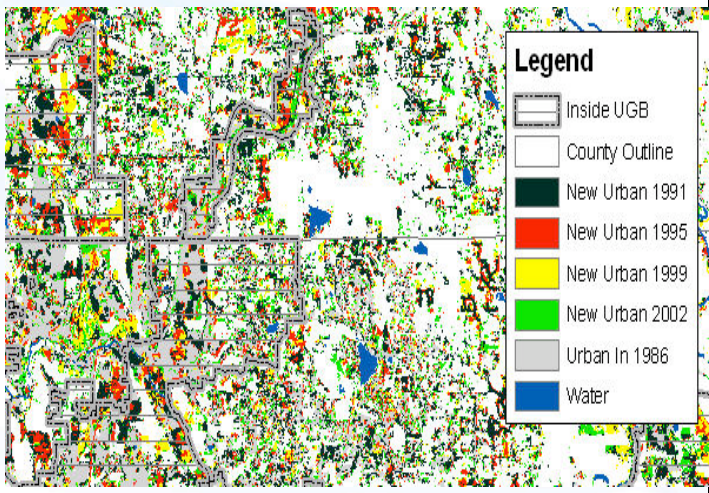

HyspIRI VSWIR/TIR composite land cover change data set

(quantitative integrative measurement of urban surface reflectances, temperatures, and emissivity across the urban ecosystem as they change through time)

HyspIRI Combined "Integrated" Advanced Product for Urban Ecosystems Analysis

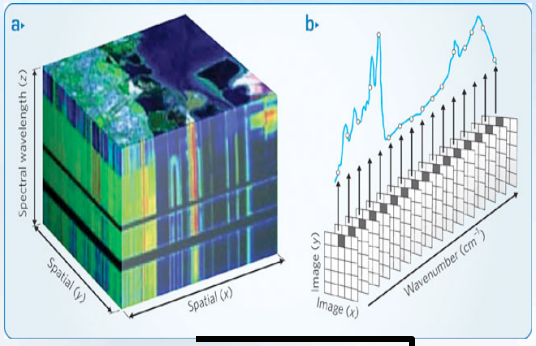

HyspIRI Hyperspectral VSWIR Level II Product
(NDVI, fPAR, surface reflectance characteristics)

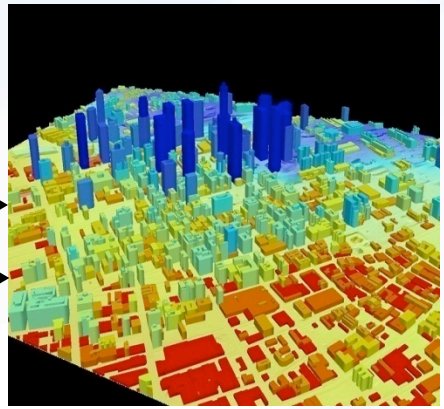

Lidar Data

=

HyspIRI VSWIR/TIR and Lidar composite data set
(X, y, z surface reflectance/thermal interactions of urban ecosystem processes)

HyspIRI TIR multispectral Level II product (8 TIR Bands)
(surface temperature, radiance, [day/night], emissivity)

HyspIRI Combined "Integrated" Topographic Advanced Product for Urban Ecosystems Analysis

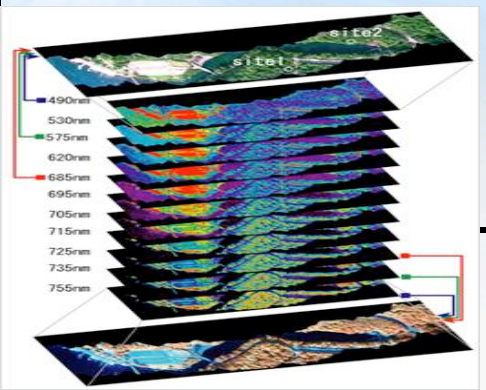

Hyperspectral VSWIR Level II Product
(NDVI, fPAR, surface reflectance characteristics)

Digital Topographic Data
(DEM)

=

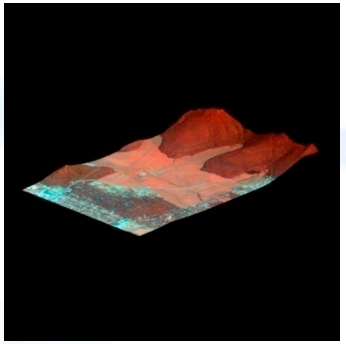

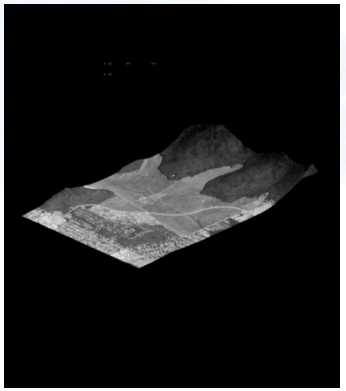

HyspIRI VSWIR/TIR and DEM composite data set
(hyperspctral/day/night TIR digital elevation model data sets))

HyspIRI TIR multispectral Level II product (8 TIR Bands)
(surface temperature, radiance, [day/night], emissivity)

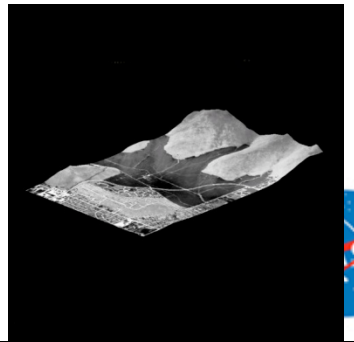

Analysis of the urban surface radiative budget and urban heat islands: How can HyspIRI data be used?

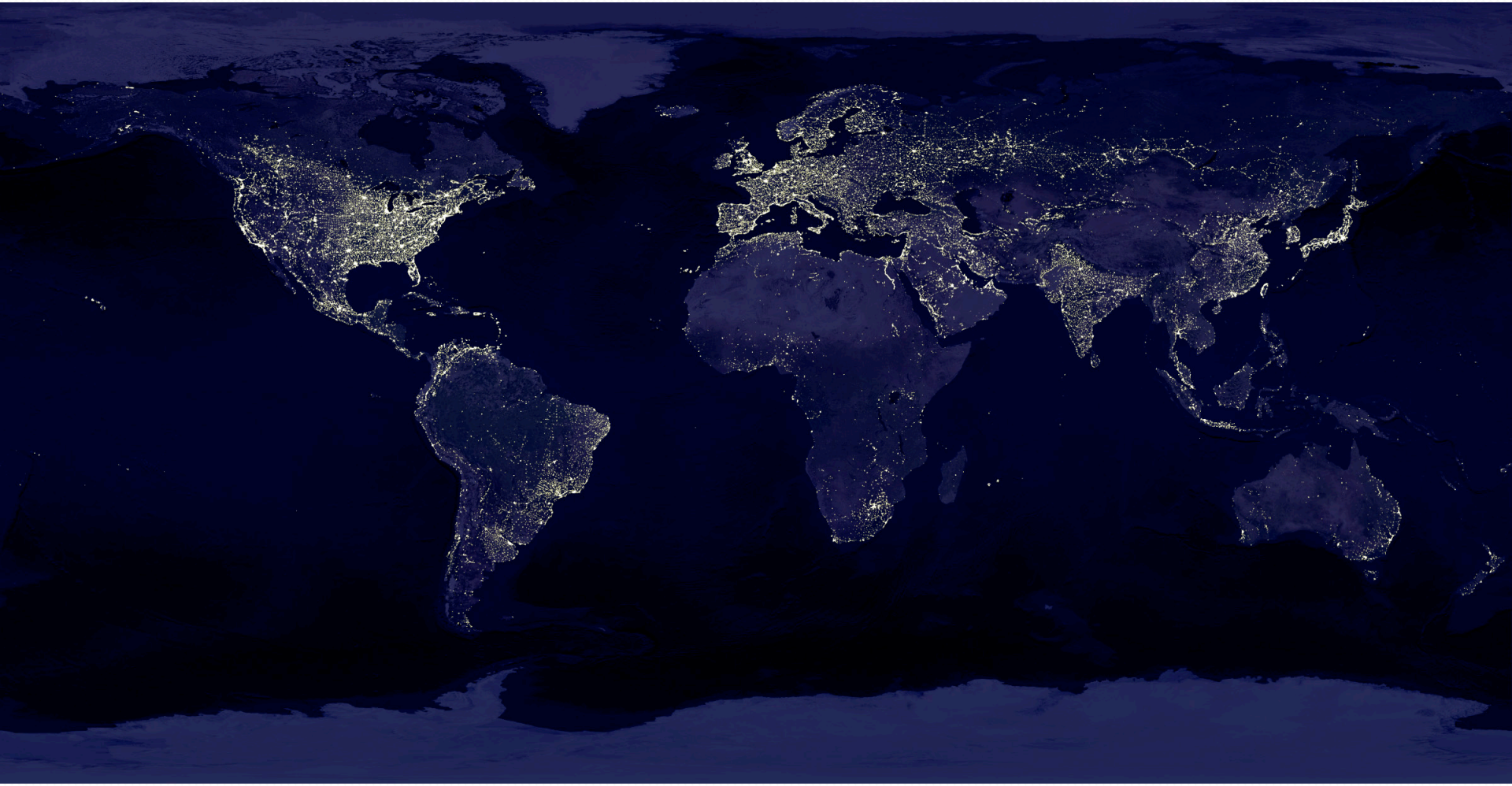

Jeffrey C. Luvall
NASA Marshall Space Flight Center

Solar and Heliospheric Observatory (SOHO) EIT Image of the Sun Obtained on September 14, 1999

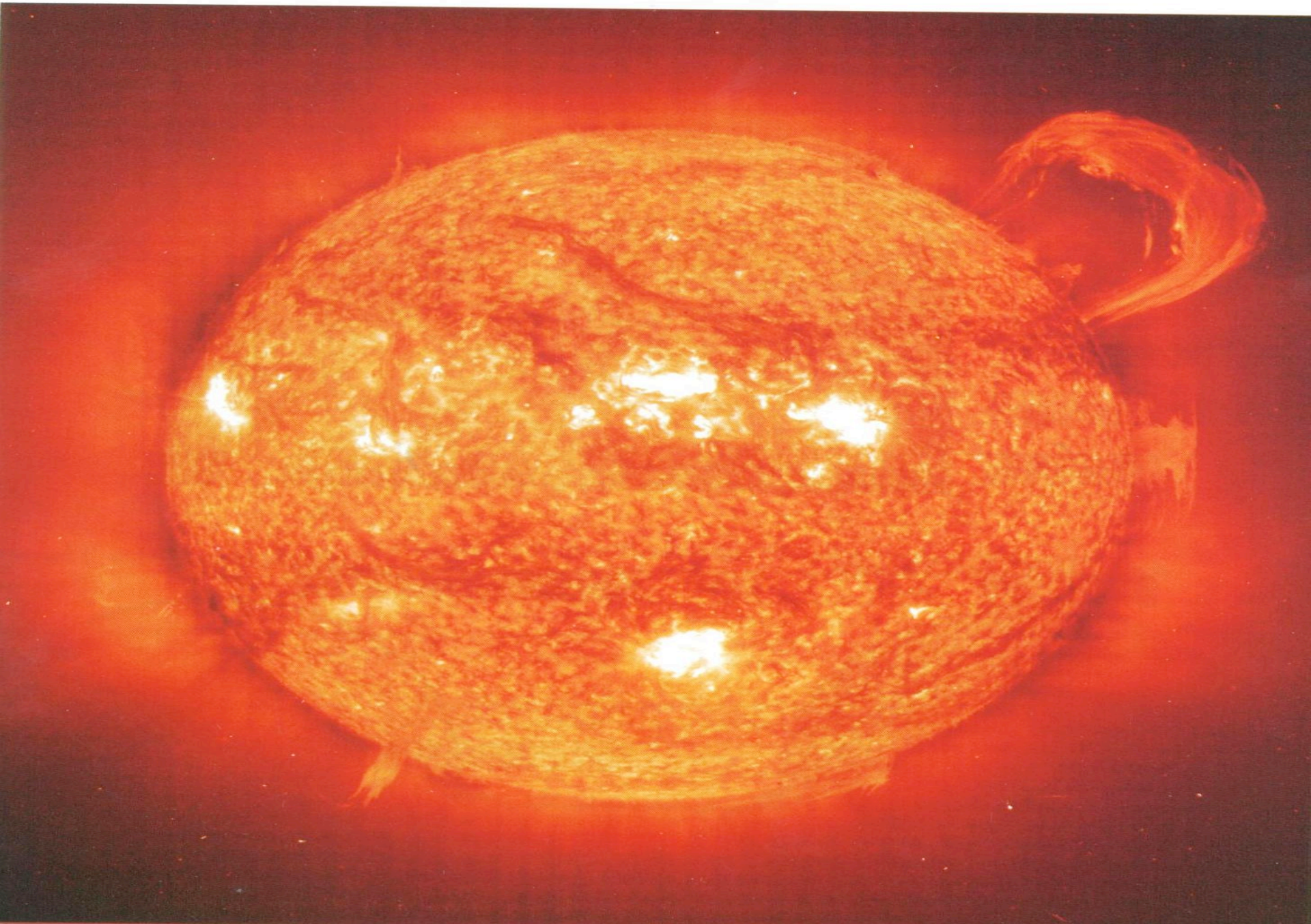

What Happens to the Sun's Energy ?

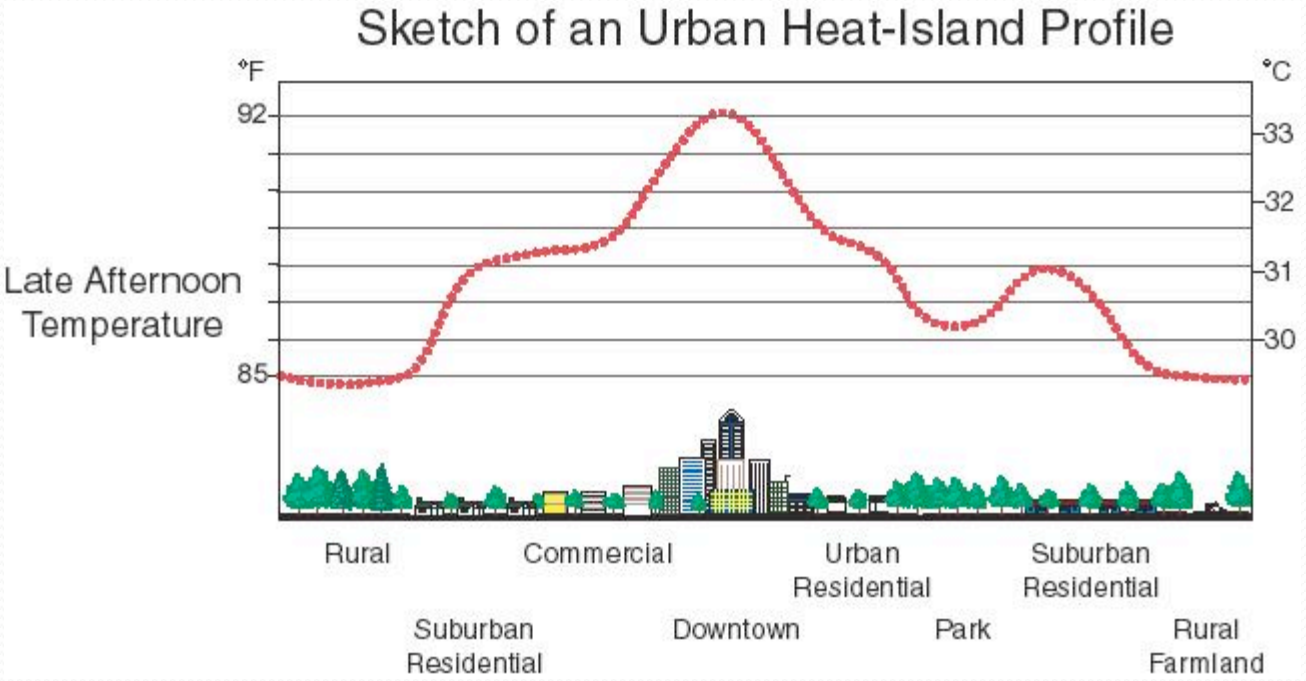
Sketch of an Urban Heat-Island Profile
°F
92
85
°C
33
32
31
30
Late Afternoon Temperature
Rural
Commercial
Urban Residential
Suburban Residential
Suburban Residential
Downtown
Park
Rural Farmland

ion to Planet Earth
nal Aeronautics and Space Administration

Urban Remote Sensing and Air Quality Models

Volatile Organic Compounds
+ Nitrogen Oxides
+ Sunlight

→ Ozone

- Air pollution remains a National issue.
- Temperature increases the ozone levels.
- Urban heat island has major effect on temperature and height of mixing layer.
- Measurement program is defining land use patterns and relationship to heat production.
- Remote sensing data are being used to improve air quality modeling.

TRMM Precipitation Radar Study of Urban-Induced Rainfall Featured in August 11th, 2003 Issue of TIME magazine

AUGUST 11, 2003
TIME

METEOROLOGY

How Cities Make Their Own Weather

WHEN HOUSTON IS HIT BY A SUDden storm, the city may be partly to blame. Increasingly, urban centers don't merely endure bad weather; they help create it. Researchers believe the phenomenon may be more common now than ever before.

Scientists have known for 200 years that the temperature in a city can be higher than that in its environs—something they learned when an amateur weather watcher detected a 1.58°F temperature difference between London and its suburbs. Modern cities, with their cars and heat-trapping buildings, can create an even bigger temperature gap, sometimes as much as 10°F.

Islands of urban heat can do funny things with weather. Hot city air, like hot air anywhere else, rises—even more so because of the turbulence caused by tall buildings. When that air is damp enough and collides with colder layers above it, water can condense out as a sudden burst of rain, especially if there are few frontal systems to disrupt the layers, as in summer. In a spot storm above a city or just downwind of it, it's likely that nature alone isn't behind the downpour.

NASA and the University of Arkansas have been using satellite mapping and ground-based temperature readings to determine how widespread this phenomenon is. This spring researchers got a surprise when they turned their attention to Houston. Because it's near a coast and sea breezes tend to cool and disperse hot air, Houston was thought to be comparatively safe from homemade rain. Now it appears that the opposite may be true. "The sea breeze may exacerbate the rainfall," says research meteorologist Marshall Shepherd of NASA's Goddard Space Flight Center. The warm air and sea air collide, he explains, and "move straight up like the front ends of two cars that hit head on, providing a pump of moist air that helps thunderstorms develop."

Hot, waterlogged cities can be cooled off in the usual ways—by limiting auto exhaust, for example. Using light-colored roofing and paving materials in place of black, heat-absorbing tar will also help. As a bonus, the cooler roof will reduce the need for air conditioning. —*By Jeffrey Kluger*

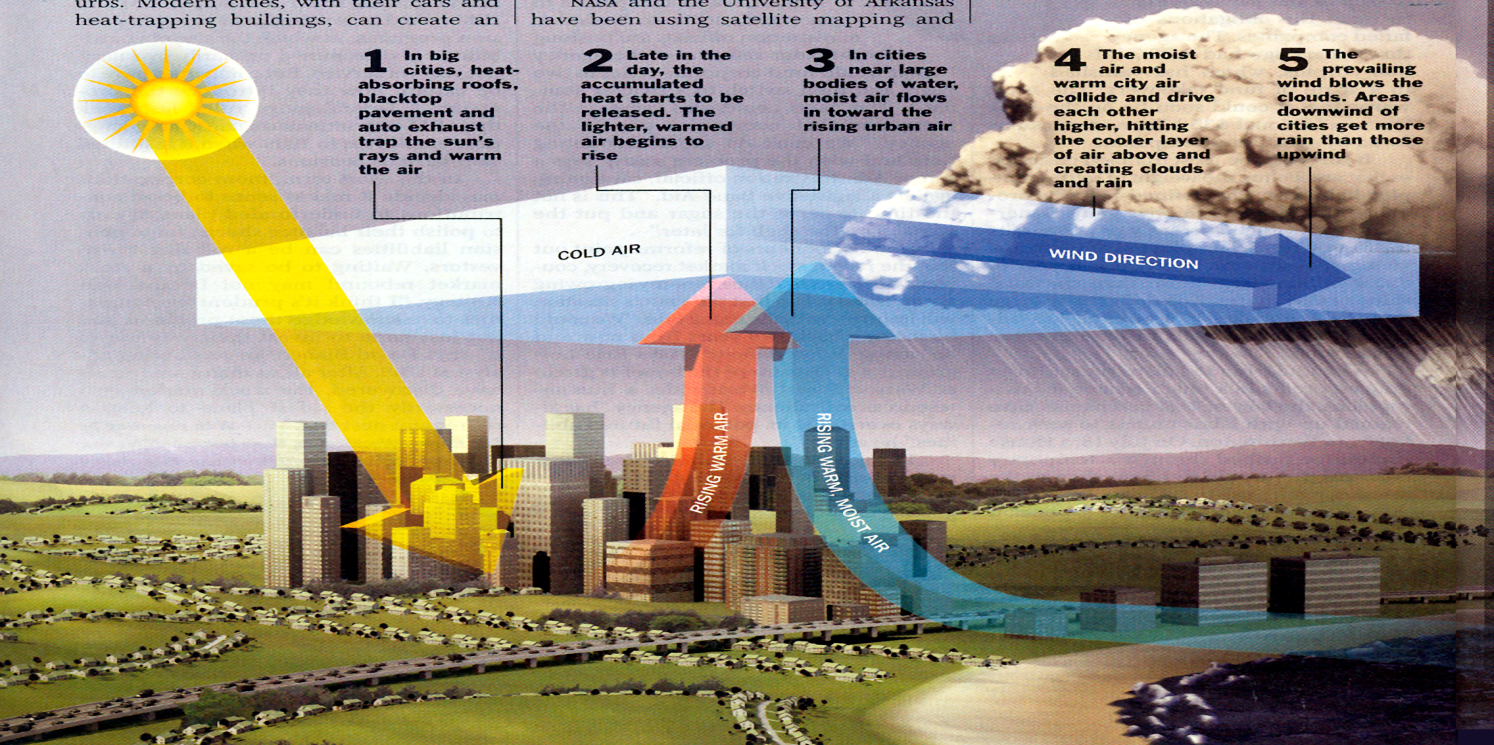

Jeffrey C. Luvall, Marshall Space Flight Center, Earth Science Department

HOT ZONE

High concentrations of buildings, roads and other artificial structures retain heat, leading to warmer temperatures. A NASA snapshot of Houston taken one evening in August 2000 demonstrates this urban heat-island effect: the hot zone downtown stands in sharp contrast to the cooler suburbs to the south

70°F (21°C) — 90°F (32°C)

Source: NASA/Goddard Space Flight Center
TIME diagram by Joe Lertola

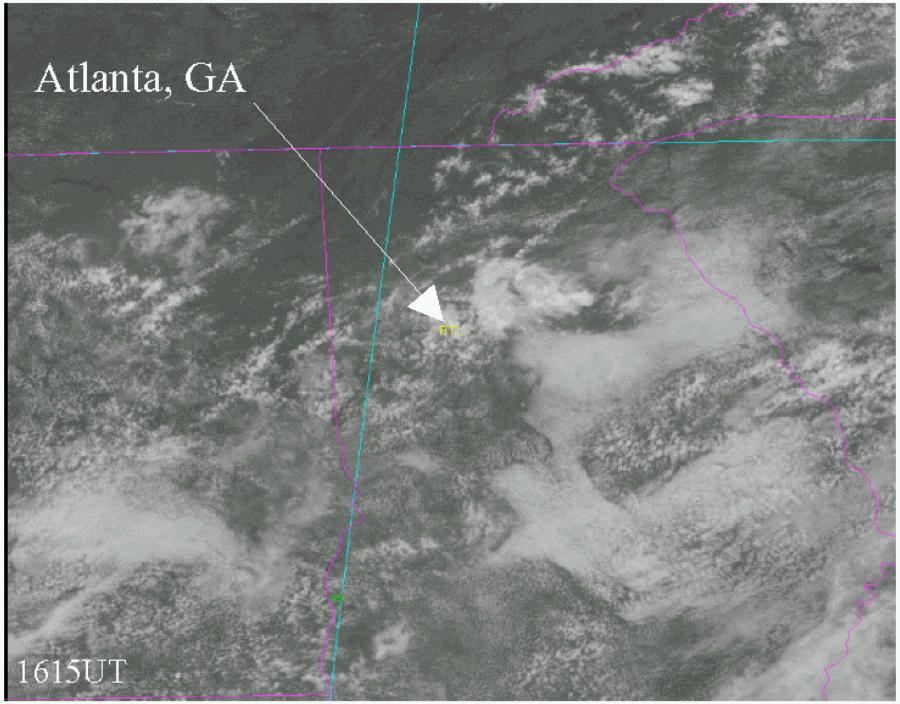
Atlanta, GA
1615UT

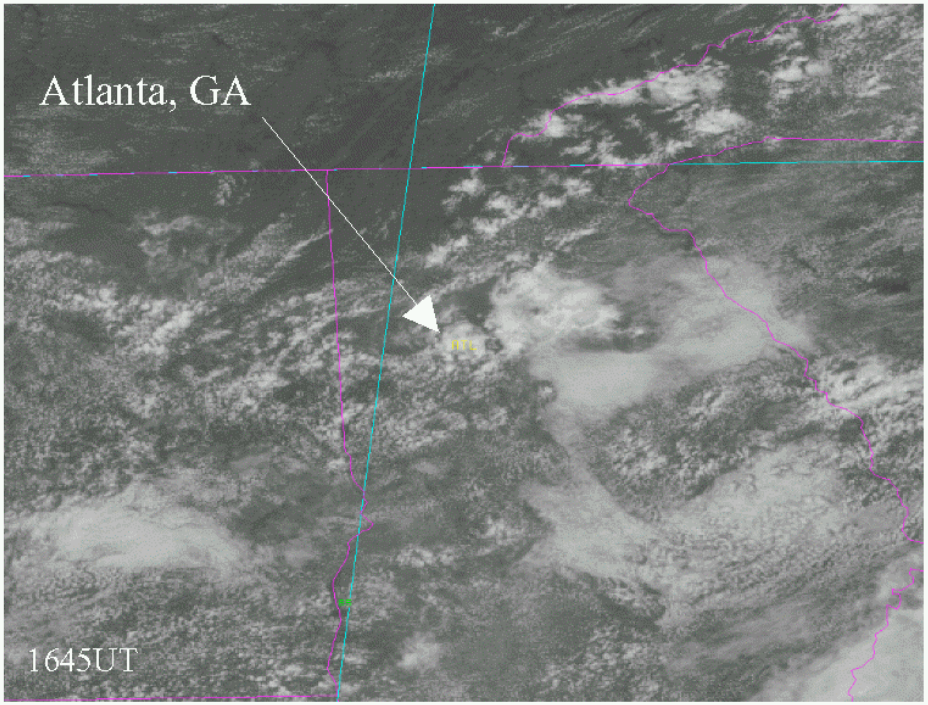
Atlanta, GA
1645UT

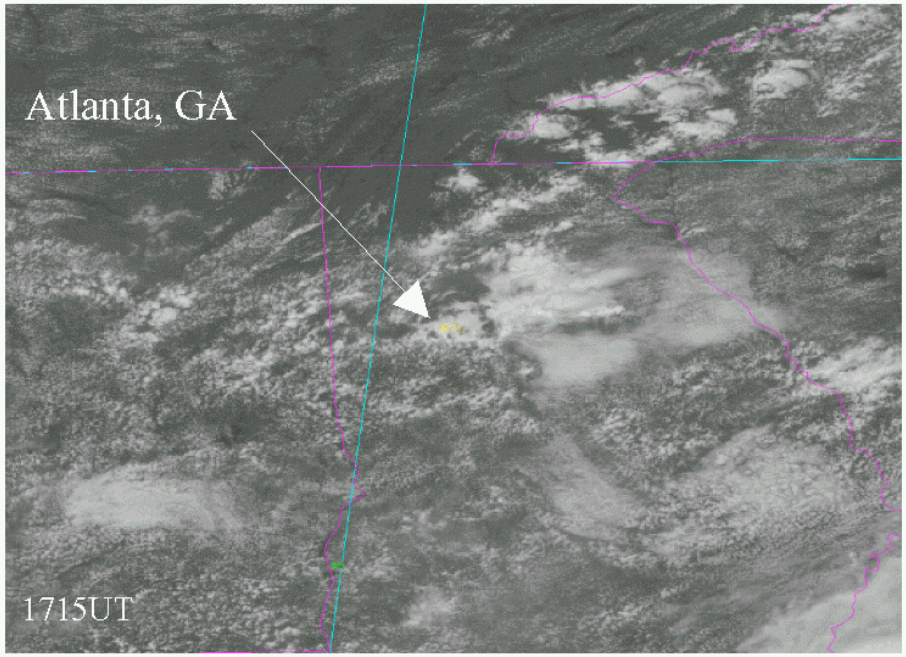
Atlanta, GA
1715UT

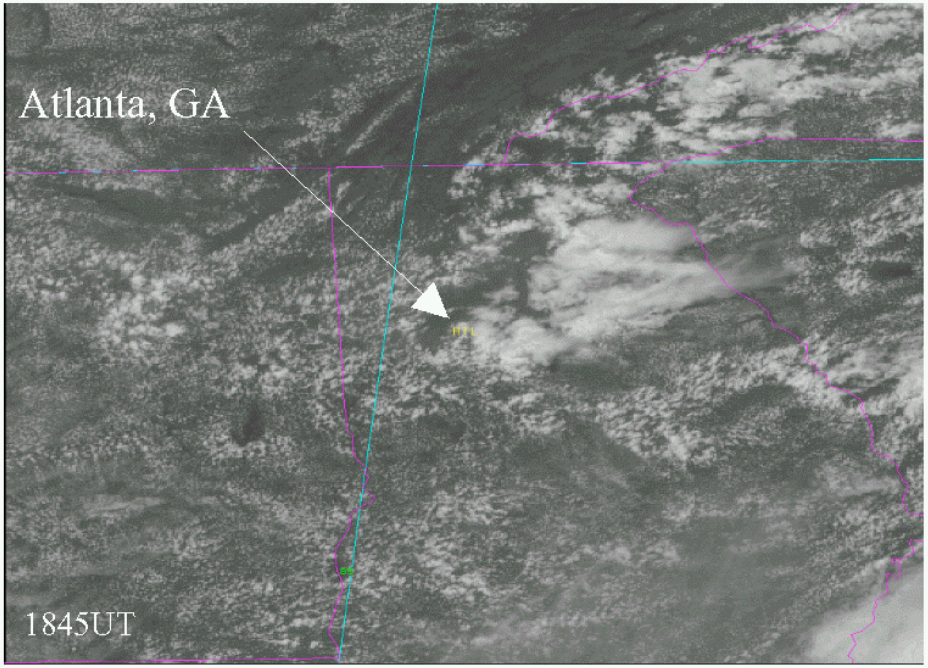
Atlanta, GA
1845UT

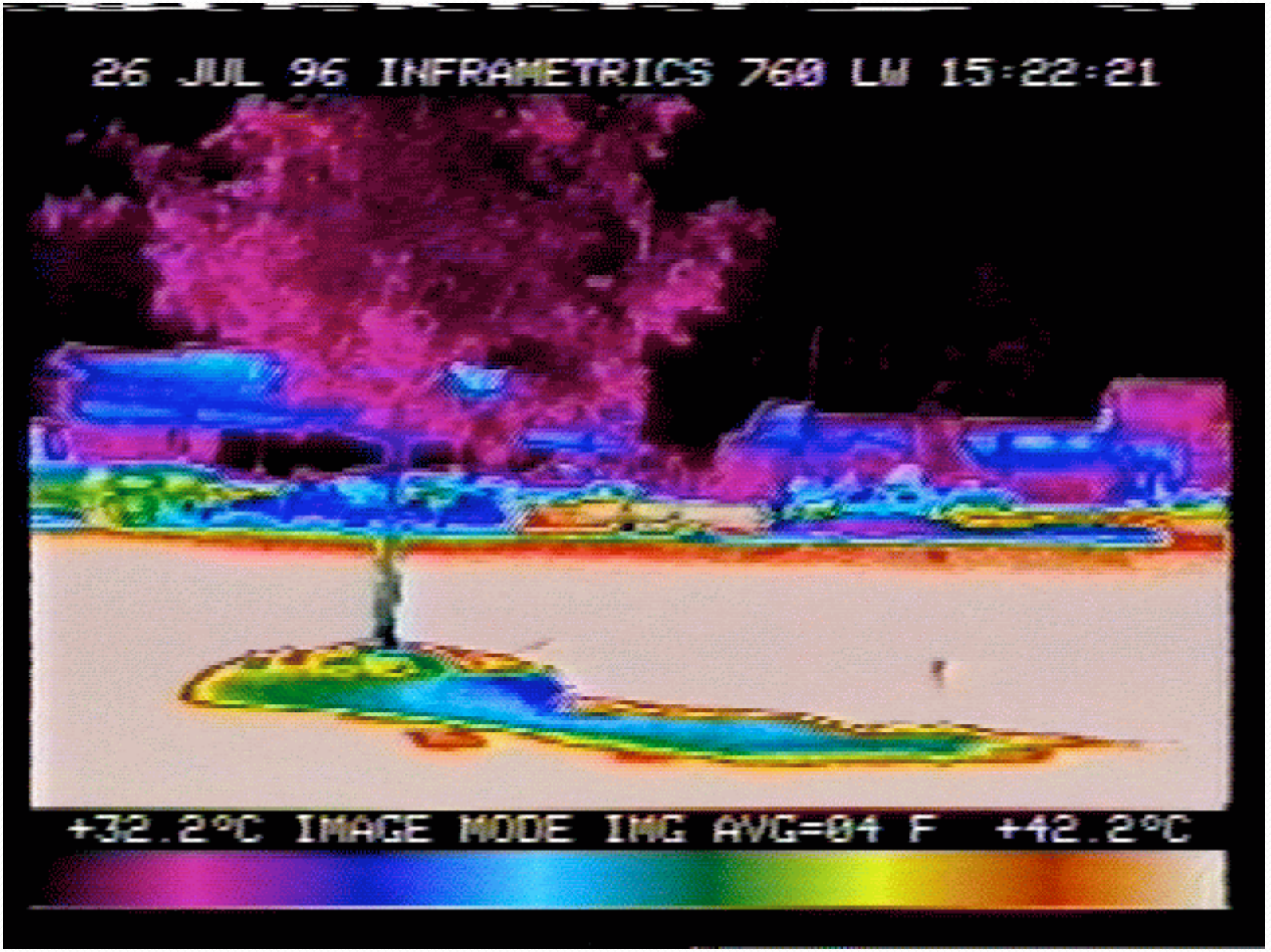
26 JUL 96 INFRAMETRICS 760 LW 15:22:21
+32.2°C IMAGE MODE IMG AVG=04 F +42.2°C

Surface Radiation Budget

$$Q^* = (K_{in} + K_{out}) + (L_{in} + L_{out})$$

Q^* = Net Radiation

K_{in} = Incoming Solar

K_{out} = Reflected Solar

L_{in} = Incoming Longwave

L_{out} = Emitted Longwave

Surface Energy Budget

$$Q^* = H + LE + G$$

H = Sensible Heat Flux

LE = Latent Heat Flux

G = Storage (maybe + or -)

Natural Surface Albedo

Surface	*Albedo*
Soils	0.05-0.40
Desert	0.20-0.45
Grass	0.16-0.26
Crops	0.18-0.25
Forests-deciduous	0.15-0.20
Forests-coniferous	0.05-0.15
Water (small zenith angle)	0.03-0.10
Snow (fresh)	0.40-0.95

Albedo of Typical Urban Mateials & Surfaces

Surface	*Albedo*
Asphalt Roads	0.05-0.20
Concrete	0.10-0.35
Brick	0.20-0.40
Tar & Gravel Roofs	0.08-0.18
Tile Roofs	0.10-0.35
Corrugated Iron Roofs	0.10-0.16
White Membrane	0.64-0.84
Paint-White	0.50-0.90
Paint- Red,Brown,Green	0.20-0.35
Urban Areas	0.10-0.27 (0.15)

NASA
N933NA

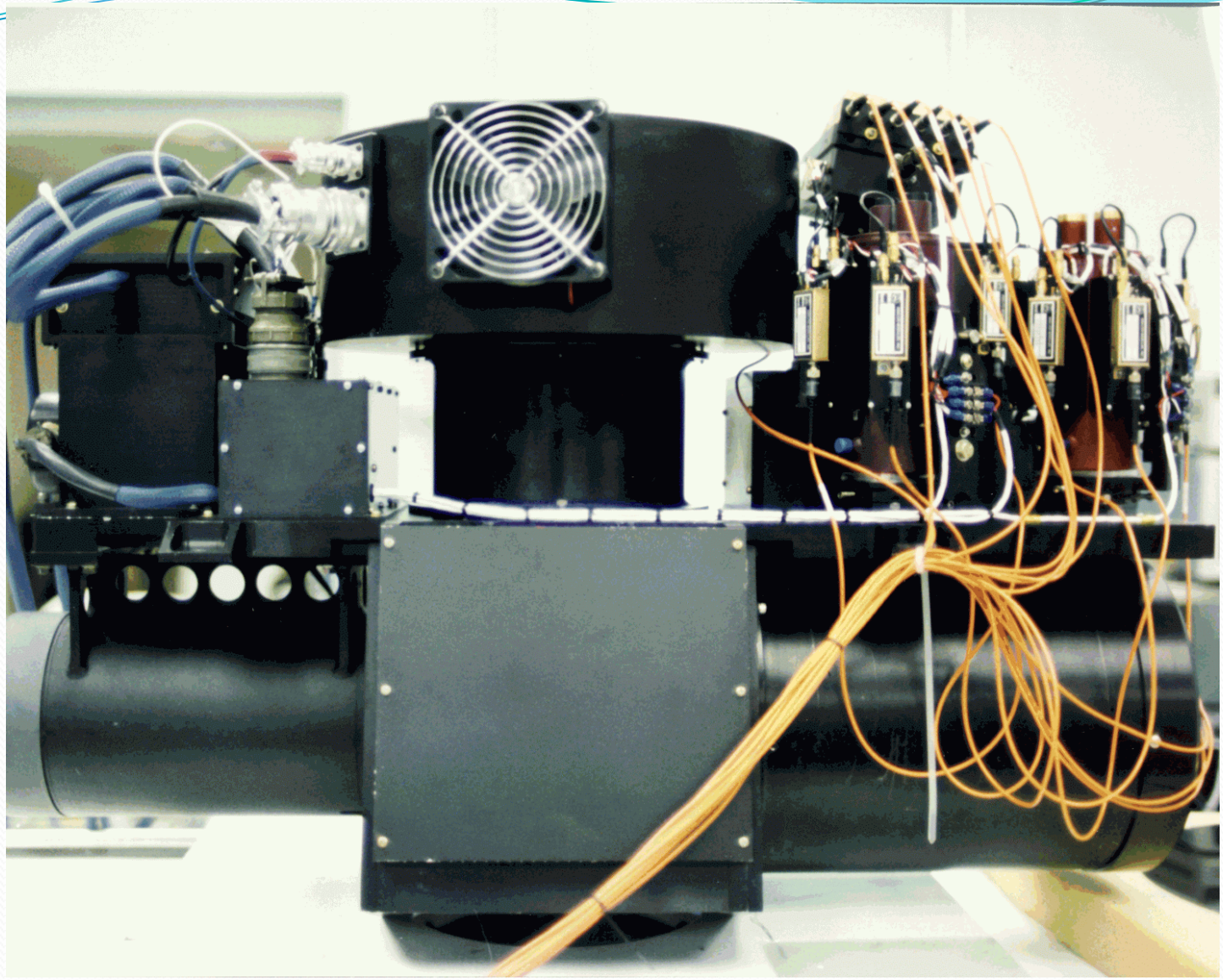

ATLAS

Typical Spectral Response Curves

Reflected Bands

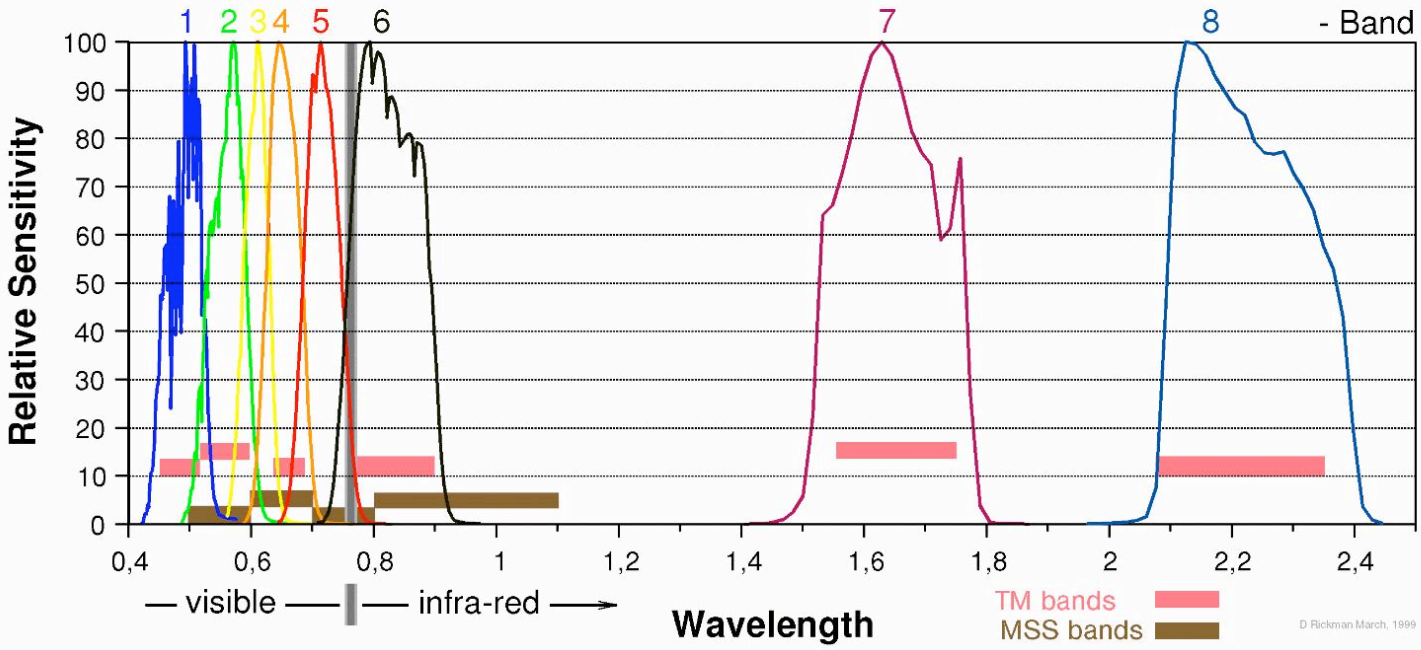

D. Rickman, et al., Nov. 9,1999

ATLAS

Typical Spectral Response Curves

Thermal Bands

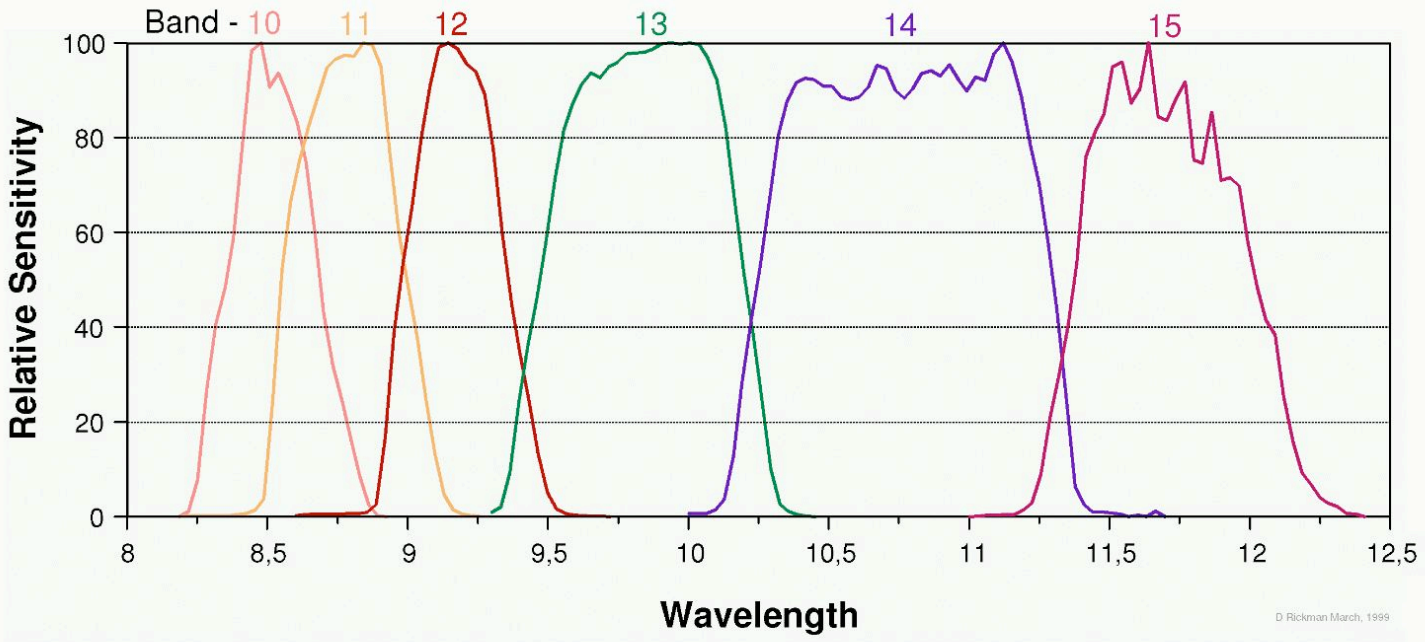

D. Rickman, et al., Nov. 9,1999

Emissivity Differences in Natural Surfaces

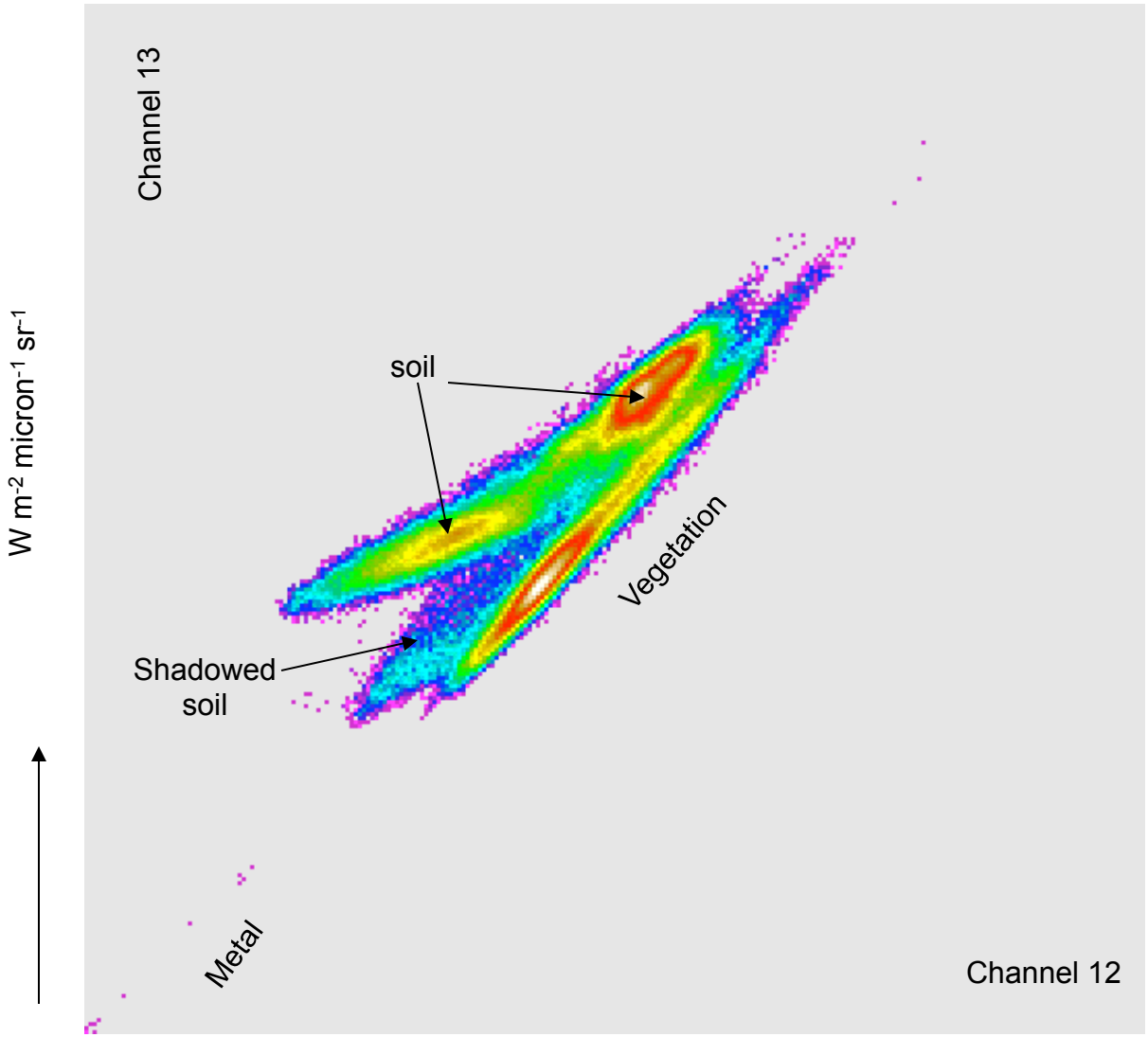

San Juan

CH 10 vs CH 11

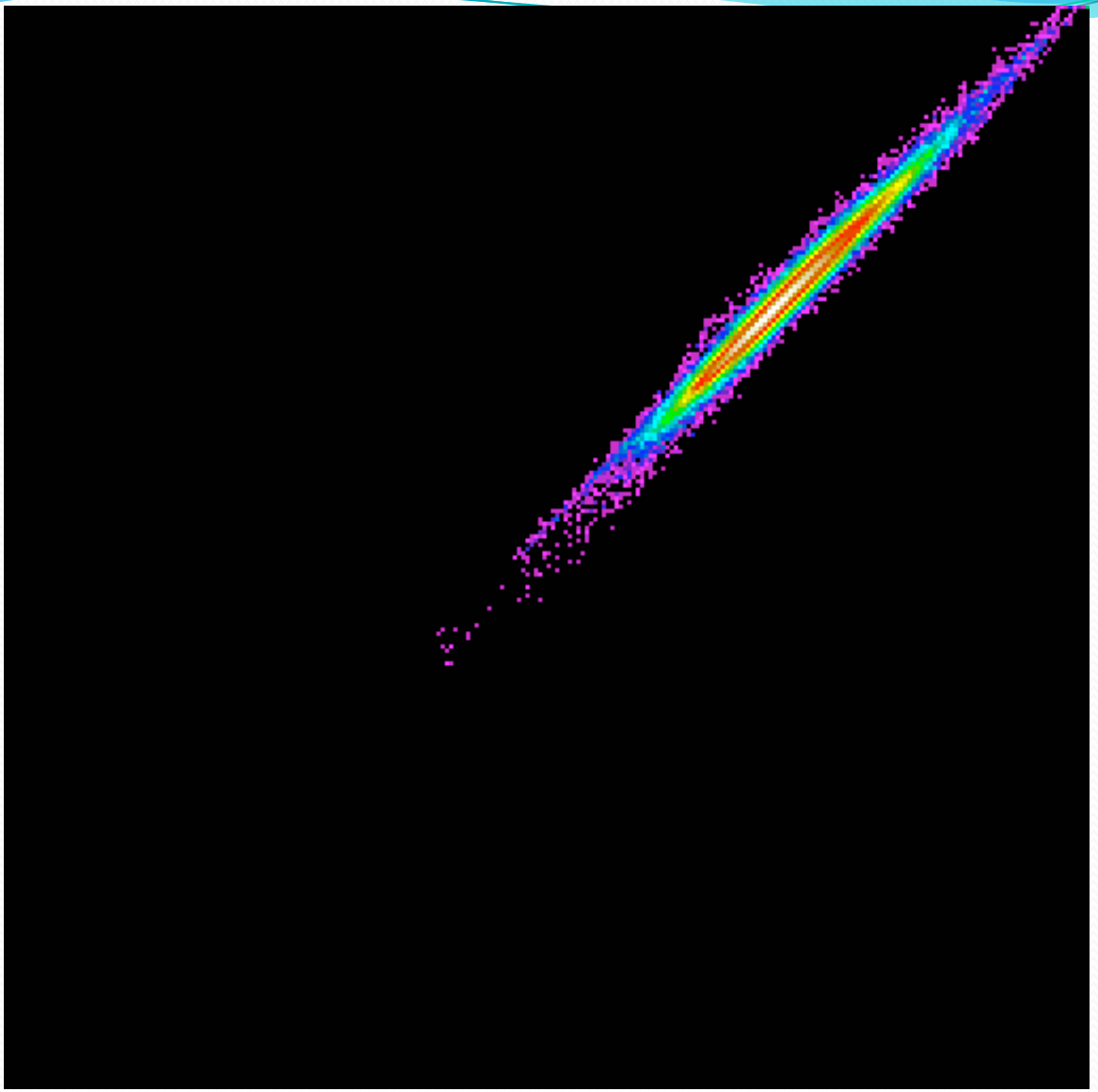

Energy

W m-2 sr-1 micron

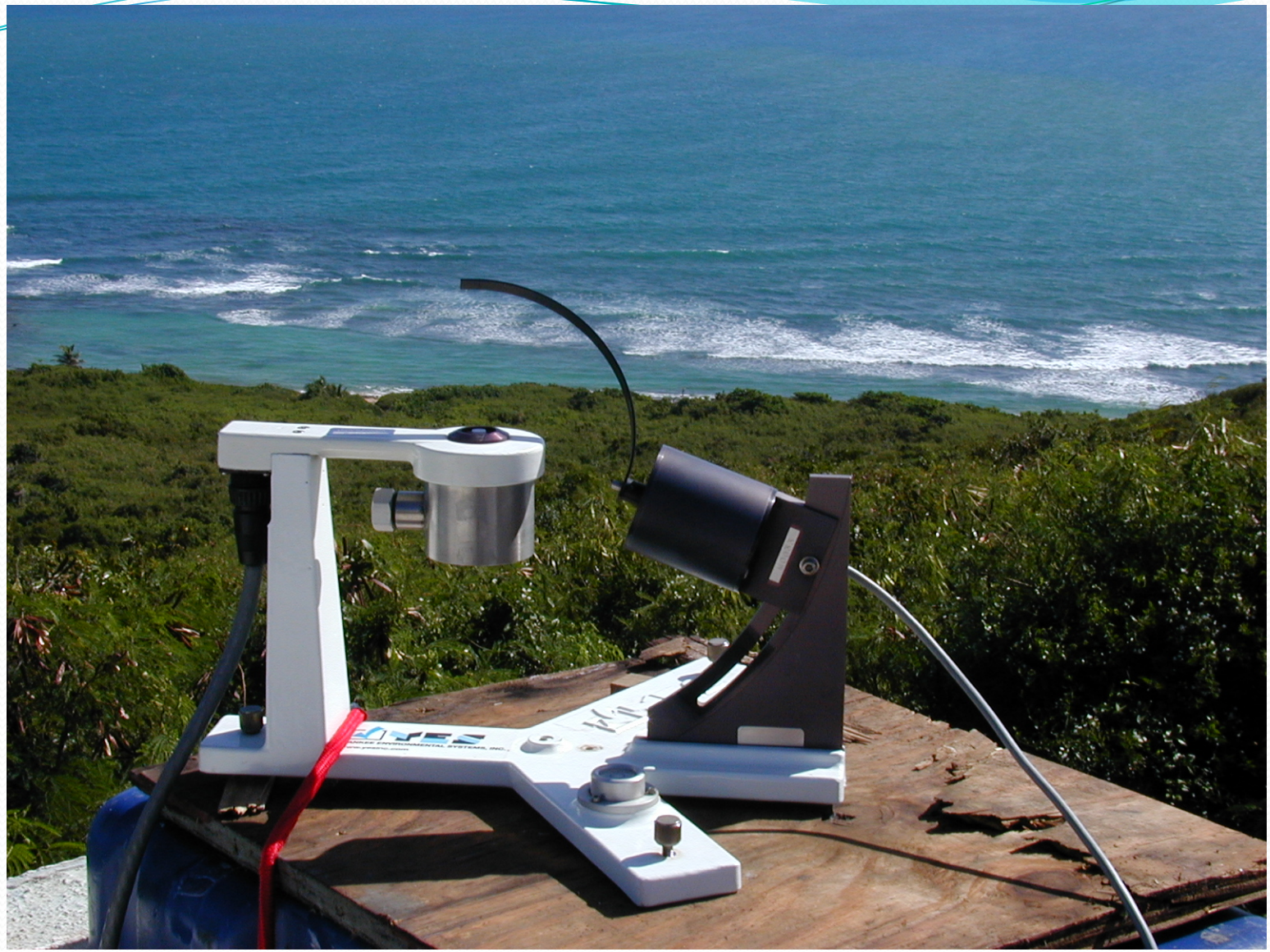

Overall Process Flow

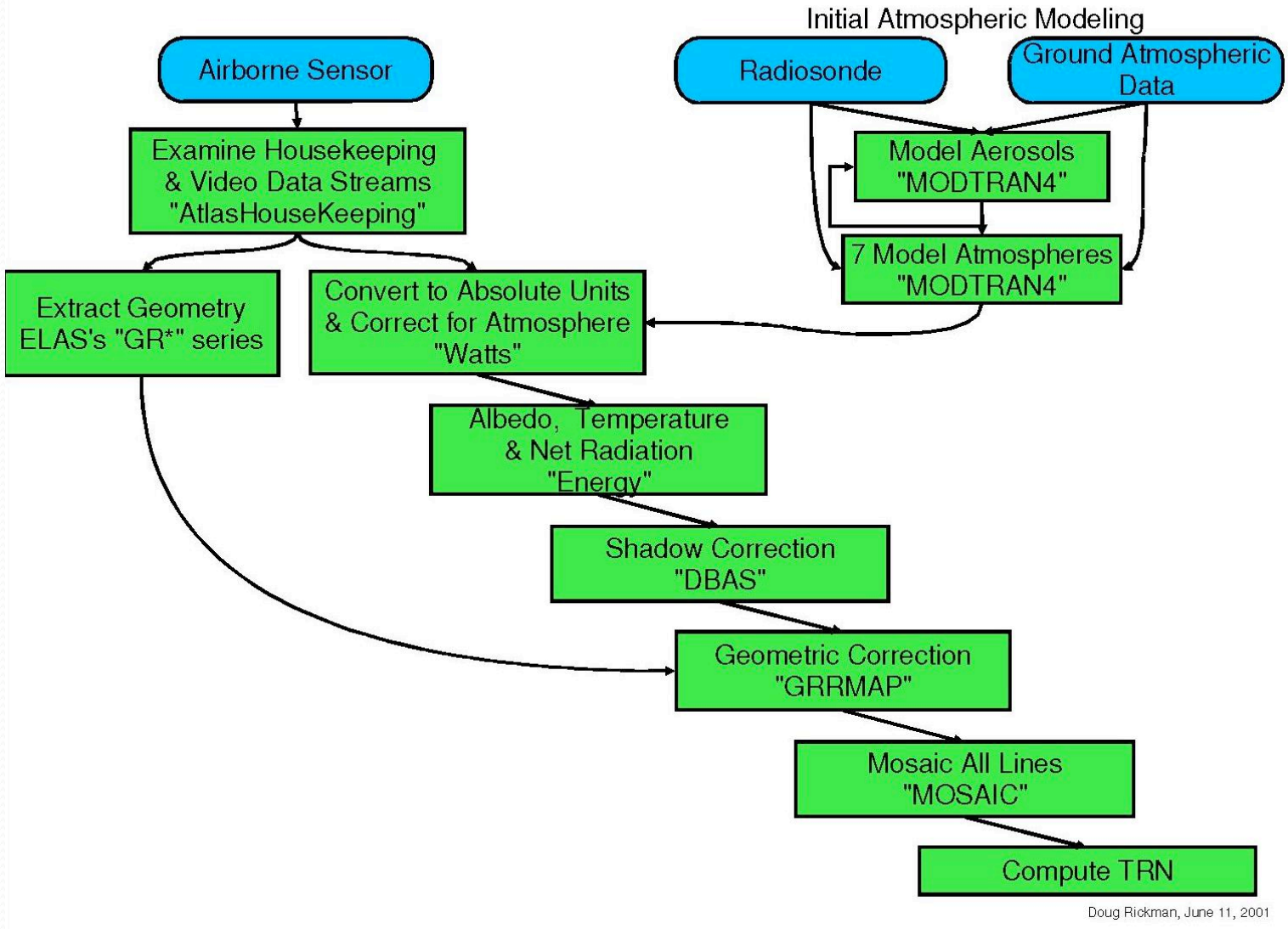

San Juan F5 Mosaic True Color

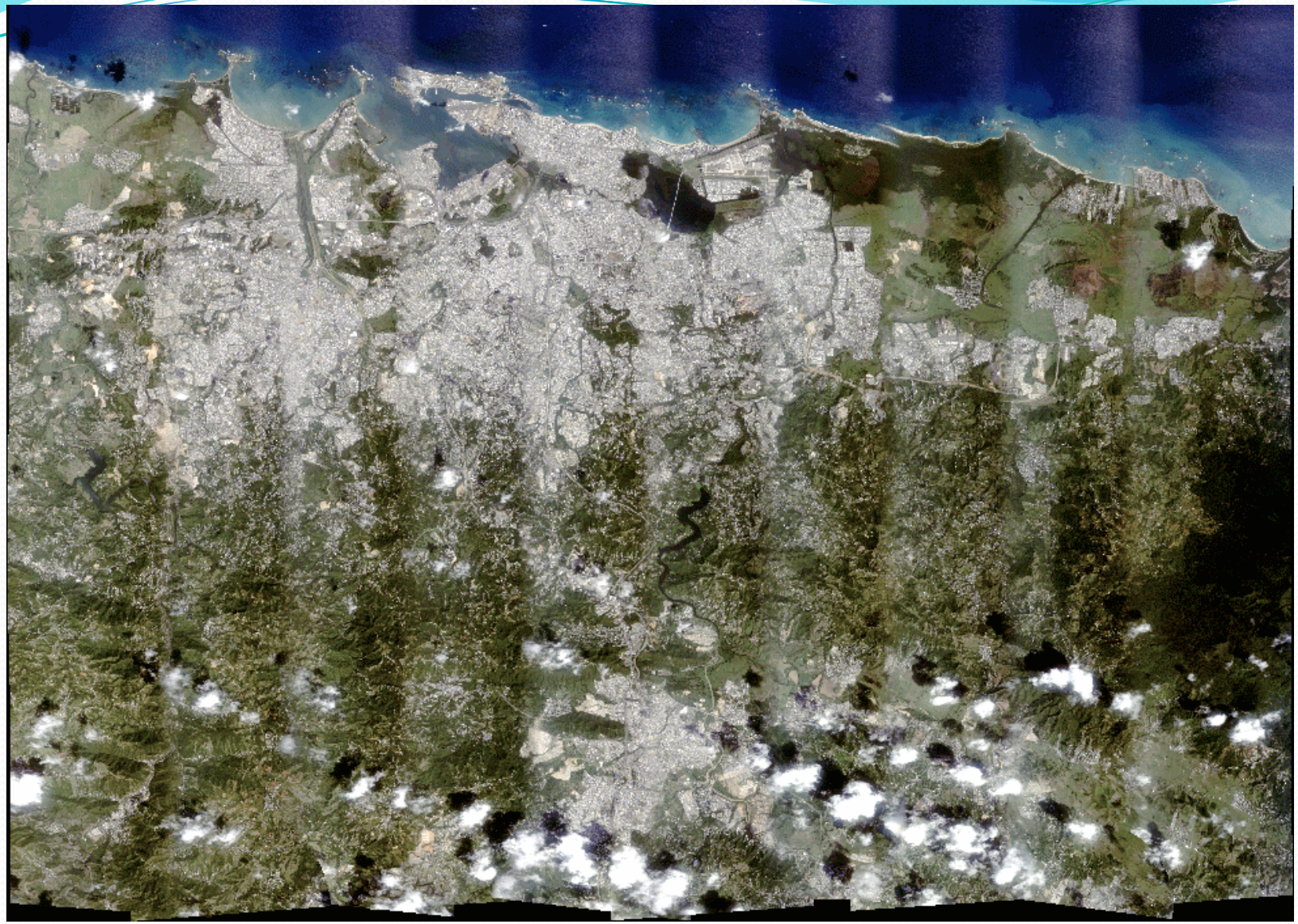

San Juan F5 Mosaic Albedo

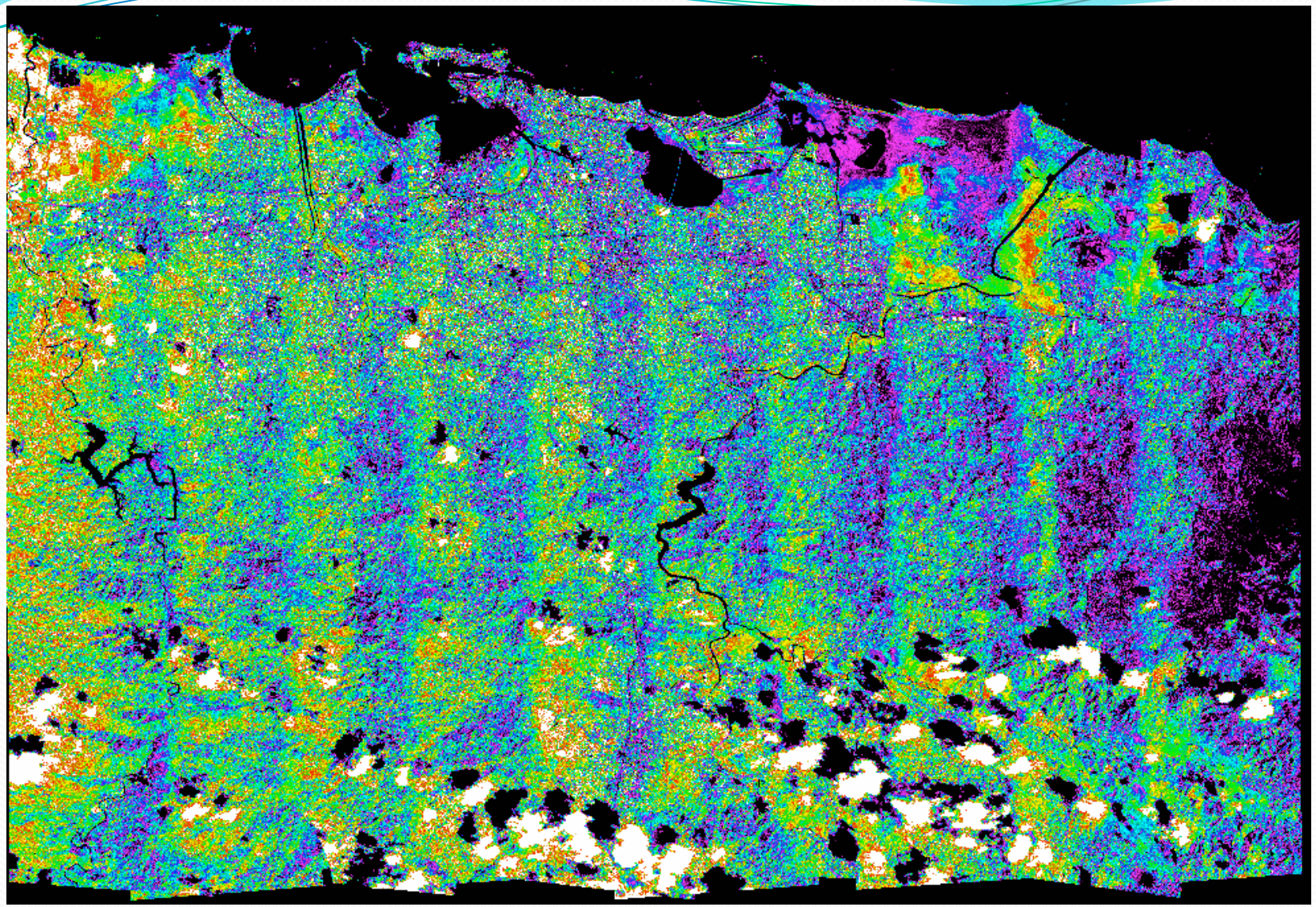

San Juan F5 Mosaic Temperature

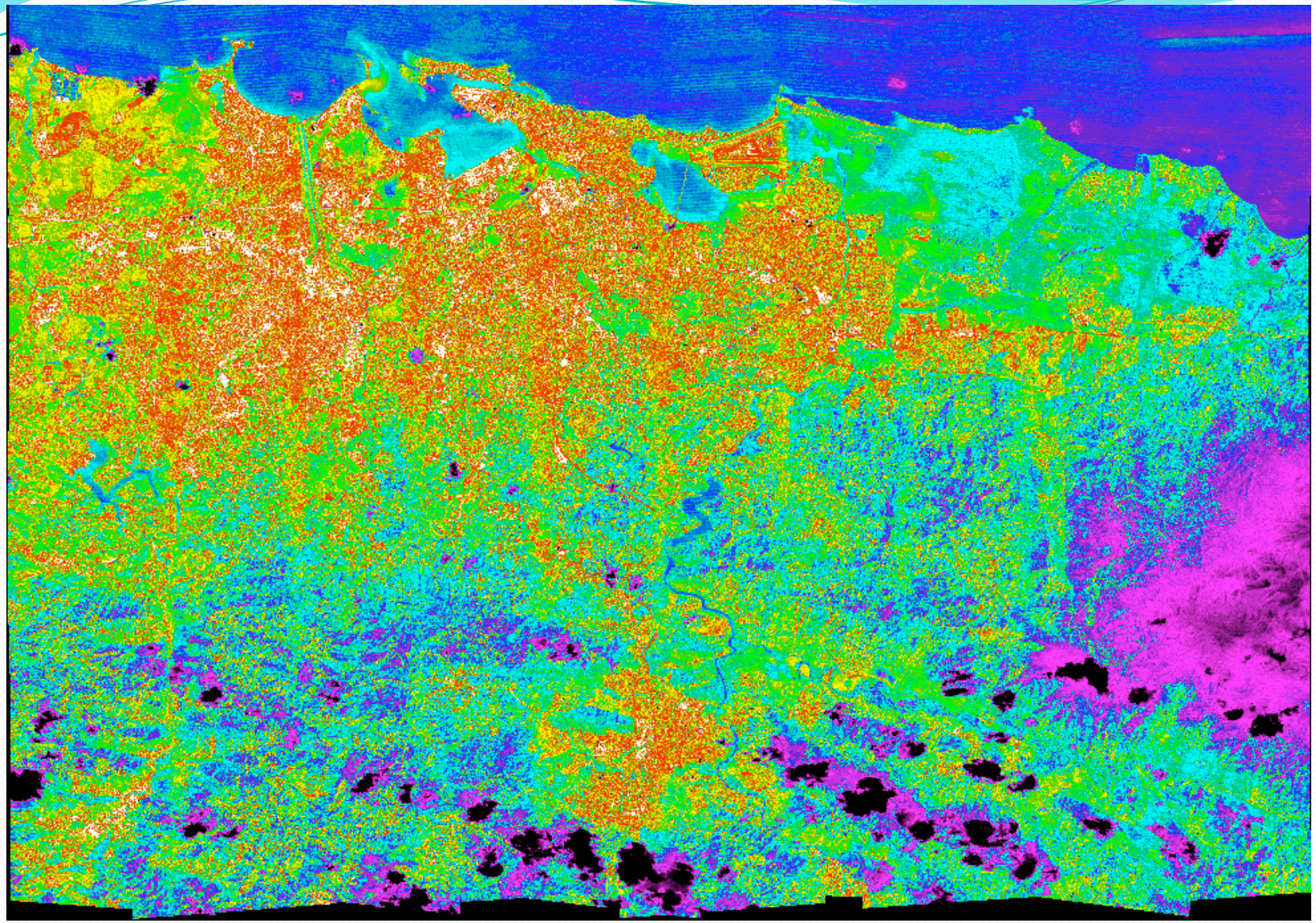

^{o}C 10 20 26 27 28 32 39 41 48

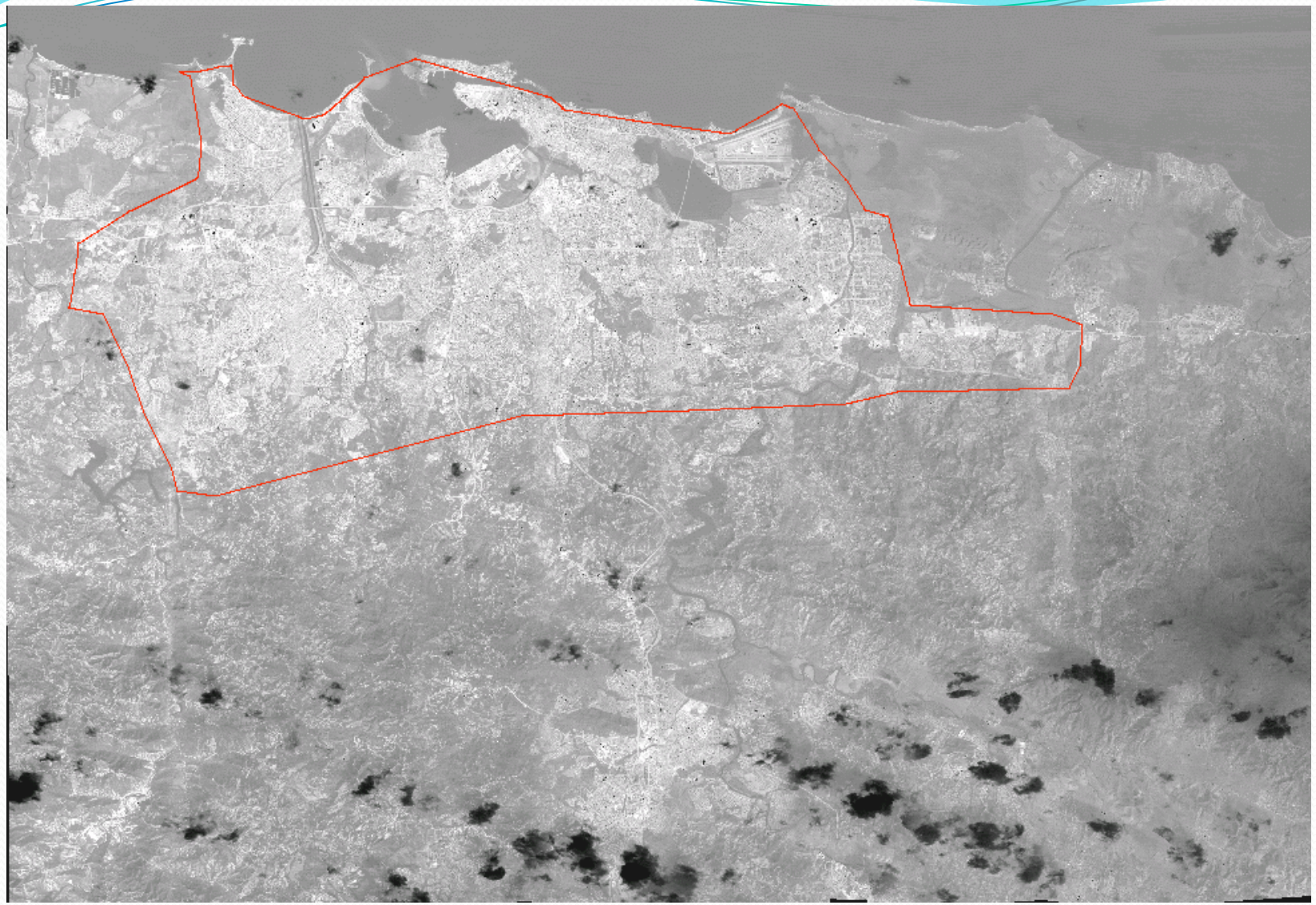

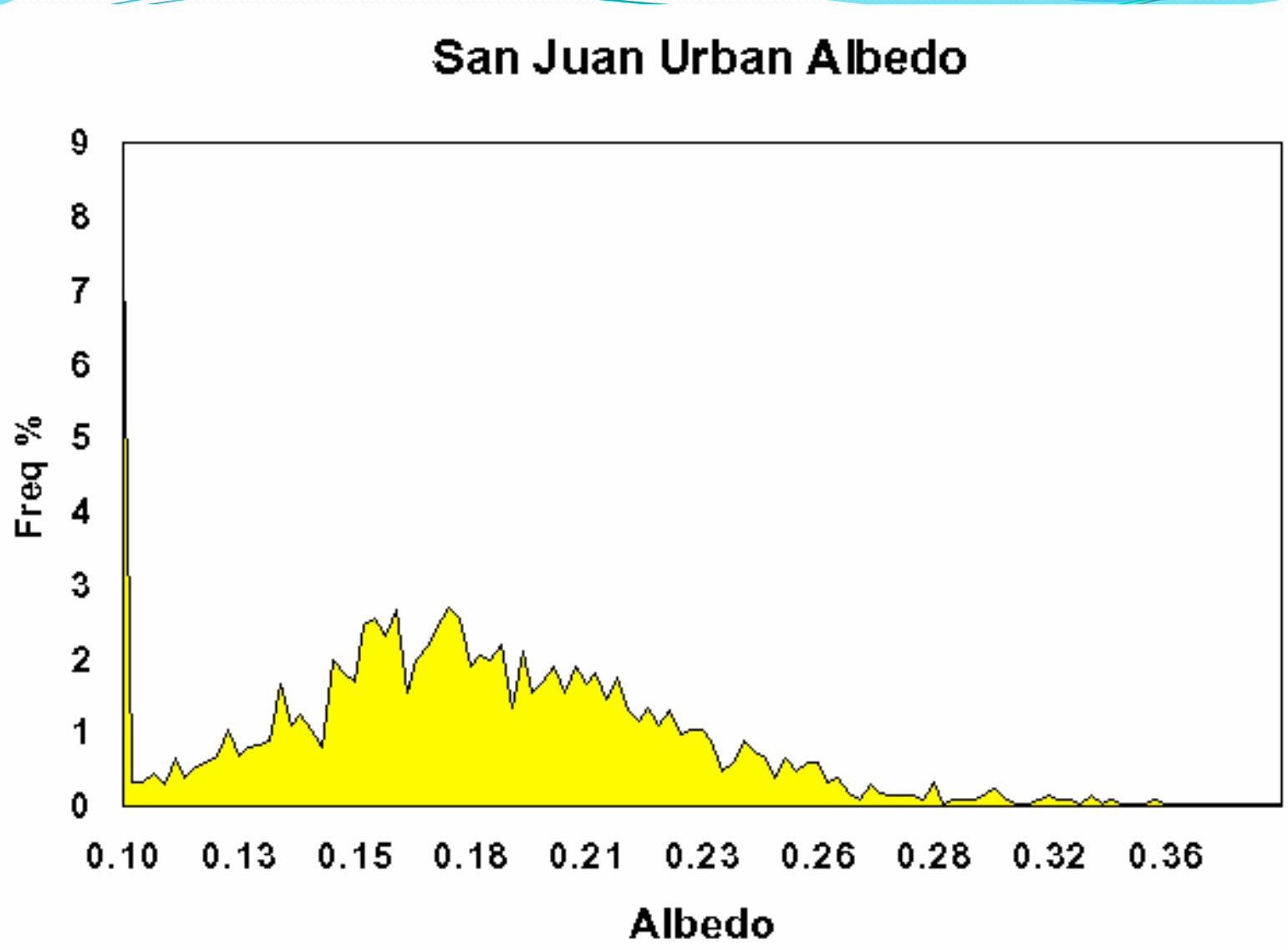
San Juan Urban Albedo
Freq %
9
8
7
6
5
4
3
2
1
0
0.10
0.13
0.15
0.18
0.21
0.23
0.26
0.28
0.32
0.36
Albedo

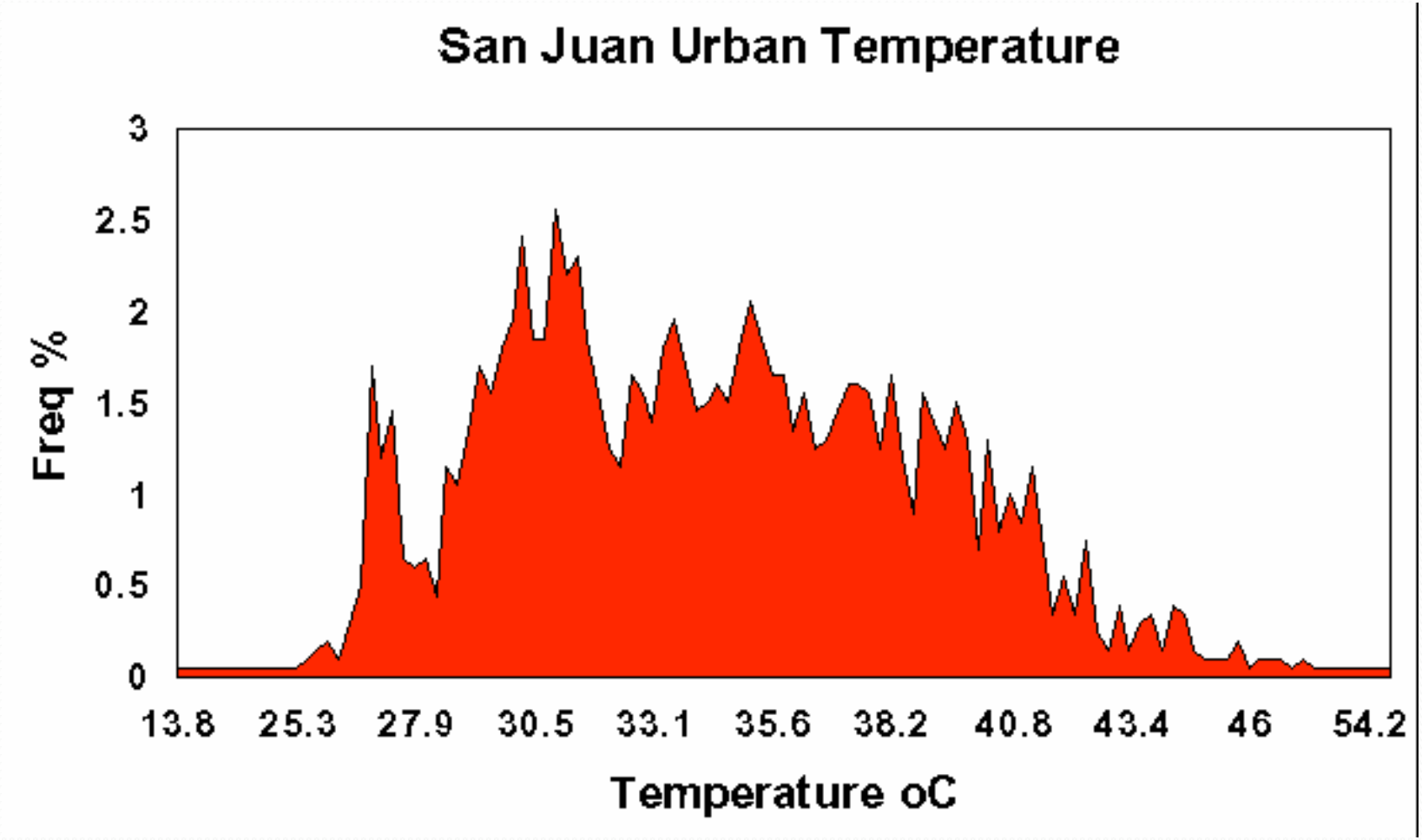
San Juan Urban Temperature
Freq %
3
2.5
2
1.5
1
0.5
0
13.8
25.3
27.9
30.5
33.1
35.6
38.2
40.8
43.4
46
54.2
Temperature oC

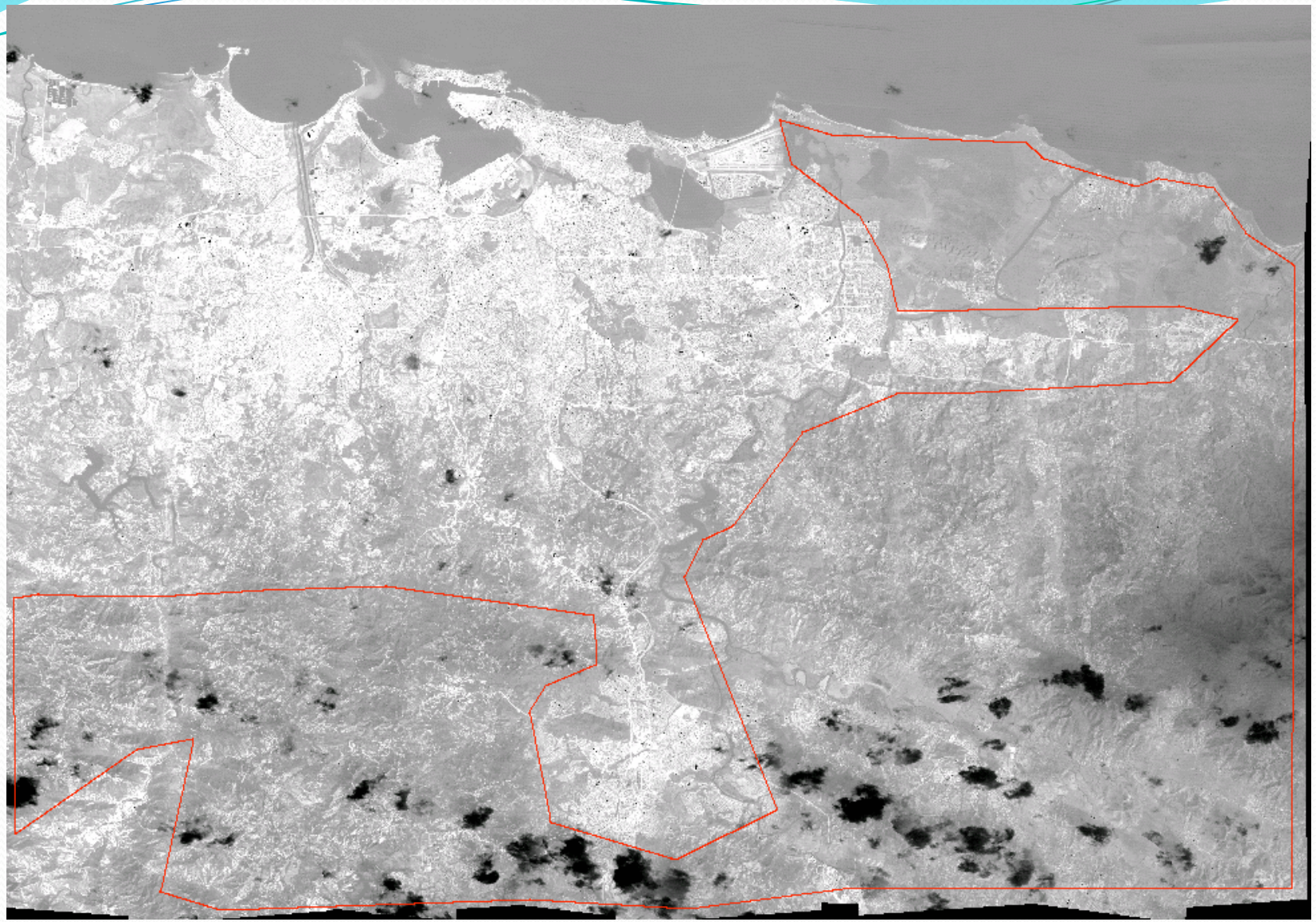

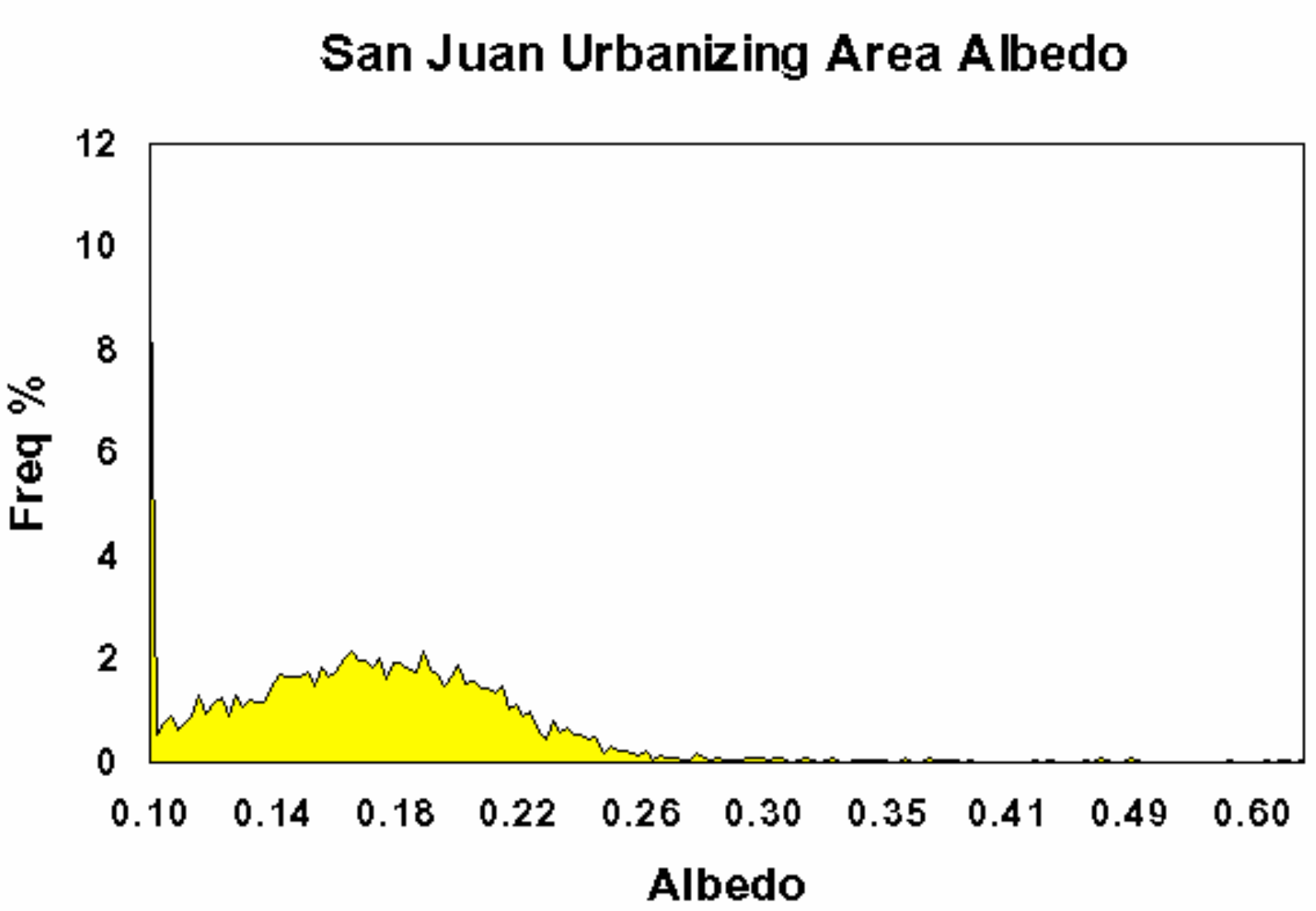
San Juan Urbanizing Area Albedo
Freq %
12
10
8
6
4
2
0
0.10
0.14
0.18
0.22
0.26
0.30
0.35
0.41
0.49
0.60
Albedo

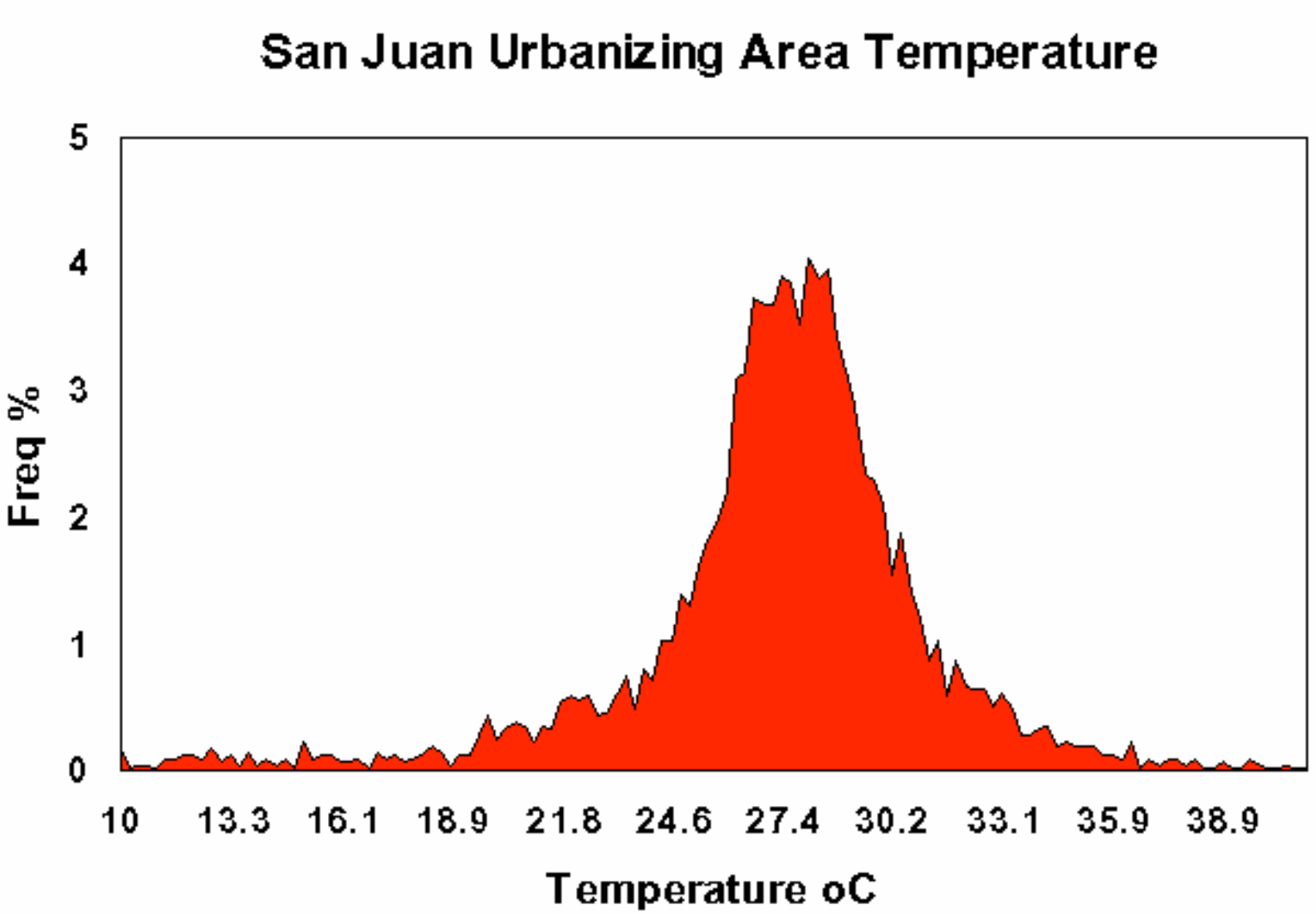
San Juan Urbanizing Area Temperature
Freq %
0
1
2
3
4
5
10
13.3
16.1
18.9
21.8
24.6
27.4
30.2
33.1
35.9
38.9
Temperature oC

San Juan Puerto Rico
Albedo vs Temperature

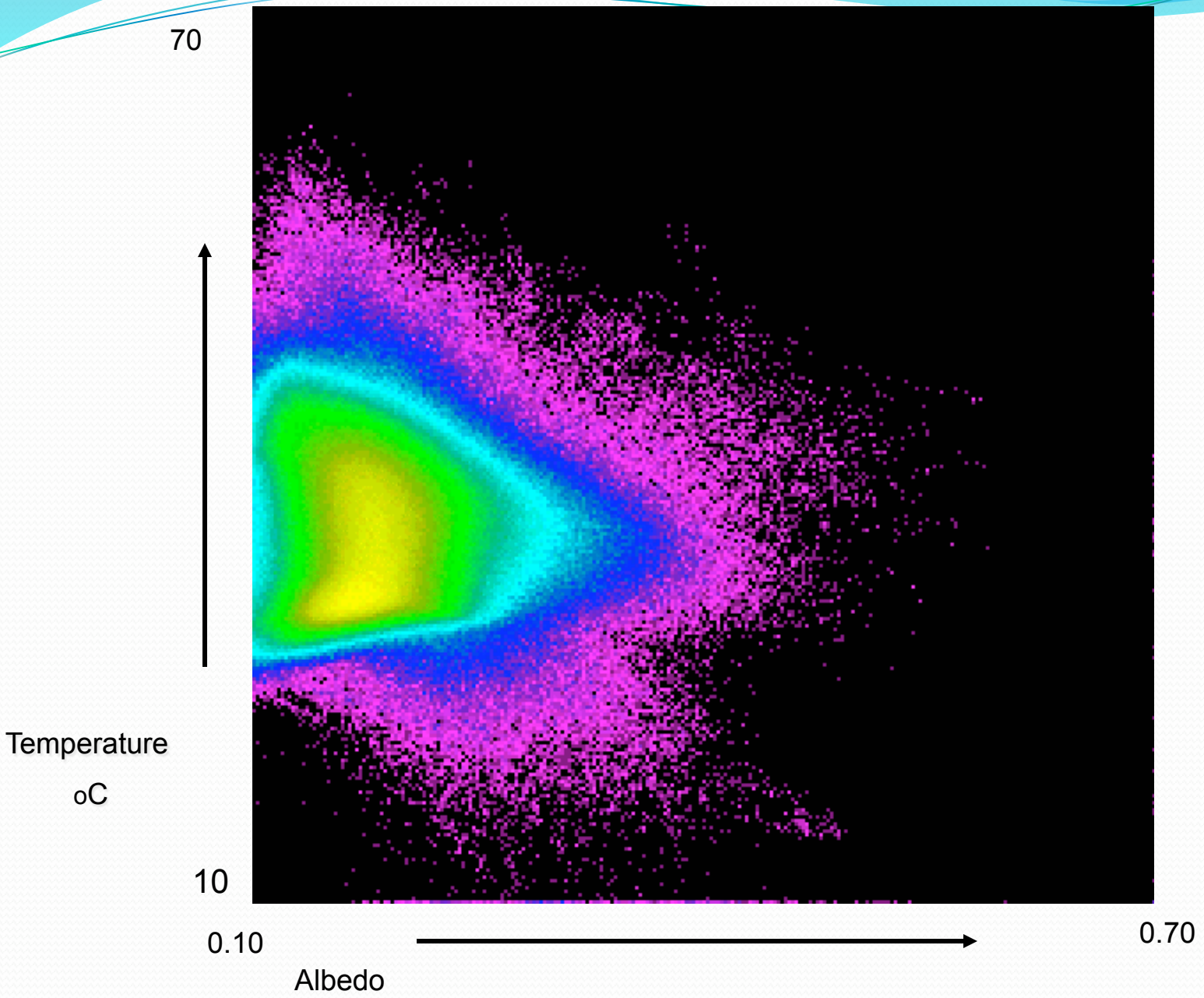

San Juan Puerto Rico Urbanizing Area
Albedo vs Temperature

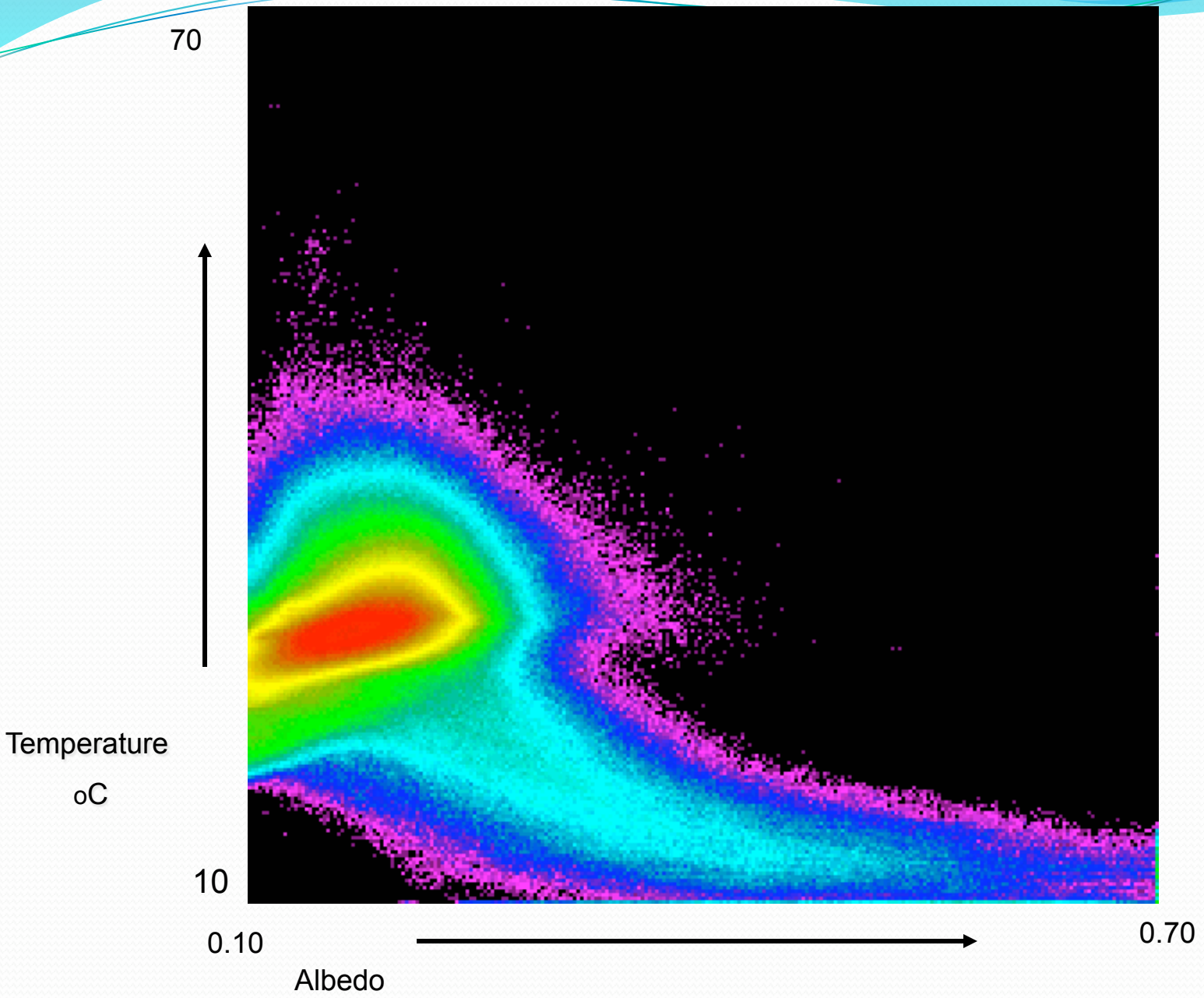

El Yunque F4 Mosaic True Color

El Yunque F4 Mosaic Albedo

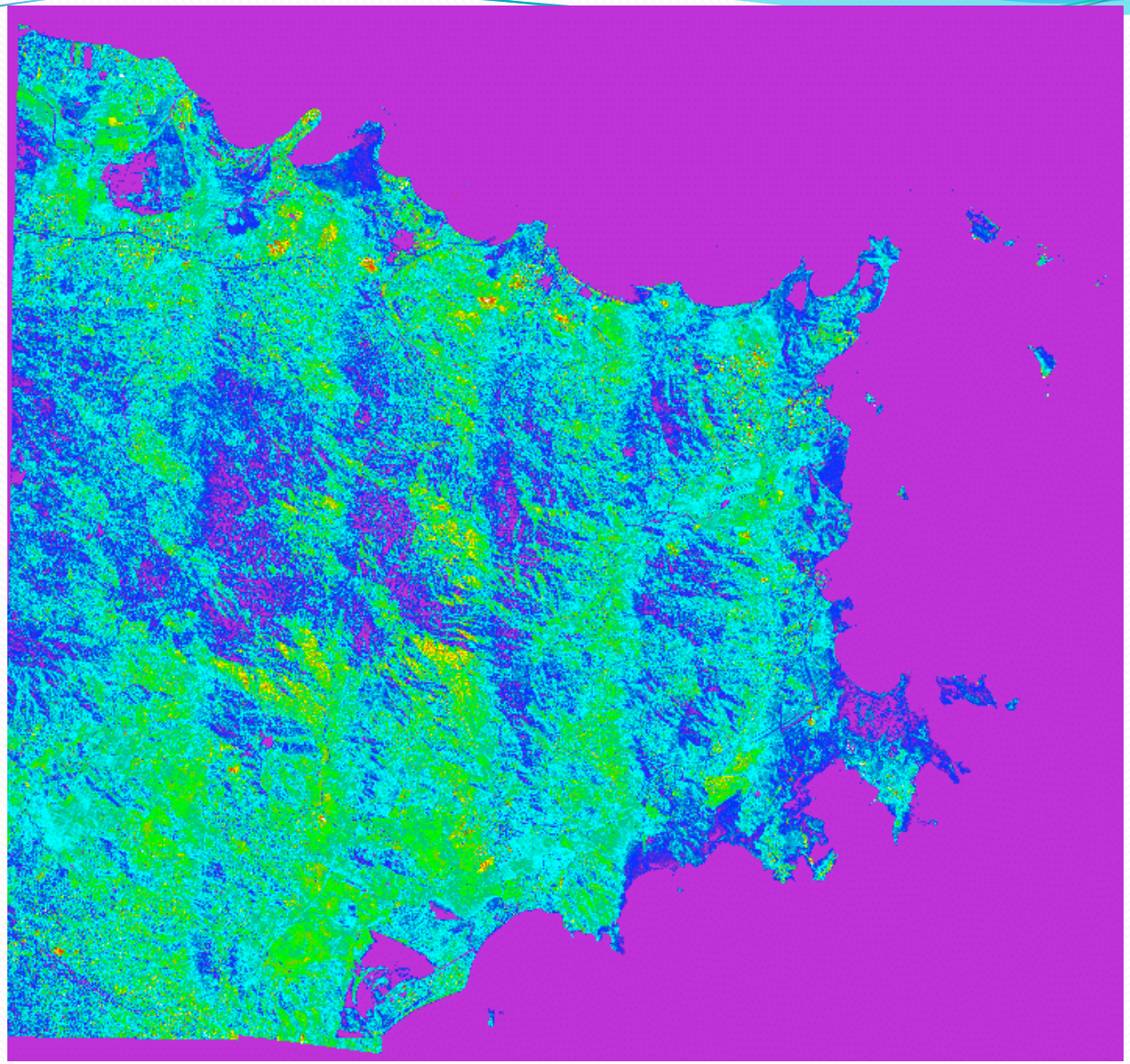

El Yunque F4 Mosaic Temperature

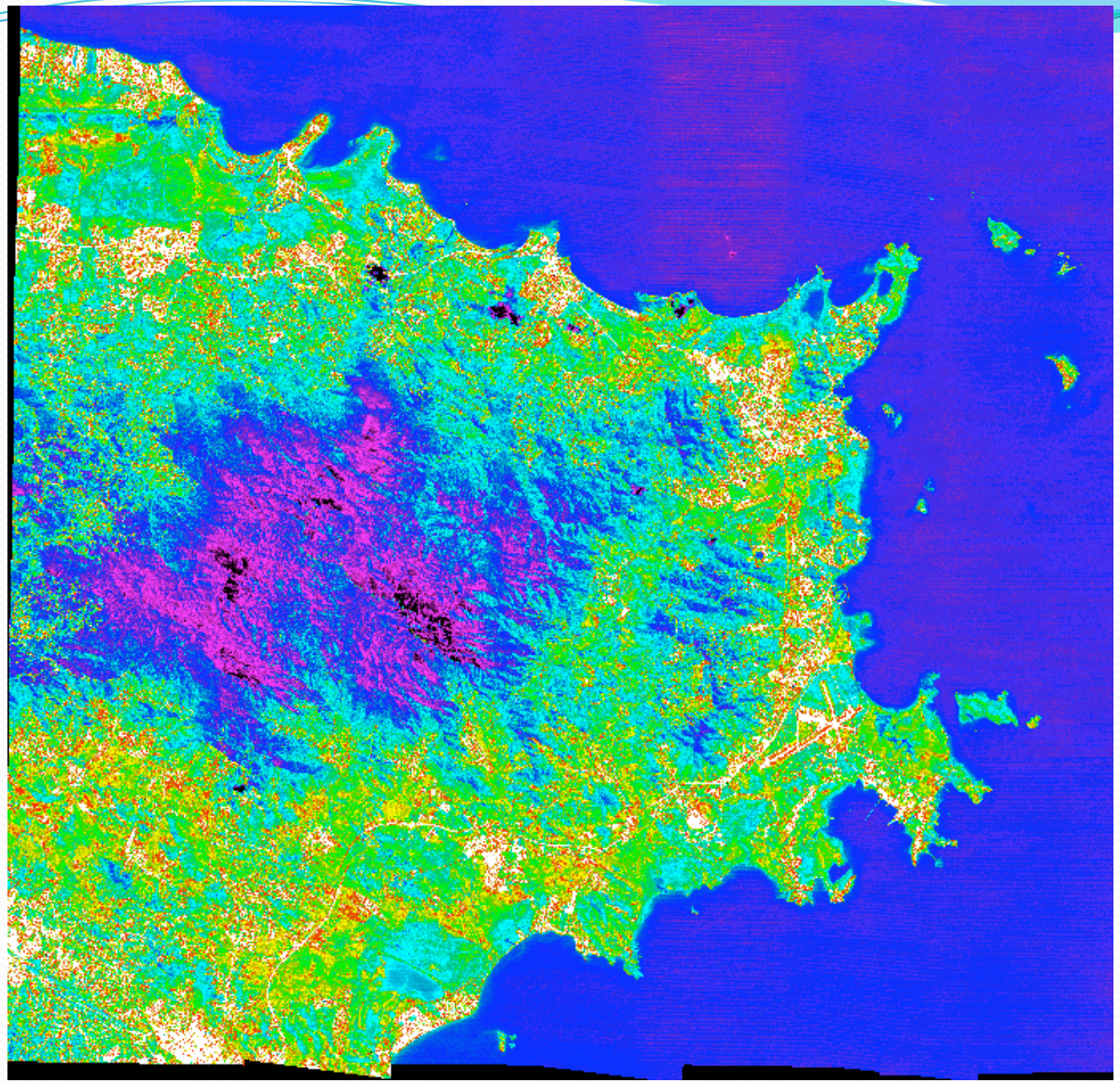

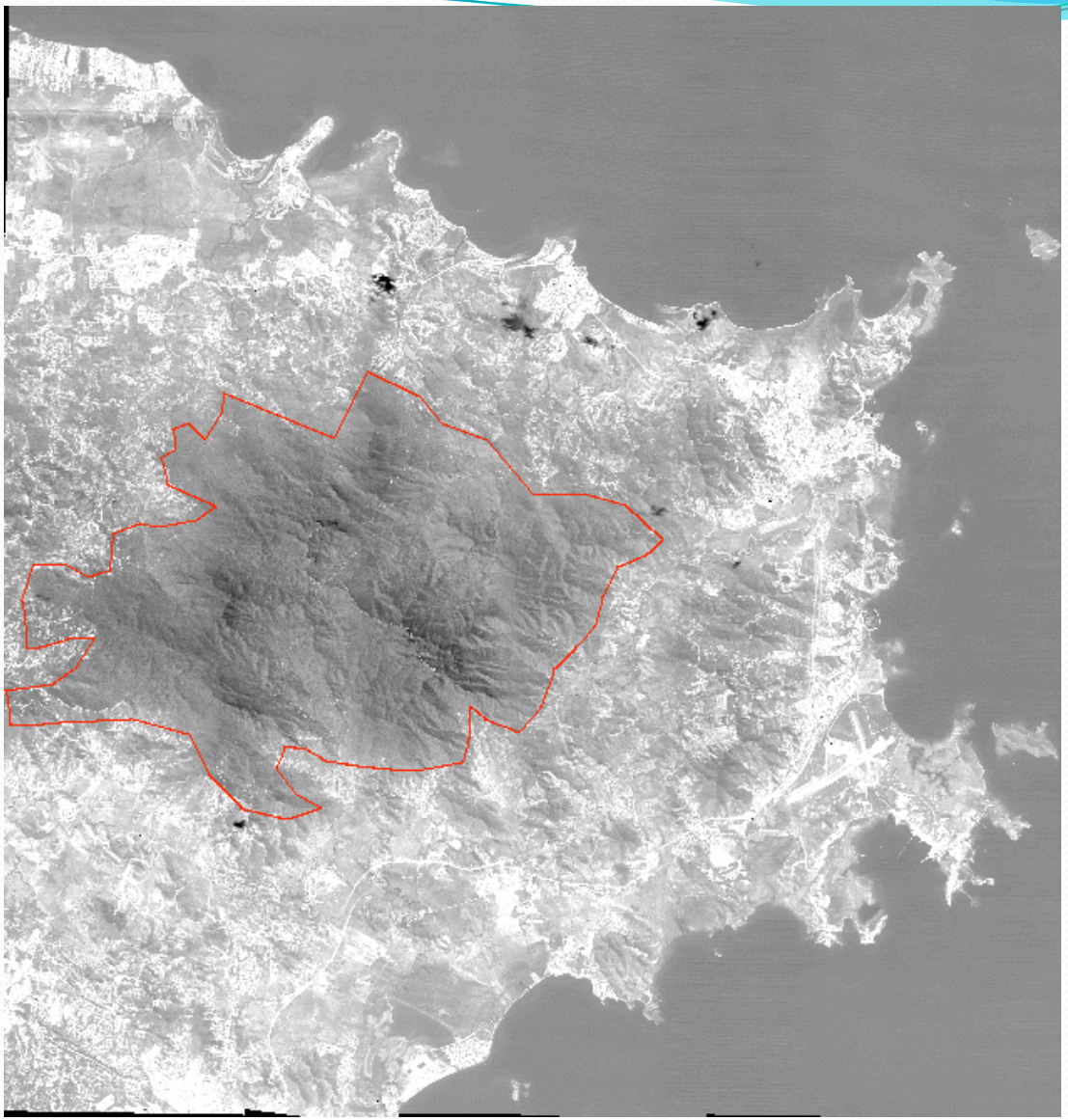

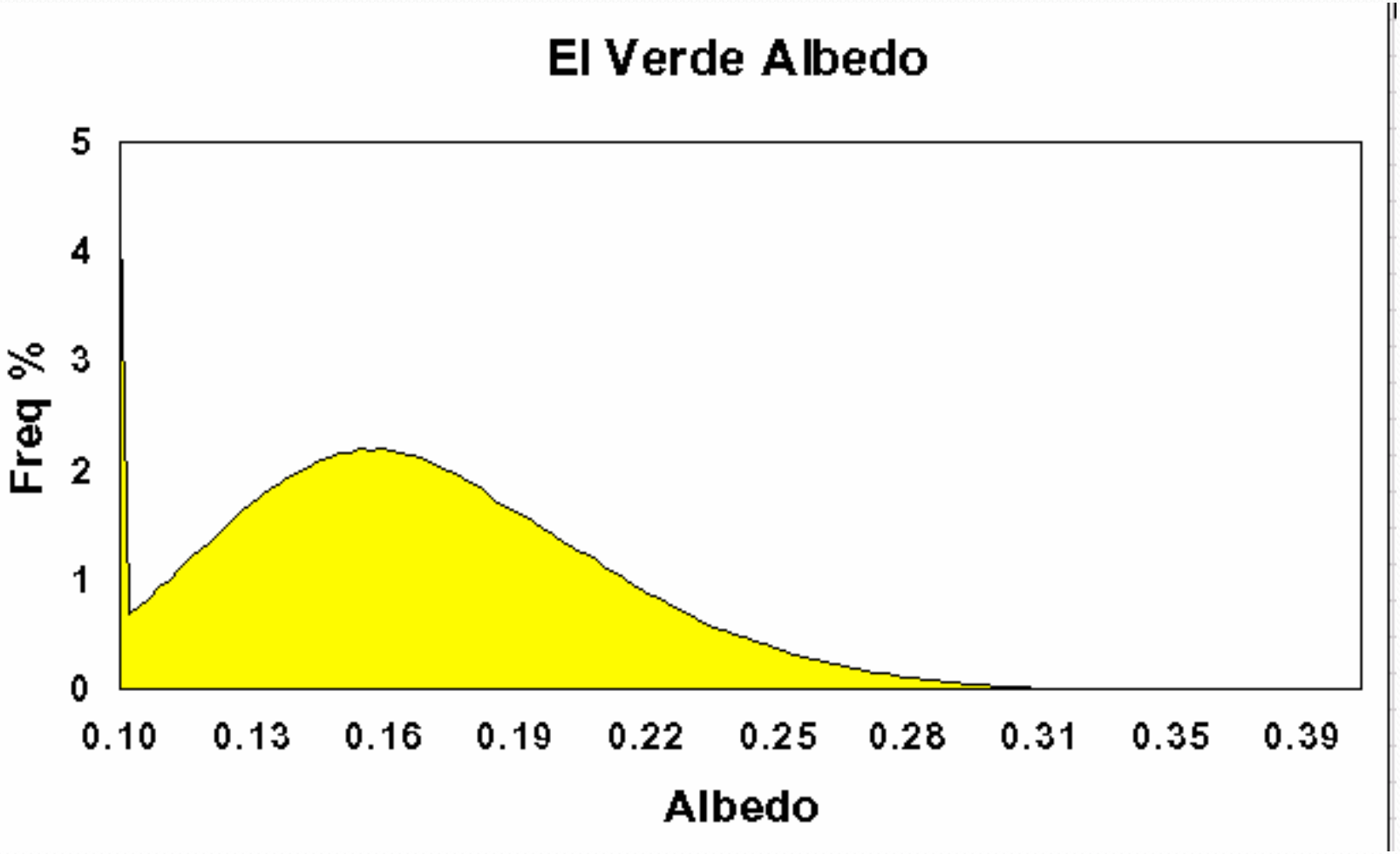
El Verde Albedo
Freq %
5
4
3
2
1
0
0.10
0.13
0.16
0.19
0.22
0.25
0.28
0.31
0.35
0.39
Albedo

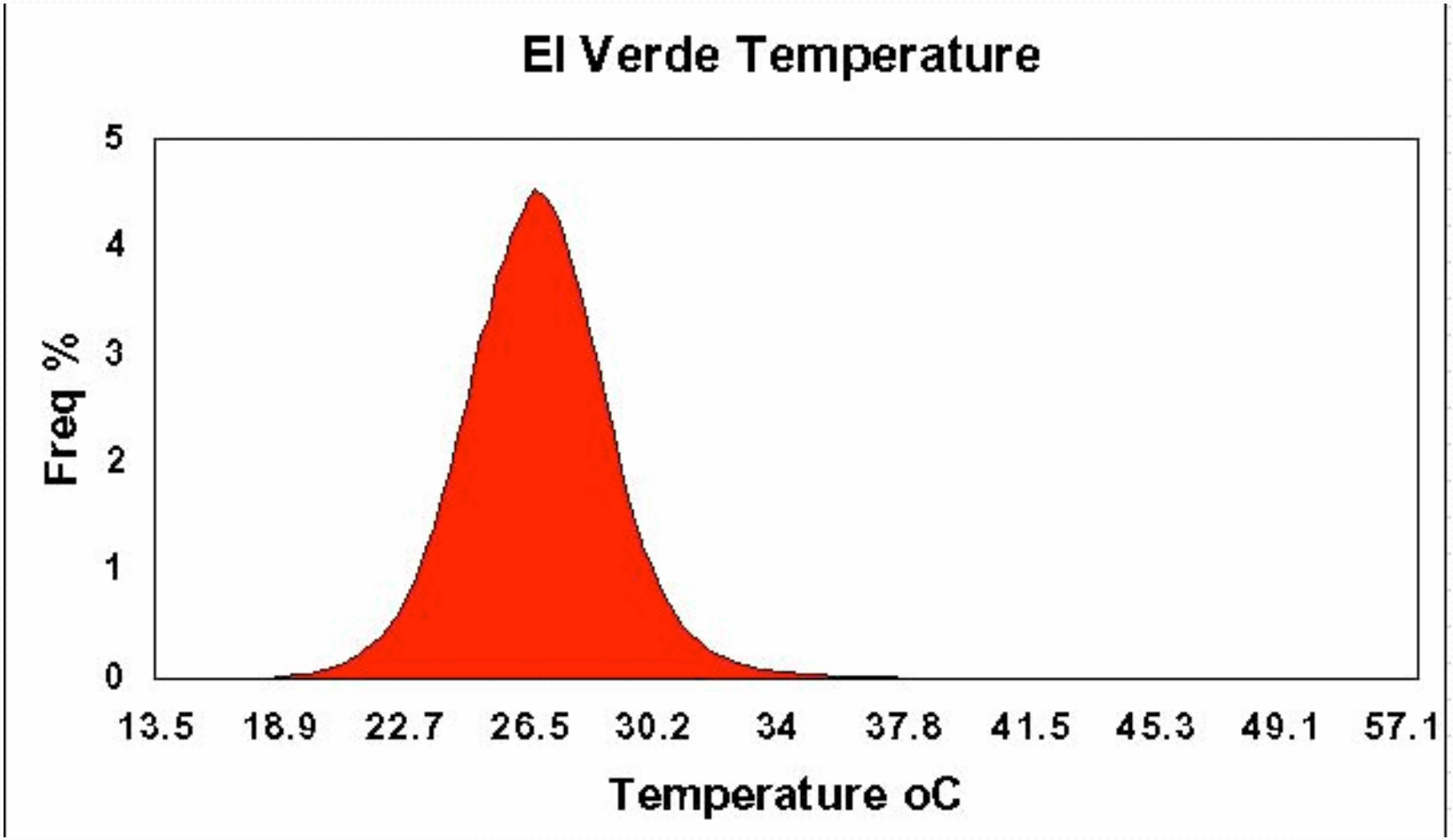
El Verde Temperature
Freq %
5
4
3
2
1
0
13.5
18.9
22.7
26.5
30.2
34
37.8
41.5
45.3
49.1
57.1
Temperature oC

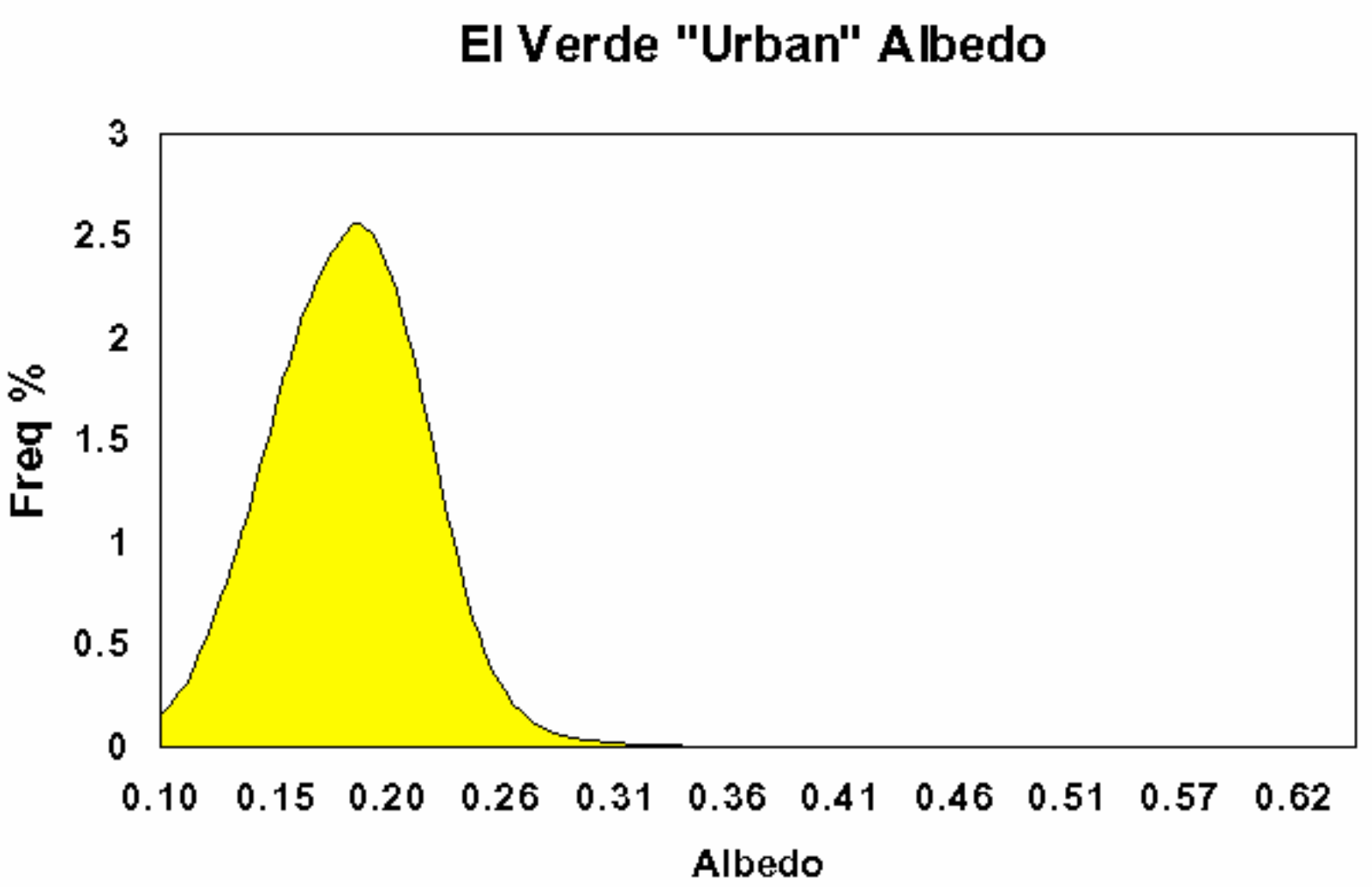
El Verde "Urban" Albedo
Freq %
3
2.5
2
1.5
1
0.5
0
0.10
0.15
0.20
0.26
0.31
0.36
0.41
0.46
0.51
0.57
0.62
Albedo

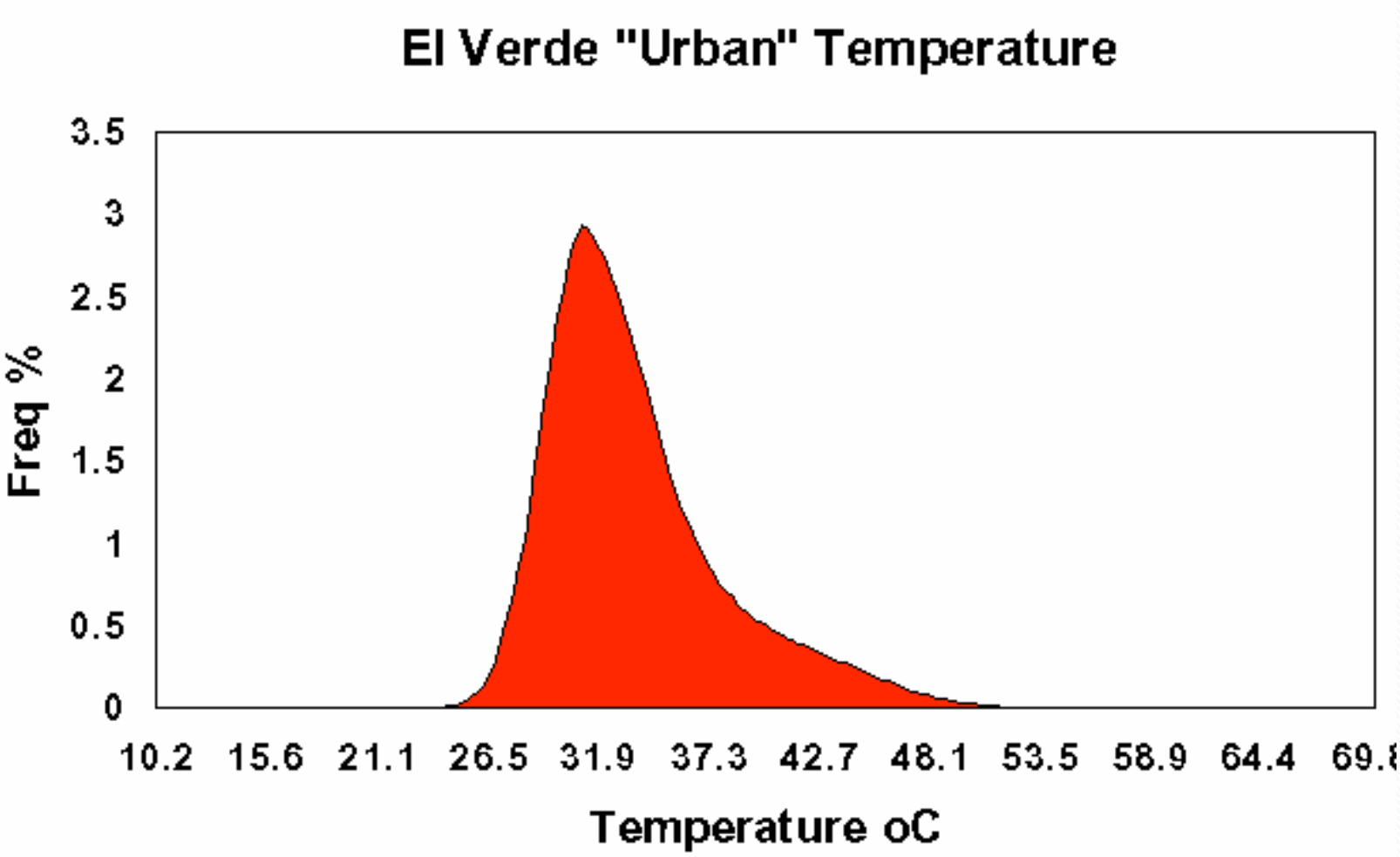
El Verde "Urban" Temperature
Freq %
3.5
3
2.5
2
1.5
1
0.5
0
10.2
15.6
21.1
26.5
31.9
37.3
42.7
48.1
53.5
58.9
64.4
Temperature oC

El Yunque
Albedo vs Temperature

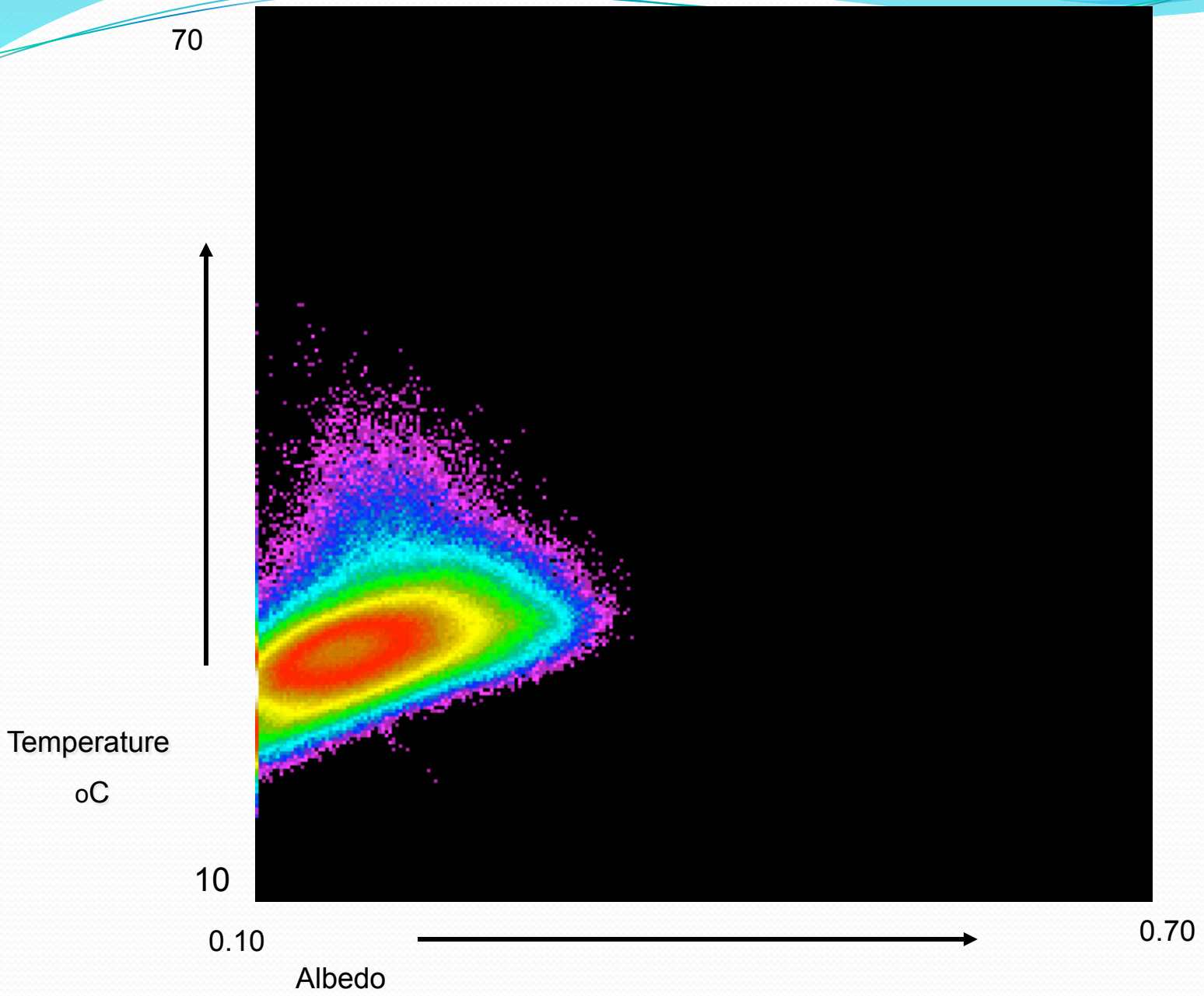

Urban Heat Island Mitigation Pilot Project

EPA/NASA Marshall Space Flight Center
Jeffrey C. Luvall
Dale Quattrochi
Maury Estes
Doug Rickman

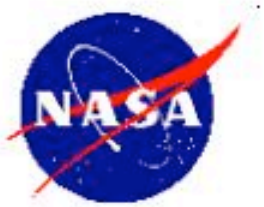

Urban Heat Island Mitigation Strategies

- Albedo Modification
  - Lighter colored roofs and pavements
  - New materials/coatings
- Plant trees and increase green space
  - Shade buildings, rooftops, parking lots and roads
  - Cool the air through transpiration
- Rooftop gardens
  - Keep roofs cool by shading and/or transpiration
  - storm water reduction

SMUD's Urban Heat Island mitigation efforts

- ✓ Increased Vegetation– SMUD's Shade Tree program (1990)
- ✓ Increased Roof's Albedo—SMUD's Cool Roof program (2001)
- ❑ Light colored pavements (i.e. Cool Parking Lots)– Sacramento Cool Community Project (1999)

SMUD Shade Tree Program

- started in 1990
- implemented in collaboration with the Sacramento Tree Foundation (STF)
- over 100,000 program participants
- approximately 300,000 trees planted
- annual budget over $1.5 million
- over $20 million invested since 1990
- received several national and state awards
- pay-for-performance contract with STF based on observed Present Value Benefits (PVB)

SMUD Shade Tree Program

Estimates of Savings for mature trees

- Average energy cooling load savings are 153 kWh/year/ per tree
- Average demand savings are 0.056 kW
- When 300,000 trees are mature = about 16 MW

SMUD Cool Roof Program

Program Objectives

- **Load Reduction-- reduce electricity peak demand and air conditioning energy load associated with high solar energy absorbed on the surface of roofs and rooftop ducts during the summer months**
- **Urban heat island effect mitigation**
- **Market Transformation-- expand the commercial retrofit and new construction roofing marketplace for highly reflective and emissive roof coatings and materials.**

SMUD
SACRAMENTO MUNICIPAL UTILITY DISTRICT
The Power To Do More.SM

SMUD Cool Roof Program

Estimates of Savings

- Average energy cooling load savings of 20%
- Average energy cooling load savings are 0.15 kWh/year/Sq.Ft.
- Average demand savings are 0.25 W/Sq.Ft.

Sacramento Skattergrams
Albedo vs Temperature

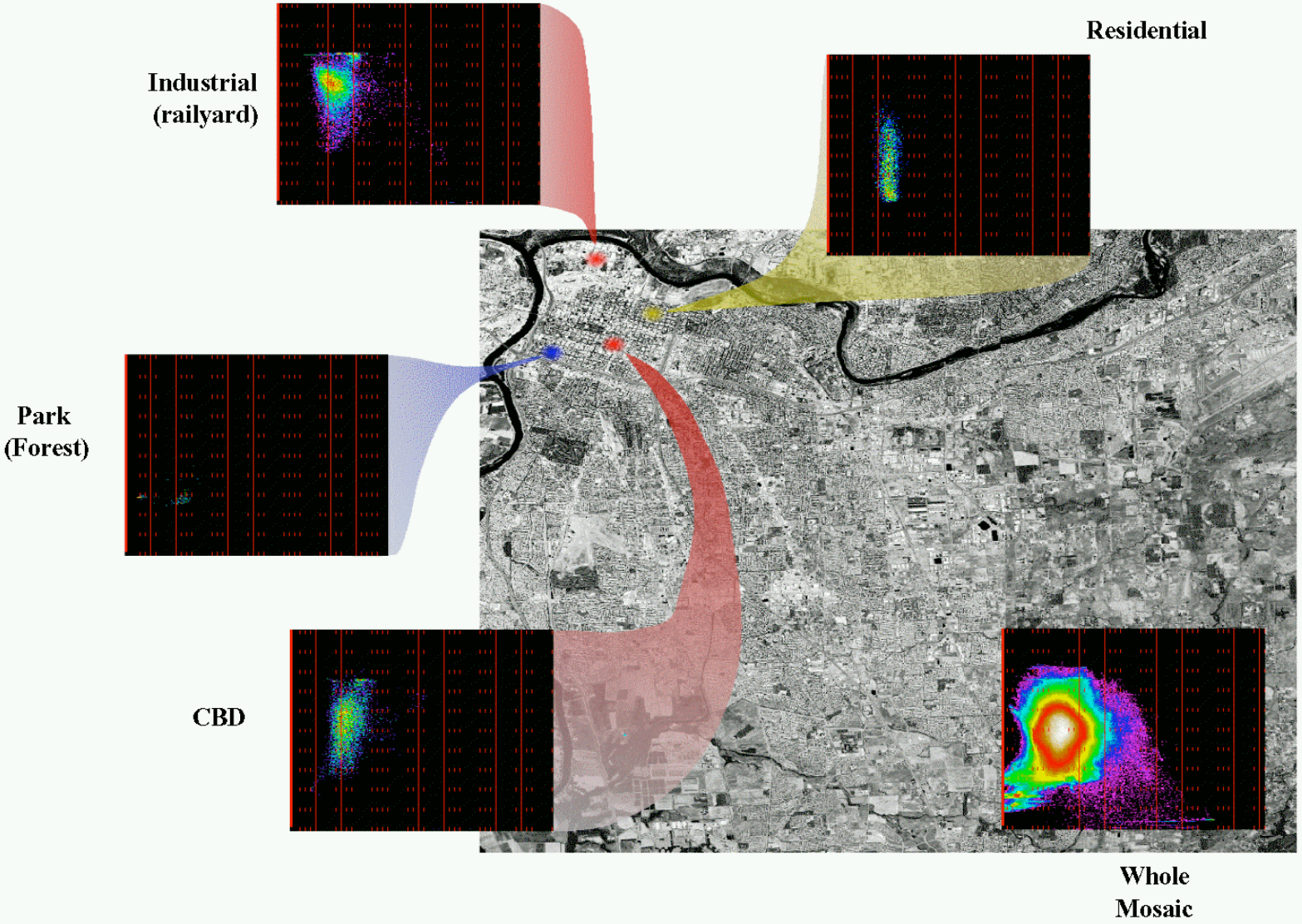

Spatial Growth Models

- Empirical
  - statistically matching temporal trends and/or spatial patterns with a set of predictor variables
- Dynamic Process
  - Interactions between agents/organisms and environment (Cellular Automata, SLEUTH)
  - Cells can represent parcels of land with unique characteristics and each changing as a result of rules on both the cell's state and state of neighbors
- Agent-based
  - Micro-scale behaviors of individuals (farmers, ranchers, etc.) or institutions (industries, gov't, etc. with feedback loops (Research)

Surface Temperature by Land Use Class

Based on ATLAS aircraft data, May 1997

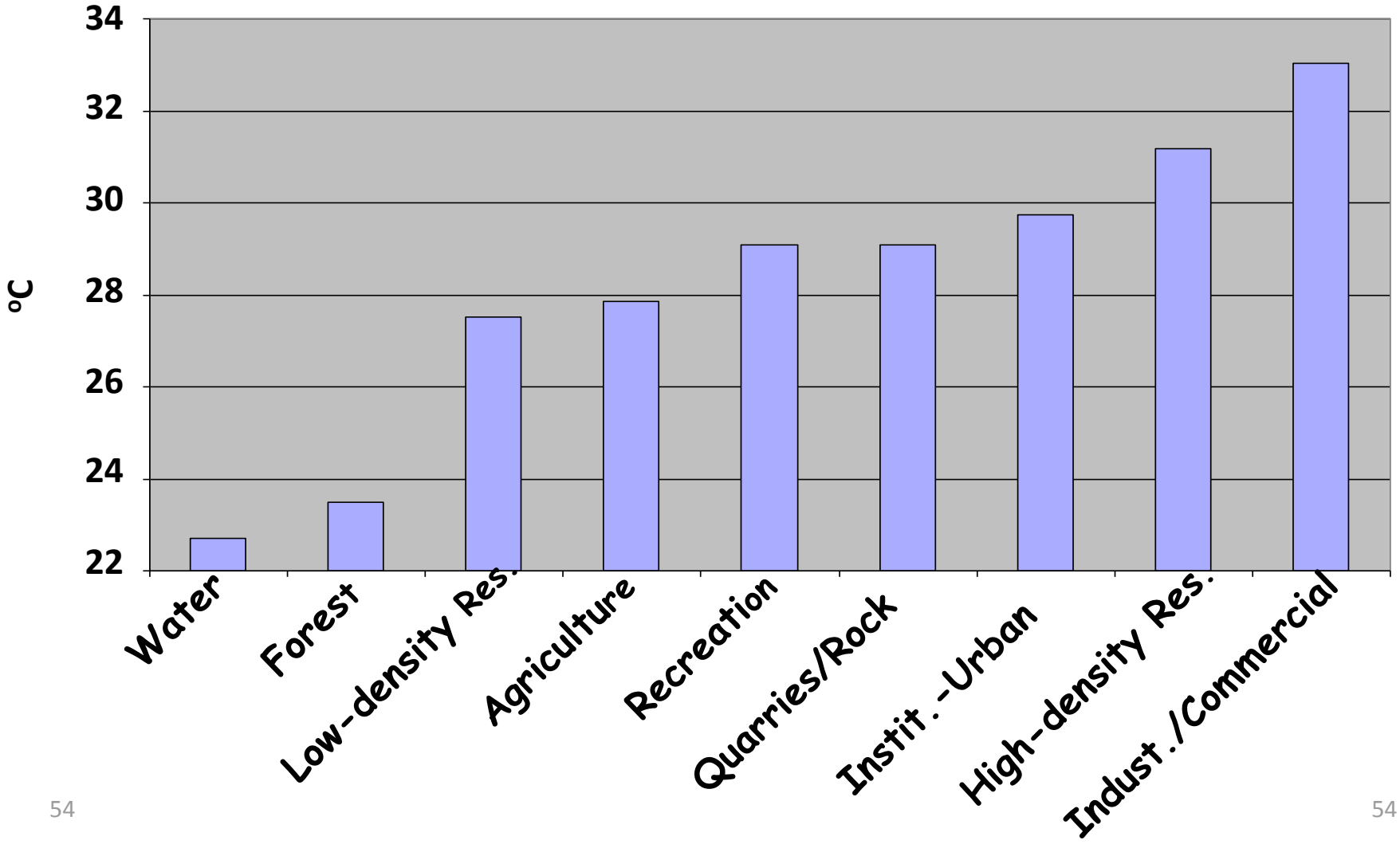

54

Problem description

- Istanbul is the largest city in turkey
  - Population 11 million
- Traffic congestion:
  - 600 cars enter the system every day
- Infrastructure project under consideration includes construction of **a third bridge** across the Bosporus, north of the city
  - How would the proposed infrastructure project affect the ecologically sensitive area located in the north?
  - Answer needed in days!!
  - This project is the **first step** towards a DSS that would provide an answer to such questions

Istanbul, Turkey
Ataturk Airport
20.2 km
Image © 2008 DigitalGlobe
Image © 2008 TerraMetrics
©2008 Google™

Fatih Sultan Mehmet Bridge
Istanbul, Turkey
3.87 km
Image © 2008 DigitalGlobe
© 2006 Google

1986 LandSat Image

Land Processes Research Application Team, NASA Marshall Space Flight Center, Huntsville, AL

2007 LandSat Image

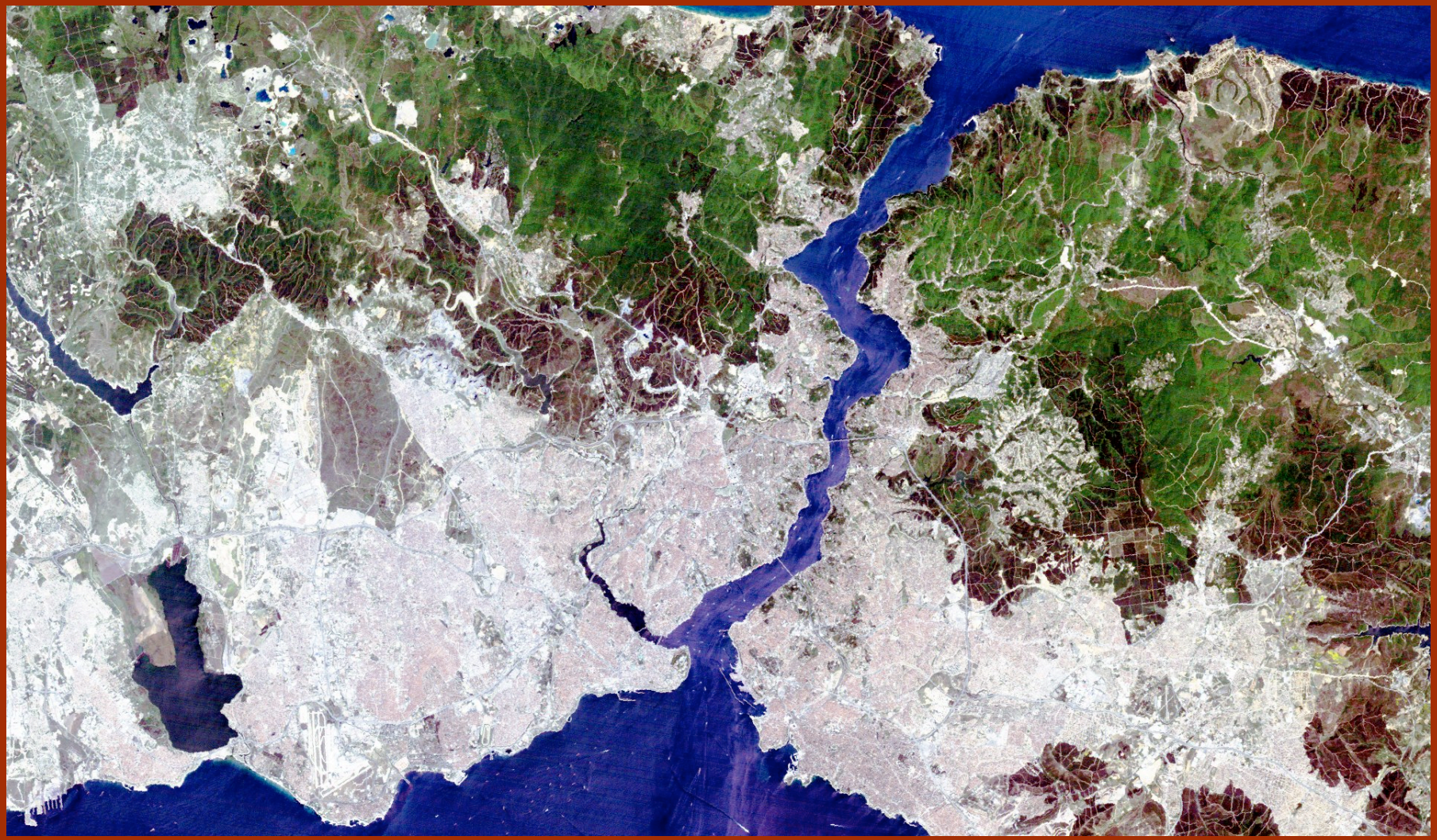

Land Processes Research Application Team, NASA Marshall Space Flight Center, Huntsville, AL

1986 Land Use

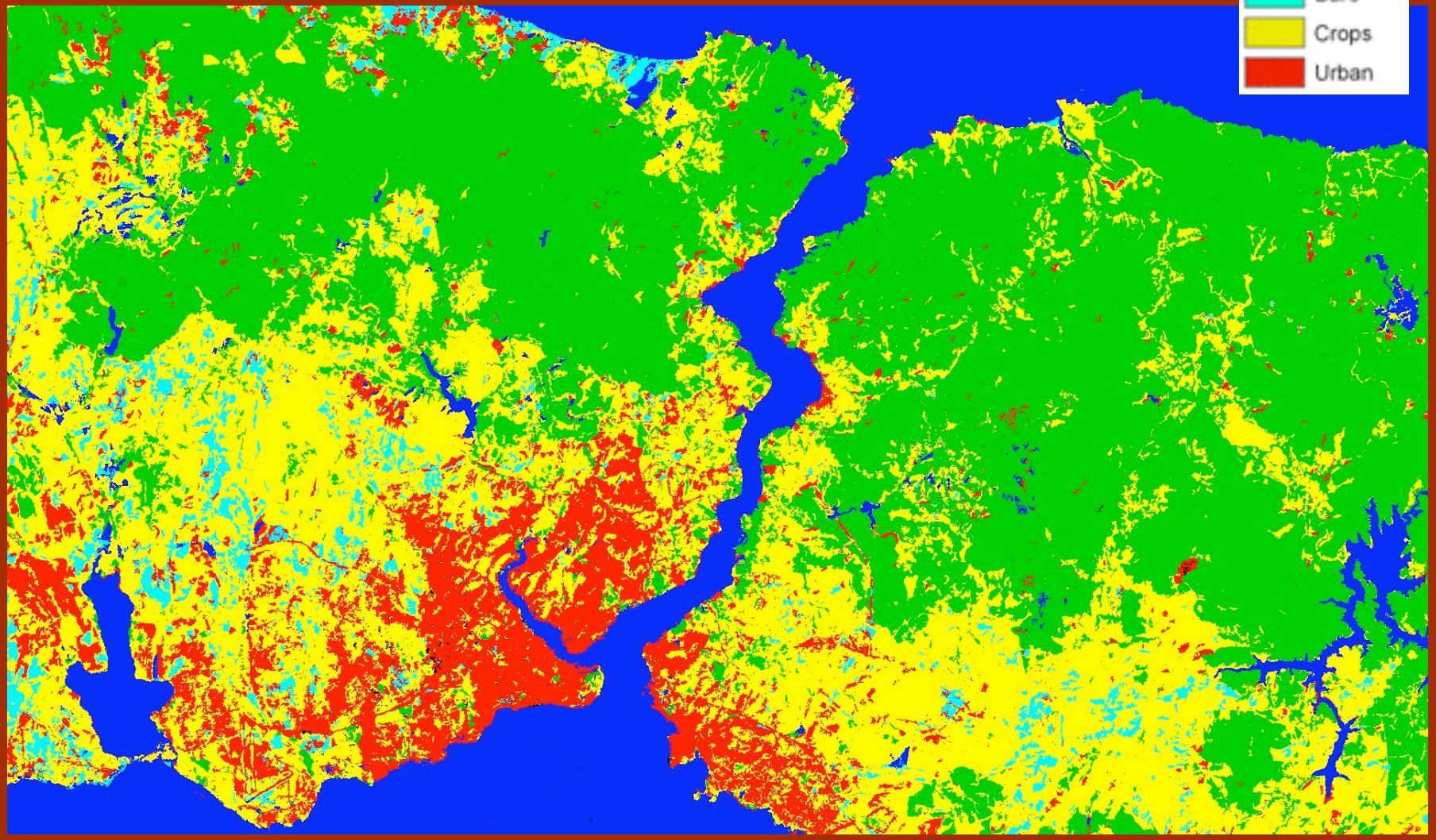

2007 Land Use

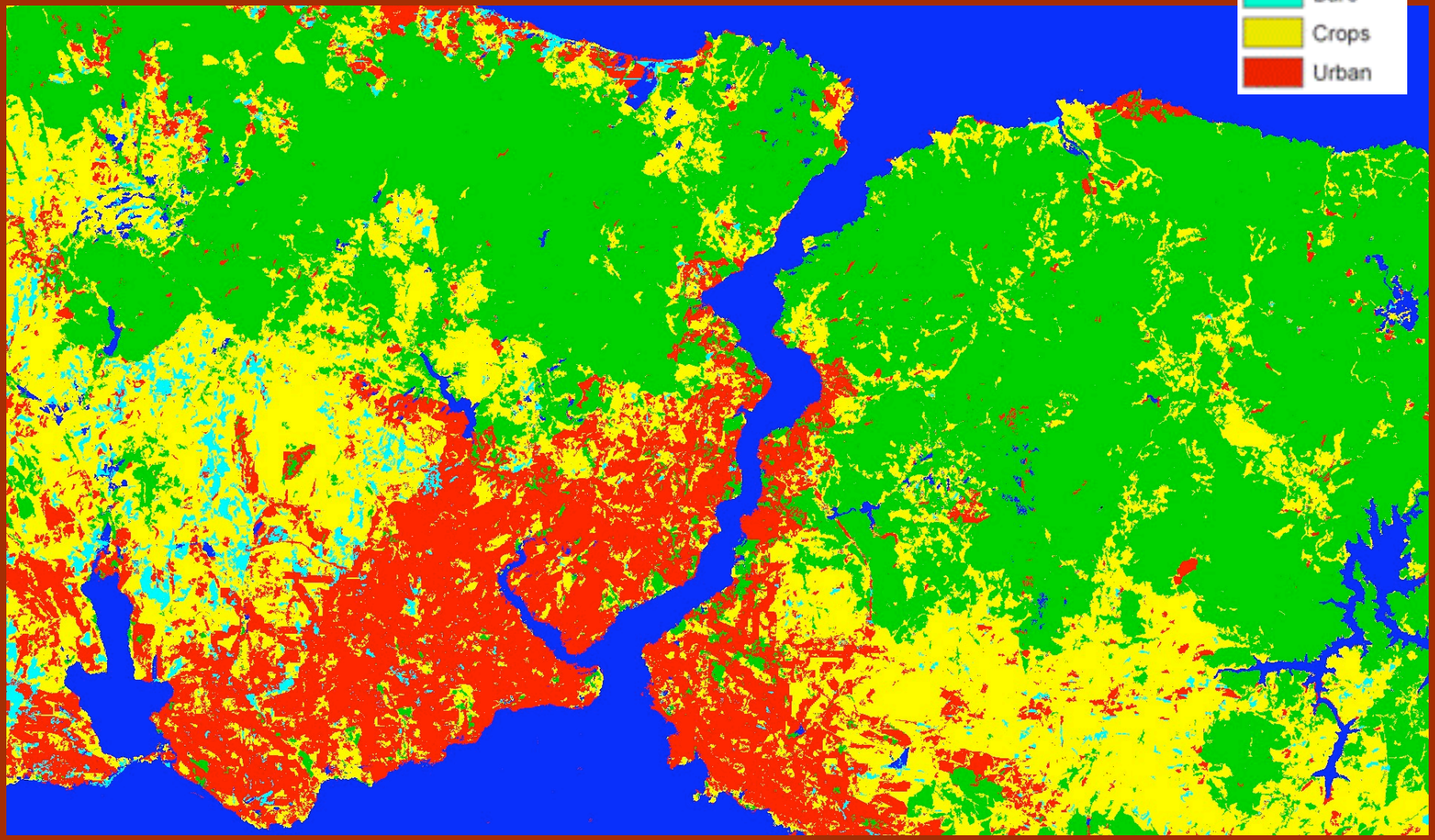

LULC statistics for Istanbul

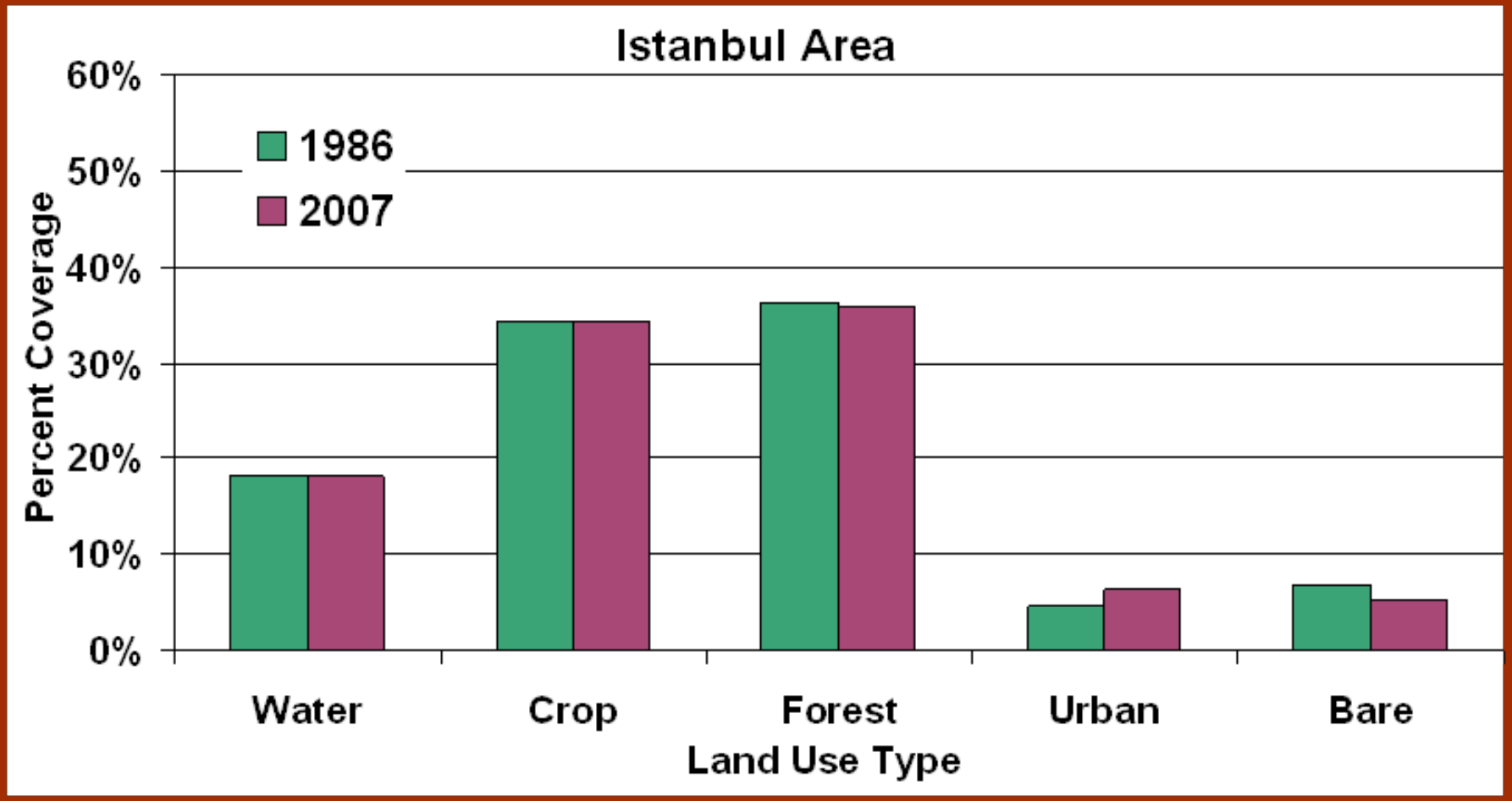

Land Processes Research and Applications Team, NASA Marshall Space Flight Center, Huntsville, AL

1986 Land Use – Bridge Area

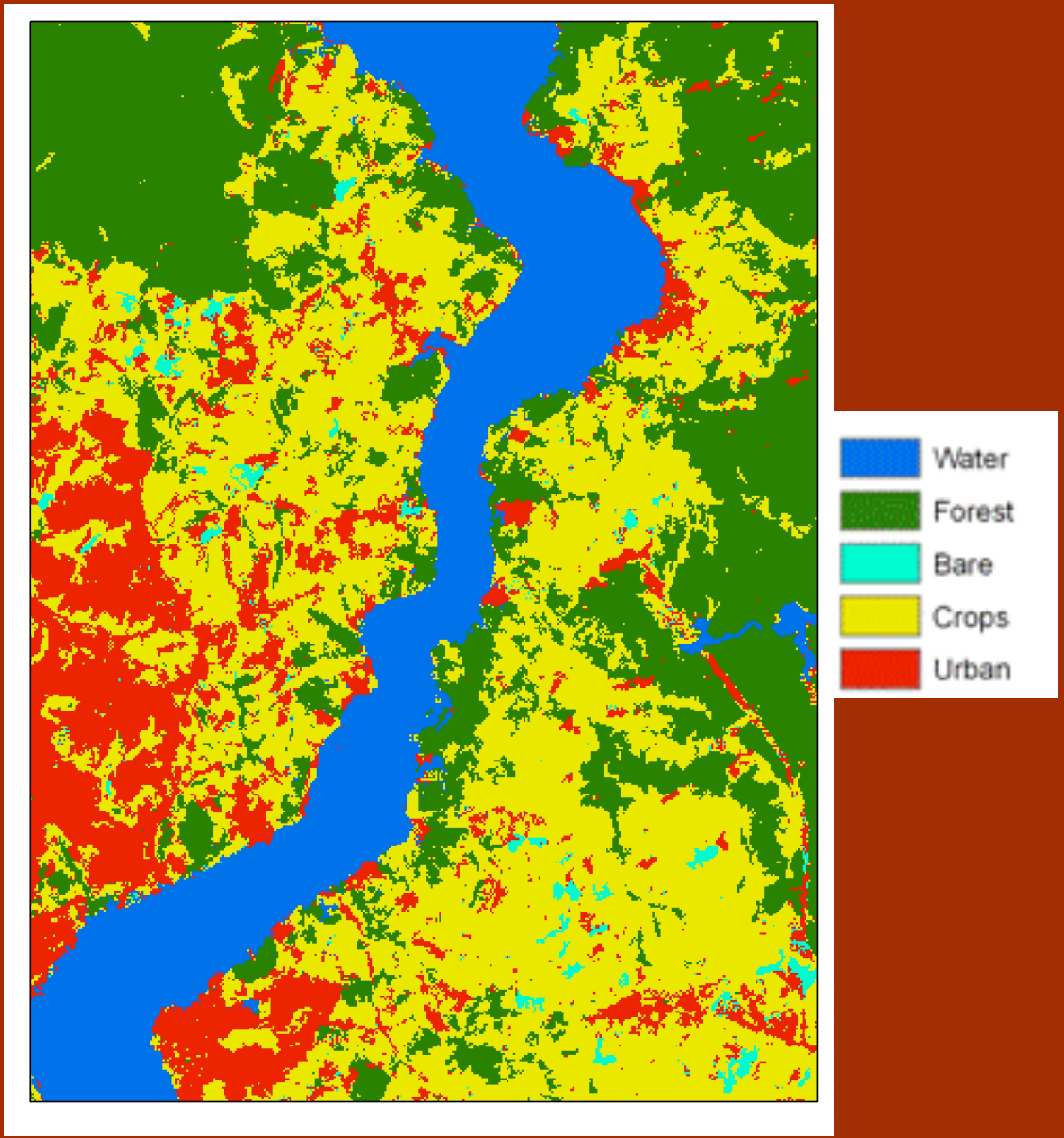

Land Processes Research and Applications Team, NASA Marshall Space Flight Center, Huntsville, AL

2007 Land Use – Bridge Area

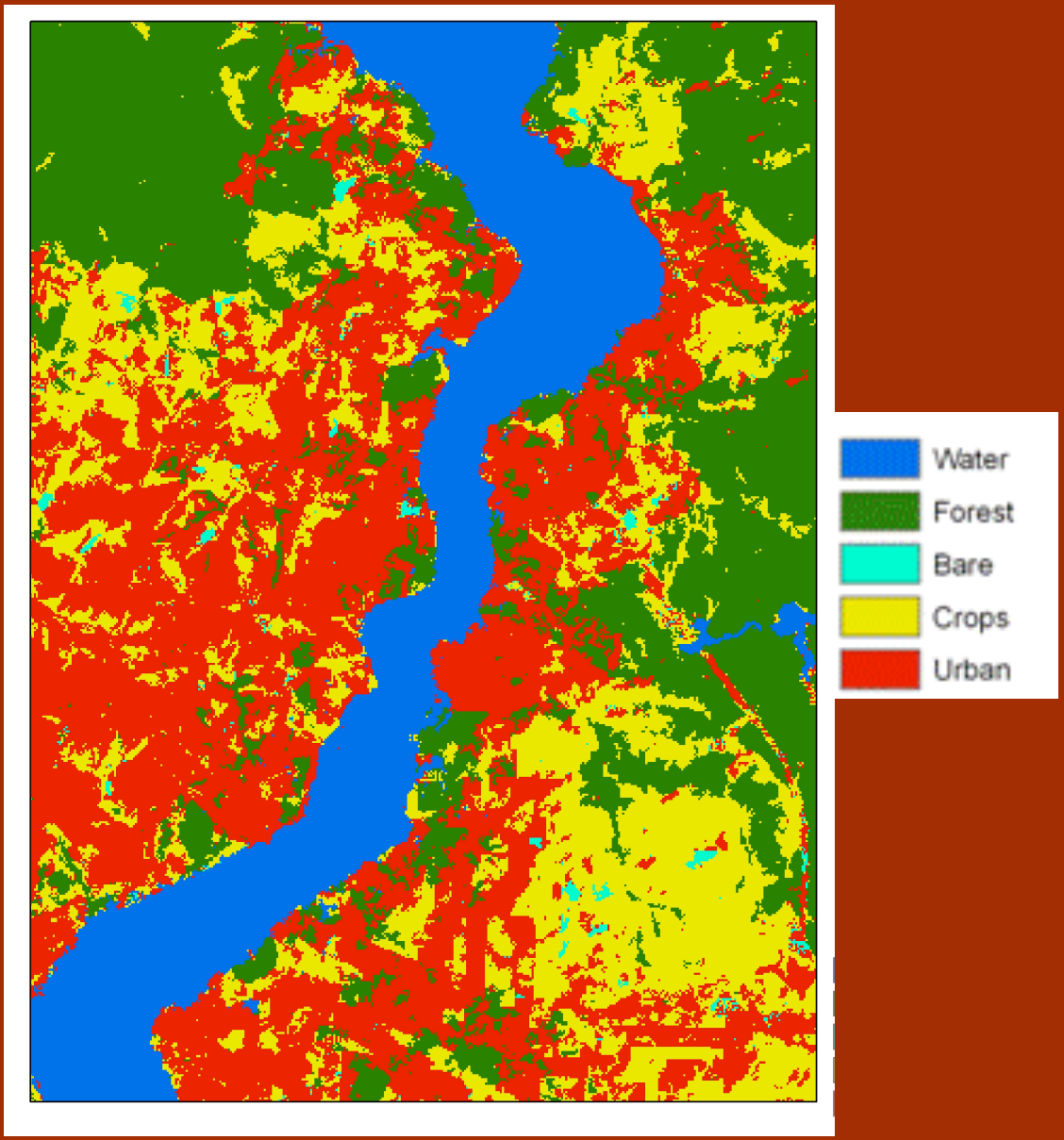

Land Processes Research and Applications Team, NASA Marshall Space Flight Center, Huntsville, AL

LULC statistics around the bridge

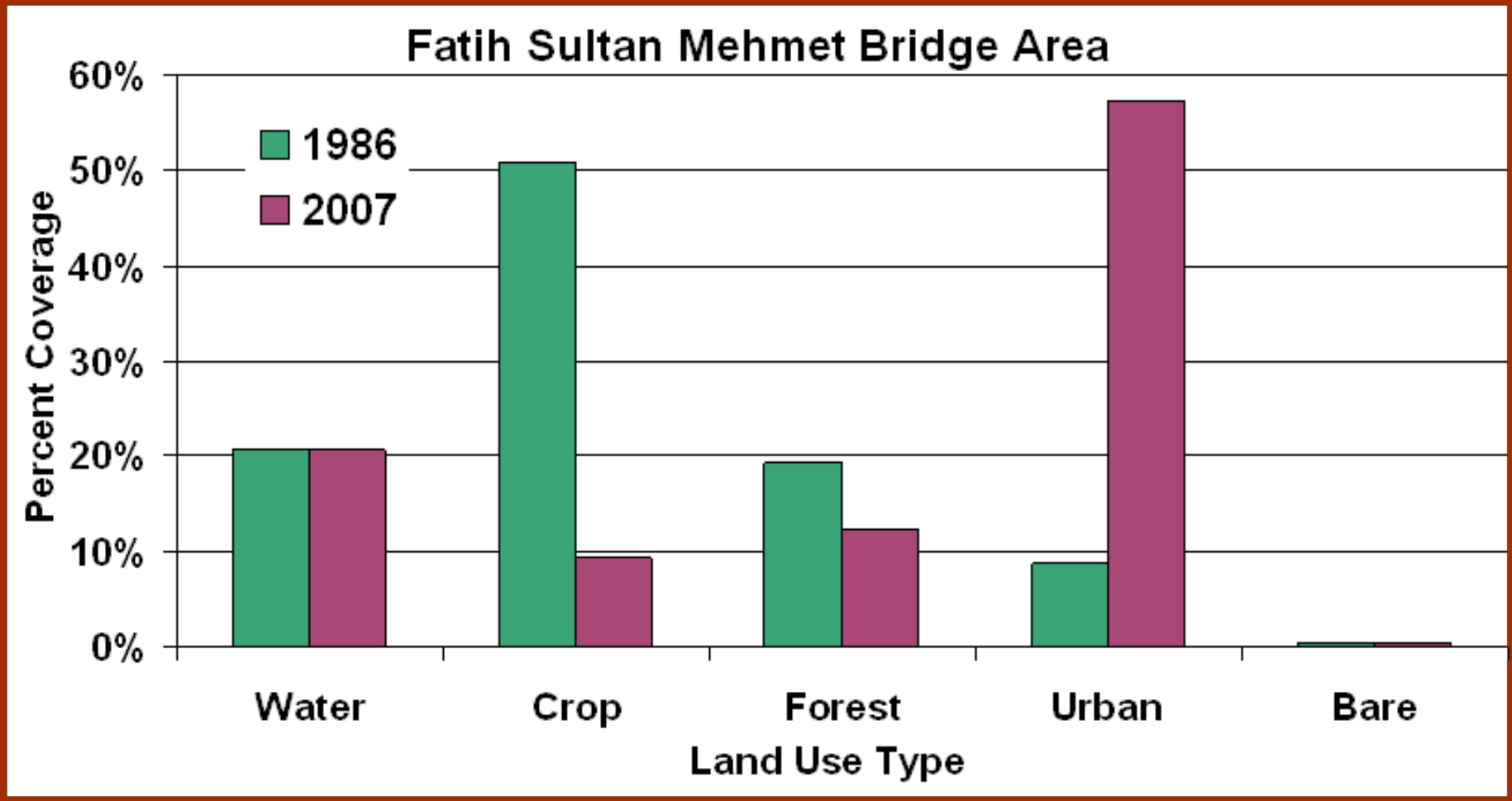

Land Processes Research and Applications Team, NASA Marshall Space Flight Center, Huntsville, AL

LST as a function of LULC and season

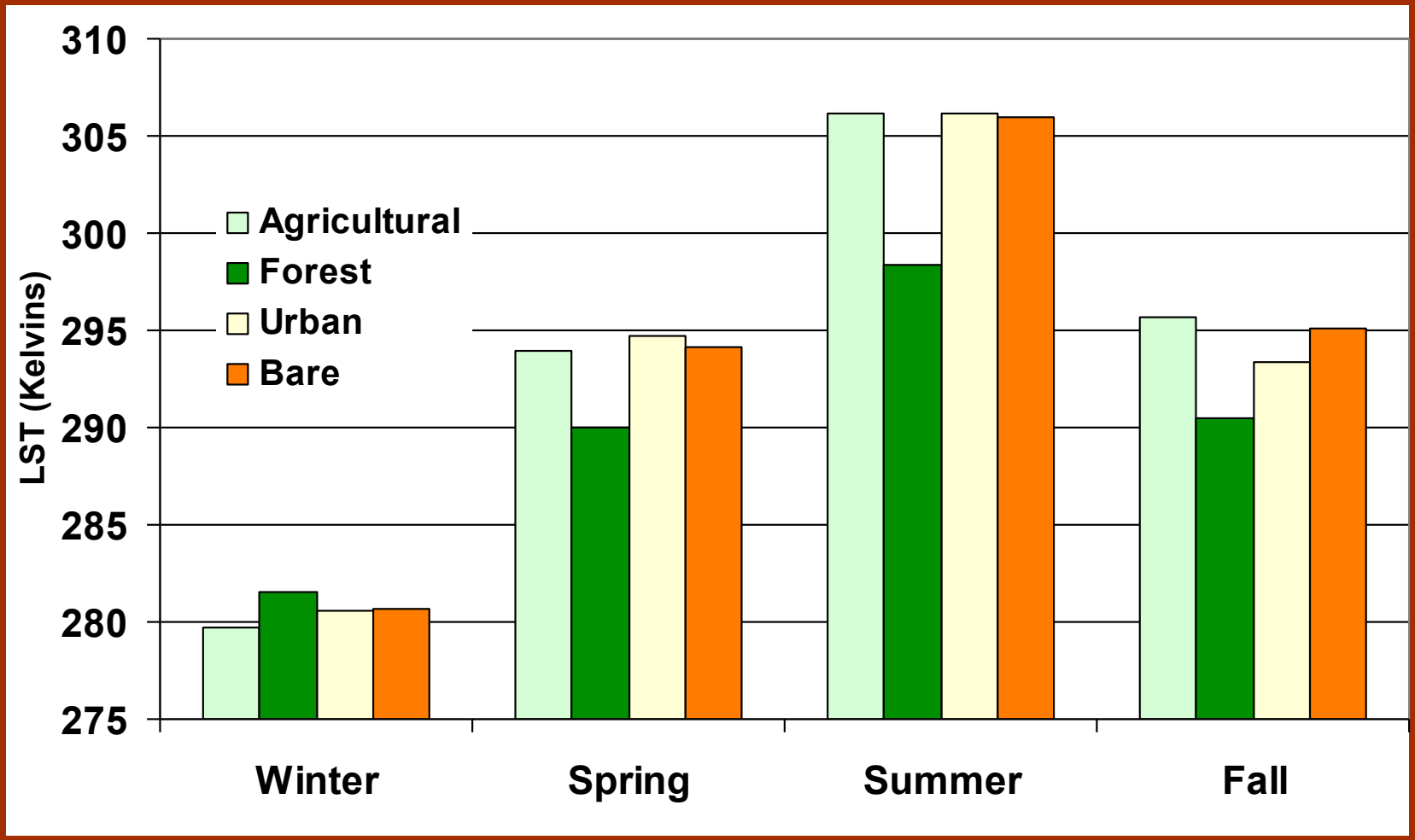

Mean land surface temperature by season and land use type, from all Aqua and Terra MODIS observations, 2003-2006.

Land Processes Research and Applications Team, NASA Marshall Space Flight Center, Huntsville, AL

LST differences due to urbanization, 1986-2007

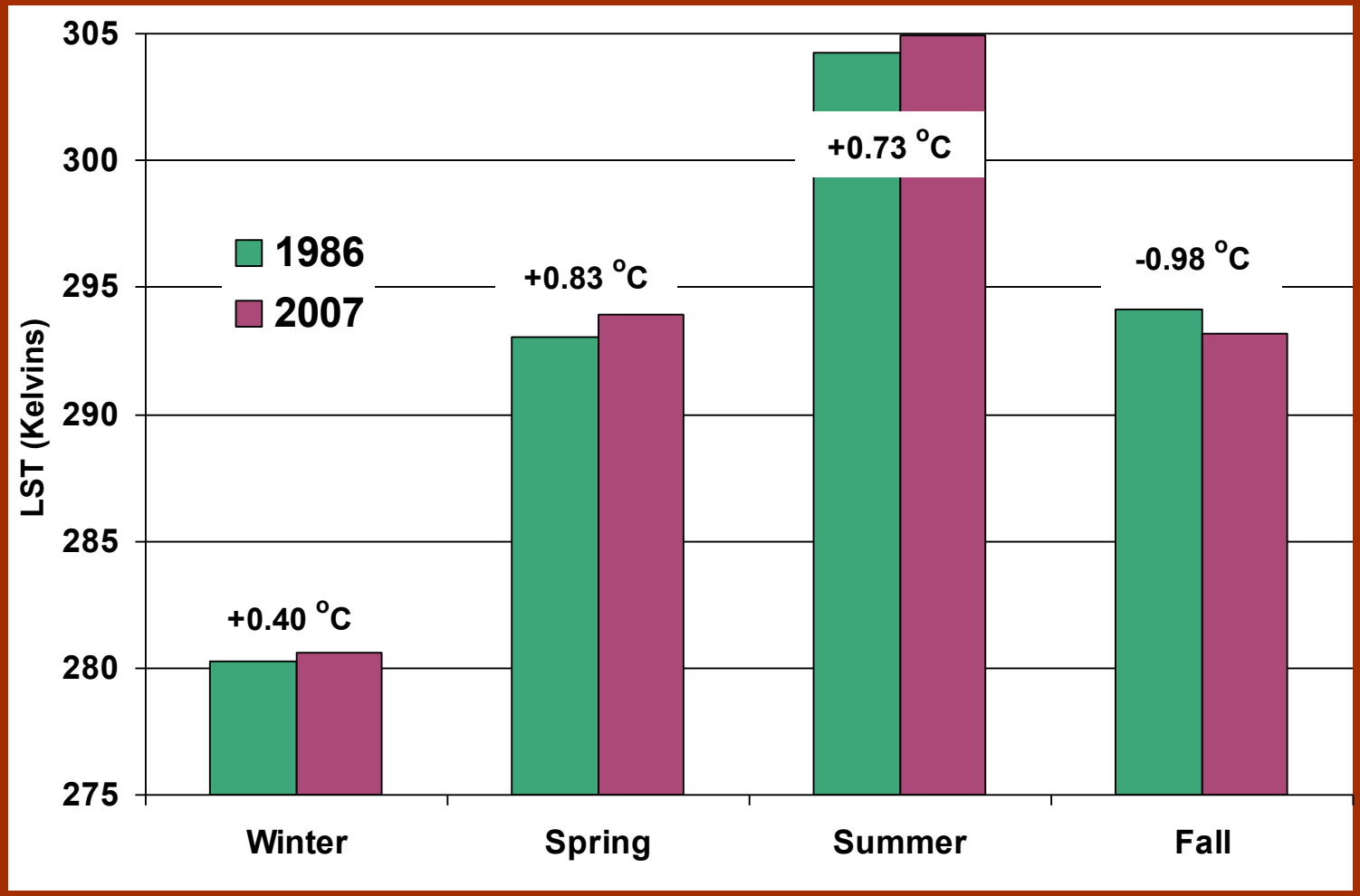

Inferred relative differences in seasonal LST attributed to LULC changes in vicinity of the second bridge between 1986 and 2007.
2007 LST based on 2003-2006 mean MODIS LST for each LULC type and 2007 Landsat LULC.
1986 LST estimated from the different proportions of LULC from the 1986 Landsat LULC.

Land Processes Research and Applications Team, NASA Marshall Space Flight Center, Huntsville, AL

Modeled 2-m air temperature Bridge Area

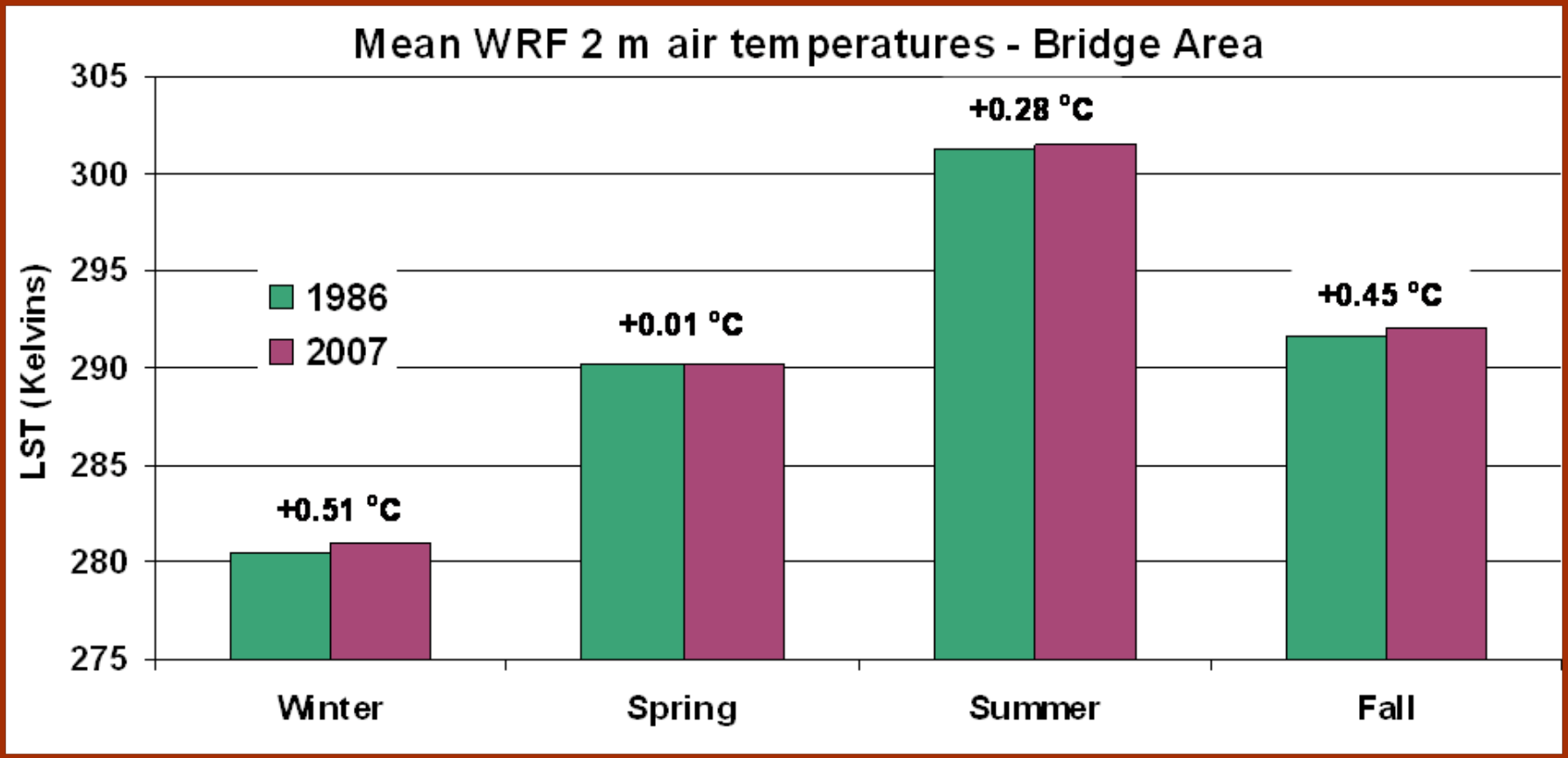

What can HysplRI dsata provide for urban heat island research and applications ?

- Scale consistance with complex urban surfaces
- Well calibrated data allows quantifiable radiative & energy budgets:
  - Analysis of albedo
  - Analysis of surface temperature
  - Analysis of emissivity
- Scale consistant to plan alteration of the urban fabric to mitigate the urban heat island
- Swath width scale for urban climatiolgy studies - urbanization of RAMS.
- Global cities.
- Only mutispectral thermal at 60 m
- 5 day repeat for thermal for short & long term trend analysis
- Allow for functional classification of urban surfaces

Mineral Mapping Using Simulated HysplRI Data

Partially Sponsored by NASA Grant NNX10AF99G
(HyspIRI Preparatory Research Activities)

F. A. Kruse, Research Professor
Department of Physics and Remote Sensing Center
Naval Postgraduate School, Monterey, CA 93943

Acknowledgments

- **Portions of this research were supported by:**
  - **The Arthur Brant Laboratory for Exploration Geophysics at the University of Nevada, Reno**
  - **The Remote Sensing Center at the Naval Postgraduate School**
- **Research contributions by M. Coolbaugh, J. V. Taranik, W. M. Calvin, E. Littlefield, and J. Michaels, B. Martini (Ormat, Reno, NV)**

Presentation Summary

- Objectives
- Introduction to Geothermal/Hydrothermal Systems
- Mineral Spectroscopy
- Temperature Mapping Example
- Simulation Approach and Methods
- Selected Results
- Summary and Conclusions

HysplRI Precursor Project Objectives

Generate HysplRI-like remote sensing datasets from existing NASA HSI and MSI remote sensing data

1. **Airborne Visible Infrared Imaging Spectrometer (AVIRIS) for HysplRI VSWIR simulations**
   - **Original Data: 0.38 – 2.52 μm, 224 spectral bands, 10nm spectral resolution, various spatial resolutions**
   - **Simulated Data: 0.4 – 2.5 μm, 213 spectral bands, ~10nm spectral resolution, 60m spatial resolution**
2. **MODIS/ASTER Airborne Simulator (MASTER) for HysplRI TIR simulations**
   - **Original Data, 50 bands 0.4 – 12.9 μm, various spatial resolutions (~3 to 35m)**
   - **Simulated Data: 7 bands 7.3 – 12.03 μm per response curves, 60m spatial resolution**

HysplRI Precursor Project Objectives

Evaluate HysplRI-simulated data's capabilities to:

1. Identify, characterize, and map mineral assemblages associated with surface exposures of active and fossil hydrothermal systems
2. Measure surface temperatures and temperature variability associated with active geothermal systems
3. Detect, characterize, and monitor surface changes associated with geothermal resources

F. A. Kruse ♦ 303-499-9471 ♦ fakruse@nps.edu ♦http://www.nps.edu/Academics/Centers/RemoteSensing

Geothermal (hydrothermal) Systems

Fossil Hydrothermal System

F. A. Kruse ♦ 303-499-9471 ♦ fakruse@nps.edu ♦http://www.nps.edu/Academics/Centers/RemoteSensing

Why Remote Sensing of Hydrothermal/Geothermal Systems?

- **High beneficial impact: Ore deposits provide raw materials for industrialized society, while geothermal systems provide abundant energy without many of the problems of fossil fuels**
- **These two are highly related. Surface mineral assemblages and distributions often provide key information about their origin and nature. Many minerals associated with these systems can be mapped using remote sensing**
- **For geothermal systems, surface temperature also provides clues to underlying processes**

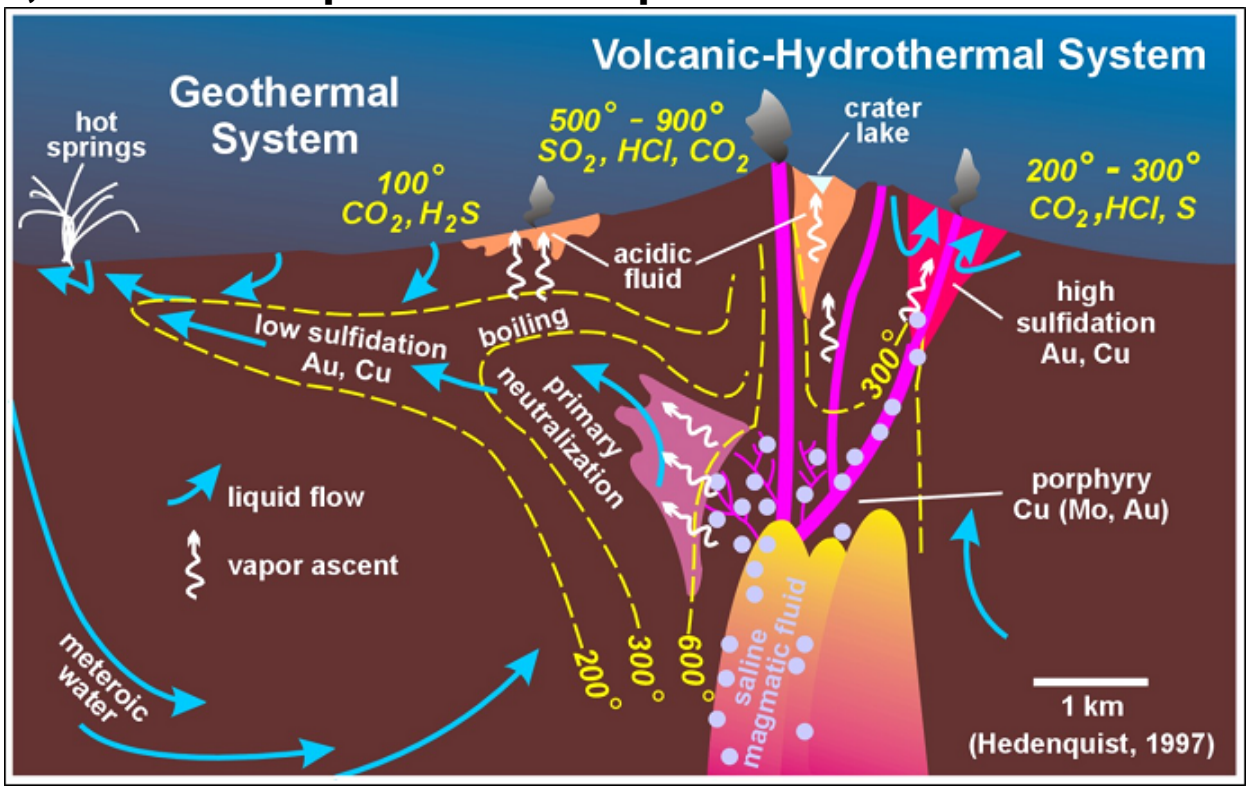

- **VNIR/SWIR spectrometry has clearly demonstrated its capability to identify minerals based on molecular physics**
- **LWIR spectrometry has unique capabilities based on fundamental molecular vibrations**

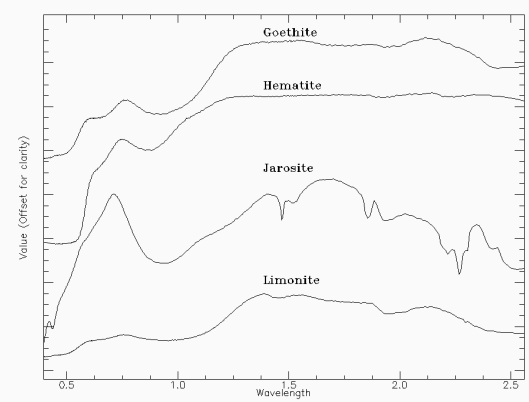

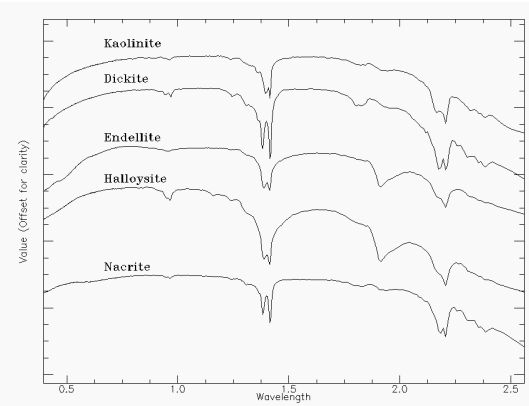

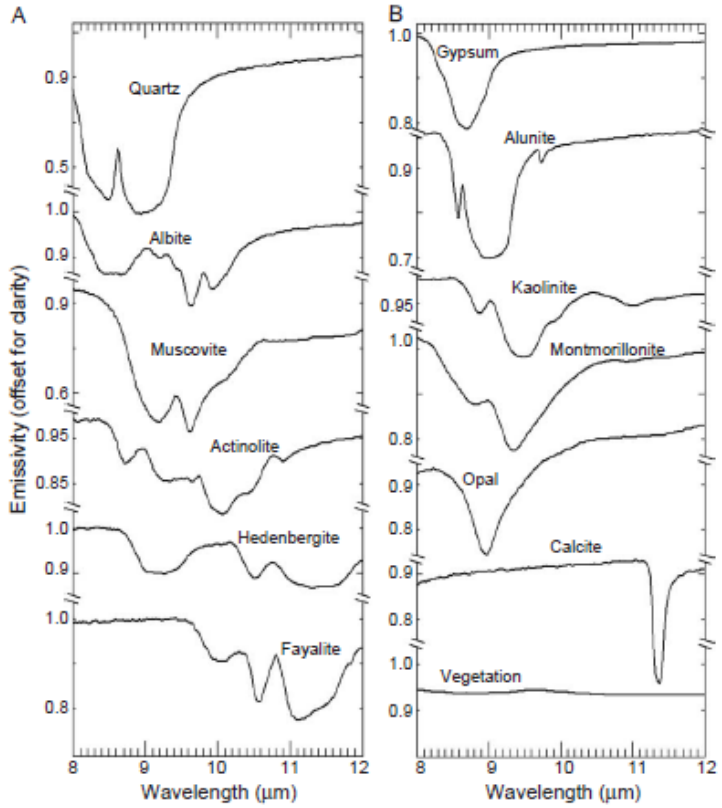

USGS Spectral Library

Vaughan et al., 2005

F. A. Kruse ♦ 303-499-9471 ♦ fakruse@nps.edu ♦http://www.nps.edu/Academics/Centers/RemoteSensing

Surface Temperature Mapping at Geothermal Systems

- **LWIR Multispectral data provide the additional capability to estimate surface temperature**
- **Improved understanding of known systems by detecting/ mapping**
  - **Distribution of heat anomalies and links to subsurface**
  - **Structural control**
  - **Outflow areas**
- **Provide new exploration tools**
  - **Temperature anomalies and magnitudes**
  - **"Blind" Systems**
- **Develop Methods for Monitoring**
  - **System characteristics and Natural variability**
  - **Exploitation Changes**

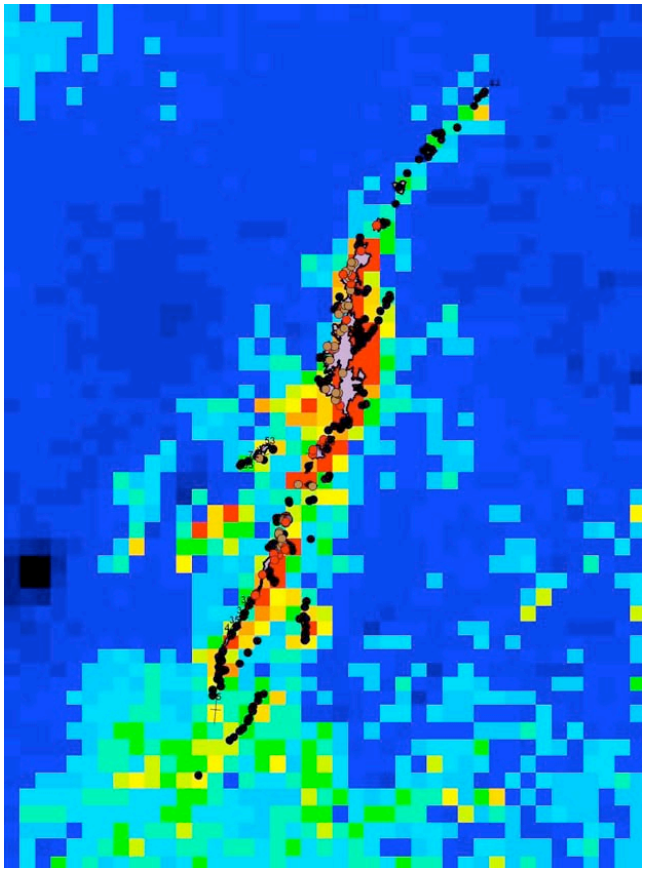

Coolbaugh, 2007 – Temperature Anomalies at Brady Hot Springs Using ASTER. Small black and brown points indicate field located steam vents or surface hot spots.

F. A. Kruse ♦ 303-499-9471 ♦ fakruse@nps.edu ♦http://www.nps.edu/Academics/Centers/RemoteSensing

HysplRI Simulation: Methods

- **Generate orthorectified ASTER base image at 15m spatial resolution**
- **AVIRIS Reflectance**
  - **Resample AVIRIS to HysplRI bands using band centers and FWHM**
  - **Perform Reflectance Conversion using ACORN**
  - **Geocorrect AVIRIS full dataset @15m to ASTER base**
  - **Spatially resample to 60m (aggregate pixels)**
- **MASTER Emissivity and Temperature**
  - **Resample MASTER Emissivity to HysplRI using band responses**
  - **Atmospherically correct using ISAC**
  - **Perform emissivity-temperature separation**
  - **Scale emissivity x 10000. to roughly match VSWIR reflectance range and convert to Integer**
  - **Geocorrect MASTER full dataset @15m to ASTER base**
  - **Spatially resample to 60m (aggregate pixels)**

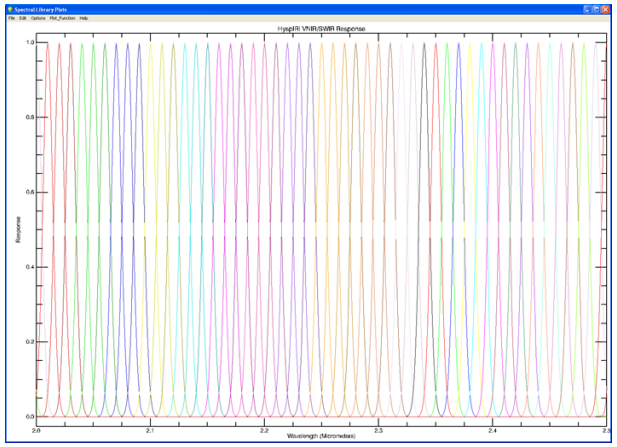

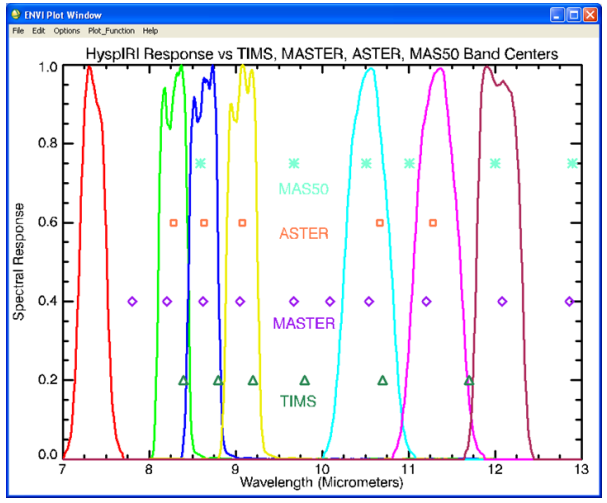

Study Areas

- **Generate Simulated HysplRI Data and Analysis Results for:**
  - **Cuprite, NV (fossil hydrothermal system)**
  - **Steamboat Springs, NV (geothermal)**
  - **Long Valley, CA (geothermal)**
  - **Fish Lake Valley, NV (geothermal)**
  - **Yellowstone, WY (geothermal)**

F. A. Kruse ♦ 303-499-9471 ♦ fakruse@nps.edu ♦http://www.nps.edu/Academics/Centers/RemoteSensing

Cuprite, NV, HysplRI Simulation

ASTER VNIR (15m)
04-28-2007 Ortho

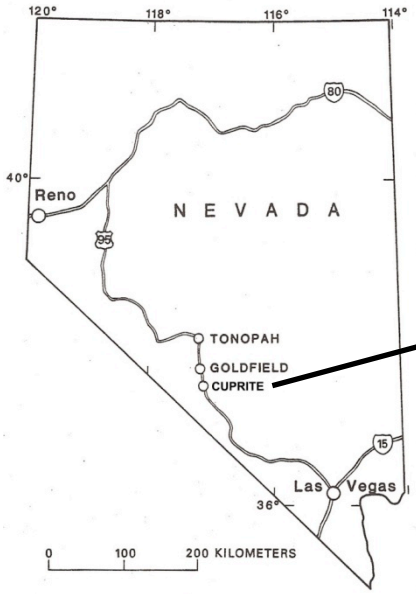

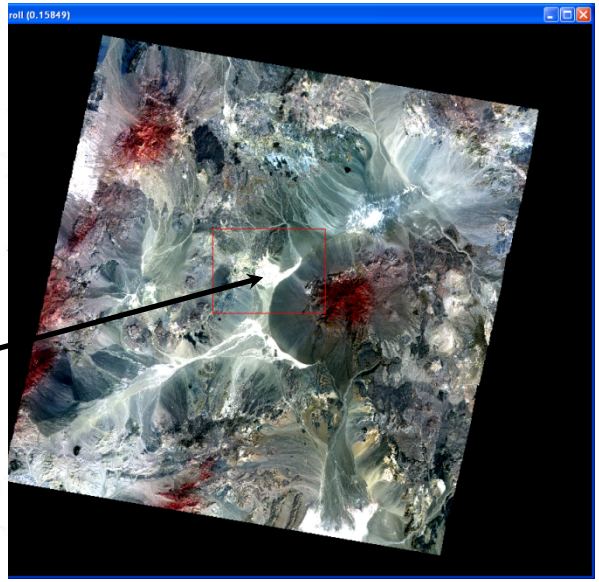

~60km

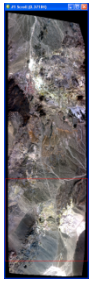

AVIRIS VNIR (15m)
09-20-2006 Ortho

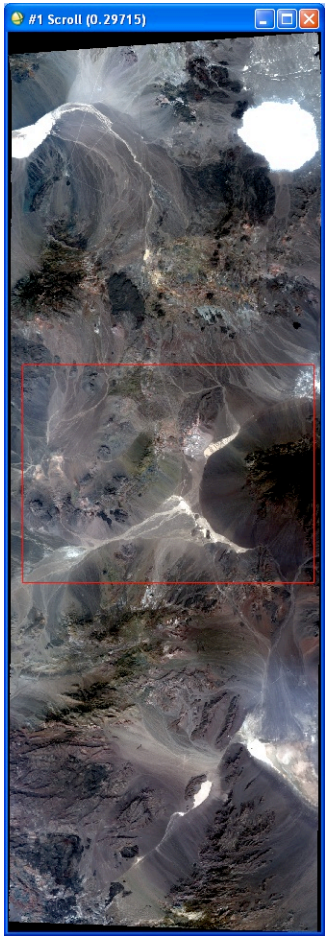

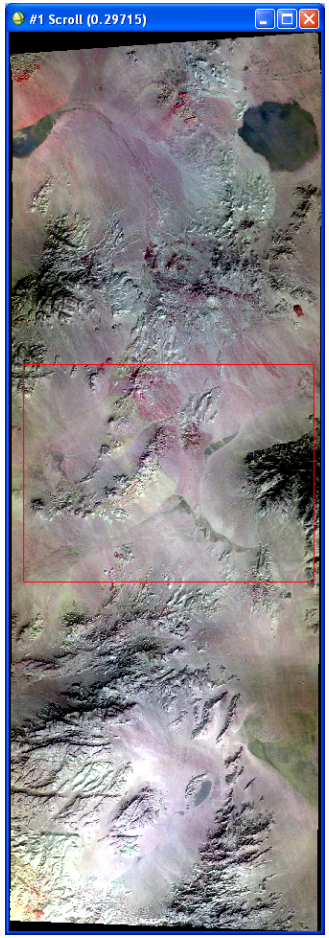

MASTER VNIR and LWIR (34m),
09-20-2006 GLT-Corrected

F. A. Kruse ♦ 303-499-9471 ♦ fakruse@nps.edu ♦http://www.nps.edu/Academics/Centers/RemoteSensing

Cuprite, NV Simulation: We end up with several small simulated datasets !

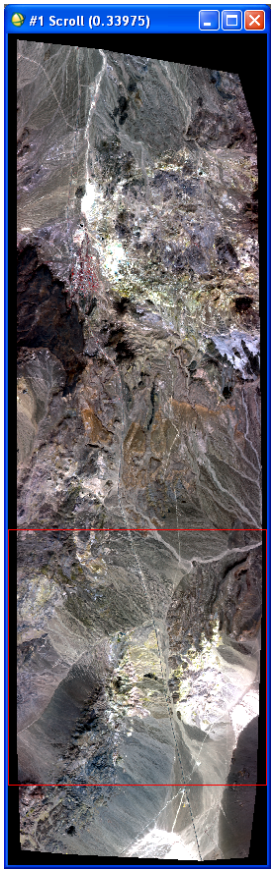

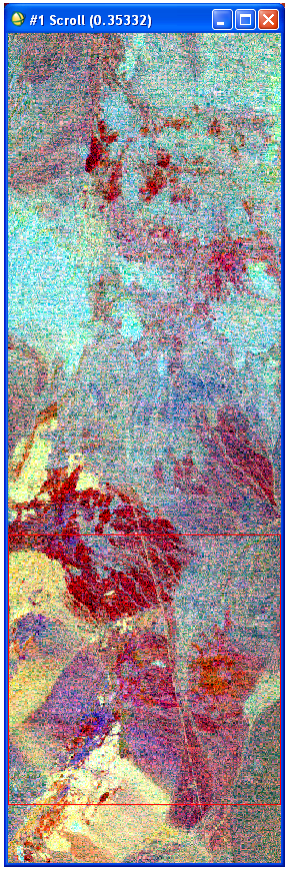

772 x 2493 Left: AVIRIS VNIR (15m) 09-20-2006 Ortho Warped to ASTER Ortho at 15m spatial resolution; Right Master Emissivity @HyspIRI bands

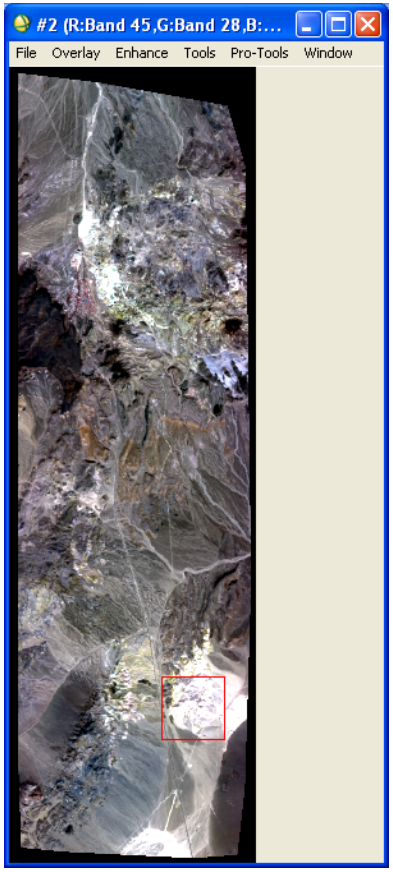

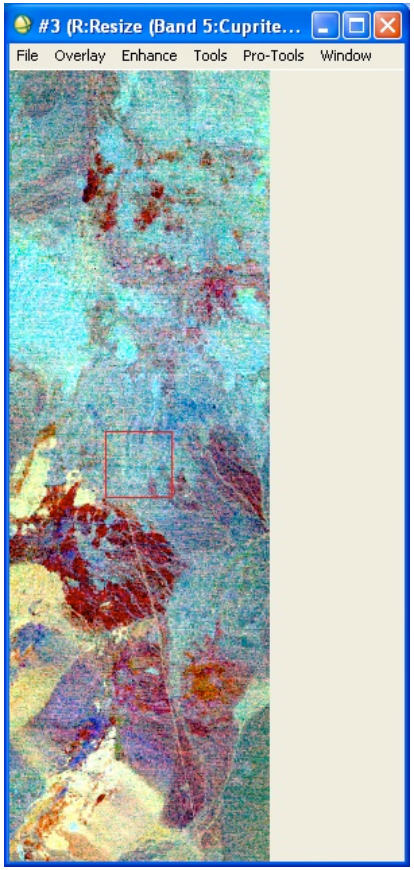

193 x 623 Left: HyspIRI simulated dataset from AVIRIS VNIR (15m) 09-20-2006 Ortho Warped to ASTER Ortho at 60m spatial resolution. Right: MASTER Emissivity @HyspIRI bands and 60m

F. A. Kruse ♦ 303-499-9471 ♦ fakruse@nps.edu ♦http://www.nps.edu/Academics/Centers/RemoteSensing

Cuprite, NV, 2006 AVIRIS
15m-derived SWIR MTMF Mineral Map (Kruse, 2011)

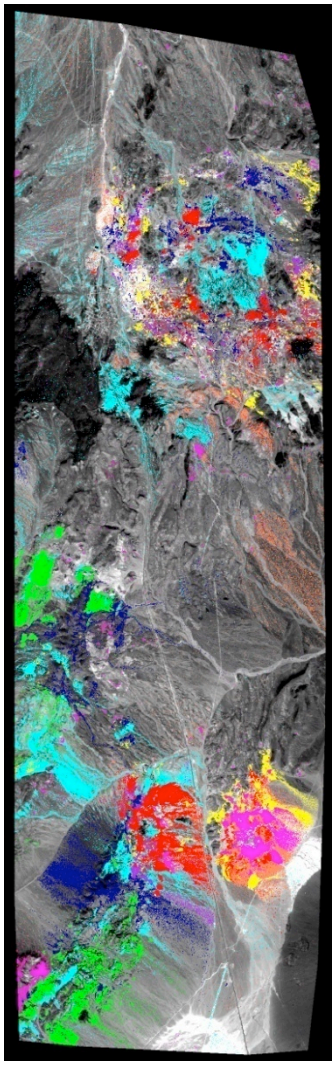

AVIRIS MTMF (60m)

Endmembers

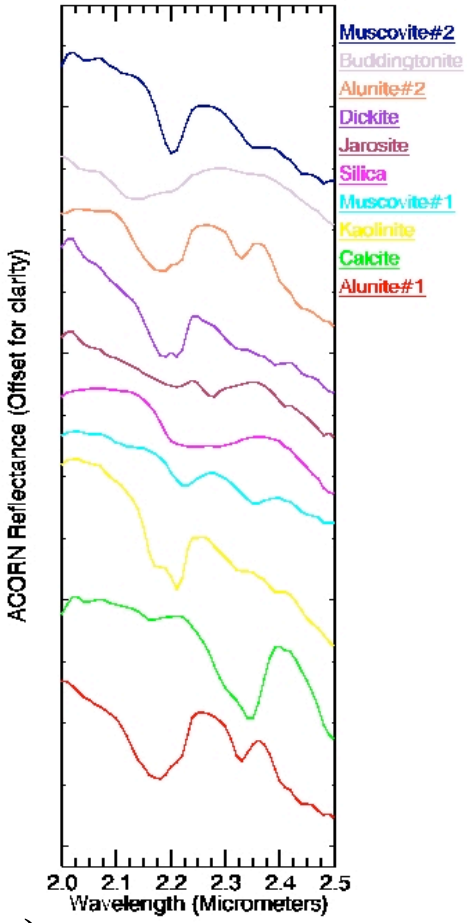

AVIRIS MTMF (60m)

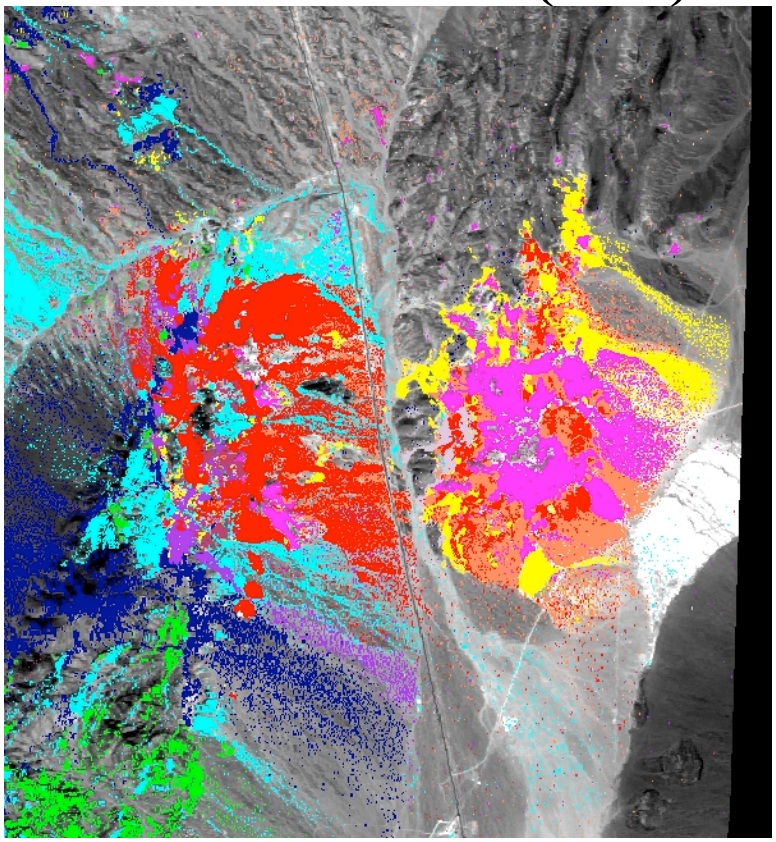

F. A. Kruse ♦ 303-499-9471 ♦ fakruse@nps.edu ♦http://www.nps.edu/Academics/Centers/RemoteSensing

Cuprite, NV, HysplRI-Simulated 60m-derived SWIR MTMF Mineral Map (Kruse, Unpublished)

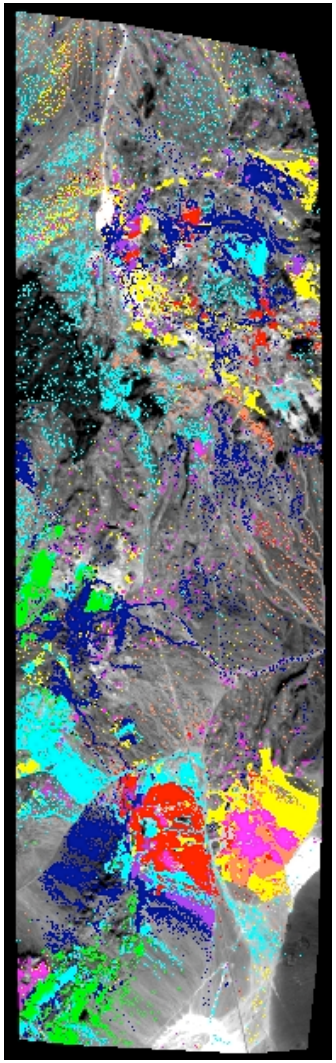

Endmembers

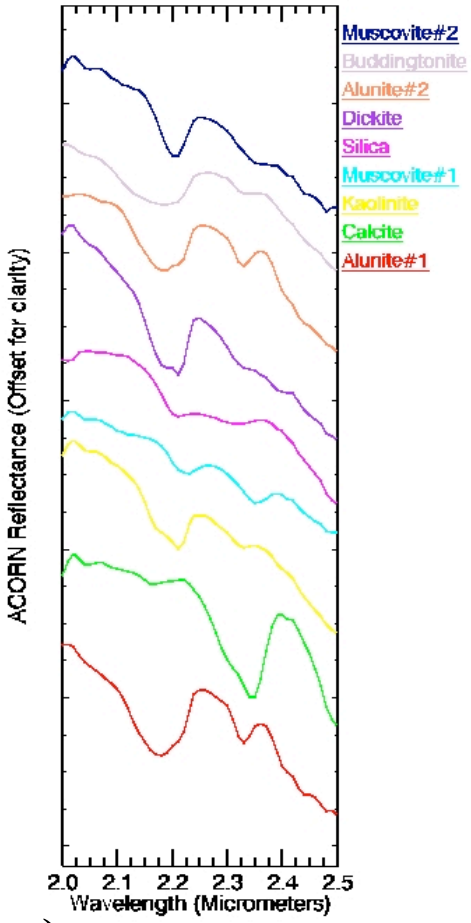

HyspIRI MTMF (60m)

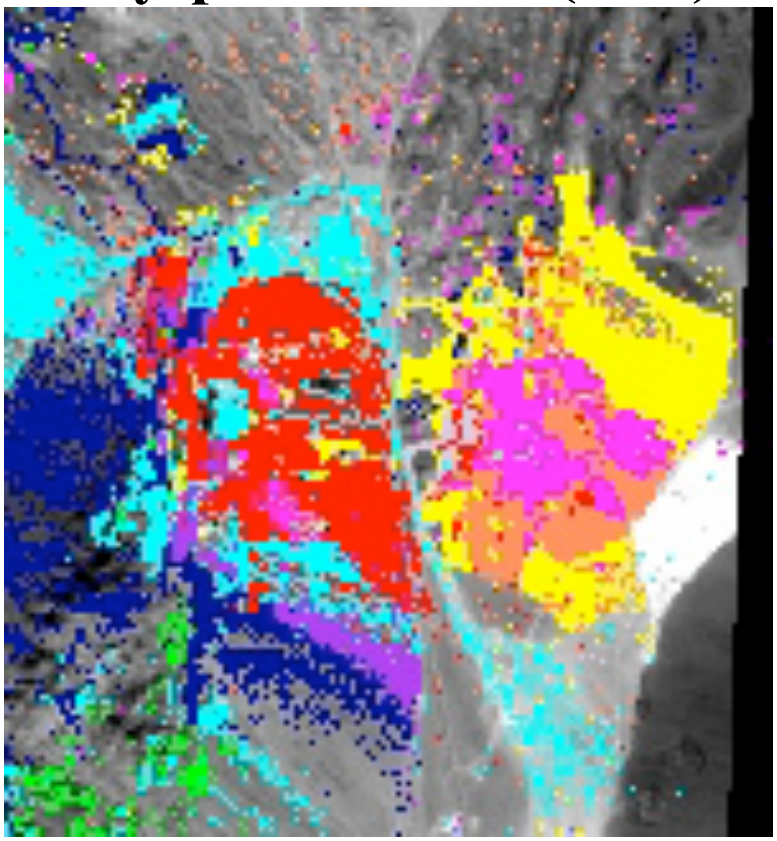

HyspIRI MTMF (60m)

F. A. Kruse ♦ 303-499-9471 ♦ fakruse@nps.edu ♦http://www.nps.edu/Academics/Centers/RemoteSensing

Table 1. Confusion matrix for Cuprite, Nevada, 15 m *versus* 60 m HyspIRI simulation. Overall Accuracy = (1533947/1905364) 80.5068%. Kappa Coefficient = 0.4627.

	Ground	**Truth**									
Class	Unclass	Alun#1	Calcite	Kaolinite	Musc#1	Silica	Dickite	Alun#2	Budding.	Musc#2	Total
Unclass	**84.01**	16.52	24.99	5.83	32.64	11.25	22.85	42.74	51.74	19.22	74.82
Alun#1	0.52	**63.83**	0.02	0.91	1.07	0.44	2.71	8.21	2.54	0.21	1.98
Calcite	0.63	0.02	**66.58**	0.01	0.55	0.09	0.09	0.02	0.56	0.35	1.80
Kaolinite	2.42	3.36	0.22	**84.84**	2.85	11.50	5.03	10.53	4.01	0.93	3.58
Musc#1	4.20	2.42	5.63	0.73	**57.25**	1.78	3.56	1.75	9.35	0.44	6.19
Silica	0.89	0.22	0.14	0.13	0.34	**67.63**	0.14	2.41	1.52	0.28	1.53
Dickite	0.45	1.67	0.00	4.21	0.51	0.01	**53.93**	0.16	0.14	0.72	0.86
Alun#2	1.35	9.03	0.05	1.16	0.64	6.50	0.32	**32.47**	0.84	0.19	2.08
Budding.	0.09	0.51	0.06	0.29	0.16	0.01	0.06	0.21	**24.11**	0.04	0.16
Musc#2	5.43	2.42	2.31	1.90	3.99	0.79	11.31	1.49	5.20	**77.62**	7.01
Total	100.00	100.00	100.00	100.00	100.00	100.00	100.00	100.00	100.00	100.00	**100.00**

Class	**Commission**	**Omission**	**Prod. Acc.**	**User Acc.**
	Percent	**Percent**	**Percent**	**Percent**
Unclass	5.28	15.97	84.03	94.72
Alun#1	34.91	36.17	63.83	65.09
Calcite	31.27	33.42	66.58	68.73
Kaol	73.24	15.16	84.84	26.76
Musc#1	61.56	42.75	57.25	38.44
Silica	54.59	32.37	67.63	45.41
Dickite	58.42	46.07	53.93	41.58
Alun#2	69.22	67.53	32.47	30.78
Budding.	65.21	75.89	24.11	34.79
Musc#2	71.08	22.38	77.62	28.92

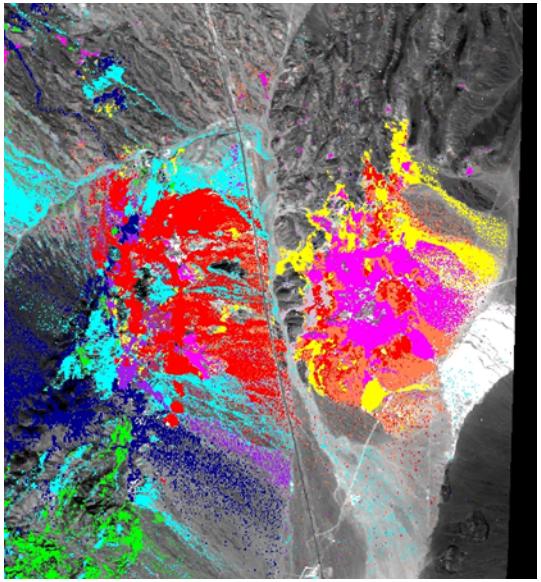

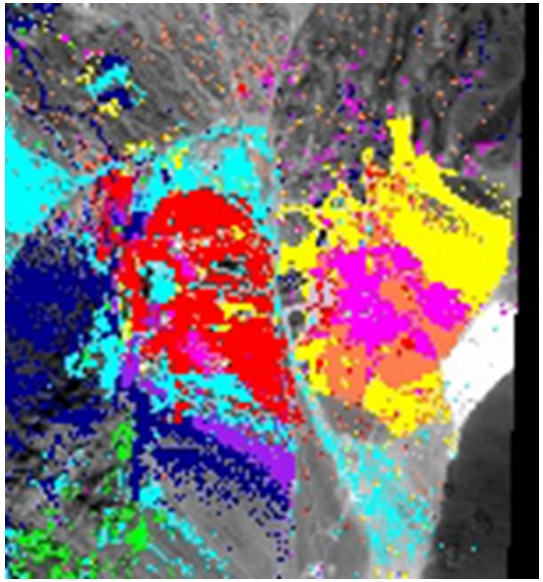

F. A. Kruse ♦ 303-499-9471 ♦ fakruse@nps.edu ♦http://www.nps.edu/Academics/Centers/RemoteSensing

Cuprite, NV 2006 MASTER LWIR (34m)

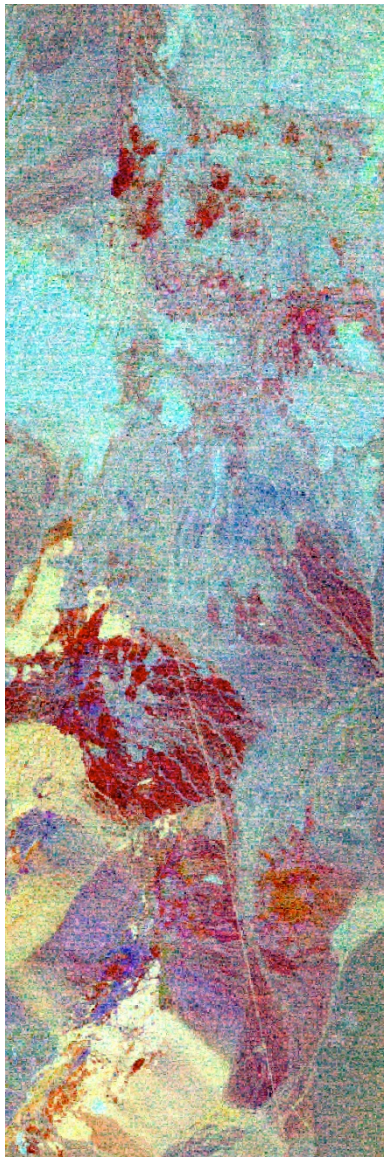

Emissivity

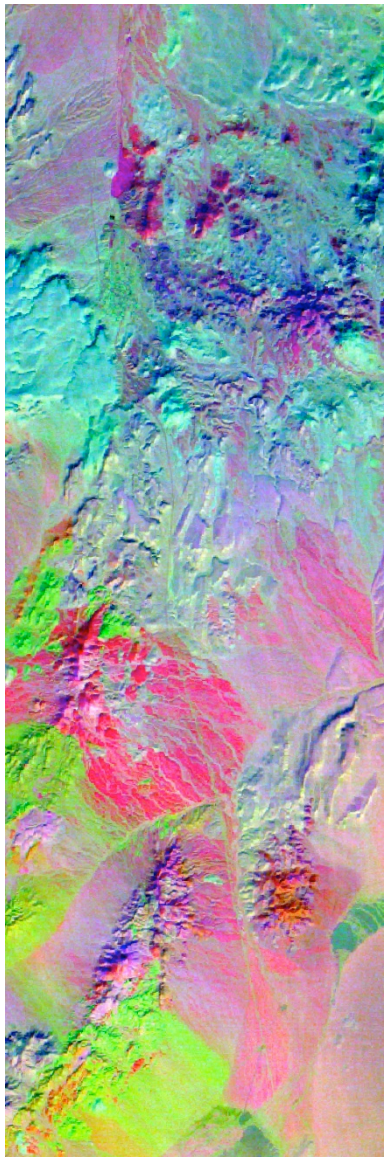

MNF 1, 2, 3

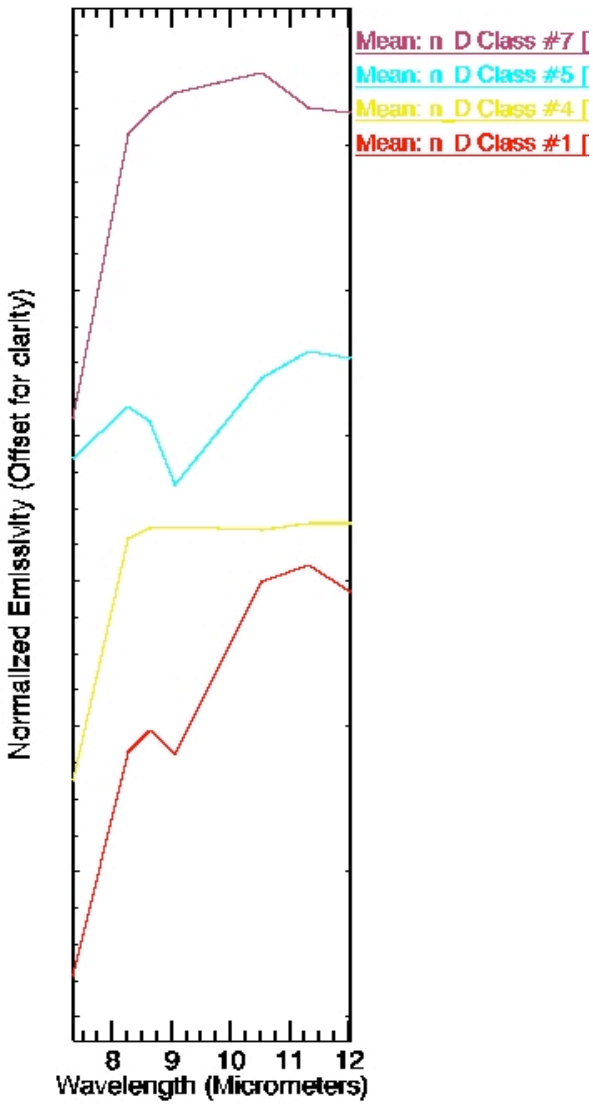

Endmembers

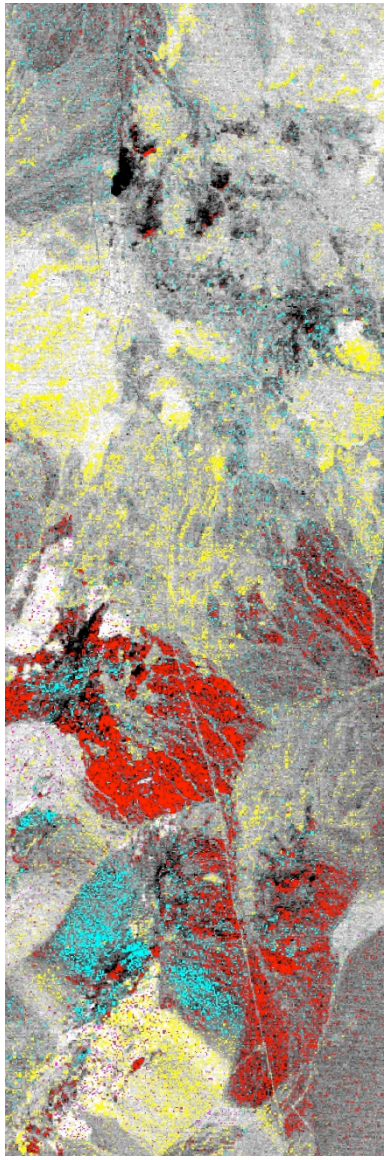

Classification

F. A. Kruse ♦ 303-499-9471 ♦ fakruse@nps.edu ♦http://www.nps.edu/Academics/Centers/RemoteSensing

Cuprite, NV 2006 HysplRI-Simulated LWIR (60m)

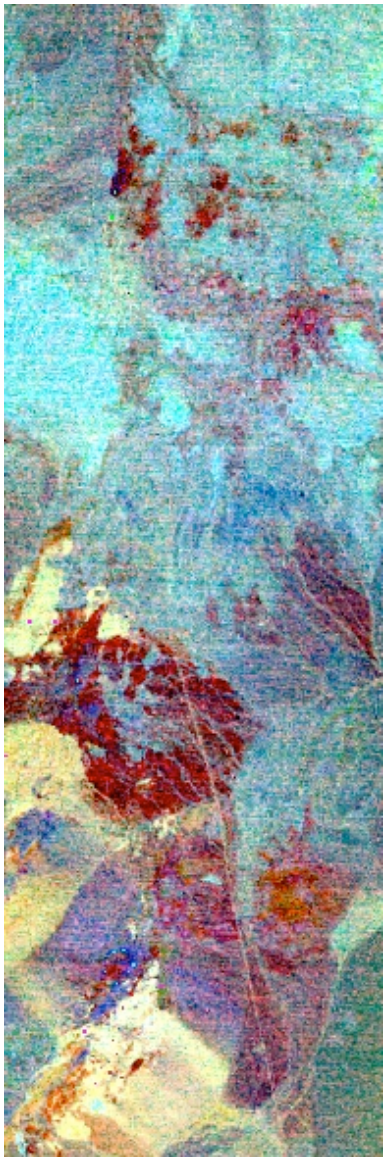

Emissivity

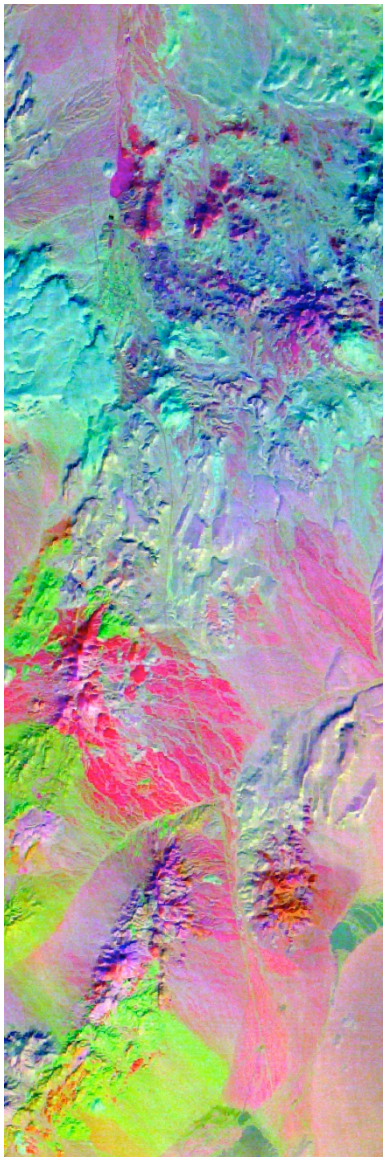

MNF 1, 2, 3

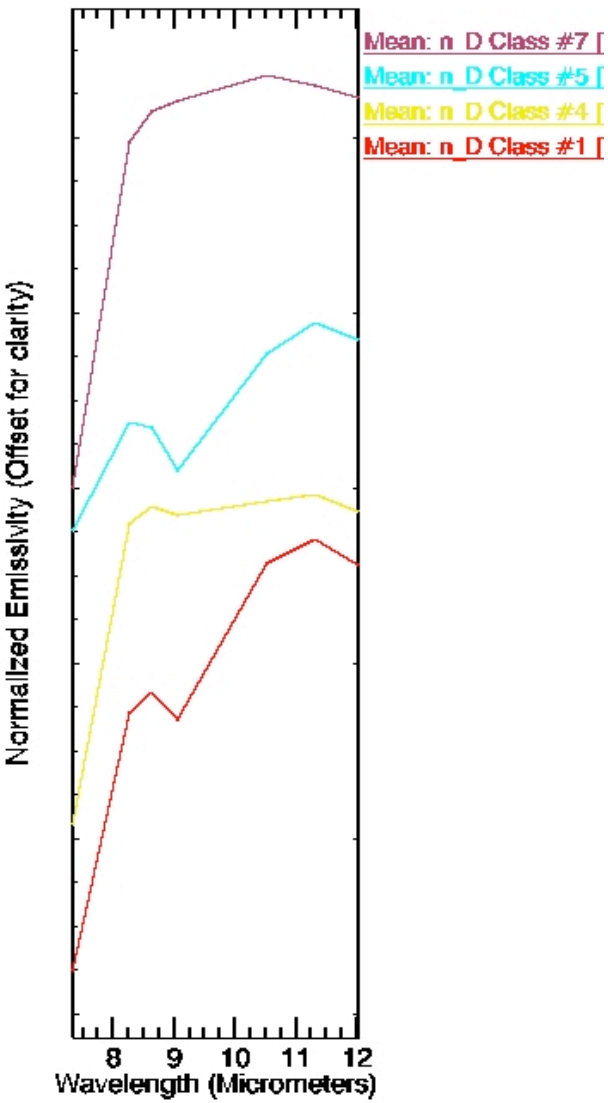

Endmembers

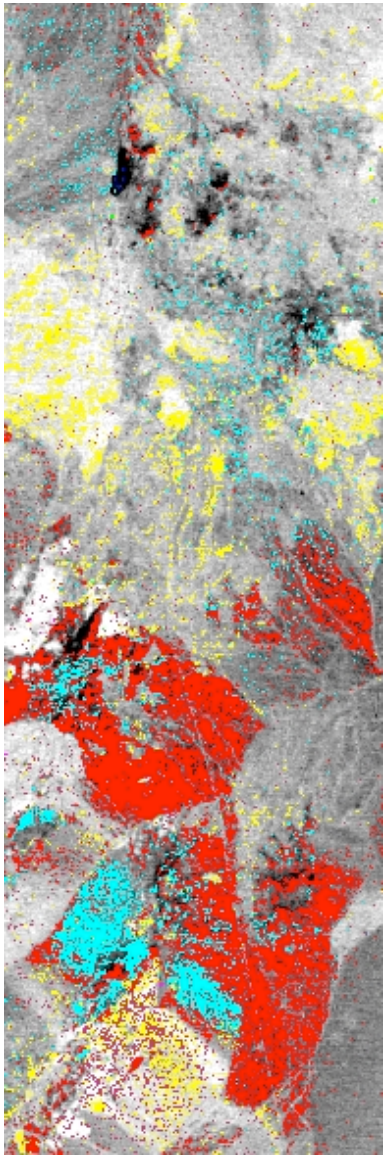

Classification

F. A. Kruse ♦ 303-499-9471 ♦ fakruse@nps.edu ♦http://www.nps.edu/Academics/Centers/RemoteSensing

Steamboat Springs, NV Simulation

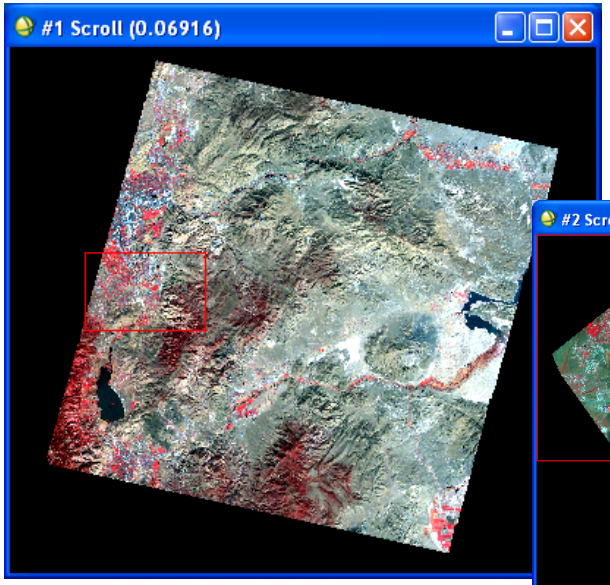

ASTER VNIR (15m)
10-23-2006 Ortho

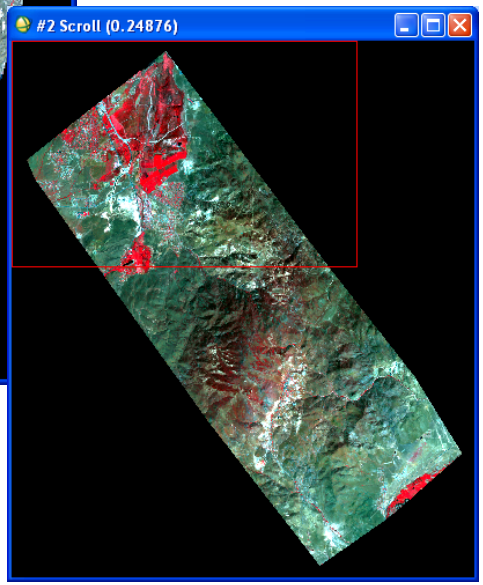

AVIRIS VNIR (15m)
07-22-1995, Warped
to ASTER Ortho

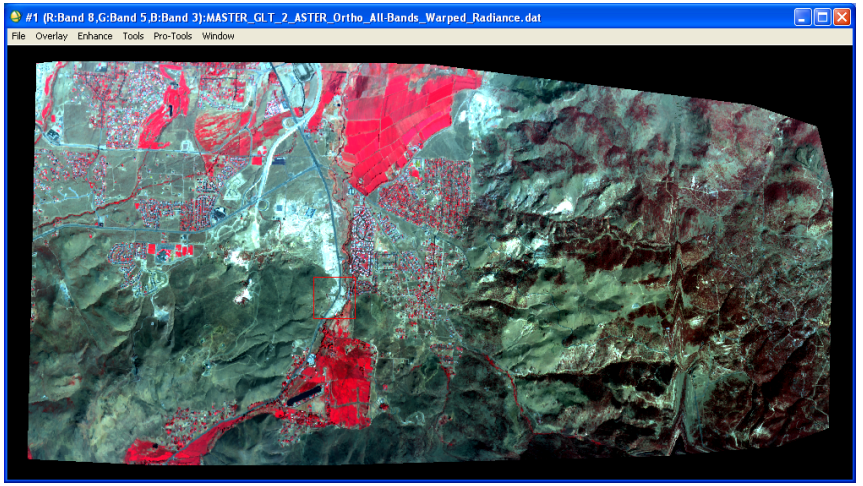

MASTER VNIR (9m @15m), 09-19-1999
GLT-Corrected, Warped to Ortho ASTER

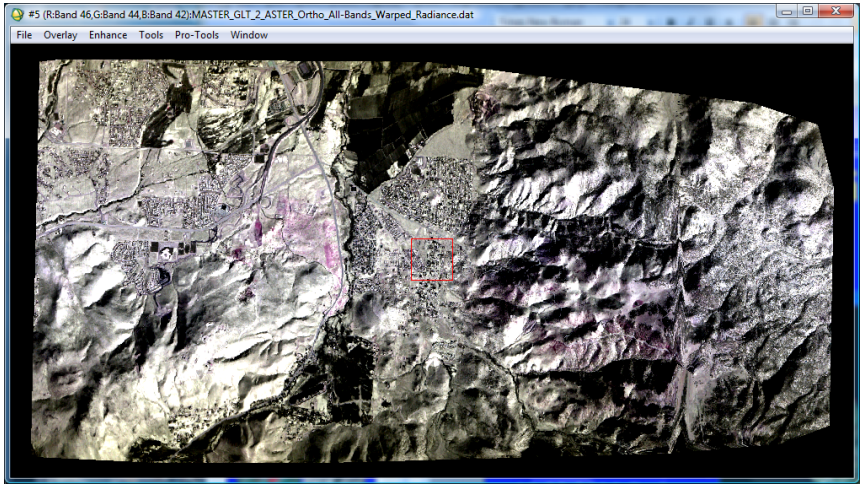

MASTER LWIR (9m @15m), GLT-Cor
09-19-1999, Warped to ASTER Ortho

F. A. Kruse ♦ 303-499-9471 ♦ fakruse@nps.edu ♦http://www.nps.edu/Academics/Centers/RemoteSensing

Steamboat Springs, NV Simulation

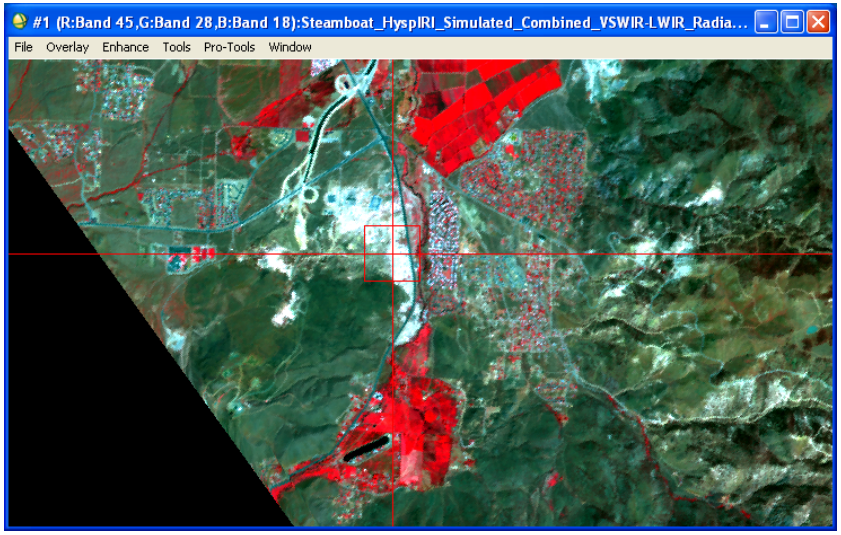

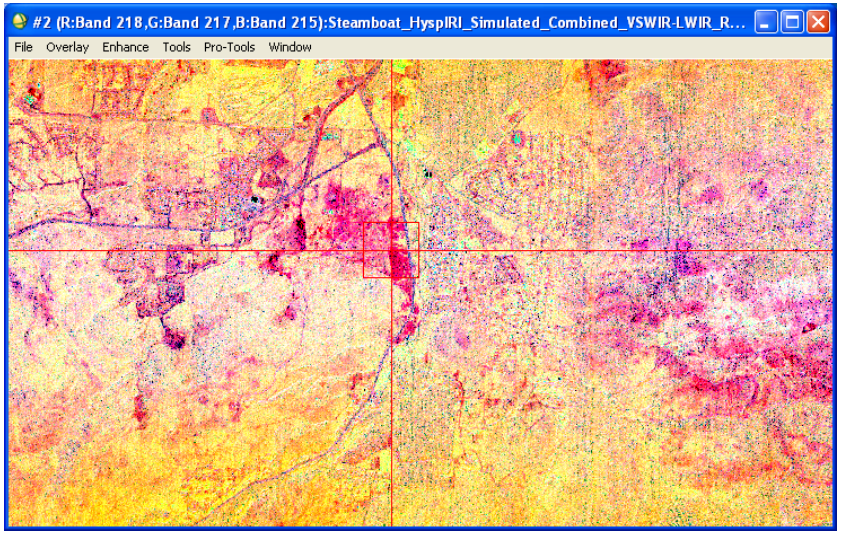

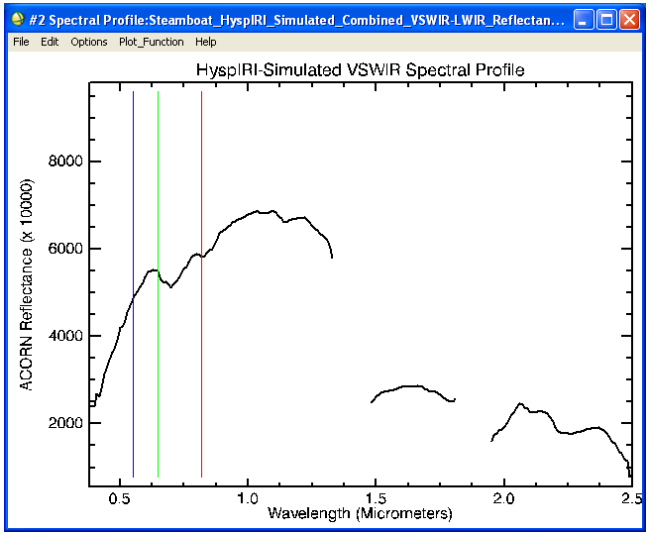

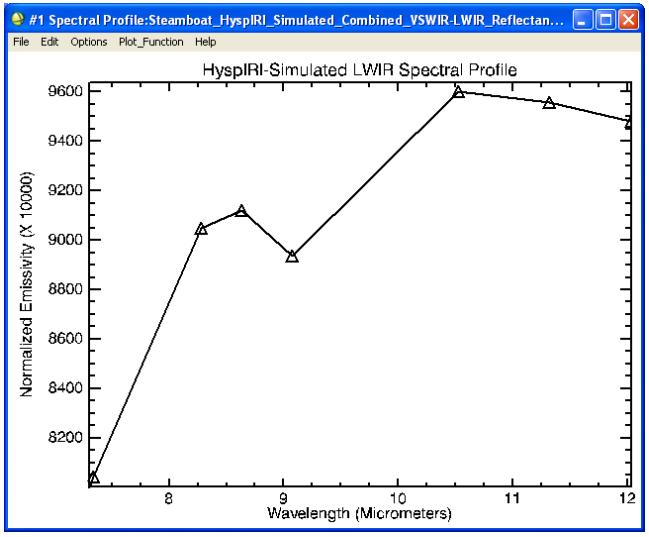

HyspIRI-Simulated VSWIR Reflectance (15m)

HyspIRI-Simulated LWIR Emissivity (15m)

F. A. Kruse ♦ 303-499-9471 ♦ fakruse@nps.edu ♦http://www.nps.edu/Academics/Centers/RemoteSensing

Steamboat Springs, NV Simulation

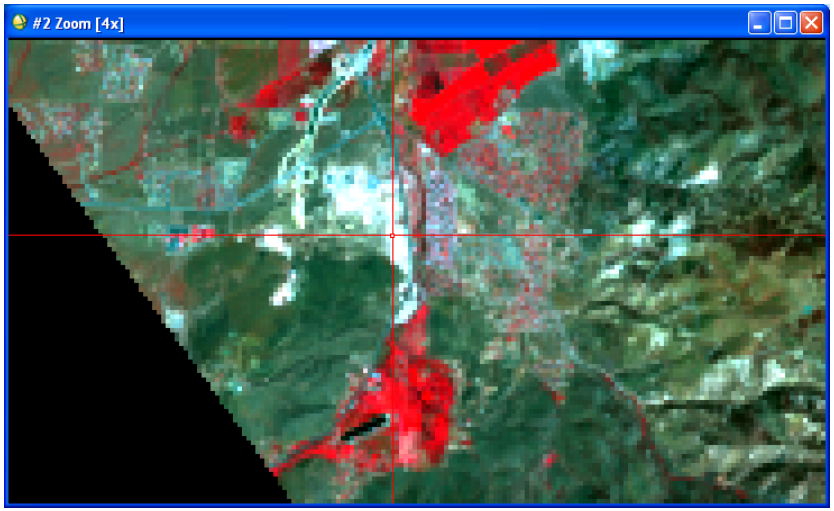

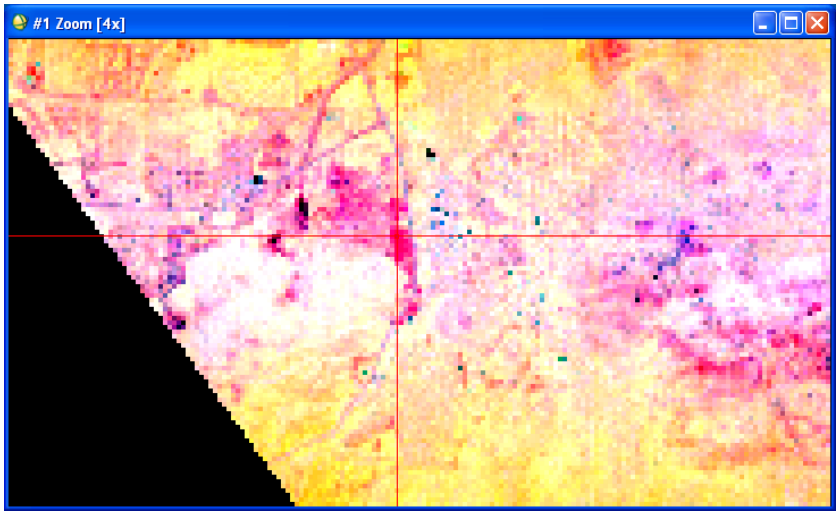

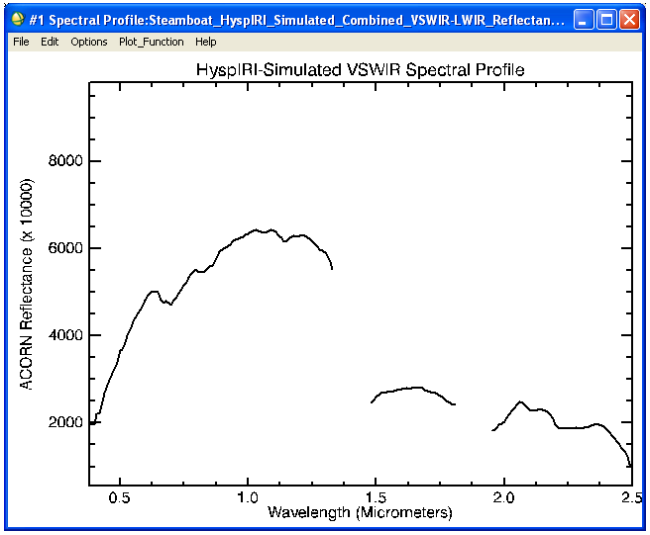

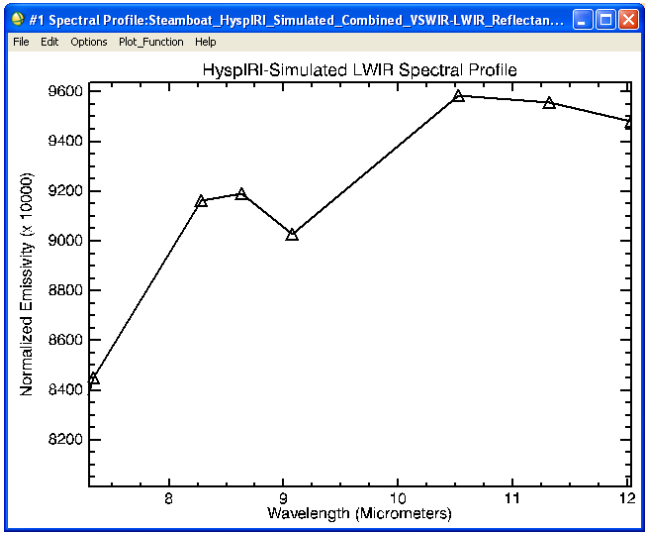

HyspIRI-Simulated VSWIR Radiance (60m)

HyspIRI-Simulated LWIR Radiance (60m)

F. A. Kruse ♦ 303-499-9471 ♦ fakruse@nps.edu ♦http://www.nps.edu/Academics/Centers/RemoteSensing

Steamboat Springs, NV Spectral Maps

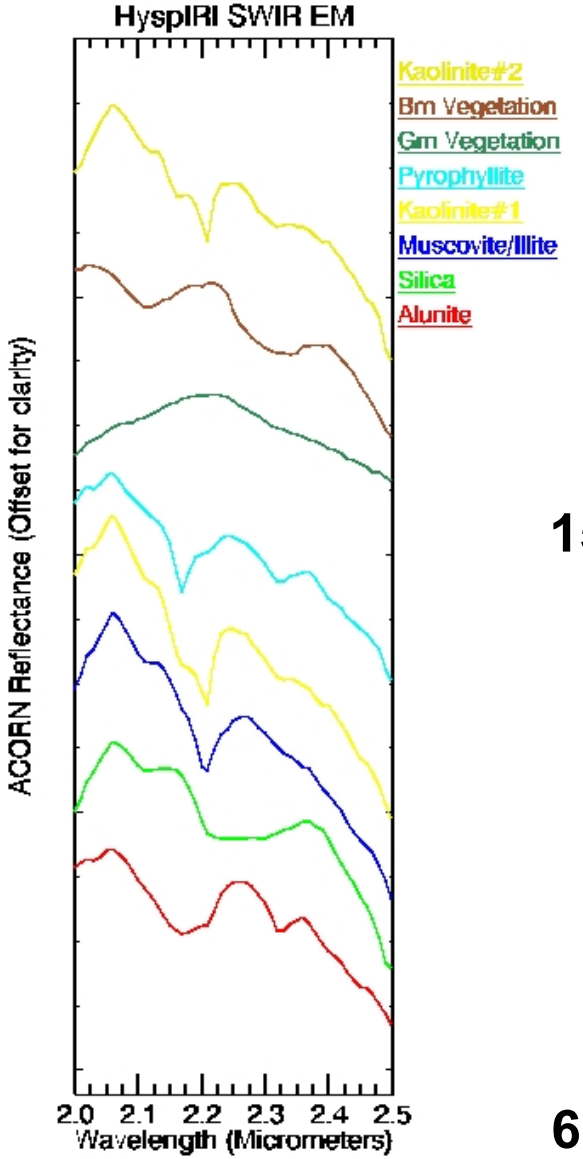

15m

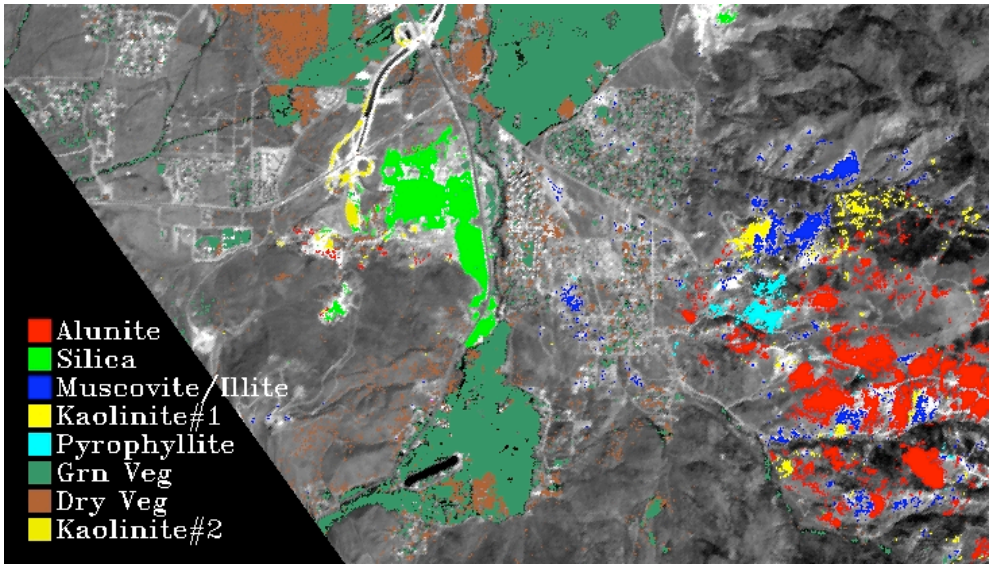

60m

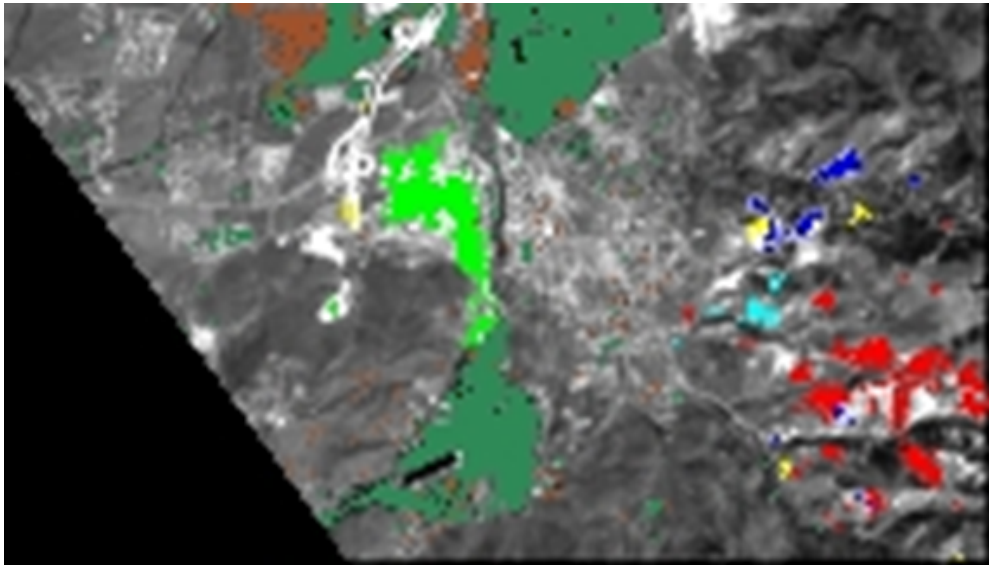

F. A. Kruse ♦ 303-499-9471 ♦ fakruse@nps.edu ♦http://www.nps.edu/Academics/Centers/RemoteSensing

Steamboat Springs, NV Accuracy Assessment

Table 2. Confusion matrix for Steamboat Springs, Nevada, 15 m *versus* 60 m HyspIRI simulation. Overall Accuracy = (278492/302217) 92.1497% Kappa Coefficient = 0.6859.

	Ground Truth									
Class	Unclass	Alunite	Silica	Mus/Ill	Kaol#1	Pyroph	G. Veg	D. Veg	Kaol#2	Total
Unclass	**98.02**	55.35	20.06	75.08	83.11	58.39	18.77	60.21	77.21	88.43
Alunite	0.20	**44.58**	0.00	0.20	0.07	0.13	0.00	0.01	0.00	1.30
Silica	0.19	0.01	**79.73**	0.00	0.00	0.00	0.00	0.19	0.00	1.31
Mus/Ill	0.08	0.04	0.00	**24.56**	0.83	0.00	0.00	0.00	0.00	0.28
Kaol#1	0.03	0.00	0.00	0.08	**15.15**	0.00	0.00	0.00	1.33	0.10
Pyroph	0.03	0.01	0.00	0.00	0.00	**41.49**	0.00	0.00	0.00	0.13
G. Veg	0.95	0.00	0.14	0.00	0.00	0.00	**80.41**	4.77	0.00	7.03
D. Veg	0.48	0.00	0.02	0.08	0.00	0.00	0.82	**34.82**	0.00	1.38
Kaol#2	0.01	0.00	0.05	0.00	0.83	0.00	0.00	0.00	**21.46**	0.05
Total	100.00	100.00	100.00	100.00	100.00	100.00	100.00	100.00	100.00	**100.00**

Class	Commission	Omission	Prod. Acc.	User Acc.
	Percent	Percent	Percent	Percent
Unclass	6.76	1.98	98.02	93.24
Alunite	13.34	55.42	44.58	86.66
Silica	12.63	20.27	79.73	87.37
Mus/Ill	25.96	75.44	24.56	74.04
Kaol#1	28.29	84.85	15.15	71.71
Pyroph	19.00	58.51	41.49	81.00
G. Veg	13.18	19.59	80.41	86.82
D. Veg	33.93	65.18	34.82	66.07
Kaol#2	32.64	78.54	21.46	67.36

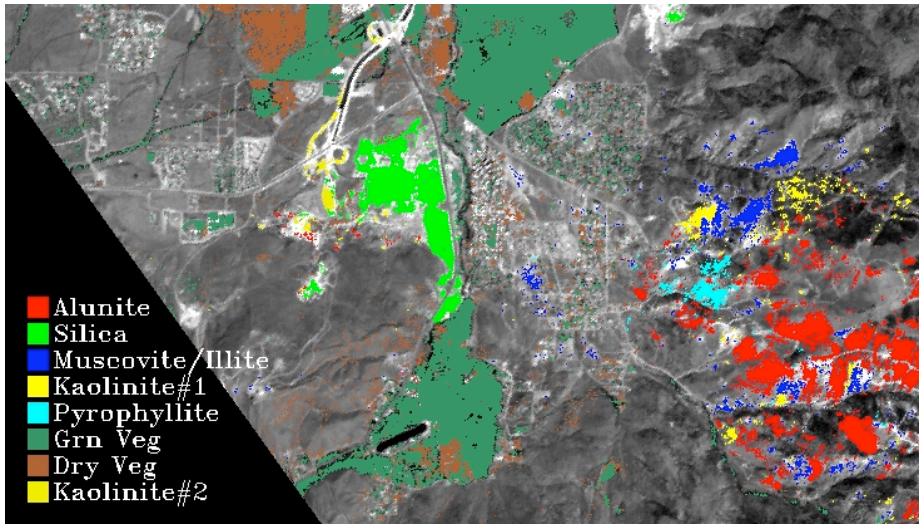

15m

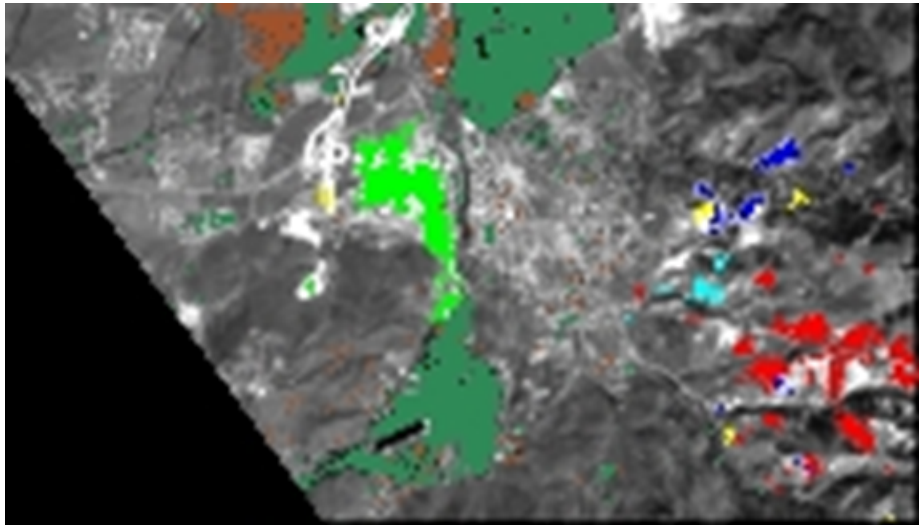

60m

F. A. Kruse ♦ 303-499-9471 ♦ fakruse@nps.edu ♦http://www.nps.edu/Academics/Centers/RemoteSensing

Yellowstone WY Example

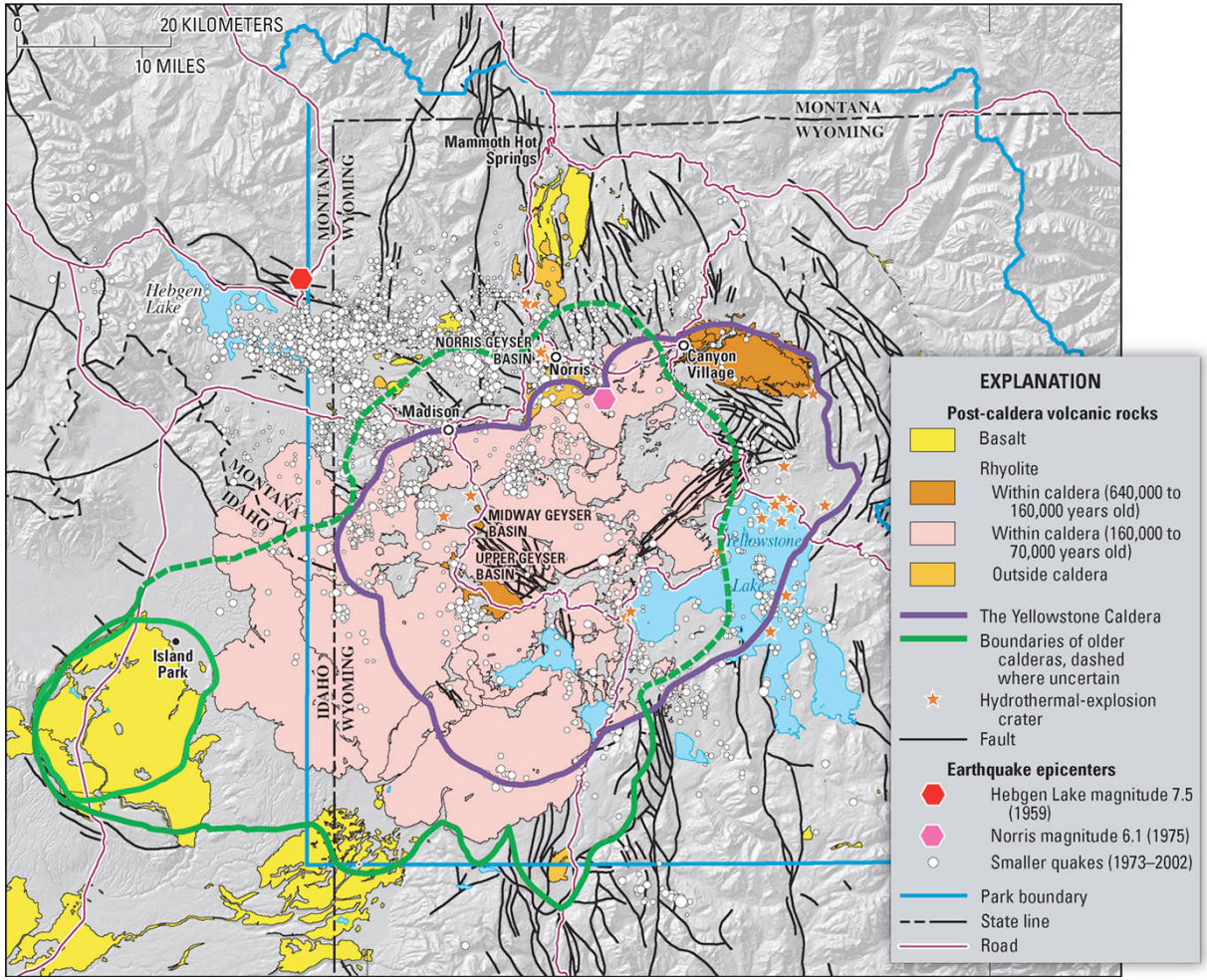

F. A. Kruse ♦ 303-499-9471 ♦ fakruse@nps.edu ♦http://www.nps.edu/Academics/Centers/RemoteSensing

Yellowstone, WY HyspIRI Simulation

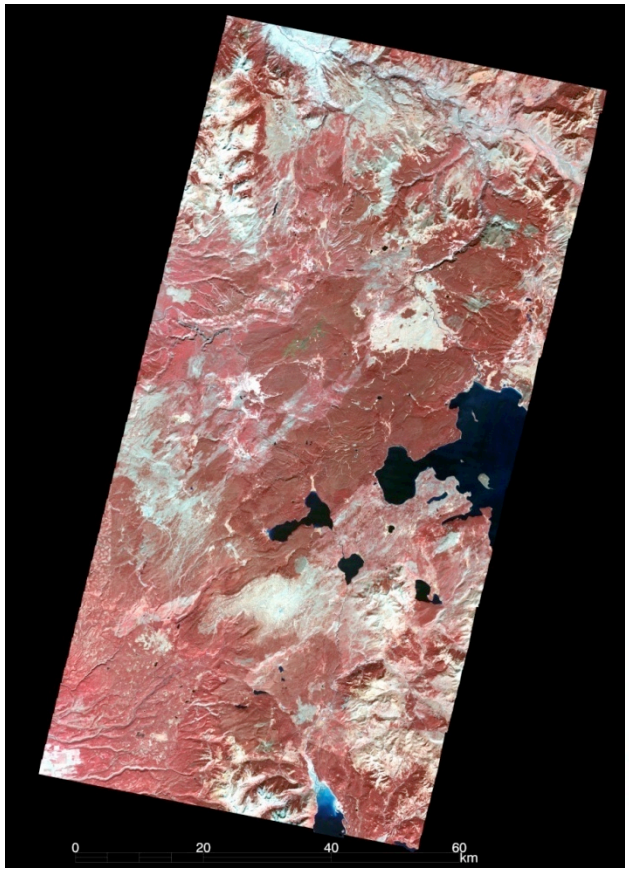

ASTER VNIR (15m)
09-08-2000 Ortho

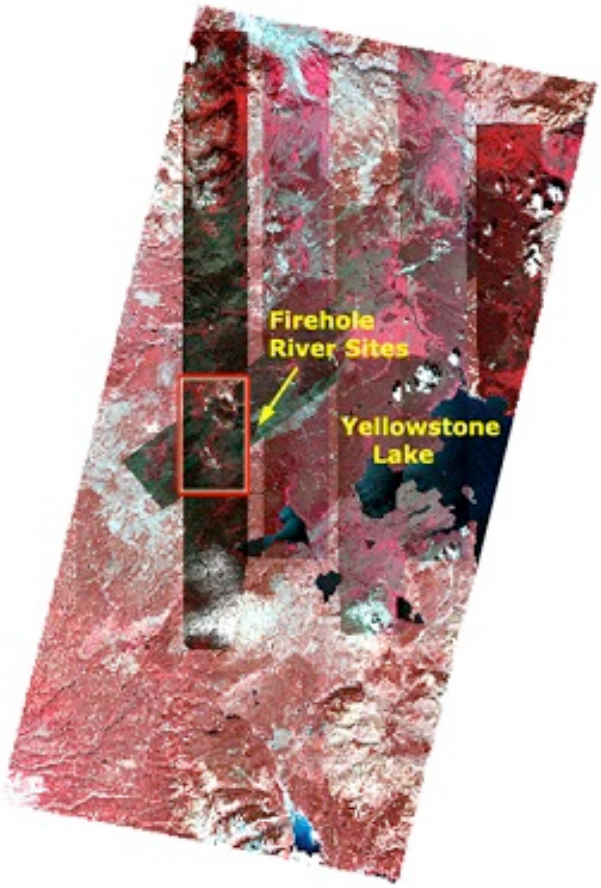

AVIRIS VNIR (15m)
07-14-1997, 08-06-1996

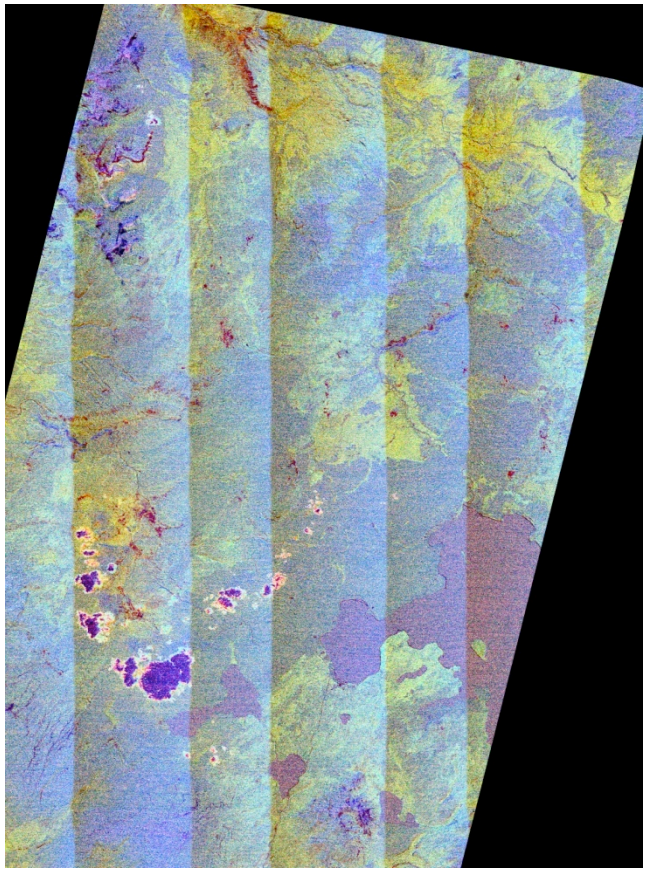

MASTER LWIR Emissivity
09-25-2006

F. A. Kruse ♦ 303-499-9471 ♦ fakruse@nps.edu ♦http://www.nps.edu/Academics/Centers/RemoteSensing

AVIRIS Results (15m) Firehole River Alkaline, with Acid Sulfate on margins

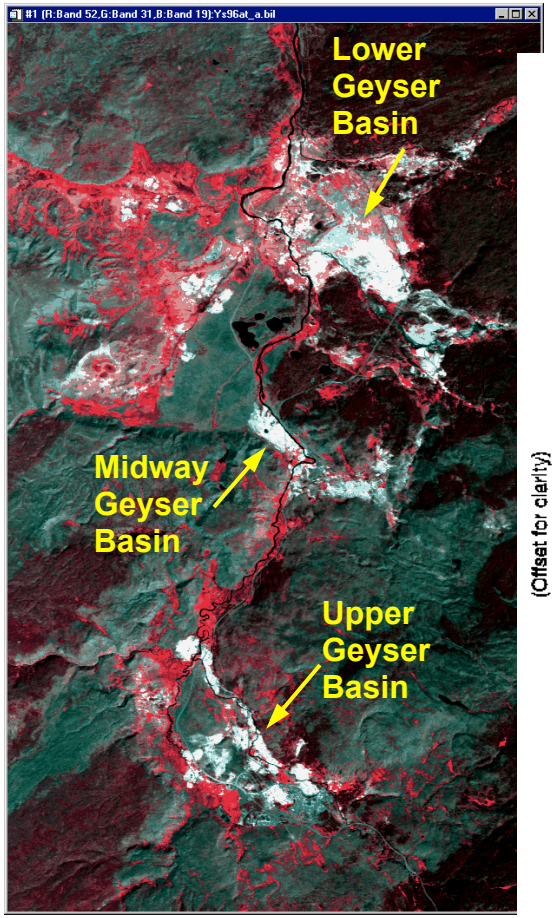

Color Infrared Composite

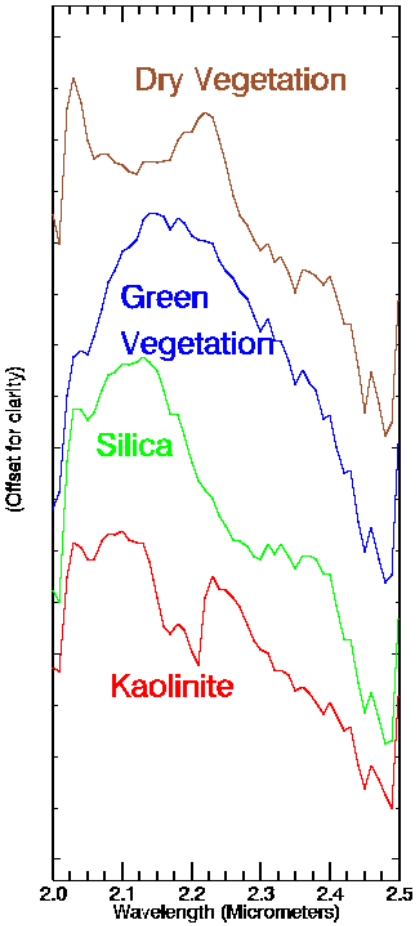

Endmember Spectra

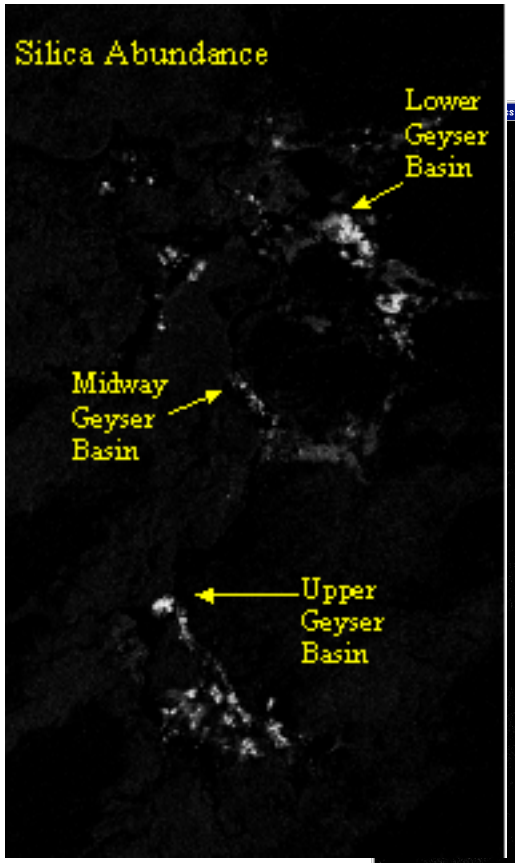

Silica

Kaolinite

F. A. Kruse ♦ 303-499-9471 ♦ fakruse@nps.edu ♦http://www.nps.edu/Academics/Centers/RemoteSensing

Compare AVIRIS Results (15m) and HyspIRI-Sim (60m) Firehole River Alkaline, with Acid Sulfate on margins

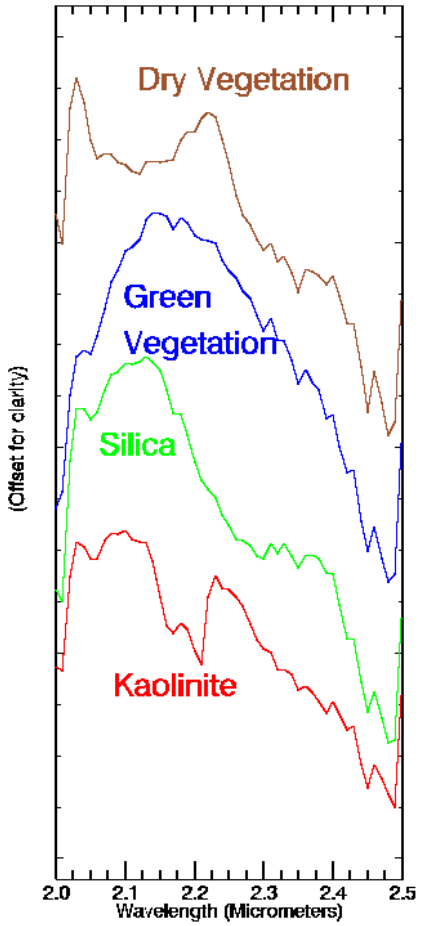

Endmembers

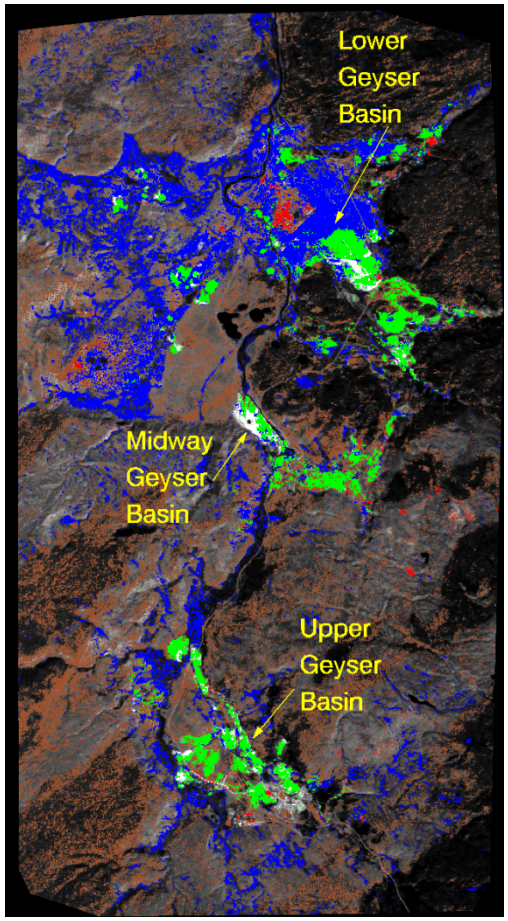

AVIRIS (15m)

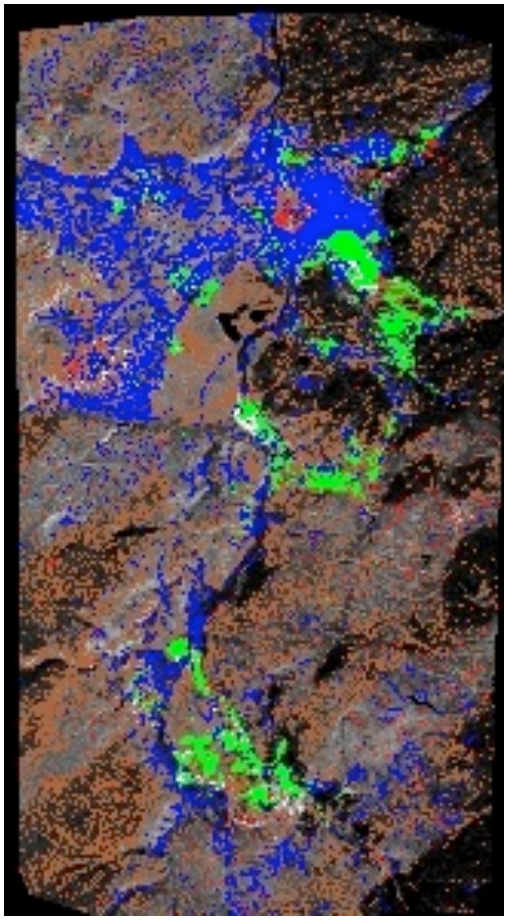

HyspIRI-Sim (60m)

Table 3. Confusion matrix for Yellowstone, Wyoming, 15 m *versus* 60 m HyspIRI simulation. Overall Accuracy = (542160/775992) 69.8667%. Kappa Coefficient = 0.3471.

	Ground	**Truth**				
Class	Unclass	Kaolinite	Silica	Grn Veg	Dry Veg	Total
Unclass	**76.89**	49.41	12.86	35.44	51.63	68.03
Kaolinite	1.12	**19.15**	0.36	0.45	1.03	1.11
Silica	0.93	3.18	**69.17**	2.34	1.41	2.84
Grn Veg	5.62	5.61	8.76	**56.01**	3.06	9.82
Dry Veg	15.44	22.65	8.85	5.77	**42.66**	18.20
Total	100.00	100.00	100.00	100.00	100.00	**100.00**

Class	**Commission**	**Omission**	**Prod. Acc.**	**User Acc.**
	Percent	**Percent**	**Percent**	**Percent**
Unclass	15.93	23.11	76.89	84.07
Kaolinite	92.49	80.85	19.15	7.51
Silcia	39.09	30.83	69.17	60.91
Grn Veg	49.33	43.99	56.01	50.67
Dry Veg	67.65	57.34	42.66	32.35

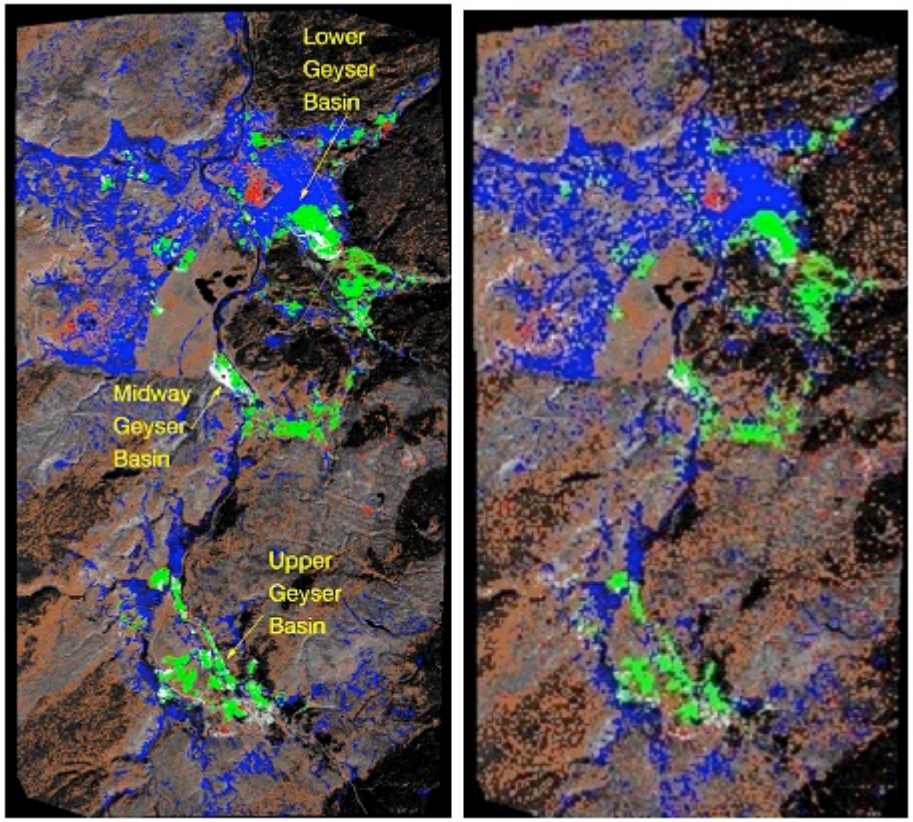

F. A. Kruse ♦ 303-499-9471 ♦ fakruse@nps.edu ♦http://www.nps.edu/Academics/Centers/RemoteSensing

MASTER Mineralogy YS (Firehole River) 2006
35m Native Spatial Resolution

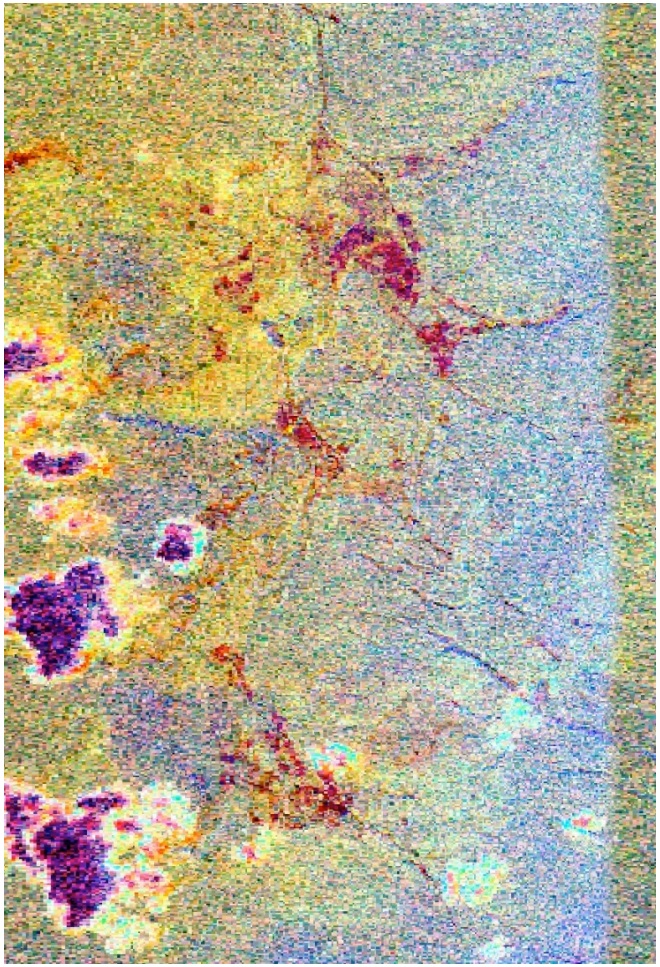

Emissivity (10.5, 9.1, 8.3 μm, RGB)
Note Clouds and Shadows (purple)

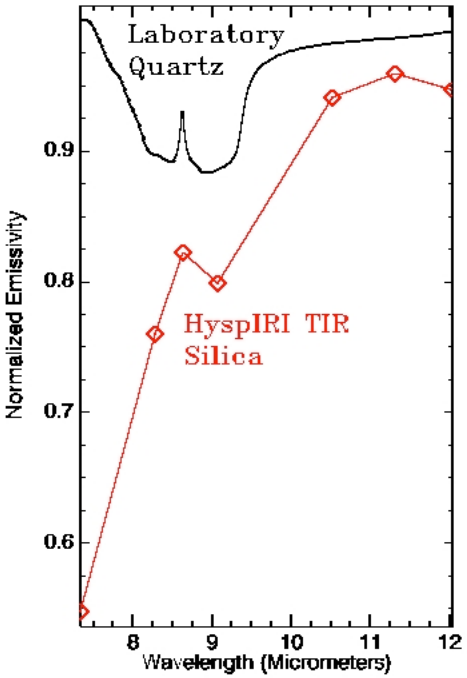

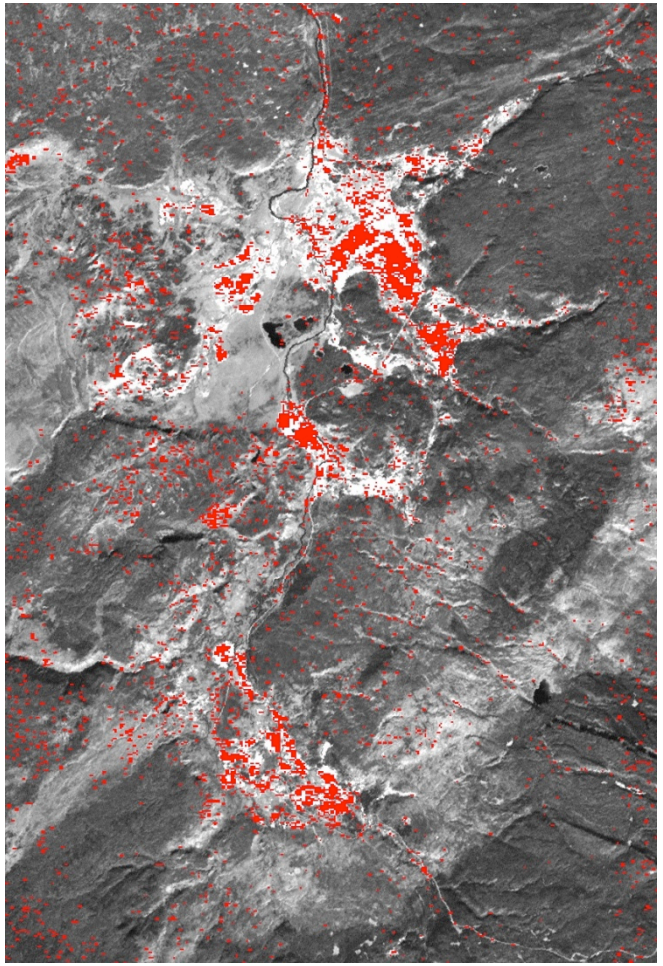

MTMF LWIR Silica Map

F. A. Kruse ♦ 303-499-9471 ♦ fakruse@nps.edu ♦http://www.nps.edu/Academics/Centers/RemoteSensing

MASTER Mineralogy YS (Firehole River) 2006
60m HyspIRI-Sim Spatial Resolution

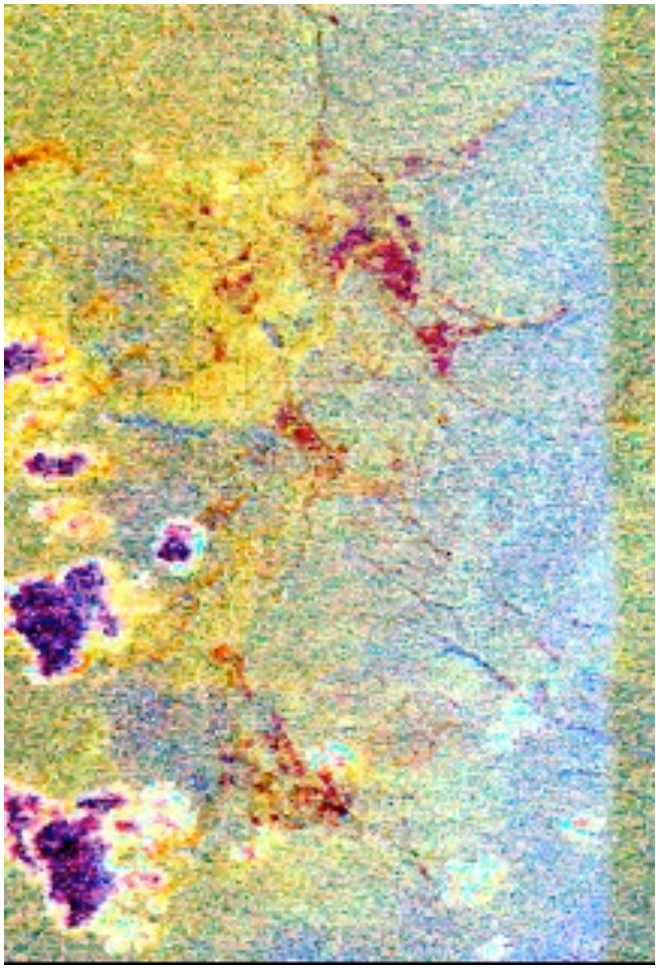

Emissivity (10.5, 9.1, 8.3 μm, RGB)
Note Clouds and Shadows (purple)

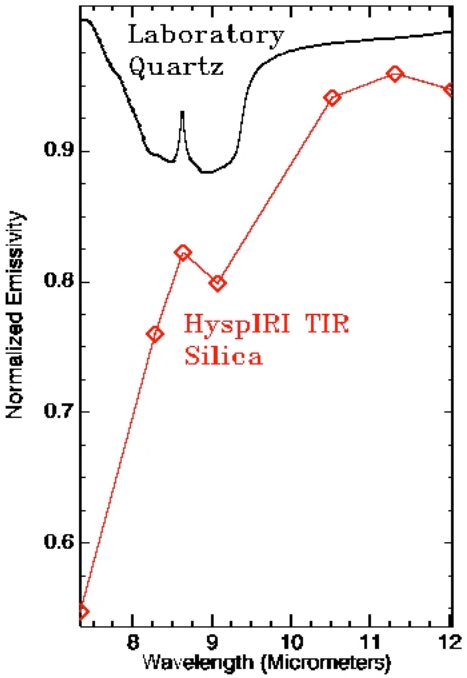

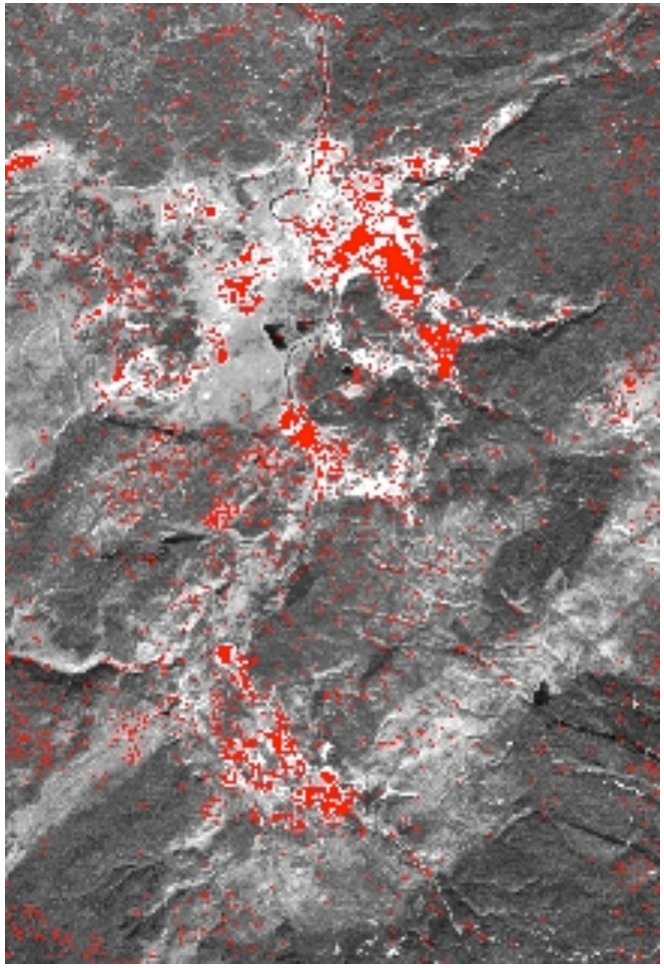

MTMF LWIR Silica Map

F. A. Kruse ♦ 303-499-9471 ♦ fakruse@nps.edu ♦http://www.nps.edu/Academics/Centers/RemoteSensing

MASTER Temperature YS (Firehole River) 2006
35m Native Spatial Resolution

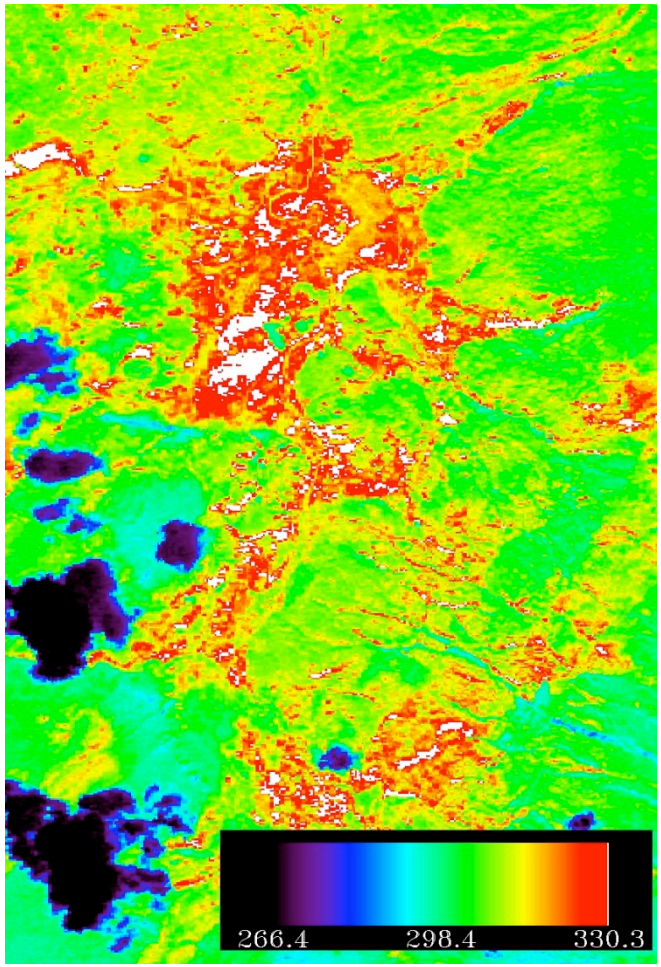

MASTER LWIR Temperature
(Density Sliced)

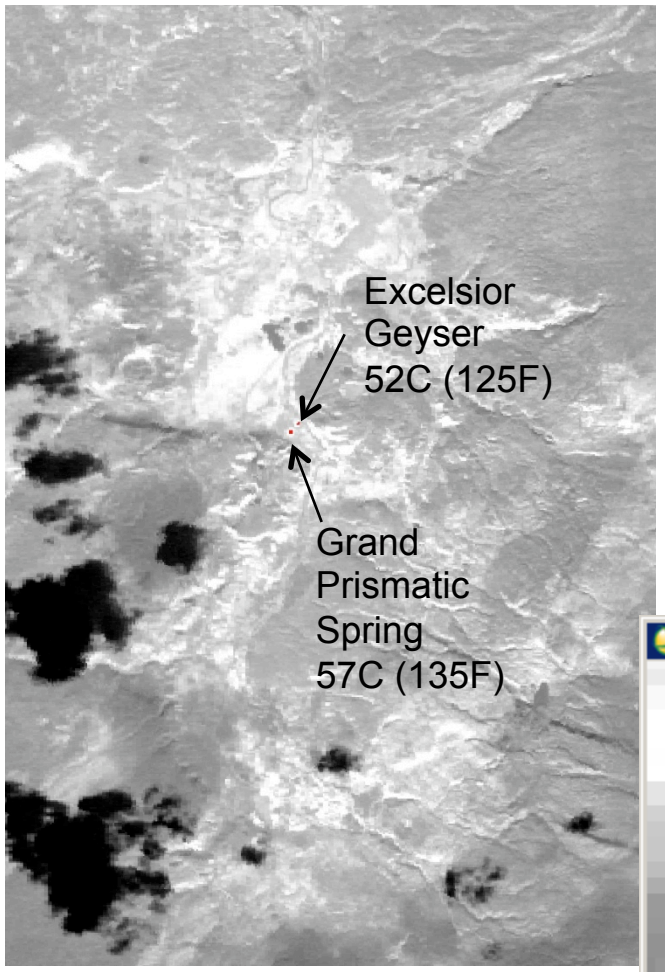

MASTER LWIR Temperature
(Temperatures >50C)

Ground-Observed
Temperatures

GP: 64 – 97C
EG: 93C

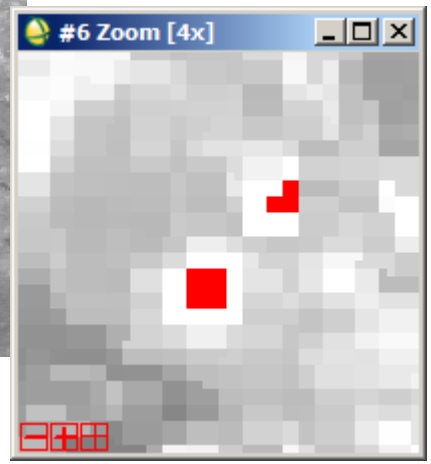

F. A. Kruse ♦ 303-499-9471 ♦ fakruse@nps.edu ♦http://www.nps.edu/Academics/Centers/RemoteSensing

MASTER Temperature YS (Firehole River) 2006
60m HyspIRI-Sim Spatial Resolution

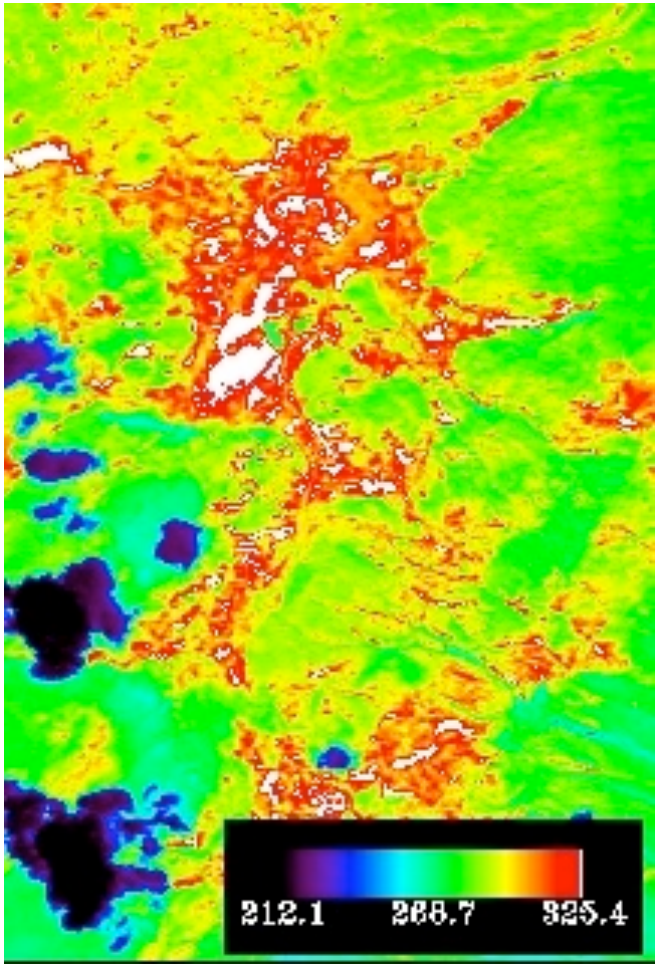

MASTER LWIR Temperature
(Density Sliced)

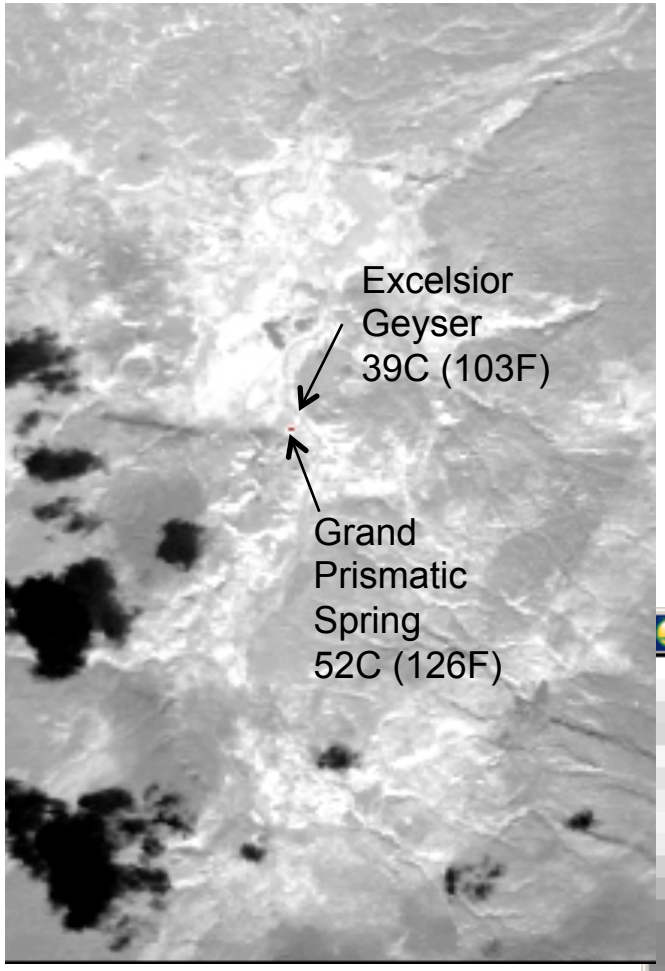

MASTER LWIR Temperature
(Temperatures >50C)

Ground-Observed
Temperatures

GP: 64 – 97C
EG: 93C

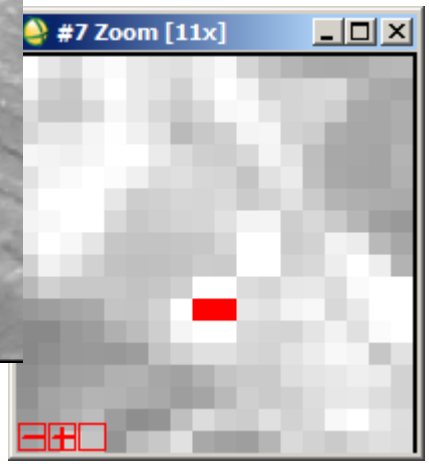

Summary and Conclusions

- **Simulations demonstrate HysplRI as a remote sensing tool for characterizing, mapping, and monitoring hydrothermal systems**
  - **SWIR spectral bands (reflectance) at ~10nm spectral resolution perform moderately well for mineral mapping**
  - **HysplRI simulated SWIR data successfully detected and mapped a wide variety of characteristic minerals, including jarosite, alunite, kaolinite, dickite, muscovite-illite, montmorillonite, pyrophyllite, calcite, buddingtonite, and hydrothermal silica at several fossil and active hydrothermal systems**
  - **60m spatial resolution doesn't strongly affect SWIR mineral mapping for most hydrothermal systems (though some smaller features lost)**

Summary and Conclusions

- **Errors of commission and omission provide insight to the causes of misclassification**
  - **Similar minerals and smaller areas of alteration are not mapped well by the simulated 60m HysplRI data**
  - **Confusion matrix analyses of the SWIR datasets show overall classification accuracy ranging from 70 to 92% for the 60m HysplRI simulated data relative to 15m AVIRIS data**
  - **Scale dependent spectral mixing due to spectral mixing with adjacent pixels appears to be the cause of most errors**

Summary and Conclusions

- **HysplRI simulated TIR bands complement the VSWIR bands**
  - **LWIR spectral bands (emissivity) provide additional mineral information**
  - **Temperature extraction provides surface temperature information critical for geothermal applications**
  - **60m spatial resolution doesn't strongly affect LWIR mineral mapping for most hydrothermal systems (though some smaller features lost)**
  - **60m spatial resolution negatively impacts temperature determinations for active geothermal systems (thermal mixing for small targets)**

Last Words

- **What will HysplRI give us that other sensors can't provide?**
  - **Combined, simultaneous VSWIR hyperspectral and TIR multispectral**
  - **Global coverage at scale that will allow development of a geographic database "inventory" of hydro/geothermal systems**
  - **Temporal monitoring (of active geothermal systems and other dynamic geologic systems)**
- **Acceptable tradeoff = principally loss of spatial detail linked to spectral mixing**

Additional Documentation

- **SWIR results published in:**

  – Kruse, F.A., Taranik, J.V., Coolbaugh, M., Michaels, J., Littlefield, E.F., Calvin, W.M., and Martini, B.A., 2011, Effect of Reduced Spatial Resolution on Mineral Mapping Using Imaging Spectrometry – Examples Using HyspIRI-Simulated Data: *Remote Sensing*, v. 3, p. 1584-1602. http://www.mdpi.com/2072-4292/3/8/1584/ (Open Access)

- **HyspIRI simulated datasets available on request**

2011 HyspIRI Science Workshop
Aug 23-25, 2011 Washington DC

Current Status of Hyperspectal Imager Suite (HISUI)

翡　翠

Tsuneo Matsunaga (National Institute for Environmental Studies)
and
Satoshi Tsuchida (AIST), Akira Iwasaki (University of Tokyo),
Jun Tanii (JAROS), Osamu Kahimura (ERSDAC),
Shuichi Rokugawa (University of Tokyo)

What is HISUI?
A Successor of Terra ASTER and ALOS AVNIR-2

- **HISUI** is a spaceborne instrument suite which consists of hyperspectral and multispectral imagers.

- **HISUI** is being developed by Japanese Ministry of Economy, Trade, and Industry (METI) as its third spaceborne optical imager mission.

  1) OPS onboard JERS-1 satellite (1992 – 1998)
  2) ASTER onboard NASA's Terra satellite (1999 -)

- **HISUI** will be launched by H-IIA rocket in 2015 or later as one of mission instruments onboard JAXA's ALOS-3 satellite

  1) ALOS (2006 -) : Optical imagers (PRISM and AVNIR-2) and L-band SAR
  2) ALOS-2 (2013 -) : L-band SAR

Targets / Objectives of HISUI Mission

1) Global energy and resource related applications
   - Oil, gas, metal, ...
   - Observations for environmental assessments which are indispensable to resource developments

2) Other applications such as environmental monitoring, agriculture, and forestry

3) Promotion of domestic space and space utilization industry through wider applications of HISUI data

"What's new" since 2010 HyspIRI Workshop

- Great East Japan Earthquake
- Instrument PDR was completed.
- Progress of operation and mission planning study
- See HISUI posters behind you
  1) Ogawa et al. "planning for Japanese future hyperspectral and multispectral senor: HISUI"
  2) Kamei et al. "Long term cal/val plan for Hyperspectral Imager Suite (HISUI)"

Great East Japan Earthquake

- On March 11, 2011, Great East Japan Earthquake occurred.
  - See Tonooka's poster behind you!
- The restoration from the earthquake and succeeding nuclear powerplant troubles requires tremendous amount of money.
- Japanese goverment is now reprioritizing the national investments on science and technology. As for space missions, the draft reprioritizing plan was issued on August 8th and being discussed.

The priorities of earth obervation satellites (draft):
- High priority missions = ASNARO 1/2, ALOS-2, GCOM-W, GPM DPR, EarthCARE CPR,,,,
- Medium priority mission = ALOS-3
- Low priority mission = GCOM-C
- HISUI's priority is currently (a little bit) higher than ALOS-3 itself.

HISUI Project Structure

METI

JOGMEC

JAROS / NEC

AIST/ERSDAC

ERSDAC

Instrument development

Calibration and data processing

Application research

Scientists from universities and national research institutes

HISUI Project

HISUI Project Team and Working Groups

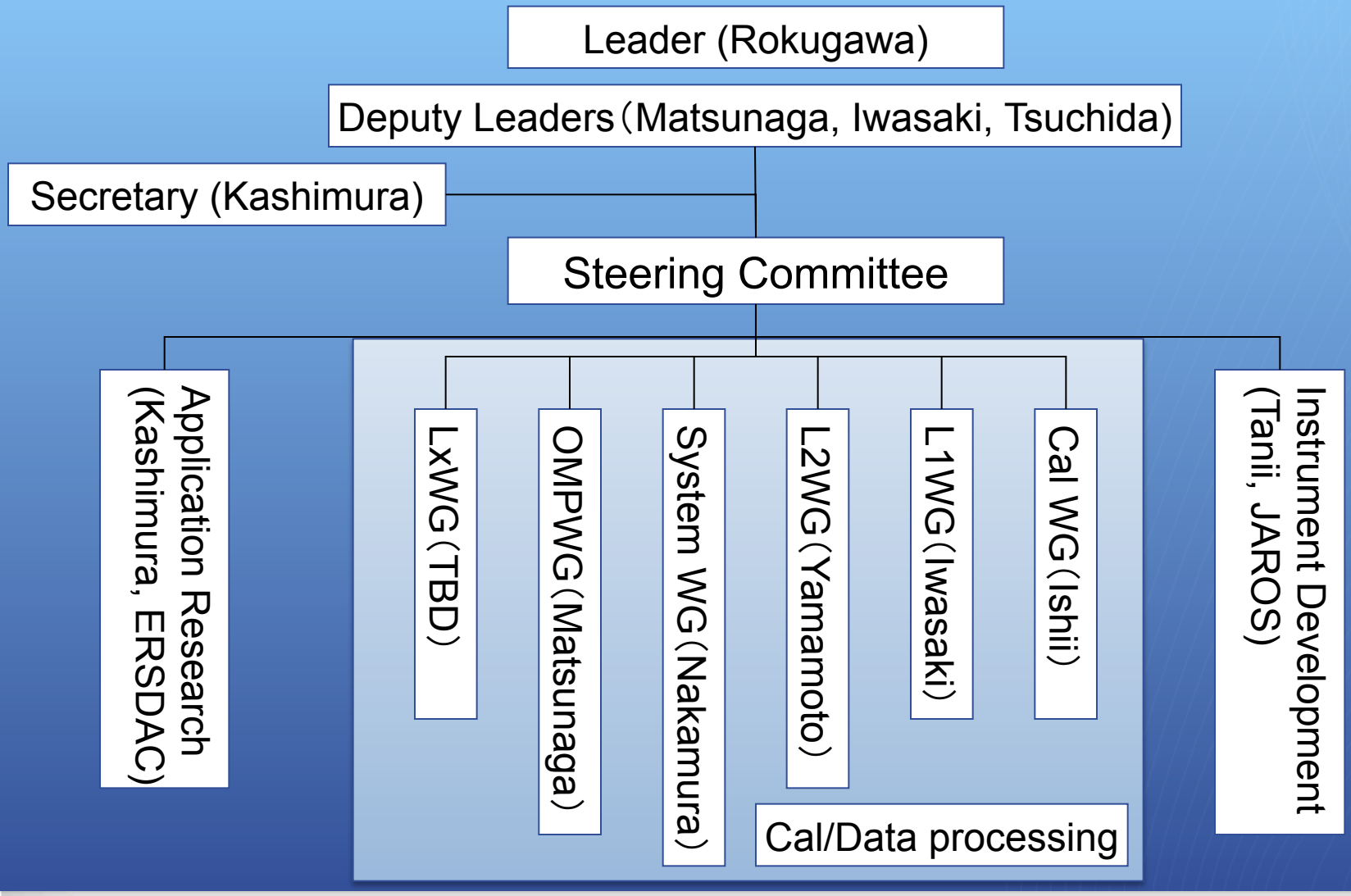

Timeline of HISUI Project

	FY2006	FY2007	FY2008	FY2009	FY2010	FY2011	FY2012	FY2013	FY2014	FY2015	FY2016
Instrument Develop-ment(NEDO/ JAROS/NEC)		*Conceptual Design*	*Preliminary Design*		*Detail Design*	PDR2	*Maintenance Design*			**Launch**	
		Evaluation Model				*PFM*					
In-flight Verification (TBD)									*Integration*		
							Development of Data Receiving / Instrument Monitoring System			*Inflight verification*	*Nominal operation*
Application Research (METI/ ERSDAC)		*Application Research*									
		Developement of Spectral Database									
Metal Resource Exploration (METI/ JOGMEC)				*Developement of Data Analysis Methodologies*							
Calibration /Data Processing (METI/ AIST/ ERSDAC)					*Research on calibration and data processing*						
					Ground Data System Study						
					Operation / Mission Planning Study						

JAXA's ALOS-3 and HISUI

HISUI

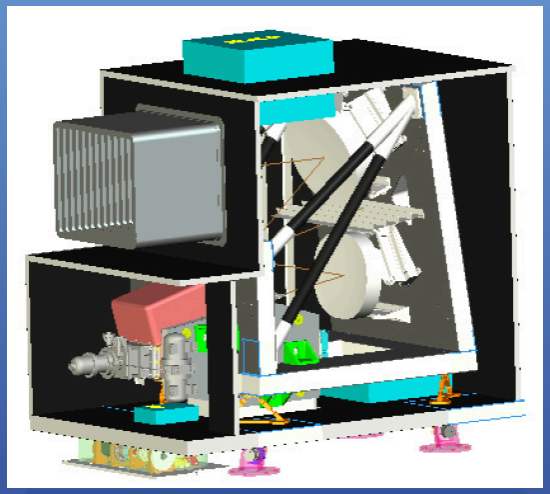

Hyperspectral Imager

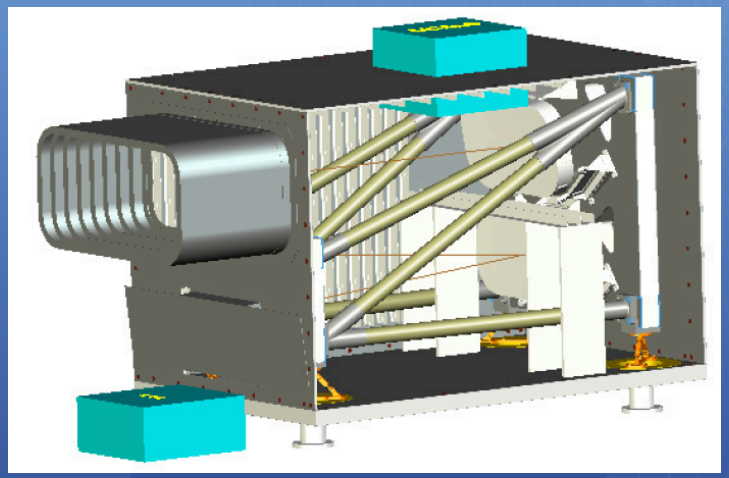

Multispectral Imager

HISUI Requirements: Hyperspectral Imager

Parameter		Requirement
Spatial Resolution and Swath Width		30 m and 30 km
Spectral	Bands	185 (VNIR:57 SWIR:128)
	Range	0.4 - 2.5 μm VNIR:0.4-0.97 μm SWIR:0.9-2.5 μm
	Resolution	10 nm (VNIR), 12.5 nm (SWIR)
Signal to Noise Ratio (30% albedo)		≥ 450 @620 nm ≥ 300 @2100 nm
MTF		≥ 0.2
Dynamic Range		≥ 10 bits (current design=12bit)
Data Compression		Lossless (70%)
Pointing Capability		≈ ±3 ° (±30 km)

HISUI Requirements: Multispectral Imager

Parameter	Requirement
Spatial Resolution and Swath Width	5 m and 90 km
Number of Bands and Spectral Coverage	4 and 0.45 – 0.90 μm
Signal to Noise Ratio (30% albedo) and MTF	≥ 200 and ≥ 0.3
Dynamic Range	≥ 8 bits (current design = 12bits)
Data Compression	Lossless (70%)

Specification of JAXA's ALOS-3 and Panchromatic Stereo Camera

Orbit Type and Altitude	Sun Synchronous, ≈ 618 km
Local Time At Descending Node	10:30 (TBD)
Orbits per Day	15 orbits/day (TBD)
Repeat Cycle and Interval between Orbits	60 days and 45 km(TBD)
Launch Vehicle	H II-A
Downlink Capability	800 Mbps (TBD)
Onboard Storage	> 200 GB (TBD)

Parameters of JAXA's Panchromatic Stereo Camera	Requirement
Spatial Resolution and Swath Width	0.8 m(nadir) and 50 km
Data Compression	Lossy (22%)

Instrument Development

Chracterization of VNIR Spectrometer Engineering Model

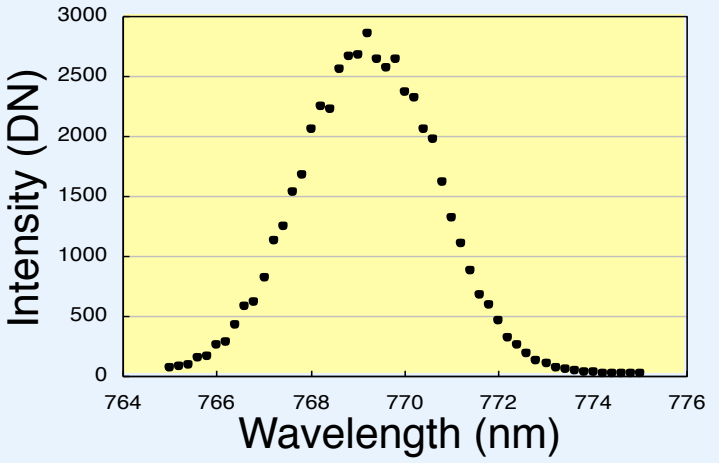

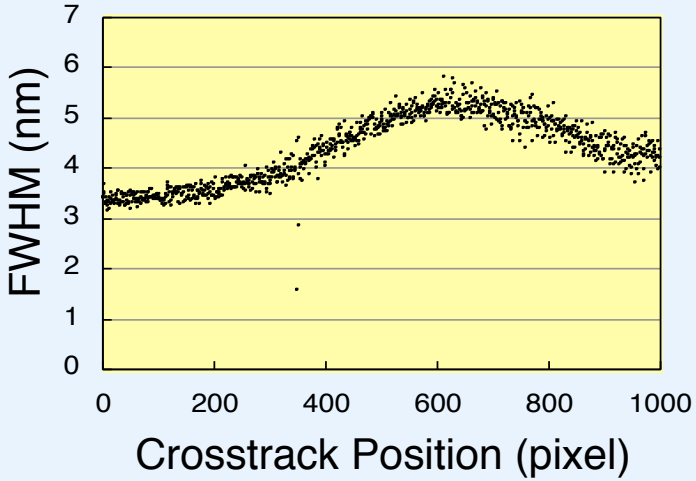

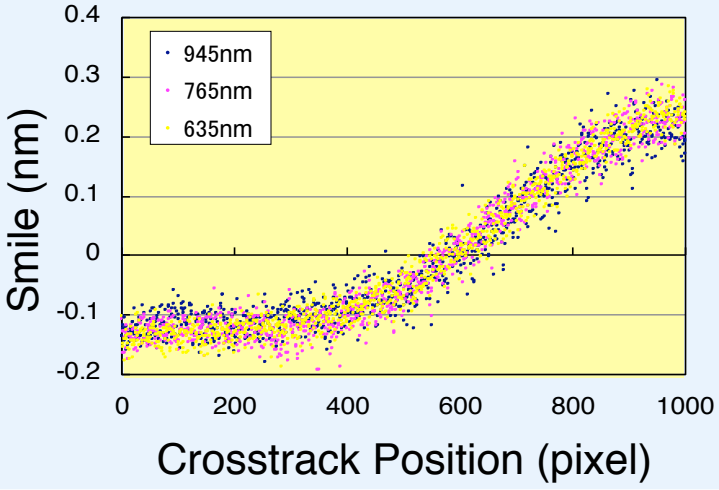

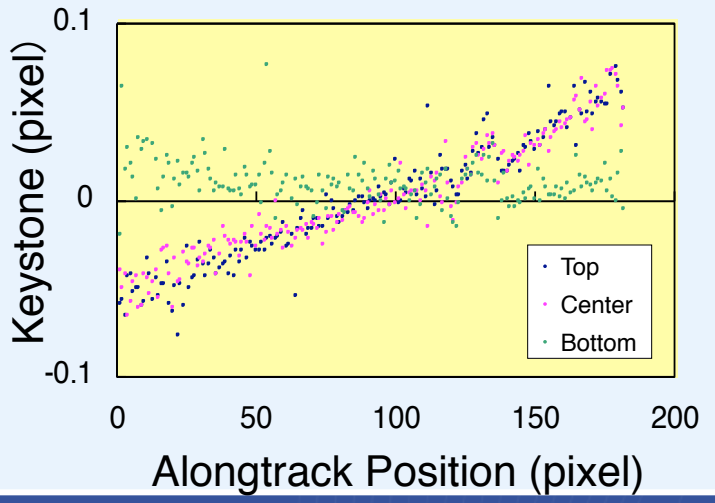

HISUI and ALOS-3
Data Amount and Downlink

	Data Rate (70% Comp.)	Maximum Observation Time per Orbit	Maximum Data Amount per Orbit	Maximum Data Amount per Day
HISUI - Hyper	0.4 Gbps	15 min.	46 Gbyte	690 Gbyte
HISUI - Multi	1 Gbps	15 min.	110 Gbyte	1600 Gbyte

	Downlink Speed	Downlink Time per Day	Data Amount per Day
Ground Station	800 Mbps	20 min.	120 Gbyte
Relay Satellite	800 Mbps	220 min.	1320 Gbyte

- HISUI will share ALOS-3's downlink capability with JAXA's panchromatic camera.
- Allocation of ALOS-3 downlink capability to HISUI is a critical issue.

HISUI Operation / Mission Planning Study
Simulation of HISUI Hyperspectral Observation

- Hyperspectral observation baseline
  - Periodical calibration data acquisition (once in a week)
  - Observation of priority areas in earliest oppotunity
    ≈ 24 % of whole land surface and shallow sea
  - Periodical nighttime SWIR observation of volcanoes
    ≈ 100 high priority and ≈ 900 low priority volcanoes from ASTER STAR database.
  - Global land mapping using remaining resources

- Major constraints
  - Opertion time = 15 minutes/orbit
  - Downlink = Six cases (50, 100, 150, 200, 250, and 300 GByte/day)
  - Cross track pointing frequency => In this study, only for to fill gaps between orbits.

- Other constraints and conditions
  - Five observation segments in one orbit
  - Avoid sunglint for shallow sea observation
  - Simulation period = one year starting from Autumnal Equinox
  - Mid- and high latitude zones are observed only in summer.

HISUI Operation / Mission Planning Study

Tentative Global Priority Map

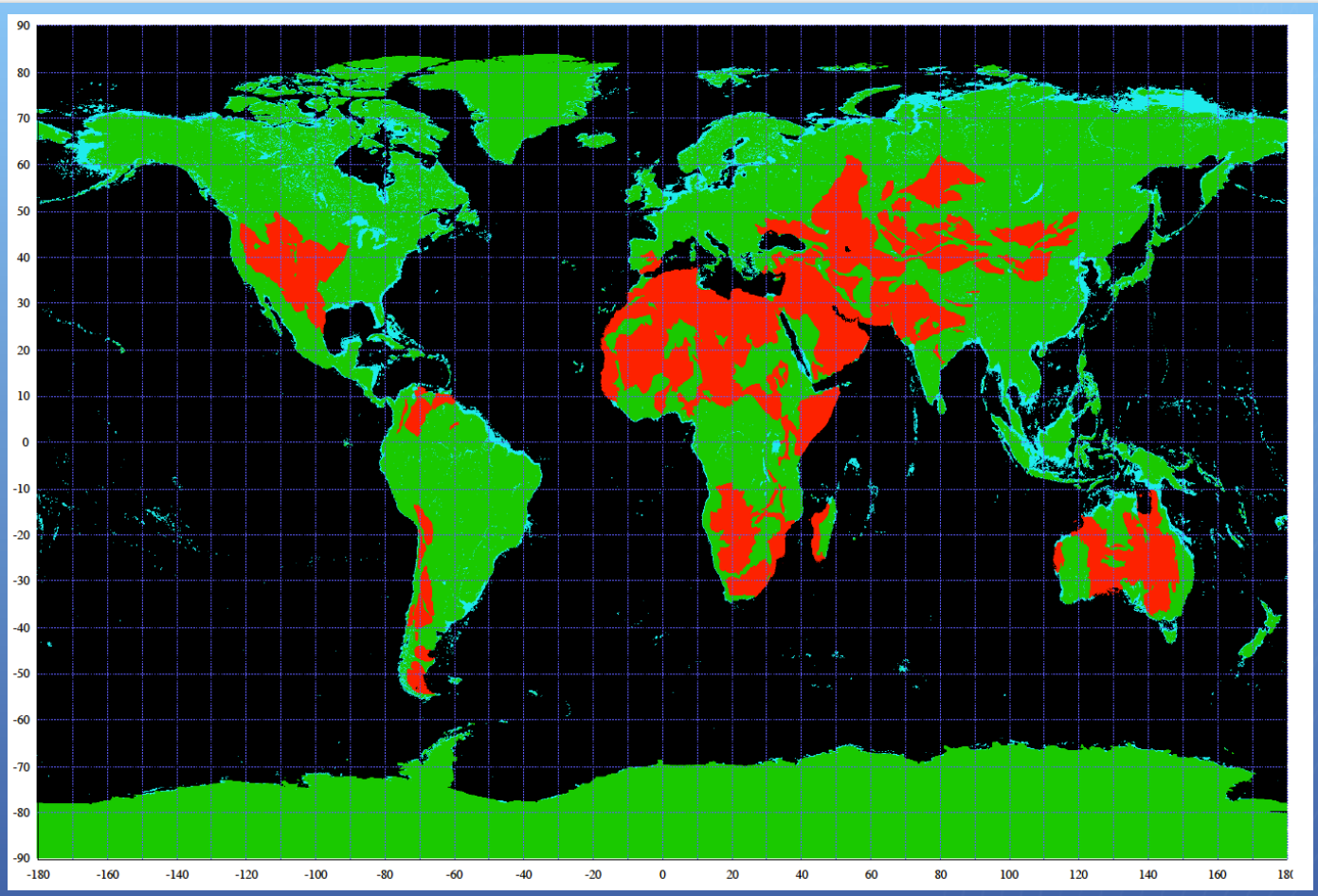

Red : Priority areas, Green : Other land areas, Light blue : Shallow sea

HISUI Operation / Mission Planning Study

Global Land Cover Type and Volcanoes

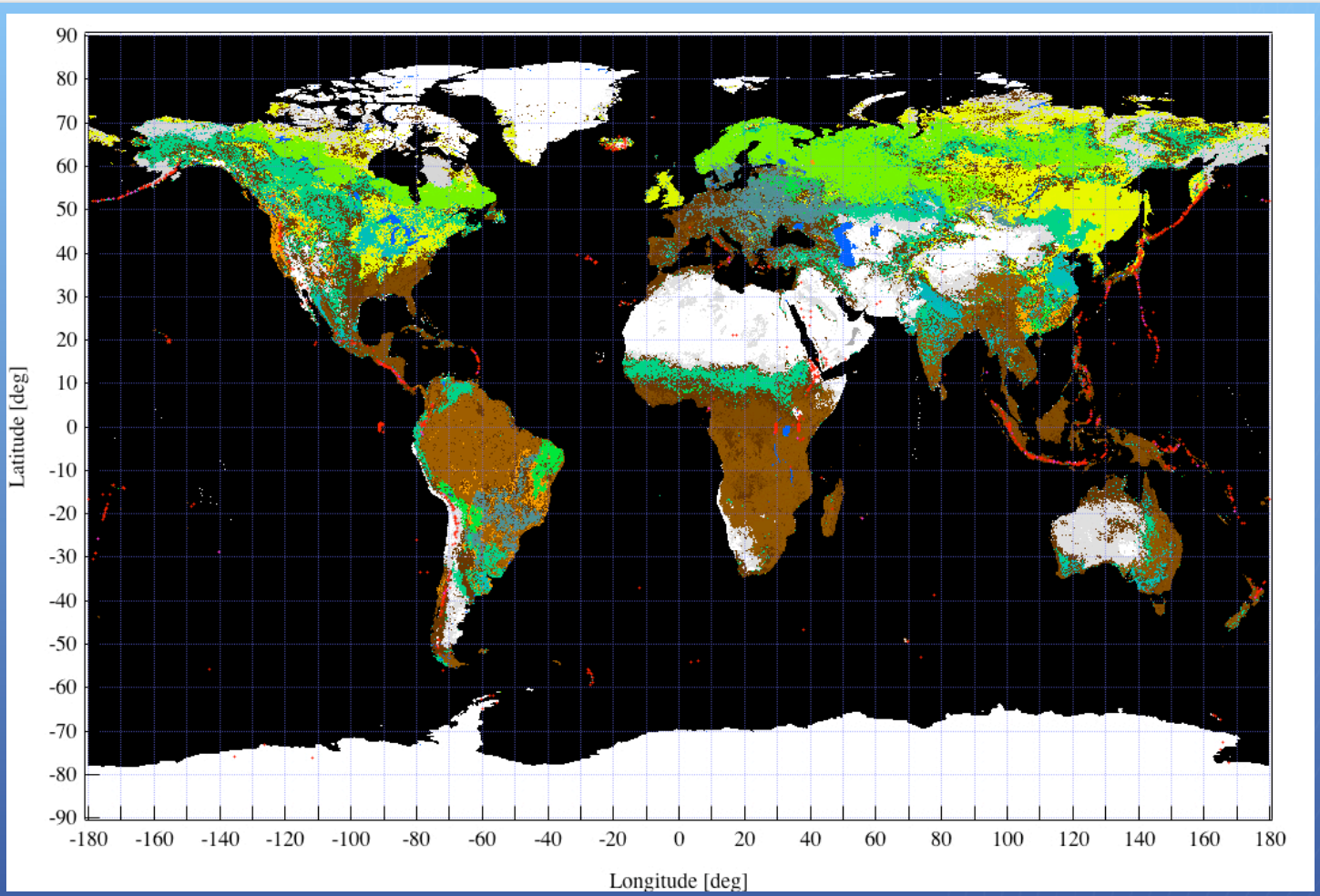

Red points : Volcanoes from ASTER STAR database

HISUI Operation / Mission Planning Study

Achievement of Priority Areas Mapping

Days	Achivement of priority areas mapping		
	50G	100G	200G
60	22.56	46.19	78.22
120	43.75	78.93	79.62
180	49.23	91.01	99.74
240	61.06	99.50	100.00
300	81.87	99.72	100.00
360		99.90	100.00

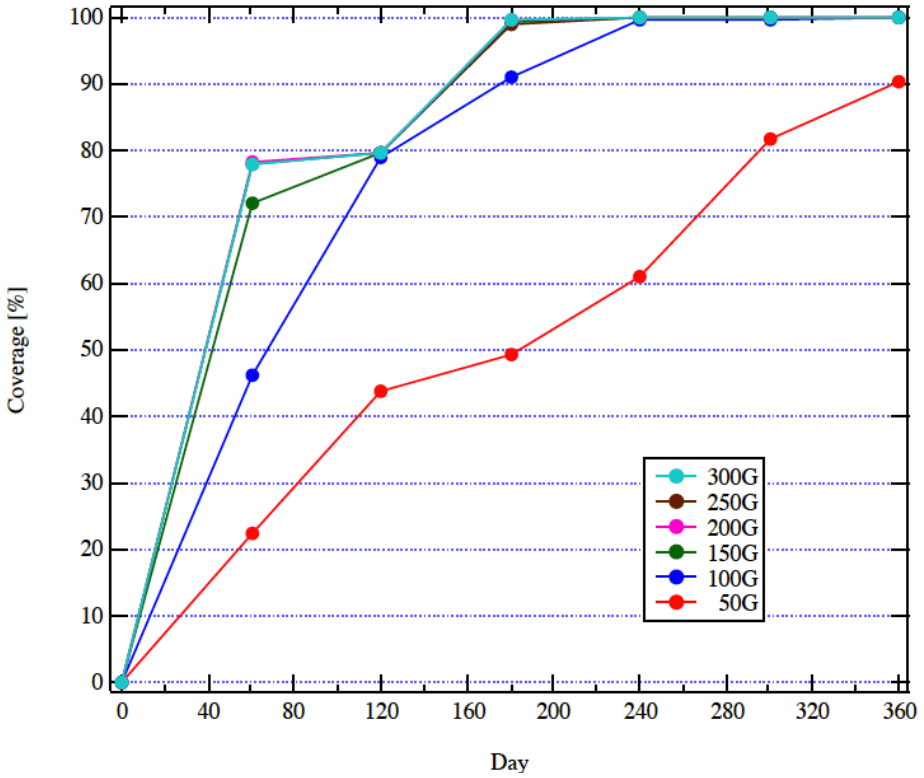

One-time observation of priority areas can be achieved within 6-8 months in case of 100 GB/day or more downlink.

HISUI Operation / Mission Planning Study
Nighttime SWIR Volcano Monitoring

50 GB/Day

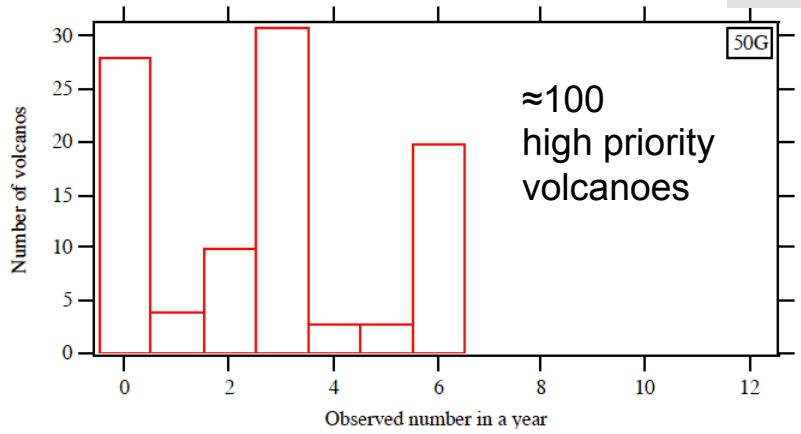

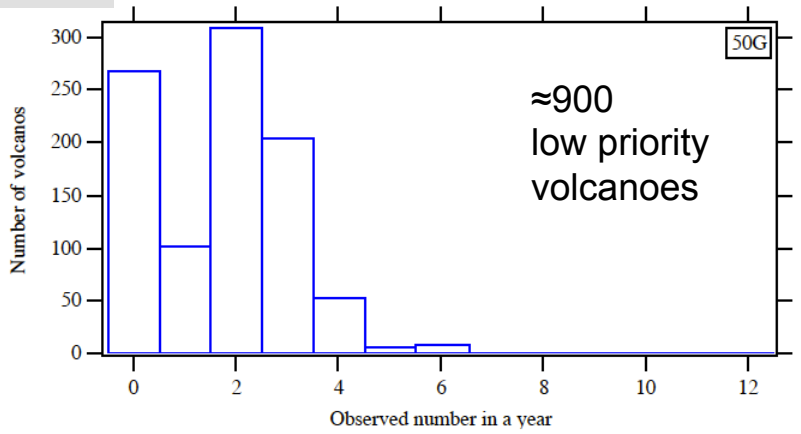

250 GB/Day

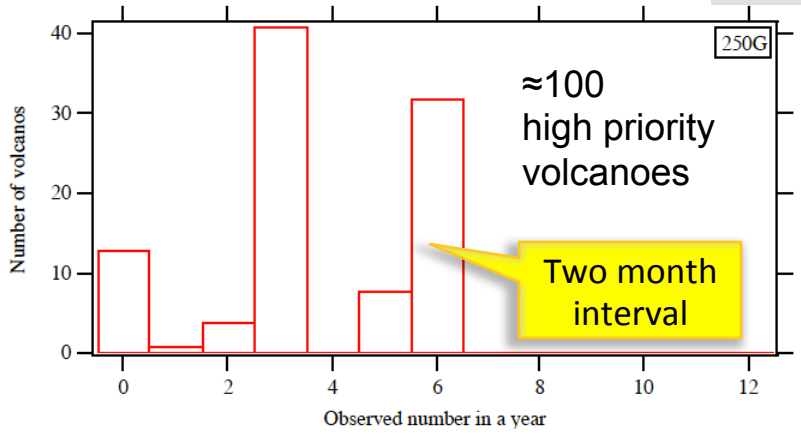

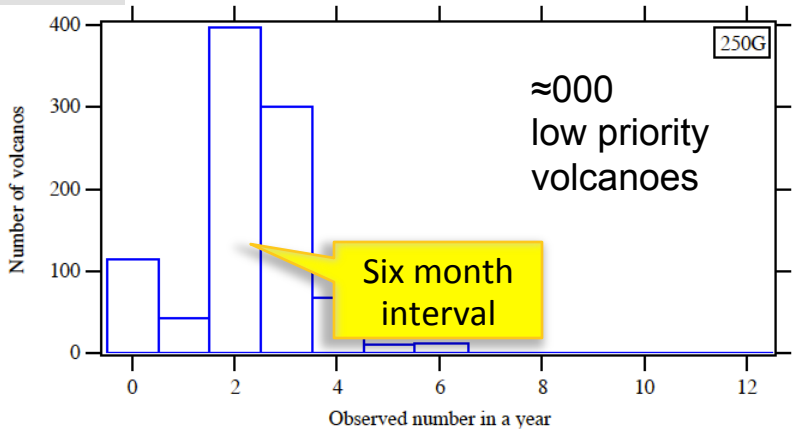

HISUI Operation / Mission Planning Study

Achievement of Global Mapping

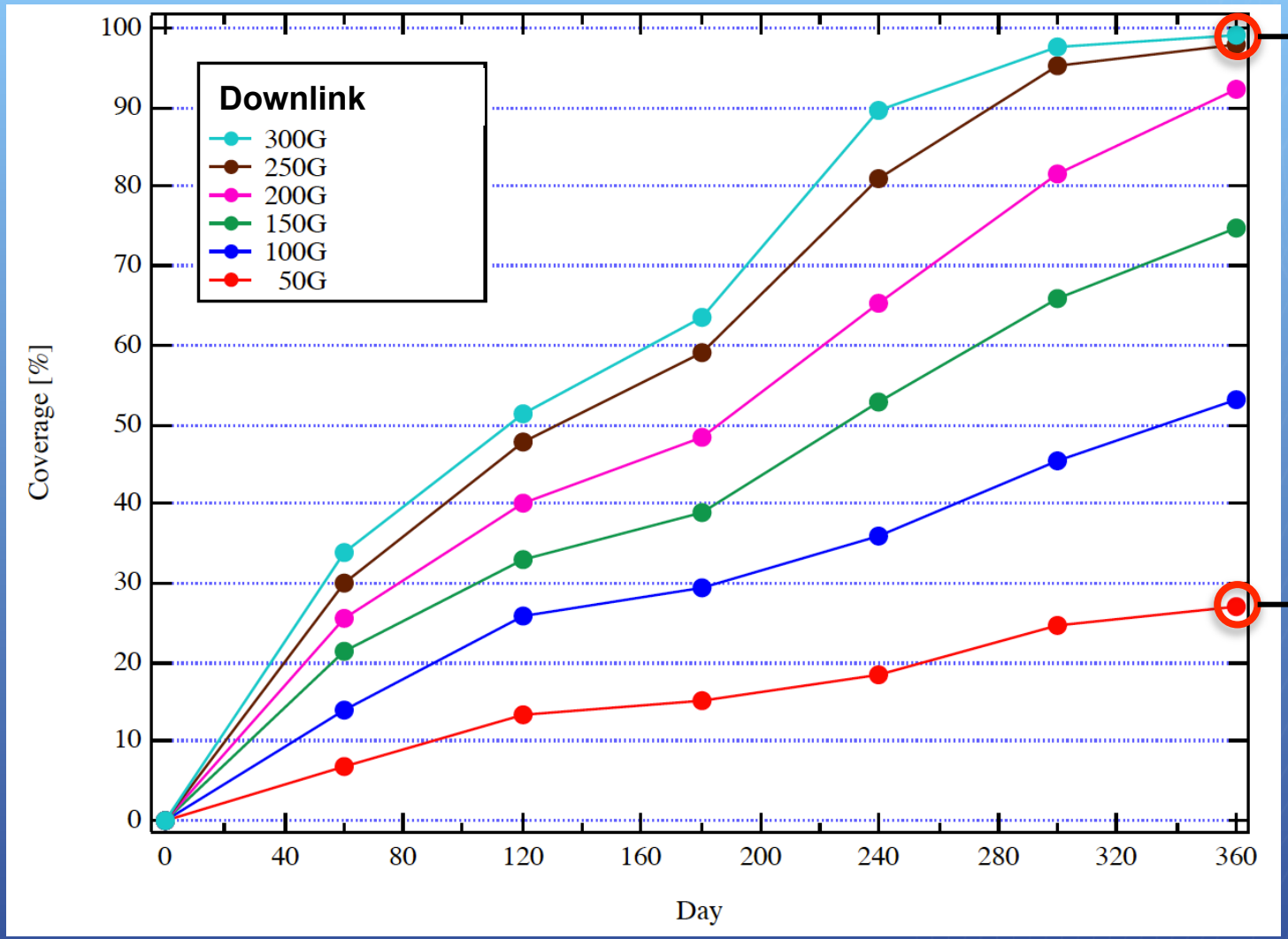

HISUI Operation / Mission Planning Study

Month of Observation (300 GB/Day case,1 year)

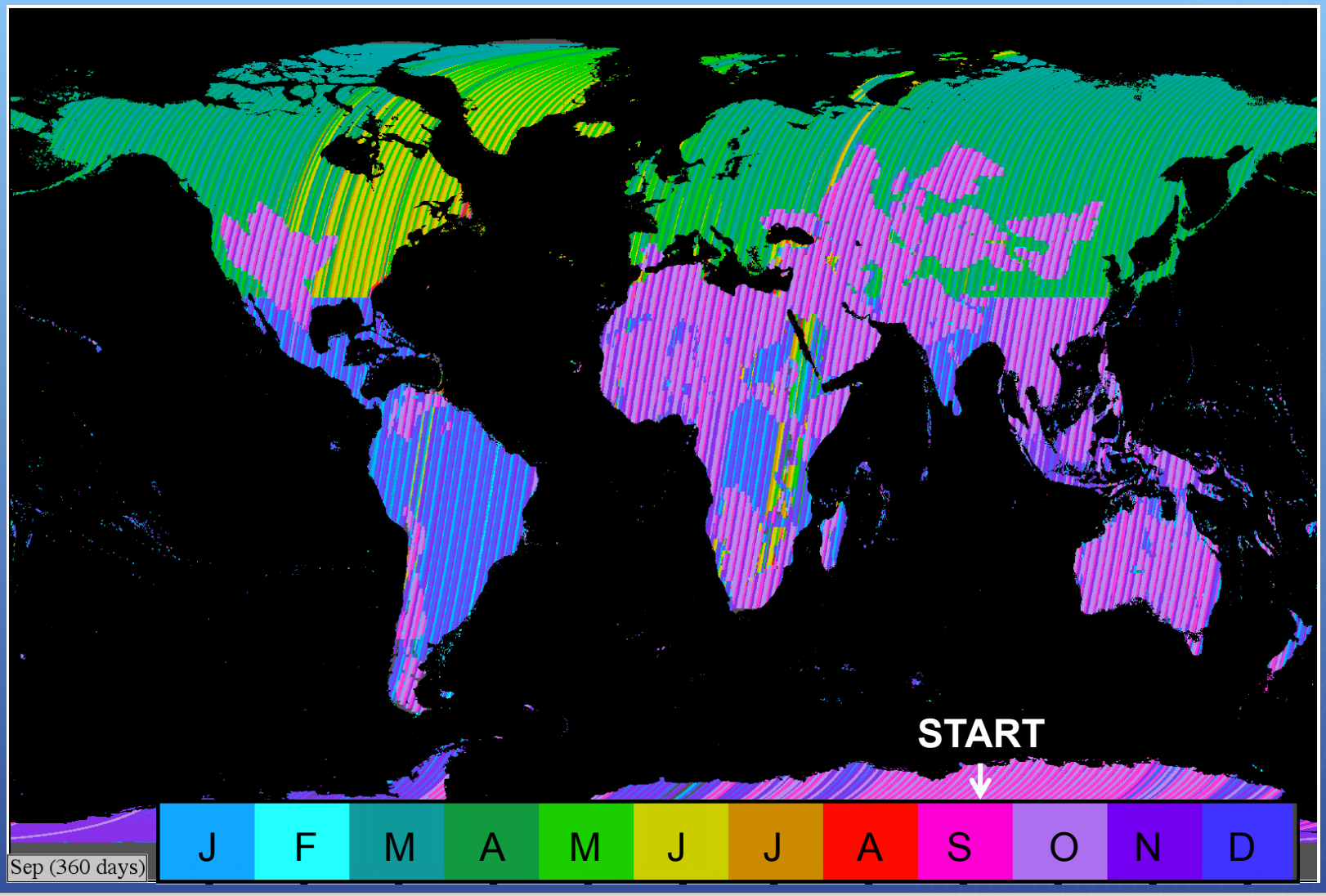

HISUI Operation / Mission Planning Study

Month of Observation (50 GB/Day case, 1 year)

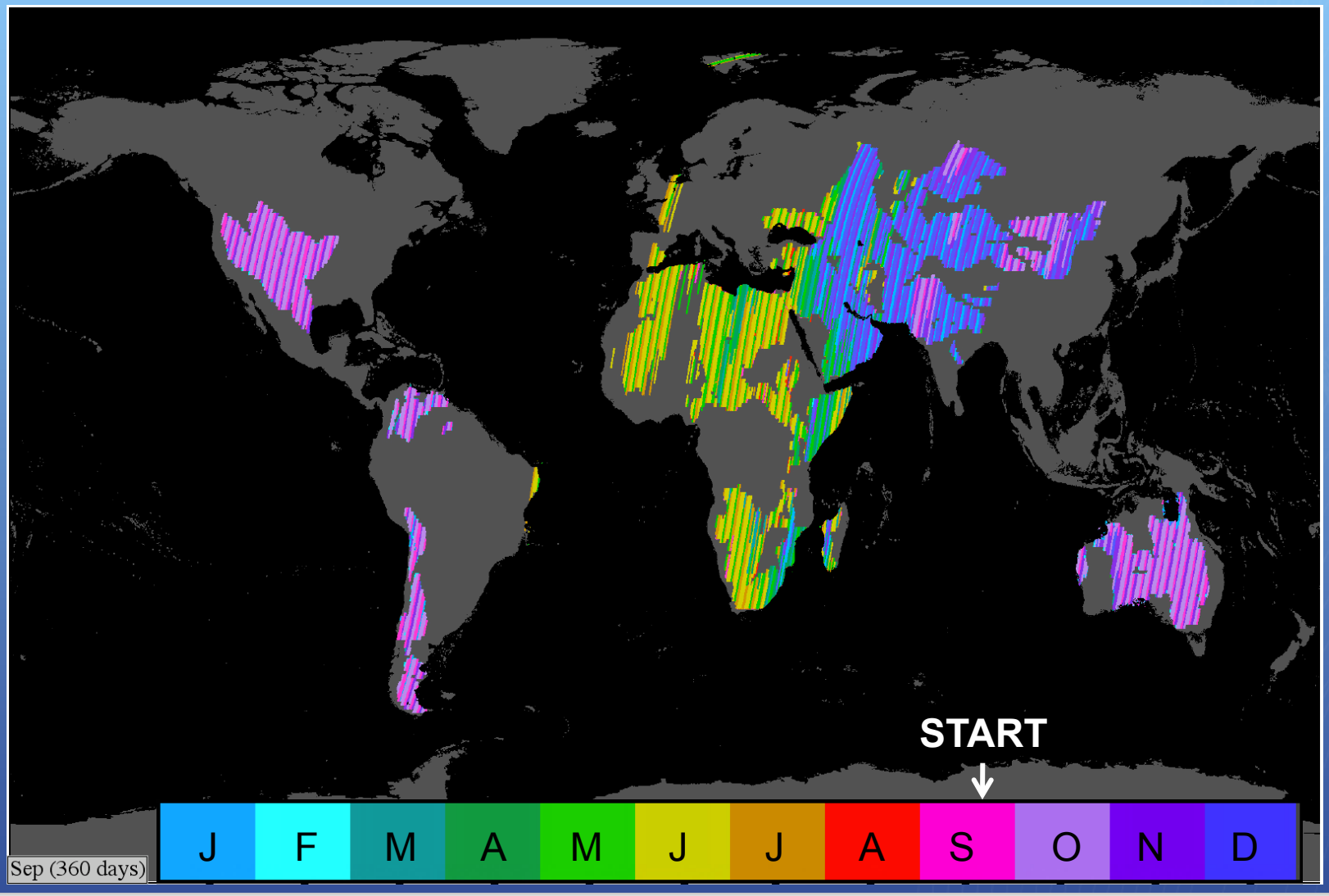

Thank you

Onboard Instrument Processing Concepts for the HyspIRI Mission

Steve Chien, Dorothy Silverman, David Mclaren,
Gregg Rabideau, Ashley Davies
Jet Propulsion Laboratory, California Institute of Technology

Daniel Mandl, Goddard Space Flight Center

Jerry Hengemihle, Microtel LLC

© Copyright 2011, California Institute of Technology, Government sponsorship acknowledged.
JPL Clearance # CL 10-2396.

Direct Broadcast Heritage

- Direct Broadcast is a technology which enables downlink of instrument data during acquisition (e.g., MODIS)
- In current use, DB downlinks all of the data acquired by the instrument

HyspIRI Direct Broadcast

- HyspIRI TIR + VSWIR will produce 800 x 10^6 bits per second (raw uncompressed)

- In order to use heritage technology groundstations HyspIRI DB will have an effective rate of 10 x 10^6 bits per second (uncompressed)
  - Even assuming 4:1 compression we have a 20x oversubscription

HyspIRI DB Concept

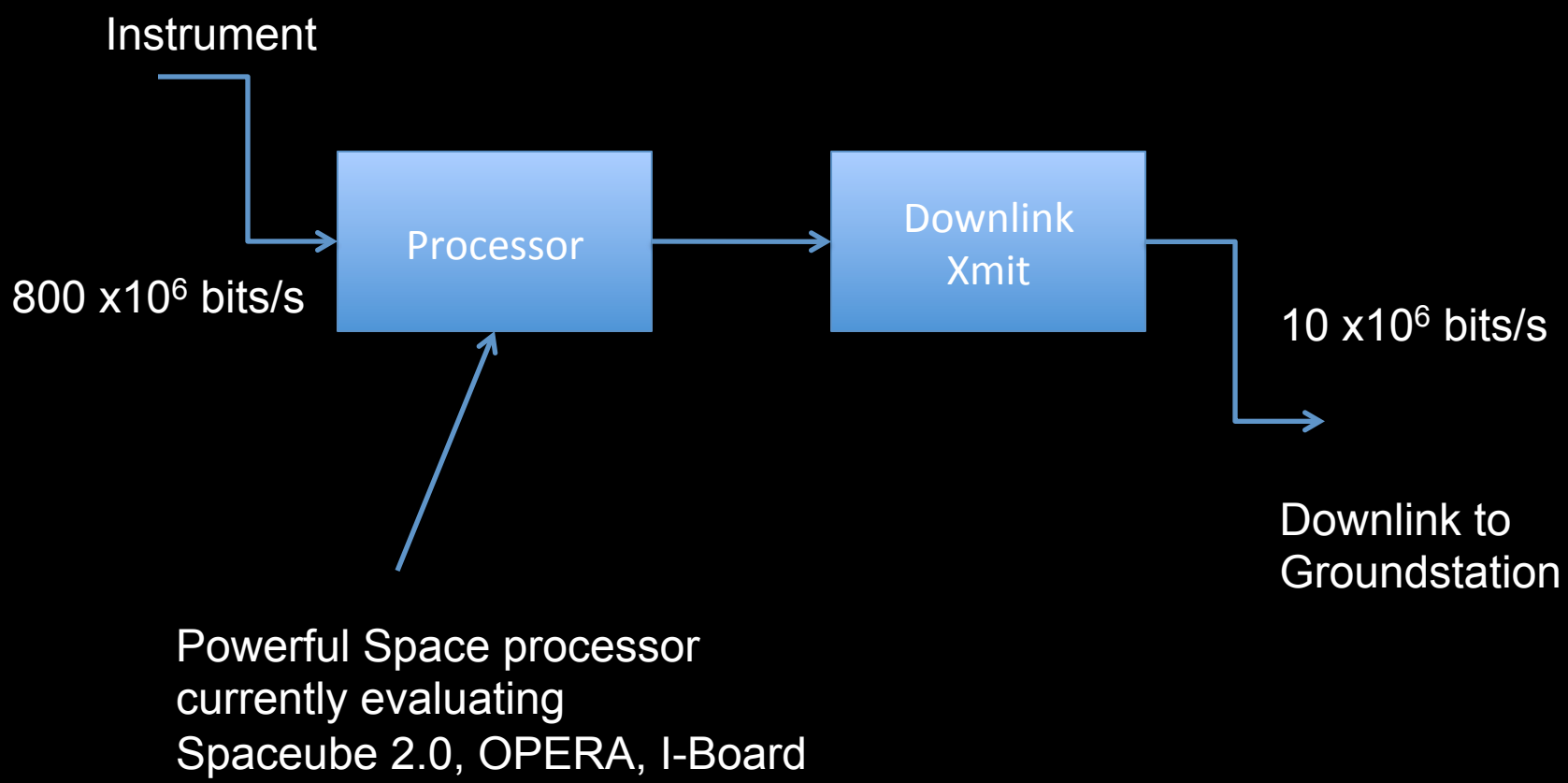

Operations for HysplRI DB

- Users specify “areas of interest” which are
  - geographical regions (polygon on surface of Earth)
  - product, (e.g. normalized burn index)
  - priority, (e.g. 50 on 1-100 scale)
  - Constraint (sun must be at least 20 degrees above horizon)
- In generic tool (e.g. Google Earth)

Instrument Swaths

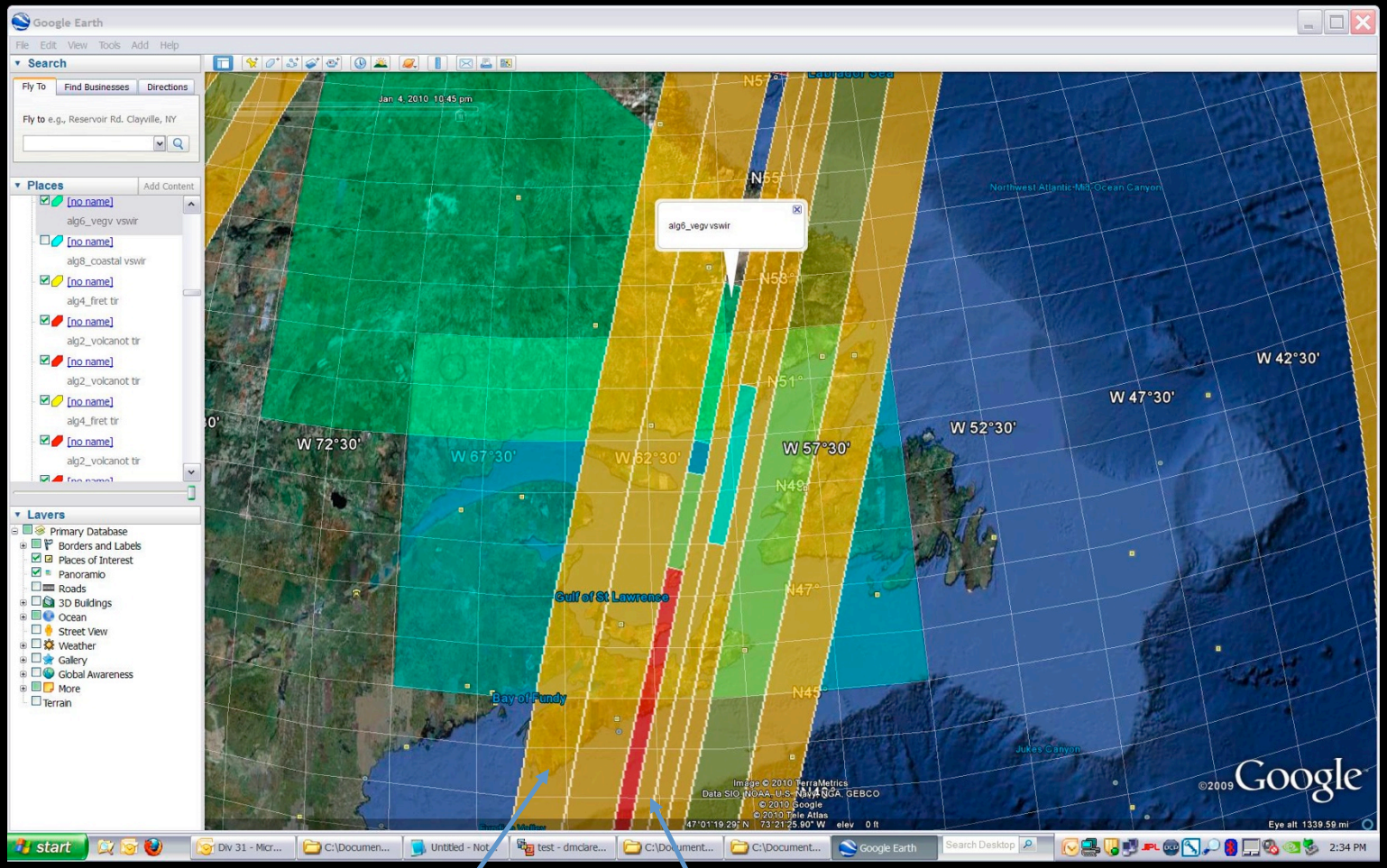

4 x 112.5.5 km wide –TIR only

4 x 37.5 km wide – VSWIR + TIR

Automated Operations Planning

- Automated Planning tool selects highest priority products while respecting
  - Visibility (instrument swaths)
  - Onboard CPU limits
  - Downlink data limits
- Result is a time ordered sequence of commands to process instrument data from each of 8 instrument swaths

Sample Plans

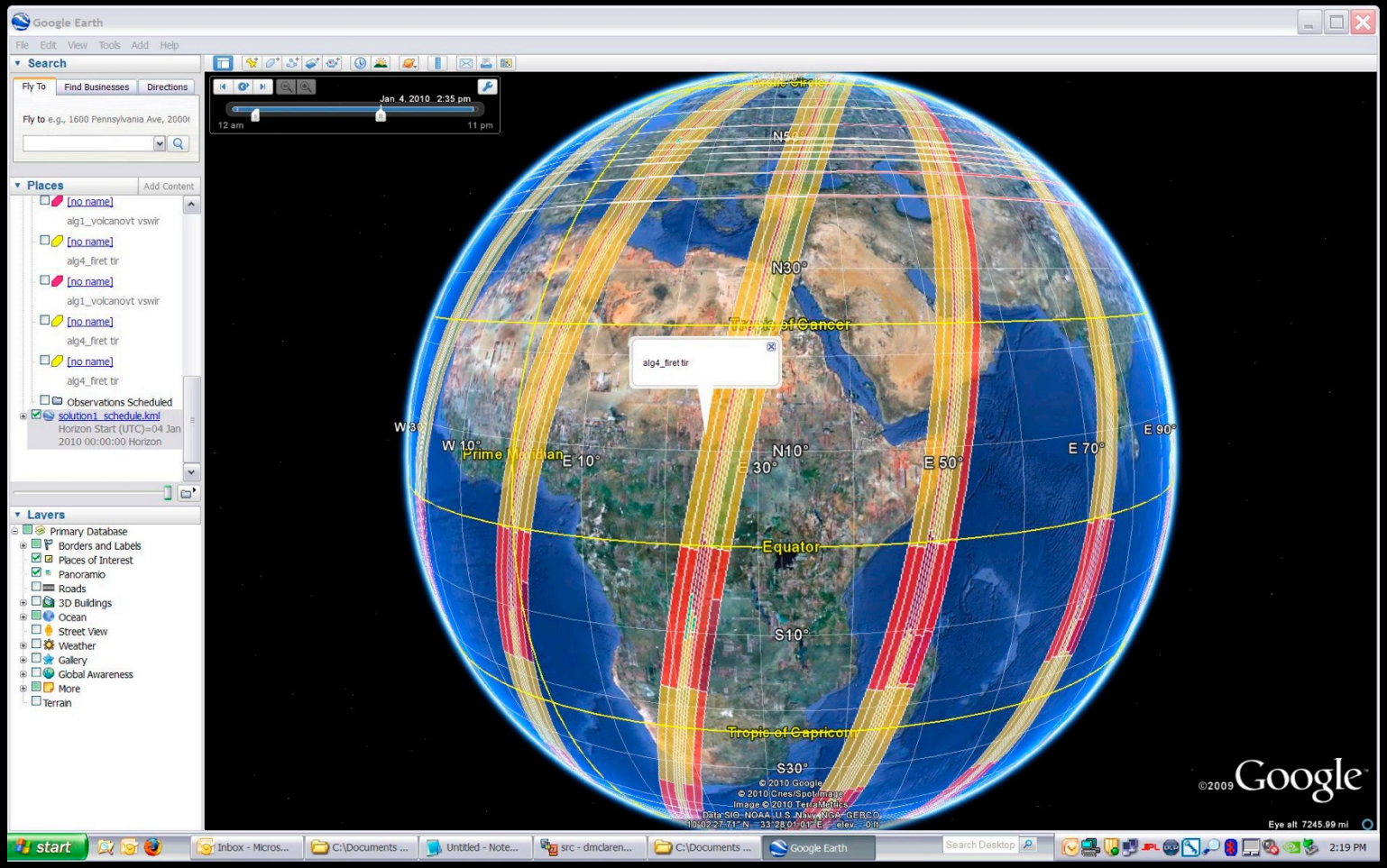

More Plans

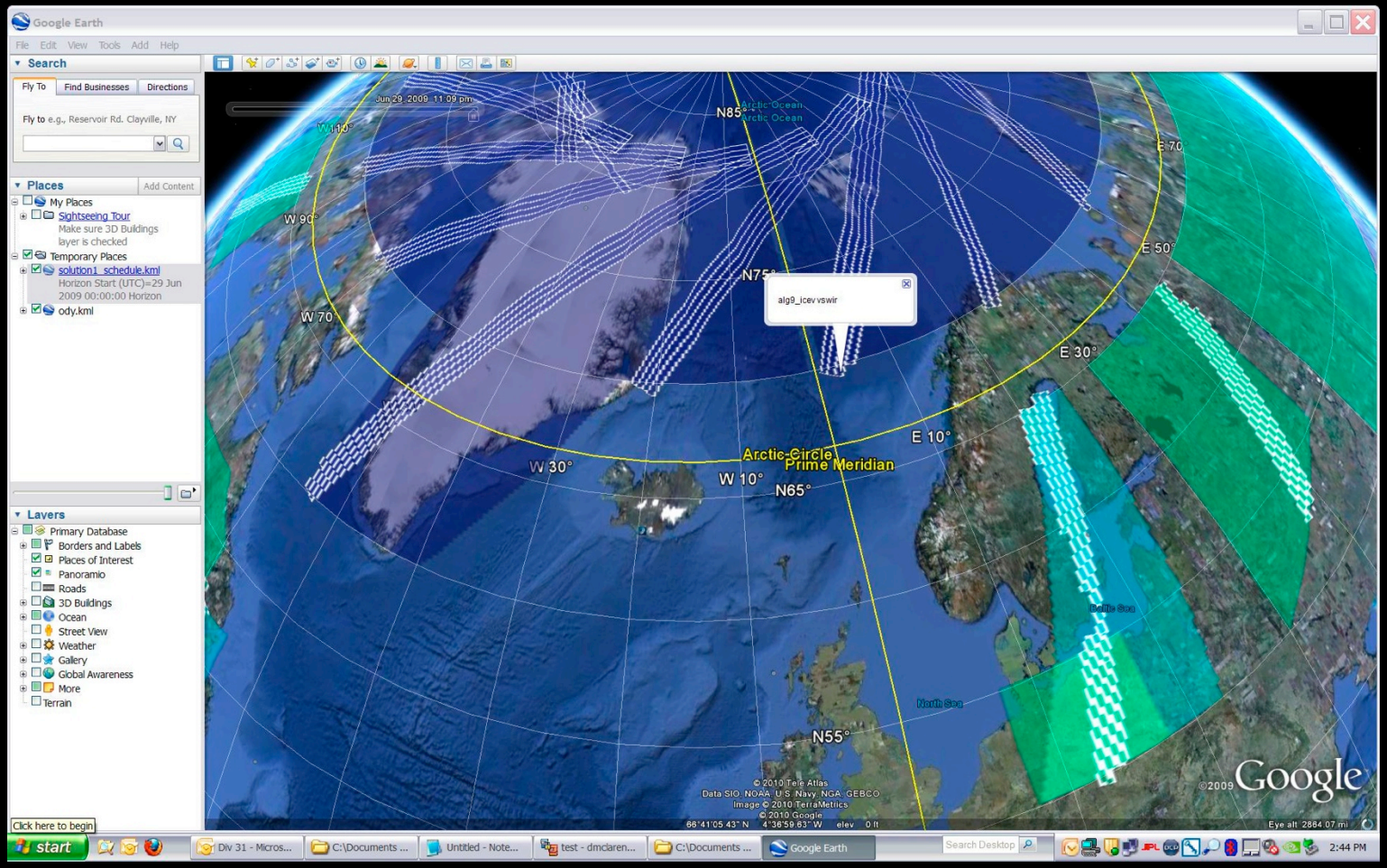
Google Earth
File Edit View Tools Add Help
Search
Fly To
Find Businesses
Directions
Fly to e.g., Reservoir Rd. Clayville, NY
Places
Add Content
My Places
Sightseeing Tour
Make sure 3D Buildings layer is checked
Temporary Places
solution1_schedule.kml
Horizon Start (UTC)=29 Jun 2009 00:00:00 Horizon
ody.kml
Layers
Primary Database
Borders and Labels
Places of Interest
Panoramio
Roads
3D Buildings
Ocean
Street View
Weather
Gallery
Global Awareness
More
Terrain
Click here to begin
Jun 29, 2009 11:09 pm
Arctic Ocean
N85°
W 110°
E 70°
W 90°
E 50°
N75°
alg9_icev vswir
W 70°
E 30°
E 10°
Arctic Circle
Prime Meridian
W 30°
W 10°
N65°
Baltic Sea
North Sea
N55°
© 2010 Tele Atlas
Data SIO, NOAA, U.S. Navy, NGA, GEBCO
Image © 2010 TerraMetrics
© 2010 Google
66°41'05.43" N 4°38'59.83" W elev 0 ft
Eye alt 2884.07 mi
©2009 Google
start
Div 31 - Micros...
C:\Documents ...
Untitled - Note...
test - dmclaren...
C:\Documents ...
Google Earth
Search Desktop
2:44 PM

HysplRI DB Applications

- Volcanos
- Fires
- Flooding
- Cryosphere
- Ocean

- Applications allows spatial and spectral subsampling (bands and products) to reduce needed downlink volume, and prior heritage

Heritage (onboard) – EO-1/ASE Thermal Detection

- EO-1
  - Onboard thermal event detection in use since 2004 based on onboard Hyperion spectral signature
  - Uses spectral slope in 1.65-2.28μ
  - Onboard event detection can trigger:
    - Subsequent imaging
    - Alert Notices
    - Generation of thermal summary and quicklook context images
    - Ground-based automatic data product generation and distribution

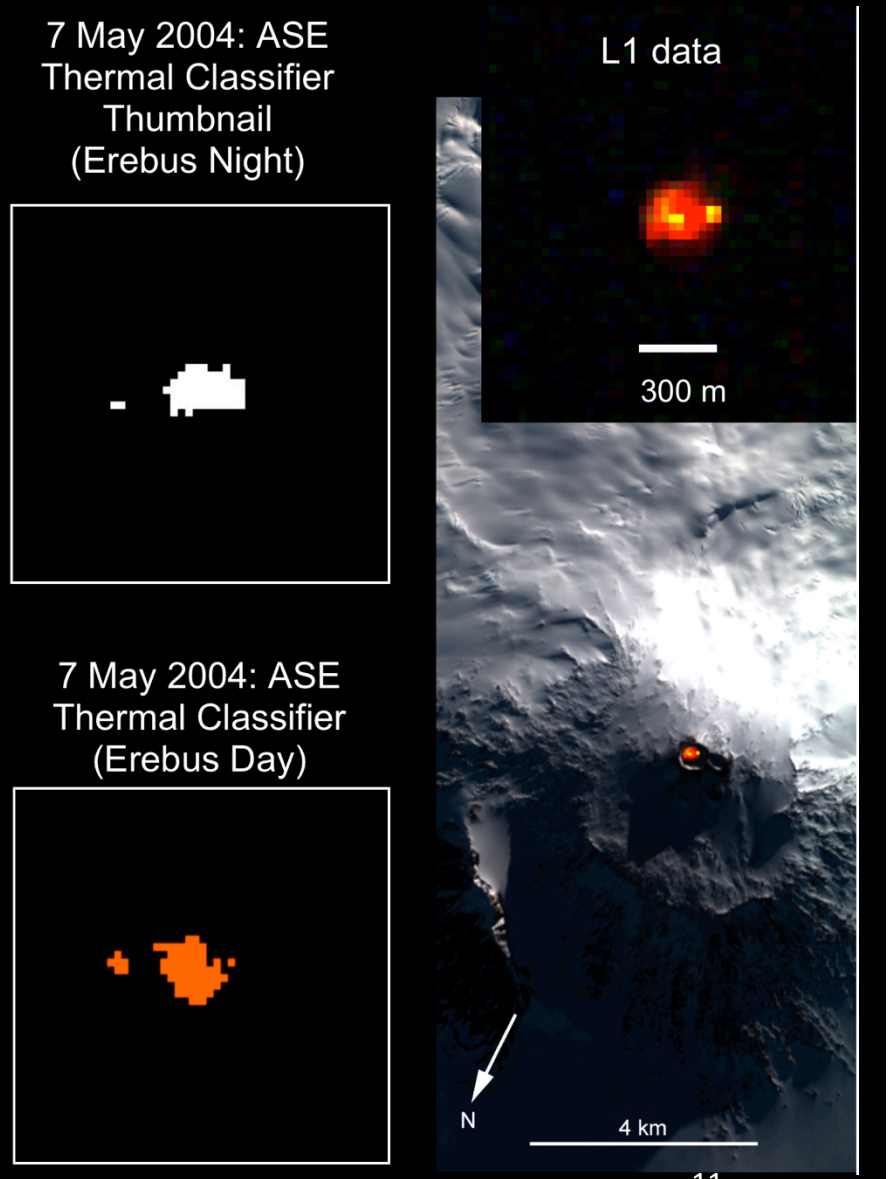

Courtesy [Davies et al. 2006]

Heritage – ground-based MODIS Active Fire Detection

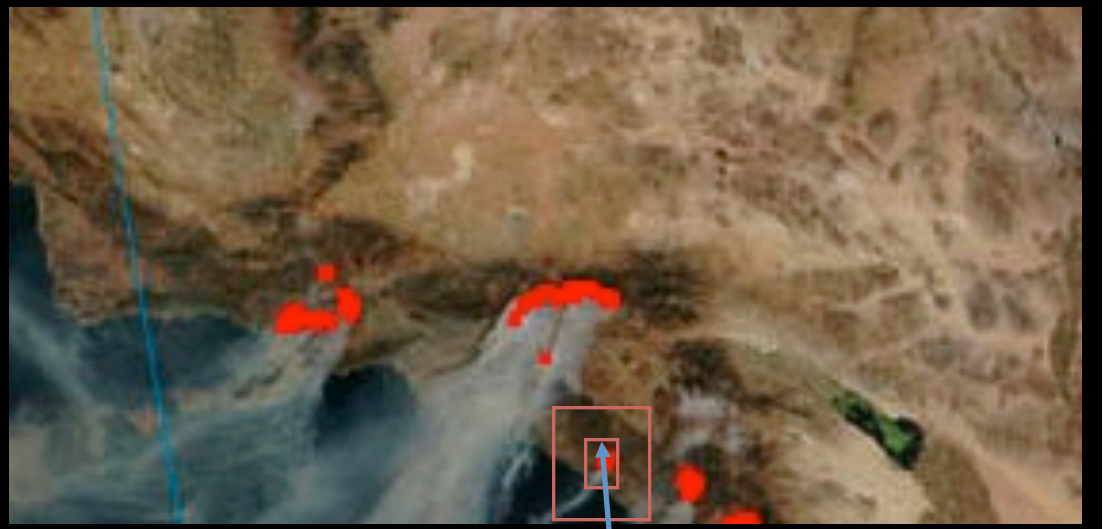

- Detects hotspots using
  - absolute threshold
    - T_4>360K, 330K(night) or
    - T_4>330K, 315K(night) and T_4-T_{11}>25K(10K @ night)
  - and relative threshold
    - $T_4 > \text{mean}(T_4) + 3\text{stddev}(T_4)$ and $T_4 - T_{11} > \text{median}(T_4-T_{11}) + 3\text{stddev}(T_4-T_{11})$

Looks for areas significantly hotter than surrounding area (requires 6 surrounding pixels cloud, water, fire free → 21x21)

C. Justice et al.

Fires – Burn Scar

Visible and burn scar enhanced images from ALI instrument on EO-1 of Station Fire near Los Angeles 03 September 2009

Images courtesy EO-1 Mission NASA GSFC

Burn scar: 0.76-0.90μm, 2.08-2.35μm

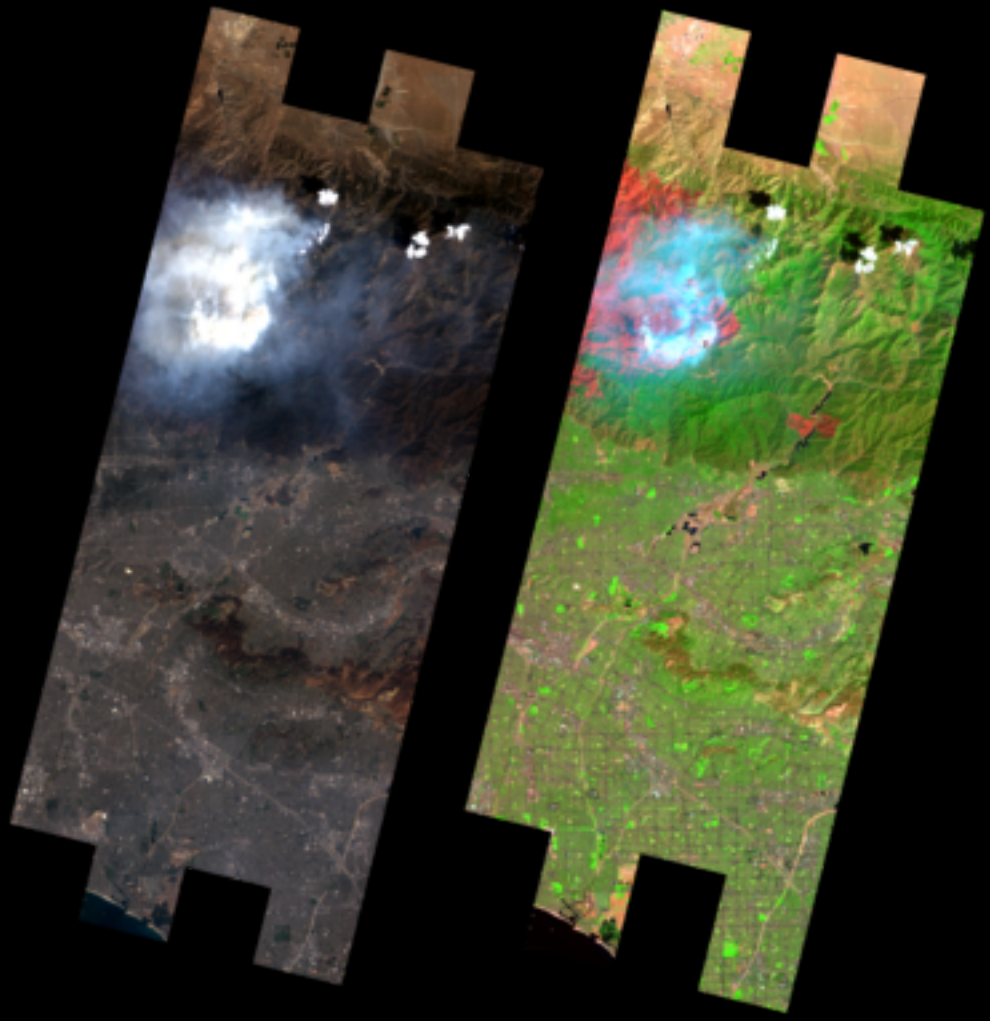

Flooding – Heritage (Ground) MODIS/UMD

- UMD Flood tracking of Myanmar using MODIS bands 1,2,5,7 (620-2155 nm)

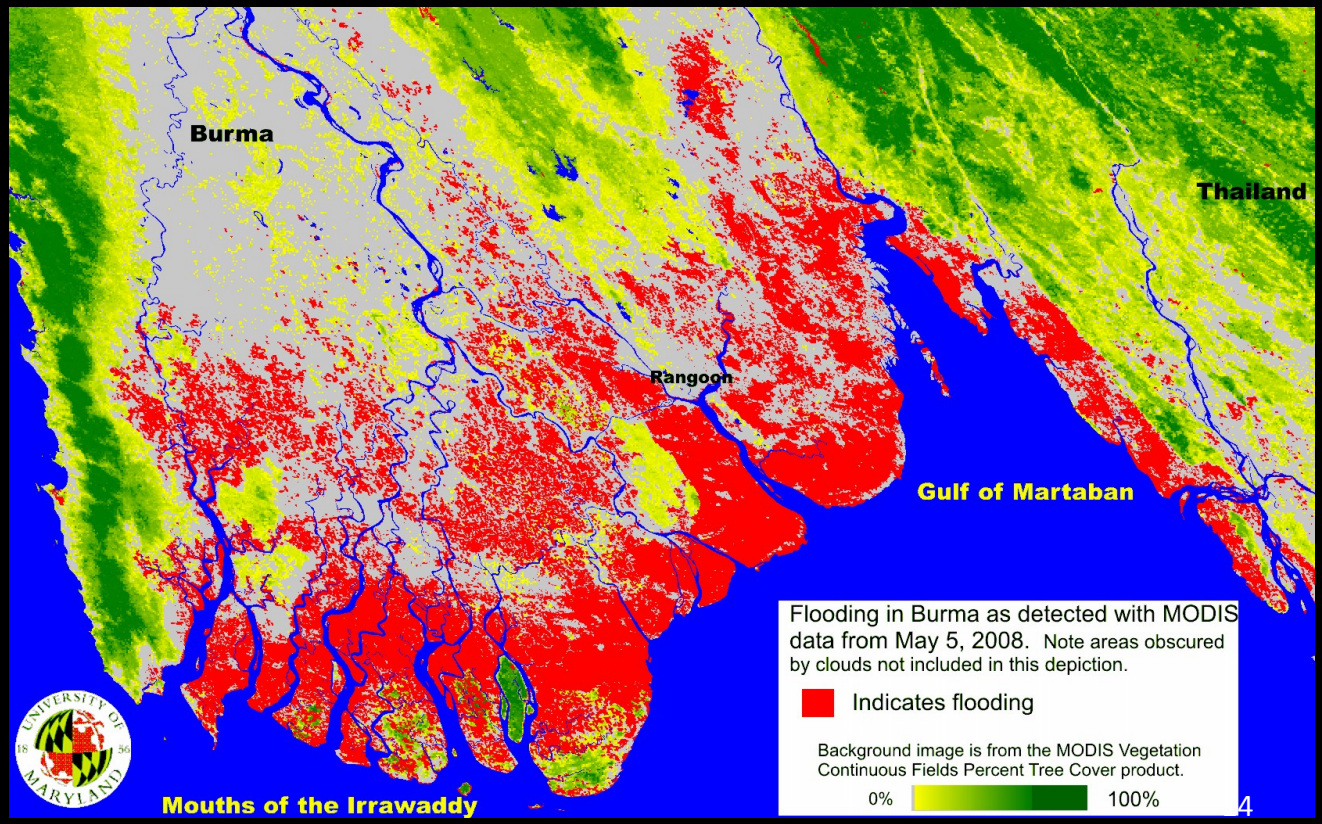

M. Carroll et al.

Flooding - Heritage (Flight) – EO-1/ASE

Onboard Detection of a Rare Major Flood on Australia's Diamantina River

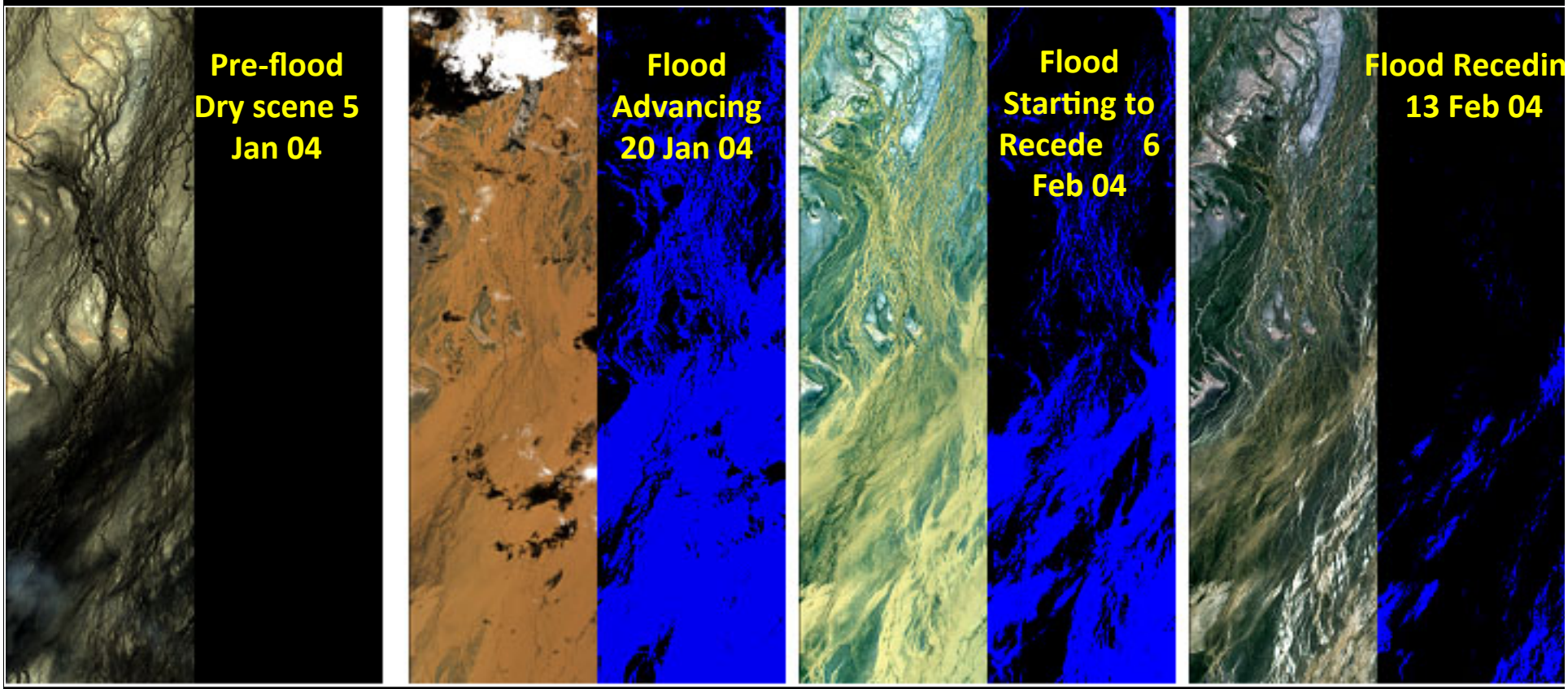

Cause of flooding: Monsoonal rain

EO-1 Hyperion. Wavelengths used: 0.86 µm and 0.99 µm

F. Ip, V. Baker, et al., University of Arizona

Cryosphere (Ground)

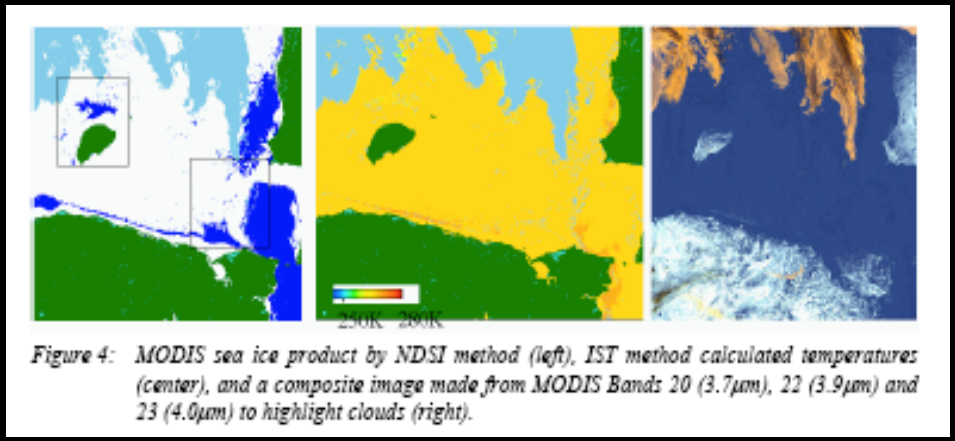

Figure 4: MODIS sea ice product by NDSI method (left), IST method calculated temperatures (center), and a composite image made from MODIS Bands 20 (3.7μm), 22 (3.9μm) and 23 (4.0μm) to highlight clouds (right).

Image courtesy of [Scharfen and Kalsa 2003]

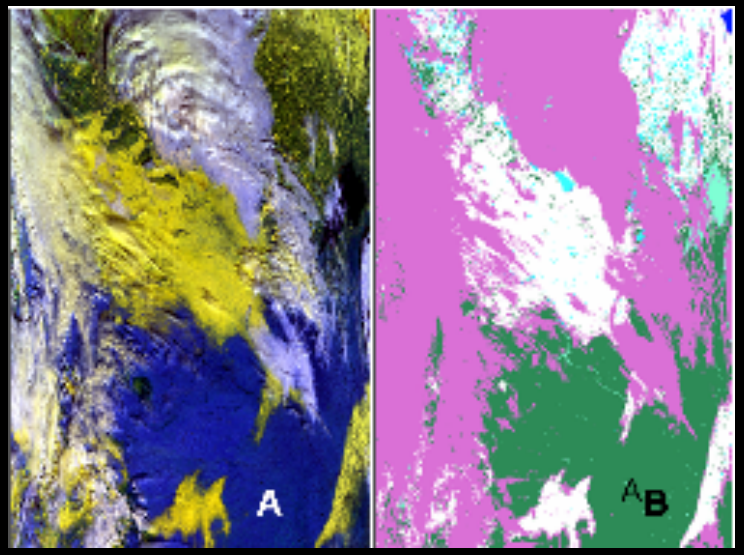

Figure 1 MODIS at-satellite reflectance image from swath of MOD02HKM for 3 January 2003 (A). Snow cover appears as yellow in this display of bands 1, 4 and 6. Snow cover map of the swath (B) and the snow cover map in sinusoidal projection (C).

Courtesy of *MODIS Snow Products User Guide*

Heritage (onboard) EO-1/ASE Hyperion Cryosphere Classifier

Deadhorse (Prudhoe Bay), Alaska

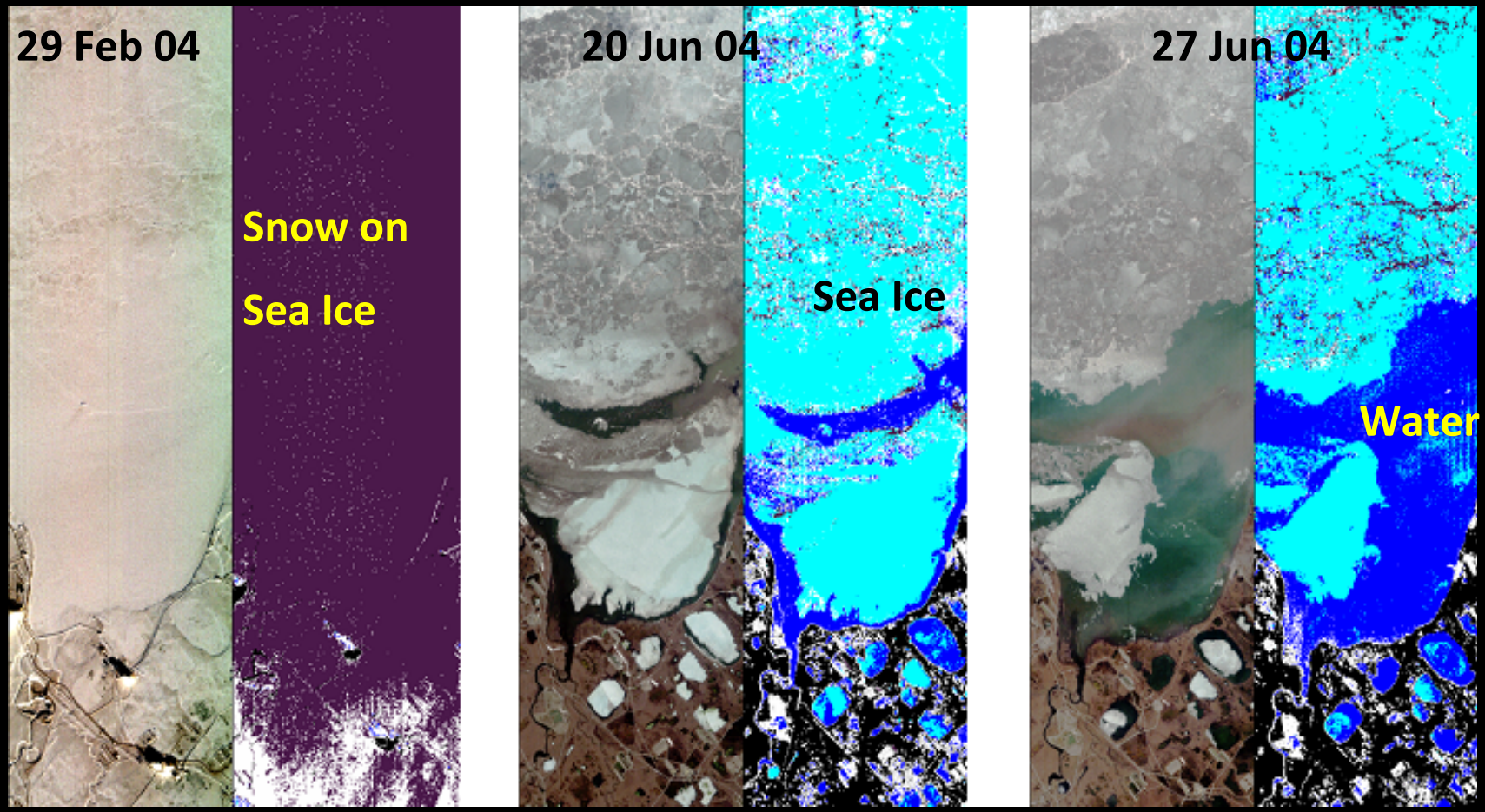

Snow
Water
Ice
Land
Unclassified

EO1/Hyperion data
Wavelengths used in classifier:
0.43, 0.56, 0.66, 0.86 and 1.65 µm

Arizona State University
Planetary Geology Group

Coastal

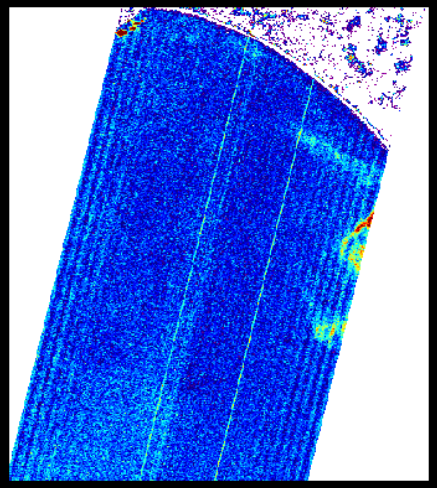

Maximum Chlorophyll Index derived from Hyperion imagery acquired 21 October 2008 of Monterey Bay [Chien et al. 2009] using 660, 681, 711, 752, nm. (ack J. Ryan/MBARI)

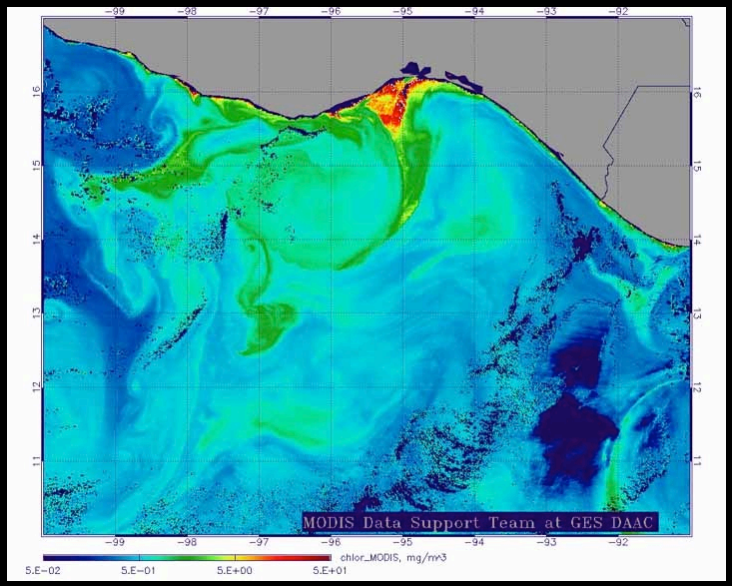

Uses 490nm/555nm or 490nm/565 nm MODIS reflectance data
Courtesy GSFC DAAC

Dust

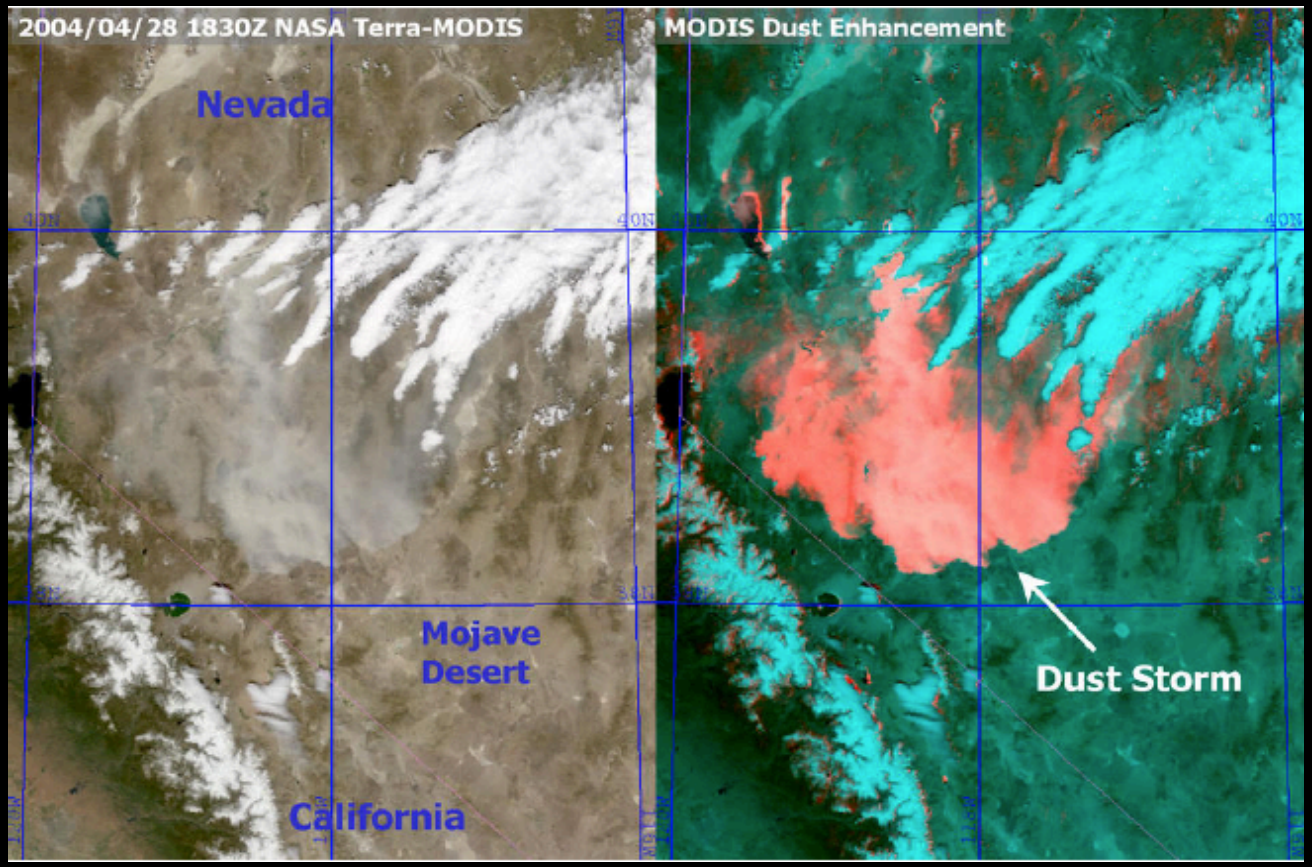

Image (processed MODIS) courtesy of *Satellite Product Tutorials: Desert Dust Storms, S. Miller et al.*

Vegetation

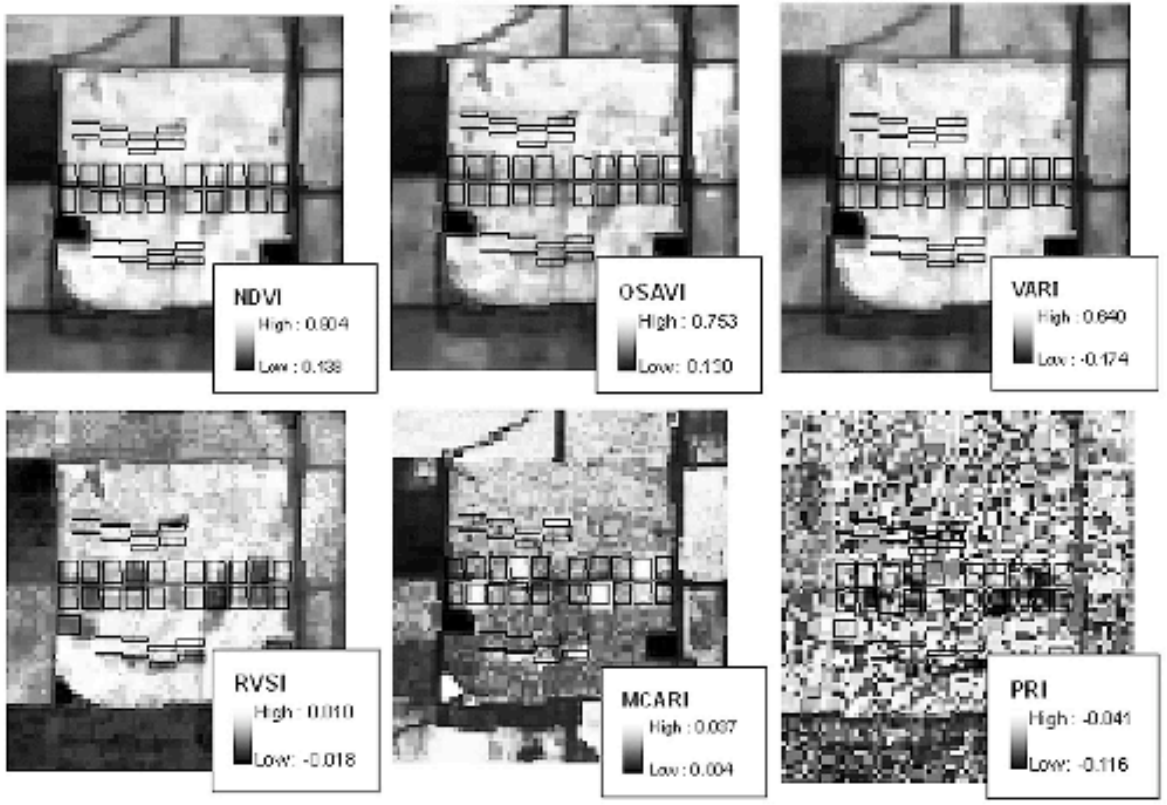

Fig. 3. Comparison of selected indices derived from 6 July Airborne Visible/Infrared Imaging Spectrometer (AVIRIS) imagery (18-m spatial resolution) with locations of N trial plots and subpixel plots shown. The corresponding classification accuracies are shown in Table 7. Note the differences between the appearance of the subpixel areas and the classification accuracies. For example, the subpixel stressed areas for the Normalized Difference Vegetation Index (NDVI) and the Modified Chlorophyll Absorption in Reflectance Index (MCARI) are quite apparent, although the classification accuracies (Table 7) for the Photochemical Reflectance Index (PRI) are generally higher.

Aviris measurement of plant stress using NDVI, MCARI, and PRI [Perry & Roberts 2008] describes 22 measures using 500-1200 nm.

Conclusions

- Direct broadcast can provide key data at low latency
- Onboard computing can address issues to downselect and process data to fit within reduced downlink
- Operations can be simple, web-based and automated
- For further information see poster and refs IGARSS 2010, IEEE Int. Sys., and 2009/2010 HyspIRI workshops

High-Speed FLAASH Atmospheric Correction for NASA Spectral Imagery

SBIR Phase I Program

Tim Perkins and Steve Adler-Golden

Spectral Sciences, Inc., Burlington, MA 01803

Pat Cappelaere

Vightel Corp., Ellicott City, MD

HyspIRI Science Workshop, Washington D.C.

25 August 2011

SBIR Program Objectives

- **Problem**
  - High duty cycle of upcoming missions such as HyspIRI will require high accuracy, fully automated, low latency, near real-time atmospheric correction (AC) processing
  - NASA's current AC algorithms are, or will soon be, outdated in both the science and the coding
- **Solution**
  - Transition NASA's current and future (HyspIRI) AC processing to a fast version of the C++ language FLAASH code
- **Objectives**
  - Port FLAASH to the Elastic Cloud or IAAS
  - Develop look-up tables (LUT) for near-real-time FLAASH processing
  - Phase II: port to prototype flight hardware
- **Team: SSI + Vightel**
  - Thanks to Dan Mandl, Technical Monitor

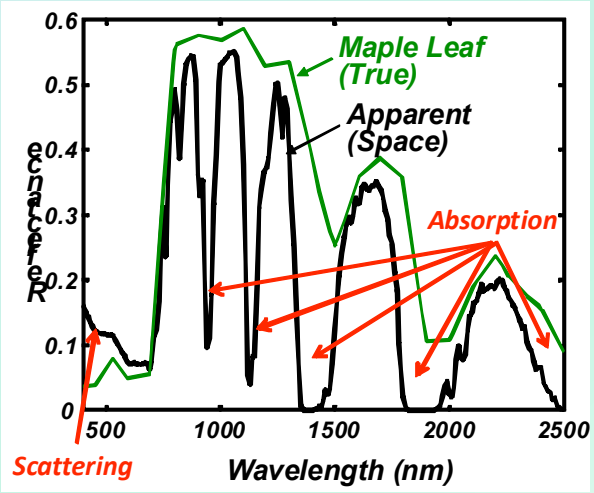

Processing Concept

- ***Ground-based system:***
  - Will support Hyperion, Landsat, ALI, MODIS, ASTER
- ***On-board system:***
  - For direct broadcast of products from HyspIRI, LDCM in near real-time

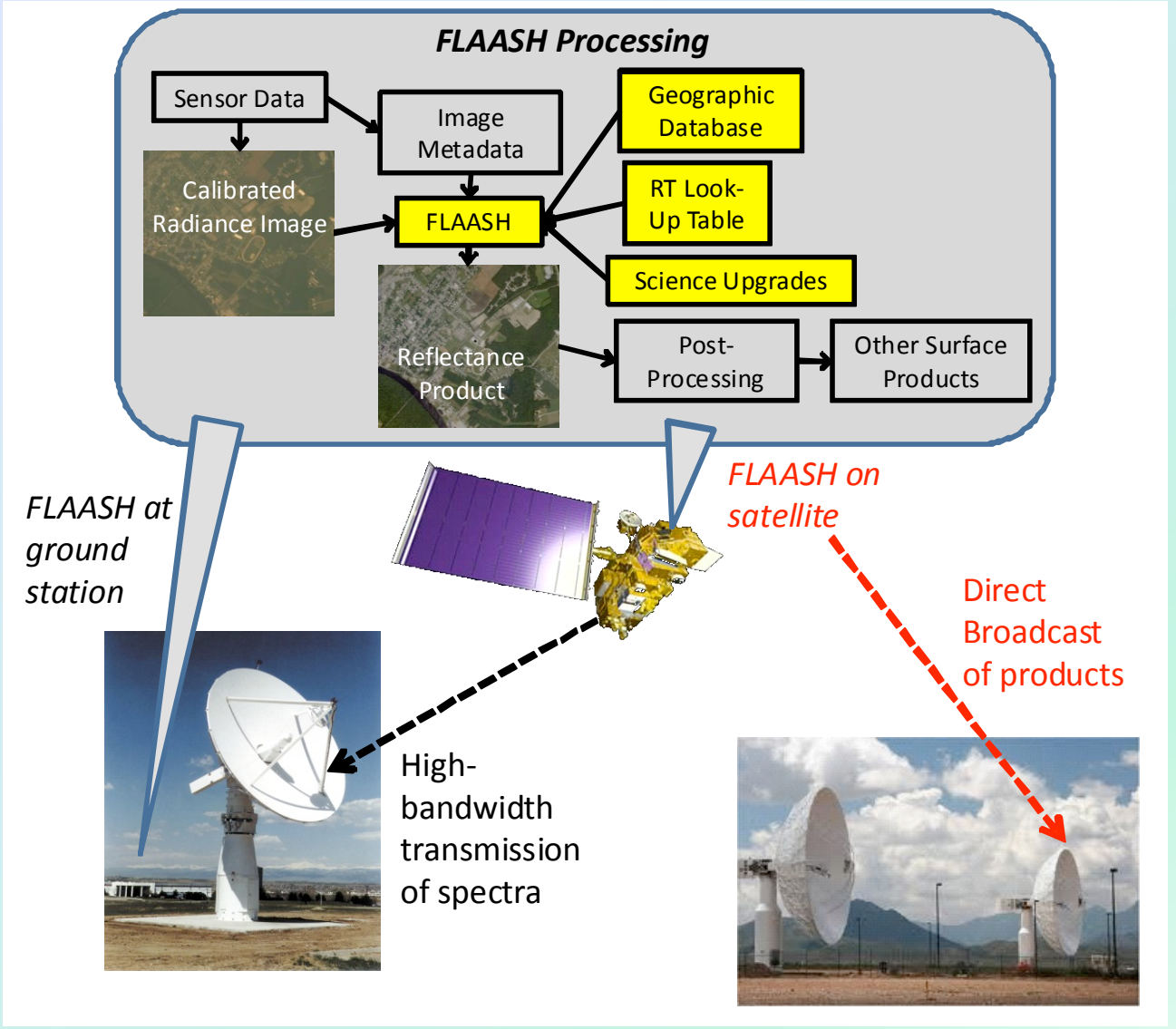

FLAASH Overview

- **Development**
  - Code developed by SSI with primary support from AFRL, additional support from NGA, NASA, SSI
  - ENVI commercial product developed from original IDL code
  - FLAASH-C developed for NGA parallel processing system; latest version approved for public release May 2011
- **Science/Features**
  - MODTRAN radiative transfer; pixel-by-pixel water retrieval; scene visibility retrieval; adjacency effect and spectral smile compensation; spectral polishing; wavelength self-calibration
- **Operating Modes**
  - Interactive (IDL) or batch (FLAASH-C)
  - High-speed MODTRAN LUT option (ongoing development)
- **Demonstrated Sensor Support**
  - AISA-ES, ALI, ARTEMIS, ASAS, ASTER, AVHRR, AVIRIS, CASI, Compass, GeoEye-1, HYDICE, HyMap, Hyperion, IKONOS, Landsat, LASH, MaRS, MASTER, MODIS, MTI, Probe-1, QuickBird, RapidEye, SPOT, TRWIS, WorldView-2

State-of-the-Art FLAASH Science

- RT equation

$$L^* = \frac{a\,\rho}{1-\rho_e S} + \frac{b\,\rho_e}{1-\rho_e S} + L_a^*$$

MODTRAN-derived

Validation with Ground Truth

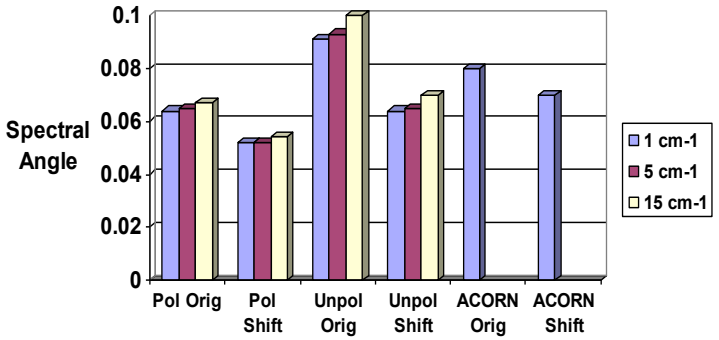

- Adjacency compensation improves accuracy

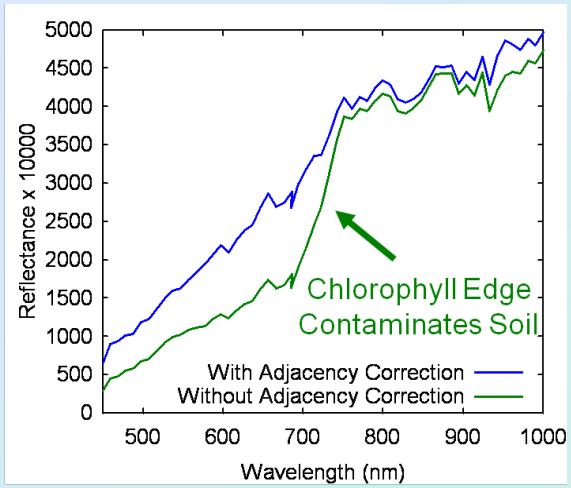

- Visibility retrieval from small dark areas

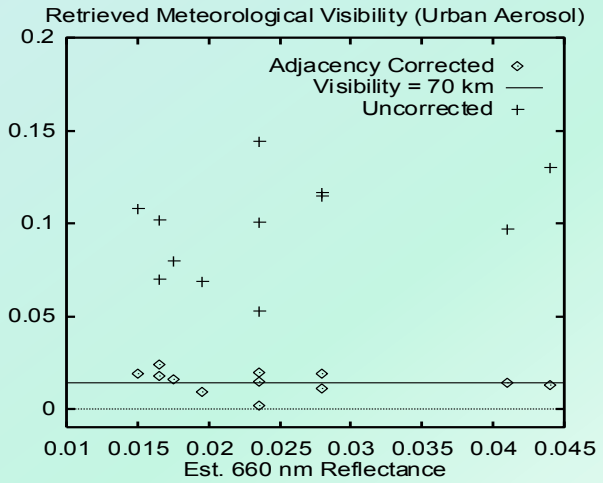

Technical Approach: Speedup via Look-up Tables (LUTs)

- **Large pre-calculated LUTs replace the custom MODTRAN calculations in FLAAASH**
  - *Eliminates the Fortran module and around half the FLAASH run time*
- **Feasibility previously demonstrated (2000 Ph 1 program)**
  - *LUTs containing MODTRAN radiance spectra were built for nadir viewing from 3 km and 20 km (e.g. AVIRIS) altitudes*
- **LUTs have now been built for TOA nadir and off-nadir viewing**
  - *Utilize PCA compression to save storage*
  - *Current LUTs developed for rural aerosol model (5-300 km visibility)*
    - *Water vapor to 1.6xTropical, view angle to 30 deg off nadir, solar angle 0-70 deg, surface elevation 0-3.5 km*

Phase I Accomplishments

- **Initial LUT Development**
  - Developed LUT for rural aerosol – ~ 1CPU-week of MODTRAN calculations
  - >100-fold compression with PCA (16 Gbytes → 100 Mbytes)
- **FLAASH-C Development**
  - Support compressed LUT files
  - Timing study: MODTRAN vs. LUT time comparison for MSI and HSI
  - New feature: atmospherically corrected radiance (shows blackbody source in "hot" pixels for characterizing fires, volcanoes, etc.)
- **Demonstrations:** EO-1 Data (Hyperion and ALI) - LUT and/or MODTRAN versions
  - On Elastic Cloud automatically processing new scenes
  - As a WCPS algorithm re-processing scenes on-demand as a
  - On IPM Telera (but not yet multicore)

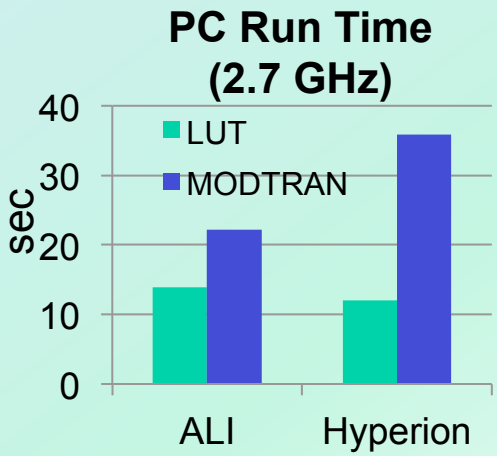

LUT Evaluation

- LUT is a compressed spectral database supporting off-nadir viewing from the TOA
  - 145000 table entries, 350 – 2500 nm, 5 cm^{-1} resolution
  - After compression, roughly the size of a single Hyperion image
- Retrieved hyperspectral reflectance values agree closely with direct results from MODTRAN

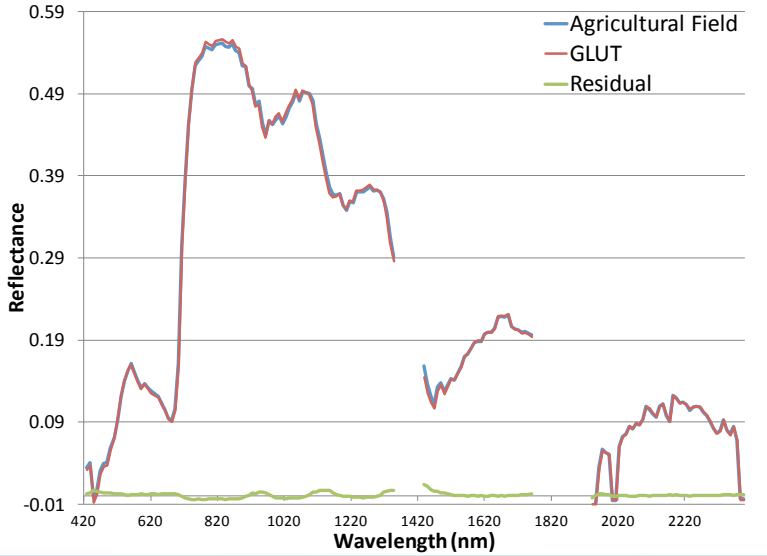

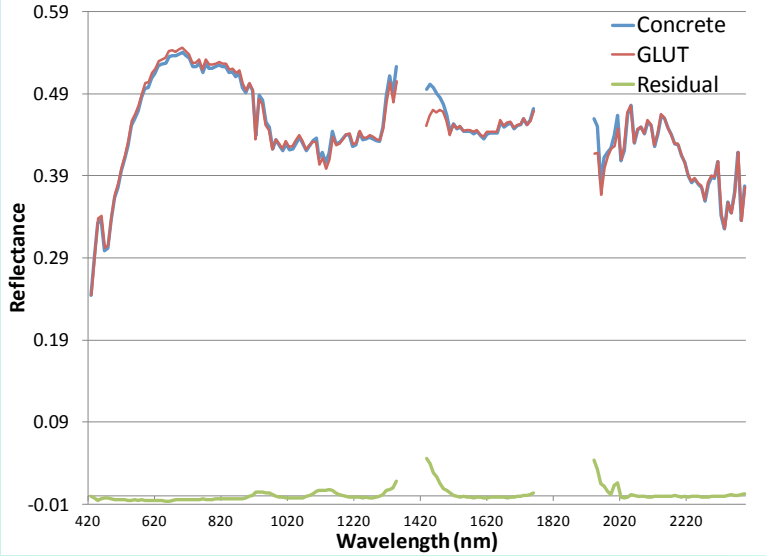

Hyperion Reflectance Spectra

Data Product Generation

- Many data products could be generated from the atmospherically corrected data in near-real time
- Bringing the coding into FLAASH would avoid time- and memory-consuming cube I/O
- A prototype of a flood map product is shown here

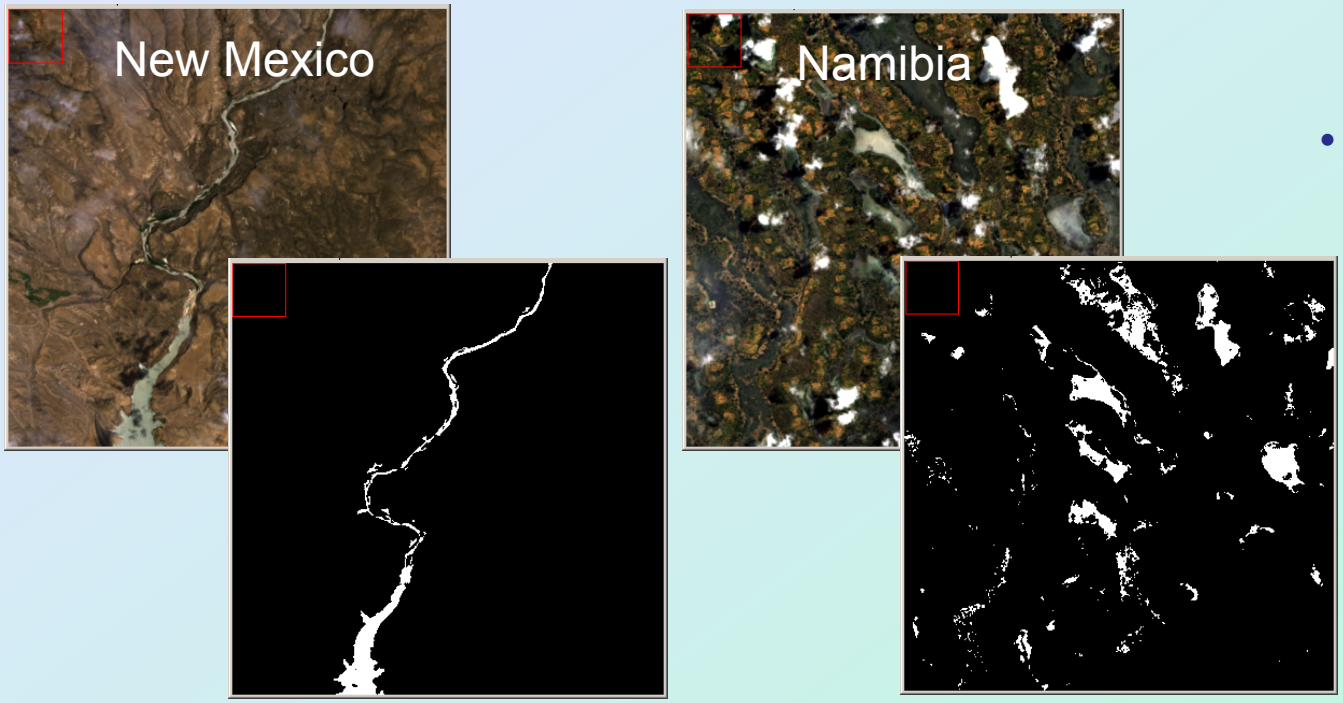

- Spectral Angle Mapper finds turbid water in two different ALI reflectance scenes

Phase II Plans

- Code Development
  - LUTs for standard aerosols/dusts (rural, maritime, urban, desert)
  - Extend to lower altitudes for aircraft (e.g. EMAS)
  - Parallelize for multiprocessor systems
  - Aerosol retrieval improvements, e.g. geographically dependent aerosol type, spatially varying AOD
  - Low-latency data product generation within FLAASH
    - Thermal IR data product(s) taking advantage of fusion with VNIR/SWIR
  - Radiance modeling for low-latency sensor calibration with cal/val sites
- Code Integration
  - Fully operational Sensor Web and IAAS data processing, distribution
  - Prototype HyspIRI flight system demo (Space Cube, Maestro)
  - Integrate with external data product codes
- Validation
  - Demonstrate accurate, automated atmospheric correction and data product generation across a variety of sensors, scenes, platforms

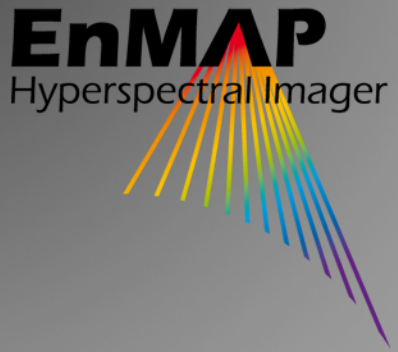

EnMAP – Technical Update and future Science Issues

Hermann Kaufmann, Karl Segl, Luis Guanter, Christian Rogass, Saskia Förster
Stefan Hofer, Bernhard Sang
Andreas Müller, Rudolf Richter, Uta Heiden
Christian Chlebek, Godela Rossner

HyspIRI Science Workshop 2011, Washington DC

Outline

- Mission introduction and current status
- Updates on instrument
- Calibration and validation activities
- Recent Advances
- Scientific program activities
- Synergies to HysplRI (Hisui)

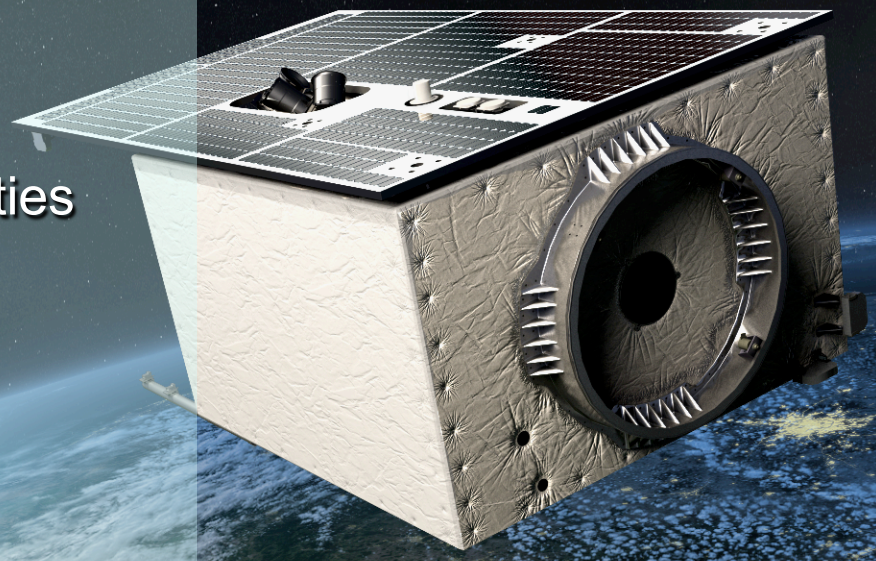

Science Program / Fields of Applications

Co-operative international Networks

management of agricultural and forest ecosystems

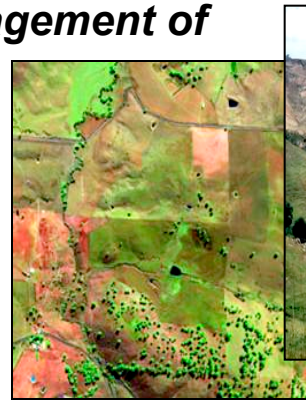

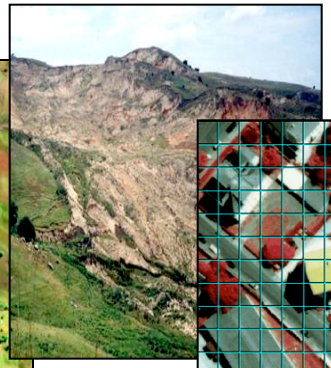

hazard assessment

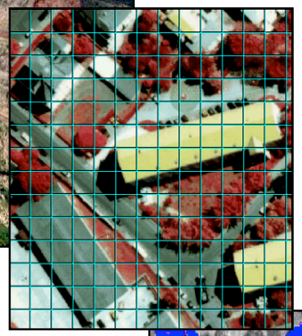

urban develop-ment

Retrieval of bio-geochemical and geophysical variables

inland & coastel waters

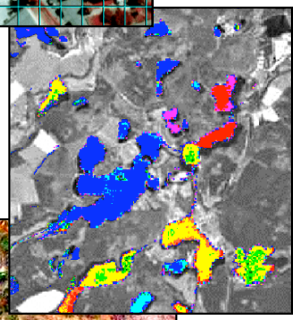

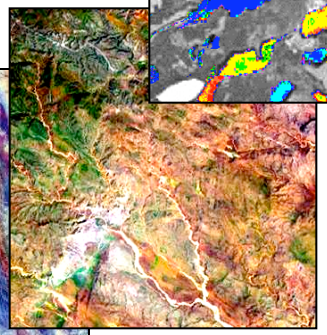

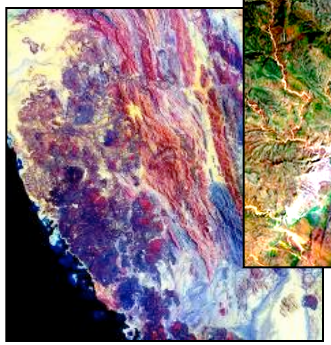

mineral exploration

dry-land degradation

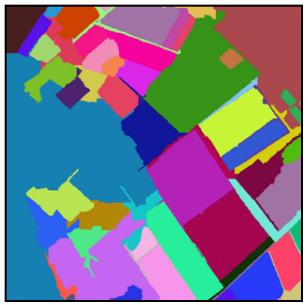

- *methodological development*
- *synergies to xs and radar (InSAR)*

Project Partners

EnMAP Hyperspectral Imager

DLR

Universität Trier

Helmholtz-Zentrum Geesthacht
Zentrum für Material- und Küstenforschung

LMU LUDWIG-MAXIMILIANS-UNIVERSITÄT MÜNCHEN

HUMBOLDT-UNIVERSITÄT ZU BERLIN

University of Lethbridge
FIAT LUX

esa

Scientific Principal Investigator
GFZ-Potsdam

Core Science Team
ECST

Project Management
DLR Agency

Space Segment
Kayser-Threde - Spectrometer
OHB Bremen - Bus Technology

Ground Segment
DLR-Oberpfaffenhofen

Status: Aug. 2011

Introduction - History and Current Status

- 2005 Phase A study accomplished
- 2006 Start of phase B
- 2007 End of phase B
- 2008 Start of phase C/D
- 2010 CDR Ground Segment
- 2011 CDR Space Segment
- 2015 Launch date

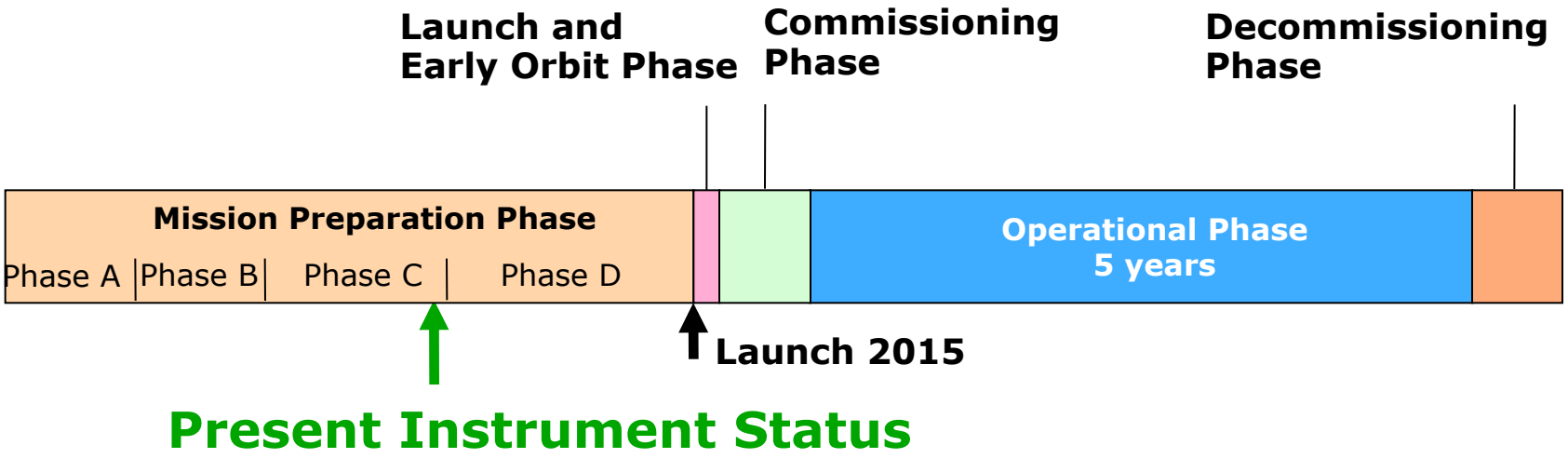

Instrument - Main Sensor/Orbit Parameters

Signal-to-noise ratio (SNR) at 30% reflectance; 30° sun zenith angle; visibility 21 km; target 500 m a.s.l.	VNIR: > 500:1 (at 495 nm) SWIR: > 150:1 (at 2200 nm)
Quantification / Radiometric stability	14 bit / < 2.5 %
Spectral Sampling	6.5 nm VNIR; 10 nm SWIR
Ground sampling distance (GSD)	30 m x 30 m (at nadir; s. l.)
Swath width	30 km
Swath length	1000 km /orbit; 5000 km /day
Geometric co-registration	≤ 0.2 x GSD
Data Rate / Compression method	860 Mbit/s / loss less
Downlink rate (X-band) / Daily downlink	300 Mbit/s / 389 Gbit
Inclination	97.96°
Repeat cycle	23 days
Repeat rate	4 days (± 30° tilt)
LTDN	11:00 ± 15 min

Instrument Optics Unit (IOU) - Main Elements

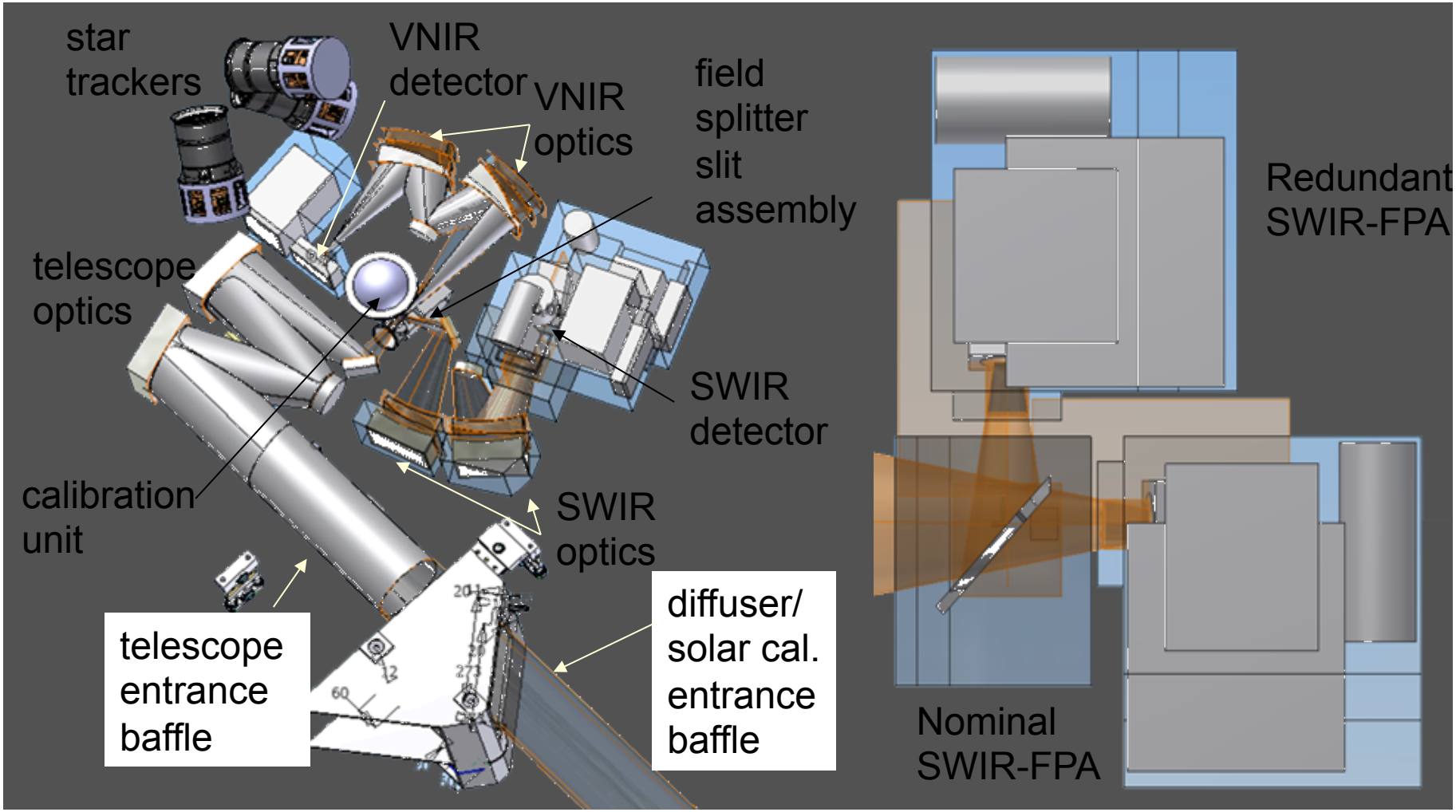

Instrument - CADs and STDM of Current Instrument Design Status

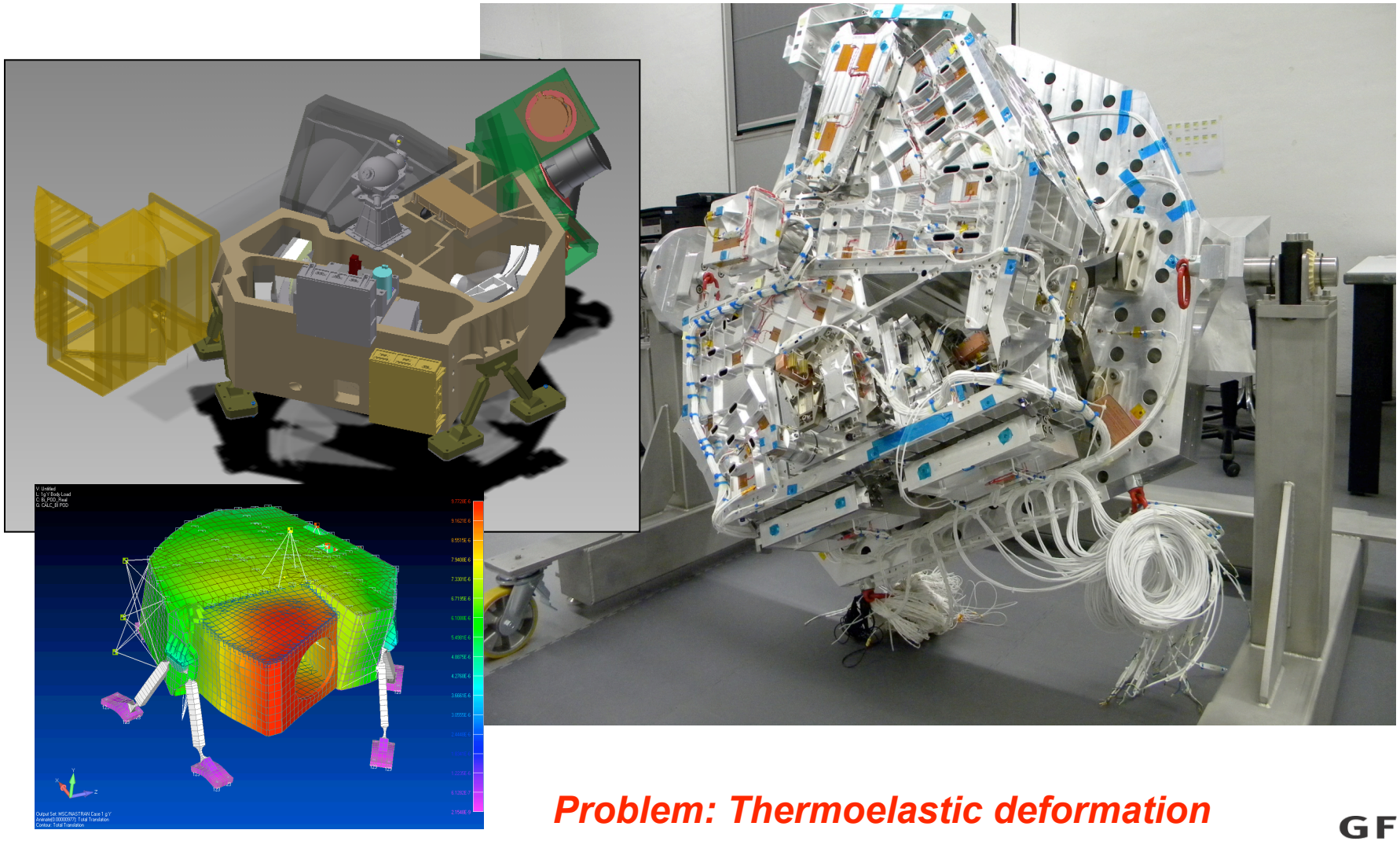

Problem: Thermoelastic deformation

Calibration and Validation

Objectives

- Data quality check and incidence reporting
- Assurance of L1 & L2 products traceability to international standards

Onboard calibration and long term monitoring

Validation

- Image-based analysis: image processing techniques to assess EnMAP instrument performance and data quality (e.g. SRFs, PSF, MTF assessment)
- Field-based validation using in-situ measurements of atmospheric and surface parameters for the validation of L1 and L2 products.
- Validation plan being framed in the internat. Cal/Val scenario (CEOS/WGCV)

Establishment of international partnerships in progress:

USA/JPL: White Sands; Australia/CSIRO: Lancelin & LJCO; Israel/Tel Aviv Uni.: Negev

Guanter, L., Segl, K., Sang, B., Alonso, L., Kaufmann, H., and Moreno, J., 2009, Scene-based spectral calibration assessment of high spectral resolution imaging spectrometers. *Optics Express,*17-14, 11594-11606, 10.1364/OE.17.011594.

Ground Segment

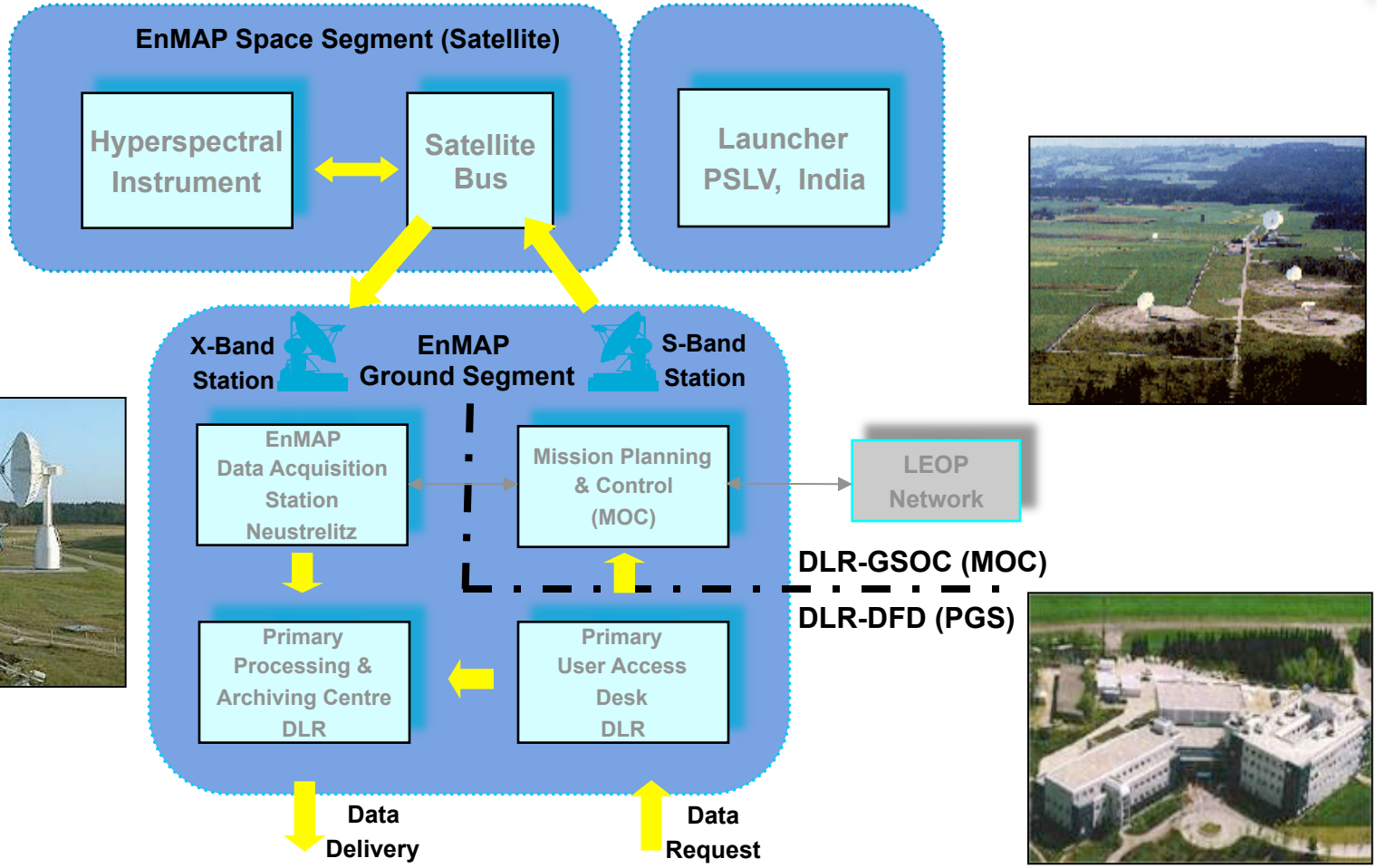

International EnMAP User Community

EeteS: an End-to-End Image Simulation Tool for the EnMAP Mission

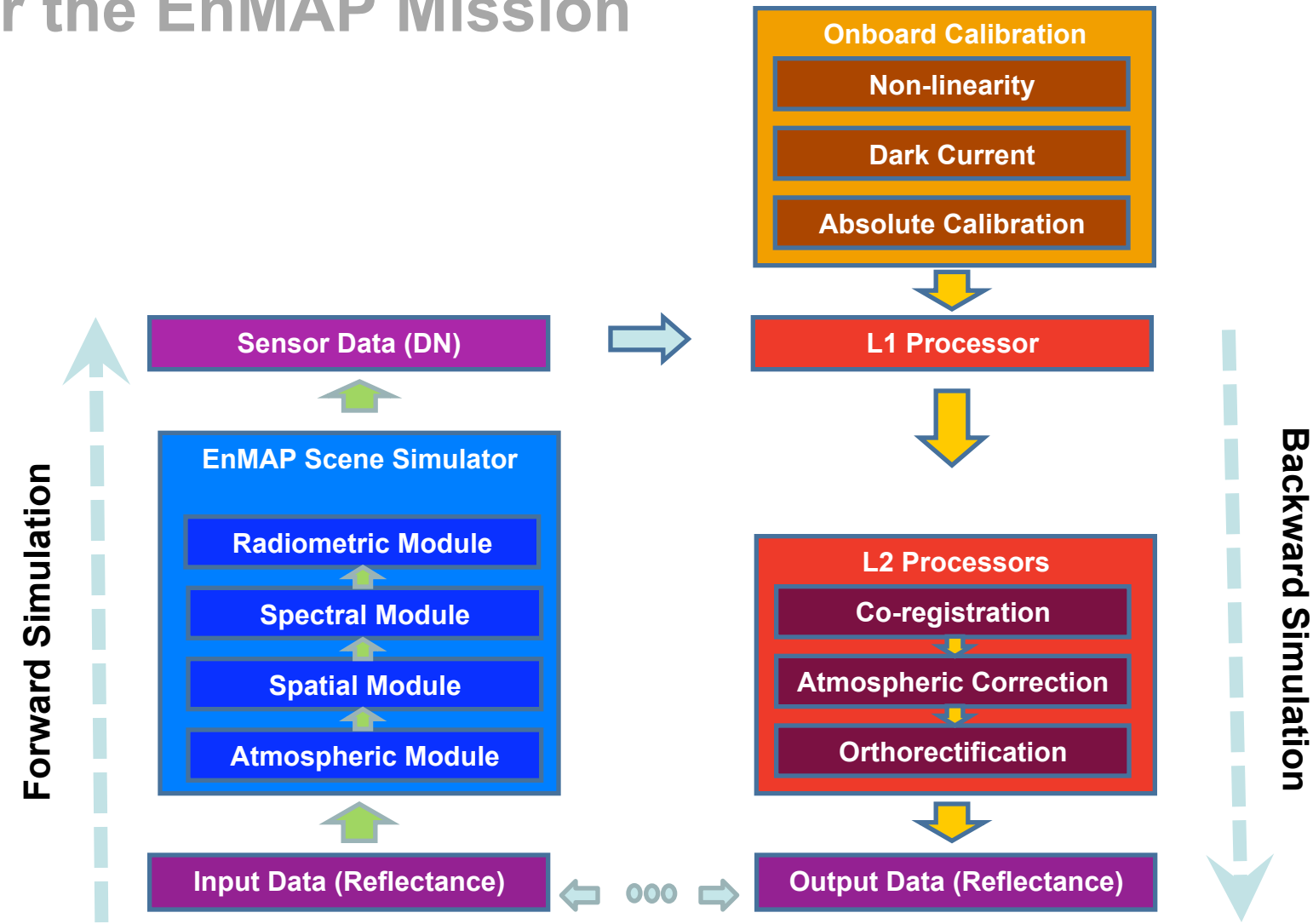

Simulated EnMAP Data – M. Ramon, Israel

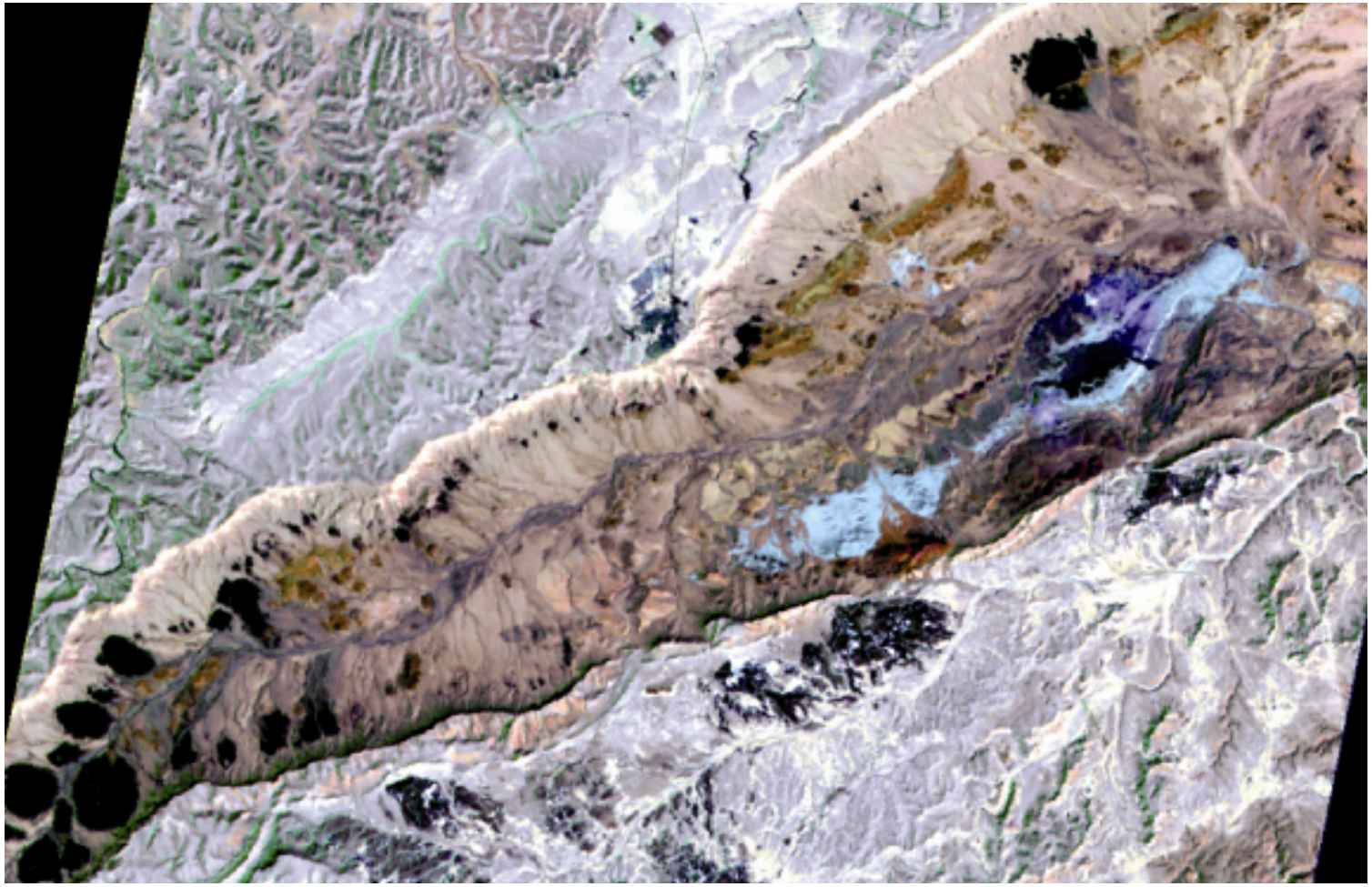

Guanter, L., Segl, K., Kaufmann, H. (2009): Simulation of Optical Remote-Sensing Scenes With Application to the EnMAP Hyperspectral Mission. - IEEE Transactions on Geoscience and Remote Sensing, 47, 7, 2340-2351

BRDF Issues

→ Simulation of any canopy structure (e.g. row distance, plant density)
→ Simulation of each growth stage
→ Simulation of plant stress and disease

MATERIAL ASSIGNMENT

Leaf spectra

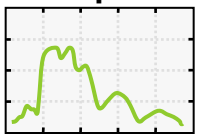

Stem spectra

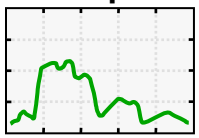

Soil spectra

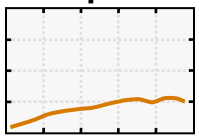

3D GEOMETRY

4D plant model

Plant positions within the canopy

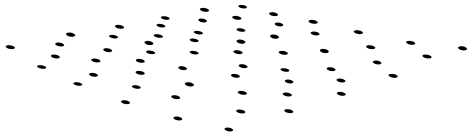

3D soil surface model

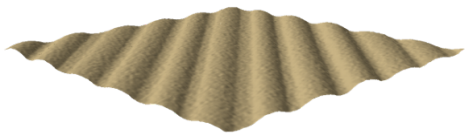

RAY TRACING

Illumination position (azimuth, altitude)

Viewing position (azimuth, altitude)

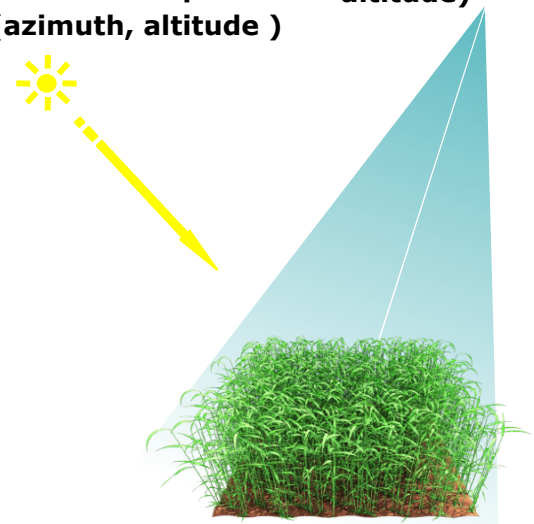

RESULTING CANOPY SPECTRUM

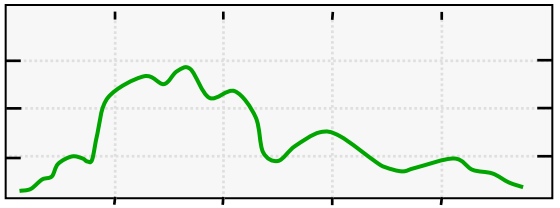

Science activities - Core Science Team (ECST)

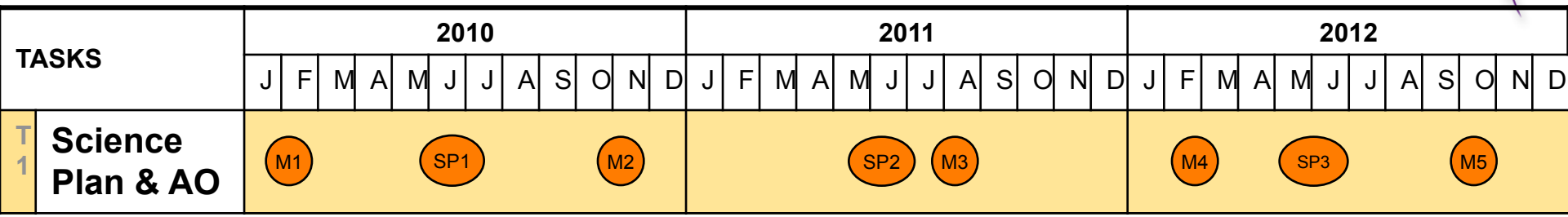

Geology and Soil Science	**Prof. Dr. Hermann Kaufmann (Principle Investigator and Chair) GFZ German Research Centre for Geosciences**
Coastal and Inland Waters	**Dr. Roland Doerffer** **HCG Research Centre**
Forest and Vegetation	**Prof. Dr. Joachim Hill** **University of Trier**
Ecosystems and Gradual Transitions	**Prof. Dr. Patrick Hostert** **Humboldt-University Berlin**
Agriculture	**Prof. Dr. Wolfram Mauser** **Ludwig-Maximilian-University München**
Urban Areas	**Andreas Mueller** **DLR German Aerospace Establishment**

Themes within the young EnMAP Program

Hdhhd

kskks

Science activities - Core Science Team (ECST)

TASKS		2010												2011												2012											
		J	F	M	A	M	J	J	A	S	O	N	D	J	F	M	A	M	J	J	A	S	O	N	D	J	F	M	A	M	J	J	A	S	O	N	D
T1	Science Plan & AO	M1					SP 1					M2								SP 2		M3																	
T2	Summer Schools									S1										S2												S3							

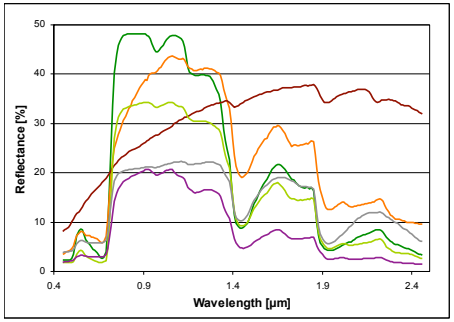

2010: 1st Summer School, Trier: Introduction to hyperspectal image analysis

2011: 2nd Summer School, Munich: Hyperspectral field campaigns: Methods, Instruments, Planning Strategies

2012: 3rd Summer School, Berlin

Science activities - Core Science Team (ECST)

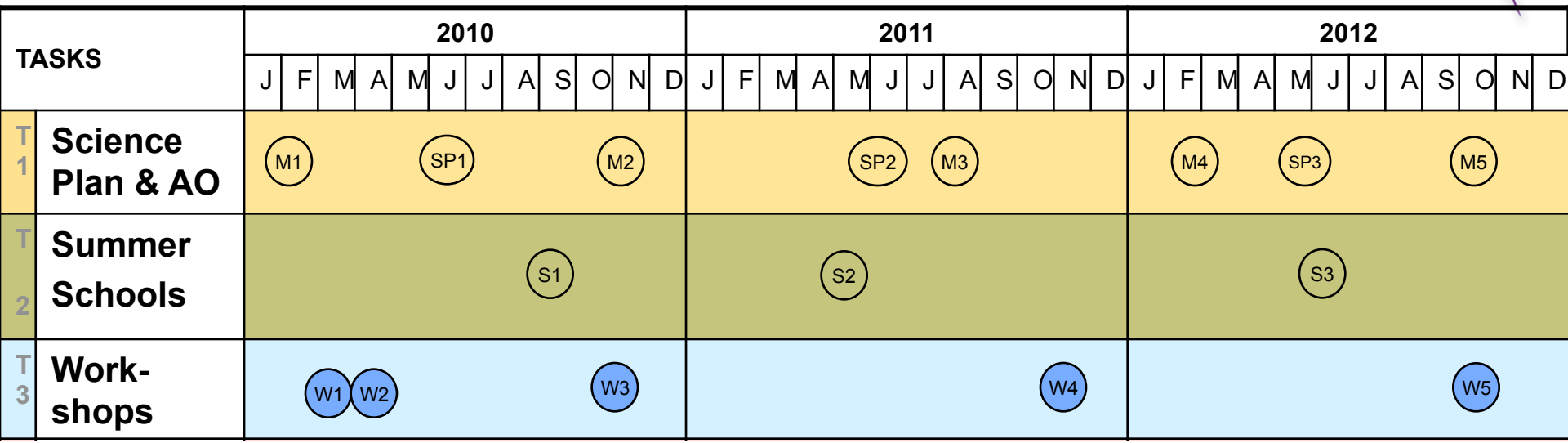

W1 Int. Hyperspectral Workshop 2010 (Frascati, Italy)

W2 Soil Workshop (GFZ)

W3 National Workshop 2010 (GFZ Potsdam)

W4 National Workshop 2011 (GFZ Potsdam)

shifted to Feb. 2012

EnMAP Toolbox

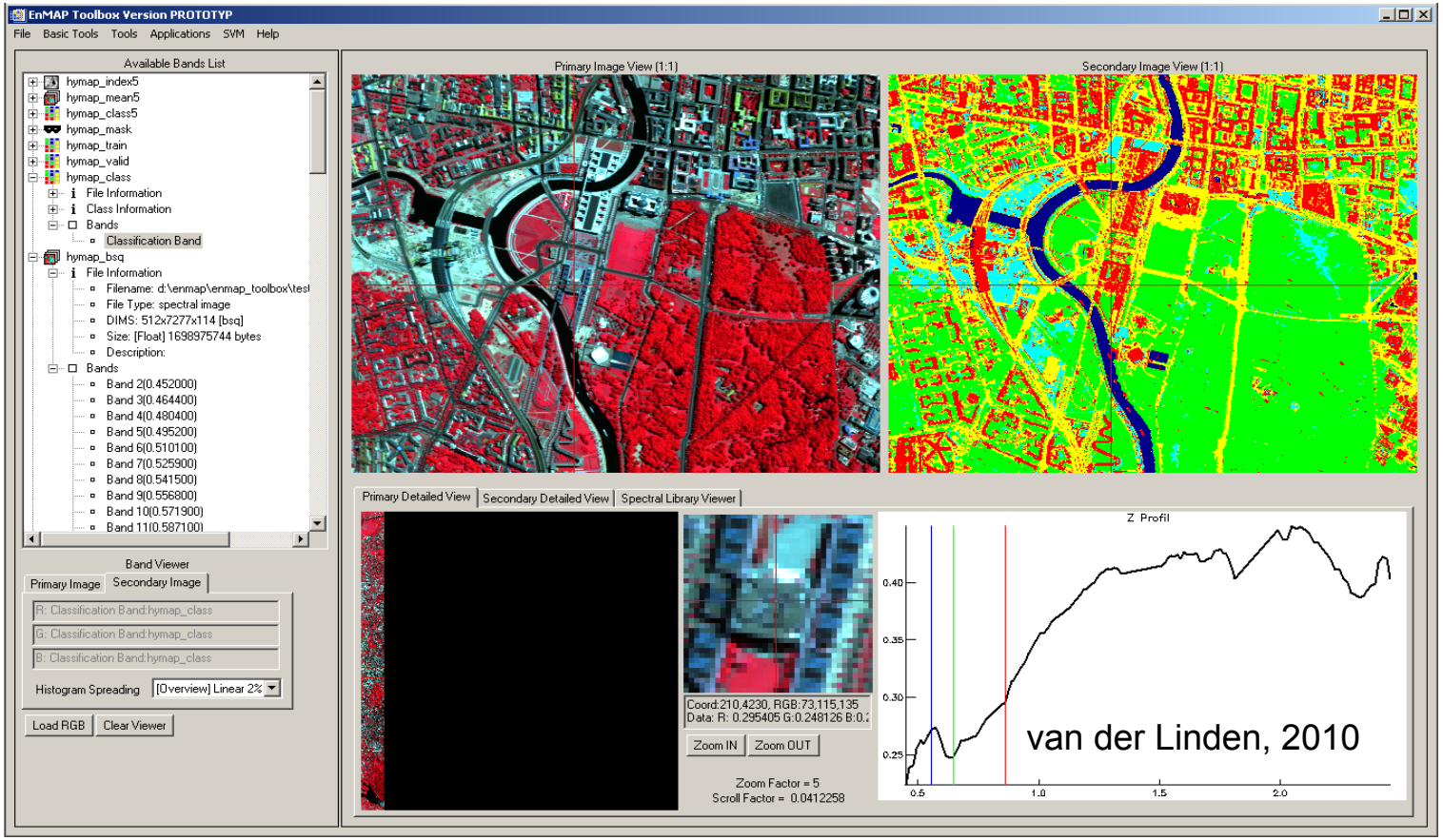

- License free and platform independent processing environment
- Optimized for EnMAP/hyperspectral processing
- Shortly (autumn) available via www.enmap.org
- Developed by Humboldt-Universität zu Berlin, Geomatic Section

User Portal

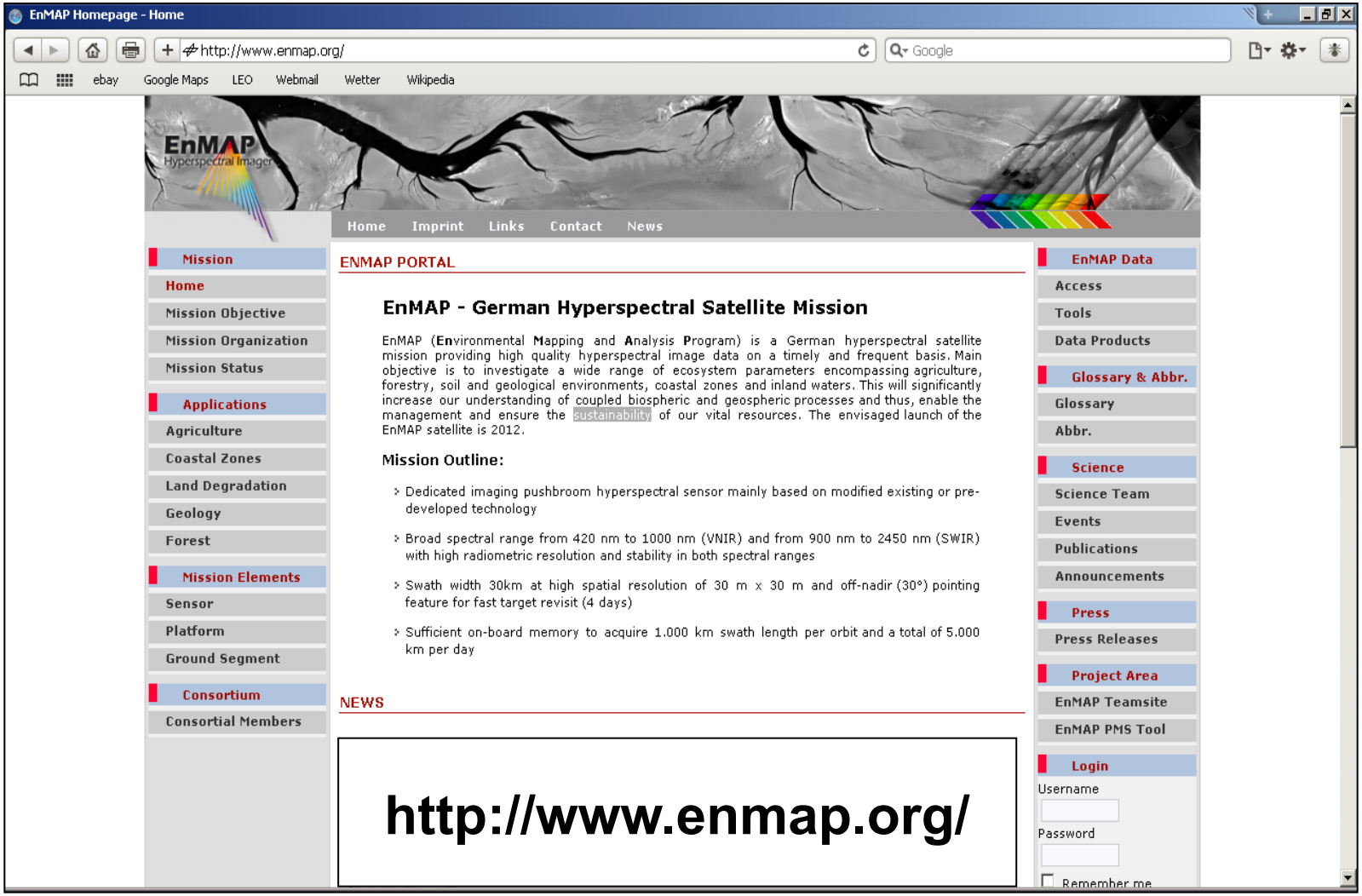
EnMAP Homepage - Home
http://www.enmap.org/
Google
ebay
Google Maps
LEO
Webmail
Wetter
Wikipedia
EnMAP
Hyperspectral Imager
Home
Imprint
Links
Contact
News
Mission
Home
Mission Objective
Mission Organization
Mission Status
Applications
Agriculture
Coastal Zones
Land Degradation
Geology
Forest
Mission Elements
Sensor
Platform
Ground Segment
Consortium
Consortial Members
ENMAP PORTAL
EnMAP - German Hyperspectral Satellite Mission
EnMAP (Environmental Mapping and Analysis Program) is a German hyperspectral satellite mission providing high quality hyperspectral image data on a timely and frequent basis. Main objective is to investigate a wide range of ecosystem parameters encompassing agriculture, forestry, soil and geological environments, coastal zones and inland waters. This will significantly increase our understanding of coupled biospheric and geospheric processes and thus, enable the management and ensure the sustainability of our vital resources. The envisaged launch of the EnMAP satellite is 2012.
Mission Outline:
Dedicated imaging pushbroom hyperspectral sensor mainly based on modified existing or pre-developed technology
Broad spectral range from 420 nm to 1000 nm (VNIR) and from 900 nm to 2450 nm (SWIR) with high radiometric resolution and stability in both spectral ranges
Swath width 30km at high spatial resolution of 30 m x 30 m and off-nadir (30°) pointing feature for fast target revisit (4 days)
Sufficient on-board memory to acquire 1.000 km swath length per orbit and a total of 5.000 km per day
NEWS
http://www.enmap.org/
EnMAP Data
Access
Tools
Data Products
Glossary & Abbr.
Glossary
Abbr.
Science
Science Team
Events
Publications
Announcements
Press
Press Releases
Project Area
EnMAP Teamsite
EnMAP PMS Tool
Login
Username
Password
Remember me

Cooperation with HysplRI (and Hisui)

- Common identification of environmental relevant core themes and resp. sites for long term observation and analyses
- Common aircraft campaigns (esp. TIR capability)
- Exchange program for seniors and young academics

- Technical issues
  - Sensitivity studies to
    different GDS's (30m<->60m) for various applications
    compatibility for long term observations
    extended end to end simulation for TIR range
  - Cross calibration of systems
  - .....

Thank you
for listening

Contact:

Hermann Kaufmann

charly@gfz-potsdam.de

www.gfz-potsdam.de

Calibration and Validation

Objectives

- Data quality check and incidence reporting
- Assurance of L1 & L2 products traceability to international standards

Onboard calibration and long term monitoring

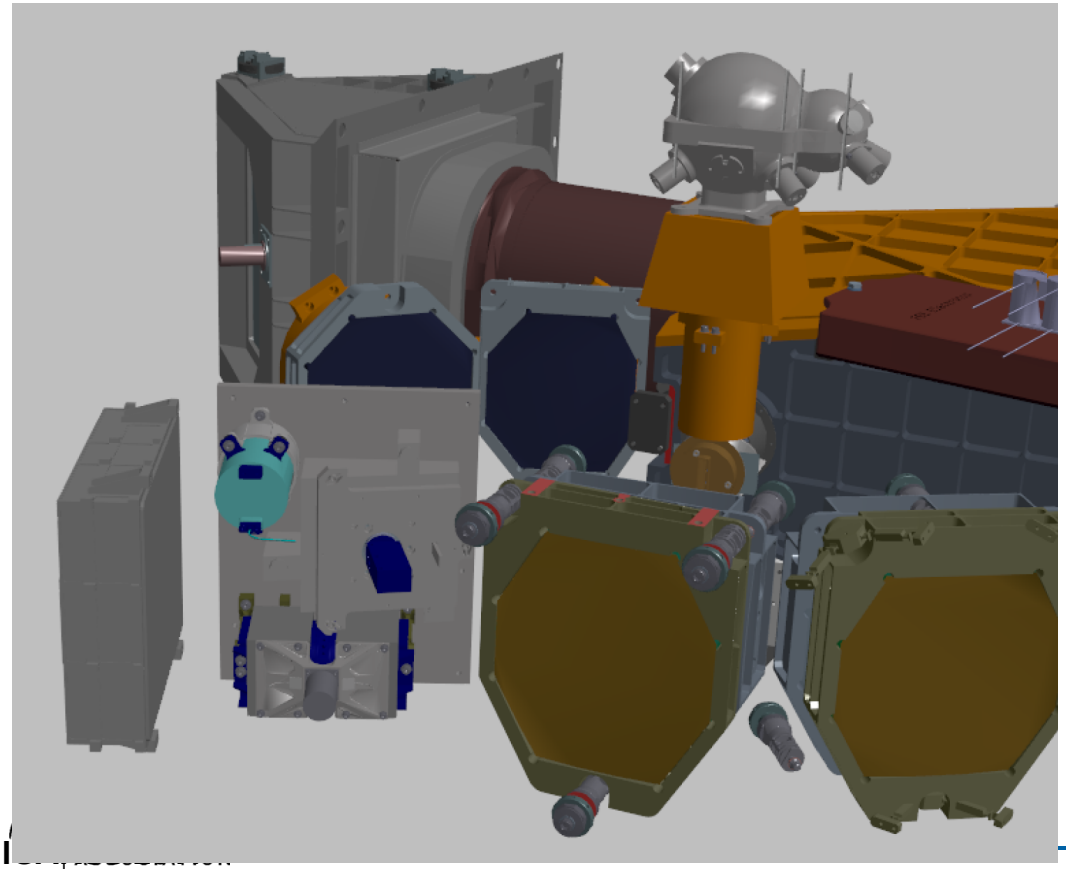

Radiometric and spectral calibration

- Dark value
- Relative radiometric calibration
- Sun calibration
- Spectral calibration
- Linearity measurements
- House keeping data analysis

Agricultural Greenhouse Gas Flux Determination via Remote Sensing and Modeling

Guy Serbin[1], E. Raymond Hunt Jr.[2], David J. Brown[3], Cesar Izaurralde[4], Keith Paustian[5], Tristram O. West[4], Heather McNairn[6], Bonny Schumaker[7], Charles W. Rice[8], Robert O. Green[7]

[1] InuTeq, LLC, Washington, DC
[2] USDA/ARS Hydrology and Remote Sensing Lab, Beltsville, MD
[3] Dept. of Crop and Soil Sciences, Washington State University, Pullman, WA
[4] Joint Global Change Research Institute, Pacific Northwest National Lab, College Park, MD
[5] Dept. of Soil and Crop Sciences, Colorado State University, Ft. Collins, CO
[6] Eastern Cereal and Oilseed Research Centre, Agriculture and Agri-Food Canada, Ottawa, ON, Canada
[7] NASA Jet Propulsion Lab, Pasadena, CA
[8] Dept. of Agronomy, Kansas State University, Manhattan, KS

Introduction

- Increasing levels of atmospheric greenhouse gases (GHGs) and associated climate change are of serious global concern:
  - For every degree in global temperature increase, grain production yields are expected to decrease 10%;
  - Global human population continues to increase by roughly 80 million per year.
- These increasing temperatures and GHGs, coupled with increasing food demand, present significant environmental, economic, and political challenges in the years to come.

Soils and GHGs

- Of these GHGs, carbon (C) is of the most concern as it is released:
  - Through the combustion of fossil fuels;
  - From agricultural soils by conventional agricultural management practices.
- Soils represent largest global C stock.
  - Hold the greatest potential to sequester atmospheric C.

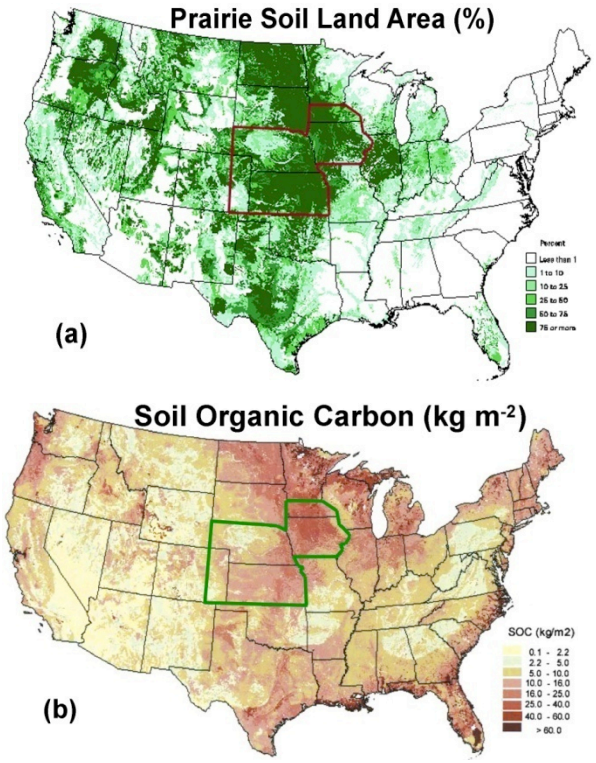

Figure 2. Prairie soils (USDA Mollisol Order) account for (a) 27% of the conterminous US land surface and (b) 31-39% of SOC stocks. The majority of US cropping acreage can be found on prairie soils, with these fertile soils hosting "bread baskets" in the central US, the South American Pampas, and the Russian steppe.

- In North America, 30 – 50% of soil organic carbon (SOC) was lost in prairie soils since conversion to agriculture 150 years ago.

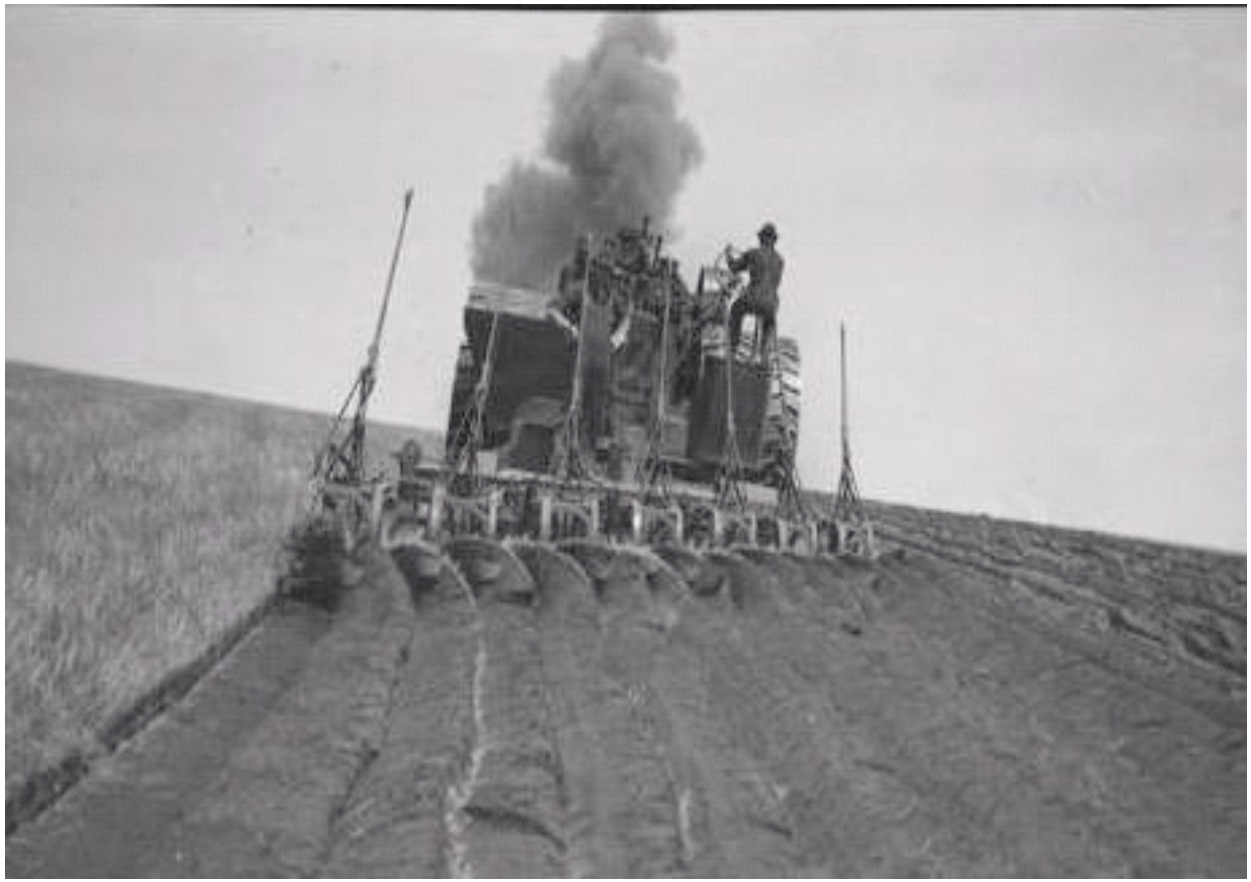

Steam plow breaking native prairie in early 1900s in ND. Institute for Regional Studies, NDSU.

Tillage Method and Agricultural Carbon Fluxes

- Conventional intensive tillage methods:
  - Remove crop residues (plant litter/ non-photosynthetic vegetation) from the surface;
  - Expose soil to erosion;
  - Destroy the natural soil structure;
  - Expose soil to SOC-destroying oxygen.

Tillage Method and Agricultural Carbon Fluxes

- Modern reduced- and conservation-tillage methods:
  - Preserve increased amounts of crop residues on the soil surface;
  - Decrease soil erosion;
  - Disturb the soil less;
  - Preserve the natural soil structure;
  - Help increase SOC;
  - Require fewer passes with farm machinery, using less fossil fuels.

Remote Sensing Tillage Method

- Tillage method is best sensed by determining areal crop residue cover fraction.
- Broad Landsat TM/ LDCM OLI/ Sentinel-2 bands cannot discriminate narrow spectral features of dry vegetation components.
- Landsat TM band 7 is very sensitive to live vegetation:
  - Does not contrast well among crop residues, soils, and live vegetation.

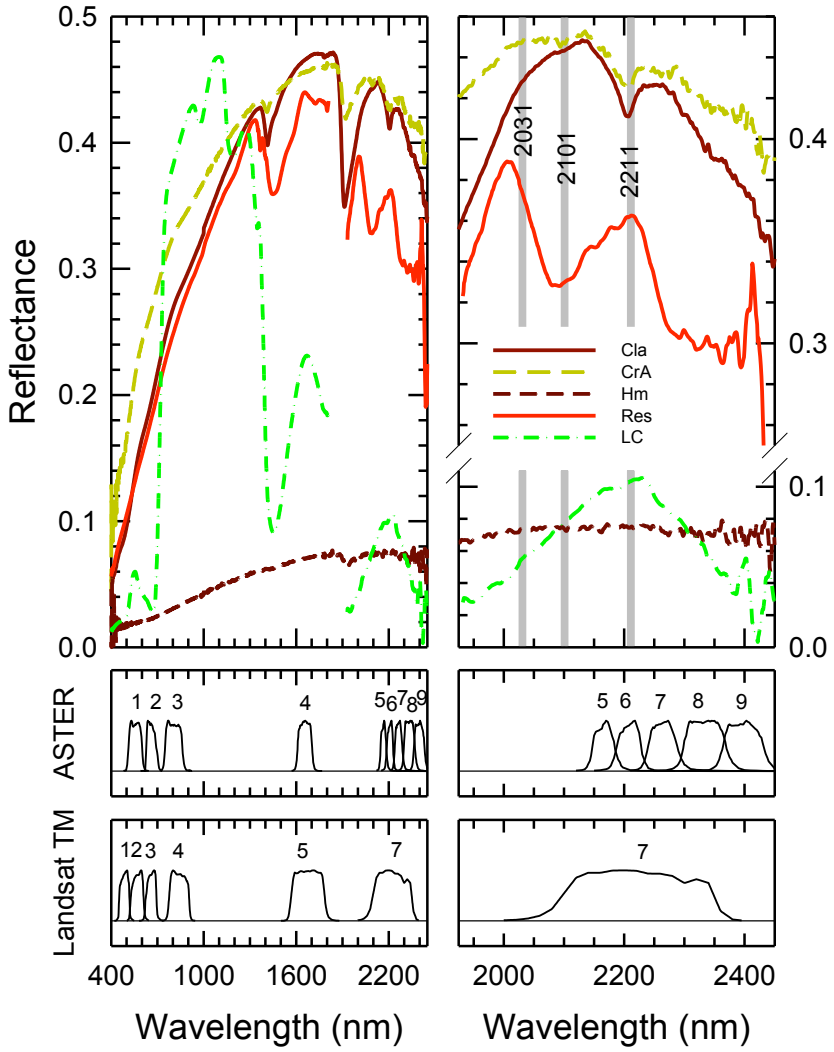

Remote Sensing Tillage Method

- The Cellulose Absorption Index (CAI) ideal for sensing dry vegetation:
  - Targets an absorption occurring at 2101 nm present for all sugars, including cellulose, but rare for soil minerals.
  - Has a linear relationship between bare soil, 100% residue cover.
  - Contrasts crop residues well among soils, live vegetation.

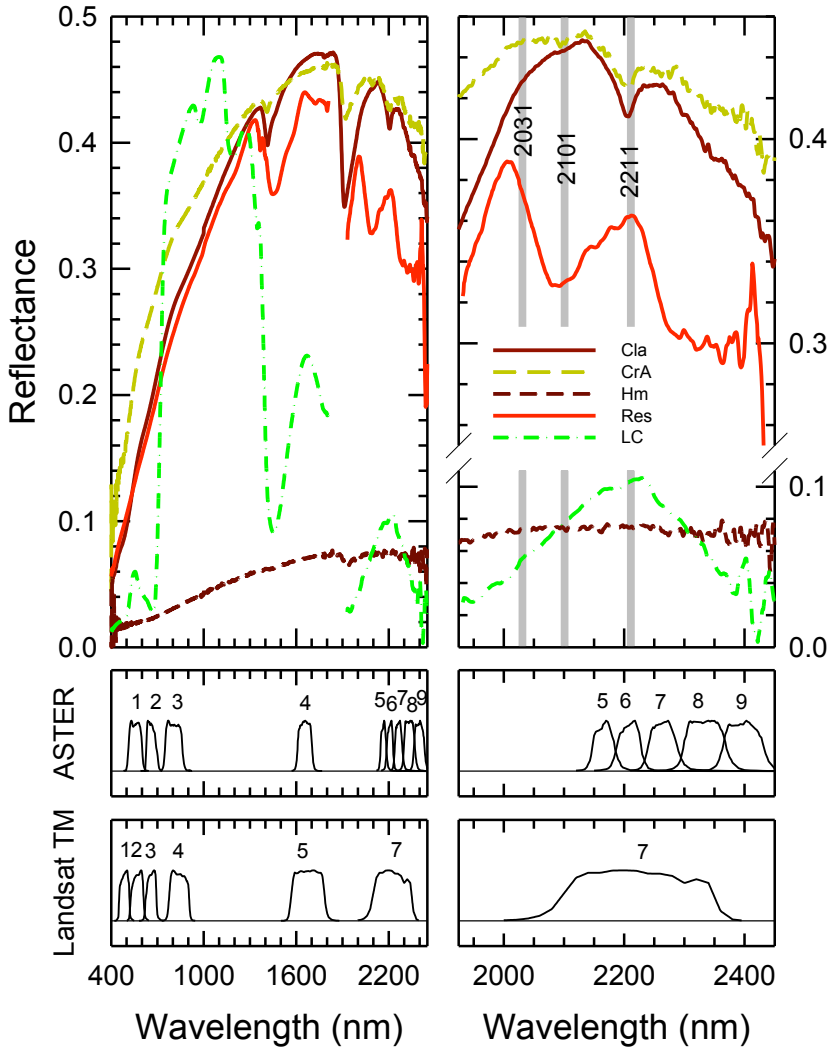

Narrowband CAI Best for Sensing Crop Residues

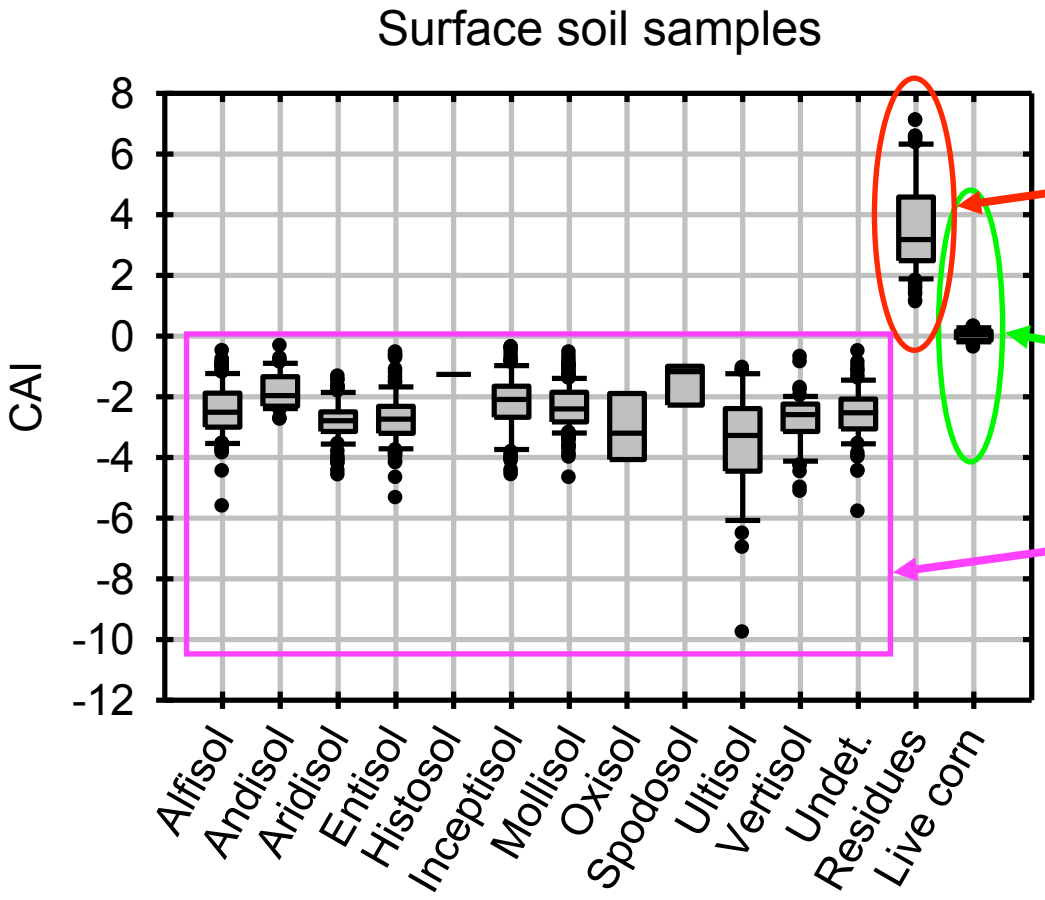

Crop residues > 0, n = 83.

Green vegetation ≈ 0, n = 40.

Soils < 0, n = 893.

$$CAI = 100\left(\frac{R_{2031} + R_{2211}}{2} - R_{2101}\right)$$

- Crop residues contrast well with all soils, green vegetation.

ASTER SWIR Normalized Difference Residue Index (SINDRI) Also Good

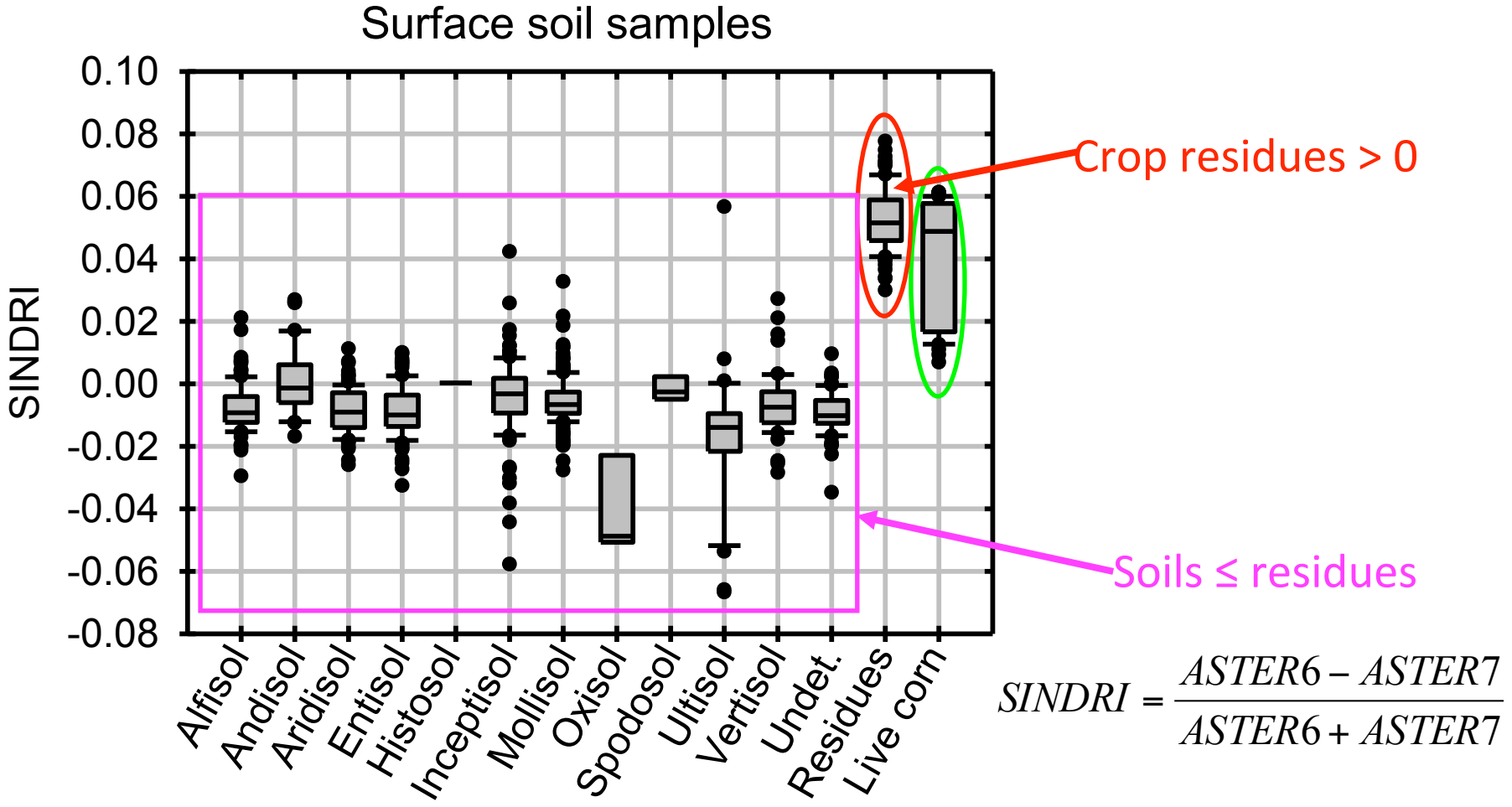

- 9 soils have SINDRI > 0.02, lacking contrast.
- Residues and green vegetation also lack contrast.

Landsat TM Bands not so Good

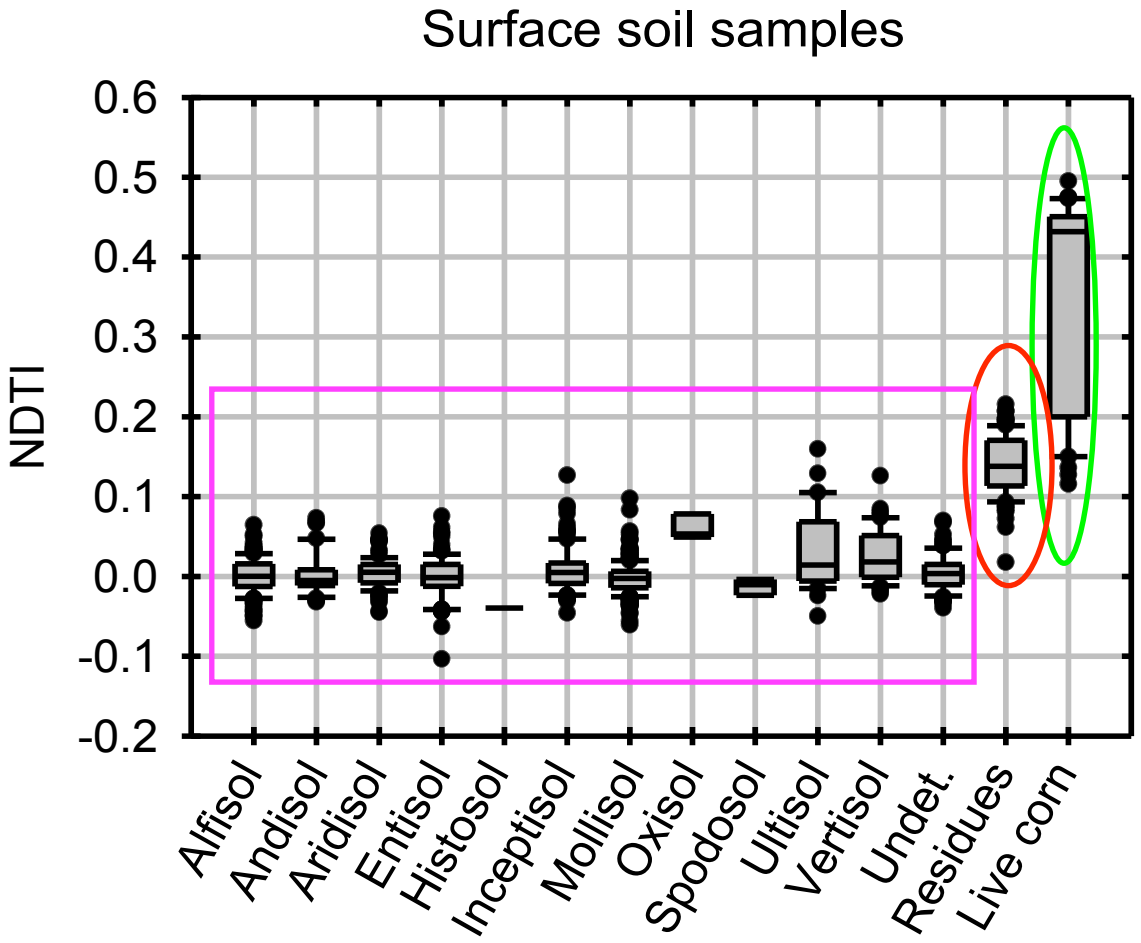

$$NDTI = \frac{TM5 - TM7}{TM5 + TM7}$$

- Many soils, residues lack contrast.
- Green vegetation has a much stronger signal than residues or soils- will strongly bias mixed pixels.

Remote Sensing Crop Residue: Indiana 2006

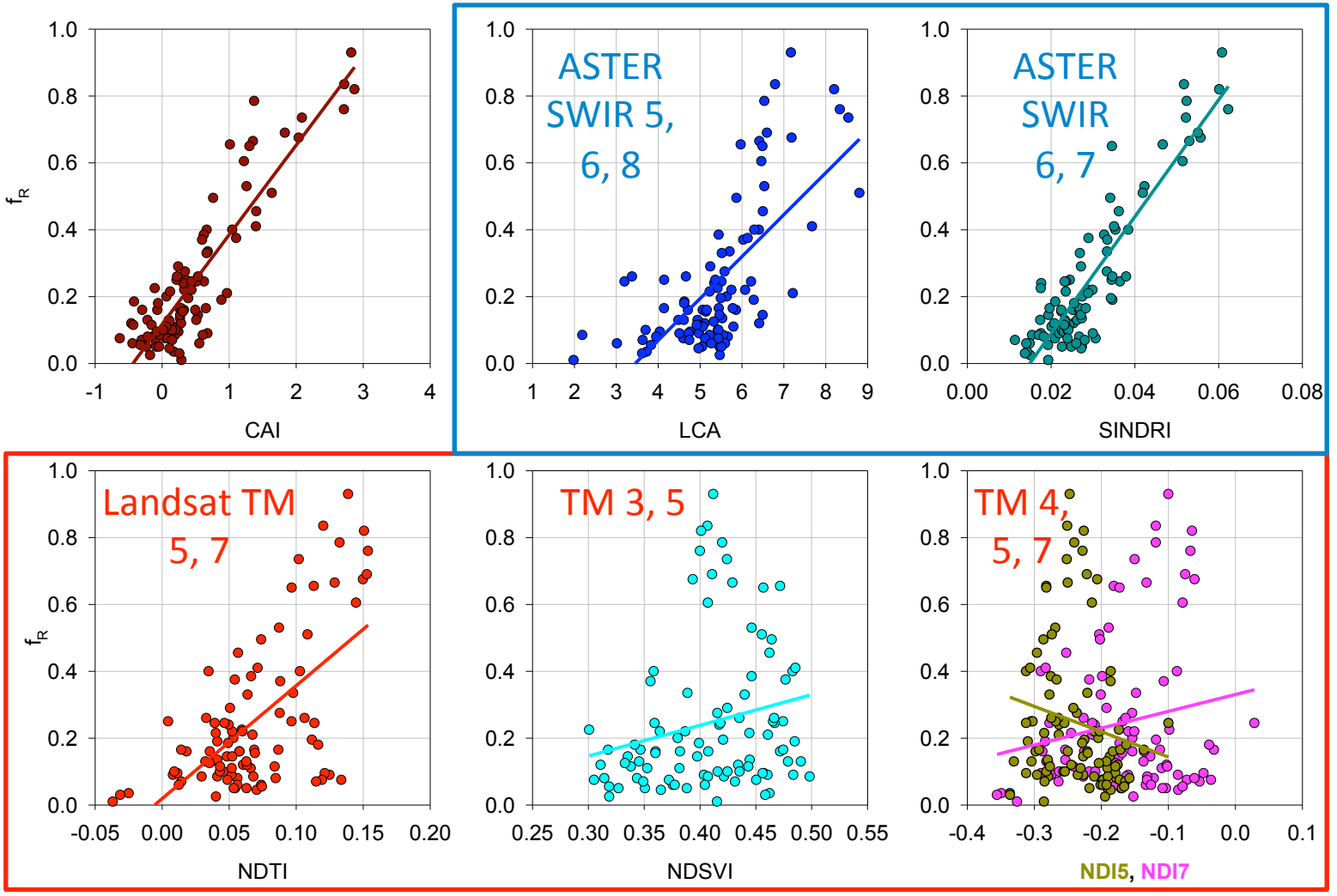

- ASTER SWIR-based indices work well, but are more affected by soils than CAI.
- Landsat TM- based indices do not separate well between residues, soils.

Remote Sensing Crop Residue: Ames, IA, 2007

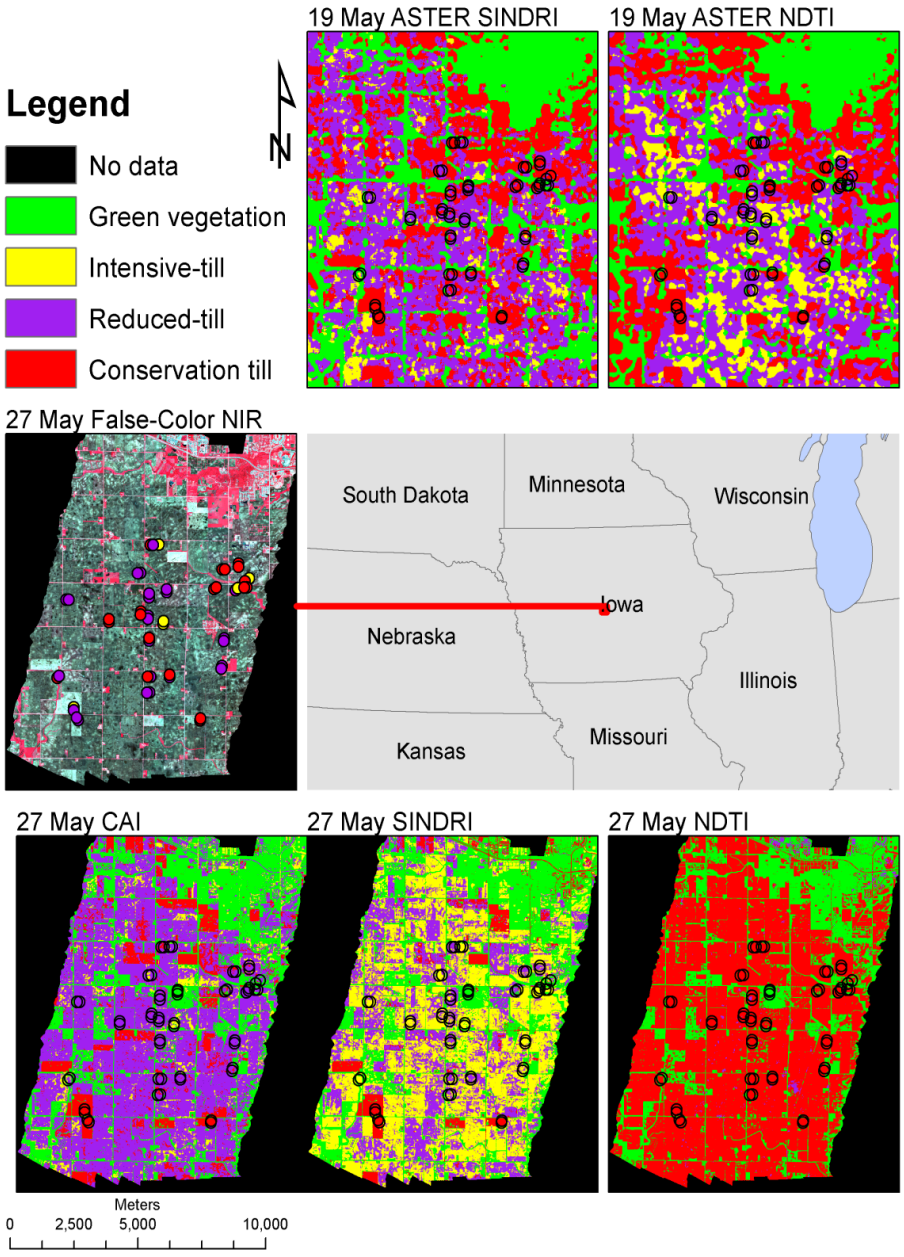

USDA/NRCS Tillage classes (% residue cover):

- Intensive: 0 – 15
- Reduced: 15 – 30
- Conservation: 30 – 100

Figure to left contains:

- Multispectral ASTER imagery, 27 May 2007.
- Hyperspectral imagery acquired by SpecTIR LLC (Sparks, NV):
  - Convolved to equivalent ASTER and Landsat TM bands.
- Circles denote ground-truth locations.

Remote Sensing of Plant Cover and Chlorophyll

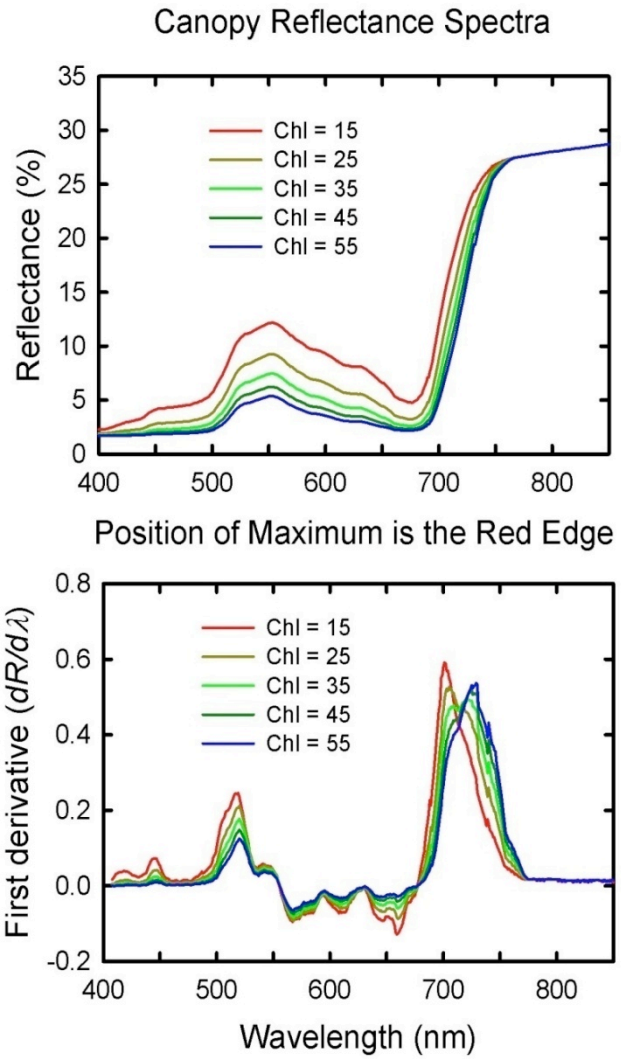

- Most plant cover/ condition remote sensing use Normalized Difference Vegetation Index (NDVI):

$$NDVI = \frac{NIR - red}{NIR + red}$$

- NDVI not overly sensitive to chlorophyll.
- Red edge indices are sensitive to chlorophyll/ leaf nitrogen.
- The position of the Red Edge can indicate nitrogen stress conditions.

Remote Sensing Crop Canopy Characteristics

- Growing season biophysical characteristics:

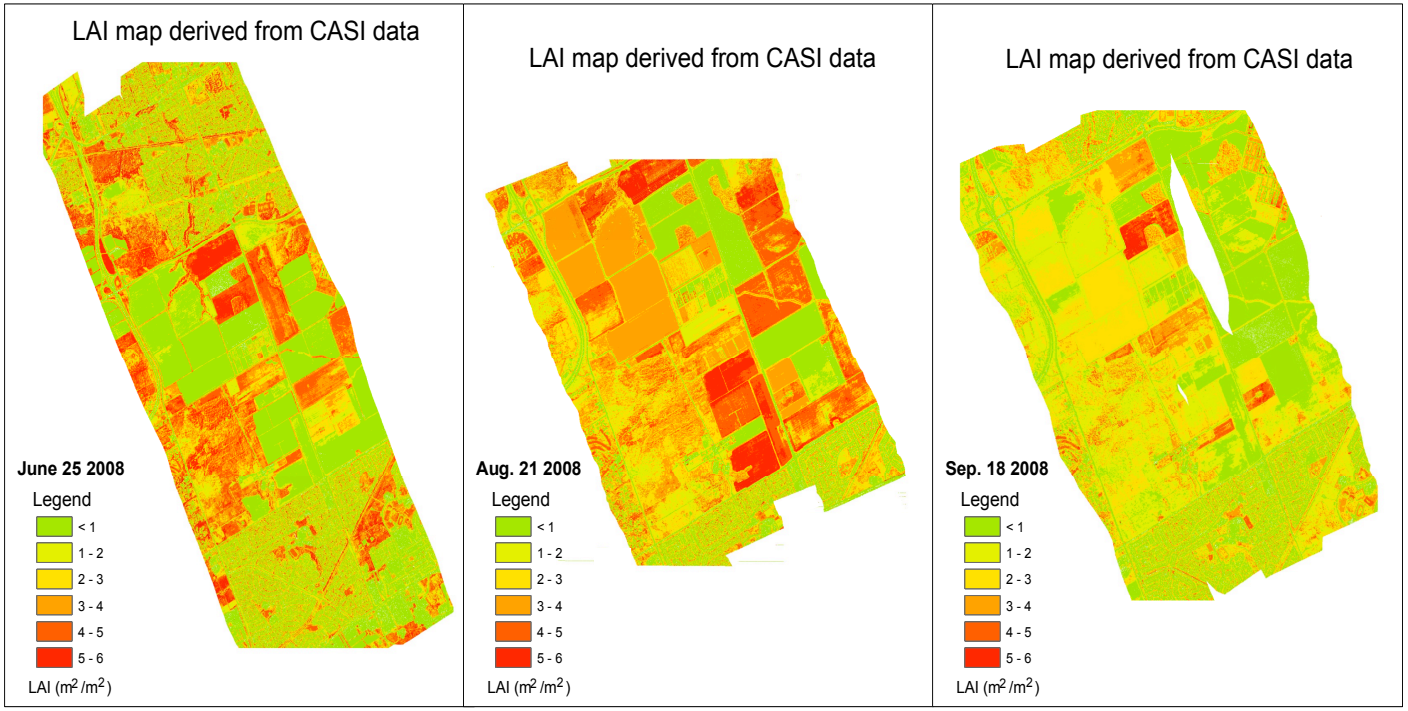

CASI (Itres Research Ltd., Calgary, AB)- derived leaf area index (LAI) maps throughout the summer 2008 growing season near Ottawa, ON. Data acquired by York University (Toronto, ON).

Remote Sensing of Canopy Water and Evapotranspiration

- Soil moisture deficiencies cause leaf stomata to close up:
  - Evapotranspiration and photosynthesis decrease;
  - Vegetation heats up;
  - Yields can be negatively impacted.
- NIR and SWIR band at 1610 – 1650 nm can be used to estimate canopy water content:
  - SWIR band reflectance inversely related to leaf water content.
- HyspIRI's thermal infrared (TIR) bands (10.8 and 12.0 μm) will allow for estimation of canopy evapotranspiration (ET).

Agricultural Greenhouse Gas Monitoring via Remote Sensing

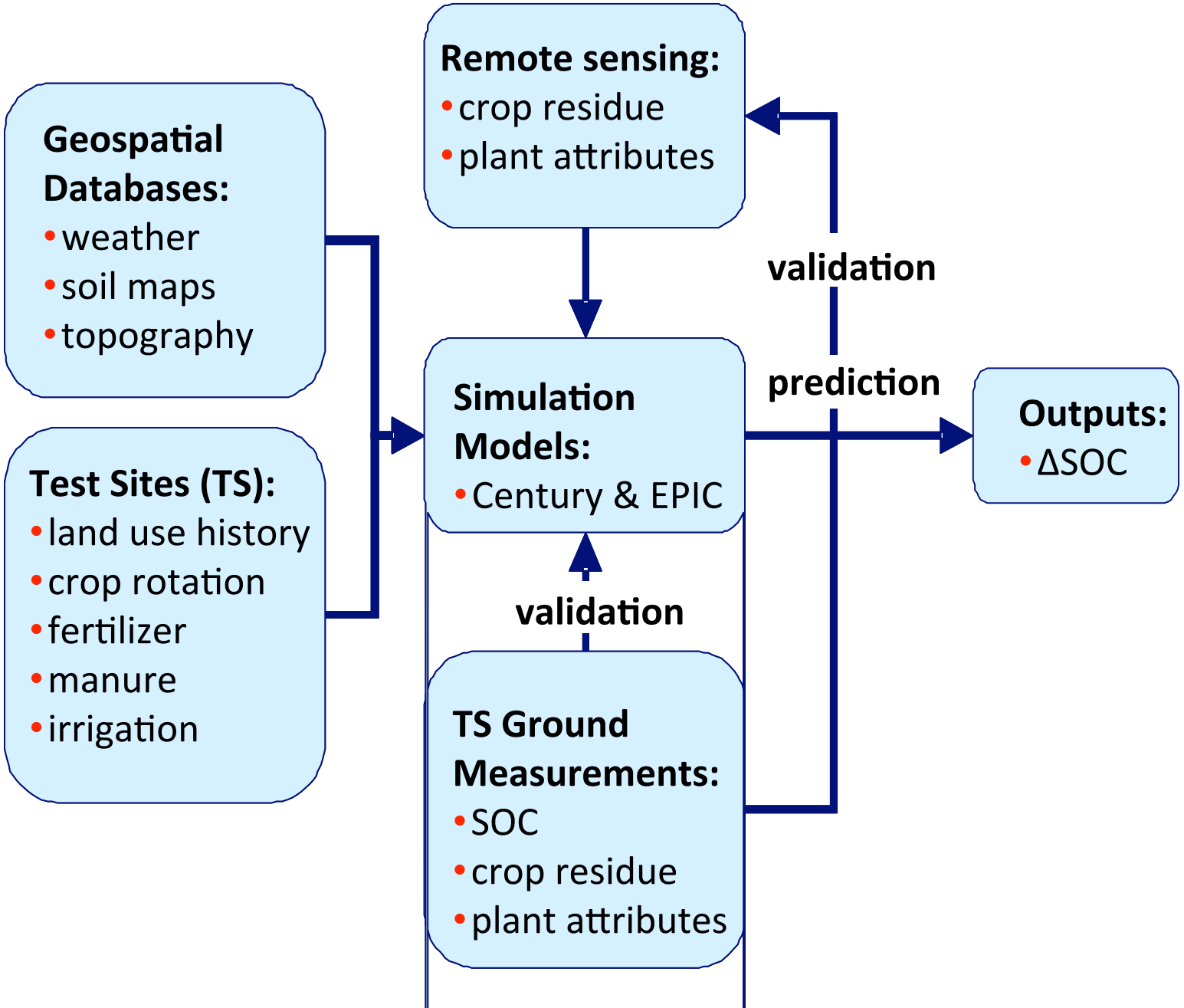

Conclusions

- Agricultural GHG fluxes can be monitored by combining remote sensing and other geospatial data into simulation models such as EPIC or Century.
  - These can be calibrated against field measurements of SOC.
- Most operational multispectral satellite sensors such as Landsat, SPOT, Sentinel-2, etc. do not have appropriate sensor bands for measuring tillage, a critical input to GHG models.
- Hyperspectral systems such as HyspIRI will allow for high-quality measurements of tillage and other crop canopy characteristics, and advance GHG monitoring efforts.
  - These systems will also allow for calibration of future advanced multispectral sensors.

Airborne TIR Hyperspectral Imaging with High Spatial Resolution and Wide Area Coverage

David M. Tratt and Jeffrey L. Hall
Space Science Applications Laboratory
Physical Sciences Laboratories
The Aerospace Corporation

HyspIRI Science Workshop
Washington, DC
August 23-25, 2011

© The Aerospace Corporation 2011

Mako: a New Thermal IR Imager

- Airborne spectral imager operating in the thermal infrared (7.8 to 13.4 μm)
  - *Deploys aboard Twin Otter aircraft*
- 128-band grating-based spectrometer
  - *0.044 μm per channel (or ~4 cm^{-1} resolution at 10 μm)*
- Large area coverage mode
  - *Scan to ± 40° around nadir*
    - 20 km^2 per minute (at 2-m GSD) from 12,500 ft (3.8 km) AGL
    - 8-minute duration datasets demonstrated
- Follow-on to SEBASS sensor
  - *Uses whiskbroom rather than pushbroom scanning*
  - *0.5 mrad pixel IFOV (vs. 1.0 mrad for SEBASS)*

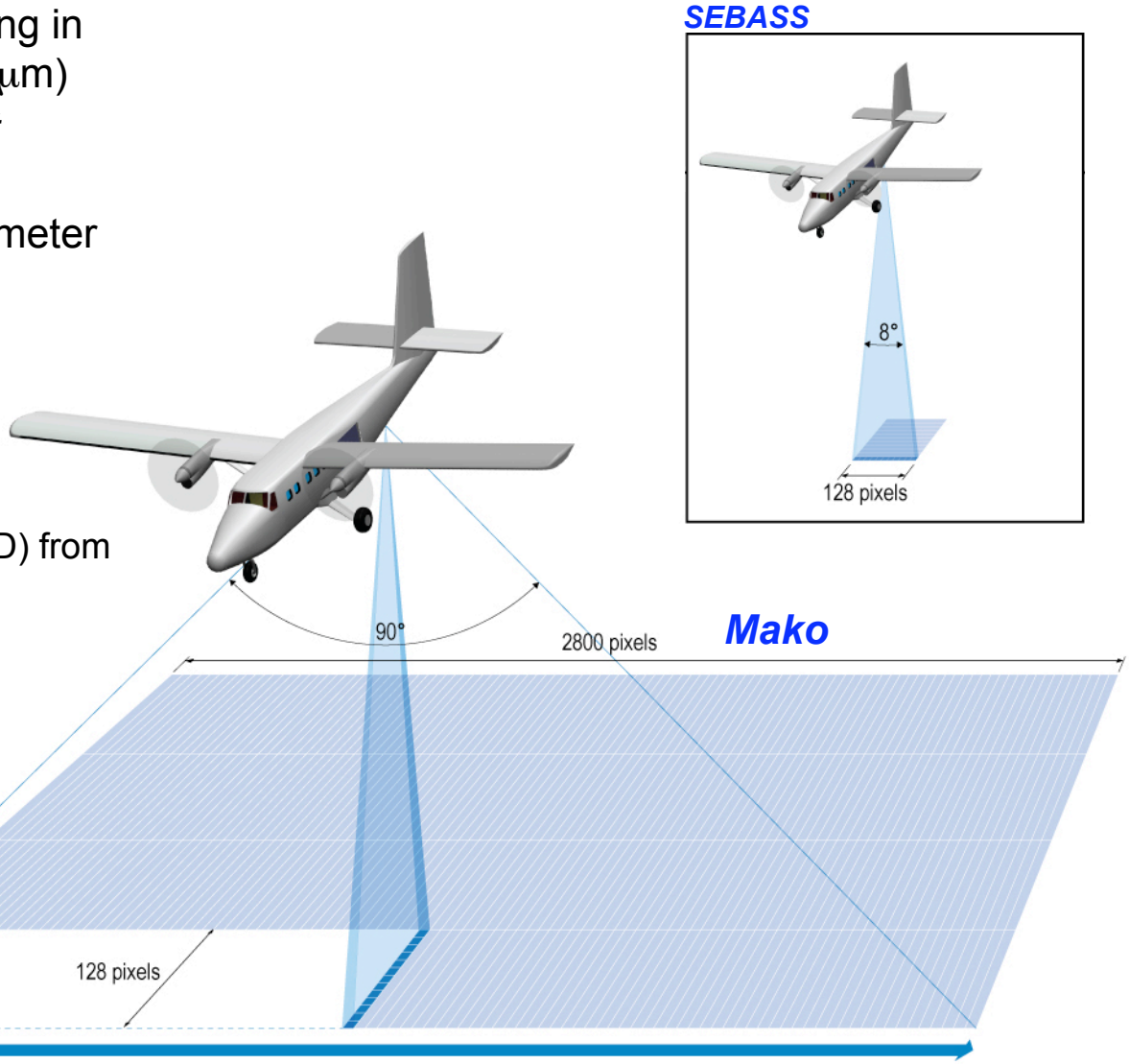

AEROSPACE

Sensor Details (cont.)

- Uses a commercial 3-axis stabilization mount
  - *Intergraph Z/I mount*
  - *High frequency jitter removed by physical vibration dampeners*
  - *Low frequency jitter removed by active control*
    - Stabilizes up to ±5° range in pitch and roll
  - *Up to ±12° yaw offset can be accommodated in Mako installation*

- Sensor attitude measured with Litton LN-100G INS and KVH DSP-3000 fiber-optic gyros (x3)
  - *Estimated pixel geolocation uncertainty is <10 meters from 12,000 ft AGL*
    - With separate differential GPS

- Gimbal mirror pitch control provides additional capability
  - *Bi-directional whisking*
  - *High-sensitivity (low area coverage) scans ("stare" mode)*

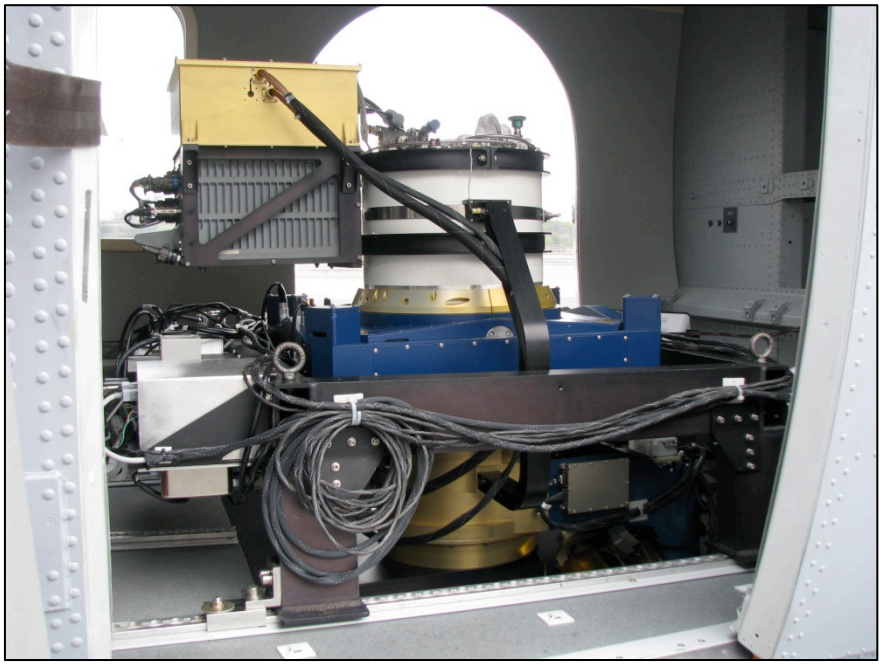

AEROSPACE

Sensor Details

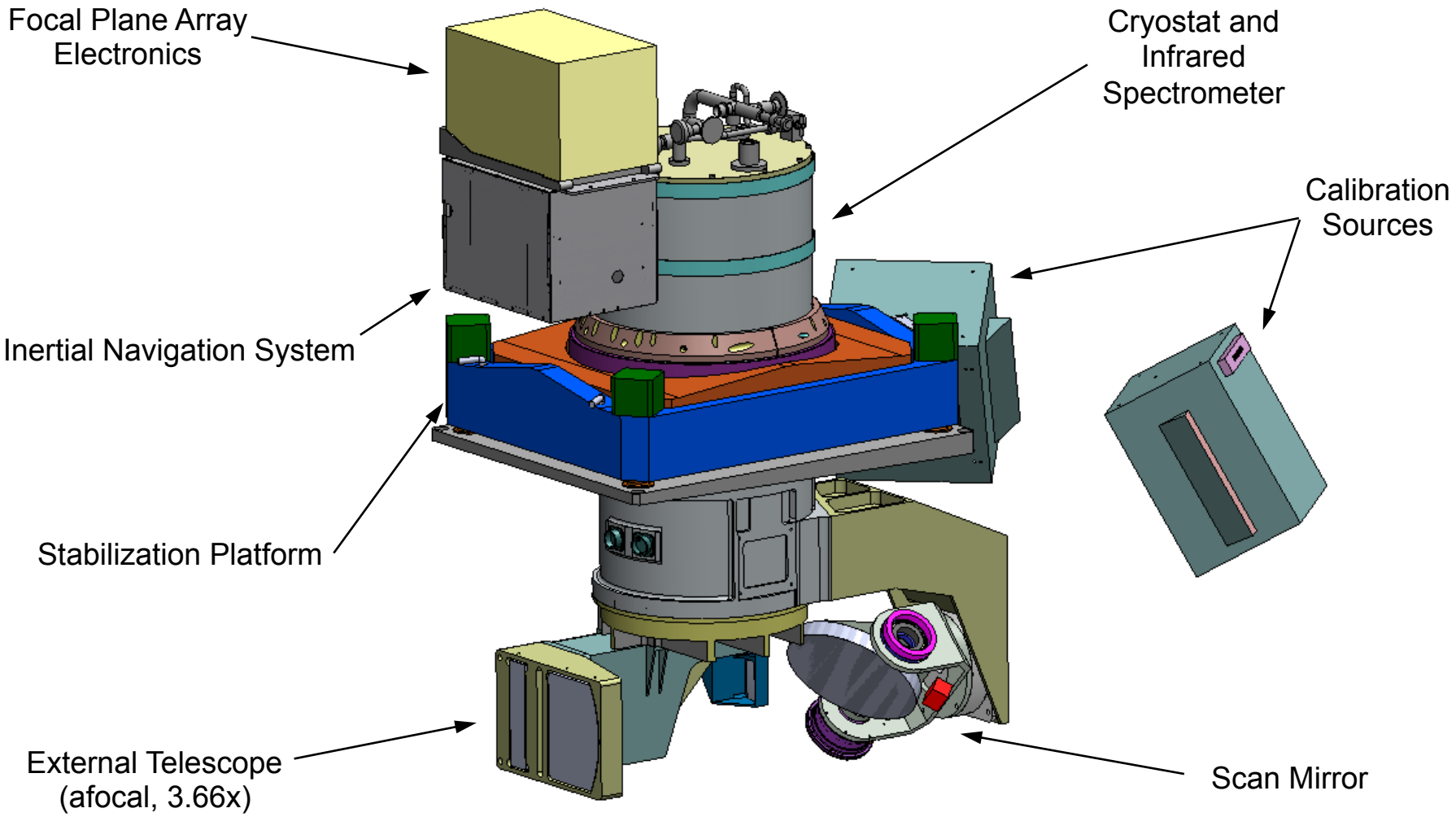

AEROSPACE

Spectrometer Details

- *Mako* uses a DRS Si:As Blocked Impurity Band 128x128 FPA
  - *75 μm pixels*
  - *Cooled to 10K using LHe*
  - *99.93% operable*
  - *4 kHz max. frame rate (Mako currently at 800 Hz); 16 output taps*

- Spectrometer based on Dyson lens and concave grating
  - *Low distortions ("smile" and "keystone") at fast f-numbers*
    - *Mako* is an f/1.25 system

- Cooled optics (LHe blow-off) for improved sensitivity and increased dynamic range
  - *48-hour dewar hold time*

AEROSPACE

Quickbird - True Color Image

Urban Mapping: Los Angeles

Whisk Footprints

Image Courtesy:
Digital Globe - 06/18/2009
Universal Transverse Mercator Projection
Zone 11 - North - WGS84 Datum/Spheroid

0 0.25 0.5 1 Miles

Latitude / Longitude Graticule

MAKO 23 WHISK MOSAIC - PRIMARY COLLECTION

12k ft. AGL - ~2m GSD
El Segundo, CA - 09/15/2010
Flat Field Corrected - 10.6 μm Thermal Band

MAKO Overview

- 3 year corporate IR&D
- Highly capable LWIR HSI airborne sensor
- Si:As array for best operability
  - *DRS 128x128x75μm pixel 16.4.3MHz outputs = 4000Hz maximum frame rate*
  - *10K operating temperature == liquid helium cryostat*
- Maximize optical throughput
  - *At fast f/ratio (f/1.25) Dyson spectrometer is best for image quality & distortion*
  - *128 Spectral bands 7.8-13.4μm*
  - *128 x 1m GSD from 6000 ft AGL*
- Agile pointing system
  - *Extra(~16x)signal can be allocated between area coverage and improved S/N*

MAKO Twin Otter Flight Configuration

MAKO Pointing System/Scan Geometry

- ±45° X-track (Roll)
- ±10° In-track (Pitch)
- Nominal Whisk Scan 25°/sec in Roll ±45° =3.6sec
- 0.55sec Flyback (Roll)
- Pre-programmed Rolls To View Cal Blackbodies

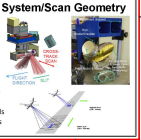

UTM Easting and Northing Grid

Mako Science Flights

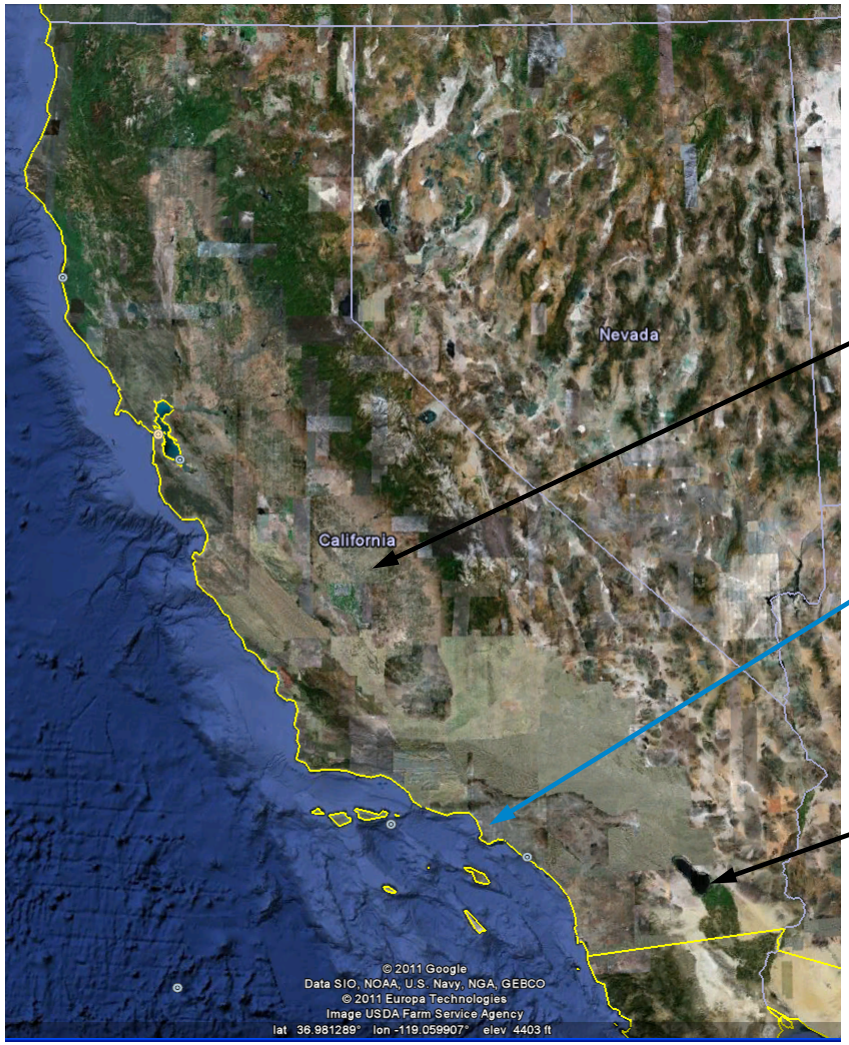

San Joaquin Valley

(Home base in Los Angeles)

Salton Sea Geothermal Field (SSGF)

(*Google Earth*)

AEROSPACE

SSGF – SE shore of Salton Sea, Background Image

AEROSPACE

SSGF – *Mako* Thermal Radiance Overlay (1-m GSD)

AEROSPACE

SSGF – Thermal Radiance and Ammonia Retrievals

AEROSPACE

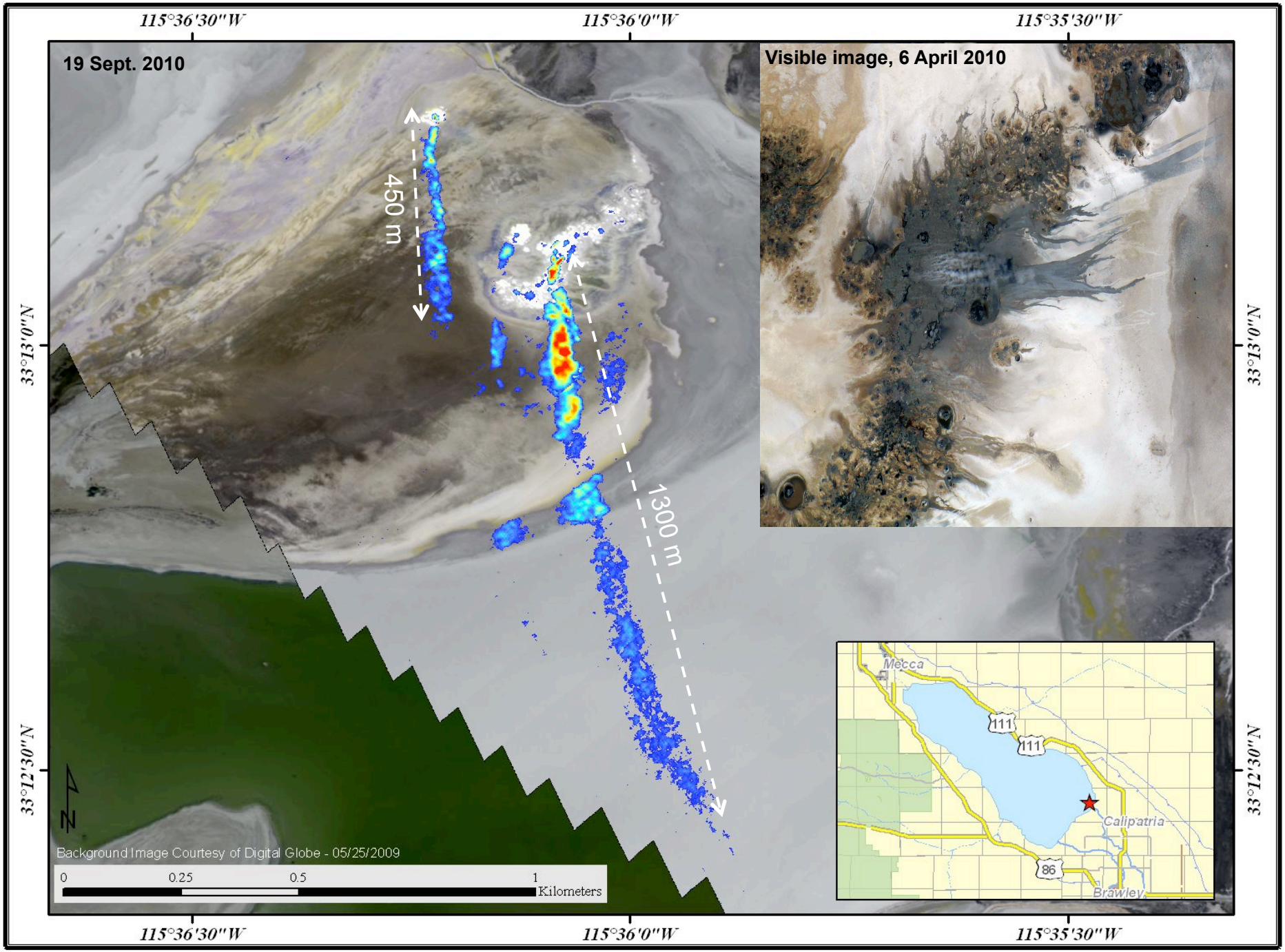
115°36'30"W
115°36'0"W
115°35'30"W
33°13'0"N
33°12'30"N
19 Sept. 2010
450 m
1300 m
Visible image, 6 April 2010
Mecca
111
111
Calipatria
86
Brawley
N
Background Image Courtesy of Digital Globe - 05/25/2009
0
0.25
0.5
1
Kilometers

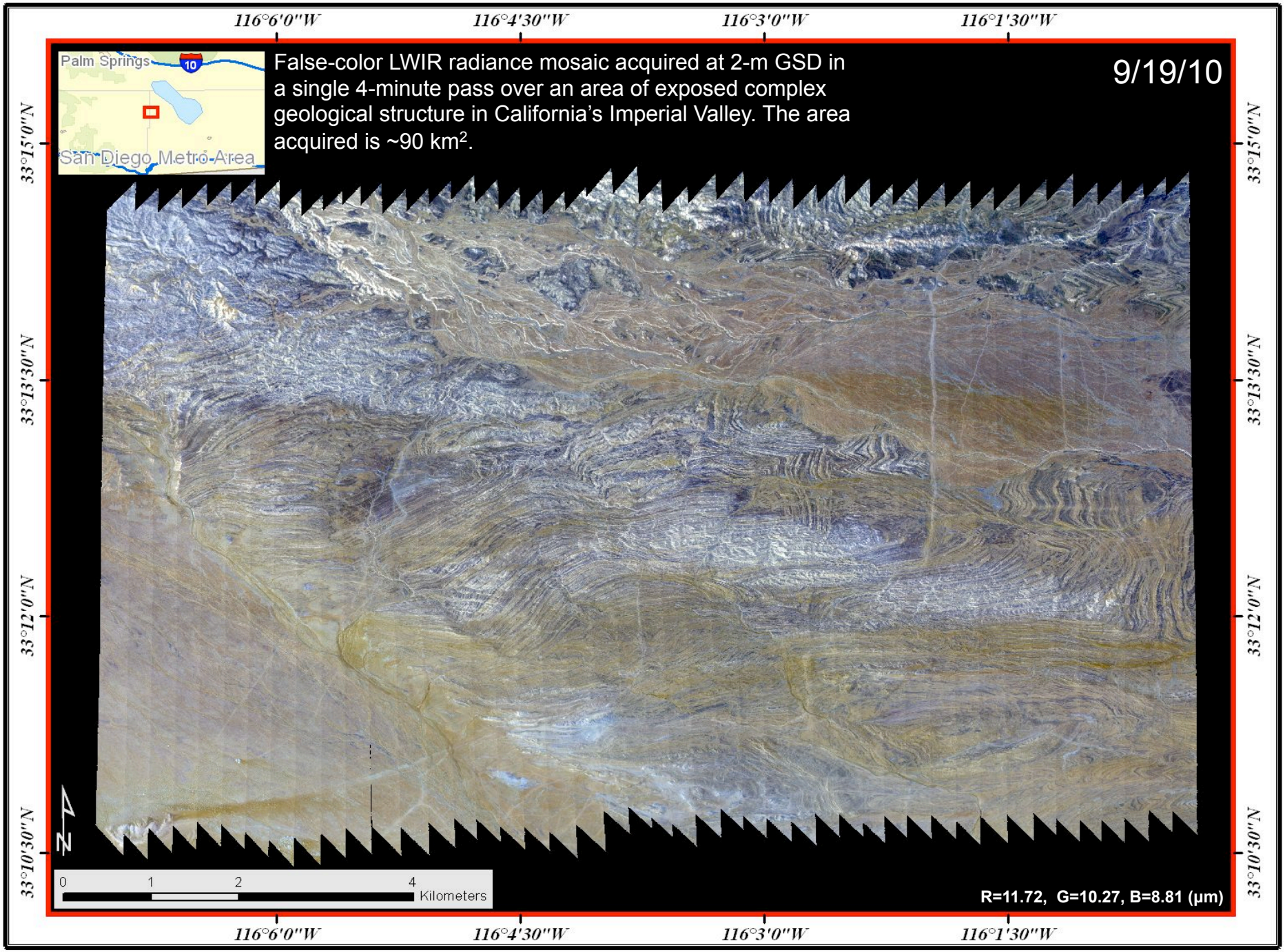
116°6'0"W
116°4'30"W
116°3'0"W
116°1'30"W
33°15'0"N
33°13'30"N
33°12'0"N
33°10'30"N
Palm Springs
10
San Diego Metro Area
False-color LWIR radiance mosaic acquired at 2-m GSD in a single 4-minute pass over an area of exposed complex geological structure in California's Imperial Valley. The area acquired is ~90 km².
9/19/10
N
0
1
2
4
Kilometers
R=11.72, G=10.27, B=8.81 (µm)

Agricultural Ammonia in the San Joaquin Valley

- *Mako* was flown over California's Central Valley on 17 Sept. 2010
- Flights were conducted in Tulare and Kings Counties primarily between the towns of Visalia and Delano
- Altitude was 3.8 km AGL → 2-m GSD
- Collections coordinated with overflights of the European IASI (Infrared Atmospheric Sounding Interferometer) sensor aboard Europe's MetOp-A
- Integrated ammonia column densities in the dairy farm regions near Visalia varied between 25 and 45 ppm-meters
- The airborne data clearly showed prominent plumes of ammonia emanating from some of the dairy facilities

This work being done in collaboration with the IASI team based at *l'Université Libre de Bruxelles* in Belgium

IASI annual average for 2010

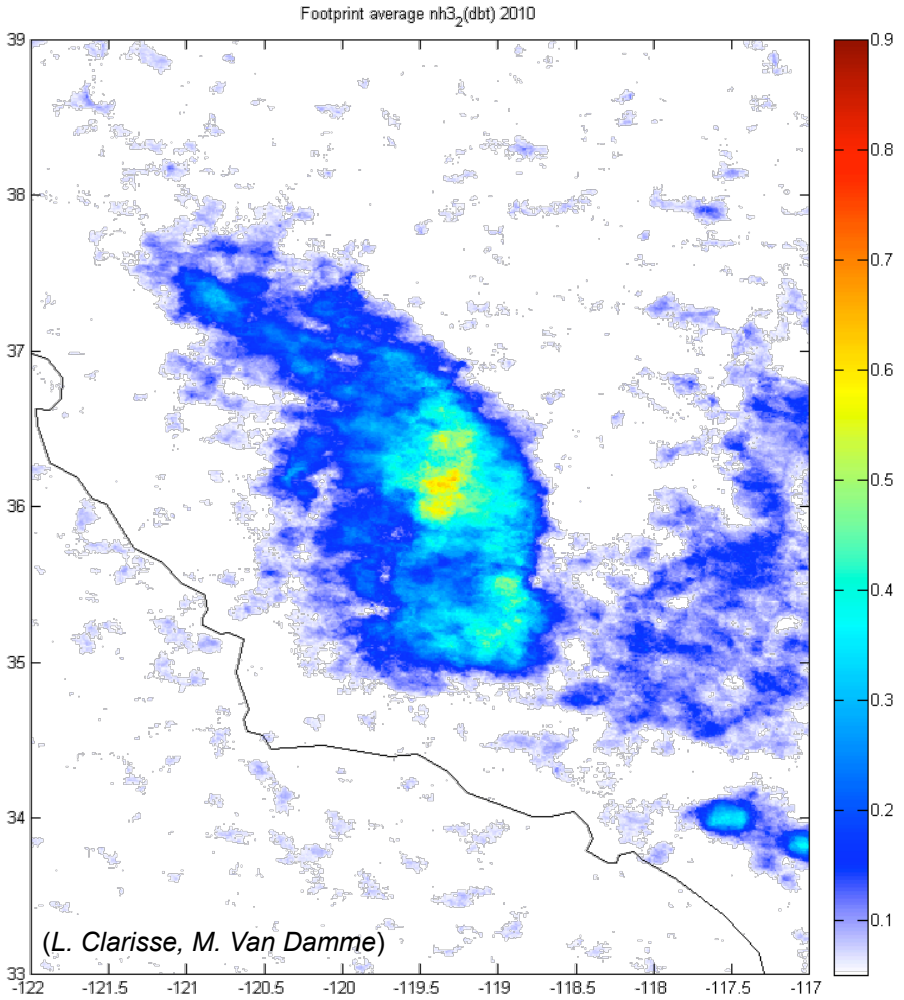

AEROSPACE

Google Earth Image for Flight CV01

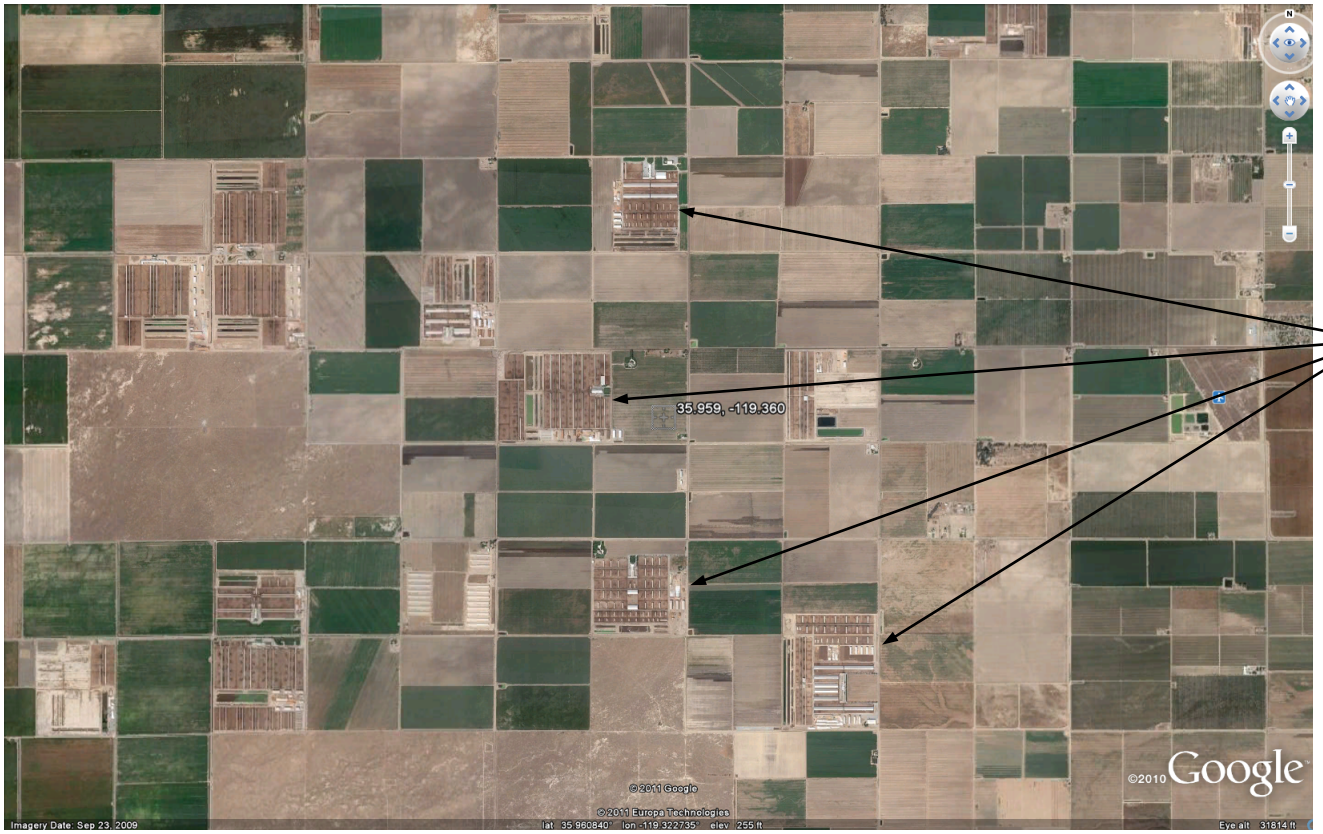

Dairy farms

AEROSPACE

CV01 – Brightness Temperature Map

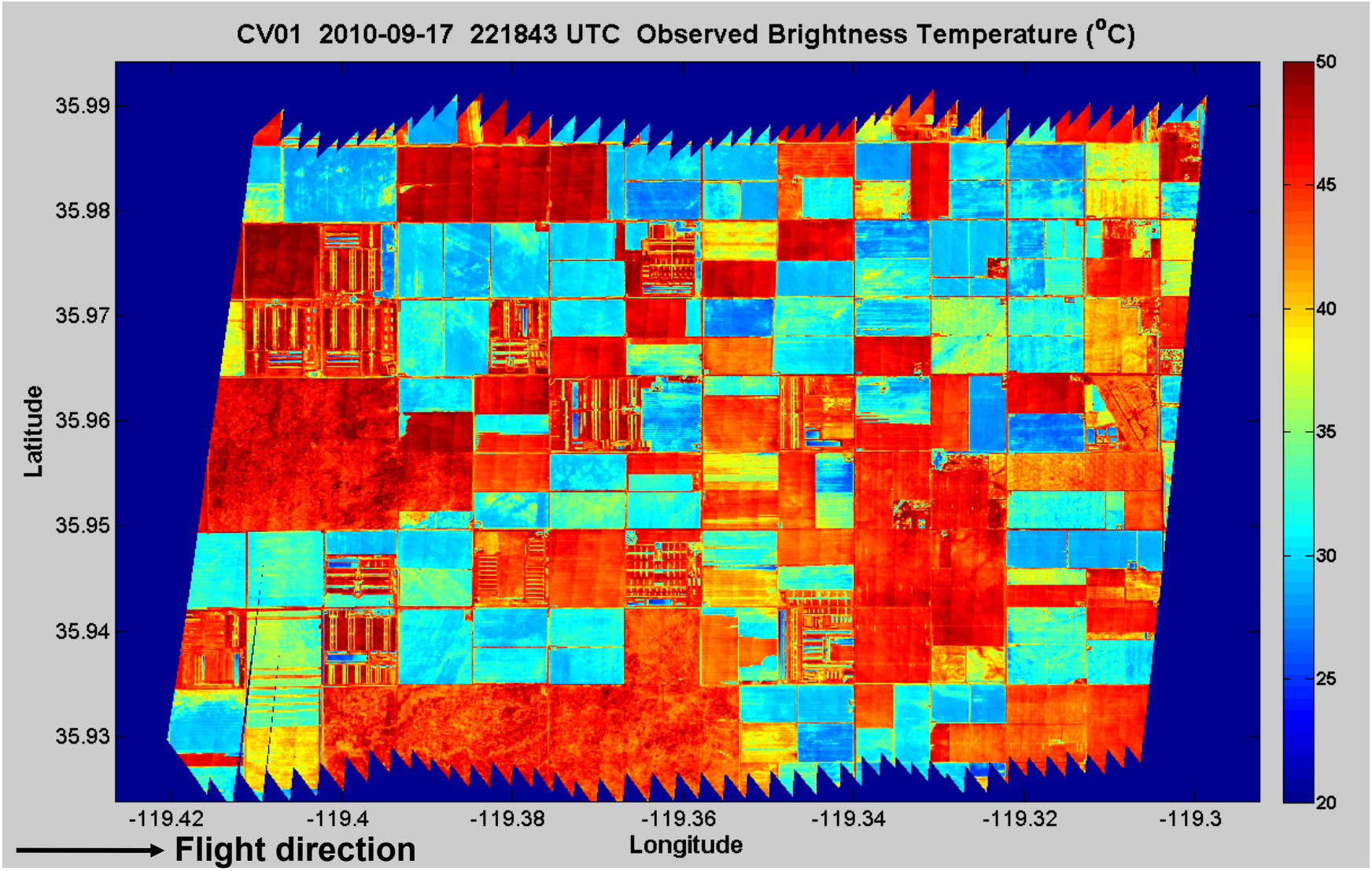

AEROSPACE

CV01 – Computed Column Density Map

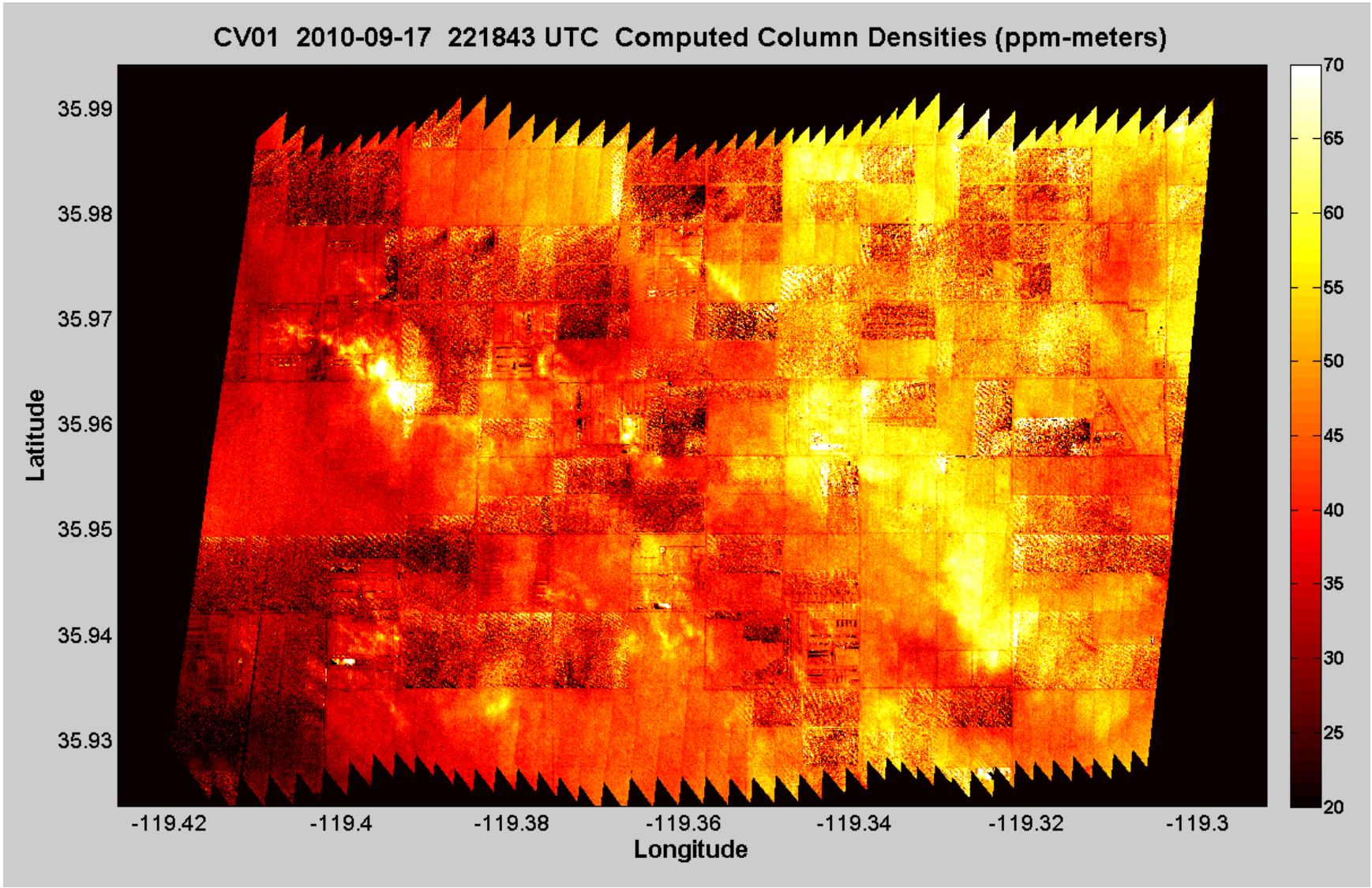

AEROSPACE

Regional comparison between IASI and *Mako* NH_3

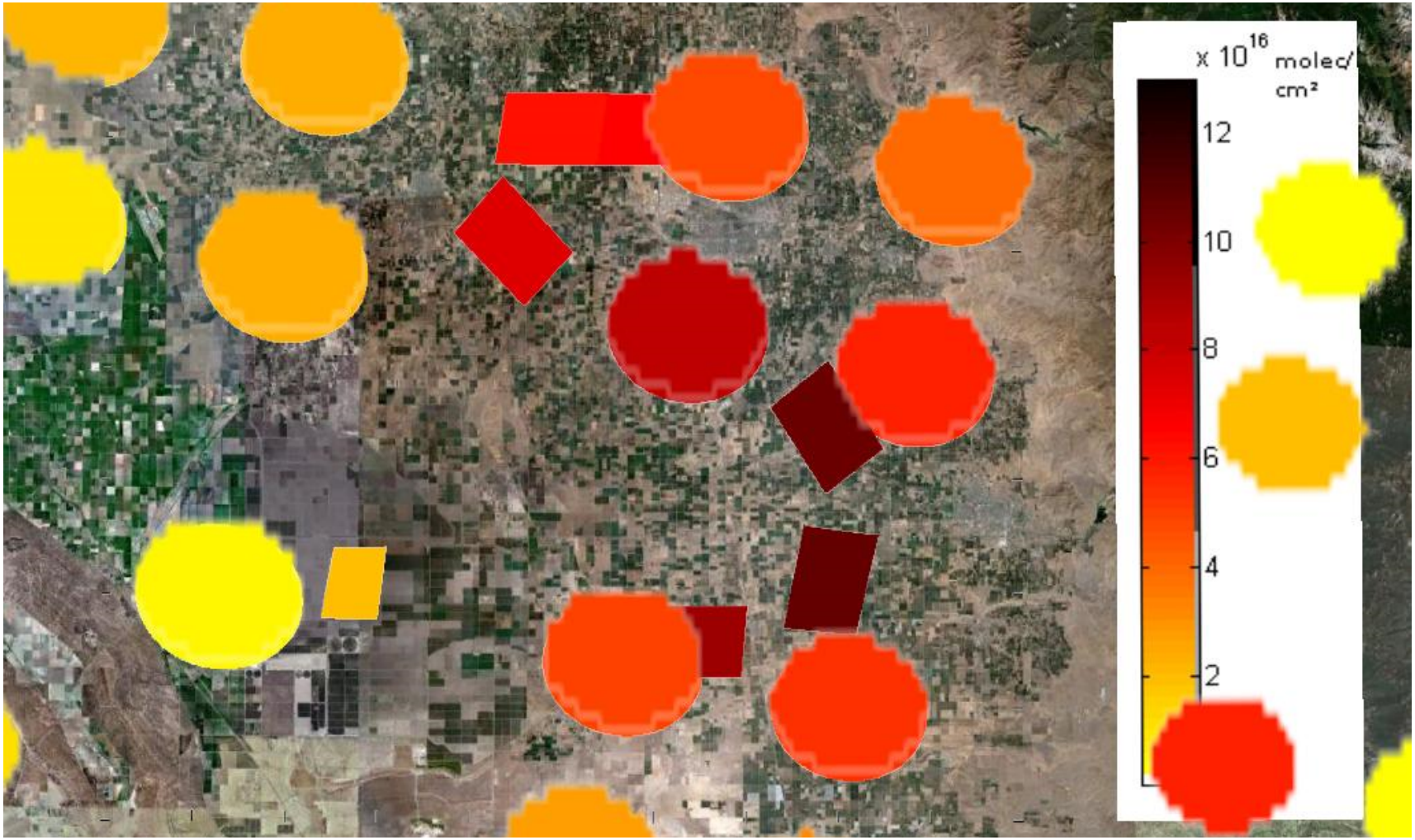

(*L. Clarisse, M. Van Damme*)

IASI: Polka dots
Mako: Parallelograms

AEROSPACE

09/16/2010 19:55:42

Thermal image

Plume tracking from 12 kft (3.8 km) AGL (GSD 2 m)

200 m

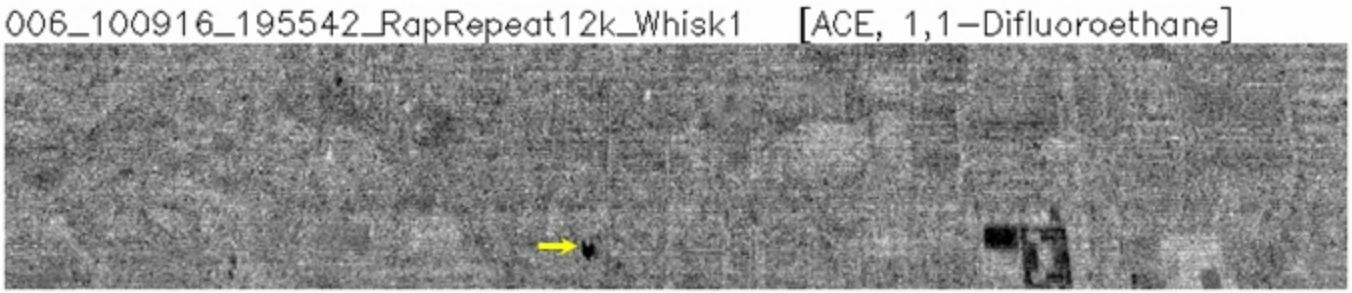

ACE filter

Continuous tracking of controlled tracer release

AEROSPACE

Summary & Future Plans

- A new high-performance thermal infrared spectral imaging sensor has successfully completed its inaugural flights
- Flights over California's Imperial and San Joaquin Valleys have demonstrated the utility of large area coverage
- Modifications ongoing to improve the frame rate and sensitivity
  - *Current NEΔT is ~0.1 K at 10 μm*
- *Mako* is available to participate in field studies

AEROSPACE

Acknowledgements

- Assistance of the following personnel of The Aerospace Corporation is gratefully acknowledged:
  - *Richard Boucher*
  - *Kerry Buckland*
  - *David Gutierrez*
  - *Steven Hansel*
  - *Patrick Johnson*
  - *Brian Kasper*
  - *Eric Keim*
  - *Nery Moreno*
  - *Mark Polak*
  - *Mazaher Sivjee*
  - *David Warren*
  - *Stephen Young*

All trademarks, service marks, and trade names are the properties of their respective owners.

Atmospheric Correction Algorithms for Surface Reflectance Retrievals from VSWIR Measurements

Bo-Cai Gao[1], Robert O. Green[2], and Sarah Lundeen[2]

[1]Remote Sensing Division, Naval Research Lab, Washington, DC USA

[2]Jet Propulsion Lab, California Institute and Technology, Pasadena, CA USA

INTRODUCTION

- Timeline of algorithm development:
  - ATREM – 1st land version (~1991, band model) to support the AVIRIS/HIRIS Project. A Paper was published in 1993 on RSE.
  - ATREM - upgraded land version (~1997, line-by-line model) to support the Navy COIS/NEMO Project. Reported in a 1997 SPIE extended abstract.
  - ATREM – 1st ocean version (~1999, line-by-line, spectrum matching using ***channels above 0.86 μm for Case 2 waters***, based on R. Fraser's formulation and multi-layer atmospheric model). A paper was published in 2000 on Applied Optics.
- Activities on prototyping the HyspIRI VSWIR Level 2 Algorithms
  Porting over a land version of algorithm to an AVIRIS computer, plus other functional versions of algorithms for hyperspectral data processing, including routines for refining wavelength calibrations, signal to noise ratio estimates, spectral convolution, and spectral smoothing.
- Sample results from AVIRIS and HICO data.
- Processing speed on an AVIRIS server computer.
- Summary

Selected Publications from Analysis of AVIRIS Data

- **1993** - Gao, B.-C., K. H. Heidebrecht, and A. F. H. Goetz, Derivation of scaled surface reflectances from AVIRIS data, *RSE., 44*, 165-178. (Cited by **260**).
- **2000** - Gao, B.-C., et al., Atmospheric correction algorithm for hyperspectral remote sensing of ocean color from space, Appl. Opt., 39, 887-896. (Cited by **103).**
- **2009** - Atmospheric correction algorithms for hyperspectral remote sensing data of land and ocean, RSE, 113, S17-S24. (Cited by 21).
- **1990** - Gao, B.-C., and A. F. H. Goetz, Column atmospheric water vapor and vegetation liquid water retrievals from airborne imaging spectrometer data, *JGR.*, *95*, 3549-3564. (Cited by **236**).
- **1993** - Gao, B.-C., A. F. H. Goetz, and W. J. Wiscombe, Cirrus cloud detection from airborne imaging spectrometer data using the 1.38 μm water vapor band, *GRL, 20*, 301-304. (Cited by **96**).
- **1996** - Gao, B.-C., NDWI - A normalized difference water index for remote sensing of vegetation liquid water from space, *RSE, 58*, 257-266 (Cited by **555**).
- **2003** - Li, R.-R., Y. J. Kaufman, B.-C. Gao, and C. O. Davis, Remote sensing of suspended sediments and shallow coastal waters, TGRS, 41, 559-566, 2003. (Cited by 58).
- **2007** - Gao, B.-C., M. J. Montes, R.-R. Li, H. M. Dierssen, and C. O. Davis, An atmospheric correction algorithm for remote sensing of bright coastal waters using MODIS land and ocean channels in the solar spectral region, TGRS, 45, 1835-1843. (Cited by 10).

Atmospheric Correction Over Land

An AVIRIS Spectrum

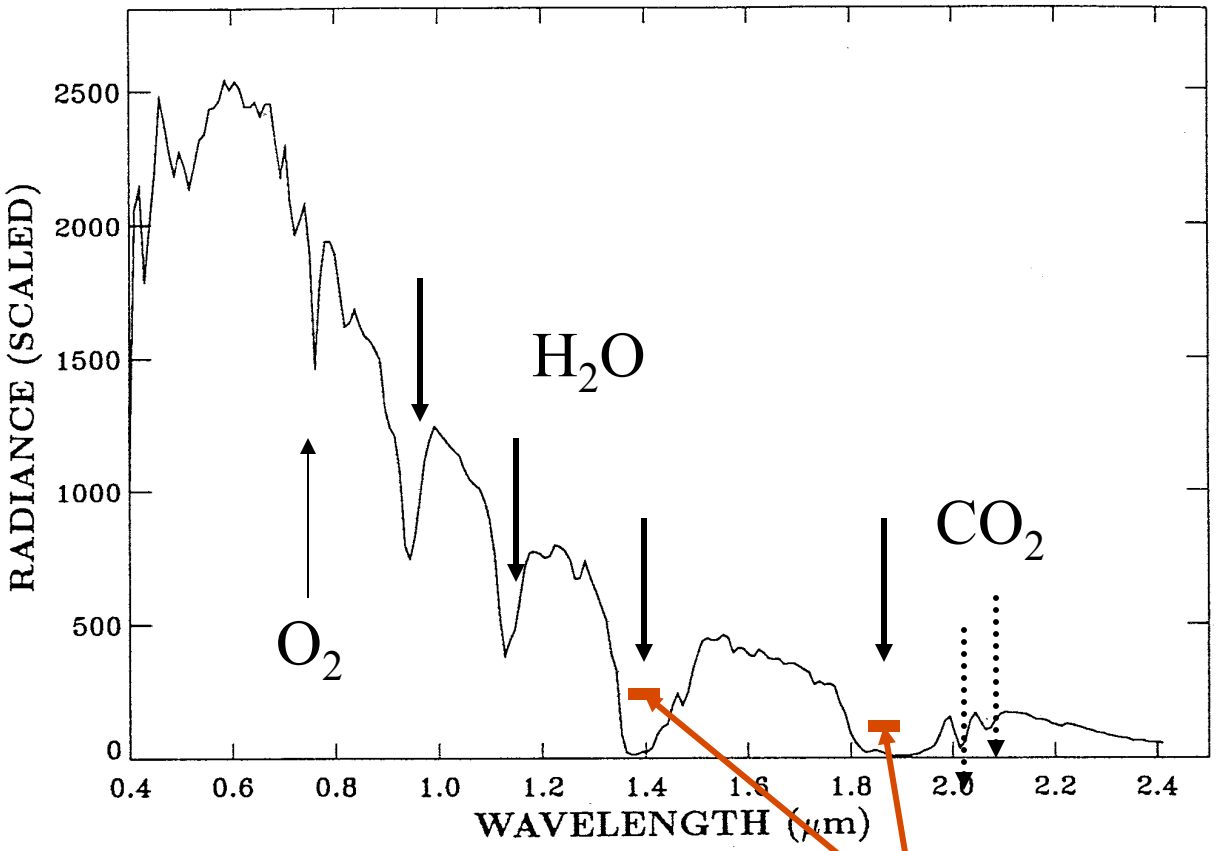

The AVIRIS spectrum is affected by atmospheric absorption and scattering effects. In order to obtain the surface reflectance spectrum, the atmospheric effects need to be removed.

Strong water vapor bands are located near 1.38 and 1.88 micron. No signals are detected under clear sky conditions.

Aerosol Scattering Effects

True Color Image
(R: 0.66, G: 0.55, B: 0.47 μm)

False Color Image
(R: 2.13, G: 1.24, B: 1.64 μm)

(A)

(B)

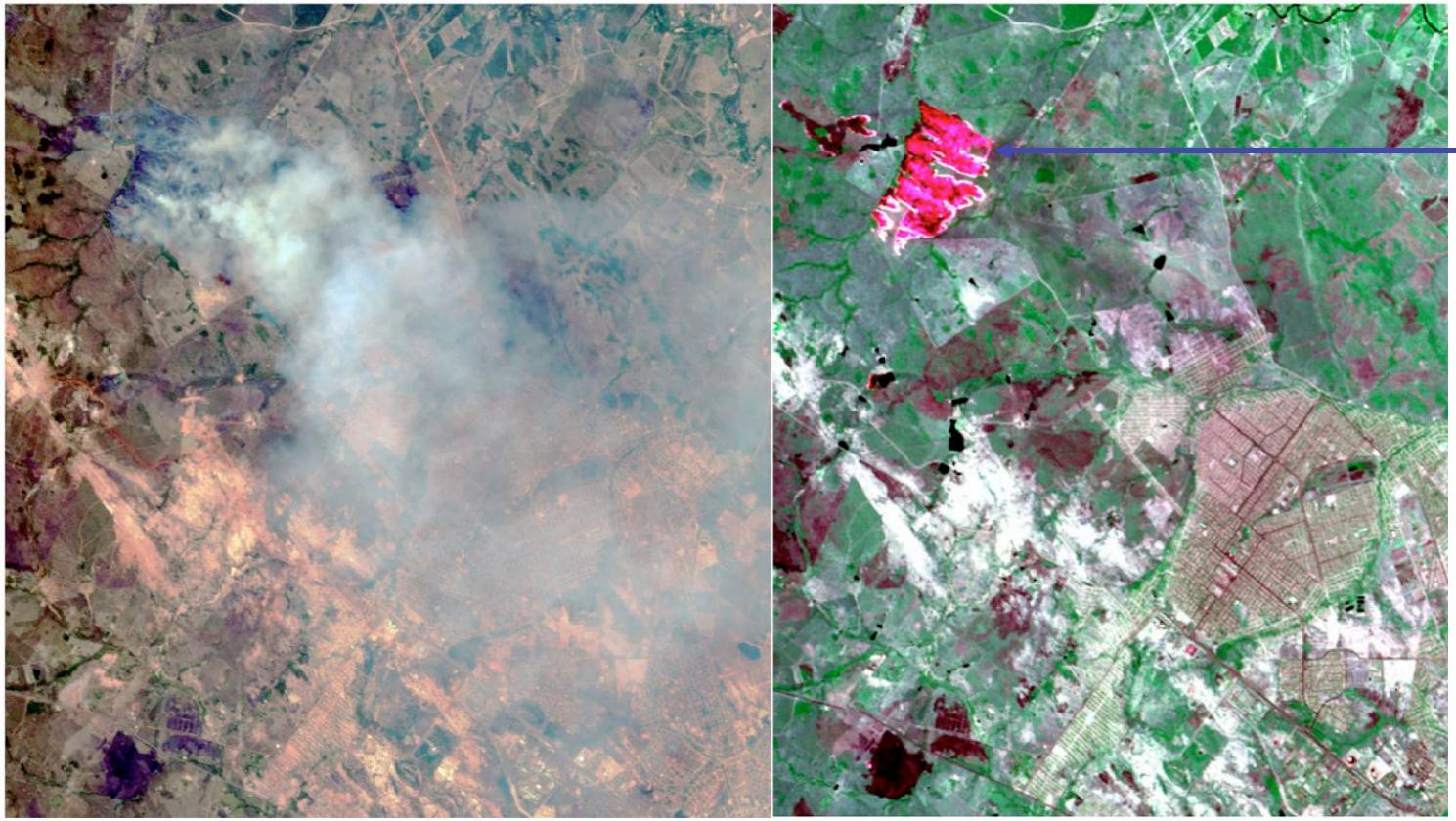

Smoke is seen in visible channel images, but disappears in the near-IR channel images. Smoke particle size is ~0.1 – 0.2 μm.

Equations For Atmospheric Correction Over Land

The measured radiance at the satellite level can be expressed as:

$$L_{obs} = L_a + L_{sun}\, t\, \rho \qquad (1)$$

L_a: path radiance;
ρ : surface reflectance;
L_{sun}: solar radiance above the atmosphere;
t: *2-way transmittance for the Sun-surface-sensor path*

Define the satellite apparent reflectance as

$$\rho^*_{obs} = \pi\, L_{obs} / (\mu_0\, E_0) \qquad (2)$$

$$\rho^*_{obs} = T_g\, [\, \rho_a + t\, \rho / (1 - \rho\, s)\,] \qquad (3)$$

By inverting Eq. (3) for ρ, we get:

$$\rho = (\rho^*_{obs}/T_g - \rho^*_a) / [t + s\, (\rho^*_{obs}/T_g - \rho^*_a)\,] \qquad (4)$$

Gao, B.-C., K. H. Heidebrecht, and A. F. H. Goetz, Derivation of scaled surface reflectances from AVIRIS data, *Remote Sens. Env., 44*, 165-178, 1993.

SAMPLE REFLECTANCE RETRIEVALS OVER MINERAL

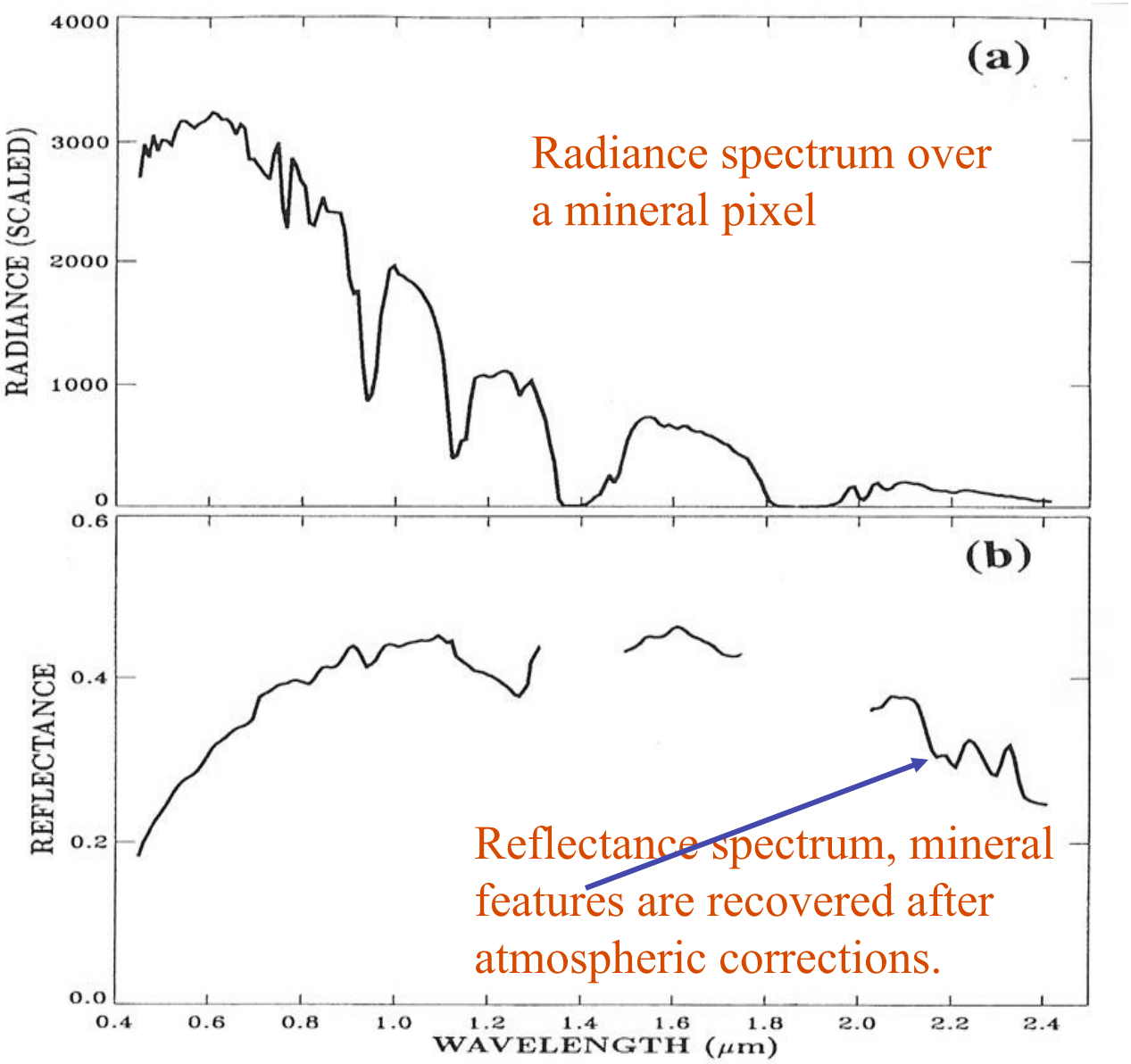

A Case of Glint Removal Using AVIRIS Data Over Kaneohe Bay, HI

Before

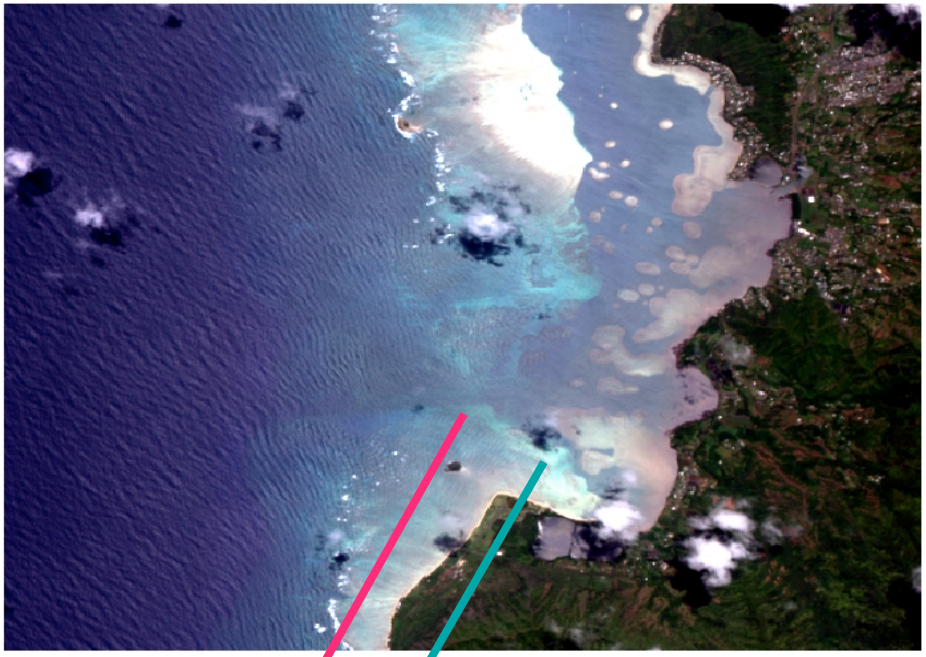

After

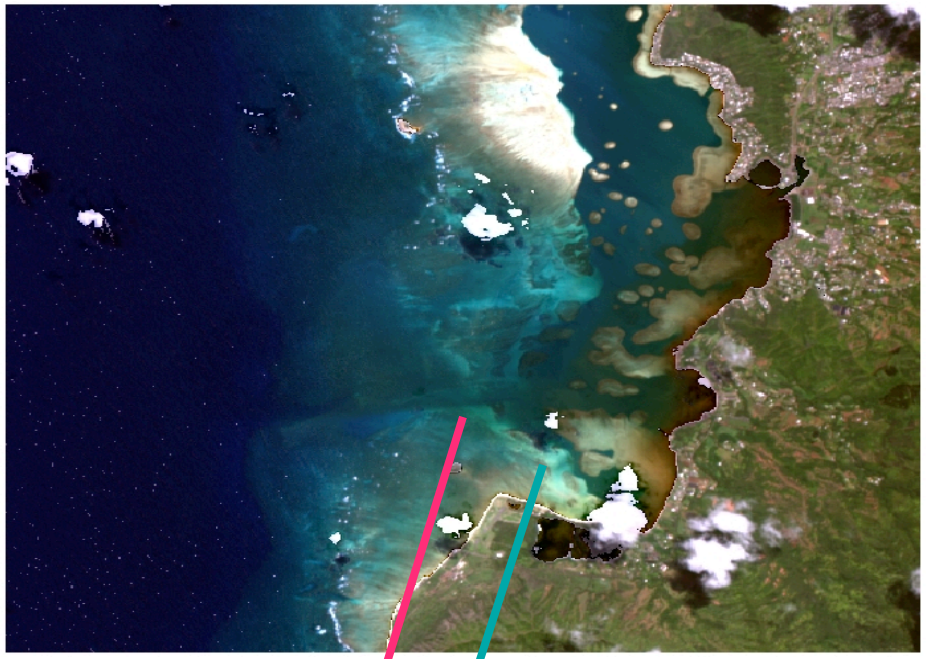

Sample Radiance Spectra

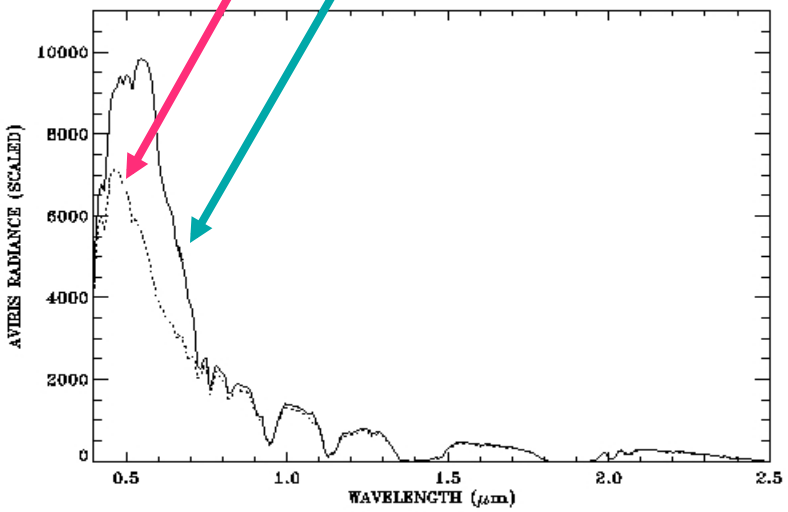

Sample Derived Reflectance Spectra

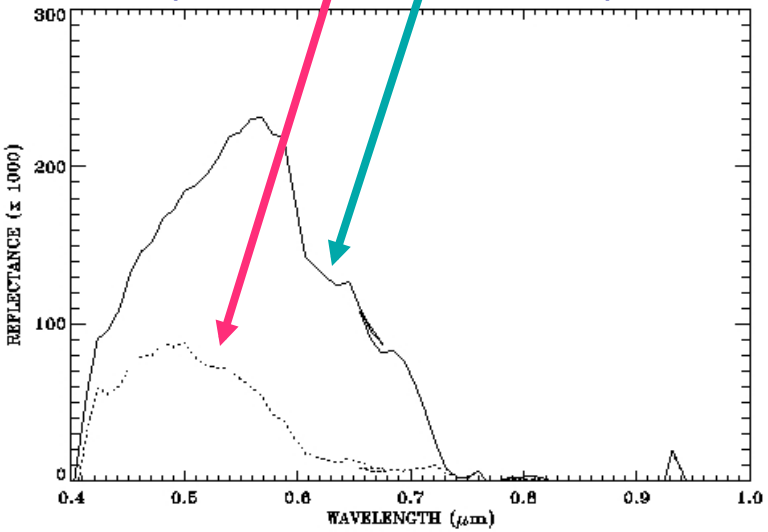

AVIRIS Image & Spectra Over Ivanpah, California (April 26, 2010)

AVIRIS Ivanpah Image

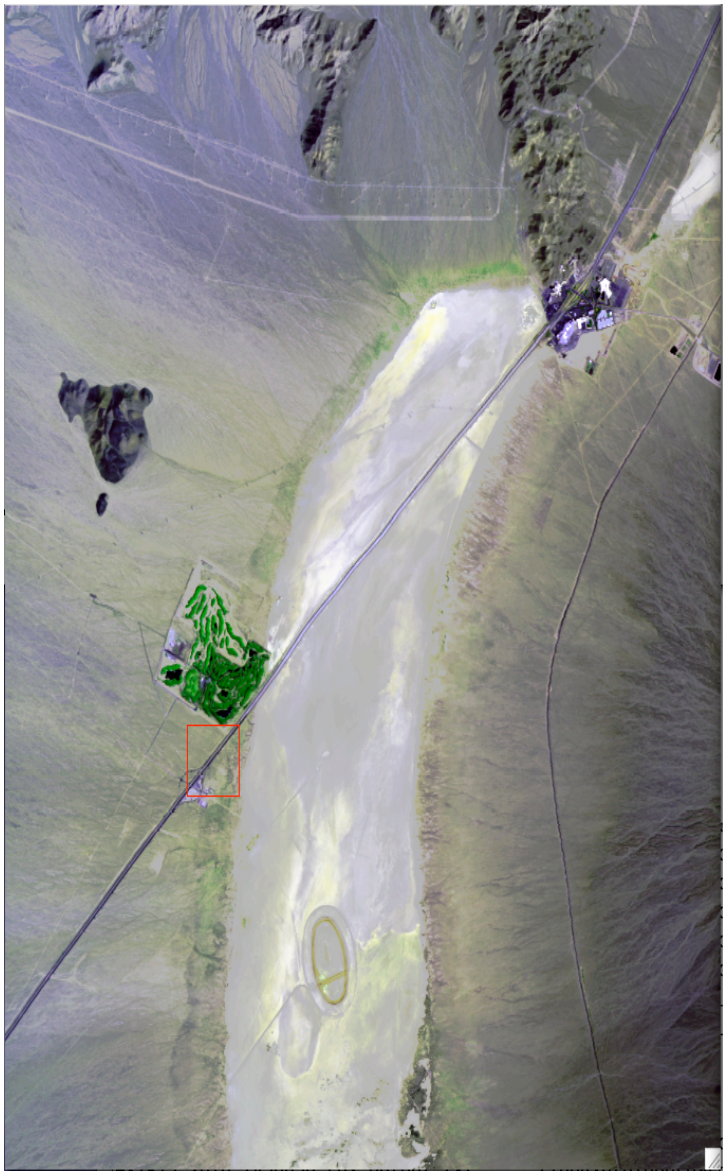

Sample Retrieved Spectra

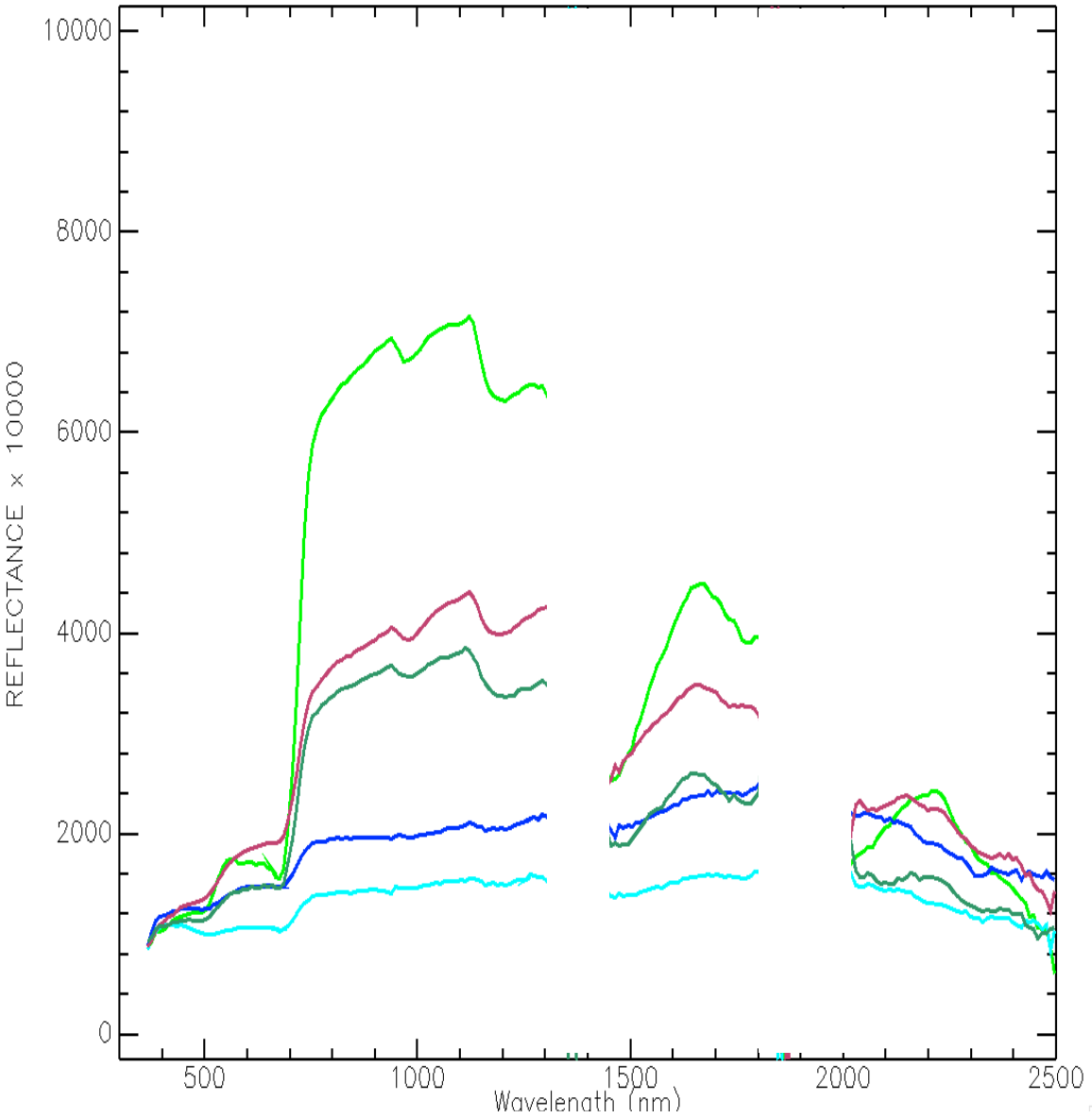

AVIRIS Image & Spectra Over The Gulf of Mexico (Oil Spill, 5/17/2010)

RGB IMAGES

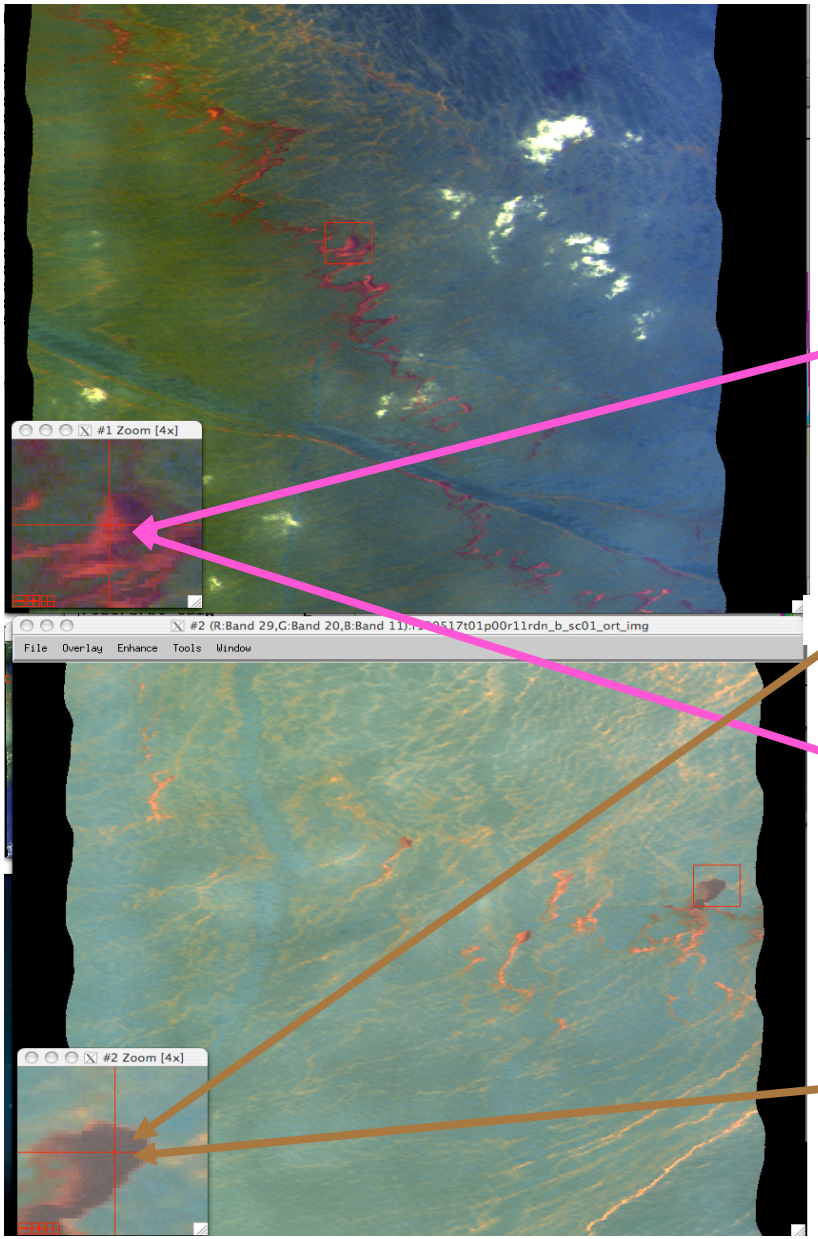

RADIANCE

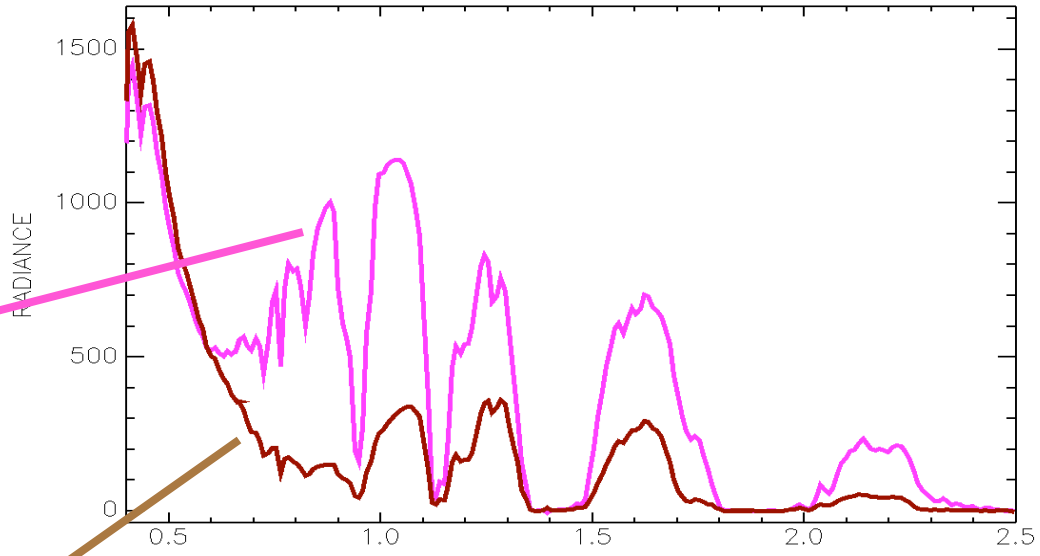

REFLECTANE (RETRIEVED)

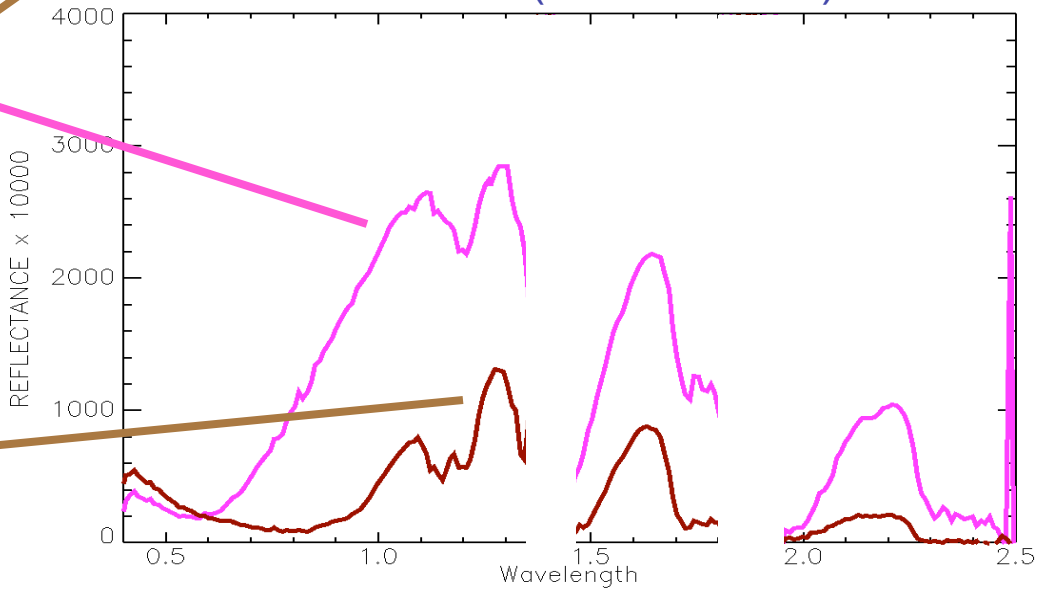

SPECTRAL COMPARISONS

Lab Reflectance Spectra of Optically Thick Oil Emulsion (From R. Clark et al., USGS)

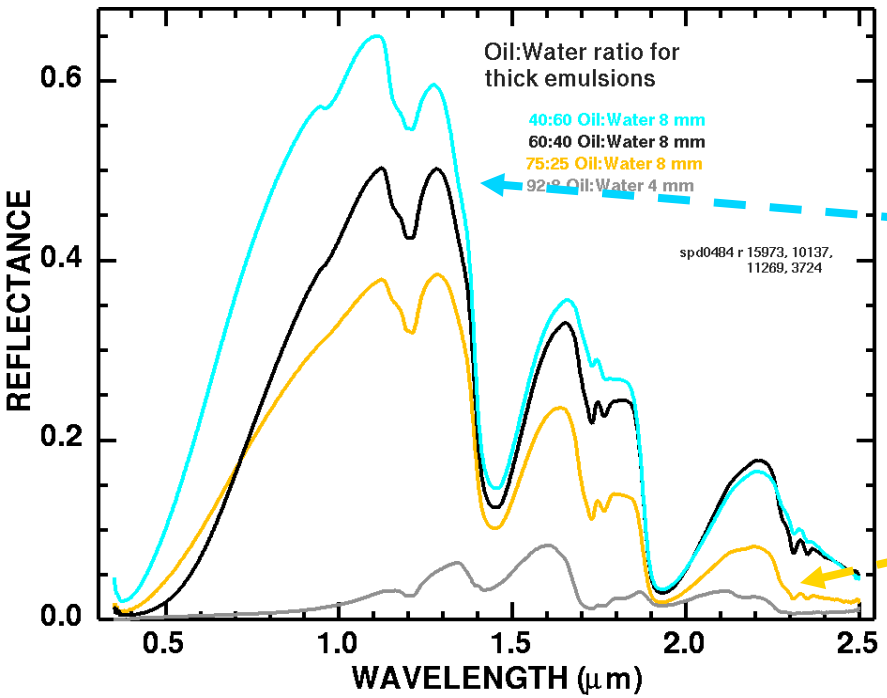

Reflectance Spectra Derived From AVIRIS Data

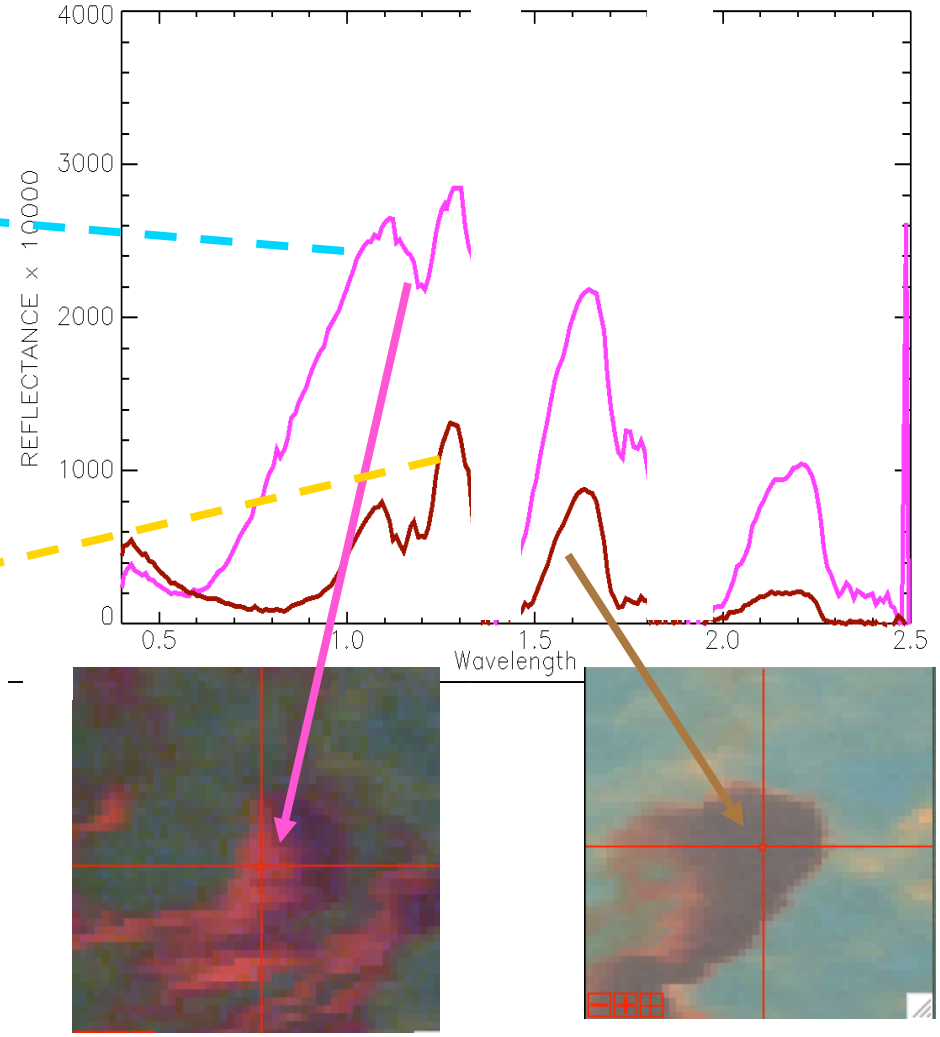

Earth Surface Images from HICO

Images are about 43 km wide and 190 km long
Orientations are given below

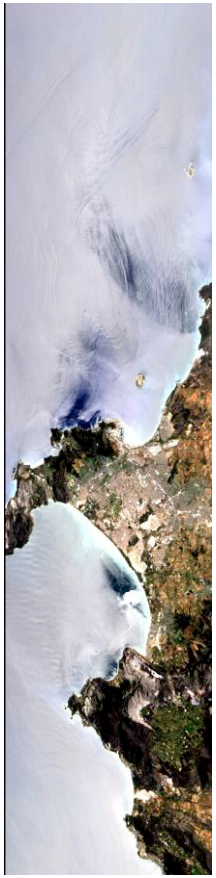

Cape Town, South Africa, Oct. 3, 2009. Orientation is from NW at top to SE at bottom.

Lower Chesapeake Bay, Oct. 7, 2009. Orientation is from NW at top to SE at bottom.

Coast of South China Sea, near Hong Kong, China, Oct. 2, 2009. Orientation is from SW at bottom to NE at top.

Part of the Grand Canyon, Sept. 27, 2009. The center of the image is at 35° 50' N, 111° 23' W and the orientation is from SW at bottom to NE at top.

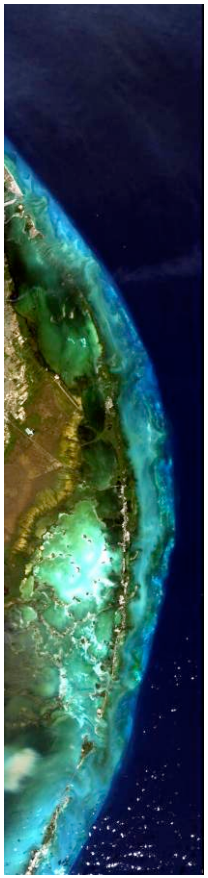

Florida Keys, over Key Largo, Sept. 27, 2009. Orientation is from SW at bottom to NE at top.

Sahara Desert over Egypt, Sept. 27, 2009. Orientation is from SW at bottom to NE at top.

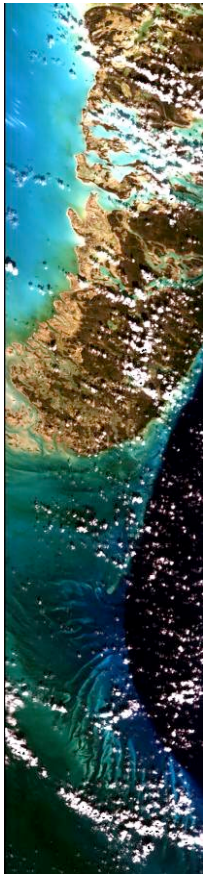

Taken over the Bahamas, Oct. 2, 2009. Orientation is from NW at top to SE at bottom.

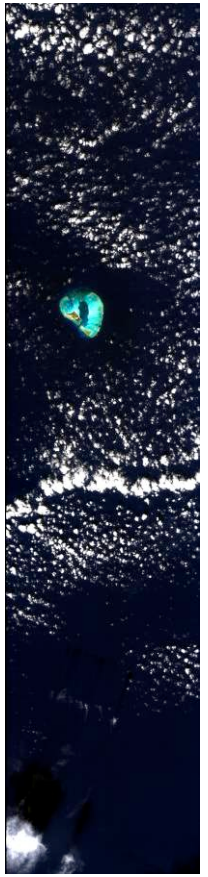

Gem of the Pacific. Midway Island, Sept. 27, 2009. Orientation is from NW at top to SE at bottom.

http://hico.coas.oregonstate.edu/

What is HICO?

The Hyperspectral Imager for the Coastal Ocean (HICO™) is an imaging spectrometer based on the PHILLS airborne imaging spectrometers. HICO is the first spaceborne imaging spectrometer designed to sample the coastal ocean. HICO will sample selected coastal regions at 90 m with full spectral coverage (380 to 960 nm sampled at 5.7 nm) and a very high signal-to-noise ratio to resolve the complexity of the coastal ocean. HICO is sponsored by the Office of Naval Research as an Innovative Naval Prototype (INP), and will demonstrate coastal products including water clarity, bottom types, bathymetry and on-shore vegetation maps. As an INP, HICO also demonstrates innovative ways to reduce the cost and schedule of this space mission by adapting proven PHILLS aircraft imager architecture and using Commercial Off-The-Shelf (COTS) components where possible.

Sample Water Leaving Reflectance Retrievals Over Lake Eyre, Australia

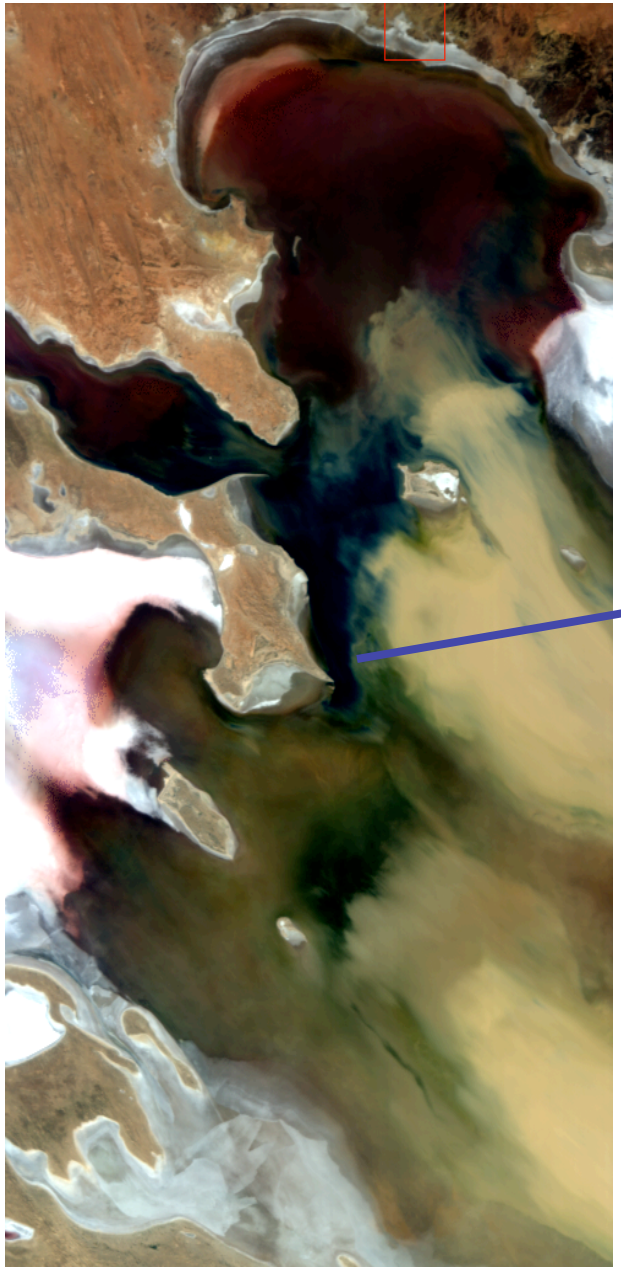

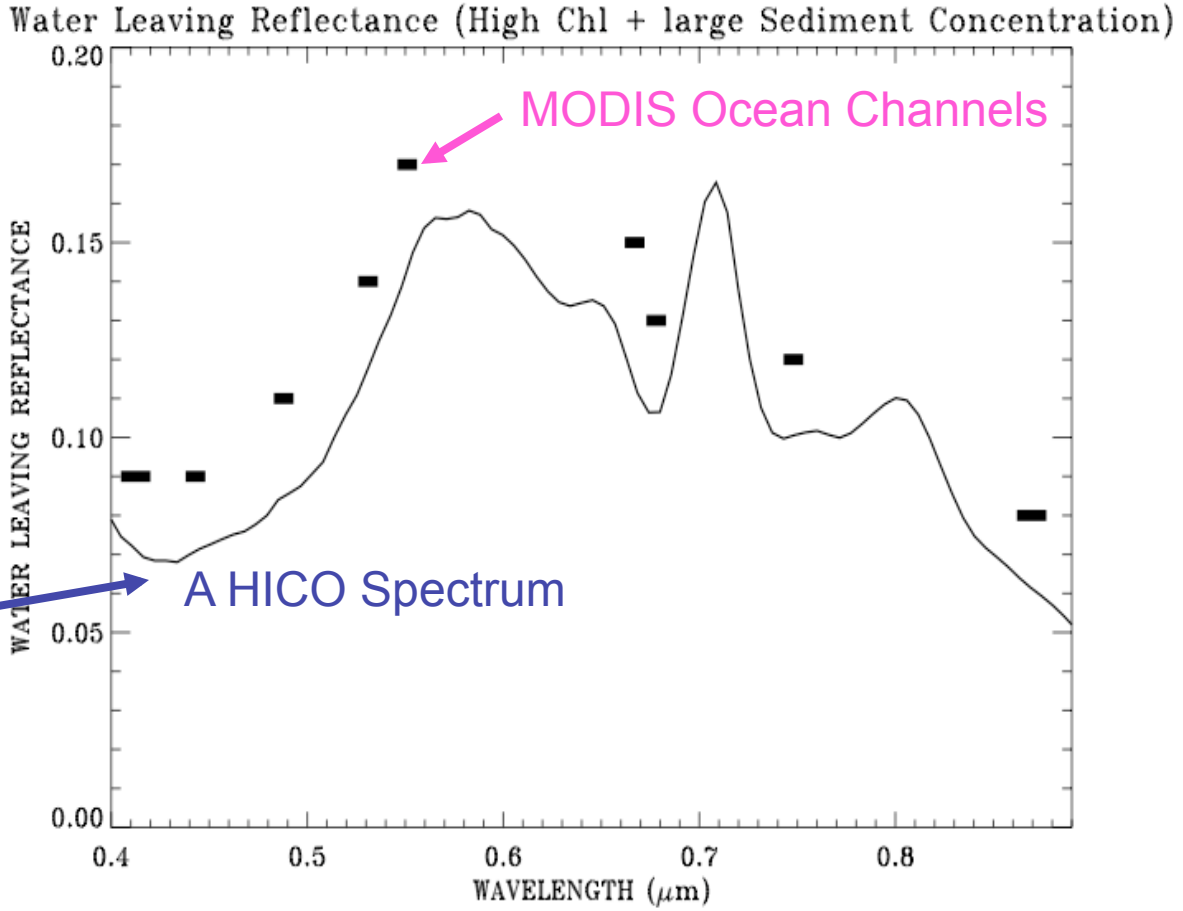

The discrete MODIS ocean channels missed several peaks in the HICO reflectance spectrum. Therefore, MODIS cannot fully characterize the shapes of the spectra acquired over the complex Case 2 waters.

Estimation of Chlorophyll-a Concentration From HICO data Acquired over The Sea of Azov Using Narrow Channels within & Around the 700-nm Refl. Peak and the Method of Gitelson et al. (ERL, 2011, doi:10.1088/1748-9326/6/2/024023)

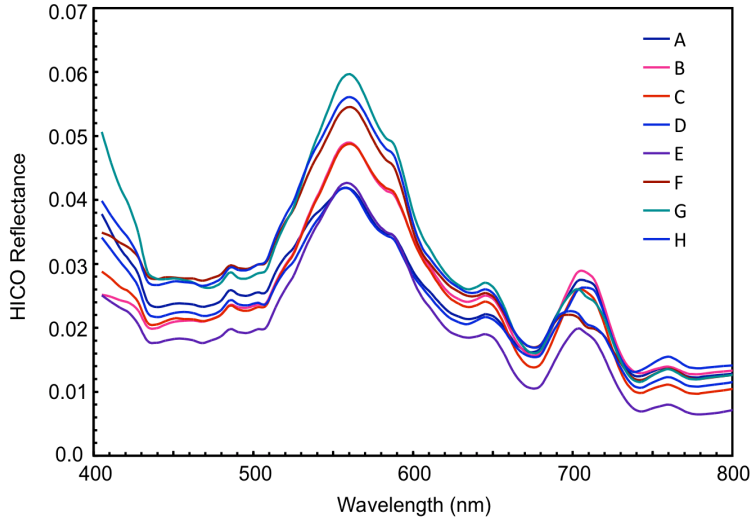

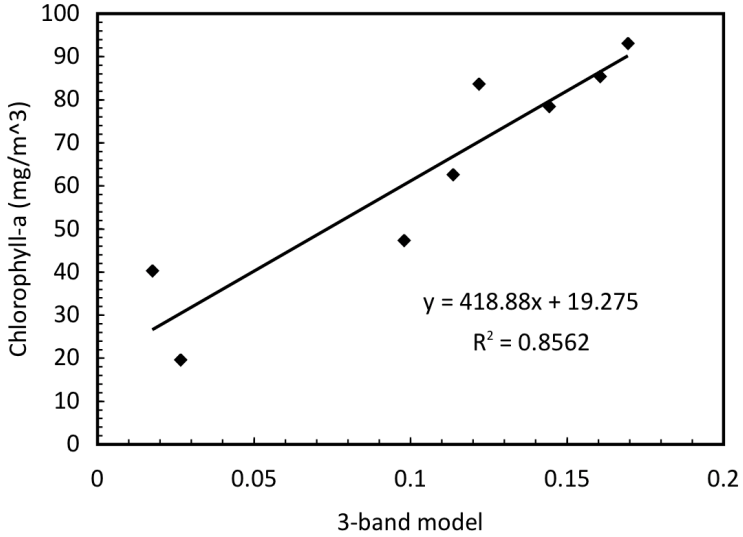

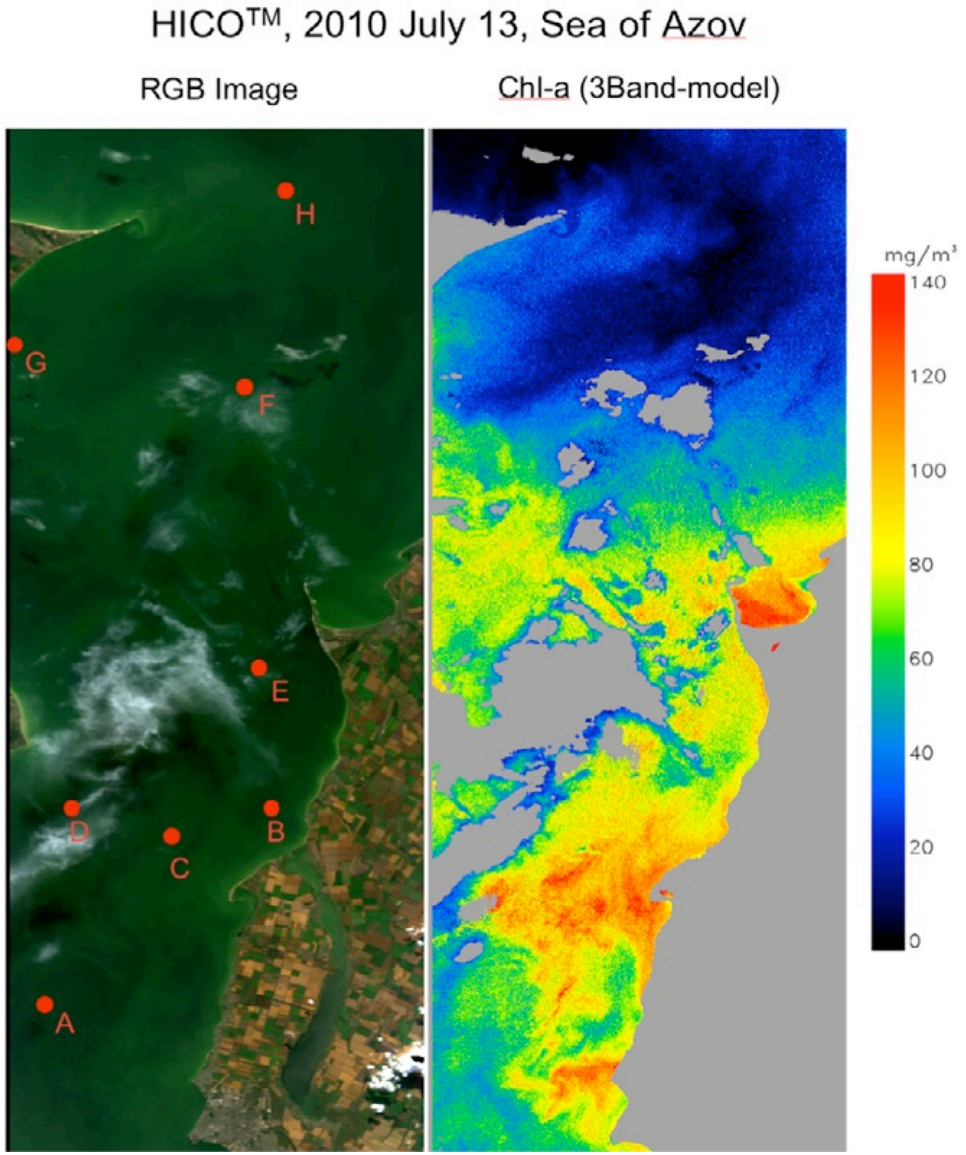

Illustration of the Spectrum-Matching Technique (for HICO Post-Launch Wavelength Calibrations)

A Sample ISS HICO Spectrum

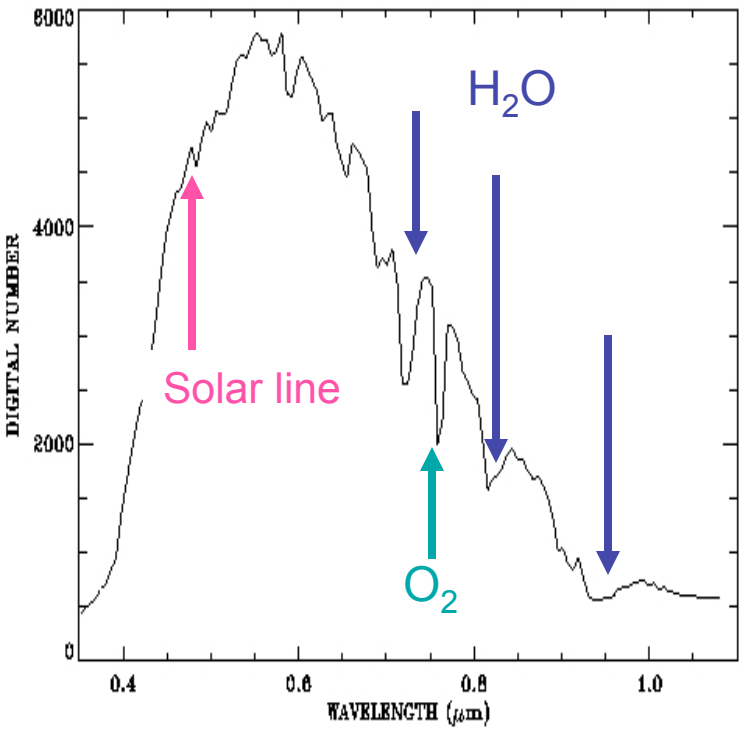

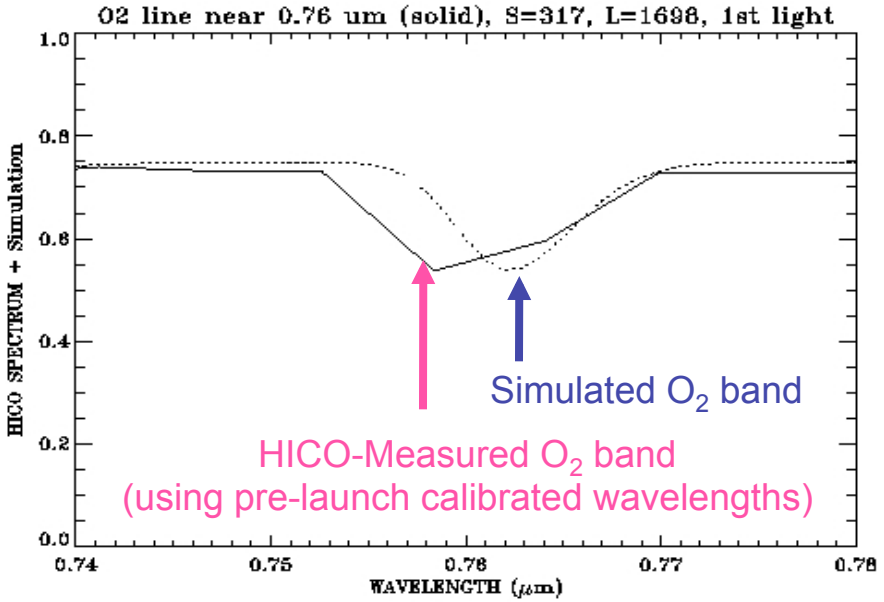

HICO Post-Launch Wavelength Shift (~1.7 nm)

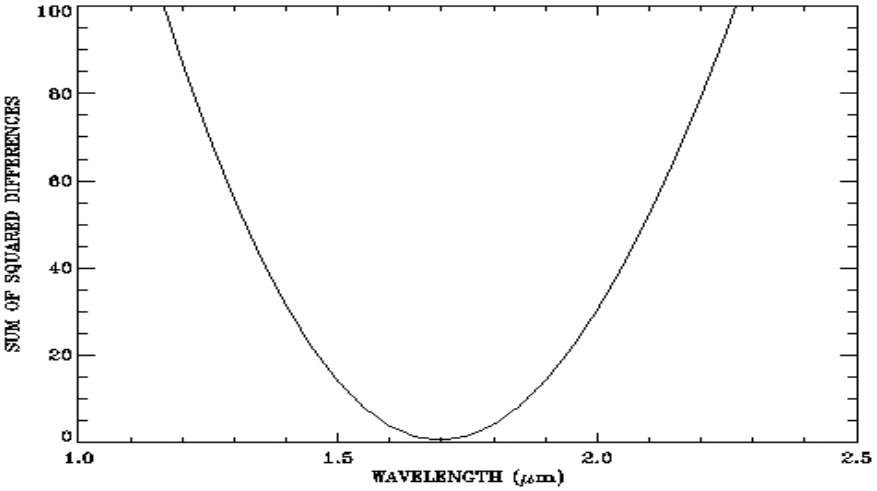

Post-launch FWHM remained the same

Cubic Spline Smoothing – Post Processing

ATREM Refl Spectra

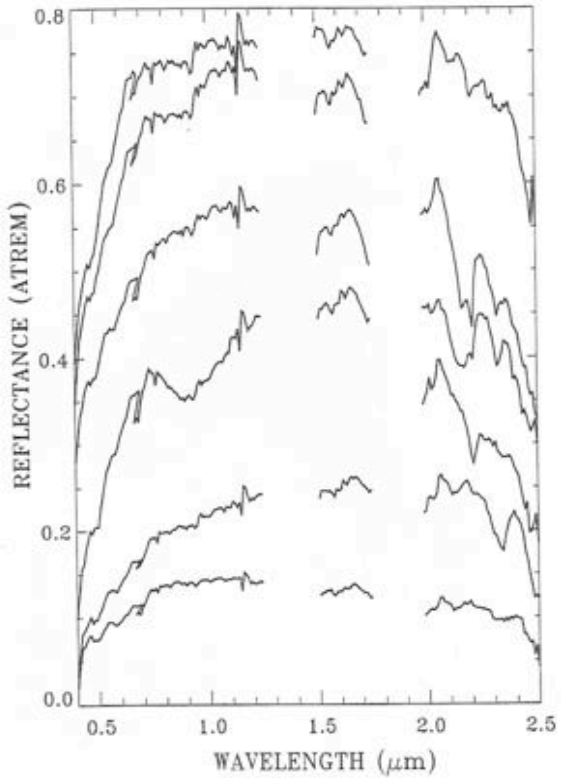

Spectra Derived with Empirical Line Method

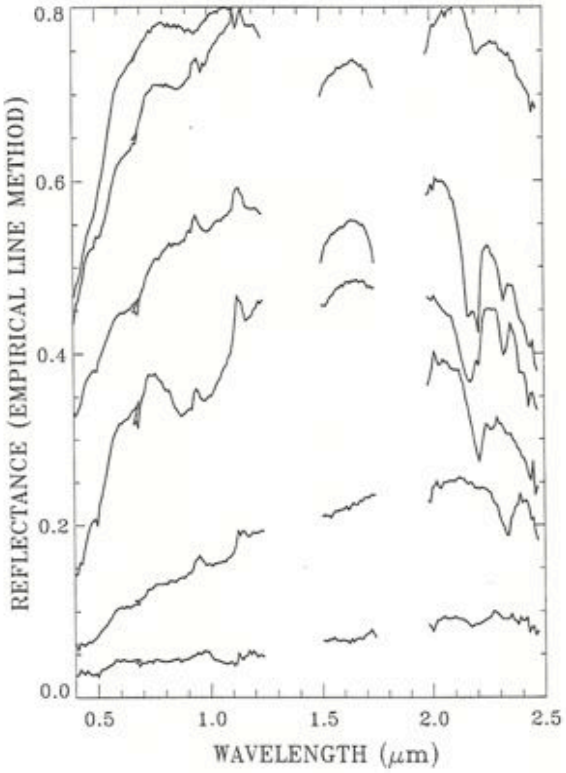

ATREM Refl Spectra + Cubic Spline Smoothing

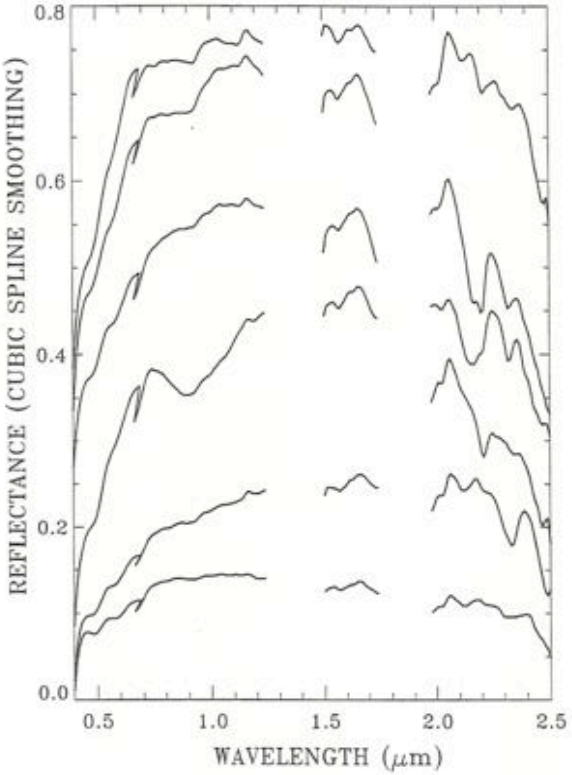

Porting Over Algorithms to Mac and PC

- In order to support the processing of HICO data collected from the International Space Station, we ported over most algorithms from an old SGI workstation to a Mac in 2010.
- We have just finished porting over all the routines to an AVIRIS PC computer, and made it possible to do batch processing of large volumes of AVIRIS data. The tasks we conducted include:
  - Replacing old Fortran IV statements with F90 compatible statements in some of the routines
  - Developing a perl script to automate the process of generating input files for ATREM code (date, time, latitude, longitude, input and output file names, etc.)
  - Developing a new Fortran 90 I/O routine for ATREM to handle AVIRIS file names, which are often longer than 80 characters. The original I/O routine was written in mixed Fortran77 and C, and was unable to handle files with names longer than 80 characters.

HyspIRI VSWIR Level 2 Algorithm Prototyping -
ATREM Processing Speed

- **AVIRIS Server**
  OS: 64-bit Windows Server 2008
  Processor: Dual Intel Xeon X5560 2.80GHz Quad-Core Processors
  Installed memory (RAM): 24.0 GB ECC DDR3

- **Storage**
  4 RAID arrays populated with 24, 2TB 7200 RPM 64 MB Cache Enterprise Class SATA II HDD's
  4Gb Fibre Channel to SAS/SAS(SATA) Controller RAID unit
  Total of 156 TB usable storage

- After processing large batches of 2010 AVIRIS data through ATREM, the average processing speed is ~9 mb/s.

- In a rough estimate -

ATREM 2011 daily rate:	864 GB/day
HyspIRI VSWIR daily rate:	1500 GB/day

SUMMARY

- We have Ported over a land version of ATREM algorithm to an AVIRIS computer, plus other functional versions of algorithms for hyperspectral data processing, such as routines for refining wavelength calibrations, signal to noise ratio estimates, spectral convolution, and spectral smoothing.

- We have developed a new Fortran 90 I/O routine for ATREM and a perl script for generating input files needed by ATREM. Batch processing of large volumes of AVIRIS data is now possible on an AVIRIS PC computer.

- Upgrades to ATREM code are still needed. For examples, adding absorbing aerosol models to ATREM and implementing new techniques for aerosol retrievals using UV channels (380 nm, 400 nm) are necessary.

HyspIRI Level-2 Thermal Infrared Preparatory Activities

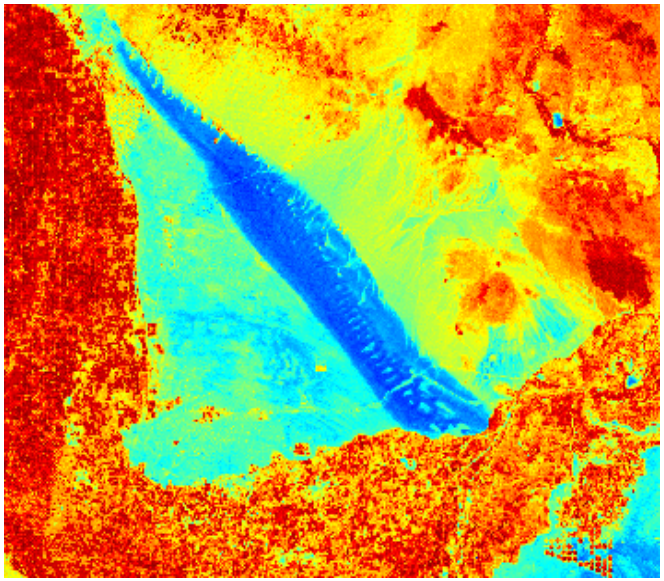

Glynn Hulley, Simon Hook

Jet Propulsion Laboratory, California Institute of Technology, Pasadena, CA

(c) 2011 California Institute of Technology. Government sponsorship acknowledged.

Introduction

- **Land Surface Emissivity:** ratio between actual emitted radiation, and radiation emitted by a blackbody at the same temperature (typically varies from 0.6 – 0.99)

$$\epsilon_\lambda = \frac{L_\lambda}{L_\lambda(BB)}$$

- **Land Surface Temperature (LST):**

  how 'hot' the skin surface of the Earth feels at any given time

Brightness temperautre (radiometric) $T_b = B_\lambda^{-1}(L_\lambda)$

Kinetic temperature (LST) $L_\lambda = \varepsilon_\lambda \cdot B_\lambda(T_s)$

- LST and emissivity closely coupled variables, BUT are independent measurements!
  - Emissivity is intrinsic property of the Earth's surface
  - LST varies with local atmospheric conditions and irradiance history
  - Emissivity error of 0.015 = 1 K LST error

- Basic concepts, but large uncertainties between different sensors (e.g. MODIS, ASTER, AIRS)

HyspIRI Land Surface Temperature (LST) and Emissivity Relevance

- Temperature/emissivity => key components for HyspIRI:
  - Fire research (Randerson, Dennison, Giglio, Veraverbeke)
  - Evapotranspiration modeling (Anderson, Kustas, French, Ustin)
  - Urban studies (Luvall, Roberts, Quattrochi)
  - Volcano monitoring, thermal anomalies (Abrams, Realmuto, Vaughan, Wright, Pieri, Ramsey)
  - Surface composition (Ramsey, Mars, Kruse)

Broader Context: Uncertainty Analysis

Emissivity

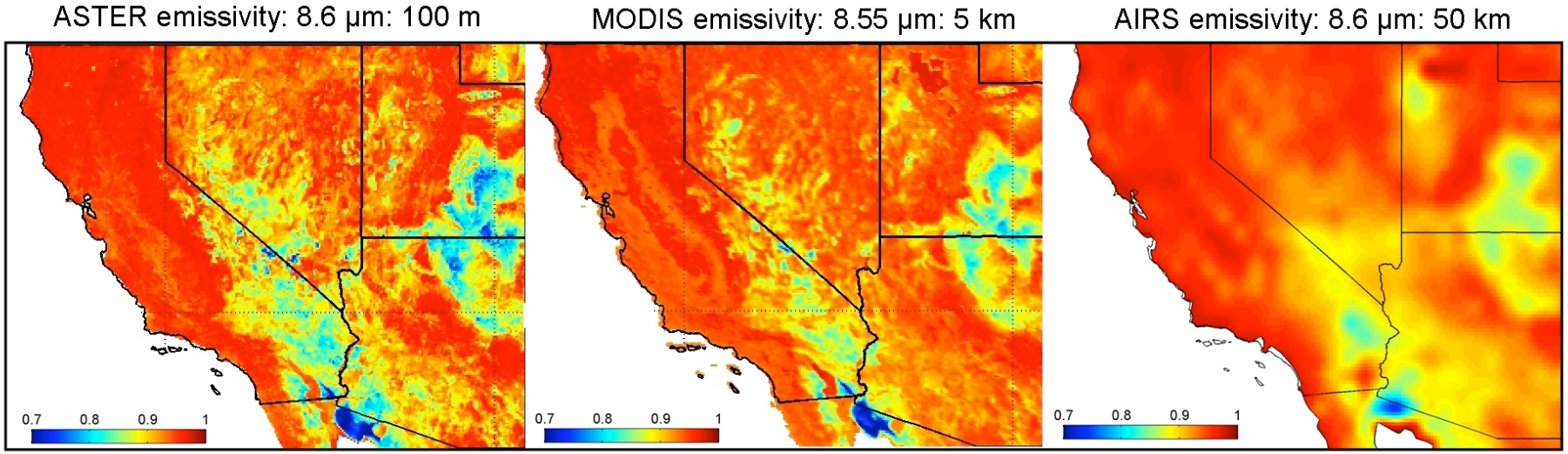

Land Surface Temperature (LST)

MODIS – AIRS daytime LST (K)

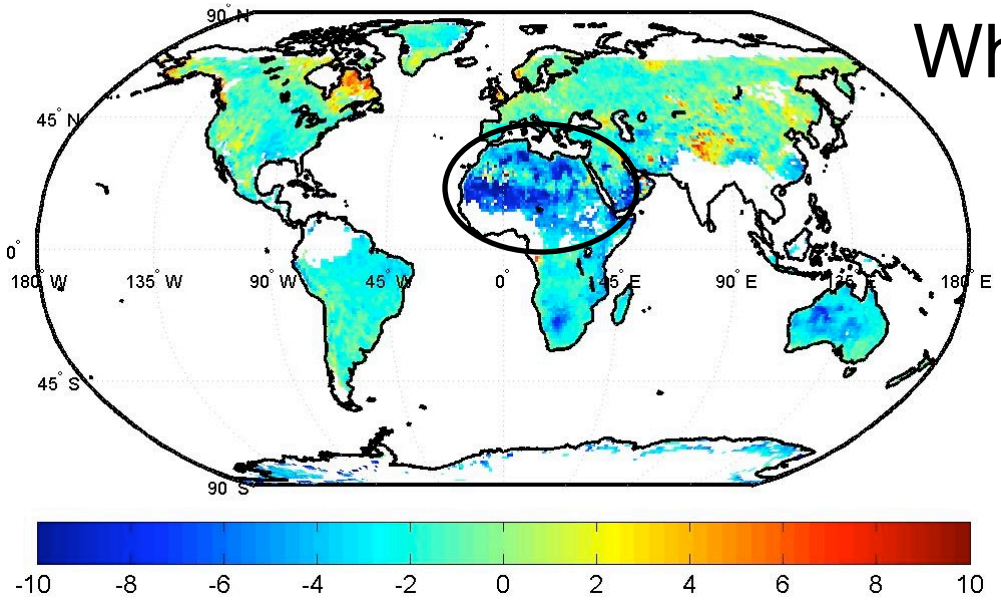

Who is Correct?

Thermal Infrared Radiative Transfer

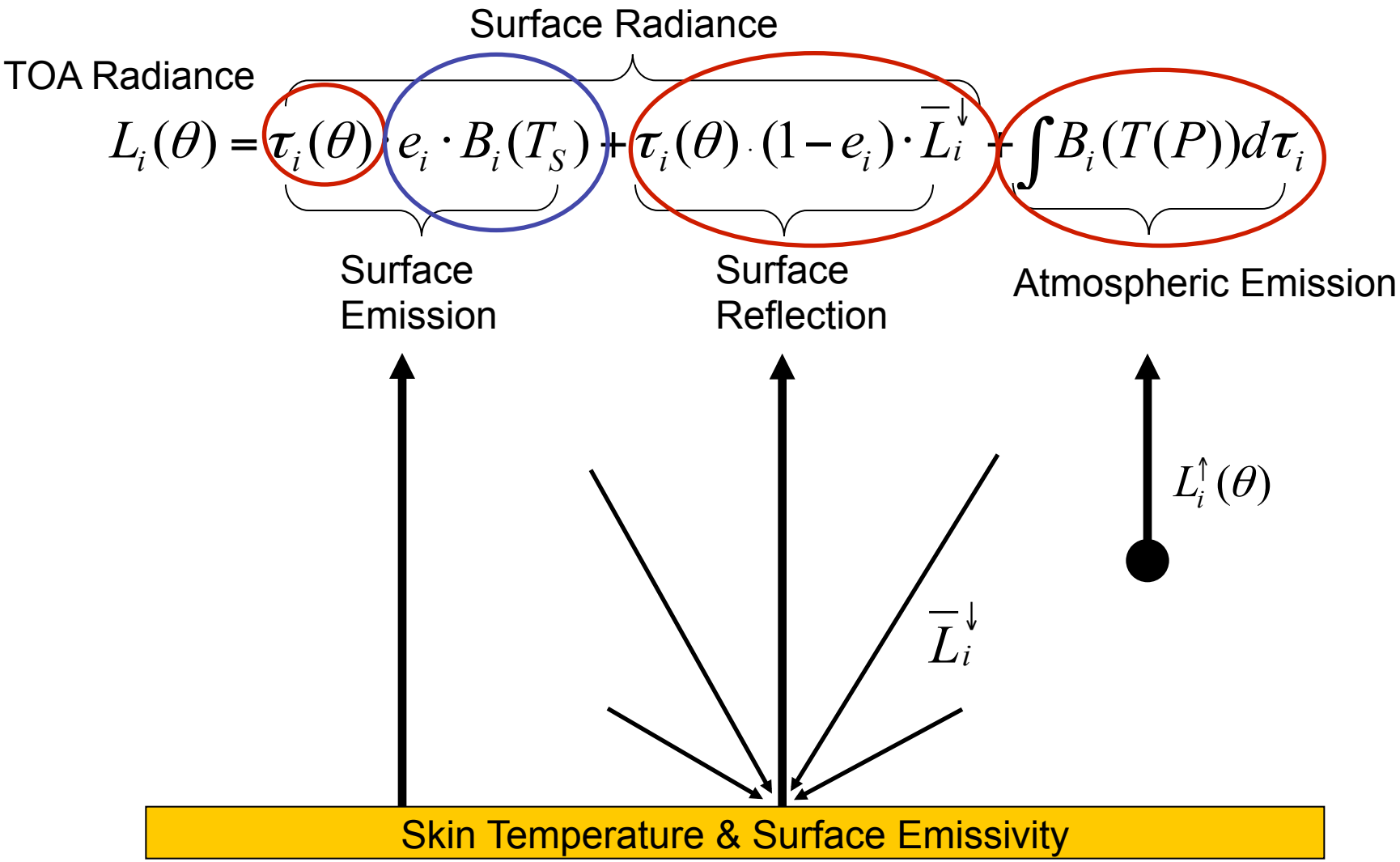

	ASTER Simulated Data	HysplRI
Characteristics	90m, 16-day, 5 bands	60m, 5-day, 8 bands
Level-2 Core Products	1. Emissivity (5 bands) 2. Surface Temperature	1. Emissivity in 8 bands 2. Surface Temperature
Cloud Mask	v3.2 (Landsat, ASTER, MODIS heritage)	Development in progress….
Atmospheric Profiles	Terra MODIS (MOD07) - Coincident - 5 km - MOD07 ozone	Contingent upon data available at launch. NPP/NPOESS (JPSS) Back up: NWP models
Atmospheric Correction	Water Vapor Scaling (WVS) (Tonooka, 2005) MODTRAN™5.2 (Berk et al. 2005)	WVS (new model coefficients required) MODTRAN**
Temperature **E**missivity **S**eparation (TES) algorithm	Standard TES (Gillespie et al. 1998)	Standard TES (Gillespie et al. 1998) New Calibration curve

Water Vapor Scaling (WVS) Method

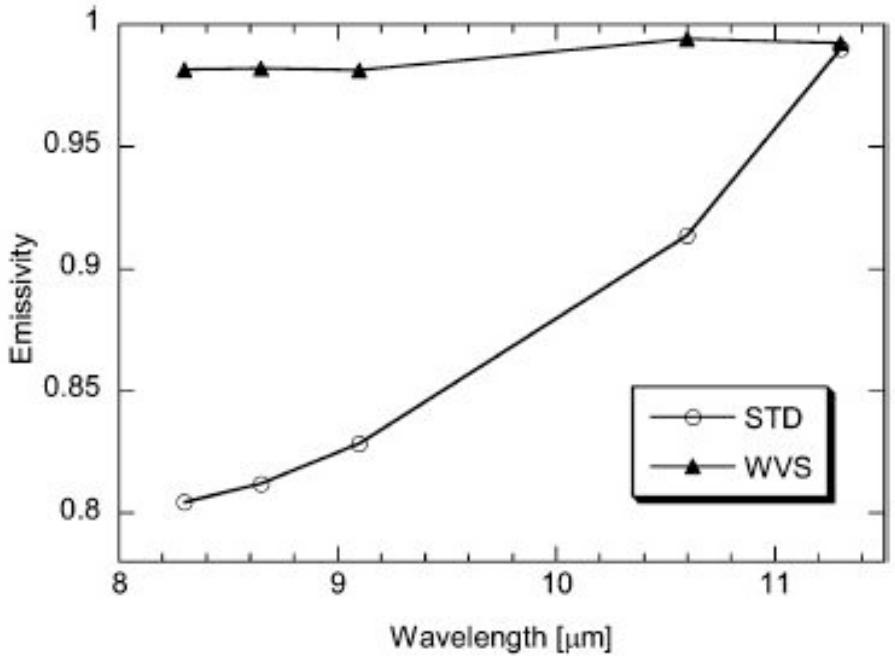

Fig. 9. Water surface emissivity spectra retrieved by the standard algorithm and by the WVS method, obtained from Lake Volta, Ghana, on October 1, 2003.

TABLE IV
LAKE SURFACE TEMPERATURE (CELSIUS) ON LAKE VOLTA, GHANA, RETRIEVED BY THE STANDARD ALGORITHM (STD) AND BY THE WVS METHOD, DERIVED FROM THE MODIS SST PRODUCT, AND GIVEN BY THE CLIMATIC REPORT

STD	WVS	MODIS	Climate
37.4	29.2	29.0	29.4

**Tonooka, 2005

North American ASTER Land Surface Emissivity Database (NAALSED)

Mean Summer Emissivity (Jul-Aug-Sep 2000-2010), Band 12 (9.1 μm)

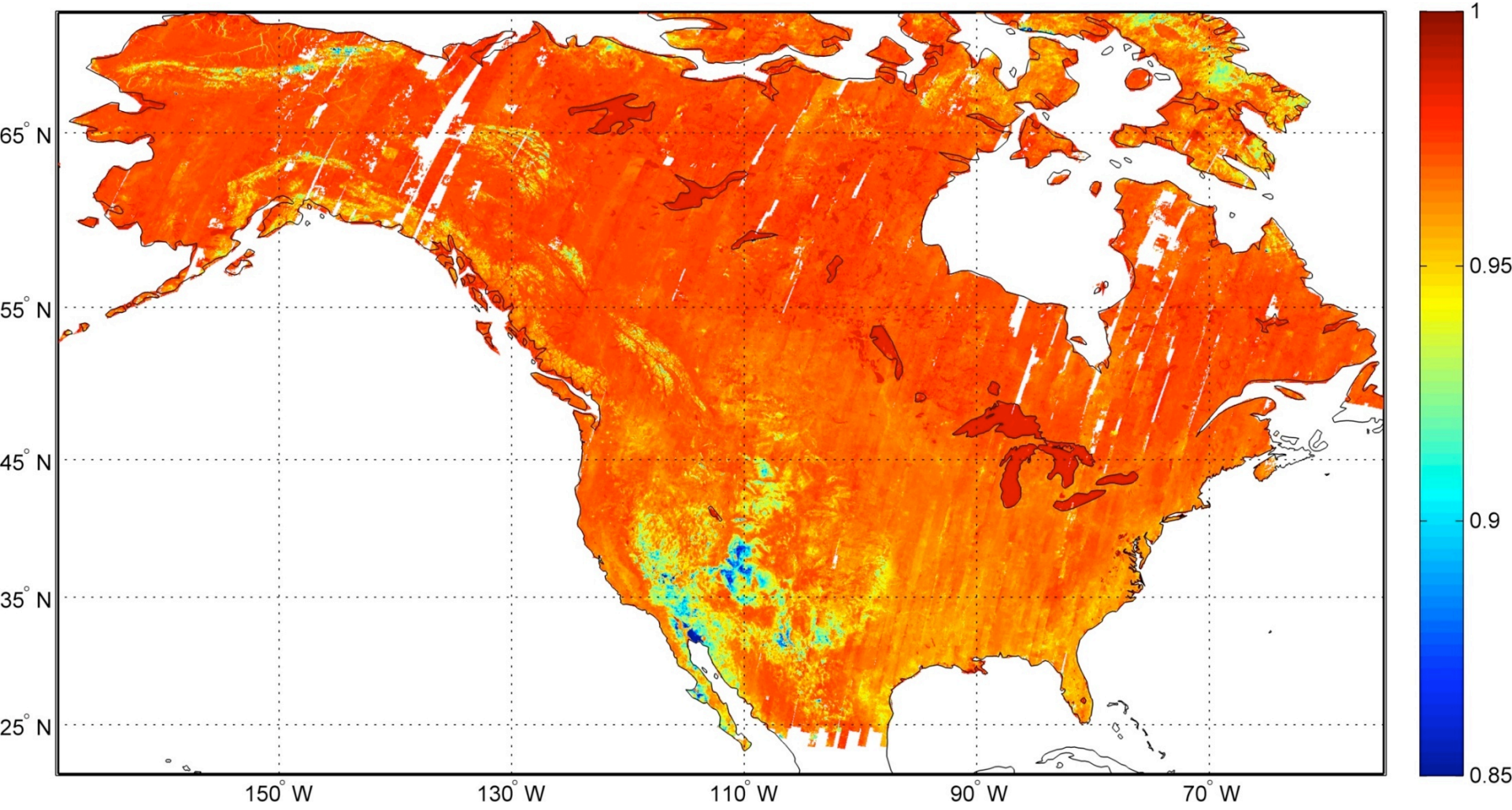

http://emissivity.jpl.nasa.gov

Jet Propulsion Laboratory
California Institute of Technology

+ View the NASA Portal

JPL HOME | EARTH | SOLAR SYSTEM | STARS & GALAXIES | TECHNOLOGY

North American Land Surface Emissivity Project

Home | Order | Publications | Validation | Examples | USCRN | Links

Log in

You are here: Home

Navigation

- Home
- Order
- Publications
- Validation
- Examples
- USCRN
- Links

« June 2010 »

Mo	Tu	We	Th	Fr	Sa	Su
	1	2	3	4	5	6
7	8	9	10	11	12	13
14	15	16	17	18	19	20
21	22	23	24	25	26	27
28	29	30				

North American Land Surface Emissivity Project

Welcome to the website for the North American Land Surface Emissivity Project. The goal of the project is to create a seamless database of emissivity from standard ASTER emissivity products for use in climate research. The Earth emits energy at wavelengths we cannot normally see, that energy is a function of the temperature and the emissivity of the surface. The surface emissivity primarily depends on the composition of the surface. Thus as the surface composition changes through, for example, land cover land use change, so does the surface emissivity. The land surface emissivity is measured by several instruments mounted on satellites and aircraft. Some of the most well known satellite sensors are AIRS, ASTER and MODIS.

Of these three satellite sensors, ASTER provides the most detailed emissivtiy images with a pixel spatial resolution of 90m. The image below was created by merging together all the ASTER emissivity data ever acquired over California, Nevada, Arizona and Utah under clear skies from 2000-2008 for the months July, August and September.

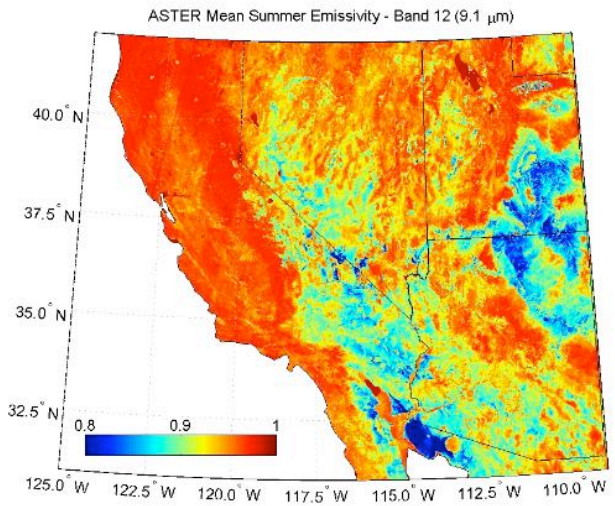

African ASTER Land Surface Emissivity Database (AALSED)

North Africa/Arabian Peninsula
- 134,662 ASTER scenes
- 49,977 MOD07 scenes

Progress:
- ✓ Data delivered from EROS
- ✓ Cloud masking completed
- ✓ TES completed
- ✓ Gridding in progress..

Southern Africa
- ~70,000 ASTER scenes
- 24,821 MOD07 scenes

Progress:
- ✓ Data delivered from EROS
- ✓ Cloud masking in progress

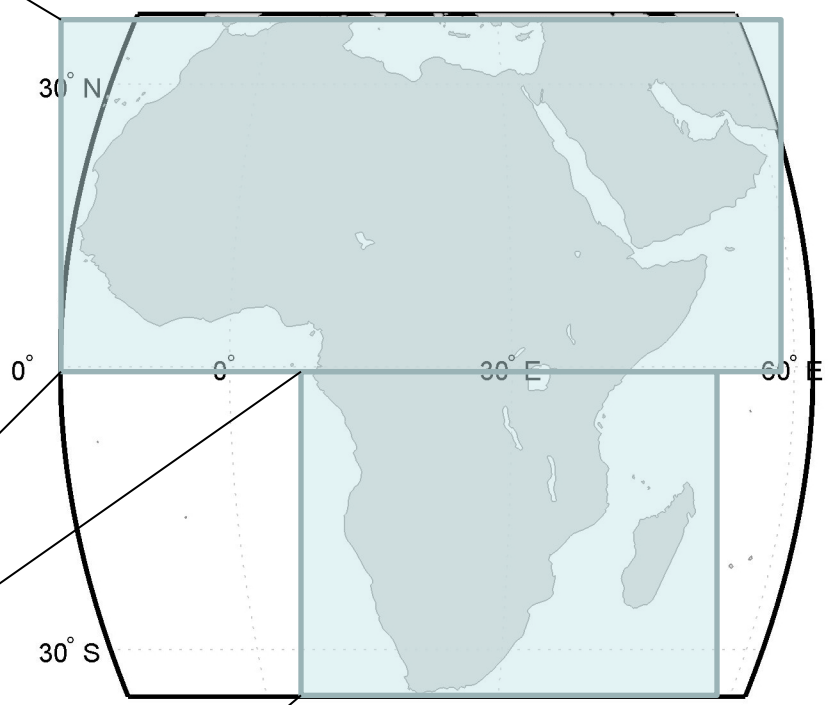

Algorithm Updates
- Updated WVS coefficients for MODTRAN5.2
- Included dust/smoke mask
- Improved no-SWIR cloud (post-2008) detection over desert

Egypt Test Area

ASTER Band 11 (8.6 μm), 2000-2009 (4,888 scenes)

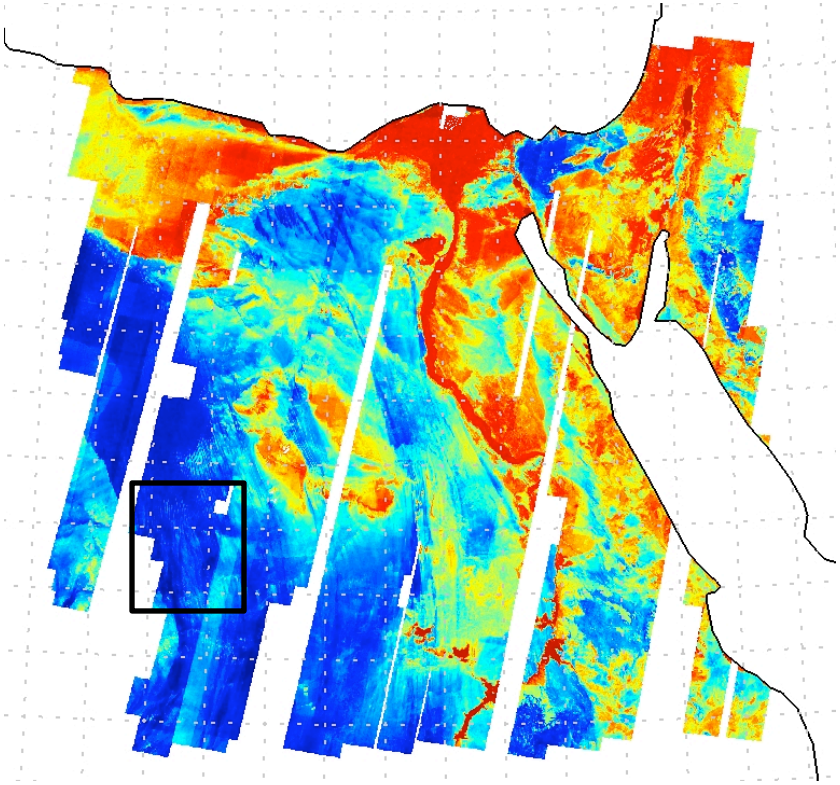

MODIS Band 29 (8.55 μm), MOD11C3, 5km

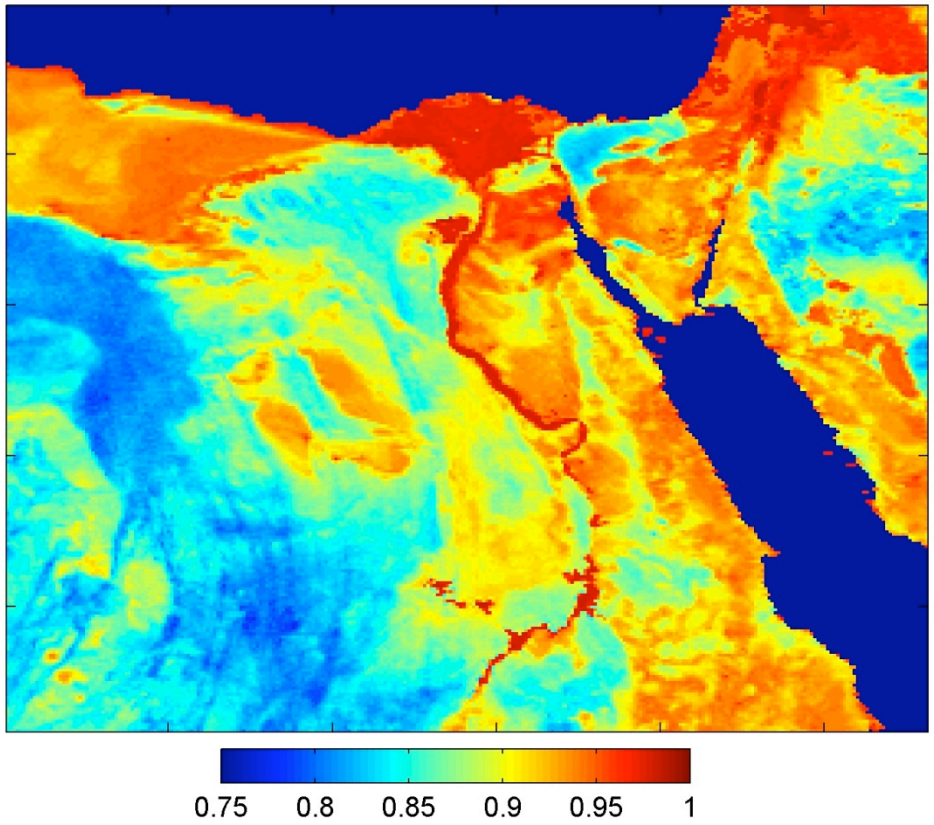

Cloud Detection?

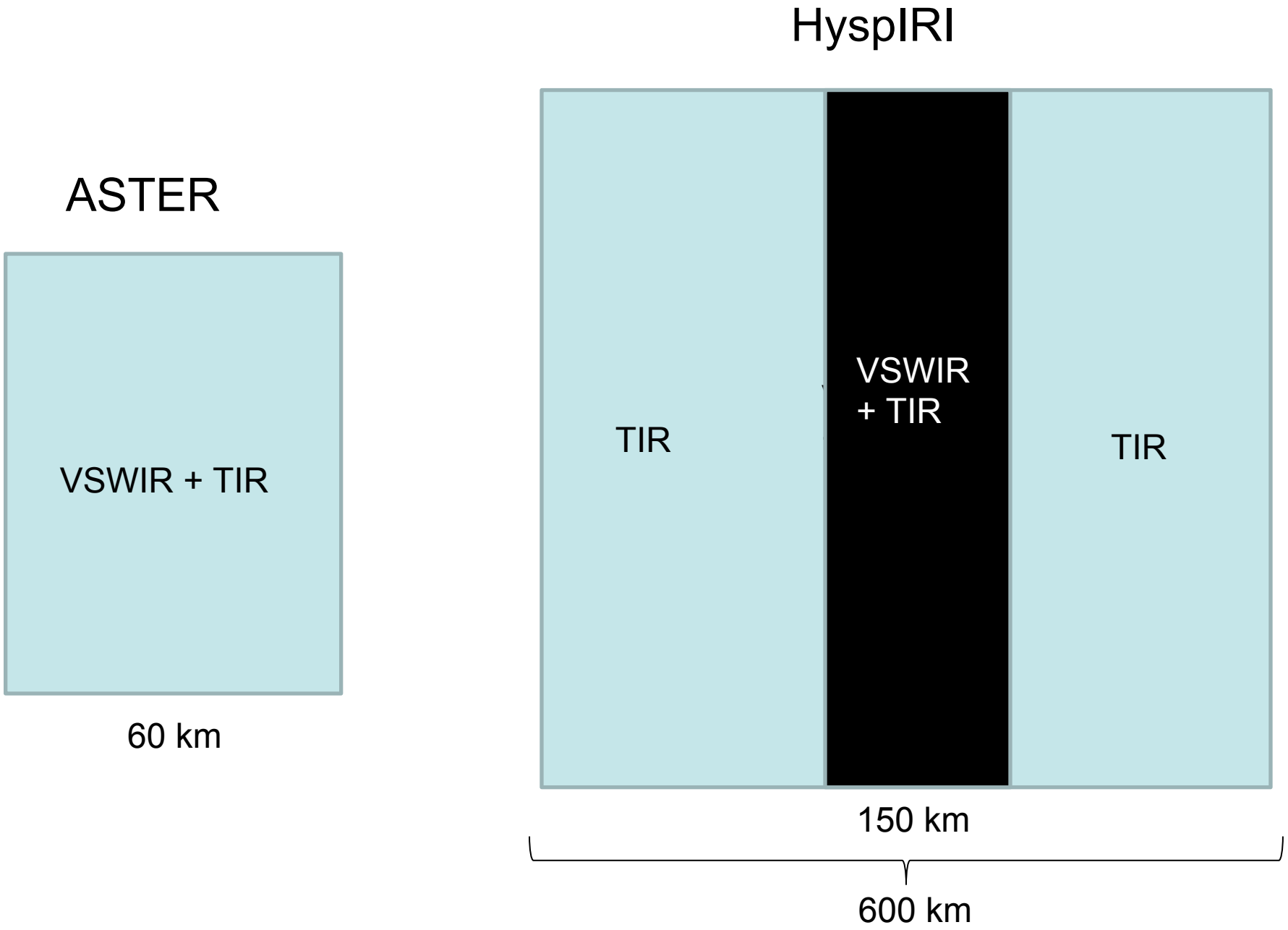

ASTER visible RGB

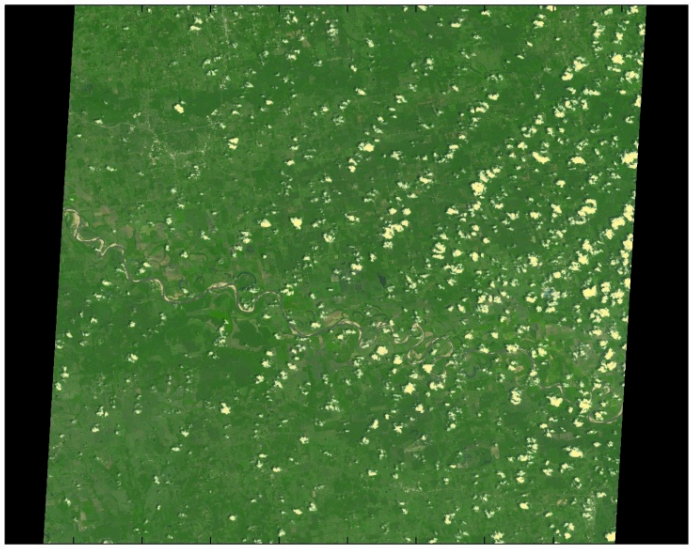

HyspIRI Simulated Pass-1

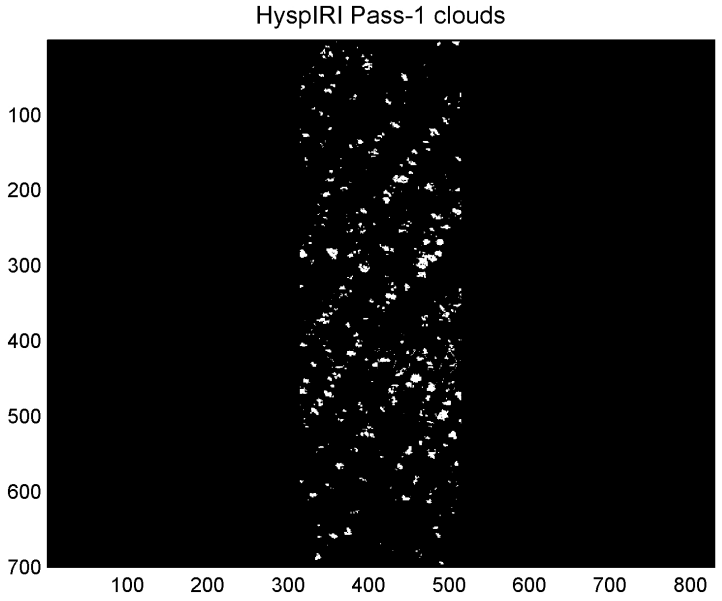

HyspIRI Simulated Pass-2

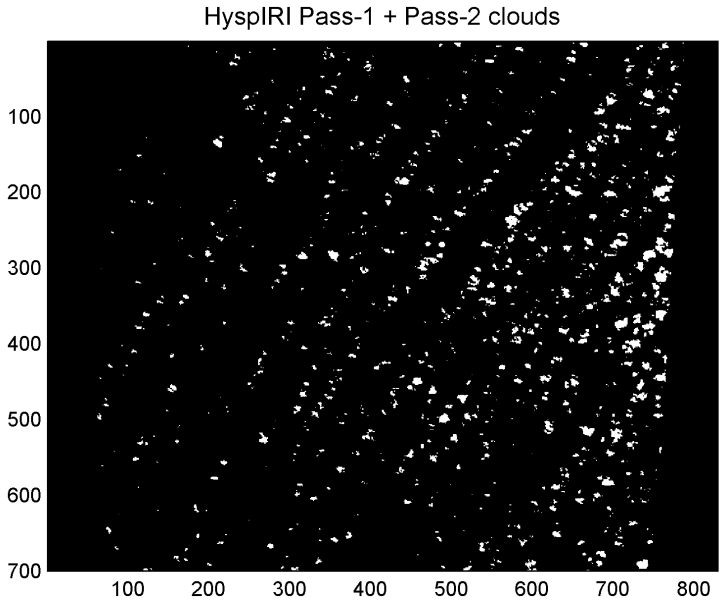

VSWIR + TIR Data

↓

Mean Temperature: 292.22 K
Max Temperature: 299.96 K
Min Temperature: 287.89 K
Standard Deviation: 2.2 K
Skewness: 0.848

↓

Statistical + TIR Data

←

ASTER visible RGB

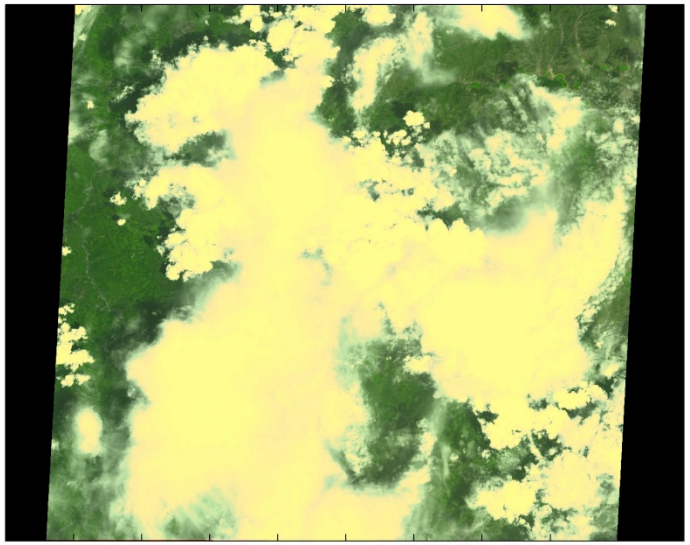

HyspIRI Simulated Pass-1

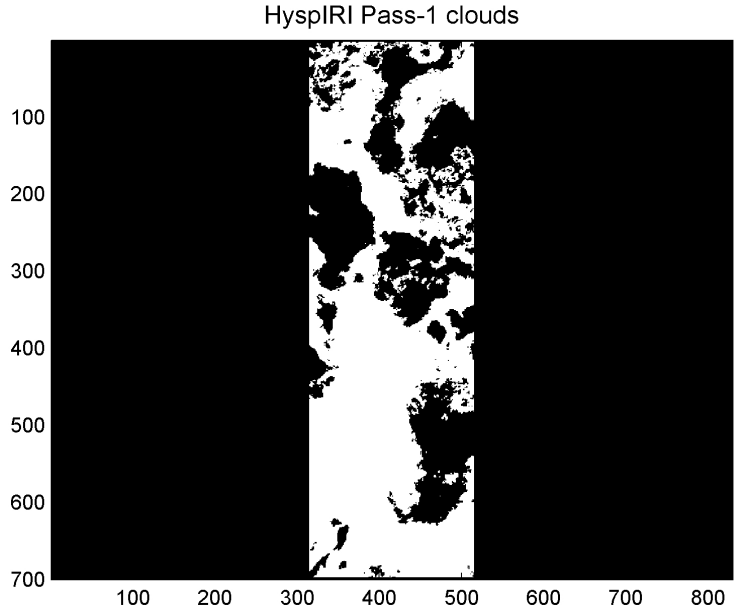

VSWIR + TIR Data

HyspIRI Simulated Pass-2

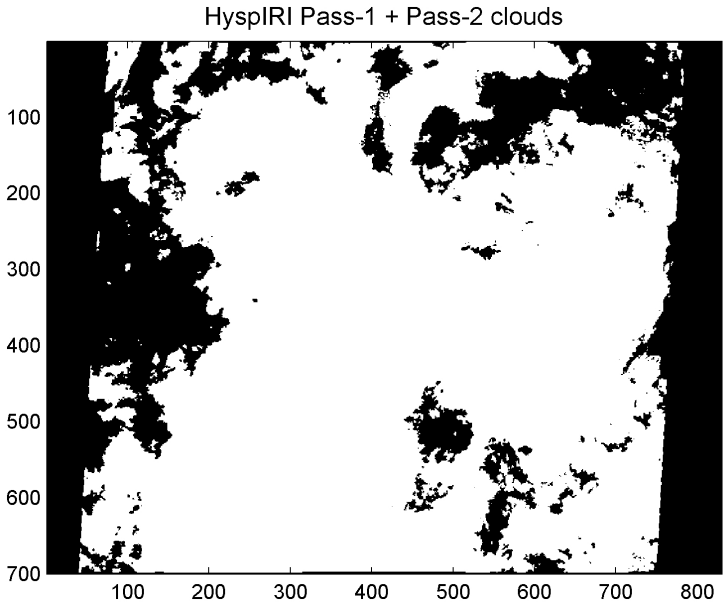

Mean Temperature: 252.42 K
Max Temperature: 299.88 K
Min Temperature: 231.52 K
Standard Deviation: 10.7 K
Skewness: 0.357

Statistical + TIR Data

HyspIRI ATBD's

2. JPL Publication XX-XX

HyspIRI Level-2 TIR Surface Radiance Algorithm Theoretical Basis Document, Version 1.0

HyspIRI Group

Prepared for National Aeronautics and Space Administration

By G. C. Hulley, S. J. Hook

Jet Propulsion Laboratory
California Institute of Technology
Pasadena, California

Jan 2010

Cleared and Released

2. JPL Publication XX-XX

HyspIRI Level-2 TIR Land Surface Temperature and Emissivity Algorithm Theoretical Basis Document, Version 1.0

HyspIRI Group

Prepared for National Aeronautics and Space Administration

By G. C. Hulley, S. J. Hook

Jet Propulsion Laboratory
California Institute of Technology
Pasadena, California

Jan 2010

In review: release imminent

- Oldest
- Aridity
- 10-85 r
- Occupi
- Primaril

Current Issue
June 2011
Table of Contents »

NATIONAL GEOGRAPHIC

ngm.com
Search

HOME | FEATURES | PHOTOGRAPHY | YOUR SHOT | MY SHOT | VIDEO | INTERACTIVES | NOW | NEXT | ARCHIVES | SUBSCRI

Feature Article | Photo Gallery | Behind the Lens: Photograph or Painting? | My Shot Gallery | Video: Hyena Steals a Meal

Africa's Super Park

Facebook Twitter More »

In 1990 the new nation of Namibia wrote wilderness protection into its constitution. Today nearly half of its land is set aside.

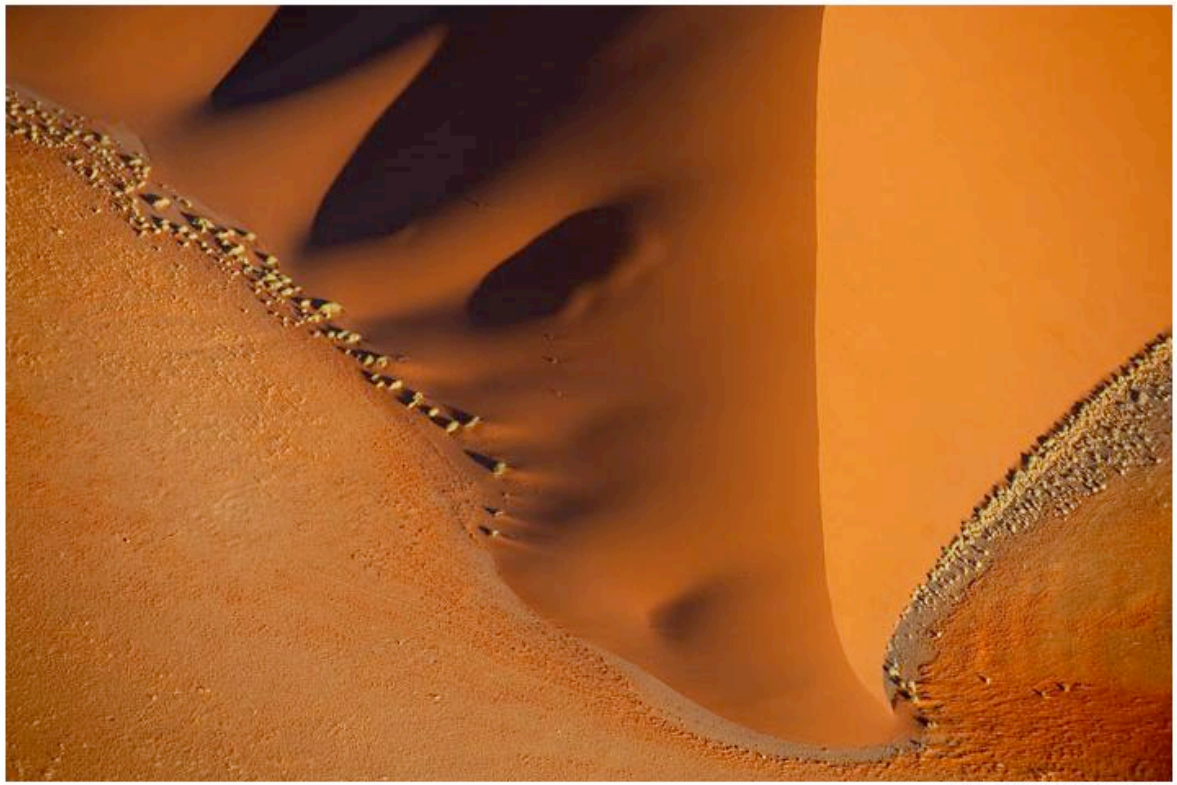

Photograph by Frans Lanting

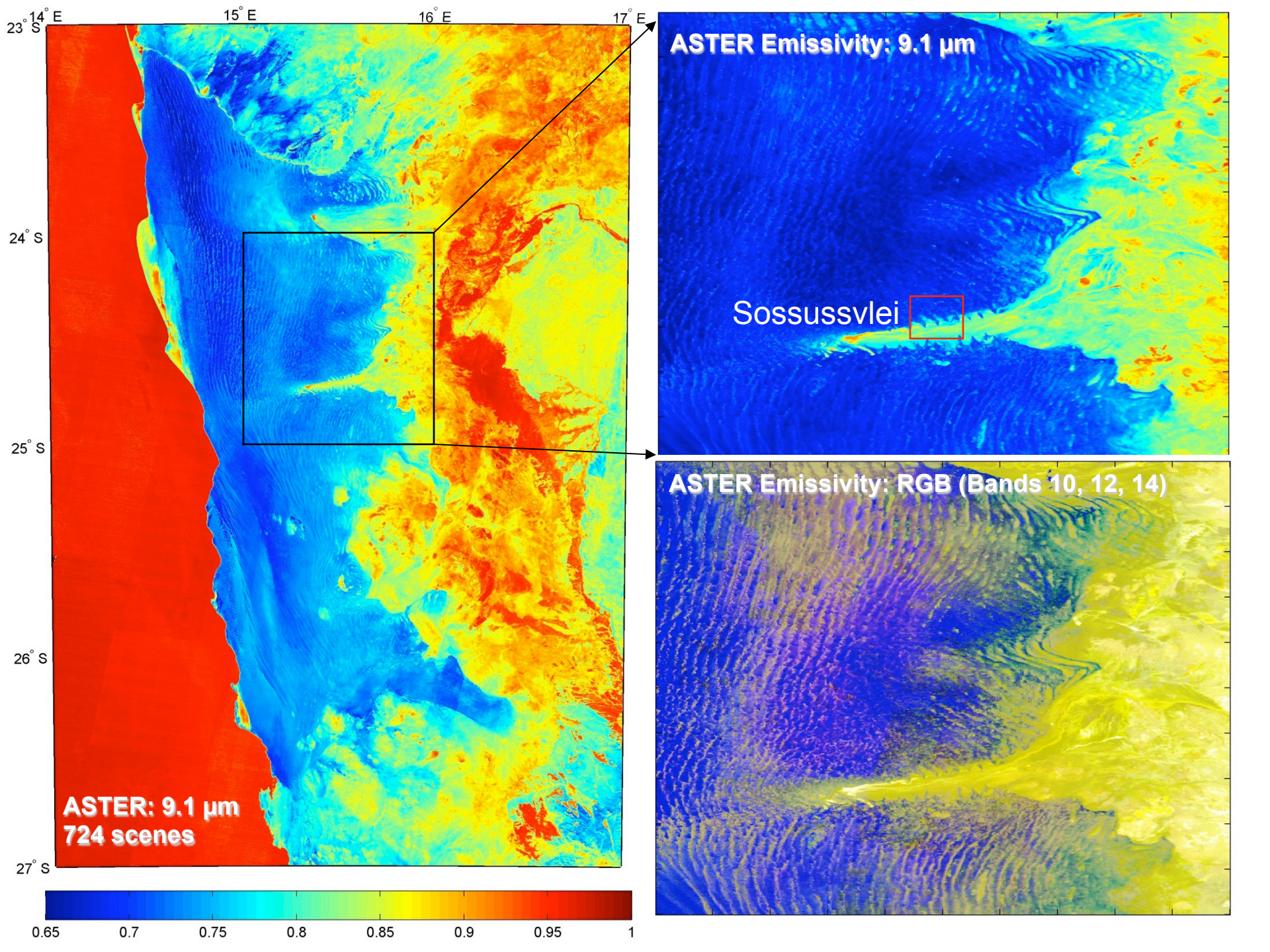
14° E
15° E
16° E
17° E
23° S
24° S
25° S
26° S
27° S
ASTER: 9.1 µm
724 scenes
0.65
0.7
0.75
0.8
0.85
0.9
0.95
1
ASTER Emissivity: 9.1 µm
Sossussvlei
ASTER Emissivity: RGB (Bands 10, 12, 14)

Sossussvlei – Namib Naukluft Park

*Credit: ASTER Science Team

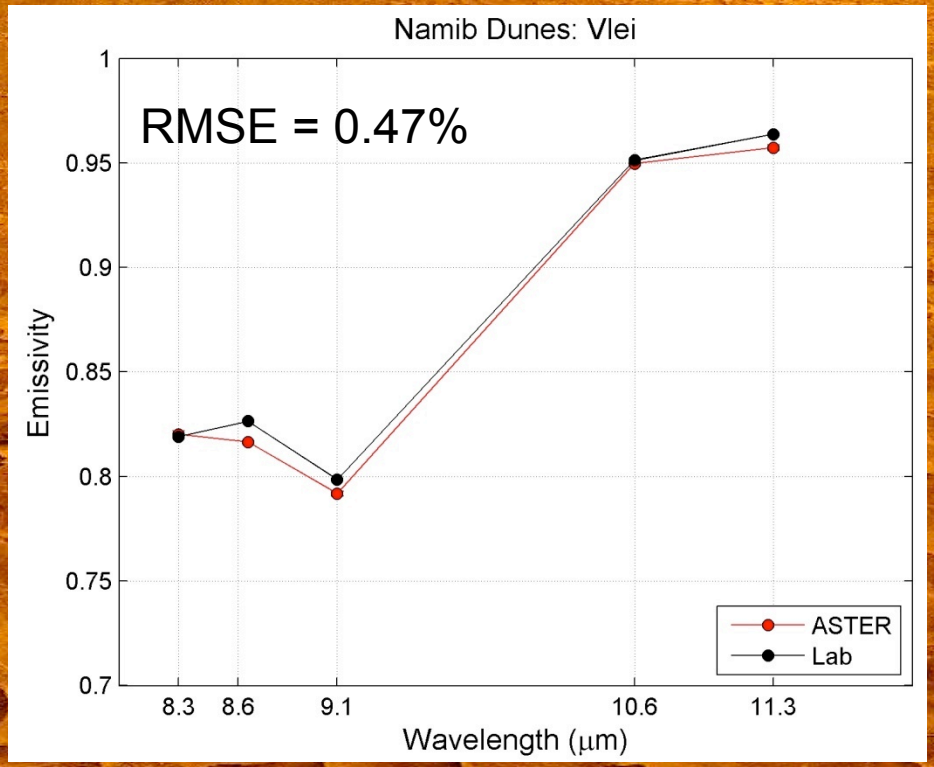

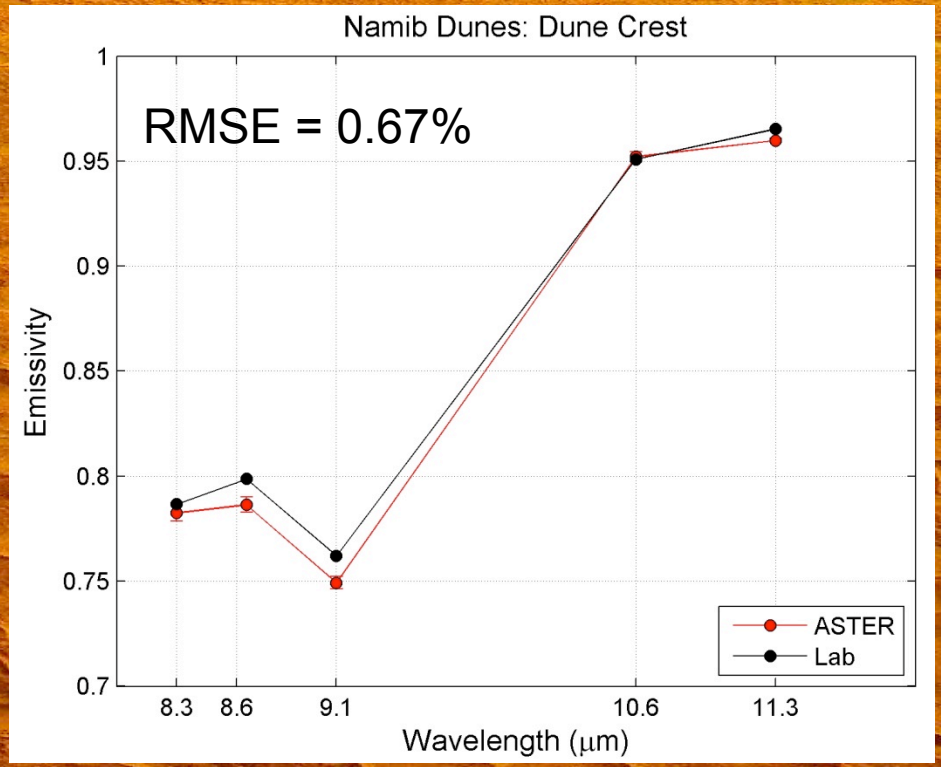

Val site 1: Interdune (vlei)
2 samples

Val site 2: Dune crest
6 samples

Dead Vlei
'Riverved'

1 km

Summary and Future Work

- Simulated emissivity database being generated for HyspIRI TIR products
- Algorithm theoretical basis documents and procedures continue to be developed for generating HyspIRI Level-2 products (Cloud Mask, Surface Radiance, Temperature and Emissivity)

- Complete and release HyspIRI Cloud Mask ATBD
- Complete Africa and Australia ASTER Emissivity maps
- Validate emissivity using sand samples from large dune sites
- Validate temperature using in-situ and radiance-based methods

The End

National Aeronautics and Space Administration

Jet Propulsion Laboratory
California Institute of Technology
Pasadena, California

www.nasa.gov

JPL 400-1278 7/06

Atmospheric Infrared Sounder (AIRS, Aqua) v5 Land Surface Emissivity Validation

Validation Targets:

- Namib Desert (desert)
- Kalahari Desert (semi-arid)

AIRS emissivity validation requires large, homogeneous sites with known composition.

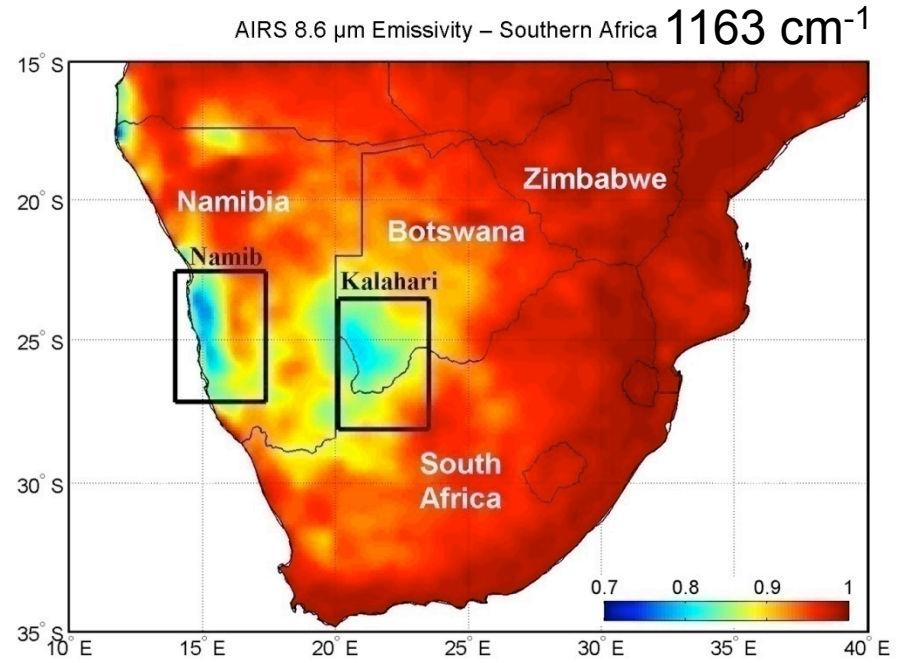

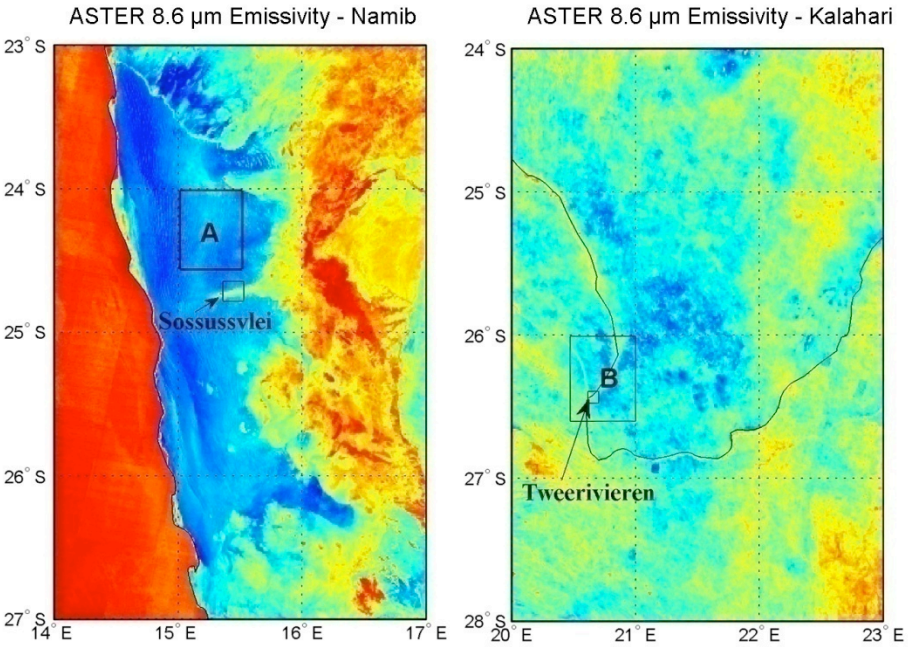

Hulley, G.C., S.J. Hook, E. Manning, S. Lee, E. Fetzer, 2009, Validation of the Atmospheric Infrared Sounder (AIRS) Version 5 Land Surface Emissivity Product over the Namib and Kalahari Desert, *Journal of Geophysical Research Atmospheres*, VOL. 114, D19104, doi:10.1029/2009JD012351

Kalahari Desert

- 20 sand samples collected at Kgalagadi National Park (17-21 November 2008)
- Sampling areas included dune crests, troughs, dry riverbeds

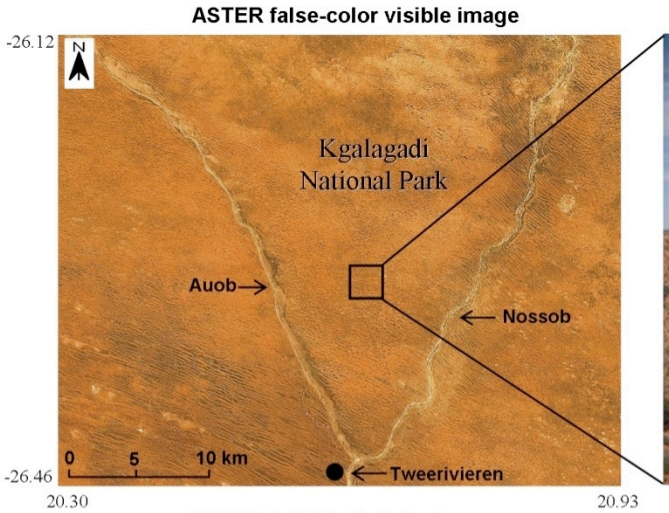

Major: Quartz
Minor: Hematite

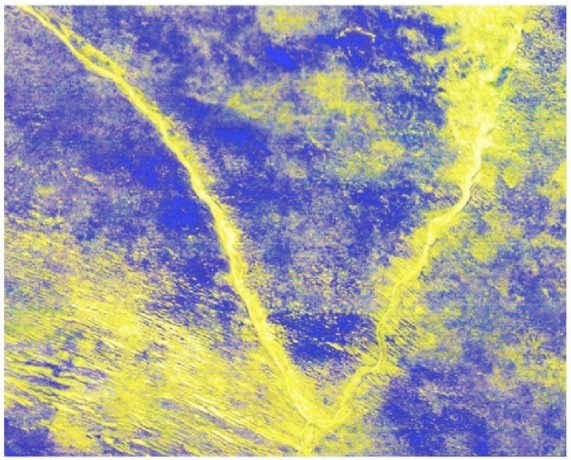

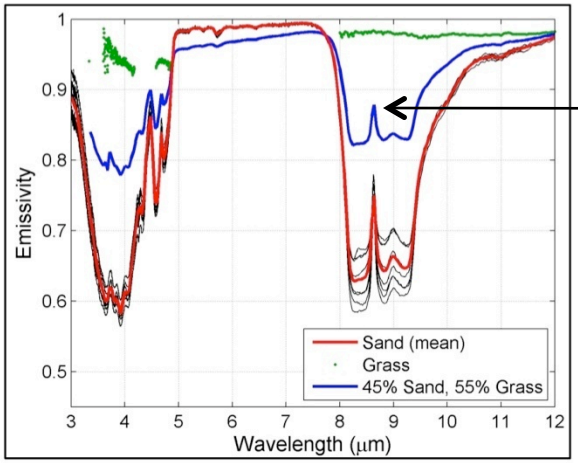

SAFARI 2000
Kalahari transects
- 55% Vegetation
- 45% Sand

Namib Desert

- Sand samples collected at Sossussvlei in Namib-Naukluft park
- 10 samples from a dune crest and interdune area

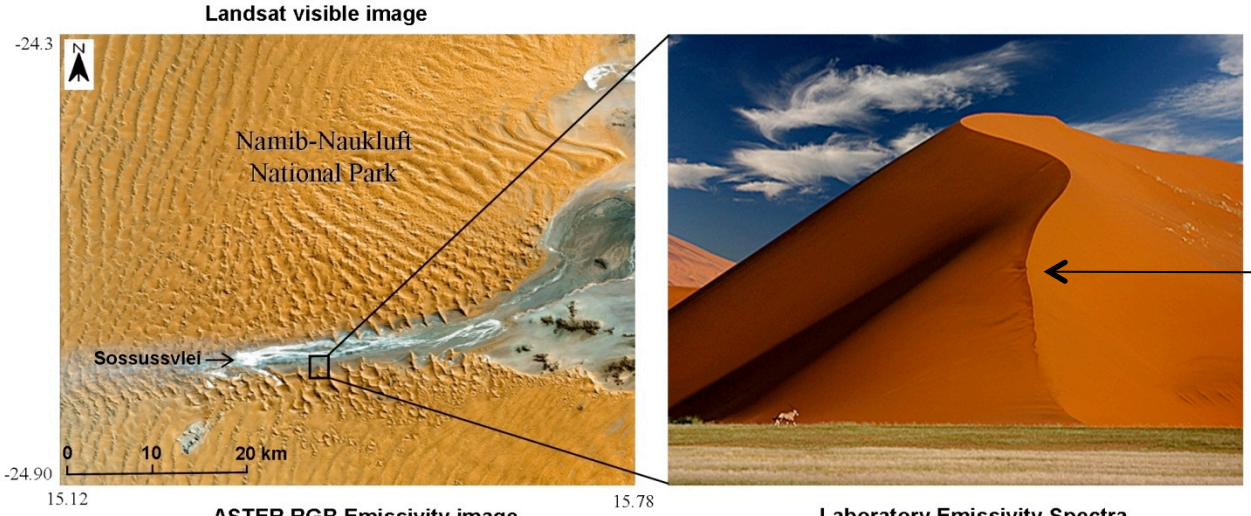

Major: Quartz
Minor: Feldspar, Magnetite

ASTER RGB Emissivity image

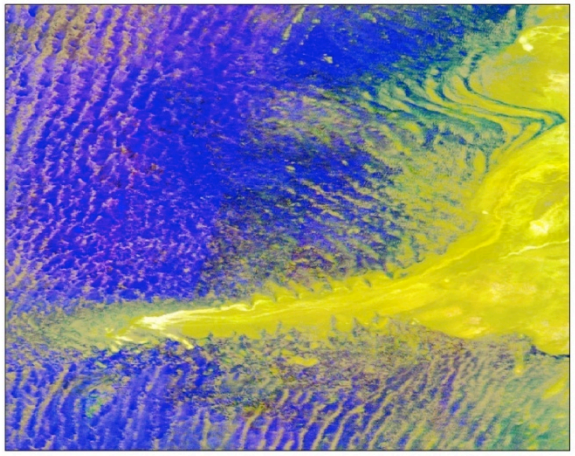

Laboratory Emissivity Spectra

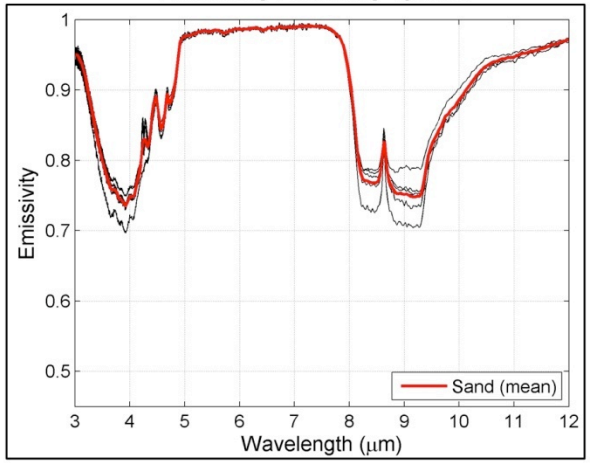

NAALSED overlays in Google Earth - Colorado Plateau
Useful for geological mapping, resource exploration
Each color represents different rock types (eg. Red = quartz)

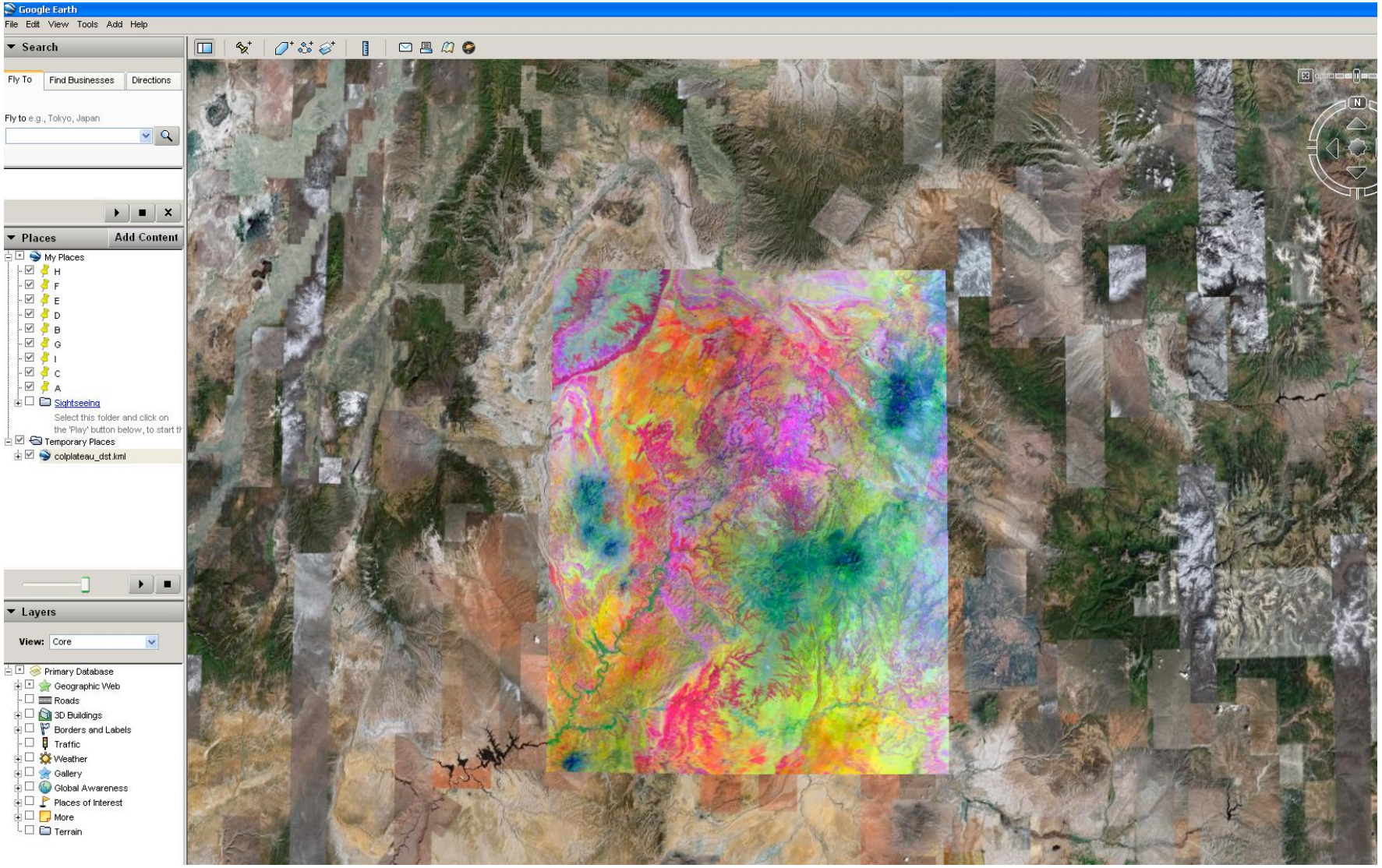

HysplRI Coverage Requirement and Cloud Analyses

Michael Mercury

2011 HysplRI Workshop

Jet Propulsion Laboratory
California Institute of Technology

Image courtesy of Krish Dulal from WikiMedia

Probability of Cloud Free View

$$P_{CloudFree} = \frac{\#_{CloudFreeMODISViews}}{\#_{MODISViews}}(100)$$

MODIS Terra views clouds at same time of day as HyspIRI since its orbit has a 10:30 AM descending node

Cloud Free MODIS View

BIT FIELD	DESCRIPTION KEY	RESULT
1-2	Unobstructed FOV Confidence Flag	00 = cloudy 01 = uncertain 10 = probably clear 11 = confident clear

$P_{CloudFree}$

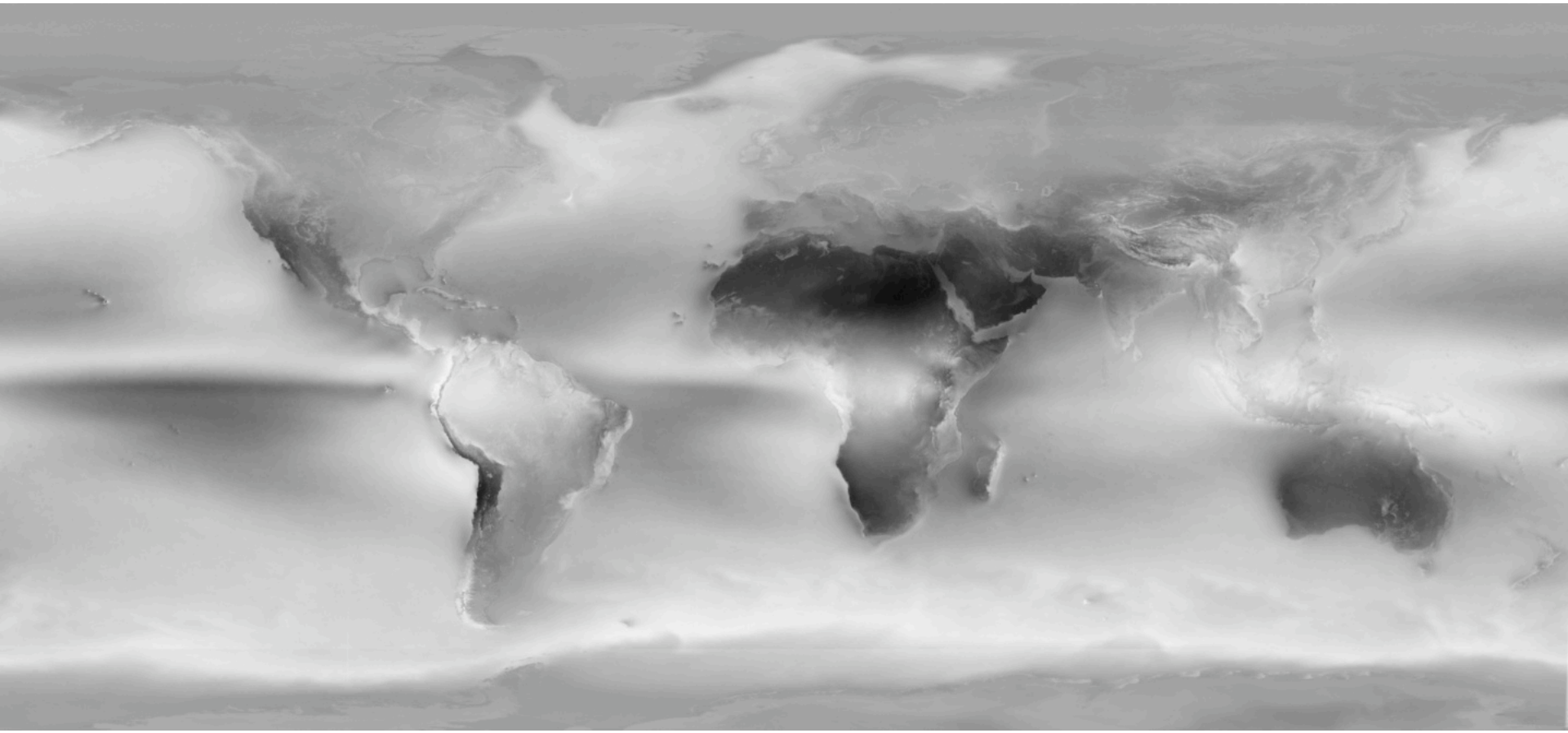

MODIS MOD35 Day 5km Cloud Mask from 2001-2007

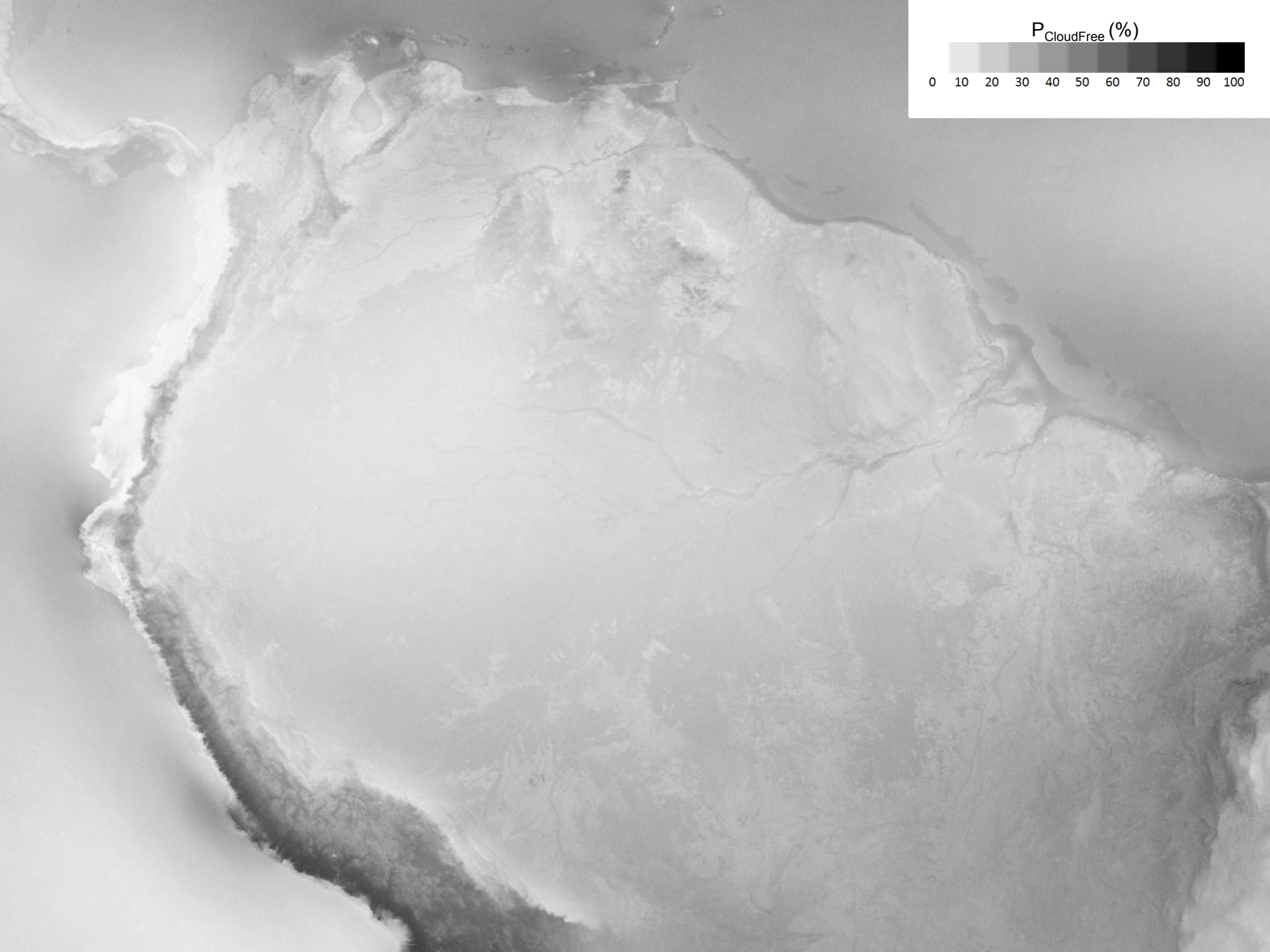
$P_{CloudFree}$ (%)
0 10 20 30 40 50 60 70 80 90 100

Oddities in MOD35 Cloud Mask

West Saharan sand showing up as habitual cloudiness

Clear cut areas of the Amazon showing up as habitual cloudiness

Correlation to MODIS Global Product

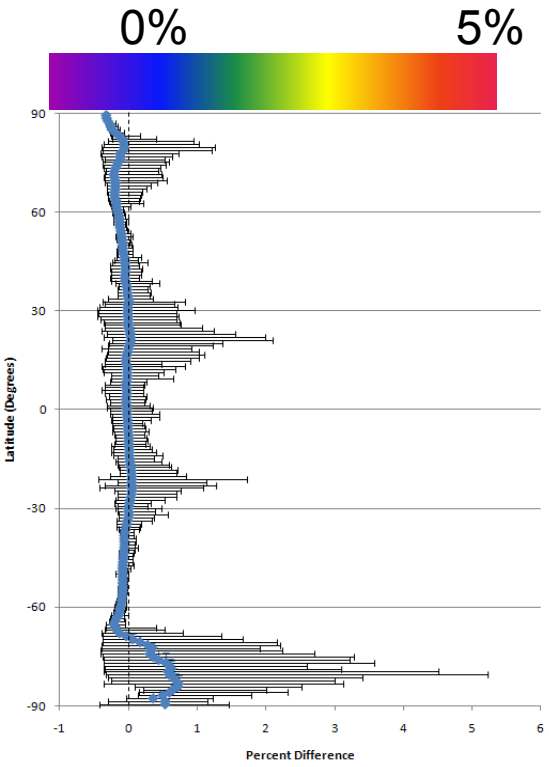

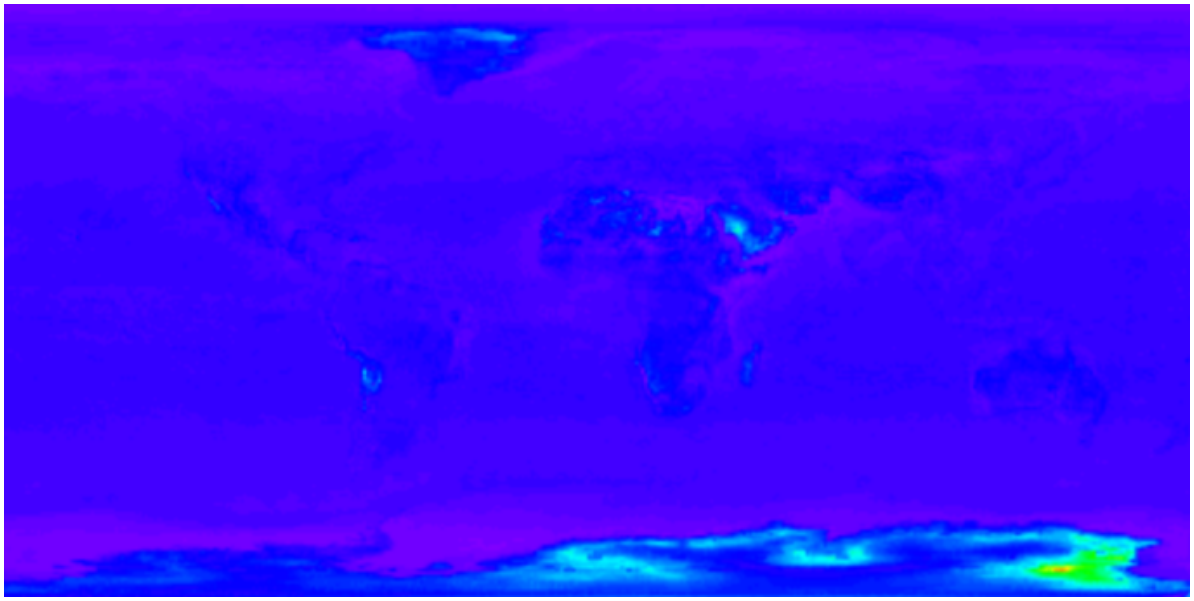

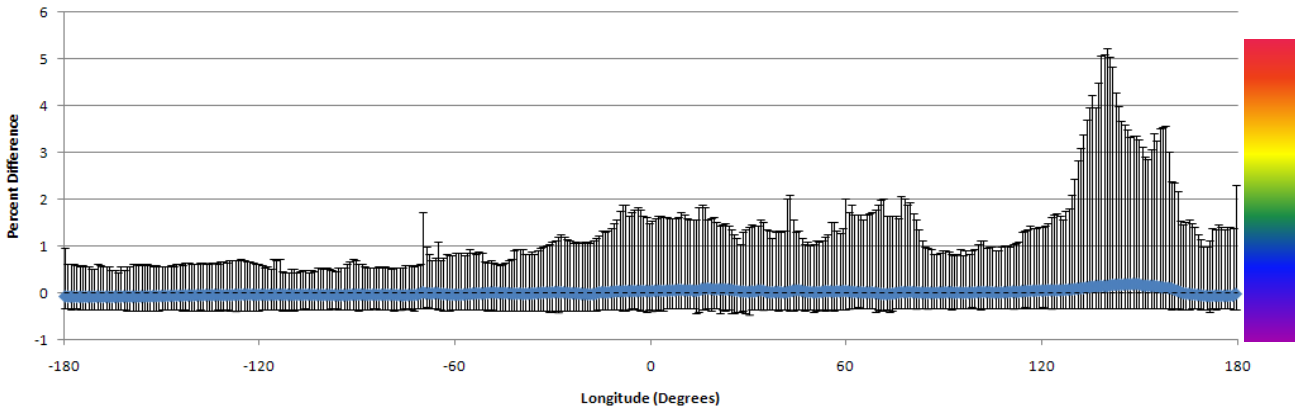

Number of Cloud Free Views by Each HyspIRI Instrument

$$\#_{CloudFreeViews} = P_{CloudFree} \#_{ViewsByInstrument}$$

TIR Daytime Views

Yearly Cloud Free Views	0	12	24+
[Days Between Views]	[-]	[30]	[<15]

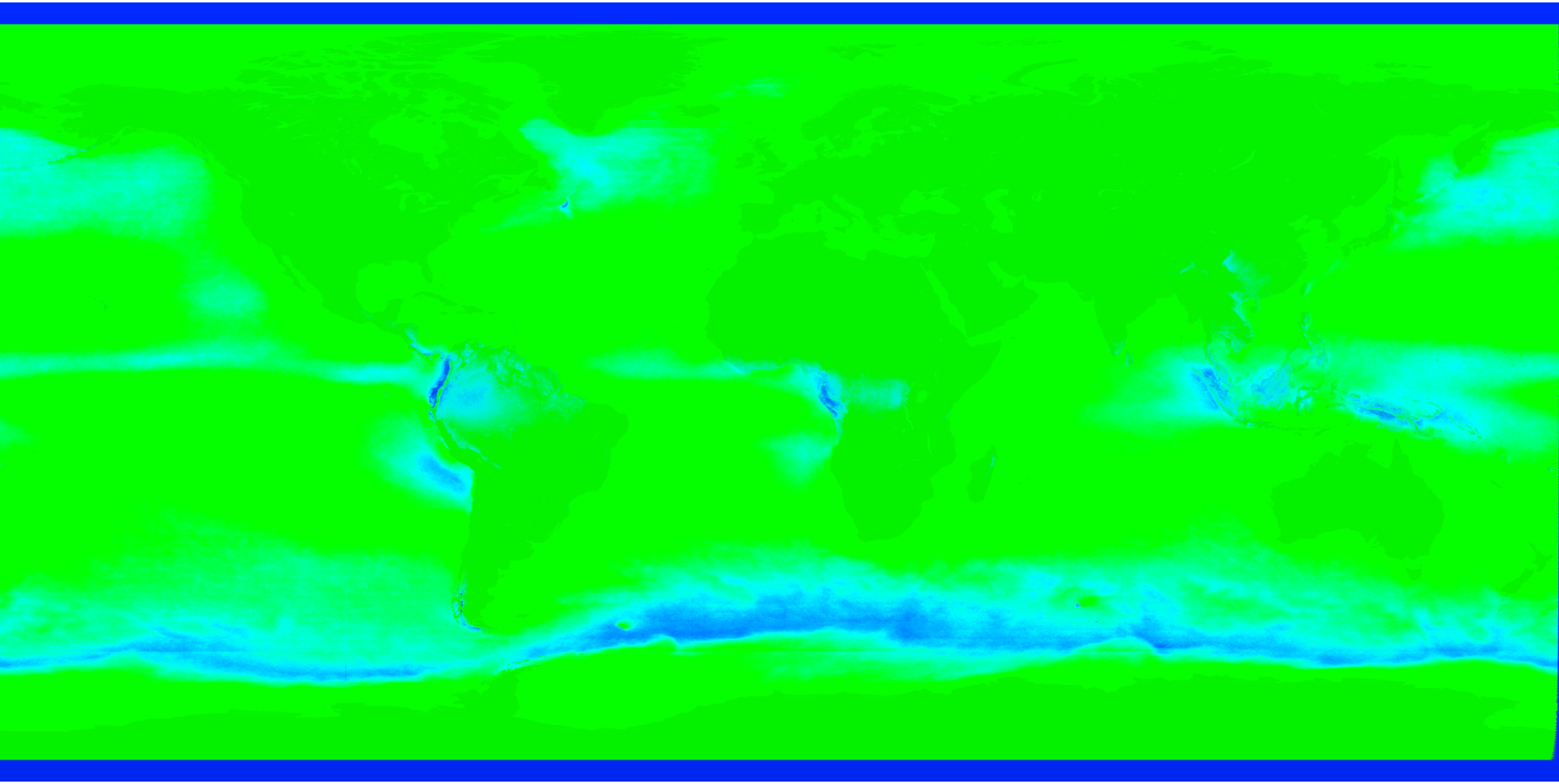

TIR Daytime Views

Yearly Cloud Free Views	0	36.5	73+
[Days Between Views]	[-]	[10]	[<5]

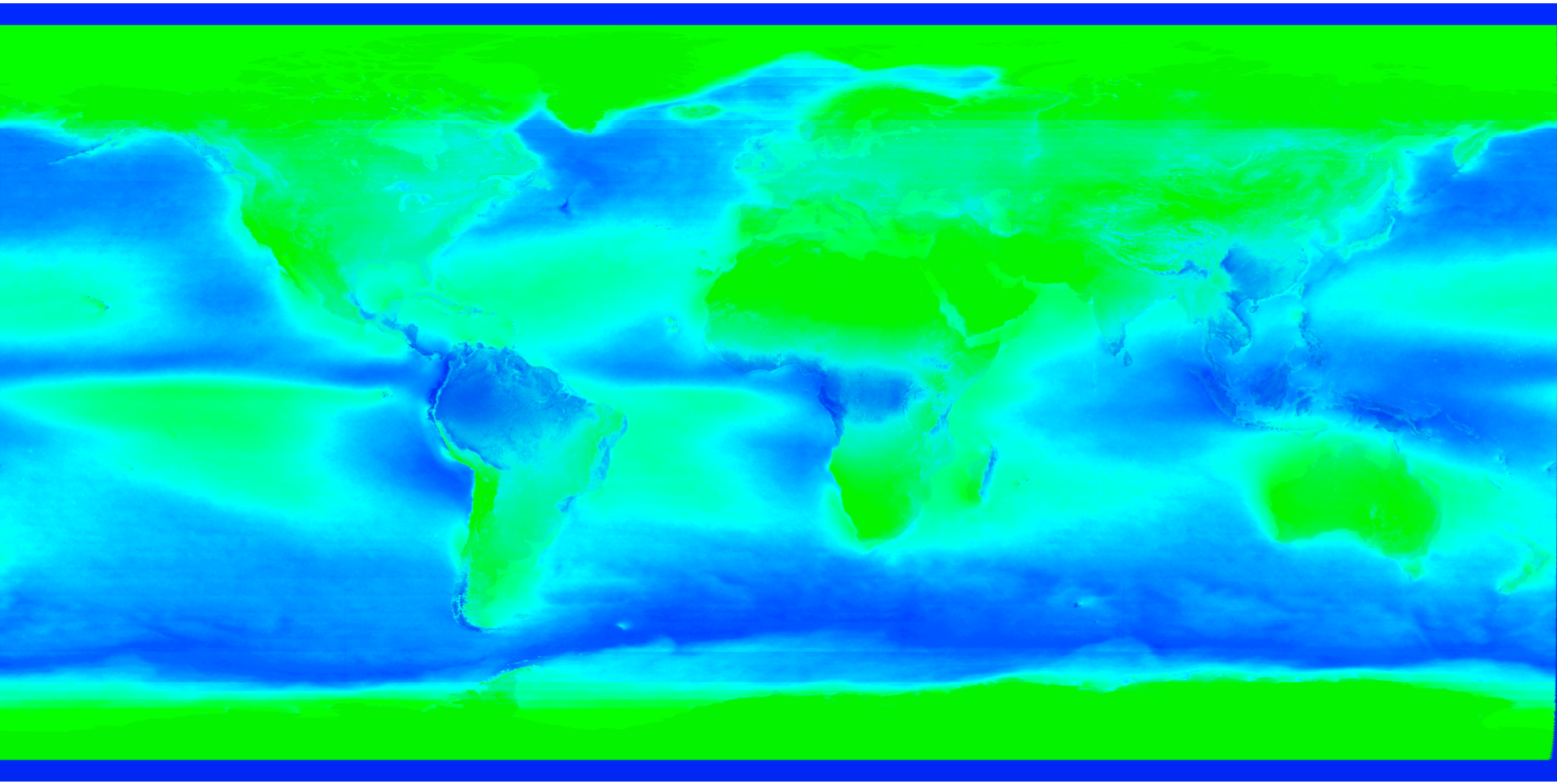

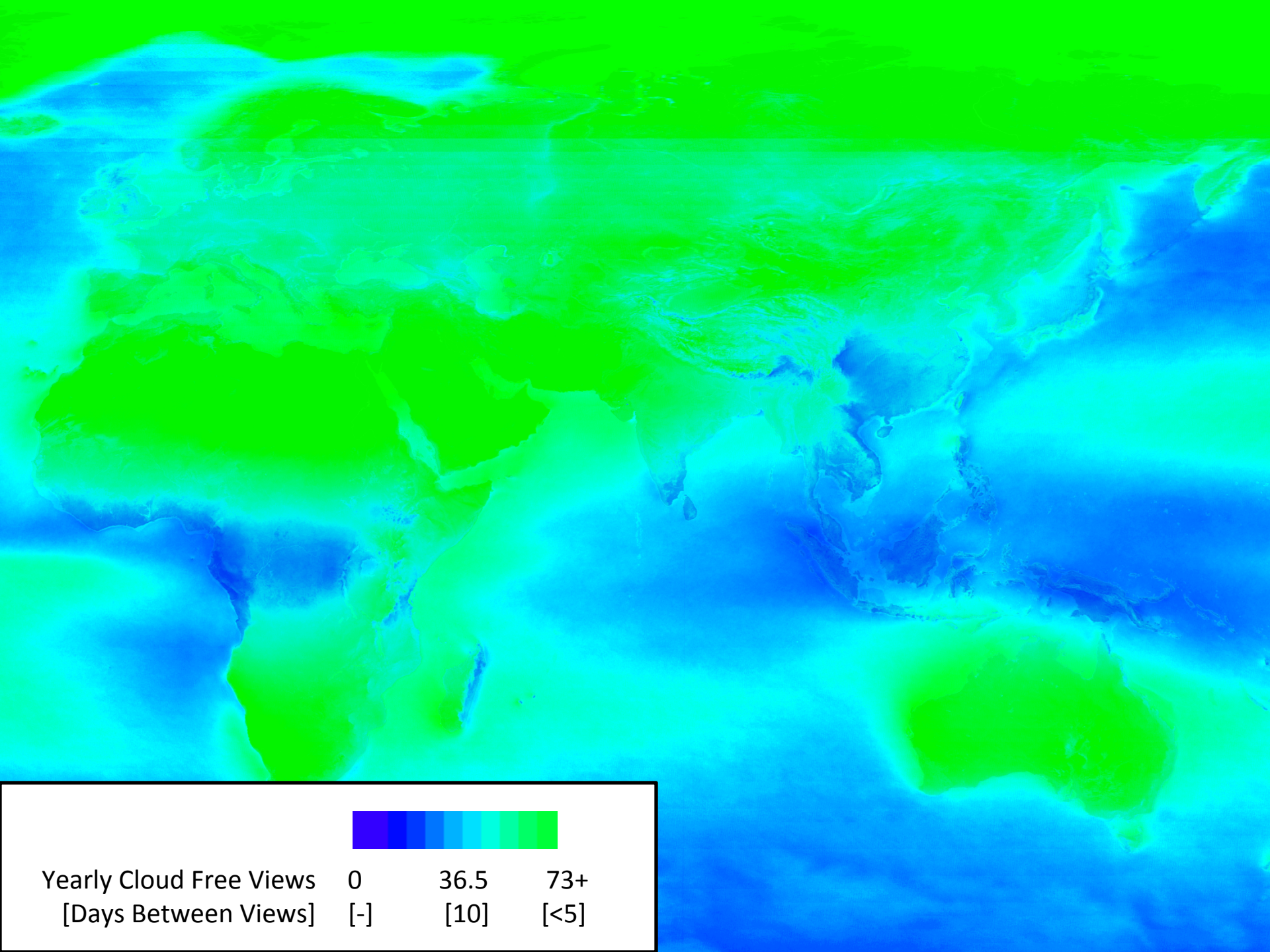
Yearly Cloud Free Views
[Days Between Views]
0
[-]
36.5
[10]
73+
[<5]

VSWIR

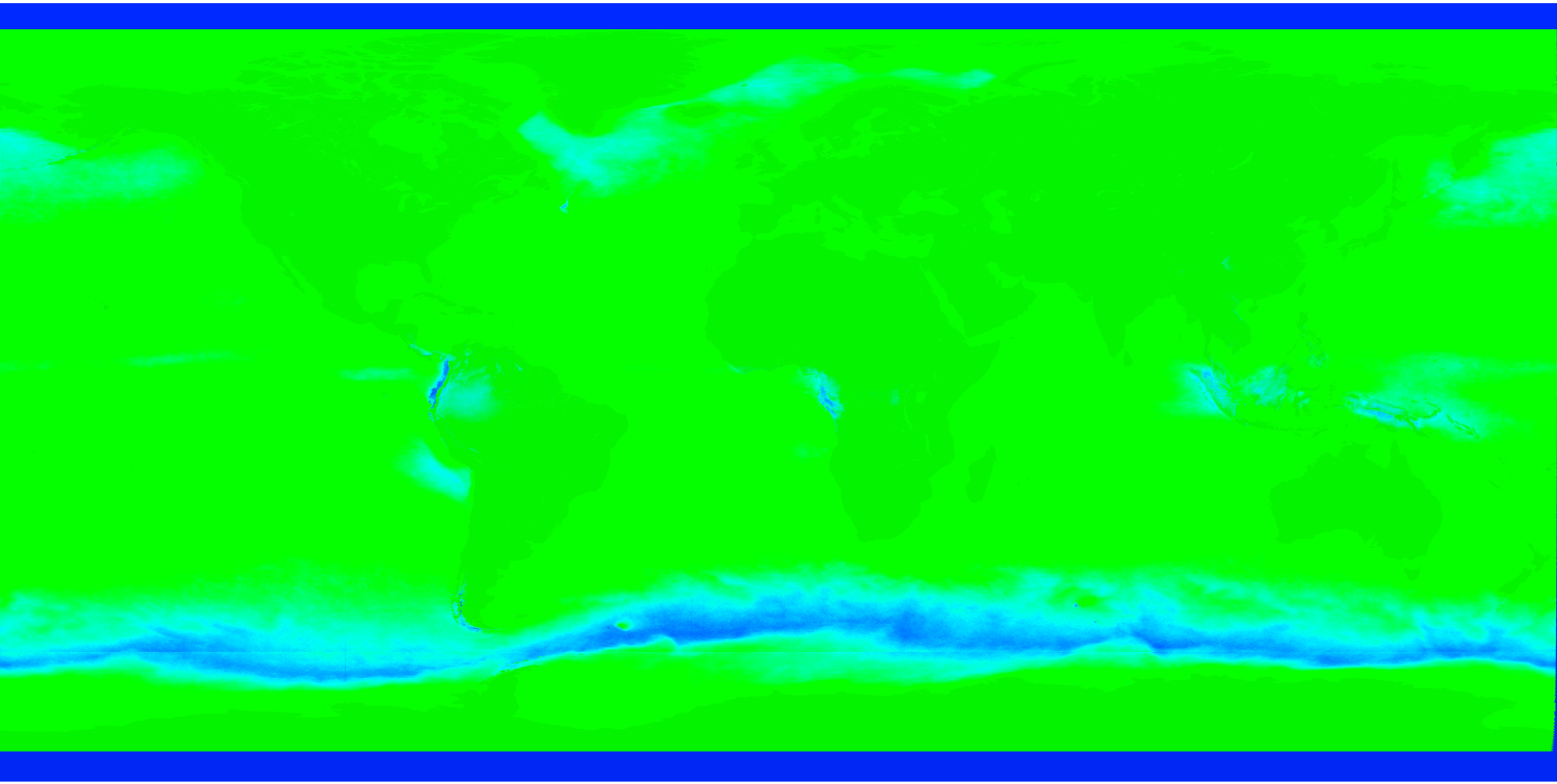

VSWIR

Yearly Cloud Free Views	0	9.5	19+
[Days Between Views]	[-]	[38]	[<19]

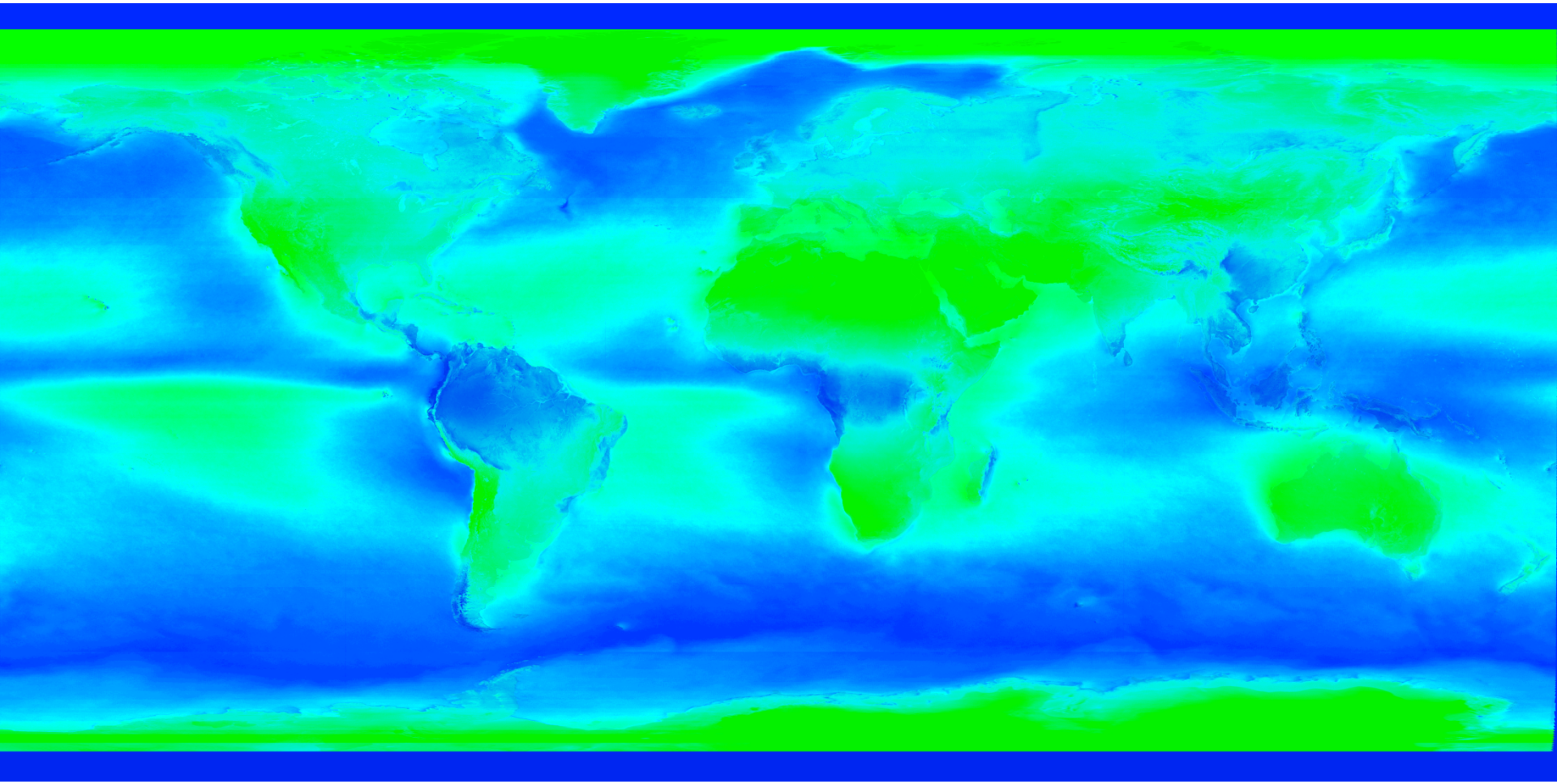

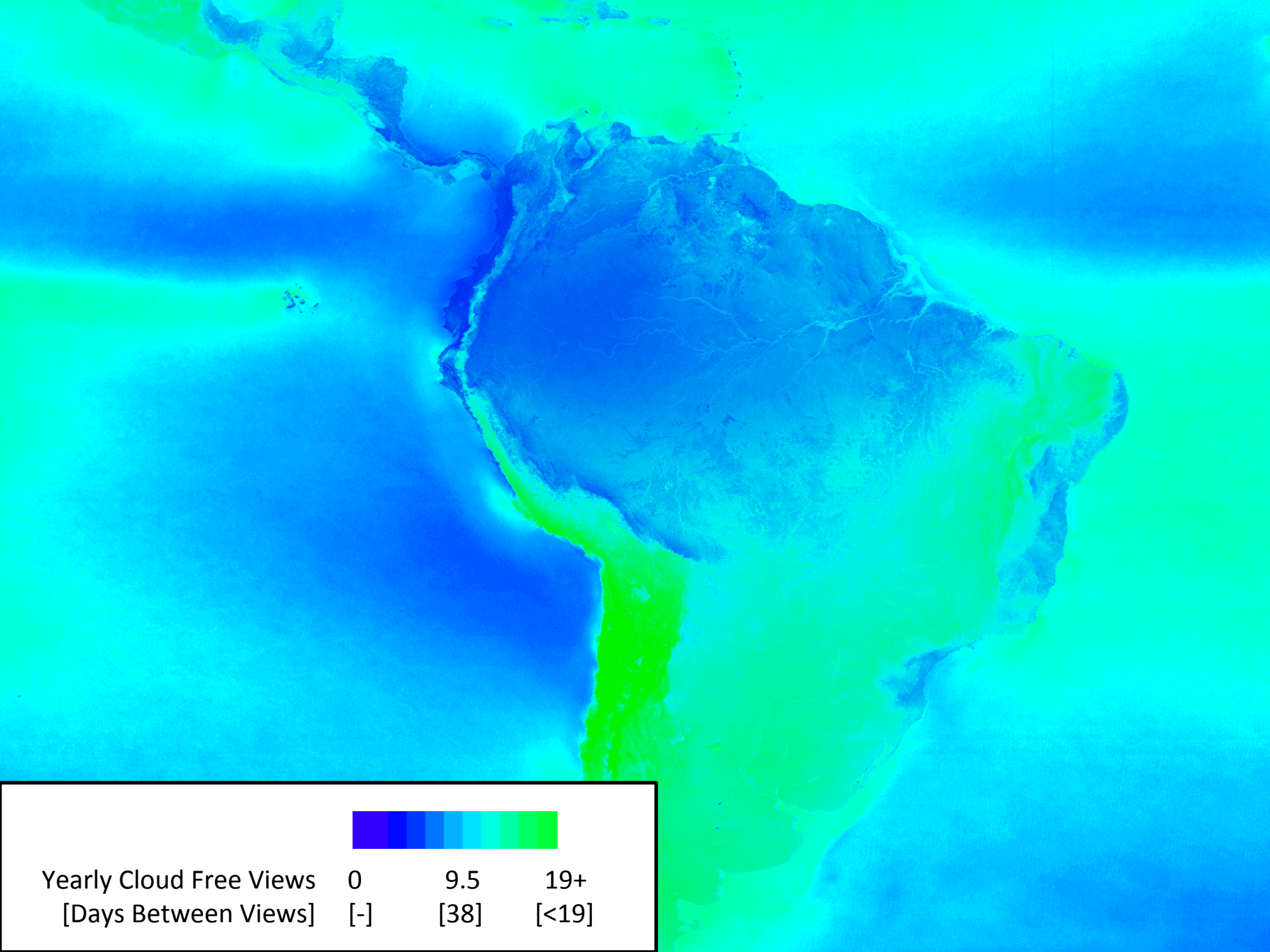
Yearly Cloud Free Views
[Days Between Views]
0
[-]
9.5
[38]
19+
[<19]

Coral Reef Remote Sensing Science Objectives and Requirements

Eric J. Hochberg
Bermuda Institute of Ocean Sciences

2011 HyspIRI Science Workshop
25 August 2011

Coral Reefs: Global Distribution and Importance

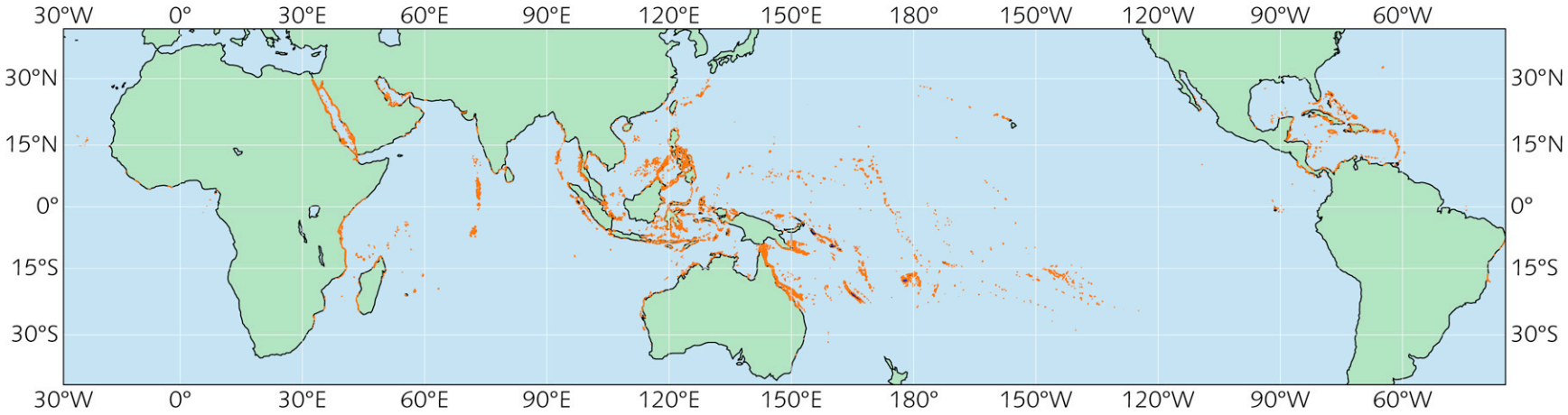

Focus for traditional culture and food source for innumerable small subsistence economies

Protection to shorelines from storm and wave damage and barriers that provide safe passage for shipping

Superlative recreational resource and the foundation of a multibillion dollar tourist industry worldwide

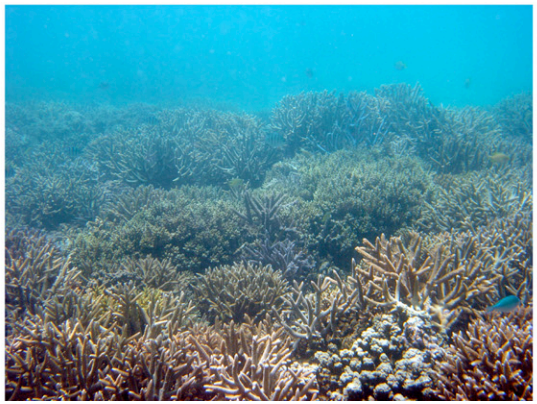

Major locus of global biodiversity, providing an ecological reserve of genetic complexity

IPCC AR4: Coral reefs are one of four cross-chapter case studies

Parry, M.L., O.F. Canziani, J.P. Palutikof, P.J. van der Linden and C.E. Hanson, Eds., 2007: Cross-chapter case study. In: Climate Change 2007: Impacts, Adaptation and Vulnerability. Contribution of Working Group II to the Fourth Assessment Report of the Intergovernmental Panel on Climate Change, Cambridge University Press, Cambridge, UK, 843-868.

C2 Impacts of climate change on coral reefs

C2.1 Present-day changes in coral reefs
- C2.1.1 Observed changes in coral reefs (Chapter 1, Section 1.3.4.1)
- C2.1.2 Environmental thresholds and observed coral bleaching (Chapter 6, Box 6.1)

C2.2 Future impacts on coral reefs
- C2.2.1 Are coral reefs endangered by climate change? (Chapter 4, Box 4.4)
- C2.2.2 Impacts on coral reefs (Chapter 6, Section 6.4.1.5)
- C2.2.3 Climate change and the Great Barrier Reef (Chapter 11, Box 11.3)
- C2.2.4 Impact of coral mortality on reef fisheries (Chapter 5, Box 5.4)

C2.3 Multiple stresses on coral reefs
- C2.3.1 Non-climate-change threats to coral reefs of small islands (Chapter 16, Box 16.2)

Global Stresses to Reefs

SST: Increased Coral Bleaching

SST: Increased Coral Disease

Ocean Acidicifation: Decreases in Calcification Rates

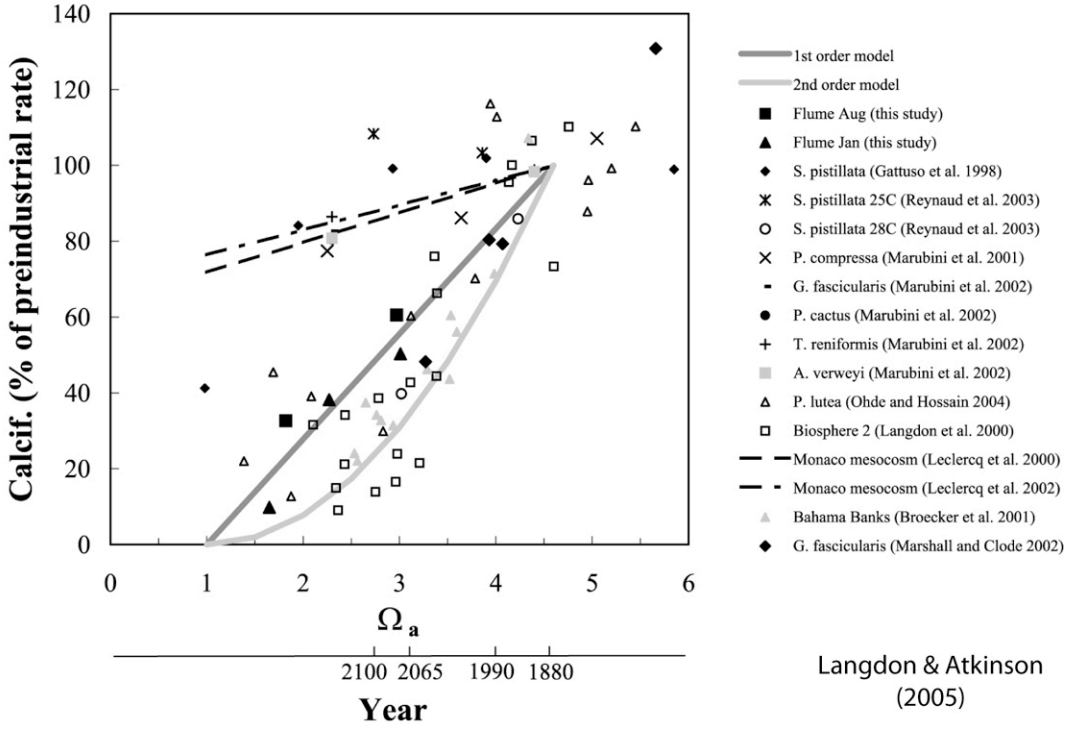

Langdon & Atkinson (2005)

Synergistic Effects

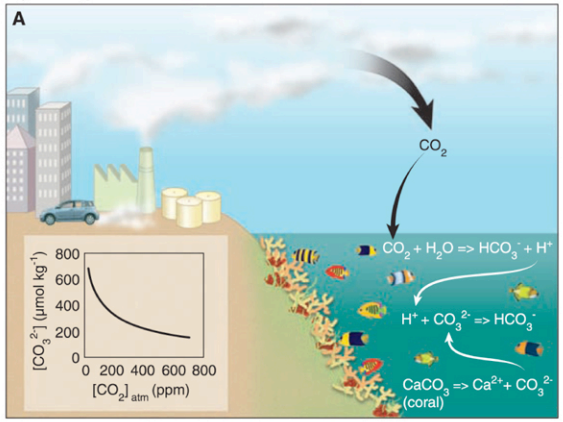

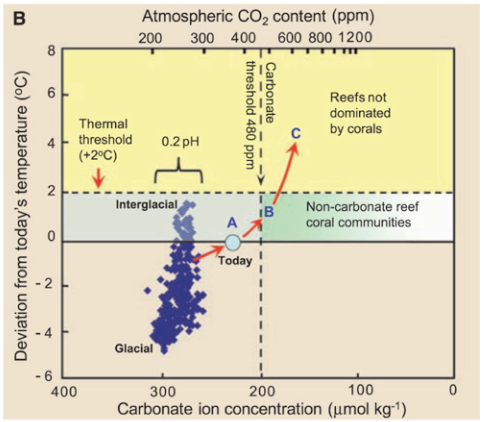

Hoegh-Gulberg et al. (2007)

The Primary Coral Reef Problem:
Phase Shifts from Coral-Dominated to Algae-Dominated

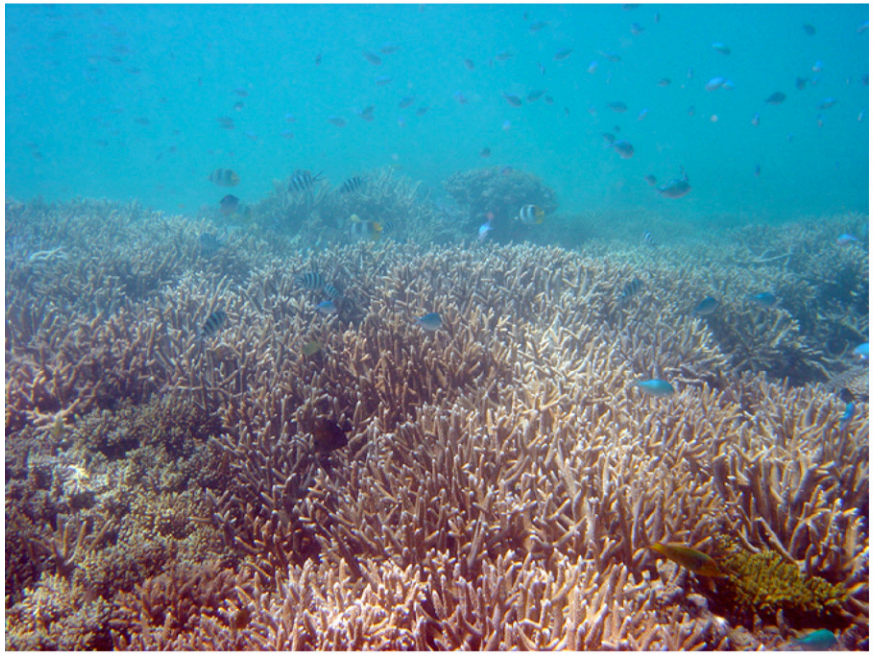

- Rough
- High productivity/calcification
- "Healthy"

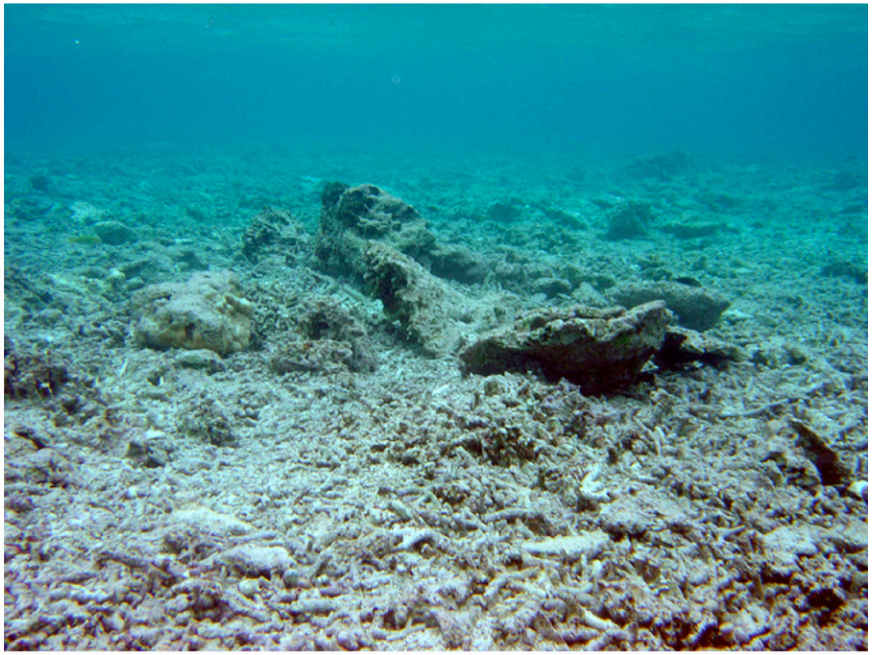

- Smooth
- Low productivity/calcification
- Not "healthy"

State of the Art in Coral Reef Structure Assessment: Resource Inventory

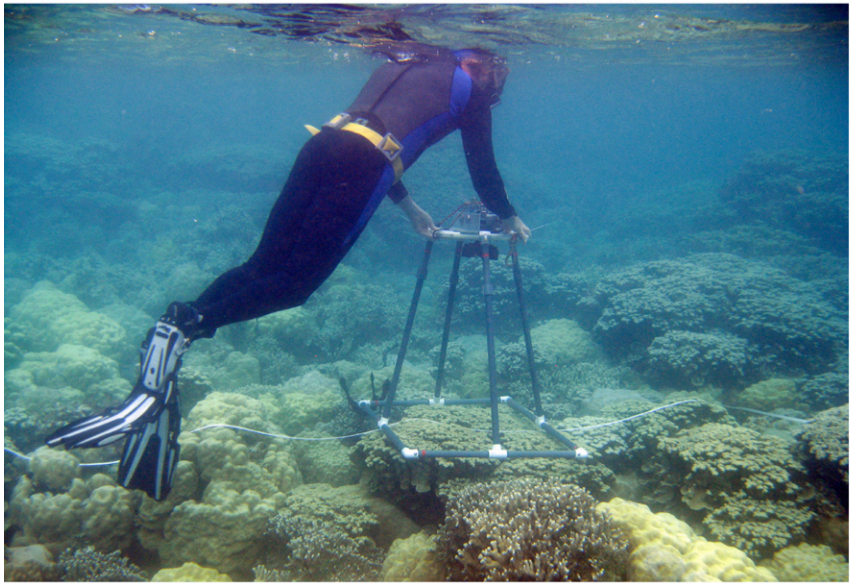

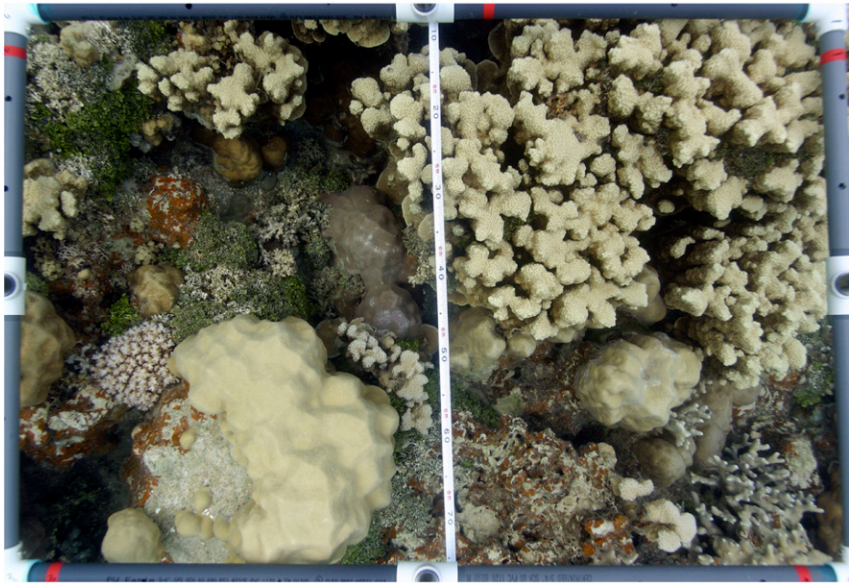

Photoquadrat Transects: detailed, laborious, small footprint

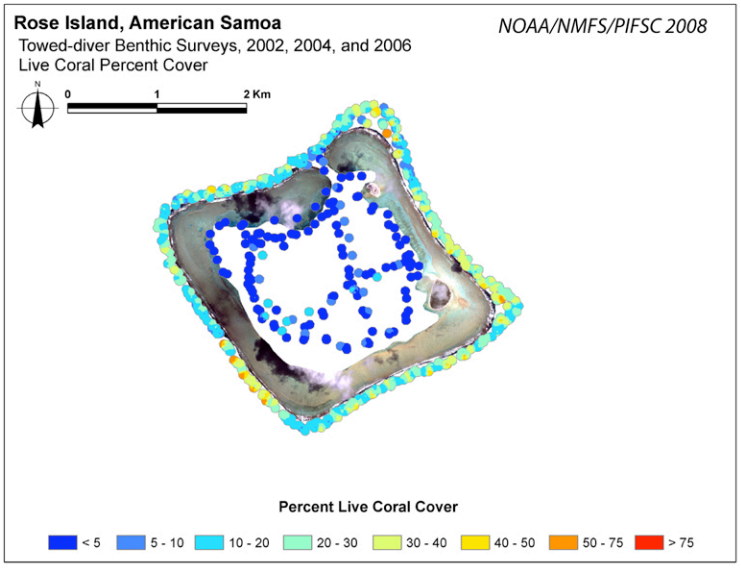

"Manta-Tows": quick, semi-quantitative, large footprint

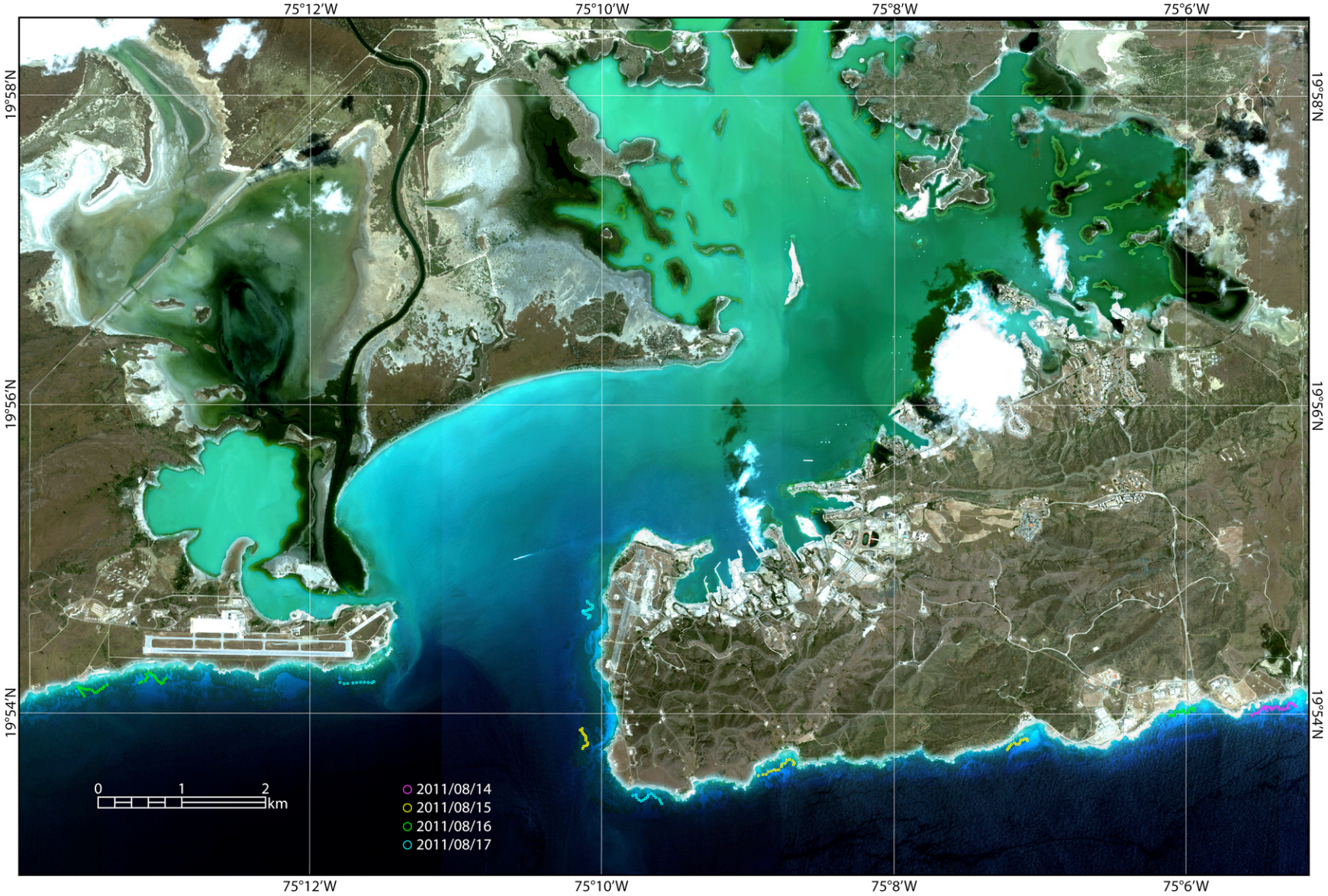
75°12′W
75°10′W
75°8′W
75°6′W
19°58′N
19°56′N
19°54′N
0
1
2
km
2011/08/14
2011/08/15
2011/08/16
2011/08/17

Coral Reefs: Sampling Problem

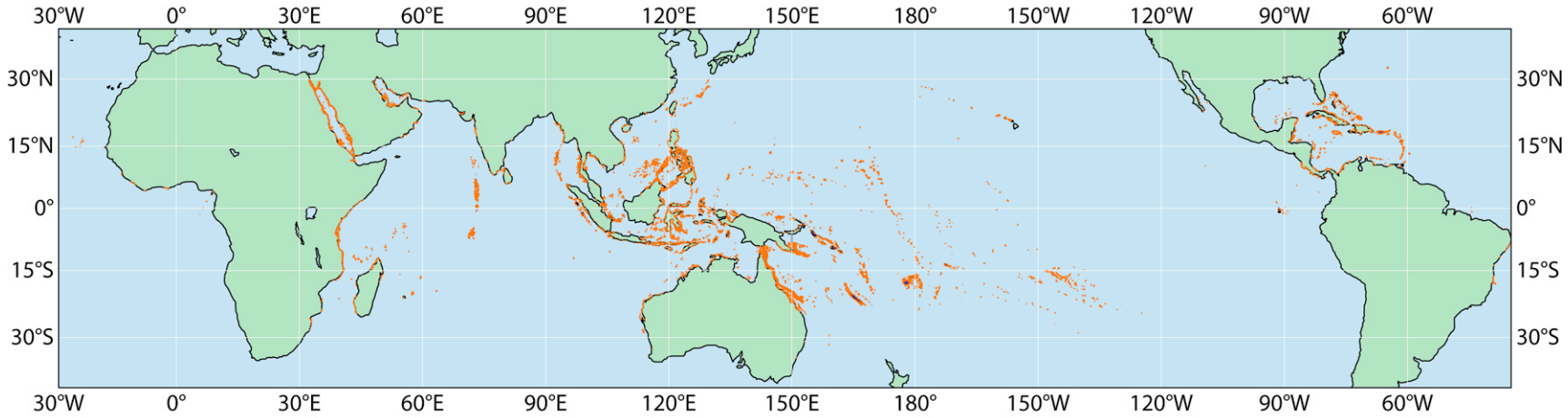

- ~9,000 reefs in the world, covering 500,000 km^2
- spread across 200,000,000 km^2 of ocean
- Quantitative in situ surveys cover only 10s to 100s of km^2 worldwide
- *Current estimates of reef loss are based on direct observation of only 0.01–0.1% of the world's reef area*
- **Only satellite remote sensing can provide the uniform data set required for assessment of the global status of coral reefs**

Five sources of light received by a remote sensor pointed at a coral reef.

Only light reflected at the reef surface can provide information about the reef.

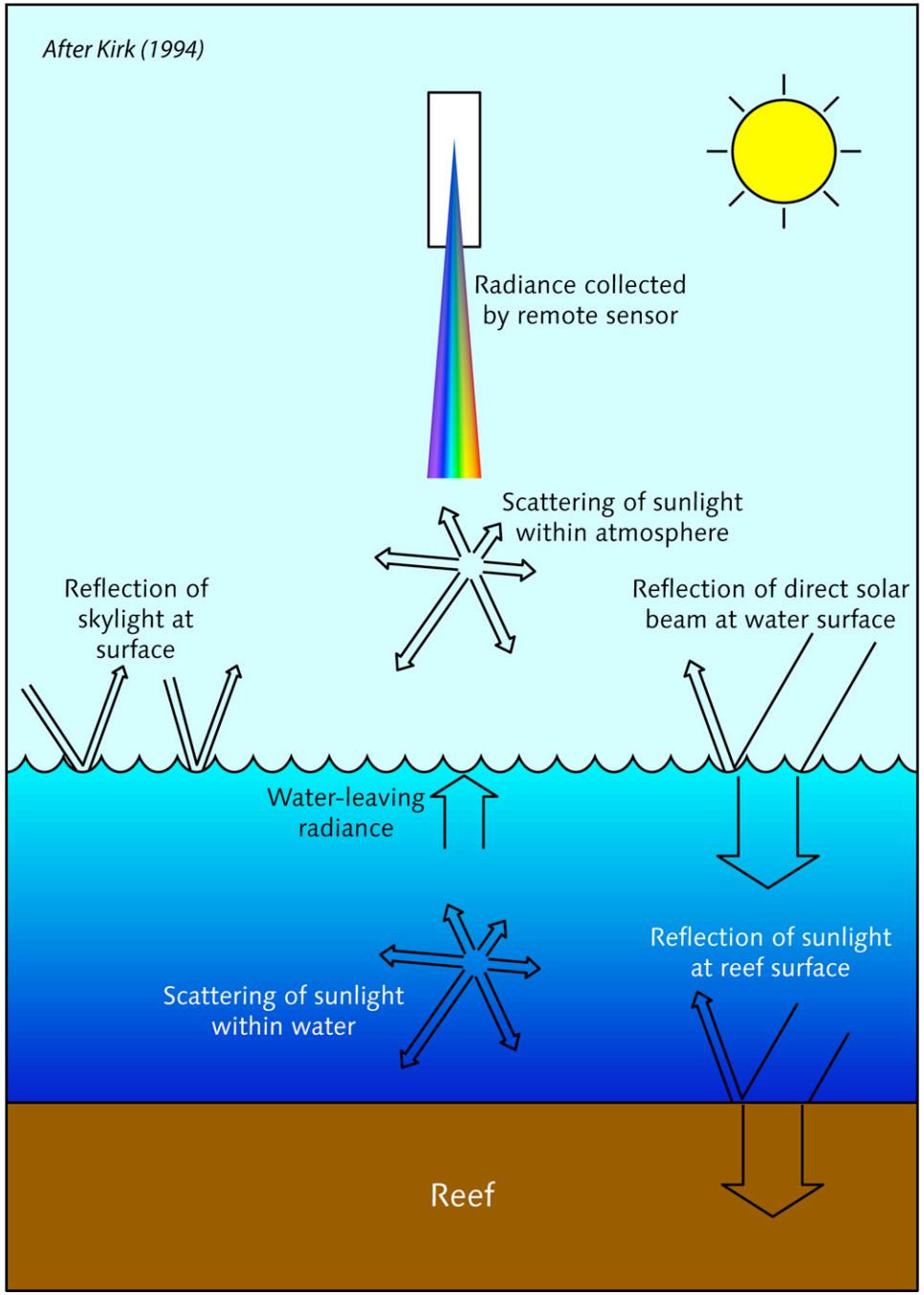

sand vs. coral+algae: sand is bright

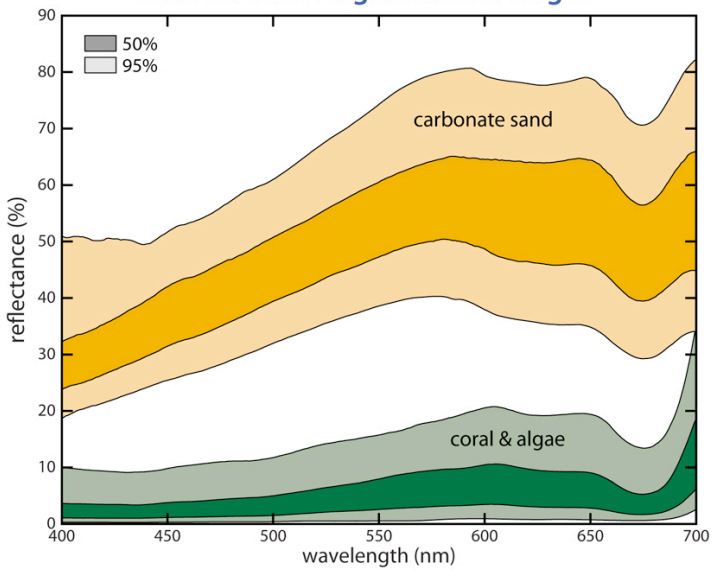

coral vs. algae: coral has peridinin

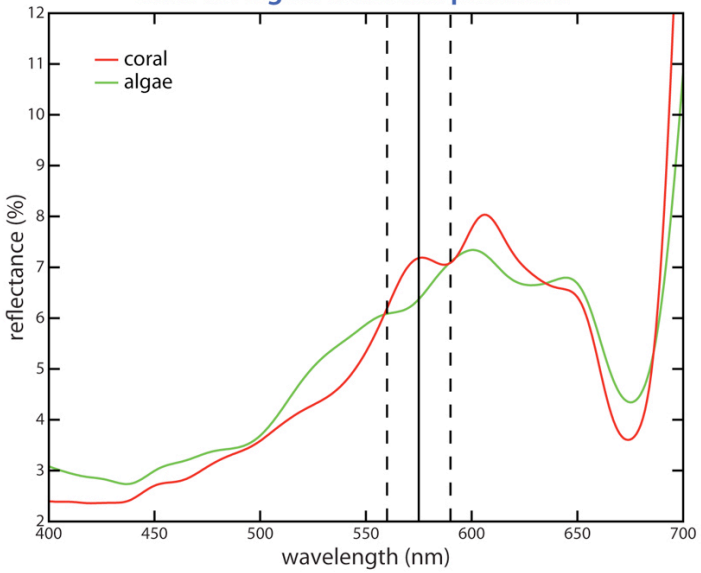

coral vs. algae: coral has peridinin

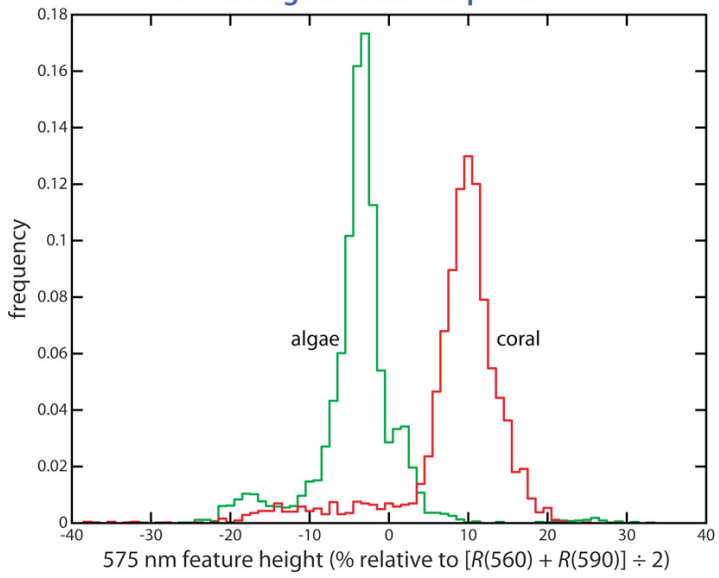

overall classification rates: very good for four wavebands

		Actual Class		
		algae	coral	sand
Predicted Class	algae	5,086 (92.5)	556 (12.4)	0 (0.0)
	coral	407 (7.4)	3,934 (87.6)	0 (0.0)
	sand	7 (0.1)	0 (0.0)	642 (100.0)

Integer values are numbers of spectra classified. Decimal values are classification rates in percent.

Hochberg & Atkinson (2003)

Table 1
Classification error matrices for in situ spectral reflectances of three coral reef classes: coral, algae, and carbonate sand

(A) Full-resolution: overall accuracy = 98%

		Actual class		
		Algae	Coral	Sand
Predicted class	Algae	2726 (99.2)	75 (3.3)	1 (0.3)
	Coral	23 (0.8)	2168 (96.6)	0 (0.0)
	Sand	0 (0.0)	1 (0.0)	320 (99.7)

(C) AVIRIS: overall accuracy = 98%

		Actual class		
		Algae	Coral	Sand
Predicted class	Algae	2725 (99.1)	74 (3.3)	1 (0.3)
	Coral	24 (0.9)	2170 (96.7)	0 (0.0)
	Sand	0 (0.0)	0 (0.0)	320 (99.7)

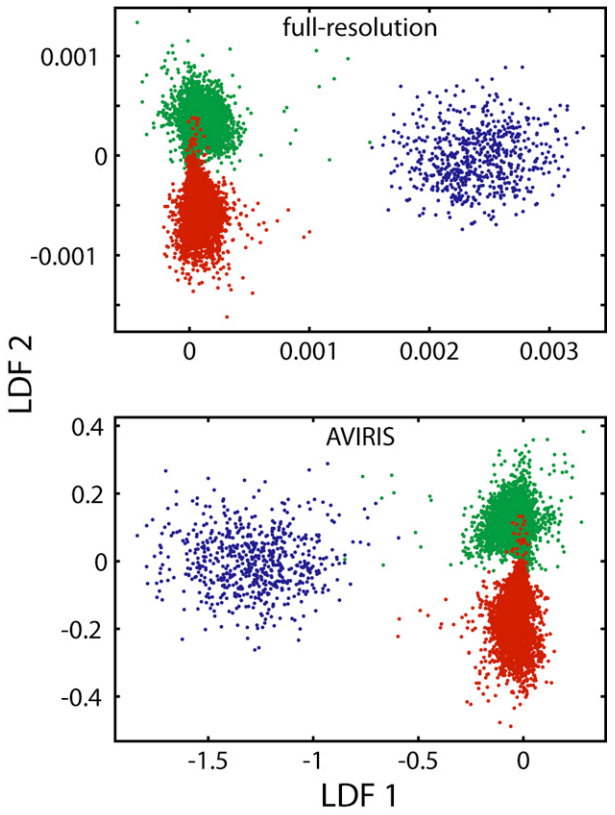

Conclusion: Contiguous, 10-nm-wide wavebands over range 400–700 nm provides excellent spectral discrimination between coral, algae, and sand

Lee & Carder (2002)

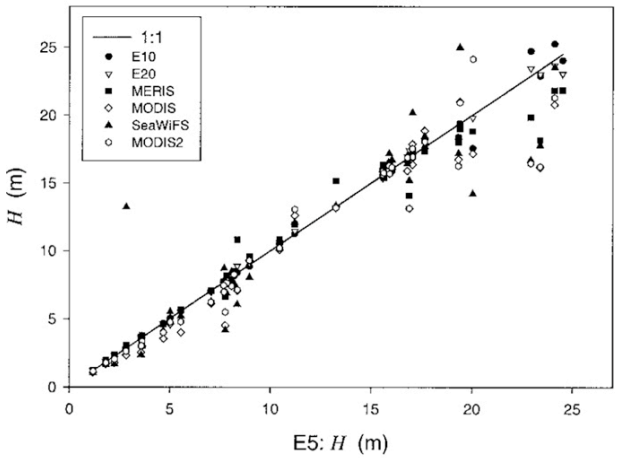

Lee et al. (2007)

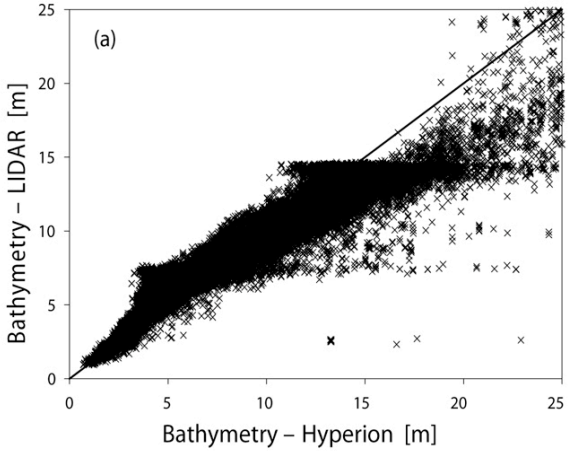

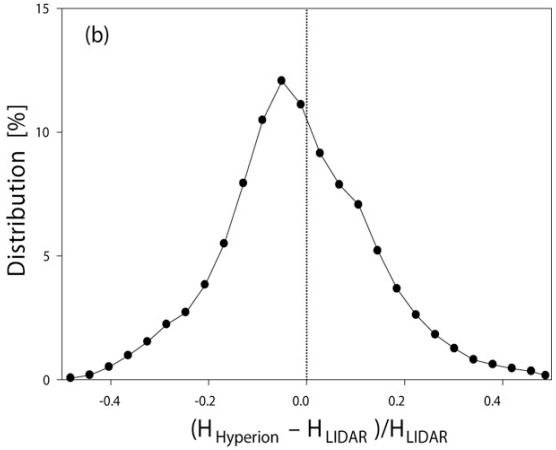

Conclusion: Contiguous, 10-nm-wide wavebands over range 400–800 nm is excellent band set for retrieval of shallow water bathymetry

Gao et al. (2007)

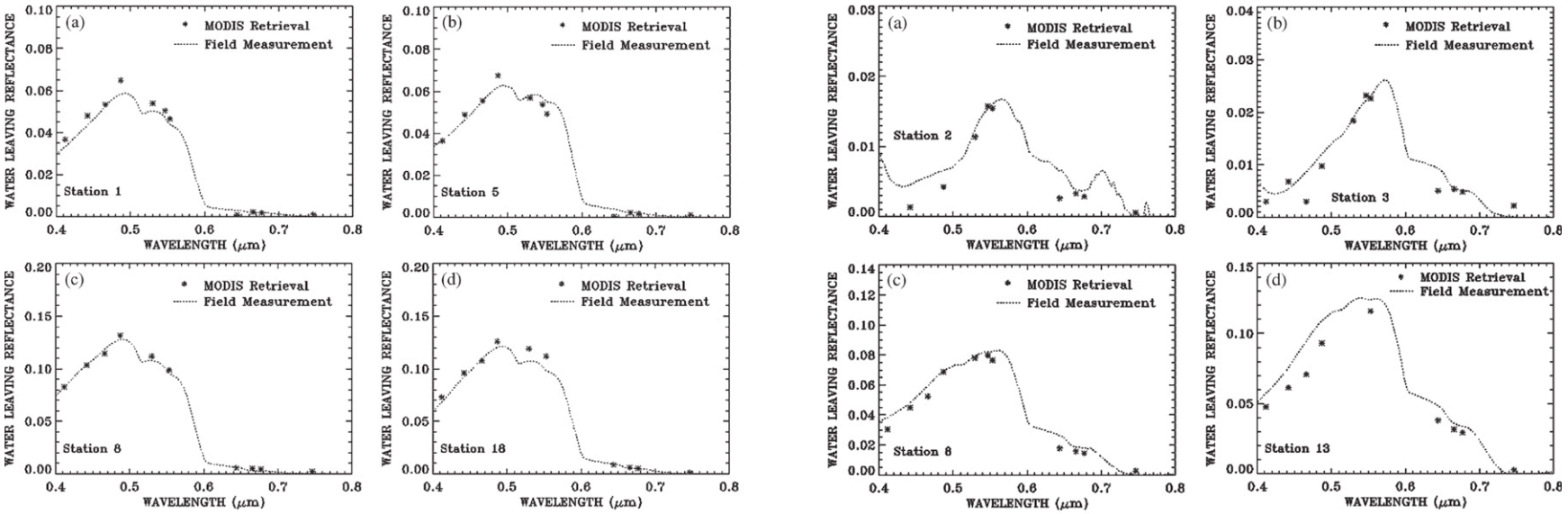

Conclusion: Combined wavebands across both NIR and SWIR (i.e., 0.865, 1.04, 1.24, 1.64, and 2.25 μm) provide very good atmospheric correction

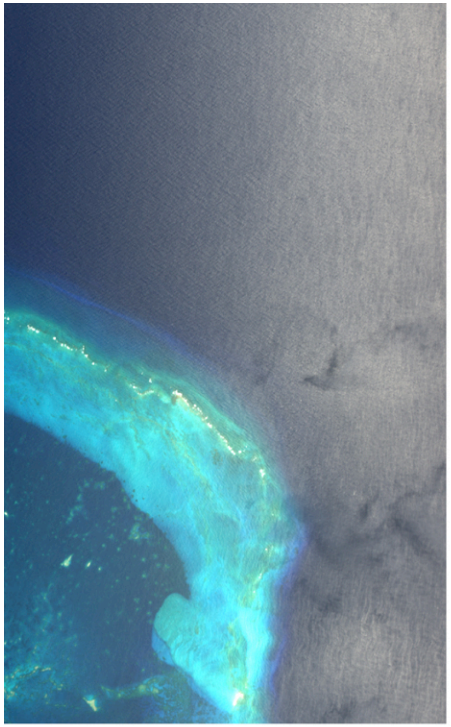

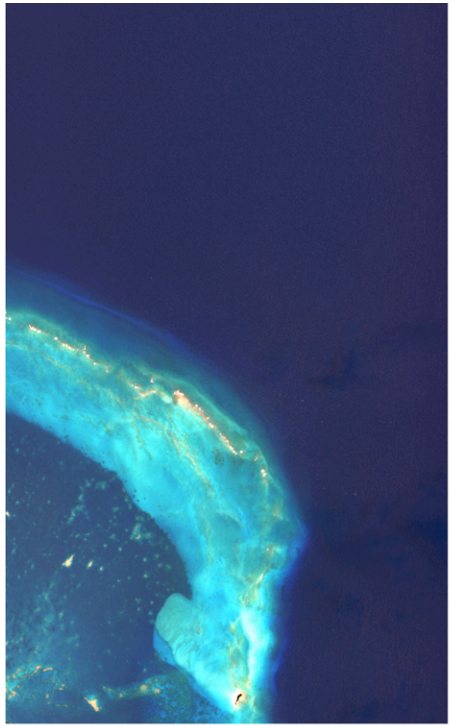

Various Workers & HyspIRI Sun Glint Subgroup

Conclusion: Glint is readily correctable, provided (1) suitable reference waveband(s) at wavelengths > 900 nm and (2) good atmospheric correction

Summarizing Waveband Requirements for a Coral Reef Satellite

- Accurate atmospheric correction is crucial to provide accurate water-leaving radiances in the VIS that are used as input to water column correction.
- Accurate water column correction is crucial to provide accurate seafloor optical properties that are used to discriminate between coral reef bottom-types.
- The most accurate atmospheric correction for shallow waters—including coral reefs requires SWIR wavebands. NIR wavebands can be used alone, but the guaranteed result is underestimates of VIS water-leaving radiance. Errors in VIS water-leaving radiance will cascade to errors in retrieval of seafloor optical properties. Errors in seafloor optical properties will result in misclassifications of coral reef bottom-types.
- The most accurate water column correction for shallow waters—including coral reefs—requires wavebands distributed across VIS wavebands. A narrower range of wavebands can be used, but the result will be less accurate retrievals of seafloor optical properties. Errors in seafloor optical properties will result in misclassifications of coral reef bottom-types.
- **Using a wavelength range 0.4-2.5 µm does not guarantee perfect classification of coral reef bottom-types, but it does guarantee the best possible results.**

Reef Remote Sensing Map Product

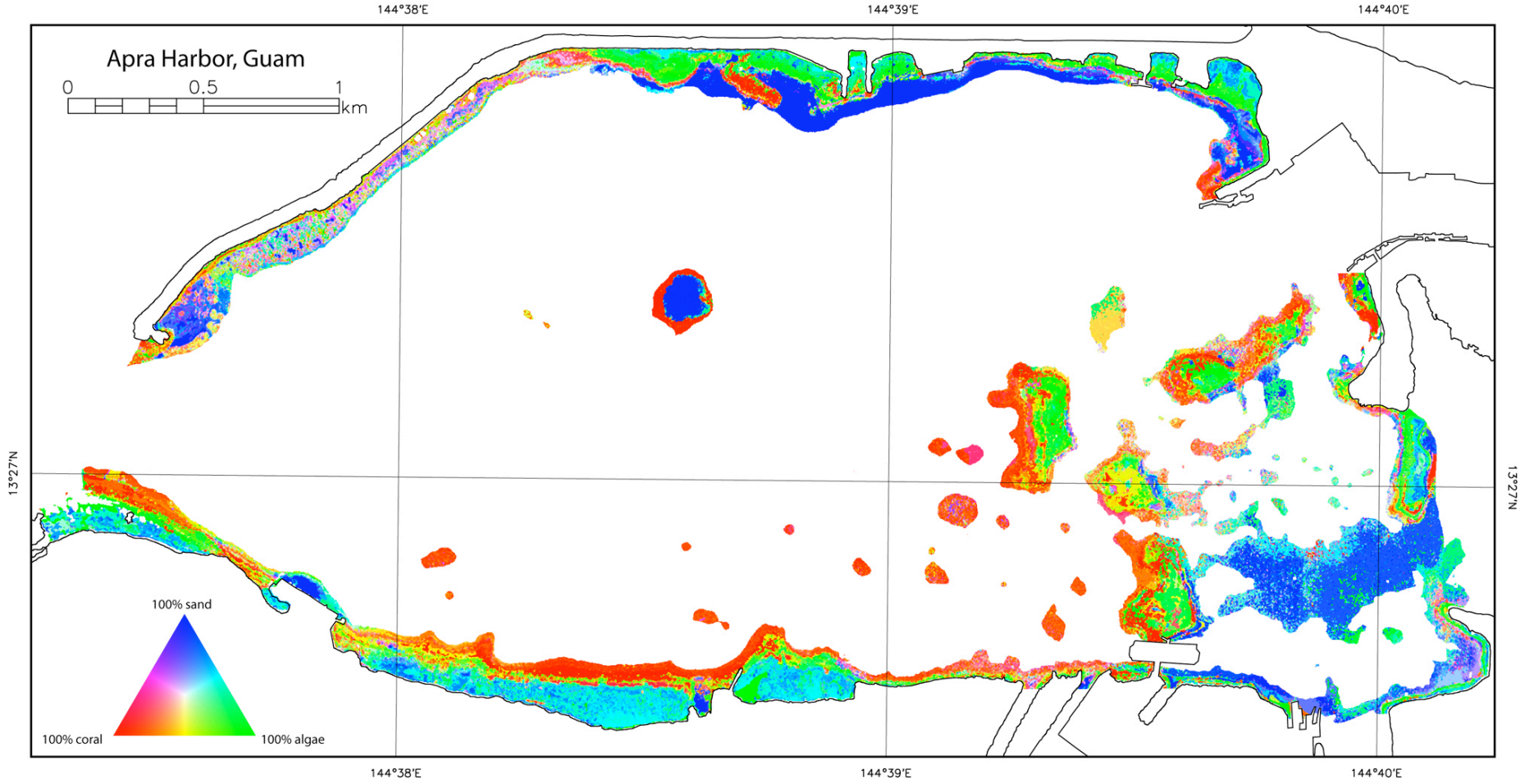

State of the Art in Coral Reef Functional Assessment: Biogeochemistry

Benthic Chamber

Flow Respirometry

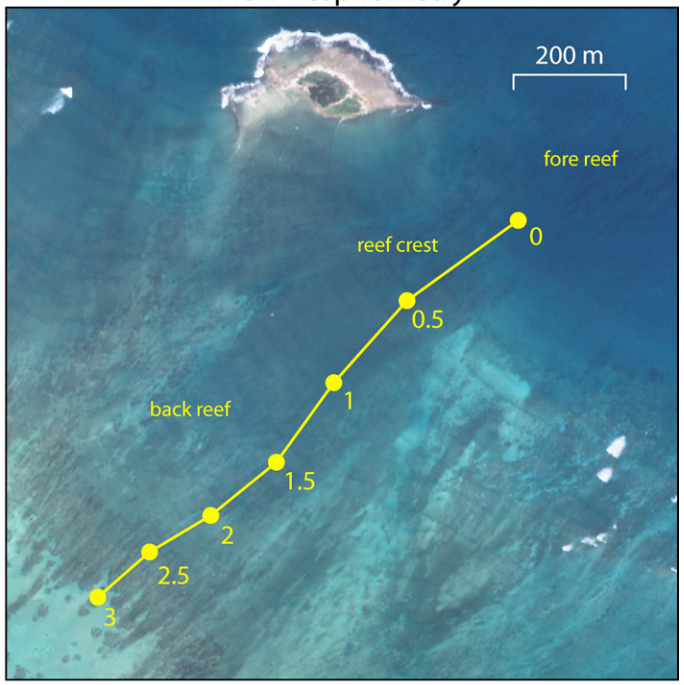

Control Volume

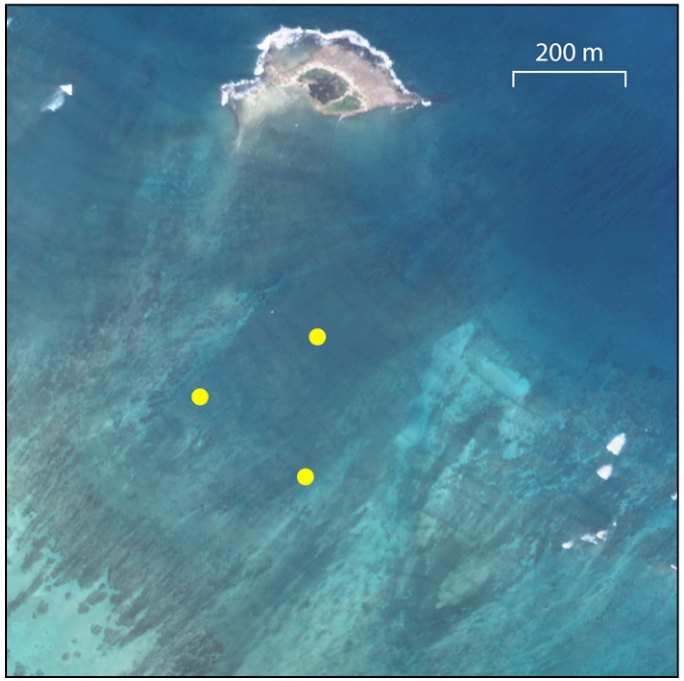

Control Volume Data

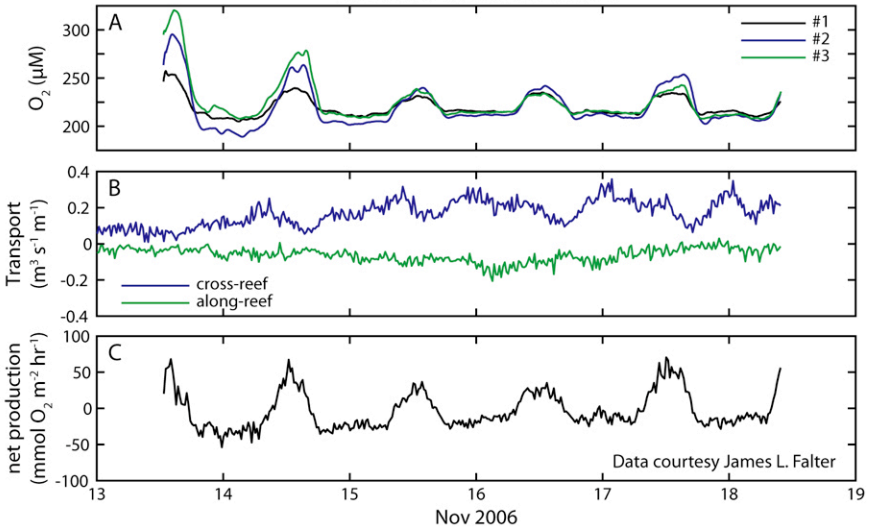

Remote Sensing of Reef Biogeochemistry

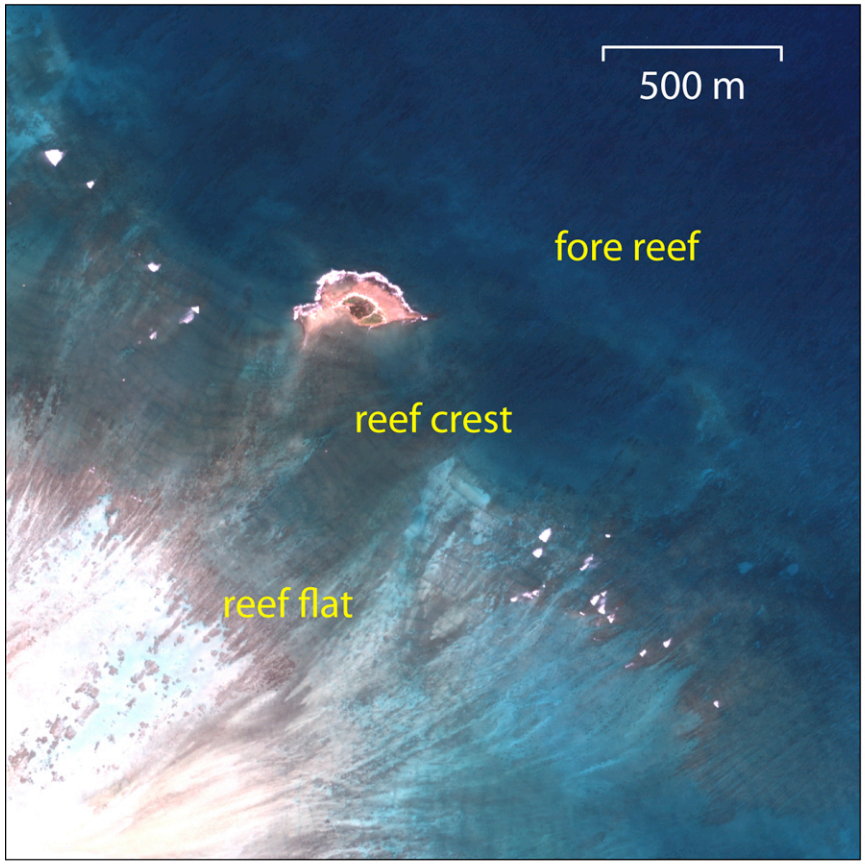

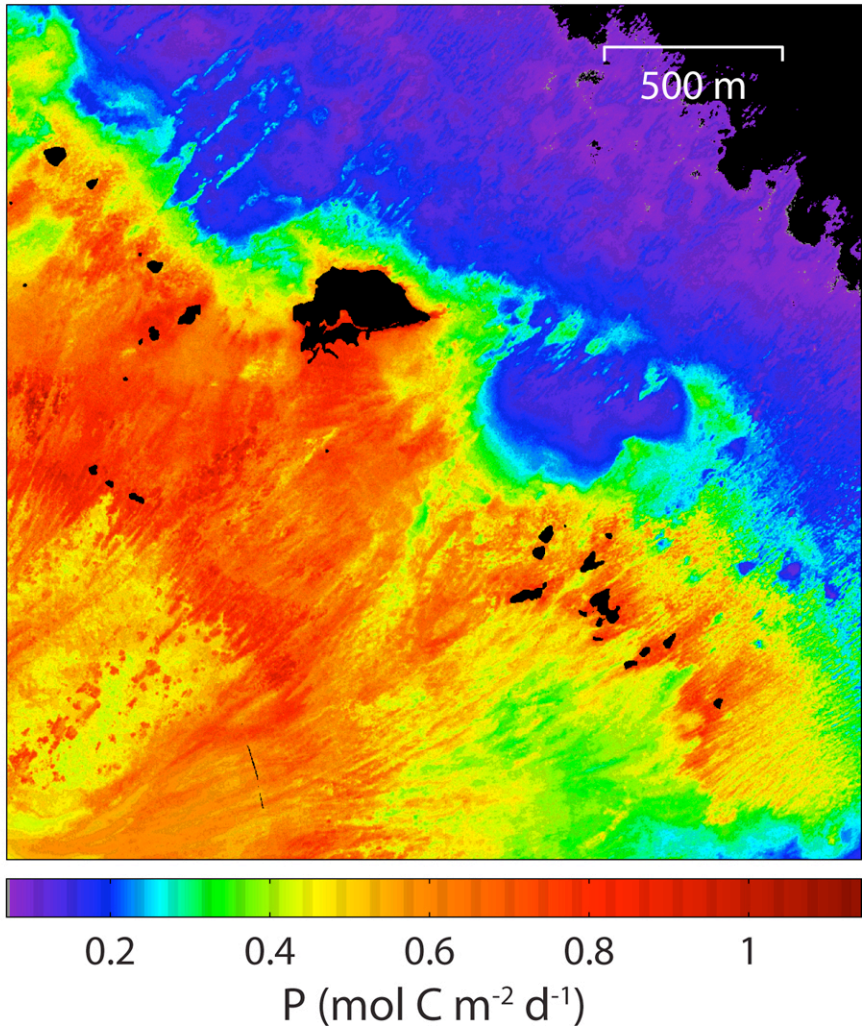

Reef Remote Sensing: Next Steps

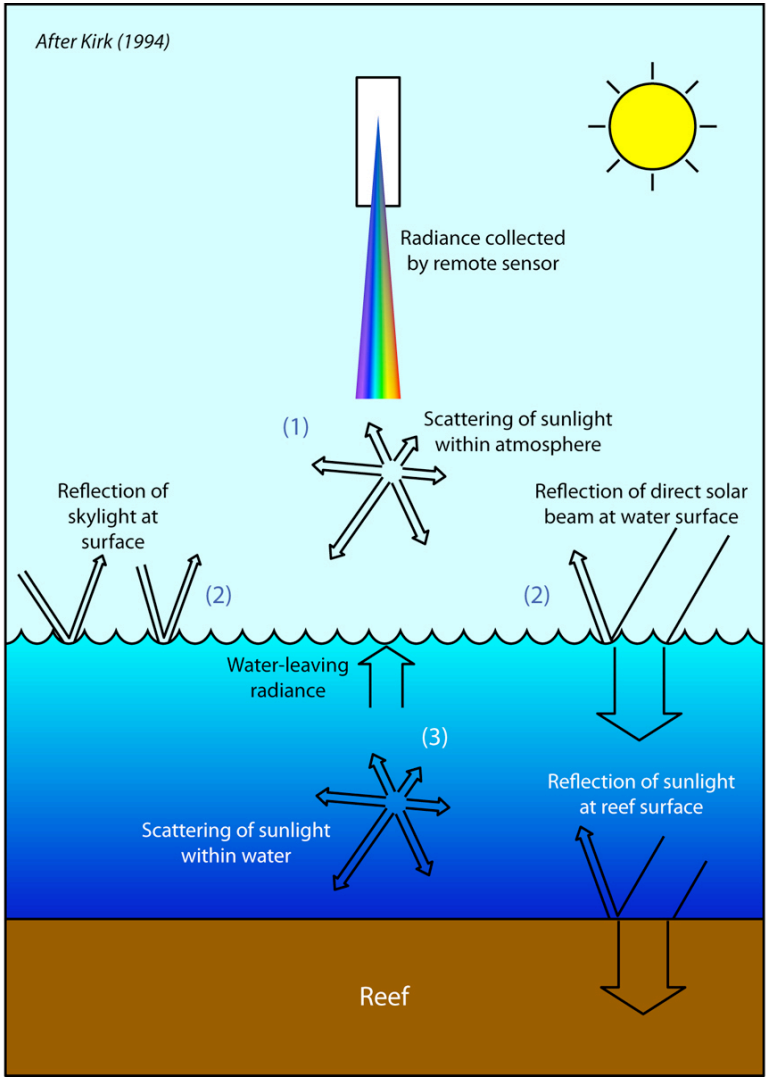

(1) Atmospheric Correction
- ATREM
- FLAASH
- Tafkaa
- Glint-Aerosol Discrimination
- ???

(2) Glint Correction
- NIR-VIS Empirical Linear Relationship
- Subtraction of NIR Reflectance
- Uniform Spectral Offset Approach
- Glint-Aerosol Discrimination

(3) Water Column Correction
- Optimization
- Look-Up Tables
- ???

(4) Successful Integration of 1 + 2 + 3
- ???

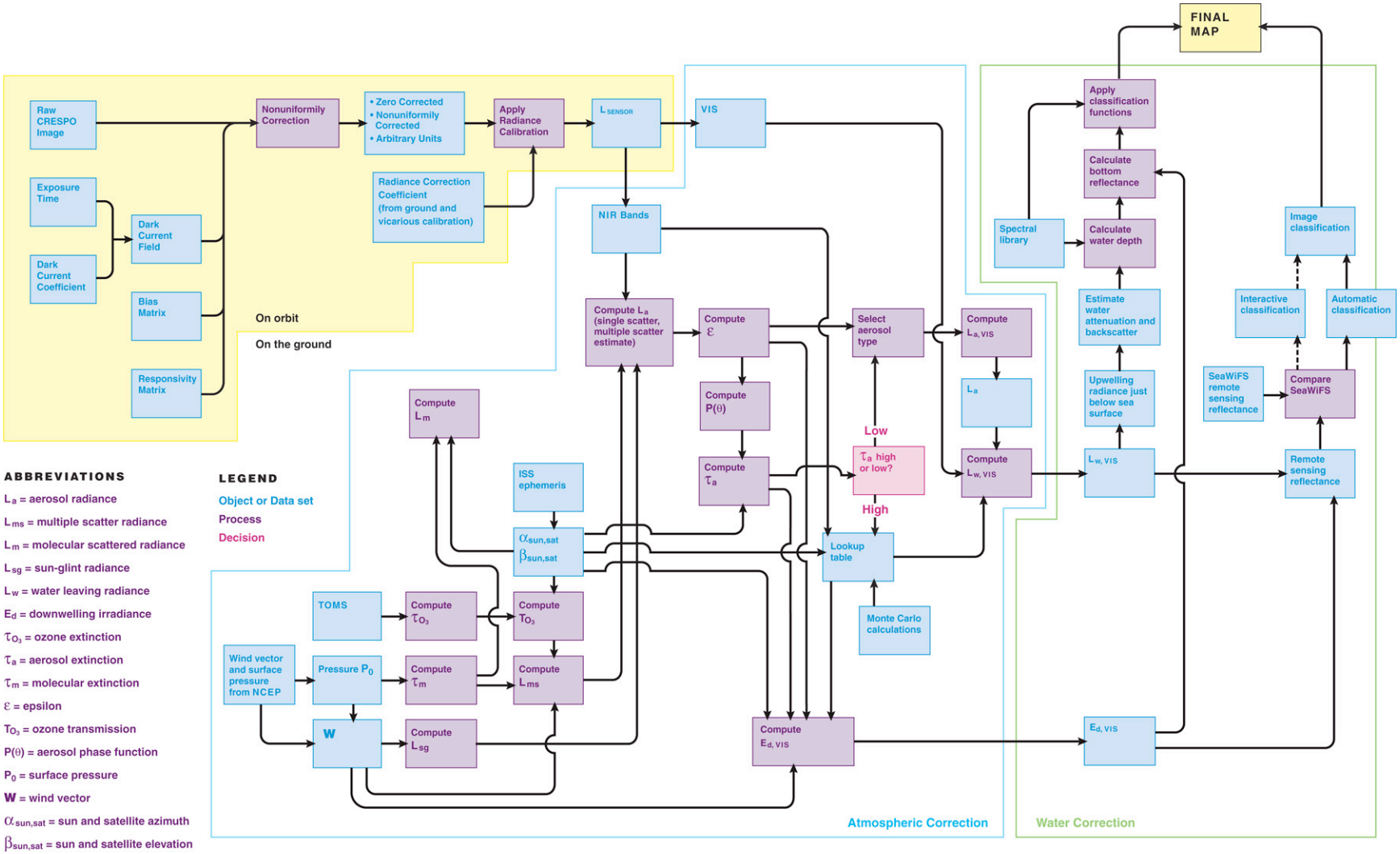

FO2-2: Algorithm Processing Flow

HyspIRI Coral Reef Science

HyspIRI data will be used to pursue the following objectives:

- Measure distributions of coral, algae and sand for ≥25% of reefs worldwide. This will be an unprecedented survey of the current status of coral reefs, and the results will serve as a baseline for future change detection.
- Examine trends of coral, algae and sand for pristine reefs versus human-impacted reefs. This comparison of reefs will enable scientists to identify a set of conditions that define a "healthy" reef (no such definition exists).
- Determine how distributions of coral, algae and sand vary with reef morphology, underlying geology, latitude, and oceanographic conditions of wind, waves, and nutrients. To understand reef health, it is important to understand how environmental factors influence the amounts of coral, algae and sand that are present.
- Generate map products to help regional and local monitoring and scientific investigation. Such maps can be used to identify sites that are crucial for conservation, as well as sites that require more intensive study to understand the ecosystem.
- Provide ancillary data for management and science. Several secondary products will be of great use for monitoring and investigating hydrodynamics and biogeochemistry of reef systems.

Coral Reef Satellite Mission Success Criteria

Minimum Success

Maps showing the distributions of coral, algae and sand for 10% of the world's reefs over the course of a single year

Targeted Success

Maps and secondary products for 25% of the world's reefs over a two-year period

Ideal Success

Maps and secondary products for 50% of the world's reefs over a two-year period

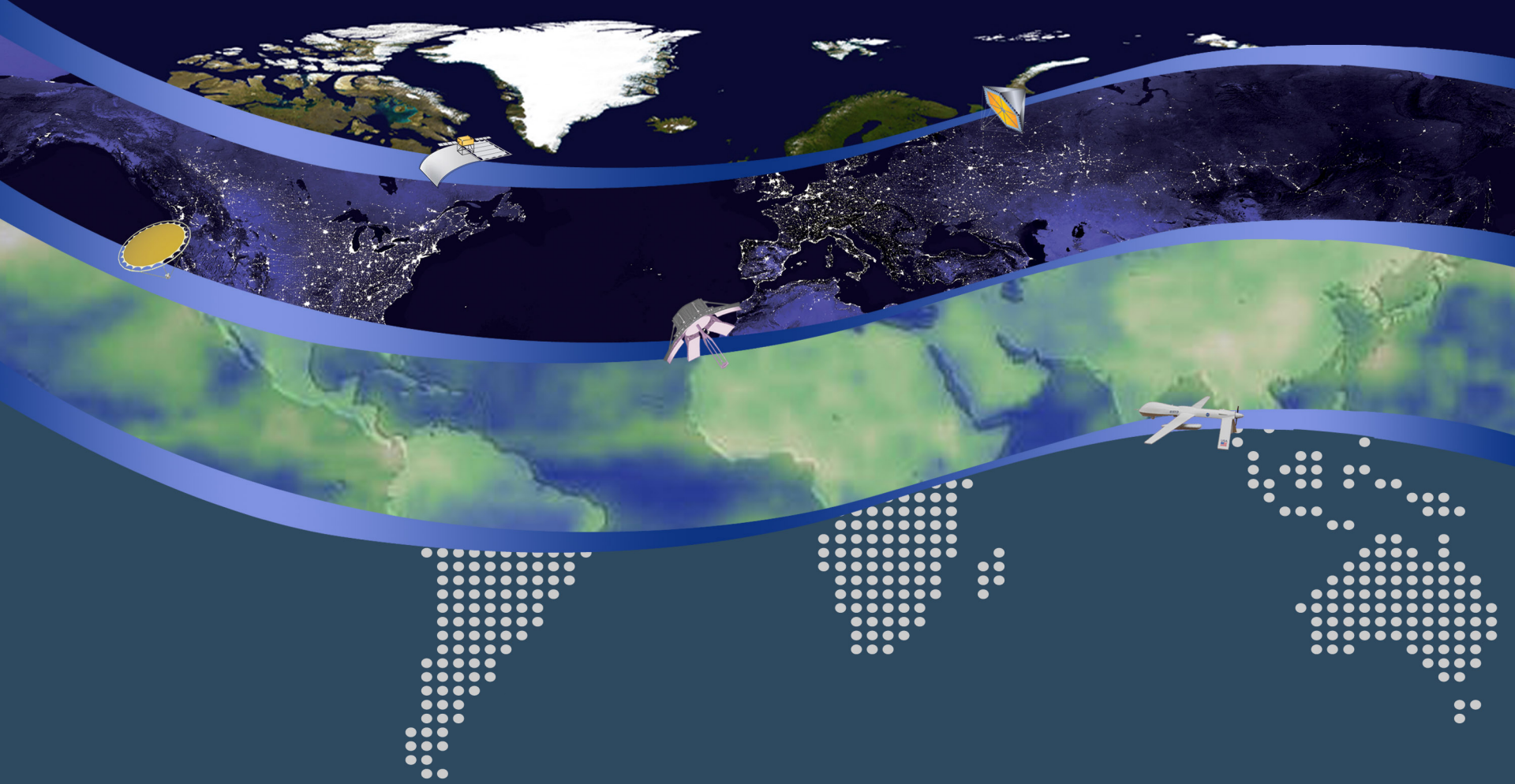

Spaceborne Flight Validation of NASA ESTO Technologies: HyspIRI IPM

August, 2011

Dr. Charles D. Norton

NASA Earth Science Technology Office and

Jet Propulsion Laboratory, California Institute of Technology

© 2011 California Institute of Technology. Government sponsorship acknowledged.

Earth Science Technology:
Overview and Program Elements

The Earth Science Technology Office (ESTO) is a ***targeted, science-driven, competed, actively managed, and dynamically communicated technology program*** and serves as a model for technology development.

Competitive, peer-reviewed proposals enable selection of best-of-class technology investments that ***retire risk*** before major dollars are invested: a cost-effective approach to technology development and validation.

ESTO investment elements include:

Observation Technologies:

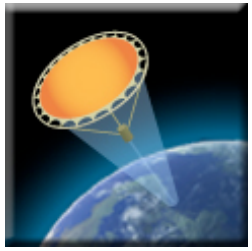

Instrument Incubator Program (IIP)
provides robust new instruments and measurement techniques

Advanced Component Technologies (ACT)
provides development of critical component and subsystem technologies for instruments and platforms

Information Technologies:

Advanced Information Systems Technology (AIST)
provides innovative on-orbit and ground capabilities for communication, processing, and management of remotely sensed data and the efficient generation of data products and knowledge

Earth Science Technology:
New Investments Enabling the Decadal Survey

Upon publication of the Earth Science Decadal Survey in 2007, ESTO investments **already supported all 18 of the recommended mission concepts**. Since then, ESTO has awarded **73** additional technology projects representing an investment of ***over $172M directly related to the Earth Science priorities outlined by the Decadal Survey.***

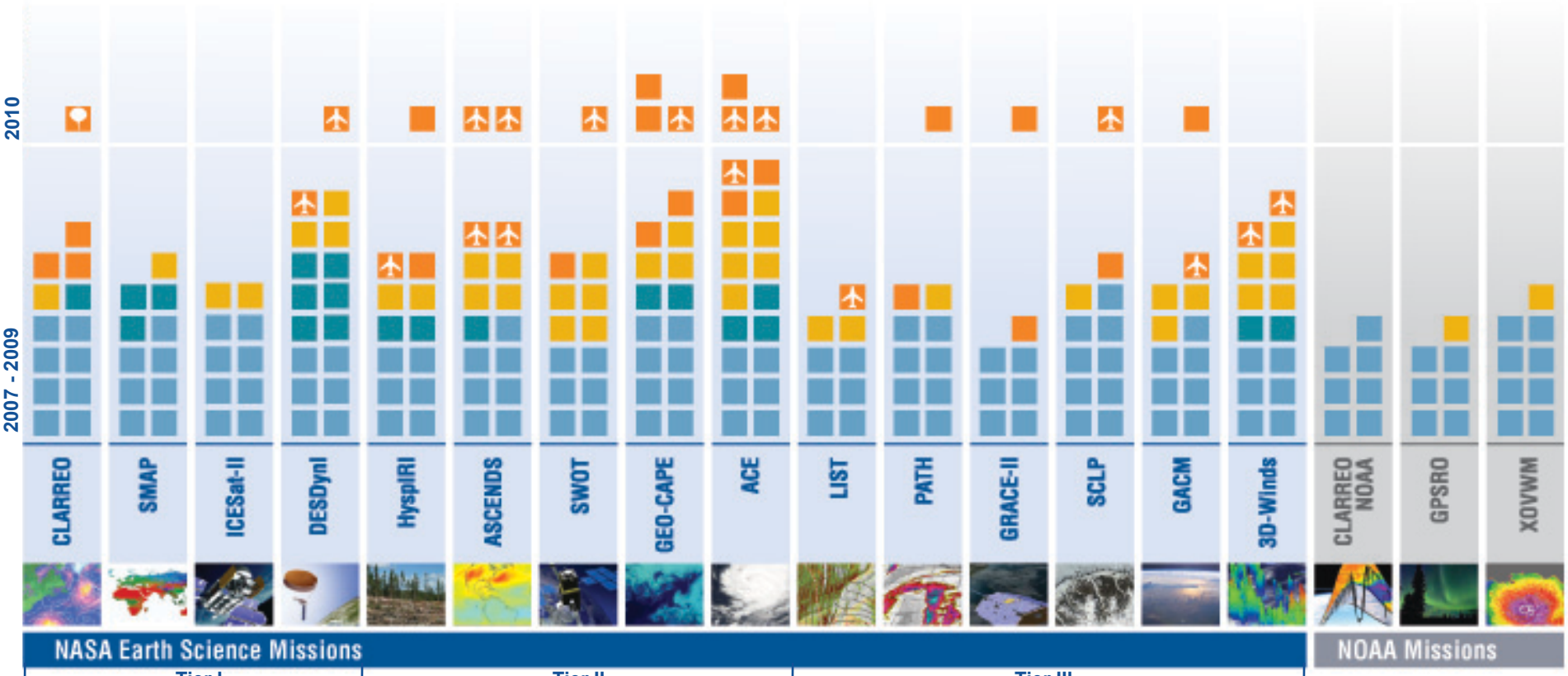

Pre-decisional – for Planning and Discussion Purposes Only

Earth Science Technology:
Incremental TRL Advancement Strategy

Current ESTO program lines generally advance technologies to TRL-6: System/ subsystem prototype demonstration in the relevant environment (ground or space)

ESTO now seeks to develop a new program line to **flight qualify** technologies through successful spaceborne demonstrations to TRL-8/9

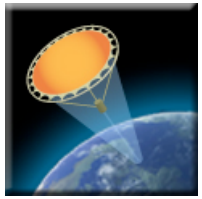

Concept Formulation — Component Demo (Relevant Environment)

Advanced Component Technology (ACT)
TRL 2 - 5

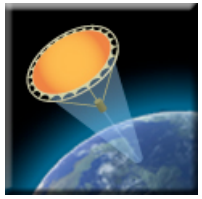

Characteristic Proof of Concept — (Sub)-System Prototype Demo (Operational Environment)

Instrument Incubator Program (IIP)
TRL 3 - 6

Concept Formulation — System Prototype Demo (Operational Environment)

Advanced Information Systems Technology (AIST)
TRL 2 - 7

Component Demo (Lab Environment) — Flight Qualified

Technology Flight Validation (ATI)
TRL 4 – 8/9

TRLs defined by NASA Procedural Requirements 7120.8 (Exp. Feb., 2013)

Technology Space Flight Validation

- Non-validated technology is generally acknowledged as a primary cause of NASA and DoD mission delays and cost overruns. For SMD, instrument development problems occur in > 60% of all missions, leading to cost and schedule delays.
- We propose a nimble, competitive program which takes advantage of recent advances in alternative opportunities to access space to retire risk and validate technologies. (*No requirement for science data campaign).*
- ESTO was requested to put some "skin in the game" to demonstrate this capability.

Onboard Processing – Two orders of magnitude data reduction for the Multiangle Spectro-Polarimetric Imager (MSPI)

Realtime Onboard Processing for MSPI (AIST)

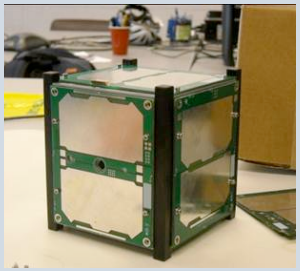

CubeSat Flight Validation (U Michigan/JPL) MRR 6/11

Launch on NPP

Phase Change Temperature Calibration - Black Body Calibration to 0.01K for Radiance Measurements

Phase Change Cells from Utah State and Wisconsin (IIP)

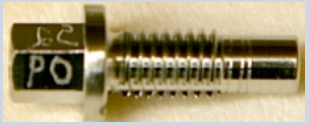

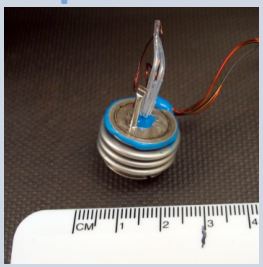

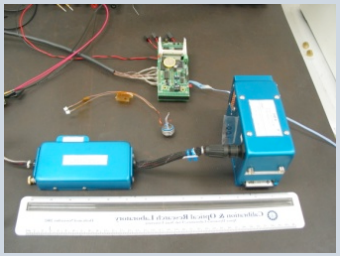

Flight Housing with Utah State Cell

Launch to ISS in 2011 & 2012

Flight Validation Drivers

Increased number of flight opportunities for secondary payloads

- NASA Launch Services' CubeSat Launch Initiative (CLI) Program also known as Educational Launch of Nano-Satellites (ELaNa)
- DOD Space Evaluation Research Board (SERB)
- US Government Rideshare Working Group (USGRWG)

Cost effectiveness of CubeSat platforms

- 18-24 months from concept formulation to deployment
- Approximately $1M including launch and basic operations

Rapid TRL advancement and risk reduction

- Meaningful risk reduction for hardware components and information systems developed for future flight instruments
- Demonstrated success stories across industry and educational institutions with substantial future growth

Emergence of industry standards

- 1U and 3U bus designs
- Orbital deployment mechanisms (P-POD) and others

ULA Delta II

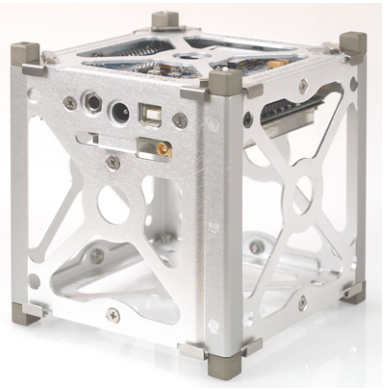

CubeSat Kit (Pumpkin Inc.)

1U: 10 cm x 10 cm x 10 cm

ESTO Technology Space Flight Validation

Partnering to flight qualify technologies through successful spaceborne demonstrations

- MCubed/COVE – Paula Pingree
  - CubeSat spaceborne validation of ACE/MSPI instrument signal processing algorithm on new Xilinx Rad-hard by design FPGA reducing data downlink by 2-orders of magnitude per camera
  - Partners: JPL, U. Michigan, Xilinx

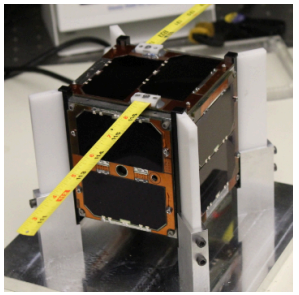

- IPEX – Steve Chien
  - CubeSat spaceborne validation of Intelligent Payload Module (IPM) capability providing a 20-times reduction in data volume for low-latency urgent production generation planned for HyspIRI
  - Partners: JPL, GSFC, Cal Poly San Luis Obispo

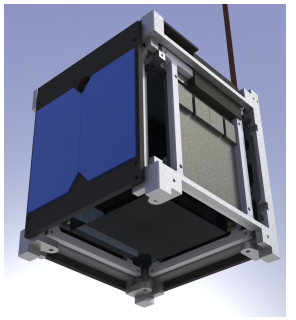

- GRIFEX – David Rider
  - CubeSat spaceborne validation of state-of-the-art ROIC/FPA assessing functionality and data integrity for high frame rate imaging planned for GEO-CAPE
  - Partners: JPL, U. Michigan

- First Launch with NPOESS Preparatory Project
  - MCubed/COVE: Secondary payload on NPP (VAFB on Oct 25, 2011)
  - IPEX: Awaiting ELaNa manifest (2012/2013)
  - GRIFEX: TBD (2013?)

ESTO CubeSat Flight Validation for Multiangle Spectropolarimetric Imager (MSPI) Processing for ACE

David Diner, Paula Pingree et al., JPL

MSPI Ground-based measurements

470, 660, 865 nm Intensity

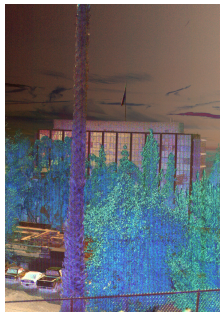

470, 660, 865 nm DOLP

MSPI Airborne engineering flight testing

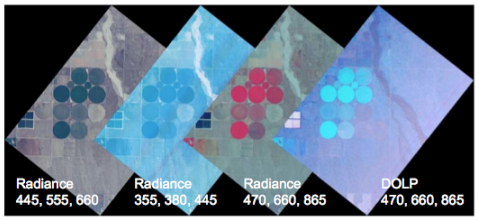

MSPI algorithms/FPGA on CubeSat operating in space environment

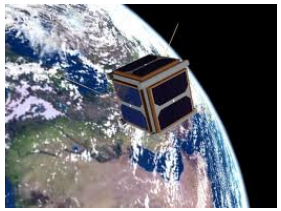

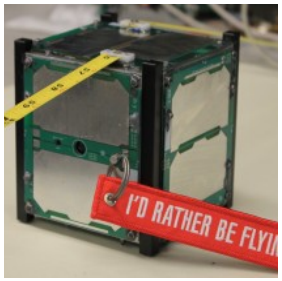

Multiangle polarimetric spectroscopy

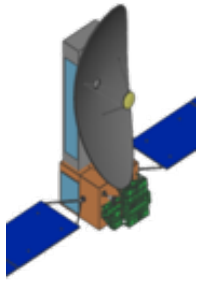

MSPI on ACE

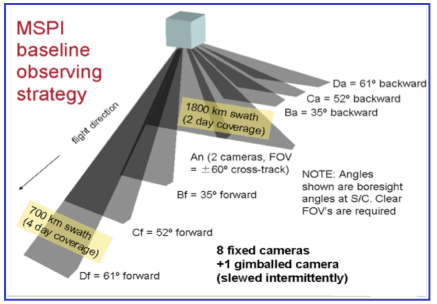

2011 Flight Validated MSPI instrument processor and algorithms

On-board instrument processing enables downlink by reducing data rate by 2-orders of magnitude in real time with no science data lost

IIP-07 and AIST-08 Ground Testbed Development and Demonstration

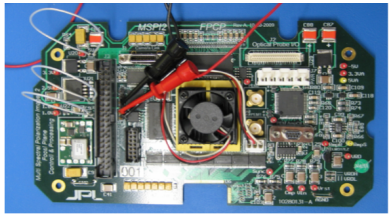

AIST-08 AirMSPI board with algorithms on Xilinx Virtex-5 FPGA

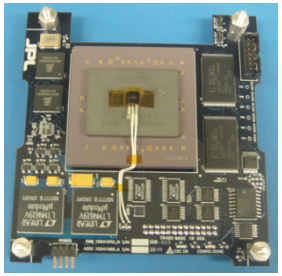

ATI-10 COVE CubeSat board with algorithms on Xilinx SIRF FPGA

XILINX

UNIVERSITY OF MICHIGAN

IPEX: Intelligent Payload Flight Experiment
PI: Steve Chien, JPL

Objective

- Demonstrate hybrid onboard and ground capability (Intelligent Payload Module) for HyspIRI to deliver high value low-latency products via Direct Broadcast with at least 20x reduction in Gbps instrument raw data rate.
  - Spaceborne technology validation of the SpaceCube Mini hardware onboard computing platform.
  - Demonstrate web-based autonomous payload operations with event/overflight-based onboard product generation.
- Enhance NASA/University partnerships by engaging students and faculty in small satellite mission operations.

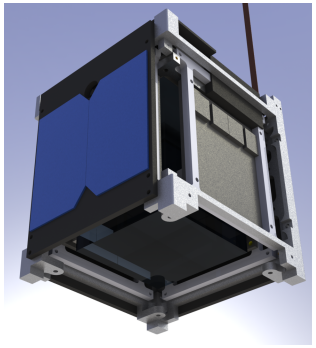

1U IPEX CubeSat carries:
- 2 Imaging cameras
- SpaceCube mini onboard processor
- IPM autonomy software

Candidate HyspIRI Low-latency Product

'09 Station Fire Burn Scar Severity Product (EO-1)

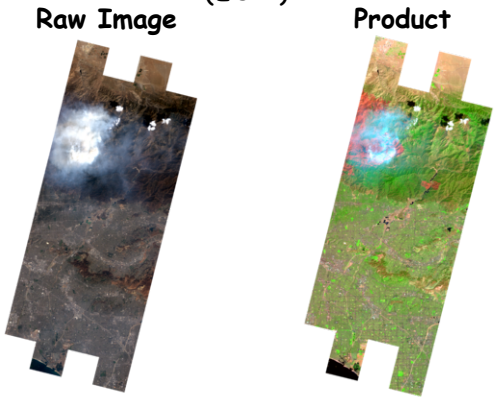

20x reduction via prioritization/compression

Approach

- Integrate SpaceCube Mini, high data rate camera, and autonomy algorithms into a 1U Cubesat as the onboard processing payload.
- Manifest CubeSat flight on a NASA, or other, launch vehicle.
- Downlink on-board derived and raw data for verification against ground tests.
- Validate onboard processing reliability and error rate on orbit.

Co-Is/Partners:

T. Flatley, GSFC, J. Puig-Suari, J. Bellardo, Cal Poly SLO

Key Milestones

• Hold preliminary design review; confirm CubeSat provider	06/11
• Hold critical design review	10/11
• Complete hardware subsystems; flight software operational on testbed	12/11
• Complete assembly and integration	03/12
• Complete integrated test; Flight readiness review	05/12
• First opportunity launch date (pending manifest)	06/12
• Nominal operations complete (pending launch)	12/12

$TRL_{in} = 4$ $TRL_{current} = 4$

ESTO Earth Science Technology Office

ESTO CubeSat Technology Validation of Intelligent Payload Modul for HyspIRI (IPEX)

Intelligent Payload Module (IPM) for HyspIRI Decadal Survey Mission

- Provides low-latency Direct Broadcast mechanism for urgent products
- Visible to Shortwave Infrared Hyperspectral Spectrometer (VSWIR) and Thermal Infrared Imager (TIR) acquire 5 Tb/day of data
- IPM will provide 20x reduction in data volume for low-latency products

SpaceCube 1.5

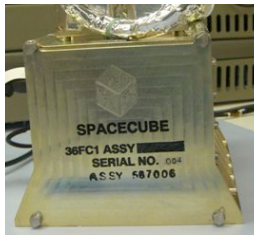

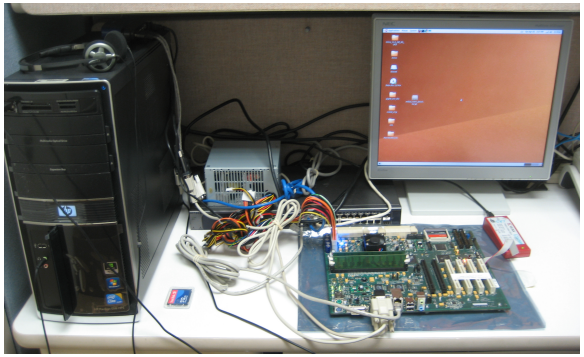

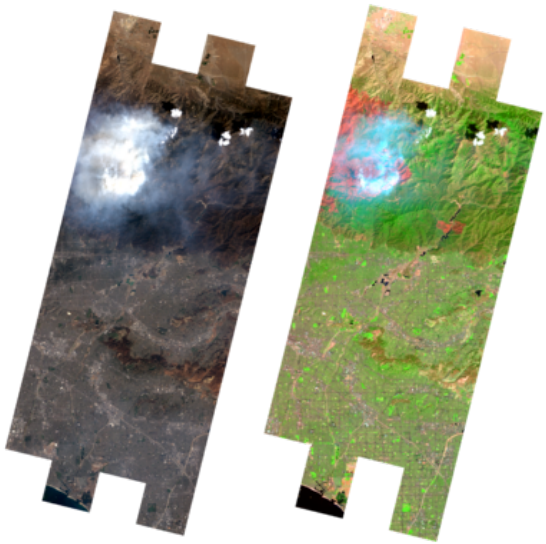

Burn Scar Severity Product (EO-1 ALI)
2009 Station Fire
Candidate HyspIRI Low-latency Product

SpaceCube Mini

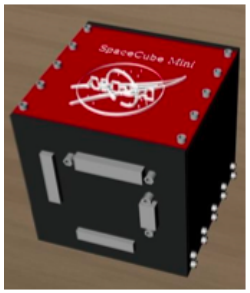

Spacecube Mini used for instrument data processing for Direct Broadcast downlink

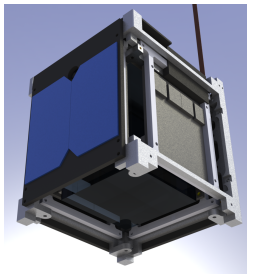

Ground Test

Development board with autonomous processing in laboratory environment

Spaceborne Validation

IPEX CubeSat will verify on-board product selection for the HyspIRI mission

IPEX System Design

Onboard Processing

- Process images on ATMEL and SC Mini 2
- Compare products
- For some very small percentage, downlink products and raw data to verify (planned, or anomalies in compared results)
- For vast majority of products, downlink status of comparison (e.g. all checked out, same results)

OBP Candidate Algorithms

- Normalized Difference Vegetation Index
- Normalized Burn Ratio
- Brightness Temperature
- Support Vector Machine Classification Algorithms
- Others in evaluation

Autonomous Ground/Space Operations

- ASPEN (ground): Creates baseline schedule producing observations and processing activities
- CASPER (flight): Creates on-board science schedule based on previous observations

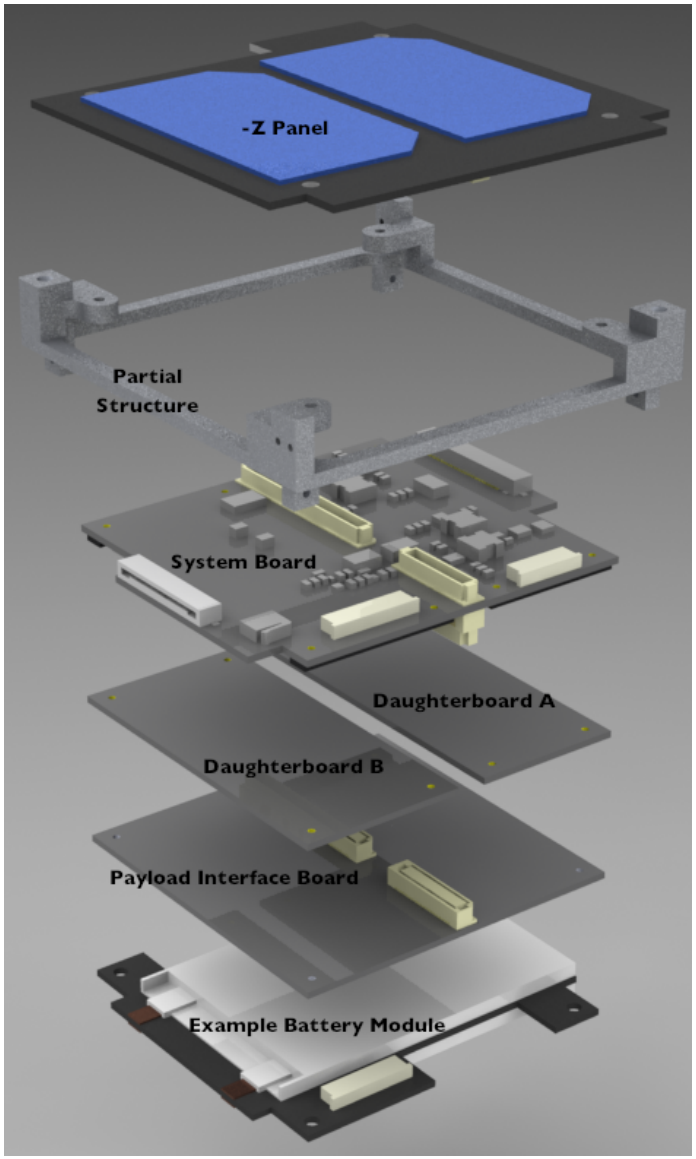

Engineering Model Design

Path-to-Flight Challenges

Spacecraft and Payload Design and Testing

- Parts acquisition and fabrication
- Safety and Mission Assurance signed agreements
- ITAR / Export Control for specific parts and CubeSat spacecraft
- Testing and “safe-to-mate” procedures

Documentation

- Interface Control Documents (ICDs)
- FCC licensing
- End-of-Life (EOL) de-orbit plan
- NOAA licensing for Earth observing missions

NASA Launch Services Requirements

- CubeSat Interface Review (CIR)
- Launch Services Program Standard Material List
- Orbital Debris Assessment Report (ODAR)
- CubeSat Transmitter Characteristics Survey
- ELaNa Requirements Verification Documentation

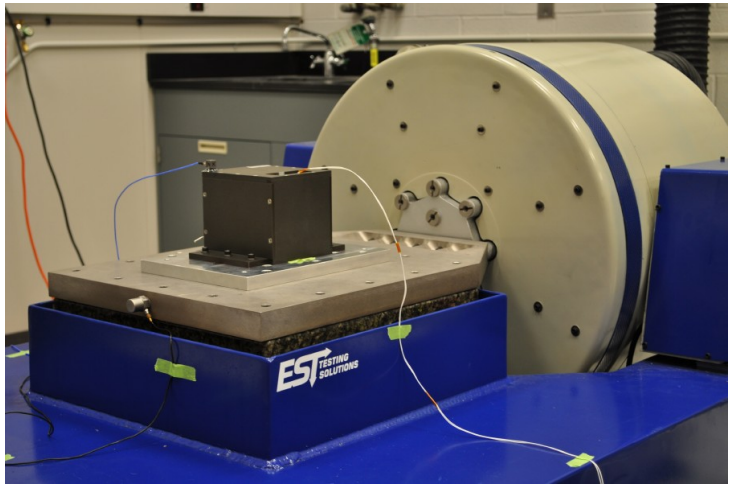

Mcubed/COVE mounted for vibration test

Qualification random vibe: (23.68 G’s for 104s)

Protoflight random vibe: (16.74 G’s for 180s)

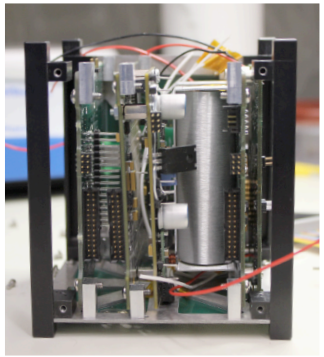

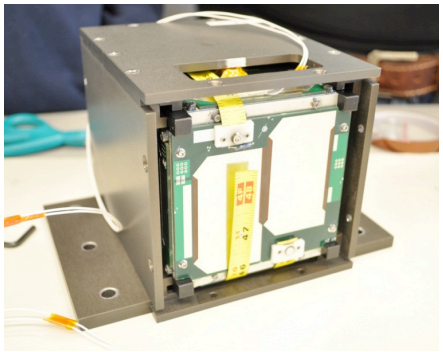

Contact Information

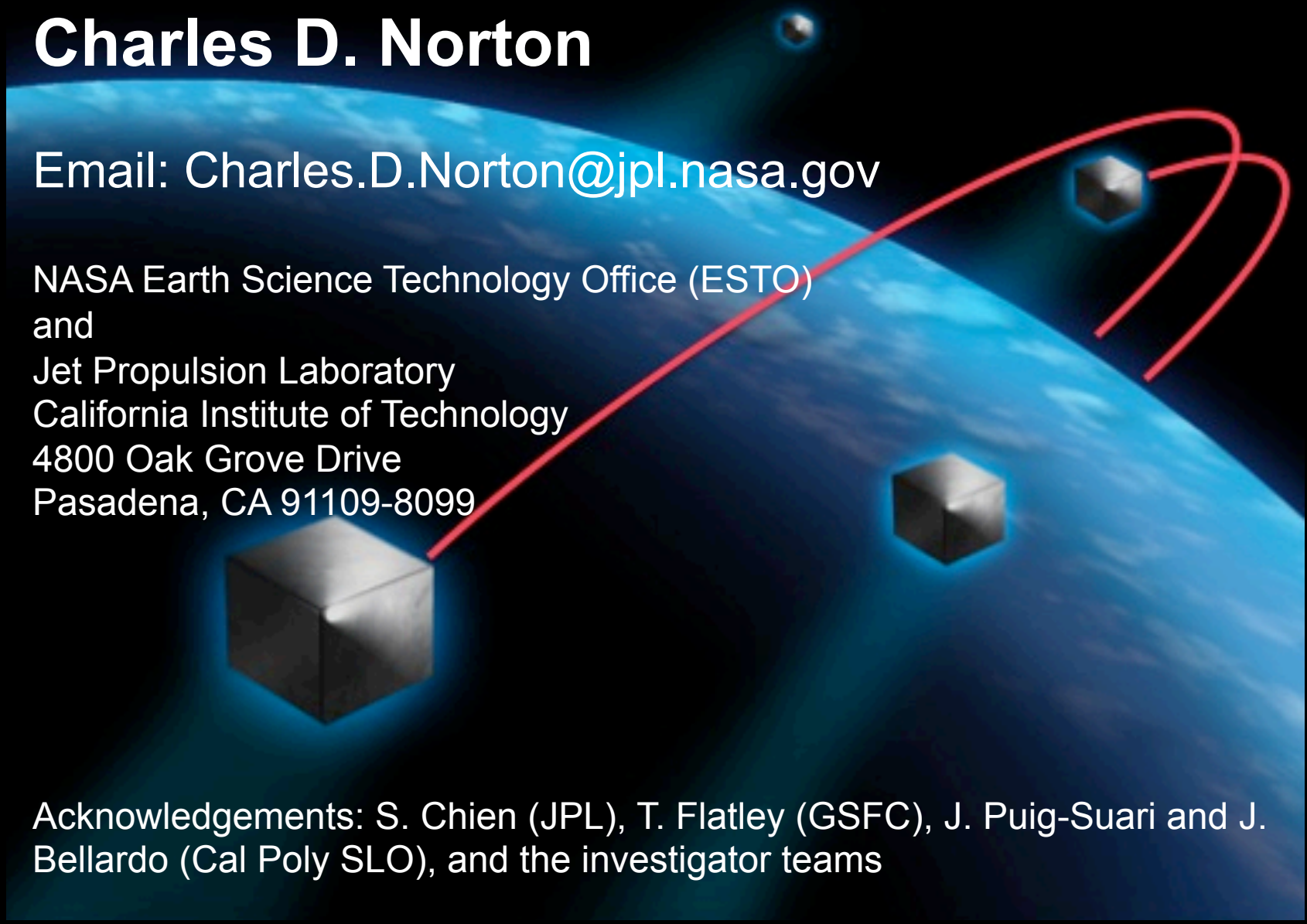

Charles D. Norton

Email: Charles.D.Norton@jpl.nasa.gov

NASA Earth Science Technology Office (ESTO)
and
Jet Propulsion Laboratory
California Institute of Technology
4800 Oak Grove Drive
Pasadena, CA 91109-8099

Acknowledgements: S. Chien (JPL), T. Flatley (GSFC), J. Puig-Suari and J. Bellardo (Cal Poly SLO), and the investigator teams

Baseline vs Minimum (Threshold)

Baseline	Minimum (Threshold)
380 to 2500 nm at ≤10 nm sampling at the specified signal-to-noise ratio and accuracy with >95% spectral/spatial uniformity at ≤60 m nadir spatial sampling with <20 day revisit to provide	380 to 2500 nm at ≤10 nm sampling at >80% of the specified signal-to-noise ratio and accuracy with >90% spectral/spatial uniformity at ≤60 m nadir spatial sampling with <20 day revisit to provide
>60% seasonal and >80% annual coverage of the terrestrial and shallow water regions of the Earth	> 50% seasonal and >70% annual coverage of the terrestrial and shallow water regions of the Earth
three years with a subset of measurements available near-real-time for designated science and applications.	two years.
8 spectral bands from the 3-5 micron and 8-12 micron regions of the spectrum at the specified noise-equivalent-delta-temperature and accuracy at ≤60 m nadir spatial sampling	8 spectral bands from the 3-5 micron and 8-12 micron regions of the spectrum at >80% the specified noise-equivalent-delta-temperature and accuracy at ≤60 m nadir spatial sampling with ≤5 day revisit
>60% Monthly, >70% seasonal and >85% annual coverage of the terrestrial and shallow water regions of the Earth	> 40% Monthly, > 60% seasonal and >70% annual coverage of the terrestrial and shallow water regions of the Earth
Note: We will keep you informed of any changes such as the change in the saturation limit of the MIR band to 1200K	

© 2011 California Institute of Technology. Jet Propulsion Laboratory, California Institute of Technology. Government sponsorship acknowledged.